VOLUME 23 / NUMBER 24
DECEMBER 23, 1985
ACC. NOS. N85-35152 TO N85-36162

STAR
AN ABSTRACT JOURNAL

Scientific and Technical Aerospace Reports

PRODUCED BY THE
SCIENTIFIC AND TECHNICAL
INFORMATION
BRANCH

NASA

NATIONAL AERONAUTICS AND SPACE ADMINISTRATION

WHAT YOU CAN DO FOR *STAR*

All users of this abstract service are urged to forward reports to be considered for announcement in *STAR*. This will aid NASA in its efforts to provide the fullest possible coverage of all scientific and technical publications that might support aeronautics and space research and development. If you have prepared relevant reports (other than those that you will transmit to NASA, DoD, or DOE through the usual contract- or grant-reporting channels), please send them for consideration to the NASA Scientific and Technical Information Facility, P.O. Box 8757, B.W.I. Airport, Maryland 21240.

Reprints of journal articles, book chapters, and conference papers are also welcome. These will be considered for announcement in *STAR's* companion journal, *International Aerospace Abstracts*.

You may specify a particular source to be included in a report announcement if you wish; otherwise the report will be placed on public sale at the National Technical Information Service. Copyrighted publications will be announced but not distributed or sold.

PURCHASE OF *STAR*

The semimonthly issues are available for sale by the Superintendent of Documents, U.S. Government Printing Office, Washington, D.C. 20402.

PUBLISHED BY:

UNITED STATES GOVERNMENT
NATIONAL AERONAUTICS AND SPACE ADMINISTRATION
SCIENTIFIC AND TECHNICAL INFORMATION BRANCH
Scientific and Technical Aerospace Reports, Volume 23, is prepared by the NASA Scientific and Technical Information Facility operated for the National Aeronautics and Space Administration by RMS Associates.

The Administrator of the National Aeronautics and Space Administration has determined that the publication of this periodical is necessary in the transaction of the public business required by law of this Agency. Use of funds for printing this periodical has been approved by the Director of the Office of Management and Budget through March 22, 1988.

US ISSN 0036-8741

INTRODUCTION

Scientific and Technical Aerospace Reports (STAR) is a major component of a comprehensive National Aeronautics and Space Administration information system covering aeronautics, space, and supporting disciplines. *STAR* is issued on the 8th and 23rd of each month and announces current publications of the following types:

- NASA, NASA contractor, and NASA grantee reports
- Reports issued by other U.S. Government agencies, domestic and foreign institutions, universities, and private firms
- Translations in report form
- NASA-owned patents and patent applications
- Dissertations and theses

Cumulative index volumes are published annually.

Journal, book, and conference literature, cover-to-cover journal translations, and certain foreign dissertations are announced in a companion journal, *International Aerospace Abstracts (IAA)*, available on subscription from the American Institute of Aeronautics and Astronautics, Technical Information Service, 555 West 57th Street, 12th Floor, New York, New York 10019.

SUBJECT SCOPE

Subject scope of *STAR*, and *IAA* includes all aspects of aeronautics and space research and development, supporting basic and applied research, and applications. Aerospace aspects of earth resources, energy development, conservation, oceanography, environmental protection, urban transportation, and other topics of high national priority are also covered.

OTHER NASA PUBLICATIONS

Other NASA publications and information services are described in the publication, *The NASA Scientific and Technical Information System ... and How to Use It*, available without charge from the NASA Scientific and Technical Information Facility, P.O. Box 8757, B.W.I. Airport, Maryland 21240.

HOW TO USE *STAR* SUBJECT CATEGORIES

STAR is categorized by 10 major subject divisions divided into 74 specific subject categories and one general category/division. The major subject divisions are listed in the Table of Contents, together with a note for each that defines its scope and provides any cross-references. For example:

AERONAUTICS

Includes aeronautics (general); aerodynamics; air transportation and safety; aircraft communications and navigation; aircraft design, testing and performance; aircraft instrumentation; aircraft propulsion and power; aircraft stability and control; and research and support facilities (air).

For related information see also *Astronautics*.

Each major division is further divided into as many as nine specific categories, which are identified by category numbers.

Abstracts in *STAR* are grouped by specific category, the categories appearing in sequential order. Category breaks in the abstract section are identified by the category number and title, and a scope note. Cross-references to other categories are provided as appropriate. For example:

02 AERODYNAMICS

Includes aerodynamics of bodies, combinations, wings, rotors, and control surfaces; and internal flow in ducts and turbomachinery.

For related information see also *34 Fluid Mechanics and Heat Transfer*.

CROSS-REFERENCES

Individual *STAR* abstracts are not ordinarily cross-referenced, except for certain conference reports or book translations that have had separate abstracts written for their component papers or chapters. Citations and abstracts of the components follow immediately after those of the parent document. When the subject content of a component differs sufficiently from the general content of the parent, a cross-reference citation also is printed at the end of the category to which it normally would have been assigned if it were independent.

DOCUMENTS ON MICROFICHE

Documents on microfiche(1) are designated by a pound sign (#) following the accession number. The pound sign is used without regard to the source or quality of the microfiche.

AVAILABILITIES

One or more sources from which a document announced in *STAR* is available to the public is given in each citation. The most commonly indicated sources and their acronyms or abbreviations are listed below. If the publication is available from a source other than those listed, the publisher and his address will be displayed on the availability line or in combination with the corporate source line.

(1) A microfiche is a transparent sheet of film, 105 by 148 mm in size, containing as many as 60 to 98 pages of information reduced to micro images (not to exceed 26:1 reduction).

Avail: NTIS. Sold by the National Technical Information Service. Prices for hard copy (HC) and microfiche (MF) are indicated by a price code following the letters HC or MF in the *STAR* citation. Current values for the price codes are given in the tables on page vii.

Initially distributed microfiche under the NTIS SRIM (Selected Research in Microfiche) is available at greatly reduced unit prices. For this service and for information concerning subscription to NASA printed reports, consult the NTIS Subscription Section, Springfield, Va. 22161.

NOTE ON ORDERING DOCUMENTS: When ordering NASA publications (those followed by the * symbol), use the N accession number. NASA patent applications (only the specifications are offered) should be ordered by the US-Patent-Appl-SN number. Non-NASA publications (no asterisk) should be ordered by the AD, PB, or other *report* number shown on the last line of the citation, not by the N accession number. It is also advisable to cite the title and other bibliographic identification.

Avail: SOD (or GPO). Sold by the Superintendent of Documents, U.S. Government Printing Office, in hard copy. The current price and 'order number are given following the availability line. (NTIS will fill microfiche requests, as indicated above, for those documents identified by a # symbol.)

Avail: NASA Public Document Rooms. Documents so indicated may be examined at or purchased from the National Aeronautics and Space Adminstration, Public Documents Room (Room 126), 600 Independence Ave., S.W., Washington, D.C. 20546, or public document rooms located at each of the NASA research centers, the NASA Space Technology Laboratories, and the NASA Pasadena Office at the Jet Propulsion Laboratory.

Avail: DOE Depository Libraries. Organizations in U.S. cities and abroad that maintain collections of Department of Energy reports, usually in microfiche form, are listed in *Energy Research Abstracts*. Services available from the DOE and its depositories are described in a booklet, *DOE Technical Information Center - Its' Functions and Services* (TID-4660), which may be obtained without charge from the DOE Technical Information Center.

Avail: Univ. Microfilms. Documents so indicated are dissertations selected from *Dissertation Abstracts* and are sold by University Microfilms as xerographic copy (HC) and microfilm. All requests should cite the author and the Order Number as they appear in the citation.

Avail: USGS. Originals of many reports from the U.S. Geological Survey, which may contain color illustrations, or otherwise may not have the quality of illustrations preserved in the microfiche or facsimile reproduction, may be examined by the public at the libraries of the USGS field offices whose addresses are listed in this Introduction. The libraries may be queried concerning the availability of specific documents and the possible utilization of local copying services, such as color reproduction.

Avail: HMSO. Publications of Her Majesty's Stationery Office are sold in the U.S. by Pendragon House, Inc. (PHI), Redwood City, California. The U.S. price (including a service and mailing charge) is given, or a conversion table may be obtained from PHI.

Avail: BLL (formerly NLL): British Library Lending Division, Boston Spa, Wetherby, Yorkshire, England. Photocopies available from this organization at the price shown. (If none is given, inquiry should be addressed to the BLL.)

Avail: Fachinformationszentrum, Karlsruhe. Sold by the Fachinformationszentrum Energie, Physik, Mathematik GMBH, Eggenstein Leopoldshafen, Federal Republic of Germany, at the price shown in deutschmarks (DM).

Avail: Issuing Activity, or Corporate Author, or no indication of availability. Inquiries as to the availability of these documents should be addressed to the organization shown in the citation as the corporate author of the document.

Avail: U.S. Patent and Trademark Office. Sold by Commissioner of Patents and Trademarks, U.S. Patent and Trademark Office, at the standard price of 50 cents each, postage free. (See discussion of patents and patent applications below.)

Avail: ESDU. Pricing information on specific data, computer programs, and details on ESDU topic categories can be obtained from ESDU International Ltd. Requesters in North America should use the Virginia address while all other requesters should use the London address, both of which are on page vi.

NASA PATENTS AND PATENT APPLICATIONS

Patents and patent applications owned by NASA are announced in *STAR* under appropriate subject categories and are referenced in the *STAR* indexes. In the Report/Accession Number Index, patents are indexed by the NASA Case Number (which appears in lieu of the report number in other indexes), the U.S. Patent Number, the U.S. Patent Application Serial Number, and the U.S. Patent Class. Patent applications for which patents have not yet been issued are indexed by the NASA Case Number and the U.S. Patent Application Serial Number.

NASA *patent application specifications* are sold in paper copy by the National Technical Information Service at price code A02 ($9.95 domestic; $19.90 foreign). Microfiche are sold at price code A01 ($5.95 domestic; $11.90 foreign). The US-Patent-Appl-SN- number should be used in ordering either paper copy or microfiche from NTIS. Printed copies of *patents* (which are not microfiched) are available for purchase at 50 cents per copy from:

Commissioner of Patents and Trademarks
U.S. Patent and Trademark Office
Washington, D.C. 20231

When ordering patents, the U.S. Patent Number should be used, and payment must be remitted in advance, preferably by money order or check payable to the Commissioner of Patents and Trademarks. Prepaid purchase coupons for ordering are also available from the Patent and Trademark Office. The patents and patent applications announced in *STAR* are owned by NASA and are available for royalty-free licensing. Requests for licensing terms and further information should be addressed to:

Assistant General Counsel for Patent Matters/Code GP-1
National Aeronautics and Space Administration
Washington, D.C. 20546

ELIGIBILITY AND REGISTRATION FOR NASA INFORMATION PRODUCTS AND SERVICES

A variety of services is available to organizations of the following types that have registered with NASA to receive specific services or products:

1. NASA offices, research centers, contractors, subcontractors, grantees, and consultants;
2. Other U.S. Government agencies and their contractors;
3. Libraries in the United States that have arrangements with NASA to maintain collections of NASA documents for public reference;
4. Other organizations in the United States having a need for NASA documents in work related to aeronautics and space research;
5. Organizations abroad that have established reciprocal document exchange arrangements with NASA.

Only the central service points or central points of document acquisition and control within qualified organizations are eligible to register for NASA products and services. Domestic organizations that may be eligible to receive various classes of NASA publications and services should address their requests for registration or for further information to:

NASA Scientific and Technical Information Facility
ATTN: Registration Activity
P.O. Box 8757
B.W.I. Airport, Maryland 21240

Organizations abroad should direct requests to the same address, but to the attention of: International Exchange Program.

AVAILABILITY OF *STAR* ABSTRACTS ON MICROFICHE

Microfiche of the abstract sections of this issue and other issues of *STAR* are available on annual subscription from NTIS, Attn: Subscriptions, 5285 Port Royal Road, Springfield, Virginia 22161. Annual subscription rates are $60.00 North America; $120.00 foreign. Abstract sections for previous years retroactive to 1964 are available at the current rates. Microfiche for individual *STAR* issue abstract sections are not available.

PUBLIC COLLECTIONS OF NASA DOCUMENTS

DOMESTIC: NASA and NASA-sponsored documents and a large number of aerospace publications are available to the public for reference purposes at the library maintained by the American Institute of Aeronautics and Astronautics, Technical Information Service, 555 West 57th Street, 12th Floor, New York, New York 10019.

EUROPEAN: An extensive collection of NASA and NASA-sponsored publications is maintained by the British Library Lending Division, Boston Spa, Wetherby, Yorkshire, England for public access. The British Library Lending Division also has available many of the non-NASA publications cited in *STAR*. European requesters may purchase facsimile copy or microfiche of NASA and NASA-sponsored documents, those identified by both the symbols # and * from ESA - Information Retrieval Service European Space Agency, 8-10 rue Mario-Nikis, 75738 Paris CEDEX 15, France.

FEDERAL DEPOSITORY LIBRARY PROGRAM

In order to provide the general public with greater access to U.S. Government publications, Congress established the Federal Depository Library Program under the Government Printing Office (GPO), with 50 regional depositories responsible for permanent retention of material, inter-library loan, and reference services. Over 1,300 other depositories also exist. A list of the regional GPO libraries appears on the inside back cover of *STAR*.

ADDRESSES OF ORGANIZATIONS

American Institute of Aeronautics and Astronautics
Technical Information Service
555 West 57th Street, 12th Floor
New York, New York 10019

British Library Lending Division,
Boston Spa, Wetherby, Yorkshire,
England

Commissioner of Patents and Trademarks
U.S. Patent and Trademark Office
Washington, D.C. 20231

Department of Energy
Technical Information Center
P.O. Box 62
Oak Ridge, Tennessee 37830

ESA-Information Retrieval Service
ESRIN
Via Galileo Galilei
00044 Frascati (Rome) Italy

ESDU International, Ltd.
1495 Chain Bridge Road
McLean, Virginia 22101

ESDU International, Ltd.
251-259 Regent Street
London, W1R 7AD, England

Fachinformationszentrum Energie, Physik, Mathematik GMBH
7514 Eggenstein Leopoldshafen
Federal Republic of Germany

Her Majesty's Stationery Office
P.O. Box 569, S.E. 1
London, England

NASA Scientific and Technical Information Facility
P.O. Box 8757
B.W.I. Airport, Maryland 21240

National Aeronautics and Space Administration
Scientific and Technical Information Branch (NIT-1)
Washington, D.C. 20546

National Technical Information Service
5285 Port Royal Road
Springfield, Virginia 22161

Pendragon House, Inc.
899 Broadway Avenue
Redwood City, California 94063

Superintendent of Documents
U.S. Government Printing Office
Washington, D.C. 20402

University Microfilms
A Xerox Company
300 North Zeeb Road
Ann Arbor, Michigan 48106

University Microfilms, Ltd.
Tylers Green
London, England

U.S. Geological Survey Library
National Center – MS 950
12201 Sunrise Valley Drive
Reston, Virginia 22092

U.S. Geological Survey Library
2255 North Gemini Drive
Flagstaff, Arizona 86001

U.S. Geological Survey
345 Middlefield Road
Menlo Park, California 94025

U.S. Geological Survey Library
Box 25046
Denver Federal Center, MS 914
Denver, Colorado 80225

NTIS PRICE SCHEDULES

(Effective October 1, 1985)

Schedule A
STANDARD PRICE DOCUMENTS AND MICROFICHE

PRICE CODE	PAGE RANGE	NORTH AMERICAN PRICE	FOREIGN PRICE
A01	Microfiche	$ 5.95	$11.90
A02-A03	001-050	9.95	19.90
A04-A05	051-100	11.95	23.90
A06-A09	101-200	16.95	33.90
A10-A13	201-300	22.95	45.90
A14-A17	301-400	28.95	57.90
A18-A21	401-500	34.95	69.90
A22-A25	501-600	40.95	81.90
A99	601-up	*	*
NO1		$40.00	70.00
NO2		40.00	70.00

Schedule E
EXCEPTION PRICE DOCUMENTS AND MICROFICHE

PRICE CODE	NORTH AMERICAN PRICE	FOREIGN PRICE
E01	$ 7.50	15.00
E02	10.00	20.00
E03	11.00	22.00
E04	13.50	27.00
E05	15.50	31.00
E06	18.00	36.00
E07	20.50	41.00
E08	23.00	46.00
E09	25.50	51.00
E10	28.00	56.00
E11	30.50	61.00
E12	33.00	66.00
E13	35.50	71.00
E14	38.50	77.00
E15	42.00	84.00
E16	46.00	92.00
E17	50.00	100.00
E18	54.00	108.00
E19	60.00	120.00
E20	70.00	140.00
E99	*	*

*Contact NTIS for price quote.

IMPORTANT NOTICE

NTIS Shipping and Handling Charges (effective June 1, 1985)

U.S., Canada, Mexico — ADD $3.00 per TOTAL ORDER

All Other Countries — ADD $4.00 per TOTAL ORDER

Exceptions — Does NOT apply to:

ORDERS REQUESTING NTIS RUSH HANDLING
ORDERS FOR SUBSCRIPTION OR STANDING ORDER PRODUCTS *ONLY*

NOTE: Each additional delivery address on an order requires a separate shipping and handling charge.

VOLUME 23 NUMBER 24 / DECEMBER 23, 1985

TABLE OF CONTENTS

AERONAUTICS

Includes aeronautics (general); aerodynamics; air transportation and safety; aircraft communications and navigation; aircraft design, testing and performance; aircraft instrumentation; aircraft propulsion and power; aircraft stability and control; and research and support facilities (air).

For related information see also *Astronautics*.

01 AERONAUTICS (GENERAL) 4059

02 AERODYNAMICS 4059

Includes aerodynamics of bodies, combinations, wings, rotors, and control surfaces; and internal flow in ducts and turbomachinery.

For related information see also *34 Fluid Mechanics and Heat Transfer*

03 AIR TRANSPORTATION AND SAFETY 4062

Includes passenger and cargo air transport operations; and aircraft accidents.

For related information see also *16 Space Transportation* and *85 Urban Technology and Transportation*.

04 AIRCRAFT COMMUNICATIONS AND NAVIGATION 4063

Includes digital and voice communication with aircraft; air navigation systems (satellite and ground based); and air traffic control.

For related information see also *17 Spacecraft Communications, Command and Tracking* and *32 Communications*.

05 AIRCRAFT DESIGN, TESTING AND PERFORMANCE 4063

Includes aircraft simulation technology.

For related information see also *18 Spacecraft Design, Testing and Performance* and *39 Structural Mechanics*.

06 AIRCRAFT INSTRUMENTATION N.A.

Includes cockpit and cabin display devices; and flight instruments.

For related information see also *19 Spacecraft Instrumentation* and *35 Instrumentation and Photography*.

07 AIRCRAFT PROPULSION AND POWER 4065

Includes prime propulsion systems and systems components, e.g., gas turbine engines and compressors; and on-board auxiliary power plants for aircraft.

For related information see also *20 Spacecraft Propulsion and Power, 28 Propellants and Fuels*, and *44 Energy Production and Conversion*.

08 AIRCRAFT STABILITY AND CONTROL 4066

Includes aircraft handling qualities; piloting; flight controls; and autopilots.

09 RESEARCH AND SUPPORT FACILITIES (AIR) 4067

Includes airports, hangars and runways; aircraft repair and overhaul facilities; wind tunnels; shock tube facilities; and engine test blocks.

For related information see also *14 Ground Support Systems and Facilities (Space)*.

ASTRONAUTICS

Includes astronautics (general); astrodynamics; ground support systems and facilities (space); launch vehicles and space vehicles; space transportation; spacecraft communications, command and tracking; spacecraft design, testing and performance; spacecraft instrumentation; and spacecraft propulsion and power.

For related information see also *Aeronautics*

12 ASTRONAUTICS (GENERAL) 4068

For extraterrestrial exploration see *91 Lunar and Planetary Exploration*.

13 ASTRODYNAMICS N.A.

Includes powered and free-flight trajectories; and orbit and launching dynamics.

14 GROUND SUPPORT SYSTEMS AND FACILITIES (SPACE) 4068

Includes launch complexes, research and production facilities; ground support equipment, e.g., mobile transporters; and simulators.

For related information see also *09 Research and Support Facilities (Air)*.

15 LAUNCH VEHICLES AND SPACE VEHICLES 4068

Includes boosters; manned orbital laboratories; reusable vehicles; and space stations.

16 SPACE TRANSPORTATION N.A.

Includes passenger and cargo space transportation, e.g., shuttle operations; and rescue techniques.

For related information see also *03 Air Transportation and Safety* and *85 Urban Technology and Transportation*.

17 SPACECRAFT COMMUNICATION, COMMAND AND TRACKING N.A.

Includes telemetry; space communications networks; astronavigation; and radio blackout.

For related information see also *04 Aircraft Communications and Navigation* and *32 Communications*.

18 SPACECRAFT DESIGN, TESTING AND PERFORMANCE 4069

Includes spacecraft thermal and environmental control; and attitude control.

For life support systems see *54 Man/System Technology and Life Support*. For related information see also *05 Aircraft Design, Testing and Performance* and *39 Structural Mechanics*.

19 SPACECRAFT INSTRUMENTATION 4069

For related information see also *06 Aircraft Instrumentation* and *35 Instrumentation and Photography*.

20 SPACECRAFT PROPULSION AND POWER 4070

Includes main propulsion systems and components, e.g., rocket engines; and spacecraft auxiliary power sources.

For related information see also *07 Aircraft Propulsion and Power, 28 Propellants and Fuels*, and *44 Energy Production and Conversion*.

CHEMISTRY AND MATERIALS

Includes chemistry and materials (general); composite materials; inorganic and physical chemistry; metallic materials; nonmetallic materials; and propellants and fuels.

23 CHEMISTRY AND MATERIALS (GENERAL) 4071
Includes biochemistry and organic chemistry.

24 COMPOSITE MATERIALS 4072
Includes laminates.

25 INORGANIC AND PHYSICAL CHEMISTRY 4075
Includes chemical analysis, e.g., chromatography; combustion theory; electrochemistry; and photochemistry.
For related information see also *77 Thermodynamics and Statistical Physics.*

26 METALLIC MATERIALS 4077
Includes physical, chemical, and mechanical properties of metals, e.g., corrosion; and metallurgy.

27 NONMETALLIC MATERIALS 4081
Includes physical, chemical, and mechanical properties of plastics, elastomers, lubricants, polymers, textiles, adhesives, and ceramic materials.

28 PROPELLANTS AND FUELS 4083
Includes rocket propellants, igniters, and oxidizers; storage and handling; and aircraft fuels.
For related information see also *07 Aircraft Propulsion and Power, 20 Spacecraft Propulsion and Power,* and *44 Energy Production and Conversion.*

ENGINEERING

Includes engineering (general); communications; electronics and electrical engineering; fluid mechanics and heat transfer; instrumentation and photography; lasers and masers; mechanical engineering; quality assurance and reliability; and structural mechanics.
For related information see also *Physics.*

31 ENGINEERING (GENERAL) 4084
Includes vacuum technology; control engineering; display engineering; and cryogenics.

32 COMMUNICATIONS 4085
Includes land and global communications; communications theory; and optical communications.
For related information see also *04 Aircraft Communications and Navigation* and *17 Spacecraft Communications, Command and Tracking.*

33 ELECTRONICS AND ELECTRICAL ENGINEERING 4088
Includes test equipment and maintainability; components, e.g., tunnel diodes and transistors; microminiaturization; and integrated circuity.
For related information see also *60 Computer Operations and Hardware* and *76 Solid-State Physics.*

34 FLUID MECHANICS AND HEAT TRANSFER 4092
Includes boundary layers; hydrodynamics; fluidics; mass transfer; and ablation cooling.
For related information see also *02 Aerodynamics* and *77 Thermodynamics and Statistical Physics.*

35 INSTRUMENTATION AND PHOTOGRAPHY 4096
Includes remote sensors; measuring instruments and gages; detectors; cameras and photographic supplies; and holography.
For aerial photography see *43 Earth Resources.* For related information see also *06 Aircraft Instrumentation* and *19 Spacecraft Instrumentation.*

36 LASERS AND MASERS 4098
Includes parametric amplifiers.

37 MECHANICAL ENGINEERING 4098
Includes auxiliary systems (non-power); machine elements and processes; and mechanical equipment.

38 QUALITY ASSURANCE AND RELIABILITY 4099
Includes product sampling procedures and techniques; and quality control.

39 STRUCTURAL MECHANICS 4100
Includes structural element design and weight analysis; fatigue; and thermal stress.
For applications see *05 Aircraft Design, Testing and Performance* and *18 Spacecraft Design, Testing and Performance.*

GEOSCIENCES

Includes geosciences (general); earth resources; energy production and conversion; environment pollution; geophysics; meteorology and climatology; and oceanography.
For related information see also *Space Sciences.*

42 GEOSCIENCES (GENERAL) 4103

43 EARTH RESOURCES 4107
Includes remote sensing of earth resources by aircraft and spacecraft; photogrammetry; and aerial photography.
For instrumentation see *35 Instrumentation and Photography.*

44 ENERGY PRODUCTION AND CONVERSION 4109
Includes specific energy conversion systems, e.g., fuel cells and batteries; global sources of energy; fossil fuels; geophysical conversion; hydroelectric power; and wind power.
For related information see also *07 Aircraft Propulsion and Power, 20 Spacecraft Propulsion and Power, 28 Propellants and Fuels,* and *85 Urban Technology and Transportation.*

45 ENVIRONMENT POLLUTION 4113
Includes air, noise, thermal and water pollution; environment monitoring; and contamination control.

46 GEOPHYSICS 4114
Includes aeronomy; upper and lower atmosphere studies; ionospheric and magnetospheric physics; and geomagnetism.
For space radiation see *93 Space Radiation.*

47 METEOROLOGY AND CLIMATOLOGY 4119
Includes weather forecasting and modification.

48 OCEANOGRAPHY 4125
Includes biological, dynamic and physical oceanography; and marine resources.

LIFE SCIENCES

Includes sciences (general); aerospace medicine; behavioral sciences; man/system technology and life support; and planetary biology.

51 LIFE SCIENCES (GENERAL) 4126
Includes genetics.

52 AEROSPACE MEDICINE 4128
Includes physiological factors; biological effects of radiation; and weightlessness.

53 BEHAVIORAL SCIENCES 4133
Includes psychological factors; individual and group behavior; crew training and evaluation; and psychiatric research.

54 MAN/SYSTEM TECHNOLOGY AND LIFE SUPPORT 4134
Includes human engineering; biotechnology; and space suits and protective clothing.

55 PLANETARY BIOLOGY N.A.
Includes exobiology; and extraterrestrial life.

MATHEMATICAL AND COMPUTER SCIENCES

Includes mathematical and computer sciences (general); computer operations and hardware; computer programming and software; computer systems; cybernetics; numerical analysis; statistics and probability; systems analysis; and theoretical mathematics.

59 MATHEMATICAL AND COMPUTER SCIENCES (GENERAL) 4135

60 COMPUTER OPERATIONS AND HARDWARE 4135
Includes computer graphics and data processing.
For components see *33 Electronics and Electrical Engineering.*

61 COMPUTER PROGRAMMING AND SOFTWARE 4136
Includes computer programs, routines, and algorithms.

62 COMPUTER SYSTEMS 4141
Includes computer networks.

63 CYBERNETICS 4141
Includes feedback and control theory.
For related information see also *54 Man/System Technology and Life Support.*

64 NUMERICAL ANALYSIS 4141
Includes iteration, difference equations, and numerical approximation.

65 STATISTICS AND PROBABILITY 4144
Includes data sampling and smoothing; Monte Carlo method; and stochastic processes.

66 SYSTEMS ANALYSIS 4144
Includes mathematical modeling; network analysis; and operations research.

67 THEORETICAL MATHEMATICS N.A.
Includes topology and number theory.

PHYSICS

Includes physics (general); acoustics; atomic and molecular physics; nuclear and high-energy physics; optics; plasma physics; solid-state physics; and thermodynamics and statistical physics.
For related information see also *Engineering.*

70 PHYSICS (GENERAL) 4144
For geophysics see *46 Geophysics.* For astrophysics see *90 Astrophysics.* For solar physics see *92 Solar Physics.*

71 ACOUSTICS 4145
Includes sound generation, transmission, and attenuation.
For noise pollution see *45 Environment Pollution.*

72 ATOMIC AND MOLECULAR PHYSICS 4146
Includes atomic structure and molecular spectra.

73 NUCLEAR AND HIGH-ENERGY PHYSICS 4149
Includes elementary and nuclear particles; and reactor theory.
For space radiation see *93 Space Radiation.*

74 OPTICS 4153
Includes light phenomena.

75 PLASMA PHYSICS 4154
Includes magnetohydrodynamics and plasma fusion.
For ionospheric plasmas see *46 Geophysics.* For space plasmas see *90 Astrophysics.*

76 SOLID-STATE PHYSICS 4160
Includes superconductivity.
For related information see also *33 Electronics and Electrical Engineering* and *36 Lasers and Masers.*

77 THERMODYNAMICS AND STATISTICAL PHYSICS N.A.
Includes quantum mechanics; and Bose and Fermi statistics.
For related information see also *25 Inorganic and Physical Chemistry* and *34 Fluid Mechanics and Heat Transfer.*

SOCIAL SCIENCES

Includes social sciences (general); administration and management; documentation and information science; economics and cost analysis; law and political science; and urban technology and transportation.

80 SOCIAL SCIENCES (GENERAL) N.A.
Includes educational matters.

81 ADMINISTRATION AND MANAGEMENT 4163
Includes management planning and research.

82 DOCUMENTATION AND INFORMATION SCIENCE 4164
Includes information storage and retrieval technology; micrography; and library science.
For computer documentation see *61 Computer Programming and Software.*

83 ECONOMICS AND COST ANALYSIS N.A.
Includes cost effectiveness studies.

84 LAW AND POLITICAL SCIENCE 4166
Includes space law; international law; international cooperation; and patent policy.

85 URBAN TECHNOLOGY AND TRANSPORTATION 4166
Includes applications of space technology to urban problems; technology transfer; technology assessment; and surface and mass transportation.
For related information see *03 Air Transportation and Safety, 16 Space Transportation,* and *44 Energy Production and Conversion.*

SPACE SCIENCES

Includes space sciences (general); astronomy; astrophysics; lunar and planetary exploration; solar physics; and space radiation.
For related information see also *Geosciences.*

88 SPACE SCIENCES (GENERAL) N.A.

89 ASTRONOMY 4166
Includes radio and gamma-ray astronomy; celestial mechanics; and astrometry.

90 ASTROPHYSICS 4167
Includes cosmology; and interstellar and interplanetary gases and dust.

91 LUNAR AND PLANETARY EXPLORATION 4169
Includes planetology; and manned and unmanned flights.
For spacecraft design see *18 Spacecraft Design, Testing and Performance.* For space stations see *15 Launch Vehicles and Space Vehicles.*

92 SOLAR PHYSICS 4169
Includes solar activity, solar flares, solar radiation and sunspots.

93 SPACE RADIATION 4170
Includes cosmic radiation; and inner and outer earth's radiation belts.
For biological effects of radiation see *52 Aerospace Medicine.* For theory see *73 Nuclear and High-Energy Physics.*

GENERAL

99 GENERAL N.A.

Note: N.A. means that no abstracts were assigned to this category for this issue.

SUBJECT INDEX I-1
PERSONAL AUTHOR INDEX I-67
CORPORATE SOURCE INDEX I-77
CONTRACT NUMBER INDEX I-91
REPORT / ACCESSION NUMBER INDEX I-93

TYPICAL CITATION AND ABSTRACT

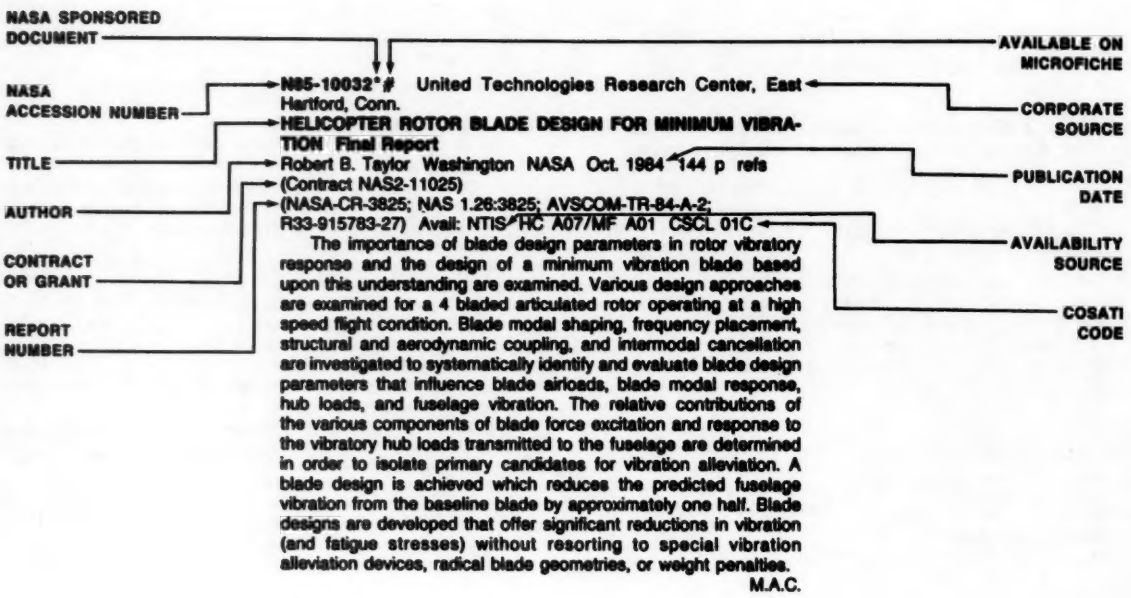
NASA SPONSORED DOCUMENT
AVAILABLE ON MICROFICHE
NASA ACCESSION NUMBER
N85-10032*# United Technologies Research Center, East Hartford, Conn.
CORPORATE SOURCE
TITLE
HELICOPTER ROTOR BLADE DESIGN FOR MINIMUM VIBRATION Final Report
AUTHOR
Robert B. Taylor Washington NASA Oct. 1984 144 p refs
PUBLICATION DATE
CONTRACT OR GRANT
(Contract NAS2-11025)
REPORT NUMBER
(NASA-CR-3825; NAS 1.26:3825; AVSCOM-TR-84-A-2; R33-915783-27) Avail: NTIS HC A07/MF A01 CSCL 01C
AVAILABILITY SOURCE
COSATI CODE
The importance of blade design parameters in rotor vibratory response and the design of a minimum vibration blade based upon this understanding are examined. Various design approaches are examined for a 4 bladed articulated rotor operating at a high speed flight condition. Blade modal shaping, frequency placement, structural and aerodynamic coupling, and intermodal cancellation are investigated to systematically identify and evaluate blade design parameters that influence blade airloads, blade modal response, hub loads, and fuselage vibration. The relative contributions of the various components of blade force excitation and response to the vibratory hub loads transmitted to the fuselage are determined in order to isolate primary candidates for vibration alleviation. A blade design is achieved which reduces the predicted fuselage vibration from the baseline blade by approximately one half. Blade designs are developed that offer significant reductions in vibration (and fatigue stresses) without resorting to special vibration alleviation devices, radical blade geometries, or weight penalties.
M.A.C.

VOLUME 23 NUMBER 24 / DECEMBER 23, 1985

Scientific and Technical Aerospace Reports

A Semimonthly Publication of the National Aeronautics and Space Administration

01 AERONAUTICS (GENERAL)

N85-35152* National Aeronautics and Space Administration, Washington, D. C.
AERONAUTICAL ENGINEERING: A CONTINUING BIBLIOGRAPHY WITH INDEXES, SUPPLEMENT 190
Aug. 1985 140 p
(NASA-SP-7037(190); NAS 1.21:7037(190)) Avail: NTIS HC $6.00 CSCL 01A

This bibliography lists 510 reports, articles and other documents introduced into the NASA scientific and technical information system in July 1985. Author

N85-35153# Federal Aviation Agency, Washington, D.C. Office of Management Systems.
U.S. CIVIL AIRMEN STATISTICS FOR CALENDAR YEAR 1984 Annual Report
31 May 1985 44 p
(AD-A156326) Avail: NTIS HC A03/MF A01 CSCL 01/2

The U.S. Civil Airmen Statistics is an annual study published to meet the demands of FAA, other government agencies, and industry for more detailed airmen statistics than those published in other FAA reports. Statistics pertaining to airmen, both pilot and nonpilot, were obtained from the official airman certification records maintained at the FAA Aeronautical Center, Oklahoma City, Oklahoma. An active airmen is one who holds both an airmen certificate and a valid medical certificate. Airmen who must have a valid medical to exercise the privileges of their certificate are all airplane pilots, control tower operators, flight navigators, flight engineers, and flight instructors. The glider and lighter-than-air pilots are not required to have a medical examination but the numbers represent only those who had a valid medical certificate. Mechanics, parachute riggers, ground instructors, and dispatchers certificates represent all certificates on record at the aeronautical center. GRA

02 AERODYNAMICS

Includes aerodynamics of bodies, combinations, wings, rotors, and control surfaces; and internal flow in ducts and turbomachinery.

For related information see also *34 Fluid Mechanics and Heat Transfer.*

N85-35154 Iowa Univ., Iowa City.
FINITE ANALYTIC SOLUTIONS OF SUPERSONIC FLOWS IN TWO-DIMENSIONAL NON-SYMMETRICAL CHANNELS Ph.D. Thesis
Wen-Chung Chen 1984 332 p
Avail: Univ. Microfilms Order No. DA8507927

A finite analytic (FA) numerical solution for steady supersonic flows with and without shock waves formation in two-dimensional non-symmetric channels is derived. The FA method utilizes the analytic solution which is based on method of characteristics for hyperbolic equations to formulate the algebraic approximation of governing partial differential equations in each small element. The solution of the system of FA algebraic equations assembled from all elements thus provides the solution of the problem. The FA solution is shown to preserve the analytic nature of characteristic solution in the numerical solution. A body-fitted coordinate system based on interpolation is used to map a non-symmetric physical domain into a rectangular computational domain which is discretized with regular grids. Dissert. Abstr.

N85-35155 Stanford Univ., Calif.
ADVERSE PRESSURE GRADIENT AND SEPARATING TURBULENT BOUNDARY-LAYER FLOWS: THE EFFECT OF DISEQUILIBRIUM IN INITIAL CONDITIONS Ph.D. Thesis
Andrew David Cutler 1985 394 p
Avail: Univ. Microfilms Order No. DA8506175

This report documents an experimental study of detaching and reattaching boundary layers and boundary layers downstream of a reattachment. Three low Mach number, fully turbulent boundary layers flowing on a flat surface have been investigated, Cases 1, 2, and 3. Cases 1 and 2 both flow towards detachment in a strong adverse pressure gradient, pass through incipient detachment, closely approach detachment, and then fully reattach. Case 1 is nearly at equilibrium at the start of the pressure gradient, whereas Case 2 has been manipulated so that, at the start of the adverse pressure gradient, its structure is far from equilibrium, with very high turbulence levels. Case 3 is a boundary layer downstream of a reattachment, initially far from equilibrium but relaxing in an adverse pressure gradient towards an equilibrium structure. Measurements have been made of the wall static-pressure distributions, percent backflow at the walls, total pressure profiles and mean-velocity and turbulence quantities.
Dissert. Abstr.

N85-35156 North Carolina State Univ., Raleigh.
A STREAM FUNCTION APPROACH TO SOLVING THE CONSERVATIVE EULER EQUATIONS FOR TRANSONIC FLOWS Ph.D. Thesis
Harold Lee Atkins 1984 121 p
Avail: Univ. Microfilms Order No. DA8506981

An approach to obtaining steady state solutions to the conservative Euler equations in two dimensions is presented. The approach makes use of the adiabatic assumption, and employs the stream function and the density as dependent variables, thus eliminating one equation and one unknown. The present approach is implemented in two different ways. In the first method, the conservative Euler equations are recast in terms of the density and the stream function to yield a system of two partial differential equations. The resulting equations are stiff, and hence, are solved by a fully implicit method for a geometrically simple internal flow problem. In the second method, the partial differential equation for density is replaced by an algebraic relation. Thus the resulting formulation involves solving one second order partial

differential equation for the stream function. The second method is applied to airfoils at transonic speeds. Dissert. Abstr.

N85-35157 Texas Univ., Austin.
THE APPLICATION OF BISPECTRAL ANALYSES TO AEROELASTIC PHENOMENA Ph.D. Thesis
Jung-Hua Chang 1984 159 p
Avail: Univ. Microfilms Order No. DA8508256

A physical system which is described by a set of differential equations with periodic time varying coefficients is sometimes referred to as an auto-parametric system. Many times the classical linear aeroelastic responses of a structure may be contaminated by auto-parametric and nonlinear responses. A positive experimental identification of such auto-parametric and nonlinear responses is desirable. The present study introduces the digital bispectral identification technique to investigate these auto-parametric and nonlinear responses. Since classical flutter and divergence are limiting cases of auto-parametric resonances, a subcritical flutter testing technique is proposed and investigated which employs this bispectral identification technique. A parametrically excited thin cantilever beam with a finite base motion is employed as a model for analyzing experimental data associated with flutter, auto-parametric and nonlinear response phenomena. Discrete frequency parametric excitation is analyzed first so a comparison can be made between the results of experimental study and the theoretical analyses. The bispectral study is then applied to a case of random parametric excitation. Dissert. Abstr.

N85-35158*# Braun (Willis H.), Berea, Ohio.
UNSTEADY FLOW IN A SUPERSONIC CASCADE WITH TWO IN-PASSAGE SHOCKS Final Report
Willis H. Braun Sep. 1985 90 p refs
(Contract NAS3-24100)
(NASA-CR-3925; E-2129; NAS 1.26:3925) Avail: NTIS HC A05/MF A01 CSCL 01A

A model for a supersonic blade row with two in-passage shock waves is developed. It accounts for three-dimensional effects in real flows by using an altered blade shape in a two-dimensional cascade. There is enough flexibility in the choice of blade shape to accommodate a desired entrance angle, exit angle, boundary-layer thickness and stage pressure ratio at a given entrance Mach number. The model divides the mean flow into regions of uniform or one-dimensional flow in which the solutions for the unsteady flow may be formed successively. The analysis makes use of previous solutions for unsteady flow in cascades and over an oscillation wedge. Six flow conditions are chosen in the range of parameters for which the two-shock model is valid for studies of flutter in torsion and bending. It is found, in keeping with previous results from a single-shock model, that in each case there is increasing instability with decreasing frequency. Author

N85-35159*# Stanitz (John D.), University Heights, Ohio.
GENERAL DESIGN METHOD FOR 3-DIMENSIONAL, POTENTIAL FLOW FIELDS. PART 2: COMPUTER PROGRAM DIN3D1 FOR SIMPLE, UNBRANCHED DUCTS Final Report
John D. Stanitz Washington NASA Sep. 1985 88 p refs
(Contract NAS3-21991)
(NASA-CR-3926; E-2388; NAS 1.26:3926) Avail: NTIS HC A05/MF A01 CSCL 01A

The general design method for three-dimensional, potential, incompressible or subsonic-compressible flow developed in part 1 of this report is applied to the design of simple, unbranched ducts. A computer program, DIN3D1, is developed and five numerical examples are presented: a nozzle, two elbows, an S-duct, and the preliminary design of a side inlet for turbomachines. The two major inputs to the program are the upstream boundary shape and the lateral velocity distribution on the duct wall. As a result of these inputs, boundary conditions are overprescribed and the problem is ill posed. However, it appears that there are degrees of compatibility between these two major inputs and that, for reasonably compatible inputs, satisfactory solutions can be obtained. By not prescribing the shape of the upstream boundary, the problem presumably becomes well posed, but it is not clear how to formulate a practical design method under this circumstance. Nor does it appear desirable, because the designer usually needs to retain control over the upstream (or downstream) boundary shape. The problem is further complicated by the fact that, unlike the two-dimensional case, and irrespective of the upstream boundary shape, some prescribed lateral velocity distributions do not have proper solutions. Author

N85-35160*# GMAF, Inc., Freeport, N.Y.
NUMERICAL STUDIES OF 2-DIMENSIONAL FLOWS Final Report
Gino Moretti Washington NASA Sep. 1985 23 p refs
(Contract NAS1-17262)
(NASA-CR-3930; NAS 1.26:3930) Avail: NTIS HC A02/MF A01 CSCL 01A

A formulation of the lambda scheme for the analysis of two dimensional inviscid, compressible, unsteady transonic flows is presented. The scheme uses generalized Riemann variables to determine the appropriate two point, one sided finite difference approximation for each derivative in the unsteady Euler equations. These finite differences are applied at the predictor and corrector levels with shock updating at each level. The weaker oblique shocks are captured, but strong near normal shocks are fitted into the flow using the Rankine-Hugoniot relations. This code is demonstrated with a numerical example of a duct flow problem with developing normal and oblique shock waves. The technique is implemented in a code which has been made efficient by streamlining to a minimal number of operations and by eliminating branch statements. The scheme is shown to provide an accurate analysis of the flow, including formation, motions, and interactions of shocks; the results obtained on a relatively coarse mesh are comparable to those obtained by other methods on much finer meshes.Author

N85-35161*# National Aeronautics and Space Administration, Washington, D. C.
PRESENTATION OF THE ACOUSTIC AND AERODYNAMIC RESULTS OF THE ALADIN 2 CONCEPT QUALIFICATION TESTING
M. Collard, C. Doyotte, and M. Sagner Jul. 1985 30 p refs
Transl. into ENGLISH of Presentation des Resultats Aerodyn. et Acoust. des Essais de Qualification du Concept Aladin 2, (France), In: AGARD CP-143, Apr. 1974 10 p Original language doc. was announced in IAA as A75-13803 Transl. by Scientific Translation Services, Santa Barbara Calif. Original doc. prep. by Bertin and Cie Company
(Contract NASw-4004)
(NASA-TM-77883; NAS 1.15:77883; CP-143) Avail: NTIS HC A03/MF A01 CSCL 01A

Wind tunnel tests were conducted of a scale model of the Aladin 2 aircraft. The propulsion system configuration is described and the air flow caused by jet ejection is analyzed. Three dimensional flow studies in the vicinity of the engine installation were made. Diagrams of the leading and trailing edge flaps are provided. Graphs are developed to show the aerodynamic performance under conditions of various airspeed and flap deflection.
Author

N85-35162*# Douglas Aircraft Co., Inc., Long Beach, Calif.
CALCULATION OF COMPRESSIBLE FLOW ABOUT THREE-DIMENSIONAL INLETS WITH AUXILIARY INLETS, SLATS AND VANES BY MEANS OF A PANEL METHOD Final Contractor Report, 17 Feb. 1983 - 15 Aug. 1985
J. L. Hess, D. M. Friedman, and R. W. Clark Jun. 1985 197 p refs
(Contract NAS3-22250)
(NASA-CR-174975; NAS 1.26:174975; MDC-J3789) Avail: NTIS HC A09/MF A01 CSCL 01A

An efficient and user oriented method was constructed for calculating flow in and about complex inlet configurations. Efficiency is attained by: (1) the use of a panel method; (2) a technique of superposition for obtaining solutions at any inlet operating condition; and (3) employment of an advanced matrix iteration technique for solving large full systems of equations, including the nonlinear

equations for the Kutta condition. User concerns are addressed by the provision of several novel graphical output options that yield a more complete comprehension of the flowfield than was possible previously. E.A.K.

N85-35163*# National Aeronautics and Space Administration, Washington, D. C.
SUPERSONIC FLOW WITH FEEDING OF ENERGY
W. Zaremba Aug. 1985 12 p Transl. into ENGLISH from Tech. Lotnicza i Astronautyczna (Poland), v. 30, Feb. 1975 p 13-16 Original language document was announced in IAA as A75-24826 Transl. by The Corporate Word, Inc., Pittsburgh, Pa.
(Contract NASw-4006)
(NASA-TM-77912; NAS 1.15:77912) Avail: NTIS HC A02/MF A01 CSCL 01A

The present work discusses the results of some experimental studies on the possibility of attenuating shock waves in a supersonic flow. The shock waves were formed by an external source of electrical energy. An electromechanical method is described that permits partial recovery of the expended energy. P.T.H.

N85-35164*# National Aeronautics and Space Administration, Washington, D. C.
DECELERATION OF A SUPERSONIC FLOW BEHIND A CURVED SHOCK WAVE WITH ISENTROPIC PRECOMPRESSION
V. G. Dulov and V. A. Shchepanovskiy Sep. 1985 13 p refs Transl. into ENGLISH from Sibirsk. Otd., Izv. Ser. Tekhn. Nauk (USSR), no. 8, Jun. 1977 p 72-78 Original language document was announced in IAA as A78-18986 Transl. by The Corporate Word, Inc., Pittsburgh, Pa.
(Contract NASw-4006)
(NASA-TM-77920; NAS 1.15:77920) Avail: NTIS HC A02/MF A01 CSCL 01A

Three-dimensional supersonic flows of an ideal fluid in the neighborhood of bodies formed by being cut out along the streamlines of an axisymmetric flow are investigated. The flow consists of a region of isoentropic compression and a region of vortex flow. An exact solution with variable entropy is used to describe the flow in the vortex region. In the continuous flow region an approximate solution is constructed by expanding the solution in a series in a small parameter. The effect of the shape of the excision and the vorticity of the flow on compression of the jet and and the total pressure loss coefficient is studied. P.T.H.

N85-35165# European Space Agency, Paris (France).
LECTURES OF A FLIGHT MECHANICS CONFERENCE
Jul. 1984 116 p refs Transl. into ENGLISH of "Vortraege eines Flugmechanik-Kolloquiums" rept. DFVLR-Mitt-83-05 DFVLR, Brunswick, Jul. 1983 128 p Conf. held at Brunswick, Dec. 1981 Original language document was announced as N84-16120
(ESA-TT-831; DFVLR-Mitt-83-05) Avail: NTIS HC A06/MF A01; original German version available from DFVLR, Cologne DM 39.20

The development of flight mechanical research at the Technical University Braunschweig is surveyed. Activities of a US liaison office for research support in Europe are reported. Flight mechanical problems of the pilot-aircraft system due to the introduction of new technologies are discussed. The influence of measuring section parameters on the results of a flight mechanical system identification is treated. Flight mechanical motion characteristics are estimated with Kalman filters. Gust producers for flight mechanical investigations in wind tunnels are considered. For individual titles, see N85-35166 through N85-35172.

N85-35166# European Space Agency, Paris (France).
DEVELOPMENT OF FLIGHT MECHANICS RESEARCH IN BRUNSWICK
Werner Schulz *In its* Lectures of a Flight Mech. Conf. (DFVLR-Mitt-83-05) Jul. 1984 p 7-17 Transl. into ENGLISH from "Vortraege eines Flugmechanik-Kolloquiums" rept. DFVLR-Mitt-83-05 DFVLR, Brunswick, Jul. 1983 p 9-19 Original language document was announced as N84-16121 (For primary document see N85-35165 24-02)
Avail: NTIS HC A06/MF A01; original German version available from DFVLR, Cologne DM 39.20

The development of flight mechanics research at the Technical University Braunschweig, for the period 1909 to 1981 is described. Author (ESA)

N85-35167# European Space Agency, Paris (France).
RESEARCH REPORT PROGRAM OF THE US ARMY IN EUROPE c81
Siegfried H. Lehnigk *In its* Lectures of a Flight Mech. Conf. (DFVLR-Mitt-83-05) Jul. 1984 p 18-24 Transl. into ENGLISH from "Vortraege eines Flugmechanik-Kolloquiums" rept. DFVLR-Mitt-83-05 DFVLR, Brunswick, Jul. 1983 p 21-27 Original language document was announced as N84-16122 (For primary document see N85-35165 24-02)
Avail: NTIS HC A06/MF A01; original German version available from DFVLR, Cologne DM 39.20

The US research liaison office for in Europe is described. Activities include chemistry, biology, computer sciencs, electronics, mechanics, fluid mechanics, materials science, mathematics, physics, and behavioral science. Author (ESA)

N85-35168# European Space Agency, Paris (France).
NEW TECHNOLOGIES AT THE FOREFRONT OF INDUSTRIAL DEVELOPMENTS c81
Helmut Ulke *In its* Lectures of a Flight Mech. Conf. (DFVLR-Mitt-83-05) Jul. 1984 p 25-41 Transl. into ENGLISH from Vortraege eines Flugmechanik-Kolloquiums" rept. DFVLR-Mitt-83-05 DFVLR, Brunswick, Jul. 1983 p 29-46 Original language document was announced as N84-16123 (For primary document see N85-35165 24-02)
Avail: NTIS HC A06/MF A01; original German version available from DFVLR, Cologne DM 39.20

Dornier's efforts to introduce the findings of aeronautics and astronautics into a broad spectrum of technical processes are described. Development trends in electronics using microprocessors are reviewed. They result in a higher technical performance, a cost reduction, and savings of energy and raw materials. In the domain of energy technology, heat pipes developed for satellites are used in solar energy systems; an energy saving system to produce hydrogen from water using high temperature vapor phase electrolysis (Hot Elly) was developed. Medical equipment for renal calculus therapy using shock waves was developed. Author (ESA)

N85-35169# European Space Agency, Paris (France).
THE CONTRIBUTION MADE BY FLIGHT MECHANICS TO CIVIL AVIATION c03
Peter Hamel *In its* Lectures of a Flight Mech. Conf. (DFVLR-Mitt-83-05) Jul. 1984 p 42-58 Transl. into ENGLISH from "Vortraege eines Flugmechanik-Kolloquiums" rept. DFVLR-Mitt-83-05 DFVLR, Brunswick, Jul. 1983 p 47-64 Original language document was announced as N84-16124 (For primary document see N85-35165 24-02)
Avail: NTIS HC A06/MF A01; original German version available from DFVLR, Cologne DM 39.20

Flight mechanical problems of the pilot-aircraft system due to the introduction of new technologies are discussed. These technologies (e.g., active control technology) are used to reduce fuel costs. Research on an evaluating improving flight characteristics using an Airbus in-flight simulator is discussed. Author (ESA)

N85-35170# European Space Agency, Paris (France).
THE EFFECT OF INSTRUMENTATION SYSTEM PARAMETERS ON THE RESULTS OF A FLIGHT MECHANICAL SYSTEM IDENTIFICATION
Martin Marchand *In its* Lectures of a Flight Mech. Conf. (DFVLR-Mitt-83-05) Jul. 1984 p 59-79 refs Transl. into ENGLISH from Vortraege eines Flugmechanik-Kolloquiums" rept. DFVLR-Mitt-83-05 DFVLR, Brunswick, Jul. 1983 p 65-84 Original language document was announced as N84-16125 (For primary document see N85-35165 24-02)
Avail: NTIS HC A06/MF A01; original German version available

from DFVLR, Cologne DM 39.20

The influence of measuring section parameters on the identification of the flight-mechanical derivatives of a free flying DO-28-TNT model was investigated. The results are considerably influenced and altered by a time delay in the pitch velocity measuring section, imposing a system of third order in the mathematical description of the flight. The derivatives calculated with this mathematical model agree well with those derived from the measured signals. This extended model requires 5 to 10 times more calculation time. The possibility of reducing this time by compensating the measuring section dynamics in the data evaluation are discussed.

Author (ESA)

N85-35171# European Space Agency, Paris (France).
ESTIMATION OF FLIGHT MECHANICAL VARIABLES BY MEANS OF KALMAN FILTERS

Ermin Plaetschke *In its* Lectures of a Flight Mech. Conf. (DFVLR-Mitt-83-05) Jul. 1984 p 80-92 refs Transl. into ENGLISH from "Vortraege eines Flugmechanik-Kolloquiums" rept. DFVLR-Mitt-83-05 DFVLR, Brunswick, Jul. 1983 p 85-99 Original language document was announced as N84-16126 (For primary document see N85-35165 24-02)

Avail: NTIS HC A06/MF A01; original German version available from DFVLR, Cologne DM 39.20

A data evaluation system was developed to estimate flight-mechanical characteristics. The measurements concern specific aerodynamic forces, angular velocities, and air data (flight velocity, angle of attack, and sliding angle). The measurement data are incompatible due to zero point drift, false calibrations, and noise. The data evaluation system uses the redundancy between the data through the equations or motion to estimate the errors, resulting in a compatible set of data. The state variables are Kalman filter estimated. Author (ESA)

N85-35172# European Space Agency, Paris (France).
GUST SIMULATION FOR FLIGHT MECHANICAL WIND TUNNEL TESTS

Bernd Krag *In its* Lectures of a Flight Mech. Conf. (DFVLR-Mitt-83-05) Jul. 1984 p 93-115 refs Transl. into ENGLISH from "Vortraege eines Flugmechanik-Kolloquiums" rept. DFVLR-Mitt-83-05 DFVLR, Brunswick, Jul. 1983 p 101-126 Original language document was announced as N84-16127 (For primary document see N85-35165 24-02)

Avail: NTIS HC A06/MF A01; original German version available from DFVLR, Cologne DM 39.20

Gust producers in the low velocity domain were tested in a wind tunnel. The gust field and flow direction were measured with a grid consisting of five differential pressure probes. A frequency dependent propagation velocity of the gusts is found in all cases. An open measuring section leads to higher gust amplitude. The amplitude decreases away from the gust producer in the case of a closed measuring section. Any vortex developing in the boundary layers leads to a deterioration of the gust quality. The measurements show that a defined and usable gust field for measuring purposes can be produced in a wind tunnel with relatively simple means. Author (ESA)

N85-35173# Naval Postgraduate School, Monterey, Calif.
ANALYSIS OF INCOMPRESSIBLE CASCADE FLOWS USING STATE-OF-THE-ART COMPUTER PROGRAMS M.S. Thesis

P. E. Genskow Mar. 1985 65 p
(AD-A155850) Avail: NTIS HC A04/MF A01 CSCL 09/2

Two state-of-the-art computer programs, Q3DFLOW and a standard Cebeci boundary layer program as applied to aerodynamic flows in a cascade are examined. Q3DFLOW is a quasi three-dimensional finite element turbomachinery program. Only the incompressible blade-to-blade module of this program is used. The Cebeci boundary layer program is for incompressible, two dimensional, and constant viscosity flows. It is used to calculate boundary layers on a few isolated airfoils and airfoils/blades in a cascade. Experimental data and other analytical computations are compared for both programs. Additionally, the theory and operation of the Cebeci boundary layer program are presented. GRA

N85-35174# Naval Postgraduate School, Monterey, Calif.
THE INFLUENCE OF HELICOPTER TAIL SHAPE ON DRAG: AN AERODYNAMIC STUDY USING A LOW SPEED WIND TUNNEL M.S. Thesis

C. L. Sargent Mar. 1985 91 p
(AD-A156304) Avail: NTIS HC A05/MF A01 CSCL 20/4

This thesis examines the effect of helicopter tail shape on drag using a low speed wind tunnel at the Naval Postgraduate School. A modification to the Aeronautical Engineering Department's 3.5 ft x 5 ft. wind tunnel was made to update facilities and allow this work. Major R. Scott Mair worked simultaneously to study the effect of nose shape on drag, a result of the 2-man requirement for wind tunnel work. The existing external balance was replaced with an internal balance and a variable angle-of-attack support system was constructed as well. Quantitative data was collected with this balance, and qualitative information was obtained by tufting the models and visualizing the airflow. The equipment built was adequate with the exception of one component of the balance, which will require a new balance to be built. This single deficiency was significant enough to invalidate the output of the balance and as a result any quantitative discussion of how a helicopter's tail shape affects drag. Without this data the explanation of drag using flow visualization is also not practical. GRA

03 AIR TRANSPORTATION AND SAFETY

Includes passenger and cargo air transport operations; and aircraft accidents.

For related information see also *16 Space Transportation* and *85 Urban Technology and Transportation.*

N85-35175# Air Force Inst. of Tech., Wright-Patterson AFB, Ohio.
INVESTIGATION OF EXPERIMENTAL LIGHTWEIGHT FIREWALL MATERIALS FOR A/C ENGINE BAY APPLICATIONS Final Report, 1 Oct. 1983 - 2 May 1984

J. J. Moyer Wright-Patterson AFB, Ohio AFWAL Apr. 1985 119 p
(AD-A155765; AFWAL-TR-84-2082) Avail: NTIS HC A06/MF A01 CSCL 11/7

An evaluation of fire-resistant materials was conducted to identify possible replacements for stainless steel for use as aircraft firewalls. The materials were subjected to the standard firewall (MIL-I-83294), fire-penetration test. In addition, each sample passing this test was further evaluated on weight, thermal protection, and maintenance requirements. An attempt was made to correlate physical properties to fire penetration test performance, but was not successful due to the lack of physical property information. The report identifies those materials which should be developed for use as firewalls and fire-hardening materials on the aircraft. Author (GRA)

N85-35176# Air Command and Staff Coll., Maxwell AFB, Ala.
INTRODUCTION TO EUROPEAN AIR TRAFFIC CONTROL

I. J. Hayes Apr. 1985 51 p
(AD-A156328; ACSC-85-1095) Avail: NTIS HC A04/MF A01 CSCL 17/7

The Strategic Air Command's authoritative source for instrument flight procedures, SAC Instrument Flight Course (SIFC), has no comprehensive vehicle with which to introduce the European flight environment to crews that may deploy into the unfamiliar airspace. The study acquaints the reader with the overall nature of flying in the European theater and introduces some procedural differences. The study also looks at how the European system is organized, by examining the airspace structure. The study concludes with a look at the military/civilian dichotomy of airspace control in Europe. GRA

N85-35177# Air Command and Staff Coll., Maxwell AFB, Ala.
INTERNATIONAL FLIGHT PLANNING HANDBOOK

H. J. Garvin Apr. 1985 71 p
(AD-A156330; ACSC-85-0915) Avail: NTIS HC A04/MF A01

CSCL 01/2

This handbook has been developed to instruct pilots and navigators on basic planning procedures and operations within the international environment. It provides a consolidated source of information to facilitate planning for international flights. The handbook is developed in four chapters covering: (1) an overview of the international environment, followed by checklists with item-by-item amplification of, (2) pre-flight planning, (3) enroute operations, and (4) services and facilities at foreign destinations. GRA

N85-35169# European Space Agency, Paris (France).
THE CONTRIBUTION MADE BY FLIGHT MECHANICS TO CIVIL AVIATION
Peter Hamel *In its* Lectures of a Flight Mech. Conf. (DFVLR-Mitt-83-05) Jul. 1984 p 42-58 Transl. into ENGLISH from "Vortraege eines Flugmechanik-Kolloquiums" rept. DFVLR-Mitt-83-05 DFVLR, Brunswick, Jul. 1983 p 47-64 Original language document was announced as N84-16124 (For primary document see N85-35165 24-02)
Avail: NTIS HC A06/MF A01; original German version available from DFVLR, Cologne DM 39.20

04 AIRCRAFT COMMUNICATIONS AND NAVIGATION

Includes digital and voice communication with aircraft; air navigation systems (satellite and ground based); and air traffic control.

For related information see also *17 Spacecraft Communications, Command, and Tracking* and *32 Communications.*

N85-35178 Purdue Univ., Lafayette, Ind.
NONLINEAR DIGITAL PHASE-LOCKED LOOPS WITH APPLICATION TO LORAN-C RECEIVERS Ph.D. Thesis
William Bruce McCain 1984 149 p
Avail: Univ. Microfilms Order No. DA8507725

This thesis is concerned with the application of nonlinear digital phase locked loops (DPLL's) to the tracking of the Loran-C radio navigation signal. This problem is characterized by the presence of nongaussian noise, which suggests the use of nonlinear processing to improve the performance of currently designed marine receivers to a level adequate for land based uses of the Loran-C system. Several methods of determining the performance of a DPLL are reviewed. A detailed development of the finite Markov chain analysis of a DPLL is presented, along with a new performance measure and an extension of the results for a second order loop. A computer simulation of the loop operations is also performed, and the close agreement between analytic and simulation results shows the value of such a simulation. Because of the noise contaminating the Loran-C signal is atmospheric (heavy tailed) and therefore nongaussian, the use of robust estimation is discussed. Dissert. Abstr.

N85-35179# Mitre Corp., McLean, Va.
FAA REQUIREMENTS FOR MODEL TO SUPPORT CAPACITY, DELAY, NOISE AND ENERGY PROGRAMS
J. N. Barrer and W. E. Weiss Mar. 1985 63 p
(Contract DTFA01-84-C-00001)
(AD-A155815; MTR-WP-85W00174; FAA-DL5-85-1) Avail: NTIS HC A04/MF A01 CSCL 17/7

This paper was written at the request of the FAA Management Steering Group on System Capacity/Airport Capacity in an effort to answer the recurring question, why should the FAA invest resources in the development and maintenance of models? It summarizes the FAA's requirements for modeling capability to analyze the issues of capacity, delay, noise and fuel burn. It concludes that there is a continuing need for such models and an additional need for airspace model(s) to address these issues in a complex terminal environment. The paper includes a detailed summary of those models related to capacity and delay which are currently owned by the FFA. GRA

N85-35180# Army Engineer Topographic Labs., Fort Belvoir, Va.
DETERMINING AN AZIMUTH WITH A NORTH SEEKING GYRO
K. P. Logan Feb. 1985 6 p
(AD-A155880; ETL-R-070) Avail: NTIS HC A02/MF A01 CSCL 17/7

Surveyors frequently require an independent means of determining an azimuth. Traditional methods, a magnetic compass reading or stellar observation, suffer from limitations of accuracy or availability. Another possibility is the use of the North Seeking Gyro which overcomes both of these defects. This paper gives a brief description of how the gyro works, effective observing procedures for its use, and results of some field observations made by the Mobile District. The gyro is shown to be an efficient and precise way for obtaining geodetic north even in situations where other techniques cannot be used. Author (GRA)

N85-35181# Maryland Univ., College Park. Center for Automation Research.
VISUAL POSITION DETERMINATION FOR AUTONOMOUS VEHICLE NAVIGATION
F. P. Andresen and L. S. Davis Nov. 1984 66 p
(Contract DAAK70-83-K-0018; DARPA Order 3206)
(AD-A156007; CAR-TR-100; CSC-TR-1458) Avail: NTIS HC A04/MF A01 CSCL 17/7

This report describes a system by which an autonomous land vehicle might improve its estimate of its current position. This system selects visible landmarks from a database of knowledge about its environment and controls a camera's direction and focal length to obtain images of these landmarks. The landmarks are then located in the images using a modified version of the generalized Hough transform and their locations are used to triangulate to obtain the new estimate of vehicle position and position uncertainty. GRA

N85-35182# Air Command and Staff Coll., Maxwell AFB, Ala.
A GUIDE TO USAF HELICOPTER INSTRUMENT FLIGHT PROCEDURES
L. O. Stendahl Apr. 1985 36 p
(AD-A156102; ACSC-85-2610) Avail: NTIS HC A03/MF A01 CSCL 01/2

This report presents information concerning USAF helicopter instrument procedures. This guide consolidates existing and new guidance into an up-to-date, single-source document for use by USAF helicopter pilots. If approved by HQ USAF Instrument Flight Center (IFC), portions of this guide will be incorporated into AFM 51-37. The paper first discusses the need for consolidated guidance, unique helicopter characteristics requiring changes to instrument procedures and how airspace design has been adjusted to accommodate helicopter operations. It then outlines procedures for performing basic helicopter instrument flight, and concludes with a chronological approach to helicopter instrument mission planning and accomplishment. Also included are proposed future changes to helicopter airspace design. GRA

05 AIRCRAFT DESIGN, TESTING AND PERFORMANCE

Includes aircraft simulation technology.

For related information see also *18 Spacecraft Design, Testing and Performance* and *39 Structural Mechanics.*

N85-35183 North Carolina State Univ., Raleigh.
AN AUTOMATED TECHNIQUE FOR ENCASING SPECIFIC PAYLOADS WITH LOW-DRAG FAIRINGS Ph.D. Thesis
Stanley Roscoe Fox 1984 492 p
Avail: Univ. Microfilms Order No. DA8507365

The energy crisis and the recent advances in technology have provided the incentive to develop an automated analytical technique

that will design low-speed, low-drag vehicles which encase specific payloads. The present work represents an effort to develop such a technique by the coupling of a flow analysis method, an optimization method, a shape perturbation scheme, and a three-dimensional plotting routine. This technique, which is applicable or easily adaptable to both aerodynamic and submerged hydrodynamic vehicle designs, orchestrates shape modifications to an arbitrary circumscribing body within the constraints stipulated by the specific payload. The evidence to date indicates that with astute modeling the present technique can produce low-drag, cost-effective designs. Dissert. Abstr.

N85-35184*# Simula, Inc., Phoenix, Ariz.
DESIGN AND TESTING OF AN ENERGY-ABSORBING CREWSEAT FOR THE F/FB-111 AIRCRAFT. VOLUME 2: DATA FROM SEAT TESTING Final Report, May 1983 - May 1985
S. Joseph Shane Washington NASA Sep. 1985 337 p 3 Vol.
(Contract NAS1-17387)
(NASA-CR-3917; NAS 1.26:3917; TR-84428-Vol-2) Avail: NTIS HC A15/MF A01 CSCL 01C

The unacceptably high injury rate during the escape sequence (including the ejection and ground impact) of the crew module for F/FB-111 aircraft is reviewed. A program to determine if the injury potential could be reduced by replacing the existing crewseats with energy absorbing crewseats is presented. An energy absorbing test seat is designed using much of the existing seat hardware. An extensive dynamic seat test series, designed to duplicate various crew module ground impact conditions is conducted at a sled test facility. Comparative tests with operational F-111 crewseats are also conducted. After successful dynamic testing of the seat, more testing is conducted with the seats mounted in an F-111 crew module. Both swing tests and vertical drop tests are conducted. The vertical drop tests are used to obtain comparative data between the energy absorbing and operational seats. Volume 1 describes the energy absorbing test seat and testing conducted, and evaluates the data from both test series. Volume 2 presents the data obtained during the seat test series, while Volume 3 presents the data from the crew module test series. Author

N85-35185*# SKF Industries, Inc., King of Prussia, Pa.
PLANETARY-GEAR-SUPPORT BEARING TEST RIG DESIGN Contractor Report, 8 Feb. 1983 - 8 Jan. 1985
J. W. Rosenlieb Mar. 1985 81 p
(Contract NAS3-23702)
(NASA-CR-174927; NAS 1.26:174927; AT85T004) Avail: NTIS HC A05/MF A01 CSCL 01C

A test rig was designed to evaluate the performance of a spherical roller bearing with a geared outer ring operating under conditions similar to those of a planet bearing in a helicopter transmission. The configuration is an extension of the widely accepted four-square gearbox arrangement. It provides for testing of two bearings simultaneously with outer ring rotation, misalignment, diametrically opposed loading through the gear teeth, and under race lubrication. Instrumentation permits the measurement of inner and outer ring temperature, bearing drag torque, degree of misalignment, outer ring speed, cage speed, and applied load. Author

N85-35186*# Virginia Polytechnic Inst. and State Univ., Blacksburg. Dept. of Aerospace and Ocean Engineering.
ENERGY MANAGEMENT OF THREE-DIMENSIONAL MINIMUM-TIME INTERCEPT Interim Report
H. G. Visser, H. J. Kelley, and E. M. Cliff Jul. 1983 121 p refs
(Grant NAG1-203)
(NASA-CR-176174; NAS 1.26:176174) Avail: NTIS HC A06/MF A01 CSCL 01C

A real-time computer algorithm to control and optimize aircraft flight profiles is described and applied to a three-dimensional minimum-time intercept mission. Author

N85-35187# Aeronautical Research Labs., Melbourne (Australia).
FATIGUE LIVES OF SPECIMENS REPRESENTING CRITICAL LOCATIONS IN MIRAGE 3 SPARS UNDER AUSTRALIAN AND SWISS TEST SPECTRA
J. Y. Mann and G. W. Revill 1985 68 p refs
(ARL-Struc-R-415; AR-003-998) Avail: NTIS HC A04/MF A01

Full scale flight by flight fatigue tests on Mirage 3 fighter aircraft wings carried out at the Australian Aeronautical Research Laboratories (ARL) and the Swiss Eidgenossisches Flugzeugwerk (F+W) indicated much greater differences in the flights to failure than were expected. This problem has been investigated by conducting fatigue tests on specimens representing the major failure locations in the test wings - a blind anchor nut hole in the Australian case and an interference fit bolt hole in the Swiss case - under flight by flight loading sequences corresponding to those used in the full scale tests. Constant amplitude fatigue tests were also carried out on the blind hole specimens to provide information for life estimation purposes, and fractographic crack propagation studies were conducted on selected blind hole specimens. The experimentally determined lives of both types of specimen were greater under the Australian than the Swiss stress spectrum. Depending on the stress scaling factor considered the life ratio (Australian/Swiss flights) obtained by grouping together the two stress spectra and the two types of specimens were between 3 and 4.2. For the blind anchor nut hole specimens the predicted fatigue lives were less than those obtained experimentally at high stress scaling factors, but at low stress scaling factors the converse was the case. Author

N85-35188# Army Test and Evaluation Command, Aberdeen Proving Ground, Md.
LABORATORY VIBRATION SCHEDULES Final Report
11 Mar. 1985 243 p Supersedes TOP-1-2-601
(AD-A155856; ITOP-1-2-601; TOP-1-2-601-Rev) Avail: NTIS HC A11/MF A01 CSCL 14/2

This ITOP describes two types of vibration tests conducted in the laboratory: first, a mission/field secured cargo test to simulate the transportation of Army material as secured cargo during logistical shipments; and second, an application-induced vibration test to simulate the tactical vibration environment experienced by equipment installed in/on ground vehicles or helicopters. No attempt is made to address the vibration environments for equipment installed in fixed-wing aircraft, missiles, and ships (marine equipment). GRA

N85-35189# Naval Postgraduate School, Monterey, Calif.
THE EFFECTS OF PARAMETER VARIATION ON HELICOPTER PERFORMANCE M.S. Thesis
C. K. Kim Mar. 1985 65 p
(AD-A156027; AD-E900451) Avail: NTIS HC A04/MF A01 CSCL 21/7

Six different cases of helicopter main rotor parameter variation are considered for each of three different forward velocities - hover, sixty knots and one-hundred fifty knots in order to consider the effects of the changes on the total power required for the helicopter. The six cases included variations in rotor radius, rotor chord, solidity disc area, rotational velocity and tip velocity. Although strong positive or negative effects may be observed at some velocities, these trends are generally not the same at all velocities, indicating that trade-offs must be made in the design process in order to optimize the level flight performance. GRA

N85-35190# Naval Postgraduate School, Monterey, Calif.
DEVELOPMENT OF NATOPS (NAVAL AIR TRAINING AND OPERATING PROCEDURE STANDARDIZATION) PERFORMANCE SOFTWARE FOR THE H-46D HELICOPTER M.S. Thesis
J. M. Caram Mar. 1985 74 p
(AD-A156089) Avail: NTIS HC A04/MF A01 CSCL 09/2

This thesis generates closed-form equations for significant and frequently used Naval Air Training and Operating Procedure Standardization (NATOPS) performance charts for the H-46D and H-46A (with T58-GE-10 engines) helicopters. These equations are developed into interactive software for the Hewlett-Packard HP-41CV hand-held programmable calculator. With this software installed in the calculator the user is able to calculate numerous

NATOPS performance parameters (expeditiously, with reduced risk of error) both prior to and in flight. Author (GRA)

N85-35191# Air Command and Staff Coll., Maxwell AFB, Ala.
RAFTS: A T-38 REPLACEMENT FOR THE 21ST CENTURY
R. C. Chapman, Jr. Apr. 1985 35 p
(AD-A156103; ACSC-85-0435) Avail: NTIS HC A03/MF A01 CSCL 01/3

The Reconnaissance Attack Fighter Training System (RAFTS) is designed to bridge the performance and systems gap between the T-46A and the Advanced Tactical Fighter (ATF). This training system will replace the T-38 now used in undergraduate pilot training. The study addresses the probable training environment, technology, training requirements, syllabi, and embedded training systems in the late 1990's. The study concludes with a conceptual design of the T-38 aircraft replacement for the 21st century.
Author (GRA)

N85-35192# Naval Postgraduate School, Monterey, Calif.
DEVELOPMENT OF NATOPS PERFORMANCE SOFTWARE FOR THE SH-3D AND SH-3H HELICOPTERS M.S. Thesis
J. T. Curtis Mar. 1985 107 p
(AD-A156140) Avail: NTIS HC A06/MF A01 CSCL 01/2

This thesis generates closed form equations for significant and frequently used Naval Air Training and Operating Procedure Standardization (NATOPS) performance charts for the SH-3D and SH-3H helicopters. These equations are developed into interactive software for the Hewlett-Packard HP-41CV hand-held programmable calculator. With this software installed in the calculator the user is able to calculate numerous NATOPS performance parameters (expeditiously, with reduced risk of error) both prior to and in flight. Author (GRA)

N85-35193# Air Command and Staff Coll., Maxwell AFB, Ala.
NEXT GENERATION GUNSHIP
W. F. Holloway Apr. 1985 39 p
(AD-A156361; AD-E900463; ACSC-85-1235) Avail: NTIS HC A03/MF A01 CSCL 01/3

Special Operations Forces (SOF) possess requirements for unique air-to-ground attack and reconnaissance capabilities. Conventional air assets do not possess these capabilities. The present SOF air-to-ground attack weapon system, the AC-130 gunship, suffers from inherent tactical and system limitations. The study explores the requirements, the tactical employment concepts, and design considerations for a new gunship. The study concludes that a new gunship must not be a modified conventional airplane, but a dedicated weapon system designed and built for SOF.
Author (GRA)

N85-35544# Deutsche Forschungs- und Versuchsanstalt fuer Luft- und Raumfahrt, Oberpfaffenhofen (West Germany). Inst. fuer Physik der Atmosphaere.
TYPICAL AND HISTORICAL ASPECTS OF MOTOR GLIDERS AS METEOROLOGICAL MEASURING AIRCRAFT [TYPISCHES UND GESCHICHTLICHES ZUM MOTORSEGLER ALS METEOROLOGISCHES MESSFLUGZEUG]
Manfred E. Reinhardt *In its* Proc. of Meteorol. Motor Glider (MEMO) Workshop '84 Jan. 1985 p 15-28 refs In GERMAN (For primary document see N85-35542 24-47)
Avail: NTIS HC A10/MF A01

06 AIRCRAFT INSTRUMENTATION

Includes cockpit and cabin display devices; and flight instruments.

For related information see also *19 Spacecraft Instrumentation* and *35 Instrumentation and Photography.*

No abstracts in this category.

07 AIRCRAFT PROPULSION AND POWER

Includes prime propulsion systems and systems components, e.g., gas turbine engines and compressors; and on-board auxiliary power plants for aircraft.

For related information see also *20 Spacecraft Propulsion and Power, 28 Propellants and Fuels,* and *44 Energy Production and Conversion.*

N85-35194* National Aeronautics and Space Administration. Langley Research Center, Hampton, Va.
WINGTIP VORTEX PROPELLER Patent
James C. Patterson, Jr., inventor (to NASA) Issued 6 Aug. 1985 9 p Filed 2 Feb. 1984 Supersedes N84-20495 (22 - 11, p 1602)
(NASA-Case-LAR-13019-1; US-Patent-4,533,101;
US-Patent-Appl-SN-576308; US-Patent-Class-244-199;
US-Patent-Class-244-55) Avail: US Patent and Trademark Office CSCL 01C

A device which increases the energy efficiency of aircraft wherein a wingtip pusher propeller is positioned aft of the wingtip to rotate in the crossflow of the wingtip vortex is presented. The propeller rotates against the vortex swirl creating additional thrust from and attenuating the wingtip vortex by simultaneously extracting energy from the vortex and converting it to propeller blade induced thrust while injecting its high energy wake into the vortex axial flow to dissipate the vortex. The device increases aircraft fuel efficiency by simultaneously increasing thrust and decreasing vortex induced drag. By attenuating the vortex safety to following aircraft is maximized.
Official Gazette of the U.S. Patent and Trademark Office

N85-35195* National Aeronautics and Space Administration. Lewis Research Center, Cleveland, Ohio.
FLOW MODIFYING DEVICE Patent
James S. Kelm (General Electric Co., Cincinnati), Edward C. Vickers (General Electric Co., Cincinnati), Jesse J. Williams (General Electric Co., Cincinnati), and Jack R. Taylor, inventors (to NASA) (General Electric Co., Cincinnati) Issued 13 Aug. 1985 10 p Continuation of abandoned US-Patent-Appl-SN-192677 filed 1 Oct. 1980
(NASA-Case-LEW-13562-2; US-Patent-4,534,166;
US-Patent-Appl-SN-500651; US-Patent-Class-60-39.23;
US-Patent-Class-60-748; US-Patent-Class-239-402.5) Avail: US Patent and Trademark Office CSCL 21E

A swirler for a gas turbine engine combustor is disclosed for simultaneously controlling combustor flow rate, swirl angle, residence time and fuel-air ratio to provide three regimes of operation. A first regime is provided in which fuel-air ratio is less than stoichiometric, NOx is produced at one level, and combustor flow rate is high. In a second regime, fuel-air ratio is nearly stoichiometric, NOx production is less than that of the first regime, and combustor flow rate is low. In a third regime, used for example at highoff, fuel-air ratio is greater than stoichiometric and the combustor flow rate is less than in either of the other regimes.
Author

N85-35196 Purdue Univ., Lafayette, Ind.
OPTIMALLY DESIGNED PROPELLERS CONSTRAINED BY NOISE Ph.D. Thesis
Christopher John Miller 1984 191 p
Avail: Univ. Microfilms Order No. DA8507731

A design tool is developed that will produce an optimum propeller geometry for a given trade-off between noise and performance. A vortex model is used for the aerodynamics and a subsonic compact source model for the noise analysis. Optimizing the twist, chord and sweep distributions produced blades with favorable tradeoffs between noise and performance. The techniques used for noise reduction include: an inboard loading shift, diameter reduction, rotational speed reduction, increased blade sweep, and blade number increase. The trade-offs for the optimized blades show that, for the straight blade, the most effective noise

reduction method is to increase the blade number which both increases efficiency and decreases the blade number which both increases efficiency and decreases the noise. This is followed by blade sweep, which can decrease the noise up to 3 dBA with no efficiency loss, and rotational speed reduction, which reduces noise by 4 dBA per percent in efficiency loss. Results demonstrate that this design tool is not only effective, but useful in the search for more efficient and lower noise propulsion methods. Dissert. Abstr.

N85-35197*# Pratt and Whitney Aircraft, East Hartford, Conn. Engineering Div.
ENERGY EFFICIENT ENGINE PROGRAM TECHNOLOGY BENEFIT/COST STUDY, VOLUME 1 Executive Summary
D. E. Gray and W. B. Gardner Oct. 1983 19 p 2 Vol.
(Contract NAS3-20646)
(NASA-CR-174766-Vol-1; NAS 1.26:174766-Vol-1;
PWA-5594-258-Vol-1) Avail: NTIS HC A02/MF A01 CSCL 21E

Turbofan engine technologies required for the years 2000 to 2010 were studied, to assess the benefits of those technologies, and to formulate programs for developing the technologies required for that time period. Preliminary technology concepts that might be amenable to future development were ranked. Cycle studies, flowpath definition studies, and mechanical configuration studies were used to identify and establish the feasibility of the technologies that would be required in the 2000 to 2010 time frame. It is shown that a turbofan engine with advancements in aerodynamics, mechanical arrangements, and materials offer significant performance improvements over 1988 technology. The benefits of technologies are assessed using fuel burn and direct operating cost plus interest (DOC+I). The concepts could yield thrust specific fuel consumption benefits of almost 16%, fuel burn benefits of up to 24% and DOC+I benefits up to 14% in a long-range airplane relative to energy efficient engine technology levels. Technology development programs are formulated and recommended to realize those benefits E.A.K.

N85-35198*# Pratt and Whitney Aircraft, East Hartford, Conn. Engineering Div.
ENERGY EFFICIENT ENGINE PROGRAM TECHNOLOGY BENEFIT/COST STUDY, VOLUME 2
D. E. Gray and W. B. Gardner Oct. 1983 109 p refs 2 Vol.
(Contract NAS3-20646)
(NASA-CR-174766-Vol-2; NAS 1.26:174766-Vol-2;
PWA-5594-251-Vol-2) Avail: NTIS HC A06/MF A01 CSCL 21E

The benefit/cost study to identify turbofan engine technologies required for the years 2000 to 2010, the benefits of those technologies were formulated, and programs for developing the technologies required for that time period were formulated. It is shown that there are still many potential benefits to be realized from the advancement of gas turbine engine technology. Preliminary technology concepts that might be amenable to future development were ranked. Cycle studies, flowpath definition studies, and mechancial configuration studies were used to identify and establish the feasibility of the technologies that would be required in the 2000 to 2010 time frame. It is shown that a turbofan engine with advancements in aerodynamics, mechanical arrangements, and materials offers significant performance improvements over 1988 technology. The benefits of the technologies are assessed using fuel burn and direct operating cost plus interest (DOC+I). E.A.K.

N85-35199*# General Electric Co., Cincinnati, Ohio. Aircraft Engine Business Group.
ENERGY EFFICIENT ENGINE, HIGH PRESSURE TURBINE THERMAL BARRIER COATING. SUPPORT TECHNOLOGY REPORT
E. C. Duderstadt and P. Agarwal May 1983 128 p refs
(Contract NAS3-20643)
(NASA-CR-168037; NAS 1.26:168037; R82AEB293) Avail: NTIS HC A07/MF A01 CSCL 21E

This report describes the work performed on a thermal barrier coating support technology task of the Energy Efficient Engine Component Development Program. A thermal barrier coating (TBC) system consisting of a Ni-Cr-Al-Y bond cost layer and ZrO2-Y2O3 ceramic layer was selected from eight candidate coating systems on the basis of laboratory tests. The selection was based on coating microstructure, crystallographic phase composition, tensile bond and bend test results, erosion and impact test results, furnace exposure, thermal cycle, and high velocity dynamic oxidation test results. Procedures were developed for applying the selected TBC to CF6-50, high pressure turbine blades and vanes. Coated HPT components were tested in three kinds of tests. Stage 1 blades were tested in a cascade cyclic test rig, Stage 2 blades were component high cycle fatigue tested to qualify thermal barrier coated blades for engine testing, and Stage 2 blades and Stage 1 and 2 vanes were run in factory engine tests. After completion of the 1000 cycle engine test, the TBC on the blades was in excellent condition over all of the platform and airfoil except at the leading edge above midspan on the suction side of the airfoil. The coating damage appeared to be caused by particle impingement; adjacent blades without TBC also showed evidence of particle impingement. B.W.

08 AIRCRAFT STABILITY AND CONTROL

Includes aircraft handling qualities; piloting; flight controls; and autopilots.

N85-35200* National Aeronautics and Space Administration. Langley Research Center, Hampton, Va.
DUAL TOWLINE SPIN-RECOVERY DEVICE Patent
William L. White, inventor (to NASA) Issued 3 Sep. 1985 9 p Filed 15 Sep. 1983 Supersedes N83-34934 (21 - 23, p 3738)
(NASA-Case-LAR-13076-1; US-Patent-4,538,778;
US-Patent-Appl-SN-532342; US-Patent-Class-244-75-R;
US-Patent-Class-244-139; US-Patent-Class-244-113) Avail: US Patent and Trademark Office CSCL 01C

A device which corrects aerodynamic spin is described wherein a parachute exerts antispin forces on an aircraft to effect spin recovery. The dual parachute towlines and are each attached to the parachute and are attached to the rear fuselage equidistant to and on opposite sides of the aircraft centerline. As the parachute is deployed during spin, the parachute force acts through only the towing and exerts its force outboard of center on the aircraft. As a result, the parachute exerts not only an antispin torque, but additionally causes the aircraft to roll, creating a gyroscopic antispin rolling moment. The additional antispin rolling moment facilitates spin recovery by permitting a relatively smaller parachute to accomplish spin recovery equivalent to that of a larger parachute attached to the center of the rear fuselage.
Official Gazette of the U.S. Patent and Trademark Office

N85-35201*# Purdue Univ., Lafayette, Ind. School of Aeronautics and Astronautics.
THE INTEGRATED MANUAL AND AUTOMATIC CONTROL OF COMPLEX FLIGHT SYSTEMS Semiannual Status Report, Jan. - Aug. 1985
David K. Schmidt 17 Sep. 1985 112 p refs
(Grant NAG4-1)
(NASA-CR-176166; NAS 1.26:176166) Avail: NTIS HC A06/MF A01 CSCL 01C

Pilot/vehicle analysis techniques for optimizing aircraft handling qualities are presented. The analysis approach considered is based on the optimal control frequency domain techniques. These techniques stem from an optimal control approach of a Neal-Smith like analysis on aircraft attitude dynamics extended to analyze the flared landing task. Some modifications to the technique are suggested and discussed. An in depth analysis of the effect of the experimental variables, such as prefilter, is conducted to gain further insight into the flared land task for this class of vehicle dynamics. E.R.

N85-35202*# Purdue Univ., Lafayette, Ind.
ANALYSIS OF FLEXIBLE AIRCRAFT LONGITUDINAL DYNAMICS AND HANDLING QUALITIES. VOLUME 1: ANALYSIS METHODS
Martin R. Waszak and David S. Schmidt Jun. 1985 111 p refs (Grant NAG1-254)
(NASA-CR-177943-Vol-1; NAS 1.26:177943-Vol-1) Avail: NTIS HC A06/MF A01 CSCL 01C

As aircraft become larger and lighter due to design requirements for increased payload and improved fuel efficiency, they will also become more flexible. For highly flexible vehicles, the handling qualities may not be accurately predicted by conventional methods. This study applies two analysis methods to a family of flexible aircraft in order to investigate how and when structural (especially dynamic aeroelastic) effects affect the dynamic characteristics of aircraft. The first type of analysis is an open loop model analysis technique. This method considers the effects of modal residue magnitudes on determining vehicle handling qualities. The second method is a pilot in the loop analysis procedure that considers several closed loop system characteristics. Volume 1 consists of the development and application of the two analysis methods described above. B.W.

N85-35203*# Purdue Univ., Lafayette, Ind.
ANALYSIS OF FLEXIBLE AIRCRAFT LONGITUDINAL DYNAMICS AND HANDLING QUALITIES. VOLUME 2: DATA
Martin R. Waszak and David K. Schmidt Jun. 1985 243 p (Grant NAG1-254)
(NASA-CR-177943-Vol-2; NAS 1.26:177943-Vol-2) Avail: NTIS HC A11/MF A01 CSCL 01C

Two analysis methods are applied to a family of flexible aircraft in order to investigate how and when structural (especially dynamic aeroelastic) effects affect the dynamic characteristics of aircraft. The first type of analysis is an open loop modal analysis technique. This method considers the effect of modal residue magnitudes on determining vehicle handling qualities. The second method is a pilot in the loop analysis procedure that considers several closed loop system characteristics. Both analyses indicated that dynamic aeroelastic effects caused a degradation in vehicle tracking performance, based on the evaluation of some simulation results. Volume 2 consists of the presentation of the state variable models of the flexible aircraft configurations used in the analysis applications mode shape plots for the structural modes, numerical results from the modal analysis frequency response plots from the pilot in the loop analysis and a listing of the modal analysis computer program. B.W.

N85-35204*# National Aeronautics and Space Administration. Langley Research Center, Hampton, Va.
A PRELIMINARY EVALUATION OF A FAILURE DETECTION FILTER FOR DETECTING AND IDENTIFYING CONTROL ELEMENT FAILURES IN A TRANSPORT AIRCRAFT
W. Thomas Bundick Jul. 1985 85 p refs
(NASA-TM-87576; NAS 1.15:87576) Avail: NTIS HC A05/MF A01 CSCL 01C

The application of the failure detection filter to the detection and identification of aircraft control element failures was evaluated in a linear digital simulation of the longitudinal dynamics of a B-737 Aircraft. Simulation results show that with a simple correlator and threshold detector used to process the filter residuals, the failure detection performance is seriously degraded by the effects of turbulence. Author

09 RESEARCH AND SUPPORT FACILITIES (AIR)

Includes airports, hangars and runways; aircraft repair and overhaul facilities; wind tunnels; shock tube facilities; and engine test blocks.

For related information see also *14 Ground Support Systems and Facilities (Space).*

N85-35205 Texas Univ., Austin.
A STUDY OF THE CONTROL OF PARTICULATE EMISSIONS FROM TURBINE ENGINE TEST CELLS Ph.D. Thesis
John Edward Stevens, Jr. 1984 197 p
Avail: Univ. Microfilms Order No. DA8508364

The United States Air Force has been cited in California for violation of visible opacity standards by the test cell buildings used for aircraft engine run-up during major engine overhaul. Recommendations to control emissions by conventional means, such as electrostatic precipitation or high-energy scrubbers with demisters, were deemed non-cost-effective (130 test cells at more than 1 million dollars per cell). As an alternative control measure, EPA Method 5 particulate sampling was used to characterize stack emissions during the incremental addition of cooling water to the engine exhaust/augmentator air discharge. Six water increments, from 230 (baseline) to 1200 gallons per minute, were tested. Increasing water injection rates to 801 gallons per minute significantly reduced engine-contributed test cell emissions for the J75-17 engine to 0.05 pounds particulate per million Btu. Water injection at 801 gallons per minute therefore represents the best available control technology for turbine engine test cells testing the J75 engine. Dissert. Abstr.

N85-35206* National Aeronautics and Space Administration. Goddard Space Flight Center, Greenbelt, Md.
THE ISAVF OPTO-MECHANICAL TEST BED
D. J. Grant Oct. 1984 34 p
(NASA-TM-87505; NAS 1.15:87505; X-725-84-18) Avail: Issuing Activity CSCL 04B

The opto-mechanical test bed (OTB) is the primary subsystem of the instrument systems analysis and verification facility (ISAVF). It is designed to provide a precise stable input stimulus to an individual detector or an array of detectors to characterize the performance of these items. The current OTB enables work in the visible and near infrared regions of the electromagnetic spectrum. Future capability will enable use in the short wave infrared region (TBD). E.A.K.

N85-35207# Army Test and Evaluation Command, Aberdeen Proving Ground, Md.
ANALYZER, FLIGHT LINE Final Report
15 Apr. 1985 24 p Supersedes AD-718642
(AD-A155777; TOP-6-2-090) Avail: NTIS HC A02/MF A01 CSCL 14/2

General guidance for determining and evaluating the technical performance and technical characteristics of Flight Line Analyzers is presented. The cumulative test results together with the results of the appropriate Common Engineering Tests will allow an estimate of the test items' capabilities and the suitability of the equipment to meet the required military needs. GRA

N85-35208# Naval Surface Weapons Center, White Oak, Md.
MACH 14 FLOW RESTRICTOR THERMAL STRESS ANALYSIS Final Report, Jan. - Apr. 1984
E. J. Becker Aug. 1984 380 p Original contains color illustrations
(AD-A156215; NSWC/TR-84-364) Avail: NTIS HC A17/MF A01 CSCL 14/2

The objective of this study was to determine the effects of heating and mechanical pressure loading on the flow restrictor plate used in the Mach 14 leg of NSWC/WO hypervelocity Wind Tunnel. Included in this report are the procedures for model generation using PATRAN-G, model translation into ABAQUS format, transient heat transfer analysis, thermal stress analysis, results translation from ABAQUS to PATRAN-G, and the method used to determine the heat transfer film coefficients needed for ABAQUS. The results of these analyses are reviewed and recommendations are made for future analyses. GRA

12 ASTRONAUTICS (GENERAL)

For extraterrestrial exploration see *91 Lunar and Planetary Exploration.*

N85-35209* National Aeronautics and Space Administration, Washington, D. C.
TECHNOLOGY FOR LARGE SPACE SYSTEMS: A BIBLIOGRAPHY WITH INDEXES
Jul. 1985 146 p
(NASA-SP-7046(12); NAS 1.21:7046(12)) Avail: NTIS HC $14.50 CSCL 22A

A bibliography listing 516 reports, articles and other documents introduced into the NASA scientific and technical information system between July 1, 1984 and December 31, 1984 is presented. Its purpose is to provide helpful information to the researcher, manager, and designer in technology development and mission design in the area of Large Space System Technology. Subject matter is grouped according to system, interactive analysis and design, structural and thermal analysis and design, structural concepts and control systems, electronics, advanced materials, assembly concepts, propulsion, and solar power satellite systems. Author

N85-35210*# National Aeronautics and Space Administration. Ames Research Center, Moffett Field, Calif.
SPACE MISSIONS FOR AUTOMATION AND ROBOTICS TECHNOLOGIES (SMART) PROGRAM
Donald L. Cliffone and Henry Lum, Jr. Aug. 1985 10 p refs
(NASA-TM-86820; NAS 1.15:86820; Rept-85375) Avail: NTIS HC A02/MF A01 CSCL 22A

NASA is currently considering the establishment of a Space Mission for Automation and Robotics Technologies (SMART) Program to define, develop, integrate, test, and operate a spaceborne national research facility for the validation of advanced automation and robotics technologies. Initially, the concept is envisioned to be implemented through a series of shuttle based flight experiments which will utilize telepresence technologies and real time operation concepts. However, eventually the facility will be capable of a more autonomous role and will be supported by either the shuttle or the space station. To ensure incorporation of leading edge technology in the facility, performance capability will periodically and systematically be upgraded by the solicitation of recommendations from a user advisory group. The facility will be managed by NASA, but will be available to all potential investigators. Experiments for each flight will be selected by a peer review group. Detailed definition and design is proposed to take place during FY 86, with the first SMART flight projected for FY 89. Author

13 ASTRODYNAMICS

Includes powered and free-flight trajectories; and orbit and launching dynamics.

No abstracts in this category.

14 GROUND SUPPORT SYSTEMS AND FACILITIES (SPACE)

Includes launch complexes, research and production facilities; ground support equipment, e.g., mobile transporters; and simulators.

For related information see also *09 Research Support Facilities (Air).*

N85-35211# Stanford Linear Accelerator Center, Calif.
OBSERVATIONS OF ACCELERATED HIGH CURRENT LOW EMITTANCE BEAMS IN THE SLC LINAC
J. T. Seeman, M. C. Ross, J. C. Sheppard, and R. F. Stiening May 1985 4 p refs Presented at the Particle Accelerator Conf., Vancouver, British Columbia, 13 May 1985
(DE85-013073; SU-SLAC-PUB-3673; CONF-850504-85) Avail: NTIS HC A02/MF A01

The Linac of the SLAC Linear Collider (SLC) is required to accelerate several intense single electron and positron bunches to high energy while not enlarging their small transverse emittances. The improvements needed by the SLAC Linac to meet these goals have very stringent design criteria. Partial systems have become available, and beam tests were performed to confirm the designs. The results of the beam tests are discussed. DOE

N85-35712# California Univ., Davis. Dept. of Physics.
FRACTIONAL CHARGE RESOLUTION IN MUSIC
J. L. Romero, F. P. Brady, B. Christie, C. Tull, E. Barasch, C. M. Castaneda, J. Drummond, M. L. Webb, J. C. Young, H. J. Crawford (California Univ., Berkeley. Lawrence Berkeley Lab.) et al *In* California Univ., Berkeley. Lawrence Berkeley Lab. Proc. of the Workshop on Detectors for Relativistic Nucl. Collisions Aug. 1984 p 135-143 refs (For primary document see N85-35700 24-72) Avail: NTIS HC A08/MF A01

15 LAUNCH VEHICLES AND SPACE VEHICLES

Includes boosters; manned orbital laboratories; reusable vehicles; and space stations.

N85-35212# Air Command and Staff Coll., Maxwell AFB, Ala.
ARMS CONTROL AND THE PRESIDENT'S STRATEGIC DEFENSE INITIATIVE
J. J. Bon Apr. 1985 28 p
(AD-A156334; ACSC-85-0240) Avail: NTIS HC A03/MF A01 CSCL 05/4

The President's Strategic Defense Initiative (SDI) provides the hope for eliminating the threat from ballistic missiles. This study evaluates the impact of SDI on existing and future arms control agreements. Because new or modified space-related treaties are a probable result of the SDI, this study concludes that the best single strategy for arms control negotiations is to preserve overall US interests and maintain open technological options vice severely limiting any space technology that might some day become part of a space-based defensive system. Author (GRA)

16 SPACE TRANSPORTATION

Includes passenger and cargo space transportation, e.g., shuttle operations; and rescue techniques.

For related information see also *03 Air Transportation and Safety* and *85 Urban Technology and Transportation.*

No abstracts in this category.

17 SPACECRAFT COMMUNICATIONS, COMMAND AND TRACKING

Includes telemetry; space communications networks; astronavigation; and radio blackout.

For related information see also *04 Aircraft Communications and Navigation* and *32 Communications.*

No abstracts in this category.

18 SPACECRAFT DESIGN, TESTING AND PERFORMANCE

Includes spacecraft thermal and environmental control; and attitude control.

For life support systems see *54 Man/System Technology and Life Support.* For related information see also *05 Aircraft Design, Testing and Performance* and *39 Structural Mechanics.*

N85-35213* Colorado Univ., Boulder. Lab. for Atmospheric and Space Physics.

STUDIES OF THE SOLAR MESOSPHERE EXPLORER: DYNAMICS AND HORIZON SENSOR PERFORMANCE. PART A: SPIN AXIS PRECESSION AND ATMOSPHERIC DRAG. PART B: CLOUDS Final Report, 1984

G. M. Lawrence, J. R. Cowley, Jr., T. P. Sparn, P. E. Arlton, and W. K. Tobiska Mar. 1985 58 p Original contains color illustrations

(Contract NAS5-28037)

(NASA-CR-175308; NAS 1.26:175308; SME-ENG-HOR3) Avail: Issuing Activity CSCL 22B

The precession rate of the spin axis of the Solar Mesosphere Explorer (SME) was studied. Data from 947 days were analyzed. Data on atmospheric density were derived from the decay rate of SME's orbit, relating torque to drag through the Jacchia 1977 model. Four density determinations from orbit decay, the 10.7 cm solar index, the Lyman Alpha solar flux, and the observed precession rate were compared. The effect of clouds on the trigger altitude of SME's horizon sensors was studied. The spatial and spectral aspects of the problem are discussed. E.A.K.

N85-35214*# Virginia Polytechnic Inst. and State Univ., Blacksburg. Dept. of Engineering Science and Mechanics.

IDENTIFICATION AND CONTROL OF STRUCTURES IN SPACE Progress Report, 1 Jan. - 30 Jun. 1985

Leonard Meirovitch 30 Jun. 1985 23 p refs

(Grant NAG1-225)

(NASA-CR-176175; NAS 1.26:176175) Avail: NTIS HC A02/MF A01 CSCL 22B

Work during the period January 1 to June 30, 1985 has concentrated on the completion of the derivation of the equations of motion for the Spacecraft Control Laboratory Experiment (SCOLE) as well on the development of a control scheme for the maneuvering of the spacecraft. The report consists of a paper presented at the Fifth Symposium on Dynamics and Control of Large Structures, June 12 to 14, 1985 at Blacksburg, VA. Author

N85-35215*# Smithsonian Astrophysical Observatory, Cambridge, Mass.

THE INVESTIGATION OF TETHERED SATELLITE SYSTEM DYNAMICS Quarterly Report, 15 May - 14 Aug. 1985

Enrico Lorenzini Sep. 1985 71 p

(Contract NAS8-36160)

(NASA-CR-176180; NAS 1.26:176180; QR-4) Avail: NTIS HC A04/MF A01 CSCL 22B

Progress in tethered satellite system dynamics research is reported. A retrieval rate control law with no angular feedback to investigate the system's dynamic response was studied. The initial conditions for the computer code which simulates the satellite's rotational dynamics were extended to a generic orbit. The model of the satellite thrusters was modified to simulate a pulsed thrust, by making the SKYHOOK integrator suitable for dealing with delta functions without loosing computational efficiency. Tether breaks were simulated with the high resolution computer code SLACK3. Shuttle's maneuvers were tested. The electric potential around a severed conductive tether with insulator, in the case of a tether breakage at 20 km from the Shuttle, was computed. The electrodynamic hazards due to the breakage of the TSS electrodynamic tether in a plasma are evaluated. E.A.K.

N85-35216# Bolt, Beranek, and Newman, Inc., Cambridge, Mass.

PLURIBUS SATELLITE IMP (INTERFACE MESSAGE PROCESSORS) DEVELOPMENT MOBILE ACCESS TERMINAL NETWORK Quarterly Technical Report, 1 Nov. 1984 - 31 Jan. 1985

S. Blumenthal Feb. 1985 12 p

(Contracts MDA903-80-C-0353; N00039-81-C-0408; F08606-73-C-0027; F08606-75-C-0032)

(AD-A155754; BBN-5977; QTR-36) Avail: NTIS HC A02/MF A01 CSCL 17/2

This quarterly technical report is the current edition in a series of reports which describe the work being performed at BBN in fulfillment of several ARPA work statements. This QTR covers work on several ARPA-sponsored projects including: (1) development of the Pluribus Satellite IMP; and (2) development of the Mobile Access Terminal Network. This work is described in this single quarterly technical report with the permission of the Defense Advanced Research Projects Agency. The work on the Mobile Access Terminal Network has been completed. GRA

N85-35217# Naval Postgraduate School, Monterey, Calif.

TARGET OBSERVABILITY FOR SATELLITE-BASED SENSORS M.S. Thesis

R. E. L. Bond Mar. 1985 130 p

(AD-A156139) Avail: NTIS HC A07/MF A01 CSCL 17/7

The purpose of this thesis is to discuss the observability of targets moving on or near the Earth's surface when viewed from space by an orbiting satellite. A simplified derivation of the satellite's orbital mechanics is undertaken, when taken in conjunction with a description of the target's motion allows for the derivation of a system of relative coordinates. An observability analysis is then performed on the resulting series of nonlinear equations, which in turn forms the basis for the design of a deterministic nonlinear observer and an Extended Kalman Filter to track the target. GRA

N85-35218# National Environmental Satellite Service, Washington, D. C.

SPACE STATION POLAR PLATFORM: INTEGRATING RESEARCH AND OPERATIONAL MISSIONS

J. H. McElroy and S. R. Schneider Jan. 1985 27 p

(PB85-195279; NOAA-TR-NESDIS-19) Avail: NTIS HC A03/MF A01 CSCL 22B

This report describes how an operational payload proposed by NOAA for the Space Station Polar Platform may be merged together with the research sensors scheduled to be carried on the Platform as part of NASA's Earth Observing System (EOS). This is the third in a series of NOAA/NESDIS Technical Reports on the space station project. Issues addressed include studies of solar terrestrial interactions, as well as monitoring of the Earth's atmosphere, oceans and land masses using both operational and R&D sensors. GRA

19 SPACECRAFT INSTRUMENTATION

For related information see also *06 Aircraft Instrumentation* and *35 Instrumentation and Photography.*

N85-35219*# Jet Propulsion Lab., California Inst. of Tech., Pasadena.

NOISELESS CODING FOR THE GAMMA RAY SPECTROMETER
Robert Rice and Jun-ji Lee Jun. 1985 37 p refs
(Contract NAS7-918)
(NASA-CR-176201; NAS 1.26:176201; JPL-Pub-85-53) Avail: NTIS HC A03/MF A01 CSCL 22B

The payload of several future unmanned space missions will include a sophisticated gamma ray spectrometer. Severely constrained data rates during certain portions of these missions could limit the possible science return from this instrument. This report investigates the application of universal noiseless coding techniques to represent gamma ray spectrometer data more efficiently without any loss in data integrity. Performance results demonstrate compression factors from 2.5:1 to 20:1 in comparison to a standard representation. Feasibility was also demonstrated by implementing a microprocessor breadboard coder/decoder using an Intel 8086 processor. Author

20 SPACECRAFT PROPULSION AND POWER

Includes main propulsion systems and components, e.g., rocket engines; and spacecraft auxiliary power sources.

For related information see also *07 Aircraft Propulsion, 28 Propellants and Fuels,* and *44 Energy Production and Conversion.*

N85-35220*# Lockheed Missiles and Space Co., Huntsville, Ala. Research and Engineering Center.
VERIFICATION OF THE SRB MOTOR CASE PIN RETAINER BAND TIPS
Zain S. Karu Mar. 1980 42 p ref
(Contract NAS8-32982)
(NASA-CR-170882; NAS 1.26:170882; LMSC-HREC-TM-D697818) Avail: NTIS HC A03/MF A01 CSCL 21H

The pin retainer band is a 1-1/4 in. wide by about 1/32 in. thick steel band that is stretched over the pins circumferentially at the joints of the solid rocket booster (SRB) motor case segments. Its purpose is to hold the retaining pins in place during flight. Since the band is thin and is mounted stretched, or under tension, over the pins which are greased in place, it is necessary to protect it thermally. Three typical areas of the band location on the SRB motor case joints were chosen for verifying the cork thermal prection system (TPS) performance on the band: the joint in front of the attach ring, at the aft skirt joint in front of the kick ring and in an unperturbed area at the forward segments of the SRB motor cases. The kick ring area pin retainer band cork TPS passed the test requirements in the region where there are no phenolic splice caps. In the splice cap areas where the band TPS is closed out around the splice with K5NA, additional amounts of K5NA material is required to adequately protect the steel band. TPS requirements were easily met in the one location where the ends of the steel band are joined together after installation and tensioning. The attack ring area pin retainer band TPS did not quite pass the heat load requirements with the .375 in. thick cork TPS as used for the kick ring area band. It is recommended that the cork thickness here be increased to .50 in. The unperturbed area band TPS presented no problems. R.J.F.

N85-35221*# Lockheed Missiles and Space Co., Huntsville, Ala. Research and Engineering Center.
RESULTS OF TESTS ON A SPECIMEN OF THE SRB AFT SKIRT HEAT SHIELD CURTAIN IN THE MSFC LRLF
W. G. Dean Jun. 1980 59 p refs
(Contract NAS8-32982)
(NASA-CR-170883; NAS 1.26:170883; LMSC-HREC-TM-D697896) Avail: NTIS HC A04/MF A01 CSCL 21H

A full scale segment of the actual Solid Rocket Booster aft skirt heat shield curtain was tested in the Large Radiant Lamp Facility (LRLF) at Marshall Space Flight Center. The curtain was mounted in the horizontal position in the same manner as it is to be mounted on the SRB. A shaker rig was designed and used to provide a motion of the curtain, simulating that to be caused in flight by vehicle acoustics. Thermocouples were used to monitor curtain materials temperatures. Both ascent and reentry heat loads were applied to the test specimen. All aspects of the test setup performed as expected, and the test was declared successful. Author

N85-35222*# Lockheed Missiles and Space Co., Huntsville, Ala. Heat Protection Systems Group.
SRB TPS CLOSEOUT MATERIALS CHARACTERIZATION
Zain S. Karu Nov. 1979 10 p refs
(Contract NAS8-32982)
(NASA-CR-170885; NAS 1.26:170885; LMSC-HREC-TN-D697757) Avail: NTIS HC A02/MF A01 CSCL 21H

The recession characteristics of the materials used to closeout the Thermal Protection System (TPS) on the Space Shuttle Solid Rocket Booster (SRB) were assessed. Two candidate closeout materials namely, K5NA and MTA2 is the Marshall Trowelable Ablator. Test panels of each of these two materials were subjected to aerodynamic heat and shear in the NASA Hot Gas Facility. Pretest and Post-test measurements were taken and the rate of recession (R) thus determined was correlated with the heating rate. A least squares curve fit of the data together with another least squares 95% confidence level fit, was performed. The characteristics of the two materials when compared showed that both materials performed equally well at the higher heating rates ($10 < q < 30$ Btu/sq ft/sec) but MTA2 was slightly better, not receding as fast, at the lower q values. The comparison of the R versus q curves for K5NA and MTA2 with that of primary TPS P-50 cork on the SRB Aft Skirt was good. B.W.

N85-35223*# Lockheed Missiles and Space Co., Huntsville, Ala. Research and Engineering Center.
RESULTS OF TESTS OF THE SRB AFT SKIRT HEAT SHIELD CURTAIN IN THE MSFC HOT GAS FACILITY
W. G. Dean Feb. 1982 64 p ref
(Contract NAS8-32982)
(NASA-CR-170888; NAS 1.26:170888; LMSC-HREC-TM-D784643) Avail: NTIS HC A04/MF A01 CSCL 21H

During the first two space shuttle flights the aft skirt heat shield curtain performed well during ascent but failed during reentry. This exposed the inside of the skirt and its subsystems to reentry heating. The resulting exposure damaged various expensive systems items and therefore a curtain reassessment is required. As a part of this reassessment, tests were conducted in the MSFC Hot Gas Facility (HGF). The purposes of these tests were to determine if the curtain would fail in a manner similar to that in flight and to demonstrate that meaningful tests of the curtain can be conducted in the HGF. Author

N85-35224*# Lockheed Missiles and Space Co., Huntsville, Ala. Research and Engineering Center.
RESULTS OF TESTS OF MTA-2 TPS ON THE SRB HOLD-DOWN BOLT BLAST CONTAINER
W. G. Dean 30 Jun. 1982 13 p
(Contract NAS8-32982)
(NASA-CR-170891; NAS 1.26:170891; LMSC-HREC-TN-D867571) Avail: NTIS HC A02/MF A01 CSCL 21H

The four solid rocket booster (SRB) hold-down posts are fastened to the mobile launch platform (MLP) with four large nuts. At liftoff the nuts are split with explosive changes to release the SRB/Shuttle. A blast container is placed over the nuts to protect the vehicle from flying debris. The blast container is a reusable part and has to be protected from aerodynamic heating during flight. The thermal protection system (TPS) used to protect these blast containers is cork. Fitting the flat cork sheet to this hemispherical shaped blast container is both time consuming and expensive. Another problem is removing the charred cork and epoxy glue from the blast containers. Replacements of this cork with another TPS material such as MTA-2 was examined. Heating rates along the centerline of the forward facing areas of the blast container were determined. The feasibility of using 1/2 in.

MTA-2 on the SRB blast containers for protection from ascent, plume impingement and reentry heating is demonstrated. E.A.K.

N85-35225*# National Aeronautics and Space Administration. Lewis Research Center, Cleveland, Ohio.
STATUS OF ADVANCED ORBITAL TRANSFER PROPULSION
Larry P. Cooper 1985 26 p refs Proposed for presentation at the 36th Intern. Astronautics Federation Congr., Stockholm, 7-12 Oct. 1985
(NASA-TM-87069; E-2638; NAS 1.15:87069; IAF-85-164) Avail: NTIS HC A03/MF A01 CSCL 21H

A new Orbital Transfer Vehicle (OTV) propulsion system that will be used in conjunction with the Space Shuttle, Space Station and Orbit Maneuvering Vehicle is discussed. The OTV will transfer men, large space structures and conventional payloads between low Earth and higher energy orbits. Space probes carried by the OTV will continue the exploration of the solar system. When lunar bases are established, the OTV will be their transportation link to Earth. Critical engine design considerations based upon the need for low cost payload delivery, space basing, reusability, aeroassist maneuvering, low g transfers of large space structures and man rating are described. The importance of each of these to propulsion design is addressed. Specific propulsion requirements discussed are: (1) high performance H2/O2 engine; (2) multiple engine configurations totalling no more than 15,000 lbf thrust 15 to 20 hr life; (3) space maintainable modular design; (4) health monitoring capability; and (5) safety and mission success with backup auxiliary propulsion. E.A.K.

N85-35226# Ogden Air Logistics Center, Hill AFB, Utah. Propellant Analysis Lab.
DISSECTED MOTORS-PROPELLANTS MOTOR NUMBER STM-012. PHASE 15: SURVEILLANCE REPORT, STAGE 1 Final Test Results
J. A. Thompson Apr. 1985 176 p
(AD-A156088; MANPA-506(85)) Avail: NTIS HC A09/MF A01 CSCL 21/8

This is the final report for Dissected Motor STM-012 and covers propellant and case bond test data. Planned dissection of additional selected motors will provide samples for continued component test and analysis for future evaluation. Testing was performed to determine the useful shelf/service life for LGM-30 Stage 1 Rocket Motors. A three year storage program for propellant and components was started in May 1961. This program was then extended to a ten year study and later continued indefinitely to assure that a deterioration in motor physical characteristics could be detected in time to take some corrective actions before the weapon system performance deteriorated below an acceptable level. The data is presented in the form of regression analysis and the trends are projected 24 months beyond the last test data. From the statistical analysis of all data tested to date, significant degradation of the propellant does not appear likely for at least two years past the oldest data point. Further testing and reporting will be conducted on individual dissected motors. GRA

23 CHEMISTRY AND MATERIALS (GENERAL)

Includes biochemistry and organic chemistry.

N85-35227* National Aeronautics and Space Administration. Pasadena Office, Calif.
PRODUCTION OF BUTANOL BY FERMENTATION IN THE PRESENCE OF COCULTURES OF CLOSTRIDIUM Patent
Sheryl L. Bergstrom (JPL, Pasadena, Calif.) and Gary L. Foutch, inventors (to NASA) (JPL, Pasadena, Calif.) Issued 3 Sep. 1985 4 p Filed 10 May 1983 Supersedes N83-29806 (21 - 18, p 2962)
(NASA-Case-NPO-16203-1; US-Patent-4,539,293; US-Patent-Appl-SN-493179; US-Patent-Class-435-160; US-Patent-Class-435-842) Avail: US Patent and Trademark Office CSCL 07C

Sugars are converted to a mixture of solvents including butanol by a fermentation process employing a coculture of microorganisms of the Clostridium genus, one of said microorganisms favoring the production of butyric acid and the other of which converts the butyric acid so produced to butanol. The use of a coculture substantially increases the yield of butanol over that obtained using a culture employing only one microorganism.
Official Gazette of the U.S. Patent and Trademark Office

N85-35228# Oak Ridge National Lab., Tenn.
CHEMISTRY DIVISION REPORT Annual Progress Report, period ending 31 Jan. 1985
May 1985 208 p
(Contract DE-AC05-84OR-21400)
(DE85-010586; ORNL-6152) Avail: NTIS HC A10/MF A01

An overview of the work of the chemistry division of ORNL is presented. This work was directed at broadening the base of fundamental understanding of materials and phenoma of relevance to future energy technologies. Some subdisciplines covered are: (1) coal chemistry; (2) aqueous chemistry at high temperatures and pressures; (3) geochemistry; (4) high temperature chemistry and thermodynamics of structural materials; (5) chemistry of transuranium elements and compounds; (6) separations chemistry; (7) electrochemistry; (8) catalysis; (9) chemical physics; (10) theoretical chemistry; (11) nuclear waste chemistry, and (12) chemical applications of artificial intelligence. E.R.

N85-35229# North Carolina Univ., Chapel Hill.
HEATS OF FORMATION OF GAS PHASE ORGANOSULFUR MOLECULES, RADICALS AND IONS MEASURED BY PEPICO AND APPLICATION OF (17)O AND (33)S NMR SPECTROSCOPY TO STRUCTURE DETERMINATION OF ORGANOSULFUR COMPOUNDS Progress Report, Jun. 1984 - Mar. 1985
T. Baer and S. A. Evans, Jr. 1985 17 p refs
(Contract DE-AS05-80ER-10641)
(DE85-010558; DOE/ER-10641/T1) Avail: NTIS HC A02/MF A01

The photoionization studies resulted in the determination of new heats of formation of the following molecules or ions: H2S2, C2H5S, C4H9SH(+), C3H7S(+). In addition, the dissociation mechanisms of diethyldisulfide and t-butyl sulfide were investigated. These data clearly show that the ion t-butyl disulfide dissociates via a two component rate indicating that there exists an isomer which is lower in energy than that of t-butyl disulfide. The (17)O and (33)S NMR spectral properties of numerous organosulfur compounds were examined in an effort to identify substituent effects and trends which might serve as predictive parameters for the identification and verification of unknown organosulfur compounds. The analytical potential of both (17)O and (33)S NMR were established as useful methods for determining the composition of mixtures containing various oxidized organosulfur constituents. The (33)S NMR technique was applied to the evaluation of organosulfur components in extracted coal samples, successfully observing a (33)S resonance consistent with a family of aryl sulfonates. DOE

N85-35230# Notre Dame Univ., Ind. Dept. of Chemical Engineering.
FTIR STUDIES OF HYDROCARBON SYNTHESIS ON Pd/ZSM5 CATALYSTS Quarterly Progress Report
E. E. Wolf 15 May 1985 8 p refs
(DE-FG22-84PC-70788)
(DE85-012430; DOE/PC-70788/T1) Avail: NTIS HC A02/MF A01

Reaction rate data were obtained in both the Pd/ZSM5 and Pd/SiO2 catalysts, and infrared spectrum was obtained of CO/H2 mixtures in both of the above catalysts. The results indicate that both catalysts exhibit CO hydrogenation activity but different selectivities. The reaction rate and the selectivities are affected by pressure and temperature. The infrared spectrum of CO on the Pd/ZSM5 catalyst under reaction conditions exhibit several bands which are different than those of adsorbed CO. DOE

N85-35231# Purdue Univ., Lafayette, Ind. School of Chemical Engineering.
CO + H2 REACTION OVER NITROGN-MODIFIED IRON CATALYSTS Quarterly Technical Progress Report, 1 Oct. - 31 Dec. 1984
W. N. Delgass 1985 25 p refs
(Contract DE-FG22-82PC-50804)
(DE85-013791; DOE/PC-50804/9) Avail: NTIS HC A02/MF A01

Preoxidizing a freshly prepared zeta-Fe2N catalyst resulted in unique Fischer-Tropsch behavior. Characterization of this catalyst by Mossbauer spectroscopy indicated contributions from both zeta-Fe2N and Fe3O4. The kinetic behavior of this preoxidized catalyst revealed a remarkable enhancement in the C4 and C5 hydrocarbons as compared to the kinetics over the zeta nitride. Transient kinetic studies by mass spectrometry determined the bulk stoichiometry of a prenitrided catalyst after 12 hours of reaction in 3/1 H2/CO at 523 K by monitoring the H2O, NH3 and CH4 produced during temperature programmed reduction in H2. The epsilon-Fe/sub 2.7/n catalyst lost 24% of its nitrogen. The zeta-Fe2N catalyst lost 15% of its nitrogen. DOE

N85-35232# Oak Ridge National Lab., Tenn.
SYSTEM FOR THE CONTINUOUS GENERATION OF PHOSPHOROUS AEROSOLS FROM RED PHOSPHORUS-BUTYL RUBBER Final Report
R. W. Holmberg, J. H. Moneyhun, and T. M. Gayle Jun. 1985 39 p refs
(Contract DE-AC05-84OR-21400)
(DE85-013527; ORNL/TM-9649) Avail: NTIS HC A03/MF A01

A system for the continuous generation of phosphoric acid aerosols from burning Red Phosphorus Butyl Rubber (RPBR) is described. The system is primarily intended for inhalation toxicology experiments using high aerosol concentrations (ca. 0.3 to 3 g/m(3)), but is adaptable to other studies where a time independent concentration of the aerosol is desired in a flowing system. The RPBR formulation is softened by addition of a small amount of hexane and extruded at a controlled rate at high pressure through an orifice. A precision hydraulic extrusion system using a micrometer adjustable high pressure hydraulic pump has been developed to control the extrusion rate. The emerging filament is ignited and burned in a flowing air stream for delivery to chambers. In addition to the extrusion combustion system for aerosol generation, devices for recovering the spent aerosol and for monitoring its concentration are described. DOE

24 COMPOSITE MATERIALS

Includes laminates.

N85-35233* National Aeronautics and Space Administration. Lewis Research Center, Cleveland, Ohio.
THERMAL BARRIER COATING SYSTEM Patent
Stephan Stecura, inventor (to NASA) Issued 13 Aug. 1985 5 p Filed 14 Aug. 1984 Supersedes N84-33595 (22 - 23, p 3724) Continuation-in-part of US Patent-4,485,151, US Patent-Appl-SN-523297, filed 16 Aug. 1983, and continuation-in-part of abandoned US Patent-Appl-SN-375784, filed 6 May 1982
(NASA-Case-LEW-14057-1; US-Patent-4,535,033; US-Patent-4,485,151; US-Patent-Appl-SN-640712; US-Patent-Appl-SN-523297; US-Patent-Appl-SN-375784; US-Patent-Class-428-633; US-Patent-Class-428-656; US-Patent-Class-428-678; US-Patent-Class-428-679; US-Patent-Class-428-680; US-Patent-Class-428-681; US-Patent-Class-428-682) Avail: US Patent and Trademark Office CSCL 11D

An oxide thermal barrier coating comprises ZrO3-Yb2O3 that is plasma sprayed onto a previously applied bond coating. The zirconia is partially stabilized with about 124 w/o ytterbia to insure cubic, monoclinic, and terragonal phases.

Official Gazette of the U.S. Patent and Trademark Office

N85-35234 North Carolina State Univ., Raleigh.
MECHANICAL CHARACTERIZATION AND FAILURE MODES OF FIBER REINFORCED ANGLE-PLY COMPOSITES Ph.D. Thesis
Mark Alan Elkins 1984 152 p
Avail: Univ. Microfilms Order No. DA8507364

Experimental and theoretical characterization of material properties were conducted for unidirectional and angle-ply laminates and comparison made. The materials used in this study were T300 Graphite/Rigidite 5209, Kevlar 49/C/Rigidite 5216, and E- Glass/Rigidite 5216. Analysis of pertinent stresses, particularly the interlaminar shear stress was performed and their relation to laminate failure observed. Failure criteria formulated for anisotropic materials were discussed and scrutinized for their use in failure predictions of angle-ply laminates. The criteria discussed include the maximum stress and maximum strain theories, the Tsai-Hill Theory, and the Tsai-Wu Theory. The Tsai-Hill Theory was applied to experimental data. Laminates in all three material systems were pulled to failure in uniaxial tension and their failure mechanisms studied. Each failure mode was related to the stresses present in the laminate at the time of failure. Special emphasis was focused on the interlaminar shear stress throughout this work. Special samples were designed and manufactured to isolate interlaminar failures and show their relation to fiber orientation.

Dissert. Abstr.

N85-35235 Virginia Polytechnic Inst. and State Univ., Blacksburg.
DAMAGE INDUCED STRESS REDISTRIBUTION IN COMPOSITE LAMINATES Ph.D. Thesis
Alton Lee Highsmith 1984 226 p
Avail: Univ. Microfilms Order No. DA8507186

During the laod history of a laminated composite, several damage modes, including matrix cracking, delamination, fiber fracture, and fiber-matrix debonding, may contribute to the eventual failure of the material. The first problem studied was the so-called crossed crack problem. Moire interferometry was used to measure surface deformation in graphite epoxy laminates which contained both transverse cracks in the 90 degree plies and longitudinal splits in the zero degree piles. The interaction between the two matrix cracks was found to be significant, particularly with respect to the interlaminar stresses. The second problem studied was the delamination problem. In those laminates containing load induced delaminations embedded within undelaminated surroundings, significant strain concentrations were observed at the delamination fronts. These strain concentrations appear to be the result of large concentrations in axial stress at the delamination fronts.

Dissert. Abstr.

N85-35236*# Lockheed Missiles and Space Co., Huntsville, Ala. Research and Engineering Center.
SRB THERMAL PROTECTION SYSTEMS MATERIALS TEST RESULTS IN AN ARC-HEATED NITROGEN ENVIRONMENT
C. J. Wojciechowski Aug. 1979 62 p refs
(Contract NAS8-32982)
(NASA-CR-170881; NAS 1.26:170881; LMSC-HREC-TM-D697786)
Avail: NTIS HC A04/MF A01 CSCL 11D

The external surface of the Solid Rocket Booster (SRB) will experience imposed thermal and shear environments due to aerodynamic heating and radiation heating during launch, staging and reentry. This report is concerned with the performance of the various TPS materials during the staging maneuver. During staging, the wash from the Space Shuttle Main Engine (SSME) exhust plumes impose severe, short duration, thermal environments on the SRB. Five different SRB TPS materials were tested in the 1 MW Arc Plasma Generator (APG) facility. The maximum simulated heating rate obtained in the APG facility was 248 Btu/sq ft./sec, however, the test duration was such that the total heat was more than simulated. Similarly, some local high shear stress levels of 0.04 psia were not simulated. Most of the SSME plume impingement area on the SRB experiences shear stress levels of 0.02 psia and lower. The shear stress levels on the test specimens were between 0.021 and 0.008 psia. The SSME plume stagnation conditions were also simulated. B.W.

N85-35237*# Lockheed Missiles and Space Co., Huntsville, Ala. Research and Engineering Center.
RESULTS OF VARIABLE ENTHALPY TESTS OF CPR-488 TIP PANELS IN MSFC HOT GAS FACILITY
W. G. Dean 22 Feb. 1982 37 p
(Contract NAS8-32982)
(NASA-CR-170889; NAS 1.26:170889; LMSC-HREC-TM-D784773) Avail: NTIS HC A03/MF A01 CSCL 11D

Tests were conducted to determine the effects of variable enthalpy levels on CPR-488 foam performance and/or recession. Also to be determined was whether the BX-250 thickness indicator plugs (TIP) concept is feasible for measuring recession rates of CPR-488 foam during external tank flight. The tests determined that the TIP plug idea works. The accuracy of the indicated recession depth is approximately + or - 1.16 in. The BX-250 plugs with TiO2 work better than the regular BX-250 plugs. Also, there is an effect of enthalpy on CPR-488 foam performance. E.R.

N85-35238*# Lockheed Missiles and Space Co., Huntsville, Ala. Research and Engineering Center.
RESULTS OF TESTS OF K5NA AND A REVISED FORMULATION OF EPDM/CORK PATCH MATERIAL IN MSFC HOT GAS FACILITY
W. G. Dean 30 Jun. 1982 13 p
(Contract NAS8-32982)
(NASA-CR-170890; NAS 1.26:170890; LMSC-HREC-TN-D867570) Avail: NTIS HC A02/MF A01 CSCL 11D

During prelaunch procedures at Kennedy Space Center some of the EPDM Thermal Protection System material was damaged on the Solid Rocket Booster stiffener stubs. The preferred solution was to patch the damaged areas with a cork-filled epoxy patching compound. Before this was done, however, it was requested that this patching technique be checked out by testing it in the MSFC Hot Gas Facility. Two tests were run in the HFG in 1980. The results showed the patch material to be adequate. Since that time, the formulation of the cork-filled epoxy material has been changed. It became necessary to retest this concept to be sure that the new material is as good as or better than the original material. In addition to the revised formulation material, tests were also made using K5NA as the patch material. The objectives of the tests reported herein were to: (1) compare the thermal performance of the original and the new cork-filled epoxy formulations, and (2) compare the K5NA closeout material to these epoxy materials. Material specifications are also discussed. B.W.

N85-35239*# Lockheed Missiles and Space Co., Huntsville, Ala. Research and Engineering Center.
RESULTS OF TESTS OF WEATHERED K5NA CLOSEOUT MATERIAL IN THE MSFC HOT GAS FACILITY
W. G. Dean 6 Aug. 1982 24 p
(Contract NAS8-32982)
(NASA-CR-170893; NAS 1.26:170893; LMSC-HREC-TN-D867576) Avail: NTIS HC A02/MF A01 CSCL 11D

The application of K5NA over hypolon was investigated. The effects of using K5NA over painted cork surfaces, the effects of weathering on the unpainted K5NA surfaces are determined, and the use of water versus solvent for tooling K5NA in place were compared. It is concluded that: (1) K5NA can be applied to hypalon surfaces; (2) K5NA can be left unpainted; and (3) K5NA can be tested with water or solvent. E.A.K.

N85-35240*# Lockheed Missiles and Space Co., Huntsville, Ala. Research and Engineering Center.
EVALUATION OF SRB PHENOLIC TPS MATERIAL MADE BY AN ALTERNATE VENDOR
Zain S. Karu 11 Oct. 1982 29 p ref
(Contract NAS8-32982)
(NASA-CR-170894; NAS 1.26:170894; LMSC-HREC-TN-D867581) Avail: NTIS HC A03/MF A01 CSCL 11D

Tests conducted to evaluate the adequacy of solid rocket booster (SRB) phenolic thermal protection system (TPS) material supplied by an alternate vendor chosen by United Space Boosters, Inc. (USBI), to replace the current phenolic TPS sections used thus far on the first four Shuttle flights. The phenolic TPS is applied mainly to the attach and kick rings of the solid rocket booster (SRB). Full-scale sectional models of both the attach and kick ring structure were made up with 0.0265 in. thick stainless steel thin skin covers with thermocouples on them to determine the heating rates. Such models were made up for both the forward and rear faces of the kick ring which has a different configuration on each side. The thin skins were replaced with the alternate phenolic TPS sections cut from flight hardware configuration phenolic parts as supplied by the new vendor. Two tests were performed for each configuration of the attach and kick rings and the samples were exposed to the flow for a duration that gave a heat load equivalent to that obtained in the series of runs made for the current line of phenolic TPS. The samples performed very well with no loss of any phenolic layers. The post-test samples looked better than those used to verify the current phenolic TPS. R.J.F.

N85-35241*# Lockheed-California Co., Burbank.
FUEL CONTAINMENT AND DAMAGE TOLERANCE FOR LARGE COMPOSITE PRIMARY AIRCRAFT STRUCTURES. PHASE 1: TESTING Contractor Report, Oct. 1981 - Jan. 1983
J. P. Sandifer Mar. 1983 501 p refs
(Contract NAS1-16856)
(NASA-CR-166091; NAS 1.26:166091; LR-30380-Phase-1) Avail: NTIS HC A22/MF A01 CSCL 11D

Technical problems associated with fuel containment and damage tolerance of composite material wings for transport aircraft were identified. The major tasks are the following: (1) the preliminary design of damage tolerant wing surface using composite materials; (2) the evaluation of fuel sealing and lightning protection methods for a composite material wing; and (3) an experimental investigation of the damage tolerant characteristics of toughened resin graphite/epoxy materials. The test results, the test techniques, and the test data are presented. E.A.K.

N85-35242*# National Aeronautics and Space Administration, Washington, D. C.
METHOD FOR MEASURING SURFACE ACTIVITY OF SILICON NITRIDE POWDER
Yoshinori Kanno and Hisao Imai Sep. 1985 10 p refs Transl. into ENGLISH from Yogyo Kyokaishi (Japan), v. 92, no. 10, 1984 p 600-603 Transl. by Scientific Translation Associates, Santa Barbara, Calif.
(Contract NASw-4004)
(NASA-TM-77906; NAS 1.15:77906) Avail: NTIS HC A02/MF A01 CSCL 11D

Amorphous, alpha-, and beta-Si3N4 powders were activated by vibration ball milling in purified MeOH, and the surface activity of ground powders was determined by the temperature programmed desorption (TPD) method using NH3 gas. The concentration of active sites with a potential energy equivalent to the peak temperature in the spectrum increased was markedly by ball milling the amorphous Si3N4. The alpha- and beta-Si3N4 also had active sites produced by ball milling. The concentration of active site increased with increased ball milling time. A method for measuring surface activity of ceramic raw materials by TPD is proposed. Author

N85-35243*# PRC Kentron, Inc., Hampton, Va. Aerospace Technologies Div.
CHEMOVISCOSITY MODELING FOR THERMOSETTING RESINS, 2 Final Report
T. H. Hou Aug. 1985 36 p refs
(Contract NAS1-18000)
(NASA-CR-177958; NAS 1.26:177958) Avail: NTIS HC A03/MF A01 CSCL 11D

A new analytical model for simulating chemoviscosity of thermosetting resin was formulated. The model is developed by modifying the Williams-Landel-Ferry (WLF) theory in polymer rheology for thermoplastic materials. By assuming a linear relationship between the glass transition temperature and the degree of cure of the resin system under cure, the WLF theory can be

modified to account for the factor of reaction time. Temperature dependent functions of the modified WLF theory constants were determined from the isothermal cure data of Lee, Loos, and Springer for the Hercules 3501-6 resin system. Theoretical predictions of the model for the resin under dynamic heating cure cycles were shown to compare favorably with the experimental data reported by Carpenter. A chemoviscosity model which is capable of not only describing viscosity profiles accurately under various cure cycles, but also correlating viscosity data to the changes of physical properties associated with the structural transformations of the thermosetting resin systems during cure was established. Author

N85-35244*# Washington Univ., St. Louis, Mo. Lab. for Ultrasonics.
QUANTITATIVE NON-DESTRUCTIVE EVALUATION OF COMPOSITE MATERIALS BASED ON ULTRASONIC WAVE PROPAGATION Semiannual Progress Report, 15 Mar. - 15 Sep. 1985
James G. Miller 15 Mar. 1984 20 p refs
(Grant NsG-1601)
(NASA-CR-176176; NAS 1.26:176176) Avail: NTIS HC A02/MF A01 CSCL 11D

The size, shape, and orientation of damage correlates well between the polar backscatter technique and the deply technique. There is good quantitative correlation between the areas of damage indicated by the two techniques. These results suggest that the polar backscatter technique is sensitive to specific orientations of damage. The polar backscatter technique provides a good qualitative image of the size and shape of the largest zone of damage in each of the principal orientations. A quantitative estimate of the extent of these largest damage zones is obtained from the polar backscatter technique. The selective sensitivity of polar backscatter provides a useful tool for further studies of the mechanisms of impact damage in graphite fiber reinforced composite laminates. Author

N85-35245*# National Aeronautics and Space Administration, Washington, D. C.
ULTRASONIC INSPECTION OF CARBON FIBER REINFORCED PLASTIC BY MEANS OF SAMPLE-RECOGNITION METHODS
R. Bilgram Aug. 1985 29 p refs Transl. into ENGLISH of conf. paper "Ultraschallpruefung von CFK mittels methoden der Mustererkennung" Messerschmitt-Boelkow-Blohm G.m.b.H., 1984 p 1-27 Presented at Intern. Wehrtech. Symp. ueber CKF Eigenschaften, Pruefung und Bewertung von Kohlefaserverstaerkten Kunststoffen, Erding, West Germany, 8-10 May 1984 Transl. by Kanner (Leo) Associates, Redwood City, Calif. Original doc. prep. by Messerschmitt-Boelkow-Blohm G.m.b.H.
(Contract NASw-4005)
(NASA-TM-77896; NAS 1.15:77896) Avail: NTIS HC A03/MF A01 CSCL 11D

In the case of carbon fiber reinforced plastic (CFRP), it has not yet been possible to detect nonlocal defects and material degradation related to aging with the aid of nondestructive inspection method. An approach for overcoming difficulties regarding such an inspection involves an extension of the ultrasonic inspection procedure on the basis of a use of signal processing and sample recognition methods. The basic concept involved in this approach is related to the realization that the ultrasonic signal contains information regarding the medium which is not utilized in conventional ultrasonic inspection. However, the analytical study of the phyisical processes involved is very complex. For this reason, an empirical approach is employed to make use of the information which has not been utilized before. This approach uses reference signals which can be obtained with material specimens of different quality. The implementation of these concepts for the supersonic inspection of CFRP laminates is discussed. G.R.

N85-35246# European Space Agency, Paris (France).
CONTRIBUTION TO THE PROPERTIES OF CARBON FIBER REINFORCED COMPOSITES
Jul. 1984 287 p refs Transl. into ENGLISH of "Beitraege zum Verhalten kohlefaserverstaerkter Verbundstruckturen" rept. DFVLR-Mitt-83-16 DFVLR, Brunswick, Jan. 1983 265 p Original language document was announced as N84-19480
(ESA-TT-849; DFVLR-Mitt-83-16) Avail: NTIS HC A13/MF A01; original German version available from DFVLR, Cologne DM 89

Environmental effects on carbon fiber reinforced composite mechanical properties, analysis of acoustic emissions, progression of defects in laminates, and development of a special finite element technique for the analysis of defects in composite structures are surveyed. For individual titles, see N85-35247 through N85-35250.

N85-35247# European Space Agency, Paris (France).
DETERMINATION OF CHARACTERISTIC VALUES FOR FIBER REINFORCED MATERIALS
M. Gaedke *In its* Contrib. to the Properties of Carbon Fiber Reinforced Composites (DFVLR-Mitt-83-16) Jul. 1984 p 7-104 refs Transl. into ENGLISH from "Beitraege zum Verhalten kohlefaserverstaerkter Verbundstrukturen" rept. DFVLR-Mitt-83-16 DFVLR, Brunswick, Jan. 1983 p 9-99 Original language document was announced as N84-19481 (For primary document see N85-35246 24-24)
Avail: NTIS HC A13/MF A01; original German version available from DFVLR, Cologne DM 89

Environmental conditions in aeronautics and astronautics for fiber reinforced plastics and their effects are presented. Test measurements of temperature and moisture effects on mechanical properties of unidirectional carbon fiber reinforced plastics (CFRP) laminates loaded by tension, compression and shear were performed. Numerical transfer of results to get a forecast of multilayer laminates behavior under environmental conditions is discussed. Thermal cycling tests were performed to demonstrate the capacity of resistance of CFRP against thermal fatigue problems in spacecraft applications. Author (ESA)

N85-35248# European Space Agency, Paris (France).
METHODS FOR NONDESTRUCTIVE TESTS OF CFRP LAMINATES
J. Block *In its* Contrib. to the Properties of Carbon Fiber Reinforced Composites (DFVLR-Mitt-83-16) Jul. 1984 p 105-154 Transl. into ENGLISH from "Beitraege zum Verhalten kohlefaserverstaerkter Verbundstrukturen" rept. DFVLR-Mitt-83-16 DFVLR, Brunswick, Jan. 1983 p 101-144 Original language document was announced as N84-19482 (For primary document see N85-35246 24-24)
Avail: NTIS HC A13/MF A01; original German version available from DFVLR, Cologne DM 89

Nondestructive testing of Carbon Fiber Reinforced Plastics (CFRP) laminates is discussed. Ultrasonic techniques, X-ray techniques, and acoustic emission analysis were employed. It is found that ultrasonic testing is particularly suited for the detection of delaminations and that X-ray techniques are suited for crack detection. Acoustic emission (AE) is suited for location and, with limitations, for the classification of AE sources. Author (ESA)

N85-35249# European Space Agency, Paris (France).
DAMAGE MECHANISMS IN DAMAGED CFRP LAMINATES c39
L. Kirschke *In its* Contrib. to the Properties of Carbon Fiber Reinforced Composites (DFVLR-Mitt-83-16) Jul. 1984 p 155-204 Transl. into ENGLISH from "Beitraege zum Verhalten kohlefaserverstaerkter Verbundstrukturen" rept. DFVLR-Mitt-83-16 DFVLR, Brunswick, Jan. 1983 p 145-189 Original language document was announced as N84-19483 (For primary document see N85-35246 24-24)
Avail: NTIS HC A13/MF A01; original German version available from DFVLR, Cologne DM 89

Damage mechanisms in damaged carbon fiber reinforced plastics (CFRP) are described. Damages are delaminations and notches. The stacking sequence of the laminates is uni and multidirectional. Growth of delaminations by tension, compression and fatigue loads is reported. Crack propagation in notched laminates by tension load is shown. Damage tolerance, and the influence of environmental conditions are discussed. Author (ESA)

N85-35250# European Space Agency, Paris (France).
COMPUTATIONAL TECHNIQUES FOR FIBER REINFORCED COMPONENTS
H. Eggers *In* Contrib. to the Properties of Carbon Fiber Reinforced Composites (DFVLR-Mitt-83-16) Jul. 1984 p 205-287 refs Transl. into ENGLISH from "Beitraege zum Verhalten kohlefaserverstaerkter Verbundstrukturen" rept. DFVLR-Mitt-83-16 DFVLR, Brunswick, Jan. 1983 p 191-264 (For primary document see N85-35246 24-24)
Avail: NTIS HC A13/MF A01; original German version available from DFVLR, Cologne DM 89

Numerical investigations of damaged fiber reinforced structures are reviewed. Tridimensional stress state around a flaw within a larger structure was calculated. A finite layer element, which describes delaminations and layer cracks is developed.
Author (ESA)

N85-35251# Naval Postgraduate School, Monterey, Calif.
EFFECTS OF TEMPERATURE ON THE TENSILE STRENGTH AND ELASTIC MODULUS OF COMPOSITE MATERIAL M.S. Thesis
H. R. Bae Mar. 1985 80 p
(AD-A156112) Avail: NTIS HC A05/MF A01 CSCL 11/4

An experimental investigation was made to determine the ultimate tensile strength and elastic modulus of HMF 330/34 woven style graphite epoxy exposed to elevated temperatures: (16 C, 50 C, 80 C, 110 C, 140 C, and 170 C). Specimen were of three different layups: (0/45/ to 45/90)s, (45/0/ to 45/90)s and (45/90/ to 45/0)s. An instron universal testing machine with 20,000 lb maximum load capacity was used to apply the uniaxial tensile loading. A Marshall clamshell furnace was used for maintaining the elevated temperatures. Results of the investigation indicate that ultimate tensile strength decreases with temperature increase in the (0/45/ to 45/90)s orientation panel. For (45/0/ to 45/90)s and (45/90/ to 45/0)s orientation panels, ultimate tensile strength increases with temperature up to 140 C, and decreases above 140 C. In all cases, the elastic modulus decreases as temperature increases.
GRA

N85-35252# Massachusetts Univ., Amherst.
CRYSTALLIZATION OF POLYETHERETHERKETONE (PEEK) IN CARBON FIBER COMPOSITES Interim Technical Report
Y. C. Lee and R. S. Porter 25 Apr. 1985 27 p
(Contracts N00014-77-C-1234; N00014-83-K-0228)
(AD-A156316; TR-26) Avail: NTIS HC A03/MF A01 CSCL 11/4

The tendency of carbon fiber to nucleate the crystallization of PEEK has been evaluated by DSC and other techniques. As the carbon fiber content was increased, the supercooling necessary for PEEK crystallization decreased. The repeated melting (at 396 C) of the same PEEK sample results in a decrease of the number of nuclei for crystallization. At equivalent thermal histories, PEEK with carbon fiber was found to have a higher nucleation density than PEEK itself. The surface growth of carbon fiber and nuclei in the PEEK matrix compete for crystallization growth. As the holding time in melt was increased, the number of matrix spherulites formed on cooling decreased, hence a more pronounced transcrystalline region was developed. Correspondingly, the composites preheated in the melt for 100 min. showed about two times the transverse tensile strength and strain-to-failure of those preheated for only 30 min. Corresponding fracture surface produced in tension showed that the former samples had a greater matrix adhesion to the carbon fiber than the latter. A strong interfacial bond is thus developed by crystallization on carbon fiber surface. Destroying nuclei in the PEEK matrix by long preheating enhances crystallization on the carbon fiber.
GRA

25 INORGANIC AND PHYSICAL CHEMISTRY

Includes chemical analysis, e.g., chromatography; combustion theory; electrochemistry; and photochemistry.

For related information see also *77 Thermodynamics and Statistical Physics.*

N85-35253* National Aeronautics and Space Administration. Pasadena Office, Calif.
FLUIDIZED BED DESULFURIZATION Patent
Maddury Ravindram (JPL, Pasadena, Calif.) and John J. Kallvinskas, inventors (to NASA) (JPL, Pasadena, Calif.) Issued 16 Apr. 1985 16 p Filed 26 Aug. 1983 Supersedes N83-36122 (21 - 24, p 3923)
(NASA-Case-NPO-15924-1; US-Patent-4,511,362; US-Patent-Appl-SN-526768; US-Patent-Class-44-1-SR; US-Patent-Class-201-17) Avail: US Patent and Trademark Office CSCL 07D

High sulfur content carbonaceous material, such as coal is desulfurized by continuous fluidized suspension in a reactor with chlorine gas, inert dechlorinating gas and hydrogen gas. A source of chlorine gas, a source of inert gas and a source of hydrogen gas are connected to the bottom inlet through a manifold and a heater. A flow controler operates servos in a manner to continuously and sequentially suspend coal in the three gases. The sulfur content is reduced at least 50% by the treatment.
Official Gazette of the U.S. Patent and Trademark Office

N85-35254 Central Electricity Generating Board, London (England).
RADIATION MEASUREMENTS ON MAGNESIUM FLAMES
F. Roessler [1985] 16 p refs Transl. into ENGLISH from Opt. Acta (West Germany), v. 15, no. 3, 1968 p 257-269
(BLL-CE-Trans-8110-(9022.09)) Avail: British Library Lending Div., Boston Spa, Engl.

The radiation of a diffusely radiating MgO flame is characterized by four parameters, which are initially unknown. These are the true temperature, optical thickness and dispersion (wavelength dependence) of the absorption and scattering coefficients. The black body temperature and color temperature can be measured. However, a prerequisite is that the flame is optically thin, otherwise reflection is ineffective. Such an optically thin flame burning constantly is demonstrated. The spectra are investigated. The equipment for measuring the black body temperature and color temperature is described and calibrated. Measurements show that the effect of reflection on the color temperature is only very small, so that the 4th parameter cannot be determined and the dispersion of the scattering coefficient could be specified only very inaccurately.
B.W.

N85-35255# California Univ., Berkeley. Dept. of Chemistry.
THE PHOTODISSOCIATION OF ACETYLENE AT 193.3 NM
A. M. Wodtke and Y. T. Lee 21 May 1985 54 p
(Contract N00014-83-K-0069)
(AD-A155775) Avail: NTIS HC A04/MF A01 CSCL 07/5

The translational energy release was measured for processes 1 and 2 using the Molecular Beam Time-of-Flight method: (1)-C2H2 in the 193 nm range yields C2H + H; (2)-C2H in the 193nm range yields C2 + H. By measuring the maximum release of transitional energy for process 1 it was determined that the C-H bond energy in acetylene, D sub o(C2H-H) is 132 + or - 2 Kcal/Mol. Since the translational energy distribution peaks well away from zero, it is quite unlikely that internal conversion of the electronically excited C2H2 is an important channel for dissociation in product rotation, it is possible to get information on the vibrational structure of C2H radical from the translational energy distribution and it is found that the bending frequency in C2H is 550 + or - 100/cm. Our experiment is consistent with earlier work on fluorescence.
GRA

N85-35256# Yale Univ. Observatory, New Haven, Conn.
THE DETECTION AND STUDY OF MOLECULAR SPECIES

USING TIME RESOLVED LASER SPECTROSCOPY Final Report, 1 Jan. 1983 - 31 Dec. 1984
S. D. Colson and P. M. Rentzepis 31 Dec. 1984 5 p
(Contract DAAG29-83-K-0032)
(AD-A155910; ARO-19748.2-CH) Avail: NTIS HC A02/MF A01 CSCL 07/4

New nsec and psec laser spectroscopic techniques are being developed for detect of specific molecular species. In the interest of general applicability, the efficiencies of the methods are being studied and improved by changing from nsec to psec excitation conditions. For specific applications to certain types of agents, we are studying photodecomposition as a method for producting a particular fragment characteristic of that agent-type and which can be detected with high sensitivity and specificity. GRA

N85-35257# Dayton Univ., Ohio.
ASPECTS OF HIGH-RESOLUTION GAS CHROMATOGRAPHY AS APPLIED TO THE ANALYSIS OF HYDROCARBON FUELS AND OTHER COMPLEX ORGANIC MIXTURES. VOLUME 1 Final Report, Jan. - Sep. 1980
W. A. Rubey Wright-Patterson AFB, Ohio AFWAL Feb. 1985 213 p
(Contract F33615-77-C-2004)
(AD-A156154; UDR-TR-82-156-Vol-1; AFWAL-TR-84-2096-Vol-1) Avail: NTIS HC A10/MF A01 CSCL 21/4

Turbine engine fuels are complex mixtures of hydrocarbons which have until recently, been obtained almost exclusively from petroleum. There is growing interest in developing alternative feedstocks for the eventual production of high-quality turbine engine fuels. The major analytical technique for separating the chemical constituents and analyzing fuels and synfuel feedstocks is high-resolution gas chromatography (HRGC), and the extreme chemical complexity of these hydrocarbon mixtures continues to challenge even the most sophisticated HRGC techniques. Therefore, the principal objective of this research was to identify and evaluate advanced HRGC instrumental procedures which show potential for improving the analysis of hydrocarbon jet fuels and various feedstocks. A gas chromatograph can be viewed as an assembly of individual components arranged to form a time invariant linear system. Accordingly, a systems approach has been used in this investigation to study, refine, and modify HRGC instrumentation. GRA

N85-35258# Defence Research Establishment Suffield, Ralston (Alberta).
THE IDENTIFICATION OF COMPOUNDS IN MUSTARD HYDROLYSATE
P. A. DAgostino and L. R. Provost Apr. 1985 37 p
(AD-A156381; DRES-412) Avail: NTIS HC A03/MF A01 CSCL 15/2

The mustard stored at the Defence Research Establishment Suffield was disposed of by hydrolysis during the 1970's. Samples of the liquid and sludge hydrolysate were analyzed by gas chromatography with flame ionization and mass spectral detection. Hydrolysis was essentially complete since only trace levels of mustard were detected. Thiodiglycol, a hydrolysis product of mustard, was found as a major component in the hydrolysate. A number of other compounds were identified (or tentatively identified) in both the liquid and sludge hydrolysate samples. GRA

N85-35259# Sandia Labs., Albuquerque, N. Mex.
PRESSURE MEASUREMENTS IN A HYDROGEN COMBUSTION ENVIRONMENT: HYDROGEN-AIR COMBUSTION TEST SERIES 1 AND 2 IN THE FITS TANK, VOLUME 1
S. F. Roller Mar. 1985 53 p
(TI85-009899; NUREG/CR-3721-1-Vol-1) Avail: NTIS HC A04/MF A01

Hydrogen combustion tests were performed in the Fully Instrumented Test Site (FITS) tank under the Hydrogen Behavior Program performed by Sandia National Laboratories under contract with the US Nuclear Regulatory Commission. Test series 1 and 2 examined the effects of a number of parameters on hydrogen-air combustion: the initial temperature and pressure of the gases, the effect of added steam or carbon dioxide as diluents, and the percent hydrogen in air. For tests in the range of 20% to 40% hydrogen in air, recorded peak pressures were equal to adibatic, isochoric, complete combustion (AICC) values within an experimental error of 15%. This was contrary to the results of tests at a number of other facilities. The pre-ignition temperature had a strong effect on the peak pressure, while pre-ignition pressure in the range examined had no effect on combustion pressure ratios. Calculations showed that, although the effect of dynamic head on the peak pressure was a few percent or less, interactions of the wave preceding the flame front with the flame and with the vessel walls may be apparent in the experimental records. DOE

N85-35260# California Univ., Berkeley. Lawrence Berkeley Lab.
CHARACTERIZATION OF THE OPTICAL AND THERMAL PROPERTIES OF MATTER BY PHOTOTHERMAL TECHNIQUES
N. M. Amer Apr. 1985 14 p refs Presented at the Workshop on the Phys. Properties of Ceram., Soverato, Italy, 20 Sep. 1984
(Contract DE-AC03-76SF-00098)
(DE85-012607; LBL-19538; CONF-8409243-1) Avail: NTIS HC A02/MF A01

When an intensity modulated beam of electromagnetic radiation is incident upon an absorbing medium, heating will occur. Typical temperature rise associated with this process is on the order of (0.00001-0.0001)C. In recent years we have exploited such a small temperature rise to develop a novel and powerful class of spectroscopy called photothermal spectroscopy. This experimental tool provides a highly sensitive and noninvasive probe of the optical and thermal properties of matter. There are two primary ways of implementing photothermal spectroscopy: photothermal deflection, and photothermal displacement. The experimental details of both approaches are described and brief examples of their application are given. The applicability of the technique to the investigation of thermal properties of solids is described. DOE

N85-35261# California Univ., Berkeley. Lawrence Berkeley Lab.
AQUEOUS VOLATILE WEAK ELECTROLYTE EQUILIBRIA TO 300 C
S. I. Phillips May 1985 16 p refs Presented at the AIChE Ann. Meeting, San Francisco, 25 Nov. 1984
(Contract DE-AC03-76SF-00098)
(DE85-013840; LBL-19619; CONF-841121-22) Avail: NTIS HC A02/MF A01

Values of equilibrium constants for ionization of selected volatile weak electrolytes and for iodine hydrolysis are given up to 300 C. The data are calculated based on values for thermodynamics of the reaction at 25 C. The model used assumes a constant heat capacity of reaction for ammonia, carbon dioxide, sulfur dioxide, hydrogen sulfide and iodine. Criteria valid for a constant heat capacity are given, and resulting equilibrium data compared with other work. Emphasis is on data at zero ionic strength. DOE

N85-35262# Oklahoma Univ., Norman. School of Chemical Engineering and Materials Science.
EQUATION OF STATE STUDY FOR POLAR FLUIDS Final Report, Nov. 1980 - Oct. 1984
K. E. Starling, L. L. Lee, T. H. Chung, M. H. Li, and C. K. So Nov. 1984 294 p refs Sponsored by Gas Research Inst.
(PB85-204345; GRI-85/0002) Avail: NTIS HC A13/MF A01 CSCL 07D

A highly accurate equation of state for polar fluids and mixtures that is applicable to natural gas systems and a wide range of fluids was developed. Advances were made in the molecular theory of mixtures, i.e., in the formulation of a statistical mechanical focal composition theory. In applications, the applicability of the equation to 51 pure fluids and 83 mixture systems that are highly nonideal is demonstrated. GRA

N85-35263# Texas Univ., Austin. Dept. of Chemistry.
VECTORIAL ELECTRON TRANSFER ON DESIGNED SURFACES Annual Report, Jan. 1984 - Jan. 1985
A. J. Bard, A. Campion, M. A. Fox, S. E. Webber, and J. M. White 15 Mar. 1985 94 p

(Contract GRI-5082-260-0756)
(PB85-204600; GRI-85/0053) Avail: NTIS HC A05/MF A01 CSCL 21D

Several systems have been investigated for photochemical water systems and the chemical and physical factors that govern their efficiencies have been studied. For platinized CdS particles immobilized in a polymer (Nation) matrix the induction period for H2 formation has been shown to correlate with the extent of reduction of the initially, partially oxidized Pt catalyst. The crystalline form of the CdS can be controlled by the precipitation conditions. Cubic CdS, which is more active for H2 generation, has a much rougher surface that is rich in sulfate. On the other hand, hexagonal CdS has a much smoother surface, which is covered by sulfide. A novel mixed semiconductor system ZnS-CdS was discovered, which is nearly as active as the platinized CdS system. This is the first example of efficient photocatalysis for this reaction that does not require a noble metal to catalyze H2 evolution.

Author (GRA)

N85-35264# SRI International Corp., Menlo Park, Calif.
LASER PROBES OF NATURAL GAS IGNITION CHEMISTRY Annual Report, Jan. - Dec. 1984
D. R. Crosley Jan. 1985 37 p refs Sponsored by Gas Research Inst.
(PB85-200210; SRI-MP-85-024; GRI-85/0023) Avail: NTIS HC A03/MF A01 CSCL 21D

The research described is aimed at developing laser induced fluorescence of various hydrocarbon species for use as probes in natural gas combustion chemistry. The radiative and collisional properties of CH were extensively studied. A two dimensional imaging experiment reveals much different CH and OH distributions in flames. Spectroscopic investigations on acetylene, formaldehyde, and methoxy were undertaken with some difficulty, and the latter tentatively identified in a flame. To identify observables with the chemistry, a model has been assembled with particular theoretical attention paid to radical-radical reactions such as methyl plus methyl. In addition, laser pyrolysis experiments have been used to follow portions of the high temperature chemistry in a time resolved fashion to confirm ignition and flame mechanisms. Profiles of OH, CH, and C2 were obtained. GRA

N85-35265# Battelle Columbus Labs., Ohio.
BASIC RESEARCH ON PULSE-COMBUSTION PHENOMENA Annual Report, Nov. 1983 - Nov. 1984
J. M. Corliss and A. A. Putnam 15 Apr. 1985 62 p
(PB85-200228; GRI-85/0029) Avail: NTIS HC A04/MF A01 CSCL 13A

The objective of this program is to study the basic fluid mechanics, kinetics, and pollutant formation phenomena occurring in pulse combustion systems. To meet the objective, nonobstrusive optical diagnostic techniques are being employed in addition to more conventional combustion diagnostics. Two pulse combustor systems are described. One is constructed from steel tubing and is used for conventional diagnostic studies. The second pulse combustor is constructed from quartz tubing and is used for the optical diagnostics. Results of the experiments indicate that cyclic reignition in the combustion chamber occurs as a result of flame stabilization at the step expansion between the mixing chamber and the combustion process never ceases from cycle to cycle.

GRA

N85-35266# Stanford Univ., Calif. Dept. of Chemical Engineering.
MOLECULAR AND MACROMOLECULAR SIEVING BY ASYMMETRIC ULTRAFILTRATION MEMBRANES Final Report
Channing R. Robertson Sep. 1984 315 p refs
(Contract DI-14-34-0001-8548)
(PB85-157766; BU-REC-C-80292-S(1)) Avail: NTIS HC A14/MF A01 CSCL 07A

The seiving of dilute solutions of low molecular weight saccharides, proteins, and a polysaccharide, dextran, by several asymmetric ultrafiltration membranes was studied as a function of transmembrane pressure, drop or solvent flux (J(sub v)) in a stirred cell device. Scanning or transmission electron microscopy were used to examine the skin layer and substructure of each membrane. The flow patterns and specific mass transfer characteristics of the Amicon 52 stirred cell were studied under the turbulent flow conditions employed in all experiments. A one dimensional mass transfer model was found adequate to describe the boundary layer concentration polarization, thereby permitting the intrinsic membrane rejection coefficient (R) to be related to the experimentally measured rejection coefficient. GRA

26 METALLIC MATERIALS

Includes physical, chemical, and mechanical properties of metals, e.g., corrosion; and metallurgy.

N85-35267* National Aeronautics and Space Administration. Lewis Research Center, Cleveland, Ohio.
OXIDATION RESISTANT SLURRY COATING FOR CARBON-BASED MATERIALS Patent
James L. Smialek and George C. Rybicki, inventors (to NASA) Issued 13 Aug. 1985 6 p Filed 17 Jan. 1984 Supersedes N84-16266 (22 - 7, p 0967)
(NASA-Case-LEW-13923-1; US-Patent-4,535,035; US-Patent-Appl-SN-571617; US-Patent-Class-428-698; US-Patent-Class-427-191; US-Patent-Class-427-228; US-Patent-Class-427-294; US-Patent-Class-427-376.2; US-Patent-Class-427-380; US-Patent-Class-427-397.7; US-Patent-Class-428-704) Avail: US Patent and Trademark Office CSCL 11F

An oxidation resistant coating is produced on carbon-base materials, and the same processing step effects an infiltration of the substrate with silicon containing material. The process comprises making a slurry of nickel and silicon powders in a nitrocellulose lacquer, spraying onto the graphite or carbon-carbon substrate, and sintering in vacuum to form a fused coating that wets and covers the surface as well as penetrates into the pores of the substrate. Optimum wetting and infiltration occurs in the range of Ni-60 w/o Si to Ni-90 w/o Si with deposited thicknesses of 25-100 mg/sq. cm. Sintering temperatures of about 1200 C to about 1400 C are used, depending on the melting point of the specific coating composition. The sintered coating results in Ni-Si intermetallic phases and SiC, both of which are highly oxidation resistant.

Official Gazette of the U.S. Patent and Trademark Office

N85-35268 British Library Lending Div., Boston Spa (England).
DECOMPOSITION OF MARTENSITE IN R6M5 AND R6AM5 STEELS AFTER DIRECT IMMERSION IN LIQUID NITROGEN
A. N. Popandopulo and L. T. Zhukova [1985] 5 p refs Transl. into ENGLISH from Izv. Vyssh. Ucheb. Zaved., Chernaya Met. (USSR), no. 12, 1984 p 76-79
(BLL-M-36305) Avail: British Library Lending Div., Boston Spa, Engl.

Specimens of R6M5 steel were subjected to sub-zero treatment (direct immersion in liquid nitrogen) after annealing and also after quenching from 800 to 1250 C. Triple immersion in liquid nitrogen at =196 C was used with holding for 15 min. in each case. The treatment is complex as it involves heat treatment proper (the continuation of austenite transformation) and deformation heat treatment resulting in martensite decomposition and formation of finite carbides. Author

N85-35269 Central Electricity Generating Board, London (England).
ELECTROCHEMICAL METHOD FOR INVESTIGATION OF THE SUSCEPTIBILITY OF CORROSION-RESISTANT STEELS TO INTERCRYSTALLINE CORROSION
V. Cihal, J. Furychova, and J. Kubelka 16 Jul. 1985 18 p refs Transl. into ENGLISH from Werkstoffe Korrosion (Weinheim), v. 27, 1976 p 782-787
(BLL-CE-Trans-8082-(9022.09)) Avail: British Library Lending Div., Boston Spa, Engl.

A potentiodynamic reactivation method is modified and compared with regard to the standard test in the presence of copper chips. The ratio of the charge during reactivation with diminishing potential to the charge during activation with increasing potential expressed in percent is used for the quantitative evaluation. Author

N85-35270 British Library Lending Div., Boston Spa (England).
INFLUENCE OF YTTRIUM ON EUTECTOID TRANSFORMATION IN IRONS
A. A. Anikin 14 Aug. 1985 6 p refs Transl. into ENGLISH from Izv. Vysshikh Uchebn. Zavedenii, Chernaya Met. (Moscow), no. 12, 1983 p 78-81
(BLL-M-35787-(5828.4)) Avail: British Library Lending Div., Boston Spa, Engl.

Five alloys with different additions of yttrium inoculant were investigated. The yttrium contents ranged from 0 to 0.45%. The effect of yttrium on the critical points Ac sup s sub 1, Ac sup f sub 1, Ar sup s sub 1 and Ar sup f sub 1, was ascertained. Yttrium was also found to increase the hardenability of iron and promote pearlite formation. Use of yttrium is recommended for cylinder-piston assemblies in engines and wear-prone agricultural components such as plough shares. Author

N85-35271 United Kingdom Atomic Energy Authority, Risley (England).
TESTS ON ZIRCONIUM NITRIDE COATINGS APPLIED TO SW 18 STEEL USING THE CHEMICAL VAPOR DEPOSITION METHOD
Jerzy Nowacki 20 Nov. 1984 15 p refs Transl. into ENGLISH from Zeszyty Naukowe Politech. Lodzkiej-Mech. (Poland), v. 60, 1980 p 101-115
Copyright. Avail: British Library Lending Div., Boston Spa, Engl.

The results of tests on zirconium nitride coatings applied to SW 18 steel using the chemical vapor deposition method with a mixture of zirconium chloride vapors, nitrogen and hydrogen are discussed. The structure of the coating is determined and the nature of the parting plane between the coating is determined and the nature of the parting plane between the coating and the base. A high resistance to wear and a low coefficient of friction for interaction with steel is identified for the coatings. A model of the physiochemical phenomena occurring during the process of synthesis of the coatings is given. Author

N85-35272*# National Aeronautics and Space Administration, Washington, D. C.
STUDIES OF THE CRYSTALLIZATION PROCESS OF ALUMINUM-SILICON ALLOYS USING A HIGH TEMPERATURE MICROSCOPE Thesis
Stefan Justi Sep. 1985 67 p refs Transl. into ENGLISH of German Thesis p 1-76 Original language document was announced as N72-20488 Transl. by Scientific Translation Service, Santa Barbara, Calif.
(Contract NASw-4004)
(NASA-TM-77869; NAS 1.15:77869) Avail: NTIS HC A04/MF A01 CSCL 11F

It is shown that primary silicon crystals grow polyhedral in super-eutectic AlSi melts and that phosphorus additives to the melt confirm the strong seeding capacity. Primary silicon exhibits strong dendritic seeding effects in eutectic silicon phases of various silicon alloys, whereas primary aluminum does not possess this capacity. Sodium addition also produces a dendritic silicon network growth in the interior of the sample that is attributed to the slower silicon diffusion velocity during cooling. Transl. by G.G.

N85-35273# United Kingdom Atomic Energy Authority, Harwell (England). Materials Development Div.
PITTING CORROSION OF FERROUS ALLOYS
C. Westcott Apr. 1985 54 p refs
(AERE-R-11490) Avail: NTIS HC A04/MF A01

The failure of metallic components by localized corrosion is of major technological importance. Failure can occur by a number of mechanisms, one of the most common being pitting corrosion. Pitting corrosion is known to occur in many alloy systems when in contact with a wide variety of environments. Against this background many workers have investigated pitting corrosion with a view to both understanding its mechanism, and preventing the occurrence. The majority of this work has been carried out on ferrous metals, reflecting their preeminent position as constructional materials, and their propensity to fail by pitting attack. The literature on this subject is reviewed. What can be observed in a variety of experimental methods commonly used to investigate pitting corrosion is covered. The effects of material and environmental parameters on the pitting process are discussed, and a number of proposed mechanisms are described. Author

N85-35274# United Kingdom Atomic Energy Authority, Harwell (England). Materials Development Div.
THE DYNAMIC STRAIN AGEING OF A533B CLASS 1 NUCLEAR PRESSURE VESSEL STEEL
E. A. Little and J. A. Hudson Feb. 1985 35 p refs
(AERE-R-11485) Avail: NTIS HC A03/MF A01

The dynamic strain aging behavior of A533B nuclear grade low alloy steel was evaluated as a function of initial heat treatment, based on determination of the tensile properties at temperatures in the range 50 to 100 C and strain rates varying from 8.3 x 0.00001 to 5.3 x 0.001/s. Residual levels of interstitial nitrogen present in the steel under standard heat treatment conditions are sufficient to induce measurable susceptibility to dynamic strain aging, as evidenced by serrated yielding and flow in the temperature range 150 to 275 C and peaks in proof and ultimate tensile strength in the range 250 to 300 C. The temperatures dependence for onset of serrations is associated with an activation energy higher than that for simple diffusion of nitrogen in ferrite, and it is suggested that the process is controlled by nitrogen manganese atom interactions. Modified heat treatments which result in coarse prior austenite grain sizes lead to diminution of the strain aging effects, whereas quenching treatments give enhanced strengthening, principally in the temperature range 50 to 250 C. R.J.F.

N85-35275# United Kingdom Atomic Energy Authority, Harwell (England). Materials Physics and Metallurgy Div.
EFFECT OF THERMAL AGEING ON THE MECHANICAL PROPERTIES OF PWR PRESSURE VESSEL STEELS AND WELDMENTS
S. G. Druce, G. Gage, G. R. Jordan, and J. A. Hudson Apr. 1985 17 p refs
(AERE-R-11460) Avail: NTIS HC A02/MF A01

The effects on mechanical properties of aging treatments in the temperature range 300 to 550 C for durations up to 2 x 10 to the 4 and their significance to PWR operational conditions are discussed. The materials investigated include A533B plate and A508 forging materials, simulated heat-affected-zone-microstructures and actual weldments. Changes in hardness, tensile properties, the ductile-brittle-transition-temperature (DBTT) and upper-shelf crack growth resistance was assessed, together with associated changes in fracture mode and grain boundary chemistry. The results indicate little or no change in mechanical properties other than DBTT. Three separate embrittlement mechanisms have been identified: strain-aging at 300 C, grain boundary segregation at 400 to 500 C and matrix softening at 500 C and above. Author

N85-35276# United Kingdom Atomic Energy Authority, Harwell (England). Materials Development Div.
THE PREPARATION OF TEM SPECIMENS SHOWING OXIDE SCALES IN TRANSVERSE CROSS-SECTION
D. P. Moon Apr. 1985 37 p refs
(AERE-R-11579) Avail: NTIS HC A03/MF A01

Detailed investigation of the microstructure and microchemistry of oxide scales formed at high temperature requires examination by analytical electron microscopy. Techniques were developed for the routine presentation of electron transparent transverse cross sections of oxidized specimens. The rationale for the adoption of individual procedures is presented, and the merits of alternative approaches are discussed. Electron microscopy results from CeO2 particle dispersed NiO are used to demonstrate the advantage of

transverse section geometry for the unambiguous characterization of thick multilayered scales. Author

N85-35277# Wayne State Univ., Detroit, Mich. Dept. of Metallurgical Engineering.
FATIGUE DAMAGE DETECTION IN STEELS BY OPTICAL CORRELATION Final Report, 15 Jun. 1981 - 31 Dec. 1984
W. L. Haworth Mar. 1985 6 p
(Contract DAAG29-81-K-0114)
(AD-A155830; ARO-17870.6-MS) Avail: NTIS HC A02/MF A01 CSCL 20/6

This study investigated the use of optical correlation (holography) as a tool for the detection of surface changes, including those induced by fatigue, and its applicability for the nondestructive evaluation of strain and fatigue damage, and the prediction of impending failure in structural alloys. GRA

N85-35278# Army Materials and Mechanics Research Center, Watertown, Mass.
MICROSHRINK, TENSILE PROPERTIES, AND THE DETECTION OF MICROSHRINK Final Report
P. R. Smoot Nov. 1984 16 p
(AD-A155875; AMMRC-TR-84-43) Avail: NTIS HC A02/MF A01 CSCL 20/11

The unknown effects of microshrink on the tensile properties of cast nickel-base alloys were investigated. The objectives of this investigation were to study the effect of microshrink on the tensile properties of nickel alloy 713C and to find nondestructive methods of detecting microshrink at any significant level. Alloy bars were cast, the microshrinkage was measured metallographically, and tensile tests were run at 1000 F. A large number of sources were searched for information on methods to detect microshrink. Within the range of 2.5% to 9%, measured in the local area having the greatest amount present, microshrink did not have any significant effect on tensile properties. A number of methods to detect microshrink nondestructively were found, but those other than conventional X-ray radiography would require development. The effect of microshrink on fatigue and creep properties was not investigated. Consideration should be given to making such an investigation of these effects. GRA

N85-35279# Naval Postgraduate School, Monterey, Calif.
THE CHARACTER OF OBSERVED POROSITY AND ITS POSSIBLE EFFECTS ON ROLLING CONTACT FATIGUE LIFE OF M-50 STEEL M.S. Thesis
J. L. Perry Mar. 1985 72 p
(AD-A155930) Avail: NTIS HC A04/MF A01 CSCL 11/6

This thesis studied a warm-rolling of AISI M-50 steel at 750 C (1382 F). Samples of both warm-rolled and as-received (spheroidized annealed) M-50 were austenitized at 1036 C (1897 F) for various times and subsequently tempered. The heat treated samples were subjected to rolling contact fatigue (RCF) testing. In all cases prior warm-rolling degraded the RCF life at both the L(10) and L(50) levels. Scanning electron microscopy was used to examine the microstructure of the as-received and warm-rolled material between 4000X and 10,000X magnification. It is thought that the increase in the void diameters accounts for the decrease in RCF performance of warm-rolled M-50. The degraded RCF performance is due to both the increase in mean void diameter and the increase in larger sized voids that accompany warm rolling. A qualitative model was developed to account for the origin of voids in as-received material and for the increase in void diameter in warm-rolled material. GRA

N85-35280# California Univ., Berkeley. Dept. of Materials Science and Mineral Engineering.
CLUSTER VARIATION STUDY OF COHERENT ORDERING IN FCC AND BCC SOLID SOLUTIONS Final Report, 15 Jun. 1980 - 15 May 1984
D. DeFontaine May 1985 8 p
(Contract DAAG29-80-K-0044)
(AD-A156039; ARO-16964.8-MS) Avail: NTIS HC A02/MF A01 CSCL 11/6

The primary objective of this investigation was the derivation of binary phase diagrams by means of a statistical mechanical model called the Cluster Variation Method. In particular, phase equilibrium as a function of the ratio between the values of second and first neighbor effective pair interactions, the ratio being the only physical input to the computer codes. The resulting phase diagrams are important for the purpose of analyzing experimentally determined alloy phase diagrams. GRA

N85-35281# Naval Postgraduate School, Monterey, Calif.
EFFECT OF PRIOR WARM ROLLING ON THE RETAINED AUSTENITE CONTENT AND HARDENING RESPONSE OF VIM-VAR (VACUUM-INDUCTION MELTED-VACUUM-ARC REMELTED) AISI M-50 STEEL M.S. Thesis
N. H. Camerino, Jr. Mar. 1985 47 p
(AD-A156145) Avail: NTIS HC A03/MF A01 CSCL 11/6

The objective of warm rolling M-50 bearing steel is microstructural refinement which may lead to increases in rolling contact fatigue life. A consequence of this refinement is that the austenitizing temperature used in the final hardening cycle should be reduced. This is because warm rolling leads to faster dissolution of finer soluble carbides at the austenitizing temperature. This thesis effort determined the temperature decrease that warm rolling allows in austenitizing to produce a microstructure of finer grain and carbide size but equivalent carbide dissolution. Here, this has been inferred by measurement of the volume fraction of retained austenite being a function of the amount of carbides taken into solution during austenitization. It was found that the standard austenitizing temperature of 1106 C used to harden stock M-50 can be reduced by 63 centrigrade degrees with warmrolled M-50 steel. GRA

N85-35282# Oak Ridge National Lab., Tenn.
THERMODYNAMICS OF THE CORROSION OF CHROMIUM IN MOLTEN CARBONATES
H. S. Hsu and J. H. DeVan 1985 24 p refs Presented at the Natl. Assoc. of Corrosion Engr. Ann. Meeting and Mater. Performance and Corrosion Show, Boston, 25 Mar. 1985
(Contract DE-AC05-84OR-21400)
(DE85-011407; CONF-850311-14-Draft) Avail: NTIS HC A02/MF A01

To define and study the mechanisms that control the corrosion of current collector materials in molten carbonate fuel cells (MCFC), the corrosion of chromium in Li2CO3-K2CO3 has been investigated from a thermodynamic point of view. Thermochemical calculations with the computer program are used to establish equilibrium phase relationships. Phase stability diagrams of Cr-Li2CO3, Cr-K2CO3, and Cr-(Li,K)2CO3 systems are considered at 650 C. The condensed phases at equilibrium are mapped as functions of log a(sub O2) and log a(sub CO2) for the gas mixture C2, CO2, and Ar at 1.0 atm (1.01 x 10(5) Pa) total pressure; where a(sub O2) and a(sub CO2) are the activities (partial pressures) of O2 and CO2, respectively. In the system Cr-(Li,K)2CO3, a mixture of (Li,K)2CO3 and (Li,K)2CrO4 should exist under oxidizing environments when log a(sub O2) > -5.0 and log a(sub CO2) > -4.6, and a mixture (Li,K)2CO3 and LiCrO2 is stable in reducing atmospheres when log a(sub O2) < -8.0 and log a(sub CO2) > -4.6. The concentration of (Li,K)2CrO4 is dependent on the concentration of (Li,K)2CO3. The ternary phase boundary of (Li,K)2CO3-(Li,K)2CrO4-LiCrO2 varies when the concentration of (Li,K)2CO3 changes. These predicted phase relationships are checked experimentally by thermogravimetric analysis (TGA) and differential thermal analysis (DTA). The results of TGA and DTA are self consistent with respect to the reaction products from the calculated phase stability diagrams. DOE

N85-35283# Argonne National Lab., Ill. Materials Science and Technology Div.
EFFECT OF TEMPERATURE AND IONIC IMPURITIES AT VERY LOW CONCENTRATIONS ON STRESS CORROSION CRACKING OF TYPE 304 STAINLESS STEEL
W. E. Ruther, W. K. Sopper, and T. F. Kassner Nov. 1984 16 p refs Presented at the CORROSION/85, Boston, 25-29 Mar. 1985

Sponsored in part by Nuclear Regulatory Commission
(Contract W-31-109-eng-38)
(TI85-003048; CONF-850311-1) Avail: NTIS HC A02/MF A01

The relative effect of approx. 12 anion species, in conjunction with hydrogen and sodium cations, on the stress-corrosion-cracking (SCC) behavior of lightly sensitized Type 304 stainless steel was investigated in constant-extension-rate-tensile (CERT) tests at 289 C in water with 0.2 ppm dissolved oxygen at total conductivity values of < 1 micron S/cm. The results show that the sulfur species, either in acid or sodium form, produce the highest degree of IGSCC relative to other anions. The effect of temperature on the SCC behavior of the material was investigated in CERT tests over the range 110 to 320 C in high-purity water and in water containing 0.1 and 1.0 ppm sulfate as H2SO4 at a dissolved oxygen concentration of 0.2 ppm. The CERT parameters were correlated with impurity concentration (i.e., conductivity) and the electrochemical potential of platinum and Type 304 stainless steel electrodes in the high-temperature environments. DOE

N85-35284# Rockwell International Corp., Golden, Colo.
INTERACTION OF TRACE ELEMENTS AND WELDING PARAMETERS ON GTA WELD SHAPE
P. Burgardt and C. R. Heiple [1985] 4 p
(Contract DE-AC04-76DP-03533)
(DE85-004046; RFP-3728) Avail: NTIS HC A02/MF A01

Good penetration and poor penetration steels have different responses to changes in temperature distribution on the weld pool surface. Penetration of 304 SS was varied using S and Se dopants. The weld parameter was the electrode tip angle. Results of bead-on-plate gas tungsten arc welding (GTA) welds show that there is a difference in response of weld pool shape to tip angle depending on penetration: low penetration base metal show no dependence, intermediate penetration steel show a small linear decrease of weld depth-to-width ratio (d/w) with tip angle, and high penetration steel show an increase of d/w up to a maximum at about 50 deg, followed by a decrease in d/w. DOE

N85-35285# Virginia Univ., Charlottesville. Dept. of Materials Science.
EFFECT OF MICROSTRUCTURE ON THE FATIGUE BEHAVIOR OF Fe-C-X ALLOYS Final Report, 1 Jul. 1983 - 16 Nov. 1984
G. J. Shiflet, K. V. Jata, and B. A. Starke, Jr. Mar. 1985 71 p
(Contract DE-AS05-83ER-45035)
(DE85-011749; DOE/ER-45035/1) Avail: NTIS HC A04/MF A01

The effect of microstructure on fatigue behavior is established by controlling the relationship between ferrite, martensite, and carbides in ternary steels. Three alloys are being studied: Fe-0.2C-1Mn; Fe-02.C-2Mo; Fe-0.2C-4Mo. The roles of austenite (martensite) and ferrite are being studied. DOE

N85-35286# Brookhaven National Lab., Upton, N. Y.
NOBLE METALS AS INCIPIENT TRANSITION METALS
R. E. Watson and L. H. Bennett 1985 13 p Presented at the 114th AIME Ann. Meeting (includes Soc. of Mining Eng.), New York, 24 Feb. 1985 Prepared in cooperation with National Bureau of Standards, Washington, D.C.
(Contract DE-AC02-76CH-00016)
(DE85-013283; BNL-36570; CONF-850211-9) Avail: NTIS HC A02/MF A01

Two classes of experiments are inspected; impurity Moessbauer isomer shifts and photoemission of core and valence electron levels. At first glance they would appear to be in conflict concerning the direction of any charge transfer. In noble metal alloys this is associated with changes in d-electron count which are compensated by the non-d electrons. The sign of the change in d occupation is readily understood in terms of d band hydridization. The normalized isomer shifts show that the balance of d and non-d transfer terms must vary across a transition metal row and that while the noble metals, when acting as impurities, act much like the transition elements immediately adjacent to them, the charge transfer, when the noble metals are hosts, is quite different. These observations indicate that three charge transfer terms have visible effects on alloying properties. The long standing discrepancy is considered between the elemental fcc-bcc structural energy differences of Kaufman and Bernstein which are standardly employed in phase diagram constructs versus those appropriate to the Engel-Brewer model of transition and noble metals. DOE

N85-35287# Oak Ridge National Lab., Tenn.
CHARACTERIZATION OF MODIFIED 9 r-1 Mo STEEL SAND CASTINGS
V. K. Sikka Apr. 1985 33 p
(Contract DE-AC05-84OR-21400)
(DE85-012057; ORNL/TM-9573) Avail: NTIS HC A03/MF A01

Experience with the sand casting of modified 9 Cr-1 Mo steel at several foundries is presented. The castings included simple blocks, elbows, valve bodies, and a steam chest. Castings were characterized by tensile and Charpy impact tests, for the effects of thermal aging on Charpy impact properties and hardness, and by creep, fatigue, and microstructure. Properties of the castings were compared with those observed for wrought material. In general, mechanical properties of castings were slightly lower than those of the wrought material. DOE

N85-35288# Allied Bendix Aerospace, Kansas City, Mo.
X-RAY FLUORESCENCE ANALYSIS OF 304L STAINLESS STEEL Final Report
L. L. Lantz May 1985 25 p
(Contract DE-AC04-76DP-00613)
(DE85-013254; BDX-613-3260) Avail: NTIS HC A02/MF A01

This project was undertaken to develop a faster, more accurate method to determine the composition of 304L vacuum and remelted (VAR), corrosion resistant steel. An accurately measured composition is required to predict the 304L ferrite content, which must be controlled to produce crack resistant welds. An X-ray fluorescence spectrometry method has been developed for the analysis of 12 elements in 304L steel. The sample composition is calculated using the XRF-11 fundamental parameters computer program (Criss Software, Incorporated, Largo, MD) for X-ray fluorescence analysis. Absolute accuracies within + or - 0.1 wt % are obtained for chromium and nickel in certified standards analyzed as samples by using program standards having composition close to sample composition and by making matrix corrections for all elements in the standards and samples. A comparison is made of the chromium concentration in 24 304L samples determined by the X-ray method and by wet chemical analysis. DOE

N85-35289# California Univ., Livermore. Lawrence Livermore Lab.
DYNAMIC COMPACTION OF A MONOSIZED SPHERICAL TUNGSTEN POWDER
W. H. Gourdin and S. L. Weinland 28 Jun. 1985 15 p Presented at the Am. Phys. Soc. Topical Conf. on Shock Waves in Condensed Matter, Spokane, 22 Jul. 1985
(Contract W-7405-eng-48)
(DE85-014808; UCRL-92855; CONF-850736-22) Avail: NTIS HC A02/MF A01

A limited number of measurements is presented of the Hugoniot of a 45 to 74-(MU)m spherical tungsten powder in the stress range 0 to 7 GPa. From these data it is inferred that compaction to the solid density occurs at about 4 GPa. Examination of recovered specimens shows that interparticle bonding does not occur at stresses as high as 6.2 GPa. This is consistent with calculations based on the energy flux at powder particle surfaces during compaction, which suggest that interparticle melting will not occur at stresses less than about 9.0 GPa. DOE

N85-35290# Bureau of Mines, Avondale, Md.
SPECTRAL CHARACTERISTICS OF GRINDING SPARKS USED FOR IDENTIFICATION OF SCRAP METALS
W. D. Riley, B. W. Dunning, and D. M. Soboroff 1985 20 p
(PB85-198570; BM-RI-8932; LC-84-600301) Avail: NTIS HC A02/MF A01 CSCL 11F

The Bureau of Mines is conducting research on methods for the rapid identification and sorting of mixed scrap metals and alloys so that domestic scrap resources can be fully utilized. One

method, spark testing, is the examination of the pattern of sparks that results when a metal or alloy is ground on an abrasive wheel. This technique requires experienced sorters. Bureau researchers have shown that spectrophotometric methods can be used in lieu of the highly skilled sorter. The spectra of a mild steel, an HSLA steel, several stainless steels, and four nickel-base alloys have been measured. Differences in the spectra that are sufficient for identification are apparent. Author (GRA)

N85-35291# Bureau of Mines, Rolla, Mo.
DEPOSITION OF NICKEL-COBALT ALLOYS BY CONTROLLED-POTENTIAL ELECTROLYSIS Report of Investigations
J. L. Holman and L. A. Neumeier 1985 24 p
(PB85-198562; BM-RI-8931; LC-84-600281) Avail: NTIS HC A02/MF A01 CSCL 11F

The Bureau of Mines is conducting research to improve technology for the recovery of strategic and critical metals, such as cobalt, nickel, and chromium, that are lost in bulk and particulate superalloy-type scrap because it has not been possible to process mixed contaminated scrap efficiently. The research approach involves melting and casting mixed superalloy scrap into soluble anodes for electrodeposition of Ni-Co alloys by controlled-potential electrolysis. This basic research assessed the effects of cathode potential, SO4:Cl electrolyte ratio, electrolyte pH, stirring rate, deposition time, cathode current density, and chromium concentration on cathode cathode current efficiency, alloy deposit composition, and deposition potential at a cell temperature of 55C.
Author (GRA)

27 NONMETALLIC MATERIALS

Includes physical, chemical, and mechanical properties of plastics, elastomers, lubricants, polymers, textiles, adhesives, and ceramic materials.

N85-35292 United Kingdom Atomic Energy Authority, Risley (England).
ACTION OF WEAR-INHIBITING Al2O3-COATINGS WHEN APPLIED TO HARD METAL CUTTING TOOLS
B. Lux and H. Schachner 25 Nov. 1984 17 p refs Transl. into ENGLISH from High Temp. - High Pressure (England), v. 10, 1978 p 315-323 Presented at the 9th Plansee Seminar, Reutte, Austria, 23-26 May 1977
(BLL-Risley-TR-5041-(9091.9F)) Copyright. Avail: British Library Lending Div., Boston Spa, Engl.

Reversible hard metal cutting tips coated with Al2O3 were utilized as an example to demonstrate that through the selective combination of two materials, whose respective properties do as far as possible meet the requirements for the surface and the substrate material, it was possible to improve fundamentally the performance of a cutting tool. It is believed that the principle which has been illustrated here, the separate optimization of the substrate material and the surface, can be applied more widely both in technical and economic respects for many material development projects. Author

N85-35293 United Kingdom Atomic Energy Authority, Risley (England).
WEAR-RESISTANT COATINGS FOR TOOLS INTENDED FOR COLD WORKING
M. Kuebert and R. Roska 25 Nov. 1984 23 p refs Transl. into ENGLISH from Werkstatt und Betrieb (West Germany), v. 116, no. 2, 1983 p 91-96
(BLL-Risley-TR-5040-(9091.9F)) Copyright. Avail: British Library Lending Div., Boston Spa, Engl.

For some time now, tools have been treated using the classical methods of nitriding and hard chroming, and more recently use has been made of boriding and the deposition from the gaseous phase of nitrides and carbides with the aid of Chemical Vapor Deposition. The Physical Vapor Deposition method which originates from the field of high vacuum technology has also been employed. The objective of these protective coatings is to combat the effects of wear, while the substrate absorbs the mechanical loads. The increase in the number of surface treatment methods has resulted in uncertainty among both users and coaters as to which method is the most suitable for the particular conditions in question. A discussion is presented of the principal surface treatment methods for the prevention of wear and of the most important process parameters with account taken of the substrate material. Author

N85-35294*# Lockheed Missiles and Space Co., Huntsville, Ala. Heat Protection Systems Group.
SPACE SHUTTLE SRB TPS PROTECTIVE PAINT TEST AND EVALUATION IN NASA HOT GAS FACILITY AND AEDC TUNNEL C
Zain S. Karu 13 Jul. 1979 25 p ref
(Contract NAS8-32982)
(NASA-CR-170884; NAS 1.26:170884; LMSC-HREC-TN-D697613) Avail: NTIS HC A02/MF A01 CSCL 11C

The results and outcome of thermal tests conducted to evaluate the performance of the protective coat of paint on the solid rocket booster (SRB) thermal protection system are discussed. A problem was uncovered during a series of tests on the SRB instrumentation islands in AEDC Tunnel C on 13 January 1979. The white protective paint or the Turco coating on the thermal protection system panels began to flow soon after the panels were exposed to the flow. This presented a serious problem especially since the critical pressure sensing, parachute opening baroswitches located on the frustum of the SRB were most likely to be contaminated by the paint flowing down the sides of the SRB nose cone. Because the first two flight articles were already completed, it was necessary to find a solution to the existing paint problem. It was found that all the coatings tested, except the Hypalon, had similar undesirable flow characteristics. Also even the Hypalon, which did not flow, would bubble up and disintegrate when it was applied on top of the new Turco. Recently, the Turco coating was removed from an MSA-:11 panel by dissolving the paint with a certain agent. This was done in two ways, by dissolving and removing almost all of the paint on one side of the panel and dissolving and removing about 50% of the paint on the other. The panel was then coated with Hypalon and tested as before in the Hot Gas Facility. No evidence of any paint flow nor any adverse performance of MSA was observed. R.J.F.

N85-35295*# Lockheed Missiles and Space Co., Huntsville, Ala. Research and Engineering Center.
RESULTS OF TESTS OF INSTA-FOAM THERMAL PROTECTION SYSTEM (TPS) MATERIAL FOR PROTECTION OF EQUIPMENT INSIDE THE SRB AFT SKIRT
W. G. Dean 3 Aug. 1982 16 p
(Contract NAS8-32982)
(NASA-CR-170892; NAS 1.26:170892; LMSC-HREC-TN-D867582) Avail: NTIS HC A02/MF A01 CSCL 11C

The objective of these tests was to determine whether Insta-Foam can be used successfully to protect items inside the solid rocket booster aft skirt during reentry. On some of the early Space Shuttle flights the aft skirt heat shield curtain failed during reentry. This allowed the hot gases to damage some of the equipment, etc., inside the skirt. For example, some of the propellant lines were overheated and ruptured and some of the NSI (nozzle severance) cables were damaged. It was suggested that the Insta-Foam thermal protection system be sprayed over these lines, etc., to protect them during future flights in case of a curtain failure. The tests presented were devised and run to check out the feasibility of this idea. R.J.F.

N85-35296*# National Aeronautics and Space Administration, Washington, D. C.
DETERMINATION OF THE VISCOSITY NUMBER OF THERMOPLASTICS IN DILUTE SOLUTION; POLYAMIDES (PA)
Sep. 1985 13 p Transl. into ENGLISH of DIN Standard no. 53-727, Berlin, West Germany, Jan. 1980 4 p Transl. by RMS Associates, BWI Airport, Md. Original document prepared by German Inst. of Standards, Standards Committee, Berlin, West

Germany
(Contract NASw-4070)
(NASA-TM-77673; NAS 1.15:77673) Avail: NTIS HC A02/MF A01 CSCL 11G

This West German Standard presents a test used to determine the viscosity number of polyamides and copolyamides which are easily diluted in sulfuric acid, and for other polyamides which are less easily diluted in sulfuric acid, and which are diluted in m-cresol. As formic acid is often used in industry instead of sulfuric acid, this solvent is also presented as an alternative, however, sulfuric acid is preferred because of the thermodynamic solubility characteristics of the polyamides and the handling safety. In addition, it is shown which solvent should be used for each polyamide. Finally, determinations concerning the preparation of the samples are presented. Using the viscosity number, a determination of the molar mass of the polyamides is possible. Author

N85-35297# Utah Univ., Salt Lake City. Dept. of Physics.
NOISE IN SILVER BETA ALUMINA CERAMICS
S. W. Smith and J. J. Brophy Sep. 1985 14 p
(Contract N00014-82-K-0603)
(AD-A156135; TR-6) Avail: NTIS HC A02/MF A01 CSCL 09/1

Voltage fluctuations at ohmic electrodes to silver beta alumina ceramic samples are observed both at contacts and in the bulk over the frequency interval 0.001 to 10000 Hz. Contact noise power in the absence of current varies as 2/F at low frequencies and is dominated by Nyquist noise of the sample at frequencies greater than 100 Hz. Bulk current noise measured at transverse contacts has a f to the minus 3/2 power spectrum and increases with the square of the current. Low-frequency contact noise, sample Nyquist noise and bulk current noise are all thermally activated with activation energies of -0.96, 0.14, and 0.61 eV, respectively. These experimental results are very similar to those previously reported for sodium beta alumina ceramics. GRA

N85-35298# Massachusetts Univ., Amherst. Dept. of Polymer Science and Engineering.
SOLID-STATE CO-EXTRUSION OF NYLON 6 GEL Interim Report
H. H. Chuah and R. S. Porter 25 Mar. 1985 38 p
(Contract N00014-83-K-0228)
(AD-A156187; TR-24) Avail: NTIS HC A03/MF A01 CSCL 13/8

A partially dried Nylon 6 gel has been drawn at 150 C and to draw ratio 5.7X, by a split billet co-extrusion technique in an Instron capillary rheometer. The gel was prepared by dissolving Nylon 6 in benzyl alcohol at 165 C and cooled to gel at room temperature. On removing solvent, preorientation was introduced into the gel with the b-chain axis weakly oriented perpendicular to the gel surface. Drawing produces double orientation as shown by wide-angle X-ray diffraction. One population of the crystals are oriented with chain axes in the draw direction, as in the usual uniaxial drawing. The second population have their chain axes oriented perpendicular to draw direction. From birefringence, wide- and small-angle X-ray scattering studies, a deformation mechanism for the double orientation was proposed. Thermal and mechanical properties were also studied. Annealing at 190 C produced partial reorientation of the second crystals resulting in a more complex orientation. GRA

N85-35299# Oak Ridge National Lab., Tenn.
DEVELOPMENT AND CHARACTERIZATION OF CARBON-BONDED CARBON FIBER INSULATION FOR RADIOISOTOPE SPACE POWER SYSTEMS
G. C. Wei and J. M. Robbins Jun. 1985 44 p
(Contract DE-AC05-84OR-21400)
(DE85-013365; ORNL/TM-9381) Avail: NTIS HC A03/MF A01

The General-Purpose Heat Source (GPHS), an improved radioisotope heat source, employs a unique thermal insulation material, carbon-bonded carbon fiber (CBCF), to protect the fuel capsule and to help achieve the highest possible specific power. The CBCF insulation is made from chopped rayon fiber about 10 micrometer in diameter and 250 micrometer long, which is carbonized and bonded with phenolic resin particles. The CBCF shapes, both tubes and plates, are formed in a multiple molding facility by vacuum molding a water slurry of the carbonized chopped-rayon fiber (54 wt %) and phenolic resin (46 wt %). The molded shapes are subsequently dried and cured. Final carbonization of the resin is at 1600 C. Machining to close tolerances (+ or - 0.08 mm) is accomplished by conventional tooling and fixturing. The resulting material is an excellent lightweight insulation with a nominal density of 0.2 Mg/cu. m. and a thermal conductivity of 0.24 W(m.K) in vacuum at 2000 C. Several attributes that make CBCF superior to other known high-temperature insulation materials for the GPHS application have been identified. DOE

N85-35300# Department of Energy, Washington, D. C.
METHOD OF PREPARING THIN POROUS SHEETS OF CERAMIC MATERIAL Patent Application
T. E. Swarr, R. C. Nickols, and M. Krasij, inventors (to DOE) Filed 23 May 1984 15 p
(Contract DE-AC21-79ET-15440)
(DE85-006399; US-Patent-Appl-SN-612952) Avail: NTIS HC A02/MF A01

A method of forming thin porous sheets of ceramic material for use as electrodes or other components in a molten carbonate fuel cell is presented. The method involves spray drying a slurry of fine ceramic particles in liquid carrier to produce generally spherical agglomerates of high porosity and a rough surface texture. The ceramic particles may include the electrode catalyst and the agglomerates can be calcined to improve mechanical strength. After slurrying with suitable volatile material and binder tape casting is used to form sheets that are sufficiently strong for further processing and handling in the assembly of a high temperature fuel cell. DOE

N85-35301# Department of Energy, Washington, D. C.
ELECTRICALLY CONDUCTIVE DOPED BLOCK COPOLYMER OF POLYACETYLENE AND POLYISOPRENE Patent Application
M. Aldissi, inventor (to DOE) Filed 27 Jun. 1984 9 p
(Contract W-7405-eng-36)
(DE85-006500; US-Patent-Appl-SN-625323) Avail: NTIS HC A02/MF A01

An electrically conductive block copolymer of polyisoprene and polyacetylene and a method of making the same are disclosed. The polymer is prepared by first polymerizing isoprene with n-butyllithium in a toluene solution to form an active isoprenyllithium polymer. The active polymer is reacted with an equimolar amount of titanium butoxide and subsequently exposed to gaseous acetylene. A block copolymer of polyisoprene and polyacetylene is formed. The copolymer is soluble in common solvents and may be doped with I2 to give it an electrical conductivity in the metallic regime. DOE

N85-35302# Sandia Labs., Albuquerque, N. Mex.
DANGLING BONDS AND SUB-GAP OPTICAL ABSORPTION IN SILICON
C. H. Seager, P. M. Lenahan, K. L. Brower, and R. E. Mikawa 1985 7 p refs Presented at 2nd Spring Meeting of the Mater. Res. Soc., San Francisco, 15 Apr. 1985
(Contract DE-AC04-76DP-00789)
(DE85-011752; SAND-84-2287C; CONF-850421-5) Avail: NTIS HC A02/MF A01

The silicon dangling bond defect plays a large part in controlling the electronic properties of a-Si, polycrystalline silicon, and Si/SiO2 interface. Jackson et al. have suggested that transitions of electrons occupying this defect produce the Urbach-like sub-gap absorption tail seen in two of these materials. Optical and electron spin resonance measurements were performed on polycrystalline silicon, plastically deformed silicon, and Si/SiO2 interfaces to further examine this contention. In addition to seeing no measurable absorptance due to dangling bond interface states in the latter system, it is concluded from the poor correlation of ESR signals with optical data that the Urbach tail in polycrystalline and deformed silicon is not due to transitions of dangling bond electrons. DOE

N85-35303# Pittsburgh Univ., Pa. Dept. of Metallurgical and Materials Engineering.
HIGH TEMPERATURE CORROSION OF CERAMICS
J. R. Blachere and F. S. Pettit Mar. 1985 52 p
(Contract DE-FG02-84ER-45117)
(DE85-013481; DOE/ER-45117/1) Avail: NTIS HC A04/MF A01

The high temperature corrosion of Si3N4, SiC, Al2O3 and SiO2 in presence of sodium sulfate deposits is discussed. For exposures up to 168 hours, all ceramics are quite resistant to high temperature corrosion at 1000 C. High purity Al2O3 (single crystal) shows essentially no corrosion under basic or acid high temperature corrosion with 5 mg/sq. cm. of Na2SO4. The more impure aluminas reacted more under basic conditions because of the presence of silicate second phases. The SiO2 and SiO2 formers deteriorate mostly through crystallization and spalling of SiO2 layers. The oxidation of Si3N4 and SiC is greatly enhanced by the sodium of the deposit. This oxidation and the crystallization of the SiO2 layers are both enhanced by high activity of Na2O in the deposit (basic conditions: 5 mg/sq. cm. of Na2SO4 in pure O2). This reaction is only superficial and localized under acid hot corrosion (5 mg/sq. cm. of Na2SO4 in 1% SO2 in O2 mixture, gas composition at room temperature); however, crystallization of the SiO2 under the Na2SO4 drops may result in nonprotective behavior of the scale. Spalling can be associated with this localized acid corrosion. DOE

N85-35304# Oak Ridge National Lab., Tenn.
INFRARED GENERATION AND WAVE-MIXING STUDIES IN CESIUM
W. Christian, J. A. D. Stockdale, A. Dodhy, and R. N. Compton 1985 7 p Presented at the Conf. on Lasers and Electro-Optics, Baltimore, 21 May 1985 Prepared in cooperation with Davidson Coll., N.C.
(Contract DE-AC05-84OR-21400)
(DE85-012883; CONF-850558-2) Avail: NTIS HC A02/MF A01

A Nd-YAG pumped dye laser and heat pipe is used to investigate stimulated infrared production, wave mixing, and ionization in cesium vapor near the one photon resonant 7P(sub 1/2,3/2) fine structure states. DOE

N85-35305# California Univ., Livermore. Lawrence Livermore Lab.
SINGLE-POINT DIAMOND CRUSHING OF ZERODUR WITH IN-SITU POLISHING AND METROLOGY ON A DIAMOND TURNING MACHINE
J. B. Bryan and D. L. Carter 1 Apr. 1985 11 p Presented at the Glancing Incident Opt.-Fabric. Workshop, Annapolis, 1 Apr. 1985
(Contract W-7405-eng-48)
(DE85-012918; UCRL-92682; CONF-8504139-1) Avail: NTIS HC A02/MF A01

Large, complicated, aspherical optical elements of glass are presently used in many astronomical devices, both on land and in space. Grazing incident mirrors are envisioned for use in such missions as the proposed Advanced X Ray Astrophysical Facility (AXAF), the Far Ultraviolet Spectroscopic Explorer (FUSE), and others. These elements are very expensive to fabricate because a great deal of time and labor are required to shape a glass blank. The fabrication of these mirrors can best be achieved by applying precision machining techniques and precision machines for figuring and finishing low expansion glasses such as Zerodur. DOE

N85-35306*# National Bureau of Standards, Gaithersburg, Md.
STRUCTURE AND PROPERTIES OF POLYETHYLENE FILMS USED IN HEAVY LIFT BALLOONS Report, Jan. - May 1984
F. Khoury, J. M. Crissman, B. M. Fanconi, H. L. Wagner, and L. H. Botz Mar. 1985 105 p refs
(NASA Order-501834D)
(NASA-CR-176227; NAS 1.26:176227; PB85-204717; NBSIR-84/2989-NASA) Avail: NTIS HC A06/MF A01 CSCL 11J

The following features of five polyethylene films used by NASA in the construction of heavy lift balloons have been examined: molecular weight, molecular weight distribution, branching, melting behavior, density, surface texture, birefringence, orientation of crystalline regions, unlaxial deformation in the machine and transverse directions, and the effect of sample geometry and strain rate on deformation behavior. The goal of this exploratory study was to determine whether there are significant differences in any of the above mentioned features, or combination of features between the films. The acquisition of such information is a first step towards determining whether there are any specific correlations between film characteristics and the incidence of catastrophic failure of balloons during ascent through the troposphere. This exploratory study has resulted in the identification of similarities and differences between various features of the films. Author

28 PROPELLANTS AND FUELS

Includes rocket propellants, igniters, and oxidizers; storage and handling; and aircraft fuels.

For related information see also *07 Aircraft Propulsion and Power, 20 Spacecraft Propulsion and Power,* and *44 Energy Production and Conversion.*

N85-35307*# National Aeronautics and Space Administration. Langley Research Center, Hampton, Va.
SOUND SPEED MEASUREMENTS IN LIQUID OXYGEN-LIQUID NITROGEN MIXTURES
Allan J. Zuckerwar and David S. Mazel (Old Dominion Univ.) Sep. 1985 22 p refs
(NASA-TP-2464; L-15965; NAS 1.60:2464) Avail: NTIS HC A02/MF A01 CSCL 21D

The sound speed in liquid oxygen (LOX), liquid nitrogen (LN2), and five LOX-LN2 mixtures was measured by an ultrasonic pulse-echo technique at temperatures in the vicinity of -195.8C, the boiling point of N2 at a pressure of I atm. Under these conditions, the measurements yield the following relationship between sound speed in meters per second and LN2 content M in mole percent: c = 1009.05-1.8275M+0.0026507 M squared. The second speeds of 1009.05 m/sec plus or minus 0.25 percent for pure LOX and 852.8 m/sec plus or minus 0.32 percent for pure LN2 are compared with those reported by past investigators. Measurement of sound speed should prove an effective means for monitoring the contamination of LOX by Ln2. Author

N85-35308# Air Force Wright Aeronautical Labs., Wright-Patterson AFB, Ohio.
NITROGEN ANALYSIS BY CHEMILUMINESCENCE Final Report, Aug. 1982 - Dec. 1983
R. C. Striebich Apr. 1985 37 p
(AD-A156197; AFWAL-TR-84-2089) Avail: NTIS HC A03/MF A01 CSCL 21/4

With high overall accuracy, a chemiluminescent detector can easily measure low ppm nitrogen levels in model mixtures and shale-derived jet fuel distillates. Forty model mixtures were analyzed using an Antek Model 720C chemiluminescent detector to demonstrate the absolute accuracy and precision of the instrument. A severely hydrotreated shale JP-4 jet fuel was blended with selected model mixtures to obtain six fuels ranging from less than 1 to approximately 150 parts-per-million added nitrogen. Total nitrogen analysis was then accomplished by two different chemiluminescent detection systems, as well as by the micro-Kjeldahl and microcombustion methods. Results clearly point out the ability of the chemiluminescent method to measure the nitrogen level of low ppm shale-derived aviation turbine fuel. GRA

N85-35309# Mound Lab., Miamisburg, Ohio.
FRICTION, IMPACT, AND ELECTROSTATIC DISCHARGE SENSITIVITIES OF ENERGETIC MATERIALS
P. S. Wang and G. F. Hall 31 May 1985 21 p refs
(Contract DE-AC04-76DP-00053)
(DE85-013321; MIM-3252) Avail: NTIS HC A02/MF A01

Impact, friction, and electrostatic discharge sensitivities of energetic materials (explosives and pyrotechnics) used or manufactured at Mound were tested by the one-shot method. The Bruceton statistical method was used to derive 50% initiation levels, and the results were compared. The materials tested include: PETN, HMX, Elastic Bonded Explosives (PEX), CP, TATB, RX26BB, RX26BH, barium styphnate, LX-15, LX-16, Ti/KC1O4, TiH(sub 0.65)/KC1O4, TiH(sub 1.65)/KC1O4, Fe/KC1O4, TiH(sub 1.75)(B) CaCrO4, Ti(B)CaCrO4, E/CaCrO4, TiH(sub 0.65)/2B, TiH(sub 0.65)/3B, 2Ti/B, TiH(sub 1.67)/2B, Ti/2B, TiH(sub 1.67)/3B, Ti/B, and Ti/3B. Some samples were investigated for aging effects, physical variables, and the effect of manufacturing parameters on sensitivities. The results show that in both friction and impact tests, CP and barium styphnate are the most sensitive; TiH(sub 1.65)KC1O4, LX-15, TATB and its related materials are the least sensitive, and other materials such as PETN and HMX are in the mid-range. In the electrostatic tests of Ti based pyrotechnics, a decrease of sensitivity with increasing hydrogen concentration was observed. DOE

N85-35310# Virginia Polytechnic Inst. and State Univ., Blacksburg.
MICROBIOLOGICAL AND BIOCHEMICAL STUDIES TOWARDS OPTIMIZATION OF SUBSTRATE UTILIZATION BY METHANOGENIC BACTERIA Annual Report, Dec. 1983 - Dec. 1984
J. G. Ferry 31 Dec. 1984 55 p refs
(PB85-188332; GRI-85/0004) Avail: NTIS HC A04/MF A01 CSCL 21D

The pathway of acetate conversion to methane and carbon dioxide was studied in Methanosarcina strain TM-1. It was shown that the methyl group of ecetate was transferred to coenzyme M which unequivocally demonstrates that methyl coenzyme M is an intermediate in the pathway. The levels of an enzyme system that demethylates methyl coezyme M and requires carbon monoxide was correlated with growth on acetate which implicates this system in the pathway of acetate to methane. However, free carbon monoxide was shown not to be an intermediate in the pathway which suggests that carbon monoxide may be bound to a site which forms a reduced C1 intermediate from the carboxyl group of acetate. Biotin, Fe, Co and Ni were shown to be required for growth of methanococcoides methylutens on methylotrophic substrates. Author (GRA)

N85-35311# Georgia State Univ., Atlanta. Dept. of Biology.
BIODEGRADATION OF JET FUEL BY AQUATIC MICROBIAL COMMUNITIES
J. C. Spain and C. C. Sommerville 1985 22 p refs
(Grant EPA-R-809370)
(PB85-191971; EPA-600/D-85-084) Avail: NTIS HC A02/MF A01 CSCL 06A

Laboratory experiments are described that studied the fate of jet fuel in several types of situations that could be encountered in the field. Benzene, toulene, and p-xylene were the only components of the fuel that dissolved in the water to significant concentrations. All three compounds volatilized within 24 h and, thus, did not remain in the water long enough for microbial deg radiation to affect their fate. Inclusion of sediment (500 mg/1 dry weight) did not retard the disappearance of the fuel components, and rates of disappearance were identical in controls sterilized with HgCl2. GRA

31 ENGINEERING (GENERAL)

Includes vacuum technology; control engineering; display engineering; and cryogenics.

N85-35312 North Carolina State Univ., Raleigh.
MEMBRANE REINFORCEMENT IN CONCRETE SHELLS: DESIGN VERSUS NONLINEAR BEHAVIOR Ph.D. Thesis
Habibollah Akbar 1985 288 p
Avail: Univ. Microfilms Order No. DA8507409

The design of membrane reinforcement in concrete shells versus their ultimate behavior is studied. The present method of design is reviewed in which the reinforcement design is based on the pointwise elemental ultimate behavior in the shell, using the stresses obtained from the elastic analysis. The adequacy of this method of design is examined both on the elemental level and on the global level. On the elemental level, the adequacy of the design method is confirmed based on the study of experimental results. It is noted that, when the conventional cracking model for reinforced concrete structures is used on the elemental level, the design and the nonlinear behavior are not, in general, consistent. A cracking model is proposed which is consistent with the design and the nonlinear behavior on the elemental level. The model is verified using several experimental results. Dissert. Abstr.

N85-35313# International Association of Fire Chiefs, Washington, D.C.
FIRE SERVICE EMERGENCY MANAGEMENT HANDBOOK Final Report, Apr. 1983 - Jan. 1985
Jan. 1985 287 p
(Contract EMW-C-0743)
(AD-A155780) Avail: NTIS HC A13/MF A01 CSCL 13/12

This planning guide was prepared for the Federal Emergency Management Agency by the International Association of Fire Chiefs as part of an effort to update and improve emergency management information available to the fire service. Intended as a primary source for fire chiefs, fire executives, and planners, it incorporates the following main topic areas: instruction for the use of the handbook; description of the emergency management process; and checklists for specific hazards. The volume includes a self evaluation form for determining community risk, concepts of emergency management, and specific steps in community risk reduction in the four phases of emergency management process. Sample forms, tables, and letters of agreement are also included. GRA

N85-35314# Energy and Environmental Analysis, Inc., Arlington, Va.
ASSESSMENT OF METAL HEATING TECHNOLOGIES FOR FERROUS FORGING: A PILOT STUDY OF THE FORM VALUE OF NATURAL GAS
T. M. Desai and S. Y. Salama Jan. 1985 120 p refs
(PB85-204394; GRI-85/0019) Avail: NTIS HC A06/MF A01 CSCL 13H

The major steps of this study are: select sample applications representative of the market segment under study and characterize applicable technologies in terms of performance and cost data; evaluate and compare economics of competing technologies for sample applications to assess gas form value in each case; perform sensitivity analysis for various market factors and evaluate their significance to the form value; explore R&D concepts to improve gas technology's form value. GRA

N85-35315# Midland-Ross Corp., Toledo, Ohio. Energy Technology Div.
ADVANCED REGENERATIVE HEAT RECOVERY SYSTEM Final Report, Sep. 1982 - Apr. 1984
R. G. Whitbeck Aug. 1984 106 p refs Sponsored by Gas Research Inst.
(PB85-199602; MR-RX-5377; GRI-85/0022) Avail: NTIS HC A06/MF A01 CSCL 13A

A new concept heat wheel regenerator was developed to recover heat from a wide range of industrial heating processes. The heat wheel design separates the heat transfer matrix from the areas to be sealed so that better sealing performance can be expected and ceramic heat transfer matrix materials can be used. The design is expected to make it possible to expand the usage of heat wheel regenerators to high temperature (2000F and higher), high flow industrial processes. Two proof of concept heat wheels were installed and laboratory tested. Author (GRA)

N85-35316# Midland-Ross Corp., Toledo, Ohio.
HIGH TEMPERATURE HEATING SYSTEM (HTHS) Final Report, Mar. 1982 - Nov. 1984

S. R. Huebner Nov. 1984 132 p Sponsored by Gas Research Inst.
(PB85-188340; GRI-85/0014) Avail: NTIS HC A07/MF A01 CSCL 13A

Natural gas has potential to become an energy alternative to electrical resistance heating for process temperatures above 1800F in furnaces where controlled process atmospheres are required. This program is intended to develop and integrate into a system, a radiant tube gas fired heating element, burner and energy recovery device. A thermal analysis is performed and shows that the heat flux of radiant tubes may be increased by application of a high combustion intensity burner and a heat transfer enhancement mechanism to increase the rate of heat transfer from the combustion products to the heating element. A radiant burner is developed which is capable of burning ten (10) times as much fuel per unit of volume as conventional radiant tube burners. The burner and radiant tube combination has demonstrated a 200 to 300 percent increase in heat flux compared to conventional systems. GRA

N85-35317# National Bureau of Standards, Gaithersburg, Md. Center for Fire Research.
PROCEEDINGS OF THE 7TH JOINT PANEL MEETING OF THE UJNR PANEL ON FIRE RESEARCH AND SAFETY
N. H. Jason and K. Davis Mar. 1985 652 p refs Meeting held in Gaithersburg, Md., 24-28 Oct. 1983
(PB85-199545; NBSIR-85/3118) Avail: NTIS HC A99/MF A01 CSCL 13L

The 7th Joint Panel Meeting of the United States-Japan Panel on Fire Research and Safety was held jointly with the Combustion Toxicity and 2nd Expert Meeting of the U.S.-Japan-Canada Cooperative Research Group on Toxicity of Combustion Products from Building Materials and Interior Goods at the National Bureau of Standards, Gaithersburg, Maryland, October 24 to 28, 1983. Technical sessions were in the areas of: Fire Hazard/Risk Management Methods; Fire Growth Prediction; Materials Fire Properties and Test Methods; Measurement Methods; Combustion Toxicity. Progress reports were presented in each area, in addition to state-of-the-art papers. Author (GRA)

N85-35318# Thermo Electron Corp., Waltham, Mass.
DEVELOPMENT OF A HIGH-EFFICIENCY, GAS-FIRED, HEAT PIPE, WARM-AIR HEATING SYSTEM Final Report, Jan. 1983 - Dec. 1984
S. Feldman and F. Becker Jan. 1985 128 p refs Sponsored by Gas Research Inst.
(PB85-199636; TE-4367-24-85; GRI-85/0062) Avail: NTIS HC A07/MF A01 CSCL 13A

With the introduction by Borg-Warner of the Heatpipe Furnace, one of the major goals of this program was achieved. This milestone was reached after a 105,000 Btu/hr, 85 percent efficient manufacturing prototype heat pipe furnace was designed, fabricated, and tested by Thermo Electron. Other prototype units of different capacities were also designed. The prototypes underwent extensive field testing and in-house accelerated life-cycle testing, indicating that they were reliable, safe, and cost-competitive. Specific issues like freeze protection and oil contamination were addressed. Two different prototype ultrahigh-efficiency condensing furnaces were designed, fabricated and tested. One approach utilized a fluorocarbon-filled heat pipe as a secondary-stage heat exchanger; the other used a plate finned tube coil as the heat exchanger. Author (GRA)

32 COMMUNICATIONS

Includes land and global communications; communications theory; and optical communications.

For related information see also *04 Aircraft Communications and Navigation* and *17 Spacecraft Communications, Command and Tracking.*

N85-35319 North Carolina State Univ., Raleigh.
ON THE CONVERGENCE OF AN ITERATIVE FORMULATION OF THE ELECTROMAGNETIC SCATTERING FROM AN INFINITE GRATING OF THIN WIRES Ph.D. Thesis
Jerry Clyde Brand 1985 99 p
Avail: Univ. Microfilms Order No. DA8507412

Contraction theory is applied to an iterative formulation of electromagnetic scattering from periodic structures and a computational method for insuring convergence is developed. A short history of spectral (or k-space) formulation is presented with an emphasis on application to periodic surfaces. The mathematical background for formulating an iterative equation is covered using straightforward single variable examples including an extension to vector spaces. To insure a convergent solution of the iterative equation, a process called the contraction corrector method is developed. Convergence properties of previously presented iterative solutions to one-dimensional problems are examined utilizing contraction theory and the general conditions for achieving a convergent solution are explored. The contraction corrector method is then applied to several scattering problems including an infinite grating of thin wires with the solution data compared to previous works. Dissert. Abstr.

N85-35320*# Illinois Univ., Urbana. Electromagnetics Lab.
NORMAL MODES IN AN OVERMODED CIRCULAR WAVEGUIDE COATED WITH LOSSY MATERIAL
C. S. Lee, S. W. Lee, and S. L. Chuang Sep. 1985 55 p refs (Grant NAG3-475)
(NASA-CR-176186; NAS 1.26:176186; TR-85-8) Avail: NTIS HC A04/MF A01 CSCL 20N

The normal modes in an overmoded waveguide coated with a lossy material are analyzed, particularly for their attenuation properties as a function of coating material, layer thickness, and frequency. When the coating material is not too lossy, the low-order modes are highly attenuated even with a thin layer of coating. This coated guide serves as a mode suppressor of the low-order modes, which can be particularly useful for reducing the radar cross section (RCS) of a cavity structure such as a jet inlet. When the coating material is very lossy, low-order modes fall into two distinct groups: highly and lowly attenuated modes. However, as a/lambda (a = radius of the cylinder; lambda = the free-space wavelength) increases, the separation between these two groups becomes less distinctive. The attenuation constants of most of the low-order modes become small, and decrease as a function of lambda sup 2/a sup 3. Author

N85-35321*# Case Western Reserve Univ., Cleveland, Ohio. Dept. of Electrical Engineering and Applied Physics.
PERTURBATION-ITERATION THEORY FOR ANALYZING MICROWAVE STRIPLINES
Brian E. Kretch Sep. 1985 137 p refs
(Grant NCC3-29)
(NASA-CR-176189; NAS 1.26:176189; WGR-85-5) Avail: NTIS HC A07/MF A01 CSCL 20N

A perturbation-iteration technique is presented for determining the propagation constant and characteristic impedance of an unshielded microstrip transmission line. The method converges to the correct solution with a few iterations at each frequency and is equivalent to a full wave analysis. The perturbation-iteration method gives a direct solution for the propagation constant without having to find the roots of a transcendental dispersion equation. The theory is presented in detail along with numerical results for the effective dielectric constant and characteristic impedance for a wide range of substrate dielectric constants, stripline dimensions, and frequencies. Author

N85-35322*# Jet Propulsion Lab., California Inst. of Tech., Pasadena.
MICROWAVE PROPERTIES OF A QUIET SEA
Joe Stacey 15 May 1985 74 p refs
(Contract NAS7-918)
(NASA-CR-176199; NAS 1.26:176199; JPL-Pub-85-33) Avail:

NTIS HC A04/MF A01 CSCL 20N

The microwave flux responses of a quiet sea are observed at five microwave frequencies and with both horizontal and vertical polarizations at each frequency--a simultaneous 10 channel receiving system. The measurements are taken from Earth orbit with an articulating antenna. The 10 channel responses are taken simultaneously since they share a common articulating collector with a multifrequency feed. The plotted flux responses show: (1) the effects of the relative, on-axis-gain of the collecting aperture for each frequency; (2) the effects of polarization rotation in the output responses of the receive when the collecting aperture mechanically rotates about a feed that is fixed; (3) the difference between the flux magnitudes for the horizontal and vertical channels, at each of the five frequencies, and for each pointing position, over a 44 degree scan angle; and (4) the RMS value of the clutter--as reckoned over the interval of a full swath for each of the 10 channels. The clutter is derived from the standard error of estimate of the plotted swath response for each channel. The expected value of the background temperature is computed for each of the three quiet seas. The background temperature includes contributions from the cosmic background, the downwelling path, the sea surface, and the upwelling path. Author

N85-35323*# Jet Propulsion Lab., California Inst. of Tech., Pasadena.

A NEW DESCRIPTION OF COMBINED TRELLIS CODING WITH ASYMMETRIC MODULATION

M. K. Simon 15 Jul. 1985 34 p refs

(Contract NAS7-918)

(NASA-CR-176197; NAS 1.26:176197; JPL-Pub-85-45) Avail: NTIS HC A03/MF A01 CSCL 17B

The combination of rate k/(k+t) trellis codes with digital modulations described by an asymmetric 2 sup k+1-point signal constellation has been recently shown to yield performance improvement over the traditional symmetric constellation combined with the same trellis code. The approach taken is to specify an underlying trellis code and then map the output code symbols into the fixed signal constellation based on a rule called mapping by set partitioning. The latter process is tantamount to assigning signals from the constellation to the trellis code transitions so as to maximize the free Euclidean distance of the code. Recently, a new description of trellis codes has been given that combines the above two steps into one. The ideas introduced are further explored, placing particular emphasis on the optimization of the signal constellation asymmetry. It can be concluded that the trellis-coded amplitude modulation (AM) designs given are very close to being optimum. Author

N85-35324*# Jet Propulsion Lab., California Inst. of Tech., Pasadena.

DMSK: A PRACTICAL 2400-BPS RECEIVER FOR THE MOBILE SATELLITE SERVICE: AN MSAT-X REPORT

Faramaz Davarian, Marvin K. Simon, and Joe Sumida 15 Jun. 1985 42 p refs

(Contract NAS7-918)

(NASA-CR-176194; NAS 1.26:176194; JPL-Pub-85-51) Avail: NTIS HC A03/MF A01 CSCL 17B

The partical aspects of a 2400-bps differential detection minimum-shift-keying (DMSK) receiver are investigated. Fundamental issues relating to hardware precision, Doppler shift, fading, and frequency offset are examined, and it is concluded that the receiver's implementation at baseband is more advantageous both in cost and simplicity than its IF implementation. The DMSK receiver has been fabricated and tested under simulated mobile satellite environment conditions. The measured receiver performance in the presence of anomalies pertinent to the link is presented in this report. Furthermore, the receiver behavior in a band-limited channel (GMSK) is also investigated. The DMSK receiver performs substantially better than a coherent minimum-shift-keying (MSK) receiver in a heavily fading environment. The DMSK radio is simple and robust, and results in a lower error floor than its coherent counterpart. Moreover, this receiver is suitable for burst-type signals, and its recovery from deep fades is fast. Author

N85-35325*# Jet Propulsion Lab., California Inst. of Tech., Pasadena.

SECOND-GENERATION MOBILE SATELLITE SYSTEM. A CONCEPTUAL DESIGN AND TRADE-OFF STUDY

M. K. Sue and Y. H. Park 1 Jun. 1985 502 p refs

(Contract NAS7-918)

(NASA-CR-176195; NAS 1.26:176195) Avail: NTIS HC A22/MF A01 CSCL 17B

In recent years, interest has grown in the mobile satellite (MSAT) system, a satellite-based communications system capable of providing integrated voice and data services to a large number of users. To explore the potential of a commercial mobile satellite system (MSS) beyond the horizon of the first generation, using technologies of the 1990's and to assist MSAT-X in directing its efforts, a conceptual design has been performed for a second-generation system to be launched around the mid-1990's. The design goal is to maximize the number of satellite channels and/or minimize the overall life-cycle cost, subject to the constraint of utilizing a commercial satellite bus with minimum modifications. To provide an optimal design, a series of trade-offs are performed, including antenna sizing, feed configurations, and interference analysis. Interference is a serious problem for MSAT and often an overlapping feed design is required to reduce interbeam interference. The trade-off studies will show that a simple non-overlapping feed is sufficient for the second-generation system, thus avoiding the need for the complicated beam-forming network that is associated with the overlapping feed designs. In addition, a system that operates at L-band, an alternative frequency band that is being considered by some for possible MSAT applications, is also presented. B.W.

N85-35326# Syracuse Univ., N. Y. Dept. of Electrical and Computer Engineering.

CHARACTERISTIC MODES FOR SLOTS IN A GROUND PLANE TE CASE

K. Y. Kabalan, R. F. Harrington, H. A. Auda, and J. R. Mautz May 1985 83 p

(Contract N00014-85-K-0082)

(AD-A155757; SYRU/DECE/TR-85/1) Avail: NTIS HC A05/MF A01 CSCL 20/14

Consider an infinitely long slot in a ground plane in an unbounded medium illuminated by a uniform TE (to the slot axis) plane wave. The theory of characteristic modes for slots is applied for solution of the problem. The characteristic currents and fields, as well as the equivalent magnetic current, transmission coefficient, and transmitted field pattern, of the slot are computed for different slot widths. Analytic expressions for the special case of a narrow slow are also given. Author (GRA)

N85-35327# Army Missile Command, Redstone Arsenal, Ala. Test and Evaluation Directorate.

ACTUATOR RIGGING TEST SET ELECTROMAGNETIC INTERFERENCE TEST (CE03)

B. Hooks Apr. 1985 27 p

(AD-A155819; AD-E950713; AMSMI/RT-85-7-TR) Avail: NTIS HC A03/MF A01 CSCL 13/7

The results of electromagnetic interference tests to MIL-STD-461 requirements are presented for the Actuator Rigging Test Set for the B1 Bomber. Test techniques and results for procedure CE03 are presented. This test was performed for Metric Systems. Author (GRA)

N85-35328# Illinois Univ., Urbana. Electromagnetic Communication Lab.

AN EXPERIMENTAL STUDY OF DIELECTRIC ROD ANTENNAS FOR MILLIMETER-WAVE IMAGING APPLICATIONS

S. H. Doran and R. Mittra Mar. 1985 24 p

(Contract DAAG29-82-K-0084)

(AD-A155832; EC-85-3; UILU-ENG-85-2543; ARO-18054.14-EL) Avail: NTIS HC A02/MF A01 CSCL 09/5

In this report, the results of an experimental investigation of dielectric antennas for application in an imaging radar at millimeter wavelengths are presented. Several designs for the antenna were

tested for use at 81 or 220 GHz and critical design features for these antennas were studied. A simple design for an imaging radar using dielectric antennas was also implemented and field maps were obtained for a series of simple test objects. GRA

N85-35329# Scientific Research Center, Los Angeles, Calif.
FEASIBILITY STUDY OF RADAR-TRANSMITTING MATERIALS Final Technical Report
M. Sparks 15 Mar. 1985 58 p
(Contract N00019-84-C-0356)
(AD-A155839; RNASCHQ8401) Avail: NTIS HC A04/MF A01 CSCL 20/14

It is shown that it is unlikely that the principles that were originally identified for investigation in this study can be used to obtain a practical material having high microwave transmittance. Electron plasmas in solids are too highly damped at room temperature to give high transmittance. Low-frequency phonon modes conceivably could have frequencies in the microwave region, but the frequency at which the refractive index is equal to one would still be in the infrared region, not the microwave region. After the research on the program was completed, it was suggested that the possibility of attaining high microwave transmittance in ionic conductors should be considered. Although there was no time for such a study, a brief investigation indicated that some ionic conductors possibly could be able to provide high microwave transmittance. They should be studied further. Author (GRA)

N85-35330# Naval Weapons Center, China Lake, Calif.
A PLANAR VERSION OF A 4.0 GIGAHERTZ REACTIVELY STEERED ADAPTIVE ARRAY Interim Report
R. J. Dinger Mar. 1985 23 p
(AD-A156029; AD-E900451; NWC-TP-6621) Avail: NTIS HC A02/MF A01 CSCL 09/1

A planar (two-dimensional) reactively steered adaptive array which includes a single active microstrip element and eight closely coupled parasitic strip elements were designed and tested. Steering of a null towards a single incident jammer is accomplished by adaptive control of reactive terminations on the parasitic elements using a guided random search algorithm. The planar array can steer a null in both the elevation and azimuth directions with a depth of 30 decibels. GRA

N85-35331# National Telecommunications and Information Administration, Boulder, Colo.
MILLIMETER-WAVE PROPAGATION IN MOIST AIR: MODEL VERSUS PATH DATA
H. J. Liebe, K. C. Allen, G. R. Hand, R. H. Espeland, and E. J. Violette Mar. 1985 48 p
(Contract MIPR-ARO-111-85)
(AD-A156040; NTIA-85-171; ARO-21677.1-GS) Avail: NTIS HC A03/MF A01 CSCL 04/1

A practical atmospheric millimeter-wave propagation model (MPM) is updated and tested with experimental data from horizontal, line-of-sight links when there is no precipitation. The MPM computer program predicts attenuation and delay properties of moist air over ranges in frequency from 1 to 1000 GHz and in height from 0 to 30 km. Input variables are radio path distributions of pressure, temperature, relative humidity, and a suspended droplet concentration simulating haze and fog conditions. Terrestrial path data from millimeter-wave propagation experiments, including those from a 27 km link operated at 11.4, 28.8, and 96.1 GHz by the Institute for Telecommunication Sciences (ITS), have been analyzed. Calibrated mean signal levels permitted studies of water vapor losses. In addition, a spectral analysis was performed of clear-air scintillations caused by turbulence. In general, good agreement is obtained with the MPM for test frequencies up to 430 GHz. Author (GRA)

N85-35332# Massachusetts Inst. of Tech., Cambridge. Lab. for Information and Decision Systems.
COMMUNICATION COMPLEXITY OF DISTRIBUTED SHORTEST PATH ALGORITHMS
B. Awerbuch and R. G. Gallager Jun. 1985 34 p
(Contract N00014-84-K-0357; DARPA Order 3045)
(AD-A156049; LIDS-P-1473) Avail: NTIS HC A03/MF A01 CSCL 17/2

A new distributed shortest path algorithm for an asynchronous communication network with unit edges, of the number of elementary messages used in finding shortest paths form a given root to all other nodes is $0(V1.6+E)$ where V is the number of nodes and E the number of edges. For dense networks, with $E > \text{or} = V$ to 1.6 power, this order of complexity is optimum. Author (GRA)

N85-35333# Air Force Geophysics Lab., Hanscom AFB, Mass.
A MULTI-CHANNEL RADAR RECEIVER Instrumentation Papers
A. W. Bishop and J. I. Metcalf 7 Jan. 1985 16 p
(AD-A156058; AFGL-TR-85-0006; AFGL-IP-328) Avail: NTIS HC A02/MF A01 CSCL 17/9

A radar receiver design is presented that yields logarithmic and coherent signals of two orthogonal polarizations derived from each of two S-band transmitted frequencies. The radar is to be used for measuring Doppler velocity and polarization parameters of meteorological backscatter. The receiver design goals include phase and amplitude balance of 5 degrees and 0.5 dB between signals of opposite polarization. The logarithmic amplifiers are specified to have linearity of + or - 0.5 dB over a dynamic range of 90 dB. High-power ferrite switching devices are to be used to alternate the polarization of transmitted signals between orthogonal states on a pulse-to-pulse basis and to permit reception of co-polarized and cross-polarized signal components. GRA

N85-35334# Georgia Tech Research Inst., Atlanta.
POLARIZATION DIVERSITY ADDITION TO THE 10 CENTIMETER DOPPLER WEATHER RADAR Final Report, 1 Apr. 1982 - 31 Jul. 1984
J. S. Ussailis and H. L. Bassett Aug. 1984 81 p
(Contract F19628-82-K-0038)
(AD-A156062; A-3226; AFGL-TR-84-0239) Avail: NTIS HC A05/MF A01 CSCL 17/9

The research performed was that of providing antenna modifications for a polarization diversity addition to the; AFGL 10 centimeter DOPPLER WEATHER RADAR. Described within are the ANTENNA FEED DESIGN (POTTER HORN), the conversion of the antenna form a prime focus to a Cassegrain Configuration, the results of the feed horn RF measurements, the construction of the POLARIZER ASSEMBLY, and the installation and testing of the antenna system. GRA

N85-35335# Syracuse Univ., N. Y. Dept. of Electrical and Computer Engineering.
SIGNAL SPACE MODELS FOR ANTENNA ARRAYS Final Technical Report, Oct. 1983 - Sep. 1984
S. S. Sandler Griffiss AFB, N.Y. RADC Apr. 1985 23 p
(Contract F30602-81-C-0169)
(AD-A156063; RADC-TR-85-50) Avail: NTIS HC A02/MF A01 CSCL 06/4

Some concepts in retinal vision are related here to the area of antennas and antenna arrays. In particular, the principles of insect motion detection based on visual cues have been applied to time-domain radar analysis. Using an example in which simple specular scattering applies, relative velocities are shown to be directly calculable in the case of short temporal pulse radar from phase-independent information for either a moving radar or a moving target. GRA

N85-35336# Air Force Geophysics Lab., Hanscom AFB, Mass.
A RAY TRACE PROGRAM FOR LINE-OF-SIGHT MICROWAVE COMMUNICATION LINKS
J. F. Morrissey 18 Oct. 1984 21 p
(AD-A156168; AD-E440284; AFGL-TR-84-0293; AFGL-ERP-893) Avail: NTIS HC A02/MF A01 CSCL 17/2

A ray trace program tailored to Line-of-Sight (LOS) communication links is described. The principal products of the program are the following: (1) a ray trace diagram, (2) a time of arrival plot,

and (3) an angle of arrival plot. The ray trace allows for a complex terrain, multiple meteorological profiles, and has options for the type of reflection to be used. GRA

N85-35337# SRI International Corp., Menlo Park, Calif.
INTERPROCESS COMMUNICATION Final Report
L. Lamport 11 Jun. 1985 47 p
(Contract N00014-84-C-0621)
(AD-A156337) Avail: NTIS HC A03/MF A01 CSCL 17/2

Interprocess communication is studied without assuming any lower-level communication primitives. Three classes of communication registers are considered, and several constructions are given for implementing one class of register with a weaker class. A formalism is developed for reasoning about concurrent systems that does not assume an atomic grain of action. GRA

N85-35338# Sandia Labs., Albuquerque, N. Mex.
MOMENT-METHOD FORMULATION OF THE CAVITY-PROBE APERTURE ANTENNA
J. M. Jarem Aug. 1958 61 p
(Contract DE-AC04-76DP-00789)
(DE85-013264; SAND-85-0132) Avail: NTIS HC A04/MF A01

The electromagnetic moment method formulation which is used to determine the fields in a cavity probe aperture ground plane antenna is presented. The formulation consists of the submatrix equations which describe the aperture fields and the probe currents. The aperture submatrix is derived using reaction matching and K space theory, and the probe equations are derived using pulse and modal function expansions. A numerical example of the probe solution, indications of how to couple the probe and aperture fields, and complete listing of the cavity Green's functions are given. DOE

N85-35339# Technische Hogeschool, Eindhoven (Netherlands).
MICROWAVE PROPAGATION STUDIES, MEASUREMENTS AND EDUCATION IN SURABAYA, INDONESIA Final Report
J. Dijk (ed.), I. V. Bruza (ed.), L. J. M. Wijdemans (ed.), H. J. J. Cuppen, R. J. Deenen, P. F. Maartense, A. A. J. Otten, Aries Purnomo, Prawiro Sugondo, F. J. M. Vincent et al 1983 385 p refs Sponsored by Netherlands Univ. Foundation for International Cooperation and Indonesian Post and Telecommunications Prepared in cooperation with Surabaya Inst. of Tech., Indonesia
(B8464633; ISBN-90-6144-999-5) Avail: NTIS HC A17/MF A01

A Netherlands-Indonesia development/cooperation project in telecommunication is described. A microwave line-of-sight link Gunung Sandangan - Surabaya and a troposcatter link Situbondo - Surabaya were realized. Measurements at 4 and 7 GHz line-of-sight and 4 GHz troposcatter (main and crosspolar components) were made and meteorological satellite signals were revieved. Seasonal atmospherical influences were investigated. A microwave laboratory, mechanical and electronics workshops, a meteorological station, and an electrical engineering and electronics basic library were set up. Author (ESA)

N85-35340# National Telecommunications and Information Administration, Annapolis, Md.
NECESSARY BANDWIDTH AND SPECTRAL PROPERTIES OF DIGITAL MODULATION
D. J. Cohen Feb. 1985 62 p refs
(PB85-185387; NTIA-84-168) Avail: NTIS HC A04/MF A01 CSCL 17B

The National Telecommunications and Information Administration (NTIA) and the Interdepartment Radio Advisory Committee (IRAC) require, for their management of the spectrum, technical guidance concerning the necessary bandwidth and spectral characteristics of digital modulation. The necessary bandwidth is the minimum emission bandwidth required for an acceptable quality of service. The concept of necessary bandwidth is applied to digital modulation. The necessary bandwidths for several digital modulations are considered in detail. These are phase shift keying (PSK), minimum shift keying (MSK), and frequency shift keying (FSK). The techniques used to determine the necessary bandwidths are general and could be extended to other digital modulations. For digital modulation systems, the necessary bandwidth signal power, and bit error rate are all interrelated and tradeoffs among these factors are possible. Author (GRA)

N85-35481# Swedish Telecommunications Administration, Farsta. Radio Div.
TELEVISION INTERFERENCE MEASUREMENT AT KALKUGNEN (SWEDEN) TEST WINDMILL
Ulf Tegth *In* Kernforschungsanlage Implementing Agreement for Cooperation in the Develop. of Large Scale Wind Energy Conversion Systems Nov. 1984 p 97-104 refs (For primary document see N85-35473 24-44)
Avail: NTIS HC A11/MF A01

33 ELECTRONICS AND ELECTRICAL ENGINEERING

Includes test equipment and maintainability; components, e.g., tunnel diodes and transistors; microminiaturization; and integrated circuitry.

For related information see also *60 Computer Operations and Hardware* and *76 Solid-State Physics.*

N85-35341 North Carolina State Univ., Raleigh.
TWO-DIMENSIONAL NUMERICAL MODELING OF ION IMPLANTED GaAs MESFET DEVICES Ph.D. Thesis
Mustafa Fituri Abusaid 1984 196 p
Avail: Univ. Microfilms Order No. DA8506969

The purpose is to investigate the two-dimensional, numerical modeling of experimental ion-implanted MESFETs using a conventional finite difference approach and static velocity-field characteristics. In the numerical model, different velocity-field relationships and velocity-field data generated from Monte Carlo calculations were used. Electron traps were included in the basic numerical model. Calculated I sub ds-V sub ds transfer characteristics of a MESFET device are compared with experimental data to investigate the effects of using various velocity models, various trap densities, and different impurity profiles on the over-all I-V characteristics. In addition, numerical calculations have been made of I sub ds-V sub ds characteristics and of small signal parameters for several applied drain and gate voltages. These calculations have been carried out for two devices having different impurity profiles and for different velocity models. In each case the calculations were done with and without traps included. Improvements in the cut-off frequency of GaAs MESFET devices by modification of device geometries such as contact spacing and channel length were studied. Dissert. Abstr.

N85-35342*# Illinois Univ., Urbana. Electromagnetic Communication Lab.
CHARACTERIZATION OF MICROSTRIP DISCONTINUITIES IN THE TIME AND FREQUENCY DOMAINS
U. Feldman and R. Mittra Sep. 1985 49 p refs
(Grant NCC3-38)
(NASA-CR-176190; NAS 1.26:176190; UILU-ENG-85-2565; Rept-85-6) Avail: NTIS HC A03/MF A01 CSCL 09C

A number of impedance transitions and interconnections to a microstrip were designed and investigated. The double-step discontinuity on a microstrip was studied in detail, and a procedure was developed to design these structures. Their response was determined by making measurements in both the frequency and time domains in a consistent and repeatable manner. The time-domain presentation of the data was the most useful feature of the measuring system. All undesirable signal components were filtered out through the use of gating functions. Theoretically computed results were verified experimentally. Author

N85-35343*# Carnegie-Mellon Univ., Pittsburgh, Pa. Dept. of Electrical and Computer Engineering.
ADVANCED DETECTORS AND SIGNAL PROCESSING Final Report

D. W. Greve, P. H. L. Rasky, and M. H. Kryder 1985 28 p refs (Grant NAG1-395)
(NASA-CR-176193; NAS 1.26:176193) Avail: NTIS HC A03/MF A01 CSCL 09C

Continued progress is reported toward development of a silicon on garnet technology which would allow fabrication of advanced detection and signal processing circuits on bubble memories. The first integrated detectors and propagation patterns have been designed and incorporated on a new mask set. In addition, annealing studies on spacer layers are performed. Based on those studies, a new double layer spacer is proposed which should reduce contamination of the silicon originating in the substrate. Finally, the magnetic sensitivity of uncontaminated detectors from the last lot of wafers is measured. The measured sensitivity is lower than anticipated but still higher than present magnetoresistive detectors. Author

N85-35344# Institut Franco-Allemand de Recherches, St. Louis (France).
MATERIALS USED BY INDUSTRY FOR THE PRODUCTION OF PIEZOELECTRIC TRANSDUCERS. THE STATE OF THE ART OF RESEARCH WORK PERFORMED IN THE FIELD OF PZT CERAMICS AND FERROELECTRIC POLYMERS
Francois Bauer, Lucien Eyraud (Inst. National des Sciences Appliquees de Lyon, Villeurban, France), and Paul Eyraud (Inst. National des Sciences Appliquees de Lyon, Villeurban, France) 25 Jun. 1984 41 p refs Presented at 86th Am. Ceramic Soc. Ann. Meeting, Pittsburgh, 29 Apr.-3 May 1984 and 107th Acoust. Soc. of Am. Meeting, Norfolk, Va., 7-10 May 1984
(ISL-CO-211/84) Avail: NTIS HC A03/MF A01

Research into piezoelectric transducers, conduction and aging of piezoelectric PZT ceramics, and ferroelectric homopolymer PVF2 and P (VDF-TrFe) copolymers are discussed. For individual titles, see N85-35345 through N85-35347.

N85-35345# Institut Franco-Allemand de Recherches, St. Louis (France).
PIEZOELECTRIC TRANSDUCERS, STATE OF RESEARCH
Lucien Eyraud, Paul Eyraud, and Francois Bauer *In its* Mater. Used by Ind. for the Production of Piezoelec. Transducers. The State of the Art of Res. Work Performed in the Field of PZT Ceramics and Ferroelec. Polymers 25 Jun. 1984 p 3-11 refs (For primary document see N85-35344 24-33)
Avail: NTIS HC A03/MF A01

Methods for preparing, treating and sintering powders to be used in the production of ceramic elements (coprecipitation, isostatic compression, sintering under shock loading) are reviewed. Faults inherent in a piezoelectric ceramic element are outlined. Perovskite type compounds, analogous to PbTiO3, which are strongly anisotropic and have a very low k31 coupling factor; lead compounds which are strongly anisotropic and give strongly attenuated ceramic elements; PVDF type polymers; electrostrictive materials; composite materials; and polar glass materials and electrets are described. Techniques for metallizing elements to improve the adhesive power of the electrodes and contacts; and adhesives and glues used for manufacturing transducers and composites are considered. Author (ESA)

N85-35346# Institut Franco-Allemand de Recherches, St. Louis (France).
CONDUCTION AND AGING OF PIEZOELECTRIC PZT CERAMICS
Lucien Eyraud, Paul Eyraud, and Francois Bauer *In its* Mater. Used by Ind. for the Production of Piezoelec. Transducers. The State of the Art of Res. Work Performed in the Field of PZT Ceramics and Ferroelec. Polymers 25 Jun. 1984 p 12-24 refs (For primary document see N85-35344 24-33)
Avail: NTIS HC A03/MF A01

In order to lower the electrical conductivity and increase resistance to aging of piezoelectric PZT ceramics, solid solutions containing as few vacancies as possible were made. The usual dry process through reaction between solids was unsuitable owing to the volatility of lead oxide at the high temperatures of reaction (900 C) and of sintering (1300 C) but using a coprecipitation method all the cations initially brought in the process are present in the final solid. A model of a superstructure polarizable through electron transfer between cationic sites suffices to justify the space charge compensation in polarized ceramics, and therefore the stability of these ferroelectrics. A lead vacancy should also induce the creation of a Pb4(+) ion, but here both vacancy and Pb4(+) ion can move under stress, which decreases the stability of polarization phases. Author (ESA)

N85-35347# Institut Franco-Allemand de Recherches, St. Louis (France).
FERROELECTRIC HOMOPOLYMER PVF2 AND P (VDF-TrFe) COPOLYMERS
Francois Bauer and Lucien Eyraud *In its* Mater. Used by Ind. for the Production of Piezoelec. Transducers. The State of the Art of Res. Work Performed in the Field of PZT Ceramics and Ferroelec. Polymers 25 Jun. 1984 p 25-40 refs (For primary document see N85-35344 24-33)
Avail: NTIS HC A03/MF A01

The ferroelectric and piezoelectric properties of PVF2 polymer are summarized. The physical properties of PVDF piezoelectric film are given. Polarization of PVF2 is described. Ferroelectric polarization of VF2/C2F3H copolymers; influence of X rays on PVF2 elements; and the effects of uniaxial compression on the piezoelectric activity of PVF2 are discussed. The performance of PVF2 transducers is compared with PZT transducers. The maximum energy input achieved in PVF2 is 10 times in excess of the energy input attainable in a PZT ceramic in which the coefficiency of electromechanical conversion is 10 times higher. Considering that for PVF2 acoustic matching to propagating media is better than for PZT and that polymer properties (easy handling, surface, thickness, lightness , random shapes) are important, it is suggested that PVF2 can fill the gaps left by PZT in loudspeakers and earphones, hydrophones, and probes used for echography.
Author (ESA)

N85-35348# Naval Surface Weapons Center, White Oak, Md.
ANALOG, STILL WITHOUT FEAR Final Report
A. D. Delagrange 1 Sep. 1984 38 p
(AD-A155920; NSWC/TR-84-360) Avail: NTIS HC A03/MF A01 CSCL 09/5

This report is an update of one issued in 1977 which predicted that the predicted death of analog circuitry (also called linear) would not occur; in fact, the patient appeared remarkably healthy. The report proved correct. We have the same situation again today: the same predictions and counter-prediction. Each year brings significant advances in the field of analog integrated circuitry. Many of the traditional arguments against analog circuitry are no longer valid. This report attempts to summarize what is available now, and what can (and cannot) be done with analog integrated circuits. It defines analog and makes some comparisons with digital. The most common types of analog integrated circuits are then listed and discussed. Lastly, some design and trouble-shooting hints are given, and the state-of-the-art is discussed.
Author (GRA)

N85-35349# Naval Postgraduate School, Monterey, Calif.
COMPUTER SIMULATION OF A CRUISE MISSILE USING BRUSHLESS dc MOTOR FIN CONTROL M.S. Thesis
G. C. Franklin Mar. 1985 61 p
(AD-A155935) Avail: NTIS HC A04/MF A01 CSCL 09/5

This thesis describes a computer simulation developed in order to provide a method of establishing the potential of brushless dc motors for applications to tactical cruise missile control surface positioning. In particular, an altitude hold controller has been developed that provides an operational load test condition for the evaluation of the electromechanical actuator. A proportional integral control scheme in conjunction with tachometer feedback provides the position control for the missile tailfin surfaces. The fin control system is further imbedded in a cruise missile model to allow altitude control of the missile. The load on the fin is developed from the dynamic fluid environment that the

missile will be operating in and is proportional to such factors as fin size and air density. The program written in CSMP language is suitable for parametric studies including motor and torque load characteristics, and missile and control system parameters. GRA

N85-35350# Hazeltine Corp., Greenlawn, N. Y.
CYLINDRICAL LENS-ARRAY ANTENNA FOR WIDEBAND ELECTRONIC SCANNING Final Report, Oct. 1981 - Jun. 1984
E. M. Newman and C. M. Ruskowski Griffiss AFB, N.Y. RADC Mar. 1985 165 p
(Contract F19628-80-C-0110)
(AD-A156085; Rept-6546; RADC-TR-84-225) Avail: NTIS HC A08/MF A01 CSCL 09/5

This report describes the fabrication and testing of a lens antenna that is designed to have wideband scanning capabilities for wide angle scanning in any plane. The lens has a 30 by 40 wavelength aperture. Far field patterns were measured in both azimuth and elevation planes over and eleven percent bandwidth. The azimuth scan angles were 0 deg, 15 deg, 30 deg and 45 deg and the elevation angles 0 deg and 15 deg. The quality of the patterns is fairly good with the average power level from + 50 deg to - 50 deg close to 44 dB in the sidelobe region (excluding the 7 or 8 close in sidelobes). These lobes have peak values about 30 dB. Author (GRA)

N85-35351# Aerospace Corp., El Segundo, Calif. Engineering Group.
A METHODOLOGY FOR THE DESIGN OF TESTABLE CUSTOM LARGE-SCALE INTEGRATED CIRCUITS Final Report, 1 Jan. 1983 - 30 Jul. 1984
31 Jan. 1985 69 p
(Contract F04701-83-C-0084)
(AD-A156098; TR-0084A(5902-04)-1; SD-TR-85-33) Avail: NTIS HC A04/MF A01 CSCL 09/5

This report summarizes the main concepts in the design for testability of custom large-scale integrated circuits (CLSICs) and concepts involved in testing for physical faults in actual hardware. Important problems and issues which should be considered in designing a testable CLSIC, including test structures and design style, test strategies, test strategy measures, and testable design methodologies are introduced. A general methodology for designing a testable CLSIC is presented, which includes partitioning a chip into circuit structures, and imbedding each circuit structure into a suitable testable design structure. Measures are introduced so that different test methodologies can be quantitatively compared. Author (GRA)

N85-35352# Naval Postgraduate School, Monterey, Calif.
CERENKOV RADIATION FROM PERIODIC ELECTRON BUNCHES FOR FINITE EMISSION LENGTH IN AIR M.S. Thesis
V. Milorad Dec. 1984 117 p
(AD-A156156) Avail: NTIS HC A06/MF A01 CSCL 20/3

The physical mechanism of Cerenkov radiation in air caused by the periodic electron bunches is presented here in a simplified and exact mathematical form, as well as some applications and evidence. The experiment is an effort to verify the theoretical prediction of the power increase and fall off with discrete harmonic frequency in the microwave region. The radiation diagrams and absolute power measurements in the far field for the first four harmonics are provided by the improvements such as: frequency selection by the YIG filter, power amplification by the TWT amplifiers, high sensitivity of the signal detection by the oscilloscope vertical differential amplifier along with the noise reduction and radiation shielding is presented. The suggested experimental method may be expanded to the higher harmonics with appropriate equipment. The experimental data reveals the unexpected spikes in the radiation diagrams. The absolute power results reasonably to the theoretical ones. The experimental method closely satisfies this Cerenkov experiment and may be improved. Further research may provide usable information for the electron beam monitoring or Cerenkov source at higher micorwave frequencies, for which a certain interest exists. Author (GRA)

N85-35353# Science Applications International Corp., Boulder, Colo. Plasma Research Inst.
RF STABILIZATION OF INTERCHANGE-BALLOONING MODES
J. R. Myra and D. A. Dippolito Apr. 1985 13 p refs
(Contract DE-AC03-76ET-53057)
(DE85-012080; SAIC-85/1676-PRI-91) Avail: NTIS HC A02/MF A01

A fully electromagnetic theory describing the interaction of radio frequency waves with low frequency curvature driven modes in mirror geometry is presented. The theory includes the direct ponderomotive force terms and sideband mode coupling on an equal footing. Tandem mirror stabilization and experiments are discussed and the further measurements that would enable a more definitive comparison of theory and experiment are emphasized. DOE

N85-35354# Sandia Labs., Albuquerque, N. Mex.
STATISTICAL DISTRIBUTION OF BREAKDOWN VOLTAGES IN REP-RATE SPARK GAPS
L. F. Rinehart and M. T. Buttram 1985 16 p Presented at the 5th IEEE Pulsed Power Conf., Washington, D.C., 10 Jun. 1985
(Contract DE-AC04-76DP-00789)
(DE85-012813; SAND-84-2578C; CONF-850616-6) Avail: NTIS HC A02/MF A01

The correlation of various breakdown voltage distributions with conditions in a rep-rated spark gap is shown. This study is extended to include effects of a wider range of rep-rates (up to 120 pps), electrode-gas combinations (brass with SF6 and argon), and gas temperature. The behavior of some of the distributions in terms of basic gas breakdown processes is explained. DOE

N85-35355# Sandia Labs., Albuquerque, N. Mex.
INJECTOR LOSSES ON MITE
H. N. Woodall and R. W. Stinnett 1985 16 p Presented at the 5th IEEE Pulsed Power Conf., Washington, D.C., 10 Jun. 1985
(Contract DE-AC04-76DP-00789)
(DE85-012356; SAND-84-2458C; CONF-850616-4) Avail: NTIS HC A02/MF A01

One of the most critical areas in a magnetically-insulated power feed is the injector section. In this portion of the feed, the electric field at the cathode becomes sufficient to cause cathode plasma formation and electron flow in the gap. We have used Faraday cups and filtered 4-chlorostyrene monitors to measure losses in this initial portion of the Mite (2 MV, 4.8 ohm) magnetically-insulated transmission line. Electron losses in the injector are measurable and last through most of the pulse. The propagation of the magnetic insulation wave through the injector region is slower in the injector region (approx..4c) than in the rest of the line (approx..6c). These experiments were performed using both carbon-coated and bead-blasted aluminum surfaces. DOE

N85-35356# Stanford Linear Accelerator Center, Calif.
SOLID STATE HIGH POWER AMPLIFIER FOR DRIVING THE SLC INJECTOR KLYSTRON
J. G. Judkins, J. E. Clendenin, and H. D. Schwarz Mar. 1985 3 p refs Presented at the Particle Accelerator Conf., Vancouver, British Columbia, 13 May 1985
(Contract DE-AC03-76SF-00515)
(DE85-013063; SU-SLAC-PUB-3610; CONF-850504-127) Avail: NTIS HC A02/MF A01

The SLC injector klystron RF drive is now provided by a recently developed solid-state amplifier. The high gain of the amplifier permits the use of a fast low-power electronic phase shifter. Thus the SLC computer control system can be used to shift the phase of the high-power RF rapidly during the fill time of the injector accelerator section. These rapid phase shifts are used to introduce a phase-energy relationship in the accelerated electron pulse in conjunction with the operation of the injection bunch compressor. The amplifier, the method of controlling the RF phase, and the operational characteristics of the system are described. DOE

N85-35357# Sandia Labs., Albuquerque, N. Mex.
DEVELOPMENT AND EVALUATION OF SULFONATED POLYSULFONE MEMBRANES FOR THE ZINC-FERRICYANIDE BATTERY
C. Arnold, Jr. and R. A. Assink 1985 22 p refs Presented at the Spring Natl. Meeting of AIChE, Houston, Tex., 24 Mar. 1985
(Contract DE-AC04-76DP-00789)
(DE85-009104; SAND-85-05080; CONF-850357-7) Avail: NTIS HC A02/MF A01

The successful commercialization of the zinc/ferricyanide battery being developed by Lockheed depends in part on the availability of an inexpensive, chemically stable membrane. Other essential membrane properties include low area resistivity (1 - 5 (UC OMEGA) cm(2)) and a low rate of iron permeation (4 x 10(-5) millimoles Fe(cm (2))h). A cast membrane which contained one sulfonate group per repeating unit in th backbone exhibited good stability in the alkaline ferricyanide electrolyte and satisfied the membrane requirements cited above. In ongoing single cell cycling tests, average energy efficiencies of 77% were achieved over 85 charge discharge cycles with this membrane. If sulfonate polysulfone membranes can be mass produced by extrusion, they can be considered as viable candidates to replace the expensive perfluorsulfonate membranes that were used to demonstrate the technical feasibility of the zinc/ferricyanide battery. The feasibility of preparing composite sulfonated polysulfone membranes by impregnation of microporous PTFE was also demonstrated. The manufacture of composite membranes should be possible using chemical coating equipment. DOE

N85-35358# Brookhaven National Lab., Upton, N. Y.
TUNING SYSTEM FOR CAPACITIVELY LOADED 1/4 ACCELERATING CAVITY
R. B. McKenzie-Wilson 1985 3 p Presented at the Particle Accelerator Conf., Vancouver, British Columbia, 13 May 1985
(Contract DE-AC02-76CH-00016)
(DE85-012516; BNI-36479; CONF-850504-81) Avail: NTIS HC A02/MF A01

The Brookhaven National Laboratory NSLS X-ray and vuv rings currently use capacitively loaded lambda/4 RF accelerating cavities. These cavities are manufactured from copper clad plate steel and require a tuning system with a considerable range. Three separate tuning systems are provided, each having its own specific problems, and interactions occur between the three systems. A single capacitive tuning system is proposed which will vary the capacitance loading of the cavity directly. The system employs a vacuum balance mechanically driven diaphragm. The control system allows 6 mm of motion at a maximum slewing rate of 1.0 mm per sec and yields a dynamic tuning range of 480 kHz. Design and fabrication details are presented together with early testing and operating experience. DOE

N85-35359# Los Alamos Scientific Lab., N. Mex.
SYSTEM EXPECTATIONS FOR PIONEER 1 FOIL IMPLOSION EXPERIMENTS
A. E. Greene, J. H. Brownell, R. S. Caird, D. J. Erickson, J. H. Goforth, I. R. Lindemuth, T. A. Oliphant, and D. L. Weiss 1985 5 p Presented at the 5th IEEE Pulsed Power Conf., Washington, D.C., 10 Jun. 1985
(Contract W-7405-eng-36)
(DE85-014129; LA-UR-85-1994; CONF-850616-55) Avail: NTIS HC A02/MF A01

Prior to the beginning of the Pioneer 1 shot of the Los Alamos National Laboratory TRAIL-MASTER project, numerous computational simulations were run to provide ball-park estimates for the electrical currents and voltages in the circuit, the timing of the implosion, the kinetic energy, temperature, and radiation output of the load. The purpose of these calculations was to provide guidance in setting the timings of the various switches within the circuit and to establish operating ranges for the various diagnostics. DOE

N85-35360# Los Alamos Scientific Lab., N. Mex.
PHOTOCONDUCTIVE PULSE POWER SWITCHES: A REVIEW
W. C. Nunnally 1985 29 p Presented at the 5th IEEE Pulsed Power Conf., Washington, D.C., 10 Jun. 1985
(Contract W-7405-eng-36)
(DE85-014125; LA-UR-85-2014; CONF-850616-65) Avail: NTIS HC A03/MF A01

This paper reviews the state of development and discusses the operational considerations of photoconductive power switch (PCPS) technology that has recently been used to generate very fast rising, high-power pulses. The rationale for using PCPSs is discussed along with the advantages of this type of switch in high-power pulse systems. The operational considerations are discussed, and the resultant operational characteristics that are dependent on the material parameters of several photoconductive materials are presented and compared. Areas for additional research and development of PCPSs are also presented. DOE

N85-35361# Valvo Roehren- und Halbleiterwerke der Philips G.m.b.H., Hamburg (West Germany). Unternehmensbereich Bauelemente.
DEVELOPMENT OF POSITION SENSORS FOR MICROCOMPUTER-ORIENTED SENSOR SYSTEMS Final Report, Dec. 1983
Heinz Sauermann and Uwe Dobbern (Philips G.m.b.H., Hamburg) Bonn Bundesministerium fuer Forschung und Technologie Mar. 1985 72 p refs In GERMAN; ENGLISH summary Sponsored by Bundesministerium fuer Forschung und Technologie
(BMFT-FB-T-85-021; ISSN-0340-7608) Avail: NTIS HC A04/MF A01; Fachinformationszentrum, Karlsruhe, West Germany DM 15

A position sensor using the magnetoresistive effect in ferromagnetic metal thin films was developed. This allows sensors of higher sensitivities than those based on other principles. The range of linearity may be adjusted between 0.9 and 20 kA/m by varying the thin film dimensions. The sensors are linearized by barber poles. It is shown that barber poles made from aluminium are cheaper than those of gold and are more efficient, and sensors are more corrosion resistant. The hard magnetic layer is a thick film layer with a hard ferrite powder, deposited by a spin-on process or by screen printing. This technique is not fully developed. Mounting and encapsulation are similar to those used for transistors, holding costs low. Measurements performed on these sensors show the results expected. Lifetime behavior is like that of other electronic components. Author (ESA)

N85-35362# Technische Hogeschool, Eindhoven (Netherlands). Dept. of Electrical Engineering.
ASPECTS OF INPUT SIGNAL DESIGN FOR ORDER AND PARAMETER ESTIMATION IN LINEAR DYNAMICAL SYSTEMS
Andrzej Krolikowski and Pieter Eykhoff 1983 7 p refs
(ER-83/05) Avail: NTIS HC A02

It is shown that a close relationship between the input signal design and model order estimation procedures (possibly with an expansion to structure determination procedures of multivariable systems) exists in linear dynamical systems. This implies that the input sequence is selected in order to improve the accuracy for the parameter estimates (e.g., in D-optimality or A-optimality sense) and at the same time can make the order tests more powerful. An overall identification algorithm, including the amplitude constrained input sequence design, estimation procedure, and an alternative instrumental determinant ratio test is proposed. Simulation results show that the algorithm works satisfactorily for the relatively short identification horizon. Author (ESA)

N85-35363# National Bureau of Standards, Gaithersburg, Md.
CENTER FOR ELECTRONICS AND ELECTRICAL ENGINEERING TECHNICAL PROGRESS BULLETIN COVERING CENTER PROGRAMS, JULY-SEPTEMBER WITH 1985 CEEE EVENTS CALENDAR
J. F. May-Wells Dec. 1984 25 p
(PB85-191393; NBSIR-84/2877-3) Avail: NTIS HC A02/MF A01 CSCL 09C

This is the eighth issue of a quarterly abstract journal covering the work of the National Bureau of Standards Center for Electronics and Electrical Engineering. This issue of the Center for Electronics

and Electrical Engineering Technical Progress Bulletin covers the third quarter of calendar year 1984. Abstracts are provided by technical area for both published papers and papers approved by NBS for publication. GRA

N85-35364# National Bureau of Standards, Boulder, Colo. Electromagnetic Fields Div.
THEORY OF MUTUAL IMPEDANCES AND MULTIPLE REFLECTIONS IN AN N-ELEMENT ARRAY ENVIRONMENT
L. A. Muth Feb. 1985 36 p refs
(PB85-191419; NBS-TN-1078) Avail: NTIS HC A03/MF A01; also available from SOD as SN003-003-02632-8 CSCL 09E

A general theoretical approach is formulated to describe the complex electromagnetic environment of an N-element array. The theory reveals the element-to-element interactions and multiple reflections within the array. From the formulation, it is found that the interaction between an excited element and an open-circuited element can be viewed as the sum of terms describing all possible signal paths within the array environment which start from the radiating element and terminate on the element under observation. Within all paths except the most direct one, multiple reflections between subgroups of elements take place. The resulting solution is highly structured and recursive and is discussed in detail. Illustrative examples are provided to facilitate understanding of these ideas. Author (GRA)

34 FLUID MECHANICS AND HEAT TRANSFER

Includes boundary layers; hydrodynamics; fluidics; mass transfer; and ablation cooling.

For related information see also *02 Aerodynamics* and *77 Thermodynamics and Statistical Physics.*

N85-35365 Arizona State Univ., Tempe.
HEAT TRANSFER CHARACTERISTICS FOR TWO-DIMENSIONAL ARRAYS OF IMPINGING JETS WITH INITIAL CROSSFLOW Ph.D. Thesis
Chiung-Chieh Jack Su 1984 252 p
Avail: Univ. Microfilms Order No. DA8501324

Two-dimensional arrays of circular air jets impinging on a heat transfer surface parallel to the jet orifice plate are considered. The jet flow, after impingement, is constrained to exit in a single direction along the channel formed by the jet orifice plate and heat transfer surface. In addition to the crossflow that originates from the jets following impingement, an initial crossflow is present that approaches the array through an upstream extension of the channel. The configurations considered are intended to model the impingement cooled midchord region of gas turbine airfoils in cases where an initial crossflow is also present. Spanwise averaged heat fluxes, resolved in the streamwise direction to one streamwise jet hole spacing, referred to as regional average fluxes, were measured for twelve arrays each having a different combination of geometric parameter values (streamwise hole spacing, spanwise hole spacing, and channel height each measured relative to jet hole diameter). Measurements were made over a range of jet flow rates and also for a range of initial crossflow rates relative to jet flow rate.
Dissert. Abstr.

N85-35366 Iowa Univ., Iowa City.
PREDICTION OF TURBULENT INTERNAL RECIRCULATING FLOWS WITH K-EPSILON MODELS Ph.D. Thesis
Sen-Ming Chang 1984 247 p
Avail: Univ. Microfilms Order No. DA8507926

The finite analytic numerical method is incorporated with both the K-epsilon-E (turbulent kinetic energy-dissipation-eddy viscosity) model and the K-epsilon-A (turbulent kinetic energy-dissipation-algebraic stress) model to predict turbulent internal recirculating flows. Three problems are solved, the first problem is turbulent flow in a cavity. Predictions are made for a square cavity with a Reynolds number of 480,000 and a rectangular cavity with an aspect ratio of 3 with a Reynolds number of 200,000. The second problem deals with flow passing through a symmetric backward step having an expansion ratio of 1.5 and a Reynolds number of 200,000. The third problem studys flow separation in front of a flat plate in a confined region. The prediction of these flows is made with the finite analytic method which utilizes the local analytic solution of the governing equation in formulating the approximate algebraic equations. Dissert. Abstr.

N85-35367 North Carolina State Univ., Raleigh.
ANALYTIC SOLUTIONS OF INVERSE HEAT CONDUCTION PROBLEMS Ph.D. Thesis
Najem Mohammad Al-Najem 1984 177 p
Avail: Univ. Microfilms Order No. DA8507348

A direct analytic approach is systematically developed for solving inverse heat conduction problems in multi-dimensional finite regions. The inverse problems involve the determination of the surface conditions from the knowledge of the time variation of the temperature at an interior point in the region. In the present approach, the unknown surface temperature is represented by a polynominal in time and a splitting-up procedure is employed to develop a rapidly converging inverse solution. The least square technique is then utilized to estimate the unknown parameters associated with the solution. The method is developed first for the analysis of one-dimensional cases, and then it is generalized to handle two- and three-dimensional situations. It provides an efficient, stable and systematic approach for inverse heat condition problems. The stability and accuracy of the current method of analysis are demonstrated by several numerical examples chosen to provide a very strict test. Dissert. Abstr.

N85-35368 Rutgers - The State Univ., New Brunswick, N. J.
AN ANALYTICAL AND NUMERICAL MODEL OF RADIATION HEAT TRANSFER IN DIRECT INJECTION-TYPE DIESEL COMBUSTION Ph.D. Thesis
Shen-Lin Chang 1984 279 p
Avail: Univ. Microfilms Order No. DA8507099

The research has been directed to a better understanding of the processes of particulate formation and radiation that transfer in direct injection type diesel engine combustion. The dissertation considers an analytical and numerical model of radiation heat transfer in a combustion reactor containing soot laden flames as an immediate application to the direct injection type diesel engine. The governing equation of the radiation heat flux and the coordinate transformation that replaces the geometric factors are analytically derived by employing unique techniques, e.g., a new radiation integral function. And the final form of equations are solved by using the Gauss numerical integration technique. The present model enables one to compute the spectral emissivity of a given volume of combustion products, and further, to find, for the individual optical paths, the spectral incident radiation flux on the wall of a combustion chamber with known species distribution.
Dissert. Abstr.

N85-35369 Rutgers - The State Univ., New Brunswick, N. J.
SOME ASPECTS OF INTERNAL GRAVITY WAVES IN A MULTI-LAYERED MOVING STRATIFIED FLOW Ph.D. Thesis
Paul C. Shang 1984 204 p
Avail: Univ. Microfilms Order No. DA8507152

Experiments have examined the two-dimensional waveforms generated by a flap-type wavemaker in a moving, three-layer fluid bounded by rigid walls. Results show that the observed modulation in waveforms could be predicted accurately for low frequencies and that if the two interfaces are sufficiently close together both mode-1 waves (whose amplitude varies in the vertical such that it is non-vanishing except at the boundaries) and mode-2 waves (with a vertical amplitude structure that contains one zero in addition to the boundary points) are generated of similar amplitude. This results in downstream shifts from sinuous to varicose modes of oscillation. Also, a study has been made of some resonant wave interactions in layered fluids with non-zero mean velocity. It has been found that resonant interactions between internal gravity waves in moving fluids can occur under conditions which are not

possible in still fluids. This is based on the computation of resonant interactions for the moving fluid case. Dissert. Abstr.

N85-35370 California Univ., Davis.
HEAT TRANSFER COEFFICIENTS FOR PARTICLES IN LIQUID IN AXIALLY ROTATING CANS Ph.D. Thesis
Bakri Hussein Hassan 1984 172 p
Avail: Univ. Microfilms Order No. DA8507306

A theoretical analysis was carried out to determine the nondimensional parameters and corresponding correlations for the overall heat transfer coefficient (between the external steam and internal rotating liquid) and the liquid-particle film heat transfer coefficient for spherical particles in liquid in axially rotating 303 x 406 cans undergoing steam heating. The correlations were obtained from dimensional analysis of the equations of continuity, motion and energy, together with the thermal energy balances and the particle-fluid dynamics of the system. The theoretical solutions for the temperature distribution in spherical particles with a time varying boundary condition were presented. Dissert. Abstr.

N85-35371*# Universities Space Research Association, Columbia, Md.
STUDIES ON EFFECTS OF BOUNDARY CONDITIONS IN CONFINED TURBULENT FLOW PREDICTIONS
M. Nallasamy and C. P. Chen Washington NASA Sep. 1985 37 p refs
(Contract NAS8-35918)
(NASA-CR-3929; M-499; NAS 1.26:3929) Avail: NTIS HC A03/MF A01 CSCL 20D

The differences in k epsilon model predictions of plane and axisymmetric expansion flows is investigated. The prediction of the coaxial jet for different velocity ratios of the annular to central jet is presented. The effects of inlet kinetic energy and the energy dissipation rate profiles are investigated for swirling and nonswirling flows. The effects of expansion ration and Reynolds number on the reattachment length are also presented. The results show that the inlet k and epsilon profiles have the most significant effect on the reattachment length and flow redevelopment for the case of coaxial jet of high velocity ratio. A comparison of k epsilon model predictions for the pipe expansion flow by the PHOENICS and TEACH codes reveals some discrepancies in the predicted results. TEACH prediction seems to produce unrealistic kinetic energy profiles in some regions of the flow. PHOENICS code produces a long tail in the recirculation region under certain conditions. Author

N85-35372*# National Aeronautics and Space Administration. Ames Research Center, Moffett Field, Calif.
COMPUTATION OF THREE-DIMENSIONAL SHOCK WAVE AND BOUNDARY-LAYER INTERACTIONS
Ching-mao Hung Aug. 1985 15 p refs
(NASA-TM-86780; NAS 1.15:86780; Rept-85350) Avail: NTIS HC A02/MF A01 CSCL 20D

Computations of the impingement of an oblique shock wave on a cylinder and a supersonic flow past a blunt fin mounted on a plate are used to study three dimensional shock wave and boundary layer interaction. In the impingement case, the problem of imposing a planar impinging shock as an outer boundary condition is discussed and the details of particle traces in windward and leeward symmetry planes and near the body surface are presented. In the blunt fin case, differences between two dimensional and three dimensional separation are discussed, and the existence of an unique high speed, low pressure region under the separated spiral vortex core is demonstrated. The accessibility of three dimensional separation is discussed. E.A.K.

N85-35373*# Imperial Coll. of Science and Technology, London (England).
VORTEX BOUNDARY-LAYER INTERACTIONS Semiannual Status Report, 1 Mar. - 31 Aug. 1985
P. Bradshaw 31 Aug. 1985 15 p
(Grant NAGw-581)
(NASA-CR-176192; NAS 1.26:176192) Avail: NTIS HC A02/MF A01 CSCL 20D

The interaction of a turbulent boundary layer on a flat plate with a strong artificially generated longitudinal vortex which may or may not actually enter the boundary layer is studied. The vortices are generated by a delta wing suspended ahead of the test plate, so that the configuration is approximately that of a close coupled carnard with zero main-wing sweep and an invisible body. All necessary configuration and parametric checks are completed, and data acquisition and analysis on the first configuration chosen for detailed study, in which the vortex starts to merge with the boundary layer a short distance downstream of the leading edge of the test plate, are nearly complete. Author

N85-35374*# National Aeronautics and Space Administration. Langley Research Center, Hampton, Va.
THE EFFECT OF POWER LAW BODY FORCES ON A THERMALLY-DRIVEN FLOW BETWEEN CONCENTRIC ROTATING SPHERES
Michele G. Macaraeg Aug. 1985 12 p refs Submitted for publication
(NASA-TM-87596; NAS 1.15:87596) Avail: NTIS HC A02/MF A01 CSCL 20D

A numerical study is conducted to determine the effect of power-law body forces on a thermally-driven axisymmetric flow field confined between concentric co-rotating spheres. This study is motivated by Spacelab geophysical fluid-flow experiments, which use an electrostatic force on a dielectric fluid to simulate gravity; this force exhibits a (1/r)sup 5 distribution. Meridional velocity is found to increase when the electrostatic body force is imposed, relative to when the body force is uniform. Correlation among flow fields with uniform, inverse-square, and inverse-quintic force fields is obtained using a modified Grashof number. Author

N85-35375*# National Aeronautics and Space Administration. Langley Research Center, Hampton, Va.
LONG-TIME ASYMPTOTICS OF A SYSTEM FOR PLASMA DIFFUSION Final Report
Philip Rosenau and Eli Turkel Jul. 1985 21 p refs
(Contract NAS1-17070)
(NASA-CR-177947; ICASE-85-34; NAS 1.26:177947) Avail: NTIS HC A02/MF A01 CSCL 20D

A system of parabolic nonlinear equations that describe the diffusion of a fully collisional plasma across a strong magnetic field is discussed. It is demonstrated that the solution to this system tends to a time asymptotic state which is of space-time separable form, theta(t)f(x). Furthermore, f(x) is independent of the initial conditions and theta(t) depends slightly on the initial conditions. The rate of decay of the temporal part is governed by a nonlinear eigenvalue problem. Since the equations are considered in a bounded domain we are able to analyze the effect of boundary conditions on the evolution of the system. Additional effects on radiation, heating, and particle injection can also be accounted for. Essential differences between the behavior of a fully-coupled system and a scalar equation are observed. Author

N85-35376# Wisconsin Univ., Madison. Mathematics Research Center.
COUETTE FLOW OF TWO FLUIDS BETWEEN CONCENTRIC CYLINDERS
Y. Renardy and D. D. Joseph 1985 16 p Repr., J. of Fluid Mech., v. 150, 1985 p 381-394
(Contract DAAG29-80-C-0041)
(AD-A155827; ARO-16415.735-MA) Avail: NTIS HC A02/MF A01 CSCL 20/4

The flow of two immiscible fluids lying between concentric cylinders when the outer cylinder is fixed and the inner one rotates is considered. The interface is assumed to be concentric with the cylinders, and gravitational effects are neglected. A numerical study of the effect of different viscosities, different densities and surface tension on the linear stability of the Couette flow is presented. Results indicate that, with surface tension, a thin layer of the less-viscous fluid next to either cylinder is linearly stable and that it is possible to have stability with the less dense fluid lying outside.

The stable configuration with the less-viscous fluid next to the inner cylinder is more stable than the one with the less-viscous fluid next to the outer cylinder. The onset of Taylor instability for one-fluid flow may be delayed by the addition of a thin layer of less-viscous fluid on the inner wall and promoted by a thin layer of more-viscous fluid on the inner wall. GRA

N85-35377# Levy (Salomon), Inc., Campbell, Calif.
A TWO-PHASE FLOW AND HEAT TRANSFER MODEL FOR ZERO GRAVITY Final Report, Sep. 1984 - Mar. 1985
D. Abdollahian and S. Levy Wright-Patterson AFB, Ohio AFWAL May 1985 76 p
(Contract F33615-84-C-3412)
(AD-A156097; AFWAL-TR-85-3014) Avail: NTIS HC A05/MF A01 CSCL 20/13

The power of future spacecraft are expected to grow considerably in the near future, and this will require more efficient thermal transport techniques. Due to high heat transfer coefficient, two-phase gas-liquid loops are expected to be used for removal and transport of heat to space radiators. The design of such cooling systems requires a knowledge of two-phase flow and heat transfer at reduced and zero gravities. The objective of this study was to develop or extend the earth gravity models for the two-phase friction multiplier, the void quantity relation, and the forced convective heat transfer coefficient to zero gravity situations. Turbulent mixing length theory was used to develop a model for the two-phase fluid and heat transfer parameters. The velocity, density, and temperature distributions were derived by solving the conservation equations for a continuous medium and assuming equal turbulent exchanges of momentum, density, and heat. The flow was assumed to be locally homogeneous, and the void distribution was allowed to vary within the channel. The results show that the model predicts all the correct physical trends. The model contains a free parameter which should be specified from experiments at zero gravity, simulated zero gravity, or conditions where the effect of gravity can be neglected. GRA

N85-35378# Minnesota Univ., Minneapolis.
PRESSURE CROSS SPECTRA IN TURBULENT BOUNDARY LAYERS IN WATER Interim Technical Report, Jun. 1983 - Dec. 1984
N. Narayan and R. Plunkett 14 Feb. 1985 55 p
(Contract N00014-83-K-0145)
(AD-A156153; AEM-85-1-RP) Avail: NTIS HC A04/MF A01 CSCL 20/4

The spectrum (power spectral density) of the vibration level for any linear system can be found by integrating the product of the cross spectrum of the excitation with the cross frequency response functions of the system over the area on which the excitation is acting. Measurements of the auto and cross spectra of the wall pressure fluctuations in a water tunnel are presented. It is shown that the cross spectra cannot be expressed as a product of functions of the streamwise and transverse coordinates alone but must include interaction terms. One possible parametric approximation is suggested. GRA

N85-35379# Los Alamos Scientific Lab., N. Mex.
NOISE-SUSTAINED STRUCTURE, INTERMITTENCY AND THE GINZBURG-LANDAU EQUATION
R. J. Deissler 1985 9 p Presented at the Conf. on Solitons and Coherent Struct., Santa Barbara, Calif., 11 Jan. 1985
(Contract W-7405-eng-36)
(DE85-009626; LA-UR-85-1055; CONF-850165-3) Avail: NTIS HC A02/MF A01

The time-dependent generalized Ginzburg-Landau equation is a partial differential equation that is related to many physical systems. In the stationary (i.e., laboratory) frame of reference the equation is: Partial psi/partial t = a psi - NU) (partial psi/partial x) + b (partial squared x/partial x) 2 - c (psi absolute) 2 psi where the dependent variable psi is in general complex; a, b, and c are constants which are in general complex; and NU is the group velocity. A small initial localized perturbation is considered for the equilibrium state psi = 0. A linear stability analysis reveals that there are three types of behavior which this perturbation can undergo: (1) the perturbation will be damped in any frame of reference; this behavior corresponds to the system being absolutely stable. (2) The perturbation will grow and spread such that the edges of the perturbation move in opposite directions; this behavior corresponds to the system being absolutely unstable; (3) the perturbation will be damped at any given stationary point, but a frame of reference may be found in which the perturbation is growing. DOE

N85-35380# California Univ., Berkeley. Dept. of Mechanical Engineering.
EXPERIMENTAL STUDY OF FREE AND MIXED CONVECTIVE FLOW OF AIR IN A HEATED CAVITY Final Report
Joseph A. C. Humphrey, Frederick S. Sherman, and Kang S. Chen Apr. 1985 292 p
(Contract DE-AC04-76DR-00789)
(DE85-012538; SAND-84-8192; Rept-83-1) Avail: NTIS HC A13/MF A01

Free and mixed convection in a strongly-heated rectangular open cavity have been investigated experimentally, to observe the effects of cavity shape and inclination, and of ambient wind, on the velocity and temperature distribution were observed. The long edges of the cavity were horizontal, and parallel to an axis around which the cavity could be rotated. The aperture plane was either vertical (ALPHA = 0), or inclined downward at (ALPHA = 20 deg or ALPHA = 45 deg). The height of the aperture, b, was always 0.0947 m, while the depth of the cavity, a, was set so that a/b = 0.5, 1.0, or 1.46. The bottom and back walls were electrically heated - the top wall was indirectly heated by conduction, radiation and convection. The average wall temperature and the ambient temperature were used to define the dimensionless overheat and Grashof numbers. The Prandtl number was that of air. In the studies of mixed convection, the axis of rotation was horizontal and normal to the ambient wind. The Reynolds number was varied from Re = 120 - 1100 to Re = 2000 = 8740. For both free and mixed convection, wall and gas temperature were measured with thermocouples, and shadowgraph pictures were taken. DOE

N85-35381# Los Alamos Scientific Lab., N. Mex.
ADAPTIVE REZONER IN A TWO-DIMENSIONAL LAGRANGIAN HYDRODYNAMIC CODE
J. J. Pyun, J. S. Saltzman, A. J. Scannapieco, and D. Carroll 1985 14 p refs Presented at 4th Intern. Conf. on Numerical Methods in Laminar and Turbulent Flow, Swansea, Wales, 8 Jul. 1985
(Contract W-7405-eng-36)
(DE85-010108; LA-UR-85-942; CONF-850745-1) Avail: NTIS HC A02/MF A01

In an effort of increase spatial resolution without adding additional meshes, an adaptive mesh was incorporated into a two-dimensional Lagrangian hydrodynamics code along with two-dimensional flux corrected (FCT) remapper. The adaptive mesh automatically generates a mesh based on smoothness and orthogonality, and at the same time also tracks physical conditions of interest by focusing mesh points in regions that exhibit those conditions: this is done by defining a weighting function associated with the physical conditions to be tracked. The FCT remapper calculated the net transportative fluxes based on a weighted average of two fluxes computed by a low-order scheme and a high-order scheme. This averaging procedure produces solutions which are conservative and nondiffusive, and maintains positivity. DOE

N85-35382# Hanford Environmental Health Foundation, Richland, Wash.
EXPERIMENTAL LITHIUM SYSTEM Final Report
R. Kolowith, J. D. Berg, and W. C. Miller Apr. 1985 326 p refs
(Contract DE-AC06-76FF-02170)
(DE85-013252; HEDL-TME-84-29) Avail: NTIS HC A15/MF A01

A full scale mockup of the Fusion Materials Irradiation Test (FMIT) Facility lithium system was built at the Hanford Engineering

Development Laboratory (HFDL). This isothermal mockup, called the Experimental Lithium System (ELS), was prototypic of FMIT, excluding the accelerator and dump heat exchanger. This 3.8 cu m lithium test loop achieved over 16,000 hours of safe and reliable operation. An extensive test program demonstrated satisfactory performance of the system components, including the HEDL supplied electromagnetic lithium pump, the lithium jet target, the purification and characterization hardware, as well as the auxiliary argon and vacuum systems. Experience with the test loop provided important information on system operation, performance, and reliability. This report presents a complete overview of the entire Experimental Lithium System test program and also includes a summary of such areas as instrumentation, coolant chemistry, vapor/aerosol transport, and corrosion. DOE

N85-35383# Los Alamos Scientific Lab., N. Mex.
ENHANCED HEAT TRANSFER COMPUTATIONS FOR INTERNALLY COOLED CABLE SUPERCONDUCTOR
J. D. Rogers Mar. 1985 9 p
(Contract W-7405-eng-36)
(DE85-011897; LA-10367-MS) Avail: NTIS HC A02/MF A01

Superconducting magnets are built with conductors that are pool bath cooled, internally cooled with the superconductor cable and contained within a conduit, or conduction cooled. The first two embody superconductors are in direct contact with liquid helium. Practical designs of internally cooled cable superconductor (ICCS) are not cryostable. Such superconductors have shown multiple regions of stability and instability. A computational method of adjusting the heat transfer coefficient of a one dimensional system of equations to enhance joule heat removal, primarily in the central region of a pulse heated model of ICCS, has been used to attempt simulation of the multiple stability/instability experiment. DOE

N85-35384# Kanner (Leo) Associates, Redwood City, Calif.
TRANSIENT THREE-PHASE THREE-COMPONENT SYSTEMS. PART 1: FORMULATION OF THE SYSTEM OF DIFFERENTIAL EQUATIONS
N. I. Kolev 1985 64 p Transl. into ENGLISH of "Transiente Dreiphsen Dreikomponenten Stromung. Teil 1: Formulierung des DGL-Systems" rept. KfK-3910 Kernforschungszentrum Karlsruhe G.m.b.H., West Germany
(Contract W-7405-eng-36)
(DE85-013267; LA-tr-85-26; KfK-3910) Avail: NTIS HC A04/MF A01

On the basis of the laws of conservation, the nonconservative form of a system of 18 quasi-linear partial differential equations was developed to describe a three phase, three component flow. The flow was described with three fields of velocity. Each field of flow consists of one inert and one noninert component. Full thermodynamic and mechanical nonequilibrium between the fields was modeled. The simplest possible concentrations and entropy equations were obtained, with no simplifying assumptions. Also obtained was the definition of the Mach number and of the critical mass velocity, and thus, the local criticality condition. DOE

N85-35385# Texas Univ., Austin. Inst. of Fusion Studies.
SCALE SEPARATION CLOSURE AND ALFVEN WAVE TURBULENCE
C. Y. Chen and S. M. Mahajan Apr. 1985 24 p
(Contract DE-FG05-80ET-53088)
(DE85-013124; DOE/ET-53088/179) Avail: NTIS HC A02/MF A01

Based on the concept of scale separation between coherent response function and incoherent source for renormalized turbulence theories, a closure scheme is proposed. A model problem dealing with shear-Alfven wave turbulence is numerically solved; the solution explicitly shows expected turbulence features such as frequency shift from linear modes, band-broadening, and a power law dependence for the turbulence spectrum. DOE

N85-35386# Sandia Labs., Albuquerque, N. Mex.
EXPERIMENTAL TECHNIQUE FOR MEASURING THE ISENTROPE OF HYDROGEN TO SEVERAL MEGABARS
L. M. Barker, T. G. Truncano, J. I. Wise, and J. R. Asay 1985 6 p refs Presented at the Am. Phys. Soc. Topical Conf. on Shock Waves in Condensed Matter, Spokane, 22 Jul. 1985
(Contract DE-AC04-76DP-00789)
(DE85-014332; SAND-85-0428C; CONF-850736-17) Avail: NTIS HC A02/MF A01

The experimental measurement of the Equations of State (EOS) of hydrogen has been of interest for some time because of the theoretical expectation of a transition to the metallic state in the multi-megabar pressure regime. Previous experiments have reported results which are consistent with a metallic transition, but experimental uncertainties have precluded positive identification of the metallic phase. In this paper we describe a new experimental approach to the measurement of the high-pressure EOS of hydrogen. A cryogenic hydrogen specimen, either liquid or solid, is located in the muzzle of a gun barrel between a tungsten anvil and another tungsten disk called a shim. Helium gas in the gun barrel cushions the impact and allows nearly isentropic compression of the hydrogen. The time-resolved pressure in the specimen is calculated from a laser interferometer (VISAR) measurement of the acceleration history of the anvil's free surface, and volume measurements at specific times are made by combining VISAR data, which define the position of the anvil, with flash X-ray photographs which define the shim position. DOE

N85-35387# Cologne Univ. (West Germany). Inst. fuer Geophysik und Meteorologie.
APPLICATION OF A TURBULENT CLOSURE MODEL TO THE PARAMETERIZATION OF THE VERTICAL DIFFUSION OF HEAT, MOMENTUM, AND HUMIDITY IN THE ECMWF MODEL [ANWENDUNG EINES TURBULENZSCHLIESSUNGSMODELLS AUF DIE PARAMETRISIERUNG DER VERTIKALDIFFUSION VON WAERME, IMPULS UND FEUCHTE IM EZMW-MODELL]
Lydia Duemenil 1984 104 p refs In GERMAN; ENGLISH summary
(Mitt-41; ISSN-0067-5882) Avail: NTIS HC A06

A simplified second order closure scheme was implemented in the ECMWF forecasting model and its performance was assessed. The scheme contains an additional prognostic equation for turbulent kinetic energy and computes diffusion coefficients that are not only Richardson number, but also turbulent kinetic energy dependent. The model was first tested in a simpler form without taking advection of turbulent kinetic energy into account. The quality of 10 day forecasts is only marginally improved. The advection of turbulent kinetic energy on the level and geographical distribution of turbulence have to be retained. The benefits of turbulence closure schemes in high resolution planetary boundary layer studies are counteracted in the large scale model by the effects of low resolution, large time steps, and the feedback from other parameterization schemes. The results show that a replacement of the operational scheme by the turbulent closure scheme cannot be recommended. Author (ESA)

N85-35388# Texas Univ., Austin. Ocean Engineering Program.
FURTHER STUDIES ON LIQUID SLOSHING Final Report, Sep. 1982 - Mar. 1985
Y. K. Lou, M. C. Wu, and C. K. Lee Mar. 1985 228 p refs
(Contract DTMA91-82-C-20036)
(PB85-198695; COE-277; MA-RD-760-85009) Avail: NTIS HC A11/MF A01 CSCL 13J

Sloshing is especially of concern for LNG Carriers and large oil tankers because of their tank size and geometrical configurations and the likelihood of near resonant excitation of the contained liquid. When a tank is under multidegree of freedom excitations the phase relationships among the excitations might have a significant effect on sloshing loads. An analytical solution is obtained for liquid sloshing under combined excitations with phase difference. A series of physical model tests has also been conducted to investigate the effects of the phase angle on liquid sloshing loads for tanks under combined roll and sway and roll and heave excitations. The experimental results are in general agreement with the analytical findings. GRA

35 INSTRUMENTATION AND PHOTOGRAPHY

Includes remote sensors; measuring instruments and gages; detectors; cameras and photographic supplies; and holography.

For aerial photography see *43 Earth Resources*. For related information see also *06 Aircraft Instrumentation*, and *19 Spacecraft Instrumentation*.

N85-35389*# Illinois Univ., Urbana. Dept. of Astronautics and Astronautical Engineering.
THE USE OF A LASER DOPPLER VELOCIMETER IN A STANDARD FLAMMABILITY TUBE Final Report, Jan. 1981 - May 1982
Roger A. Strehlow and Edward M. Flynn May 1985 101 p refs
(Contract NAS3-2266C)
(NASA-CR-174960; NAS 1.26:174960; TR-AAE-85-4; UILU-ENG-85-0504) Avail: NTIS HC A06/MF A01 CSCL 14B

The use of the Laser Doppler Velocimeter, (LDV), to measure the flow associated with the passage of a flame through a standard flammability limit tube (SFLT) was studied. Four major results are presented: (1) it is shown that by using standard ray tracing calculations, the displacement of the LDV volume and the fringe rotation within the experimental error of measurement can be predicted; (2) the flow velocity vector field associated with passage of an upward propagating flame in an SFLT is determined; (3) it is determined that the use of a light interruption technique to track particles is not feasible; and (4) it is shown that a 25 mW laser is adequate for LDV measurements in the Shuttle or Spacelab. E.A.K.

N85-35390*# Energy Optics, Inc., Las Cruces, N. Mex.
MINIATURE INFRARED DATA ACQUISITION AND TELEMETRY SYSTEM Final Report
J. H. Stokes and S. M. Ward Sep. 1985 95 p
(Contract NAS1-17944)
(NASA-CR-177953; NAS 1.26:177953) Avail: NTIS HC A05/MF A01 CSCL 09F

The Miniature Infrared Data Acquisition and Telemetry (MIRDAT) Phase 1 study was performed to determine the technical and commercial feasibility of producing a miniaturized electro-optical telemetry system. This system acquires and transmits experimental data from aircraft scale models for realtime monitoring in wind tunnels. During the Phase 1 study, miniature prototype MIRDAT telemetry devices were constructed, successfully tested in the laboratory and delivered to the user for wind tunnel testing. A search was conducted for commercially available components and advanced hybrid techniques to further miniaturize the system during Phase 2 development. A design specification was generated from laboratory testing, user requirements and discussions with component manufacturers. Finally, a preliminary design of the proposed MIRDAT system was documented for Phase 2 development. Author

N85-35391*# Pratt and Whitney Aircraft, East Hartford, Conn. Engineering Div.
DEVELOPMENT OF ADVANCED HIGH-TEMPERATURE HEAT FLUX SENSORS. PHASE 2: VERIFICATION TESTING Final Report
William. H. Atkinson, Marcia A. Cyr, and Richard R. Strange Aug. 1985 69 p refs
(Contract NAS3-22133)
(NASA-CR-174973; NAS 1.26:174973; PWA-5914-39) Avail: NTIS HC A04/MF A01 CSCL 14B

A two-phase program is conducted to develop heat flux sensors capable of making heat flux measurements throughout the hot section of gas turbine engines. In Phase 1, three types of heat flux sensors are selected; embedded thermocouple, laminated, and Gardon gauge sensors. A demonstration of the ability of these sensors to operate in an actual engine environment is reported. A segmented liner of each of two combustors being used in the Broad Specification Fuels Combustor program is instrumented with the three types of heat flux sensors then tested in a high pressure combustor rig. Radiometer probes are also used to measure the radiant heat loads to more fully characterize the combustor environment. Test results show the heat flux sensors to be in good agreement with radiometer probes and the predicted data trends. In general, heat flux sensors have strong potential for use in combustor development programs. Author

N85-35392# Aerodyne Research, Inc., Billerica, Mass.
HOLOSWITCH Final Progress Report
E. S. Gaynor and H. J. Caulfield May 1985 30 p
(Contract N00014-84-C-0727; DARPA Order 4941)
(AD-A155841; ARI-RR-447) Avail: NTIS HC A03/MF A01 CSCL 09/3

The purpose of this Phase 1 SBIR contract was to invent ways of using switchable holograms to change from one optical interconnect pattern to another with great speed. That is, we sought to combine the high flexibility in design and high diffraction efficiency of classical holography with the programmability of the far-less-efficient real time holography methods of four wave mixing, three wave mixing, etc. We have solved this problem in many separate and wholly satisfactory ways. A Phase 2 proposal to develop the best of these solutions is being submitted along with this report. The report organization is historical. That is, it follows the path of our thought as it evolved toward the ultimate solution. This historical matter is important in that it sets the stage for recognizing the superiority our final decision over earlier versions. GRA

N85-35393# Sandia Labs., Albuquerque, N. Mex.
CALIBRATOR FOR DISPLACEMENT GAGES USED IN THE ROCK MECHANICS LABORATORY
M. J. McNamee May 1985 24 p ref
(Contract DE-AC04-76DP-00789)
(DE85-013257; SAND-85-0548) Avail: NTIS HC A02/MF A01

A system for calibration of LVDT's (linear variable displacement transformers) was developed for use in the rock mechanics laboratory. The new calibrator system works on an electrical-mechanical principle where a mechanical translator moves a holding fixture, which has provisions for both the calibrator measurement standard, a precision gage head LVDT and the LVDT(s) of interest during the calibration procedure. Output voltages from both the calibrator standard and the gage(s) being calibrated are easily recorded by laboratory computers, making printouts and plots of data a simple task. The new system avoids measurement errors introduced by micrometer thread backlash and spindle sticking associated with previous mechanical systems. DOE

N85-35394# Pennsylvania State Univ., University Park. Dept. of Chemical Engineering.
CHARACTERIZATION OF CATALYSTS WITH METAL-SUPPORT EFFECTS AND OF THE SPECIES ADSORBED ON THEIR SURFACES Progress Report, 1 Sep. 1984 - 30 Aug. 1985
M. A. Vannice 13 Jun. 1985 13 p refs
(Contract DE-FG02-84ER-13276)
(DE85-012254; DOE/ER-13276/1) Avail: NTIS HC A02/MF A01

The influence of crystallite size and the support on heats of adsorption of H2, CO, and O2 on Pt and Pd are reported. Isothermal, integral heats of adsorption have been measured for H2 and CO adsorption on Pt and Pd dispersed on four supports, SiO2, Al2O3, and SiO2-Al2O3. These values were determined at 215K and 300 to 320K. Results are presented. For support Pt the heats of adsorption were highest on Pt/SiO2 and lowest on Pt/TiO2. However, a clear trend existed between heats of adsorption and Pt exposed with large Pt crystallites having the highest values. The Pd catalysts exhibited behavior different than those for the Pt catalysts in two major aspects. First, the heats of adsorption values tended to increase somewhat as crystallite sizes became very small. Second, the high temperature reduction step did not decrease the heats of adsorption values as significantly for Pd/TiO2. DOE

N85-35395*# University of Southern California, Los Angeles. Center for Laser Studies.
CRYOGENIC LASER CALORIMETRY FOR IMPURITY ANALYSIS Final Report, 6 Sep. 1983 - 1 Dec. 1984
R. T. Swimm May 1985 19 p refs
(Contract NAS7-100)
(NASA-CR-176179; NAS 1.26:176179; DE85-012793; DOE/JPL-956613-85/1) Avail: NTIS HC A02/MF A01 CSCL 14B

The results of a one-year effort to determine the applicability of laser-calorimetric spectroscopy to the study of deep-level impurities in silicon are presented. Critical considerations for impurity analysis by laser-calorimetric spectroscopy are discussed, the design and performance of a cryogenic laser calorimeter is described, and measurements of background absorption in high-purity silicon are presented. DOE

N85-35396# Sandia Labs., Albuquerque, N. Mex.
RASTER FUNCTIONALITY FOR A VDI
C. Pavlakos 1985 21 p refs Presented at SIGGRAPH 1985, San Francisco, 22 Jul. 1985
(Contract DE-AC04-76DP-00789)
(DE85-006734; SAND-85-0151C; CONF-850727-1) Avail: NTIS HC A02/MF A01

SVID+Raster is a Virtual Device Interface (VDI) which includes raster primitives for imaging applications. The raster functionality of SVDI+Raster provides a high degree of device-independence, while still allowing the user to customize image output for particular devices. Raster images can be mapped into arbitrary viewports, with various options available for specifying how the logical image data are to be mapped onto actual device pixels. Output primitives allow the user to pass image data as streams of individual pixels or as streams of pixel-runs for data compression. An extra benefit of the VDI+Raster is the capability to merge vector and raster graphics. The raster functions form an isolated part of the VDI which can easily be adapted to other general graphics interfaces. DOE

N85-35397# Rockwell International Corp., Golden, Colo.
MEASUREMENT CONTROL FOR PLUTONIUM ISOTOPIC MEASUREMENTS USING GAMMA-RAY SPECTROMETRY
J. G. Fleissner 10 May 1985 12 p
(Contract DE-AC04-76DP-03533)
(DE85-013394; RFP-3780) Avail: NTIS HC A02/MF A01

A measurement control (MC) program should be an integral part of every nondestructive assay measurement system used for the assay of special nuclear materials. This report describes an MC program for plutonium isotopic composition measurements using high-resolution gamma-ray spectroscopy. This MC program emphasizes the standardization of data collection procedures along with the implementation of internal and external measurement control checks to provide the requisite measurement quality assurance. This report also describes the implementation of the MC program in the isotopic analysis code GRPAUT. Recommendations are given concerning the importance and frequency of the various MC checks in order to ensure a successful implementation of the MC procedures for the user's application. DOE

N85-35398# Sandia Labs., Albuquerque, N. Mex.
ELLIPTICAL X-RAY ANALYZER SPECTROGRAPH APPLICATION TO A LASER-PRODUCED PLASMA
T. J. Tanaka, M. A. Palmer, and B. L. Benke 1985 26 p Presented at the SPIE Intern. Tech. Symp. on Optical and Electro-Optical Eng., San Diego, Calif., 18 Aug. 1985 Prepared in cooperation with Hawaii Univ., Honolulu
(Contract DE-AC04-76DP-00789)
(DE85-013790; SAND-85-0302C; CONF-850887-2) Avail: NTIS HC A03/MF A01

A spectrograph is designed to record a range of 100 to 2000 eV X-rays on calibrated Kodak Rar-2497 film. Using point calibrations and theoretical models, the spectrograph efficiency is predicted. Basic spectrograph geometry and photographic calibrations are presented in companion papers. A 20 J, 6 ns duration Nd:glass laser pulse is focussed on planar targets of gold, aluminum, teflon and boron carbide. Sample spectra for line and X-ray yields analysis are presented. DOE

N85-35399# Siemens A.G., Munich (West Germany). Technische Abt. Sensoren.
MATERIALS AND PROCESS DEVELOPMENT FOR MICROCOMPUTER-COMPATIBLE PRESSURE, TEMPERATURE, AND POSITION SENSORS Final Report, Mar. 1983
Josef Binder and Manfred Poppinger Bonn Bundesministerium fuer Forschung und Technologie Apr. 1985 75 p refs In GERMAN; ENGLISH summary Sponsored by Bundesministerium fuer Forschung und Technologie
(BMFT-FB-T-85-024; ISSN-0340-7608) Avail: NTIS HC A04/MF A01; Fachinformationszentrum, Karlsruhe, West Germany DM 16

Polysilicon pressure sensor temperature compensated within 3%/100 K with N = 10 to the 20th power/CC was made. By integrating a network of suitable polysilicon resistors on top of the chip of a standard silicon pressure sensor, an interchangeable pressure sensor is obtained. By laser trimming the offset voltage can be compensated and the temperature errors related to the signal can be reduced to better than 5 o/oo/100 K for the offset and better than 2%/100 K for the sensitivity. Author (ESA)

N85-35400# AEG-Telefunken, Frankfurt am Main (West Germany). Forschungsinst.
DEVELOPMENT OF CONTACTLESS SENSORS FOR INDUSTRIAL AND AUTOMATIVE APPLICATIONS Final Report, Aug. 1984
Ernst-August Heidler, Helmut Kanbach, and Horst Interhoff Bonn Bundesministerium fuer Forschung und Technologie Apr. 1985 96 p refs In GERMAN; ENGLISH summary Sponsored by Bundesministerium fuer Forschung und Technologie
(BMFT-FB-T-85-031; ISSN-0340-7608) Avail: NTIS HC A05/MF A01; Fachinformationszentrum, Karlsruhe, West Germany DM 20.50

Contactless speed and torque sensors were developed for power measurement and control of motors and for the investigation of their properties for applications in motor vehicle and in industrial domains. For the speed sensor a magnetic bistable wire was developed. The method of wire preparation, efforts to optimize its properties, and data of the prototypes are described. The torque sensor is based on an eddy current measuring head of relatively small dimensions. Changes of permeability at rotating ferromagnetic shafts are detected contactlessly. These changes originate from the inverse magnetostrictive effect as a result of the torsion of the loaded shaft. They are a function of the torque acting at the shaft. The measuring heads and relevant effects are described. Author (ESA)

N85-35709# Pennsylvania Univ., Philadelphia. Intensity Interferometry Sub-Group.
DETECTOR REQUIREMENTS FOR INTENSITY INTERFEROMETRY MEASUREMENTS
William Zajc *In* California Univ., Berkeley. Lawrence Berkeley Lab. Proc. of the Workshop on Detectors for Relativistic Nucl. Collisions Aug. 1984 p 121-132 refs (For primary document see N85-35700 24-72)
Avail: NTIS HC A08/MF A01

N85-35710# Max-Planck-Inst. fuer Astrophysik, Munich (West Germany).
A HOLOGRAPHIC STREAMER CHAMBER FOR RELATIVISTIC NUCLEUS-NUCLEUS COLLISION EXPERIMENTS
V. Eckardt *In* California Univ., Berkeley. Lawrence Berkeley Lab. Proc. of the Workshop on Detectors for Relativistic Nucl. Collisions Aug. 1984 p 133-134 refs (For primary document see N85-35700 24-72)
Avail: NTIS HC A08/MF A01

N85-35711# California Univ., Berkeley. Lawrence Berkeley Lab.
A LEAD GLASS TUBING DRIFT CALORIMETER

T. A. Mulera, V. Perez-Mendez, H. Hirayama (Stanford Linear Accelerator), W. R. Nelson (Stanford Linear Accelerator), R. Bellazzini (Dipartimento di Fisica, Pisa, Italy), A. DelGuerra (Dipartimento di Fisica, Pisa, Italy), and M. M. Massai (Dipartimento di Fisica, Pisa, Italy) *In its* Proc. of the Workshop on Detectors for Relativistic Nucl. Collisions Aug. 1984 p 135-138 refs (For primary document see N85-35700 24-72)
(Contracts DE-AC03-76SF-00098; DE-AC03-76SF-00515)
Avail: NTIS HC A08/MF A01

N85-35556# Technische Univ., Munich (West Germany). Lehrstuhl fuer Flugmechanik und Flugregelung.
DEVELOPMENT AND OPERATION OF A MEASURING DATA ACQUISITION SYSTEM FOR USE IN LIGHT AIRPLANES [ENTWICKLUNG UND BETRIEB EINER MESSDATENERFASSUNGSANLAGE (MEA) FUER DEN EINSATZ IN LEICHTFLUGZEUGEN]
Peter Huber *In* DFVLR Proc. of Meteorol. Motor Glider (MEMO) Workshop '84 Jan. 1985 p 157-160 In GERMAN (For primary document see N85-35542 24-47)
Avail: NTIS HC A10/MF A01

36 LASERS AND MASERS

Includes parametric amplifiers.

N85-35401# Air Force Geophysics Lab., Hanscom AFB, Mass.
LINEAR ABSORPTION AND SCATTERING OF LASER BEAMS
F. X. Kneizys, S. A. Clough, E. P. Shettle, and R. W. Fenn 27 Sep. 1984 30 p
(AF Proj. 7670)
(AD-A156167; AD-E440284; AFGL-TR-84-0265; AFGL-ERP-889) Avail: NTIS HC A03/MF A01 CSCL 20/5

The linear transmission effects of the atmosphere on laser beams is described and examples are given of high resolution (FASCODE) model predictions of transmittance for carbon dioxide, deuterium fluoride, hydrogen fluoride, neodymium - yttrium aluminum garnet, iodine, and excimer laser wavelengths. Author (GRA)

N85-35402# Naval Research Lab., Washington, D. C.
SOLID NEON SOURCES FOR PLASMA AND X-RAY LASERS
R. H. Dixon, J. L. Ford, T. N. Lee, and R. C. Elton 30 Apr. 1985 13 p
(Contract DE-AI08-79DP-40092)
(DE85-011347; NRL-MR-5534) Avail: NTIS HC A02/MF A01

A thin layer of frozen neon is condensed onto a cryogenically cooled substrate for use in generating a neon plasma for X-ray laser research. The freezing process and quasi-equilibrium state of the layer are discussed with a phase diagram. Spectral purity of a neon plasma formed by laser irradiation is demonstrated with grazing incidence X-ray spectroscopy. Control of the layer thickness is possible to the point that a substrate spectrum is also obtained. DOE

N85-35403# Illinois Univ., Chicago. Dept. of Physics.
GENERATION OF STIMULATED EMISSION IN THE SOFT X-RAY RANGE BY NONLINEAR PROCESSES WITH EXCIMER LASERS Progress Report, 1 Oct. 1984 - 15 May 1985
C. K. Rhodes, K. Boyer, T. S. Luk, U. Johann, and A. P. Schwarzenbach 1985 36 p refs
(Contract DE-AC02-83ER-13137)
(DE85-012465; DOE/ER-13137/T1) Avail: NTIS HC A03/MF A01

Studies of multiphoton ionization of atoms have revealed several unexpected characteristics. The confluence of the experimental evidence leads to the hypothesis that the basic character of the atomic response involves highly organized coherent motions of entire atomic shells. The important regime, for which the radiative field strength E is greater than an atomic unit (e/a0(2)), can be viewed in approximate correspondence with the physics of fast (approx. 10 MeV/amu) atom-atom scattering. This physical picture provides a basis for the expectation that stimulated emission in the X-ray range can be produced by direct highly nonlinear coupling of ultraviolet radiation to atoms. DOE

N85-35404# California Univ., Livermore. Lawrence Livermore Lab.
ATA UPGRADE TO 150 MeV
D. L. Birx, S. A. Hawkins, S. E. Poor, L. L. Reginato, and M. W. Smith 9 Apr. 1985 9 p
(Contract W-7405-eng-48)
(DE85-013174; UCID-20443) Avail: NTIS HC A02/MF A01

The increased interests in upgrading the ATA accelerator has warranted a preliminary look at applying the magnetic drivers to achieve both higher energy and higher average power. The goal of this upgrade is to satisfy the FEL requirements and to keep the capability of producing a higher current beam for CPE experiments at reduced energy. ATA Note 247 showed that a possible solution to obtain higher energy was simply to add additional cells, run them at higher voltage and accept a 30 ns pulse width with about 5% energy variation. Considering the recent history of the cells and the doubling of the voltage stress that would be required at the insulator, it seemed prudent to review the overall system reliability and try a different approach. DOE

N85-35405# Los Alamos National Lab., N. Mex.
LOS ALAMOS FREE-ELECTRON LASER
J. M. Watson 1985 6 p refs Presented at the Particle Accelerator Conf., Vancouver, British Columbia, 13 May 1985
(Contract W-7405-eng-36)
(DE85-012666; LA-UR-85-1611; CONF-850504-49) Avail: NTIS HC A02/MF A01

The free-electron laser (FEL) oscillator has demonstrated high peak and average power, broad-wavelength tunability, and near-ideal optical quality. An electron energy-extraction efficiency of 1% was measured. The predicted production of synchrotron sidebands was observed in the broadened optical spectrum. As shorter wavelengths and higher powers are pursued, higher currents with improved beam quality will be required. Advanced injectors and energy-recovery systems are developed to meet these demands. DOE

37 MECHANICAL ENGINEERING

Includes auxiliary systems (non-power); machine elements and processes; and mechanical equipment.

N85-35406 Purdue Univ., Lafayette, Ind.
THE COMPLIANCE OF END EFFECTOR FORCE SENSORS FOR ROBOT MANIPULATOR CONTROL Ph.D. Thesis
Randall Keith Roberts 1984 129 p
Avail: Univ. Microfilms Order No. DA8507751

This dissertation analyzes the effect of wrist force sensor mechanical stiffness on robot manipulator control. Typically, wrist force sensors for robotic systems have been designed and fabricated viewing the transducer as a isolated element, with mechanically stiff structures instrumented with strain gages being the most common configuration. Research has indicated, however, that force control system implementation with such stiff sensors is complicated by the resulting low system damping. A theoretical analysis of the manipulator system based on physical modeling was performed. The dynamic equations of motion in Cartesian coordinates for the general six link manipulator, assuming finite drive train stiffnesses at each joint, were derived. Next, the general form of the manipulator-sensor dynamics were established in a transfer function matrix formulation. From this analysis, the Cartesian stiffness of the overall robotic system was established. Dissert. Abstr.

N85-35407*# Lockheed Missiles and Space Co., Huntsville, Ala. Research and Engineering Center.
SRB ATTACH RING PHENOLIC TPS FISHTAIL SEAL EVALUATION TESTS

Zain S. Karu Feb. 1982 48 p
(Contract NAS8-32982)
(NASA-CR-170887; NAS 1.26:170887; LMSC-HREC-TM-D784769) Avail: NTIS HC A03/MF A01 CSCL 13I

The SRB attach ring is thermally protected with layered phenolic cloth fairings that are fastened to the ring. The gap between the fairings and the motor case is closed off with a rubber seal of a fishtail cross sectional shape bonded to the phenolic. On both the STS-1 and STS-2 flights this gap was discovered to vary anywhere from an intended gap of 0.375 in. to an actual measured gap of 0.60 in. due to tolerances. Tests were conducted with and without a 0.25 in. thick cork shim placed under the seal with a 0.60 in. gap under the phenolic TPS to determine and compare the performance of the seal in the two different configurations. To alleviate the difficult and costly procedure of installing the cork shim under the seal, especially after phenolic TPS mounting on the attach ring, large fishtail seals of idential Elder gray silicon material and two different hardnesses were tested. A similar matrix of tests was conducted with this new large fishtail seal, and seals with both type hardnesses performed well regardless of whether or not the seal was bonded in the phenolic at the front of the seal groove. Similar results had been obtained with the original small fishtail seal which performed adequately with the 0.25 in. cork shim under it. Author

N85-35408# Hayes-Albion Corp., Mich.
DEVELOPMENT OF A HIGH STRENGTH ISOTHERMALLY HEAT-TREATED NODULAR IRON ROAD WHEEL ARM Final Report, Mar. 1983 - Mar. 1985
A. R. Moore and L. Geer 31 Mar. 1985 98 p
(Contract DAAE07-83-C-R051)
(AD-A155755; TACOM-TR-13091) Avail: NTIS HC A05/MF A01 CSCL 19/3

This report describes the redesign, material characterization, material selection, manufacture, and testing of a proposed road wheel arm for the M-1 tank. The material selected is bainitic ductile iron (BDI). This material, made by the casting process and heat-treatment, takes advantage of the toughness of bainite (acicular ferrite), the ability of the casting process to make a complex shape, and a 10 percent lighter than steel weight. A further advantage is its relatively low cost compared to a steel forging. A set of 14 road wheel arms were made and assembled. Dynamic tests on the design passed the 650,000 cycle specification, going beyond one million cycles. A 35 pound or 27 percent weight savings per arm was achieved, and based on figures obtained during the project, a considerable cost reduction can be effected. GRA

N85-35409# Colorado School of Mines, Golden.
UNITED STATES ARMY WELDING RESEARCH AND DEVELOPMENT TOPICAL AND COORDINATION MEETING Final Report, 7 Dec. 1984 - 6 Dec. 1985
D. L. Olson Mar. 1985 25 p
(Contract DAAG29-85-M-0101)
(AD-A155834; MT-CWR-85-001; ARO-22674.1-MS-CF) Avail: NTIS HC A02/MF A01 CSCL 13/8

The United States Army Welding Research and Development Topical and Coordination Meeting, February 5 to 8, 1985 was held at the Colorado School of Mines to achieve the following objectives: (1) identify the technical expertise at each of the U.S. Army welding research facilities and to increase communication between facilities; (2) methods for information exchange will be established (i.e., establish annual Army Welding Research meetings; (3) possible solutions to specific technical joining and assembly problems will be introduced and discussed; and (4) potential research projects will be identified which have the greatest possibility of being meaningful to the U.S. Army concerns. GRA

N85-35410# Applied Concepts Corp., Woodstock, Va.
INVESTMENT JUSTIFICATION OF ROBOTIC TECHNOLOGY IN AEROSPACE MANUFACTURING. USER'S MANUAL Final Report, 21 Feb. - 28 Sep. 1984
J. A. Simpson Oct. 1984 80 p
(Contract F33615-83-C-5080)
(AD-A156193; BRMC-83-5080-3) Avail: NTIS HC A05/MF A01 CSCL 05/3

A computer program summary of the results of a three phased research program entitled Investment Justification of Robotic Technology in Aerospace Manufacturing, whose objective was to develop a computerized economic analysis methodology appropriate for investment justification of robotics and flexible manufacturing systems (FMS) in aerospace manufacturing is presented. A microcomputer-based economic justification methodology was developed, called the Robotics Investment Decision Model (RIDM). In Phase 1 a nation-wide survey was performed of robotics investment analysis methodologies used or proposed by government, industry, and academia. The survey included discussions with financial, engineering, and management personnel at eight major U.S. aerospace corporations, to determine their needs and constraints, and how a model might best be designed. Phase 2 was the model development phase. The model was written as a Lotus 1-2-3 template, and is called the Robotics Investment Decision Model. Phase 3 was a review and field test of the model, RIDM was demonstrated to several USAF organizations, and was assessed by a major U.S. aerospace manufacturer. Internal testing continued, improving RIDM through several format changes, one minor technical change, and adding a few new features. The model is now ready for release to the aerospace industry. GRA

N85-35411# Army Engineer Waterways Experiment Station, Vicksburg, Miss. Geotechnical Lab.
STATE-OF-THE-ART CONSTRUCTION TECHNOLOGY FOR DEEP TUNNELS AND SHAFTS IN ROCK Final Report
R. D. Bennett, H. J. Hignett, S. Johansson, D. M. Patrick, and P. A. Taylor Jan. 1985 476 p
(AD-A156362; AD-E900463; WES/MP/GL-85-1) Avail: NTIS HC A21/MF A01 CSCL 08/9

This study was part of the initial planning efforts for the deep-based missile system, but the methods described are applicable to a wide range of projects and conditions. As far as possible, all the construction methods in this report are discussed from the point of view of production rates, costs, and appropriate conditions. All known methods for tunnel and shaft excavation, muck and material transport, support and lining, ground stabilization and ground-water control, and auxiliary operations are described. General guidelines are given to assist in the selection of specific methods and equipment. Manufacturer's specifications and cost and performance data are included in the appendices to assist in this selection and to support the statements and conclusions made in this report. GRA

N85-35412# Sandia Labs., Albuquerque, N. Mex.
TESTBED FOR SENSORY CONTROL OF INTELLIGENT MACHINES
G. W. Donohoe 1985 13 p Presented at EPES '85 - Energy, Power and Environ. Systems Intern. Conf., Santa Barbara, Calif., 29 May 1985
(Contract DE-AC04-76DP-00789)
(DE85-012355; SAND-85-0173C; CONF-8505122-1) Avail: NTIS HC A02/MF A01

The development of the sensory control of robots to perform human-like tasks in hostile environments, such as the remote maintenance of a nuclear reactor is described. Such a robot should be able to operate in a relatively unstructured environment. It should be able to monitor the progress of a task, verifying that things are proceeding as planned. If they are not, the robot should be able to detect this and take corrective action. A sensor-driven robot testbed for exploring these issues was constructed. DOE

38 QUALITY ASSURANCE AND RELIABILITY

Includes product sampling procedures and techniques; and quality control.

N85-35413 Texas Technological Univ., Lubbock.
RELIABILITY PREDICTION OF THE SERIES SYSTEM WITH

SPARES SUBJECT TO WEIBULL FAILURE Ph.D. Thesis
Jeh-Nan Pan 1984 196 p
Avail: Univ. Microfilms Order No. DA8507455

A mathematical model for predicting the system reliability of a series system with spares subject to Weibull failures is developed. Many modern equipment systems are designed in a series configuration with spares available when necessary. The Weibull distribution is one of the most widely applied and flexible failure distributions used to describe and model present day single component systems. Due to the theoretical intractability of the Weibull distribution in spares models, it is extremely difficult to solve the multiple integration involved in this type of model analytically. Therefore, a numerical integration method using Simpson's Rule was selected as a tool to address the problem of multiple integration of the Weibull distribution. Then, a recursive algorithm was developed for the reliability prediction of a series system with spares subject to a general failure model (including the Weibull distribution). The developed model has been validated for accuracy using a two component series system with spares. A sensitivity analysis has also been performed on the two parameters of the Weibull distribution, and the effect of adding spares or stages on the system reliability has been assessed. Dissert. Abstr.

N85-35414# Sandia Labs., Albuquerque, N. Mex.
A KINETIC MODEL FOR PREDICTING OXIDATIVE DEGRADATION RATES IN COMBINED RADIATION-THERMAL ENVIRONMENTS
K. T. Gillen and R. L. Clough 1985 10 p refs Sponsored in part by Nuclear Regulatory Commission and DOE
(TI85-002629; SAND-84-2097C) Avail: NTIS HC A02/MF A01

The use of accelerated aging tests for making predictions of material life expectancy, especially in combined radiation and temperature environments is discussed. Strong dose-rate and synergistic effects of combined radiation/temperature/air environments were observed for a stabilized polyvinyl-chloride (PVC) cable jacketing material and a polyethylene insulation material. It is shown that one major cause of these effects is a chemical mechanism involving thermally-induced breakdown of intermediate peroxides initially formed by the radiation. The complicated combined radiation-thermal aging responses for the PVC jacketing material is examined. A general theoretical kinetic model is formulated which can be utilized to explain radiation dose-rate effects, synergistic effects of radiation and temperature, and sequential aging behavior. E.A.K.

39 STRUCTURAL MECHANICS

Includes structural element design and weight analysis; fatigue; and thermal stress.

For applications see *05 Aircraft Design, Testing and Performance* and *18 Spacecraft Design, Testing and Performance.*

N85-35415 Maryland Univ., College Park.
ANALYSIS OF THE NONLINEAR EQUATIONS DESCRIBING THE ELASTIC, THERMAL, AND ELECTROMAGNETIC BEHAVIOR OF SOLIDS: EXISTENCE OF SOLUTIONS OF SEMI-INVERSE PROBLEMS Ph.D. Thesis
Robert Charles Rogers 1984 121 p
Avail: Univ. Microfilms Order No. DA8508527

The development of a properly general, unified constitutive theory for materials with elastic, thermal, and electromagnetic properties is proposed. A systematic and rational development of the equilibrium equations for such materials in material coordinates is presented. Great care is taken to link mathematical considerations (e.g., the desire to deal with a quasilinear system of partial differential equations) with physical considerations (the form of the Maxwell stress tensor). The utility of this unified formulation is demonstrated by proving the existence and regularity of solutions for a large class of semiinverse problems involving wedges and tubes of material which are deformed, heated, polarized, and magnetized. Monotonicity and compactness methods are used to handle the more intricate global problems associated with the quasilinear integro-differential equations describing media sustaining constant electric currents. In all cases, the Strong Ellipticity Condition stands out as the most important constitutive assumption. Dissert. Abstr.

N85-35416 California Inst. of Tech., Pasadena.
STRUCTURAL ANALYSIS OF IMPERFECT THREE-LEGGED TRUSS COLUMNS FOR LARGE SPACE STRUCTURES APPLICATIONS Ph.D. Thesis
Dov Elyada 1985 198 p
Avail: Univ. Microfilms Order No. DA8508458

Three-legged truss columns are basic structural components of many envisioned large outer-space structures. They constitute three longerons (legs) forming, in the column cross-section, the vertices of an equilateral triangle. Their longerons are held together by uniformly spaced battens while a shear web, usually made of diagonals, restrains shear deformation. This work deals with configurations characterized by having relatively stiff battens, longerons which are pinned to the battens and prestressed string diagonals. Considered are only simple-supported slender columns having slender longeron segments and relatively thin and lightly preloaded diagonals. The columns are allowed to have global (overall) as well as local (longeron segment) geometrical imperfections--not necessarily small ones. Investigated is the static structural behavior of such columns when loaded by purely axial compressive concentrated forces acting at the supports. Dissert. Abstr.

N85-35417 Texas Univ., Austin.
DESIGN AND BEHAVIOR OF COPED BEAMS Ph.D. Thesis
Jung-June Cheng 1984 273 p
Avail: Univ. Microfilms Order No. DA8508258

The behavior of coped beams with various coping details was examined by conducting a theoretical parametric study using the elastic and inelastic finite element programs BASP and ABAQUS. The design models and recommendations or different types of coped connections (top, bottom and double coped) are made according to the behavior and results of the analytical studies. In addition to yielding, coped beams can fail in two distinct instability modes, lateral-torsional buckling over the span and local web buckling at the cope region. Simple interaction equations, which utilize the individual lateral buckling capabilities of the coped region and the uncoped length, were developed for design of lateral buckling of top (compression) flange coped beams and double coped beams. Copes on the bottom (tension) flange reduced the lateral buckling capacity 10 percent of the uncoped case. A plate buckling model was developed to check for web buckling in compression flange coped beams and a lateral buckling model was adopted for web buckling in double flange coped beams.
Dissert. Abstr.

N85-35418 California Univ., Davis.
VIBRATIONS OF FREE HOLLOW CIRCULAR CYLINDRICAL BODIES Ph.D Thesis
Sanusi Abdelwahab El-Azhari 1984 218 p
Avail: Univ. Microfilms Order No. DA8507297

A series solution of the general three-dimensional equations of linear elasticity is developed and used to find accurate natural frequencies for the vibrations of isotropic elastic hollow circular cylindrical bodies with traction-free surfaces. The present approach involves combining exact solutions of the governing equations, which term-by-term satisfy most of the shear stress boundary conditions. The boundary conditions on the normal stress, and the remaining shear stress are satisfied by orthogonalization. This leads to an eigenvalue matrix the size of which is equal to the number of terms in each series. The frequencies at which the determination of this matrix is zero are the natural frequencies of the cylindrical body. The accuracy of the final solution depends on how well the boundary conditions are satisfied by orthogonalization. It is found that the solution converges monotonically as more

terms in the series are chosen, and it is shown that very few terms produce excellent results for some frequencies.
Dissert. Abstr.

N85-35419 Syracuse Univ., N. Y.
STRESS ANALYSIS OF AXISYMMETRIC SANDWICH SHELLS OF VARIABLE THICKNESS Ph.D. Thesis
Renjie Mao 1984 214 p
Avail: Univ. Microfilms Order No. DA8508230

An axisymmetric sandwich shell is considered that is made of two face sheets and a honeycomb-type core, the thicknesses of which may vary longitudinally. Both core and face sheets may be orthotropic, with principal directions of orthotropy in the meridian and latitude directions. Based on an energy principle, a complete set of first-order partial differential equations are derived for the sandwich shell, taking into account the contribution of the face sheets in carrying transverse shear. Transverse normal strain of the core and thermal effects are also taken into account. For the case of a closed shell, the Fourier series method combined with a finite-difference scheme is used to reduce the partial differential equations to a set of linear algebraic equations, which is solved by the Riccati transfer-matrix method. For shell segments, the finite-difference method, the finite-difference energy method and the finite-element energy method are used and compared with each other. The systems of linear algebraic equations resulting from these methods are solved by the method of chasing.
Dissert. Abstr.

N85-35420 Connecticut Univ., Storrs.
DEVELOPMENT AND APPLICATION OF A UNIFIED VISCO-ELASTIC CONSTITUTIVE MODEL FOR THE PREDICTION OF MATERIAL RESPONSE UNDER THERMOMECHANICAL LOADING Ph.D. Thesis
Vito Moreno, Jr. 1984 193 p
Avail: Univ. Microfilms Order No. DA8508759

Results of a research program conducted to develop and apply a unified constitutive model to the prediction of material stress-strain behavior at elevated temperatures are presented. Specifically, a model that represents inelastic behavior as coupled plastic and creep response was developed for a nickel base alloy, Hastelloy X, subjected to thermomechanical cycles in which both the mechanical strain and temperature are simultaneously changing. The basis for the constitutive model is the unified approach first proposed by Bodner who demonstrated the capability to predict the time-dependent isothermal inelastic behavior of a wide range of metal alloys. Adaptation of the approach to Hastelloy X for variable temperature loading cycles required significant modification of the original model. Among the issues addressed are the methods of determination of model constants for proper strain rate dependence, formulation of the internal state variable for the prediction of cyclic thermal recovery effects, and the necessity of a transient temperature rate formulation for the internal state variable.
Dissert. Abstr.

N85-35421 Defence Research Information Centre, Orpington (England).
STRAIN MEASUREMENT USING POINT RECOGNITION PICTURE PROCESSING
G. Yagawa, S. Matsuura, and Y. Ando Mar. 1985 25 p refs Transl. into ENGLISH of Japan Soc. Mech. Eng., Ser. A., v. 49, no. 447 (1983) p 1435-1443
(DRIC-T-7407; BR94271) Copyright. Avail: Issuing Activity

A technique for measuring the deformation of metal plate specimens under high rates of strain and high temperature is described. A grid of punchmarks is monitored by a television camera whose image is digitized and computer processed. Comparison with predictions of a finite element code shows satisfactory agreement.
Author (ESA)

N85-35422 Defence Research Information Centre, Orpington (England).
1983 REVIEW OF EXPERIMENTAL STRESS AND STRAIN ANALYSIS
T. Fujiyoshi Apr. 1985 33 p refs Transl. into ENGLISH of Japan. J. of NDI, v. 33, no. 6, 1984 p 426-433
(DRIC-T-7469; BR94501) Copyright. Avail: Issuing Activity

Stress and strain measurement using computers, in high temperature environments measurement of residual stress and impact stress, ultrasonic stress and strain measurement, stress amplification factor measurement, evaluation of static fracture properties evaluation fatigue and dynamic fracture properties, crack detection, photoelasticity, strain gages, and moire methods are discussed.
Author (ESA)

N85-35423*# Lockheed Missiles and Space Co., Huntsville, Ala. Research and Engineering Center.
STUDY OF NSI AND RELATED CABLE PERFORMANCE DURING TESTS PERFORMED IN THE NASA HOT GAS FACILITY
Zain S. Karu Jan. 1982 32 p
(Contract NAS8-32982)
(NASA-CR-170886; NAS 1.26:170886; LMSC-HREC-TM-D784644)
Avail: NTIS HC A03/MF A01 CSCL 20K

Some seven different configurations of the NSI and other cables were tested in the NASA-MSFC Hot Gas Facility (HGF). The tests were conducted to study what happens to the cables when they are exposed to hot flow as was the case in the first two Shuttle flights, the STS-1 and STS-2. Protection of these components is vital for various functions especially to attain proper nozzle separation. The tests in the HGF demonstrated the severity of the aerodynamic forces combined with aero heating environment on the test cables and helped, in general, to evaluate the cable wrap materials and cable mounting hardware and technique. Blastape 2 cable wrap which is adequate for thermal protection of the cables must be properly clamped at its ends. The nylon clamps (or ties) used to secure cables to metal components inside the skirt could not withstand the heating. K5NA closeout material used on the outboard surface of the aft skirt when troweled over the cables performed excellently in protecting the cables and mounting hardware.
Author

N85-35424*# National Aeronautics and Space Administration. Langley Research Center, Hampton, Va.
STRESS-INTENSITY FACTORS FOR CIRCUMFERENTIAL SURFACE CRACKS IN PIPES AND RODS UNDER TENSION AND BENDING LOADS
I. S. Raju (Analytical Services and Materials, Inc.) and J. C. Newman, Jr. Aug. 1985 36 p refs
(NASA-TM-87594; NAS 1.15:87594) Avail: NTIS HC A03/MF A01 CSCL 20K

The purpose of this paper is to present stress-intensity factors for a wide range of nearly semi-elliptical surface cracks in pipes and rods. The configurations were subjected to either remote tension or bending loads. For pipes, the ratio of crack depth to crack length (a/c) ranged from 0.6 to 1; the ratio of crack depth to wall thickness (a/t) ranged from 0.2 to 0.8; and the ratio of internal radius to wall thickness (R/t) ranged from 1 to 10. For rods, the ratio of crack depth to crack length also ranged from 0.6 to 1; and the ratio of crack depth to rod diameter (a/D) ranged from 0.05 to 0.35. These particular crack configurations were chosen to cover the range of crack shapes (a/c) that have been observed in experiments conducted on pipes and rods under tension and bending fatigue loads. The stress-intensity factors were calculated by a three-dimensional finite-element method. The finite-element models employed singularity elements along the crack front and linear-strain elements elsewhere. The models had about 6500 degrees of freedom. The stress-intensity factors were evaluated using a nodal-force method.
B.W.

N85-35425# Airtech Precision Shot Peening, Livonia, Mich.
DEVELOPMENT OF A MATHEMATICAL MODEL FOR PREDICTING THE PERCENTAGE FATIGUE LIFE INCREASE RESULTING FROM SHOT PEENED COMPONENTS Final Report, Sep. 1983 - Apr. 1984
R. S. Simpson Wright-Patterson AFB, Ohio AFWAL Apr. 1985 47 p
(Contract F33615-83-C-3252)

(AD-A155774; AFWAL-TR-84-3116) Avail: NTIS HC A03/MF A01 CSCL 12/1

Shot peening is used extensively in many aircraft structural and engine applications to enhance fatigue life and stress corrosion resistance. Recent research indicates that high shot peening intensities can produce a phenomenon called peened surface extrusion folds (PSEF) which is hypothesized to result in fatigue life reductions. In this investigation more than one hundred specimens of 7075-T6 and 7075-T73 aluminum material were manufactured and treated at various levels of shot peening intensity, almen saturation level, and peening media size. Specimens were subsequently fatigue tested under axial loading conditions. The longest fatigue life was obtained at relatively low almen intensities with the smallest size glass bead at 100 to 110% almen saturation. Intensity vs fatigue life patterns were similar for both materials. The optimum intensity level was substantially below that specified in MIL-STD-852. Scanning electron microscopy and metallography showed increasing depth and quantity of PSEF and embedded glass bead particles at the surface as peening intensity increased. Test work demonstrated statistically significant effects of PSEF, embedded glass particles, percent of almen saturation, part material hardness, and peening media size on specimen fatigue life. Multiple linear statistical regression of these four variables accounted for a high percentage of the variance in specimen fatigue life. Author (GRA)

N85-35426# Harvard Univ., Cambridge, Mass. Div. of Applied Sciences.

ON SIZE EFFECTS IN PLANE STRESS CRACK-GROWTH RESISTANCE

B. Budiansky and E. E. Sumner, Jr. Apr. 1985 9 p
(Contract N00014-84-K-0510; Grant NSF MEA-82-13925)
(AD-A155926; MECH-68) Avail: NTIS HC A02/MF A01 CSCL 20/11

For a ductile material, the tearing resistance curve represented by the dependence of the fracture parameter J on crack extension delta(a) is a material property only for the small-scale yielding conditions that are approached for very large specimen size. In this paper the influence of size on crack-growth resistance is studied theoretically for single-edge-notch (SEN) specimens of ideally-plastic materials in plane stress. The calculations are based on the Dugdale model in conjunction with a crack-growth criterion defined by an invariant crack-opening shape. Over a large range of specimen sizes, results are exhibited for materials having low-to-moderate values of initial tearing resistance. GRA

N85-35427# Naval Weapons Center, China Lake, Calif.

EXPERIMENTAL DATA FOR CHARACTERIZING PERFORATING IMPACTS: FRAGMENTATION PROCESSES Technical Publication, Fiscal Year 1981 - 1982

M. E. Backman and S. A. Finnegan May 1985 99 p
(ZR0-0001)
(AD-A156370; AD-E900463; NWC-TP-6490) Avail: NTIS HC A05/MF A01 CSCL 19/1

The impact of compact projectiles against plates has been investigated to improve the phenomenological description of the impact and perforation processes, especially at those speeds at which the projectile and target show significant breakup. This investigation identifies and characterizes the internal failure processes involved in perforation and fragmentation. It employs momentum and energy balances to characterize the dynamics of the system of fragments expelled following perforation. GRA

N85-35428# Army Engineer Waterways Experiment Station, Vicksburg, Miss.

USER'S GUIDE: A COMPUTER PROGRAM FOR STRENGTH ANALYSIS OF NON-HYDRAULIC CONCRETE STRUCTURAL ELEMENTS. REPORT 1. CONCRETE GENERAL STRENGTH INVESTIGATION (CGSI) Instruction Report

W. A. Price, III, M. D. Davister, and M. E. George Sep. 1984 48 p
(AD-A156392; WES/IR/K-84-10-1) Avail: NTIS HC A03/MF A01 CSCL 09/2

Strength investigation on nonhydraulic beams and columns defines the program described in this user's guide. The program, obtained from another agency and adapted to Corps of Engineers usage, applies a fundamental theory and, therefore, is not code-dependent. This program Concrete General Strength Investigation (CGSI), and another program, Portland Cement Association's PCAUC, complement each other in their capabilities and their equipment requirements. Author (GRA)

N85-35429# Army Engineer Waterways Experiment Station, Vicksburg, Miss.

USER'S GUIDE: A COMPUTER PROGRAM FOR STRENGTH ANALYSIS OF NON-HYDRAULIC CONCRETE STRUCTURAL ELEMENTS. REPORT 2. STRENGTH DESIGN OF REINFORCED CONCRETE COLUMN SECTIONS (PCAUC) Instruction Report

C. C. Hamby, D. K. Martin, and W. E. Galyean Sep. 1984 40 p
(AD-A156393; WES/IR/K-84-10-2) Avail: NTIS HC A03/MF A01 CSCL 09/2

Strength investigation on nonhydraulic beams and columns and strength design of nonhydraulic columns define the program described in this user's guide. The program Strength Design of Reinforced Concrete Column Sections (PCAUC) obtained from the Portland Cement Association and adapted to Corps of Engineers usage, applies a fundamental theory and, therefore, is not code-dependent. This program, Portland Cement Association's PCAUC, and another program, Concrete General Strength Investigation (CGSI), complement each other in their capabilities and their equipment requirements. Program PCAUC may be used to design and/or investigate reinforced concrete compression members. There is no graphics output for results from this program. Program CGSI investigates the strength of a reinforced concrete member with cross sections subjected to combined axial load and biaxial bending. Results are presented in graphical form. Neither of the programs considers shear. GRA

N85-35430# George Washington Univ., Washington, D.C. School of Engineering and Applied Science.

PREDICTION OF PLASTICITY CHARACTERISTICS FOR THREE-DIMENSIONAL FRACTURE SPECIMENS COMPARISON WITH EXPERIMENT

E. T. Moyer, Jr., P. K. Poulose, and H. Liebowitz 1985 40 p
(Contract N00014-84-K-0027)
(AD-A156425) Avail: NTIS HC A03/MF A01 CSCL 11/9

A center-cracked panel of 7075-Aluminum alloy which has overaged from the T651 condition was loaded in tension and subsequently unloaded to zero applied load. The permanent surface deformation was measured close to the intersections of the crack front with the free surfaces. The permanent deformation (being a good indicator of the extent of plastic deformation) was used to measure the accuracy of finite element analysis. The same specimen was modeled using 20-node three-dimensional isoparametric elements. A fully incremental elastic-plastic formulation was employed in the stress analysis. The residual surface deformations after unloading were compared to the experimental results. The average experimental results compare quite favorably with the finite element predictions. The average results were employed to minimize the influence of material inhomogeneity, load misalignment, and lack of symmetry in the fatigue crack. The scatter in the results from measuring the different sides is discussed.
Author (GRA)

N85-35431# Los Alamos National Lab., N. Mex.

EVALUATION OF THE CRACK PLANE EQUILIBRIUM MODEL FOR PREDICTING PLASTIC FRACTURES

T. A. Butler and F. W. Smith 1985 17 p refs Presented at the ASME Pressure Vessel and Piping Div. Conf., New Orleans, 24 Jun. 1985
(DE85-005558; LA-UR-84-4017; CONF-850670-1) Avail: NTIS HC A02/MF A01

The Crack Plane Equilibrium (CPE) model is a simple model for predicting the initiation of crack growth in ductile materials. The CPE model is evaluated for center-crack tension specimens and for pipe specimens containing part-through circumferential

cracks emanating from the inside surface of the pipe. The model is based upon requiring equilibrium between the applied loads and an assumed stress distribution in the uncracked ligament near the crack tip. Required fracture parameters are the ultimate tensile strength and a process zone size at the crack tip that is determined from simple fracture tests. Crack growth initiation for the crack and specimen geometries studied is predicted with sufficient accuracy to warrant extending the CPE model for investigating other geometries and for predicting stable crack growth and the onset of unstable crack growth. DOE

N85-35432# Argonne National Lab., Ill.
RESPONSE OF A BWR MARK 2 CONTAINMENT VESSEL HEAD TO LOADS BEYOND THE DESIGN BASIS
R. F. Kulak, J. E. Ash, J. M. Kennedy, and B. J. Hsieh 1985 13 p refs Presented at the 8th Intern. Conf. on Struct. Mech. in Reactor Technol., Brussels, 19 Aug. 1985
(Contract W-31109-eng-38)
(DE85-010524; CONF-850809-55) Avail: NTIS HC A02/MF A01

A simulation of the macrodeformations of the sealing surfaces between the removable drywell head and the conical shell of a Mark 2 containment vessel head during a severe accident is presented. This junction contains two continuous gaskets in a configuration classified as nonpressure seating. The behavior of this junction to pressure and thermal loadings is examined. DOE

N85-35433# South Carolina Univ., Columbia. Dept. of Civil Engineering.
STATIC AND CYCLIC BEHAVIOR OF SEMI-RIGID STEEL BEAM-COLUMN CONNECTIONS Final Report
A. Azizinamini, J. H. Bradburn, and J. B. Radziminski Mar. 1985 234 p refs
(Grant NSF CEE-81-15014)
(PB85-194363; NSF/ENG-85003) Avail: NTIS HC A11/MF A01 CSCL 13M

The behavior of semirigid beam to column connections subjected to static and cyclic loadings was investigated. Bolted connections comprised of top and seat beam flange angles and double web angles, to evaluate cyclic performance under constant amplitude and variable amplitude displacements and to determine moment rotation behavior under static loading. From the constant amplitude cyclic tests, linear log-log equations were established. Empirical relationships established by the tests were applied to a linear cumulative damage model and the results of several variable amplitude block cyclic tests are compared with damage summations predicted by the model. Geometric parameters which affect connection performance were quantified by the static tests and are compared with analytical models to predict initial stiffness and complete nonlinear moment rotation behavior of the connections. Author

N85-35434# Agbabian Associates, El Segundo, Calif.
AN EVALUATION OF A CLASS OF PRACTICAL OPTIMIZATION TECHNIQUES FOR STRUCTURAL DYNAMICS APPLICATIONS Final Report, 18 Apr. 1982 - 31 Mar. 1985
S. F. Masri and S. D. Werner Mar. 1985 74 p refs
(Grant NSF CEE-81-11964)
(PB85-195766; NSF/ENG-85007; AA-R-8222-5817) Avail: NTIS HC A04/MF A01 CSCL 13B

This report evaluates a class of practical optimization techniques for parameter identification of realistic structural dynamic systems. The techniques involve quasi-Newton methods together with an efficient procedure for estimating complicated error functions. The optimization procedures are verified through their application to several representative examples, including finite element models of realistic structural systems. Extensive numerical and graphical results demonstrate the effects of various optimization algorithm parameters on the rate of convergence of the objective function, the parameter vector error norm, and the gradient norm. Guidelines are presented as an aid for addressing several significant issues in the practical application of structural dynamics optimization procedures. GRA

N85-35249# European Space Agency, Paris (France).
DAMAGE MECHANISMS IN DAMAGED CFRP LAMINATES
L. Kirschke *In its* Contrib. to the Properties of Carbon Fiber Reinforced Composites (DFVLR-Mitt-83-16) Jul. 1984 p 155-204 Transl. into ENGLISH from "Beitraege zum Verhalten kohlefaser-verstaerkter Verbundstrukturen" rept. DFVLR-Mitt-83-16 DFVLR, Brunswick, Jan. 1983 p 145-189 Original language document was announced as N84-19483 (For primary document see N85-35246 24-24)
Avail: NTIS HC A13/MF A01; original German version available from DFVLR, Cologne DM 89

42 GEOSCIENCES (GENERAL)

N85-35435# Geological Survey, Alexandria, Va.
USGS RESEARCH ON MINERAL RESOURCES, 1985
Kathleen Krafft, ed. 1985 81 p refs Proc. of the 1st V. E. McKelvey Forum on Mineral and Energy Resources, Alexandria, Va., 6-7 Feb. 1985
(Circ-949) Avail: NTIS HC A05/MF A01

Various topics related to mineral resources are discussed. Mineral exploration, brines, geochemistry, underwater resources, magnetic signatures, gas analysis are discussed. For individual titles, see N85-35436 through N85-35460.

N85-35436# Chevron Oil Field Research Co., La Habra, Calif.
CHEMISTRY OF ORE-FORMING FLUIDS Abstract Only c46
Robert J. Bodnar, I-Ming Chou, and Edwin Roedder *In* Geological Survey USGS Res. on Mineral Resources, 1985 1985 p 1-3 (For primary document see N85-35435 24-42)
Avail: NTIS HC A05/MF A01

The phase relations of such fluid inclusions, which may contain many daughter crystals formed during cooling, can provide semiquantitative and in part, quantitative data on their composition. Knowledge of the chemistry of such fluids is essential to understanding the processes involved in ore transport and deposition. However, the interpretation of fluid inclusion data is hindered by the lack of data on salt solubilities and on volumetric properties of brines at elevated temperature. Volumetric (PVTX) properties of H2O-NaCl compositions of 30, 50, and 70 weight percent NaCl have been determined experimentally over the range 20 to 900 C and 0.5 to 5 kbar. These results were combined with other available volumetric data for H2O-NaCl to generate a single equation for specific volume as a function of temperature pressure and composition. R.J.F.

N85-35437# Geological Survey, Alexandria, Va.
AEROMAGNETIC AND RADIOMETRIC SIGNATURES OF A POSSIBLE PORPHYRY SYSTEM IN THE WESTERN TUSHAR MOUNTAINS, UTAH Abstract Only c43
David L. Campbell, James A. Pitkin, Joseph S. Duval, Thomas A. Steven, Charles G. Cunningham, and C. W. Naeser *In its* USGS Res. on Mineral Resources, 1985 1985 p 3-4 (For primary document see N85-35435 24-42)
Avail: NTIS HC A05/MF A01

Geologic mapping, petrologic analysis, isotopic dating, geochemical sampling, and geophysical studies have identified several areas in the western Tushar Mountains, Utah, that may be underlain by mineralized intrusive systems containing molybdenum, uranium, and other valuable metals. One of these areas is near Indian Creek, 18 km north of Beaver, Utah, where there may be a multiple intruded mineralized stock. Several lines of evidence were pulled together to make this interpretation, providing a good example of synergism in geological research. The geophysical component of these studies is focused upon. R.J.F.

N85-35438# Geological Survey, Alexandria, Va.
SOME GEOPHYSICAL GUIDES TO ORE IN SOUTHERN AND SOUTHWESTERN ALASKA Abstract Only c46
In its USGS Res. on Mineral Resources, 1985 1985 p 5-7 (For

primary document see N85-35435 24-42)
Avail: NTIS HC A05/MF A01

In southern Alaska, massive sulfide deposits are associated with Late Cretaceous Paleogene pillow basalt, sheeted dikes, and overlying flysch deposits. Most such mafic assemblages in Prince William Sound are characterized by prominent positive gravity anomalies. Magnetic anomalies over the volcanic belts are positive, but their amplitudes range widely. Where massive sulfide deposits occur on Knight Island and the Ellamar Peninsula, magnetic anomalies are relatively flat or negative--a strong indication of hydrothermal alteration accompanying mineralization. To the north and west, a belt of late Mesozoic gabbros, diorites, and ultramafic rocks of the northern Chugach Range and western Kenai Peninsula is indicated by large positive gravity and magnetic anomalies. These rocks may contain chromite, massive sulfide, magnetite, and gold deposits. The gravity and magnetic anomalies show that the complex continues beneath glaciers, alluvial cover, and water covered areas. R.J.F.

N85-35439# Geological Survey, Alexandria, Va.
MARINE PHOSPHORITE DEPOSITS MODEL FOR EXPLORATION, WITH EMPHASIS ON DEPOSITS IN THE US ATLANTIC COASTAL PLAIN Abstract Only **c43**
James B. Cathcart *In its* USGS Res. on Mineral Resources, 1985 1985 p 7 (For primary document see N85-35435 24-42)
Avail: NTIS HC A05/MF A01

Phosphorus is an essential element for growth in plants and animals; its principal source is deposits of phosphate rock. Onshore deposits of phosphorite, a marine sedimentary rock, constitute about 80 percent of the world's phosphate resources and are the source for about 80 percent of world production. Identified resources (reserve base) of phosphorite in the world are estimated to be about 69 billion metric tons containing at least 25 percent P2O5, and resources in deposits that may become economic are thought to be about double the identified resources. Deposits on the sea floor form an additional, probably enormous, resource. R.J.F.

N85-35440# Geological Survey, Alexandria, Va.
THE ROLE OF REGIONAL SUBSURFACE GEOCHEMISTRY IN RESOURCE ASSESSMENT IN THE CENTRAL UNITED STATES Abstract Only **c46**
R. L. Erickson, E. L. Mosier, J. G. Viets, and M. S. Erickson *In its* USGS Res. on Mineral Resources, 1985 1985 p 10-11 (For primary document see N85-35435 24-42)
Avail: NTIS HC A05/MF A01

Regional subsurface geochemical studies are an integral part of the U.S. Geological Survey program for assessing the mineral resource potential of platform carbonates in the Central United States. Much of this area is flat to gently rolling agricultural land, outcrops are few, and the known favorable host rocks are at depths ranging from a few hundred meters to more than a kilometer. Thus, traditional surface geochemical techniques are of little use in this area for evaluating the potential for the occurrence of concealed or undiscovered mineral deposits. Geochemical studies of subsurface Cambrian strata in the Rolla 1 deg X 2 deg quadrangle. Missouri, completed in 1980, and current geochemical studies in the Springfield Joplin, and Harrison 1 deg X 2 deg quadrangles, which cover about 80,000 km2 in parts of Missouri, Kansas, and Arkansas, indicate that insoluble residues of carbonate rocks are a useful and informative geochemical sample medium in a carbonate environment. R.J.F.

N85-35441# Geological Survey, Alexandria, Va.
HEAT TRANSFER AND BRINE EVOLUTION IN MAGMA-HYDROTHERMAL SYSTEMS Abstract Only **c46**
Robert O. Fournier *In its* USGS Res. on Mineral Resources, 1985 1985 p 13 (For primary document see N85-35435 24-42)
Avail: NTIS HC A05/MF A01

The anism (or mechanisms) by which heat is transferred from magma to a surrounding hydrothermal system is discussed. Mechanisms that have been proposed include: (1) conduction, (2) transfer of heat by movement of water and volatiles out of the magma, and (3) circulation of meteoric water into a thin zone of thermal cracking that migrates inward towards the magma with time as the rocks cool. Our present knowledge of hydrothermal mineral deposits and active geothermal systems demonstrates the importance of interaction between shallow dilute meteoric water and deeper brines. The highly concentrated brines thus far encountered in active hydrothermal systems are all in environments in which the waters may have interacted with evaporites. Experimental data, however, indicate that highly saline as well as moderately concentrated brines may evolve from a crystallizing magma, depending on the initial water and chloride contents and the depth of crystallization. R.J.F.

N85-35442# Geological Survey, Alexandria, Va.
AEROMAGNETIC AND GRAVITY MODELS OF THE PLUTON BELOW THE LAKE CITY CALDERA, COLORADO Abstract Only **c43**
V. J. S. Grauch *In its* USGS Res. on Mineral Resources, 1985 1985 p 15-16 (For primary document see N85-35435 24-42)
Avail: NTIS HC A05/MF A01

Aeromagnetic and gravity data collected over the Lake City caldera, San Juan Mountains, Colorado, were used to calculate models of the pluton below the caldera. Magnetic data are from a draped airborne survey and are in digital form. Gravity data were assembled from the Department of Defense files and were combined with more recent data collected across the caldera. Both data sets were gridded and contoured in map form and also examined in profile form. Regional trends were removed where necessary and data were continued upward mathematically, to enhance the effect of the subsurface pluton over the effects of shallow sources. Geologic mapping revealed isolated outcrops of quartz syenite inside the caldera. It was inferred that these rocks were intruded at the time of resurgence of the caldera. R.J.F.

N85-35443# Geological Survey, Alexandria, Va.
ORIGIN OF SEDIMENTARY HUMIC ACIDS, POTENTIAL CARRIERS OF ORE-FORMING ELEMENTS Abstract Only **c46**
Patrick G. Hatcher *In its* USGS Res. on Mineral Resources, 1985 1985 p 21-22 (For primary document see N85-35435 24-42)
Avail: NTIS HC A05/MF A01

Humic acids are complex, macromolecular organic components of sediments and are defined by their solubility in dilute alkali insolubility in dilute acid. Because of their general structural characteristics (for example, their high proportion of oxygen functional groups), humic acids can complex with inorganic cations and may be important in forming ore deposits. In some instances (such as uranium ores), ore bodies are believed to have originated by mobilization of an ore-forming element complexed with humic acids and subsequent precipitation. Knowledge of the mechanism for the formation of humic acids is being applied to two major ore deposits. Carlin-type gold ores from Nevada show that humic acids may have been precursors. This suggests that the humic acids could have played a major role in the transport and accumulation of the ore. R.J.F.

N85-35444# Geological Survey, Alexandria, Va.
COBALT-RICH FERROMANGANESE CRUSTS IN THE OCEANS Abstract Only **c48**
James R. Hein and Frank T. Manheim *In its* USGS Res. on Mineral Resources, 1985 1985 p 23-24 (For primary document see N85-35435 24-42)
Avail: NTIS HC A05/MF A01

Ferromanganese crusts form on hard substrates in three general geotectonic environments: flanks of midplate seamounts, ridges, and plateaus (chiefly hydrogenous crusts); active oceanic spreading ridges (hydrothermal crusts); and convergent margins such as island arcs (combinations of hydrothermal and hydrogenous processes). Crusts commonly have botryoidal surfaces and laminar internal development on a continuous substrate or around isolated nuclei. Since the West German Midpac cruise of 1981, hydrogenous crusts have been recognized as potential offshore mineral resources owing to their valuable metal content. They are of special interest to the United States since many crust areas lie within the

U.S. Exclusive Economic Zones. The principal exploratory cruises devoted to crust investigations are listed. R.J.F.

N85-35445# Geological Survey, Alexandria, Va.
NEW SILVER RESOURCE MAP OF THE UNITED STATES: POTENTIAL FOR INCREASED DOMESTIC SILVER PRODUCTION Abstract Only **c43**
Allen V. Heyl and Robert B. Hall *In its* USGS Res. on Mineral Resources, 1985 1985 p 24-25 (For primary document see N85-35435 24-42)
Avail: NTIS HC A05/MF A01

A new silver resource map of the United States was compiled in 1984 to replace the out of print U.S. Geological Survey Map MR-34 published in 1962. Estimated past production (in troy ounces) plus estimated resources of each district are indicated on the new map by the size of the dot representing the district. The text includes brief summaries of mining history, geologic setting and character of the ores for each district, an improvement over the one line descriptions of districts that accompanied the 1962 map. Many locations have been added, especially in the Eastern United States. R.J.F.

N85-35446# Geological Survey, Alexandria, Va.
MASSIVE SULFIDE DEPOSITS FROM THE SOUTHERN JUAN DE FUCA RIDGE Abstract Only **c48**
Randolph A. Koski, David A. Clague, James L. Bischoff, and Robert A. Zierenberg *In its* USGS Res. on Mineral Resources, 1985 1985 p 27-28 (For primary document see N85-35435 24-42)
Avail: NTIS HC A05/MF A01

Six hydrothermal vent sites and associated benthic communities were located in the axial valley of the southern Juan de Fuca Ridge in 1981, by means of transponder navigated bottom photography. The hydrothermal deposits form chimneys, spires, and mounds within a central zone characterized by a linear bathymetric depression and numerous collapse features. The flat valley floor adjacent to the central zone consists of ferrobalsalt lobate sheetflows sediment cover is minimal. Vent sites are characterized by concentrations of tube worms, clams, limpets, gastropods, and several unidentified fauna. Two types of massive sulfide were dredged from one of the vent sites. Type A samples are angular slabs of dark gray Zn rich sulfide with interlayers and a thin, partly oxidized crust of Fe sulfide. Type B sulfide samples are subrounded, spongy textured fragments composed almost entirely of dendritic aggregates of pale Fe poor colloform sphalerite and opaline silica. R.J.F.

N85-35447# Geological Survey, Alexandria, Va.
GAS ANALYSIS OF ORE-FORMING FLUIDS Abstract Only **c46**
G. P. Landis *In its* USGS Res. on Mineral Resources, 1985 1985 p 28 (For primary document see N85-35435 24-42)
Avail: NTIS HC A05/MF A01

Precise analysis of the volatiles or gaseous fluids trapped in fluid inclusions during mineralization is used to determine physical and chemical parameters of metal transport and deposition and to better understand the environments of ore formation. Knowledge of the abundance of such gases as CO2, CH4, SO2, H2S, N2, O2, NH3, AR, H2, H2O in mineralizing fluids enables researchers to significantly refine ore genesis models. The new mass spectrometer instrumentation developed for these analyses will also permit isotopic analyses of both stable isotopes (C, O, S, H, N) and radiogenic isotopes (Ar, Ne, Xe, Kr, He) for very small samples extracted from fluid inclusions. R.J.F.

N85-35448# Geological Survey, Alexandria, Va.
MINERAL DEPOSIT MODELS: THEORY AND PRACTICE Abstract Only **c43**
Steve Ludington and Paul Barton *In its* USGS Res. on Mineral Resources, 1985 1985 p 30-31 (For primary document see N85-35435 24-42)
Avail: NTIS HC A05/MF A01

New exploration targets for gold, molybdenum, tungsten, and tin are indicated by the systematic distribution of metals in soil and plants of the Red Mountain stockwork and its environs. Metal anomalies in soil of a gridded area 3,600 ft (1,100 m) by 8,400 ft (2,600 m) are mostly weak and small. In contrast, metal anomalies in plants are strong and large. Gold in ashed sapwood of Douglas fir (Pseudosuga menziesli) indicates a major Au anomaly, peak value 14.2 ppm, associated with granodiorite in an unexplored area south of the exposed stockwork. Locally, the Au anomaly is accompanied by a sizable tin anomaly peak value 100 ppm, in Douglas fir Molybdenum concentrations in ashed leaf samples of beargrass (Xerophyllum tenax) indicate an extensive anomaly within a 2 mi long (5 km long) semielliptical belt in which Mo values exceed the median value 20 ppm. The maximum Mo concentration is 500 ppm. R.J.F.

N85-35449# Geological Survey, Alexandria, Va.
EARLY AND MIDDLE CENOZOIC VOLCANIC SYNTHESIS Abstract Only **c46**
Robert G. Luedke *In its* USGS Res. on Mineral Resources, 1985 1985 p 31 (For primary document see N85-35435 24-42)
Avail: NTIS HC A05/MF A01

Maps for the middle and early Cenozoic volcanic centers (16 to 55 Ma) in the western conterminous United States are now being compiled in a manner similar to a series of seven maps showing the distribution, composition, and age of late Cenozoic volcanic centers (0 to 16 Ma) in the Western United States, Alaska, and Hawaii, which are published or in the process of publication (USGS Miscellaneous Investigations Series Maps 1 to 1091). Analysis of the temporal and spatial relations among igneous rock types, their tectonic relations, and their relation to ore deposits is fundamental to present and future progress in research on ore deposition, tectonism, and magnetism. Synthesis of the geological and geochemical data illustrated on this new series of maps will be used to produce models that will guide exploration for ore deposits and improve resource assessment. R.J.F.

N85-35450# Geological Survey, Alexandria, Va.
EXPERT SYSTEMS RESEARCH IN REGIONAL RESOURCE EVALUATION: EXPERIENCES IN THE APPLICATION OF MICROCOMPUTER TECHNOLOGIES Abstract Only **c43**
Richard B. McCammon *In its* USGS Res. on Mineral Resources, 1985 1985 p 32 (For primary document see N85-35435 24-42)
Avail: NTIS HC A05/MF A01

The muPROSPECTOR, patterned after SRI's expert system PROSPECTOR, is designed to aid the geologist in evaluating the mineral resources within a given geographic area. The central idea of the system is matching deposit models encoded by expert economic geologists against observations made by field geologists. The muPROSPECTOR is a microcomputer based system that can be applied to problems in regional mineral resource evaluation. Included are models for volcanogenic massive sulfide, sediment hosted lead zinc silver, tin greisen, porphyry copper, vein type uranium, uraniferous peat, and tin placer deposits. These models are represented in the knowledge base as a set of rules derived from recognition criteria developed for each deposit type. Author

N85-35451# Geological Survey, Alexandria, Va.
APPLICATIONS OF THE MINERAL RESOURCES DATA SYSTEM AND THE INTERNATIONAL STRATEGIC MINERALS INVENTORY IN MINERAL-RESOURCE ASSESSMENTS BY REGION AND COMMODITY Abstract Only **c43**
Antoinette L. Medlin, David M. Sutphin, and John H. DeYoung, Jr. *In its* USGS Res. on Mineral Resources, 1985 1985 p 32-33 (For primary document see N85-35435 24-42)
Avail: NTIS HC A05/MF A01

From 1972 to 1982, the USGS developed the Computerized Resources Information Bank (CRIB). CRIB, a centralized data base, was initiated to meet the growing need for rapid access to data on mineral deposits and occurrences. Regional and commodity information was collected from geologists and commodity specialists at the USGS, other Federal agencies, and State geological agencies. In 1982, CRIB was used as the basis for establishing the Mineral Resources Data System (MRDS), which applies computerized data to mineral resource assessments. MRDS

includes the capability of storing data on mineral deposits and occurrences for use in deposit type studies. Another of the goals of the MRDS is to have data coverage by area and commodity for the major comestic and foreign deposits. Author

N85-35452# Geological Survey, Alexandria, Va.
A COMPARISON OF LANDSAT THEMATIC MAPPER, MULTISPECTRAL SCANNER AND AIRBORNE SENSORS FOR MAPPING THE DISTRIBUTION OF ALTERATION MINERALS: EXAMPLES FROM THE SOUTHWESTERN UNITED STATES Abstract Only **c43**
M. H. Podwysocki, M. S. Power, O. D. Jones, M. H. Koslow, and William E. Collins *In its* USGS Res. on Mineral Resources, 1985 1985 p 43 (For primary document see N85-35435 24-42)
Avail: NTIS HC A05/MF A01

Spaceborne geologic remote sensing capabilities have progressed over the years from the relatively simple four channel LANDSAT Multispectral Scanner (MSS), which operates in the visible and near infrared region and is capable of few mineralogic distinctions, to the present seven channel LANDSAT Thematic Mapper (TM), which has additional channels in the near and mid infrared regions, allowing further mineralogic distinctions. Airborne spectroradiometers, precursors to future spaceborne systems, contain 64 or more narrow channels that can be used to identify individual species in some mineral groups. Data from these instruments are compared to determine their effectiveness for mapping hydrothermally altered rocks in Nevada and Utah. Author

N85-35453# Geological Survey, Alexandria, Va.
SOME RECENT DEPOSIT MODELING EFFORTS Abstract Only **c43**
D. A. Singer and D. P. Cox *In its* USGS Res. on Mineral Resources, 1985 1985 p 52 (For primary document see N85-35435 24-42)
Avail: NTIS HC A05/MF A01

A compilation of 62 descriptive and 37 gradetonnage models, which was published in 1983, provides a starting point for a larger deposit modeling effort useful for resource assessment and exploration. The classification of deposits is empirical rather than genetic and is based on a study of well known deposits. Use of data from many deposits increases the robustness of the models, and emphasis on lithologic-tectonic associations allows the use of geology to indicate which resources are possible in a region. The deposit models make possible effective project design for assessments and exploration and provide a basis for quantitative assessments. Author

N85-35454# Geological Survey, Alexandria, Va.
PRELIMINARY RESULTS OF AN ALVIN DIVE PROGRAM ON ACTIVE HYDROTHERMAL VENTS AT THE SOUTHERN JUAN DE FUCA RIDGE Abstract Only **c48**
W. R. Normark, J. L. Morton, J. L. Bischoff, R. Brett, R. T. Holcomb, E. S. Kappel, R. A. Koski, S. L. Ross, W. C. Shanks, III, J. F. Slack et al *In its* USGS Res. on Mineral Resources, 1985 1985 p 54-55 (For primary document see N85-35435 24-42)
Avail: NTIS HC A05/MF A01

In September 1984, the USGS Juan de Fuca Study Group conducted 8 ALVIN submersible dives to investigate hydrothermal activity on the southern Juan de Fuca Ridge. Three primary vent sites along a 6 km segment of ridge are sampled and mapped. Traverses across the axial valley floor confirm the general volcanic and tectonic features mapped by deep towed photography in 1983. From the inner valley walls to the axis, the 1 km wide, symmetric valley floor is characterized by the following sequence of volcanic features: smooth lobate sheetflows, lobate sheetflows with numerous small collapse pits, a subsided lava lake, and a 10 to 30 m deep, 50 m wide cleft along the center of the valley floor. Author

N85-35455# Geological Survey, Alexandria, Va.
PROCESSING OF LANDSAT IMAGERY TO MAP SURFACE MINERAL ALTERATION ON THE ALASKA PENINSULA, ALASKA Abstract Only **c43**
Frederic H. Wilson and James E. York *In its* USGS Res. on Mineral Resources, 1985 1985 p 56-57 (For primary document see N85-35435 24-42)
Avail: NTIS HC A05/MF A01

LANDSAT images are digitally processed to facilitate assessment of the mineral resources of the Port Moller, Stepovak Bay, and Simeonof Island (Alaska) areas. Field mapping and assessment of these quadrangles were begun in 1983 as part of the Alaska Mineral Resource Assessment Program (AMRAP). It was realized that time and budget constraints would limit mapping coverage. Therefore existing LANDSAT multispectral scanner imagery was used to aid in locating surface alteration, which could be field checked or related to stream sediment or hand sample geochemical data. Author

N85-35456# Geological Survey, Alexandria, Va.
MINERAL RESOURCES PROGRAMS Abstract Only **c43**
In its USGS Res. on Mineral Resources, 1985 1985 p 58 (For primary document see N85-35435 24-42)
Avail: NTIS HC A05/MF A01

A series of extended abstracts is presented that briefly explain the various Mineral Resource Programs of the U.S. Geological Survey (U.S.G.S.). The programs have the following goals: to assess the mineral resource potential of specific areas in the United States (particularly Federal lands) for resource management and Congressional action; to provide timely assessments of the Nation's mineral resources; to identify new areas for exploration and develop new concepts of ore formation and distribution to increase our known mineral resources, particularly the strategic and critical minerals; to improve current methodology and develop new techniques for identifying and evaluating mineral resources and analyzing resource data more efficiently and more precisely. Author

N85-35457# Geological Survey, Alexandria, Va.
THE DEVELOPMENT OF ASSESSMENT TECHNIQUES PROGRAM Abstract Only **c43**
Charles G. Cunningham *In its* USGS Res. on Mineral Resources, 1985 1985 p 60 (For primary document see N85-35435 24-42)
Avail: NTIS HC A05/MF A01

The Development of Assessment Techniques (DAT) Program is a program of basic and applied research on the origin and the geological geochemical, and geophysical expression of mineral deposit systems. The objectives are to develop concepts and techniques to improve the capability of identifying and evaluating mineral resources. To achieve these objectives, the program supports multidisciplinary field and laboratory studies directed toward understanding the processes by which mineral deposits form and developing new technology and models to assess the mineral resource potential in areas of concealed deposits. The studies are organized under the following major categories: ore deposit models; geophysical exploration techniques; district and deposit studies; and laboratory studies. Author

N85-35458# Geological Survey, Alexandria, Va.
THE CONTERMINOUS UNITED STATES MINERAL ASSESSMENT PROGRAM Abstract Only **c43**
Gary C. Curtin *In its* USGS Res. on Mineral Resources, 1985 1985 p 61-63 (For primary document see N85-35435 24-42)
Avail: NTIS HC A05/MF A01

Regional assessments of the mineral and energy potential of the conterminous United States are being made under the Conterminous United States Mineral Assessment Program (CUSMAP). This program is providing up to date, systematic assessments of areas that have identified resources or are throught to have potential for mineral occurrences, especially strategic and critical minerals. Areas are assessed for their mineral and energy potential by integrating existing information, reevaluating known mineral occurrences and acquiring new data through coordinated geologic, geochemical, geophysical, and related studies. The results are published in format tailored to meet the needs of existing and potential users such as industry, the public, Congress, other Federal agencies, and State and local governments. Author

N85-35459# Geological Survey, Alexandria, Va.
FEDERAL MINERAL LAND INFORMATION SYSTEM Abstract Only **c82**
Richard L. Kleckner *In its* USGS Res. on Mineral Resources, 1985 1985 p 65-66 (For primary document see N85-35435 24-42)
Avail: NTIS HC A05/MF A01

The U.S. Geological Survey is developing the Federal Mineral Land Information System (FMLIS), which will allow land managers, policy makers, and others to rapidly retrieve, display, and analyze minerals information on Federal lands at regional, State, and National levels. This capability is being developed in order to input, manipulate, analyze, and output digital data through a geographic information system (GIS). A GIS is a tool for integrating and analyzing spatial data functions with a GIS allow for changes in map scale and projection, data editing, registration and overlay, selection, retrieval, and display of data tabulation of acreages; and measurement of distances. In an interactive environment, the user can rapidly analyze data, examine alteratives, and test hypotheses. Author

N85-35460# Geological Survey, Alexandria, Va.
THE ALASKA MINERAL RESOURCES ASSESSMENT PROGRAM Abstract Only **c43**
Gary R. Winkler *In its* USGS Res. on Mineral Resources, 1985 1985 p 66-68 (For primary document see N85-35435 24-42)
Avail: NTIS HC A05/MF A01

AMRAP (Alaska Mineral Resources Assessment Program), the prototype U.S. Geological Survey regional resource assessment program, enters its second decade with the continuing goal to provide comprehensive information on the mineral and energy resource endowment of Alaska to the public, the private sector the academic community and those who are concerned with national mineral policy. The program is designed: (1) to provide information to land management agencies for decisions regarding the classification and allocation of Alaska's Federal lands; (2) to produce systematic, state of the art geoscience information to the mineral and energy industries, Alaska natives, and other public and private interests; and (3) to expand the general knowledge of Alaska's complex geological setting, much of which is known presently only in reconnaissance. Author

43 EARTH RESOURCES

Includes remote sensing of earth resources by aircraft and spacecraft; photogrammetry; and aerial photography.

For instrumentation see *35 Instrumentation and Photography.*

N85-35461 Washington Univ., Seattle.
PARAMETRIC STABILITY OF ANALYTICAL CLOSE-RANGE PHOTOGRAMMETRY Ph.D. Thesis
Abbas Zedan Khalaf 1984 366 p
Avail: Univ. Microfilms Order No. DA8508064

In close range photography, metric cameras are limited in their range of focus, and when they are designed to fill the needs of some application, they are often unsuitable in other applications. Therefore, photogrammetrists turned their attention to the use of nonmetric cameras. However, these cameras were produced primarily not for metric purposes and to utilize them for such purposes becomes the new challenge. One immediate problem is their unknown interior orientation and the stability of such interior orientations. In this research a new approach has been developed to determine the interior projection geometry of non-metric cameras which is called the Stability Control System SCS. This represents a control system placed inside the camera (between lens and the image plane) having the capability of recovering the inner perspective center coordinates (principal distance, principal point coordinates) for any focusing independently from lens distortion and the object being photographed. Dissert. Abstr.

N85-35462 Iowa Univ., Iowa City.
THE GEOSTATISTICAL APPROACH TO THE INVERSE PROBLEM IN TWO-DIMENSIONAL STEADY STATE GROUND-WATER MODELING Ph.D. Thesis
Robert James Hoeksema 1984 169 p
Avail: Univ. Microfilms Order No. DA8507946

In general the inverse problem is that of estimating some spatially varying aquifer property field based on point measurements of the property of interest, other aquifer properties, and measures of the system outputs. The scope of this work is that of estimating the transmissivity field for a two-dimensional model of a confined aquifer under steady flow conditions. The estimation procedure uses point measuremetns of transmissivity and hydraulic head. The geostatistical approach to this problem is founded on the assumption that the aquifer property and system variable distributions can be modeled as realizations of random processes. The geostatistical approach has five steps. Dissert. Abstr.

N85-35463*# Purdue Univ., Lafayette, Ind. Lab. for Application of Remote Sensing.
LANDSAT-4/5 IMAGE DATA QUALITY ANALYSIS Final Report, 9 Aug. 1982 - 8 Dec. 1984
Erick Malaret, Luis A. Bartolucci, D. Fabian Lozano, Paul E. Anuta, and Clare D. McGillem 8 Dec. 1984 80 p refs Original contains imagery. Original photography may be purchased from the EROS Data Center, Sioux Falls, S.D. 57198 ERTS
(Contract NAS5-26859)
(E85-10105; NASA-CR-176264; NAS 1.26:176264;
LARS-CR-060185) Avail: NTIS HC A05/MF A01 CSCL 05B

A LANDSAT Thematic Mapper (TM) quality evaluation study was conducted to identify geometric and radiometric sensor errors in the post-launch environment. The study began with the launch of LANDSAT-4. Several error conditions were found, including band-to-band misregistration and detector-to detector radiometric calibration errors. Similar analysis was made for the LANDSAT-5 Thematic Mapper and compared with results for LANDSAT-4. Remaining band-to-band misregistration was found to be within tolerances and detector-to-detector calibration errors were not severe. More coherent noise signals were observed in TM-5 than in TM-4, although the amplitude was generally less. The scan direction differences observed in TM-4 were still evident in TM-5. The largest effect was in Band 4 where nearly a one digital count difference was observed. Resolution estimation was carried out using roads in TM-5 for the primary focal plane bands rather than field edges as in TM-4. Estimates using roads gave better resolution. Thermal IR band calibration studies were conducted and new nonlinear calibration procedures were defined for TM-5. The overall conclusion is that there are no first order errors in TM-5 and any remaining problems are second or third order.
Author

N85-35464*# Environmental Research Inst. of Michigan, Ann Arbor. Infrared and Optics Div.
STUDY OF SPECTRAL/RADIOMETRIC CHARACTERISTICS OF THE THEMATIC MAPPER FOR LAND USE APPLICATIONS Quarterly Status Technical Progress Report, 21 Dec. 1984 - 20 Mar. 1985
William A. Malila and Michael D. Metzler, Principal Investigators May 1985 74 p refs ERTS
(Contract NAS5-27346)
(E85-10106; NASA-CR-176265; NAS 1.26:176265;
ERIM-164000-18-P) Avail: NTIS HC A04/MF A01 CSCL 08B

Progress during ERIM's tenth quarter of effort under the LANDSAT-4 and 5 Image Data Quality Assessment program for the Thematic Mapper is described. Coincident LANDSAT-4 and 5 fully corrected (CCT-PT) TM data are analyzed in more detail and revised band-by-band relationships between the two sensors derived. An analysis technique employing the matching of cumulative distributions is developed and used and is believed to offer advantages over the histogram matching procedure currently used to produce LANDSAT data. Multiplicative factors ranging from 0.987 to 1.145 and offsets ranging from -2.7 to -6.2 video quantum levels are required to cause LANDSAT-5 data to match LANDSAT-4

data values. Evidence of low level clipping is found in TM Bands 5 and 7 of LANDSAT-5 but not LANDSAT-4. Analysis of the information content of LANDSAT TM and MSS data is continued. Components of information loss are identified and quantified and the effects of coarsened quantization are explored. Author

N85-35465# Geological Survey, Washington, D.C.
USGS COASTAL RESEARCH, STUDIES AND MAPS: A SOURCE OF INFORMATION FOR COASTAL DECISION MAKING
J. T. Sun, ed. 1985 84 p
(USGS-Circ-883) Avail: NTIS HC A05/MF A01

The tasks of the U.S. Geological Survey (USGS) coastal research, an information resource for coastal decision making, are outlined. The different projects include: coastal zone management, national mapping, geologic and water resources investigation and research, and activities applicable to coastal states. E.A.K.

N85-35466 Texas Univ., Austin.
HYDROGEOLOGY OF THE LOWER GLEN ROSE AQUIFER, SOUTH-CENTRAL TEXAS Ph.D. Thesis
Weldon Woolf Hammond, Jr. 1984 344 p
Avail: Univ. Microfilms Order No. DA8508274

The lower member of the Glen Rose Formation contains one of the most productive and laterally extensive aquifers in the region. The lower member is divided into an upper and lower unit on the basis of lithologic and hydrologic differences. Ground water in the Lower Glen Rose aquifer is under confined and unconfined conditions. Two types of systems of groundwater flow are present, a regional system dominated by syndepositional permeability and porosity, and many local systems produced by later solutional activity. Isotopic dating of samples of ground water from the Lower Glen Rose aquifer by C yields modern apparent ages for ground water of the local systems and old apparent ages (8,490 to 28,980 years) for ground water of the regional system. Velocity of ground water movement in the regional system as determined by C analyses ranges from 4.2 to 4.9 m/year. Velocities obtained from hydrologic parameters compare favorably with these values. A similar range of velocity of ground water movement was determined for the Floridan aquifer of Florida and the Pahasapa Limestone of South Dakota and Wyoming. Dissert. Abstr.

N85-35467# Pennsylvania State Univ., University Park. Office of Remote Sensing of Earth Resources.
REMOTE SENSING OF HYDROLOGIC TRANSPORT PROCESSES USING SPOT SIMULATION DATA Final Report, 1 Aug. 1983 - 30 Apr. 1985
T. W. Gardner, G. W. Petersen, K. F. Connors, and G. M. Baumer Apr. 1985 125 p refs
(Contract DE-AC02-83ER-60182)
(DE85-012412; DOE/ER-60182/1) Avail: NTIS HC A06/MF A01

The utility of the next generation of high resolution, digital satellite imagery was evaluated to characterize surface hydrology and geomorphology in both arid and humid regions. The simulated data have three multispectral (MS) bands. Resolution of the SPOT system allows for landscape classification at level three and occasionally level four across distinctly different climatic zones and in areas disturbed by different types of energy exploitation. Given the SPOT feature recognition and the extensive data base on Quaternary history and rates of surficial geomorphic procsses for the two study sites, it was possible to recognize and classify critical components of the hydrologic system and landspace stability. These component maps include: (1) infiltration/ potential runoff rate maps; (2) groundwater recharge/discharge site maps: (3) landscape stability maps; and (4) fluvial erosion intensity maps. Eight analytic techniques, including manual interpretation of four analog imagery and statistical analyses of digital imagery are evaluated. E.A.K.

N85-35468# New Mexico Inst. of Mining and Technology, Socorro. Petroleum Recovery Research Center.
STEAMFLOOD PILOTS IN THE O'CONNELL RANCH FIELD AND THE T-4 RANCH FIELD Final Report
F. D. Martin Apr. 1985 101 p refs
(DE85-901363; NMERDI-2-71-4333) Avail: NTIS HC A06/MF A01; also available from NMERDI-Information Center, New Mexico Univ., 117 Richmond Dr., N.E., Albuquerque, New Mex. 87106

Field results and geological information on two small steamflood projects in Guadalupe County, New Mexico are given. Both projects, the O'Connell Ranch and T-4 Ranch Pilots, were operated by Rio Petro, Dallas, TX. Water injection rates at these pilots were low and intermittent. Since the oil sands are relatively thin, heat was lost to adjacent rock, and no substantial temperature increase in produced fluids was observed. Through September 1984, the O'Connell Ranch Pilot produced 337 barrels of oil; no oil was produced at the T-4 Ranch Pilot. Three developmental techniques are suggested for use in these projects, and each is being considered. DOE

N85-35469# Geological Survey, Denver, Colo.
SIMULATED EFFECTS OF INCREASED RECHARGE ON THE GROUND-WATER FLOW SYSTEM OF YUCCA MOUNTAIN AND VICINITY, NEVADA-CALIFORNIA
J. B. Czarnecki 1985 38 p refs
(Contract DE-AI08-78ET-44802)
(DE85-012985; USGS/WRI-84-4344) Avail: NTIS HC A03/MF A01

A study was performed to assess the potential effects of changes in future climatic conditions on the ground-water system in the vicinity of Yucca Mountain, the site of a potential mined geologic repository for high-level nuclear wastes being evaluated by the US Department of Energy. These changes probably would result in greater rates of precipitation and, consequently, greater rates of recharge. The study was performed by simulating the ground-water system using a two-dimensional, finite-element ground-water flow model. The simulated position of the water table rose as much as 130 meters near the primary repository area at Yucca Mountain for a simulation involving a 100-percent increase in precipitation compared to modern-day conditions. Despite the water-table rise, no flooding of the potential repository would occur at its current proposed location. According to the simulation, springs would discharge south and west of Timber Mountain; along Fortymile Canyon; in the Amargosa Desert near Lathrop Wells and Franklin Lake playa; and near Furnace Creek Ranch in Death Valley, where they presently discharge. Simulated directions of ground-water flow paths near the potential repository area generally would be the same for the baseline (modern-day climate) and the increased-recharge simulations, but the magnitude of flow would increase by 2 to 4 times that of the baseline-simulation flux. DOE

N85-35470# Dennett, Muessing, Ryan and Associates Ltd., Iowa City, Iowa.
EVALUATION: CLOSE-RANGE PHOTOGRAMMETRY FOR SLOPE INVENTORY AND MONITORING Final Report
H. Muessig Sep. 1984 43 p refs Sponsored by Pennsylvania Dept. of Transportation
(PB85-192755; FHWA/PA-84-012) Avail: NTIS HC A03/MF A01 CSCL 13B

The use of close-range photogrammetry as a rock slope inventory procedure for the inspection, identification, and classification of slope stability was studied. A geotechnical description and evaluation form is supplemented by photogrammetric measurements and a contour map and profiles of the slope are illustrated which were prepared from a single stereopair using an analytical stereoplotter. Slope stability monitoring, using close-range photogrammetry, is discussed and compared with other measurement procedures and several metric camera systems and analytical stereoplotters are compared. Implementation of a close-range photogrammetric inventory and monitoring program is recommended. GRA

N85-35437# Geological Survey, Alexandria, Va.
AEROMAGNETIC AND RADIOMETRIC SIGNATURES OF A POSSIBLE PORPHYRY SYSTEM IN THE WESTERN TUSHAR MOUNTAINS, UTAH Abstract Only

David L. Campbell, James A. Pitkin, Joseph S. Duval, Thomas A. Steven, Charles G. Cunningham, and C. W. Naeser *In its* USGS Res. on Mineral Resources, 1985 1985 p 3-4 (For primary document see N85-35435 24-42)
Avail: NTIS HC A05/MF A01

N85-35439# Geological Survey, Alexandria, Va.
MARINE PHOSPHORITE DEPOSITS MODEL FOR EXPLORATION, WITH EMPHASIS ON DEPOSITS IN THE US ATLANTIC COASTAL PLAIN Abstract Only
James B. Cathcart *In its* USGS Res. on Mineral Resources, 1985 1985 p 7 (For primary document see N85-35435 24-42)
Avail: NTIS HC A05/MF A01

N85-35442# Geological Survey, Alexandria, Va.
AEROMAGNETIC AND GRAVITY MODELS OF THE PLUTON BELOW THE LAKE CITY CALDERA, COLORADO Abstract Only
V. J. S. Grauch *In its* USGS Res. on Mineral Resources, 1985 1985 p 15-16 (For primary document see N85-35435 24-42)
Avail: NTIS HC A05/MF A01

N85-35445# Geological Survey, Alexandria, Va.
NEW SILVER RESOURCE MAP OF THE UNITED STATES: POTENTIAL FOR INCREASED DOMESTIC SILVER PRODUCTION Abstract Only
Allen V. Heyl and Robert B. Hall *In its* USGS Res. on Mineral Resources, 1985 1985 p 24-25 (For primary document see N85-35435 24-42)
Avail: NTIS HC A05/MF A01

N85-35448# Geological Survey, Alexandria, Va.
MINERAL DEPOSIT MODELS: THEORY AND PRACTICE Abstract Only
Steve Ludington and Paul Barton *In its* USGS Res. on Mineral Resources, 1985 1985 p 30-31 (For primary document see N85-35435 24-42)
Avail: NTIS HC A05/MF A01

N85-35450# Geological Survey, Alexandria, Va.
EXPERT SYSTEMS RESEARCH IN REGIONAL RESOURCE EVALUATION: EXPERIENCES IN THE APPLICATION OF MICROCOMPUTER TECHNOLOGIES Abstract Only
Richard B. McCammon *In its* USGS Res. on Mineral Resources, 1985 1985 p 32 (For primary document see N85-35435 24-42)
Avail: NTIS HC A05/MF A01

N85-35451# Geological Survey, Alexandria, Va.
APPLICATIONS OF THE MINERAL RESOURCES DATA SYSTEM AND THE INTERNATIONAL STRATEGIC MINERALS INVENTORY IN MINERAL-RESOURCE ASSESSMENTS BY REGION AND COMMODITY Abstract Only
Antoinette L. Medlin, David M. Sutphin, and John H. DeYoung, Jr. *In its* USGS Res. on Mineral Resources, 1985 1985 p 32-33 (For primary document see N85-35435 24-42)
Avail: NTIS HC A05/MF A01

N85-35452# Geological Survey, Alexandria, Va.
A COMPARISON OF LANDSAT THEMATIC MAPPER, MULTISPECTRAL SCANNER AND AIRBORNE SENSORS FOR MAPPING THE DISTRIBUTION OF ALTERATION MINERALS: EXAMPLES FROM THE SOUTHWESTERN UNITED STATES Abstract Only
M. H. Podwysocki, M. S. Power, O. D. Jones, M. H. Koslow, and William E. Collins *In its* USGS Res. on Mineral Resources, 1985 1985 p 43 (For primary document see N85-35435 24-42)
Avail: NTIS HC A05/MF A01

N85-35453# Geological Survey, Alexandria, Va.
SOME RECENT DEPOSIT MODELING EFFORTS Abstract Only
D. A. Singer and D. P. Cox *In its* USGS Res. on Mineral Resources, 1985 1985 p 52 (For primary document see N85-35435 24-42)
Avail: NTIS HC A05/MF A01

N85-35455# Geological Survey, Alexandria, Va.
PROCESSING OF LANDSAT IMAGERY TO MAP SURFACE MINERAL ALTERATION ON THE ALASKA PENINSULA, ALASKA Abstract Only
Frederic H. Wilson and James E. York *In its* USGS Res. on Mineral Resources, 1985 1985 p 56-57 (For primary document see N85-35435 24-42)
Avail: NTIS HC A05/MF A01

N85-35456# Geological Survey, Alexandria, Va.
MINERAL RESOURCES PROGRAMS Abstract Only
In its USGS Res. on Mineral Resources, 1985 1985 p 58 (For primary document see N85-35435 24-42)
Avail: NTIS HC A05/MF A01

N85-35457# Geological Survey, Alexandria, Va.
THE DEVELOPMENT OF ASSESSMENT TECHNIQUES PROGRAM Abstract Only
Charles G. Cunningham *In its* USGS Res. on Mineral Resources, 1985 1985 p 60 (For primary document see N85-35435 24-42)
Avail: NTIS HC A05/MF A01

N85-35458# Geological Survey, Alexandria, Va.
THE CONTERMINOUS UNITED STATES MINERAL ASSESSMENT PROGRAM Abstract Only
Gary C. Curtin *In its* USGS Res. on Mineral Resources, 1985 1985 p 61-63 (For primary document see N85-35435 24-42)
Avail: NTIS HC A05/MF A01

N85-35460# Geological Survey, Alexandria, Va.
THE ALASKA MINERAL RESOURCES ASSESSMENT PROGRAM Abstract Only
Gary R. Winkler *In its* USGS Res. on Mineral Resources, 1985 1985 p 66-68 (For primary document see N85-35435 24-42)
Avail: NTIS HC A05/MF A01

44 ENERGY PRODUCTION AND CONVERSION

Includes specific energy conversion systems, e.g., fuel cells and batteries; global sources of energy; fossil fuels; geophysical conversion; hydroelectric power; and wind power.

For related information see also *07 Aircraft Propulsion and Power, 20 Spacecraft Propulsion and Power, 28 Propellants and Fuels,* and *85 Urban Technology and Transportation.*

N85-35471*# Giner, Inc., Waltham, Mass.
DEVELOPMENT OF ELECTRODES FOR THE NASA IRON/CHROMIUM Final Report
Larry Swette and Vinod Jalan Jun. 1984 285 p refs
(Contracts DEN3-262; DE-AI04-80AL-12726)
(NASA-CR-174724; DOE/NASA/0262-1; NAS 1.26:174724) Avail: NTIS HC A13/MF A01 CSCL 10A

This program was directed primarily to the development of the negative (Cr3+/Cr2+) electrode for the NASA chromous/ferric Redox battery. The investigation of the effects of substrate processing and gold/lead catalyzation parameters on electrochemical performance were continued. In addition, the effects of reactant cross-mixing, acidity level, and temperature were examined for both Redox couples. Finally, the performance of optimized electrodes was tested in system hardware (1/3 square foot single cell). The major findings are discussed: (1) The recommended processing temperature for the carbon felt, as a substrate for the negative electrode, is 1650 to 1750 C, (2) The recommended gold catalyzation procedure is essentially the published NASA procedure (NASA TM-82724, Nov. 1981) based on deposition from aqueous methanol solution, with the imposition of a few controls such as temperature (25 C) and precatalyzation pH of the felt (7), (3) Experimental observations of the gold catalyzation process

and subsequent electron microscopy indicate that the gold is deposited from the colloidal state, induced by contact of the solution with the carbon felt, (4) Electrodeposited lead appears to be present as a thin uniform layer over the entire surface of the carbon fibers, rather than an discrete particles, and (5) Cross-mixing of reactants (Fe-2+ in negative electrode solution or Cr-3+ in the positive electrode solution) did not appear to produce significant interference at either electrode. Author

N85-35472*# Michigan Univ., Ann Arbor.
PRACTICAL ASPECTS OF PHOTOVOLTAIC TECHNOLOGY, APPLICATIONS AND COST (REVISED) Final Report
Louis Rosenblum Aug. 1985 247 p refs Previously announced as N83-34450
(Grant NAG3-185)
(NASA-CR-174963; NAS 1.26:174963) Avail: NTIS HC A11/MF A01 CSCL 10A

The purpose of this text is to provide the reader with the background, understanding, and computational tools needed to master the practical aspects of photovoltaic (PV) technology, application, and cost. The focus is on stand-alone, silicon solar cell, flat-plate systems in the range of 1 to 25 kWh/day output. Technology topics covered include operation and performance of each of the major system components (e.g., modules, array, battery, regulators, controls, and instrumentation), safety, installation, operation and maintenance, and electrical loads. Application experience and trends are presented. Indices of electrical service performance - reliability, availability, and voltage control - are discussed, and the known service performance of central station electric grid, diesel-generator, and PV stand-alone systems are compared. PV system sizing methods are reviewed and compared, and a procedure for rapid sizing is described and illustrated by the use of several sample cases. The rapid sizing procedure yields an array and battery size that corresponds to a minimum cost system for a given load requirement, insulation condition, and desired level of service performance. PV system capital cost and levelized energy cost are derived as functions of service performance and insulation. Estimates of future trends in PV system costs are made. Author

N85-35473# Kernforschungsanlage, Juelich (West Germany). Project Management for Energy Research.
IMPLEMENTING AGREEMENT FOR COOPERATION IN THE DEVELOPMENT OF LARGE SCALE WIND ENERGY CONVERSION SYSTEMS
Nov. 1984 242 p refs Proc. of 11th Experts Meeting on Gen. Environ. Aspects of Large Scale Wind Energy Utilization, Munich, 7-9 May 1984; organized by Kernsforschungsanlage, Juelich, West Ger. and Tech. Univ. of Denmark; sponsored by West Germany Ministry of Research and Technology Previously announced in IAA as A84-21445
(Juel-Spez-278; ISSN-0343-7639) Avail: NTIS HC A11/MF A01

The effects of megawatt wind energy converters on noise pollution, television reception, birds, agriculture, and scenery were discussed. Site selection, performance assessment, and safety factors were considered. For individual titles, see N85-35474 through N85-35487.

N85-35474# Aeronautical Research Inst. of Sweden, Stockholm.
GENERAL ENVIRONMENTAL ASPECTS OF LARGE SCALE WIND ENERGY UTILIZATION
S. Engstroem (Swedish National Energy Administration) and A. Gustafsson *In* Kernforschungsanlage Implementing Agreement for Cooperation in the Develop. of Large Scale Wind Energy Conversion Systems Nov. 1984 p 1-8 (For primary document see N85-35473 24-44)
Avail: NTIS HC A11/MF A01

Safety, noise, television interference, visual impact, agricultural, and bird population effects of megawatt wind energy converters are reviewed. Actions to investigate these effects are suggested. Author (ESA)

N85-35475# Technical Univ. of Denmark, Lyngby. Dept. of Fluid Mechanics.
CALCULATION OF TRAJECTORIES OF DETACHED WIND TURBINE BLADES AND PREDICTION OF SITE RISK LEVELS ASSOCIATED WITH FAILURES OF HAWT'S
Jens Noerkaer Soerensen *In* Kernforschungsanlage Implementing Agreement for Cooperation in the Develop. of Large Scale Wind Energy Conversion Systems Nov. 1984 p 9-32 refs (For primary document see N85-35473 24-44)
Avail: NTIS HC A11/MF A01

The risk of a wind turbine blade or blade fragment hitting a person was calculated. For the prediction of trajectories of detached wind turbine blades, the governing equations of the full motion, which includes translation and rotation of the blade, are derived. The aerodynamic forces and moments, acting on the blade, are determined by strip theory and constructed airfoil data, which take into account that the blade can be exposed to all possible angles of the relative free stream velocity. The sensitivity of trajectories and throw distances to changes in the conditions by which the blade is detached, was studied. A statistical model by which the damage to people, under assumption of detachment of a blade/blade-fragment, can be determined is presented. The results for a 2 MW, 60 m diameter unit are shown. Author (ESA)

N85-35476# Maschinenfabrik Augsburg-Nuernberg A.G., Munich (West Germany).
GROWIAN: FIRST OBSERVATIONS OF THE ENVIRONMENTAL IMPACT AT THE GROWIAN SITE
Friedrich Koerber *In* Kernforschungsanlage Implementing Agreement for Cooperation in the Develop. of Large Scale Wind Energy Conversion Systems Nov. 1984 p 33-37 (For primary document see N85-35473 24-44)
Avail: NTIS HC A11/MF A01

Sound emission and television interference by a megawatt wind energy converter were measured. Noise from the rotor in idle operation is perceptible 2 km downwind, 1 km upwind. Projections predict 56 dBA at 3 MW power at 250 m on the ground. Tests with a television receiver show a 2 x vertical jump of picture per rotor rotation; interference at vertical or horizontal rotor blade position (depending on polarization of the transmitter); only shading effects, no reflection; no interference on TV sound; and no ghosts or double images on TV screen. Author (ESA)

N85-35477# Aeronautical Research Inst. of Sweden, Stockholm.
WIND TURBINE NOISE: PREDICTION TOOLS AND DESIGN PARAMETER DEPENDENCE
Staffan Meijer *In* Kernforschungsanlage Implementing Agreement for Cooperation in the Develop. of Large Scale Wind Energy Conversion Systems Nov. 1984 p 39-63 (For primary document see N85-35473 24-44)
Avail: NTIS HC A11/MF A01

Wind turbine aerodynamic noise sources are described, and noise predictions and measurements are compared. The influence of design parameters and variable running speed on noise emission is discussed. Results show that prediction tools for blade tower passage noise predict noise emission reasonably well. Prediction tools for high frequency noise are not sufficient. Reliable noise measurements for different machines are needed. It is important to take background noise levels into account when noise criteria are decided. Noise emission is highly dependent on rotational speed and running a turbine with variable rpm lowers noise emission for low wind speeds. Author (ESA)

N85-35478# Central Electricity Generating Board, London (England).
ENVIRONMENTAL ASPECTS OF LARGE-SCALE WIND-POWER SYSTEMS IN THE UK
A. Robson *In* Kernforschungsanlage Implementing Agreement for Cooperation in the Develop. of Large Scale Wind Energy Conversion Systems Nov. 1984 p 65-70 refs (For primary document see N85-35473 24-44)
Avail: NTIS HC A11/MF A01

Environmental issues relating to the introduction of large,

MW-scale wind turbines at land-based sites in the UK are discussed. Noise, television interference, hazards to bird life, and visual effects are considered. Areas of uncertainty are identified, but enough is known from experience elsewhere in the world to enable the first UK machines to be introduced in a safe and environmentally acceptable manner. Research to establish siting criteria more clearly, and significantly increase the potential wind-energy resource is mentioned. Studies of the comparative risk of energy systems are shown to be overpessimistic for UK wind turbines. Author (ESA)

N85-35479# Central Electricity Generating Board, London (England). Scientific Services Dept.
A PROGRAMMABLE AUTOMATIC NOISE DATA AND OTHER RELATED PARAMETER ACQUISITION SYSTEM (PANDORA)
P. J. Nairne and M. R. Burt *In* Kernforschungsanlage Implementing Agreement for Cooperation in the Develop. of Large Scale Wind Energy Conversion Systems Nov. 1984 p 71-85 refs (For primary document see N85-35473 24-44)
Avail: NTIS HC A11/MF A01

A microprocessor controlled sampling system for wind turbines was developed and used in field studies for the unattended collection of noise, wind, humidity, and machine data, in digital and analog formats, within programmable limits using a range of control parameters. The system saves skilled manpower time on site. Data collection in digital and analog form permits a variety of analytical techniques to be applied (statistical, and time and frequency domain). Programmable data collection minimizes subsequent analysis effort. Field investigations demonstrate the suitability and effectiveness of the equipment. Author (ESA)

N85-35480# Sydkraft AB (Sydsvenska Kraft- och Vaerme Aktiebolaget), Malmoe (Sweden).
TELEVISION INTERFERENCE AT THE MAGLARP (SWEDEN) WIND TURBINE
Mats Agrell and Ulf Teght (Swedish Telecommunications Administration) *In* Kernforschungsanlage Implementing Agreement for Cooperation in the Develop. of Large Scale Wind Energy Conversion Systems Nov. 1984 p 87-95 refs (For primary document see N85-35473 24-44)
Avail: NTIS HC A11/MF A01

Severe television interference from a wind turbine when the unit is running was investigated. The disturbed area is mainly behind the wind turbine seen from the transmitter, but interference is reported outside this area. Interference is probably caused by the lightning protection tape on the blades. The tape protects the cables to the strain gages and is oriented as a grid. The interference problems can be solved by installing a TV-transmitter close to the wind turbine at a place where the transmitter can recieve an undisturbed signal. Author (ESA)

N85-35481# Swedish Telecommunications Administration, Farsta. Radio Div.
TELEVISION INTERFERENCE MEASUREMENT AT KALKUGNEN (SWEDEN) TEST WINDMILL c32
Ulf Tegth *In* Kernforschungsanlage Implementing Agreement for Cooperation in the Develop. of Large Scale Wind Energy Conversion Systems Nov. 1984 p 97-104 refs (For primary document see N85-35473 24-44)
Avail: NTIS HC A11/MF A01

Television reception interference from a windmill was analyzed. Reflections from rotating metal blades result in TV-picture intensity fluctuations for signal-to-interference ratios < 28 dB, and synchronization jumps below 20 dB. The contour described by just perceptible interference for a given amount of locations is a sinusoid for forward scatttering relative to the transmitter and a cardioid for backscattering. The interfernce radii for the metallic blade for forward scattering is 370 m and for backscattering 215 m estimated for 90% of the locations that are free from interference on a circle dividing the coverage area for UHF TV into two equal areas. Corresponding radii for the next generation of wind turbine generators are 7.2 and 2.8 km. taking the worst case forward scattering area as 30% of the physical blade area like the present case. The backscatter radii are reduced by the receiver antenna front-to-back ratio fo 15 dB. The radii causing interference for 50% of the locations are 205 and 120 m (for the next generation 6.5 and 1.6 km). Author (ESA)

N85-35482# North of Scotland Hydro-Electric Board.
ENVIRONMENTAL MONITORING BURGER HILL, ORKNEY WIND TURBINE GENERATOR SITE AND SIMILAR WORK AT OTHER UK WTG SITES
W. G. Stevenson *In* Kernforschungsanlage Implementing Agreement for Cooperation in the Develop. of Large Scale Wind Energy Conversion Systems Nov. 1984 p 105-127 (For primary document see N85-35473 24-44)
Avail: NTIS HC A11/MF A01

Television reception interference, hazards to birds, noise, and visual impact of wind energy converters (250 and 350 kW, 3 MW) are discussed. Programs to investigate these aspects are outlined. Author (ESA)

N85-35483# National Agency for Physical Planning (Denmark).
SITING OF LARGE SCALE WIND TURBINES IN DENMARK
Soeren Rasmussen *In* Kernforschungsanlage Implementing Agreement for Cooperation in the Develop. of Large Scale Wind Energy Conversion Systems Nov. 1984 p 129-146 (For primary document see N85-35473 24-44)
Avail: NTIS HC A11/MF A01

General siting investigations for wind turbines, pilot projects for siting wind farms, and site selection for 500 to 800 wind turbines are summarized. General investigations include mapping of wind conditions; mapping and describing conflicting land use interests; survey of potential siting areas for siting models which are different in their respect to other land use interests; and deciding siting criteria (especially distance from buildings) and their importance in how many turbines may be sited in a certain area. Pilot projects investigate how the turbines can best be sited with respect to landscape and recreative and agricultural interest. Author (ESA)

N85-35484# Lahmeyer International (West Germany).
SPECIAL QUESTIONS OF SITING WIND TURBINE ARRAYS AND NETWORKS
H. Ernst and L. Henke *In* Kernforschungsanlage Implementing Agreement for Cooperation in the Develop. of Large Scale Wind Energy Conversion Systems Nov. 1984 p 147-154 ref (For primary document see N85-35473 24-44)
Avail: NTIS HC A11/MF A01

The effect of siting criteria on wind turbine site selection in West Germany is summarized. About 50% of the reference siting potential can be gained by cutting the safety spacing range from 1000 to 250 m to 500 to 250 m. In parks and areas of scenic beauty, wind energy converters could be installed if standard spacing was increased. In areas classified as excellent wind energy potential, > 50% total potential is excluded because of conflict with higher priority uses, e.g., military installations or airports. Author (ESA)

N85-35485# Kema (N. V.), Arnhem (Netherlands).
ENVIRONMENTAL ASPECTS OF THE NETHERLANDS WIND FARM PROJECT
J. A. Kuipers *In* Kernforschungsanlage Implementing Agreement for Cooperation in the Develop. of Large Scale Wind Energy Conversion Systems Nov. 1984 p 155-192 refs (For primary document see N85-35473 24-44)
Avail: NTIS HC A11/MF A01

Safety factors, noise pollution, television interference, visual impact, and impact on farming of wind farms are discussed. Failsafe design, strict quality assurance, and rigorous monitoring during operation are advocated. Noise emission of small wind turbines is acceptable, but must be reduced for medium and megawatt units. It is possible to site the turbines so that they do not interfere with television reception. Visual impact is judged from artists impressions and photomontages, but no results on the acceptability of many small units versus a few large units are

available. Impact on farming varies considerably between sites.
Author (ESA)

N85-35486# GROWIAN Co. (West Germany).
VISUAL IMPACT OF GROWIAN AND RESULTING RECOMMENDATIONS FOR SITING OF LARGE WIND ENERGY CONVERTERS
H. Zwahr *In* Kernforschungsanlage Implementing Agreement for Cooperation in the Develop. of Large Scale Wind Energy Conversion Systems Nov. 1984 p 193-201 (For primary document see N85-35473 24-44)
Avail: NTIS HC A11/MF A01

The distance at which a large wind energy converter dominates its surroundings was subjectively assessed using photographs. Results show that it becomes dominant from < 3 km. Light colors should be used to make it less visible. To avoid an accumulating effect, the turbines should not be placed too closely together. Masts 50 m high (standing 400 m apart) disappear at a distance of 2 km, because perspective makes them look smaller and the intervening air dissolves the contours. It is pointed out that rotating shadows from the turbines can be very irritating to people in nearby houses. Author (ESA)

N85-35487# Voith (J. M.) G.m.b.H., Herdenhern (West Germany).
VISIT TO TEST FACILITY STOETTEN (WEST GERMANY) MAY 9, 1984, INCLUDING THE VOITH WIND ENERGY CONVERTER (WEC) 520 TURBINE. THE ANNUAL PRODUCTION OF VARIOUS WIND ENERGY PLANTS IN SELECTED LOCATIONS
Hans-Ulrich Banzhaf and Wolfgang Weber *In* Kernforschungsanlage Implementing Agreement for Cooperation in the Develop. of Large Scale Wind Energy Conversion Systems Nov. 1984 p 203-216 refs (For primary document see N85-35473 24-44)
Avail: NTIS HC A11/MF A01

Design possibilities for wind energy plants which differ from each other in terms of specific power are described. The annual energy output figures of two wind turbine designs with an installed power of 316 kW each, 1 in the interior and 1 in a coastal region, are compared. The larger plant, which is designed to a lower specific power, gives a 2 to 3.5 times greater energy yield than the design with the higher specific power. Because, however, the larger plant also demands a higher price, not only the installed power, but also the great difference in annual energy production must be considered in comparisons. Author (ESA)

N85-35488# Naval Civil Engineering Lab., Port Hueneme, Calif.
SOLAR POND TECHNOLOGY FOR NAVY APPLICATIONS Final Report, Oct. 1982 - Aug. 1984
L. C. P. Huang and W. R. Major Apr. 1985 37 p
(NR Proj. Z03-71)
(AD-A155877; NCEL-TN-1723) Avail: NTIS HC A03/MF A01 CSCL 10/3

Many of the Navy and Marine Corps bases have potential for thermal solar pond systems that can cost-effectively displace existing thermal and electrical loads. The salt-gradient solar pond offers a simple method of collecting solar insulation while providing its own storage medium for the energy collected. The economic attractiveness of a solar pond is enhanced by this feature; however, the viability of a given application is dependent on site attributes and requirements. For the salt-gradient solar pond, site specific features such as solar radiation, siting area, type of load to be displaced, and availability of salt, clay, and water are important factors affecting the success of each application. An investigation of current salt-gradient solar pond technology was conducted and a preliminary technical and economic analysis was performed for a proposed application at the Marine Corps Logistics Base, Barstow, California. Author (GRA)

N85-35489# Castle Technology Corp., Woburn, Mass.
CATIONIC EXCHANGE MEMBRANE FOR THE ZINC-FERRICYANIDE BATTERY Final Report
J. Paul Pemsler and Michael D. Dempsey May 1985 47 p
(Contract DE-AC04-76DP-00789)
(DE85-013152; SAND-85-7194) Avail: NTIS HC A03/MF A01

In this one year effort of research into supported liquid membrane (SLM) separators for the zinc ferricyanide battery systems, at least one SLM separator (80% LT27/M80 cn 0.13 mm PTFE), has been found that approaches the required specifications with separator resistance in the 2 to 3 ohm sq cm range, 1 x 10 to the -3 power mmoles Fe/h-sq cm iron transport and 2 x 10 to the -4 power mmoles Zn/hsq cm zinc transport. This separator is still being tested in a 60 sq cm zinc ferricyanide battery and is exhibiting encouraging results. DOE

N85-35490# Utah Geological and Mineralogical Survey, Salt Lake City.
EVALUATION OF LOW-TEMPERATURE GEOTHERMAL POTENTIAL IN NORTH-CENTRAL BOX ELDER COUNTY, UTAH
M. C. Davis and P. T. Kolesar Dec. 1984 113 p refs
(Contract DE-AS07-77ET-28393)
(DE85-009541; DOE/ET-28393/T8) Avail: NTIS HC A06/MF A01

The low-temperature geothermal resources of north-central Box Elder County, Utah were assessed. Exploration techniques used included chemical analyses of water from wells and springs, temperature surveys, and temperature-depth measurements in unused wells within the study area. The highest water temperatures (31, 30, and 29 C) recorded in this research were located in three separate geographic regions, suggesting that no single warm water occurrence dominates the study area. Total dissolved solid (TDS) concentrations ranged 294 to 11,590 mg/1. Areas of warm water occurrences generally had TDS values of greater than 1100 mg/1. Reservoir temperatures were estimated using chemical geothermometers. Calculated temperatures ranged between 50 and 100 C. Temperature-depth measurements were logged in 16 unused wells. Thermal gradients calculated from the profiles ranged from isothermal to 267 C/km. The background gradient for the study area appears to be slightly above the verage Basin and Range gradient of 35 C/km. The highest gradients were calculated for the area approximately eight kilometers west of Snowville, Utah, which is also an area of warm water. DOE

N85-35491# Wyoming Univ., Laramie. Dept. of Geology and Geophysics.
GEOTHERMAL RESOURCES OF THE WASHAKIE AND GREAT DIVIDE BASINS, WYOMING
H. P. Heasler and K. L. Buelow 1985 63 p refs
(Contract DE-FC07-79ID-12026)
(DE85-013004; DOE/ID-12026/T11) Avail: NTIS HC A04/MF A01

The geothermal resources of the Great Divide and Washakie Basins of southern Wyoming are described. Oil well bottomhole temperatures, thermal logs of wells, and heat flow data were interpreted within a framework of geologic and hydrologic constraints. It was concluded large areas in Wyoming are underlain by water hotter than 120 F. Isolated areas with high temperature gradients exist within each basin. DOE

N85-35492# Midwest Research Inst., Golden, Colo.
ENERGY FROM LOW TEMPERATURE DIFFERENCES
B. K. Parsons May 1985 8 p Presented at the 22nd Space Congr., Cocoa Beach, Fla., 23 Apr. 1985
(Contract DE-AC02-83CH-10093)
(DE85-008817; SERI/TP-252-2693; CONF-8504137-1) Avail: NTIS HC A02/MF A01

A number of energy conservation and alternative energy approaches utilize a low temperature heat source. Applications in this category include: solar ponds, ocean thermal energy conversion (OTEC), low temperature solar thermal, geothermal, and waste heat recovery and bottoming cycles. Low temperature power extraction techniques are presented and the differences between closed and open Rankine power cycles are discussed. Specific applications and technical areas of current research in OTEC along with a breakdown of plant operating conditions and a rough cost estimate illustrate how the use of low temperature power conversion technology can be cost effective. DOE

N85-35493# Conservation and Renewable Energy Inquiry and Referral Service, Silver Spring, Md.
PHOTOVOLTAICS TECHNOLOGY PROGRAM SUMMARY
May 1985 5 p
(Contract DE-AC01-83CE-30780)
(DE85-013098; DOE/CE-0106) Avail: NTIS HC A02/MF A01

An adequate supply of energy at reasonable price is discussed. Economic efficiency and the following strategies to obtain it are suggested: (1) minimization of federal regulation in energy pricing; and (2) promote a balanced and mixed energy resource system. The development of photovoltaic energy conversion technology is summarized. DOE

N85-35494# California Univ., Berkeley. Lawrence Berkeley Lab.
TWO-DIMENSIONAL INVERSION OF RESISTIVITY MONITORING DATA FROM THE CERRO PRIETO GEOTHERMAL FIELD
N. E. Goldstein, Y. Sasaki, and M. J. Wilt Mar. 1985 11 p refs Presented at the Intern. Symp. on Geothermal Energy, Kailua Kona, Hawaii, 26 Aug. 1985
(Contract DE-AC03-76SF-00098)
(DE85-012554; LBL-19150; CONF-850801-39) Avail: NTIS HC A02/MF A01

Two dimensional iterative, least-squares inversions were performed on dc resistivity data obtained over the geothermal field at five successive times during the 1979-1983 period. The solutions gave the percent change in resistivity within each of 47 rectangular blocks representing the reservoir and recharge regions. The changes are consistent with hydrogeologic and recharge models, on the basis of geophysical well logs, well cuttings, well production, geochemical and reservoir engineering data. The solutions support the model of a reservoir that is recharged mainly by cooler, less saline water, causing changes in both pore fluid resistivity and the extent of boiling near the wells. There may be a component of high-temperature recharge from below and to the east, but flow may be impeded by a two-phase zone. Notwithstanding the various sources of error and uncertainty in the data acquisition and 2-D inversions, repetitive, high precision dc resistivity monitoring seems to be a useful method for assessing reservoir conditions when used in conjunction with production and reservoir engineering data and analysis. DOE

N85-35495# General Electric Co., Schenectady, N. Y. Corporate Research and Development Dept.
DESIGN AND CONSTRUCTION OF AN ADVANCED POWER CONDITIONING SUBSYSTEM FOR SMALL PHOTOVOLTAIC APPLICATIONS
R. I. Steigerwald, B. K. Bose, and P. M. Szczesny Mar. 1985 92 p Prepared in cooperation with Sandia National Lab., Albuquerque, N. Mex.
(Contract DE-AC04-76DP-00789)
(DE85-013940; SAND-83-7037) Avail: NTIS HC A05/MF A01

The power inverter development is described and the high-frequency transformer-link power conditioning system was selected as the preferred approach. The details of a microcomputer-controlled 4 kW inverter design intended for residential applications are described. The theory of operation, detailed design, and some operational results are given. The inverter was designed to deliver utility quality power to the residential grid. Total harmonic current distortion of less than 5% and efficiencies around 90% were achieved. Reliability and cost analyses of the inverter and an equivalent circuit of the inverter useful for system analysis are presented. DOE

N85-35496# Siemens A.G., Munich (West Germany). Werk fuer Diskrete Halbleiter.
MONOLITHIC PHOTOVOLTAIC SERIES ARRAY FOR AN ENERGY COUPLER Final Report, Mar. 1984
Werner Kuhlmann Bonn Bundesministerium fuer Forschung und Technologie Mar. 1985 66 p refs In GERMAN; ENGLISH summary Sponsored by Bundesministerium fuer Forschung und Technologie
(BMFT-FB-T-85-023; ISSN-0340-7608) Avail: NTIS HC A04/MF A01; Fachinformationszentrum, Karlsruhe, West Germany DM 14

A monolithic photovoltaic series array of 16 interconnected, but physically seperated photodiodes used within an energy coupler was developed. The process steps needed were investigated, and optimized, and based on these concepts, element arrays were fabricated and electrically measured. The obtained electrical performances fulfill expectations and prove the feasibility of the concept. Arrays of this type can be used as an energy source to control a MOS power transistor or to drive an isolated CMOS circuit. Author (ESA)

45 ENVIRONMENT POLLUTION

Includes air, noise, thermal and water pollution; environment monitoring; and contamination control.

N85-35497 California Inst. of Tech., Pasadena.
STUDIES IN PHOTOCHEMICAL SMOG CHEMISTRY. 1: ATMOSPHERIC CHEMISTRY OF TOULENE. 2: ANALYSIS OF CHEMICAL REACTION MECHANISMS FOR PHOTOCHEMICAL SMOG Ph.D. Thesis
Joseph Anthony Leone 1985 649 p
Avail: Univ. Microfilms Order No. DA8501337

This study focuses on two related topics in the gas phase organic chemistry of importance in urban air pollution. An experimental effort aimed at developing a new explicit reaction mechanism for the atmospheric photooxidation of toluene is described. This mechanism is tested using experimental data from both indoor and outdoor smog chamber facilities. The predictions of the new reaction mechanism are found to be in good agreement with both sets of experimental data. Additional simulations performed with the new mechanism are used to investigate various mechanistic paths. A theoretical analysis of lumped chemical reaction mechanisms for photochemical smog is presented. Included is a description of a new counter species analysis technique which can be used to analyze any complex chemical reaction mechanism. When applied to mechanisms for photochemical smog, this analysis is shown capable of providing answers to previously inaccessible questions such as the relative contributions of individual organics to photochemical ozone formation. Dissert. Abstr.

N85-35498# Air Command and Staff Coll., Maxwell AFB, Ala.
A GUIDE FOR NEW ENVIRONMENTAL COORDINATORS
J. F. Karasek Apr. 1985 49 p
(AD-A156327; ACSC-85-1405) Avail: NTIS HC A03/MF A01 CSCL 05/1

This guide provides introductory information about the environmental coordinator's role in the implementation of pollution abatement policy, programs, and requirements. It was written for new environmental coordinators. The guide doesn't replace any document, nor is it a substitute for more detailed information. It identifies requirements, programs, agencies, and sources of information necessary for the environmental coordinator to perform his/her duties. GRA

N85-35499# Rhode Island Univ., Narragansett. Graduate School of Oceanography.
ELEMENTAL TRACERS OF SOURCE REGIONS OF CONTAMINANTS IN PRECIPITATION Quarterly Report
K. A. Rahn and B. Beaton 1 Jun. 1985 11 p
(Contract DE-FG22-84PC-71253)
(DE85-012858; DOE/PC-71253/2; QR-2) Avail: NTIS HC A02/MF A01

Eight precipitation events, each with daily aerosol samples before, during, and after were sampled. Analytical data are complete for the first five events. Improvements in sampling and analytical blank and analytical procedures are reported. DOE

N85-35500# JACA Corp., Fort Washington, Pa.
LAND DISPOSAL OF HAZARDOUS WASTE Final Report, Jul. 1984 - Jul. 1985

Apr. 1985 385 p refs Proc. of the 11th Ann. Res. Symp., Cincinnati, 29 Apr. - 1 May 1985
(Contract EPA-68-03-3131)
(PB85-196376; EPA-600/9-85-013) Avail: NTIS HC A17/MF A01 CSCL 13B

Land disposal, remedial action, incineration, and treatment of hazardous waste was discussed. Significant research findings of ongoing and recently completed projects concerned with hazardous waste management were presented. Hazardous waste land disposal and abstracts in the areas of: (1) remedial action; (2) pollutant assessment; and (3) pollutant control were compiled. Subjects discussed include landfill design and operation, waste leaching and analyses, pollutant migration and control, waste modification, surface impoundments, flexible membrane liners, remedial action techniques and underground mine disposal. Author

N85-35501# Radian Corp., Research Triangle Park, N.C.
REVIEW OF US NOx ABATEMENT TECHNOLOGY
J. David Mobley and Gary D. Jones 1985 27 p refs
(Contract EPA-68-02-3994)
(PB85-193522; EPA-600/D-85-105) Avail: NTIS HC A03/MF A01 CSCL 13B

The paper describes U.S. research efforts, demonstration projects, and commercial applications designed to control nitrogen oxide (NOx) emissions from stationary sources. Research and development of NOx control techniques in the U.S. has included a variety of combustion-related techniques, as well as selective catalytic reduction (SCR) of NOx with ammonia (NH3). Current U.S. emission standards or both utility and industrial boilers will require either low NOx burners or combustion modifications to achieve compliance. The State of California has more stringent regulations that, in some cases, require the use of SCR to achieve compliance; however, there have been no commercial applications to utility boilers. Results from pilot unit testing of SCR have allowed the costs of full scale systems to be estimated. Current research is directed toward processes that remove NOx and sulfur oxides (SOx) simultaneously. Author (GRA)

N85-35502# Georgia Inst. of Tech., Atlanta. School of Geophysical Sciences.
ATMOSPHERIC NITROGEN OXIDES: THEIR DETECTION AND CHEMISTRY Final Annual Report, 1 Jul. 1983 - Aug. 1984
D. Davis Mar. 1985 98 p Prepared for Coordinating Research Council, Inc., Atlanta, Ga.
(PB85-193910; CRC-APRAC-CAPA-23-83-01) Avail: NTIS HC A05/MF A01 CSCL 14B

The development of new instrumental capability for measuring key atmospheric nitrogen species; and the improvement of the understanding of the cycling of atmospheric nitrogen were investigated. Two of the pivotal species in the atmospheric cycling of nitrogen are NO and NO2. Major design changes were made to the ground-based, field-operational two photon/laser-induced fluorescence NO sensor which resulted in two major technological advances in this instrument: (1) the sensitivity was improved by a factor of five; and (2) the ground-based NO system was made aircraft compatible. A modified laboratory prototype photofragmentation laser-induced fluorescence NO2 sensor was field-tested; a more sensitive sensor to be used in making airborne NO2 measurements is in the design stage. The field measurements involved both airborne platforms, with sampling occurring over remote Pacific Ocean regions, and ground-based sampling. Author

N85-35503# Massachusetts Inst. of Tech., Cambridge. Energy Lab.
INCORPORATING METEOROLOGICAL DATA INTO RECEPTOR ANALYSIS: RAPS (REGIONAL AIR POLLUTION STUDY) REVISITED
S. A. Batterman, J. A. Fay, and D. Golomb 1985 21 p refs
(Grant EPA-R-811534)
(PB85-188944; EPA-600/D-85-061) Avail: NTIS HC A02/MF A01 CSCL 13B

An analysis of data collected in the St. Louis Regional Air Pollution Study indicates that about 72% of the annual average PM-15 aerosol is background material, presumably of regional origin. The fine and coarse fractions are composed largely of sulfate and crustal material, respectively. About 29% of the particle mass is unaccounted for assuming the measured elements are present as stable oxides. The ratio between PM-15 and TSP concentrations varied considerable among sites depending on averaging time and percentile. Dispersion model results corroborate the regional origin of the bulk of the aerosol. Annual average dispersion modeling can reproduce the observed annual concentrations from from local sources emitting trace elements; however, only about 14% of the PM-15 mass can be accounted for by local point sources. Author

46 GEOPHYSICS

Includes aeronomy; upper and lower atmosphere studies; ionospheric and magnetospheric physics; and geomagnetism.

For space radiation see *93 Space Radiation.*

N85-35504 Oregon State Univ., Corvallis.
SUBSEASONAL VARIABILITY IN A TWO-LEVEL ATMOSPHERIC GENERAL CIRCULATION MODEL Ph.D. Thesis
Yochanan Kushnir 1984 190 p
Avail: Univ. Microfilms Order No. DA8508403

The dynamical processes which maintain atmospheric disturbances in regions of strong wintertime variability of the Northern Hemisphere are examined using data from a GCM simulation. Time series of the dependent variables and diabatic heating components from 10 Northern Hemisphere winters simulated by the Oregon State University two-level GCM are used. Variance and covariance analyses are performed to determine the geographical distribution of the intensities and transport properties of high-frequency (periods between 2.5 and 10 days) and low-frequency (periods between 10 days and a season) eddies. These are compared with existing observations and the discrepancies are discussed in terms of their dynamical consistency with the time-mean circulation. The energetics of high-frequency and low-frequency eddies are studied. It is found that the behavior of high-frequency eddies is consistent with baroclinic instability theory. Low-frequency eddies appear to be maintained mainly by a high-latitude baroclinic energy cycle. Dissert. Abstr.

N85-35505 Texas Univ., Austin.
DEPOSITIONAL SYSTEMS AND COAL OCCURRENCE IN THE FORT UNION FORMATION (PALEOCENE), POWDER RIVER BASIN, WYOMING AND MONTANA Ph.D. Thesis
Walter Barton Ayers, Jr. 1984 226 p
Avail: Univ. Microfilms Order No. DA8508246

The Powder River Basin is a Laramide foreland basin which was formed as a structural and depositional entity in the Paleocene and was filled by fluvial-deltaic, paludal, and lacustrine sediments of the Fort Union Formation. A regional subsurface study shows that, as a result of rapid subsidence in the middle paleocene, a lake (Lebo Shale Member) formed along the axis of the Powder River Basin and rapidly transgressed an area greater than 10,000 sq mi. (25,900 sq km). From middle through late Paleocene, Lake Lebo was filled peripherally by fluvially dominated deltas (Tongue River Member). Primary fill was from: (1) the east by elongate deltas fed by suspended-load fluvial systems issuing from the Black Hills and; (2) the southwest by lobate deltas fed by mixed-to-bed-load streams sourced to the west. Secondary fill was from the northwest by an elongate delta fed by a suspended-load fluvial system flowing through the Bull Mountain trough. A detailed study of Tongue River coal seams near the center of the basin shows that coal occurrence is facies controlled. Dissert. Abstr.

N85-35506 California Univ., Davis.
GEOLOGY: STRUCTURAL HISTORY AND FLUVIAL GEOMORPHOLOGY OF THE SOUTHERN DEATH VALLEY FAULT ZONE, INYO AND SAN BERNARDINO COUNTIES, CALIFORNIA

Ph.D. Thesis
Paul Ray Butler 1984 151 p
Avail: Univ. Microfilms Order No. DA8507292

Estimates of offset along the southern Death Valley fault zone range from 8 to 80 km of right-lateral slip. In order to determine the amount of offset, an area of approximately 200 square km was mapped in southern Death Valley between the Owishead Mountains and the southern Black Mountains, focusing primarily on late-cenozoic deposits. Field mapping was supplemented by age determinations of volcanic rocks and geophysical studies, including a gravity and magnetic line across the fault zone and paleomagnetic determinations to assist in correlation and age control of lacustrine deposits. By matching offset alluvial fan gravel with its source area, 20 to 35 km of right-lateral slip is documented for the last 10 to 12 million years. The geometry of the pull-apart-basin model that has been proposed for Death Valley requires that there be approximately 20 km of right-lateral slip along the southern Death Valley fault zone. Virtually all of the right-lateral slip took place prior to 0.9 million years ago along western traces of the southern Death Valley fault zone. Dissert. Abstr.

N85-35507 Texas A&M Univ., College Station.
SEISMIC STRATIGRAPHIC ANALYSIS OF THE MISSISSIPPI FAN Ph.D. Thesis
Mary Hart Feeley 1984 247 p
Avail: Univ. Microfilms Order No. DA8504663

Examination of extensive multichannel and single channel data across the Mississippi Fan, Gulf of Mexico reveals that at least eight seismic sequences comprise the Pliocene/Pleistocene section. The sequence boundaries are basin wide uncomformities identified on the basis of truncation and reflector terminations. Isopach and structure maps compiled for each of the sequences indicates a seaward and eastward migration in the fan depocenter. Mapping of the orientation of the axis of maximum thickness for each sequence indicates a major eastward shift in the depocenter during the Lake Pleistocene. This shift suggests a major influx of sediment from sources other than the Mississippi River Embayment, possibly from the DeSoto Canyon. Seven seismic facies were identified within the fan unit each with one or more facies types. A depositional mechanism was proposed for each based on the reflection pattern, position within each sequence, and lateral facies relationships. Channel, overbank, mass transport, and turbidity flow deposits were interpreted.
Dissert. Abstr.

N85-35508 North Carolina Univ., Chapel Hill.
STRUCTURAL DEVELOPMENT OF THE WEST-CENTRAL GRANT RANGE, NYE COUNTY, NEVADA Ph.D. Thesis
Joan Esther Fryxell 1984 232 p
Avail: Univ. Microfilms Order No. DA8508583

The Grant Ridge in east central Nevada shows a complex history of Mesozoic and Cenozoic deformation. The oldest structure in the range is a major east vergent overturned anticline, possibly related to a thrust fault at depth. Most of the lower to upper Cambrian rocks exposed in the study area are part of the overturned limb of the anticline. After folding, the Cambrian rocks were metamorphosed, locally to staurolite grade; neomineralization dies out upward through the fold. The older set dips to the southeast, and generally placed slightly to unmetamorphosed units upon more severely deformed units. The younger fault set dips west, cutting east dipping faults and syntectonic conglomerates likely correlative with the Mio-Pliocene Horse Camp Formation. These faults are therefore Pliocene or younger in age. These relationships indicate that, folding, metamorphism, ductile shearing, and low angle normal faulting were geometrically and chronologically independent of each other. Post late Cretaceous and pre late Oligocene low angle north directed shearing occurred, but the relationship of this shearing to the regional structural history is uncertain.
Dissert. Abstr.

N85-35509 Wyoming Univ., Laramie.
THERMAL EVOLUTION OF COASTAL CALIFORNIA WITH IMPLICATIONS FOR HYDROCARBON MATURATION Ph.D. Thesis
Henry Peter Heasler 1984 85 p
Avail: Univ. Microfilms Order No. DA8508867

The thermal constraints imposed by plate subduction, cooling oceanic lithosphere, and the migration of a fault-fault-trench triple junction are numerically modeled using finite differences in order to better understand the thermal evolution of coastal California. Numerical solutions for steady state heat transfer are used to estimate the effect of plate subduction in lowering temperatures in coastal California. Numerical solutions for time dependent heat transfer estimate the thermal effect of the passage of the Mendocino triple junction with consequent upwelling of asthenosphere. Calculated heat flow values from the models result in a heat flow distribution similar to measured values from north of Cape Mendocino to the Garlock fault zone. When the calculated paleotemperatures are applied to the Pismo Basin, the basal 300 meters of source rocks are predicted to have entered or be near the liquid oil window. Trends suggested by the thermal models indicate that the more southern basins and basins closer to the North American plate Pacific plate boundary have experienced higher paleotemperatures. Consequently, these basins potentially contain a greater amount of generated hydrocarbons.
Dissert. Abstr.

N85-35510 Oregon State Univ., Corvallis.
ORE GENESIS AT THE MONTERROSAS DEPOSIT IN THE COASTAL BATHOLITH, ICA, PERU Ph.D. Thesis
Gary Brian Sidder 1984 247 p
Avail: Univ. Microfilms Order No. DA8508413

Monterosas is a hydrothermal deposit of copper and for that is hosted by gabbro-diorites of the Upper Cretaceous Patap Superunit within the Coastal Batholith of central Peru. The ore body is localized by fractures and splays related to a nearby regional fault and is composed of massive chalcopyrite, magnetite, and pyrite. Ore and alteration minerals such as actinolite, sodic scapolite, epidotes, sphene, magnetite, apatite, tourmaline, chlorites, hematite, and quartz formed dominantly as replacements of magmatic diosside, labradorite-andesine, and ilmenite. Hydrothermal mineralization was characterized by the exchange of major, minor, and trace elements between hot saline fluids and gabbro-diorite wall rocks. Geochemical data suggest that the ore and gangue minerals were deposited at high temperatures from saline fluids derived from a magma. The evidence includes fluid inclusions within gangue quartz that exhibit homogenization temperatures of 400 to 500 C, salinites of 32 to 56 wt percent NaCl and the halite trend, and magmatic like sulfur isotopic compositions that range from 1.6 to 3.3 permit in gyrite and chalcopyrite. Dissert. Abstr.

N85-35511 Purdue Univ., Lafayette, Ind.
GEOLOGY AND GEOMORPHOLOGY OF THE RORAIMA GROUP, SOUTHEASTERN VENEZUELA Ph.D. Thesis
Galo YanezPintado 1984 267 p
Avail: Univ. Microfilms Order No. DA8507778

A moderately detailed, accurate geologic geomorphologic map of the Roraima region at a 1:250,000 scale was prepared. This provides a suitable base for future, more detailed studies. It is recommended that the Roraima Formation be raised to Group status and include three apparently conformable but lithogically separable Formations from the base upwards, these are the Canaima, Gualaquinima, and Auyantepui formation. Two composite stratigraphic sections are established and formational thicknesses determined near Santa Elena de U. and Canaima. Radar imagery and aerial photo interpretation allows improved mapping of regional and local structures. Broad, gentle, postdepositional folding of the Roraima into anteclises and syneclises apparently was followed by intrusion of basic dikes and sills; the principal host is the Canaima Formation. Diamond bearing places in the present alluvial valleys are the result of continuous deposition, reworking and redeposition of older, more geographically disjunct floodplain and deltaic sediments. Dissert. Abstr.

N85-35512 California Inst. of Tech., Pasadena.
CRUSTAL STRUCTURE IN SOUTHERN CALIFORNIA FROM ARRAY DATA Ph.D. Thesis
Thomas Martin Hearn 1985 140 p
Avail: Univ. Microfilms Order No. DA8508461

Crustal structure in Southern California is investigated using travel times from over 200 stations and thousands of local earthquakes. The data are divided into two sets of first arrivals representing a two layer crust. The Pg arrivals have paths that refract at depths near 10 km and the Pn arrivals refract along the Moho discontinuity. These data are used to find lateral and azimuthal refractor velocity variations and to determine refractor topography. Pn raypaths are modeled using linear inverse theory. This enables statistical verification that static delays, lateral slowness variations and anisotropy are all significant parameters. However, because of the inherent size limitations of inverse theory, the full array data set could not be processed and the possible resolution was limited. The tomographic backprojection algorithm developed avoids these size problems. This algorithm allows the processing of the data sequentially and to iteratively refine the solution. The variance and resolution for tomography are determined empirically using synthetic structures. Dissert. Abstr.

N85-35513 Wisconsin Univ., Madison.
ATTENUATION PROPERTIES OF THE PETATLAN REGION, MEXICO, AND A LOCAL MAGNITUDE SCALE FOR MICROEARTHQUAKES IN THIS AREA Ph.D. Thesis
Mehrdad Mahdyiar 1984 270 p
Avail: Univ. Microfilms Order No. DA8500834

The attenuation properties of the Petation region which is part of the Middle America subduction zone on the coast of Mexico by estimating P-, S-, and coda wave quality factors. Through a general formulation of a single scattering model for the coda wave, it was found that the coda wave amplitude decay strongly depends on the distribution of the scatterers, and that Q sub c in part is a measure of the difference between the assumed and the actual geometrical spreading of the coda waves. A magnitude scale based on the peak horizontal velocity (V) and a velocity hypocentral distance (F) function was developed. This function was determined using an empirical relationship between moment, V, and R for the earthquakes in the Petatian region so that the magnitude and the moment magnitude scales for these earthquakes, on an average, are the same. Because Richter's magnitude scale which was developed for southern California is widely used throughout the world, the probable error was investigated in the estimation of Richter's scale of earthquakes outside southern California. This error is a function of the magnitude itself, because the scaling law between moment and peak Wood-Anderson response for earthquakes in different regions is not the same. Dissert. Abstr.

N85-35514 California Univ., San Diego.
APPLICATIONS OF THE GALERKIN FORMALISM IN THE COUPLING OF THE EARTH'S FREE OSCILLATIONS Ph.D. Thesis
Jeffrey John Park 1985 227 p
Avail: Univ. Microfilms Order No. DA8502479

How free oscillation coupling calculations can be incorporated into the search for global lateral structure in the deep earth is shown. A discussion of the methods of performing coupling calculations is given, followed by recipes and examples of the construction of synthetic seismograms. Examples of coupling due to rotational Coriolis force that are clearly observable are given and shown to correspond to coupling calculations in a qualitative manner. Coupling kernels are discussed, whose form will determine the ability to resolve structure. Various degrees of coupling interaction are demonstrated and compared in coupled fundamental mode synthetic seismograms. The mechanical problem of two coupled pendula is examined. Dissert. Abstr.

N85-35515 California Inst. of Tech., Pasadena.
APPLICATIONS OF THE KIRCHOFF-HELMHOLTZ INTEGRAL TO PROBLEMS IN BODY WAVE SEISMOLOGY Ph.D. Thesis
Patricia Frances Scott 1985 187 p
Avail: Univ. Microfilms Order No. DA8508469

A procedure is described for evaluating the Kirchhoff Helmholtz integral and presents applications of it which involve the interpretation of amplitude and travel time anomalies of body waves. The method of integration is a summation of single point evaluations of the integrand and requires that spacing of these evaluations on the surface be small compared to the wavelength of the incident disturbance. The technique predicts amplitudes, travel times and waveforms of acoustic potentials that propagate through a homogeneous medium and interact with three dimensional curved boundaries. Results from test models compare well with optical solutions for reflections of planar interfaces and rigid spheres and transmissions through planar interfaces. Dissert. Abstr.

N85-35516* Colorado Univ., Boulder.
SUBCRITICAL FRACTURE PROPAGATION IN ROCKS: AN EXAMINATION USING THE METHODS OF FRACTURE MECHANICS AND NON-DESTRUCTIVE TESTING Ph.D. Thesis
Peter Lee Swanson 1984 282 p
Avail: Univ. Microfilms Order No. DA8508975

An experimental investigation of tensile rock fracture is presented with an emphasis on characterizing time dependent crack growth using the methods of fracture mechanics. Subcritical fracture experiments were performed in moist air on glass and five different rock types at crack velocities using the double torsion technique. The experimental results suggest that subcritical fracture resistance in polycrystals is dominated by microstructural effects. Evidence for gross violations of the assumptions of linear elastic fracture mechanics and double torsion theory was found in the tests on rocks. In an effort to obtain a better understanding of the physical breakdown processes associated with rock fracture, a series of nondestructive evaluation tests were performed during subcritical fracture experiments on glass and granite. Comparison of the observed process zone shape with that expected on the basis of a critical normal principal tensile stress criterion shows that the zone is much more elongated in the crack propagation direction than predicted by the continuum based microcracking model alone. Dissert. Abstr.

N85-35517*# Aerospace Corp., El Segundo, Calif. Space Sciences Lab.
TWO-DIMENSIONAL QUASINEUTRAL DESCRIPTION OF PARTICLES AND FIELDS ABOVE DISCRETE AURORAL ARCS
A. L. Newman, Y. T. Chiu, and J. M. Cornwall 15 Jul. 1985 44 p refs
(Contract NASw-3839)
(NASA-CR-176170; NAS 1.26:176170; ATR-85(7083)-8) Avail: NTIS HC A03/MF A01 CSCL 04A

Stationary hot and cool particle distributions in the auroral magnetosphere are modelled using adiabatic assumptions of particle motion in the presence of broad-scale electrostatic potential structure. The study has identified geometrical restrictions on the type of broadscale potential structure which can be supported by a multispecies plasma having specified sources and energies. Without energization of cool thermal ionospheric electrons, a substantial parallel potential drop cannot be supported down to altitudes of 2000 km or less. Observed upward-directed field-aligned currents must be closed by return currents along field lines which support little net potential drop. In such regions the plasma density appears significantly enhanced. Model details agree well with recent broad-scale implications of satellite observations. Author

N85-35518# Commonwealth Scientific and Industrial Research Organization, Mordialoc (Australia). Div. of Atmospheric Research.
A STRATEGY FOR CALIBRATING ATMOSPHERIC TRANSPORT MODELS
I. G. Enting 1985 28 p refs
(CSIRO-DAR-TP-9; ISBN-0-643-03866-3) Avail: NTIS HC A03/MF A01

The distribution of long-lived atmospheric constituents is strongly influenced by the extent to which they are transported by large-scale atmospheric circulations. At present the knowledge of

the effects of these circulations is incomplete and can in principle be improved by incorporating information on tracer distributions. Since each tracer cycle has its own inherent uncertainties as well as the uncertainties in the atmospheric transports, the overall model calibration problem becomes one of considerable complexity once a number of different tracers are considered. The application of transformations developed for analyzing seismic data can separate the calibration problem into a number of essentially independent parts, reducing the complexity to a more manageable level and allowing for systematic inclusion of additional tracer information as it becomes available. Author

N85-35519# Ohio State Univ., Columbus. Dept. of Geodetic Science and Surveying.
OPTIMAL ESTIMATION OF A HIGH DEGREE GRAVITY FIELD FROM A GLOBAL SET OF 1 DEG X 1 DEG ANOMALIES TO DEGREE AND ORDER 250
D. P. Hajela Hanscom AFB, Mass. AFGL Aug. 1984 69 p
(Contract F19628-82-K-0022)
(AD-A156008; OSU/DGSS-358; AFGL-TR-84-0263; SR-7) Avail: NTIS HC A04/MF A01 CSCL 08/5

An algorithm developed by Colombo (1981) for the optimal estimation of potential coefficients has been implemented with global 1 deg X 1 deg gravity anomalies. The reformulation of the algorithm, and the modifications, have been described. The effect of changes in anomaly error estimates, and change in the anomaly data, on the optimally estimated potential coefficients has been examined. Potential coefficients were estimated complete to degree and order 250 with present realistic anomaly error estimates, and also with idealized anomaly error estimates. A comparison with the current set of potential coefficients complete to degree and order 180 shows a realistic coefficient percentage improvement of about 8% at degree 60, increasing to about 33% at degree 180. The cumulative undulation and anomaly difference to degree 180 is 1.51 meters and 2.7 mgals respectively. The present coefficient error estimates are better by a factor of about two when compared to the current coefficient error estimates. GRA

N85-35520# Dikewood Corp., Albuquerque, N. Mex.
AIR CHEMISTRY MEASUREMENTS 2 Final Report, Jan. 1983 - Aug. 1984
D. K. Davies and P. J. Chantry May 1985 66 p
(Contract F29601-81-C-0044)
(AD-A156041; DC-TN-2030.308-2; AFWL-TR-84-130) Avail: NTIS HC A04/MF A01 CSCL 04/1

This report describes a comprehensive set of measurements of electron, negative-ion, and positive-ion mobilities together with attachment and ionization rate coefficients for dry air and mixtures of dry air with water vapor. These measurements were made for values of E/N (the ratio of electric field to gas density) ranging from about 10 to the -22nd power Vm2 to about 3x10 to the -19th power Vm2. This range of E/N corresponds to values of electric field at atmospheric pressure from about 10 thousand to 10 million V/m and covers values of electron mean energy from near thermal to values well above the onset of impact ionization. GRA

N85-35521# Air Force Geophysics Lab., Hanscom AFB, Mass.
ION COMPOSITION MEASUREMENTS OF THE DISTURBED AND QUIET D-REGION IN 1980 - 1981 Environmental Research Papers
W. Swider, L. Wlodyka, G. S. Federico, A. D. Bailey, and R. Rossi 21 Nov. 1984 28 p
(AD-A156055; AFGL-TR-84-0316; AFGL-ERP-901) Avail: NTIS HC A03/MF A01 CSCL 04/1

Mass-spectrometric data were obtained from rocket-borne instruments flown from Poker Flat, Alaska, during October 1980 and 1981 under disturbed and quiet conditions, respectively. The positive ion spectra for both events appear to be compatible with our current understanding of the D-region. The instrument configuration (cone front) yielded poor negative ion currents. Much more work is needed to develop a D-region mass spectrometer which accurately observes in situ negative ions. This need is underscored by the fact that only light negative ions, possibly mostly contaminants, were present near 80 km. Ions two to three times heavier were obtained in earlier flights with a blunt front end configuration. Nitric oxide profiles derived for both cases were within the range expected. The 1980 flight, under disturbed conditions, yielded higher concentrations than did the 1981 flight. GRA

N85-35522# Analytic Sciences Corp., Reading, Mass.
GRAVITY GRADIOMETER SURVEY DATA PROCESSING
J. V. White and J. D. Goldstein 30 Jul. 1984 37 p
(Contract F19628-83-C-0053)
(AD-A156165; AFGL-TR-84-0198; SR-2) Avail: NTIS HC A03/MF A01 CSCL 09/2

This Technical Report describes a practical methodology for processing airborne gravity gradiometer survey data to estimate gravity disturbance vectors at the surface of the Earth. The methodology also provides an error analysis of the disturbance estimates. Special consideration is given to the data processing and data documentation required for testing of the airborne Gravity Gradiometer Survey System (GGSS). As an example of the data processing methodology, a prototype data template is defined for the simplified problem of estimating the z (vertical) gravity disturbance from measurements of the zz gradient. This template is an interim example of the types of templates that are being developed in this study for processing real survey data. Gravity and measurement error covariance matrices (for the AWN worldwide gravity disturbance model) were computed for this prototype template. These matrices are sufficient for designing the optimal gravity disturbance estimator for the template and for computing its rms accuracy. Author (GRA)

N85-35523# Weston Observatory, Mass.
PROCEDURE FOR EDITING THE FLUXGATE MAGNETOMETER DATA OF THE AFGL (AIR FORCE GEOPHYSICS LABORATORY) MAGNETOMETER NETWORK Scientific Report, 1 Jul. 1983 - 28 Sep. 1984
A. J. Paboojian 30 Oct. 1984 73 p
(Contract F19628-82-K-0040)
(AD-A156331; AFGL-TR-84-0275; SR-1) Avail: NTIS HC A04/MF A01 CSCL 09/2

The procedure for producing the edited data base of the AFGL Magnetometer Network is described in detail. The input to the procedure is the series of archive tapes on which the raw data from the seven network stations are recorded; the output is several series of tapes containing the edited data from the fluxgate magnetometer only. Each series has either a one-second or a one-minute (averaged) sampling interval and is written in a tape format selected for compatibility with one or more specific computer types used at the Air Force Geophysics Laboratory, The World Data Center, and other scientific institutions. Detailed instructions are given for the execution of each of the computer programs employed in the procedure as well as for the basic operation of the network minicomputer on which the procedure is carried out. The procedure is highly automated and the description provided is sufficient to permit its being carried out by an untrained operator. GRA

N85-35524# Aerodyne Research, Inc., Billerica, Mass.
A STUDY OF THE CHEMISTRY OF ALKALI METALS IN THE UPPER ATMOSPHERE
J. A. Silver and C. E. Kolb Jan. 1985 71 p
(Contract F19628-83-C-0010)
(AD-A156349; ARI-RR-441; AFGL-TR-85-0008; SR-2) Avail: NTIS HC A04/MF A01 CSCL 04/1

The reactions of metallic species introduced into the atmosphere by meteor ablation may play a significant role in mesospheric and stratospheric chemistry. During this second year of a three year program to investigate these phenomena, we have completed measurements for the reactions of atomic sodium with ozone, and of NaO with ozone. Preliminary measurements of the rate constant for the reaction of NaO_2 + HCl have been done, as well as an initial photodissociation cross section determination

for NaCl at 193 nm. We have also begun to investigate the means by which neutral gas phase alkali species may be removed from the mesosphere and stratosphere. GRA

N85-35525# Los Alamos Scientific Lab., N. Mex.
THREE-DIMENSIONAL GRAVITY IDEAL BODY STUDIES IN ROUGH TERRAIN
M. E. Ander and S. P. Huestis 1985 5 p refs Presented at the Intern. Meeting on Potential Fields in Rugged Topography, Lausanne, Switzerland, 28 Jul. 1985 Prepared in cooperation with New Mexico Univ., Albuquerque
(Contract W-7405-eng-36)
(DE85-014097; LA-UR-85-2171; CONF-850763-1) Avail: NTIS HC A02/MF A01

An approach to the interpretation of potential field anomaly data is to maximize or minimize some nonlinear scalar property of solutions fitting the data. As an example, a comparison of 2-D and 3-D gravity ideal body results from the Lucero Uplift, a westward-tilted fault block located on the western flank of the Rio Grande rift, is discussed. The anomaly was analyzed to obtain bounds on the density contrast, depth of burial, and minimum thickness of its sources. Based on a synthesis of the gravity data with structural analysis and geomorphology, a shallow mafic intrusion is proposed to account for the positive gravity anomaly. DOE

N85-35526# National Bureau of Standards, Gaithersburg, Md.
DEVELOPMENT OF AN NBS (NATIONAL BUREAU OF STANDARDS) POLYMER GAGE FOR DYNAMIC SOIL STRESS MEASUREMENT
R. M. Chung, A. J. Bur, and E. Reasner Apr. 1985 89 p Sponsored by Air Force Armament Lab. and Air Force Engineering and Services Center
(PB85-208494; NBSIR-85/3135) Avail: NTIS HC A05/MF A01 CSCL 08M

Polymer gages developed by the National Bureau of Standards (NBS) have been tested extensively in the NBS Geotechnical Engineering Laboratory to evaluate their capability and reliability for use in determining dynamic soil stresses generated by blast loadings. Penetration of soil grains into the gage surface was found to be the major concern and a major effort was undertaken to develop the most appropriate protective covering. Gages were dynamically loaded to develop their corresponding calibration curves. Author (GRA)

N85-35527# California Univ., Richmond. Earthquake Engineering Research Center.
SIMPLIFIED PROCEDURES FOR THE EVALUATION OF SETTLEMENTS IN SANDS DUE TO EARTHQUAKE SHAKING
K. Tokimatsu and H. B. Seed Jan. 1984 48 p
(Grant NSF CEE-81-10734)
(PB85-197887; EERC-84/16; NSF/CEE-84027) Avail: NTIS HC A03/MF A01 CSCL 08M

On the basis of previous studies it appears that the primary factors controlling earthquake-induced settlement are the cyclic stress ratio for saturated sands with pore pressure generation and the cyclic shear strain for dry or partially saturated sands, together with the N-value for the sand and the magnitude of the earthquake. This report reviews previous studies, summarizes available information concerning the settlements of sands during earthquakes and proposes simplified methods of analysis to predict earthquake-induced settlement in both saturated and nonsaturated clean sands. Comparison of the numerical results with several case histories indicates that the methods presented in this report can be used in many cases as a first approximation for evaluating the volume changes and settlements of sands due to earthquake shaking. GRA

N85-35528# University of Southern California, Los Angeles. Geophysics Lab.
CARBON FIBER STRAINMETER STUDIES IN SOUTHERN CALIFORNIA
P. C. Leary and T. L. Henyey Mar. 1985 29 p
(Contract DI-14-08-0001-21240)
(PB85-196889; TR-85-4) Avail: NTIS HC A03/MF A01 CSCL 08K

Apart from the short interval of time encompassing a great earthquake rupture, deformation of the crust along the locked segment of the San Andreas fault system in southern California can be characterized by slow steady accumulation of strain punctuated by sporadic episodes of microslip. The microslip episodes are insignificant in relation to the overall strain budget, but are important for what they may reveal about the origins and state of stress at depth. Long baseline but infrequently surveyed geodetic nets serve well to define the systematics of long term crustal strain: rate, magnitude, orientation, and possible excursions from uniformity of these descriptive variables. Author (GRA)

N85-35529# University of Southern California, Los Angeles. Geophysics Lab.
GROUNDWATER RADON STUDIES FOR EARTHQUAKE PRECURSORS IN SOUTHERN CALIFORNIA
T. Teng Mar. 1985 22 p
(Contract DI-14-08-0001-21193)
(PB85-196871; TR-85-2) Avail: NTIS HC A02/MF A01 CSCL 08K

Accomplishments in radon monitoring program are reported. They are completion of the design and construction of 10 microprocessor-based continuous radon monitors (CRMs) that have significantly augmented the field radon monitoring and downstream data processing capability. The instrumentation of 10 continuous radon monitoring stations in southern California along the San Andreas fault from Tejon to Cajon, and in the Transverse Mountains were improved. It is believed that fluids in the crust play an important role in the generation of shallow earthquakes. GRA

N85-35530# Bureau of Mineral Resources, Geology and Geophysics, Canberra (Australia).
WORKSHOP PROCEEDINGS: INTERPRETATION OF SEISMIC WAVE PROPAGATION IN LATERALLY HETEROGENEOUS STRUCTURES
D. M. Finlayson, comp. and J. Ansorge, comp. 1984 216 p Workshop held in Einsiedeln, Switzerland, 7-12 Aug. 1983
(BMR-258; ISSN-0084-7100; ISBN-0-644-03541-2) Avail: NTIS HC A10/MF A01

New methods to determine two-dimensional velocity distributions in the lithosphere from a rapidly growing amount of experimental data were reported. A synthetic set of data serves as the most suitable basis to reveal the power of the presently available analysis methods. The laterally heterogeneous structures and the treatment of seismic refraction and reflection data were discussed. The distributed data and a description on how they were generated are reported. The complete range of presently available techniques of interpretation was applied to these data. The combined treatment of seismic refraction and reflection data from the same area include the detection of structural features like low-velocity zones and gradient layers. E.A.K.

N85-35436# Chevron Oil Field Research Co., La Habra, Calif.
CHEMISTRY OF ORE-FORMING FLUIDS Abstract Only
Robert J. Bodnar, I-Ming Chou, and Edwin Roedder *In* Geological Survey USGS Res. on Mineral Resources, 1985 1985 p 1-3 (For primary document see N85-35435 24-42)
Avail: NTIS HC A05/MF A01

N85-35438# Geological Survey, Alexandria, Va.
SOME GEOPHYSICAL GUIDES TO ORE IN SOUTHERN AND SOUTHWESTERN ALASKA Abstract Only
In its USGS Res. on Mineral Resources, 1985 1985 p 5-7 (For primary document see N85-35435 24-42)
Avail: NTIS HC A05/MF A01

N85-35440# Geological Survey, Alexandria, Va.
THE ROLE OF REGIONAL SUBSURFACE GEOCHEMISTRY IN RESOURCE ASSESSMENT IN THE CENTRAL UNITED STATES

Abstract Only
R. L. Erickson, E. L. Mosier, J. G. Viets, and M. S. Erickson *In its* USGS Res. on Mineral Resources, 1985 1985 p 10-11 (For primary document see N85-35435 24-42)
Avail: NTIS HC A05/MF A01

N85-35441# Geological Survey, Alexandria, Va.
HEAT TRANSFER AND BRINE EVOLUTION IN MAGMA-HYDROTHERMAL SYSTEMS Abstract Only
Robert O. Fournier *In its* USGS Res. on Mineral Resources, 1985 1985 p 13 (For primary document see N85-35435 24-42)
Avail: NTIS HC A05/MF A01

N85-35443# Geological Survey, Alexandria, Va.
ORIGIN OF SEDIMENTARY HUMIC ACIDS, POTENTIAL CARRIERS OF ORE-FORMING ELEMENTS Abstract Only
Patrick G. Hatcher *In its* USGS Res. on Mineral Resources, 1985 1985 p 21-22 (For primary document see N85-35435 24-42)
Avail: NTIS HC A05/MF A01

N85-35447# Geological Survey, Alexandria, Va.
GAS ANALYSIS OF ORE-FORMING FLUIDS Abstract Only
G. P. Landis *In its* USGS Res. on Mineral Resources, 1985 1985 p 28 (For primary document see N85-35435 24-42)
Avail: NTIS HC A05/MF A01

N85-35449# Geological Survey, Alexandria, Va.
EARLY AND MIDDLE CENOZOIC VOLCANIC SYNTHESIS Abstract Only
Robert G. Luedke *In its* USGS Res. on Mineral Resources, 1985 1985 p 31 (For primary document see N85-35435 24-42)
Avail: NTIS HC A05/MF A01

47 METEOROLOGY AND CLIMATOLOGY

Includes weather forecasting and modification.

N85-35531 Wyoming Univ., Laramie.
THE KINEMATIC STRUCTURE OF COLD FRONTAL RAINBANDS Ph.D. Thesis
Bruce William Johnson 1984 140 p
Avail: Univ. Microfilms Order No. DA8508868

A new method for the analysis of single Doppler radar data called Band-Velocity-Processing (BVP) is presented. The BVP method was designed to exploit the two-dimensional nature of banded precipitation systems with crossband length values of 5 to 50 km. The BVP method offers improved horizontal (crossband) resolution over existing volume scan methods (VAD/VVP), plus the ability to extract band perpendicular vertical cross sections from a single volume scan. The BVP analysis yields a more complete kinematic structure than RHI analyses, providing estimates for both horizontal wind components, both horizontal divergence components, the shearing deformation, and the vertical shear vector. The bias and variance errors for the BVP method are shown to be acceptably small. The application of the BVP method to narrow and wide cold frontal rainbands reveals important kinematic features. The mesoscale structure of the low level jet ahead of the narrow cold frontal rainband is examined along with the evolution of the kinematic structure during the dissipation stage. Dissert. Abstr.

N85-35532 North Carolina State Univ., Raleigh.
TIME-DEPENDENT RESPONSE OF THE CLIMATE TO INCREASING ATMOSPHERIC CARBON DIOXIDE Ph.D. Thesis
Kerry Harrison Cook 1984 178 p
Avail: Univ. Microfilms Order No. DA8507361

The thesis describes the development of an intermediate level, primitive equation climate model and the application of the model to the transient CO2-climate problem. The model solves the equations of large scale motion in two atmospheric layers. Longitudinal dependence is expressed as a highly truncated Fourier series. Meridional derivatives are finite differenced with a 3 degree latitude interval. The time step of integration is 2 hours. The surface has stylized geography, and an immobile, isothermal ocean with latitudinally-dependent heat capacity. Radiative processes are highly parameterized in this version of the model. Sensitivity experiments are performed to test the effects of two different assumptions about the amount of ocean that is thermally involved with the atmosphere over the time scale of the atmospheric CO2 increase. To simulate the time-dependent nature of the climate response to increasing CO2, the model is integrated in time for 100 years. Dissert. Abstr.

N85-35533*# Pennsylvania State Univ., University Park. Dept. of Meteorology.
KINEMATIC ANALYSIS OF HURRICANE FREDERICK (1979) USING SATELLITE, AIRCRAFT AND RAWINSONDE DATA Final Report
William M. Frank [1984] 90 p refs
(Grant NAG5-102)
(NASA-CR-176167; NAS 1.26:176167) Avail: NTIS HC A05/MF A01 CSCL 04B

Results of kinematic analyses of Hurricane Frederick (1979) performed using satellite wind vectors, aircraft measurements and rawinsonde data are presented. The data were gathered, reduced, preliminarily integrated and used to analyze the structure of the storm in the inflow and outflow layers. The mean structure at large radii is in good agreement with composite analyses of tropical cyclones. Changes in the storm structure from 11 to 12 Sep. 1979 suggests that remote sensing techniques may be useful in monitoring storm intensity. Author

N85-35534*# PRC Planning and Economics, Inc., Lake Success, N.Y.
COMPARATIVE ANALYSIS OF OPERATIONAL FORECASTS VERSUS ACTUAL WEATHER CONDITIONS IN AIRLINE FLIGHT PLANNING, VOLUME 1
John F. Keitz Apr. 1982 83 p 5 Vol.
(Contract NAS3-22748)
(NASA-CR-167862; NAS 1.26:167862) Avail: NTIS HC A05/MF A01 CSCL 04B

The impact of more timely and accurate weather data on airline flight planning with the emphasis on fuel savings is studied. This volume of the report discusses the results of Task 1 of the four major tasks included in the study. Task 1 compares flight plans based on forecasts with plans based on the verifying analysis from 33 days during the summer and fall of 1979. The comparisons show that: (1) potential fuel savings conservatively estimated to be between 1.2 and 2.5 percent could result from using more timely and accurate weather data in flight planning and route selection; (2) the Suitland forecast generally underestimates wind speeds; and (3) the track selection methodology of many airlines operating on the North Atlantic may not be optimum resulting in their selecting other than the optimum North Atlantic Organized Track about 50 percent of the time. Author

N85-35535*# PRC Planning and Economics, Inc., Lake Success, N.Y.
COMPARATIVE ANALYSIS OF OPERATIONAL FORECASTS VERSUS ACTUAL WEATHER CONDITIONS IN AIRLINE FLIGHT PLANNING, VOLUME 2
John F. Keitz Apr. 1982 54 p 5 Vol.
(Contract NAS3-22748)
(NASA-CR-167863; NAS 1.26:167863) Avail: NTIS HC A04/MF A01 CSCL 04B

The impact of more timely and accurate weather data on airline flight planning with the emphasis on fuel savings is studied. This volume of the report discusses the results of Task 2 of the four major tasks included in the study. Task 2 compares various catagories of flight plans and flight tracking data produced by a simulation system developed for the Federal Aviation Administrations by SRI International. (Flight tracking data simulate actual flight tracks of all aircraft operating at a given time and provide for rerouting of flights as necessary to resolve traffic conflicts.) The comparisons of flight plans on the forecast to flight plans on

the verifying analysis confirm Task 1 findings that wind speeds are generally underestimated. Comparisons involving flight tracking data indicate that actual fuel burn is always higher than planned, in either direction, and even when the same weather data set is used. Since the flight tracking model output results in more diversions than is known to be the case, it was concluded that there is an error in the flight tracking algorithm. Author

N85-35536*# PRC Planning and Economics, Inc., Lake Success, N.Y.
COMPARATIVE ANALYSIS OF OPERATIONAL FORECASTS VERSUS ACTUAL WEATHER CONDITIONS IN AIRLINE FLIGHT PLANNING, VOLUME 3
John F. Keitz Apr. 1982 96 p 5 Vol.
(Contract NAS3-22748)
(NASA-CR-167864; NAS 1.26:167864) Avail: NTIS HC A05/MF A01 CSCL 04B

The impact of more timely and accurate weather data on airline flight planning with the emphasis on fuel savings is studied. This volume of the report discusses the results of Task 3 of the four major tasks included in the study. Task 3 compares flight plans developed on the Suitland forecast with actual data observed by the aircraft (and averaged over 10 degree segments). The results show that the average difference between the forecast and observed wind speed is 9 kts. without considering direction, and the average difference in the component of the forecast wind parallel to the direction of the observed wind is 13 kts. - both indicating that the Suitland forecast underestimates the wind speeds. The Root Mean Square (RMS) vector error is 30.1 kts. The average absolute difference in direction between the forecast and observed wind is 26 degrees and the temperature difference is 3 degree Centigrade. These results indicate that the forecast model as well as the verifying analysis used to develop comparison flight plans in Tasks 1 and 2 is a limiting factor and that the average potential fuel savings or penalty are up to 3.6 percent depending on the direction of flight. Author

N85-35537*# PRC Planning and Economics, Inc., Lake Success, N.Y.
COMPARATIVE ANALYSIS OF OPERATIONAL FORECASTS VERSUS ACTUAL WEATHER CONDITIONS IN AIRLINE FLIGHT PLANNING, VOLUME 4
John F. Keitz Apr. 1982 93 p 5 Vol.
(Contract NAS3-22748)
(NASA-CR-167865; NAS 1.26:167865) Avail: NTIS HC A05/MF A01 CSCL 04B

The impact of more timely and accurate weather data on airline flight planning with the emphasis on fuel savings is studied. This volume of the report discusses the results of Task 4 of the four major tasks included in the study. Task 4 uses flight plan segment wind and temperature differences as indicators of dates and geographic areas for which significant forecast errors may have occurred. An in-depth analysis is then conducted for the days identified. The analysis show that significant errors occur in the operational forecast on 15 of the 33 arbitrarily selected days included in the study. Wind speeds in an area of maximum winds are underestimated by at least 20 to 25 kts. on 14 of these days. The analysis also show that there is a tendency to repeat the same forecast errors from prog to prog. Also, some perceived forecast errors from the flight plan comparisons could not be verified by visual inspection of the corresponding National Meteorological Center forecast and analyses charts, and it is likely that they are the result of weather data interpolation techniques or some other data processing procedure in the airlines' flight planning systems. Author

N85-35538*# PRC Planning and Economics, Inc., Lake Success, N.Y.
COMPARATIVE ANALYSIS OF OPERATIONAL FORECASTS VERSUS ACTUAL WEATHER CONDITIONS IN AIRLINE FLIGHT PLANNING: SUMMARY REPORT
J. F. Keitz Apr. 1982 47 p 5 Vol.
(Contract NAS3-22748)
(NASA-CR-167866; NAS 1.26:167866) Avail: NTIS HC A03/MF A01 CSCL 04B

The impact of more timely and accurate weather data on airline flight planning with the emphasis on fuel savings is studied. This summary report discusses the results of each of the four major tasks of the study. Task 1 compared airline flight plans based on operational forecasts to plans based on the verifying analyses and found that average fuel savings of 1.2 to 2.5 percent are possible with improved forecasts. Task 2 consisted of similar comparisons but used a model developed for the FAA by SRI International that simulated the impact of ATc diversions on the flight plans. While parts of Task 2 confirm the Task I findings, inconsistency with other data and the known impact of ATC suggests that other Task 2 findings are the result of errors in the model. Task 3 compares segment weather data from operational flight plans with the weather actually observed by the aircraft and finds the average error could result in fuel burn penalties (or savings) of up to 3.6 percent for the average 8747 flight. In Task 4 an in-depth analysis of the weather forecast for the 33 days included in the study finds that significant errors exist on 15 days. Wind speeds in the area of maximum winds are underestimated by 20 to 50 kts., a finding confirmed in the other three tasks. Author

N85-35539*# University Corp. for Atmospheric Research, Boulder, Colo.
A PRELIMINARY INTERCOMPARISON BETWEEN NUMERICAL UPPER WIND FORECASTS AND RESEARCH AIRCRAFT MEASUREMENTS OF JET STREAMS
M. A. Shapiro 15 Apr. 1982 10 p Sponsored by NASA
(NASA-CR-167884; NAS 1.26:167884) Avail: NTIS HC A02/MF A01 CSCL 04B

During the past several years, research on the structure of extra-tropical jet streams has been carried out with direct measurements with instrumented research aircraft from the National Center for Atmospheric Research (NCAR). These measurements have been used to describe the wind, temperature, turbulence and chemical characteristics of jet streams. A fundamental question is one of assessing the potential value of existing operational numerical forecast models for forecasting the meteorological conditions along commercial aviation flight routes so as to execute Minimum Flight Time tracks and thus obtain the maximum efficiency in aviation fuel consumption. As an initial attempt at resolving this question, the 12 hour forecast output from two models was expressed in terms of a common output format to ease their intercomparison. The chosen models were: (1) the Fine-Mesh Spectral hemispheric and (2) the Limited Area Fine Mesh (LFM) model. Author

N85-35540*# Dayton Univ., Ohio. Research Inst.
THE PHYSICAL AND EMPIRICAL BASIS FOR A SPECIFIC CLEAR-AIR TURBULENCE RISK INDEX Final Report
John L. Keller Aug. 1985 47 p refs
(Contract NAS8-34678)
(NASA-CR-178522; NAS 1.26:178522; UDR-TR-85-94) Avail: NTIS HC A03/MF A01 CSCL 04B

An improved operational CAT detection and forecasting technique is developed and detailed. This technique is the specific clear air turbulence risk (SCATR) index. This index shows some promising results. The improvements seen using hand analyzed data, as a result of the more realistic representation of the vertical shear of the horizontal wind, are also realized in the data analysis used in the PROFS/CWP application. The SCATR index should improve as database enhancements such as profiler and VAS satellite data, which increase the resolution in space and time, are brought into even more sophisticated objective analysis schemes. E.R.

N85-35541# Danish Meteorological Inst., Copenhagen.
AN ATMOSPHERIC BOUNDARY LAYER MODEL FORCED BY THE OPERATIONAL ECMWV-MODEL
Bent Hansen Sass 1985 49 p refs
(WSR-3; ISBN-87-7478-247-9) Avail: NTIS HC A03/MF A01

A 1-dimensional boundary layer model forced by the 3-dimensional global ECMWF-model is briefly introduced. The model equations are presented and results of 3 model simulations are shown to illustrate the behavior of the model. Operational output is described and forecasts of temperature, humidity and wind in July and August 1984 for one location (Beldringe) in Denmark are compared with observations. The predictions of temperature are also compared with output from the ECMWF-model. Author

N85-35542# Deutsche Forschungs- und Versuchsanstalt fuer Luft- und Raumfahrt, Oberpfaffenhofen (West Germany). Inst. fuer Physik der Atmosphaere.

PROCEEDINGS OF METEOROLOGICAL MOTOR GLIDER (MEMO) WORKSHOP '84

Jan. 1985 213 p refs Partly in ENGLISH and GERMAN Proc. held at Oberpfaffenhofen, West Ger., 1-5 Oct. 1985 Report will also be announced as translation (ESA-TT-945)
(DFVLR-Mitt-85-04; ISSN-0176-7739) Avail: NTIS HC A10/MF A01

Motor glider meteorology and the history of motor gliders used for meteorological flight are reviewed. Vertical wind velocity determination using aircraft motion is discussed. Meteorological data from the Falcon aircraft and the ASK 16 motor glider are compared. Atmospheric boundary layer turbulence is investigated. Environmental meteorological data in urban areas are examined. The concept of Lagrangian partitioning was applied to turbulent energy transport. Horizontal and vertical structure of the boundary layer, and the energy budgets above rural and urban areas are treated. Lee circulation in a Foehn wind is studied. Meteorological measuring campaigns with instrumented motor gliders in Poland are reviewed. A data acquisition system for meteorological measurements onboard light aircraft is developed. Accuracy and error analysis of meteorological measuring data is considered. The principles of wind velocity measurements onboard research aircraft are presented. For individual titles, see N85-35543 through N85-35558.

N85-35543# Bonn Univ. (West Germany). Inst. fuer Meteorologie.

MOTOR GLIDER METEOROLOGY [MOTORSEGLER-METEOROLOGIE]

Helmut Kraus *In* DFVLR Proc. of Meteorol. Motor Glider (MEMO) Workshop '84 Jan. 1985 P 11-13 In GERMAN (For primary document see N85-35542 24-47)
Avail: NTIS HC A10/MF A01

Methods of dividing meteorological sciences in partial domains are given, and the requirements and tasks of motor glider meteorology are depicted. It is explained that motor gliders are especially suited for the experimental determination of processes and structures on a micro and mesoscale and of micro-mesoscale interactions. Author (ESA)

N85-35544# Deutsche Forschungs- und Versuchsanstalt fuer Luft- und Raumfahrt, Oberpfaffenhofen (West Germany). Inst. fuer Physik der Atmosphaere.

TYPICAL AND HISTORICAL ASPECTS OF MOTOR GLIDERS AS METEOROLOGICAL MEASURING AIRCRAFT [TYPISCHES UND GESCHICHTLICHES ZUM MOTORSEGLER ALS METEOROLOGISCHES MESSFLUGZEUG] c05

Manfred E. Reinhardt *In its* Proc. of Meteorol. Motor Glider (MEMO) Workshop '84 Jan. 1985 p 15-28 refs In GERMAN (For primary document see N85-35542 24-47)
Avail: NTIS HC A10/MF A01

The history of motor gliders used for meteorological flight since 1920 is depicted. Motor glider is defined. Historical requirements for gliding aircraft with built-in motor are mentioned. The characteristics of motor gliders, their wing loading, and motor power are shown. The milestones marked by these motor gliders are explained. The expectations for meteorological measurements with motor gliders are outlined. Author (ESA)

N85-35545# Eidgenoessisches Inst. fuer Reaktorforschung, Wuerenlingen (Switzerland).

DETERMINATION OF VERTICAL AIR VELOCITY USING MEASUREMENTS OF THE AIRCRAFT MOTION [BESTIMMUNG DER VERTIKALGESCHWINDIGKEIT DER LUFT MIT HILFE VON MESSUNGEN DER FLUGZEUGBEWEGUNG]

Markus Hutter *In* DFVLR Proc. of Meteorol. Motor Glider (MEMO) Workshop '84 Jan. 1985 p 29-42 refs In GERMAN (For primary document see N85-35542 24-47)
Avail: NTIS HC A10/MF A01

Absolute air velocity is determined from the movements of an aircraft. Determination of aircraft motion in a vertical plane is described; the vertical equation of motion and the calculation of an average position angle are discussed. Good agreement is found between measured and calculated angles. The sensitivity of the results to the position angle is discussed. Author (ESA)

N85-35546# Technische Univ., Brunswick (West Germany). Inst. fuer Flugfuehrung.

CONTROL VARIABLES IN VERTICAL WIND DETERMINATION USING SIMPLE FLIGHT-MECHANICAL EQUATIONS [EINFLUSSGROESSEN BEI DER VERTIKALWINDBESTIMMUNG MIT EINFACHEN FLUGMECHANISCHEN GLEICHUNGEN]

Klaus-Uwe Hahn and Chang-Jiang Jin *In* DFVLR Proc. of Meteorol. Motor Glider (MEMO) Workshop '84 Jan. 1985 p 43-60 refs In GERMAN (For primary document see N85-35542 24-47)
Avail: NTIS HC A10/MF A01

A measuring method for the determination of the vertical wind velocity using small measuring aircraft (e.g., motor gliders) is developed. During the flight through a wind field, wind velocity fluctuations act on the aircraft in the form of additional forces. Aircraft reactions to these perturbations depend strongly on the steering maneuvers of the pilot. From this response behavior of the aircraft conclusions can be drawn as to the wind behavior if the aircraft dynamics are precisely known. The wind determination procedure can be simplified if only vertical wind is taken into account and if stationary behavior is assumed. The validity domain of these simplifying assumptions and the effect of measuring quantity errors (investigated by simulations) are discussed.
Author (ESA)

N85-35547# Deutsche Forschungs- und Versuchsanstalt fuer Luft- und Raumfahrt, Oberpfaffenhofen (West Germany). Inst. fuer Physik der Atmosphaere.

A COMPARISON BETWEEN FALCON DATA AND MOTOR GLIDER DATA [EIN VERGLEICH VON FALCON-DATEN MIT MOTORSEGLER-DATEN]

Hermann Willeke *In its* Proc. of Meteorol. Motor Glider (MEMO) Workshop '84 Jan. 1985 p 61-68 refs In GERMAN (For primary document see N85-35542 24-47)
Avail: NTIS HC A10/MF A01

The data of the Falcon aircraft and the ASK 16 motor glider meteorological flight under the same meteorological conditions are compared to estimate errors in the determination of the vertical wind component. Flight data and equipment of both aircraft are listed. The flight programs, data evaluation, and comparison method are described. The parameters measured by both aircraft are listed. The power spectra to the vertical velocity show good agreement. The differing relative deviations in heat fluxes shows that at least one unknown effect occurs. Author (ESA)

N85-35548# Deutsche Forschungs- und Versuchsanstalt fuer Luft- und Raumfahrt, Oberpfaffenhofen (West Germany). Inst. fuer Physik der Atmosphaere.

CASE STUDIES FOR FLUX MEASUREMENTS ALONG A LOW-FLYING ROUTE TO THE SOUTH OF MUNICH [FALLSTUDIEN ZU FLUSSMESSUNGEN ENTLANG EINER TIEFFLUGSTRECKE SUEDLICH VON MUENCHEN]

Manfred E. Reinhardt *In its* Proc. of Meteorol. Motor Glider (MEMO) Workshop '84 Jan. 1985 p 69-79 refs In GERMAN (For primary document see N85-35542 24-47)
Avail: NTIS HC A10/MF A01

Turbulent, sensible, and latent heat fluxes along low flying

motor glider routes are measured to study the atmospheric boundary layer. The behavior of sensible and latent heat fluxes on days with different meteorological conditions is discussed. Normalized frequency distributions of all measured vertical accelerations during measuring of flights are shown. Improvements of the measuring strategy are proposed to allow deeper analysis of the fine structure of atmospheric boundary layer phenomena. Author (ESA)

N85-35549# Eidgenoessisches Inst. fuer Reaktorforschung, Wuerenlingen (Switzerland).
ENVIRONMENTAL-PHYSICAL MEASUREMENTS AND DETERMINATION OF ATMOSPHERIC TURBULENCE WITH THE ASK-16 MOTOR GLIDER [UMWELTPHYSIKALISCHE MESSUNGEN UND ERFASSUNG ATMOSPHAERISCHER TURBULENZ MIT DEM MOTORSEGLER ASK-16]
Markus Hutter *In* DFVLR Proc. of Meteorol. Motor Glider (MEMO) Workshop '84 Jan. 1985 p 81-89 refs In GERMAN (For primary document see N85-35542 24-47)
Avail: NTIS HC A10/MF A01

Meteorological motor glider flights are performed to determine environmental and atmospheric turbulence parameters. Temperature and humidity probes used in the project CLIMOD (climate modification) studying the effect of increasing urbanization and planned nuclear power plants with their cooling system on the climate, and the results of the measurements and model calculations are discussed. Ozone in the lower troposphere due to the existence of smog reactions in the neighborhood of Zurich is investigated in ground stations and with two captive balloons; the regional ozone distribution was measured by motor gliders; the measurements strongly point at the Zurich agglomeration as the origin of the ozone-rich air. The motions of motor gliders due to air flows are used to determine atmospheric turbulence in the wavelength domain between 10 and 100 m; the measurements confirm previous results: agreement between the measurements and a mathematical turbulence parameterization model is found. Author (ESA)

N85-35550# Deutsche Forschungs- und Versuchsanstalt fuer Luft- und Raumfahrt, Oberpfaffenhofen (West Germany). Inst. fuer Physik der Atmosphaere.
MEASUREMENTS FOR THE DETERMINATION OF THE VERTICAL STRUCTURE OF THE CONVECTIVE BOUNDARY LAYER [MESSUNGEN ZUR VERTIKAL STRUKTUR DER KONVEKTIVEN GRENZSCHICHT]
Anne M. Jochum *In its* Proc. of Meteorol. Motor Glider (MEMO) '84 Workshop Jan. 1985 p 91-97 refs In GERMAN (For primary document see N85-35542 24-47)
Avail: NTIS HC A10/MF A01

A meteorological measuring compaign with motor gliders is performed to investigate turbulent vertical transport in the convective boundary layer and the spatial structure of thermal air fields. The measuring procedures are described. The vertical profiles measured and normalized (mixed-layer scaling) can be well integrated in the framework of similar profiles. Author (ESA)

N85-35551# Bonn Univ. (West Germany). Inst. fuer Meteorologie.
PARTITIONING OF THE VERTICAL TURBULENT ENERGY TRANSPORT INTO POSITIVE AND NEGATIVE CONTRIBUTIONS [AUFSPALTUNG DER VERTIKALEN TURBULENTEN ENERGIETRANSPORTE IN POSITIVE UND NEGATIVE BEITRAEGE]
Joerg M. Hacker *In* DFVLR Proc. of Meteorol. Motor Glider (MEMO) Workshop '84 Jan. 1985 p 99-114 refs In GERMAN (For primary document see N85-35542 24-47)
Avail: NTIS HC A10/MF A01

The concept of Lagrangian partitioning is applied to motor glider meteorological flight measuring series in order to study which single processes contribute to the turbulent net vertical transport of sensible and latent heat. Normalization and data evaluation procedures are described. It is found that in the upper level of the inversion layer the net fluxes consist of much higher single contributions than in the lower level, especially for the sensible heat flux. At both levels the moist, then hot, wakes give the largest contribution to the direct circulations, while the hot wakes give the largest contribution to the indirect circulations. For sensible heat the intensities of the processes due to hot air dominate at both levels. For latent heat the intensities of the processes due to moist air only dominate at the lower level. Author (ESA)

N85-35552# Bonn Univ. (West Germany). Inst. fuer Meteorologie.
AIRCRAFT MEASUREMENTS DURING THE BONN EXPERIMENT (BONEX 1) [DIE FLUGZEUGMESSUNGEN WAEHREND DES EXPERIMENTES BONEX 1]
Volker Kespe *In* DFVLR Proc. of Meteorol. Motor Glider (MEMO) Workshop '84 Jan. 1985 p 115-133 refs In GERMAN (For primary document see N85-35542 24-47)
Avail: NTIS HC A10/MF A01

Meteorological measurements are performed to investigate the horizontal and vertical structure of the atmospheric boundary layer. Two captive balloon systems, an energy budget station, and instrumented motor gliders are used. The synoptic measuring situation is described. The effect of the mask on the motor glider measurements of the lowest flight level is discussed. The spatial and temporal variation of the standard deviations of vertical wind velocity, potential temperature, and specific humidity, and of the correlation coefficients, as well as the turbulent fluxes of sensible and latent heat are obtained. The profile of the standard deviations are discussed. Author (ESA)

N85-35553# Bonn Univ. (West Germany). Inst. fuer Meteorologie.
MOTOR GLIDER MEASUREMENTS DURING THE URBAN ATMOSPHERE ENERGY BUDGET EXPERIMENT (EESA 1) [MOTORSEGLERMESSUNGEN WAEHREND DES EXPERIMENTES EESA 1]
Joerg M. Hacker *In* DFVLR Proc. of Meteorol. Motor Glider (MEMO) Workshop '84 Jan. 1985 p 135-141 refs In GERMAN (For primary document see N85-35542 24-47)
Avail: NTIS HC A10/MF A01

Meteorological measurements to compare energy budgets in rural and urban areas, and to study terms in the energy budget of sensible and latent heat are performed. The measurements of several ground stations, a radiosonde, two captive balloons, and a motor glider are combined. The model on which the investigation is based and the measuring strategy are described. The measured energy fluxes above the city and the surroundings are presented. The differences in the energy budgets of the boundary layer above the two areas are discussed. Author (ESA)

N85-35554# Deutsche Forschungs- und Versuchsanstalt fuer Luft- und Raumfahrt, Oberpfaffenhofen (West Germany). Inst. fuer Physik der Atmosphaere.
THE DETERMINATION OF LEE CIRCULATION DURING THE FOEHN WIND [ZUR BESTIMMUNG DER LEE-ZIRKULATION BEI FOEHN]
Klaus P. Hoinka *In its* Proc. of Meteorol. Motor Glider (MEMO) Workshop '84 Jan. 1985 p 143-149 ref In GERMAN (For primary document see N85-35542 24-47)
Avail: NTIS HC A10/MF A01

A field experiment, including measurements with motor gliders, are conducted to determine the circulation above and in the lee of the Alps during the foehn wind. Pressure, temperature, and humidity are measured and the isentropes are analyzed. Flow lines and trajectories agree with the isentropes, under the assumption that the flow is two-dimensional, frictionless, and adiabatic. The results show that motor gliders can provide an important contribution to the investigation of partial problems, as in the case of foehn, especially in connection with other measurements and investigation methods. Author (ESA)

N85-35555# Warsaw Univ. (Poland). Inst. of Geophysics.
METEOROLOGICAL MEASUREMENTS WITH MOTOR GLIDERS IN POLAND
Szymon P. Malinowski *In* DFVLR Proc. of Meteorol. Motor Glider

(MEMO) Workshop '84 Jan. 1985 p 151-156 refs (For primary document see N85-35542 24-47)
Avail: NTIS HC A10/MF A01

Meteorological measuring campaigns with instrumental motor gliders study small scale humidity and temperature inhomogeneities caused by dissipating cumulus clouds; and the invisible parts of cooling tower plumes. A program to investigate entrainment and mixing processes in small cumulus clouds is outlined. The motor glider instrumentation and the specification of the measuring unit are presented. The motor glider SZD-45 Ogar is described.
Author (ESA)

N85-35556# Technische Univ., Munich (West Germany). Lehrstuhl fuer Flugmechanik und Flugregelung.
DEVELOPMENT AND OPERATION OF A MEASURING DATA ACQUISITION SYSTEM FOR USE IN LIGHT AIRPLANES [ENTWICKLUNG UND BETRIEB EINER MESSDATENERFASSUNGSANLAGE (MEA) FUER DEN EINSATZ IN LEICHTFLUGZEUGEN] c35
Peter Huber *In* DFVLR Proc. of Meteorol. Motor Glider (MEMO) Workshop '84 Jan. 1985 p 157-160 In GERMAN (For primary document see N85-35542 24-47)
Avail: NTIS HC A10/MF A01

A data acquisition system weighing 35 kg is developed for use onboard light aircraft. The basic concept of the system (task definition, requirements) is given. Development status (onboard components, special systems, ground components, measuring data recorder, technical data, and data evaluation software) is presented. The performed measurements are reviewed.
Author (ESA)

N85-35557# Deutsche Forschungs- und Versuchsanstalt fuer Luft- und Raumfahrt, Oberpfaffenhofen (West Germany). Inst. fuer Flugmechanik.
ACCURACY AND ERROR ANALYSIS [GENAUIGKEITS- UND FEHLERANALYSE]
Jean Skudridakis *In its* Proc. of Meteorol. Motor Glider (MEMO) Workshop '84 Jan. 1985 p 161-194 ref In GERMAN (For primary document see N85-35542 24-47)
Avail: NTIS HC A10/MF A01

Accuracy estimation and error analysis of physical quantities measured during flights are treated. The standard deviation of the Gaussian distribution as criterion for the uncertainty of the measured quantity is discussed. Accuracy estimates via the covariance matrices of the state and measurement equations, and via system identification are explained. The effect of the measurement precision, and a dynamic angle of attack equation are given. The example of air and recovery temperature measurement is presented.
Author (ESA)

N85-35558# Technische Univ., Brunswick (West Germany). Inst. fuer Flugfuehrung.
THE PRINCIPLES OF WIND MEASUREMENT WITH THE HELP OF AIRCRAFT [GRUNDLAGEN DER WINDMESSUNG MIT HILFE VON FLUGZEUGEN]
Peter Voersmann *In* DFVLR Proc. of Meteorol. Motor Glider (MEMO) Workshop '84 Jan. 1985 p 195-205 refs In GERMAN; ENGLISH summary (For primary document see N85-35542 24-47)
Avail: NTIS HC A10/MF A01

The three components of the wind vector are computed in real time by taking the difference between the inertial velocity and the true airspeed. To perform this calculation, it is necessary to transform the true airspeed from the aerodynamic to the Earth-fixed coordinate system. This coordinate transformation contains numerous trigonometric functions (sine and cosine functions), which yield nonlinear relations for the determination of the wind vector components. These relations present the theoretical principles for measuring winds onboard an aircraft. Author (ESA)

N85-35559# Battelle Pacific Northwest Labs., Richland, Wash.
TURBULENT STRUCTURE OF STABLY STRATIFIED NOCTURNAL SLOPE FLOWS Final Report, 1 Mar. 1983 - 28 Feb. 1985
J. C. Doran and T. W. Horst Apr. 1985 54 p
(Contract DAAG29-83-K-0052)
(AD-A155845; ARO-19862.2-GS) Avail: NTIS HC A04/MF A01 CSCL 20/4

Turbulence characteristics of wind and temperature fields in drainage flows over a simple slope were studied. Data was collected on a simple, nearly two-dimensional mountain ridge with little vegetation. Anemometers, thermistors, and thermometers were used to collect mean and turbulent wind and temperature data 150 m below the ridgeline. Evidence for katabatically driven winds was found for a wide range of ambient conditions whenever a surface inversion was formed. When a velocity jet characteristic of good slope flows was present, the vertical profiles of turbulence were found to differ significantly from those over flat terrain, with the turbulent kinetic energy no longer a monotonically decreasing function of height. Richardson number profiles revealed a value well in excess of critical values in the region of the jet. The existence of an internal mixing layer, found by other investigators in deeper drainage flows, was not confirmed. Calculations of turbulent kinetic energy budgets showed a close balance between shear production and viscous dissipation, with buoyancy forces playing a relatively minor role. Above the jet, the contribution from the vertical heat flux was only a few percent of the shear production term and resulted from a near-calculation of the contributions from the heat flux normal to the sloping surface and flux parallel to the surface. In this region, the heat flux parallel to the slope was upslope, resulting in an energy production term, while below the jet it was downslope, resulting in an energy loss.
GRA

N85-35560# Naval Postgraduate School, Monterey, Calif.
METEOROLOGICAL DATA FROM THE OPTOMA (OCEAN PREDICTION THROUGH OBSERVATIONS, MODELING AND ANALYSIS) PROGRAM OPTOMA 2, LEG D2. 30 JUN. - 10 JUL. 1984 M.S. Thesis
M. C. Colton and C. N. K. Mooers May 1985 79 p
(AD-A156134; NPS68-85-017) Avail: NTIS HC A05/MF A01 CSCL 04/2

The OPTOMA (Ocean Prediction Through Observations, Modeling and Analysis) Program seeks to understand the mesoscale (front, eddies, and jets) variability and dynamics of the California Current System and to determine the scientific limits to practical mesoscale ocean forecasting. This report presents the meteorological data acquired by twenty-six radiosondes launched during the hydrographic cruise OPTOMA11, Leg DII (30 June to 10 July, 1984). To compare the prevailing atmospheric and oceanic conditions, the radiosonde potential temperature and specific humidity profiles are plotted with nearly coincident XBT temperature profiles. Also included are: (1) time series plots of hourly dry-bulb and wet-bulb temperatures and hourly wind velocities, (2) an AVHRR image, and (3) National Weather Service surface pressure analyses for the cruise period.
GRA

N85-35561# Hawaii Univ., Honolulu. Dept. of Meteorology.
MEAN CLOUDINESS OVER THE GLOBAL TROPICS FROM SATELLITE OBSERVATIONS Final Report, 15 Jun. 1983 - 14 Dec. 1984
J. C. Sadler, B. Kilonsky, L. Oda, and A. Hori Dec. 1984 142 p
(Contract N00014-83-K-0496; NR Proj. F59-553)
(AD-A156188; UHMET-84-1; NEPRF-CR-84-09) Avail: NTIS HC A07/MF A01 CSCL 04/2

Charts of mean monthly cloudiness over the global tropics, based on satellite observations during the period February 1965 through July 1973, are provided. Estimates of cloud amounts are based on daily nephanalyses for the eight-year period, assessing cloud cover in 2.5 degree latitude-longitude intervals. Time-latitude sections are included for selected representative longitudes, to aid in summarizing seasonal variations of mean cloudiness. Mean cloudiness is particularly useful in describing the seasonal variability of cloud systems. Both mesoscale and synoptic features of clear and cloudy areas are revealed by these analyses, including windward-leeward cloudiness changes resulting from island barrier effects. This realistic assessment of cloud amount variability in the tropics will be useful in regional climatologies and in studies involving air-sea interaction.
GRA

N85-35562# Oak Ridge National Lab., Tenn.
CARBON DIOXIDE AND CLIMATE: A WORKING GLOSSARY
1985 48 p
(Contract DE-AC05-84OR-21400)
(DE85-013535; ORNL/CDIC-10) Avail: NTIS HC A03/MF A01

A glossary is presented which provides a reference to definitions of CO2-related terms and units of conversion. General principles are emphasized and are presented in a format that can be used by both the specialist and the generalist. DOE

N85-35563# California Univ., Livermore. Lawrence Livermore Lab.
INVESTIGATION OF THE LIGHTNING VULNERABILITY OF NUCLEAR EXPLOSIVE TEST SYSTEMS AT THE NEVADA TEST SITE
R. T. Hasbrouck 4 Oct. 1985 16 p refs Presented at the Intern. Conf. on Lightning and Static Elec., Paris, 10 Jun. 1985
(Contract W-7405-eng-48)
(DE85-011761; UCRL-91626; CONF-8506121-1) Avail: NTIS HC A02/MF A01

The underground detonation of nuclear explosive test devices is discussed. To assure safety, all components, systems and procedures are analyzed and subjected to nuclear explosive safety study. All sources and paths of energy that could conceivably initiate an unwanted detonation are considered. One of the energy sources considered is lightning. Several lightning hazard were studied. It was concluded that the magnitude of lightning energy reaching the high explosive or the detonators was small compared to that required to produce a detonation. The lightning vulnerability of the nuclear explosive test systems was reexamined. Simulated lightning tests are used to provide verification of the safety claims. Although underground nuclear testing is unique, the overall method and results of this investigation should be of use to those faced with a lightning threat in a large, cable-interconnected system. E.A.K.

N85-35564# Sandia Labs., Albuquerque, N. Mex.
APPLICATION OF PULSED POWER IN THE SIMULATION OF SEVERE NATURAL LIGHTNING
R. A. White 1985 5 p Presented at the 5th IEEE Pulsed Power Conf., Washington, D.C., 10 Jun. 1985
(Contract DE-AC04-76DP-00789)
(DE85-012866; SAND-84-2374C; CONF-850616-13) Avail: NTIS HC A02/MF A01

Pulsed-power technology has application in the laboratory simultation of severe natural lightning. The value of pulsed-power approaches in safety assessment testing, and for evaluating lightning induced hazards and transient effects were confirmed. Performance capability examples are presented to substantiate the practicality of using crowbarred Marx impulse generators for lightning simultation testing. Severe, double-pulse, direct-stroke environments with continuing current were applied to full-size aircraft and a variety of other test items. A typical double-pulse test simulation of severe lightning has a first-current peak in excess of 200 kiloamps, a rise time of about one microsecond, and a half-amplitude pulse width of about 200 microseconds. DOE

N85-35565# Bureau of Reclamation, Denver, Colo.
PROJECT SKYWATER, 1983-84 SCPP (SIERRA COOPERATIVE PILOT PROJECT) DATA INVENTORY
Oct. 1984 181 p
(PB85-187052) Avail: NTIS HC A09/MF A01 CSCL 05B

An inventory of all data collected from October 15, 1983, through April 1984, in association with the SCPP (Sierra Cooperative Pilot Project), a weather modification research project in winter orographic cloud seeding. It is subdivided into an introduction plus 12 sections and appendixes A, B, C and D. Forecasting, Radar, Satellite, Aircraft, Rawinsondes, Surface Meteorological Observations, Precipitation Gage Network, Ground based Microphysical Observations, Radiometer, Cooperative and Operational Seeding Activities, Snow Chemistry Measurements, National Weather Service, Federal Aviation Administration, and National Climatic Center Products, and Sierra PROBE Data Availability, SCPP Operations for 1983-84, University of Wyoming King Air Flight Summary Notes. GRA

N85-35566# National Oceanic and Atmospheric Administration, Washington, D. C. National Environmental Satellite, Data and Information Service.
SURFACE CYCLOGENESIS AS INDICATED BY SATELLITE IMAGERY
F. J. Smigielski and G. P. Ellrod Mar. 1985 37 p refs
(PB85-191815; NOAA/TM-NESDIS-9) Avail: NTIS HC A03/MF A01 CSCL 04B

Indications of extratropical cyclogenesis which can be observed in infrared, visible or 6.7 micrometers moisture channel satellite imagery are summarized. These include semi-quantitative techniques for estimating the minimum central pressure and the location and strength of maximum surface winds accompanying the low. Satellite analysis of extratropical storm systems is invaluable over oceanic regions where conventional data is limited. GRA

N85-35567# National Center for Atmospheric Research, Boulder, Colo.
MAINTENANCE OF BLOCKING ANTICYCLONES IN A GENERAL CIRCULATION MODEL Ph.D. Thesis
S. L. Mullen 1985 293 p refs Sponsored by NSF
(PB85-190866; NCAR/CT-86) Avail: NTIS HC A13/MF A01 CSCL 04B

Blocking anticyclones that appear in perpetual January simulations of a general circulation model are examined. Blocks in three geographical regions are studied: the North Pacific, the North Atlantic and Western North America. Local time-averaged balances of vorticity and heat are evaluated for composite cases of blocking. The following common relationships emerged from these budgets. The time-mean divergence term is, in general, a first order term throughout the troposphere and its pattern over severe orography is closely related to the underlying topography. The horizontal advection of the time-mean temperature field by the mean wind throughout the troposphere is a first order term and is mainly responsible for maintaining the block's thermal perturbations. The mountains appear capable of influencing the shape of the model blocks through the divergence term, but preliminary results indicate that orographic forcing may not be absolutely essential for the blocking process to occur in the model. GRA

N85-35568# National Center for Atmospheric Research, Boulder, Colo.
TWO-POINT CLOSURE STUDY OF COVARIANCE BUDGETS FOR TURBULENT RAYLEIGH-BENARD CONVECTION Ph.D. Thesis
W. P. Dannevik 1985 78 p refs Sponsored by NSF Prepared in cooperation with St. Louis Univ., Mo.
(PB85-189108; NCAR/CT-85) Avail: NTIS HC A05/MF A01 CSCL 04B

Statistical properties of turbulent Rayleigh-Benard convection in a laterally periodic domain between free slip boundaries are investigated. Ensemble mean dynamics of this system are studied by means of a non-Markovian two-point closure obtained from the Direct Interaction Approximation by application of a two time perturbation formalism and nonequilibrium fluctuation-dissipation relation. The computations are economized by use of Pade approximation methods to estimate the modal response function and triad relaxation time. Comparisons at the level of second- and third-order moments are made between the closure predictions and averages obtained from Direct Spectral Simulation (DSS) solutions of the full Naiver-Stokes-Boussinesq equations. The final state convective heat flux and volume integrated kinetic energy and thermal variance are predicted to 0(5%) accuracy with the closure model. GRA

N85-35569# National Oceanic and Atmospheric Administration, Washington, D. C. Environmental Research Lab.
PROGRAM FOR REGIONAL OBSERVING AND FORECASTING SERVICES (PROFS) Annual Report, 1 Oct. 1983 - 30 Sep. 1984

Jan. 1985 25 p refs
(PB85-188050) Avail: NTIS HC A02/MF A01 CSCL 04B

The Program for Regional Observing and Forecasting Services (PROFS) enjoyed its fifth year as a NOAA organization in FY 1984. It has been initiated in FY 1980 as a part of the Environmental Research Laboratories. The mission of the program is to improve short range operational weather services by the development, testing, and transfer of scientific and technological advances. Management suggested two areas of focus: Forecasting research and development: a test program and joint research efforts with other NOAA laboratories. Technology transfer: direct work with operational programs such as the National Weather Service's AWIPS-90 (Advanced Weather Interactive Processing System for the 1990s), NESDIS's VISSR Atmospheric Sounder (VAS), and the NEXRAD (Next Generation Weather Radar program). GRA

N85-35570# National Oceanic and Atmospheric Administration, Seattle, Wash. Pacific Marine Environmental Lab.

CURRENT INVENTORY OF ANTHROPOGENIC CARBON DIOXIDE IN THE NORTH PACIFIC SUBARCTIC GYRE

J. D. Cline, R. A. Feely, K. Kelly-Hanson, J. F. Gendron, and D. P. Wisegarver Mar. 1985 52 p refs
(PB85-187938; NOAA-TM-ERL-PMEL-60) Avail: NTIS HC A04/MF A01 CSCL 04B

The atmospheric increase of carbon dioxide is the result of the burning of fossil fuels and massive deforestation currently underway. Since 1958, the atmosphere CO2 concentration has risen from about 315 ppm to about 343 ppm. The major repositories for anthropogenic CO2 are the oceans and the atmosphere. The distributions of freon-11, as a surrogate tracer, have been combined with precise measurements of total carbon dioxide, total alkalinity oxygen, nutrient and hydrography in order to estimate the amount of excess CO2 in the subarctic water of the North Pacific gyre. Calculations indicate that approximately 4 x 10 to the 1b power g of excess carbon, or about 2% of the total estimated fossil-fuel derived carbon input now resides in the mixed layer and thermocline waters of the North Pacific gyre. GRA

N85-35571# National Oceanic and Atmospheric Administration, Boulder, Colo. Environmental Sciences Group.

AIRBORNE INVESTIGATIONS OF MESOSCALE CONVECTIVE SYSTEMS (AIMCS), 1984: OPERATIONAL SUMMARY AND DATA INVENTORY

Jan. 1985 82 p
(PB85-187904; NOAA-TM-ERL-ESG-9) Avail: NTIS HC A05/MF A01 CSCL 04B

The Airborne Investigations of Mesoscale Convective Systems (AIMCS) Program-1984 are summarized; type, amount, and frequency are listed for the data obtained. Highlights and outlook for the future are discussed. Each flight mission and the six subprograms are described in detail. Author (GRA)

48 OCEANOGRAPHY

Includes biological, dynamic and physical oceanography; and marine resources.

N85-35572# Defence Research Information Centre, Orpington (England).

SEASONAL VARIABILITY AND SPATIAL NON-UNIFORMITY OF BIOLUMINESCENCE IN THE MEDITERRANEAN SEA

E. P. Bityukov Jun. 1985 24 p refs Transl. into ENGLISH of Ekol. Morya (USSR), v. 8, 1982 p 10-20
(DRIC-T-7545; BR96067) Avail: NTIS HC A02/MF A01

The bioluminescence of individual planktonic organisms and the integral effect of this feature of pelagic communities were studied in the Mediterranean. Analysis of the structure of the bioluminescent emission field suggests the presence of alternating layers with high and low bioluminescence, pointing to nonuniform vertical distribution of plankton. There is seasonal variation in the intensity of bioluminescence both in the entire expanse of water, and in layers of elevaters luminosity whose location depth is in most cases stable. A general trend of the spatial distribution of bioluminescence towards an increase in its level in a westward direction is established. Author (ESA)

N85-35573*# National Aeronautics and Space Administration. Ames Research Center, Moffett Field, Calif.

SEA SURFACE AND REMOTELY SENSED TEMPERATURES OFF CAPE MENDOCINO, CALIFORNIA

L. C. Breaker (NOAA, Redwood City, Calif.), J. C. Arvesen, D. Frydenlund (Coast Guard, San Francisco), J. S. Myers (ATAC), and K. Short (Northwest Ocean Services Center) Sep. 1985 29 p refs
(NASA-TM-86712; Rept-85208; NAS 1.15:86712) Avail: NTIS HC A03/MF A01 CSCL 08J

During September 3 to 5, 1979, a multisensor oceanographic experiment was conducted off Cape Mendocino, California. The purpose of this experiment was to validate the use of remote sensing techniques over an area along the U.S. west coast where coasted upwelling is known to be intense. Remotely sensed mutlispectral data, including thermal infrared imagery, were collected above an upwelling feature off Cape Mendocino. Data were acquired from the TIRNOS-N and NOAA-6 polar orbiting satellites, the NASA Ames Research Center's high altitude U-2 aircraft, and a U.S. Coast Guard C-130 aircraft. Supporting surface truth data over the same feature were collected aboard the National Oceanic and Atmospheric Administration (NOAA) ship, OCEANOGRAPHER. Atmospheric soundings were also taken aboard the ship. The results indicate that shipboard measurements of sea surface temperatures can be reproduction within 1 C or better through remote observation of absolute infrared radiance values (whether measured aboard the NOAA polar orbiting satellite, the U-2 aircraft, or the Coast Guard aircraft) by using appropriate atmospheric corrections. Also, the patterns of sea surface temperature which were derived independently from the various remote platforms provide a consistent interpretation of the surface temperature field. Author

N85-35574# Committee on Tidal Hydraulics (Army), Washington, D.C.

BIBLIOGRAPHY ON TIDAL HYDRAULICS. REPORT 2. SUPPLEMENT 9: SUPPLEMENTARY MATERIAL COMPILED FROM JUNE 1980 - JUNE 1983. TIDAL FLOWS IN RIVERS AND HARBORS

K. M. Kennedy and A. S. Clark Jun. 1985 125 p
(AD-A155990; Rept-2-Suppl-9) Avail: NTIS HC A06/MF A01 CSCL 08/3

This 9th supplement contains approximately 440 references. Topics include: theoretical considerations; sedimentation; salinity effects; contamination; regulation and improvement; modeling and other laboratory experiments; surveys and instruments; and basic physical data is presented. GRA

N85-35575# Coastal Engineering Research Center, Vicksburg, Miss.

ATLANTIC COAST HINDCAST. PHASE 2: WAVE INFORMATION, ADDITIONAL EXTREMAL ESTIMATES Final Report

W. D. Corson and B. A. Tracy May 1985 39 p
(AD-A156137; WIS-15) Avail: NTIS HC A03/MF A01 CSCL 08/3

Estimates of extreme wave heights for 73 open-ocean locations on the US East Coast are presented. The estimates include the median wave heights and interquartile ranges for 100-, 50-, 20-, 10-, and 5- year return periods. Only waves generated by extra-tropical storms are considered. Hurricane generated waves will be analyzed in future work. GRA

N85-35576# Naval Ocean Research and Development Activity, Bay St. Louis, Miss.

A TOWED INSTRUMENT VEHICLE FOR DEEP OCEAN SAMPLING Final Report

C. R. Rein, D. A. Wiesenburg, and D. M. Lavoie Jan. 1985 50 p
(AD-A156322; NORDA-90) Avail: NTIS HC A03/MF A01 CSCL 13/10

A vehicle that can take instrumentation into the ocean while being towed by a surface craft has been built. The vehicle body is a flooded, 8-foot-long cylinder stabilized at the tail and depressed by a short wing. Most of the structural loads are borne by four full-length radius plates. These plates divide the cylindrical body lengthwise into four wet compartments that have quadrant cross sections. Each quadrant can hold instrument payloads as large as 5-1/2-in. in diameter. Each quadrant can be uncovered independently to service the payload. These features are improvements over previous designs for carrying an assortment of payloads. Construction cost was only $3200. Design criteria, details of the construction, and results of an initial tow test of the towed body are presented. GRA

N85-35577# Naval Ocean Research and Development Activity, Bay St. Louis, Miss.
THE NORDA/FNOC (NAVAL OCEAN RESEARCH AND DEVELOPMENT ACTIVITY'S/FLEET NUMERICAL OCEANOGRAPHY CENTER) POLAR ICE PREDICTION SYSTEM (PIPS)-ARCTIC: A TECHNICAL DESCRIPTION Final Report
R. Preller May 1985 66 p
(AD-A156332; NORDA-108) Avail: NTIS HC A04/MF A01 CSCL 08/12

The hydrodynamic/thermodynamic sea ice model designed by W.D. Hibler was modified to run operationally at the Fleet Numerical Oceanography Center (FNCC). Changes were made to adapt the model to the Cyber 205 system and to allow easy interfacing between the model and the data base needed to drive the model, the Navy Operational Global Atmospheric Prediction System (NOGAPS). The Polar Ice Prediction System (PIPS) contains the most recently updated thermodynamic version of the model. Improved numerics have been included in the model relaxation routine, which increases the model efficiency by a factor of three. A long-term simulation of the ice model was run using the NOGAPS forcing fields from 18 January 1983 to 18 January 1984. The model was run for three years and used the 1983 data repeatedly. This repetition allows the model to spin up from its initial conditions, a 3.3 m thick layer of ice, to an appropriate ice thickness for 1983. Results from the third year of integration are compared to previous model results and observations. GRA

N85-35444# Geological Survey, Alexandria, Va.
COBALT-RICH FERROMANGANESE CRUSTS IN THE OCEANS Abstract Only
James R. Hein and Frank T. Manheim *In its* USGS Res. on Mineral Resources, 1985 1985 p 23-24 (For primary document see N85-35435 24-42)
Avail: NTIS HC A05/MF A01

N85-35446# Geological Survey, Alexandria, Va.
MASSIVE SULFIDE DEPOSITS FROM THE SOUTHERN JUAN DE FUCA RIDGE Abstract Only
Randolph A. Koski, David A. Clague, James L. Bischoff, and Robert A. Zierenberg *In its* USGS Res. on Mineral Resources, 1985 1985 p 27-28 (For primary document see N85-35435 24-42)
Avail: NTIS HC A05/MF A01

N85-35454# Geological Survey, Alexandria, Va.
PRELIMINARY RESULTS OF AN ALVIN DIVE PROGRAM ON ACTIVE HYDROTHERMAL VENTS AT THE SOUTHERN JUAN DE FUCA RIDGE Abstract Only
W. R. Normark, J. L. Morton, J. L. Bischoff, R. Brett, R. T. Holcomb, E. S. Kappel, R. A. Koski, S. L. Ross, W. C. Shanks, III, J. F. Slack et al *In its* USGS Res. on Mineral Resources, 1985 1985 p 54-55 (For primary document see N85-35435 24-42)
Avail: NTIS HC A05/MF A01

51 LIFE SCIENCES (GENERAL)

Includes genetics.

N85-35578*# National Aeronautics and Space Administration. Ames Research Center, Moffett Field, Calif.
NASA DEVELOPMENTAL BIOLOGY WORKSHOP: A SUMMARY
Kenneth A. Souza, ed. and Thora W. Halstead, ed. (NASA, Washington) Sep. 1985 94 p refs Workshop held in Arlington, Va., 2-4 May 1984
(NASA-TM-86756; Rept-85264; NAS 1.15:86756) Avail: NTIS HC A05/MF A01 CSCL 06C

The Life Sciences Division of the National Aeronautics and Space Administration (NASA) as part of its continuing assessment of its research program, convened a workshop on Developmental Biology to determine whether there are important scientific studies in this area which warrant continued or expanded NASA support. The workshop consisted of six panels, each of which focused on a single major phylogenetic group. The objectives of each panel were to determine whether gravity plays a role in the ontogeny of their subject group, to determine whether the microgravity of spaceflight can be used to help understand fundamental problems in developmental biology, to develop the rationale and hypotheses for conducting NASA-relevant research in development biology both on the ground and in space, and to identify any unique equipment and facilities that would be required to support both ground-based and spaceflight experiments. For individual titles, see N85-35579 through N85-35586.

N85-35579*# National Aeronautics and Space Administration. Ames Research Center, Moffett Field, Calif.
EFFECTS OF MICROGRAVITY AND HYPERGRAVITY ON INVERTEBRATE DEVELOPMENT
Jaime Miquel *In its* NASA Develop. Biol. Workshop Sep. 1985 p 7-34 refs (For primary document see N85-35578 24-51)
Avail: NTIS HC A05/MF A01 CSCL 06C

Data suggest that abnormal gravity loads do not increase the rate of mutations in lower animals. Insects such as Drosophila melanogaster and Tribolium confusum have been able to reproduce aboard unmanned and manned space satellites, though no precise quantitative data have been obtained on mating competence and various aspects of development. Research with Drosophila flown on Cosmos spacecraft suggests that flight behavior is seriously disturbed in insects exposed to microgravity, which is reflected in increased oxygen utilization and concomitant life shortening. The decrease in longevity was less striking when the flies were enclosed in space, which suggests that they could adapt to the altered gravitational environment when maturation of flight behavior took place in microgravity. The reviewed data suggest that further research on the development of invertebrates in space is in order for clarification of the metabolic and behavioral effects of microgravity and of the development and function of the orientation and gravity sensing mechanisms of lower animals. Author

N85-35580*# Case Western Reserve Univ., Cleveland, Ohio. Dept. of Anatomy.
VERTEBRATE DEVELOPMENT IN SPACE: GRAVITY IS A DRAG (AND HAS BEEN FOR EONS AND EONS)
J. Richard Keefe *In* NASA. Ames Research Center NASA Develop. Biol. Workshop Sep. 1985 p 35-43 refs (For primary document see N85-35578 24-51)
Avail: NTIS HC A05/MF A01 CSCL 06C

Brief sketches of developmental biology studies during spaceflight presented are intended to be complete in scope and to provide the reader with an overview of the present status of such studies. Means of evaluating both the direct role of gravity on all processes of mammalian reproduction and development as well as defining the means of assessing indirect transplacemental aspects are considered. The potential present in the development of a spaceflight system/program specifically designed to provide chronic exposure of a representative variety of mammalian species with periodic sampling for multiple generations to fully assess the potential impact of an altered gravitational vector on general mammalian development is also considered. E.R.

N85-35581*# Case Western Reserve Univ., Cleveland, Ohio. Dept. of Anatomy.
REPORT OF THE NASA MAMMALIAN DEVELOPMENTAL BIOLOGY WORKING GROUP
J. Richard Keefe *In* NASA. Ames Research Center NASA Develop. Biol. Workshop Sep. 1985 p 45-63 refs (For primary document see N85-35578 24-51)
Avail: NTIS HC A05/MF A01 CSCL 06C

Development is considered to encompass all aspects of the mammalian life span from initial initial germ cell production through the complete life cycle to death of the organism. Thus, gamete production, fertilization, embryogenesis, implantation, fetogenesis, birth, peri- and postnatal maturation, and aging were all considered as stages of a development continuum relevant to problems of Space Biology. Deliberations thus far have been limited to stages of the development cycle from fertilization to early postnatal life. The deliberations are detailed. E.R.

N85-35582*# Wisconsin Univ., Madison. Dept. of Anatomy.
REPORT OF THE AVIAN DEVELOPMENT WORKING GROUP
John F. Fallon *In* NASA. Ames Research Center NASA Develop. Biol. Workshop Sep. 1985 p 65-68 (For primary document see N85-35578 24-51)
Avail: NTIS HC A05/MF A01 CSCL 06C

The anteroposterior axis of the avian embryo is established before it is laid. Baer's rule states that the cephalic end of the avian embryo will be away from the observer when the pointed end of the shell is on the observer's right. There are experimental data available which indicate gravity has a role in the establishment of the anteroposterior axis while the egg is in the uterus; this results in Baer's rule. The influence of gravity on egg development is studied. Author

N85-35583*# Indiana Univ., Bloomington. Dept. of Biology.
REPORT OF AMPHIBIAN DEVELOPMENT GROUP
George Malacinski *In* NASA. Ames Research Center NASA Develop. Biol. Workshop Sep. 1985 p 69-73 refs (For primary document see N85-35578 24-51)
Avail: NTIS HC A05/MF A01 CSCL 06C

Amphibian and fish embryos are extremely well suited for studies on pattern specification, whereas other systems (e.g., avian or mammalian) might be just as well suited for studies on differentiation or growth. Those distinctions are important for at least two reasons: (1) More precise focus regarding underlying mechanisms is called for when those distinctions are made. That facilitates the formulation of specific models or hypotheses; and (2) stress effects (i.e., the effects of weightlessness on structures (e.g., bones) which normally bear a load) are distinguished as being indirect, in contrast to direct effects of microgravity, which would be expected to act on pattern specification. That is, direct gravity effects are distinguished from indirect stress effects. Author

N85-35584*# Rockstein (Morris), Coral Gables, Fla.
REPORT OF THE INSECT DEVELOPMENT GROUP
Morris Rockstein *In* NASA. Ames Research Center NASA Develop. Biol. Workshop Sep. 1985 p 75-77 (For primary document see N85-35578 24-51)
Avail: NTIS HC A05/MF A01 CSCL 06C

Drosophila metanogaster was chosen as the insect species of choice, in regard to gravity response experiments involving normal reproduction and develop different strains. The specific gravity responses which might be affected by microgravity and are exhibited in normal reproduction and development include normal flight for courtship, mating and oviposition, tropisms for pupating or emergency of the adult, and crawling for gettering food by the larval instars at the organismic level. At the suborganismic elevel, it is believed that maturation of developing eggs in the virgin female and embryonic development of the developing egg could be affected by microgravity and warrant study. Author

N85-35585*# Millsaps Coll., Jackson, Miss.
AQUATIC INVERTEBRATE DEVELOPMENT WORKING GROUP
Dewey Meyers *In* NASA. Ames Research Center NASA Develop. Biol. Workshop Sep. 1985 p 79-81 refs (For primary document see N85-35578 24-51)
Avail: NTIS HC A05/MF A01 CSCL 06C

Little definitive evidence exists to show that gravity plays a major role in embyrogenesis of aquatic invertebrates. Two reasons for this may be: (1) few studies have been done that emphasize the role of gravity; and (2) there simply may not be any gravity effect. The buoyant nature of the aquatic environment could have obscured any evolutionary effect of gravity. The small size of most eggs and their apparent lack of orientation suggests reduced gravitational influence. Therefore, it is recommended that the term development, as applied to aquatic invertebrates, be loosely defined to encompass behavioral and morphological parameters for which baseline data already exist. Author

N85-35586*# Jet Propulsion Lab., California Inst. of Tech., Pasadena.
REPORT OF THE MICROBIAL DEVELOPMENT WORKING GROUP
Gregory Nelson *In* NASA. Ames Research Center NASA Develop. Biol. Workshop Sep. 1985 p 83-89 refs (For primary document see N85-35578 24-51)
Avail: NTIS HC A05/MF A01 CSCL 06C

In formulating ideas on the relationship of gravity to the development, growth, and reproduction of microorganisms, a rather liberal definition of microorganisms is used which includes bacteria, yeasts, protists, filamentous fungi, and single cells in culture. A principal advantage of microorganisms as experimental subjects is the rigor with which they can be defined and controlled. As single cells, each cell may be regarded as identical to the others in the population. This property applies to the morphology, physiology, and genetic parameters of the cells. The growth and development of the population is subject to precise manipulation as the nutritional requirements are known and minimal media formulations have been developed. Growth and differentiation can be manipulated in a variety of ways, such as alteration of the culture temperature and food supply, or by use of mutants. Finally, the short generation times of microorganisms provide the opportunity to conduct multigenerational studies within practical time limits and, in a similar vein, cellular responses to various stimuli or stresses are conveniently monitored because of the rapid response times of single cells. Author

N85-35587# Commonwealth Scientific and Industrial Research Organization, Aspendale (Australia). Div. of Atmospheric Research.
THE MEASUREMENT OF NITROGEN OXIDE (NO, NO2) EXCHANGE OVER PLANT/SOIL SURFACES
I. E. Galbally, C. R. Roy (Australian Radiation Lab.), C. M. Elsworth, and H. A. Rabich 1985 26 p refs Document includes Microfiche supplement
(CSIRO-DAR-TP-8; ISBN-0-643-03867-1) Avail: NTIS HC E03/MF A01

A chamber technique for evaluating fluxes of NO and NOX (NO + NO2) over soil/plant surfaces is described. A mathematical model involving a constant exhalation rate of NO from the soil/plant surface coupled with a competing concentration dependent uptake process is formulated. This model provides a good fit to the data obtained from chamber measurements and allows the quantitative determination of both net and gross NO and NOX fluxes over the plant/soil surfaces examined. Measurements of these fluxes and supporting data from a grazed pasture at the Agricultural Research Center, Victoria during 2 weeks in April 1978 are presented. Author

N85-35588*# Arizona Univ., Tucson. Dept. of Biochemistry.
POSSIBLE MECHANISM FOR CHANGES IN GLYCOGEN METABOLISM IN UNLOADED SOLEUS MUSCLE
Erik J. Henriksen and Marc E. Tischler [1985] 2 p
(Grant NAGw-227)
(NASA-CR-176184; NAS 1.26:176184) Avail: NTIS HC A02/MF A01 CSCL 06C

Carbohydrate metabolism has been shown to be affected in a

number of ways by different models of hypokinesia. In vivo glycogen levels in the soleus muscle are known to be increased by short-term denervation and harness suspension. In addition, exposure to 7 days of hypogravity also caused a dramatic increase in glycogen concentration in this muscle. The biochemical alterations caused by unloading that may bring about these increases in glycogen storage in the soleus were sought. G.L.C.

N85-35589*# Arizona Univ., Tucson. Dept. of Biochemistry.
RESPONSE OF AMINO ACIDS IN HINDLIMB MUSCLES TO RECOVERY FROM HYPOGRAVITY AND UNLOADING BY TAIL-CAST SUSPENSION
Marc E. Tischler, Erik J. Henriksen, Stephan Jacob, and Paul H. Cook [1985] 2 p refs
(Grant NAGw-227)
(NASA-CR-176183; NAS 1.26:176183) Avail: NTIS HC A02/MF A01 CSCL 06C

Concentrations of glutamine, glutamate, aspartate (+ asparagine) and alanine were compared in hindlimb muscles of SL-3 and ground control rats. Alanine was lower in the soleus of flown rats but not of suspended animals, with no response in other muscles except a slight increase in the unloaded plantaris. With recovery, alanine in the soleus was elevated. Since no differences in alanine metabolism were found by isolated muscle, changes in muscle alanine are probably due to altered body use of this amino acid leading to varied plasma levels. G.L.C.

N85-35590*# Arizona Univ., Tucson. Dept. of Biochemistry.
RESPONSE OF RAT HINDLIMB MUSCLES TO 12 HOURS RECOVERY FROM TAIL-CAST SUSPENSION
Marc. E. Tischler, Erik J. Henriksen, Stephan Jacob, and Stephen R. Jaspers [1985] 2 p refs
(Grant NAGw-227)
(NASA-CR-176182; NAS 1.26:176182) Avail: NTIS HC A02/MF A01 CSCL 06C

Previous work has shown a number of biochemical changes which accompany atrophy or reduced muscle growth in hindlimb of tail-casted, suspended rats. These results clearly show that altered muscle growth was due to changes in protein turnover. Accordingly, the rise in soleus tyrosine following unloading reflects the more negative protein balance. Other major changes we found included slower synthesis of glutamine as indicated by lower ratios of glutamine/glutamate and reduced levels of aspartate which coincide with slower aspartate and ammonia metabolism in vitro. In conjunction with the study of SL-3 rats, which were subjected to 12 h of post-flight gravity, a study of the effects of 12 h eight bearing on metabolism of 6-day unloaded hindlimb muscles was carried out. G.L.C.

N85-35591*# Arizona Univ., Tucson. Dept. of Biochemistry.
MUSCLE PROTEIN AND GLYCOGEN RESPONSES TO RECOVERY FROM HYPOGRAVITY AND UNLOADING BY TAIL-CAST SUSPENSION
Erik J. Henriksen, Marc E. Tischler, Stephan Jacob, and Paul H. Cook [1985] 2 p refs
(Grant NAGw-227)
(NASA-CR-176181; NAS 1.26:176181) Avail: NTIS HC A02/MF A01 CSCL 06C

Previous studies in this laboratory using the tail-bast hindlimb suspension model have shown that there are specific changes in protein and carbohydrate metabolism in the soleus muscle due to unloading. For example, 6 days of unloading caused a 27% decrease in mass and a 60% increase in glycogen content in the soleus muscle, while the extensor digitorum longus muscle was unaffected. Also, fresh tissue tyrosine and its in vitro release from the muscle are increased in the unloaded soleus, indicating that this condition causes a more negative protein balance. With these results in mind, studies to investigate the effect of hypogravity on protein and carbohydrate metabolism in a number of rat hindlimb muscles were carried out. G.L.C.

N85-35592# Systems and Applied Sciences Corp., Hyattsville, Md.
LITERATURE SEARCH FOR NEW PHYSICAL METHODS FOR BIOLOGICAL AEROSOL DETECTION Contractor Report, Aug. 1982 - Sep. 1984
L. Shapiro Apr. 1985 216 p
(Contract DAAK11-82-C-0113)
(AD-A155883; CRDC-CR-84132) Avail: NTIS HC A10/MF A01 CSCL 06/13

Microbiological entities in the atmosphere can be viewed as particles and studied for their particle properties, as packages of chemicals such as proteins, glucosides, DNA or RNA carriers, as potentially fluorescent or stainable entities or are as viable cells capable of reaction with an environment to produce detectable products. This report presents a discussion of each of the techniques found suitable to deal with some aspect of detection. In addition, a brief presentation is made of experimental probes of two unique approaches made within the time frame of the project. The final section presents the bibliography developed in the study. The reference material presented are those actually looked at and almost all were photocopied for convenient review. In each category they are arranged chronologically, the most recent first. GRA

N85-35593# Chicago Univ., Ill.
MOLECULAR BIOLOGY OF ENVIRONMENTAL AROMATIC HYDROCARBONS Progress Report, 1 Sep. 1984 - 31 Jun. 1985
S. B. Weiss Jul. 1985 13 p refs
(Contract DE-AC02-80EV-10328)
(DE85-015036; DOE/EV-10328/4) Avail: NTIS HC A02/MF A01

The biological activities of the (+)- and (-)-enantiomers of anti-BPDE (benzoapyrene diol epoxide) and BePe (benzoepyrene epoxide) were examined for their capacity to inhibit infectious single- and double-stranded 0X174 phage DNAs. For both activated PAH derivatives, the (+)-isomer was more inhibitory using either single- or double-stranded 0X DNAs. Both PAH derivatives showed a higher inhibition potency with single-strended 0X DNA than with duplex DNA; this difference between the two phage DNA forms was much greater for BePe than with anti-BPDE. A model viral DNA system was used, containing short oligonucleotide inserts as targets for PAH alkylation, to detect sequence modifications induced by anti-BPDE. A 10-base-pair oligomer (Bam HI linker) was treated with anti-BPDE and inserted into phage M13 replicative from DNA. E. coli was transfected with the recombinant DNA containing the alkylated oligomer, progeny viral plaques were selected, and their DNAs subjected to DNA sequence analysis at the region of oligomer insertion. For the alkylated inserts used in our study, the DNA sequence analysis of progeny viral DNA showed that nucleotide deletions were present in all the clones examined. DOE

N85-35602# European Space Agency, Paris (France).
ARE LIVING CELLS GENERALLY SENSITIVE TO GRAVITY?
Wolfgang Briegleb *In its* Proc. of a Sci. Meeting on the Occasion of the Inauguration of New Buildings for the DFVLR Inst. for Aerospace Med. (DFVLR-Mitt-83-19) Nov. 1984 p 92-105 refs Transl. into ENGLISH from "Vortraege eines flugmed. Kolloq. aus Anlass der Vorstellung des Naubaues des DFVLR-inst. fuer Flugmed." rept. DFVLR-Mitt-83-19 DFVLR, Cologne, 1983 p 87-97 Original language document was announced as N84-27425 (For primary document see N85-35595 24-52)
Avail: NTIS HC A07/MF A01; original German version available from DFVLR, Cologne DM 43

52 AEROSPACE MEDICINE

Includes physiological factors; biological effects of radiation; and weightlessness.

N85-35594*# Arizona Univ., Tucson. Dept. of Biochemistry.
RESPONSES OF SKELETAL MUSCLE TO UNLOADING, A REVIEW

Marc E. Tischler, Stephen R. Jaspers, Erik J. Henriksen, and Stephan Jacob [1985] 4 p refs Sponsored in part National Inst. of Arthritis, Diabetes and Digestive and Kidney Diseases (Grant NAGw-227)
(NASA-CR-176177; NAS 1.26:176177) Avail: NTIS HC A02/MF A01 CSCL 06P

Suspension models were used to study muscle response to reduced activity. During 6 days of tail casting, the soleus (SOL) atrophies while the extensor digitorum longus grows relatively normally. After discounting those changes in both muscles due primarily to increased secretion of adrenal hormones, the following conclusions regarding the specific responses of the SOL could be drawn: (1) Atrophy is probably due primarily to increased protein degradation; (2) Decreased synthesis of glutamine may result from reduced availability of ammonia due to diminished use of ATP; (3) Greater muscle glycogen seems to reflect an increased response to insulin of glucose uptake which leads to greater glucose metabolism; and (4) Faster catabolism of branched-chain amino acids can be attributed to enhanced flux through ketoacid dehydrogenase. Studies by others using tail casted suspended rats showed in the SOL: (1) a gradual switch from type 1 to type 2 fibers; (2) increased acid protease activity; and (3) altered muscle function and contractile duration. Using harness suspended rats, others showed in the SOL: (1) significant atrophy; (2) increased numbers of glucocorticoid receptors; and (3) no change in muscle fatigability. Author

N85-35595# European Space Agency, Paris (France).
PROCEEDINGS OF A SCIENTIC MEETING ON THE OCCASION OF THE INAUGURATION OF NEW BUILDINGS FOR THE DFVLR INSTITUTE FOR AEROSPACE MEDICINE
Nov. 1984 142 p refs Transl. into ENGLISH of "Vortraege eines flugmed. Kolloq. aus Anlass der Vortstellung des Naubaues des DFVLR-Inst. Fuer Flugmed." rept. DFVLR-Mitt-83-19 DFVLR, Cologne, 1983 130 p Meeting held at Cologne, 10 Mar. 1982 Original language document was announced as N84-27418
(ESA-TT-857; DFVLR-Mitt-83-19) Avail: NTIS HC A07/MF A01; original German version available from DFVLR, Cologne DM 43

Analogies of control mechanisms in flight guidance and medicine; a mathematical model of the human body; models for assessing flight crew workloads; the relationship between personality and performance; cardiovascular responses to weightlessness and orthostatism; cell sensitivity to gravity; radiobiology of space flight; deep diving; and the effect of an unphysiological oxygen supply on the organism were discussed. For individual titles, see N85-35596 through N85-35605.

N85-35596# European Space Agency, Paris (France).
THE RESEARCH PROGRAMME OF THE INSTITUTE FOR AEROSPACE MEDICINE
Karl Egon Klein *In its* Proc. of a Sci. Meeting on the Occasion of the Inauguration of New Buildings for the DFVLR Inst. for Aerospace Med. (DFVLR-Mitt-83-19) Nov. 1984 p 6-11 Transl. into ENGLISH from "Vortraege eines flugmed. Kolloq. aus Anlass der Vorstellung des Naubaues des DFVLR-Inst. fuer Flugmed." rept. DFVLR-Mitt-83-19 DFVLR, Cologne, 1983 p 9-14 original language document was announced as N84-27419 (For primary document see N85-35595 24-52)
Avail: NTIS HC A07/MF A01; original German version available from DFVLR, Cologen DM 43

Research into the medical, biological, physiological, and psychological effects of air travel, space flight, and deep sea diving is summarized. Biodynamic effects of helicopter vibration; biorhythm effects of jet travel; pilot performance; and space environment effects on cells and tissues are studied. Author (ESA)

N85-35597# European Space Agency, Paris (France).
ANALOGIES OF CONTROL MECHANISMS IN FLIGHT GUIDANCE AND MEDICINE
Fred Thomas *In its* Proc of a Sci. Meeting on the Occasion of the Inauguration of New Buildings for the DFVLR Inst. for Aerospace Med. (DFVLR-Mitt-83-19) Nov. 1984 p 12-24 Transl. into ENGLISH from "Vortraege eines flugmed. Kolloq. aus Anlass der Vorstellung des Naubaues des DFVLR-Inst. fuer Flugmed." rept. DFVLR-Mitt-83-19 DFVLR, Cologne, 1983 p 15-25 Original language document was announced as N84-27420 (For primary document see N85-35595 24-52)
Avail: NTIS HC A07/MF A01; original German version available from DFVLR, Cologne DM 43

The similarities between air traffic control and flight control systems and the regulation system of the human body are discussed. It is pointed out that the increasing automation in aeronautics produces a situation where the control loop in the aircraft corresponds to the autonomic nervous system and the hormone system in the human body. It is suggested that doctors could benefit from adapting control loop analysis philosophies current in engineering, e.g., to detect overload in self regulating mechanisms before they become chronic defects. Author (ESA)

N85-35598# European Space Agency, Paris (France).
A MECHANICAL MODEL OF THE HUMAN BODY AND ITS APPLICATION
Hans Lorenz Vogt *In its* Proc. of a Sci. Meeting on the Occasion of the Inauguration of New Buildings for the DFVLR Inst. for Aerospace Med. (DFVLR-Mitt-83-19) Nov. 1984 p 25-43 Transl. into ENGLISH from "Vortraege eines flugmed. Kolloq. aus Anlass der Vorstellung des Naubaues des DFVLR-Inst. fuer Flugmed." rept. DFVLR-Mitt-83-19 DFVLR, Cologne, 1983 p 27-43 Original language document was announced as N84-27421 (For primary document see N85-35595 24-52)
Avail: NTIS HC A07/MF A01; original German version available from DFVLR, Cologne DM 43

The development, validation and application of a mathematical model of the human body, for vibration and impact tests are described. Nonlinear properties of the body were determined in tests with a shake table mounted on a centrifuge to combine vibration and acceleration forces. The mechanical input impedance which represents the complex resistance of the entire body when seated upright, and transmission of vibration to the head were measured. Impacts were simulated by subjecting a rough model based on the measurements to rectangular, trapezoid and sinusoid pulses. Time courses of acceleration typical of aircraft rescue systems were added. Validation tests were run on a standard laboratory computer. Author (ESA)

N85-35599# European Space Agency, Paris (France).
MODELS FOR ASSESSING WORKLOAD OF AIRCREWS ON LONG DISTANCE FLIGHTS c53
Hans Martin Wegmann *In its* Proc. of a Sci. Meeting on the Occasion of the Inauguration of New Buildings for the DFVLR Inst. for Aerospace Med. (DFVLR-Mitt-83-19) Nov. 1984 p 44-58 refs Transl. into ENGLISH from "Vortraege eines flugmed. Kolloq. aus Anlass der Vorstellung des Naubaues des DFVLR-Inst. fuer Flugmed." rept. DFVLR-Mitt-83-19 DFVLR, Cologne, 1983 p 45-56 Original language document was announced as N84-27422 (For primary document see N85-35595 24-52)
Avail: NTIS HC A07/MF A01; original German version available from DFVLR, Cologne DM 43

The Buley, Gerathewohl, Mohler, and Nicholson flight crew workload assessment models were compared using a flight from Germany to South America. The Mohler model gives the best assessments, but calculations are complex and it underassesses flights which consist only of outward and return flights. A stress index (SI) calculated from flight duty time in hours (T) night flight duty time in hours (N) (night : 01.00-07.00 h local time) coefficient for transits (CTR) coefficient for duration of the stopover (CL) (layover) and coefficient for the number of time zones flown over in the preceding section (CTZ) is proposed : SI = T + N + CTR + (CL.CTZ). Author (ESA)

N85-35600# European Space Agency, Paris (France).
THE RELATIONSHIP BETWEEN PERSONALITY AND PERFORMANCE c53
Konrad Steininger *In its* Proc. of a Sci. Meeting on the Occasion of the Inauguration of New Buildings for the DFVLR Inst. for Aerospace Med. (DFVLR-Mitt-83-19) Nov. 1984 p 59-70 refs

Transl. into ENGLISH from "Vortraege eines flugmed. Kolloq. aus Anlass der Vorstellung des Naubaues des DFVLR-Inst. fuer Flugmed." rept. DFVLR-Mitt-83-19 DFVLR, Cologne, 1983 p 57-66 Original language document was announced as N84-27423 (For primary document see N85-35595 24-52)
Avail: NTIS HC A07/MF A01; original German version available from DFVLR, Cologne DM 43

The difficulties in finding a two dimensional relationship between personality and performance are discussed. The influences of anxiety, motivation, and rigidity of outlook on performance in critical and routine situations are contrasted. The flexible personality, prepared to take risks, performs better in crises, but is less reliable at other times. Author (ESA)

N85-35601# European Space Agency, Paris (France).
CARDIOVASCULAR RESPONSES TO ORTHOSTATISM AND WEIGHTLESSNESS
Friedhelm Baisch *In its* Proc. of a Sci. Meeting on the Occasion of the Inauguration of New Buildings for the DFVLR Inst. for Aerospace Med. (DFVLR-Mitt-83-19) Nov. 1984 p 71-91 refs Transl. into ENGLISH from "Vortraege eines flugmed. Kolloq. aus Anlass der Vorstellung des Naubaues des DFVLR-Inst. fuer Flugmed." rept. DFVLR-Mitt-83-19 DFVLR, Cologne, 1983 p 67-85 Original language document was announced as N84-27424 (For primary document see N85-35595 24-52)
Avail: NTIS HC A07/MF A01; original German version available from DFVLR, Cologne DM 43

Weightlessness simulation studies during astronaut training are discussed. Tilt table and lower body negative pressure box investigations of blood redistribution and orthostatic stress are described. Space flight and zero gravity simulation demonstrate an increase in venous return from the lower limbs. Intrathoracic blood volume and central venous pressure also increase. Blood volume decreases, but urine volume increases. The negative effects of zero gravity adjustment suggest that 6 months in space should not be exceeded. Author (ESA)

N85-35602# European Space Agency, Paris (France).
ARE LIVING CELLS GENERALLY SENSITIVE TO GRAVITY?
c51
Wolfgang Briegleb *In its* Proc. of a Sci. Meeting on the Occasion of the Inauguration of New Buildings for the DFVLR Inst. for Aerospace Med. (DFVLR-Mitt-83-19) Nov. 1984 p 92-105 refs Transl. into ENGLISH from "Vortraege eines flugmed. Kolloq. aus Anlass der Vorstellung des Naubaues des DFVLR-inst. fuer Flugmed." rept. DFVLR-Mitt-83-19 DFVLR, Cologne, 1983 p 87-97 Original language document was announced as N84-27425 (For primary document see N85-35595 24-52)
Avail: NTIS HC A07/MF A01; original German version available from DFVLR, Cologne DM 43

General sensitivity of living cells to gravity is discussed. Categories of specific sensory functions for the individual cells of multicellular organisms are described. Overall regulation of metabolism, differentiation, and transport processes in cells; toxic sensory functions of cells moving autonomously during differentiation of embryos and organs, in regenerating tissue, and in blood cells and sperm; and polarization processes due to external stimuli during maturation and fertilization of ova and the early stages of segmentation in animals and plants are discussed. If the three categories are subject to direct gravitational influence, then they would all have a hypothetical primary gravitation receptor located in the smallest functional unit, i.e., the cell. Ground based and spaceborne results about general gravity sensitivity are inconclusive. Author (ESA)

N85-35603# European Space Agency, Paris (France).
BIOPHYSICAL RESEARCH IN SPACE
Horst Buecker *In its* Proc. of a Sci. Meeting on the Occasion of the Inauguration of new Buildings for the DFVLR Inst. for Aerospace Med. (DFVLR-Mitt-83-19) Nov. 1984 p 106-111 refs Transl. into ENGLISH from "Vortraege eines flugmed. Kolloq. aus Anlass der Vorstellung des Naubaues des DFVLR-Inst. fuer Flugmed." rept. DFVLR-Mitt-83-19 DFVLR, Cologne, 1983 p 99-103 Original language document was announced as N84-27426 (For primary document see N85-35595 24-52)
Avail: NTIS HC A07/MF A01; original German version available from DFVLR, Cologne DM 43

Radiobiological problems of manned space flight are discussed. Manned space flight studies deal less with quantitative extrapolation of radiobiological observations on Earth than the assessment of novel types of effects for whose actions there is neither adequate theoretical understanding nor an empirical basis. The Apollo-Soyuz Biostack experiments show that significant effects observed in the various biological test organisms resulting from the trajectory of a single heavy ion can be explained to only a small extent by theories based on ground studies. Measured by the absorbed dose, these effects are caused by only a small fraction, (0.5%) of the total radiation doses occurring on the space flights, while the component of 99.5% of weak ionizing radiation leaves no detectable effects. Control experiments carried out in a heavy ion accelerator qualitatively confirm the findings.
Author (ESA)

N85-35604# European Space Agency, Paris (France).
THE DEEP DIVING SIMULATOR TITAN: PHYSIOLOGICAL PROBLEMS ASSOCIATED WITH STAYING IN GREAT DEPTHS OF WATER
Hans Dietrich Fust *In its* Proc. of a Sci. Meeting on the Occasion of the Inauguration of New Buildings for the DFVLR Inst. for Aerospace Med. (DFVLR-Mitt-83-19) Nov. 1984 p 112-127 refs Transl. into ENGLISH from "Vortraege eines flugmed. Kolloq. aus Anlass der Vorstellung des Naubaues des DFVLR-Inst. fuer Flugmed." rept. DFVLR-Mitt-83-19 DFVLR, Cologne, 1983 p 105-119 Original language document was announced as N84-27427 (For primary document see N85-35595 24-52)
Avail: NTIS HC A07/MF A01; original German version available from DFVLR, Cologne DM 43

The similarities between the physiological effects of manned space flight and deep diving underwater, and the equipment (e.g., life support) used in both domains are pointed out. Decompression sickness, circulatory changes, disorientation, intoxication by artificial gas mixtures, and lack of external assistance in returning to the Earth's surface are hazards for astronauts and divers. Diving simulator studies (to 600 m depth) of compression, isopression, and decompression effects are outlined. Techniques used to monitor bodily functions are described. Author (ESA)

N85-35605# European Space Agency, Paris (France).
THE EFFECT OF AN UNPHYSIOLOGICAL OXYGEN SUPPLY ON THE ORGANISM
Gerhard Schaefer *In its* Proc. of a Sci. Meeting on the Occasion of the Inauguration of New Buildings for the DFVLR Inst. for Aerospace Med. (DFVLR-Mitt-83-19) Nov. 1984 p 128-139 refs Transl. into ENGLISH from "Vortraege eines flugmed. Kolloq. aus Anlass der Vorstellung des Naubaues des DFVLR-Inst. fuer Flugmed." rept. DFVLR-Mitt-83-19 DFVLR, Cologne, 1983 p 121-130 Original language document was announced as N84-27428 (For primary document see N85-35595 24-52)
Avail: NTIS HC A07/MF A01; original German version available from DFVLR, Cologne DM 43

In order to determine individual time reserves on exposure to oxygen deficiency in a low pressure chamber, the correlation between the partial pressure of O2 in the inhaled air and the pO2 in the arterial and venous blood in humans and animals was studied. Results show that while there is a close relation between the venous and arterial pO2 values and the inspiratory pO2 when a normal atmosphere is breathed, after a short exposure to conditions of reduced atmospheric pressure large differences in the pO2 in the blood occur, while the pO2 in the inhaled air is constant. Under a normal atmosphere, the mean pO2 in the arterial blood is 95 mmHg and the variations are very small. At a nominal altitude of 7,500 m, with an inhaled pO2 of 50 mmHg, the arterial pO2 values vary between 24 and 34 mmHg. The variations in the venous blood are even greater. Results are confirmed in experiments on rabbits. Author (ESA)

N85-35606# School of Aerospace Medicine, Brooks AFB, Tex.
DENTAL MULTI-PURPOSE SLOWSPEED HANDPIECES TEST AND EVALUATION Final Report, Mar. 1984 - Mar. 1985
C. D. Foster, K. D. Satrom, P. M. Callison, and T. D. Stockman Apr. 1985 37 p
(AD-A155764; USAFSAM-TR-85-23) Avail: NTIS HC A03/MF A01 CSCL 06/12

This study included the test and evaluation of three air-driven operative, three electrical operative, two air-driven surgical, and three electrical surgical handpieces. Speed and torque of the handpieces were compared by the use of a hysteresis electric dynamometer. Comparisons were also made of handpiece characteristics. User evaluations were performed in U.S. Air Force dental clinics, and results are presented. The purpose of the study was to provide assistance to the base dental surgeons for selection of dental multi-purpose slowspeed handpieces. GRA

N85-35607# Army Military Personnel Center, Alexandria, Va.
WHOLEBODY RADIATION COUNTING SYSTEM M.S. Thesis - Final Report
G. M. Fechter 1 May 1985 133 p
(AD-A155842) Avail: NTIS HC A07/MF A01 CSCL 06/18

The purpose of this research was to develop a system that would allow the Health Physics staff of the Nuclear Engineering Department of Rensselaer Polytechnic Institute to conduct wholebody radiation counting of all assigned personnel and to determine if a multiple crystal arrangement had any benefits over the single crystal system. The research had three main objectives: (1) to design and construct the electronic hardware necessary to collect data from a series of three NaI(Tl) scintilation crystals; (2) to develop the computer software necessary to interpret this data and calculate concentrations present within those individuals tested. (3) to interface the Helgeson Wholebody Counter with the Vax 11/750 Computer System. This system includes a Texas Instruments TM990-101M Microcomputer which acts as the main control unit for the operator and as the interface with the Vax computer. Additionally, the final system included a computer interface and data acquisition module and it uses a Digital Equipment Corporation VAX 11/750 Computer System for a majority of the data manipulation. This system, was all wholebody counting systems, is characterized by its ability to detect low levels of radionuclide concentration while maintaining adequate resolution to identify the exact isotopes present within the person being counted. GRA

N85-35608# Aerospace Medical Research Labs., Wright-Patterson AFB, Ohio.
THE EFFECT OF +Gx ACCELERATION ON PLATELET ACTIVATION AS DETERMINED BY PLASMA PLATELET FACTOR 4 LEVELS Technical Report
F. S. Cramer, T. J. Jennings, C. T. Olson, G. A. McDonald, and L. L. Howell Apr. 1985 15 p
(AF Proj. 7231)
(AD-A155881; AFAMRL-TR-85-038) Avail: NTIS HC A02/MF A01 CSCL 06/19

Six healthy men were exposed to a +Gx acceleration (chest to back) profile with peak +Gx levels of 5, 8, and 9 G. Platelet factor 4 levels and platelet counts were measured prior to and immediately following the acceleration exposure. The +Gx acceleration exposure did not affect either parameter, however elevated pre-acceleration platelet factor 4 levels were found in five of six subjects. The possible significance of this is discussed. Future space missions will expose man to unique combinations of environmental stresses. Decompression and +Gx acceleration exposure is one such combination. It is important to determine if there are some features of these stresses which by themselves are benign, but in combination can result in problems for the astronaut. At acceleration levels greater +4 Gx, the subject experiences chest pain. Breathing becomes difficult, causing the subject to become dyspneic and to breathe using his abdominal muscles. Above +6Gx, pulmonary volumes are reduced, and the subject is unable to move his arms and legs. GRA

N85-35609# Naval Air Development Center, Warminster, Pa. Aircraft and Crew Systems Technology Directorate.
MATCHED FILTERING OF VISUAL EVOKED POTENTIALS TO DETECT ACCELERATION (+Gz) INDUCED BLACKOUT Final Report
J. G. Nelson, L. Hrebien, and J. p. Cammarota 3 Jan. 1985 29 p
(DA Proj. WR0-4101)
(AD-A155912; NADC-85040-60) Avail: NTIS HC A03/MF A01 CSCL 06/19

In air-combat maneuvering and on human centrifuges, moderate levels of positive acceleration (+ Gz), coupled with moderate rates of onset, produce visual symptoms which are ordinarily progressive: Decreasing visual sensitivity, dimming of the visual field, peripheral light-loss, and central light-loss (black-out). Since these symptoms provide warning of impending loss of consciousness, subjective visual symptoms are the most commonly used tolerance end point in acceleration research. In order to provide an Objective indication of the integrity of the visual system, we have developed (and continue to improve) a method for real-time monitoring of the steady-state visual evoked potential(VEP). Since significant degradation of visual functioning must be recognized in less than approximately four seconds, we required a previously unattained efficiency in producing and measuring the VEP. Using the Fast Fourier Transform (FFT), we developed a method for maximizing the signal-to-noise ratio: A digital, frequency domain, non-white-noise-matched filter, with evaluation only at the expected response peak. The coefficients of the matched filter are determined empirically by analysis of test data obtained in a static run, just prior to the dynamic (+ Gz) run. Experiments on the Navy's Human Centrifuge demonstrated that the response does progressively decrease, disappearing at black-out. Improved computer facilities have permitted evaluation of alternative methods of processing, and the effectiveness of such processing. GRA

N85-35610# Aerospace Medical Research Labs., Wright-Patterson AFB, Ohio.
SIMULATION OF HIGH +GZ ONSET IN THE DYNAMIC ENVIRONMENT SIMULATOR
W. B. Albery, T. Jennings, M. Roark, J. Frazier, and D. Ratino Apr. 1985 29 p
(AF Proj. 7231)
(AD-A155963; AD-E301698; AFAMRL-TR-85-030) Avail: NTIS HC A03/MF A01 CSCL 06/19

This report documents a unique approach of coupling the cab-axis degree of freedom to the main arm motion of the Air Force Aerospace Medical Research Laboratory human centrifuge, or DES (Dynamic Environment Simulator). This technique of simulating high +Gz/sec to 2.875 Gz/sec was investigated and eleven subjects completed the study. Peripheral light loss (PLL), a precursor to loss of consciousness, was recorded in all eleven subjects using this technique. Three G-tolerance scenarios were investigated; relaxed subject/no anti-G suit inflation, relaxed subject/anti-G suit inflation and straining subject/anti-G suit inflation. A semi-circular light bar was used in the DES cab to monitor peripheral light loss of subjects. The PLL results compare favorably with similar results in the NADC centrifuge where subjects faced tangentially and were subjected to +Gz only rather than +Gx and then +GZ as in this experiment. These results give a strong indication that this technique can be used to stimulate high + Gz onset in the evaluation of anti G-valves, suits and straining maneuvers. GRA

N85-35611# Canyon Research Group, Inc., Westlake Village, Calif.
A REVIEW OF MOTION SICKNESS WITH SPECIAL REFERENCE TO SIMULATOR SICKNESS Final Interim Report, 1 Sep. 1981 - 15 Apr. 1985
R. S. Kennedy and L. H. Frank 15 Apr. 1985 51 p
(Contract N61339-81-C-0105)
(AD-A155975; NAVTRAEQUIPC-81-C-0105-16) Avail: NTIS HC A04/MF A01 CSCL 06/19

The incidence of simulator sickness is increasing. As many incidents have been reported since 1980 as in all of time before

then, and there are implications for training and safety. The present paper reviews: the signs and symptoms, stimuli and response characteristics, anatomical structures, and susceptibility factors. The prevalent theories of the genesis of this malady are put forth and an integrating theory is proposed which suggests that simulator sickness is a form of motion sickness and may be best understood as a special case of sensory rearrangement. Other works in this series describe the scope of the problem, report the incidence in over 4500 exposures, and list more than 2000 relavent references. This correlation theory which is offered suggests that motion sickness is a result of decorrelation between and within sensory input channels of information. This correlation theory is in general agreement with the perceptual conflict or cue mismatch theories, and implies that the central nervous system (CNS) perceives decorrelated stimulations as toxic events. This CNS interpretation of toxicity causes the constellation of symptoms associated with motion sickness to be released. GRA

N85-35612# Army Research Inst. of Environmental Medicine, Natick, Mass.

WEIGHT LOSS, RECTAL TEMPERATURE AND HEART RATES FOLLOWING THE 1984 BOSTON MARATHON

W. L. Daniels, B. H. Jones, W. T. Matthew, P. I. Fitzgerald, and P. Szlyk May 1985 23 p

(AD-A155984; USARIEM-M29/85) Avail: NTIS HC A02/MF A01 CSCL 06/19

This report summarizes the physiological changes that occurred in runners following the 1984 Boston Marathon. The marathon took place under cool and rainy weather conditions (WBGT range 6.5 to 10.5). Subjects for this study consisted of 57 males and 10 females. Their average age was 40.5 years (range 22 to 61 years). Average marathon pace was 219.1 m/min (X time = 3 hrs 12 min 36 sec). During the race, these runners drank an average of 581 mls of fluid. As a result of running a marathon, heart rate increased from 61.3 bts/min to 91.2 bts/minute; body weight decreased from 67.3 kg to 65.7 kg., and rectal temperature (T sub Re)was not significantly changed. Post-heart rate and T sub Re were affected by how soon after finishing the race an individual was measured. Runners who reported to the post-test site soonest tended to be younger and faster than those reporting later. Age and average weekly mileage correlated significantly with mean marathon pace. Our results with heart rate and T sub Re provide medical personnel with some guidance on the effect of the marathon on these parameters in uninjured runners. GRA

N85-35613# Human Engineering Labs., Aberdeen Proving Ground, Md.

THE HUMAN ENGINEERING EYE MOVEMENT MEASUREMENT RESEARCH FACILITY Final Report

J. Mazurczak and R. S. Pillalamarri Apr. 1985 31 p

(AD-A156099; HEL-TM-6-85) Avail: NTIS HC A03/MF A01 CSCL 06/5

Visual perception plays a critical role in many tasks the soldier is asked to perform. One key component of these tasks where visual perception is critical is visual search. An example is the acquisition of key information in monitoring displays and directing fire at targets. How should the individual soldier in any given task allocate his attention to optimize performance and what tasks or operator factor affect visual search performance are some of the questions to be answered. There is a need for developing a body of data on the principles governing human visual search. This knowledge has direct application to such diverse aspects of the Army's mission as the optimal design of visual information displays in various systems, techniques for intelligent interpretation of reconnaissance photographs, and the design of automatic electronic target acquisition devices. Driven by this need a system facility has been developed for monitoring eye movement behavior unobtrusively which imposes no mechanical constraints on the subject. The system utilizes the pupil-center/corneal-reflection measurement technique and features a high speed on-line data processing capability. The purpose of this report is to describe the HEL Eye-Movement Research Facility; including the subject viewing studio, the projection room, and the master control room. GRA

N85-35614# Army Research Inst. of Environmental Medicine, Natick, Mass.

AN ANALYSIS OF AEROBIC CAPACITY IN A LARGE UNITED STATES POPULATION

J. A. Vogel, J. F. Patton, R. P. Mello, and W. L. Daniels 29 Apr. 1985 34 p

(AD-A156200; USARIEM-M28/85) Avail: NTIS HC A03/MF A01 CSCL 06/16

A description of aerobic capacity in a large U.S. population comprised of 1,514 males and 375 females is presented. Such influencing factors as age, training state, occupation and body composition were evaluated. The population consisted of new recruits entering the U.S. Army from civilian life as well as soldiers in a variety of assignments and physical training programs. Age ranged from 17 through 55. Aerobic capacity was determined as maximal oxygen uptake measured directly by the Douglas bag technique during a standard discontinuous treadmill running procedure with the exception of one older aged group. New male and female recruits, representing a young civilian population, entered the service with VO2 max of 51 and 37 ml/kg/BW/min, respectively, and thereafter increased 5-10% during initial basic training. The difference between genders, 30% on an absolute basis, was 14% when expressed as a function of lean body mass. Aerobic capacity was less after occupational training and continued to decrease with age at an average yearly rate of 10%. Aerobic capacity varied with intensity of the occupational physical demand except in groups with significant physical training programs. This first large U.S. population study of aerobic capacity, using a direct treadmill procedure, demonstrates levels consistent with any previously reported population. Author (GRA)

N85-35615# Army Research Inst. of Environmental Medicine, Natick, Mass.

THIRST AND FLUID INTAKE FOLLOWING GRADED HYPOHYDRATION LEVELS IN HUMANS

D. B. Engell, O. Maller, M. N. Sawka, R. N. Francesconi, and L. Drolet 6 Jun. 1985 38 p

(AD-A156201) Avail: NTIS HC A03/MF A01 CSCL 06/19

The relationship among changes in thirst sensations, blood variables, and differential fluid intake in hypohydrated humans was examined. Seven subjects were hypohydrated by 0%, 3%, 5% and 7% of their body weight on four separate trials which were systematically randomized between subjects. Hypohydration levels were achieved with a regimen of restricted food and fluid intake and moderate heat-exercise stress. Statistically significant linear and quadratic trends were found for the intensity of several sensations with progressive hypohydration levels. In general plasma osmolality and renin activity increased and plasma volume decreased with increasing hypohydration levels. During a one hour period of ad-libitum drinking, all subjects consumed insufficient fluid to rehydrate back to baseline body weights. Using regression analyses, fluid intake was predicted by the magnitude of subjective and physiological indices of hypohydration. Results demonstrate that both hypovolemia and plasma osmolality contribute significantly to fluid intake in hypohydrated humans. The results also indicate that thirst sensations are not epiphenomena but make a substantial contribution to differential fluid intake in humans. GRA

N85-35616# Naval Submarine Medical Research Lab., Groton, Conn.

IMMEDIATE VISIBILITY AFTER RED AND WHITE ADAPTATION Interim Report

S. M. Luria and D. A. Kobus 26 Apr. 1985 12 p

(NR Proj. M01-00)

(AD-A156271; AD-F630668; NSMRL-1045) Avail: NTIS HC A02/MF A01 CSCL 06/16

The ability to see simulated ship silhouettes and shadows within 10 seconds of looking away from either red or white light of equal brightness was measured. There were no significant differences in the ability to see such targets after adaptation to

red or white light at either 0.1 or .01 fL, or when the background illumination was .09 fc or .006 fc. GRA

N85-35617# Massachusetts Univ., Amherst. Dept. of Microbiology.
GENETIC AND PHYSIOLOGICAL CONTROL OF PROTECTIVE ANTIGEN SYNTHESIS BY BACILLUS ANTHRACIS Annual Progress Report, 1 Jan. - 31 Dec. 1984
C. B. Thorne Dec. 1984 51 p
(Contract DAMD17-80-C-0099; DA Proj. 3M1-61102-BS-12)
(AD-A156324; APR-5) Avail: NTIS HC A04/MF A01 CSCL 06/13

The primary objective of the research is to gain information and to develop genetic systems that will contribute to the development of an improved vaccine for anthrax. Genetic and physiological factors controlling the synthesis and accumulation of protective antigen as well as the two other components of anthrax toxin are being investigated. During the past year attention was focused on: (1) further development and application of a mating system for transfer of plasmids among Bacillus species: and (2) studies of a newly discovered plasmid which encodes capsule formation in B. anthracis. The mating system for transfer of plasmids among B. anthracis, B. cereus, and B. thuringiensis is very useful for assessing the biological significance of plasmids found in the three species. GRA

N85-35618# Oak Ridge National Lab., Tenn.
TRITIUM HAZARD VIA THE INGESTION PATHWAY
C. C. Travis 1985 10 p refs Presented at the 2nd Natl. Topical Meeting on Tritium Technol. in Fission, Fusion and Isotopic Appl., Dayton, Ohio, 30 Apr. 1985
(Contract DE-AC05-84OR-21400)
(DE85-012897; CONF-850405-9) Avail: NTIS HC A02/MF A01

The classic methodology for estimating dose to man from environmental tritium ignores the fact that organically bound tritium in foodstuffs may be directly assimilated in the bound compartment of tissues without previous oxidation. A four-compartment model that allows for the ability to input organically bound tritium in foodstuffs directly into the organic compartments of the model is proposed. It is found that organically bound tritium in foodstuffs can increase the total body dose by a factor of 1.7 to 4.5 times the free body water dose alone, depending on the bound to loose ratio of tritium in the diet. DOE

53 BEHAVIORAL SCIENCES

Includes psychological factors; individual and group behavior; crew training and evaluation; and psychiatric research.

N85-35619# Federal Aviation Agency, Washington, D.C. Office of Aviation Medicine.
PHYSIOLOGICAL RESPONSES TO UNVARYING (STEADY) AND 2-2-1 SHIFTS: MIAMI INTERNATIONAL FLIGHT SERVICE STATION
C. E. Melton Feb. 1985 33 p
(AD-A155751; FAA-AM-85-2) Avail: NTIS HC A03/MF A01 CSCL 05/9

Two types of shift rotation in the same air traffic facility were investigated in order to determine the relative advantages and disadvantages of nonrotating shift work (steady shift) and rotating shift work. The rotating shift work chosen for comparison was a 2-2-1 pattern often preferred by air traffic controllers, and which consists of a schedule of progressively earlier work periods throughout the workweek, with 9 to 14 hours off duty between 8-hour work periods, and an extended off-duty period of 80 hours between workweeks. Objective differences, as judged by urine biochemistry, between workers on the two shift patterns are minimal and insignificant statistically. Generally, however, greater fatigue was reported in connection with the 2-2-1 rotation than with the steady shift, both preshift and postshift. When prework to postwork changes in subjective fatigue were compared for the two shift patterns, no statistically significant differences were noted. Within the 2-2-1 schedule, there was (1) significantly greater excretion of catecholamines on the day watch as compared to the evening watch; and (2) significantly greater preshift fatigue reported on day shift than evening shift. Despite the observed differences between and within the steady and rotating shift patterns, employee participation in shift pattern choice may have contributed greatly to worker contentment and willingness to accept the observed stressors. GRA

N85-35620# Idaho Univ., Moscow. Dept. of Psychology.
MANUAL AND COMPUTER-AIDED SEQUENTIAL DIAGNOSTIC INFERENCE Final Report, May - Aug. 1984
S. E. Gordon Jun. 1985 16 p
(AD-A156229; AFHRL-TP-84-51) Avail: NTIS HC A02/MF A01 CSCL 09/2

This paper describes a pilot study on how human subjects process information during a diagnostic inference task. The objective was a descriptive/predictive model of the inference task and how that task could be affected by implementation of an automated system. The study directly supported research being conducted by AFHRL on quantitative techniques to predict the impacts that automation may have on operator performance, by defining its interaction with the operator's information processing (Modelling Impacts of Automation on Non-Automated Tactical Command and Control Systems). The pilot study involved testing human subjects who had to infer the identity of two fictitious diseases by sampling up to eight symptom dimensions. A set of process and performance variables were selected for measurement. Signal detection theory served as the data collection design. Results were in line with anticipated outcomes (i.e., certainty increased as more cues were sampled); however, certainty rate of increase was highest for trials where subjects sampled four cues and lowest for trials where subjects sampled eight cues (total number of cues was eight). The pilot study helped formulate a list of critical variables expected to affect the operator's information processing and define plausible relationships between those processes and automation assistance. Author (GRA)

N85-35621# Air Command and Staff Coll., Maxwell AFB, Ala.
RELAXATION TECHNIQUES
R. Marconi-Dooley Apr. 1985 43 p
(AD-A156248; ACSC-85-1725) Avail: NTIS HC A03/MF A01 CSCL 06/16

The project consists of two parts, the written text and the videotape. The text describes how the project idea was formulated, the sources of data used, and how the videotape script was developed. The script describes the concept of relaxation techniques, and the techniques of deep breathing, progressive muscle relaxation, and visualization. Then through a short demonstration, the viewer has the opportunity to experience each of these three techniques. The videotape is used in the Air War College (AWC) noontime film series in conjunction with the AWC Executive Health Assessment and Fitness block of instruction. The videotape can, however, be used to introduce relaxation techniques to any adult. Author (GRA)

N85-35622# Air Command and Staff Coll., Maxwell AFB, Ala.
AIR UNIVERSITY COMMANDER'S AND SUPERVISOR'S GUIDE ON SUBSTANCE ABUSE
H. E. Booker Apr. 1985 40 p
(AD-A156336; ACSC-85-0245) Avail: NTIS HC A03/MF A01 CSCL 06/5

The use of mood altering substances has become part of our modern way of life. According to a study prepared by the Social Research Group at George Washington University, nearly 80% of adult Americans use some alcohol. The impact this lost work time has on military readiness is my primary motivation for developing this handbook on substance abuse for Air University supervisors and commanders. It is designed to be a ready reference guide to assist in the identification and treatment of substance abuse. Although Air Force Regulation 30-2 (Social Actions Programs) is

the primary source, other materials such as books, pamphlets and material from substance abuse guides from other commands and bases are used along with suggestions and recommendations based on my training and eight years of experience as the author, a Social Actions Officer. This guide will give an explanation of Air Force policy on substance abuse, followed by a chapter on your responsibility as a commander and supervisor. There is also discussion of the substance abuser and the evaluation/ rehabilitation process. GRA

N85-35599# European Space Agency, Paris (France).
MODELS FOR ASSESSING WORKLOAD OF AIRCREWS ON LONG DISTANCE FLIGHTS
Hans Martin Wegmann *In its* Proc. of a Sci. Meeting on the Occasion of the Inauguration of New Buildings for the DFVLR Inst. for Aerospace Med. (DFVLR-Mitt-83-19) Nov. 1984 p 44-58 refs Transl. into ENGLISH from "Vortraege eines flugmed. Kolloq. aus Anlass der Vorstellung des Naubaues des DFVLR-Inst. fuer Flugmed." rept. DFVLR-Mitt-83-19 DFVLR, Cologne, 1983 p 45-56 Original language document was announced as N84-27422 (For primary document see N85-35595 24-52)
Avail: NTIS HC A07/MF A01; original German version available from DFVLR, Cologne DM 43

N85-35600# European Space Agency, Paris (France).
THE RELATIONSHIP BETWEEN PERSONALITY AND PERFORMANCE
Konrad Steininger *In its* Proc. of a Sci. Meeting on the Occasion of the Inauguration of New Buildings for the DFVLR Inst. for Aerospace Med. (DFVLR-Mitt-83-19) Nov. 1984 p 59-70 refs Transl. into ENGLISH from "Vortraege eines flugmed. Kolloq. aus Anlass der Vorstellung des Naubaues des DFVLR-Inst. fuer Flugmed." rept. DFVLR-Mitt-83-19 DFVLR, Cologne, 1983 p 57-66 Original language document was announced as N84-27423 (For primary document see N85-35595 24-52)
Avail: NTIS HC A07/MF A01; original German version available from DFVLR, Cologne DM 43

54 MAN/SYSTEM TECHNOLOGY AND LIFE SUPPORT

Includes human engineering; biotechnology; and space suits and protective clothing.

N85-35623*# National Aeronautics and Space Administration. Ames Research Center, Moffett Field, Calif.
IMPROVED OXYGEN SOURCES FOR BREATHING APPARATUS Final Report, Apr. 1974 - Sep. 1982
Peter C. Wood (San Jose State Univ.) and Theodore Wydeven Aug. 1983 160 p refs
(NASA-TM-86671; NAS 1.15:86671) Avail: NTIS HC A08/MF A01 CSCL 06K

Research is described which is directed toward the preparation of chemical oxygen sources which exhibited improved O2 storage and reaction characteristics when compared to potassium superoxide (KO2). The initial focus of the research was the preparation of calcium superoxide (Ca(O2)2) by the disproportionation of calcium peroxide diperoxyhydrate. the Ca(O2)2 was characterized by chemical, thermal, and x ray analyses. Several methods for scaling up the Ca(O2)2 syntheis process were studied. The reactivity of Ca(O2)2 toward humidified carbon dioxide (CO2) was evaluated and was compared to that of KO2 under flow test conditions approximating those existing in portable breathing apparatus. The reactivities of mixtures of KO2 and Ca(O2)2 or lithium peroxide towards humidified CO2 were also studied. Finally, an analysis of two commercial, KO2-based, self contained self rescuers was conducted to determine the potential weight and volume savings which would be possible if Ca(O2)2 or a mixture of KO2 and Ca(O2)2 were used as a replacement for KO2. Author

N85-35624# National Resource Analysis Center, Washington, D.C. Committee on Human Factors.
RECOMMENDATIONS FOR CONTENT REVISION AND ALTERNATE DELIVERY MODES FOR THE HUMAN ENGINEERING GUIDE TO EQUIPMENT DESIGN (HEGED)
Mar. 1985 8 p
(Contract N00014-85-G-0093)
(AD-A155781) Avail: NTIS HC A02/MF A01 CSCL 05/5

As its meeting on October 4-6, 1983, the Department of Defense Human Factors Engineering Technical Advisory Group (HFE-TAG) recommended that the National Research Council (NRC) consider the need for and an approach to revising the Human Engineering Guide to Equipment Design (HEGED). At the November 1983 meeting of the Committee on Human Factors, the Air Force representative of HFE-TAG requested the committee's advice on whether a revision of the Guide was appropriate and, if so, what its general contents and format should be for the greatest availability to users. The committee does not feel it can undertake or supervise the work of revision. However, it shows willingness to prepare recommendations on the format and content of such a revision, as well as its desire to suggest some possibilities for alternate forms of publication. The purpose of the Guide is to assist designers, engineers, human factors specialists, researchers, system developers, and others in the understanding and application of human factors engineering principles. Since its last publication in 1972, extensive additional useful data and technological innovations have been generated. The committee suggests that the Guide be revised under the guidance of an editorial board. This letter covers suggested areas of coverage and suggests that NRC would make the information available to the general scientific and technical community and should be enabled to receive inputs from this community. In addition, there should be organizations within the military services and other government agencies responsible for maintaining access appropriate to their special needs. GRA

N85-35625# Naval Postgraduate School, Monterey, Calif.
THE USE OF AUSTENITIC STAINLESS STEEL VERSUS MONEL (NI-CU) ALLOY IN PRESSURIZED GASEOUS OXYGEN (GOX) LIFE SUPPORT SYSTEMS M.S. Thesis
B. Marsh Mar. 1985 133 p
(AD-A156305) Avail: NTIS HC A07/MF A01 CSCL 06/11

Gaseous oxygen (GOX) must be stored at pressures up to 24 MPa (3500 psi) to provide the flow rates required to support the metabolic needs of a diver. A review of the literature concerned with materials compatibility in pressurized oxygen systems were conducted, with emphasis on metallic structural materials. Review of experimental and theoretical work on combustion of austenitic stainless steels and nickel-copper alloys revealed a consensus that Monel nominal (63 % Ni-34% Cu) is preferred in high pressure oxygen systems, when its strength and weight are acceptable. At the intermediate pressures, 0.7 to 10.3 MPa (100 to 1500 psi), the relative safety of stainless steel as a structural material is unclear. This thesis reviewed the following testing methods: friction rubbing, particle impact, fresh metal exposure to heated flowing GOX, promoted ignition and resonance. An experimental apparatus was used to simulate the conditions of GOX flow found in an operational diving set and to compare the flame propagation rates for austenitic stainless steel (AISI 316), Monel (63% Ni -34% Cu) and carbon steel (AMS 5050) tubing in this environment. GRA

55 PLANETARY BIOLOGY

Includes exobiology; and extraterrestrial life.

No abstracts in this category.

59 MATHEMATICAL AND COMPUTER SCIENCES (GENERAL)

N85-35626# Massachusetts Inst. of Tech., Cambridge. Artificial Intelligence Lab.
JUSTIFIED GENERALIZATION: ACQUIRING PROCEDURES FROM EXAMPLES Ph.D. Thesis
P. M. Andreae Jan. 1985 163 p
(Contract N00014-80-C-0505)
(AD-A156408; AI-TR-834) Avail: NTIS HC A08/MF A01 CSCL 05/9

This thesis describes an implemented system called NODDY for acquiring procedures from examples presented by a teacher. Acquiring procedures from examples involves several different generalization tasks. Generalization is an underconstrained task, and the main issue of machine learning is how to deal with this underconstraint. The thesis presents two principles; one is to exploit domain based constraints. The second principle is to avoid spurious generalizations by requiring justification before adapting a generalization NODDY demonstrates several different ways of justifying a generalization and proposes a way of ordering and searching a space of candidate generalizations based on how much evidence would be required to justify each generalization. Acquiring procedures also involves three types of constructive generalization: inferring loops (a kind of group), inferring complex reactions and state variables, and inferring predicates. The NODDY demonstrates three constructive generalization for these kinds of generalization. GRA

60 COMPUTER OPERATIONS AND HARDWARE

Includes computer graphics and data processing.

For components see *33 Electronics and Electrical Engineering.*

N85-35627# Naval Research Lab., Washington, D. C.
AN APPROACH TO DETERMINING COMPUTER SECURITY REQUIREMENTS FOR NAVY SYSTEMS Final Report, May 1984 - Jan. 1985
C. E. Landwehr and H. O. Lubbes 13 May 1985 14 p
(AD-A155750; NRL-8897) Avail: NTIS HC A02/MF A01 CSCL 09/2

The DoD Trusted Computer System Evaluation Criteria (The Orange Book) define requirements corresponding to specified levels of security functions and assurance. These do not (The Orange Book), however, help determine what level system is required for a specific environment. It is at present left to the system is expected to be used. This report proposes a straightforward technique a developer can use to map a specific system architecture and application environment to a particular requirement level as defined in the Criteria. This technique is applicable throughout the system life cycle, so that security requirements can be updated as changes to system structure and function occur. Author (GRA)

N85-35628# Army Military Personnel Center, Alexandria, Va.
OPTIMIZE COMPUTER THROUGHPUT USING ARRAY PROCESSORS M.S. Thesis - Final Report
M. W. Moakler, Jr. 1 May 1985 163 p
(AD-A155843) Avail: NTIS HC A08/MF A01 CSCL 09/2

The nuclear industry, as with other industries, is faced with a computational dilemma. While there are increasing requirements for the real time processing of data and for batch execution of long running, complex computer codes to meet operational commitments, there is usually a shortage of computer resources. The industry is forced to pursue various alternatives to meet their processing needs or to augment their computer resources. Large, expensive computers may be purchased. Time may be leased on other computer systems. The supercomputers, such as the CRAY, may be used to improve code run times. All of these alternatives are very expensive. Minicomputers may also be purchased. The minicomputer, although comparatively inexpensive, performs the number crunching operations much slower. The purpose of this thesis is to present another alternative, which may be classified as a composite blend of the above alternatives: the purchase of minicomputers such as the VAX family of computers augmented by modular array processors to speed up their throughput. GRA

N85-35629# Naval Postgraduate School, Monterey, Calif.
DSS/MIS (DECISION SUPPORT SYSTEMS/MANAGEMENT INFORMATION SYSTEMS) DESIGN AND IMPLEMENTATION FOR LAMPS Mk 3 UTILIZING A MICROCOMPUTER AND A MAINTENANCE PERSONNEL ASSIGNMENT PROGRAM M.S. Thesis
T. C. Jones, II and J. E. Dolenti Mar. 1985 122 p
(AD-A155852) Avail: NTIS HC A06/MF A01 CSCL 09/2

This thesis is intended to act as an aid in the incorporation of a microcomputer into the daily activities of a LAMPS Mk III helicopter squadron; specifically HSL-43. It includes an application program utilizing a Pascal driver interfacting with a DBMS (Database Management System) to optimize the assignment of maintenance personnel to deploying detachments subject to time constraints. Several future Management Information Systems (MIS) and Decision Support Systems (DSS) applications are addressed, but not specified, in hopes that other individuals will investigate and expand on this preliminary effort. GRA

N85-35630# Stanford Univ., Calif. Dept. of Computer Science.
EDGE DETECTION AND GEOMETRIC METHODS IN COMPUTER VISION
A. P. Blicher Feb. 1985 267 p
(Contracts MDA903-80-C-0102; N00039-82-C-0250)
(AD-A155873; SU-STAN-CS-85-1041; SU-AIM-352) Avail: NTIS HC A12/MF A01 CSCL 12/1

Basic problems of vision are studied form the viewpoint of modern differential topology and geometry; primarily: edge detection, stereo matching, picture representation at multiple scales, and motion. Some mathematical background is provided for the nonexpert. Some new edge detection techniques are introduced, including a nonlinear operator based on a symmetry principle, a variational approach to global edge finding, and a least-squares localization method. A theorem is proved which shows that localizing edge position and orientation requires at least 2 orientation dependent families of convolution operators. A unifying mathematical structure is presented for vision, notably stereo, motion stereo, optic flow (apparent flow of visual space under motion), and matching. The general matching problem is analyzed, and it is proved that generically, general matching is highly degenerate for monochrome pictures, but has a unique solution for 2 or more color dimensions. The result is extended to pictures with bias and gain. Small diagrams and level set topology are introduced as invariants useful for matching, reducing the problem to graph or tree making. The level set topology tree is also proposed as a method of multi-scale description of the picture, and shown to be and invariant generalization of the scale space technique. GRA

N85-35631# Naval Postgraduate School, Monterey, Calif.
VLSI (VERY LARGE SCALE INTEGRATED) TUTORIALS THROUGH THE VIDEO-COMPUTER COURSEWARE IMPLEMENTATION SYSTEM M.S. Thesis
L. R. Muth Mar. 1985 150 p
(AD-A155889) Avail: NTIS HC A07/MF A01 CSCL 05/9

An overview of the University of Utah Video-computer Courseware Implementation System (VCIS) programs is presented. A tutorial is included which is designed to provide an author with enough knowledge to create a simple lesson containing test and graphic frames. VCIS was used in creating two tutorials, which exercise most of the functions in the authoring system. One tutorial is only text and is an introduction to the Berkeley UNIX operating system and its vieditur. The other tutorial contains both text and

graphics and is an introduction to Very Large Scale Integrated (VLSI) circuit design. GRA

N85-35632# Naval Training Equipment Center, Orlando, Fla.
AN EXPLORATORY STUDY OF THE EFFECT OF SCREEN SIZE AND RESOLUTION ON THE LEGIBILITY OF GRAPHICS IN AUTOMATED JOB PERFORMANCE AIDS Final Report, Oct. 1981 - Dec. 1983
D. J. Dwyer 30 May 1985 47 p Prepared in cooperation with Air Force Human Resources Lab.
(DA Proj. 236-2)
(AD-A155989; NAVTRAEQUIPC-IH-355; AFHRL-TR-84-55) Avail: NTIS HC A03/MF A01 CSCL 05/8

The electronic delivery of technical information in computer-based job performance aids (JPAs) for maintenance will rely heavily on graphic displays of schematics, printed circuit (PC) boards, illustrated parts breakdowns (IPBs), and locator diagrams. Optimal levels of critical visual display parameters such as screen size and resolution must be identified to maximize the efficiency and effectiveness of task performance and to determine device design requirements. The purpose of this experiment was to determine how locator task performance varied as a function of changes in display screen size and resolution when information needed to perform a task is presented in a graphic format. Graphic displays of PC boards were presented on a cathode ray tube (CRT) under varying conditions of screen size and resolution. Students were asked to locate test points on an actual PC board, based on test points identified by a flashing arrow on a graphic display of the PC board. The results demonstrated that screen size affected response accuracy only when the graphic display contained a large number of highly similar, densely packed test points (i.e., there was low descriminability among the test points). In this case, the largest screen size produced the highest accuracy rates. Screen size did not affect response accuracy when the test points on the graphic display were of many different shapes and sizes (i.e., there was high discriminability among the test points). GRA

N85-35633# Mitre Corp., Bedford, Mass.
A QUICKLY TESTED PASCAL RANDOM NUMBER GENERATOR FOR MICROCOMPUTERS Final Report
C. J. Colwell, R. A. Dramstad, and M. E. Lopez May 1985 53 p
(Contract F19628-84-C-0001)
(AD-A156059; MTR-9067; ESD-TR-84-202) Avail: NTIS HC A04/MF A01 CSCL 09/2

An assembly language subroutine that uses a shifting mask to generate pseudo-random numbers has been written for use with Apple II microcomputer Pascal. The routine is nearly 80 times faster than a direct Pascal multiplicative congruence scheme. With the recommended starting parameters, the resulting stream has passed 10 different statistical tests for density and randomness. An efficient extension to the normal distribution is also presented. Author (GRA)

N85-35634# Lincoln Lab., Mass. Inst. of Tech., Lexington.
SELECTED PUBLICATIONS IN IMAGE UNDERSTANDING AND COMPUTER VISION FROM 1974 TO 1983
J. G. Verly 18 Apr. 1985 100 p
(Contract F19628-85-C-0002; ARPA Order 4881)
(AD-A156196; TR-716; ESD-TR-85-180) Avail: NTIS HC A05/MF A01 CSCL 09/2

A list of selected publications in image understanding and computer vision is presented. The list was compiled as part of work for the DARPA-sponsored Autonomous IR Sensor Technology program, and the choice of references was directly influenced by the needs of that program. Therefore, emphasis was placed on theories, techniques, and systems for interpreting complex imagery; the more classical fields of image processing, e.g., filtering, enhancement, restoration, coding, and reconstruction, were not included. The topics of edge detection and region segmentation as well as the well-known scene analysis problems of shape recognition from stereo, shading, texture, and motion were also excluded. The bibliography covers the last decade (1974-1983) and is based on the yearly surveys published by A. Rosenfeld in the Journal initially called Computer Graphics and Image Processing (CGIP) and now Computer Vision, Graphics, and Image Processing (CVGIP). GRA

N85-35635# Illinois Univ., Urbana. Computer Systems Group.
DESIGN FOR MISP: A MULTIPLE INSTRUCTION STREAM SHARED PIPELINE PROCESSOR M.S. Thesis
L. M. Pedersen Dec. 1984 194 p
(Contract N00039-80-C-0556)
(AD-A156314; CSG-37) Avail: NTIS HC A09/MF A01 CSCL 09/2

The multiple stream shared pipeline processor is an eight-segment pipelined processor and is designed to allow eight essentially independent instruction streams to execute concurrently. This allows the hardware resources of the pipeline to be shared among the eight instruction streams. The basic hardware design for the MISP processor is presented. Methods for accomplishing process control are discussed and a description of the operating system is given. A mechanism for trap and interrupt handling is presented and the control structure is described. An appropriate system configuration is given for the MISP processor. The feasibility of a VLSI implementation of the MISP processor is evaluated. MISP has several advantages over a conventional microprocessor implementation. MISP has a higher pin utilization over a single processor, since it has one address bus and one bidirectional data bus which is shared by all of the processes. It also maximizes hardware resource utilization, since much of the hardware in the segments is shared and only the process state needs to be replicated for each process. Thus, for a modest cost increase, the MISP processor architecture achieves nearly an eight times speed-up over a conventional single stream microprocessor architecture. MISP represents a cost-effective alternative to conventional multiprocessor architectures. GRA

61 COMPUTER PROGRAMMING AND SOFTWARE

Includes computer programs, routines, and algorithms.

N85-35636 California Inst. of Tech., Pasadena.
ERROR-CORRECTING CODES FOR COMPUTER MEMORIES Ph.D. Thesis
Mario Blaum 1985 88 p
Avail: Univ. Microfilms Order No. DA8508455

A generalization of the birthday surprise problem is presented, i.e., how many people need to be interviewed on the average until either r birthdays occur k times each or one birthday occurs $k + 1$ times. If $r = 1$, the usual birthday surprise number is obtained. Asymptotic estimates for the birthday surprise number using a theorem proved in appendix 1 are given. Accurate and easily evaluated estimates for the average lifetime of a semiconductor RAM memory protected by a single error correcting, doubly error detecting (SEC-DED) code are presented. Two methods for increasing the lifetime of a computer memory: adding s rows of spare chips and implementing 2-ECC. A class of burst error correcting array codes is described. The fundamental properties of these codes are proved. A code that can correct any track error or two track erasures in a 9-track magnetic tape is constructed. The construction is extended to codes and erasures. The result is a new family of codes, the B(n,m)-codes.
Dissert. Abstr.

N85-35637*# National Aeronautics and Space Administration. Langley Research Center, Hampton, Va.
TRICCS: A PROPOSED TELEOPERATOR/ROBOT INTEGRATED COMMAND AND CONTROL SYSTEM FOR SPACE APPLICATIONS
Ralph W. Will Jul. 1985 31 p refs
(NASA-TM-87577; NAS 1.15:87577) Avail: NTIS HC A03/MF A01 CSCL 09B

Robotic systems will play an increasingly important role in

space operations. An integrated command and control system based on the requirements of space-related applications and incorporating features necessary for the evolution of advanced goal-directed robotic systems is described. These features include: interaction with a world model or domain knowledge base, sensor feedback, multiple-arm capability and concurrent operations. The system makes maximum use of manual interaction at all levels for debug, monitoring, and operational reliability. It is shown that the robotic command and control system may most advantageously be implemented as packages and tasks in Ada. Author

N85-35638# Sherbrooke Univ. (Quebec). Dept. de Geographie.
CALCULATION OF THE DIFFUSION OF LIGHT BY AEROSOLS: DESCRIPTION OF THE MIELOR SOFTWARE AND RESULTS OBTAINED [CALCUL DE DIFFUSION DE LA LUMIERE PAR LES AEROSOLS: DESCRIPTION DES PROGRAMMES MIELOR ET RESULTATS OBTENUS]
Alain Royer, Robert Bernier, Uta Adler, and Daniel Pilon Mar. 1985 77 p refs In FRENCH; ENGLISH summary
(Rept-80) Avail: NTIS HC A05/MF A01

The MIELOR software package was developed to compute the MIE's scattering function. A summary of the MIE's theory used for a given size distribution and refractive index of microparticles (aerosols) is presented. The computer programs for the determination of the phase functions, the efficiency factors for scattering and extinction, the single scattering albedo and the asymmetry factor are described. Author

N85-35639*# Informatics-PMI, Inc., Palo Alto, Calif.
CRAYCDC
Clayton J. Guest Mar. 1985 12 p
(Contract NAS2-11555)
(NASA-CR-177374; NAS 1.26:177374; TN-84-7104-101-16) Avail: NTIS HC A02/MF A01 CSCL 09B

The CRAYCDC is a FORTRAN subroutine which runs on the CDC Cyber 205. It converts 64 bit binary data from a Cray computer (1S or X-MP) to the corresponding 64 bit binary data for a Cyber 205. The purpose, usage, storage, timing consideration, access to CRAYCDC, are outlined. E.A.K.

N85-35640*# Informatics-PMI, Inc., Palo Alto, Calif.
CDCCRAY
Clayton J. Guest Mar. 1985 11 p
(Contract NAS2-11555)
(NASA-CR-177375; NAS 1.26:177375; TN-84-7104-101-13) Avail: NTIS HC A02/MF A01 CSCL 09B

The CDCCRAY is a FORTRAN subroutine which runs on the Cray and converts 32 or 64 bit binary data from the CDC Cyber 205 to the corresponding 64 bit binary data for the Cray X-MP. The CDCCRAY's purpose, usage, storage, timing consideration, and linkage editing are discussed. E.A.K.

N85-35641*# Avco Systems Div., Wilmington, Mass.
ENHANCEMENT OF THE FLEXIBLE SPACECRAFT DYNAMICS PROGRAM FOR OPEN SPACECRAFT Final Report
15 Mar. 1985 36 p ref
(Contract NAS5-28128)
(NASA-CR-175309; NAS 1.26:175309) Avail: NTIS HC A03/MF A01 CSCL 09B

The modifications and additions made to the Flexible Spacecraft Dynamics (FSD) Program are described. The principal addition to the program was the capability to simulate a single axis gimble platform nadir pointing despin control system. The formulation for the single axis gimble equations of motion is a modification of the formulation. The details of the modifications made to the FSD Program are presented. Modifications to existing subroutines are briefly described and a detailed description of new subroutines is given. In addition, e program variables in new labelled COMMON blocks are described in detail. A description of new input symbols for the FSD Program is given. G.L.C.

N85-35642*# Charles River Analytics, Inc., Cambridge, Mass.
STUDY OF FAULT TOLERANT SOFTWARE TECHNOLOGY FOR DYNAMIC SYSTEMS
Alper K. Caglayan and Greg L. Zacharias Sep. 1985 97 p refs
(Contract NAS1-17705)
(NASA-CR-172618; NAS 1.26:172618) Avail: NTIS HC A05/MF A01 CSCL 09B

The major aim of this study is to investigate the feasibility of using systems-based failure detection isolation and compensation (FDIC) techniques in building fault-tolerant software and extending them, whenever possible, to the domain of software fault tolerance. First, it is shown that systems-based FDIC methods can be extended to develop software error detection techniques by using system models for software modules. In particular, it is demonstrated that systems-based FDIC techniques can yield consistency checks that are easier to implement than acceptance tests based on software specifications. Next, it is shown that systems-based failure compensation techniques can be generalized to the domain of software fault tolerance in developing software error recovery procedures. Finally, the feasibility of using fault-tolerant software in flight software is investigated. In particular, possible system and version instabilities, and functional performance degradation that may occur in N-Version programming applications to flight software are illustrated. Finally, a comparative analysis of N-Version and recovery block techniques in the context of generic blocks in flight software is presented. Author

N85-35643*# Research Triangle Inst., Research Triangle Park, N.C.
AUTOSIM: AN AUTOMATED REPETITIVE SOFTWARE TESTING TOOL
J. R. Dunham and S. E. McBride Sep. 1985 98 p refs
(Contract NAS1-16489)
(NASA-CR-177930; NAS 1.26:177930) Avail: NTIS HC A05/MF A01 CSCL 09B

AUTOSIM is a software tool which automates the repetitive run testing of software. This tool executes programming tasks previously performed by a programmer with one year of programming experience. Use of the AUTOSIM tool requires a knowledge base containing information about known faults, code fixes, and the fault diagnosis-correction process. AUTOSIM can be considered as an expert system which replaces a low level of programming expertise. Reference information about the design and implementation of the AUTOSIM software test tool provides flowcharts to assist in maintaining the software code and a description of how to use the tool. Author

N85-35644# Battelle Columbus Labs., Ohio.
ESTABLISHMENT OF A COMPUTER-AIDED DESIGN (CAD)-COMPUTER-AIDED MANUFACTURING (CAM) PROCESS FOR THE PRODUCTION OF COLD FORGED GEARS Final Report, 25 May 1983 - 1 Apr. 1985
D. J. Kuhlmann, P. S. Raghupathi, and T. Altan Warren, Mich. Army Tank-Automotive Command Apr. 1985 230 p Prepared in cooperation with Eaton Corp., Willoughby Hills, Ohio
(Contract DAAE07-82-C-4063)
(AD-A155756; TACOM-TR-13090) Avail: NTIS HC A11/MF A01 CSCL 09/2

In Phase II of the program, a spur gear and a helical gear were selected to be extruded, using dies which were manufactured using the techniques developed in Phase I. The computer program, GEARDI, was used to generate the corrected die geometry for each gear. kTHe dies were made both by electrical discharge machining. Extensive trials were conducted for both the spur gear and helical gear. Twenty spur and 20 helical gears were formed in a hydraulic press. Extra extrusions were made which were sectioned and inspected for grain flow patterns. Geometrical measurements made on the extruded gears show that errors in the tooth profile are small. The extruded spur gear, which is designed to be an AGMA quality Class 7 gear, was determined to be between quality Classes 7 and 8. The helical gear, a quality Class 7 gear design, was extruded to a Class 5 gear. For the spur gear, these results indicate a high degree of accuracy in the ability of the GEARDI computer program to compensate for elastic deflection and bulk shrinkage of the extrusion dies. The rather

poor quality of the helical gears indicates that there are some technical problems which must be solved before this type of gear can be extruded successfully on a production basis. GRA

N85-35645# Naval Postgraduate School, Monterey, Calif.
ATTACKING SOFTWARE CRISIS: A MACRO APPROACH M.S. Thesis
T. N. Qureshi Mar. 1985 87 p
(AD-A155846) Avail: NTIS HC A05/MF A01 CSCL 09/2

The software crisis refers to a set of problems that are encountered in the development of computer software. The problems are not limited to software that does not function properly. Rather the software crisis includes problems attached with the development of software, and keeping pace with the ever-increasing demand of software. The software crisis is characterized by many problems: Schedules and cost estimates are often grossly inaccurate, cost overruns of an order of magnitude have been experienced, schedules slip by months or years and software quality is often suspect. This thesis attempts to provide solutions to overcome the software crisis. The basic premise of this thesis is that unless the problems at the software industry level are solved, no number of technical and project management tools can be of much help in overcoming the software crisis. The author examines the existence of the software crisis, its causes and its serious impact on every walk of life. The nature of software development is discussed, considering it as a craft and as an engineering discipline. After evaluating various alternatives, a managerial approach is emphasized. Issues like education, professionalization, programmer's productivity, and human factors are discussed. Action on these recommendations requires crossing organizational boundaries, and viewing the problem from a macro perspective. GRA

N85-35646# Naval Postgraduate School, Monterey, Calif.
SOFTWARE MAINTENANCE RELATING TO THE INPUT TRANSLATOR AND z-80 REALIZATION VOLUME OF THE COMPUTER SYSTEMS DESIGN ENVIRONMENT M.S. Thesis
R. R. Vogel Mar. 1985 122 p
(AD-A155849) Avail: NTIS HC A06/MF A01 CSCL 09/2

This thesis corrects the discrepancies between the input Translator and the Z-80 Realization Volume of the Computer System Design Environment (CSDE). It also demonstrated, for the first time, complete processing of a problem through CSDE. CSDE is a computer-aided design system for real time controllers. The Translator takes as input, a Computer System Design Language (CSDL) problem and generates a primitive list. Each primitive is matched to identically named primitive realizations in the Realization Volume. The final outputs are hardware and software listings to implement the initial design. GRA

N85-35647# Carnegie-Mellon Inst. of Research, Pittsburgh, Pa. Robotics Inst.
REACHABLE GRASPS ON A POLYGON: THE CONVEX ROPE ALGORITHM Interim Report
M. A. Peshkin and A. C. Sanderson Apr. 1985 32 p
(AD-A155913; CMU-RI-TR-85-6) Avail: NTIS HC A03/MF A01 CSCL 12/1

This document describes an algorithm which finds the externally visible vertices of a polygon, and which generates the clockwise and counter-clockwise convex ropes of each one. The convex ropes give the range of angles from which each vertex is visible, and give all the pairs of vertices which are reachable by a straight robotic finger. All of the convex ropes can be found in expected time order n, where n is the number of vertices of the polygon the application of this geometric construction to automated grasp planning is discussed. The computational complexity of the grasp selection process can be substantially reduced by its use. Author (GRA)

N85-35648# Systems and Applied Sciences Corp., Vienna, Va.
USERS GUIDE FOR OPTIMUM INTERPOLATION METHOD OF GLOBAL DATA ASSIMILATION
D. C. Norquist Hanscom AFB, Mass. AFGL 1 Nov. 1984 69 p
(AD-A155929; AFGL-TR-84-0290; SR-7) Avail: NTIS HC A04/MF A01 CSCL 09/2

This report is a manual for using the codes that produce the ASAP (AFGL Statistical Analysis Program) optimum interpolation global data analysis. It describes the procedures for running the codes and indicates necessary input and output files and their forms. It describes what variables need to be changed for desired changes in resolution, time and date of analysis, and other changes and where these variables are located in the codes. Also described are procedures for running the AFGL global spectral model and non-linear normal mode initialization in sequence with the analysis procedure to form the data assimilation cycle. The manual is designed to accompany code listings available from the author. GRA

N85-35649# Adaptive Sensors, Inc., Santa Monica, Calif.
L-STEP SEQUENTIAL DECODING Quarterly Report
I. S. Reed 31 Mar. 1985 8 p
(Contract N00014-84-C-0720)
(AD-A156121; QR-2) Avail: NTIS HC A02/MF A01 CSCL 09/4

In the final report of an earlier yearly contract with NAVAIR a new decoding technique was found for minimum error-path decoding of convolutional codes. This new technique was called piece-wise L-steps minimum-error decoding or more simply L-step decoding. In a general sense L-step decoding is a method for decoding convolutional codes which appears to bridge the gap between the full implementation of a specific ideal decoder type and its less than ideal version in which memory paths are truncated. Although L-step decoding was introduced to save steps in an error trellis decoding algorithm, it can be extended to apply to most major types of decoding algorithms for convolutional codes, including Viterbi, stack, Fano, and their associated error-trellis algorithms. GRA

N85-35650# Adaptive Sensors, Inc., Santa Monica, Calif.
PRUNED ERROR-TRELLIS DECODING OF CERTAIN NON-SYSTEMATIC CONVOLUTIONAL CODES Quarterly Report
I. S. Reed 31 Dec. 1984 34 p
(Contract N00014-84-C-0720)
(AD-A156122; QR-1) Avail: NTIS HC A03/MF A01 CSCL 09/4

In this report, pruned error-trellis decoding of systematic and nonsystematic convolutional codes with a delay-free inverse has been developed in detail, including quantitative formulas for the number of states and transitions which remain in the pruned error trellis. Currently, the problem of trellis pruning of other nonsystematic CCs is being investigated. Finally, the reduced hardware requirements for pruned error-trellis decoding versus standard Viterbi decoding is being studied, and a preliminary architecture has already been found for the dual-K decoding algorithm developed in this report. Author (GRA)

N85-35651# Naval Postgraduate School, Monterey, Calif.
BENCHMARK EVALUATION OF PC SIMSCRIPT M.S. Thesis
A. A. Deckert, Jr. Mar. 1985 88 p
(AD-A156133) Avail: NTIS HC A05/MF A01 CSCL 09/2

As senior defense managers increasingly rely on models and simulations to justify major programs, greater attention is focused on the models and how they were constructed and validated. The SIMSCRIPT language has become the language of choice for military simulations and modeling primarily due to its readability and world view use of processes and events to model the interaction of entities, attributes and sets. This thesis reviews the personal computer release of SIMSCRIPT which was made available during late 1984. Topics include results of hands-on testing, feasibility as a teaching tool at the Naval Postgraduate School, evaluating transportability of programs between different releases of SIMSCRIPT, and benchmark time trials when programs are run on different machine configurations. GRA

N85-35652# SRI International Corp., Menlo Park, Calif.
SPECIFYING AND VERIFYING CONCURRENT PROGRAMS Final Report, 15 Aug. 1983 - 14 Nov. 1984
L. Lamport Feb. 1985 94 p

(Contract DAAG29-83-K-0119)
(AD-A156190; ARO-20628.5-EL) Avail: NTIS HC A05/MF A01 CSCL 09/2

The goal of this project was the development of formal methods for the specification and verification of concurrent programs to help avoid software errors in concurrent systems. This involved research in three areas: Specification; Verification; and Semantics. GRA

N85-35653# Ballistic Research Labs., Aberdeen Proving Ground, Md.
COMPUTATIONAL METHODS FOR THE EXPLOSIVE AND IMPACT COMPACTION OF POWDERS Final Report
R. F. Benck May 1985 28 p
(DA Proj. 1L1-62618-AH-80)
(AD-A156219; BRL-MR-3448) Avail: NTIS HC A03/MF A01 CSCL 09/2

THe effects of computational cell size and slide line routines upon TROTT computer code simulations of explosive and impact powder densifications is determined. A 30 by 40 grid of quadrilateral cells is computationally adequate to describe the systems under study and the presence of a slide line does not appreciably affect the final calculated powder density. GRA

N85-35654# Naval Postgraduate School, Monterey, Calif.
PROTOTYPING WITH DATA DICTIONARIES FOR REQUIREMENTS ANALYSIS M.S. Thesis
A. F. Noel Mar. 1985 199 p
(AD-A156303) Avail: NTIS HC A09/MF A01 CSCL 09/2

The analysis of software system requirements is to develop a complete, consistent and unambiguous statement for what the software will do, but not how. Failure to correctly elicit requirements is cause for difficult and expensive correction efforts during later phases of system development. An alternative approach to interviewing and textual document preparation is the use of a functionally limited model, a prototype. This thesis will examine the feasibility of using prototypes accompanied with data dictionaries as a more effective means of communicating with users and, therefore, more correctly eliciting requirements. It will include development of a relational based, prototype data dictionary using the dBASE II database management system. GRA

N85-35655# Illinois Univ. at Urbana-Champaign, Savoy. Coordinated Science Lab.
DESIGN OF A MICROPROGRAM CONTROL UNIT WITH CONCURRENT ERROR DETECTION M.S. Thesis
M. M. Yen Aug. 1984 65 p
(Contract N00039-80-C-0556)
(AD-A156447; CSG-30) Avail: NTIS HC A04/MF A01 CSCL 09/2

This paper presents an integrated approach to the design of a microprogram control unit (MCU) with concurrent error detection (CED) capability for errors generated by VLSI physical failures. The paper first presents the design of a single-chip MCU that comprehensively detects errors due to internal physical failures during its normal operation. The AM2910 microprogram sequencer is used as a functional model for the CED MCU. Lastly, the paper presents a critical evaluation of the actual mask-level layout of the CED MCU design versus a simplex MCU without CED and a CED MCU through duplication and comparison. Author (GRA)

N85-35656# Los Alamos Scientific Lab., N. Mex.
USING AN LSI-11/23 AND RT-11 TO DIGITIZE ANALOG TAPES
J. N. Stewart 1985 7 p Presented at the Spring DECUS Symp., New Orleans, 27 May 1985
(Contract W-7405-eng-36)
(DE85-012736; LA-UR-85-1817; CONF-8505131-4) Avail: NTIS HC A02/MF A01

The design and implementation of a system on an LSI-11/23 under RT-11 that digitizes 14-channel analog tapes at given intervals and writes the digitized data to a magnetic tape are described. The analog tapes contain 13 channels of data and one channel of IRIG-B time code. A given interval is selected by entering a time and an interval. The IRIG-B time code is read from the analog tapes and used to start the digitizing. A programmable clock board is used to control the digitizer and to count the interval length. The code is written in MACRO and the magnetic tape controller is addressed directly instead of using programmed requests to achieve the needed throughput rates. DOE

N85-35657# Argonne National Lab., Ill.
SASSYS-1 COMPUTER CODE VERIFICATION WITH EBR-2 TEST DATA
D. K. Warinner and F. E. Dunn 1985 8 p Presented at the ANS/ENs Fast Reactor Safety Meeting, Knoxville, Tenn., 21 Apr. 1985
(Contract W-31-109-eng-38)
(DE85-012119; CONF-850410-46) Avail: NTIS HC A02/MF A01

The EBR-2 natural circulation experiment, XX08 Test 8A, is simulated with the SASSYS-1 computer code and the results for the latter are compared with published data taken during the transient at selected points in the core. The SASSYS-1 results provide transient temperature and flow responses for all points of interest simultaneously during one run, once such basic parameters as pipe sizes, initial core flows, and elevations are specified. The SASSYS-1 simulation results for the EBR-II experiment XX08 Test 8A, conducted in March 1979, are within the published plant data uncertainties and, thereby, serve as a partial verification/validation of the SASSYS-1 code. DOE

N85-35658# Illinois Univ., Urbana. Dept. of Computer Science.
POLYLITH: THE EARLY GOALS
J. M. Purtilo Apr. 1985 33 p refs
(Contract DE-AC02-76ER-02383)
(DE85-012534; DOE/ER-02383/0108; UILU-ENG-85-1710) Avail: NTIS HC A03/MF A01

The system Polylith is a language domain independent module interconnection grammar, together with an enhanced set of execution time services and assistance from a collection of expert tools. This report summarizes some of the early ambitious for Polylith. It draws upon many internal documents written during the specification phase of the system's development. It is intended to coalesce this material for rapid dissemination throughout the UIUC community. DOE

N85-35659# Oak Ridge National Lab., Tenn.
DEPTH-CHARGE STATIC AND TIME-DEPENDENT PERTURBATION/SENSITIVITY SYSTEM FOR NUCLEAR REACTOR CORE ANALYSIS, REVISION 1
J. R. White Apr. 1985 169 p
(Contract DE-AC05-84OR-21400)
(DE85-013103; ORNL/CSD-78/R1) Avail: NTIS HC A08/MF A01

The background theory, user input, and sample problems required for the efficient application of the DEPTH-CHARGE system - a code black for both static and time dependent perturbation theory and data sensitivity analyses are reported. The DEPTH-CHARGE system is of modular construction and was implemented within the VENTURE-BURNER computational system. The DEPTH module (coupled with VENTURE) solves for the three adjoint functions of depletion perturbation theory, and calculates the desired time dependent derivatives of the response with respect to the nuclide concentrations and nuclear data utilized in the reference model. The CHARGE code is a collection of utility routines for general data manipulation and input preparation and considerably extends the usefulness of the system through the automatic generation of adjoint sources, estimated perturbed responses, and relative data sensitivity coefficients. Combined, the DEPTH-CHARGE system provides, for the first time, a complete generalized first order perturbation/sensitivity theory capability for both static and time dependent analyses of realistic multidimensional reactor models. Minor revisions to the original DEPTH-CHARGE documentation are incorporated to reflect some new capabilities within the individual codes. DOE

N85-35660# California Univ., Berkeley. Dept. of Civil Engineering.
THREE-DIMENSIONAL FINITE DEFORMATION VISCOELASTIC MODEL ACCOUNTING FOR DAMAGE EFFECTS
J. C. Simo and R. L. Taylor Mar. 1985 44 p
(Contract W-7405-eng-48)
(DE85-012951; UCRL-15679; UCB/SESM-85/02) Avail: NTIS HC A03/MF A01

A fully three dimensional finite deformation isotropic viscoelastic model was developed with the following characteristics: (1) uncoupled bulk response over any range of deformations; (2) generalization of the classical standard solid of the linearized theory; and (3) both for relaxation times either extremely small or very large, the model exactly reduces to the classical Mooney-Rivlin model of rubber elasticity. In addition, a damage mechanism is incorporated into the model of the type previously developed by the authors in the context of the linearized theory. This is a three dimensional isotropic damage mechanism based on the maximum value attained by a scalar function of certain deviatoric Lagrangian strain measure. The resulting five parameter finite deformation damage model is implemented in the finite element computer program FEAP. The coding architecture is compatible with the NIKE2D codes. DOE

N85-35661# Los Alamos Scientific Lab., N. Mex.
RFQ MODELING COMPUTER PROGRAM
J. M. Potter 1985 4 p Presented at the Particle Accelerator Conf., Vancouver, British Columbia, 13 May 1985
(Contract W-7405-eng-36)
(DE85-012665; LA-UR-85-1612; CONF-850504-50) Avail: NTIS HC A04/MF A01

The mathematical background for a multiport network solving program is described. A method for accurately numerically modeling an arbitrary, continuous, multiport transmission line is discussed. A modification to the transmission line equations to accommodate multiple RF drives is presented. An improved model for the radio frequency quadrupole (RFQ) accelerator that corrects previous errors is given. This model permits treating the RFQ as a true eight port network for simplicity in interpreting the field distribution and ensures that all modes propagate at the same velocity in the high frequency limit. The flexibility of the multiport model is illustrated by simple modifications to otherwise two dimensional systems that permit modeling them as linear chains of multiport networks. DOE

N85-35662# California Univ., Livermore. Lawrence Livermore Lab.
SIG: A GENERAL-PURPOSE SIGNAL PROCESSING PROGRAM. USER'S MANUAL: REVISION 1
D. Lager and S. Azevedo 9 Mar. 1985 105 p Revised
(Contract W-7405-eng-48)
(DE85-013035; UCID-19912-Rev-1) Avail: NTIS HC A06/MF A01

The SIG is a general purpose signal processing, analysis, and display program. Its main purpose is to perform manipulations on time domain and frequency domain signals. The manual contains a complete description of the SIG program from the user's standpoint. A brief exercise in using SIG is shown. Complete descriptions are given for each command in the SIG core. General information about the SIG structure, command processor, and graphics options are provided. An example, usage of SIG for solving a problem is developed, and error message formats are discussed. DOE

N85-35663# Los Alamos Scientific Lab., N. Mex.
OPTIMIZING DATA ACCESS IN THE LAMPF CONTROL SYSTEM
S. C. Schaller, J. K. Corley, and P. A. Rose 1985 4 p Presented at the Particle Accelerator Conf., Vancouver, British Columbia, 13 May 1985
(Contract W-7503-eng-36)
(DE85-012653; LA-UR-85-1624; CONF-850504-55) Avail: NTIS HC A02/MF A01

The LAMPF control system data access software offers considerable power and flexibility to application programs through symbolic device naming and an emphasis on hardware independence. Optimizations aimed at improving the performance of the data access software while retaining these capabilities are discussed. The only aspects of the optimizations visible to the application programs are vector devices and aggregate devices. A vector device accesses a set of hardware related data items through a single device name. Aggregate devices allow run time optimization of references to groups of unrelated devices. Optimizations not visible on the application level include careful handling of network message traffic, the sharing of global resources, and storage allocation. DOE

N85-35664# Stanford Linear Accelerator Center, Calif.
ERROR MESSAGE RECORDING AND REPORTING IN THE SLC CONTROL SYSTEM
N. Spencer, J. Bogart, N. Phinney, and K. Thompson Apr. 1985 3 p Presented at the Particle Accelerator Conf., Vancouver, British Columbia, 13 May 1985
(Contract DE-AC03-76SF-00515)
(DE85-013057; SU-SLAC-PUB-3633; CONF-850504-84) Avail: NTIS HC A02/MF A01

Error or information messages that are signaled by control software either in the VAX host computer or the local microprocessor clusters are handled by a dedicated VAX process (PARANOIA). Messages are recorded on disk for further analysis and displayed at the appropriate console. Another VAX process (ERELOG) can be used to sort, list and histogram various categories of messages. The functions performed by these processes and the algorithms used are discussed. DOE

N85-35665# Colorado Univ., Boulder.
TOOLPACK Final Report, 1 Aug. 1980 - 31 Jul. 1984
L. J. Osterweil and L. D. Fosdick May 1985 23 p
(Contract DE-AC02-80ER-10718)
(DE85-013135; DOE/ER-10718/5) Avail: NTIS HC A02/MF A01

The Toolpack project has produced a large configuration of tightly integrated tools comprising a numerical software development environment. Major tool capabilities were created. Odin - an innovative tool integration system was implemented. The combination of research, development and definitive evaluation is characterized. The Toolpack project in the advance of the state of the art and the state of practice in the area of software tools and environments is included. Knowledge about tool integration was advanced through the development of Odin, and the widespread use of effective tools by an important software community will be advanced by the development of the Toolpack/IST prototype which has given way to the distributed Toolpack/1 system. E.A.K.

N85-35666# Edgerton, Germeshausen and Grier, Inc., Idaho Falls, Idaho.
COMPUTER CODE CALCULATIONS OF THE TMI-2 ACCIDENT: INITIAL AND BOUNDARY CONDITIONS
S. R. Behling May 1985 49 p
(Contract DE-AC07-76ID-01570)
(DE85-012613; EGG-TMI-6859) Avail: NTIS HC A03/MF A01

Initial and boundary conditions during the Three Mile Island Unit 2 (TMI-2) accident are described and detailed. A brief description of the TMI-2 plant configuration is given. Important contributions to the progression of the accident in the reactor coolant system are discussed. Sufficient information is provided to allow calculation of the TMI-2 accident with computer codes. DOE

N85-35667# Ames Lab., Iowa.
MASTER FIT USERS' GUIDE, VERSION 1.0
M. E. Nieland Jun. 1985 96 p
(Contract W-7405-eng-82)
(DE85-014199; IS-4876) Avail: NTIS HC A05/MF A01

Master Fit is a computer program for analyzing digitized pulse height spectra consisting of discrete peaks superimposed on a continuous background, such as those that occur in nuclear

physics. The program has capabilities for spectral plotting, peak finding, peak fitting, and data calibration. The peak finding section uses a second difference smoothing routine, along with other parameters, to locate the Gaussian peaks within the spectrum. The program has a skewed Gaussian fitting algorithm to calculate the intensity and energy of a peak from the area and centroid of the peak. The user may choose to store results of selected fits on a calibration data spectrum for a final calibration of peak shape parameters to be determined. Instructions are provided for the execution of the program and for the use of each of the program features. DOE

N85-35668# Telefunken Electronic G.m.b.H., Heilbronn (West Germany).
COMPUTER AIDED DESIGN (CAD) METHODS FOR VERY LARGE SCALE INTEGRATION SYSTEMS Final Report, Mar. 1981
Thomas Ricker, Heinz Rinderle, Dieter Wolff, Irmgard Blasser, Alfred Baechle, Erich Kasper, Johann Killian, Maximilian Kuisl, Otto Mank, Ulf-Guenter Schindel et al Bonn Bundesministerium fuer Forschung und Technologie Apr. 1985 168 p refs In GERMAN; ENGLISH summary Sponsored by Bundesministerium fuer Forschung und Technologie
(BMFT-FB-T-85-029; ISSN-0340-7608) Avail: NTIS HC A08/MF A01; Fachinformationszentrum, Karlsruhe, West Germany DM 33.50

Computer aided design systems were developed to treat integrated circuits (IC) as analog or geometrical systems. The Stanford University Process Engineering Modeling program for the simulation of technological processes was installed. One-dimensional numerical modeling is available with the program one-dimensional semiconductor device simulation. It was used to analyze and optimize different types of elements. The layout and circuit-check program LOCATE, was modified for use with NMOS and bipolar IC's. It was installed on VAX, Interdata and IBM computers. The development of algorithms for automated mask inspection is completed. Modules for automated placement and routing are produced. Author (ESA)

62 COMPUTER SYSTEMS

Includes computer networks.

N85-35669# Brookhaven National Lab., Upton, N. Y.
DISTRIBUTION OF COMPUTER FUNCTIONALITY FOR ACCELERATOR CONTROL AT THE BROOKHAVEN AGS
A. Stevens, T. Clifford, and B. Frankel 1985 6 p Presented at the Particle Accelerator Conf., Vancouver, British Columbia, 13 May 1985
(Contract DE-AC02-76CH-00016)
(DE85-012520; BNL-36393; CONF-850504-141) Avail: NTIS HC A02/MF A01

A set of physical and functional system components and their interconnection protocols were established for all control work. The following computer and control system elements are included: (1) a broadband local area network, which embodies MODEMS; (2) transmission systems and branch interface units; (3) a hierarchical layer, which performs certain data base and watchdog/alarm functions; and (4) a group of work station processors (Apollo's) which perform the function of traditional minicomputer host(s) and a layer, which provides both real time control and standardization functions for accelerator devices and instrumentation. Data bases and other accelerator functionalities are assigned to the most correct level within the network for both real time performance, long-term utility, and orderly growth. DOE

63 CYBERNETICS

Includes feedback and control theory.
For related information see also *54 Man/System Technology and Life Support.*

N85-35670 Purdue Univ., Lafayette, Ind.
RECURSIVE PARTITIIONING ESTIMATION Ph.D. Thesis
Ching-Fu Gau 1984 328 p
Avail: Univ. Microfilms Order No. DA8507689

The partitioned solutions for adaptive control, estimation, identification, and associated Riccati equation solutions were developed by Lainiotis. In this work, the Recursive Partitioning Algorithm (RPA), a recursive version of Lainiotis' Generalized Partitioned Algorithm (GPA) is presented. The interpretation of RPA as a combination of a nominal Kalman filter for the partial initial condition and a recursive least-squares estimator for smoothing the remaining portion of a total initial condition gives great intuitive insight into the partitioned solutions of Lainiotis. The Parallel Partitioning Algorithm (PPA) is then presented to unify various partitioning approaches for optimal linear estimation. This procedure allows the process noise to be partitioned into two parts. The resulting algorithms based on the PPA retained a two-part partitioning structure which consists of two nested suboptimal Kalman filters. Dissert. Abstr.

N85-35671# Tulane Univ., New Orleans, La.
ARTIFICIAL INTELLIGENCE IN Ada (TRADEMARK): PATTERN-DIRECTED PROCESSING Final Report
L. H. Reeker, J. Kreuter, and K. Wauchope May 1985 45 p
(Contract F49620-82-C-0035)
(AD-A156230; AFHRL-TR-85-12) Avail: NTIS HC A03/MF A01 CSCL 09/2

If the programming language Ada is to be widely used in artificial intelligence applications, it will be necessary to demonstrate to programmers that it can provide superior facilities for use in that domain. One means of doing this is to provide facilities for pattern-directed programming within Ada. This report includes three papers, of which the first is designed to serve as an introduction to pattern-directed programming and to the significance of the two papers that follow. It includes: discussions of artificial intelligence programming and the facilities provided by the Ada language, pattern-directed computation, pattern matching, and parsing. The other two papers deal with the use of Ada for pattern-directed programming. One paper deals with efficient implementation of pattern matching (within Ada) is important, because pattern matching tends to be inefficient, leading to problems with excessive processing time. Another paper treats extensions of pattern-direction from strings to more general data structures of the sort used in artificial intelligence. Author (GRA)

64 NUMERICAL ANALYSIS

Includes iteration, difference equations, and numerical approximation.

N85-35672 Wisconsin Univ., Madison.
THE FINITE ELEMENT-DIFFERENCE METHOD Ph.D. Thesis
Xianrui Huang 1984 109 p
Avail: Univ. Microfilms Order No. DA8500824

In the standard finite element method, the strain (stress) field is generally discontinuous at the element boundaries. It may happen that the standard method produces adequate answers for the displacements, but poor answers for the stresses. A new method called finite element-difference (FED for short) method is developed from the Loubignac method by introducing a finite difference technique into the formulation of the strain field. The FED method constructs a displacement field in the usual way, but for the strain field, another finite element interpolation is used to represent the strain field within an element as a linear combination of the nodal strains of the element. A finite difference technique is then

invoked to express the nodal strains in terms of the nodal displacements so that these two fields are coupled. Hence, the FED method provides both a continuous displacement field and a continuous strain field. An iterative algorithm is suggested for solving the basic equations of the method. Dissert. Abstr.

N85-35673# Bremen Univ., (West Germany). Forschungsschwerpunkt Dynamische Systeme.
A GRAPH THEORETIC PROCEDURE FOR THE DESIGN OF FEEDBACK PATTERNS
Arno Linnemann Nov. 1983 33 p refs
(Rept-110) Avail: NTIS HC A03/MF A01

Using a recent characterization of structurally fixed modes, a graph theoretic procedure is developed for the design of feedback patterns, which permits the stabilization of a given time invariant linear system. The proposed method is flexible enough to take into account various design aspects as costs of information transfers, cost of compensators, and the complexity of the closed loop system. Two examples of a large scale system are used to illustrate the procedure. Author

N85-35674# Bremen Univ., (West Germany). Forschungsschwerpunkt Dynamische Systeme.
DESIGN OF DYNAMIC COMPENSATORS OF PRESCRIBED PATTERN
Arno Linnemann Nov. 1983 24 p refs In GERMAN; ENGLISH summary
(BU-109) Avail: NTIS HC A02/MF A01

The following method to stabilize a given strongly connected system by decentralized output feedback is proposed. In a first design step some static decentralized feedback law is determined such that the closed loop system becomes controllable and observable through a single channel. In a second design step a dynamic compensator is connected to this channel to stabilize the whole system. It is shown that the above method is also feasible if feedback laws of some arbitrarily prescribed patterns are considered instead of decentralized feedback laws. For this, a new graph is introduced, which represents the structure of the system as well as the admissible feedback pattern. Subsequently, it is shown that the poles of the system may be arbitrarily assigned by the above method, if and only if the graph is strongly connected and the system has no fixed modes with respect to the prescribed feedback pattern. Author

N85-35675*# National Aeronautics and Space Administration. Langley Research Center, Hampton, Va.
A NEW THEORY FOR MULTISTEP DISCRETIZATIONS OF STIFF ORDINARY DIFFERENTIAL EQUATIONS: STABILITY WITH LARGE STEP SIZES
George Majda (Brown Univ.) Jun. 1985 72 p refs
(Contract NAS1-17070)
(NASA-CR-177941; ICASE-85-31; NAS 1.26:177941) Avail: NTIS HC A04/MF A01 CSCL 12A

A large set of variable coefficient linear systems of ordinary differential equations which possess two different time scales, a slow one and a fast one is considered. A small parameter epsilon characterizes the stiffness of these systems. A system of o.d.e.s. in this set is approximated by a general class of multistep discretizations which includes both one-leg and linear multistep methods. Sufficient conditions are determined under which each solution of a multistep method is uniformly bounded, with a bound which is independent of the stiffness of the system of o.d.e.s., when the step size resolves the slow time scale, but not the fast one. This property is called stability with large step sizes. The theory presented lets one compare properties of one-leg methods and linear multistep methods when they approximate variable coefficient systems of stiff o.d.e.s. In particular, it is shown that one-leg methods have better stability properties with large step sizes than their linear multistep counter parts. The theory also allows one to relate the concept of D-stability to the usual notions of stability and stability domains and to the propagation of errors for multistep methods which use large step sizes. Author

N85-35676*# National Aeronautics and Space Administration. Langley Research Center, Hampton, Va.
ABSORBING BOUNDARY CONDITIONS FOR EXTERIOR PROBLEMS
S. I. Hariharan (Tennessee Univ. Space Inst.) Jul. 1985 35 p refs
(Contract NAS1-17070; Grant NAG1-527)
(NASA-CR-177944; ICASE-85-33; NAS 1.26:177944) Avail: NTIS HC A03/MF A01 CSCL 12A

Elliptic and hyperbolic problems in unbounded regions are considered. These problems, when one wants to solve them numerically, have the difficulty of prescribing boundary conditions at infinity. Computationally, one needs a finite region in which to solve these problems. The corresponding conditions at infinity imposed on the finite distance boundaries should dictate the boundary condition at infinity and be accurate with respect to the interior numerical scheme. Such boundary conditions are commonly referred to as absorbing boundary conditions. A treatment is given of these boundary conditions for wave-like equations. Author

N85-35677# Montreal Univ. (Quebec). Lab. de Physique Mathematique.
ALGORITHMIC APPROACHES IN SETS OF GOOD ANSWERS IN INVERSE PROBLEMS
Pierre C. Sabatier [1984] 17 p refs
(PM/84/18) Avail: NTIS HC A02/MF A01

A very short review of methods recently used for solving applied or theoretical inverse problems and which neither belong to the class of local methods (the most well-known local method is the least squares method) or to the class of el'fand-Levitan type methods is presented. It is shown how very ill-posed inverse problems can be replaced by a set of well-posed questions. Then it is shown how the structure of certain direct problems can suggest using Backlund transformations to construct an algorithm for solving the inverse problem. G.L.C.

N85-35678# Jackson State Univ., Miss.
SMOOTHING SURFACE DATA BY SPLINE FUNCTIONS Final Report, 8 Feb. 1982 - 7 Feb. 1985
P. C. Stein and W. L. White Apr. 1985 12 p
(Grant DAAG29-82-G-0002)
(AD-A155829; ARO-18612.1-MA-H) Avail: NTIS HC A02/MF A01 CSCL 12/1

Research was performed to develop techniques based on spline functions which can be used to smooth two- and higher-dimensional data. GRA

N85-35679# Stanford Univ., Calif. Dept. of Statistics.
INVARIANT TESTS AND LIKELIHOOD RATIO TESTS FOR MULTIVARIATE ELLIPTICALLY CONTOURED DISTRIBUTIONS
T. W. Anderson and H. Hsu Jun. 1985 82 p
(Contract DAAG29-82-K-0156)
(AD-A155844; TR-14; ARO-19065.14-MA) Avail: NTIS HC A05/MF A01 CSCL 12/1

The usual assumption in multivariate hypothesis testing is that the sample consists of n independent, identically distributed Gaussian p-vectors. In this dissertation this assumption is weakened by considering a class of distributions for which the vector observation are not necessarily Gaussian or independent. The following hypothesis testing problems are considered: testing for equality between the mean vector and a specified vector, lack of correlations among different sets, equality of covariance matrices and mean vectors, equality between the correlation coefficient and a specified number, and MANOVA. For each of the above hypotheses, invariant tests and their properties are developed. These include the uniformly most powerful test, the locally most powerful test, admissibility, and null and non-null distributions. GRA

N85-35680# Virginia Univ., Charlottesville. Dept. of Systems Engineering.
CHARACTERIZATIONS OF GENERALIZED HYPEREXPONENTIAL DISTRIBUTIONS

R. F. Botta and C. M. Harris May 1985 48 p
(Contract N00014-83-K-0624)
(AD-A155855; UVA/525393/SE85/107) Avail: NTIS HC A03/MF A01 CSCL 12/1

Generalized hyperexponential (GH) distributions are linear combinations of exponential CDFs with mixing parameters (positive and negative) that sum to unity. The denseness of the class GH with respect to the class of all CDFs defined on (0, infinity) is established by showing that a GH distribution can be found that is as close as desired, with respect to a suitably defined metric, to a given CDF. The metric induces the usual topology of weak convergence so that, equivalently, there exits a sequence of GH CDFs that converges weakly to any CDF. The result follows from a similar well-known result for weak convergence of Erlang mixtures. Various set inclusion relations are also obtained relating the GH distributions to other commonly used classes of approximating distributions including generalized Erlang, mixed generalized Erlang, those with reciprocal polynomial Laplace transforms, those with rational Laplace transforms, and phase-type distributions. A brief survey of the history and use of approximating distributions in queueing theory is also included. GRA

N85-35681# Stanford Univ., Calif. Dept. of Statistics.
LARGE DEVIATIONS FOR THE MAXIMA OF SOME RANDOM FIELDS
D. Siegmund and M. L. Hogan May 1985 28 p
(Contract N00014-77-C-0306; Grant NSF MCS-80-24649)
(AD-A155909; SU-TR-33; SU-TR-233) Avail: NTIS HC A03/MF A01 CSCL 12/1

Several statistical problems which involve the distribution of the maximum of Gaussian random fields are described. Specific examples are the pinned Brownian sheet and a Brownian bridge with reflection, which arises in certain change point problems. In these concrete cases the method of Pickands is adapted to give large deviation probabilities for the maximum, both for continuous and for discrete indexing sets. A different method is used to give a second order correction for the reflected Brownian bridge and hence for reflected Brownian motion. The numerical accuracy of the approximations is studied via simulation. GRA

N85-35682# Naval Research Lab., Washington, D. C.
RELAXATION PHENOMENA AND STABILITY OF PROBABILITY DENSITIES Interim Report, Nov. - Dec. 1984
K. L. Ngai, A. K. Rajagopal, and S. Teitler 5 Jun. 1985 24 p
(AD-A155923; NRL-MR-5575) Avail: NTIS HC A02/MF A01 CSCL 12/1

A characteristic function whose positive time behavior is proportional to a step response function is constructed in such a way that: all its derivatives at t=0 are finite; it has the usual exponential decay behavior for intermediate times; it satisfies the Paley-Wiener bound for long times. The constructed characteristic function CCF is piecewise continuous with behavior determined by different exponentials of a monomial function of t, termed monomial exponentials, on appropriate segments of time. Continuity conditions at joining points provide relations among the tau sub k so only one tau sub k is an independent parameter. The occurrence of tau sub k well within a particular segment in (positive) time determines the monomial exponential that dominates the behavior of CCF and the behavior is then called k-dominant. The k-dominance property is discussed for the probability density corresponding to CCF. A formalism is developed in which the probability density for summand variable in omega-space maintains k-dominant behavior for its corresponding characteristic function. The property of k-dominant stability for probability densities is thereby introduced. At this point the identification of the positive t portion of as a step response function is used to make a comparison with a model of relaxation in complex systems which other have called the Ngai model. The latter involves the introduction of interactions that lead to a modification of a constant decay rate for a linear exponential to a time-dependence one appropriate for fractional exponential behavior. GRA

N85-35683# Naval Postgraduate School, Monterey, Calif.
A NEW METHOD FOR BOUNDARY VALUE PROBLEMS M.S. Thesis
N. F. Heredia Mar. 1985 71 p
(AD-A155934) Avail: NTIS HC A04/MF A01 CSCL 12/1

Large matrix storage constitutes a limitation on the applicability of most numerical techniques including the Finite Element Method, when very accurate results are required. This is particularly true when dealing with Boundary Value Problems. In order to surpass this difficulty a new method to solve these problems has been devised which does not require matrix storage while still providing the possibility of accuracy improvement. Although restricted to one-dimensional, linear differential equations of the form Y to the n th power (X) = f(x) this new approximating technique gives acceptable results. The method will perform equally well for problems with exact or non-exact integrable forcing functions, continuous or discontinuous, or functions existing only as a set of values at discrete points. GRA

N85-35684# Systems and Applied Sciences Corp., Vienna, Va.
TWO METHODS OF GLOBAL DATA ASSIMILATION
I. Halberstam, C. Johnson, D. C. Norquist, and S. L. Tung 1 Oct. 1984 91 p
(Contract F19628-82-C-0023)
(AD-A155981; AFGL-TR-84-0260; SR-4) Avail: NTIS HC A05/MF A01 CSCL 12/1

An optimum interpolation (OI) method and a method that fits observations to basis functions are described. The selected basis functions are the normal modes of the linearized primitive equations. In both methods the assimilation system consists of the analysis procedure, a non-linear normal mode initialization, and the AFGL global spectral NWP model. Both methods were tested using FGGE analyses for Jan. 7, 1979 OOGMT as the starting point. Successive 12 h assimilations were conducted for ten cycles for the OI and five cycles for the fitting procedure. For the OI method results showed a slight increase in error with time when compared with observations, partly attributable to the 12 h forecast length, which was excessive for the forecast error standard deviation prescribed. The fitting procedure showed significantly stronger error increases with time, due in part to faulty conversion of heights to temperature with the hydrostatic equation and to possible over smoothing by the procedure. GRA

N85-35685# Aerospace Corp., El Segundo, Calif. Engineering Group.
CONSTRAINED STIFFNESS MATRIX ADJUSTMENT USING MODE DATA Final Report, Jun. 1983 - Jan. 1984
A. M. Kabe 15 Aug. 1984 38 p
(Contract F04701-83-C-0084)
(AD-A155988; TR-0084(4409-13)-1; SD-TR-85-25) Avail: NTIS HC A03/MF A01 CSCL 12/1

A procedure is introduced that uses, in addition to mode data, structural connectivity information to optimally adjust deficient stiffness matrices. The adjustments are performed such that the percentage change to each stiffness coefficient is minimized. The physical configuration of the analytical model is preserved, and the adjusted model will reproduce exactly the modes used in the identification. The theoretical development is presented, and the procedure is demonstrated by numerical simulation of a test problem. GRA

N85-35686# Stanford Univ., Calif. Dept. of Statistics.
MODEL ROBUST RESPONSE SURFACE DESIGNS: SCALING TWO-LEVEL FACTORIALS
D. M. Steinberg 6 Jun. 1985 36 p
(Contract N00014-76-C-0475)
(AD-A156218; SU-TR-358) Avail: NTIS HC A03/MF A01 CSCL 12/1

Response surface methodology uses simple graduating functions to study the relationship between an experimental response variable and a set of continuous explanatory variables. In designing a response surface study, an experimenter must decide how far apart to set the levels of each factor; i.e., how to scale the design.

A good choice should be sensitive to the fact that the graduating function is only an approximation to the true response function. A Bayesian model is proposed that makes explicit assumptions about the inadequacy of an assumed model and a design criterion based on the model leads to reasonable choices of scale for two-level factorial designs. The choice of scale is found to be insensitive to the prior distributions in the model. GRA

65 STATISTICS AND PROBABILITY

Includes data sampling and smoothing; Monte Carlo method; and stochastic processes.

N85-35687# Tilburg Univ. (Netherlands). Dept. of Business and Economics.
RISK ANALYSIS AND SENSITIVITY: ANTITHESIS OR SYNTHESIS
J. P. C. Kleijnen 1985 11 p refs
(B8562444) Avail: NTIS HC A02

Application of risk versus sensitivity analysis, i.e., estimation of prior or posterior mean, is discussed. If a dynamic model assumes parameters constant over time, then the posterior mean (i.e., the mean conditional on specific values of these parameters) is relevant. Since parameters are unknown, they must be estimated. Sensitivity analysis quantifies the effects of incorrectly specified values of the parameters. If these effects are important then additional information on the parameters might be collected; otherwise robust solutions are to be sought. If these options do not work, then risk analysis can quantify the probability of specific outputs, incorporating the probability distribution of the estimated parameters. Sensitivity analysis changes the values of parameters systematically, whereas risk analysis samples the parameter values. Simple queuing and econometric examples illustrate the two approaches. Author (ESA)

66 SYSTEMS ANALYSIS

Includes mathematical modeling; network analysis; and operations research.

N85-35688# Bremen Univ., (West Germany). Forschungsschwerpunkt Dynamische Systeme.
SPREADING THE CONTROL COMPLEXITY IN DECENTRALIZED CONTROL OF INTERCONNECTED SYSTEMS
B. D. O. Anderson (Australian National Univ., Canberra) and Arno Linnemann Apr. 1984 24 p refs
(BU-117) Avail: NTIS HC A02/MF A01

The problem is considered for large scale interconnected systems of designing decentralized dynamic controllers so that the sum of the orders of the local controllers is approximately the system order, while the separate controller orders are more evenly spread, which generally leads to all memoryless controllers, save one of high complexity. It is shown that under certain circumstances, it is possible to design dynamic feedback controllers for each channel which introduce stable uncontrollable or unobservable modes to the overall system, thus lowering the effective order of that system. This result is then used to spread the controller complexity. Author

N85-35689# Bremen Univ., (West Germany). Forschungsschwerpunkt Dynamische Systeme.
DECENTRALIZED STABILIZATION BY HIGH GAIN FEEDBACK
Arno Linnemann Jan. 1984 14 p refs
(BU-115) Avail: NTIS HC A02/MF A01

Sufficient conditions are derived for a linear time invariant interconnected system to be stabilizable by decentralized state feedback. The conditions centralize known results in decentralized control theory and are obtained by combining a state space version of the small gain theorem on almost invariant subspaces. The stabilizing feedback is in general of high gain type and the closed loop system has nice robustness properties. Author

67 THEORETICAL MATHEMATICS

Includes topology and number theory.

No abstracts in this category.

70 PHYSICS (GENERAL)

For geophysics see *46 Geophysics*. For astrophysics see *90 Astrophysics*. For solar physics see *92 Solar physics*.

N85-35690# Deputy Chief of Staff for Research Development and Acquisition (Army), Washington, D.C.
PROCEEDINGS OF THE 14TH ARMY SCIENCE CONFERENCE. VOLUME 2: PRINCIPAL AUTHORS I THROUGH O
1984 368 p refs Conf. held at West Point, N.Y., 19-21 Jun. 1984 5 Vol.
(AD-A149201) Avail: NTIS HC A16/MF A01 CSCL 05/2

Progress and results in military science, technology, and research and development was presented at the 1984 Army Science conference. E.A.K.

N85-35691# Deputy Chief of Staff for Research Development and Acquisition (Army), Washington, D.C.
PROCEEDINGS OF THE 14TH ARMY SCIENCE CONFERENCE. VOLUME 3: PRINCIPAL AUTHORS P THROUGH Z
1984 323 p refs Conf. held at West Point, N.Y., 19-21 Jun. 1984 5 Vol.
(AD-A149202) Avail: NTIS HC A14/MF A01 CSCL 05/2

The fourteenth in a series of Army Science Conferences was held. A cross section of the many significant scientific and engineering programs carried out by the department of the army was presented, and an opportunity was provided for department of the army civilian and military scientists and engineers to present the results of their research and development efforts. E.A.K.

N85-35692# Office of Naval Research, London (England).
ELECTROMAGNETIC COMPATIBILITY CONFERENCE FEATURES BIOLOGICAL INTERACTIONS
T. C. Rozzell 29 Apr. 1985 13 p Presented at the 6th Symp. and Tech. Exhibition on Electromagnetic Compatibility, Zurich, Mar. 1985
(AD-A155813; ONRL-C-3-85) Avail: NTIS HC A02/MF A01 CSCL 20/3

The Sixth Symposium and Technical Exhibition on Electromagnetic Compatibility was held in Zurich, Switzerland, in March 1985. A session dealing with the interaction between electromagnetic (EM) waves and biological systems is discussed. Topics such as the hazards of EM fields, stationary magnetic fields, therapeutic techniques, microwave power dissipation, and measurement of specific absorption rate were also discussed. GRA

N85-35693# GTE Labs., Inc., Waltham, Mass.
NATIONAL PROGRAM FOR INSPECTION OF NON-FEDERAL DAMS. WOODWARD RESERVOIR DAM (VT 00209), CONNECTICUT RIVER BASIN, PLYMOUTH, VERMONT. PHASE 1 INSPECTION REPORT
May 1979 104 p
(AD-A156256) Avail: NTIS HC A06/MF A01 CSCL 13/13

The dam is a stone-earth fill dam with a concrete emergency spillway. The dam is about 150 ft. long with a maximum height of 30 ft. It is intermediate in size with a significant hazard potential. There were few significant conditions which should be corrected by the owner. The dam should be continuously monitored during

high flows and the gate opened as necessary to minimize flows over the spillway. GRA

71 ACOUSTICS

Includes sound generation, transmission and attenuation. For noise pollution see *45 Environment Pollution.*

N85-35694 British Broadcasting Corp., Kingswood (England). Engineering Div.
ACOUSTIC SCALING: THE DEVELOPMENT OF IMPROVED INSTRUMENTATION
C. D. Mathers, C. Eng, and K. F. L. Lansdowne Aug. 1985 16 p refs
(BBC-RD-1985/7; PH-272) Avail: BBC, Kingswood Warren, Tadworth, Surrey, England

This report describes improvements made to the instrumentation used in one-eight scale acoustic modelling at British Broadcasting Corporation Research Department. In particular it describes the design of new model loudspeakers. Problems encountered in the work are described in some detail to assist in their future avoidance, and the important factors are discussed both from theoretical and practical standpoints. It is concluded that sound quality should no longer be a significant obstacle in making subjective judgements on the modelled acoustic of a projected studio design. Author

N85-35695*# Kansas Univ. Center for Research, Inc., Lawrence. Flight Research Lab.
A RESEARCH PROGRAM TO REDUCE THE INTERIOR NOISE IN GENERAL AVIATION AIRCRAFT, INDEX AND SUMMARY
Louise Morgan, Kevin Jackson, and Jan Roskam Aug. 1985 63 p
(Grant NsG-1301)
(NASA-CR-176178; NAS 1.26:176178; KU-FRL-417-24) Avail: NTIS HC A04/MF A01 CSCL 20A

This report is an index of the published works from NASA Grant NSG 1301, entitled A Research Program to Reduce the Interior Noise in General Aviation Aircraft. Included are a list of all published reports and papers, a compilation of test specimen characteristics, and summaries of each published work. Author

N85-35696# Naval Underwater Systems Center, New London, Conn.
A COMPARISON OF MULTIPATH ARRIVAL STRUCTURES OBSERVED IN THE PRESENCE OF A SURFACE DUCT WITH PREDICTIONS OBTAINED USING CLASSICAL RAY TECHNIQUES AND THE PARABOLIC EQUATION METHOD
H. A. Freese 14 Feb. 1985 121 p
(AD-A156024; AD-E900451; NUSC-TM-811061) Avail: NTIS HC A06/MF A01 CSCL 20/1

Observations of multipath arrival structures made at sea using short pulses have indicated that energy leaking into and out of surface ducts can play a significant role in the propagation of acoustic energy. This leakage phenomenon was first reported with reference to leakage into and out of refracted-surface reflected (RSR) paths. Recent experience has indicated that this leakage phenomenon can also be of importance for energy propagating via bottom bounce modes. Observed underwater acoustic multipath arrival structures are compared with theoretical predictions based on historic sound speed profiles for the vicinity of the Mid-Atlantic Ridge (3500 m water) and the Blake Plateau (1000 m water). Examining these comparisons for surface duct environmental conditions resulted in the conclusion that wave theory is necessary for predicting the distribution of received energy and that classical ray theory (i.e., ray propagation using the high frequency assumption without sound leakage correction) is inadequate. GRA

N85-35697# Catholic Univ. of America, Washington, D.C. Dept. of Physics.
SECOND COLLOQUIM ON THE SCATTERING OF ULTRASONIC WAVES Interim Technical Report, 1 Oct. 1984 - 30 Sep. 1985
H. Uberall 29 Jan. 1985 103 p In ENGLISH and FRENCH Colloq. held at Paris, 4-7 Dec. 1984 Submitted for publication
(Contract N00014-76-C-0430; NR Proj. 384-914; RR0-1108)
(AD-A156298) Avail: NTIS HC A06/MF A01 CSCL 20/1

Contents: L'acoustique des faisceaux bornes; Scattering from fluid and elastic layers; Acoustic scattering from elastic cylinders and spheres: Surface waves (Watson transform) and transmitted waves; Helical surface waves on cylinders and cylindrical cavities; Resonance scattering theory: spherical and cylindrical cavities and inclusions; Scattering from Inhomogeneities; Scattering of short and long sound pulses: Connection with the singularity expansion method; and Inverse scattering and acoustic spectroscopy. GRA

N85-35698# Colorado School of Mines, Golden. Center for Wave Phenomena.
ANALYSIS OF TWO-PARAMETER CONSTANT BACKGROUND BORN INVERSION FOR ACOUSTIC SYNTHETIC DATA
P. B. Violette 15 May 1985 135 p
(Contract N00014-84-K-0049)
(AD-A156394; CWP-029) Avail: NTIS HC A07/MF A01 CSCL 17/10

This thesis examines the usefulness of the two-parameter Born inversion method of Clayton and Stolt under idealized conditions. We implement a constant background procedure to reconstruct line source synthetic data which simulate a stratified acoustic medium. Specifically, this investigation is an extension of the single interface work for double interface models. Since we use offset data to recover one-dimensional bulk modulus and density variations, this procedure is termed a 1.5 dimensional inversion. Implicit in these reconstructed acoustic profiles are errors related to the approximate inversion. Phase shifts inherent in the modeled wave field cause these inversion errors not only to propagate, but also to increase with depth. Since the model data are exact, we are able to examine the analytic expressions of these inversion artifacts. From this analysis, we develop an implementation which minimizes inversion errors. This is achieved by both preconditioning the offset data, and judiciously choosing a reference velocity in accordance with inversion goals. Both of these procedures however provide limited improvement, and we conclude that this constant background, frequency domain, and method should be enhanced by more sophisticated algorithms. Specifically, we suggest the implementation of either a variable background procedure, or the refinement algorithm of Hagin and Cohen. GRA

N85-35699# Argonne National Lab., Ill.
ACOUSTIC RESONANCES IN CYLINDER BUNDLES OSCILLATING IN A COMPRESSIBILE FLUID
W. H. Lin and A. C. Raptis Dec. 1984 19 p refs Presented at the Symp. on Fluid-Struct. Interaction, New Orleans, 23 Jun. 1985
(Contract W-31-109-eng-38)
(DE85-004066; CONF-850648-1) Avail: NTIS HC A02/MF A01

An analytical study on acoustic resonances of elastic oscillations of a group of parallel, circular, thin cylinders in an unbounded volume of barotropic, compressible, inviscid fluid is presented. The perturbed motion of the fluid is assumed due entirely to the flexural oscillations of the cylinders. The motion of the fluid disturbances is first formulated in a three-dimensional wave form and then casted into a two-dimensional Helmholtz equation for the harmonic motion in time and in axial space. The acoustic motion in the fluid and the elastic motion in the cylinders are solved simultaneously. Acoustic resonances were approximately determined from the secular (eigenvalue) equation by the method of successive iteration with the use of digital computers for a given set of the fluid properties and the cylinders' geometry and properties. Effects of the flexural wavenumber and the configuration of and the spacing between the cylinders on the acoustic resonances were thoroughly investigated. DOE

72 ATOMIC AND MOLECULAR PHYSICS

Includes atomic structure and molecular spectra.

N85-35700# California Univ., Berkeley. Lawrence Berkeley Lab.
PROCEEDINGS OF THE WORKSHOP ON DETECTORS FOR RELATIVISTIC NUCLEAR COLLISIONS
Aug. 1984 161 p refs Workshop held in Berkeley, Calif., 26-30 Mar. 1984
(Contract DE-AC03-76SF-00098)
(LBL-18225; CONF-8403137) Avail: NTIS HC A08/MF A01

Given that new heavy-ion facilities will be available within two years, it is both timely and necessary to start looking at the detector requirements imposed by these much higher energies well in advance of their coming on-line. The specific goals set were: (1) build on the base of information generated at previous meetings held to discuss quark matter (specifically: fixed target detectors discussed at Bielefeld (QM'82) and a SPS workshop held in late 1982: collider detectors discussed at Brookhaven (QM'83)); (2) consider detectors for both geometries, i.e., fixed target: spanning the interval 15 to 225 GeV/nucleon collider: from 2 + 2 and 100 + 100 Gev/nucleon; and (3) to identify those critical path items for detectors requiring an R and D effort. It is clear that the area of high energy nuclear collisions is one where both particle and nuclear physicists can join together in a common endeavor. For individual titles, see N85-35701 through N85-35712.

N85-35701# European Organization for Nuclear Research, Geneva (Switzerland).
DETECTORS FOR RELATIVISTIC NUCLEAR COLLISIONS (REPORT FROM THE FIXED-TARGET HADRON GROUP)
C. Gruhn and I. Otterlund (Lund Univ.) *In* California Univ., Berkeley. Lawrence Berkeley Lab. Proc. of the Workshop on Detectors for Relativistic Nucl. Collisions Aug. 1984 p 1-37 refs (For primary document see N85-35700 24-72)
Avail: NTIS HC A08/MF A01

Some predictions of multiplicities and rapidity densities in the absence of quark gluon plasma (QGP) followed by the physics motivation for probing subgroups follow and finally some concluding remarks are given. G.L.C.

N85-35702# California Univ., Berkeley. Lawrence Berkeley Lab.
EVENT PARAMETERS: FIXED TARGETS
A. Poskanzer, H-G. Ritter, B. Ludewigt, K. Foley (Brookhaven National Lab.), S. Borenstein (Brookhaven National Lab.), E. Platner (Brookhaven National Lab.), W. Love (Brookhaven National Lab.), D. Keane (California Univ., Riverside), and F. Plasil (ORNL) *In its* Proc. of the Workshop on Detectors for Relativistic Nucl. Collisions Aug. 1985 p 38-44 (For primary document see N85-35700 24-72)
Avail: NTIS HC A08/MF A01

Detectors for fixed target experiments which have full azimuthal coverage were considered. The general scope of the working group was to consider the configuration of an idealized detector, and various configurations of practical detectors that could be implemented on a relatively short time scale. The second category includes possible upgrades and modifications of existing experimental facilities. Beams of both 15 GeV/A sulphur at the AGS and 200 GeV/A oxygen at the SPS were considered. G.L.C.

N85-35703# California Univ., Los Angeles.
WORKING GROUP ON PENETRATING PROBES AT FIXED TARGET FACILITIES
J. Carroll, G. Igo, M. Goldberg (Syracuse Univ.), W. Cleland (Pittsburg Univ., Pa.), B. Cork (California Univ., Berkeley. Lawrence Berkeley Lab.), D. Hendrie (California Univ., Berkeley. Lawrence Berkeley Lab.), H. Maris (California Univ., Berkeley. Lawrence Berkeley Lab.), T. Mulera (California Univ., Berkeley. Lawrence Berkeley Lab.), G. Roche (California Univ., Berkeley. Lawrence Berkeley Lab.), L. Kluberg (Ecole Polytechnique, Palaiseau, France) et al *In* California Univ., Berkeley. Lawrence Berkeley Lab. Proc. of the Workshop on Detectors for Relativistic Nucl. Collisions Aug. 1984 p 45-60 refs (For primary document see N85-35700 24-72)
Avail: NTIS HC A08/MF A01

This subset of the overall penetrating probes working group considered possible experiment designs and concomitant difficulties in detecting the concentional directly produced electromagnetic probes (gamma, e+e-, mu+mu-) at facilities to be available in the near term. G.L.C.

N85-35704# Brookhaven National Lab., Upton, N. Y.
SUMMARY OF THE WORKING GROUP ON PENETRATING PROBES IN COLLIDER EXPERIMENTS. 1: THE COLLIDER ENVIRONMENT
T. Ludlam *In* California Univ., Berkeley. Lawrence Berkeley Lab. Proc. of the Workshop on Detectors for Relativistic Nucl. Collisions Aug. 1984 p 61-74 refs (For primary document see N85-35700 24-72)
Avail: NTIS HC A08/MF A01

Studies of experiments and their detectors considered the following range of parameters for heavy ion colliders: (1) beam energies up to approx. 100 + 100 GeV/amu; (2) ion masses up to A > 200; (3) luminosity L < 10 to the 27/cm sq sec at top energy for A = 200; and (4) collision energy can be varied down to 2 + 2 GeV/amu. G.L.C.

N85-35705# California Univ., Berkeley. Lawrence Berkeley Lab.
REPORT OF WORKING GROUP ON DETECTORS FOR HADRONS AND EVENT PARAMETERS AT COLLIDERS
W. Carrithers, D. E. Greiner, W. Myers, L. S. Schroeder, H. Steiner, T. J. M. Symons, G. Young (ORNL), D. Beavis (California Univ., Riverside), G. VanDalen (California Univ., Riverside), D. Carmony (Purdue Univ., Lafayette, Ind.) et al *In its* Proc. of the Workshop on Detectors for Relativistic Nucl. Collisions Aug. 1984 p 75-84 refs (For primary document see N85-35700 24-72)
Avail: NTIS HC A08/MF A01

This group was charged with designing detectors to cover two broad classes of experiments to be done at colliding beam machines. The first, hadron studies, includes detection of baryons, mesons and their antiparticles with a view to extracting information on strange to non-strange production ratios, baryon to antibaryon production ratios and relative yields of particles with one, two, or three unit of strangeness. Intensity inteferometry for p1p1 KK, pp and similar pairs as well as studies of multipion and multikaon systems are also included in this category. The second, event parameters, includes measurements of multiplicity (N) and energy and momentum flow as functions of rapidity (y) and azimuthal angle (phi) for both events as a whole and for specific types of particles. Correlations between, say, dN/dy and P sub perp. (which Van Hove has suggested as a phase transition signature), are to be measured. The detectors studied naturally permitted study of, for example, hadron production ratios as a function of energy flow and multiplicity. In addition, the similarities and differences between detectors that would be appropriate for the relativistic Heavy Ion Collider (RHIC) with 100 + 100 GeV/nucleon colliding beams and those of a lower energy machine (mini-collider) usable in the energy range of 3 + 3 GeV/nucleon were considered. G.L.C.

N85-35706# Lund Univ. (Sweden). Div. of Cosmic and Subatomic Physics.
A SURVEY OF MULTIPLICITIES AND RAPIDITY DENSITIES FROM EXISTING EMISSION DATA ON HADRON-NUCLEUS NUCLEUS-NUCLEUS COLLISIONS
I. Otterlund *In* California Univ., Berkeley. Lawrence Berkeley Lab. Proc. of the Workshop on Detectors for Relativistic Collisions Aug. 1984 p 85-104 refs (For primary document see N85-35700 24-72)
Avail: NTIS HC A08/MF A01

A short survey of multiplicities and rapidity densities in high energy hadron-nucleus and nucleus-nucleus collisions obtained in emulsion experiments is given and some extrapolations from proton-nucleus to nucleus-nucleus collisions are discussed. Author

N85-35707# Lund Univ. (Sweden). Div. of Cosmic and Subatomic Physics.
A SIMULATION OF ULTRA-RELATIVISTIC NUCLEUS-NUCLEUS

COLLISIONS
I. Otterlund and E. Stenlund *In* California Univ., Berkeley. Lawrence Berkeley Lab. Proc. of the Workshop on Detectors for Relativistic Nucl. Collisions Aug. 1984 p 105-114 refs (For primary document see N85-35700 24-72)
Avail: NTIS HC A08/MF A01

The number of participant (wounded) nucleons are simulated and rapidity densities are estimated from high energy proton-nucleus collisions. Author

N85-35708# Brookhaven National Lab., Upton, N. Y.
VERY HIGH ENERGY PROBES OF THE QUARK-GLUON PLASMA c75
T. Ludlam, F. Paige, and L. Madansky (John Hopkins Univ., Baltimore, Md.) *In* California Univ., Berkeley. Lawrence Berkeley Lab. Proc. of the Workshop on Detectors for Relativistic Nucl. Collisions Aug. 1984 p 115-120 refs Original language document previously announced as N86-18763 (For primary document see N85-35700 24-72)
Avail: NTIS HC A08/MF A01

Among the penetrating probes of nuclear matter the most frequently discussed are those which involve the detection of photons or leptons with m(sub T) approx. = P(sub T) 3 GeV. This is the expected range of emission from a hot, thermalized plasma of quarks and gluons. The suggestion has been made that in very high energy collisions of nuclei the properties of medium through which the parent partons have propagated just after the collision. The possible uses of such a probe are examined. DOE

N85-35709# Pennsylvania Univ., Philadelphia. Intensity Interferometry Sub-Group.
DETECTOR REQUIREMENTS FOR INTENSITY INTERFEROMETRY MEASUREMENTS c35
William Zajc *In* California Univ., Berkeley. Lawrence Berkeley Lab. Proc. of the Workshop on Detectors for Relativistic Nucl. Collisions Aug. 1984 p 121-132 refs (For primary document see N85-35700 24-72)
Avail: NTIS HC A08/MF A01

The requirements imposed on detector design by intensity interferometry measurements are briefly discussed. The question of momentum resolution is analyzed for the central region. Expected rates for typical nuclear events are estimated. Questions related to the physical significance of the extracted parameters are raised (but not answered). Author

N85-35710# Max-Planck-Inst. fuer Astrophysik, Munich (West Germany).
A HOLOGRAPHIC STREAMER CHAMBER FOR RELATIVISTIC NUCLEUS-NUCLEUS COLLISION EXPERIMENTS c35
V. Eckardt *In* California Univ., Berkeley. Lawrence Berkeley Lab. Proc. of the Workshop on Detectors for Relativistic Nucl. Collisions Aug. 1984 p 133-134 refs (For primary document see N85-35700 24-72)
Avail: NTIS HC A08/MF A01

One of the experimental difficulties in handling the events from relativistic nucleus-nucleus collisions is the extremely high multiplicity of these events. In a collision of an 160 ion with an energy of 200 GeV/A on 197Au for a minimum bias trigger the total multiplicity is expected to be 250 and can be up to 500 for a central collision. In addition to the primary produced particles secondary intractions take place and also a large number of knock-on electrons, so called delta-rays, will be created. Therefore, not only a precise position measurement, and time resolution is needed, but also a good two track separation and pattern recognition capability is desirable. An optical track detector like a conventional streamer chamber at atmospheric pressure and with film recording may meet the mentioned requirements, but there are still doubts that the detection efficiency for neutral strange particle decays will be high enough. These decays are expected to be an indication for the existence of the quark gluon plasma. A streamer chamber operation is described which improves the resolution and detection efficiency for neutral strange particles significantly. G.L.C.

N85-35711# California Univ., Berkeley. Lawrence Berkeley Lab.
A LEAD GLASS TUBING DRIFT CALORIMETER c35
T. A. Mulera, V. Perez-Mendez, H. Hirayama (Stanford Linear Accelerator), W. R. Nelson (Stanford Linear Accelerator), R. Bellazzini (Dipartimento di Fisica, Pisa, Italy), A. DelGuerra (Dipartimento di Fisica, Pisa, Italy), and M. M. Massai (Dipartimento di Fisica, Pisa, Italy) *In its* Proc. of the Workshop on Detectors for Relativistic Nucl. Collisions Aug. 1984 p 135-138 refs (For primary document see N85-35700 24-72)
(Contracts DE-AC03-76SF-00098; DE-AC03-76SF-00515)
Avail: NTIS HC A08/MF A01

A design for a drift collection calorimeter having a combined radiator and electric field shaping structure of lead glass tubing is described. Reduction of a surface layer of lead oxide in a hydrogen oven is used to form a high-resistance metallic layer on the interior of the tubes which is used as a continuous voltage divider for drift field shaping. The EGS shower Monte Carlo code was used to model the performance of the proposed calorimeter, and the effects of tube geometry, gas pressure and sampling schemes (proportional vs digital) are discussed. Author

N85-35712# California Univ., Davis. Dept. of Physics.
FRACTIONAL CHARGE RESOLUTION IN MUSIC c14
J. L. Romero, F. P. Brady, B. Christie, C. Tull, E. Barasch, C. M. Castaneda, J. Drummond, M. L. Webb, J. C. Young, H. J. Crawford (California Univ., Berkeley. Lawrence Berkeley Lab.) et al *In* California Univ., Berkeley. Lawrence Berkeley Lab. Proc. of the Workshop on Detectors for Relativistic Nucl. Collisions Aug. 1984 p 135-143 refs (For primary document see N85-35700 24-72)
Avail: NTIS HC A08/MF A01

MUSIC (MUltiple Sampling Ionization Chamber) is a large ionization chamber which can multiple-sample the energy loss of nuclear fragments. MUSIC uses time projection chamber (TPS) principles and electronics so that large multiplicites from a single event can be handled. This is done by measuring as a function of time the electrons from the ionization tracks as they reach the sampling electrodes after drifting down in the uniform electric field. The charge segments arriving at each anode wire are sampled every approx. 100 ns via charged-coupled devices so that a time projection of the charge cloud is obtained thus allowing the vertical distance of the track centroid to be located accurately, and to allow its separation from the tracks formed by other fragments from the same event. Using TPC electronics developed at LBL the signals are digitized and sent to a computer. The multiple sampling (along the track) of each ion track provides an energy loss distribution and one determines the mean energy loss from this distribution. G.L.C.

N85-35713*# Nebraska Univ., Lincoln. Lab. of Physics.
DISSOCIATIVE AND DOUBLE PHOTOIONIZATION CROSS SECTIONS OF NO FROM THRESHOLD TO 120 A
James A. R. Samson, T. Masuoka, and P. N. Pareek [1985] 19 p refs
(Grant NGR-28-002-01)
(NASA-CR-176185; NAS 1.26:176185) Avail: NTIS HC A02/MF A01 CSCL 20H

The partial photoionization cross sections for producing the NO(+) parent ion and the O(+), N(+), and NO2(+) fragment ions from neutral NO are presented from 120 to 614 A. The results indicate predissociation of the c(sup3) pi (21.72 eV) and B prime (sup 1) sigma (+) (22.73 eV) electronic states of NO(+). The photoionization threshold for double ionization was found to be 39.4 + or 0.12 eV. Author

N85-35714# Argonne National Lab., Ill.
HIGH-RESOLUTION SPECTROSCOPY AND DYNAMICS OF MULTIPHOTON PROCESSES IN ATOMS AND MOLECULES Annual Summary Report, 1 Oct. 1984 - 30 Sep. 1985
P. M. Dehmer and J. L. Dehmer 13 Jun. 1985 19 p
(Contract N00014-85-F-0015; NR Proj. R01-103)
(AD-A155862) Avail: NTIS HC A02/MF A01 CSCL 20/5

This report summarizes research on resonantly enhanced multiphoton absorption dissociation, and ionization processes in

atoms and molecules. Multiphoton processes are studied using from one to three independently tunable visible and/or UV laser beams in order to establish both the underlying physics and the high degree of selectivity of multiphoton processes. Measurements are made to probe both the formation of excited molecular states and the subsequent behavior of excited states either in the presence or in the abscence of further intense laser radiation. Detection methods include laser-induced fluorescence, ion mass analysis, and electron energy analysis. During the current reporting period, we have studied resonant multiphoton ionization processes for the molecules N2, CO, O2, NO, NeXe, ArXe, KrXe, and Xe2 and for the atoms C, I, and S using both mass spectrometry and photoelectron spectroscopy to analyze the products of the ionizations. In addition, we are developing three new instruments that will provide significantly enhanced resolution, collection efficiency, and versatility in both the ion mass and the electron kinetic energy detection channels. Author (GRA)

N85-35715# Office of Naval Research, London (England).
THE 2ND EUROPEAN CONFERENCE ON ATOMIC AND MOLECULAR PHYSICS
P. Roman 22 May 1985 15 p Conf. held at Amsterdam, 15-19 Apr. 1985
(AD-A155863; ONRL-C-4-85) Avail: NTIS HC A02/MF A01 CSCL 07/4

The Second European Conference on Atomic and Molecular Physics was held in Amsterdam, The Netherlands, from 15 through 19 April 1985. This report focuses on presentations dealing with Rydberg systems, clusters, and coherent vacuum ultraviolet and X-ray ultraviolet generation. It also lists the topics of all other fields covered by the meeting. GRA

N85-35716# Brush Wellman, Inc., Cleveland, Ohio.
BERYLLIUM PRODUCTION Monthly Technical Progress Report, 1 Apr. - 5 May 1985
1985 9 p
(Contract DE-AC04-82AL-18071)
(DE85-013360; DOE/AL-18071/T5) Avail: NTIS HC A02/MF A01

Progress on the Research and Development Study for the optimization of beryllium production operations for government purposes is reported. Task 4 is an operation of the subscale demonstration models of recommended alternative beryllium production processes. DOE

N85-35717# Kanner (Leo) Associates, Redwood City, Calif.
X-RAY FLUORESCENCE ANALYSIS OF URANIUM CONCENTRATES
J. P. Diaz-Guerra, A. Bayor, and M. Roca May 1985 28 p refs Transl. into ENGLISH of "Analisis de Concentrados de Uranio Mediante Fluorescencia de Rayos X" rept. JEN-400 Junta de Energia Nuclear, Madrid, 1978 Prepared for LASL
(Contract W-7405-eng-36)
(DE85-013189; IA-tr-85-27; ISSN-0081-3397) Avail: NTIS HC A03/MF A01

Uranium concentrates were analyzed by X-ray fluorescence for the following impurities: arsenic, calcium, iron, molybdenum, phosphorus, silicon, sulfur, thorium, and vanadium. All of the impurities except arsenic can be determined simultaneously. DOE

N85-35718# Brookhaven National Lab., Upton, N. Y.
COOLING HIGH INTENSITY ATOMIC HYDROGEN BEAMS TO LIQUID HELIUM TEMPERATURES
A. Hershcovitch, A. Kponou, B. DeVito, R. Meier, V. Kovarik, and T. Sluyters 1985 3 p refs Presented at the Particle Accelerator Conf., Vancouver, British Columbia, 13 May 1985
(Contract DE-AC02-76CH-00016)
(DE85-012515; BNL-36483; CONF-850504-122) Avail: NTIS HC A02/MF A01

An atomic hydrogen source, designed to operate in the viscous flow range, was built. A unique feature of this source is a miniature gap between a Teflon tube which guides the beam and an accommodator which cools it. Across this gap a step-function in temperature, with the teflon temperature exceeding 100 K and the accommodator temperature below 8 K, was successfully maintained. This configuration collimates the beam enough to prevent significant diffusive losses without subjecting it to the temperature range of high recombination. Initial results with an orifice of only one-tenth the dissociator aperture are indicative of particle density in the beam of well above 10 to the 10th power cm/-3. DOE

N85-35719# Fermi National Accelerator Lab., Batavia, Ill.
WIDTH OF NONLINEAR DIFFERENCE RESONANCES
S. Chnuma and R. L. Gluckstern May 1985 5 p refs Presented at the Particle Accelerator Conf., Vancouver, British Columbia, 13 May 1985 Prepared in cooperation with Maryland Univ., College Park
(Contract DE-AC02-76CH-03000)
(DE85-013026; FNAL-TM-1311; CONF-850504-97) Avail: NTIS HC A02/MF A01

A definition is proposed in which the concept of acceptable growth in emittance plays the essential role. A numerical table is given for some combinations of p and q which are likely to be of practical interest. DOE

N85-35720# Sandia Labs., Albuquerque, N. Mex.
QUALITY ASSURANCE CONSIDERATIONS FOR THE IMPLEMENTATION OF A PULSED POWER R AND D PROJECT
J. P. Furaus, G. W. Barr, and C. G. Shirley 1985 15 p Presented at the 5th IEEE Pulsed Power Conf., Washington, D.C., 10 Jun. 1985
(Contract DE-AC04-76DP-00789)
(DE85-012357; SAND-84-2538C; CONF-850616-3) Avail: NTIS HC A02/MF A01

The second generation Particle Beam Fusion Accelerator (PBFA II) at Sandia National Laboratories (SNLA) is a $48.15M construction project that includes conventional facilities such as buildings as well as state-of-the-art pulsed power designs and special support systems. The project also includes considerations for longer term program goals, such as breakeven fusion reactions. This project started in May 1980 and is scheduled for completion in January 1986. Implementation of Quality Assurance (QA) policies, techniques and programs, although not a straightforward problem for this complex project, has been effective as demonstrated by progress thus far. The discussion will describe key features of the QA program, their implementation and the results. DOE

N85-35721# Los Alamos National Lab., N. Mex.
USE OF A MINIMUM-ELLIPSE CRITERION IN THE STUDY OF ION-BEAM EXTRACTION SYSTEMS
R. Keller, J. D. Sherman, and P. Allison 1985 4 p refs Presented at the Particle Accelerator Conf., Vancouver, British Columbia, 13 May 1985
(Contract W-7405-eng-36)
(DE85-012670; LA-UR-85-1607; CONF-850504-95) Avail: NTIS HC A02/MF A01

Ion beam extraction systems may be optimized by ray tracing codes. As a general criterion for comparing the geometry dependent phase space distributions, we first calculate the minimum area ellipse that encloses all particles of any given two dimensional phase space distribution. Then, the relation between ellipse area and contained beam fraction is established by systematically finding and eliminating those particles that contribute most heavily to the emittance. Prescriptions for finding the minimum ellipse and beam fractions are presented. The minimum and rms ellipses are compared for two code calculated distributions that represent ion beam extraction geometries. DOE

N85-35722# Stanford Linear Accelerator Center, Calif.
REPORT ON THE SLC CONTROL SYSTEM
N. Phinney May 1985 3 p refs Presented at the Particle Accelerator Conf., Vancouver, British Columbia 13 May 1985
(Contract DE-AC03-76SF-00515)
(DE85-013076; SU-SLAC-PUB-3668; CONF-850504-137) Avail: NTIS HC A02/MF A01

The SLC control system is based on a VAX 11/780 Host computer with approximately 50 microprocessor clusters which provide distributed intelligence and control of all CAMAC interface modules. An overview is presented of the system including current status and a description of the software architecture and communication protocols. DOE

N85-35723# Stanford Linear Accelerator Center, Calif.
FORTY-FIVE YEARS OF e(+)e(-) ANNIHILATION PHYSICS: 1956 TO 2001
B. Richter Apr. 1985 19 p Presented at the 12th SLAC Summer Inst. on Particle Phys., Stanford, Calif., 23 Jul. 1984
(Contract DE-AC03-76SF-00515)
(DE85-013052; SU-SLAC-PUB-3659; CONF-8407112-9) Avail: NTIS HC A02/MF A01

The history of electron positron physics in the 1950's and 1960's is reviewed followed by some highlights of the spectacular discoveries in electron positron annihilation made during the 1970's. The consolidation of knowledge during the last few years is summarized. Some predictions are made for the field of electron positron physics for the next decade and beyond. DOE

N85-35724# Stanford Linear Accelerator Center, Calif.
STATUS OF THE ZETA(8.3)
S. T. Lowe May 1985 5 p Presented at the 20th Recontre de Moriond, Les Arcs, France, 10 Mar. 1985
(Contract DE-AC03-76SF-00515)
(DE85-013070; SU-SLAC-PUB-3683; CONF-850375-2) Avail: NTIS HC A02/MF A01

Results are presented from 22.1 pb(-1) of UPSILON 1S data, taken with the Crystal Ball detector at Doppel-Ring-Speicher (DORIS). These data were taken to further explore the zeta (8.3) signal originally seen in 10.4 pb(-1) of UPSILON 1S data. No evidence for the zeta is observed in this new sample. Data quality checks and possible explanations are discussed. DOE

N85-35725# Oak Ridge National Lab., Tenn.
CALCULATION OF HEAVY-ION TRACKS IN LIQUID WATER
R. N. Hamm, J. E. Turner, R. H. Ritchie, and H. A. Wright 1985 17 p refs
(Contract DE-AC05-84OR-21400)
(DE85-012101; CONF-8505113-1) Avail: NTIS HC A02/MF A01

Monte Carlo calculations are presented of proton and alpha-particle tracks in liquid water. The computations treat the interactions of the primary particle and all secondary electrons on a statistical, event-by-event basis to simulate the initial physical changes that accompany the passage of an ion through water. Inelastic scattering probabilities (inverse mean free paths) are derived from a complex dielectric response function constructed for liquid water, based on experimental and theoretical data. The computation of electron transport and energy loss includes exchange, elastic scattering, and a scheme for the delocalization of energy shared collectivity by a large number of electrons in the condense medium. Several examples of calculated proton and alpha-particle tracks are presented and discussed. The meaning and significance of the concept of a track core is briefly addressed in the light of this work. The present paper treats only the initial, physical changes produced by radiation in water (in approx. 10(-15)sec in local regions of a track). DOE

N85-35726# Oak Ridge National Lab., Tenn.
EXIT CHANNELS OF AUTOIONIZATION RESONANCES IN ATOMS
M. C. Krause 1985 9 p Presented at the Workshop on Autoionization of Atoms and Small Molecules, Argonne, Ill., 2 May 1985
(Contract DE-AC05-84OR-21400)
(DE85-012299; CONF-050560-4) Avail: NTIS HC A02/MF A01

In many-electron atoms with open shells strong autoionization resonances occur when an electron from an inner, weakly bound subshell is excited. Usually, the resonance state lies above several ionization thresholds and, hence, will decay into more than one exit or continuum channel. Several cases are discussed in which the resonance state is induced by synchrotron radiation, and the exit channels are differentiated and characterized by the analysis of the ejected electrons. DOE

73 NUCLEAR AND HIGH-ENERGY PHYSICS

Includes elementary and nuclear particles; and reactor theory.

For space radiation see *93 Space Radiation.*

N85-35727 United Kingdom Atomic Energy Authority, Dounreay (Scotland).
ANALYTICAL METHODS IN THE PUREX PROCESS
Dieter Ertel and Gerard Horn 1985 13 p refs Transl. into ENGLISH from Atomkernenergie Kerntech. (West Germany), v. 46, no. 2, 1985
(BLL-Dounreay-Tr-952(9091.9F)) Avail: British Library Lending Div., Boston Spa, Engl.

The extensive analytical task of the modern Purex process is discussed and some recommendations are given to solve problems arising from the special boundary conditions of nuclear research. The most important analytical methods and instruments for process control are tabulated and discussed. The development of the Karlsruhe laboratory is discussed. R.J.F.

N85-35728*# Boeing Aerospace Co., Seattle, Wash. Electrical Power Systems Technology.
APPLICABILITY OF 100kWe-CLASS OF SPACE REACTOR POWER SYSTEMS TO NASA MANNED SPACE STATION MISSIONS Final Report
Sidney W. Silverman, Harvey J. Willenberg, and Charles Robertson (General Electric Co., King of Prussia, Pa.) Aug. 1985 184 p refs
(Contract NAS3-23865)
(NASA-CR-174696; NAS 1.26:174696; D180-28461-1) Avail: NTIS HC A09/MF A01 CSCL 18I

An assessment is made of a manned space station operating with sufficiently high power demands to require a multihundred kilowatt range electrical power system. The nuclear reactor is a competitor for supplying this power level. Load levels were selected at 150kWe and 300kWe. Interactions among the reactor electrical power system, the manned space station, the space transportation system, and the mission were evaluated. The reactor shield and the conversion equipment were assumed to be in different positions with respect to the station; on board, tethered, and on a free flyer platform. Mission analyses showed that the free flyer concept resulted in unacceptable costs and technical problems. The tethered reactor providing power to an electrolyzer for regenerative fuel cells on the space station, results in a minimum weight shield and can be designed to release the reactor power section so that it moves to a high altitude orbit where the decay period is at least 300 years. Placing the reactor on the station, on a structural boom is an attractive design, but heavier than the long tethered reactor design because of the shield weight for manned activity near the reactor. Author

N85-35729# Air Force Inst. of Tech., Wright-Patterson AFB, Ohio. School of Engineering.
EVALUATION OF NUCLEAR DETONATION LOCATION CAPABILITY UNDER HIGH ATTACK SCENARIO M.S. Thesis
F. A. Zawada Mar. 1985 129 p
(AD-A155761; AFIT/OS/GST/85M-16) Avail: NTIS HC A07/MF A01 CSCL 18/3

Analysis was conducted to see how the location accuracy of a nuclear detonation (NUDET) and probability of damage (Pd) calculations were affected by high rates of attack NUDET locations were generated by random variates from horizontal cumulative distributions, a function of the number of satellites/sensors observing the NUDET. Location was calculated for target silos with cratering and impulse as the damage mechanisms. The

estimated Pd was compared to the actual Pd. System performance in correctly predicting a target as destroyed was poor. A target's Pd exceeding 50% was the criteria for a target being destroyed. Decreasing the location error by factor of 12 greatly improved the system's ability (53%) to determine a target as destroyed. However, 18% of the targets were incorrectly considered destroyed. This problem was eliminated using 90% threshold criteria, yet system performance was highly degraded. These implications have to be weighed and understood when such systems are used in the decision making process. GRA

N85-35730# Army Military Personnel Center, Alexandria, Va.
(NAT)Fe(n,n'X) SPECTRA AT 65.5 MeV Final Report
M. A. Hamilton 5 Jun. 1985 87 p
(AD-A155776) Avail: NTIS HC A05/MF A01 CSCL 20/8

The first spectra from the U.C. Davis (n,n'x) detection facility are presented for 65.5 MeV incident neutrons on a Natural iron target. The experimental system is explained along with analysis methodology. Elastic and continuum spectra are presented from 14 to 24 degrees with cross section tabulation. Cross section comparisons are made between 20 degree (n,n'x) and 20 degree (p,p'x) data at 61 MeV and the ratio of neutron to proton matrix elements has been obtained. The first evidence of a (n,n'x) giant resonance has been detected. Author (GRA)

N85-35731# Argonne National Lab., Ill.
FAST-NEUTRON INTERACTION WITH NIOBIUM
A. B. Smith, P. T. Guenther, W. P. Poenitz, D. L. Smith, J. F. Whalen, and R. J. Howerton (California Univ., Livermore. Lawrence Livermore Lab.) 1985 5 p refs Presented at the Intern. Conf. on Nucl. Data for Basic and Appl. Sci., Santa Fe, N. Mex., 13 May 1985
(Contract W-31-109-eng-38)
(DE85-011471; CONF-850507-15) Avail: NTIS HC A02/MF A01

Results of a comprehensive study of the interaction of fast neutrons with niobium are presented, including measurement and interpretation of neutron total, differential scattering and radiative capture cross sections. The experimental results are interpreted in the context of the optical statistical model, with attention to the Fermi surface anomaly. Experimental results, physical interpretations and rigorous statistical methods are used to provide a comprehensive evaluated nuclear data file suitable for use in a wide range of applied neutronic calculations. DOE

N85-35732# California Univ., Berkeley. Lawrence Berkeley Lab. Nuclear Science Div.
GAMMA-RAY PRODUCTION CROSS SECTIONS FOR ALPHA-PARTICLE INDUCED REACTIONS ON F-19 AND Na-23
E. B. Norman, K. T. Lesko (Washington Univ., Seattle), T. E. Chupp (Washington Univ., Seattle), P. Schwalbach (Washington Univ., Seattle), and M. A. DeFaccio (Washington Univ., Seattle) May 1985 6 p refs Presented at the Intern. Conf. on Nucl. Data for Basic and Appl. Sci., Santa Fe, N. Mex., 13 May 1985
(Contract DE-AC03-76SF-00098)
(DE85-012603; LBL-18944; CONF-850507-16) Avail: NTIS HC A02/MF A01

The understanding of spectra obtained from gamma ray astronomical observatories requires knowledge of gamma ray production cross sections for a large number of proton and alpha particle induced reactions. Production cross sections have been measured for GAMMA ray lines excited in ALPHA particle bombardments of a NaF target for beam energies from 4.5 to 26 MeV. DOE

N85-35733# Los Alamos Scientific Lab., N. Mex.
MEASUREMENT OF URANIUM ENRICHMENT FOR GASEOUS URANIUM AT LOW PRESSURE
D. A. Close, J. C. Pratt, H. F. Atwater, J. J. Malanify, K. V. Nixon, and L. G. Speir 1985 7 p refs Presented at 7th Symp. on Safeguards and Nucl. Mater. Management, Liege, 21 May 1985
(Contract W-7405-eng-36)
(DE85-012697; LA-UR-85-1436; CONF-850556-5) Avail: NTIS HC A02/MF A01

X-ray fluorescence determines the amount of total uranium present in gaseous UF6 inside cascade header pipes of a uranium centrifuge enrichment facility. A highly collimated source, highly collimated detctor, and a very rigid, reproducible geometry are required. Two measurements of the 185.7 keV gamma ray from U-235 using two collimators determine the amount of U-235 present only in the gas phase. The ratio of the gas only U235 signal to the total uranium gas only signal is directly proportional to the enrichment of the process UF6 gas. This measurement technique is independent of the deposit that forms on a surface in contact with UF6. This measurement technique is independent of the pressure of the gaseous UF6. This technique has the required sensitivity to determine whether the process gas is of uranium enrichment less than or equal to 20% or $> 20\%$. DOE

N85-35734# Oak Ridge National Lab., Tenn.
NEUTRONIC CALCULATIONS FOR A NEW HIGH FLUX REACTOR
F. C. Difilippo, B. A. Worley, and D. R. Vondy 1985 8 p Presented at the Intern. Conf. on Nucl. Data for Basic and Appl. Sci., Santa Fe, N. Mex., 13 May 1985
(Contract DE-AC05-84OR-21400)
(DE85-011551; CONF-850507-14) Avail: NTIS HC A02/MF A01

The Oak Ridge National Laboratory has begun the design of a new high flux reactor to be used for basic research, isotope production, and material irradiation. One of the principal goals of the design is the production of a thermal flux peak in the reflector larger than 5 x 10 to the 15th/sq. cm. sec. A theoretical analysis of this slowing-down and diffusion of neutrons produced by a spherical fission source immersed in a moderator shows that the flux per unit power is maximized by combining a very under-moderated core with a very low absorbing reflector. The theoretical model interrelates total power, power density and transport properties with the thermal flux allowing very inexpensive scoping calculations. Full scale and detailed calculations were made with a numerical model which uses the Bold Venture code system. Calculations show that a highly enriched (235)U reactor with D2O as moderator and reflector would produce the desired peak flux, and the reactor would have a reasonable core life. DOE

N85-35735# Martin Marietta Energy Systems, Inc., Oak Ridge, Tenn.
STRATEGIC DEFENSE INITIATIVE
J. P. Nichols 1985 17 p
(Contract DE-AC05-84OR-21400)
(DE85-012778; DOE/OR-21400/T124) Avail: NTIS HC A02/MF A01

The initial work in support of the strategic defense initiative (SDI) program is focused on three technologies: (1) space nuclear power; (2) flywheel energy storage; and (3) neutral particle beams. The space nuclear program will utilize the capabilities in areas of refractory materials, high-temperature alkali metal systems, shielding, and instrumentation. Space nuclear reactors capable of supplying multimegawatt levels of electrical power on a continuous and long-term basis will be required for a variety of SDI surveillance satellites and spaceborne weapons platforms. The feasibility of an alkali metal Rankine power conversion cycle which provides high power with a very low system mass is studied. DOE

N85-35736# Department of Energy, Washington, D. C.
LIMITER Patent Application
S. A. Cohen (Princeton Univ., N.J.), J. C. Hosea (Princeton Univ., N.J.), and J. R. Timberlake, inventors (to DOE) (Princeton Univ., N. J.) Filed 19 Oct. 1984 13 p
(Contract DE-AC02-76CH-03073)
(DE85-011620; US-Patent-Appl-SN-662645) Avail: NTIS HC A02/MF A01

A limiter with a specially contoured front face is provided. The front face of the limiter (the plasma side face) is flat with a central indentation. In addition, the limiter shape is cylindrically symmetric so that the limiter can be rotated for greater heat distribution. This limiter shape accommodates the various power

scrape off distances lambda p, which depend on the parallel velocity, V sub parallel, of the impacting particles. DOE

N85-35737# Brookhaven National Lab., Upton, N. Y.
ROBINSON INSTABILITY AND BEAM LOADING
B. C. Craft, III 1985 4 p ref Presented at the Particle Acclerator Conf., Vancouver, British Columbia, 13 May 1985
(Contract DE-AC02-76CH-00016)
(DE85-013301; BNL-36462; CONF-850504-149) Avail: NTIS HC A02/MF A01

The Robinson instability problem is developed in three stages. The first step is to derive the synchrotron oscillation equations in the absence of beam loading (unloaded case). Next, the equations are evaluated in the presence of beam loading at the fundamental RF frequency (statically loaded case). Finally, the system is redeveloped taking into account beam loading at the synchrotron sidebands (dynamically loaded case). Following the theoretical development, the results are applied to calculate the synchrotron frequency in the presence of beam loading, automatic gain control, and automatic tune control. The results of this calculation are compared with data from the NSLS vuv-ring, a 750 MeV electron storage ring. DOE

N85-35738# Pacific Northwest Lab., Richland, Wash.
CALIBRATION OF A HIGH-LEVEL PHOTON IRRADIATION
C. D. Hooker, P. L. Roberson, G. L. Carter, R. A. Fox, and R. T. Hogan Apr. 1985 9 p Presented at the Health Phys. Soc. Ann. Meeting, Chicago, 26 May 1985
(Contract DE-AC06-76RL-01830)
(DE85-013044; PNL-SA-12909; CONF-8505103-2) Avail: NTIS HC A02/MF A01

A high level photon facility capable of providing exposure rates of up to 85 kR/hr from co -60 and up to 500 R/hr from Cs-137 100 Ci: (3)Co,-60 600 Ci, and (4) Co,-60 5000 Ci is also described. DOE

N85-35739# Argonne National Lab., Ill.
ANALYSIS OF REACTOR MATERIAL EXPERIMENTS INVESTIGATING OXIDE FUEL CRUST STABILITY AND HEAT TRANSFER IN JET IMPINGEMENT FLOW
J. J. Sienicki and B. W. Spencer 1985 9 p Presented at the ANS/ENS Fast Reactor Safety Meeting, Knoxville, Tenn., 21 Apr. 1985
(Contract W-31-109-eng-38)
(DE85-012097; CONF-850410-50) Avail: NTIS HC A02/MF A01

An analysis is presented of the crust stability and heat transfer behavior in the CSTI-1, CSTI-3, and CWTI-11 reactor material experiments in which a jet of molten oxide fuel at approx. 160 K above its freezing temperature was impinged normally upon stainless steel plates initially at 300 and 385 K. The major issue is the existence of nonexistence of a stable solidified layer of fuel, or crust, interstitial to the flowing hot fuel and the steel substrate, tending to insulate the steel from the hot molten fuel. A computer model was developed to predict the heatup of thermocouples imbedded immediately beneath the surface of the plate for both of the cases in which a stable crust is assumed to be either present or absent during the impingement phase. Comparison of the model calculations with the measured thermocouple temperatures indicates that a protective crust was present over nearly all of the plate surface area throughout the impingement process precluding major belting of the plate steel. However, the experiments also show evidence for very localized and isolated steel melting as revealed by localized and isolated pitting of the steel surface and the response of thermocouples located within the pitted region. DOE

N85-35740# California Univ., Livermore. Lawrence Livermore Lab.
PULSED-NEUTRON-SOURCE MODELS FOR THE ASTROPHYSICAL s-PROCESS
W. M. Howard, G. J. Mathews, K. Takahashi, and R. A. Ward May 1985 7 p Presented at 20th Recontre de Moriond, Les Arcs, France, 10 Mar. 1985
(Contract W-7405-eng-48)
(DE85-012927; UCRL-92725; CONF-850375-6) Avail: NTIS HC A02/MF A01

The astrophysical s-process is a sequence of neutron-capture and beta-decay reactions on a slow time scale compared to beta-decay lifetimes near the line of stability. This detailed sequence of neutron capture, continuum and bound-state beta decay, positron decay, and electron-capture reactions that comprise the s-process for a broad range of astrophysical environments was systematically studied. Results were then compared with the solar-system abundances of heavy elements to determine the range of physical conditions responsible for their nucleosynthesis. DOE

N85-35741# Rochester Univ., N. Y.
NEUTRINO PRODUCTION OF LIKE SIGN DIMUONS
K. Lang, A. Bodek, F. Borcherding, N. Giokaris, I. R. Stockdale, P. Auchincloss, R. Blair, C. Haber, S. Mishra, and M. Ruiz 1985 8 p refs Presented at the 20th Recontre de Moriond, Les Arcs, France, 10 Mar. 1985 Prepared in cooperation with Columbus Univ., N.Y., California Inst. of Tech., Pasadena, Chicago Univ. and Fermi National Accelerator Lab.
(Contract DE-AC02-76ER-13065)
(DE85-013594; DOE/ER-13065/415; CONF-850375-8) Avail: NTIS HC A02/MF A01

Neutrino interactions with two muons in the final state were studied using the Fermilab narrow band beam. A sample of 18 like sign dimuon events with momentum P sub (MU) $>$ 9 GeV/c yields a prompt signal of 8.1 + or - 4.4 events and a rate of (1.4 + or - 0.8) x 10 to the -4 per single muon event. The kinematics of these events are compared with those of the non-prompt sources. DOE

N85-35742# Du Pont de Nemours (E. I.) and Co., Aiken, S.C.
RADIATION SAFETY PROBLEMS IN HANDLING HIGHLY ACTIVE TRITIUM TARGETS
D. Beyer, W. Friedrich, J. Knieper, and P. F. Sauermann [1985] 7 p refs Transl. into ENGLISH from rept. KFK-1638 Nuclear Research Installtion Juelich GMBH, Juelich, West Germany p 245-250 Prepared in cooperation with Kernforschungsanlage, Juelich, West Germany
(Contract DE-AC09-76SF-00001)
(DE85-014268; DP-tr-80; KFK-1638) Avail: NTIS HC A02/MF A01

Measurement of surface area contamination and air contamination as well as incorporation measurements was conducted during the exchanging of a highly active tritium target. The results show that the contamination danger and incorporation danger during the target exchange as well as in the handling of non-irradiated targets should not be underestimated. Observation of the necessary safety measures will, however, prevent endangering the operating personnel. DOE

N85-35743# California Univ., Livermore. Lawrence Livermore Lab.
GROUND MOTION MEASUREMENTS FOR THE QUESO NUCLEAR EVENT
H. D. Glenn, T. P. Stubbs, and J. A. Kalinowski Jun. 1985 8 p refs Presented at the Am. Phys. Soc. Topical Conf. on Shock Waves in Condensed Matter, Spokane, 22 Jul. 1985 Prepared in cooperation with Edgerton, Grier and Germeshausen, San Ramon, Calif.
(Contract W-7405-eng-48)
(DE85-014806; UCRL-92155; CONF-850736-26) Avail: NTIS HC A02/MF A01

QUESO was a low yield nuclear event detonated at a depth of 216.4 m in hole U 10bf at the Nevada Test Site on August 11, 1982. Shock wave histories containing the peak residual stress values were obtained for the first time in free field measurements. Radial and tangential stress measurements indicated a strong residual stress field was induced above the cavity by 200 ms after the nuclear detonation, following rebound of that region after passage of the ground shock. Free field particle velocity profiles

corresponded closely with measurements made at comparable ranges in the emplacement hole. DOE

N85-35744# Tufts Univ., Medford, Mass.
HIGH ENERGY PHYSICS AT TUFTS UNIVERSITY Progress Report, 1 Aug. 1984 - 1 Jul. 1985
1985 110 p refs
(Contract DE-AC02-83ER-40085)
(DOE/ER-40085/7) Avail: NTIS HC A06/MF A01

Work is reported in these experimental projects: Soudan-II nucleon decay project; neutrino interactions; photoproduction studies; multiparticle spectrometer studies, such as K sub s (0) K sub s (0) from (PI)(-)p interactions and phi phi final states in pp reactions; and streamer chamber study of anti K*(0) (890). Theoretical work included general kinematic description of polarization processes and applications of CQD perturbation theory. DOE

N85-35745# Johns Hopkins Univ., Baltimore, Md.
STUDIES OF RELATIVISTIC HEAVY ION COLLISIONS Annual Progress Report, 1 Jan. - 31 Jul. 1985
I. Madansky 1985 79 p
(Contract DE-AC02-76ER-03274)
(DE85-014686; DOE/ER-03275/6) Avail: NTIS HC A05/MF A01

Progress is reported on a program to study direct single electron production in relativistic p-A and A-A collisions. Another experiment reported using direct leptons as probes of the precursor quark-gluon level processes has begun with the design and construction of a di-lepton spectrometer. Subthreshold K(-) and antiproton production were studied. A proposal was made to search for quark matter and other new phenomena utilizing heavy ion collisions at the AGS. DOE

N85-35746# California Univ., Berkeley. Lawrence Berkeley Lab.
NEUTRON PRODUCTION BY Ne AND Si IONS ON A THICK Cu TARGET AT 670 MeV/A WITH APPLICATION TO RADIATION PROTECTION
J. B. McCaslin, P. R. LaPlant, A. R. Smith, W. P. Swanson, and R. H. Thomas Apr. 1985 5 p refs Presented at the Particle Accelerator Conf., Vancouver, British Columbia, 13 May 1985
(Contract DE-AC03-76SF-00098)
(DE85-014526; LBL-19648; CONF-850504-208) Avail: NTIS HC A02/MF A01

Beams of neon and silicon at 670 MeV/A from the Bevalac were stopped in a copper target. Neutron yields and angular distributions were measured with activation detectors. Attenuation of neutrons through a concrete shield was measured at 7, 54 and 72 deg. to the beam direction. Dose equivalent estimates were made in adjoining areas by using moderated BF3 proportional counters and carbon and aluminum activation detectors. Data are presented and radiation protection aspects discussed. DOE

N85-35747# Idaho National Engineering Lab., Idaho Falls.
THERMAL HYDRAULIC FEATURES OF THE TMI ACCIDENT
B. Tolman 1985 28 p Presented at the Am. Chem. Soc. Meeting, Miami, Fla., 1 May 1985
(Contract DE-AC07-76ID-01570)
(DE85-014569; EGG-M-12085; CONF-8505179-1) Avail: NTIS HC A03/MF A01

The Three Mile island (TMI)-2 accident resulted in extensive core damage and recent data confirms that the reactor vessel was challenged from molten core materials. A hypothesized TMI accident scenario is presented that consistently explains the TMI data and is also consistent with research findings from independent severe fuel damage experiments. The TMI data will prove useful in confirming our understanding of severe core damage accidents under realistic reactor systems conditions. This understanding will aid in addressing safety and regulatory issues related to severe core damage accidents in light water reactors. DOE

N85-35748# Oak Ridge National Lab., Tenn.
APPLICATIONS AND MISAPPLICATIONS OF THE CHANNEL-CAPTURE FORMALISM OF DIRECT NEUTRON CAPTURE
S. Raman and J. E. Lynn 1985 23 p refs Presented at the 4th Intern. Symp. on Neutron Induced Reactions, Smolenice, Czechoslovakia, 17 Jun. 1985 Prepared in cooperation with United Kingdom Nuclear Energy Authority, Harwell
(Contract DE-AC05-84OR-21400)
(DE85-013992; CONF-850635-1) Avail: NTIS HC A02/MF A01

The channel-capture approximation of slow neutron direct-capture theory is discussed. This approximation gives a generally good representation of the neutron capture cross sections for several electric dipole transitions in a broad range of nuclides from A = 9 to A = 136; these are mostly near-spherical nuclei. Comparison with calculations of the potential-capture cross section can be up to approx. =40% in error. In cases where the expected channel-capture cross section is much smaller than the hard-sphere capture cross-section estimate, the disagreement with potential capture can be much worse than this. Also, in these cases, compound-nucleus capture can be of comparable or greater magnitude. These affects were shown to completely undermine recent attempts to determine nuclear interaction radii for targets, such as carbon 12 and beryllium 9 by application of the channel-capture formula to capture cross-section data. DOE

N85-35876*# Minnesota Univ., Minneapolis. School of Physics and Astronomy.
STOPPING RELATIVISTIC Xe, Ho, Au AND U NUCLEI IN NUCLEAR EMULSIONS
C. J. Waddington, D. J. Fixsen, and P. S. Freier *In* NASA. Goddard Space Flight Center 19th Intern. Cosmic Ray Conf., Vol. 6 Aug. 1985 p 104-107 refs (For primary document see N85-35848 24-93)
(Grants NGR-24-005-050; NAG8-500; NSF PHY-84-05852)
Avail: NTIS HC as boxed set only $200/MF A01 per volume or E99 per entire set CSCL 18K

N85-35877*# Warsaw Technical Univ. (Poland). Inst. of Physics.
PHYSICAL MEANING OF THE MULTIPLICITIES OF EMITTED NUCLEONS IN HADRON-NUCLEUS COLLISIONS
Z. Strugalski *In* NASA. Goddard Space Flight Center 19th Intern. Cosmic Ray Conf., Vol. 6 Aug. 1985 p 108-111 refs (For primary document see N85-35848 24-93)
Avail: NTIS HC as boxed set only $200/MF A01 per volume or E99 per entire set CSCL 18K

N85-35878*# Warsaw Technical Univ. (Poland). Inst. of Physics.
HOW ARE PARTICLE PRODUCTION, NUCLEON EMISSION AND TARGET FRAGMENT EVAPORATION PROCESSES INTERRELATED IN HADRON-NUCLEUS COLLISIONS?
Z. Strugalski *In* NASA. Goddard Space Flight Center 19th Intern. Cosmic Ray Conf., Vol. 6 Aug. 1985 p 112-114 refs (For primary document see N85-35848 24-93)
Avail: NTIS HC as boxed set only $200/MF A01 per volume or E99 per entire set CSCL 18K

N85-35879*# Warsaw Technical Univ. (Poland). Inst. of Physics.
EXPERIMENTAL STUDY OF THE SPACE-TIME DEVELOPMENT OF THE PARTICLE PRODUCTION PROCESS IN HADRON-NUCLEON COLLISIONS, USING MASSIVE TARGET NUCLEUS AS A DETECTOR
Z. Strugalski *In* NASA. Goddard Space Flight Center 19th Intern. Cosmic Ray Conf., Vol. 6 Aug. 1985 p 115-116 refs (For primary document see N85-35848 24-93)
Avail: NTIS HC as boxed set only $200/MF A01 per volume or E99 per entire set CSCL 18K

N85-35880*# Warsaw Technical Univ. (Poland). Inst. of Physics.
EXPERIMENTAL EVIDENCE OF THE DECREASE OF KINETIC ENERGY OF HADRONS IN PASSING THROUGH ATOMIC NUCLEI
Z. Strugalski *In* NASA. Goddard Space Flight Center 19th Intern. Cosmic Ray Conf., Vol. 6 Aug. 1985 p 118-121 refs (For

primary document see N85-35848 24-93)
Avail: NTIS HC as boxed set only $200/MF A01 per volume or E99 per entire set CSCL 18K

N85-35881*# Warsaw Technical Univ. (Poland). Inst. of Physics.
ENERGY-RANGE RELATIONS FOR HADRONS IN NUCLEAR MATTER
Z. Strugalski *In* NASA. Goddard Space Flight Center 19th Intern. Cosmic Ray Conf., Vol. 6 Aug. 1985 p 122-124 refs (For primary document see N85-35848 24-93)
Avail: NTIS HC as boxed set only $200/MF A01 per volume or E99 per entire set CSCL 18K

N85-35882*# Warsaw Technical Univ. (Poland). Inst. of Physics.
SCATTERING AND STOPPING OF HADRONS IN NUCLEAR MATTER
Z. Strugalski *In* NASA. Goddard Space Fligt Center 19th Intern. Cosmic Ray Conf., Vol. 6 Aug. 1985 p 125-128 refs (For primary document see N85-35848 24-93)
Avail: NTIS HC as boxed set only $200/MF A01 per volume or E99 per entire set CSCL 18K

N85-35883*# Warsaw Technical Univ. (Poland). Inst. of Physics.
MEASUREMENTS OF HADRON MEAN FREE PATH FOR THE PARTICLE-PRODUCING COLLISIONS IN NUCLEAR MATTER
Z. Strugalski *In* NASA. Goddard Space Flight Center 19th Intern. Cosmic Ray Conf., Vol. 6 Aug. 1985 p 129-132 refs (For primary document see N85-35848 24-93)
Avail: NTIS HC as boxed set only $200/MF A01 per volume or E99 per entire set CSCL 18K

N85-35886*# Rivers State Univ. of Science and Technology, Port Harcourt (Nigeria). Dept. of Physics.
HEAVY FLAVOURS PRODUCTION IN QUARK-GLUON PLASMA FORMED IN HIGH ENERGY NUCLEAR REACTIONS
J. Kloskinski *In* NASA. Goddard Space Flight Center 19th Intern. Cosmic Ray Conf., Vol. 6 Aug. 1985 p 141-144 refs (For primary document see N85-35848 24-93)
Avail: NTIS HC as boxed set only $200/MF A01 per volume or E99 per entire set CSCL 18K

N85-35895*# Institute of Nuclear Physics, Krakow (Poland).
FORWARD PARTICLE PRODUCTION IN INELASTIC Ne-22 INTERACTIONS IN EMULSION AT 4.1 A Ge/c Ulan-Bator Collaboration
In NASA. Goddard Space Flight Center 19th Intern. Cosmic Ray Conf., Vol. 6 Aug. 1985 p 176-179 refs (For primary document see N85-35848 24-93)
(HE-1.4-7) Avail: NTIS HC as boxed set only $200/MF A01 per volume or E99 per entire set CSCL 18K

N85-35898*# Korea Univ., Seoul. Dept. of Physics.
INCLUSIVE ANGULAR DISTRIBUTION OF ALPHA AND LI FRAGMENTS PRODUCED IN THE Fe-C AND Fe-Pb COLLISIONS AT 1.88 GeV/u
C. O. Kim, S. N. Kim, I. K. Chae (Sookmyung Women's Univ., Seoul, Korea), and D. H. Kim (Sookmyung Women's Univ., Seoul, Korea) *In* NASA. Goddard Space Flight Center 19th Intern. Cosmic Ray Conf., Vol. 6 Aug. 1985 p 188-191 refs Sponsored in part by Korea Science and Engineering Foundation (For primary document see N85-35848 24-93)
(HE-1.4-11) Avail: NTIS HC as boxed set only $200/MF A01 per volume or E99 per entire set CSCL 18K

N85-35899*# Academy of Sciences of the Armenian SSR, Erivan (USSR).
EXPERIMENT PAMIR-3. COPLANAR EMISSION OF HIGH ENERGY GAMMA-QUANTA AT INTERACTION OF HADRONS WITH NUCLEI OF AIR ATOMS AT ENERGIES ABOVE 10 TO THE 7TH POWER GeV
T. L. Asatiani, L. E. Genina, G. T. Zatsepin (Institute for Nuclear Research, Moscow, USSR) et al *In* NASA. Goddard Space Flight Center 19th Intern. Cosmic Ray Conf., Vol. 6 Aug. 1985 p 192-195 refs (For primary document see N85-35848 24-93)
(HE-1.4-12) Avail: NTIS HC as boxed set only $200/MF A01 per volume or E99 per entire set CSCL 18K

N85-35900*# Moscow State Univ. (USSR). Inst. of Nuclear Physics.
THE EFFECT OF THE RELATIVE NUCLEAR SIZE ON THE NUCLEUS-NUCLEUS INTERACTIONS
I. N. Erofeeva, V. S. Murzin, S. Yu. Sivoklokov, and L. N. Smirnova *In* NASA. Goddard Space Flight Center 19th Intern. Cosmic Ray Conf., Vol. 6 Aug. 1985 p 196-199 refs (For primary document see N85-35848 24-93)
(HE-1.4-13) Avail: NTIS HC as boxed set only $200/MF A01 per volume or E99 per entire set CSCL 18K

N85-35901*# National Aeronautics and Space Administration. Goddard Space Flight Center, Greenbelt, Md.
JAPAN - USSR JOINT EMULSION CHAMBER EXPERIMENT AT PAMIR Japan - USSR Joint Experiment
In its 19th Intern. Cosmic Ray Conf., Vol. 6 Aug. 1985 p 200-203 refs (For primary document see N85-35848 24-93)
(HE-3.1-1) Avail: NTIS HC as boxed set only $200/MF A01 per volume or E99 per entire set CSCL 18K

N85-35905*# Academy of Sciences of the Georgian SSR, Tbilisi (USSR). Inst. of Physics.
HADRON INTENSITY AND ENERGY SPECTRUM AT 4380 m ABOVE LEVEL
S. D. Cananov, E. Kh. Chadranyan, L. A. Khizanishvili, N. K. Ladaria, and N. N. Roinishvili *In* NASA. Goddard Space Flight Center 19th Intern. Cosmic Ray Conf., Vol. 6 Aug. 1985 p 216-219 refs (For primary document see N85-35848 24-93)
(HE-3.1-7) Avail: NTIS HC as boxed set only $200/MF A01 per volume or E99 per entire set CSCL 18K

N85-35919*# Moscow State Univ. (USSR). Inst. of Nuclear Physics.
THE MULTIPLICITY AND THE SPECTRA OF SECONDARIES CORRELATED WITH THE LEADING PARTICLE ENERGY
N. A. Kruglov, A. S. Proskuryakov, L. I. Sarycheva, and L. N. Smirnova *In* NASA. Goddard Space Flight Center 19th Intern. Cosmic Ray Conf., Vol. 6 Aug. 1985 p 270-273 refs (For primary document see N85-35848 24-93)
(HE-3.2-11) Avail: NTIS HC as boxed set only $200/MF A01 per volume or E99 per entire set CSCL 18K

74 OPTICS

Includes light phenomena.

N85-35749*# Smithsonian Astrophysical Observatory, Cambridge, Mass.
A NORMAL INCIDENCE X-RAY TELESCOPE SOUNDING ROCKET PAYLOAD Semiannual Progress Report, 1 Aug. 1984 - 31 Jul. 1985
Leon Golub Sep. 1985 55 p
(Grant NAG5-626)
(NASA-CR-176169; NAS 1.26:176169; SAPR-1; SAPR-2) Avail: NTIS HC A04/MF A01 CSCL 20F

Progress is reported on the following major activities on the X-ray telescope: (1) complete design of the entire telescope assembly and fabrication of all front-end components was completed; (2) all rocket skin sections, including bulkheads, feedthroughs and access door, were specified; (3) fabrication, curing and delivery of the large graphite-epoxy telescope tube were completed; (4) an engineering analysis of the primary mirror vibration test was completed and a decision made to redesign the mirror attachment system to a kinematic three-point mount; (5) detail design of the camera control, payload and housekeeping

electronics were completed; and (6) multilayer mirror plates with 2d spacings of 50 A and 60 A were produced. E.A.K.

N85-35750*# Jet Propulsion Lab., California Inst. of Tech., Pasadena.
OPTICAL RECEIVERS USING ROUGH REFLECTORS
Victor A. Vilnrotter 1 May 1985 50 p refs
(Contract NAS7-918)
(NASA-CR-176200; JPL-Pub-85-25; NAS 1.26:176200) Avail: NTIS HC A03/MF A01 CSCL 20F

This report examines the possible use of rough, or nondiffraction-limited, reflectors for collecting optical signals. It is shown that in the absence of background radiation, the reflector's surface quality has little effect on the performance of a properly designed receiver, but that the presence of even small amounts of background radiation can lead to severe performance degradation. Techniques are suggested for improving receiver performance in high-background environments, and bounds and approximations to the exact error-probability expressions are derived. Author

N85-35751# Maryland Univ., College Park. Center for Automation Research.
EDGE INFORMATION IN COLOR IMAGES BASED ON HISTOGRAMS OF DIFFERENCES
M. Pietikainen and D. Harwood Mar. 1985 27 p
(Contract DAAK70-83-K-0018; DARPA Order 3206)
(AD-A156002; CAR-TR-112; CS-TR-1479) Avail: NTIS HC A03/MF A01 CSCL 06/4

A new measure of edge information for color images based on cumulative histograms of absolute color differences is proposed. A multispectral version of the Symmetric Nearest Neighbor filter for edge-preserving smoothing and methods for image segmentation and edge detection are developed based on this measure. Experimental results show that the performance of the new algorithms is very good. The analysis of color images has received little attention in computer vision research, in spite of the facts that color plays an important role in human vision and that color should also provide much useful information for many image analysis applications. GRA

N85-35752# Environmental Research Inst. of Michigan, Ann Arbor.
OPTICAL SYNTHETIC APERTURE TECHNIQUES Final Report
C. C. Aleksoff May 1985 58 p
(Contract DAAG29-80-K-0008)
(AD-A156151; ERIM-151200-17-F) Avail: NTIS HC A04/MF A01 CSCL 17/5

Optical synthetic aperture imaging concepts and techniques were theoretically and experimentally investigated. The theory of optical synthetic aperture imaging was extended to arbitrary geometries and to multiple sources/receivers. Scanned synthetic aperture imaging was demonstrated at a wavelength of 1.22 mm. A bandwidth compression technique was analyzed and demonstrated that gave fine range resolution with only a narrow passband receiver using mode-locked lasers. A coherent optical spectrum analyzer that uses a tapped optical fiber was conceived and experimentally demonstrated. Special backprojection concepts were conceived that can process certain types of synthetic aperture data. Grating interferometer processing techniques were also investigated. Author (GRA)

N85-35753# National Bureau of Standards, Gaithersburg, Md. National Engineering Lab.
TRANSIENT ANALYSIS OF ELECTROMAGNETIC REFLECTION FROM DISPERSIVE MATERIALS
A. G. Lieberman Mar. 1985 73 p refs
(PB85-200186; NBS/TN-1202) Avail: NTIS HC A04/MF A01; also avail: SOD as SN003-003-02651-4 CSCL 20F

Theoretical expressions are presented describing the transient and steady-state temporal evolution of an impulsive, TE-polarized, plane wave reflected into vacuum from any of a variety of frequency-dispersive material surfaces. Polar dielectrics, nonpolar dielectrics, metals and plasmas are treated using, respectively, the Debye, Lorentz, and Drude material models to investigate the effects of dispersion upon dimensional measurements performed with optical pulses of extremely short duration. The more general problem, concerning the reflection of an optical pulse of any specified waveform, is resolved by performing a convolution of the incident wave at the material surface with the previously determined reflection of an impulsive wave. Author (GRA)

N85-35754# National Bureau of Standards, Gaithersburg, Md.
SELF-STUDY MANUAL ON OPTICAL RADIATION MEASUREMENTS. PART 1: CONCEPTS. CHAPTER 12: BLACKBODIES, BLACKBODY RADIATION, AND TEMPERATURE SCALES
J. C. Richmond and F. E. Nicodemus Apr. 1985 49 p refs
(PB85-195303; NBS/TN-910-8) Avail: NTIS HC A03/MF A01; also avail: SOD as SN003-003-02847-6 CSCL 20F

A comprehensive tutorial treatment of the measurement of optical radiation that is complete enough for self-instruction is presented. Detailed chapter summaries make it also a convenient authoritative reference source. In this chapter, the radiometric treatment, and the significance for radiometric measurements, of blackbodies, blackbody radiation, and temperature scales are reviewed. Many important and interesting aspects are not treated because the primary interest is radiometry and radiometric measurements. The emphasis is on ideal blackbodies and laboratory simulators; thermal radiation from other real sources will be treated in a chapter on Thermal Radiation Properties of Materials. GRA

N85-35755# National Bureau of Standards, Washington, D.C. Electromagnetic Technology Div.
REDEFINING THE SCRATCH STANDARDS
M. Young and E. G. Johnson Feb. 1985 28 p refs Sponsored in part by Army
(PB85-194736; NBS/TN-1080) Avail: NTIS HC A03/MF A01; also avail: SOD as SN003-003-02635-2 CSCL 20F

The scratch standard (MIL-9-13830A) is a cosmetic standard that is effected by a visual comparison with a set of submasters that are in turn evaluated by comparison with a set of master standards. Both manufacture and certification of the submasters are somewhat unreliable. The submasters can be classified according to the relative power scattered at a relatively small angle. They have designed etched gratings with which to replace the submasters; these gratings have the appearance of scratches but diffract a broad peak between 5 and 10 degrees off the axis of the incident beam. Some prototpyes are classified both by comparison with the master standards and by a photoelectric measurement; agreement between the two methods is good. Such gratings used as the submasters and possibly may be classified by a photoelectric rather than visual measurement. GRA

75 PLASMA PHYSICS

Includes magnetohydrodynamics and plasma fusion.

For ionospheric plasmas see *46 Geophysics*. For space plasmas see *90 Astrophysics*.

N85-35756# Sandia Labs., Albuquerque, N. Mex..
OPERATIONS CONSIDERATIONS IN DESIGNING A HIGH SPEED MULTI-CHANNEL DATA ACQUISITION SYSTEM
F. A. Bouchier and C. R. Mattson 1985 13 p refs Presented at the 5th IEEE Pulsed Power Conf., Washington, D.C., 10 Jun. 1985
(Contract DE-AC04-76DP-00789)
(DE85-012840; SAND-84-2520C; CONF-850616-27) Avail: NTIS HC A02/MF A01

Several unique features are being implemented in the particle beam fusion accelerator 2 data acquisition system. Set up efficiency has been improved by a cable harness that easily allows any of over 700 signals to be cabled to more than 100 waveform channels. Flexibility has been increased by a trigger and fiducial patch panel switching system that quickly enables any of the 18 triggers and fidus to be connected to any of the waveform channels. Reliability

has been improved by a specially designed cooling system and a modular system design approach. DOE

N85-35757# Los Alamos National Lab., N. Mex.
CONSIDERATIONS ON COLLECTIVE ION ACCELERATION AS AN INTENSE ION INJECTOR
R. J. Faehl and W. K. Peter 1985 11 p refs Presented at the Particle Accelerator Conf., Vancouver, British Columbia, 13 May 1985
(Contract W-7405-eng-36)
(DE85-012706; LA-UR-85-1654; CONF-850504-90) Avail: NTIS HC A02/MF A01

A virtual cathode collective acceleration configuration is examined for use as a pulsed, intense ion injector. Numerical calculations of the collective acceleration show peak ion energies of several times that of the electron beam energy. The late time behavior is to accelerate ions to lower energies but at a higher current. This is characteristic of a reflex ion triode, which produces an ion beam largely charged but not current neutralized. Dynamic neutralization must be achieved if accelerator applications requiring transport and focusing are to be realized. Representative applications are simulated and discussed. DOE

N85-35758# Stanford Linear Accelerator Center, Calif.
TIME DOMAIN REFLECTOMETRY FOR SLC BPM SYSTEM
D. R. Thompson Mar. 1985 36 p refs Revised
(Contract DE-AC03-76SF-00515)
(DE85-012389; SU-SLAC-TN-84-1-Rev) Avail: NTIS HC A03/MF A01

A maintenance manual for troubleshooting installed SLC Position Monitor stripline assemblies and the associated cabling, using time Domain Reflectometry is presented. Once a technician becomes familiar with this manual's procedures, the Table of Contents can serve as a checklist. DOE

N85-35759# Brookhaven National Lab., Upton, N. Y.
HIGH VACUUM PORTABLE PUMPING STATION SUITABLE FOR ACCELERATOR USE
P. Stattel, J. Briggs, W. DeBoer, and R. Skelton 1985 3 p ref Presented at the Particle Accelerator Conf., Vancouver, British Columbia, 13 May 1985
(Contract DE-AC02-76CH-00016)
(DE85-011840; BNL-36454; CONF-850504-35) Avail: NTIS HC A02/MF A01

The need for a Portable Pump Station for Ultra High Vacuum use became apparent when the Isabelle collider was first being designed. A portable pump station had to be developed which contained the following features: maneuverability, compact size, ruggedness, self protection against various failures and capability of running unattended and of reaching 10(-9) torr. The pump station that was developed and other variations are discussed. DOE

N85-35760# Texas Univ., Austin. Inst. for Fusion Studies.
HIGH ENERGY PLASMA ACCELERATORS
T. Tajima May 1985 144 p refs
(Contract DE-FG05-80ET-53088)
(DE85-013121; DOE/ET-53088/190; ISFR-190) Avail: NTIS HC A07/MF A01

Colinear intense laser beams (LC OMEGA)0, kappa0 and (LC OMEGA)1, kappa1 shone on a plasma with frequency separation equal to the electron plasma frequency (LC OMEGA) sub pe are capable of creating a coherent large longitudinal electric field E sub L = mc (LC OMEGA) sub pe e of the order of 1 GeV/cm for a plasma density of 10 to the 18th/c.c. through the laser beat excitation of plasma oscillations. Accompanying favorable and deleterious physical effects using this process for a high energy beat-wave accelerator are discussed: the longitudinal dephasing, pump depletion, the transverse laser diffraction, plasma turbulence effects, self-steepening, self-focusing, etc. The basic equation, the driven nonlinear Schroedinger equation, is derived to describe this system. Advanced accelerator concepts to overcome some of these problems are proposed, including the plasma fiber accelerator of various variations. An advanced laser architecture suitable for the beat-wave accelerator is suggested. Accelerator physics issues such as the luminosity are discussed. Applications of the present process to the current drive in a plasma and to the excitation of collective oscillations within nuclei are also discussed. DOE

N85-35761# Washington Univ., Seattle. Dept. of Nuclear Engineering.
CONFINEMENT AND HEATING OF HIGH BETA PLASMAS WITH EMPHASIS ON COMPACT TOROIDS Annual Report, 1 Oct. 1983 - 30 Sep. 1984
F. I. Ribe 4 Oct. 1985 24 p
(Contract DE-AT06-72ET-53047)
(DE85-011459; DOE/ET-53047/21) Avail: NTIS HC A02/MF A01

The changes to the High Beta Q Machine (HBQM) which permit plasma production along a helical axis were successfully completed. The equilibrium and stability of linear heliacs with bean-shaped flux cross-sections and also the simpler linear 1=1 stellarator with nearly circular flux cross-sections were experimentally investigated. DOE

N85-35762# Los Alamos Scientific Lab., N. Mex.
BEAM POTENTIAL MEASUREMENT OF AN INTENSE H(-) BEAM BY USE OF THE EMISSIVE PROBE TECHNIQUE
J. D. Sherman, P. Allison, and H. V. Smith, Jr. 1985 4 p refs Presented at the Particle Accelerator Conf., Vancouver, British Columbia, 13 May 1985
(Contract W-7405-eng-36)
(DE85-012671; LA-UR-85-1606; CONF-850504-65) Avail: NTIS HC A02/MF A01

An emissive probe was developed to study the beam-plasma potential generated by a 20 keV, 30 mA sq cm quiescent H(-) beam propagating in Xe background gas. An axial ion trap was built, and its influence on the measured potentials is reported. The peak plasma potential at 10 to the 12th power cu cm Xe density increased from +5V to +10V when the ion-trap voltage was increased from zero to +80V. The quiescent H(-) beam rms emittance, measured 34 cm from the ion source, increased from 0.012 to 0.023 (PI) x cm x mrad when the Xe density was decreased from 2.2 x 10 to the 12th power cu cm to zero. DOE

N85-35763# Stanford Linear Accelerator Center, Calif.
BREEDING NEW LIGHT INTO OLD MACHINES (AND NEW)
J. E. Spencer and S. J. Brodsky Apr. 1985 4 p Presented at the Particle Accelerator Conf., Vancouver, British Columbia, 13 May 1985
(Contract DE-AC03-76SF-00515)
(DE85-013055; SU-SLAC-PUB-3646; CONF-850504-78) Avail: NTIS HC A02/MF A01

Photons produced by lasers or wigglers backscattered on high energy electron or proton beams can provide high energy, high luminosity photon-electron, photon-photon or photon-proton collisions. This allows the study of short-distance QCD processes such as high transverse momentum photon-photon and photo-production reactions, deep inelastic Compton scattering, the photon structure function, direct photon reactions, or searches for pseudo-Goldstone bosons and supersymmetry particles like the photino or goldstino. The relative reaction rates should be quite high since: (1) photo-production cross sections are significantly larger than the corresponding electro-production cross sections, and (2) absence of the conventional beam-beam interaction allows significantly higher currents and smaller interaction areas. It thus seems possible to have photon luminosities much larger than for electrons. Examples are given using the PEP storage ring with the SLAC linac beam. DOE

N85-35764# Argonne National Lab., Ill.
BEAM INTENSITY INCREASES AT THE INTENSE PULSED NEUTRON SOURCE ACCELERATOR
C. Potts, F. Brumwell, J. Norem, A. Rauchas, V. Stipp, and G. Volk 1985 3 p Presented at the Particle Accelerator Conf., Vancouver, British Columbia, 13 May 1985

(Contract W-31-109-eng-38)
(DE85-012377; CONF-850504-115) Avail: NTIS HC A02/MF A01

The intense pulsed neutron source (IPNS) accelerator system has managed a 40% increase in time average beam current. Currents of up to 15.6 micron A were accelerated and cleanly extracted. The high current operation demands low loss beam handling to permit hands-on maintenance. A new H(-) ion source offers the opportunity to get above 8 micron A but an instability causes unacceptable losses when attempting to operate at 10 micron A and above. Simple techniques to control the instabilities are introduced. These techniques and improvements in the regulation of various power supplies which provide improved low energy orbit stability and contribute to the increased beam current are discussed. E.A.K.

N85-35765# Los Alamos Scientific Lab., N. Mex.
MAJOR FACILITY OVERHAULS AT LAMPF
D. L. Grisham, J. E. Lambert, and W. F. Sommer, Jr. 1985 4 p Presented at the Particle Accelerator Conf., Vancouver, British Columbia, 13 May 1985
(Contract W-7405-eng-36)
(DE85-012724; LA-UR-85-1736; CONF-850504-112) Avail: NTIS HC A02/MF A01

A linear proton accelerator designed to operate at 800 MeV and 1.0 mA is discussed. It operated at power levels above 200 microamperes and now routinely operates near the design level. The problems encountered with the original target cell components, the repairs required since 1976, and specifically details the steps involved in the complete replacement of the vital target cell components are outlined. These components include target boxes, collimators, main beam line magnets, and the front-end magnets of the secondary beam lines. The A-2 target cell was replaced in the spring of 1983 and the A-1 target cell was replaced in the spring of 1984. Both have operated satisfactorily since their completion. The overhaul and total component replacement in the beam stop area (A-6) was completed and is placed in operation. The upgrade and the replacement of the beam stop and the vacuum-to-air window with state-of-the-art designs, provide an increase capability of both proton and neutron irradiation of materials. DOE

N85-35766# Los Alamos Scientific Lab., N. Mex.
ION SOURCE DEVELOPMENT FOR THE LOS ALAMOS HEAVY ION FUSION INJECTOR
H. L. Rutkowski, H. Oona, E. A. Meyer, R. P. Shurter, L. S. Engelhardt, and S. Humphries, Jr. (New Mexico Univ., Albuquerque) 1985 4 p Presented at the Particle Accelerator Conf., Vancouver, British Columbia, 13 May 1985
(Contract W-7405-eng-36)
(DE85-012682; LA-UR-85-1584; CONF-850504-152) Avail: NTIS HC A02/MF A01

A multibeam injector was designed and built for the heavy ion fusion program. Development of an aluminum-spark, pulsed plasma source is carried out. Faraday cup diagnostics are used to study current emission and to map the current profile. An aluminum oxide scintillator with photographic film is used in conjunction with a pepper-pot to obtain time integrated emittance values. DOE

N85-35767# Brookhaven National Lab., Upton, N. Y.
APPLICATIONS OF DECELERATED IONS
B. M. Johnson Mar. 1985 7 p refs Presented at the Symp. of Northeastern Accelerator Personnel, Stony Brook, N.Y., 15 Oct. 1984
(Contract DE-AC02-76CH-00016)
(DE85-011832; BNL-36417; CONF-8410172-10) Avail: NTIS HC A02/MF A01

Many facilities whose sole purpose was to accelerate ion beams are now becoming decelerators as well. The development and current status of accel-decel operations is reviewed. Applications of decelerated ions in atomic physics experiments are discussed. DOE

N85-35768# Sandia Labs., Albuquerque, N. Mex.
FOUR STAGE HELIA EXPERIMENT
J. J. Ramirez, D. E. Hasti, J. P. Corley, J. W. Poukey, K. R. Prestwich, P. W. Spence, I. D. Smith, L. G. Schlitt, H. N. Nishimoto, K. E. Nielsen et al 1985 15 p refs Presented at the 5th IEEE Pulsed Power Conf., Washington, D.C., 10 Jun. 1985 Prepared in cooperation with Pulse Sciences, Inc.
(Contract DE-AC04-76DP-00789)
(DE85-012026; SAND-84-2412C; CONF-850616-2) Avail: NTIS HC A02/MF A01

A four stage, 4 MV, 250 kA, 30 ns accelerator to demonstrate the High Energy Linear Induction Accelerator (HELIA) concept is described. HELIA uses modular, water dielectric, pulse forming lines to drive inductively isolated cavities. A cathode stalk extends the length of the accelerator, adds the voltages from the cavities, and delivers the power to a high voltage anode-cathode gap. The cathode stalk constitutes the inner electrode of a coaxial magnetically insulated transmission line (MITL). The outer electrode of the MITL is not ocntinuous but is interrupted at regular intervals by the cavity feeds. The single cavity experiment demonstrated the performance of individual cavities and pulse forming elements. The four cavity experiment demonstrated the key physics issues of the HELIA concept. The design and performance of the pulsed power driver, induction cavities, and measurements of the power delivered by the MITL to an electron beam load are presented. DOE

N85-35769# Sandia Labs., Albuquerque, N. Mex.
POWER FLOW EVALUATIONS FOR HERMES 3
D. L. Smith, J. J. Ramirez, J. P. Corley, and D. E. Hasti 1985 19 p Presented at the 5th IEEE Pulsed Power Conf., Washington, D.C., 10 Jun. 1985
(Contract DE-AC04-76DP-00789)
(DE85-013116; SAND-84-2366C; CONF-850616-22) Avail: NTIS HC A02/MF A01

A study was conducted to evaluate the transfer of electromagnetic pulses from water dielectric strip transmission lines into a diode insulator stack. The HERMES 3 Scale Model Experiments (HERMEX) included single-stage diodes as well as multistage models in which a variety of parallel/series combinations of strip transmission lines (strip lines) were used to evaluate the voltage adding efficiency at the diode. A technique was established to estimate an equivalent shunt impedance across the diode due to the nearby uncharged water volume. DOE

N85-35770# New York Univ., New York. Inst. of Mathematical Sciences.
SOME RIGOROUS RESULTS CONCERNING SPECTRAL THEORY FOR IDEAL MHD
P. Laurence May 1985 46 p
(Contract DE-AC02-76ER-03077)
(DE85-013427; DOE/ER-03077/245) Avail: NTIS HC A03/MF A01

Spectral theory for linear ideal MHD is laid on a firm foundation by defining appropriate function spaces for the operators associated with both the first and second order (in time and space) partial differential operators. Thus, it is rigorously established that a self-adjoint extension of F(xi) exists. It is shown that the operator L associated with the first order formulation satisfies the conditions of the Hille-Yosida theorem. A foundation is laid thereby within which the domains associated with the first and second order formulations can be compared. This allows future work in a rigorous setting that will clarify the differences (in the two formulations) between the structure of the generalized eigenspaces corresponding to the marginal point of the spectrum (LC OMEGA) = 0. DOE

N85-35771# Westinghouse Electric Corp., Pittsburgh, Pa. Advanced Systems Technology Div.
STUDY TO ASSESS THE EFFECTS OF MAGNETOHYDRODYNAMIC ELECTROMAGNETIC PULSE ON ELECTRIC POWER SYSTEMS, PHASE 1, VOLUME 3 Final Report
J. R. Legro, N. C. Abi-Samra, and F. M. Tesche May 1985

135 p
(Contract DE-AC05-84OR-21400)
(DE85-011301; ORNL/SUB-83/43374/1/V3) Avail: NTIS HC A07/MF A01

In addition to the initial transients designated as fast transient high-altitude EMP (HEMP) and intermediate time EMP, electromagnetic signals are also perceived at times from seconds to hundreds of seconds after a high-altitude nuclear burst. This signal was defined by the term magnetohydrodynamic-electromagnetic pulse (MHD-EMP). The MHD-EMP phenomena was detected in actual weapon tests and predicted from theoretical models. A preliminary research effort to investigate the nature and coupling of the MHD-EMP environments to electric power systems documented the construction of approximate system response network models, and the development of a unified methodology to assess equipment and systematic vulnerability are defined. The MHD-EMP environment is compared to a qualitatively similar natural event, the electromagnetic environment produced by geomagnetic storms. DOE

N85-35772# Stanford Linear Accelerator Center, Calif.
ON-LINE MODEL DRIVEN CONTROL OF THE SLC ELECTRON DAMPING RING
I. Almoq, J. Jaeger, M. Lee, and M. Woodley Mar. 1985 4 p Presented at the Particle Accelerator Conf., Vancouver, British Columbia, 13 May 1985
(Contract DE-AC03-76SF-00515)
(DE85-013377; SU-SLAC-PUB-3608; CONF-850504-73) Avail: NTIS HC A02/MF A01

Model driven procedures have been used for control of the linac, beam transport lines and storage rings at SLAC. These procedures, based upon computer models of the machine lattice, are used for on-line calculation of the strengths of beam line components which yield desired lattice parameter values. They are also used for routine operation of the machine and for diagnosing and correcting errors of various types, as well as for aiding physicists in the acquisition and presentation of data. Successful operational experience in the use of such procedures at the PEP and SPEAR storage rings had led to the decision that this method of operation will be used for control of all of the SLC subsystems: two-mile Linac, Arcs, Final Focus Region, Positron Return Line and the Damping Rings and their associated injection/extraction beam transport lines. The purpose of this paper is to describe the development of the on-line model driven control procedures and their implementation in the SLC computer control system. DOE

N85-35773# Argonne National Lab., Ill.
VACUUM SYSTEM FOR THE ARGONNE 6 GeV SYNCHROTRON LIGHT SOURCE
R. Wehrle and J. Moenich 1985 3 p Presented at the Particle Accelerator Conf., Vancouver, British Columbia, 13 May 1985
(Contract W-31-109-eng-38)
(DE85-012286; CONF-850504-43) Avail: NTIS HC A02/MF A01

The ANL vacuum system for the 6 GeV light source storage ring features nonevaporable strip getter pumps for uniform pumping around the ring within a gas desorption antechamber, and it also features lumped getter pumping directly under and above crotch radiation absorbers that are positioned after each bending magnet. Based on experiments at ANL in 1980 and by others, the technical and economical advantages have been established for the use of the distributed NeG pumps on nonmagnetic strips coated with a nonevaporable Zr Al getter matrix. The NeG strip pump lifetime approaches ten years. The antechamber improves the isolation of the gas desorption process from the main beam chamber and beam. The combination of these vacuum techniques (the NeG strip getter pumps, the gas desorption antechambers, and the lumped ion and lumped getter pumping) provide a unique and reliable system for maintaining long beam lifetime. DOE

N85-35774# Stanford Linear Accelerator Center, Calif.
HIGH RESOLUTION BEAM PROFILE MONITORS IN THE SLC
M. C. Ross, J. T. Seeman, R. K. Jobe, J. C. Sheppard, and R. F. Stiening Apr. 1985 3 p refs Presented at the Particle Accelerator Conf., Vancouver, British Columbia, 13 May 1985
(Contract DE-AC03-76SF-00515)
(DE85-013375; SU-SLAC-PUB-3640; CONF-850504-66) Avail: NTIS HC A02/MF A01

In the SLC linac, low emittance beams with typical transverse dimensions less than 0.2 mm must be accelerated without effective emittance growth. In order to monitor this, a high resolution beam profile monitor system was installed which consists of an aluminum target covered with a fine grained phosphor, a magnifying optical system, a television camera and video signal recording electronics. The image formed when the beam strikes the phosphor screen is viewed on a CRT monitor at the console and selected horizontal and vertical slices of the beam spot intensity are recorded. A 20 MHz transient waveform recorder is used to sample and digitize the raw video signal along the selected slice. The beam width is determined by fitting the background subtracted data to a Gaussian. Beam spots less than 6 x 3 mm can be viewed. Beam spot sizes sigma/sub x,y/ $<$ 80 (MU)m have been measured. DOE

N85-35775# Los Alamos Scientific Lab., N. Mex.
RECENT ADVANCES IN REMOTE HANDLING AT LAMPF
J. E. Lambert and D. L. Grisham 1985 4 p Presented at the Particle Accelerator Conf., Vancouver, British Columbia, 13 May 1985
(Contract W-7405-eng-36)
(DE85-012725; LA-UR-85-1735; CONF-850504-107) Avail: NTIS HC A02/MF A01

The Clinton P. Anderson Meson Physics Facility (LAMPF) has operated at beam currents above 200 microamperes since 1976. As a result, the main experimental beam line (Line A) has become increasingly radioactive over the years. Since 1976 the radiation levels have steadily increased from 100 mR/hr to levels that exceed 10,000 R/hr in the components near the pion production targets. During this time the LAMPF remote handling system, Monitor, has continued to operate successfully in the ever increasing radiation levels, as well as with more complex remote handling situations. The evolution of Monitor is described and specifically described is the complete rebuild of the A-6 target area, which is designated as the beam stop, but also includes isotope production capabilities and a primitive neutron irradiation facility. The new facility includes not only the beam stop and isotope production, but also facilities for proton irradiation and a ten fold expansion in neutron irradiation facilities. DOE

N85-35776# Oak Ridge National Lab., Tenn.
NEUTRAL PUMPING RATES FOR A NEXT STEP TOKAMAK IGNITION DEVICE
J. D. Galambos, Y. K. M. Peng, and D. Heifetz 1985 6 p Presented at the 6th Topical Meeting on the Technol. of Fusion Energy, San Francisco, 3 Mar. 1985 Prepared in cooperation with Princeton Univ., N.J.
(Contract DE-AC05-84OR-21400)
(DE85-012780; CONF-850310-101) Avail: NTIS HC A02/MF A01

Neutral pumping rates are calculated for pump limiter and diverter options of a next step tokamak ignition device using a method that accounts for the coupled effects of neutral transport and plasma transport. For both pump limiters and divertors the plasma flow into the channel surrounding the neutralizer plate is greatly reduced by the neutral recycling. The fraction of this flow that is pumped can be large ($>$ 50%) but in general is dependent on the particular geometry and plasma conditions. It is estimated that pumping speeds greater than or approximately 10(5) L/s are adequate for the exhaust requirements in the pump limiter and the diverter cases. DOE

N85-35777# Texas Univ., Austin. Inst. for Fusion Studies.
GENERALIZED REDUCED FLUID MODEL WITH FINITE ION-GYRORADIUS EFFECTS
C. T. Hsu, R. D. Hazeltine, and P. J. Morrison Apr. 1985 35 p
(Contract FG05-80ET-53088)

(DE85-013123; DOE/ET-53088/171; IFSR-171) Avail: NTIS HC A03/MF A01

Reduced fluid models have become important tools for studying the nonlinear dynamics of plasma in a large aspect ratio tokamak. A self consistent nonlinear reduced fluid model, with finite ion gyroradius effects is presented. The model is distinctive in allowing for arbitrary beta and in satisfying an exact, relatively simple energy conservation law. DOE

N85-35778# Los Alamos Scientific Lab., N. Mex.
PROPOSED FRX-D EXPERIMENT
K. F. McKenna, W. T. Armstrong, R. E. Chrien, W. N. Hugrass, R. K. Linford, D. J. Rej, J. L. Schwarzmeier, R. E. Siemon, and M. Tuszewski 1985 5 p Presented at the 7th US Symp. on Compact Toroid Res., Santa Fe, N. Mex., 21 May 1985
(Contract W-7405-eng-36)
(DE85-012766; LA-UR-85-1831; CONF-8505100-8) Avail: NTIS HC A02/MF A01

The field-reversed-configuration (FRC) research program is poised for a significant step forward. Resolution of the critical FRC physics issues, which must now be addressed in order to advance the development of this concept, requires experimental studies in a plasma regime closer to reactor relevance than is possible with existing devices. The purpose of FRX-D is to extrapolate the parameters of FRC's into the required regime of large plasma size relative to an ion gyroradius, i.e., large anti s. The critical issues that FRX-D will address are: (1) the FRC stability and confinement properties at large anti s; (2) the demonstration of adiabatic compression as an efficient, technologically attractive FRC heating method; (3) the identification of the dominant electron energy loss mechanism; and (4) the determination of the dependence of poloidal flux loss on electron temperature. An additional, more technologically oriented purpose of FRX-D is to demonstrate the separation of FRC formation and heating functions using the reactor-like technique of sequential formation/translation/compression. DOE

N85-35779# Los Alamos Scientific Lab., N. Mex.
LOS ALAMOS HIGH-CURRENT PROTON STORAGE RING Status Report
G. P. Lawrence, R. A. Hardekopf, A. J. Jason, P. N. Clout, and G. A. Sawyer 1985 5 p refs Presented at the Particle Accelerator Conf., Vancouver, British Columbia, 13 May 1985
(Contract W-7405-eng-36)
(DE85-012664; LA-UR-85-1613; CONF-850504-51) Avail: NTIS HC A02/MF A01

The Proton Storage Ring (PSR), whose installation was recently completed at Los Alamos, is a fast-cycling high-current accumulator designed to produce intense 800 MeV proton pulses for driving a spallation neutron source. The ring converts long beam pulses from the LAMPF linear accelerator into short bunches well matched to requirements of a high-resolution neutron-scattering materials science program. The initial performance goal for this program is to provide 100-(MU)A average current at the neutron production target within a 12-Hz pulse rate. Operation at 20 (MU)A is scheduled for September 1985, with full intensity within the next year. The storage ring was originally designed to function in a second mode in which six 1-ns bunches are accumulated and separately extracted every LAMPF macropulse. Implementation of this mode, which would serve a fast-neutron nuclear-physics program, was deferred in favor of initial concentration on the neutron-scattering program. The PSR design and status is summarized. Unique machine features include high peak current, two-step charge-stripping injection, a low-impedance buncher amplifier to counter beam-loading, and a high-repetition-rate strip-line extraction kicker. DOE

N85-35780# Sandia Labs., Albuquerque, N. Mex.
KINETIC LOSS EXPERIMENTS ON MITE
R. W. Stinnett and H. N. Woodall 1985 15 p Presented at the 5th IEEE Pulsed Power Conf., Washington, D.C., 10 Jun. 1985
(Contract DE-AC04-76DP-00789)
(DE85-012826; SAND-84-2457C; CONF-850616-7) Avail: NTIS HC A02/MF A01

Experiments on Sandia National Laboratory's Mite accelerator (2 MV, 4.8 ohms) were conducted to study the effect of geometric transitions on power flow in a magnetically insulated power feed. The effect of both changing gaps (electric convolutes) and changing line widths (magnetic convolutes) was studied. These geometric transitions caused electron losses which depended on both the abruptness of the transition and the downstream load impedance. These losses, due to perturbation of the orbits of the magnetically insulated electron flow in the anode-cathode gap, are called kinetic losses. Temporally and spatially resolved measurements of these losses were made using Faraday cups and filtered. The effect of an anode plasma on magnetically insulated electron flow was also studied. The kinetic losses measured in these experiments can be significant in some situations. DOE

N85-35781# Brookhaven National Lab., Upton, N. Y.
SYNCHRONOUS TIMING OF MULTI-ENERGY FAST BEAM EXTRACTION DURING A SINGLE AGS CYCLE
J. Gabusi and S. Naase 1985 3 p Presented at the Particle Accelerator Conf., Vancouver, British Columbia, 13 May 1985
(DE85-011829; BNL-36391; CONF-850504-31) Avail: NTIS HC A02/MF A01

Synchronous triggering of fast beams is required because the field of Kicker Magnets must rise within the open space between one beam bunch and the next. Within the Brookhaven AGS, Fast Extracted Beam (FEB) triggering combines nominal timing, based on beam energy with bunch-to-bunch synchronization, based on the accelerating RF waveform. During beam acceleration, a single bunch is extracted at 22 GeV/c and within the same AGS cycle. the remaining eleven bunches are extracted at 28.4 GeV/c. When the single bunch is extracted, a hole, which is left in the remaining circulating beam, can appear in random locations within the second extraction during successive AGS cycles. To overcome this problem, a synchronous RF/12 counting scheme and logic circuitry are used to keep track of the bunch positions relative to each other, and to place the hole in any desired location within the second extraction. The RF/12 signal is used also to synchronize experimenters triggers. DOE

N85-35782# Sandia Labs., Albuquerque, N. Mex.
SURFACE DISCHARGES AS INTENSE PHOTON SOURCES IN THE EXTREME ULTRAVIOLET
J. R. Woodworth, J. E. Maenchen, and P. F. McKay 1985 5 p Presented at the 5th IEEE Pulsed Power Conf., Washington, D.C., 10 Jun. 1985
(Contract DE-AC04-76DP-0789)
(DE85-012593; SAND-84-2443C; CONF-850616-26) Avail: NTIS HC A02/MF A01

Surface discharges were investigated as xuv photon sources for in-situ cleaning and preionizing of anode surfaces in light-ion-fusion accelerators. In these experiments the surface discharge was formed by discharging a capacitor bank across a spark gap which consisted of two copper electrodes attached to an insulator and facing each other across a 5.5-mm gap. The surface discharge and its power feeds were constructed in a stripline configuration to minimize system inductance. When the surface discharge was driven by a 2.9-(MU)F, 45-kV capacitor bank, the peak current thru the discharge was (-)250 kA. When driven at these levels, a single discharge radiated with a peak power of over 80 megawatts of 10 to 70 eV photons and had a total xuv output energy of 60 Joules per pulse. The xuv illumination of the anode on Sandia's PBFA-I Accelerator significantly improves the diode impedance characteristics. DOE

N85-35783# California Univ., Berkeley. Lawrence Berkeley Lab.
NUMERICAL STUDIES OF HIGH CURRENT BEAM COMPRESSION IN HEAVY ION FUSION
J. Bisognano, E. P. Lee, and J. W. K. Mark 10 May 1985 5 p Presented at the Particle Accelerator Conf., Vancouver, British Columbia, 13 May 1985 Prepared in cooperation with California Univ., Livermore, Lawrence Livermore Lab.
(Contract W-7405-eng-48)

(DE85-011874; UCRL-91968; CONF-850504-40) Avail: NTIS HC A02/MF A01

The process of longitudinal compression of a drifting heavy ion pulse to be used as an ICF driver is examined with the aid of particle simulation. Space charge forces play a vital role in halting compression before the final focus lens system is reached. This must take place with minimal growth of transverse emittance and momentum spread. Of particular concern is the distortion of longitudinal phase space by the rounded transverse profile of the longitudinal self-electric field. DOE

N85-35784# Los Alamos Scientific Lab., N. Mex.
RELATION BETWEEN FIELD ENERGY AND RMS EMITTANCE IN INTENSE PARTICLE BEAMS
T. P. Wangler, K. R. Crandall, R. S. Mills, and M. Reiser 1985 6 p refs Presented at the Particle Accelerator Conf., Vancouver, British Columbia, 13 May 1985 Prepared in cooperation with Maryland Univ., College Park
(Contract W-7405-eng-36)
(DE85-012655; LA-UR-85-1622; CONF-850504-58) Avail: NTIS HC A02/MF A01

An equation is presented for continuous beams with azimuthal symmetry and continuous linear focusing, which expresses a relationship between the rate of change for squared rms emittance and the rate of change for a quality we call the nonlinear field energy. The nonlinear field energy depends on the shape of the charge distribution and corresponds to the residual field energy possessed by beams with nonuniform charge distributions. The equation can be integrated for the case of an rms matched beam to yield a formula for space-charge-induced emittance growth that was tested numerically for a variety of initial distributions. The results provide a framework for discussing the scaling of rms emittance growth and an explanation for the well established lower limit on output emittance. DOE

N85-35785# Stanford Linear Accelerator Center, Calif.
ACCELERATOR PHYSICS MEASUREMENTS AT THE DAMPING RING
L. Rivkin, J. P. Delahaye, K. Wille, M. A. Allen, K. Bane, T. Fieguth, A. Hofmann, A. Button, M. Lee, and W. Linebarger May 1985 4 p Presented at the Particle Accelerator Conf., Vancouver, British Columbia, 13 May 1985 Prepared in cooperation with California Inst. of Tech., Pasadena, European Organization for Nuclear Research, Geneva, Switzerland and Deutsches Elektronen-Synchrotron (DESY), Hamburg, West Germany
(Contracts DE-AC03-76SF-00515; DE-AC03-81ER-40050)
(DE85-013373; SU-SLAC-PUB-3690; CONF-850504-151) Avail: NTIS HC A02/MF A01

Besides the optics measurements described elsewhere, machine experiments were done at the Stanford Linear Collider (SLC) damping ring to determine some of its parameters. The synchrotron radiation energy loss which gives the damping rates was measured by observing the RF-voltage dependence of the synchronous phase angle. The emittance was obtained from the synchrotron light monitor, scraper measurements and by extracting the beam through a doublet and measuring its size for different quadrupole settings. Current dependent effects such as parasitic mode losses, head tail instabilities, synchrotron and betatron frequency shifts were measured to estimate the impedance. RF-cavity beam loading and its compensation were also studied and ion collection was investigated. All results agree reasonably well with expectations and indicate no limitations to the design performance. DOE

N85-35786# Los Alamos Scientific Lab., N. Mex.
ANALYSIS OF A PULSED POWER SYSTEM CONTAINING ROTATING MACHINE
P. Chowdhuri 1985 5 p Presented at the 5th IEEE Pulsed Power Conf., Washington, D.C., 10 Jun. 1985
(Contract W-7405-eng-36)
(DE85-014128; LA-UR-85-2001; CONF-850616-56) Avail: NTIS HC A02/MF A01

Several hundred megajoules of energy lasting for several seconds are required for magnetic fusion experiments. Such high energy can be stored as inertial energy in an alternator which is brought up to speed slowly. The alternator is then discharged through a thyristor converter to magnets which produce and sustain the plasma. A major portion of the inertial stored energy, for reversed field pinch experiments in Los Alamos, will be dissipated in charging the magnetizing coil to produce the plasma. The plasma is then sustained, during the flat-top period, by energizing the magnetizing coil in the reverse direction. To hold the plasma current constant at the required level, the output voltage of the converter must be held at a prescribed level by controlling the firing angle of the thyristors. The possibility of using the same converter for both the magnetizing and the flat-top periods is discussed. The electrical requirements that will be imposed on the alternator and the converter are analyzed. DOE

N85-35787# Los Alamos Scientific Lab., N. Mex.
DIAGNOSTICS FOR PIONEER 1 IMPLODING PLASMA EXPERIMENTS
P. H. Y. Lee, R. F. Benjamin, J. H. Brownell, D. J. Erickson, J. H. Goforth, A. E. Greene, J. S. McGurn, J. F. Pecos, R. H. Price, and H. Oona 1985 5 p Presented at the 5th IEEE Pulsed Power Conf., Washington, D.C., 10 Jun. 1985
(Contract W-7405-eng-36)
(DE85-014120; LA-UR-85-2042; CONF-850616-57) Avail: NTIS HC A02/MF A01

The Pioneer 1 series of imploding plasma experiments are aimed at collapsing a thin aluminum foil with a multimegampere, submicrosecond electrical pulse produced by an explosive flux compression generator and fast plasma compression opening switch. Anticipated experimental conditions are bounded by implosion velocities of 2 x 10 to the 7 cm/s and maximum plasma temperatures of 100 eV. A comprehensive array of diagnostics have been deployed to measure implosion symmetry (gated microchannel plate array and other time-resolved imaging), temperature of the imploding plasma (visible/uv spectroscopy), stagnation geometry (X-ray pinhole imaging), radiation emission characteristics at pinch (XRD's, fast bolometry), and electrical drive history (Rogowski loops, Faraday rotation current detectors, and capacitive voltage probes). Diangostic performance is discussed and preliminary results are presented. DOE

N85-35788# Brookhaven National Lab., Upton, N. Y.
EFFECT OF Cu4Ti COMPOUND FORMATION ON THE CHARACTERISTICS OF NbTi ACCELERATOR MAGNET WIRE
M. Garber, M. Suenaga, W. B. Sampson, and R. L. Sabatini 1985 4 p Presented at the Particle Accelerator Conf., Vancouver, British Columbia, 13 May 1985
(Contract DE-AC02-76CH-00016)
(DE85-014226; BNL-36632; CONF-850504-197) Avail: NTIS HC A04/MF A01

High critical density, J sub c $>$ 2500 A/mm(2), and small filament diameter, d approx. 3 (MU)m, are required in multifilamentary NbTi wire used for superconducting accelerator magnets. Wire obtained from various commerical sources had J sub c's in the range 1000 to 2800 A/sq. mm and d's in the range 1 to 23 (MU)m. The filaments were examined by means of scanning electron microscopy in order to determine the reason for the variation in J sub c. It was found that the filaments in high J sub c wires had clean smooth surfaces and uniform cross section along their lengths. Filaments in low J sub c wires show formation of Cu4Ti compound particles on their surfaces and large variations in cross section. The lower critical current measured in these wires is believed to be largely due to this effect. The superconducting-normal state transition is relatively wide in these wires. DOE

N85-35789# Stanford Linear Accelerator Center, Calif.
SLC ARC TRANSPORT SYSTEM: MAGNET DESIGN AND CONSTRUCTION
G. E. Fischer, M. Anderson, R. Byers, and K. Halbach Mar. 1985 4 p refs Presented at the Particle Accelerator Conf., Vancouver, British Columbia, 13 May 1985

(Contract DE-AC03-76SF-00515)
(DE85-014289; SU-SLAC-PUB-3612; CONF-850504-200) Avail: NTIS HC A02/MF A01

Design and construction details of alternate gradient bending magnets, 950 of which are used in a single pass transport system to bring high energy positrons and electrons into head-on collision are described. The overall arc system is 8000 ft long, has an aperture of 1/2 inch and a circumference factor of 96%. DOE

N85-35790# Stanford Linear Accelerator Center, Calif.
SLC ENERGY UPGRADE PROGRAM AT SLAC
G. A. Loew, M. A. Allen, R. L. Cassel, N. R. Dean, G. T. Konrad, R. F. Koontz, and J. V. Lebacqz Mar. 1985 4 p Presented at the Particle Accelerator Conf., Vancouver, British Columbia, 13 May 1985
(Contract DE-AC03-76SF-00515)
(DE85-014290; SU-SLAC-PUB-3609; CONF-850504-199) Avail: NTIS HC A02/MF A01

The Stanford Linear Accelerator Center (SLAC) Linear Collider (SLC) must reach a nominal center-of-mass energy of 100 GeV to fulfill its high energy physics goals. The energy upgrade program that is being implemented on the SLAC linear accelerator to meet these goals is described. A discussion of the design requirements and available technical options, the rationale for the adopted solution, and the technical problems involved in the engineering and production of klystrons and modulators is presented. DOE

N85-35791# California Univ., Livermore. Lawrence Livermore Lab.
RESONANCE LOCALIZATION IN TOKAMAKS EXCITED WITH ICRF WAVES
G. D. Kerbel and M. G. McCoy 20 Jun. 1985 5 p Presented at the 6th Topical Conf. on Radio Frequency Plasma Heating, Pine Mountain, Ga., 13 May 1985
(Contract W-7405-eng-48)
(DE85-014559; UCRL-92236; CONF-8505130-7) Avail: NTIS HC A02/MF A01

Advanced wave model used to evaluate ICRH in tokamaks typically used warm plasma theory and allow inhomogeneity in one dimension. The majority of these calculations neglect the fact that gyrocenters experience the inhomogeneity via their motion parallel to the magnetic field. In strongly driven systems, wave damping can distort the particle distribution function supporting the wave and this produces changes in the absorption. A bounce-averaged Fokker-Planck quasilinear computational model which evolves the population of particles on more realistic orbits is presented. Each wave-particle resonance has its own specific interaction amplitude within any given volume element; these data need only be generated once, and appropriately stored for efficient retrieval. The wave-particle resonant interaction then serves as a mechanism by which the diffusion of particle populations can proceed among neighboring orbits. The local specific spectral energy absorption rate is directly calculable once the orbit geometry and populations are determined. The code is constructed in such fashion as to accommodate wave propagation models which provide the wave spectral energy density on a poloidal cross-section. Information provided by the calculation includes the local absorption properties of the medium which can then be exploited to evolve the wave field. DOE

N85-35792# Stanford Linear Accelerator Center, Calif.
MULTI-CHANNEL PULSER FOR THE SLC THERMIONIC ELECTRON SOURCE
M. J. Browne, J. E. Clendenin, P. I. Corredoura, R. K. Jobe, R. F. Koontz, and J. Sodja Jan. 1985 4 p refs Presented at the Particle Accelerator Conf., Vancouver, British Columbia, 13 May 1985
(Contract DE-AC03-76SF-00515)
(DE85-014222; SU-SLAC-PUB-3546; CONF-850504-202) Avail: NTIS HC A02/MF A01

A new pulser developed for the Stanford Linear Collider (SLC) thermionic gun has been operational since September 1984. It consists of two planar triode amplifiers with a common output triode driving the gun cathode to produce two independent pulses of up to 9A with a 3 nsec FWHM pulse width. Three long-pulse amplifiers are also connected to the cathode to produce pulses with widths controllable between 100 nsec and 1.6 (MU)sec. Each amplifier has independent timing and amplitude control through a fiber optic link to the high voltage plane of the gun cathode-grid structure. The pulser and its operating characteristics are described. DOE

N85-35793# Stanford Linear Accelerator Center, Calif.
TOSCA CALCULATIONS AND MEASUREMENTS FOR THE SLAC SLC DAMPING RING DIPOLE MAGNET
R. A. Early and J. K. Cobb Apr. 1985 4 p ref Presented at the Particle Accelerator Conf., Vancouver, British Columbia, 13 May 1985
(Contract DE-AC03-76SF-00515)
(DE85-014366; SU-SLAC-PUB-3631; CONF-850504-188) Avail: NTIS HC A02/MF A01

The SLAC damping ring dipole magnet was originally designed with removable nose pieces at the ends. Recently, a set of magnetic measurements was taken of the vertical component of induction along the center of the magnet for four different pole-end configurations and several current settings. The three dimensional computer code TOSCA, which is currently installed on the National Magnetic Fusion Energy Computer Center's Cray X-MP, was used to compute field values for the four configurations at current settings near saturation. Comparisons were made for magnetic induction as well as effective magnetic lengths for the different configurations. DOE

N85-35708# Brookhaven National Lab., Upton, N. Y.
VERY HIGH ENERGY PROBES OF THE QUARK-GLUON PLASMA
T. Ludlam, F. Paige, and L. Madansky (John Hopkins Univ., Baltimore, Md.) *In* California Univ., Berkeley. Lawrence Berkeley Lab. Proc. of the Workshop on Detectors for Relativistic Nucl. Collisions Aug. 1984 p 115-120 refs Original language document previously announced as N86-18763 (For primary document see N85-35700 24-72)
Avail: NTIS HC A08/MF A01

76 SOLID-STATE PHYSICS

Includes superconductivity.

For related information, see also *33 Electronics and Electrical Engineering* and *36 Lasers and Masers.*

N85-35794*# Eloret Corp., Sunnyvale, Calif.
SIZE AND SHAPE DEPENDENCE OF CO ADSORPTION SITES ON SAPPHIRE SUPPORTED Fe MICROCRYSTALS Final Technical Report
Ch. Papageorgopoulos and K. Heinemann Sep. 1985 27 p refs (Contract NCC2-323)
(NASA-CR-176171; NAS 1.26:176171; EI85-0923) Avail: NTIS HC A03/MF A01 CSCL 20L

The surface structure and stoichiometry of alumina substrates, as well as the size, growth characteristics, and shape of Fe deposits on sapphire substrates have been investigated by low energy electron diffraction (LEED), Auger electron spectroscopy, electron energy loss spectroscopy, and X-ray photoemission spectroscopy (XPS), as well as work function measurements, in conjunction with transition electron microscopy observations. The substrates used in this work were the following: (1) new, clean Al2O3; (2) same surface amorphized by Ar ion bombardment; (3) same surface regenerated by 650 C annealing; (4) amorphous alumina films on Ta slab; and (5) polycrystal alumina films, obtained by heating amorphous films to 600 C. Substrate cleaning was found to be most effective in producing a reproducible surface upon oxygen RF plasma treatment. The Fe nucleation and growth process was found to depend strongly on the type of substrate surface and deposition conditions. Ar ion bombardment under beam flooding,

and subsequent annealing at 650 C was found an effective means to restore the original Al2O3 (1102) surface for renewed Fe deposition. Author

N85-35795*# Jet Propulsion Lab., California Inst. of Tech., Pasadena.
TOTAL INTEGRATED DOSE TESTING OF SOLID-STATE SCIENTIFIC CD4011, CD4013, AND CD4060 DEVICES BY IRRADIATION WITH CO-60 GAMMA RAYS
Armando Roberto V. Dantas, Michael K. Gauthier, and James R. Coss 15 May 1985 60 p
(Contract NAS7-918)
(NASA-CR-176196; JPL-Pub-85-47; NAS 1.26:176196) Avail: NTIS HC A04/MF A01 CSCL 20L

The total integrated dose response of three CMOS devices manufactured by Solid State Scientific has been measured using CO-60 gamma rays. Key parameter measurements were made and compared for each device type. The data show that the CD4011, CD4013, and CD4060 produced by this manufacturers should not be used in any environments where radiation levels might exceed 1,000 rad(Si). Author

N85-35796# Stanford Univ., Calif. Electronics Lab.
LASER AND ELECTRON BEAM PROCESSING OF SEMICONDUCTORS Final Report
J. F. Gibbons Apr. 1985 97 p
(Contract MDA903-81-C-0294)
(AD-A155914) Avail: NTIS HC A05/MF A01 CSCL 20/12

Research carried out under the subject contract was undertaken to explore the potential of scanning CW beam sources for annealing ion implanted layers in silicon and for recrystallizing thin films of silicon deposited on insulators for subsequent use as layers for device fabrication. This research was a continuation of work begun under a previous DARPA contract in which a CW laser beam was the principal tool. Exploration of several different problems and approaches was undertaken in the research reported here to map out the potential of beam processing for IC and VLSI applications. The principal results are contained in a series of thirteen papers. GRA

N85-35797# California Univ., Los Angeles.
ELECTRONIC STRUCTURE AND LATTICE DYNAMICS OF DIMENSIONALLY CONSTRAINED AND DISORDERED SOLIDS Final Report, 1 Sep. 1981 - 28 Feb. 1985
R. Braunstein 28 Feb. 1985 286 p
(Contract DAAG29-81-K-0164)
(AD-A155927; ARO-17826.19-PH) Avail: NTIS HC A13/MF A01 CSCL 20/12

The techniques of infrared modulation, Raman scattering, and photoinduced transients were utilized to study bulk and surface electronic and vibrational properties of metals, insulators, and semiconductors. Results are reported on: optical properties of the surface plasmons of n(+) silicon and copper-Raman and Brillouin scattering and luminiscence studies of alkali borate tungstate glasses wavelength modulation studies of order-disorder effects on the band structure of metal alloys, bulk and surface impurities in alkali halide and alkaline earth fluorides, and deep levels in semiconductors. GRA

N85-35798# Utah Univ., Salt Lake City. Dept. of Physics.
NOISE IN SODIUM BETA ALUMINA CRYSTALS
J. J. Brophy and S. W. Smith Sep. 1985 14 p
(Contract N00014-82-K-0603)
(AD-A156025; AD-E900451; TR-7) Avail: NTIS HC A02/MF A01 CSCL 11/2

Experimental current noise spectra for single crystal sodium beta alumina are essentially identical to those previously reported for polycrystalline ceramic specimens. The measured noise power is proportional to the square of the dc sample current and varies as 1.5/f, which suggests conductivity fluctuations arising from diffusion of the mobile ions. Only a small fraction of the mobile ions appear to participate in the diffusion noise process and the number is thermally activated with an activation energy of 0.8 eV, in agreement with data from ceramic specimens. GRA

N85-35799# Santa Barbara Research Center, Calif.
HgCdTe SURFACE AND DEFECT STUDY PROGRAM Interim Technical Report, Jan. - Jul. 1984
J. A. Wilson, V. A. Cotton, J. A. Silberman, G. P. Carey, and C. K. Shih 1 Jul. 1984 159 p
(Contract MDA903-83-C-0108)
(AD-A156079; RPt50220; ITR-3) Avail: NTIS HC A08/MF A01 CSCL 20/12

This report presents program results for the six-month period ending July 1, 1984. The results presented include determination of the sources of charge at the Photox/HgCdTe interface; measurement and comparison of atomic concentration vs depth and electrical activity due to nuclear stopping for random and channeled implants using SIMS and C-V techniques respectively; evaluation of changes in bulk trapping levels near the processing altered interface by DLTS; identification and evaluation of new trap levels introduced by implantation damage by DLTS; measurement of surface band structure; continued bond length calculations; results of TEM examination of the CdTe/HgCdTe interface; and finally calculations of dislocation energy and hardness. Author (GRA)

N85-35800# California Univ., Santa Barbara. Dept. of Electrical and Computer Engineering.
RESEARCH ON GaSb/AlSb MULTI-QUANTUM WELL SUPERLATTICES Final Report
H. Kroemer Jun. 1985 24 p
(Contract N00014-76-C-1044)
(AD-A156080) Avail: NTIS HC A02/MF A01 CSCL 20/12

Multi-quantum-well Gallium Antimonide/Aluminum Antimonide superlattices (SLs) with well widths ranging from 12 mm down to 1.2 nm were grown by molecular beam epitaxy (MBE), and their photoluminescence (PL) properties were studied. From the photoluminescence data it was concluded that the gamma-valley of the GaSb band structure gets pushed above the L-valleys for well widths below 3.8 nm, rather than already below 9 nm, as was previously thought. For well widths below the direct-to-indirect crossover, the direct-gap luminescence dropped in intensity by over two orders of magnitude, but remained visible down to the narrowest wells studied, with a strength comparable to the (presumably phonon-assisted) weak indirect-gap luminescence originating from the lower L-valleys themselves, which was also clearly observed. The photoluminescence decay times of the direct-gap luminescence increased from less than 1ns in the direct-gap range to about 100 ns in the indirect-gap range, indicating that the direct-gap luminescence in the indirect-gap range cannot be due to primary electrons initially captured by the gamma-valley and surviving there, but must be due to electrons from the lower L-valleys somehow being lifted back up into the gamma-valley. The energies and temperatures involved rule out a thermal re-excitation process, and suggest an Auger-like process, but the details of the latter remain obscure. The indirect-gap luminescence from the L-valleys overlapped with a board luminescence band at lower energies, the origin of which could be traced to the defective wells near the interface between the superlattice and the AlSb buffer layer. It was absent in the remainder of the superlattice. GRA

N85-35801# Naval Postgraduate School, Monterey, Calif.
ELECTRON IRRADIATION OF N TYPE CADMIUM TELLURIDE M.S. Thesis
C. P. Bauer, Jr. Mar. 1985 75 p
(AD-A156117) Avail: NTIS HC A04/MF A01 CSCL 18/8

An experiment is described in which 30 MeV electrons were used to irradiate a sample of cadmium telluride. A brief history of irradiation studies of cadmium telluride is given, followed by the description of the construction of a laboratory used in the taking of Hall measurements and resistivity versus temperature data. The irradiation was performed at the Naval Postgraduate School linear accelerator facility and damage was observed in the CdTe sample

at doses above 10 to the 13th power electrons/sq cm. The sample was held at 100 K for the irradiation. Three results were noted from the Hall and resistivity data. First, the resistivity increased by a factor of two at radiation doses of 10 to the 15th power electrons/sq cm. Secondly, there was a 10% lowering of the electron mobility at 77 K. Finally, possible annealing was seen at 160 K for the 10 to the 13th power electrons/sq cm dose resistivity versus temperature graph. Photoluminescence measurements confirmed the existence of damage by an increase of a broad maximum associated with defects. GRA

N85-35802# Massachusetts Inst. of Tech., Cambridge. National Magnet Lab.

OPTICAL PROPERTIES OF HETEROSTRUCTURES AND SUPERLATTICES Annual Report, 15 Jun. 1984 - 14 Jun. 1985

B. Lax May 1985 39 p

(Contract N00014-84-K-0431)

(AD-A156243) Avail: NTIS HC A03/MF A01 CSCL 20/12

The investigation of the optical properties of heterostructures and quantum wells in semiconductors has produced a number of results of basic and practical importance. Experimental and theoretical studies of luminescence of a single quantum well under laser excitation established exciton transport as the mechanism for providing the electron-hole pairs which recombine within the well. This contradicts previous models of electron hole transport into quantum wells. The significance to heterojunction and quantum well lasers is obviously relevant. GRA

N85-35803# Massachusetts Univ., Amherst. Dept. of Polymer Science and Engineering.

A NEW DRAWING TECHNIQUE FOR NYLON 6 BY REVERSIBLE PLASTICIZATION WITH IODINE Interim Report

H. H. Chuah and R. S. Porter 25 Mar. 1985 29 p

(Contract N00014-83-K-0228)

(AD-A156272; AD-F630668; TR-25) Avail: NTIS HC A03/MF A01 CSCL 11/5

A new method for drawing Nylon 6 has been developed using iodine as a reversible plasticizer. This is based on the ability of the alpha-crystals is fully transform to gamma-crystals by treatment with an aqueous KI3 solution. Drawing is performed on the intermediate Nylon 6-1 complex and iodine is subsequently removed with sodium thiosulfate to generate back a transparent, drawn Nylon 6. At 55 C, a 790% elongation has been obtained, considerably higher than previously reported for Nylon 6. A dynamic mechanical study of the undrawn complex showed an alpha-transition at 41 to 53 C. Above this temperature, it is rubbery and thus readily drawn. GRA

N85-35804# University of Southern California, Los Angeles. Dept. of Materials Science.

INVESTIGATIONS OF THE MOLECULAR BEAM EPITAXIAL GROWTH AND CHARACTERISTICS OF EXTERNAL EXCITATION INDUCED NON-EQUILIBRIUM PHASES OF IMMISCIBLE 3-5 COMPOUND SEMICONDUCTORS Annual Report, 1 Nov. 1983 - 31 Oct. 1984

A. Madhukar 15 Apr. 1985 14 p

(Contract N00014-83-K-0050)

(AD-A156325) Avail: NTIS HC A02/MF A01 CSCL 20/12

This program undertakes experimental and theoretical investigation of the role of growth kinetics and mechanism(s) in molecular beam epitaxial growth of 3 to 5 semiconductors and its possible control via laser excitation to effect metastable structures and phases. The experimental work on laser induced MBE growth is collaboratively carried out. Specifically, progress is reported on: (1) Monte-Carlo computer simulations of MBE growth and predictions of the dynamics of reflection-high-energy-electron-diffraction (RHEED) intensities, (2) a theory of laser--induced-desorption, (3) Experimental studies of the RHEED intensity dynamics for GaAs/InxGa1-xAs(100) MBE growth, (4) the first realization of GaAs/InAs strained layer structures (with 7.4% lattice mismatch) and transmission electron microscopy studies showing high quality interfaces, and (5) establishment of a facility for magneto-absorption studies. GRA

N85-35805# Oak Ridge National Lab., Tenn. Physics Div.

MULTIPLE VACANCY PRODUCTION BY HIGH ENERGY HEAVY IONS

Richard L. Becker, A. L. Ford (Texas A&M Univ., College Station), and J. F. Reading (Texas A&M Univ., College Station) 1984 15 p refs Presented at the 2nd Workshop on High Energy Ion-Atom Collision Process., Debrecen, Hungary, 27-28 Aug. 1984

(DE85-004428; CONF-8408110-3) Avail: NTIS HC A02/MF A01

The theory of atomic collisions has two ingredients: collision theory and atomic structure theory. The collision theories differ with respect to the collision dynamics and the treatment of the relative motion of the projectile and target nuclei. Multiple vacancy production is a signature for and probe of strong interactions between the projectile and the target electrons. For projectiles of large nuclear charge, the interaction becomes strong enough to give a high probability of multiple vacancy production and a breakdown of perturbation theory. A nonperturbative collision theory is generally available for multiple vacancy production only in the form of the highly numerical coupled channels theory. For special problems analytically tractable models were devised. Along with earlier coupled-channels calculations and first Magnus calculations, this model describes the saturation of PL(0) with Z sub p at fixed impact speed. E.A.K.

N85-35806# Argonne National Lab., Ill. Components Technology Div.

STATE-OF-THE-ART OF SOLID-STATE MOTOR CONTROLLERS

R. A. Jaross, T. P. Mulcahey, and E. R. Koehl Sep. 1984 122 p refs

(TI85-008674; NUREG/CR-4180) Avail: NTIS HC A06/MF A01

The state-of-the-art of solid-state motor controllers (SSMCs) is assessed in terms of use, probability of Class 1E qualification, failure rate experience, and reliability prediction. Surveys of commercial availability, nuclear and nonnuclear electric utility experience, and architect-engineering use were made relative to the suitability of SSMCs for nuclear service. Reasons for the limited use of SSMCs in nuclear plants are given. Available failure rate data are meager, and are augmented by data on other solid-state power electronic devices that are shown to have subcomponents similar to those found in SSMCs. In addition to large nonnuclear solid-state adjustable-speed motor drives, the reliability of nuclear plant inverter systems and high-voltage solid-state DC transmission line converters is assessed. Class 1E environmental qualification experience with nuclear plant converter/inverters and battery chargers is shown to be directly applicable to SSMCs. DOE

N85-35807# Fermi National Accelerator Lab., Batavia, Ill.

DESIGN CONSIDERATIONS FOR PERSONNEL ACCESS PENETRATIONS FOR THE SUPERCONDUCTING SUPER COLLIDER

J. D. Cossairt Apr. 1985 13 p refs

(Contract DE-AC02-76CH-03000)

(DE85-013027; FNAL-TM-1307) Avail: NTIS HC A02/MF A01

The detailed design of the tunnel for the supersonic supercollider (SSC) are considered. Considerations concerning the design of the radiological shielding for personnel access labyrinths are documented. A conceptual design is presented which will provide the required amount of protection for use of the SSC both as a pure collider and as an accelerator used for a fixed-target experimental program. A recipe will be developed which will allow designers to adjust these calculations for small deviations from this conceptual design. DOE

N85-35808# Sandia Labs., Albuquerque, N. Mex.

SIMULATION OF LATTICE DAMAGE DUE TO DYNAMIC LOADING

R. A. Taylor and B. W. Dodson 1985 10 p refs Presented at Am. Phys. Soc. Topical Conf. on Shock Waves in Condensed Matter, Spokane, Wash., 22 Jul. 1985

(Contract DE-AC04-76DP-00789)

(DE85-008468; SAND-85-0391C; CONF-850736-1) Avail: NTIS HC A02/MF A01

By means of a dynamic simulation technique based upon the Monte Carlo method, the response of two-dimensional Lennard-Jones lattice systems to dynamic uniaxial strain paths that are either fast or slow with respect to a lattice equilibration time were investigated. The simulation of lattice response to various compression-release cycles indicates a dependence of the degree of sustained lattice damage (i.e., dislocations and defects) on the rate and maximum amplitude of applied strain. Specifically, greater lattice damage is predicted whenever the lattice is subjected to a fast-loading process and/or higher maximum strain amplitude as compared to that induced by a slow-loading process and/or lower maximum strain amplitude. DOE

N85-35809# Oak Ridge National Lab., Tenn.
IONIC CRYSTALS
G. D. Mahan Mar. 1985 26 p refs Presented at the 2nd Petra School, Amman, Jordan, Sep. 1983
(Contract DE-AC05-84OR-21400)
(DE85-009482; DOE/OR-21400/T147) Avail: NTIS HC A03/MF A01

The theory of ionic crystals such as the alkali halides is discussed. The general topics include a discussion of: the local electric fields, multipole polarizability, core level spectra, and electron energy levels. A good theory of crystal structure, since microscopic forces are not well characterized, is still not available. One concludes that other quantities which depend upon forces, such as the elastic constants, are also not well understood, although theories of them are published all of the time. A good theory of bonding is also not available. Here there are two camps: one which regards the bonding as ionic, while the other advocates significant amounts of covalency. Recently it was shown that both the elastic constants, and the amount of covalent bonding, depend significantly upon the higher multipole polarizabilities. DOE

77 THERMODYNAMICS AND STATISTICAL PHYSICS

Includes quantum mechanics; and Bose and Fermi statistics.

For related information see also *25 Inorganic and Physical Chemistry* and *34 Fluid Mechanics and Heat Transfer.*

No abstracts in this category.

80 SOCIAL SCIENCES (GENERAL)

Includes educational matters.

No abstracts in this category.

81 ADMINISTRATION AND MANAGEMENT

Includes management planning and research.

N85-35810# DOD Product Engineering Services Office, Alexandria, Va.
DOD VALUE ENGINEERING CONFERENCE REPORT. VALUE ENGINEERING (VE): A TOOL THAT BENEFITS LINE MANAGEMENT HELD AT LEESBURG, VIRGINIA ON 1-2 NOVEMBER 1984. PART 1. EXECUTIVE SUMMARY
G. Frank and L. Paulson Jun. 1985 17 p Conf. held at Leesburg, Va., 1-2 Nov. 1984
(AD-A156067) Avail: NTIS HC A02/MF A01 CSCL 05/1

This Conference Report summarizes and consolidates the proceedings from the 1984 DOD Value Engineering Conference held 1 through 2 November in Leesburg, VA. The findings and recommendations with supporting material from the five workshops are provided in addition to the complete plenary session presentations. An Executive Summary is presented in Part 1. Proposed actions include: Up-Front Funding, VECP Processing Time, VECP Approval/Disapproval, VE Training, Improvement of Communication, Accounting for VE Savings, and VE as Performance Review Item GRA

N85-35811# DOD Product Engineering Services Office, Alexandria, Va.
DOD VALUE ENGINEERING CONFERENCE REPORT. VALUE ENGINEERING (VE): A TOOL THAT BENEFITS LINE MANAGEMENT HELD AT LEESBURG, VIRGINIA ON 1-2 NOVEMBER 1984. PART 2. PLENARY SESSION
G. Frank and L. Paulson Jun. 1985 246 p Conf. held at Leesburg, Va., 1-2 Nov. 1984
(AD-A156068) Avail: NTIS HC A11/MF A01 CSCL 05/1

This Conference Report summarizes and consolidates the proceedings from the 1984 DOD Value Engineering Conference held 1 through 2 November in Leesburg, VA. The findings and recommendations with supporting material from the five workshops are provided in addition to the complete plenary session presentations. An Executive Summary is presented in Part 1. Plenary Session: Moving Value Engineering Conference, The Hughes Aircraft Company Approach to Value Engineering, E-3A Value Engineering, FMC Value Engineering Program, FAR/DoD FAR Supplement, VECPs - the IG View, Collateral Savings - The Real Challenge, Where's the Map?, and A Value Engineering Coordinator's Preception of the DOD Value Engineering Program. GRA

N85-35812# DOD Product Engineering Services Office, Alexandria, Va.
DOD VALUE ENGINEERING CONFERENCE REPORT. VALUE ENGINEERING (VE): A TOOL THAT BENEFITS LINE MANAGEMENT. PART 3, WORKSHOP A: VE IN THE PROGRAM OFFICE
G. Frank and L. Paulson Jun. 1985 39 p Workshop held at Leesburg, Va., 1-2 Nov. 1984 7 Vol.
(AD-A156069) Avail: NTIS HC A03/MF A01 CSCL 05/1

Part 3 of the 1984 DOD Value Engineering (VE) Conference held 1 to 2 November in Leesburg, Va., included reports on VE Program Managers and 'VE and the R&D Engineer.' The first of these exhorts the VE manager to make vigorous use of VE methodology to reduce defense expenditures in this area of operation. The second report recommends that the R&D Engineer share in the savings brought about through the implementation of VE. F.M.R.

N85-35813# DOD Product Engineering Services Office, Alexandria, Va.
DOD VALUE ENGINEERING CONFERENCE REPORT. VALUE ENGINEERING (VE): A TOOL THAT BENEFITS LINE MANAGEMENT. PART 4, WORKSHOP B: VE ON SPARE PARTS
G. Frank and L. Paulson Jun. 1985 190 p Workshop held at Leesburg, Va., 1-2 Nov. 1984 7 Vol.
(AD-A156070) Avail: NTIS HC A09/MF A01 CSCL 05/1

Part 4 of the 1984 DOD Value Engineering, (VE) Conference held 1 to 2 Nov. in Leesburg, Va., included the following papers concerning the procurement and utilization of spare parts: Talking Paper on Spare Parts; Spare Parts Acquisition; Buy Our Spare Parts Smart (BOSS); Contracting and Manufacturing; DLA Value Engineering and Competition; Reverse Engineering; Standardization of 400 Volt input Power Cable; and, GIDEP/VEDISARS. F.M.R.

N85-35814# DOD Product Engineering Services Office, Alexandria, Va.
DOD VALUE ENGINEERING CONFERENCE REPORT. VALUE ENGINEERING (VE): A TOOL THAT BENEFITS LINE MANAGEMENT. PART 5, WORKSHOP C: VEP/VECP ADMINISTRATION, NEGOTIATION, AND IMPLEMENTATION

G. Frank and L. Paulson Jun. 1985 24 p Workshop held at Lessburg, Va., 1-2 Nov. 1984 7 Vol.
(AD-A156071) Avail: NTIS HC A02/MF A01 CSCL 05/1

Part 5 of the 1884 DOD Value Engineering (VE) Conference held 1 to 2 Nov. in Leesburg, Va., discussed Value Engineering Program (VEP)/ Value Engineering Change Concept (VECP) Administration, Negotiation, and implementation. The VECP is a proposal from a DOD VE Project Officer that a contractor modify and element of an ongoing defense contract with a view toward reducing the latter's cost to the country. F.M.R.

N85-35815# DOD Product Engineering Services Office, Alexandria, Va.
DOD VALUE ENGINEERING CONFERENCE REPORT. VALUE ENGINEERING (VE): A TOOL THAT BENEFITS LINE MANAGEMENT. PART 6, WORKSHOP D: VE TRAINING-ORIENTATION
G. Frank and L. Paulson Jun. 1985 29 p Workshop held at Leesburg, Va., 1-2 Nov. 1984 7 Vol.
(AD-A156072) Avail: NTIS HC A03/MF A01 CSCL 05/1

This Conference Report summarizes and consolidates the proceedings from the 1984 DoD Value Engineering Conference held 1 to 2 November in Leesburg, VA. The findings and recommendations with supporting material from the five workshops are provided in addition to the complete plenary session presentations. An Executive Summary is presented in Part 1. Part 6-Workshop D: VE Training/Orientation. GRA

N85-35816# DOD Product Engineering Services Office, Alexandria, Va.
DOD VALUE ENGINEERING CONFERENCE REPORT. VALUE ENGINEERING (VE): A TOOL THAT BENEFITS LINE MANAGEMENT. PART 7, WORKSHOP E: VE IN CONSTRUCTION AND ARCHITECT ENGINEER CONTRACTS
G. Frank and L. Paulson Jun. 1985 52 p Workshop held at Leesburg, Va., 1-2 Nov. 1984 7 Vol.
(AD-A156073) Avail: NTIS HC A04/MF A01 CSCL 05/1

This Conference Report summarizes and consolidates the proceedings from the 1984 DoD Value Engineering Conference held 1 to 2 November in Leesburg, VA. The findings and recommendations with supporting material from the five workshops are provided in addition to the complete plenary session presentations. An Executive Summary is presented in Part 1. Part 7-Workshop E: VE in Construction and Architect Engineer Contracts papers include: Value Engineering Program, Scope of Work for Open-End Contract for Value Engineering Services, A/E Restrictions - Things Beyond His Control, DoD Directive 4245.8, FAR 52.248 With Recommended Changes, 1983 Annual Report of the Deputy Assistant Secretary of Defense Installations. GRA

N85-35817# Air Command and Staff Coll., Maxwell AFB, Ala.
AERONAUTICAL SYSTEMS DIVISION MANUFACTURING/ QUALITY ASSURANCE ORIENTATION
W. F. Laessig and A. Laird Apr. 1985 61 p
(AD-A156128; ACSC-85-1535) Avail: NTIS HC A04/MF A01 CSCL 13/8

Aeronautical Systems Division (ASD) Manufacturing/Quality Assurance (Mfg/QA) Orientation (videotape) includes ASD organization, program management team concept, matrix management, generic acquisition milestones with associated Mfg/QA inputs, and general sources of expertise. Intended as an overview to enhance big picture understanding of new Mfg/QA managers. Mfg/QA Orientation for the Mfg/QA Managers (sound-on-slide) expands explanation of Mfg/QA inputs to the request for proposal (RFP), source selection participation, pre/post-award contact reviews and audits, and more specific on additional help. Intended to start the new Mfg/QA manager working. Mfg/QA Orientation for Program Managers (sound-on-slide) provides an overview covering Mfg/QA requirements, expected participation, and potential sources of help covering RFP preparation, source selection, and reviews and audits. GRA

N85-35818# Oak Ridge Associated Universities, Tenn.
ELECTRONIC INFORMATION MANAGEMENT AND PRODUCTIVITY
E. B. Sigmon Apr. 1985 40 p
(Contract DE-AC05-76OR-00033)
(DE85-013362; ORAU/IEA-85-3(M)) Avail: NTIS HC A03/MF A01

Electrification leads to technological advances because its characteristic flexibility and controllability circumvent barriers inherent with other means of delivering energy to processes. Typically, the productivity impacts of electrification occur in two stages: Small gains are realized when the electric technology is directly substituted for the established non-electric technology; larger gains accrue from subsequent reorganization of the production process permitted by the superior flexibility of the electric technology. Electricity's role as an information medium is examined and parallels to its role as an energy medium are found. Electronic information technologies (e.g., robotics and word processing) permit mechanization of complex, low volume tasks formerly too expensive to mechanize. Yet experts expect the greatest gains to come from subsequent linking of individual electronically mechanized tasks into an integrated unit in which information barriers between tasks are largely eliminated. Again, the unique flexibility of electricity leads to technological progress. DOE

N85-35819# Office of Science and Technology, Washington, D.C.
PROGRESS REPORT ON IMPLEMENTING THE RECOMMENDATIONS OF THE WHITE HOUSE SCIENCE COUNCIL'S FEDERAL LABORATORY REVIEW PANEL, VOLUME 1 Summary Report
Jul. 1984 35 p
(PB85-185072) Avail: NTIS HC A03/MF A01 CSCL 14B

The White House Science Council's Federal Laboratory Review Panel looks at Federal laboratory missions, identifies any systemic impediments to performance, and determine whether this Nation is getting the optimum return on its substantial investment in talent and facilities at the Federal laboratories. GRA

N85-35167# European Space Agency, Paris (France).
RESEARCH REPORT PROGRAM OF THE US ARMY IN EUROPE
Siegfried H. Lehnigk *In its* Lectures of a Flight Mech. Conf. (DFVLR-Mitt-83-05) Jul. 1984 p 18-24 Transl. into ENGLISH from "Vortraege eines Flugmechanik-Kolloquiums" rept. DFVLR-Mitt-83-05 DFVLR, Brunswick, Jul. 1983 p 21-27 Original language document was announced as N84-16122 (For primary document see N85-35165 24-02)
Avail: NTIS HC A06/MF A01; original German version available from DFVLR, Cologne DM 39.20

N85-35168# European Space Agency, Paris (France).
NEW TECHNOLOGIES AT THE FOREFRONT OF INDUSTRIAL DEVELOPMENTS
Helmut Ulke *In its* Lectures of a Flight Mech. Conf. (DFVLR-Mitt-83-05) Jul. 1984 p 25-41 Transl. into ENGLISH from Vortraege eines Flugmechanik-Kolloquiums" rept. DFVLR-Mitt-83-05 DFVLR, Brunswick, Jul. 1983 p 29-46 Original language document was announced as N84-16123 (For primary document see N85-35165 24-02)
Avail: NTIS HC A06/MF A01; original German version available from DFVLR, Cologne DM 39.20

82 DOCUMENTATION AND INFORMATION SCIENCE

Includes information storage and retrieval technology; micrography; and library science.

For computer documentation see *61 Computer Programming and Software.*

N85-35820* National Aeronautics and Space Administration, Washington, D. C.
NASA PATENT ABSTRACTS BIBLIOGRAPHY, A CONTINUING

BIBLIOGRAPHY. SECTION 2: INDEXES (SUPPLEMENT 27)
Jul. 1985 472 p
(NASA-SP-7039(27)-Section-2; NAS 1.21:7039(27)-Section-2)
Avail: NTIS HC A20 CSCL 05B

A subject index is provided for over 4300 patents and patent applications for the period May 1969 through June 1985. Additional indexes lists personal authors, corporate authors, contract numbers, NASA case numbers, U.S. patent class numbers, U.S. Patent numbers, and NASA accession numbers. Author

N85-35821 George Washington Univ., Washington, D.C.
DATA PROCESSING PROFESSIONALS AND DP APPLICATION USERS' PERCEPTIONS AND EXPECTATIONS OF OPERATIONAL ROLES OF PERSONS WORKING IN A DP/APPLICATION USER INTERFACE GROUP Ed.D Thesis
Margaret Konzo Wolf 1985 148 p
Avail: Univ. Microfilms Order No. DA8506771

The purpose of this study is to determine the perceptions and role expectations of data processing professionals (DPP) and data processing application users (DPAU) working in a data processing/application user interface (DPAU)/application user interface (DPAU) group in an organization. From two mailings sent to each of the two subpopulations, a total of 349 computer processable questionnaires were received from 213 DPPs and 136 DPAUs. A Likert type scale is used to obtain four grouped responses for each of the 16 technical questions. The four responses corresponds with four points of view related to what DPPs and DPAUs are doing or should be doing in their daily work. It is found that DPAUs have a very low level of perceived competency and a low level of job expectancy and that DPPs have a low level of perceived competency and a high/medium high level of job expected competency. Competency training for DPPs and DPAUs should be developed and required in order to create more effective and efficient DPAU groups in organizations. Dissert. Abstr.

N85-35822# Defence Research Establishment, Ottawa. (Ontario).
LOCAT: A DATA RETRIEVAL PROGRAM
S. Y. Slinn Dec. 1984 77 p
(AD-A156004; DREO-TN-84-30) Avail: NTIS HC A05/MF A01 CSCL 09/2

LOCAT is a program used to facilitate the retrieval of data from the SARSAT Evaluation Facility (SEF) database. It is written using FORTRAN 4X and IMAGE/1000, and is intended to be used on an HP-1000 computer with a RTE IVB operating system. The SEF database was established to process Canadian SARSAT evaluation data collected from various sources including the SARSAT Local User Terminal, the Canadian Mission Control Centre located at CFB Trenton and the Rescue Coordination Centre located across Canada. Because of limitations in the SEF software, which was developed under contract, and in order to address specific evaluation requirements, it was necessary to build a package of software routines to support SARSAT studies. LOCAT was the first of a series of analytical software programs to meet these requirements. This report documents the program LOCAT in terms of the program overview which summarizes the data retrieval criteria and the output files produced, a user's guide which provides instructions on how to run the program, and finally, information on compiling and loading the program in the SEF operating environment. Appendix A contains a sample run and Appendix B documents the LOCAT source code. The SEF database is a time ordered structure containing SARSAT evaluation data from a variety of sources. During operations, SARSAT facilities detect transmissions from Emergency Locator Transmitters (ELTs) or their marine equivalent, the Emergency Position Indicating Radio Beacon (EPIRB), which may have been activated because of an air or marine distress incident. GRA

N85-35823# Naval Research Lab., Washington, D. C.
RECORDS DISPOSAL: A GUIDEBOOK FOR LABORATORY OFFICES
J. A. S. Pitts Apr. 1985 58 p
(AD-A156064; AD-E301677) Avail: NTIS HC A04/MF A01 CSCL 05/2

A guidebook for the disposal of U.S. Government laboratory records includes among the types of temporary or permanent records any that have been produced at goverment expense or on government time. They are to be reviewed periodically by a project manager or other accountable official. The records can be either stored or destroyed. Instructions are given for the separate disposal of the following types of records: general office records; scientific and technical program records; program management records; data and specifications records; technical report files; audiovisual records; and personal files. F.M.R.

N85-35824# Defense Technical Information Center, Alexandria, Va.
SOURCE HEADER LIST, SUPPLEMENT 3 Annual Report, May 1984 - May 1985
J. P. Burrell 1 Jul. 1985 224 p Supersedes AD-A143800; DTIC/TR-84/8
(AD-A156100; DTIC/TR-85/5) Avail: NTIS HC A10/MF A01 CSCL 05/2

This publication is a one volume, alphabetically arranged, compilation of corporate author names by the Defense Technical Information Center since April 1982. It is a supplement to the two volume Source Header List (AD-A115000, AD-A115001). Taken together these three volumes contain all corporate source names in the DTIC database system. Each source name is assigned a 6-digit numeric code for computer input and retrieval purposes plus a 4-digit alphanumeric geopolitical code and an alphanumeric type code. Source names displayed are included as data elements in the Technical Report, Work Unit Information System, Research and Development Program Planning, and Independent Research and Development databases maintained by DTIC. GRA

N85-35825# Defense Technical Information Center, Alexandria, Va.
SOURCE HIERARCHY LIST. VOLUME 1: A THROUGH H Annual Report, Jul. 1984 - Jun. 1985
J. Beitzell Jul. 1985 843 p Supersedes AD-A143500; DTIC/TR-84/6-Vol-1 2 Vol.
(AD-A156300; DTIC/TR-85/7-Vol-1) Avail: NTIS HC A99/MF A02 CSCL 05/2

This is the first of two volumes of an alphabetical listing of corporate authors as used for announcement of reports received in the Defense Technical Information Center (DTIC). Former names of organization are included and displayed below the current source name used by DTIC. Cross references direct the user for sub-element organizations to the major source level entry where they are also displayed. Major and subhierarchies are provided. This list is used in conjunction with and is not a replacement for DTIC's Source Header List, Volume 1, AD-115000, Volume 11, AD-A115001, and Supplement 3, AD-A156100. It displays only those source names from the source header list for which hierarchical linkages are pertinent. GRA

N85-35826# Defense Technical Information Center, Alexandria, Va.
SOURCE HIERARCHY LIST. VOLUME 2: I THROUGH Z Annual Report, Jul. 1984 - Jun. 1985
J. Beitzell Jul. 1985 858 p Supersedes Rept. no. DTIC/TR/84/6-VOL-2; AD-A143501 2 Vol.
(AD-A156301; DTIC/TR-85/7-Vol-2) Avail: NTIS HC A99/MF A02 CSCL 05/2

This is the second of two volumes of an alphabetical listing of corporate authors as used for announcement of reports received in the Defense Technical Information Center (DTIC). former names of organization are included and displayed below the current source name used by DTIC. Cross references direct the user from sub-element organizations to the major source level entry where they are also displayed. Major and sub-hierarchies are preceded and ended by a row of asterisks. This list is used in conjunction with and is not a replacement for DTIC's Source Header List, Volume 1, AD-115000, Volume 2, AD-A115001, and Supplement 3, AD-A156100. It displays only those source names from the

Source Header List for which hierarchical linkages are pertinent.
Author (GRA)

N85-35827# National Bureau of Standards, Gaithersburg, Md. Center for Fire Research.
FIRE RESEARCH PUBLICATIONS, 1984 Final Report
N. H. Jason May 1985 20 p
(PB85-208502; NBSIR-85/3153) Avail: NTIS HC A02/MF A01 CSCL 21B

Fire Research Publications (1984) is a supplement to previous editions. Information about earlier editions is available upon request. In a departure from the usual practice of citing only publications prepared by the Center for Fire Research (CFR) staff, by other National Bureau of Standards (NBS) personnel for CFR, or by external laboratories under contract or grant from the CFR, include are papers presented at the Howard Emmons' Conference, Fire Science for Safety. The CFR devoted its 1983 Annual Conference to invited papers on subject areas that have been significantly influenced by Professor Emmons and his students. The Conference was held at NBS in Gaithersburg, MD, August 23 to 24, 1983. Selected papers have been published in a special issue of Combustion Science and Technology, Vol. 39 to 40, 1984 and are cited herein. GRA

N85-35828# Computer Sciences Corp., Gulf Breeze, Fla.
EPALIT: A DATA MANAGEMENT SYSTEM APPLIED TO THE CONTROL AND RETRIEVAL OF TECHNICAL REPORTS
S. M. Means 1985 20 p refs
(Contract EPA-68-01-6639-236)
(PB85-193068; EPA-600/D-85-085) Avail: NTIS HC A02/MF A01 CSCL 05B

The EPALIT data management system is used by the EPA Environmental Research Laboratory, Gulf Breeze, FL, to preserve and manipulate information in text atabases. EPALIT provides the logical resources for data organization, analysis, and retrieval. It is completely interactive and permits natural language searching with full or truncated terms, imbedded word fragments, and Boolean search strings. The library has applied this system to the control and dissemination of its information resources. The Contribution Database, consisting of the laboratory's in-house and extramural publications, is the most sophisticated application to date. EPALIT's features are described in the context of this Contribution Database and its various report formats illustrated. GRA

N85-35459# Geological Survey, Alexandria, Va.
FEDERAL MINERAL LAND INFORMATION SYSTEM Abstract Only
Richard L. Kleckner *In its* USGS Res. on Mineral Resources, 1985 1985 p 65-66 (For primary document see N85-35435 24-42)
Avail: NTIS HC A05/MF A01

83 ECONOMICS AND COST ANALYSIS

Includes cost effectiveness studies.

No abstracts in this category.

84 LAW AND POLITICAL SCIENCE

Includes space law; international law; international cooperation; and patent policy.

N85-35829# Committee on Science and Technology (U. S. House).
THE 1986 NATIONAL AERONAUTICS AND SPACE ADMINISTRATION AUTHORIZATION
Washington GPO 1985 1543 p Hearings before the Subcomm. on Space Sci. and Appl. of the Comm. on Sci. and Technol., 99th Congr., 1st Sess., 6, 19-21, 26, 28 Feb. and 5-7, 26 Mar. 1985 (GPO-47-635) Avail: Subcommittee on Space Science and Applications

On Feb. 6, 1985, Mr. James Beggs, NASA Administrator, presented the 1986 budget for his agency before the Subcommittee of Space Science and Applications of the Committee on Science and Technology, U.S. House of Representatives. The total NASA request is $7.9 billion, of which 2.9 billion is for research and development, 3.5 billion for space flight, control and data communications, 149 million of construction of facilities, and 1.3 billion for research and program management. This budget will provide for solid progress toward the aeronautics and space objectives of the Administration and the Congress. F.M.R.

85 URBAN TECHNOLOGY AND TRANSPORTATION

Includes applications of space technology to urban problems; technology transfer; technology assessment; and surface and mass transportation.

For related information see *03 Air Transportation and Safety, 16 Space Transportation,* and *44 Energy Production and Conversion.*

N85-35830# Applied Physics Lab., Johns Hopkins Univ., Laurel, Md.
NETWORK MANAGEMENT SIMULATION OF AUTOMATED GUIDEWAY TRANSIT SYSTEMS UNDER VEHICLE-FOLLOWER CONTROL Final Report
H. Y. Chiu, D. L. Kershner, and P. J. McEvaddy Oct. 1984 154 p refs
(Contract DOT-UT-90042)
(PB85-188233; JHU/APL/CP-086/TPR/047;
UMTA-MD-06-0047-84-1) Avail: NTIS HC A08/MF A01 CSCL 13F

The use of Automated Guideway Rapid Transit (AGRT) was proposed as a means of alleviating many of the problems associated with conventional transportation modes in urban areas. The concept of AGRT requires the deployment of remotely controlled vehicles in a dedicated guideway network. Many control strategies were proposed to handle the simultaneous longitudinal control of possibly hundreds of these vehicles. One generic approach is vehicle-follower, in which vehicle state information is used to command vehicle spacing and velocity of the immediately following vehicle. The network level behavior of a vehicle-follower approach to longitudinal control in AGRT systems is presented. A computer simulation was developed for the evaluation of station operations, vehicle management techniques, and vehicle-follower longitudinal control algorithms in a full AGRT network context. The simulation was then exercised to investigate the performance characteristics of and interactions among vehicle control, network management, and station models. Author (GRA)

88 SPACE SCIENCES (GENERAL)

No abstracts in this category.

89 ASTRONOMY

Includes radio and gamma-ray astronomy; celestial mechanics; and astrometry.

N85-35831*# National Aeronautics and Space Administration. Ames Research Center, Moffett Field, Calif.
THE STRUCTURE OF HERBIG-HARO OBJECT 43 AND ORION

DARK CLOUD EXTINCTION

Richard D. Schwartz (Missouri Univ., St. Louis), Michael A. Dopita (Australian National Univ.), and Martin Cohen [1984] 32 p refs (NASA-TM-87503; NAS 1.15:87503) Avail: NTIS HC A03/MF A01 CSCL 03A

New ultraviolet and optical observations of Herbig-Haro Object No. 43 are reported. Continuum and emission line fluxes in the range 1250 A equal to or less than lambda equal to less than 7350A have been measured. The continuum fluxes are best matched by an enhanced H two photon component added to H free bound emission, assuming theta Ori extinction curve with E(B-V) = 0.2, R = 5. The strucutre and dynamics of three components within the object are discussed. The object has a radiative output of equal to or greater than 0.23 infrared luminosity in ultraviolet and optical radiation combined. The energy requirements are discussed in terms of the production of shock waves by a collimated, supersonic mass outflow from a nearby infrared source. Author

N85-35832*# National Aeronautics and Space Administration. Ames Research Center, Moffett Field, Calif.

FAR-INFRARED EMISSION LINES OF CO AND OH IN THE ORION-KL MOLECULAR SHOCK

Dan M. Watson (California Univ., Berkeley), R. Genzel (California Univ., Berkeley), C. H. Townes (California Univ., Berkeley), and J. M. V. Storey (New South Wales Univ.) Sep. 1985 37 p refs Submitted for publication

(NASA-TM-86721; Rept-85222; NAS 1.15:86721) Avail: NTIS HC A03/MF A01 CSCL 03A

Observations of far infrared rotational emission lines which arise in the shocked gas associated with Orion-KI are presented, including detections of the CO J = 34 yields 33, J = 31 yields 30, J = 26 yields 25, and OH sup 2 PI sub (3/2) J sup P = 7/2(-) yields 5/2(+) emission lines, as well as improved measurements of the CO J = 22 yields 21 and OH sup 2 PI sub (3/2) J = 5/2 yields 3/2 lines. These lines are observed to have velocity widths of Del V approx. 20 to 30 km/sec, somewhat less than either the 2 micro H sub 2 lines or the high velocity plateau component of the millimeter wave CO lines seen in this object. An H sub 2 column density of approx. 3 x 10 to the 21st power, a total mass of approx. 1 solar mass and characteristic temperature and density T approx. 750 K and approx. 2 x 10 to the 6th power per cu cm can be derived from the CO intensities. The density is too low by at least an order of magnitude for the observed infrared H sub 2 and far infrared CO emission to be accounted for by a purely hydrodynamic shock, and support is lent to hydromagnetic shock models. From the present measurements, the relative abundance of CO is estimated to be CO H sub 2 = 1.2 x .0001, corresponding to 20% of the cosmic abundance of C existing in the form of CO. The average relative abundance of OH in the shocked gas is O/H sub 2 > or = 5 x 10 to the -7th power. An upper limit to the intensity of the HD J = 1 yields 0 line is used to derive an upper limit of tau > or = 3 for the D/H relative abundance in the Orion cloud core. Author

N85-35833*# National Aeronautics and Space Administration. Ames Research Center, Moffett Field, Calif.

OBSERVATIONS OF FAR-INFRARED TRANSITIONS BETWEEN EXCITED STATES OF OH

Paul J. Viscuso (Cornell Univ.), Gordon J. Stacey (Cornell Univ.), Martin Harwit (Cornell Univ.), M. R. Haas (Mycol, Inc., Sunnyvale, Calif.), E. F. Erickson, and P. B. Duffy Sep. 1985 13 p refs Submitted for publication

(NASA-TM-86722; Rept-85223; NAS 1.15:86722) Avail: NTIS HC A02/MF A01 CSCL 03A

In observations of the Kleinmann-Low Nebula were detected of Orion 84.42 and 84.60 micron transitions between the P-2 sub 3/2 and Pi-2 sub 3/2 (J = 5/2) levels of OH with respective fluxes of 1.0 + or - 0.3 to the minus 17th power and 1.4 + or - 0.4 x 10 to the minus 17th power W cm/sq. When compared to 119 micron flux levels of OH and 153 micron flux levels of these radicals by Viscuso, these results suggest appreciable self-absorption of OH line radiation within the Nebula. It is probable that the CO emission due to the J = 31 yields 30 rotational transition at 84.411 micron makes a substantial contribution to the observed 84.42 micron flux, and that it also is at least partially absorbed at the 84.42 micron OH transition frequency. The 88.55 and 88.78 micron (J = 9/2 to 7/2) transitions of CH also were sought, but yielded only to upper limits of < 3 x 10 to the minus 18th power W /sq cm each. A search of W3-IRS5 yields upper limits to the 84.42 micron OH and 87.19 micron CO (J = 30 to 29) transitions of < 2 x 10 minus 18th power W cm/2. E.A.K.

N85-35834*# National Aeronautics and Space Administration. Ames Research Center, Moffett Field, Calif.

FAR-INFRARED OBSERVATIONS OF YOUNG CLUSTERS EMBEDDED IN THE R CORONAE AUSTRINAE AND RHO OPHIUCHI DARK CLOUDS

B. A. Wilking (Texas Univ., Austin), P. M. Harvey (Texas Univ., Austin), M. Joy (Texas Univ., Austin), A. R. Hyland (Australian National Univ.), and T. J. Jones (Minnesota Univ., Minneapolis) Oct. 1985 41 p refs

(NASA-TM-86681; Rept-85129; NAS 1.15:86681; Preprint-Ser-027) Avail: NTIS HC A03/MF A01 CSCL 03A

Multicolor far infrared maps in two nearby dark clouds, R Coronae Austrinae and rho Ophiuchi, were made in order to investigate the individual contribution of low mass stars to the energetics and dynamics of the surrounding gas and dust. Emission from cool dust associated with five low mass stars in Cr A and four in rho Oph was detected; their far infrared luminosities range from 2 far infrared luminosities L. up to 40 far infrared luminosities. When an estimate of the bolometric luminosity was possible, it was found that typically more than 50% of the star's energy was radiated longward of 20 micrometers. meaningful limits to the far infrared luminosities of an additional eleven association members in Cr A and two in rho Oph were also obtained. The dust optical depth surrounding the star R Cr A appears to be asymmetric and may control the dynamics of the surrounding molecular gas. The implications of the results for the cloud energetics and star formation efficiency in these two clouds are discussed. Author

90 ASTROPHYSICS

Includes cosmology; and interstellar and interplanetary gases and dust.

N85-35835 Wyoming Univ., Laramie.

THE NATURE AND GEOMETRY OF INFRARED REFLECTION NEBULAE Ph.D. Thesis

Michael William Castelaz 1984 129 p

Avail: Univ. Microfilms Order No. DA8508864

Infrared surface brightness maps, and polarimetric images at K (2.2 micrometers) of the objects GSS30 in the Ophiuchus dark cloud, SVS12 in the NGC 1333 dark cloud, and 75N were made with the 2.3m Wyoming Infrared telescope. At H(1.6 micrometers), K, and L(3.4 micrometers), the images of GSS30 show bilobed asymmetric reflection nebulosity, and the images of SVS12 show single-lobed reflection nebulosity. At H and K, W75N shows two separate reflection lobes illuminated by different stars. Hubble's relation states that the observed extent of the reflection nebulosity depends on the apparent brightness of the illuminating star and the limiting magnitude of the image. The apparent K magnitudes derived from Hubble's relation for all three infrared reflection nebulae are brighter than the observed K magnitudes. This is interpreted in terms of obscuring matter which is optically thick along the line of sight to the illuminating star, but optically thin between the star and the nebulosity and along the line of sight to the nebulosity. Dissert. Abstr.

N85-35836 California Inst. of Tech., Pasadena.

CIRCUMSTELLAR SHELLS OF LATE-TYPE STARS: A STUDY AT MILLIMETER AND INFRARED WAVELENGTHS Ph.D. Thesis

Raghvendra Sahai Sahai 1985 149 p

Avail: Univ. Microfilms Order No. DA8508468

An investigation of mass loss envelopes around late type stars concentrating on the high mass loss, carbon rich star IRC 10216 is described. A multitransition study is made of the SIS rotational spectrum from the IRC + 10216 envelope is made. A numerical model to calculate the excitation of molecular rotation and vibration rotation lines in circumstellar envelopes is developed. From fitting the observations, it is found that the (SIS)/H sub 2 abundance in the inner regions of the envelope to be approx. 2.4 x 10 to the -7 power, roughly 100 times smaller than predicted by chemical models. The abundance falls steeply with radius reaching one half the above value at r = 9 x 10 to the 16th power cms. We show that Si, not S depletion is responsible for the low SIS abundance, and that most of the available Si is probably used up in forming SIC grains. An investigation of the inner (r approx. 2 in) envelope of IRC + 10216 is also conducted employing an annular aperture (size 2-3.45 in) to measure extended emission due to resonant scattered photons in the 4.6 micron CO vibration rotation band. Dissert. Abstr.

N85-35837 North Carolina State Univ., Raleigh.
STUDY OF THE PARAMETERS AFFECTING THE COLLAPSE OF A ROTATING PROTOSTELLAR CLOUD Ph.D. Thesis
Chandrasekharan Tiruvannamalai Vanajakshi 1984 239 p
Avail: Univ. Microfilms Order No. DA8507405

The effect of three different processes--turbulent viscosity, initial rotation rates and random fluctuations in initial density and/or velocity fields on the collapse of an isothermal, rotating protostellar cloud was studied using Eulerian hydrodynamics in finite difference approximation and cylindrical coordinates. Specifically, it was desired to see the influence of these processes in the formation of a centrally condensed core which can eventually lead to a single star. It was found that turbulent viscosity enhances the central condensation, reduces ring radius and the ratio of ring density to central density but, except for very large viscous forces where there is a possibility of prevention ring formation, turbulent viscosity does not suppress rings completely. Turbulence also slows the collapse. Random fluctuations in initial density and/or velocity fields slow the collapse and hinder deep collapse. The effects of fluctuations in either the initial density or velocity or both have similar effects. Fluctuations in both lead to even smaller densities at the center than fluctuations in either one of the initial parameters. Dissert. Abstr.

N85-35838 Arizona Univ., Tucson.
THE NATURE AND ORIGIN OF OUTER SOLAR SYSTEM ASTEROIDS FROM REFLECTANCE SPECTROPHOTOMETRY Ph.D. Thesis
Faith Vilas 1984 213 p
Avail: Univ. Microfilms Order No. DA8506962

Narrowband spectrophotometric observations of outer solar system (semi-major axis greater than 3.2 AU) asteroids have been used to investigate the surface compositions of the D- and P-class asteroids in an effort to learn about their origins and formation conditions. Spectra of 20 outer solar system asteroids and 2 main-belt D-class asteroids were obtained using two charge-coupled device (CCD) spectrographs. No mineralogical absorption features were evident. The spectra can be divided into four groups based upon four discrete slopes among the spectra. The slope increases (reddens) with increasing heliocentric distance. All of the asteroids observed are locked in orbits driven by Jupiter's gravitational attraction. The distinct slope changes suggest that these asteroids are the remnants of a gradation in composition of planetesimals in the outer solar system, which were selectively retained in location when other material was lost. Three possible compositions based upon organic polymer materials are discussed. Dissert. Abstr.

N85-35839*# National Aeronautics and Space Administration. Goddard Space Flight Center, Greenbelt, Md.
COMET HALLEY RETURNS: A TEACHERS' GUIDE 1985-1986
Robert D. Chapman and R. Lynn Bondurant 1985 50 p refs
(NASA-EP-197; NAS 1.19:197) Avail: NTIS HC A03/MF A01 CSCL 03B

This booklet has been put together as an aid for teachers in elementary and secondary schools. It is divided into two distinct parts. The first part is a brief tutorial which introduces some of the most important concepts about comets, including their historical significance. A list of selected readings is provided at the end of the booklet. The second part of the booklet contains a number of suggested activities, built around the comet. These include both classroom exercises and carefully described field work to observe the comet. Guidance is provided on where to look for the comet, how to observe it, and to photograph it. B.W.

N85-35840*# Smithsonian Astrophysical Observatory, Cambridge, Mass.
THE HEAO-2 GUEST INVESTIGATOR PROGRAM: NON-LINEAR GROWTH OF INSTABILITIES IN LINE-DRIVEN STELLAR WINDS Semiannual Progess Report, 1 Nov. 1984 - 30 Apr. 1985
George B. Rybicki Aug. 1985 30 p refs
(Grant NAG8-463)
(NASA-CR-176168; NAS 1.26:176168; SAPR-3) Avail: NTIS HC A03/MF A01 CSCL 03B

The linear instability of line-driven stellar winds to take proper account of the dynamical effect of scattered radiation were analyzed. It is found that: (1) the drag effect of the mean scattered radiation does greatly reduce the contribution of scattering lines to the instability at the very base of the wind, but the instability growth rate associated with such lines rapidly increases as the flow moves outward from the base, reaching more than 50% of the growth rate for pure absorption lines within a stellar radius of the surface, and eventually reaching 80% of that rate at large radii; (2) perturbations in the scattered radiation field may be important for the propagation of wind disturbances, but they have little effect on the wind instability; and (3) the contribution of strongly shadowed lines to the wind instability is often reduced compared to that of unshadowed lines, but their overall effect is not one of damping in the outer parts of the wind. It is concluded that, even when all scattering effects are taken into account, the bulk of the flow in a line-driven stellar wind is still highly unstable. E.A.K.

N85-35841*# California Univ., San Diego, La Jolla. Center for Astrophysics and Space Sciences.
[DEVELOPMENT OF OBSERVATIONAL AND INSTRUMENTAL TECHNIQUES IN HARD X-RAY AND MEDIUM ENERGY GAMMA-RAY ASTRONOMY] Final Report
Michael Pelling Sep. 1985 58 p refs
(Grant NGL-05-005-003)
(NASA-CR-176172; NAS 1.26:176172) Avail: NTIS HC A04/MF A01 CSCL 03B

The technical activities, scientific results, related space hardware projects and personnel of the high energy astrophysics program are reported. The development of observational and instrumental techniques in hard X-ray (0.001 to 100 keV) and medium energy gamma-ray (0.1 to 10 MeV) astronomy are examined. Many of these techniques were developed explicitly for use on high altitude balloons where most of the scientific results were obtained. The extensive observational activity using balloons are tabulated. Virtually every research activity will eventually result in a major space hardware development effort. E.A.K.

N85-35842# California Univ., Livermore. Lawrence Livermore Lab.
SOME NUCLEAR DATA NEEDS IN ASTROPHYSICS
G. J. Mathews, R. W. Bauer, S. D. Bloom, R. C. Haight, W. M. Howard, K. Takahashi, and R. A. Ward May 1985 20 p refs Presented at the Intern. Conf. on Nucl. Data for Basic and Appl. Sci., Santa Fe, N. Mex., 13 May 1985
(Contract W-7405-eng-48)
(DE85-012916; UCRL-92672; CONF-850507-20) Avail: NTIS HC A02/MF A01

A number of astrophysical environments and how improved nuclear data could facilitate a better understanding of them is discussed. One area of interest includes proton and alpha-particle reactions with unstable nuclei which are necessary for under-

standing the nucleosynthesis and energy generation in hot hydrogen-burning environments. Efforts underway at LLNL and elsewhere to develop the technology for the measurement of these reaction rates are discussed. Heavy-element nucleosynthesis in the late stages of red-giant stars and supernovae requires a complete network of neutron capture rates and beta-decay rates for nuclei near and far from stability. Experimental and theoretical efforts at LLNL to supply the input data and to model the nucleosynthetic environments will be outlined. Suggestions are made as to which nuclear data are most critical for the various scenarios. DOE

N85-35843# Stanford Linear Accelerator Center, Calif.
HIGH ENERGY RADIATION FROM NEUTRON STARS
M. Ruderman Apr. 1985 17 p refs Presented at the Symp. on Cosmogonical Processes, Boulder, Colo., 25 Mar. 1985 Prepared in cooperation with Columbia Univ., N.Y.
(Contract DE-AC03-76SF-00515)
(DE85-014353; SU-SLAC-PUB-3658; CONF-8503145-2) Avail: NTIS HC A02/MF A01

Topics covered include young rapidly spinning pulsars; static gaps in outer magnetospheres; dynamic gaps in pulsar outer magnetospheres; pulse structure of energetic radiation sustained by outer gap pair production; outer gap radiation, Crab pulsar; outer gap radiation, the Vela pulsar; radioemission; and high energy radiation during the accretion spin up of older neutron stars. DOE

91 LUNAR AND PLANETARY EXPLORATION

Includes planetology; and manned and unmanned flights. For spacecraft design see *18 Spacecraft Design Testing, and Performance.* For space stations see *15 Launch Vehicles and Space Vehicles.*

N85-35844*# Wheaton Coll., Norton, Mass. Dept. of Physics and Astronomy.
THE IONIZATION STRUCTURE OF PLANETARY NEBULAE. PART 4: NGC 7662
Timothy Barker [1985] 39 p refs Sponsored in part by NSF (Grant NsG-5376)
(NASA-CR-176151; NAS 1.26:176151) Avail: NTIS HC A03/MF A01 CSCL 03B

Spectrophotometric observations of emission-line intensities over the spectral range 1400 to 7200 A were made in five positions in the planetary nebula NGC 7662. Standard equations used to correct for the existence of elements in other than the optically observable ionization stages show a consistent and approximate agreement with abundances calculated using ultraviolet lines. The abundances of C and N indicate that some mixing of CNO-processed material into the nebular shell may have occurred in NGC 7662; the low He abundance, however, indicates that little or no He enrichment occurred. The Ar, Ne, and O and S abundances appear to be low. It is suggested that the progenitor to NGC 7662 may have formed out of somewhat metal-poor material. E.A.K.

N85-35845*# California Inst. of Tech., Pasadena. Div. of Geological and Planetary Sciences.
A DYNAMIC MODEL OF VENUS'S GRAVITY FIELD
Walter S. Kiefer, Mark A. Richards, Bradford H. Hager, and Bruce G. Bills (Lunar and Planetary Inst.) Aug. 1984 17 p refs Submitted for publication
(Contract NASw-3389; Grant NAG5-315)
(NASA-CR-176173; NAS 1.26:176173) Avail: NTIS HC A02/MF A01 CSCL 03B

Unlike Earth, long wavelength gravity anomalies and topography correlate well on Venus. Venus's admittance curve from spherical harmonic degree 2 to 18 is inconsistent with either Airy or Pratt isostasy, but is consistent with dynamic support from mantle convection. A model using whole mantle flow and a high viscosity near surface layer overlying a constant viscosity mantle reproduces this admittance curve. On Earth, the effective viscosity deduced from geoid modeling increases by a factor of 300 from the asthenosphere to the lower mantle. These viscosity estimates may be biased by the neglect of lateral variations in mantle viscosity associated with hot plumes and cold subducted slabs. The different effective viscosity profiles for Earth and Venus may reflect their convective styles, with tectonism and mantle heat transport dominated by hot plumes on Venus and by subducted slabs on Earth. Convection at degree 2 appears much stronger on Earth than on Venus. A degree 2 convective structure may be unstable on Venus, but may have been stabilized on Earth by the insulating effects of the Pangean supercontinental assemblage. Author

92 SOLAR PHYSICS

Includes solar activity, solar flares, solar radiation and sunspots.

N85-35846# Texas Univ., Austin. Inst. for Fusion Studies.
CURRENT INTERRUPTION BY DENSITY DEPRESSION
J. S. Wagner, T. Tajima, and S. I. Akasofu (Alaska Univ., Fairbanks) Apr. 1985 25 p
(Contract DE-FG05-80ET-53088)
(DE85-013120; DOE/ET-53088/187; IFSR-187) Avail: NTIS HC A02/MF A01

Using a one dimensional electrostatic particle code, processes associated with current interruption in a collisionless plasma when a density depression is present along the current channel is examined. Current interruption due to double layers was suggested by Alfven and Carlqvist (1967) as a cause of solar flares. At a local density depression, plasma instabilities caused by an electron current flow are accentuated, leading to current disruption. The simulation study encompasses a wide range of the parameters in such a way that under appropriate conditions, both the Alfven and Carlqvist (1967) regime and the Smith and Priest (1972) regime take place. In the latter regime the density depression decays into a stationary structure (ion acoustic layer) which spaws a series of ion acoustic solutions and ion phase space holes travelling upstream. A large inductance of the current circuit tends to enhance the plasma instabilities. DOE

N85-35847# Max-Planck-Inst. fuer Aeronomie, Katlenburg-Lindau (West Germany).
PARALLEL FAST-FORWARD SHOCK WITHIN 1 AU: HELIOS-1 AND 2 OBSERVATIONS
A. K. Richter, K. C. Hsieh (Arizona Univ., Tuscon), H. Rosenbauer, and F. M. Neubauer (Cologne Univ.) 1984 40 p refs Submitted for publication Sponsored by Bundesministerium fuer Forschung und Technologie
(Grant NSF INT-82-05325)
(MPAE-W-79-84-27) Avail: NTIS HC A03

Conditions by which a set of 21 events selected from Helios solar wind data on fast-forward shocks can be considered as parallel in the strict sense of MHD theory were investigated using a very general, adaptive optimization and acceptance scheme to iterate spaceprobe data to the ideal Rankine-Hugoniot conditions for oblique and parallel shocks. Depending on the level of sophistication of this scheme, between 2 and 17 parallel shocks are found. Shock velocity, amplitudes, and normalized amplitudes of the plasma parameters are summarized, and it is shown that their values are comparable with those for oblique fast-mode shocks. With respect to the first critical Mach number 4 subcritical, 6 critical, and 11 supercritical, or, taking also the plasma beta into account, four laminar, eight quasi laminar, and nine turbulent shocks are found; in only 30 % of all cases is the ratio between the preshock electron to proton temperature >1. Author (ESA)

93 SPACE RADIATION

Includes cosmic radiation; and inner and outer Earth's radiation belts.

For biological effects of radiation see *52 Aerospace Medicine*. For theory see *73 Nuclear and High-Energy Physics*.

N85-35848*# National Aeronautics and Space Administration. Goddard Space Flight Center, Greenbelt, Md.

NINETEENTH INTERNATIONAL COSMIC RAY CONFERENCE. HE SESSIONS, VOLUME 6

Frank C. Jones, comp. Washington Aug. 1985 496 p refs Conf. held in La Jolla, Calif., 11-23 Aug. 1985 8 Vol.

(NASA-CP-2376-Vol-6; NAS 1.55:2376-Vol-6) Avail: NTIS HC as boxed set only $200/MF A01 per volume or E99 per entire set CSCL 03B

Papers contributed to the 19th International Cosmic Ray Conference which address high energy interactions and related phenomena are compiled. Particular topic areas include cross sections; particle production; nuclei and nuclear matter; nucleus-nucleus collisions; gamma ray and hadron spectra; C-jets, a-jets, and super families; and emulsion chamber simulations. For individual titles, see N85-35849 through N85-35967.

N85-35849*# New Mexico Univ., Albuquerque. Dept. of Physics and Astronomy.

PROTON-AIR AND PROTON-PROTON CROSS SECTIONS FROM AIR SHOWER DATA

John Linsley *In* NASA. Goddard Space Flight Center 19th Intern. Cosmic Ray Conf., Vol. 6 Aug. 1985 p 1-4 refs (For primary document see N85-35848 24-93)

(HE-1.1-1) Avail: NTIS HC as boxed set only $200/MF A01 per volume or E99 per entire set CSCL 03B

Data on the fluctuations in depth of maximum development of cosmic ray air showers, corrected for the effects of mixed primary composition and shower development fluctuations, yield values of the inelastic proton-air cross section for laboratory energies in the range 10 to the 8th power to 10 to the 10th power GeV. From these values of proton-air cross section, corresponding values of the proton-proton total cross section are derived by means of Glauber theory and geometrical scaling. The resulting values of proton-proton cross section are inconsistent with a well known 1n(2)s extrapolation of ISR data which is consistent with SPS data; they indicate a less rapid rate of increase in the interval 540 < sq root of s < 100000 GeV. Author

N85-35850*# Utah Univ., Salt Lake City. Dept. of Physics.

PROTON-AIR INELASTIC CROSS SECTION AT S(1/2) = 30 TeV

R. M. Baltrusaitis, G. L. Cassiday, R. Cooper, J. W. Elbert, P. R. Gerhardy, S. Ko, E. C. Loh, Y. Mizumoto, P. Sokolsky, and D. Steck *In* NASA. Goddard Space Flight Center 19th Intern. Cosmic Ray Conf., Vol. 6 Aug. 1985 p 5-8 refs (For primary document see N85-35848 24-93)

(Grant NSF PHY-82-01089)

(HE-1.1-2) Avail: NTIS HC as boxed set only $200/MF A01 per volume or E99 per entire set CSCL 03B

The distribution of the maxima of high energy cosmic ray induced extensive air showers in the atmosphere was measured as a function of atmospheric depth. From the exponential tail of this distribution, it was determined that the proton-air inelastic cross section at 30 TeV center-of-mass energy to be 540 + or - 40mb. Author

N85-35851*# Maryland Univ., College Park. Dept. of Physics and Astronomy.

HADRON CROSS SECTIONS AT ULTRA HIGH ENERGIES AND UNITARITY BOUNDS ON DIFFRACTION DISSOCIATION

G. B. Yodh and T. K. Gaisser (Delaware Univ., Newark) *In* NASA. Goddard Space Flight Center 19th Intern. Cosmic Ray Conf., Vol. 6 Aug. 1985 p 9-12 refs Supported in part by NSF and DOE (For primary document see N85-35848 24-93)

(HE-1.1-3) Avail: NTIS HC as boxed set only $200/MF A01 per volume or E99 per entire set CSCL 03B

It was shown that if unitarity bounds on diffractive cross sections are valid at ultra high energies then diffractive dominance models which ascribe the increase in total hadron-hadron cross sections to diffractive processes only are ruled out. Calculations also show that cosmic ray cross sections derived from air shower experiments at ultra high energies clearly rule out models for hadron-hadron cross sections with nat.log ns energy dependence and favor those with nat.log n(2)s variation. Author

N85-35852*# Academy of Sciences of the Armenian SSR, Erivan (USSR).

ON TOTAL CROSS SECTIONS AND SLOPES AT SUPERHIGH ENERGIES

Sh. S. Yeremian and V. M. Zhamkochian *In* NASA. Goddard Space Flight Center 19th Intern. Cosmic Ray Conf., Vol. 6 Aug. 1985 p 13-16 refs (For primary document see N85-35848 24-93)

(HE-1.1-4) Avail: NTIS HC as boxed set only $200/MF A01 per volume or E99 per entire set CSCL 03B

Hadron-hadron and hadron-nucleus interactions are investigated in the framework of the Reggeon field theory with critical and supercritical pomerons and multiple scattering theory. A good agreement is obtained with experimental data on cross sections of proton-proton and proton-nucleus interactions at high energies. Author

N85-35853*# Academy of Sciences of the Armenian SSR, Erivan (USSR).

DETERMINATION OF THE CROSS SECTION OF THE PROTON, PION AND NEUTRON INELASTIC INTERACTION WITH LEAD AND CARBON NUCLEI AT 0.5 - 5.0 TeV ENERGIES (PION EXPERIMENT)

V. V. Avakian, G. V. Karagjozian, E. A. Mamidjanian, M. I. Keropian, R. M. Martirosov, G. G. Ovsepian, and S. O. Sokhoyan *In* NASA. Goddard Space Flight Center 19th Intern. Cosmic Ray Conf., Vol. 6 Aug. 1985 p 17-20 refs (For primary document see N85-35848 24-93)

(HE-1.1-5) Avail: NTIS HC as boxed set only $200/MF A01 per volume or E99 per entire set CSCL 03B

Experimental results on the cross section of the single pion, proton and neutron inelastic interaction with carbon and lead nuclei in the 0.5 to 5.0 TeV energy interval obtained on the PION installation (Mount Aragats, Armenia, 3250 m) are presented. For this purpose the (N pi)/(N p) and inelastic (p Fe)/(pi Fe) ratios measured directly on the installation as well as the calculated inelastic (p A)/(pi A) dependence on the target nucleus atomic numbers were used. Author

N85-35854*# Punjab Univ., Lahore (Pakistan). Centre for High Energy Physics.

P(P BAR)P ELASTIC SCATTERING AND COSMIC RAY DATA

Fazal-e-Aleem and Mohammad Saleem *In* NASA. Goddard Space Flight Center 19th Intern. Cosmic Ray Conf., Vol. 6 Aug. 1985 p 21-24 refs Supported by the Pakistan Science Foundation (For primary document see N85-35848 24-93)

(Contract P-PU/Phys(11/2))

(HE-1.1-6) Avail: NTIS HC as boxed set only $200/MF A01 per volume or E99 per entire set CSCL 03B

It is shown that the total cross section for pp elastic scattering at cosmic ray energies, as well as the total cross section, the slope parameter b(s,t) and the differential cross section for small momentum transfer at ISR and collider energies for p(p)p elastic scattering can be simultaneously fitted by using a simple Regge pole model. The results of this theory is discussed in detail. Author

N85-35855*# Academia Sinica, Beijing (China). Inst. of High Energy Physics.

MEASUREMENT OF INTERACTION CROSS SECTION OF COSMIC RAY Fe NUCLEI (E<4 GeV/N) WITH Al TARGET

G. X. Ren, Y. Z. Zhou, R. Q. Huang, and M. Y. Chen *In* NASA. Goddard Space Flight Center 19th Intern. Cosmic Ray Conf.,

Vol. 6 Aug. 1985 p 25-27 refs (For primary document see N85-35848 24-93)
(HE-1.1-7) Avail: NTIS HC as boxed set only $200/MF A01 per volume or E99 per entire set CSCL 03B

Although the study of relativistic heavy ion interaction encumbered by the low intensities of the incident heavy nuclei in cosmic ray experiments, however, one can use a suitable structure of detector to attain a result with a reasonable accuracy. A cross section value of Fe(E < 4 GeV/N) with Al is presented. CR-39 was used as detector and Al as target. The cross section value is estimated using maximum likelihood method. Author

N85-35856*# Universidade Estadual de Campinas (Brazil). Inst. de Fisica.
HADRON THERMODYNAMICS IN RELATIVISTIC NUCLEAR COLLISIONS
P. Ammiraju *In* NASA. Goddard Space Flight Center 19th Intern. Cosmic Ray Conf., Vol. 6 Aug. 1985 p 28-30 refs (For primary document see N85-35848 24-93)
(HE-1.1-8) Avail: NTIS HC as boxed set only $200/MF A01 per volume or E99 per entire set CSCL 03B

Various phenomenological models based on statistical thermodynamical considerations were used to fit the experimental data at high P sub T to a two temperature distribution. Whether this implies that the two temperatures belong to two different reaction mechanisms, or consequences of Lorentz-contraction factor, or related in a fundamental way to the intrinsic thermodynamics of Space-Time can only be revealed by further theoretical and experimental investigations of high P sub T phenomena in extremely energetic hadron-hadron collisions. Author

N85-35857*# Moscow State Univ. (USSR). Inst. of Nuclear Physics.
ESTIMATION OF THE TOTAL INELASTICITY COEFFICIENT IN INTERACTION OF GREATER THAN OR EQUAL TO 20 TeV HADRONS WITH LEAD
B. L. Kanevsky, I. A. Mikhailova, I. V. Rakobolskaya, and L. G. Sveshnikova *In* NASA. Goddard Space Flight Center 19th Intern. Cosmic Ray Conf., Vol. 6 Aug. 1985 p 31-34 refs (For primary document see N85-35848 24-93)
(HE-1.1-9) Avail: NTIS HC as boxed set only $200/MF A01 per volume or E99 per entire set CSCL 03B

Experimental data on the interaction mean free path of hadrons with energy E > 20 TeV in lead obtained with multilayer X-ray emulsion chambers(XEC) are compared with results of simulation of nuclear-electromagnetic cascades in lead chamber. It is shown that, to explain experimental data, the value of the inelasticity coefficients, < K > .8 should be assumed. Author

N85-35858*# Academy of Sciences (USSR), Moscow. Physical Inst.
THE METHOD FOR THE STUDY OF THE INELASTIC CROSS-SECTION FOR HIGH ENERGY PROTONS BY MEANS OF SHOWER ARRAYS WITH THE LARGE CALORIMETRIC AREA
T. V. Danilova and A. D. Erlykin *In* NASA. Goddard Space Flight Center 19th Intern. Cosmic Ray Conf., Vol. 6 Aug. 1985 p 35-38 refs (For primary document see N85-35848 24-93)
(HE-1.1-11) Avail: NTIS HC as boxed set only $200/MF A01 per volume or E99 per entire set CSCL 03B

Proton initiated showers could be reliably separated from showers initiated by cosmic ray nuclei by means of arrays with large calorimetric area, using distributions of energy fractions for EAS electromagnetic muon and hadron components. Proton initiated showers penetrate deeper into the atmosphere and have relatively lower energy fraction in muons. Distribution of that energy fraction is sensitive to the value of the proton inelastic cross-section. It is shown that the analysis of this distribution let one distinguish between log sup 2 S -rise and log S -rise of the cross-section at energies above 10 to the 15th power eV. Author

N85-35859*# Academy of Sciences (USSR), Moscow. Physical Inst.
ON A POSSIBILITY OF INELASTICITY PARTIAL COEFFICIENT K SUB GAMMA DETERMINATION IN PI C AND PI Pb INTERACTIONS AT 10 TO THE 14TH POWER eV (EXPERIMENT PAMIR 1)
A. S. Borisov, K. V. Cherdyntseva, Z. M. Guseva, V. G. Denisova, A. M. Dunaevsky, E. A. Kanevskaya, V. M. Maximenko, R. A. Nam, S. V. Pashkov, V. S. Puchkov et al *In* NASA. Goddard Space Flight Center 19th Intern. Cosmic Ray Conf., Vol. 6 Aug. 1985 p 39-42 refs (For primary document see N85-35848 24-93)
(HE-1.1-2) Avail: NTIS HC as boxed set only $200/MF A01 per volume or E99 per entire set CSCL 03B

The investigation of hadron-nuclear interactions in Pamir experiment is carried out by means of X-ray emulsion chambers of two types: carbon (C) and lead (Pb). While comparing the results from the chambers of both types it was found a discrepancy in n sub h and E sub h(1)R values. The observed discrepancy in C and Pb chambers is connected with the difference in values of effective coefficients of energy transfer to the soft component K sub eff for C and Pb chambers. Author

N85-35860*# Georgia Univ., Athens. Dept. of Physics.
SINGLE PARTICLE MOMENTUM AND ANGULAR DISTRIBUTIONS IN HADRON-HADRON COLLISIONS AT ULTRAHIGH ENERGIES
T. T. Chou and Ning Yang Chen (State Univ. of New York, Stony Brook) *In* NASA. Goddard Space Flight Center 19th Intern. Cosmic Ray Conf., Vol. 6 Aug. 1985 p 43-46 refs (For primary document see N85-35848 24-93)
(HE-1.2-1) Avail: NTIS HC as boxed set only $200/MF A01 per volume or E99 per entire set CSCL 03B

The forward-backward charged multiplicity distribution (P n sub F, n sub B) of events in the 540 GeV antiproton-proton collider has been extensively studied by the UA5 Collaboration. It was pointed out that the distribution with respect to n = n sub F + n sub B satisfies approximate KNO scaling and that with respect to Z = n sub F - n sub B is binomial. The geometrical model of hadron-hadron collision interprets the large multiplicity fluctuation as due to the widely different nature of collisions at different impact parameters b. For a single impact parameter b, the collision in the geometrical model should exhibit stochastic behavior. This separation of the stochastic and nonstochastic (KNO) aspects of multiparticle production processes gives conceptually a lucid and attractive picture of such collisions, leading to the concept of partition temperature T sub p and the single particle momentum spectrum to be discussed in detail. Author

N85-35861*# Franklin Inst., Newark, Del.
QCD-MOTIVATED DESCRIPTION OF VERY HIGH ENERGY PARTICLE INTERACTIONS
T. K. Gaisser and F. Halzen (Wisconsin Univ., Madison) *In* NASA. Goddard Space Flight Center 19th Intern. Cosmic Ray Conf., Vol. 6 Aug. 1985 p 47-50 refs (For primary document see N85-35848 24-93)
(Contract DE-FG09-84ER-40160; Grant NSF PHY-81-09110-A01)
(HE-1.2-2) Avail: NTIS HC as boxed set only $200/MF A01 per volume or E99 per entire set CSCL 03B

Cross sections for the production of secondaries with large transverse momentum can become comparable to the total cross section in the TeV energy range. It is argued that the onset of this effect is observed at sub TeV energies via an increase of the rapidity distribution near y = 0, an increase of p sub T with energy and, most directly, via a correlation between p sub T and multiplicity. If indeed scaling violations are associated with the hard scattering of partons, then scaling violations are largely confined to the central region and have little effect on cosmic ray data which are sensitive to the forward fragmentation region. Author

N85-35862*# Lodz Univ. (Poland). Inst. of Nuclear Science and Technology.
EMPIRICAL DESCRIPTION OF THE HADRON-HADRON AND HADRON-NUCLEUS INTERACTION AT THE ACCELERATOR ENERGY RANGE
G. Kubiak, J. Szabelski, J. Wdowczyk, J. Kempa, and A. Piotrowska

In NASA. Goddard Space Flight Center 19th Intern. Cosmic Ray Conf., Vol. 6 Aug. 1985 p 51-54 refs (For primary document see N85-35848 24-93)
(HE-1.2-4) Avail: NTIS HC as boxed set only $200/MF A01 per volume or E99 per entire set CSCL 03B

Taking into account several assumptions, a formula is transformed into two expressions for kaon and baryon plus antibaryon production in proton interaction and for pion production in pion interactions. Combining both formulae, expression are obtained for the spectrum of kaons and baryons plus antibaryons produced in the meson interactions. For analysis of the cosmic ray propagation in the atmosphere in actual fact, instead of the formulae for interactions of protons and mesons with protons, formulae appropriate for interactions with air nuclei was used. Using the method outlined among others by Elias et al. (1980) simple corrections were introduced to the derived expressions to account for the fact that the target is an air nucleus. E.R.

N85-35863*# George Mason Univ., Fairfax, Va. Dept. of Physics.
MULTIPLICITY DISTRIBUTIONS IN INTERACTION MODELS USED FOR CASCADE SIMULATIONS Abstract Only
R. W. Ellsworth, T. K. Gaisser (Franklin Inst., Newark, Del.), and Todor Stanev (Franklin Inst., Newark, Del.) *In* NASA. Goddard Space Flight Center 19th Intern. Cosmic Ray Conf., Vol. 6 Aug. 1985 p 55 refs (For primary document see N85-35848 24-93)
(HE-1.2-5) Avail: NTIS HC as boxed set only $200/MF A01 per volume or E99 per entire set CSCL 03B

In cascade simulations, conservation of energy is of paramount importance. It is pointed out that it is possible to construct algorithms in which energies of secondaries are chosen from physically correct distributions in such a way as to conserve energy, and give physically correct multiplicity distributions without further adjustment. The resulting non-Poissonian nature of the distribution and the approximate KNO scaling are related to the large fluctuations in the energy available for pion production and to the detailed shape of the inclusive momentum distribution. Two multiparticle production algorithms are described which have these features. One is the algorithm used in the simulation of C jets, the other is for a hadron-nucleus interaction model used in the calculation of muon and neutrino fluxes. Author

N85-35864*# Maryland Univ., College Park. Dept. of Physics and Astronomy.
SOME REMARKS ABOUT SIMULATION OF COSMIC RAY PHENOMENA WITH USE OF NUCLEAR INTERACTION MODELS BASED ON THE CURRENT SPS PROTON-ANTIPROTON DATA
J. A. Wrotniak (Lodz Univ.) and G. B. Yodh *In* NASA. Goddard Space Flight Center 19th Intern. Cosmic Ray Conf., Vol. 6 Aug. 1985 p 56-59 refs (For primary document see N85-35848 24-93) (Grant NSF PHY-82-07425)
(HE-1.2-6) Avail: NTIS HC as boxed set only $200/MF A01 per volume or E99 per entire set CSCL 03B

The x-y controversy is studied by introducing models with as many features (except for x and y distributions) in common, as possible, to avoid an extrapolation problem, only primary energies of 500 TeV are considered. To prove the point, Monte Carlo simulations are performed of EAS generated by 500 TeV vertical primary protons. Four different nuclear interaction models were used. Two of them are described elsewhere. Two are: (1) Model M-Y00 - with inclusive x and y distributions behaving in a scaling way; and (2) Model M-F00 - at and below ISR energies (1 TeV in Lab) exactly equivalent to the above, then gradually changing to provide the distributions in rapidity at 155 TeV as given by SPS proton-antiproton. This was achieved by gradual decrease in the scale unit in x distributions of produced secondaries, as interaction energy increases. Other modifications to the M-Y00 model were made. Author

N85-35865*# Institute of Nuclear Physics, Krakow (Poland).
LOW P SUB T HADRON-NUCLEUS INTERACTIONS
R. Holynski and K. Wozniak *In* NASA. Goddard Space Flight Center 19th Intern. Cosmic Ray Conf., Vol. 6 Aug. 1985 p 60-63 refs (For primary document see N85-35848 24-93)
(HE-1.2-7) Avail: NTIS HC as boxed set only $200/MF A01 per volume or E99 per entire set CSCL 03B

The possibility of describing hadron-nucleus (hA) interactions is discussed in terms of a number of independent collisions of the projectile inside the target nucleus. This multiple rescattering may occur on a particle or quark parton level. To investigate the characteristics of hA interactions as a function of antineutrinos advantage is taken of the correlation between the average number antineutrinos of collisions of the projectile inside the nucleus and the number Ng of fast protons ejected from the struck nucleus. The relation antineutrinos vs Ng obtained in antineutrinos was used. For a given target nucleus this allows the selection of interactions occurring at different impact parameters. Author

N85-35866*# Academy of Sciences of the Armenian SSR, Erivan (USSR).
ANGULAR DISTRIBUTION AND MULTIPLICITY OF BACKWARD HADRONS IN hFe INTERACTIONS AT 0.5-5.0 TeV ENERGIES (PION EXPERIMENT)
V. V. Avakian, M. O. Azarian, K. Sh. Egiyan, E. A. Mamidjanian, G. Zh. Ohanian, and S. V. Ter-Antonian *In* NASA. Goddard Space Flight Center 19th Intern. Cosmic Ray Conf., Vol. 6 Aug. 1985 p 64-67 refs (For primary document see N85-35848 24-93)
(HE-1.2-8) Avail: NTIS HC as boxed set only $200/MF A01 per volume or E99 per entire set CSCL 03B

Based on the analysis of approximates 5 X 1000 events registered on the PION installation, data are obtained on the angular distribution and multiplicity of particles, flying back into the laboratory coordinate system (LCS) that are identified mainly as hadrons produced in the reactions of hFe yield h prime X type. The inclusively produced hadron energy is $>$ 200 MeV. The experimental data are compared to the results of the cumulative particle production in hA processes observed on accelerators at lower energies. Author

N85-35867*# Waseda Univ., Tokyo (Japan).
A TEST OF THE FEYNMAN SCALING IN THE FRAGMENTATION REGION
T. Doke, V. Innocente (Naples Univ.), K. Kasahara (Tokyo Univ.), J. Kikuchi, T. Kashiwagi, S. Lanzano (Naples Univ.), K. Masuda, H. Murakami (Rikkyo Univ.), Y. Muraki (Tokyo Univ.), and T. Nakada (SIN, Villingen, Switzerland) *In* NASA. Goddard Space Flight Center 19th Intern. Cosmic Ray Conf., Vol. 6 Aug. 1985 p 68-71 refs (For primary document see N85-35848 24-93)
(HE-1.2-9) Avail: NTIS HC as boxed set only $200/MF A01 per volume or E99 per entire set CSCL 03B

The result of the direct measurement of the fragmentation region will be presented. The result will be obtained at the CERN proton-antiproton collider, being exposured the Silicon calorimeters inside beam pipe. This experiment clarifies a long riddle of cosmic ray physics, whether the Feynman scaling does villate at the fragmentation region or the Iron component is increasing at 10 to the 15th power eV. Author

N85-35868*# Korea Univ., Seoul. Dept. of Physics.
ANGULAR DISTRIBUTION OF SHOWER PARTICLES PRODUCED IN THE COLLISIONS OF 20-GeV/c and 300-GeV NEGATIVE PIONS WITH EMULSION NUCLEI
C. O. Kim, S. N. Kim, I. G. Park, and C. S. Yoon *In* NASA. Goddard Space Flight Center 19th Intern. Cosmic Ray Conf., Vol. 6 Aug. 1983 p 72-75 refs Sponsored in part by the Korea Science and Engineering Foundation (For primary document see N85-35848 24-93)
Avail: NTIS HC as boxed set only $200/MF A01 per volume or E99 per entire set CSCL 03B

For 435 accelerator produced antipions jets of 20 GeV/c and 300 GeV, in nuclear emulsion, eta(theta)'s have been individually calculated for each jet, where eta(theta) is a kinematic parameter introduced in order to approximate the LS (laboratory system) rapidity, eta = arctan h (beta cos theta). By taking further averages by dividing the samples into groupings of the LS energy E sub pi = m cos h eta sub pi N sub h, the number of heavy prongs with

LS velocity beta < 0.7, and n $^{-}$, the number of charged shower particles with LS velocity beta > 0.7, much less than eta (theta) much greater than are obtained. By use of the KNO (Koba-Nielsen-Olesen) scaling variable, xi = n sub s/,n sub s. good fit is found of data to regression function. Author

N85-35869*# National Aeronautics and Space Administration. Marshall Space Flight Center, Huntsville, Ala.
NUCLEON-NUCLEUS INTERACTIONS FROM JACEE
T. H. Burnett (Washington Univ., Seattle), S. Dake (Kobe Univ.), M. Fuki (Okayama Univ. of Science), J. C. Gregory (Alabama Univ., Huntsville), T. Hayashi (Alabama Univ., Huntsville), R. Holynski (Louisiana State Univ.), J. Iwai (Washington Univ., Seattle), W. V. Jones (Louisiana State Univ.), A. Jurak (Louisiana State Univ.), J. J. Lord (Washington Univ., Seattle) et al *In* NASA. Goddard Space Flight Center 19th Intern. Cosmic Ray Conf., Vol. 6 Aug. 1985 p 76-79 refs Sponsored in part by DOE, NSF and JSPS (For primary document see N85-35848 24-93)
Avail: NTIS HC as boxed set only $200/MF A01 per volume or E99 per entire set CSCL 03B

Results on hadron-nucleus interactions from the Japanese-American Cooperation Emulsion Experiment experiment are presented. Angular distributions for charged particles, and angular and transverse momentum spectra for photons have been measured for a sample of events with sigma epsilon sub gamma. Results on central rapidity density and transverse energy flow are discussed. Author

N85-35870*# Academy of Sciences (USSR), Alma-Ata. High Energy Physics Inst.
A UNIFICATION OF THE INTERACTIONS AND THE DIFFRACTIVE PROCESSES
I. A. Kuchin *In* NASA. Goddard Space Flight Center 19th Intern. Cosmic Ray Conf., Vol. 6 Aug. 1985 p 80-83 refs (For primary document see N85-35848 24-93)
Avail: NTIS HC as boxed set only $200/MF A01 per volume or E99 per entire set CSCL 03B

The transition of a number of hadronic process characteristics to a certain universal regime is interpreted as an indication to the early origination of the unification regime of the interactions. Author

N85-35871*# Academy of Sciences (USSR), Alma-Ata. High Energy Physics Inst.
IS THE INELASTIC CHARGE-EXCHANGE CONTRIBUTION CONSTANT AT THE LARGE X AND SUPERHIGH ENERGIES?
J. A. Kuchin *In* NASA. Goddard Space Flight Center 19th Intern. Cosmic Ray Conf., Vol. 6 Aug. 1985 p 84-87 refs (For primary document see N85-35848 24-93)
Avail: NTIS HC as boxed set only $200/MF A01 per volume or E99 per entire set CSCL 03B

The mechanism explaining the decrease of the inelastic charge-exchange contribution at x approximately equal to I and s yields infinity has been proposed. Author

N85-35872*# Sofia Univ. (Bulgaria). Dept. of Mathematics and Mechanics.
GENERAL CONSEQUENCES OF THE VIOLATED FEYNMAN SCALING
G. Kamberov and L. Popova (Inst. of Nuclear Research and Nuclear Energy) *In* NASA. Goddard Space Flight Center 19th Intern. Cosmic Ray Conf., Vol. 6 Aug. 1985 p 88-91 refs (For primary document see N85-35848 24-93)
Avail: NTIS HC as boxed set only $200/MF A01 per volume or E99 per entire set CSCL 03B

The problem of scaling of the hadronic production cross sections represents an outstanding question in high energy physics especially for interpretation of cosmic ray data. A comprehensive analysis of the accelerator data leads to the conclusion of the existence of breaked Feynman scaling. It was proposed that the Lorentz invariant inclusive cross sections for secondaries of a given type approaches constant in respect to a breaked scaling variable x sub s. Thus, the differential cross sections measured in accelerator energy can be extrapolated to higher cosmic ray energies. This assumption leads to some important consequences. The distribution of secondary multiplicity that follows from the violated Feynman scaling using a similar method of Koba et al is discussed. Author

N85-35873*# Academy of Sciences (USSR), Moscow.
PROPAGATION OF COSMIC RAYS THROUGH THE ATMOSPHERE IN THE QUARK-GLUON STRINGS MODEL
A. D. Erlykin, N. P. Krutikova, and Yu. M. Shabelski (Leningrad Nuclear Physics Inst.) *In* NASA. Goddard Space Flight Center 19th Intern. Cosmic Ray Conf., Vol. 6 Aug. 1985 p 92-95 refs (For primary document see N85-35848 24-93)
Avail: NTIS HC as boxed set only $200/MF A01 per volume or E99 per entire set CSCL 03B

The quark-gluon strings model succeeds in the description of multiple hadron production in the central rapidity region of nucleon-nucleon interctions. This model was developed for hadron-nucleus interactions and used for calculation of the cosmic ray propagation through the atmosphere. It is shown that at energies 10 to the 11th power to the 12th power eV, this model gives a satisfactory description of experimental data. But with the increase of the energy up to approximately 10 to the 14th power eV, results of calculations and of experiments begin to differ and this difference rises with the energy. It may indicate that the scaling violation in the fragmentation region of inclusive spectra for hadron-nucleus interactions is stronger than in the quark-gluon strings model. Author

N85-35874*# Academy of Sciences (USSR), Moscow.
SCALING VIOLATION IN THE FRAGMENTATION REGION OF INCLUSIVE NUCLEON SPEKTRUM
S. K. Machavariani, S. I. Nikolsky, and A. P. Chubenko *In* NASA. Goddard Space Flight Center 19th Intern. Cosmic Ray Conf., Vol. 6 Aug. 1985 p 96-99 refs (For primary document see N85-35848 24-93)
Avail: NTIS HC as boxed set only $200/MF A01 per volume or E99 per entire set CSCL 03B

Spectra of cosmic ray showers associated with hadrons of various energies from 5 to 80 TeV were investigated. Results could be interpreted as scaling violation in the fragmentation region of secondary particles generated in inelastic interactions of primary protons at the energy above 30 TeV. Author

N85-35875*# Minnesota Univ., Minneapolis. School of Physics and Astronomy.
DETERMINATION OF PRIMARY ENERGY IN NUCLEUS-NUCLEUS COLLISIONS AND THE HIGH P(SUB)T TAIL OF ALPHA-PARTICLES
P. S. Freier and T. W. Atwater *In* NASA. Goddard Space Flight Center 19th Intern. Cosmic Ray Conf., Vol. 6 Aug. 1985 p 100-103 refs (For primary document see N85-35848 24-93)
(Grants NGR-24-005-050; NSF PHY-84-05852)
Avail: NTIS HC as boxed set only $200/MF A01 per volume or E99 per entire set CSCL 03B

A determination of primary energy is required in order to study the energy dependence of meson multiplicity in A-A collisions in cosmic rays. Various procedures which estimate the energy of a primary nucleus from its interaction were investigated. An average of two methods were used, one using the pions and wounded protons and the other using spectator protons and alpha particles. The high P sub T tail observed for Z = 2 fragments requires a modification of the latter method. Author

N85-35876*# Minnesota Univ., Minneapolis. School of Physics and Astronomy.
STOPPING RELATIVISTIC Xe, Ho, Au AND U NUCLEI IN NUCLEAR EMULSIONS c73
C. J. Waddington, D. J. Fixsen, and P. S. Freier *In* NASA. Goddard Space Flight Center 19th Intern. Cosmic Ray Conf., Vol. 6 Aug. 1985 p 104-107 refs (For primary document see N85-35848 24-93)

(Grants NGR-24-005-050; NAG8-500; NSF PHY-84-05852)
Avail: NTIS HC as boxed set only $200/MF A01 per volume or E99 per entire set CSCL 18K

Nuclei of Xe-54, Ho-67, Au-79 and U-92 accelerated at the Bevalac to energies between 1200 and 900 MeV/n were stopped in nuclear emulsions. The observed residual ranges were compared with those calculated from various models of energy loss and shown to be most consistent with a calculation that includes those higher order correction terms proposed previously to describe the energy loss of highly charged particles, for which the first Born approximation is not valid. author

N85-35877*# Warsaw Technical Univ. (Poland). Inst. of Physics.
PHYSICAL MEANING OF THE MULTIPLICITIES OF EMITTED NUCLEONS IN HADRON-NUCLEUS COLLISIONS c73
Z. Strugalski *In* NASA. Goddard Space Flight Center 19th Intern. Cosmic Ray Conf., Vol. 6 Aug. 1985 p 108-111 refs (For primary document see N85-35848 24-93)
Avail: NTIS HC as boxed set only $200/MF A01 per volume or E99 per entire set CSCL 18K

The analysis of experimental data on hadron-nucleus collisions at energies from about 2 up to about 400 GeV was performed in order to discover a physical meaning of the multiplicity of emitted nucleons. Simple relations between the multiplicities and the thickness of the nuclear matter layer involved in collisions were obtained. Author

N85-35878*# Warsaw Technical Univ. (Poland). Inst. of Physics.
HOW ARE PARTICLE PRODUCTION, NUCLEON EMISSION AND TARGET FRAGMENT EVAPORATION PROCESSES INTERRELATED IN HADRON-NUCLEUS COLLISIONS? c73
Z. Strugalski *In* NASA. Goddard Space Flight Center 19th Intern. Cosmic Ray Conf., Vol. 6 Aug. 1985 p 112-114 refs (For primary document see N85-35848 24-93)
Avail: NTIS HC as boxed set only $200/MF A01 per volume or E99 per entire set CSCL 18K

Relations between particle production, nucleon emission, and fragment evaporation processes were searched for in hadron-nucleus collisions. It was stated that: (1) the nucleon emission and target fragment evaporation proceed independently of the particle production process; and (2) relation between multiplicities of the emitted protons and of the evaporated charged fragments is expressed by simple formula. Author

N85-35879*# Warsaw Technical Univ. (Poland). Inst. of Physics.
EXPERIMENTAL STUDY OF THE SPACE-TIME DEVELOPMENT OF THE PARTICLE PRODUCTION PROCESS IN HADRON-NUCLEON COLLISIONS, USING MASSIVE TARGET NUCLEUS AS A DETECTOR c73
Z. Strugalski *In* NASA. Goddard Space Flight Center 19th Intern. Cosmic Ray Conf., Vol. 6 Aug. 1985 p 115-116 refs (For primary document see N85-35848 24-93)
Avail: NTIS HC as boxed set only $200/MF A01 per volume or E99 per entire set CSCL 18K

Experimental study of the space-time development of the particle production process in hadronic collisions at its initial stage was performed. Massive target nuclei have been used as fine detectors of properties of the particle production process development within time intervals smaller than 10 to the 22nd power s and spatial distances smaller than 10 to the 12th power cm. In hadron-nucleon collisions, in particular in nucleon-nucleon collisions, the particle production process goes through intermediate objects in 2 yields 2 type endoergic reactions. The objects decay into commonly observed resonances and paricles. Author

N85-35880*# Warsaw Technical Univ. (Poland). Inst. of Physics.
EXPERIMENTAL EVIDENCE OF THE DECREASE OF KINETIC ENERGY OF HADRONS IN PASSING THROUGH ATOMIC NUCLEI c73
Z. Strugalski *In* NASA. Goddard Space Flight Center 19th Intern. Cosmic Ray Conf., Vol. 6 Aug. 1985 p 118-121 refs (For primary document see N85-35848 24-93)
Avail: NTIS HC as boxed set only $200/MF A01 per volume or E99 per entire set CSCL 18K

Hadrons with kinetic energies higher than the pion production threshold lose their kinetic energies monotonically in traversing atomic nuclei, due to the strong interactions in nuclear matter. This phenomenon is a crude analogy to the energy loss of charged particles in their passage through materials. Experimental evidence is presented. Author

N85-35881*# Warsaw Technical Univ. (Poland). Inst. of Physics.
ENERGY-RANGE RELATIONS FOR HADRONS IN NUCLEAR MATTER c73
Z. Strugalski *In* NASA. Goddard Space Flight Center 19th Intern. Cosmic Ray Conf., Vol. 6 Aug. 1985 p 122-124 refs (For primary document see N85-35848 24-93)
Avail: NTIS HC as boxed set only $200/MF A01 per volume or E99 per entire set CSCL 18K

Range-energy relations for hadrons in nuclear matter exist similarly to the range-energy relations for charged particles in materials. When hadrons of GeV kinetic energies collide with atomic nuclei massive enough, events occur in which incident hadron is stopped completely inside the target nucleus without causing particle production - without pion production in particular. The stoppings are always accompanied by intensive emission of nucleons with kinetic energy from about 20 up to about 400 MeV. It was shown experimentally that the mean number of the emitted nucleons is a measure of the mean path in nuclear matter in nucleons on which the incident hadrons are stopped. Author

N85-35882*# Warsaw Technical Univ. (Poland). Inst. of Physics.
SCATTERING AND STOPPING OF HADRONS IN NUCLEAR MATTER c73
Z. Strugalski *In* NASA. Goddard Space Fligt Center 19th Intern. Cosmic Ray Conf., Vol. 6 Aug. 1985 p 125-128 refs (For primary document see N85-35848 24-93)
Avail: NTIS HC as boxed set only $200/MF A01 per volume or E99 per entire set CSCL 18K

It was observed, in the 180 litre xenon bubble chamber, that when hadrons with kinetic energy higher than the pion production threshold fall on a layer of nuclear matter - on an atomic nucleus in other words - in many cases they can pass through it without causing particles production but they are deflected through some deflection angles; if the energy is lower than a few GeV and the nuclear matter layer is thick enough, the hadrons can be stopped in it. The amount of the deflection at a given incident hadron energy varies with the way the hadron strikes the atomic nucleus; the probability of the occurrence of stopping depends on the incident hadron identity and energy, and on the way the hadron passed through the nucleus, as well. Author

N85-35883*# Warsaw Technical Univ. (Poland). Inst. of Physics.
MEASUREMENTS OF HADRON MEAN FREE PATH FOR THE PARTICLE-PRODUCING COLLISIONS IN NUCLEAR MATTER c73
Z. Strugalski *In* NASA. Goddard Space Flight Center 19th Intern. Cosmic Ray Conf., Vol. 6 Aug. 1985 p 129-132 refs (For primary document see N85-35848 24-93)
Avail: NTIS HC as boxed set only $200/MF A01 per volume or E99 per entire set CSCL 18K

It is not obvious a priority that the cross-section for a process in hadron collisions with free nucleons is the same as that for the process in hadron collisions with nucleons inside a target nucleus. The question arises: what is the cross-section for a process in a hadron collision with nucleon on inside the atomic nucleus. The answer to it must be found in experiments. The mean free path for particle-producing collisions of pions in nuclear matter is determined experimentally using pion-xenon nucleus collisions at

3.5 GeV/c momentum. Relation between the mean free path in question lambda sub in nucleons fm squared and the cross-section in units of fm squared/nucleon for collisions of the hadron with free nucleon is: lambda sub i = k/cross section sub i, where k = 3.00 plus or minus 0.26. Author

N85-35884*# National Aeronautics and Space Administration. Marshall Space Flight Center, Huntsville, Ala.
THE PHI-MESON AND CHIRAL-MASS-MESON PRODUCTION IN HEAVY-ION COLLISIONS AS POTENTIAL PROBES OF QUARK-GLUON-PLASMA AND CHIRAL SYMMETRY TRANSITIONS
Y. Takahashi (NAS-NRC) and P. B. Eby *In* NASA. Goddard Space Flight Center 19th Intern. Cosmic Ray Conf., Vol. 6 Aug. 1985 p 133-136 refs (For primary document see N85-35848 24-93)
Avail: NTIS HC as boxed set only $200/MF A01 per volume or E99 per entire set CSCL 03B

Possibilities of observing abundances of phi mesons and narrow hadronic pairs, as results of QGP and Chiral transitions, are considered for nucleus-nucleus interactions. Kinematical requirements in forming close pairs are satisfied in K+K decays of S(975) and delta (980) mesons with small phi, and phi (91020) mesons with large PT, and in pi-pi decays of familiar resonance mesons only in a partially restored chiral symmetry. Gluon-gluon dominance in QGP can enhance phi meson production. High hadronization rates of primordial resonance mesons which form narrow hadronic pairs are not implausible. Past cosmic ray evidences of anomalous phi production and narrow pair abundances are considered.Author

N85-35885*# National Aeronautics and Space Administration. Goddard Space Flight Center, Greenbelt, Md.
SU(2) X U(1) VACUUM AND THE CENTAURO EVENTS
D. Kazanas, V. K. Balasubrahmanyan, and R. E. Streitmatter *In its* 19th Intern. Cosmic Ray Conf., Vol. 6 Aug. 1985 p 137-140 refs (For primary document see N85-35848 24-93)
Avail: NTIS HC as boxed set only $200/MF A01 per volume or E99 per entire set CSCL 03B

It is proposed that the fireballs invoked to explain the Centauro events are bubbles of a metastable superdense state of nuclear matter, created in high energy (E approximately 10 to the 15th power eV) cosmic ray collisions at the top of the atmosphere. If these bubbles are created with a Lorentz factor gamma approximately equals 10 at their CM frame, the objections against the origin of these events in cosmic ray interactions are overcome. A relationship then between their lifetime, tau, and the threshold energy for bubble formation, E sub th, appears to be insensitive to the value of tau and always close to E sub th approximately 10 to 15th power eV. Finally it is speculated that these bubbles might be manifestations of the SU(2) x U(1) false vacuum excited in these collisions. The absence of in the Centauro events is then explained by the decay modes of these excitations. Author

N85-35886*# Rivers State Univ. of Science and Technology, Port Harcourt (Nigeria). Dept. of Physics.
HEAVY FLAVOURS PRODUCTION IN QUARK-GLUON PLASMA FORMED IN HIGH ENERGY NUCLEAR REACTIONS c73
J. Kloskinski *In* NASA. Goddard Space Flight Center 19th Intern. Cosmic Ray Conf., Vol. 6 Aug. 1985 p 141-144 refs (For primary document see N85-35848 24-93)
Avail: NTIS HC as boxed set only $200/MF A01 per volume or E99 per entire set CSCL 18K

Results on compression and temperatures of nuclear fireballs and on relative yield of strange and charmed hadrons are given . The results show that temperatures above 300 MeV and large compressions are unlikely achieved in average heavy ion collision. In consequence, thermal production of charm is low. Strange particle production is, however, substantial and indicates clear temperature - threshold behavior. Author

N85-35887*# Academy of Sciences (USSR), Moscow.
RINGLIKE INELASTIC EVENTS IN COSMIC RAYS AND ACCELERATORS
I. M. Dremin, A. M. Orlov, and M. I. Tretyakova *In* NASA. Goddard Space Flight Center 19th Intern. Cosmic Ray Conf., Vol. 6 Aug. 1985 p 145-148 refs (For primary document see N85-35848 24-93)
Avail: NTIS HC as boxed set only $200/MF A01 per volume or E99 per entire set CSCL 03B

In cosmic rays and in accelerators there were observed single inelastic processes with densely produced (azimuthally isotropic) groups of particles exhibiting spikes in the pseudorapidity plot of an individual event (i.e. ringlike events). Theoretically the existence of such processes was predicted as a consequence of Cerenkov gluon radiation or, more generally, of deconfinement radiation. Nowadays some tens of such events have been accumulated at 400 GeV and at 150 TeV. Analyzing ringlike events in proton-nucleon interactions at 400 GeV/c it is shown that they exhibit striking irregularity in the positions of pseudorapidity spikes' centers which tend to lie mostly at 55,90 and 125 deg in cms. It implies rather small deconfinement lengths of the order of some fermi. Author

N85-35888*# California Univ., La Jolla. Dept. of Physics.
PHASE SPACE FACTORS IN MULTIPARTICLE PROCESSES
Robert J. Gould *In* NASA. Goddard Space Flight Center 19th Intern. Cosmic Ray Conf., Vol. 6 Aug. 1985 p 149-151 refs (For primary document see N85-35848 24-93)
(Grant NGR-05-005-004)
Avail: NTIS HC as boxed set only $200/MF A01 per volume or E99 per entire set CSCL 03B

General phase space theorems are discussed for the cases (A) with only energy conservation applied and (B) with energy and momentum conservation applied. It is shown that in the non-relativistic limit for N particles there is a very close relationship between the multiparticle phase space integral in case B and that for case A and N-1 particles. Author

N85-35889*# National Aeronautics and Space Administration. Marshall Space Flight Center, Huntsville, Ala.
THE RESPONSE OF A SCINTILLATION COUNTER BELOW AN EMULSION CHAMBER TO HEAVY NUCLEUS INTERACTIONS IN THE CHAMBER
T. H. Burnett (Washington Univ., Seattle), S. Dake (Kobe Univ.), J. H. Derrickson, W. F. Fountain, M. Fuki (Okayama Univ. of Science), J. C. Gregory (Alabama Univ., Huntsville), T. Hayashi (Kobe Univ.), T. Hayashi (Alabama Univ., Huntsville), R. Holynski (Louisiana State Univ.), J. Iwai (Washington Univ., Seattle) et al *In* NASA. Goddard Space Flight Center 19th Intern. Cosmic Ray Conf., Vol. 6 Aug. 1985 p 152-155 refs (For primary document see N85-35848 24-93)
Avail: NTIS HC as boxed set only $200/MF A01 per volume or E99 per entire set CSCL 03B

In 1982 a hybrid electronic counter-emulsion chamber experiment was flown on a balloon to study heavy nucleus interactions in the 20 to approximately 100 GeV/AMU energy range. A gas Cerenkov counter, two solid Cerenkov counters, and a proportional counter hodoscope gave the primary energy, the primary charge and the trajectory of the particles, respectively. Using the trajectory information cosmic ray nuclei of $Z > 10$ were found reliably and efficiently, and interaction characteristics of the Fe group nuclei were measured in the chamber. A plastic scintillator below the emulsion chamber responded to showers resulting from interactions in the chamber and to noninteracting nuclei. Data on the response of the counter have been compared with simulations of hadronic-electromagnetic cascades to derive the average neutral energy fraction released by the heavy interactions, and to predict the performance of this kind of counter at higher energies. For the interacting events of highest produced particles multiplicity comparison between various simulations and the shower counter signal have been made. Author

N85-35890*# Tokyo Univ. (Japan). Inst. for Cosmic Ray Research.
HEAVY NUCLEUS COLLISIONS BETWEEN 20 AND 60 GeV/NUCLEON The JACEE Collaboration
T. H. Burnett, S. Dake (Kobe Univ.), M. Fuki (Kobe Univ.), J. C.

Gregory (Alabama Univ., Huntsville), T. Hayashi (Waseda Univ.), R. Holynski (Institute of Nuclear Physics, Krakow, Poland), J. Iwai (Washington Univ., Seattle), W. V. Jones (Louisiana State Univ., Baton Rouge), A. Jurak (Institute of Nuclear Physics, Krakow, Poland), and J. J. Lord (Washington Univ., Seattle) *In* NASA. Goddard Space Flight Center 19th Intern. Cosmic Ray Conf., Vol. 6 Aug. 1985 p 156-159 refs (For primary document see N85-35848 24-93)
(HE-1.4-2) Avail: NTIS HC as boxed set only $200/MF A01 per volume or E99 per entire set CSCL 03B

Interest in studying relativistic nucleus-nucleus interations arises from the fact that they offer an opportunity to probe nuclear matter at high density and temperature. It is expected that under such extreme conditions a transition from hadronic matter into quark-gluon plasma occurs and that in the interactions of highly relativistic nuclei such conditions are created. Cosmic rays remain a unique source of high energy heavy nuclei. The Japanese-American Cooperative Emulsion Experiment (JACEE-3) was designed to study the collisions of heavy cosmic ray nuclei with different nuclear targets at energies beyond 20 GeV/nucleon. JACEE-3 experiment was carried out using a combined electronic counters and an emulsion chamber detector, which was exposed to the cosmic rays on a balloon at an altitude of 5 g/sq cm. B.W.

N85-35891*# National Aeronautics and Space Administration. Marshall Space Flight Center, Huntsville, Ala.
CHARACTERISTICS OF CENTRAL COLLISION EVENTS IN Fe-NUCLEUS INTERACTIONS FOR 20 - 60 GeV/NUCLEON
T. H. Burnett (Washington Univ., Seattle), S. Drake (Kobe Univ.), J. H. Derrickson, W. Fountain, M. Fuki (Okayama Univ.), J. C. Gregory (Alabama Univ., Huntsville), Ta. Hayashi (Alabama Univ., Huntsville), To. Hayashi (Kobe Univ.), R. Holynski (Institute for Nuclear Physics, Krakow, Poland), and J. Iwai (Washington Univ., Seattle) *In* NASA. Goddard Space Flight Center 19th Intern. Cosmic Ray Conf., Vol. 6 Aug. 1985 p 160-163 refs (For primary document see N85-35848 24-93)
(HE-1.4-3) Avail: NTIS HC as boxed set only $200/MF A01 per volume or E99 per entire set CSCL 03B

A counter emulsion hybrid chamber in Japanese-American Cooperative Emulsion Experiment (JACEE-3) was flown on a balloon at the altitude (5.4 g/sq cm) in 1982 with the objective of probing the heavy nuclear collisions above 20 GeV per nucleon. In the energy region, it is suggested that nucleus-nucleus collisions provide dense collisions complex through compression and secondary particle production. In the lower energy region, an evidence of collective flow has been reported. And also, at higher energy region, it has been argued that nucleus has rather large stopping power. In this paper, the high multiplicity characteristics of Fe nucleus central collisions with energies 20 to 50 GeV/nucleon are presented. This is considered to be relevant to compressibility and collective flow of nuclear matter. Author

N85-35892*# National Aeronautics and Space Administration. Marshall Space Flight Center, Huntsville, Ala.
NUCLEUS-NUCLEUS INTERACTION ABOVE SEVERAL HUNDRED GeV/n The JACEE Collaboration
T. H. Burnett (Washington Univ., Seattle), S. Dake (Kobe Univ.), M. Fuki (Okayama Univ. of Science, Japan), J. C. Gregory (Alabama Univ., Huntsville), T. Hayashi (Alabama Univ., Huntsville), R. Holynski (Louisiana State Univ., Huntsville), J. Iwai (Washington Univ., Seattle), W. V. Jones (Osaka Univ.), A. Jurak (Kobe Univ.), J. J. Lord (Tokyo Univ., Japan) et al *In* NASA. Goddard Space Flight Center 19th Intern. Cosmic Ray Conf., Vol. 6 Aug. 1985 p 164-167 refs Sponsored in part by DOE, NSF, Japan Society for the Promotion of Science and Kashma Foundation (For primary document see N85-35848 24-93)
(HE-1.4-4) Avail: NTIS HC as boxed set only $200/MF A01 per volume or E99 per entire set CSCL 03B

The Japanese-American Cooperative Emulsion Experiment (JACEE) have been investigating high energy nuclear interactions of cosmic ray nuclei by means of balloon-borne emulsion chamber. Current exposure parameters are listed. Analysis of the last two experiments (JACEE4 and JACEE5) are still in progress. A result of semi-inclusive analysis of a sample set of central collision events is presented here, concerning multiplicity, rapidity fluctuation for extremely high multiplicity events and correlation between transverse momentum and estimated energy density. B.W.

N85-35893*# National Aeronautics and Space Administration. Marshall Space Flight Center, Huntsville, Ala.
OBSERVATION OF DIRECT HADRONIC PAIRS IN NUCLEUS-NUCLEUS COLLISIONS IN JACEE EMULSION CHAMBERS The JACEE Collaboration
T. H. Burnett (Washington Univ., Seattle), S. Dake (Kobe Univ.), M. Fuki (Okayama Univ. of Science, Japan), J. C. Gregory (Alabama Univ., Huntsville), T. Hayashi (Alabama Univ., Huntsville), T. Hayashi (Kobe Univ.), R. Holynski (Institute of Nuclear Physics, Krakow, Poland), J. Iwai (Washington Univ., Seattle), W. V. Jones (Louisiana State Univ., Baton Rouge), A. Jurak (Institute of Nuclear Physics, Krakow, Poland) et al *In* NASA. Goddard Space Flight Center 19th Intern. Cosmic Ray Conf., Vol. 6 Aug. 1985 p 168-171 refs (For primary document see N85-35848 24-93)
(HE-1.4-5) Avail: NTIS HC as boxed set only $200/MF A01 per volume or E99 per entire set CSCL 03B

In a number of high energy (> or = 1 TeV/amu) nucleus-nucleus collisions observed in Japanese-American Cooperative Emulsion Experiment (JACEE) emulsion chambers, nonrandom spatial association of produced charged particles, mostly hadronic pairs, are observed. Similar narrow pairs are observed in about 100 events at much low energy (20 to 60 GeV/amu). Analysis shows that 30 to 50% of Pair abundances are understood by the Hambury-Brown-Twiss effect, and the remainder seems to require other explanations. Author

N85-35894*# National Aeronautics and Space Administration. Marshall Space Flight Center, Huntsville, Ala.
EXCESSIVE PRODUCTION OF ELECTRON PAIRS BY SOFT PHOTONS IN LOW MULTIPLICITY ION INTERACTIONS The JACEE Collaboration
T. H. Burnett (Washington Univ., Seattle), S. Dake (Kobe Univ.), M. Fuki (Okayama Univ. of Science, Japan), J. C. Gregory (Alabama Univ., Huntsville), T. Hayashi (Alabama Univ., Huntsville), R. Holynski (Institute for Nuclear Physics, Krakow Poland), J. Iwai (Washington Univ., Seattle), W. V. Jones (Louisiana State Univ., Baton Rougee), A. Jurak (Institute for Nuclear Physics, Krakow, Poland), J. J. Lord (Washington Univ., Seattle) et al *In* NASA. Goddard Space Flight Center 19th Intern. Cosmic Ray Conf., Vol. 6 Aug. 1985 p 172-175 refs Sponsored in part by DOE, NSF, Japan Society for the Promotion of Science and Tokyo Univ. (For primary document see N85-35848 24-93)
(HE-1.4-6) Avail: NTIS HC as boxed set only $200/MF A01 per volume or E99 per entire set CSCL 03B

Three multiply charged primary cosmic ray interactions with carbon nuclei are reported, in which the number of materialized electron pairs within a distance of about 0.3 conversion length is larger than predicted from isospin considerations. These are the most energetic (sigma E gamma > 4 TeV) of the low multiplicity (< 15 tracks) events observed in the Japanese-American Cooperative Experiment (JACEE-2) emulsion chamber. B.W.

N85-35895*# Institute of Nuclear Physics, Krakow (Poland).
FORWARD PARTICLE PRODUCTION IN INELASTIC Ne-22 INTERACTIONS IN EMULSION AT 4.1 A Ge/c Ulan-Bator Collaboration c73
In NASA. Goddard Space Flight Center 19th Intern. Cosmic Ray Conf., Vol. 6 Aug. 1985 p 176-179 refs (For primary document see N85-35848 24-93)
(HE-1.4-7) Avail: NTIS HC as boxed set only $200/MF A01 per volume or E99 per entire set CSCL 18K

The collisions of high energy nuclei are likely to be the subject of intense experimental investigation in the near future. The results are presented on multiple meson production in forward cone in inelastic interactions of Ne-22 nuclei in emulsion at a primary momentum 4.1 GeV/c per nucleon. The detailed characteristics of particle production and the fragmentation processes in collisions of Ne-22 nuclei in emulsion are described. Author

N85-35896*# Academy of Sciences (USSR), Alma-Ata. High Energy Physics Inst.
ON THE MECHANISM OF ANOMALOUS NUCLEUS-NUCLEUS INTERACTIONS AT ENERGIES ABOVE 1 TeV/NUCLEON
S. Sh. Ameev and V. L. Shmonin *In* NASA. Goddard Space Flight Center 19th Intern. Cosmic Ray Conf., Vol. 6 Aug. 1985 p 180-183 refs (For primary document see N85-35848 24-93)
(HE-1.4-8) Avail: NTIS HC as boxed set only $200/MF A01 per volume or E99 per entire set CSCL 03B

Two anomalous interactions of cosmic ray nuclei with photo-emulsion nuclei are considered within the framework of the nuclear pionization model. It is shown that the observed regularities of nuclear collisions at the given energy range are satisfactorily reproduced by the model. Author

N85-35897*# Minnesota Univ., Minneapolis. School of Physics and Astronomy.
MESON MULTIPLICITY IN NUCLEUS-NUCLEUS COLLISIONS ABOVE 4 GeV/amu
T. W. Atwater, P. S. Freier, and M. P. Ketzman *In* NASA. Goddard Space Flight Center 19th Intern. Cosmic Ray Conf., Vol. 6 Aug. 1985 p 184-187 refs (For primary document see N85-35848 24-93)
(Grants NGR-24-005-050; NSF PHY-84-05852)
(HE-1.4-10) Avail: NTIS HC as boxed set only $200/MF A01 per volume or E99 per entire set CSCL 03B

Dependence of meson multiplicity on energy for 1486 cosmic ray nucleus-emulsion nucleus interactions is examined. Comparison is made to predictions of the Multi-Chain Model. Author

N85-35898*# Korea Univ., Seoul. Dept. of Physics.
INCLUSIVE ANGULAR DISTRIBUTION OF ALPHA AND LI FRAGMENTS PRODUCED IN THE Fe-C AND Fe-Pb COLLISIONS AT 1.88 GeV/u **c73**
C. O. Kim, S. N. Kim, I. K. Chae (Sookmyung Women's Univ., Seoul, Korea), and D. H. Kim (Sookmyung Women's Univ., Seoul, Korea) *In* NASA. Goddard Space Flight Center 19th Intern. Cosmic Ray Conf., Vol. 6 Aug. 1985 p 188-191 refs Sponsored in part by Korea Science and Engineering Foundation (For primary document see N85-35848 24-93)
(HE-1.4-11) Avail: NTIS HC as boxed set only $200/MF A01 per volume or E99 per entire set CSCL 18K

The LS (laboratory system) emission angles theta for 2188 and 298 Li fragments, produced inclusively in relativistic Fe-C and Fe-Pb collisions, have been measured in reference to incident Fe-ion beam tracks nearby in nuclear emulsion. An empirical differential frequency formula, dN(cot theta) = exp (a + b cot theta)d(cot theta) is obtained with the constant b approx. = -0.026 at 1.88 GeV/u, which seems to be independent on the kinds of target nucleus as well as on the kinds of projectile fragments. B.W.

N85-35899*# Academy of Sciences of the Armenian SSR, Erivan (USSR).
EXPERIMENT PAMIR-3. COPLANAR EMISSION OF HIGH ENERGY GAMMA-QUANTA AT INTERACTION OF HADRONS WITH NUCLEI OF AIR ATOMS AT ENERGIES ABOVE 10 TO THE 7TH POWER GeV **c73**
T. L. Asatiani, L. E. Genina, G. T. Zatsepin (Institute for Nuclear Research, Moscow, USSR) et al *In* NASA. Goddard Space Flight Center 19th Intern. Cosmic Ray Conf., Vol. 6 Aug. 1985 p 192-195 refs (For primary document see N85-35848 24-93)
(HE-1.4-12) Avail: NTIS HC as boxed set only $200/MF A01 per volume or E99 per entire set CSCL 18K

A systematic analysis of large gamma families, detected in X-ray emulsion chambers, cases of multicore halos have been observed, and among them five events in which the halo is divided into three of four separate cores with their alignment observed in the target diagram (coplanarity of axes of corresponding electron photon cascades). The halo alignment (tendency to the straight line) leads to the aximuthal asymmetry (thrust). The analysis of lateral and momentum distributions of particles in these families shows that they also have thrust that correlates with the direction of the halo core alignment. Author

N85-35900*# Moscow State Univ. (USSR). Inst. of Nuclear Physics.
THE EFFECT OF THE RELATIVE NUCLEAR SIZE ON THE NUCLEUS-NUCLEUS INTERACTIONS **c73**
I. N. Erofeeva, V. S. Murzin, S. Yu. Sivoklokov, and L. N. Smirnova *In* NASA. Goddard Space Flight Center 19th Intern. Cosmic Ray Conf., Vol. 6 Aug. 1985 p 196-199 refs (For primary document see N85-35848 24-93)
(HE-1.4-13) Avail: NTIS HC as boxed set only $200/MF A01 per volume or E99 per entire set CSCL 18K

The experimental data on the interactions of light nuclei (d, He(4), C(12)) at the momentum 4.2 GeV/cA with the carbon nuclei were taken in the 2-m propane bubble chamber. The distributions in the number of interacting nucleons, the spectra of protons, the mean energies of secondary pions and protons, the mean fractions of energy transferred to the pion and nucleon components are presented. The results of the investigation of the mechanism of nucleus-nucleus interactions can be used to calculate the nuclear cascades in the atmosphere. Author

N85-35901*# National Aeronautics and Space Administration. Goddard Space Flight Center, Greenbelt, Md.
JAPAN - USSR JOINT EMULSION CHAMBER EXPERIMENT AT PAMIR Japan - USSR Joint Experiment **c73**
In its 19th Intern. Cosmic Ray Conf., Vol. 6 Aug. 1985 p 200-203 refs (For primary document see N85-35848 24-93)
(HE-3.1-1) Avail: NTIS HC as boxed set only $200/MF A01 per volume or E99 per entire set CSCL 18K

The results are presented for the systematic measurement of cosmic ray showers in the first carbon chamber of Japan-USSR joint experiment at Pamir Plateau. The intensity and the energy distribution of electromagnetic particles, of hadrons and of families are in good agreement with the results of other mountain experiment if the relative error in energy estimation is taken into consideration. Author

N85-35902*# Academia Sinica, Beijing (China). Inst. of High Energy Physics.
INTENSITIES OF HIGH-ENERGY COSMIC RAYS AT MOUNT KANBALA
J. R. Ren, H. H. Kuang, A. X. Huo, S. L. Lu, S. Su, Y. X. Wang, Y. G. Xue, C. R. Wang (Shangdong Univ., Jinan, China), M. He (Shangdong Univ., Jinan, China), N. J. Zhang (Shangdong Univ., Jinan, China) et al *In* NASA. Goddard Space Flight Center 19th Intern. Cosmic Ray Conf., Vol. 6 Aug. 1985 p 204-207 refs Sponsored in part by Japanese Ministry of Education (For primary document see N85-35848 24-93)
(HE-3.1-2) Avail: NTIS HC as boxed set only $200/MF A01 per volume or E99 per entire set CSCL 03B

The energy spectra of atmospheric cosmic rays at Mt. Kanbala (520 g/sq cm.) are measured with emulsion chambers. The power indexes of the spectra are values of about 2.0 for both gamma-rays and hadrons. Those fluxes are consistent with the ones expected from the model of primary cosmic rays with heavy nuclei of high content in the energy around 10 to the 15th power eV. Author

N85-35903*# Hirosaki Univ. (Japan).
HIGH ENERGY GAMMA-RAYS AND HADRONS AT MOUNT FUJI
M. Amenomori, H. Nanjo, E. Konishi (Utsunomiya Univ., Japan), N. Hotta (Saitama Univ., Japan), K. Mizutani (Tokyo Univ., Tanashi, Japan), K. Kasahara (Tokyo Univ., Tanashi, Japan), T. Kobayashi (Tokyo Univ., Tanashi, Japan), E. Mikumo (Tokyo Univ., Tanashi, Japan), K. Sato (Tokyo Univ., Tanashi, Japan), T. Yuda (Tokyo Univ., Tanashi, Japan) et al *In* NASA. Goddard Space Flight Center 19th Intern. Cosmic Ray Conf., Vol. 6 Aug. 1985 p 208-211 refs (For primary document see N85-35848 24-93)
(HE-3.1-3) Avail: NTIS HC as boxed set only $200/MF A01 per volume or E99 per entire set CSCL 03B

The energy spectra of high energy gamma-rays and hadrons were obtained by the emulsion chamber with 40 c.u. thickness at Mt. Fuji (3750 m). These results are compared with the Monte Carlo calculation based on the same model which is used in a

family analysis. Our data are compatible with the model of heavy-enriched primary and scaling in the fragmentation region. Author

N85-35904*# Academia Sinica, Beijing (China). Inst. of High Energy Physics.
ON THE CHARACTERISTICS OF EMULSION CHAMBER FAMILY EVENTS PRODUCED IN LOW HEIGHTS
Guru Jing, Cailiu Jing, Qingqi Zhu, and Linkai Ding *In* NASA. Goddard Space Flight Center 19th Intern. Cosmic Ray Conf., Vol. 6 Aug. 1985 p 212-215 refs (For primary document see N85-35848 24-93)
(HE-3.1-6) Avail: NTIS HC as boxed set only $200/MF A01 per volume or E99 per entire set CSCL 03B

The uncertainty of the primary cosmic ray composition at 10 to the 14th power -10 to the 16th power eV is well known to make the study of the nuclear interaction mechanism more difficult. Experimentally considering, if one can identify effectively the family events which are produced in low heights, then an event sample induced by primary protons might be able to be separated. It is undoubtedly very meaningful. In this paper an attempt is made to simulate the family events under the condition of mountain emulsion chamber experiments with a reasonable model. The aim is to search for the dependence of some experimentally observable quantities to the interaction height. Author

N85-35905*# Academy of Sciences of the Georgian SSR, Tbilisi (USSR). Inst. of Physics.
HADRON INTENSITY AND ENERGY SPECTRUM AT 4380 m ABOVE LEVEL **c73**
S. D. Cananov, E. Kh. Chadranyan, L. A. Khizanishvili, N. K. Ladaria, and N. N. Roinishvili *In* NASA. Goddard Space Flight Center 19th Intern. Cosmic Ray Conf., Vol. 6 Aug. 1985 p 216-219 refs (For primary document see N85-35848 24-93)
(HE-3.1-7) Avail: NTIS HC as boxed set only $200/MF A01 per volume or E99 per entire set CSCL 18K

The flux value of hadrons with E (sup gamma) h > or = 5 TeV, where E (sup gamma) h > or = is the energy transferred into electromagnetic component is presented. It is shown that the energy spectrum slope beta of hadrons with E h > or = 20 TeV is equal to 1.9. Author

N85-35906*# Indian Statistical Inst., Calcutta. Physical and Earth Science Div.
SOME CHARACTERISTIC COSMIC RAY EVENTS AND AN ATTEMPT AT THEIR EXPLANATION
S. Bhattacharyya *In* NASA. Goddard Space Flight Center 19th Intern. Cosmic Ray Conf., Vol. 6 Aug. 1985 p 220-223 refs (For primary document see N85-35848 24-93)
(HE-3.1-8) Avail: NTIS HC as boxed set only $200/MF A01 per volume or E99 per entire set CSCL 03B

Some cosmic ray events with very large multiplicities and very high transverse momenta have recently been reported in balloon-borne emulsion chamber experiments. The explanation for these events by the standard approaches has become a bit problematical. An attempt has been made in this paper to understand and interpret them in the light of a dynamical model of multihadron production phenomena with power-law nature of average multiplicity and automatic scale-breaking derived in the model. Author

N85-35907*# Trondheim Univ. (Norway).
THE NUCLEON INTENSITY IN THE ATMOSPHERE AND THE Pt DISTRIBUTION
A. Liland *In* NASA. Goddard Space Flight Center 19th Intern. Cosmic Ray Conf., Vol. 6 Aug. 1985 p 224-227 refs (For primary document see N85-35848 24-93)
(HE-3.1-9) Avail: NTIS HC as boxed set only $200/MF A01 per volume or E99 per entire set CSCL 03B

The diffusion equation for cosmic ray nucleons in the atmosphere has been solved analytically, taking into account the transverse momentum distribution of nucleons produced in nucleon-air nucleus collisions. The effect of the transverse momentum distribution increases the nucleon intensity at large zenith angles and low energies. Author

N85-35908*# Moscow State Univ. (USSR). Inst. of Nuclear Physics.
ENERGY SPECTRA OF PROTON AND NUCLEI OF PRIMARY COSMIC RAYS IN ENERGY REGION > 10 TeV/PARTICLE
K. V. Mandritskaya, G. P. Sazhina, N. V. Sokolskaya, A. Ya. Varkovitskaya, E. A. Zamchalova, and V. I. Zatsepin *In* NASA. Goddard Space Flight Center 19th Intern. Cosmic Ray Conf., Vol. 6 Aug. 1985 p 228-231 (For primary document see N85-35848 24-93)
(HE-3.1-10) Avail: NTIS HC as boxed set only $200/MF A01 per volume or E99 per entire set CSCL 03B

To investigate the chemical composition of primary cosmic rays, several emulsion chambers were exposed at a 10.8 g/sq cm. depth in the stratosphere. Each chamber has the area of 0.92x0.46 sq m. and the depth of 14 c.u. The exposure time of chambers processed by now is 260 hours. The detecting layers were X-ray films and nuclear emulsions, which allowed to measure an energy of cascade and a type of primary particle. Results and techniques are described. B.W.

N85-35909*# National Aeronautics and Space Administration. Goddard Space Flight Center, Greenbelt, Md.
SCALING VIOLATION IN FRAGMENTATION REGION AT ENERGIES ABOVE 10-15 eV BASED ON THE DATA ON COSMIC RAY HADRON COMPONENT Pamir Collaboration
In its 19th Intern. Cosmic Ray Conf., Vol. 6 Aug. 1985 p 232-235 refs (For primary document see N85-35848 24-93)
(HE-3.1-11) Avail: NTIS HC as boxed set only $200/MF A01 per volume or E99 per entire set CSCL 03B

The ratio of intensity of energetic hadrons, having no visible accompaniment, to the total flux of hadrons of the same energy at 4380m above sea level is given. The ratio is much more than expected for scaling model with proton primaries. This result could not be explained by complex chemical composition of primary cosmic ray and indicates the scaling violation in fragmentation region. Author

N85-35910*# Academy of Sciences (USSR), Troitsk. Inst. of Terrestrial Magnetism, Ionosphere and Radio Wave Propagation.
CONNECTION BETWEEN VARIATIONS OF THE ATMOSPHERE TEMPERATURE PROFILE AND VARIATIONS OF THE MESON COMPONENT INTENSITY
Ya. L. Blokh and S. I. Rogovaya *In* NASA. Goddard Space Flight Center 19th Intern. Cosmic Ray Conf., Vol. 6 Aug. 1985 p 236-238 refs (For primary document see N85-35848 24-93)
(HE-3.1-12) Avail: NTIS HC as boxed set only $200/MF A01 per volume or E99 per entire set CSCL 03B

The influence of temperature effects on intensity variations of the cosmic ray meson component were studied. The connection between the temperature variation delta T and the intensity variation delta I was established by using the temperature coefficient density technique. To realize how many devices are needed on the Earth for predicting the temperature variation of the atmosphere profile with a reasonable accuracy, IO isobaric levels and IO were calculated. The set of initial elements of the cosmic ray mesons are varied and it is shown that the matrix of the coefficients B sub ij is rather sensitive to their choice. It is found that if for the calculations of the atmospheric temperature variations the model is used, the number of meson components, essentially exceeding 3, should be considered. E.A.K.

N85-35911*# Kanagawa Univ. (Japan).
HIGH SENSITIVE X-RAY FILMS TO DETECT ELECTRON SHOWERS IN 100 GeV REGION
T. Taira, T. Shirai, N. Tateyama, S. Torii, J. Nishimura (Inst. of Space and Astronautical Science), M. Fujii (Inst. of Space and Astronautical Science), A. Yoshida (Inst. of Space and Astronautical Science), H. Aizu (Kanagawa Prefectural Junior Coll.), Y. Nomura (Kanagawa Prefectural Junior Coll.), M. Kazuno (Toho Univ., Chiba) et al *In* NASA. Goddard Space Flight Center 19th Intern. Cosmic

Ray Conf., Vol. 6 Aug. 1985 p 239-242 refs (For primary document see N85-35848 24-93)
(HE-3.1-13) Avail: NTIS HC as boxed set only $200/MF A01 per volume or E99 per entire set CSCL 03B

Nonscreen type X-ray films were used in emulsion chamber experiments to detect high energy showers in cosmic rays. Ranges of the detection threshold is from about 1 to 2 TeV depending on the exposure conditions. Different types of X-ray films and sheets i.e. high sensitive screen type X-ray films and luminescence sheets were tested. The threshold of the shower detection is found to be about 200 GeV, which is much lower than that of nonscreen type X-ray films. These films are useful to detect showers in the medium energy range, a few hundred GeV, of the cosmic ray electrons. E.A.K.

N85-35912*# Universidade Estadual de Campinas (Brazil).
JETS IN AIR-JET FAMILY
C. E. Navia and K. Sawayanagi *In* NASA. Goddard Space Flight Center 19th Intern. Cosmic Ray Conf., Vol. 6 Aug. 1985 p 243-245 refs Sponsored in part by the 19th ICRC, and by Conselho Nacional de Desenvolvimento Cientifico e Tecnologico-CNPq (For primary document see N85-35848 24-93)
(HE-3.2-1) Avail: NTIS HC as boxed set only $200/MF A01 per volume or E99 per entire set CSCL 03B

The A-jet families on Chacaltaya emulsion chamber experiments were analyzed by the study of jets which are reconstructed by a grouping procedure. It is demonstrated that large-E sub J R sub J events are characterized by small number of jets and two-jet like asymmetric shape, binocular events and the other type. This type has a larger number of jets and more symmetrical shape in the P sub t plane. E.A.K.

N85-35913*# Waseda Univ., Tokyo (Japan). Science and Engineering Research Lab.
SEARCH FOR ANOMALOUS C-JETS IN CHACALTAYA EMULSION CHAMBER EXPERIMENT
H. Kumano *In* NASA. Goddard Space Flight Center 19th Intern. Cosmic Ray Conf., Vol. 6 Aug. 1985 p 246-249 refs (For primary document see N85-35848 24-93)
(HE-3.2-5) Avail: NTIS HC as boxed set only $200/MF A01 per volume or E99 per entire set CSCL 03B

Anomalous C-jets were measured in Chacaltaya emulsion chamber No.17. Measurement of 150 C-jets nuclear interactions occured in the target layer in the chamber itself with total visible energy greater than 5 TeV was completed. they are recorded in area of 11 sq m, corresponding to 17.1 sq m year exposure. Among them, seven events have no pinaught and two events are peculiar in that three showers out of four show abnormal cascade development. Two show remarkable characteristics indicating that they are coming from exotic interactions in the target layer. Illustrations of these events are presented and the thresholds of this type of event are discussed. E.A.K.

N85-35914*# National Aeronautics and Space Administration. Goddard Space Flight Center, Greenbelt, Md.
EXOTIC INTERACTIONS AMONG C-JETS AND Pb-JETS Brasil-Japan Emulsion Chamber Collaboration
In its 19th Intern. Cosmic Ray Conf., Vol. 6 Aug. 1985 p 250-253 refs (For primary document see N85-35848 24-93)
(HE-3.2-6) Avail: NTIS HC as boxed set only $200/MF A01 per volume or E99 per entire set CSCL 03B

The C-jets and Pb-jets were surveyed on the part of Chacaltaya emulsion chamber No.19 amounting to an exposure of 28.8 sq m yr. It is shown that the adopted events make up an unbiased sample of C-jets for sigma sub E gamma > TeV. Mini-Centauro interaction gives the most natural explanation for the eight pinaught-less C-jets with three or more constituent shower core. Out of the eight double-cored pinaught-less events, three are found to have visible invariant masses > 1.8 GeV/c. Three Pb-jets-lower are composed of double cores whose respective visible transverse momenta are greater than 0.5 GeV/c, suggesting that they are of Geminion origin or chiron origin. The energies of the parent particles are estimated to be 100 to 200 TeV for all three kinds of events. The implications of this energy estimate and the frequency of observed exotic events are discussed. E.A.K.

N85-35915*# Academy of Sciences (USSR), Moscow. Inst. of Physics.
X-RAY FILM CHAMBER WITH CARBON TARGET OF TIEN-SHAN COMPLEX ARRAY
K. V. Cherdyntseva, A. P. Chubenko, A. G. Dubovy, N. P. Krutikova, N. M. Nesterova, S. I. Nikolsky, N. M. Nikolskaja, E. I. Tukish, N. G. Vildanov, and T. I. Yakovleva *In* NASA. Goddard Space Flight Center 19th Intern. Cosmic Ray Conf., Vol. 6 Aug. 1985 p 254-257 refs (For primary document see N85-35848 24-93)
Avail: NTIS HC as boxed set only $200/MF A01 per volume or E99 per entire set CSCL 03B

X-ray films were exposed inside the ionization calorimeter under 74g/sq cm of carbon and 5 cm of lead. The X-ray film chamber area is 35 sq. m. Moving X-ray films were used, 50% of the events, which succeeded to determine incidence time, were identified with corresponding extensive air showers (EAS). For such events the size spectrum of associated EAS was derived. Two methods of energy measurement using X-ray films and ionization calorimeter were compared. The energy transfer from selected hadron to electromagnetic component is illustrated. It is found that in cascades with high energy release into electromagnetic components the hadron component is practically absent. E.A.K.

N85-35916*# Academy of Sciences of the Georgian SSR, Tbilisi (USSR). Inst. of Physics.
SCALING VIOLATION IN HADRON-NUCLEUS INTERACTION
Yu. G. Verbetski, L. P. Garsevanishvili, D. M. Kotlyarevski, N. K. Ladaria, N. G. Tatalashvili, P. V. Tsomaya, N. I. Sherer, Yu. M. Shabelski, and G. Z. Stemanetyan *In* NASA. Goddard Space Flight Center 19th Intern. Cosmic Ray Conf., Vol. 6 Aug. 1985 p 258-261 refs (For primary document see N85-35848 24-93)
(HE-3.2-8) Avail: NTIS HC as boxed set only $200/MF A01 per volume or E99 per entire set CSCL 03B

The scaling violation within the pionization region in the energy range of 0.2 to 2.0 TeV is shown on the basis of the analysis of angular characteristics in the interactions of the cosmic radiation hadrons with the nuclei of various substances (CH2, Al, Cu, Pb). E.A.K.

N85-35917*# Academy of Sciences of the Georgian SSR, Tbilisi (USSR). Inst. of Physics.
FEW-PARTICLES GENERATION CHANNELS IN INELASTIC HADRON-NUCLEAR INTERACTIONS AT ENERGY APPROXIMATELY EQUALS 400 GeV
P. V. Tsomaya *In* NASA. Goddard Space Flight Center 19th Intern. Cosmic Ray Conf., Vol. 6 Aug. 1985 p 262-265 refs (For primary document see N85-35848 24-93)
(HE-3.2-9) Avail: NTIS HC as boxed set only $200/MF A01 per volume or E99 per entire set CSCL 03B

The behavior of the few-particles generation channels in interaction of hadrons with nuclei of CH2, Al, Cu and Pb at mean energy 400 GeV was investigated. The values of coherent production cross-sections beta coh at the investigated nuclei are given. A dependence of coherent and noncoherent events is investigated. The results are compared with the simulations on additive quark model (AQM). E.A.K.

N85-35918*# Altai State Univ., Barnaul (USSR).
THE MODEL OF INDEPENDENT PARTICLES EMISSION IN THE MULTIPARTICLE PRODUCTION THEORY
V. V. Uchaikin and V. A. Litvinov *In* NASA. Goddard Space Flight Center 19th Intern. Cosmic Ray Conf., Vol. 6 Aug. 1985 p 266-269 refs (For primary document see N85-35848 24-93)
(HE-3.2-10) Avail: NTIS HC as boxed set only $200/MF A01 per volume or E99 per entire set CSCL 03B

The possibility to obtain the degree dependence of average multiplicity from energy, KNO-scaling and the effect of leading is shown, taking into account the law of energy preservation. E.A.K.

N85-35919*# Moscow State Univ. (USSR). Inst. of Nuclear Physics.
THE MULTIPLICITY AND THE SPECTRA OF SECONDARIES CORRELATED WITH THE LEADING PARTICLE ENERGY c73
N. A. Kruglov, A. S. Proskuryakov, L. I. Sarycheva, and L. N. Smirnova *In* NASA. Goddard Space Flight Center 19th Intern. Cosmic Ray Conf., Vol. 6 Aug. 1985 p 270-273 refs (For primary document see N85-35848 24-93)
(HE-3.2-11) Avail: NTIS HC as boxed set only $200/MF A01 per volume or E99 per entire set CSCL 18K

The spectra of leading particles of different nature in pp-collisions at E sub 0 = 33 GeV are obtained. The multiplicities and the spectra of secondaries, mesons, gamma-quanta, lambda and lambda-hyperons and protons for different leading particle energy ranges are determined. Author

N85-35920*# Academy of Sciences (USSR), Alma-Ata.
CHARACTERISTICS OF ANOMALOUSLY HIGH MULTIPLICITY COSMIC RAY INTERACTIONS
I. Ya. Chasnikov, Yu. A. Eremenko, D. T. Madigozhin, T. Kh. Sadykov, and V. G. Voinov *In* NASA. Goddard Space Flight Center 19th Intern. Cosmic Ray Conf., Vol. 6 Aug. 1985 p 274-277 refs (For primary document see N85-35848 24-93)
(HE-3.3-1) Avail: NTIS HC as boxed set only $200/MF A01 per volume or E99 per entire set CSCL 03B

Six events with the number of secondaries ranging from 250 to several thousands were registered by an installation consisting of a thin graphite target, above and under which are placed photolayers followed by the usual lead X-ray film and emulsion chambers. Data concerning the number of secondaries and their angular distribution are given. The variance of the angular distribution is compared with data obtained at accelerator energies. E.A.K.

N85-35921*# Academia Sinica, Beijing (China). Inst. of High Energy Physics.
TRANSVERSE MOMENTUM DISTRIBUTION OF PION DEG IN THE FRAGMENTATION REGION OF SUPER HIGH ENERGY INTERACTIONS
J. R. Ren, H. H. Kuang, A. X. Huo, S. L. Lu, S. Su, Y. X. Wang, Y. G. Xue, C. R. Wang (Shandong Univ.), M. He (Shandong Univ.), N. J. Zhang (Shandong Univ.) et al *In* NASA. Goddard Space Flight Center 19th Intern. Cosmic Ray Conf., Vol. 6 Aug. 1985 p 278-279 refs (For primary document see N85-35848 24-93)
Avail: NTIS HC as boxed set only $200/MF A01 per volume or E99 per entire set CSCL 03B

The lateral distribution of gamma-families observed by emulsion chamber is sensitive to test transverse momentum of high energy interaction. But most part gamma-families are succesive interation's results which makes it necessary to analyze the propagation of gamma-ray in atmosphere. A gamma-ray with energy Er and transverse momentum Pt is produced at the altitude h. In the emulsion chamber experiment, Eob is estimated by decascade method. There are 30 gamma-families observed by Ganbala emulsion Chamber. A group of Monte-Carlo simulation gamma-families are used to compare with experimental data with the same treatment. It is found that both distributions are consistent. E.A.K.

N85-35922*# Waseda Univ., Tokyo (Japan). Science and Engineering Research Lab.
STUDY OF HADRON BUNDLES OBSERVED IN CHACALTAYA TWO-STORY EMULSION CHAMBER
H. Aoki *In* NASA. Goddard Space Flight Center 19th Intern. Cosmic Ray Conf., Vol. 6 Aug. 1985 p 280-283 refs (For primary document see N85-35848 24-93)
(HE-3.3-4) Avail: NTIS HC as boxed set only $200/MF A01 per volume or E99 per entire set CSCL 03B

The existence of hadron-rich families associated with few gamma-ray emission named Centauro and Mini-Centauro phenomena was reported. It was investigated whether these are produced by the special type of interaction different from the ordinary pion multiple production or not. The experimental results are compared with simulation calculation based on ordinary multiple pion production model. Both hadron multiplicity distribution, obtained from the present observation and the simulation calculation, show almost the same distribution which means that hadron bundles of such smaller multiplicities are considered to originate from successive interactions of surviving nucleon with the nature of multiple production during passage through the atmosphere. E.A.K.

N85-35923*# Waseda Univ., Tokyo (Japan). Science and Engineering Research Lab.
PENETRATIVE NATURE OF HIGH ENERGY SHOWERS OBSERVED IN CHACALTAYA EMULSION CHAMBER
Y. Funayama and M. Tamada *In* NASA. Goddard Space Flight Center 19th Intern. Cosmic Ray Conf., Vol. 6 Aug. 1985 p 284-287 refs (For primary document see N85-35848 24-93)
(HE-3.3-5) Avail: NTIS HC as boxed set only $200/MF A01 per volume or E99 per entire set CSCL 03B

About 30% of single core showers with E (sup gamma) > 10 TeV have stronger penetrating power than that expected from electromagnetic showers (e,gamma). On the other hand, their starting points of cascades in the chamber are found to be as shallow as those of (e,gamma) components. It is suggested that those showers are very collimated bundles of hadron and (e,gamma) component. Otherwise, it is assumed that the collision mean free path of those showers in the chamber is shorter than that of hadron with geometrical value. E.A.K.

N85-35924*# Waseda Univ., Tokyo (Japan). Science and Engineering Research Lab.
ANOMALOUS CORRELATION BETWEEN HADRON AND ELECTROMAGNETIC PARTICLES IN HADRON AND GAMMA-RAY FAMILIES
M. Tamada *In* NASA. Goddard Space Flight Center 19th Intern. Cosmic Ray Conf., Vol. 6 Aug. 1985 p 288-291 refs (For primary document see N85-35848 24-93)
(HE-3.3-6) Avail: NTIS HC as boxed set only $200/MF A01 per volume or E99 per entire set CSCL 03B

Correlations between hadrons and electromagnetic particles were studied in the hadron-gamma families observed in the Chacaltaya emulsion chamber experiment. It is found that there exist a number of hadrons which associate electromagnetic showers in extraordinarily close vicinity. The probability to have such a large number of hadrons associating electromagnetic showers, expected from background calculation, is found to be negligibly small and it means there exists anomalous correlation between hadrons and electromagnetic particles in the characteristic spread of atmospheric electromagnetic cascade. E.A.K.

N85-35925*# Centro Brasileiro de Pesquisas Fisicas, Rio de Janeiro.
ATMOSPHERIC INTERACTIONS DETECTED IN BOTH THE UPPER AND THE LOWER CHAMBERS AT CHACALTAYA
N. M. Amato, N. Arata, and R. H. C. Maldonado (Univ. Federal Fluminense) *In* NASA. Goddard Space Flight Center 19th Intern, Cosmic Ray Conf., Vol. 6 Aug. 1985 p 292-295 refs (For primary document see N85-35848 24-93)
(HE-3.3-7) Avail: NTIS HC as boxed set only $200/MF A01 per volume or E99 per entire set CSCL 03B

The cosmic ray interactions in the energy region 10 to the 13th power to 10 to the 17th power eV were studied by emulsion chambers exposed at Chacaltaya, 5220 m above sea-level. The chambers have a two-storied structure, and the events observed in both chambers give important informations on these phenomena. The first Centauro event ws detected as a small shower at the bottom of the upper chamber and as a big fraction of energy deposit in the lower chamber, which indicates a high contribution of hadronic showers. Results of the events with continuation in the rather low energy region are described. E.A.K.

N85-35926*# Saitama Univ., Urawa (Japan).
LATERAL DISTRIBUTION OF HIGH ENERGY HADRONS AND GAMMA RAY IN AIR SHOWER CORES OBSERVED WITH EMULSION CHAMBERS

T. Matano, M. Machida, N. Kawasumi, I. Tsushima, K. Honda, K. Hashimoto, C. E. Navia, N. Matinic, and C. Aquirre *In* NASA. Goddard Space Flight Center 19th Intern. Cosmic Ray Conf., Vol. 6 Aug. 1985 p 296-299 refs Sponsored by Grant-in-Aid for Oversea Survey of the Ministry of Education, Science and Culture in Japan (For primary document see N85-35848 24-93)
(HE-3.3-8) Avail: NTIS HC as boxed set only $200/MF A01 per volume or E99 per entire set CSCL 03B

A high energy event of a bundle of electrons, gamma rays and hadronic gamma rays in an air shower core were observed. The bundles were detected with an emulsion chamber with thickness of 15 cm lead. This air shower is estimated to be initiated with a proton with energy around 10 to the 17th power to 10 to the 18th power eV at an altitude of around 100 gmc/2. Lateral distributions of the electromagnetic component with energy above 2 TeV and also the hadronic component of energy above 6 TeV of this air shower core were determined. Particles in the bundle are produced with process of the development of the nuclear cascade, the primary energy of each interaction in the cascade which produces these particles is unknown. To know the primary energy dependence of transverse momentum, the average products of energy and distance for various average energies of secondary particles are studied. E.A.K.

N85-35927*# Saitama Univ., Urawa (Japan). Dept. of Physics.
SIZE DISTRIBUTIONS OF AIR SHOWERS ACCOMPANIED WITH HIGH ENERGY GAMMA RAY BUNDLES OBSERVED AT MT. CHACALTAYA Abstract Only
T. Matano, M. Machida, I. Tsuchima (Yamanashi Univ.), N. Kawasumi (Yamanashi Univ.), K. Honda (Yamanashi Univ.), K. Hashimoto (Yamanashi Univ.), N. Martinic (Univ. Mayor de San Andres), J. Zapata (Univ. Mayor de San Andres), C. E. Navia (Univ. Mayor de San Andres), C. Aquirre (Univ. Mayor de San Andres) et al *In* NASA. Goddard Space Flight Center 19th Intern. Cosmic Ray Conf., Vol. 6 Aug. 1985 p 300 refs (For primary document see N85-35848 24-93)
(HE-3.3-9) Avail: NTIS HC as boxed set only $200/MF A01 per volume or E99 per entire set CSCL 03B

Size distributions of air showers accompanied with bundle of high energy gamma rays and/or large size bursts under emulsion chambers, to study the composition of primary cosmic rays and also characteristics of high energy nuclear interaction. Air showers initiated by particles with a large cross section of interaction may develop from narrow region of the atmosphere near the top. Starting levels of air showers by particles with smaller cross section fluctuate in wider region of the atmosphere. Air showers of extremely small size accompanied with bundle of gamma rays may be ones initiated by protons at lower level after penetrating deep atmosphere without interaction. It is determined that the relative size distribution according to the total energy of bundle of gamma rays and the total burst size observed under 15 cm lead absorber. Author

N85-35928*# Konan Univ., Kobe (Japan).
EAS ACCOMPANIED BY GAMMA-FAMILIES AT MT. NORIKURA AND COMPARISON WITH MONTE CARLO SIMULATION
M. Shima, To. Saito, M. Sakata, Y. Yamamoto, K. Kasahara (Tokyo Univ., Tanashi, Japan), T. Yuda (Tokyo Univ., Tanashi, Japan), S. Torii (Kanagawa Univ., Yokohama), and N. Hotta (Utsunomiya Univ.) *In* NASA. Goddard Space Flight Center 19th Intern. Cosmic Ray Conf., Vol. 6 Aug. 1985 p 301-304 refs (For primary document see N85-35848 24-93)
(HE-3.3-10) Avail: NTIS HC as boxed set only $200/MF A01 per volume or E99 per entire set CSCL 03B

The experimental data of extensive air showers (EAS) accompanied by gamma-families, with total energy greater than 10 TeV, were compared with a Monte Carlo simulation with a rising cross section proportional to E sup 0.04 for the p-air inelastic cross section. It is found that the absolute intensity of size spectrum of such EAS is strongly affected by the primary protons intensity at 10 to the 15th power approx. 10 to the 16th power eV region and the experimental size spectrum agrees with the simulated spectra for the p-poor primary composition better than the p-rich one. E.A.K.

N85-35929*# Konan Univ., Kobe (Japan).
COMPARISON OF ABSOLUTE INTENSITY BETWEEN EAS WITH GAMMA-FAMILIES AND GENERAL EAS AT MOUNT NORIKURA
T. Mitsumune, T. Nakatsuka, K. Nishikawa, To. Saito, M. Sakata, M. Shima, Y. Yamamoto, S. Dake (Kobe Univ.), M. Kawamoto (Kobe Univ.), M. Kusumose (Kochi Univ.) et al *In* NASA. Goddard Space Flight Center 19th Intern. Cosmic Ray Conf., Vol. 6 Aug. 1985 p 305-308 refs (For primary document see N85-35848 24-93)
(HE-3.3-11) Avail: NTIS HC as boxed set only $200/MF A01 per volume or E99 per entire set CSCL 03B

Gamma-families with total energy greater than 10 TeV, found in the EX chamber which was cooperated with the EAS array were combined with EAS triggered by big bursts. The absolute intensity of the size spectrum of these combined EAS was compared with that of general EAS obtained by AS trigger. The EAS with sizes greater than 2x1 million were always accompanied by gamma-families with sigma E sub gamma H $>$ 10 TeV, n sub gamma, H $>$ 2 and Emin=3 TeV, although the rate of EAS accompaning such gamma-families decreases rapidly as their sizes decrease. E.A.K.

N85-35930*# Academia Sinica, Beijing (China). Inst. of High Energy Physics.
A COSMIC RAY SUPER HIGH MULTICORE FAMILY EVENT. 1: EXPERIMENT AND GENERAL FEATURES China-Japan Emulsion Chamber Collaboration
J. R. Ren, H. H. Kuang, A. X. Huo, S. L. Lu, S. Su, Y. X. Wang, Y. G. Xue, C. R. Wang (Shandong Univ.), M. He (Shandong Univ.), N. J. Zhang (Shandong Univ.) et al *In* NASA. Goddard Space Flight Center 19th Intern. Cosmic Ray Conf., Vol. 6 Aug. 1985 p 309-312 refs (For primary document see N85-35848 24-93)
(HE-3.4-1) Avail: NTIS HC as boxed set only $200/MF A01 per volume or E99 per entire set CSCL 03B

Information on the fragmentation region in super high energy hadronic interactions can be obtained through the observations of gamma-ray families produced by cosmic rays. Gamma-ray families with the sum of E sub gamma $>$ or 1000 TeV are receiving increasing interests in emulsion chamber experiments. There exist some complications caused by the superposition of nuclear and electromagnetic cascades and the uncertainty in the nature of the primary particles. These complications usually make the conclusions drawn from various interesting phenomena observed in family events not so definite. An interesting family event KO E19, which is likely to have suffered only very slight disturbances is described. It was found in the Mt. Kambala emulsion chamber experiment. The production height of the event is determined to be H=(70 + or - 30)m and some conclusions are given. G.L.C.

N85-35931*# National Aeronautics and Space Administration. Goddard Space Flight Center, Greenbelt, Md.
A COSMIC RAY SUPER HIGH ENERGY MULTICORE FAMILY EVENT. 2: STRUCTURE AND FRAGMENTATION CHARACTERISTICS OF THE JETS China-Japan Emulsion Chamber Collaboration
In its 19th Intern. Cosmic Ray Conf., Vol. 6 Aug. 1985 p 313-316 refs (For primary document see N85-35848 24-93)
(HE-3.4-2) Avail: NTIS HC as boxed set only $200/MF A01 per volume or E99 per entire set CSCL 03B

Quarks and gluons are not directly observable, but may be displayed through fragmentation in the form of hadronic jets, the evidence of which was first revealed in cosmic ray interactions before the advent of the modern theory of strong interactions. Experimental results from ISR and SPPS collider rendered the jet phenomena more confident and definite. All the properties of jets observed up to now at ISR and SPPS collider are in agreement with the predictions of QCD. In order to make further test of QCD in still higher energy regions, detailed study of super high energy jet events in cosmic rays is very desirable. The event KO E19 observed in the Mt. Kambala emulsion chamber is an interesting event for such study. The general features of KO E19 is described. Its total visible energy is sigma E sub gamma = 1537 TeV(E sub

min = 1.5 TeV) and production height H=(70 + or - 30)m, with a hadron as its primary particle. Besides about forty small clusters, there are five super high energy cores or jets, one lying near the center of the event while the other four surrounding it, having incident directions making small angles with that of the primary particle. Detailed analysis is done on the emulsion plates inserted in the chamber, making full use of their fine granularity, superior in detecting and analyzing jet events, specially their substructures. G.L.C.

N85-35932*# Academia Sinica, Beijing (China).
OBSERVATION OF SUPER HIGH ENERGY BIG FAMILY WITH LARGE SCALE Fe EMULSION CHAMBERS China-Japan Emulsion Chamber Collaboration
In NASA. Goddard Space Flight Center 19th Intern. Cosmic Ray Conf., Vol. 6 Aug. 1985 p 317-319 refs (For primary document see N85-35848 24-93)
(HE-3.4-3) Avail: NTIS HC as boxed set only $200/MF A01 per volume or E99 per entire set CSCL 03B

In order to get higher efficiencies for detecting hadrons and to make technical improvements in the chamber structure, the Mt. Kambala Emulsion Chamber Collaboration constructed 57 sq. m. of Fe chamber, with thickness 29 c.u.(1c.u.=17.6 mm Fe), using 300 tons of Fe plates and made the first exposure from Sept., 1982 to May, 1984. The photosensitive layers consist of X-ray films of Sakura N type, Fuji No. 100 type and Tianjin III type, some of them contain also emulsion plates of Fuji ET7B type. They are inserted between the Fe plates at 2 c.u., beginning at 5 c.u. from the chamber top. In a number of blocks, 3 mm spacings are provided at every 2 c.u. of Fe plates to facilitate the replacement of photosensitive layers, without disassembling the chamber. On the bottom of the chamber Fe plates of thickness 9 mm are placed in order to shield the chamber from the radioactivities of the ground. An event, numbered K2 58 of visible energy sigma E sub gamma = 7345 TeV was found in this exposure. No obvious halo is seen in the event and all the showers are clearly separated and easy to measure. A brief report of the preliminary results is presented. G.L.C.

N85-35933*# Centro Brasileiro de Pesquisas Fisicas, Rio de Janeiro.
A HALO EVENT CREATED AT 200 m ABOVE THE CHACALTAYA EMULSION CHAMBER
N. M. Amato, N. Arata, and R. H. C. Maldonado (Univ. Federal de Fleminense, Niteroi, Brazil) *In* NASA. Goddard Space Flight Center 19th Intern. Cosmic Ray Conf., Vol. 6 Aug. 1985 p 320-323 refs (For primary document see N85-35848 24-93)
(HE-3.4-5) Avail: NTIS HC as boxed set only $200/MF A01 per volume or E99 per entire set CSCL 03B

The results of analysis on a cosmic-ray induced nuclear event with the total visible energy approx. = 1300 TeV which is characterized by the central (halo) part of a strong energy concentration and the outer part of a large lateral spread are presented. The event (named as P06) was detected in the 18th two-storied emulsion chamber exposed at Chacaltaya by Brasil-Japan Collaboration. As the nuclear emulsion plates were inserted at every layer of the concerned blocks in the upper and the lower chambers together with RR- and N-type X-ray films, it is possible to study the details of the event. Some results on P06 have already been reported [1] based on the general measurement of opacity on N-type X-ray films: (1) the total energy of halo is approx. = 1000 TeV; (2) the shower transition reaches its maximum at approx. 16 cu; and (3) the radius of halo is 6.5 mm (at the level of 10 to the 6th power electrons/sq.cm.). The results in more details will be described. G.L.C.

N85-35934*# Centro Brasileiro de Pesquisas Fisicas, Rio de Janeiro.
A BINOCULAR-TYPE ATMOSPHERIC INTERACTION GENERATING SEQUENTIAL EXOTIC FEATURES
N. M. Amato, N. Arata, and R. H. C. Maldonado (Univ. Federal de Fleminense, Niteroi, Brazil) *In* NASA. Goddard Space Flight Center 19th Intern. Cosmic Ray Conf., Vol. 6 Aug. 1985 p 324-327 refs (For primary document see N85-35848 24-93)
(HE-3.4-6) Avail: NTIS HC as boxed set only $200/MF A01 per volume or E99 per entire set CSCL 03B

A cosmic-ray induced nuclear event is presented, which is of clear binocular-type and contains several exotic features through its passage in the atmosphere and the emulsion chamber. Author

N85-35935*# Franklin Inst., Newark, Del.
GAMMA-HADRON FAMILIES AND SCALING VIOLATION
T. K. Gaisser, T. Stanev, and J. A. Wrotniak (Lodz Univ.) *In* NASA. Goddard Space Flight Center 19th Intern. Cosmic Ray Conf., Vol. 6 Aug. 1985 p 328-331 refs (For primary document see N85-35848 24-93)
(Contract DE-AC02-76ER-05007; Grant NSF PHY-84-10989)
(HE-3.4-7) Avail: NTIS HC as boxed set only $200/MF A01 per volume or E99 per entire set CSCL 03B

For three different interaction models we have simulated gamma-hadron families, including the detector (Pamir emulsion chamber) response. Rates of gamma families, hadrons, and hadron-gamma ratios were compared with experiments. Author

N85-35936*# Tokyo Univ. (Japan). Inst. for Cosmic Ray Research.
SUPER-FAMILY P2 C-96-125 OBSERVED BY JAPAN-URSS JOINT EMULSION CHAMBER EXPERIMENT Japan-URSS Joint Emulsion Chamber Experiment
Edison Hiroyuki Shibuya (Univ. Estadual de Caminas, Sao Paulo, Brazil) *In* NASA. Goddard Space Flight Center 19th Intern. Cosmic Ray Conf., Vol. 6 Aug. 1985 p 332-335 refs (For primary document see N85-35848 24-93)
(HE-3.4-8) Avail: NTIS HC as boxed set only $200/MF A01 per volume or E99 per entire set CSCL 03B

A detailed description of the event detected in the second chamber of Japan-URSS Collaboration is presented. A preliminary description was already published and from that time a careful microscopic scanning was carried out. G.L.C.

N85-35937*# Academia Sinica, Beijing (China). Inst. of High Energy Physics.
ON THE HALO EVENTS OBSERVED BY MOUNT FUJI AND MOUNT KANBALA EMULSION CHAMBER EXPERIMENTS Mount Fuji Collaboration and Japan-China Collaboration
J. R. Ren, H. H. Kuang, A. X. Huo, S. L. Lu, S. Su, Y. X. Wang, Y. G. Xue, C. R. Wang (Shandong Univ.), M. He (Shandong Univ.), N. J. Zhang (Shandong Univ.) et al *In* NASA. Goddard Space Flight Center 19th Intern. Cosmic Ray Conf., Vol. 6 Aug. 1985 p 336-339 refs (For primary document see N85-35848 24-93)
(HE-3.4-9) Avail: NTIS HC as boxed set only $200/MF A01 per volume or E99 per entire set CSCL 03B

The intensity of big gamma-ray families associated by halo is obtained from Mt. Fuji experiment (650 g/sq.cm. atmospheric depth) and Mt. Kanbala experiment (515 g/sq.cm.). The results are compared with Monte Carlo calculation based on several assumptions on interaction mechanisms and the primary cosmic ray composition. The results suggest more than 3 times lower proton abundance among primaries than that of 10 to the 12th to 10 to the 13th eV region within the framework of quasi-scaling model of multiple production. Author

N85-35938*# Academy of Sciences (USSR), Moscow. Inst. for Nuclear Research.
EXPERIMENT PAMIR-2. FIANIT: A GIANT SUPER-FAMILY WITH HALO (EPSILON SUB 0 AT APPROXIMATELY 10(17) eV) Collaboration of Experiment Pamir
G. T. Zatsepin *In* NASA. Goddard Space Flight Center 19th Intern. Cosmic Ray Conf., Vol. 6 Aug. 1985 p 340-343 refs (For primary document see N85-35848 24-93)
(HE-3.4-10) Avail: NTIS HC as boxed set only $200/MF A01 per volume or E99 per entire set CSCL 03B

A superfamily with halo of extremely high energy named Fianit was recorded in X-ray emulsion chamber (XEC) at the Pamirs (atmospheric depth 600 g/sq.cm.). Detailed description of the superfamily and results of its analysis are presented. G.L.C.

N85-35939*# Academy of Sciences (USSR), Moscow. Inst. of Nuclear Research.
EXPERIMENT PAMIR-4: ANALYSIS OF SUPERFAMILY WITH HALO OF ELECTROMAGNETIC NATURE DETECTED IN DEEP XEC Collaboration of Experiment Pamir
G. T. Zatsepin et al *In* NASA. Goddard Space Flight Center 19th Intern. Cosmic Ray Conf., Vol. 6 Aug. 1985 p 344-347 refs (For primary document see N85-35848 24-93)
(HE-3.4-11) Avail: NTIS HC as boxed set only $200/MF A01 per volume or E99 per entire set CSCL 03B

The family Pb2-11 was detected in the multilayer lead XEC with total thickness of 100 c.u. exposed at the Pamirs. Each lead layer was 1 cm thick, the first registering layer being located under 2 cm of Pb(= 4 c.u.). The family comprised a narrow group of gamma-rays which near the maximum of cascade development (= 14 c.u.) produced a dark spot of optical density D approx. > .4 over area S = 25 sq.mm. The narrow group of gamma-rays was traced up to 14th layer corresponding to 30 c.u. Deeper in the chamber, for the space of 70 c.u. no hadron cascade was observed. Thus, the pure electromagnetic halo could be assumed. Preliminary results of the analysis of the family Pb2-11 was presented. The methods of estimation of energy of primary particle and height of nuclear interaction responsible for the observed halo are considered in more detail. G.L.C.

N85-35940*# Hirosaki Univ. (Japan).
PARTICLE INTERACTIONS AT ENERGIES OVER 1000 TeV INFERRED FROM GAMMA-FAMILIES OBSERVED AT MOUNT FUJI Mount Fuji Collaboration
M. Amenomori, H. Nanjo, E. Konishi, N. Hotta (Utsunomiya Univ.), K. Mizutani (Saitama Univ.), K. Kasahara (Tokyo Univ.), T. Kobayashi (Tokyo Univ.), E. Mikumo (Tokyo Univ.), K. Sato (Tokyo Univ.), T. Yuda (Tokyo Univ.) et al *In* NASA. Goddard Space Flight Center 19th Intern. Cosmic Ray Conf., Vol. 6 Aug. 1985 p 348-351 refs (For primary document see N85-35848 24-93)
(HE-3.5-1) Avail: NTIS HC as boxed set only $200/MF A01 per volume or E99 per entire set CSCL 03B

Scaling, mean P sub t, high P sub t jets and others at energies over 1000 TeV are discussed on the basis of gamma-family data with sigma E sub gamma > 100 TeV, observed at Mt. Fuji (3750 m). These quantities were examined in connection with the primary composition. Author

N85-35941*# Waseda Univ., Tokyo (Japan).
A SEARCH FOR MINI-CLUSTERS IN JAPAN-USSR JOINT EXPERIMENT AT PAMIR Japan-USSR Joint Experiment
In NASA. Goddard Space Flight Center 19th Intern. Cosmic Ray Conf., Vol. 6 Aug. 1985 p 352-355 refs Sponsored in part by the Ministry of Education (For primary document see N85-35848 24-93)
(HE-3.5-2) Avail: NTIS HC as boxed set only $200/MF A01 per volume or E99 per entire set CSCL 03B

A search for mini-clusters, very collimated shower clusters of hadrons and electromagnetic particles, is made for the hadron and gamma families observed by Japan-USSR joint carbon chamber at Pamir. The existence of anomalous correlation between hadrons and electromagnetic particles is found. The decascading method is applied to the families and it is found that 11 clusters which include hadrons as members have smaller spread, Er < 3.5 GeV.m and larger lateral spread, E'R' > 100 GeV.m, from the family center. In the simulated events, such clusters were found to be very rare. Author

N85-35942*# Universidade Estadual de Campinas (Brazil). Inst. de Fisica Gleb Wataghin.
MINI-CLUSTERS Brazil-Japan Collaboration of Chacaltaya Emulsion Chamber Experiment
J. A. Chinellato, C. Dobrigkeit, J. BellandiFilho, C. M. G. Lattes, M. J. Menon, C. E. Navia, A. Pamilaju, K. Sawayanagi, E. H. Shibuya, A. Turtelli, Jr. et al *In* NASA. Goddard Space Flight Center 19th Intern. Cosmic Ray Conf., Vol. 6 Aug. 1985 p 356-359 refs (For primary document see N85-35848 24-93)
(HE-3.5-3) Avail: NTIS HC as boxed set only $200/MF A01 per volume or E99 per entire set CSCL 03B

Experimental results of mini-clusters observed in Chacaltaya emulsion chamber no. 19 are summarized. The study was made on 54 single core shower upper and 91 shower clusters of E(gamma) > 10 TeV from 30 families which are visible energy greater than 80 TeV and penetrate through both upper and lower detectors of the two-story chamber. The association of hadrons in mini-cluster is made clear from their penetrative nature and microscopic observation of shower continuation in lower chamber. Small P sub t (gamma) of hadrons in mini-clusters remained in puzzle. Author

N85-35943*# Universidade Estadual de Campinas (Brazil).
GIANT MINI-CLUSTERS AS POSSIBLE ORIGIN OF HALO PHENOMENA OBSERVED IN SUPER-FAMILIES Brazil-Japan Collaboration of Chacaltaya Emulsion Chamber Experiment
In NASA. Goddard Space Flight Center 19th Intern. Cosmic Ray Conf., Vol. 6 Aug. 1985 p 360-363 refs Sponsored in part by Conselho Nacional para o Desemvolvimento Cienüfico e Tecnologico, Tokyo Univ., and the Japanese Ministry of Education (For primary document see N85-35848 24-93)
(HE-3.5-4) Avail: NTIS HC as boxed set only $200/MF A01 per volume or E99 per entire set CSCL 03B

Among 91 mini-clusters from 30 high energy Chiron-type families in Chacaltaya emulsion chambers, there were observed several extremely large multiplicity clusters in the highest energy range, far beyond the average of ordinary type clusters. Some details of microscopic observation of those giant mini-clusters in nuclear emulsion plates and some phenomenological regularity found in common among them are described. Such giant mini-clusters are possible candidates for the origin of narrow symmetric single halo phenomena in X-ray films which are frequently observed in super-families of visible energy greater than 1,000 TeV. Author

N85-35944*# Waseda Univ., Tokyo (Japan). Science and Engineering Research Lab.
STRUCTURE OF SUPER-FAMILIES
S. Yamashita, A. Ohsawa (Tokyo Univ.), and J. A. Chinellato (Univ. Estadual de Campinas) *In* NASA. Goddard Space Flight Center 19th Intern. Cosmic Ray Conf., Vol. 6 Aug. 1985 p 364-367 refs (For primary document see N85-35848 24-93)
(HE-3.5-7) Avail: NTIS HC as boxed set only $200/MF A01 per volume or E99 per entire set CSCL 03B

At present the study of nuclear interactions induced by cosmic rays is the unique source of information on the nuclear interactions in the energy region above 10 to the 15th power eV. The phenomena in this energy region are observed by air shower arrays or emulsion chambers installed at high mountain. An emulsion chamber is the pile of lead plates and photo-sensitive layers (nuclear emulsion plates and/or X-ray films) used to detect electron showers. High spatial resolution of photographic material used in the emulsion chamber enables the observation of the phenomena in detail, and recent experiments of emulsion chamber with large area are being carried out at high mountain altitudes by several groups in the world. G.L.C.

N85-35945*# Waseda Univ., Tokyo (Japan). Science and Engineering Research Lab.
EXTREMELY HIGH ENERGY HADRON AND GAMMA-RAY FAMILIES(3). CORE STRUCTURE OF THE HALO OF SUPERFAMILY
S. Yamashita, A. Ohsawa (Tokyo Univ.), J. A. Chinellato (Univ. Estadual de Campinas), and E. H. Shibuya (Univ. Estadual de Campinas) *In* NASA. Goddard Space Flight Center 19th Intern. Cosmic Ray Conf., Vol. 6 Aug. 1985 p 368-371 refs (For primary document see N85-35848 24-93)
(HE-3.5-8) Avail: NTIS HC as boxed set only $200/MF A01 per volume or E99 per entire set CSCL 03B

The study of the core structure seen in the halo of Mini-Andromeda 3(M.A.3), which was observed in the Chacaltaya emulsion chamber, is presented. On the assumption that lateral distribution of darkness of the core is exponential type, i.e., D=D0exp(-R/r0), subtraction of D from halo darkness is performed

until the cores are gone. The same quantity on cores obtained by this way are summarized. The analysis is preliminary and is going to be developed. Author

N85-35946*# Altai State Univ., Barnaul (USSR).
NUMERICAL ANALYSIS OF ELECTROMAGNETIC CASCADES IN EMULSION CHAMBERS
A. V. Plyasheshnikov and K. V. Vorobyev *In* NASA. Goddard Space Flight Center 19th Intern. Cosmic Ray Conf., Vol. 6 Aug. 1985 p 372-375 refs (For primary document see N85-35848 24-93)
(HE-3.5-9) Avail: NTIS HC as boxed set only $200/MF A01 per volume or E99 per entire set CSCL 03B

A new calculational scheme of the Monte Carlo method assigned for the investigation of the development of high and extremely high energy electromagnetic cascades (EMC) in the matter was elaborated. The scheme was applied to the analysis of angular and radial distributions of EMC electrons in the atmosphere. By means of this scheme the EMC development in dense medium is investigated and some preliminary data are presented on the behavior of EMC in emulsion chambers. The results of more detailed theoretical analysis of the EMC development in emulsion chambers are discussed. G.L.C.

N85-35947*# Tashkent V. I. Lenin State Univ., Vuzgorodok (USSR).
AN EXPERIMENTAL STUDY OF CORRELATIONS IN THE DEVELOPMENT OF THE ELECTRON-PHOTON CASCADES
Yu. P. Kratenko and S. A. Caharishnikov *In* NASA. Goddard Space Flight Center 19th Intern. Cosmic Ray Conf., Vol. 6 Aug. 1985 p 376-379 refs (For primary document see N85-35848 24-93)
(HE-3.5-10) Avail: NTIS HC as boxed set only $200/MF A01 per volume or E99 per entire set CSCL 03B

In terms of the experimental data on the development of the electron photon cascades (EPC) in Pb from electrons and photons of cosmic rays in the tens GeV energy region a calculation of correlations between the characteristics of longitudinal and lateral development of the EPC as well as those between fluctuations of the cascade particle numbers at different stages of the cascade development was carried out. The results obtained are compared to the numerical EPC calculations. Author

N85-35948*# Moscow State Univ. (USSR). Inst. of Nuclear Physics.
THE ELECTROMAGNETIC COMPONENT OF ALBEDO FROM SUPERHIGH ENERGY CASCADES IN DENSE MEDIA
R. M. Golynskaya, L. A. Hein, A. V. Plyasheshnikov, and K. V. Vorobyev *In* NASA. Goddard Space Flight Center 19th Intern. Cosmic Ray Conf., Vol. 6 Aug. 1985 p 380-383 refs (For primary document see N85-35848 24-93)
(HE-3.5-11) Avail: NTIS HC as boxed set only $200/MF A01 per volume or E99 per entire set CSCL 03B

Albedo from cascades induced in iron by high energy gamma quanta were Monte Carlo simulated. Thereafter the albedo electromagnetic component from proton induced cascades were calculated analytically. The calculations showed that the albedo electromagnetic component increases more rapidly than the nuclear active component and will dominate at sufficiently high energies. Author

N85-35949*# Moscow State Univ. (USSR). Inst. of Nuclear Physics.
INTEGRAL FUNCTIONS OF ELECTRON LATERAL DISTRIBUTION AND THEIR FLUCTUATIONS IN ELECTRON-PHOTON CASCADES
I. P. Ivanenko, B. L. Kanevsky, A. A. Kirillov, I. A. Linde, and Yu. G. Lyutov *In* NASA. Goddard Space Flight Center 19th Intern. Cosmic Ray Conf., Vol. 6 Aug. 1985 p 384-387 refs (For primary document see N85-35848 24-93)
(HE-3.5-12) Avail: NTIS HC as boxed set only $200/MF A01 per volume or E99 per entire set CSCL 03B

Monte Carlo simulated lateral distribution functions for electrons of EPC developing in lead, at superhigh energies (.1-1 PeV) for depths t < or = 60 c.u. delta t=1t. c.u. are presented. The higher moment characteristics, i.e., variation, asymmetry, excess, are presented along with analytical solutions for the same characteristics at fixed observation level calculated to theory approximations A and B by using numerical inversion of the Laplace transformation. The conclusion is made of a complex, usually non-Gaussian shape of the function of the particle number distribution within a circle of given radius at fixed depth. G.L.C.

N85-35950*# Moscow State Univ. (USSR). Inst. of Nuclear Physics.
ANALYTICAL-NUMERICAL METHODS OF CALCULATIONS OF ENERGY AND THREE-DIMENSIONAL PARTICLE DISTRIBUTIONS IN ELECTROMAGNETIC CASCADES
I. P. Ivanenko, B. L. Kanevsky, T. M. Roganova, V. V. Sizov, and S. V. Triphonova *In* NASA. Goddard Space Flight Center 19th Intern. Cosmic Ray Conf., Vol. 6 Aug. 1985 p 388-391 refs (For primary document see N85-35848 24-93)
(HE-3.5-13) Avail: NTIS HC as boxed set only $200/MF A01 per volume or E99 per entire set CSCL 03B

Analytical and numerical methods of calculation of the energy and three dimensional EPS characteristics are reported. The angular and lateral functions of electrons in EPS have been obtained by the Landau and small angle approximations A and B and compared with earlier data. A numerical method of solution of cascade equations for the EPS distribution function moments has been constructed. Considering the equilibrium rms angle as an example, errors appearing when approximating the elementary process cross sections by their asymptotic expressions are analyzed. Author

N85-35951*# Academy of Sciences of the Armenian SSR, Erivan (USSR).
MULTIDIMENSIONAL ANALYSIS OF DATA OBTAINED IN EXPERIMENTS WITH X-RAY EMULSION CHAMBERS AND EXTENSIVE AIR SHOWERS
A. A. Chilingaryan, S. Kh. Galfayan, M. Z. Zazyan, and A. M. Dunaevsky *In* NASA. Goddard Space Flight Center 19th Intern. Cosmic Ray Conf., Vol. 6 Aug. 1985 p 392-395 refs (For primary document see N85-35848 24-93)
(HE-3.6-2) Avail: NTIS HC as boxed set only $200/MF A01 per volume or E99 per entire set CSCL 03B

Nonparametric statistical methods are used to carry out the quantitative comparison of the model and the experimental data. The same methods enable one to select the events initiated by the heavy nuclei and to calculate the portion of the corresponding events. For this purpose it is necessary to have the data on artificial events describing the experiment sufficiently well established. At present, the model with the small scaling violation in the fragmentation region is the closest to the experiments. Therefore, the treatment of gamma families obtained in the Pamir' experiment is being carried out at present with the application of these models. Author

N85-35952*# Academy of Sciences of the Armenian SSR, Erivan (USSR). Physics. Inst.
A NEW METHOD OF DIFFERENTIAL STRUCTURAL ANALYSIS OF GAMMA-FAMILY BASIC PARAMETERS
L. G. Melkumian, S. V. Ter-Antonian, and Yu. A. Smorodin (Academy of Sciences, USSR, Moscow) *In* NASA. Goddard Space Flight Center 19th Intern. Cosmic Ray Conf., Vol. 6 Aug. 1985 p 396-399 refs (For primary document see N85-35848 24-93)
(HE-3.6-3) Avail: NTIS HC as boxed set only $200/MF A01 per volume or E99 per entire set CSCL 03B

The maximum likelihood method is used for the first time to restore parameters of electron photon cascades registered on X-ray films. The method permits one to carry out a structural analysis of the gamma quanta family darkening spots independent of the gamma quanta overlapping degree, and to obtain maximum admissible accuracies in estimating the energies of the gamma quanta composing a family. The parameter estimation accuracy weakly depends on the value of the parameters themselves and

exceeds by an order of the values obtained by integral methods. Author

N85-35953*# Bordeaux 1 Univ., Gradignan (France). Lab. de Physique Theorique.
LPM EFFECT AND PRIMARY ENERGY ESTIMATIONS
M. F. Bourdeau and J. N. Capdevielle *In* NASA. Goddard Space Flight Center 19th Intern. Cosmic Ray Conf., Vol. 6 Aug. 1985 p 400-403 refs (For primary document see N85-35848 24-93)
(HE-3.6-4) Avail: NTIS HC as boxed set only $200/MF A01 per volume or E99 per entire set CSCL 03B

The distortion of the electron cascade development under LPM effects is now admitted; it consists of an increase of depth of showers origin, of shower maximum T sum max, a decrease of the number of particles at maximum N sub max and results in a flattening and a widening of the cascade transition curve. Connected with the influence of multiple Coulomb scattering on basic electromagnetic processes (bremstrahlung, pair production), this effect appears at high energy with a threshold dependent on the density of the medium (more than 10 TeV for lead, more than 10 sup 6 TeV in air). Consequently, the electromagnetic components of hadron induced showers in lead and EAS in air calculated for the same hadronic cascades in the different alternative, including or not the LPM effect are examined here. Author

N85-35954*# Warsaw Technical Univ. (Poland). Inst. of Physics.
EXPERIMENTAL BASIS FOR THE MODELS OF CASCADE PROPAGATION IN ATMOSPHERE
Z. Strugalski *In* NASA. Goddard Space Flight Center 19th Intern. Cosmic Ray Conf., Vol. 6 Aug. 1985 p 404-406 refs (For primary document see N85-35848 24-93)
(HE-3.6-6) Avail: NTIS HC as boxed set only $200/MF A01 per volume or E99 per entire set CSCL 03B

The picture of the hadron nucleus collision process is presented as it emerges on the basis of newly obtained experimental data. The picture is applicable to models of cascade propagation in Earth atmosphere. Author

N85-35955*# Yanagita (Tomotake), Takakura (Japan).
RELATION BETWEEN GAMMA-RAY FAMILY AND EAS CORE: MONTE-CARLO SIMULATION OF EAS CORE
Tomotake Yanagita *In* NASA. Goddard Space Flight Center 19th Intern. Cosmic Ray Conf., Vol. 6 Aug. 1985 p 407-410 refs (For primary document see N85-35848 24-93)
(HE-3.6-7) Avail: NTIS HC as boxed set only $200/MF A01 per volume or E99 per entire set CSCL 03B

Preliminary results of Monte-Carlo simulation on Extensive Air Showers (EAS) (Ne=100,000) core is reported. For the first collision at the top of the atmosphere, high multiplicity (high rapidity, density) and a large Pt (1.5GeV average) model is assumed. Most of the simulated cores show a complicated structure. Author

N85-35956*# Saitama Univ., Urawa (Japan). Dept. of Physics.
COMPARISON OF BIG EVENT WITH CALCULATIONS OF THE AIR SHOWER DEVELOPMENT Abstract Only
M. Niwa, A. Misaki, and T. Matano *In* NASA. Goddard Space Flight Center 19th Intern. Cosmic Ray Conf., Vol. 6 Aug. 1985 p 411 (For primary document see N85-35848 24-93)
(HE-3.6-8) Avail: NTIS HC as boxed set only $200/MF A01 per volume or E99 per entire set CSCL 03B

The incidence of high energy hadrons and electron-photons in air showers at various stages of development is calculated. Numerical calculation is used to solve the diffusion equation for a nuclear cascade and analytical calculation for cascade shower induced gamma rays. From these calculations, one can get the longitudinal development of the high energy hadron and electron-photon components, and the energy spectra of these components at various depths of air shower development. The total number of hadrons (N sub H) and electron-photon components (N sub gamma) are related according to stages of the air shower development and primary energy. The relation of the total energy of hadron and electron-photon component above the threshold energy is given. The energy balance between both components is also a useful parameter to study high energy events accompanying air showers. The relation of N sub H and fractional hadronic energy E (sum E sub H sup gamma/sum E sub H sup gamma + Sum E sub gamma) is calculated. This relation is helpful to understand the stage of air shower development(t) and primary energy (E sub p). Author

N85-35957*# Lodz Univ. (Poland). Inst. of Nuclear Studies.
THE LATERAL DISTRIBUTIONS OF CHARGED PARTICLES OF ENERGY GREATER THAN 0.3 E SUB CRIT IN ELECTRON-PHOTON CASCADES IN LEAD AND AIR
A. Wasilewski and E. Krys *In* NASA. Goddard Space Flight Center 19th Intern. Cosmic Ray Conf., Vol. 6 Aug. 1985 p 412-415 refs (For primary document see N85-35848 24-93)
(HE-3.6-10) Avail: NTIS HC as boxed set only $200/MF A01 per volume or E99 per entire set CSCL 03B

In recent investigations, both theoretical and experimental, the agreement between cascade theory and experimental data is pointed out. The radial distributions obtained from the Monte Carlo simulation are compared ith the results of the analytical theory for all particles in cascades. The data on the mean radius of electron lateral distribution in air are compared with those in lead. Author

N85-35958*# Lodz Univ. (Poland). Inst. of Nuclear Studies.
RESULT OF MONTE-CARLO SIMULATION OF ELECTRON-PHOTON CASCADES IN LEAD AND LAYERS OF LEAD-SCINTILLATOR
A. Wasilewski and E. Krys *In* NASA. Goddard Space Flight Center 19th Intern. Cosmic Ray Conf., Vol. 6 Aug. 1985 p 416-419 refs (For primary document see N85-35848 24-93)
(HE-3.6-11) Avail: NTIS HC as boxed set only $200/MF A01 per volume or E99 per entire set CSCL 03B

Results of Monte-Carlo simulation of electromagnetic cascade development in lead and lead-scintillator sandwiches are analyzed. It is demonstrated that the structure function for core approximation is not applicable in the case in which the primary energy is higher than 100 GeV. The simulation data has shown that introducing an inhomogeneous chamber structure results in subsequent reduction of secondary particles. Author

N85-35959*# Hiroshima Univ. (Japan).
ON MINI-CLUSTER OBSERVED BY CHACALTAYA EMULSION CHAMBER EXPERIMENT
T. Tati *In* NASA. Goddard Space Flight Center 19th Intern. Cosmic Ray Conf., Vol. 6 Aug. 1985 p 420-423 refs (For primary document see N85-35848 24-93)
(HE-3.6-12) Avail: NTIS HC as boxed set only $200/MF A01 per volume or E99 per entire set CSCL 03B

Bundles of electromagnetic showers with very small tranverse momenta (approx. 10 MeV) accompanied by decay products of Chiron-type fireballs, have been observed. These bundles are called Miniclusters. This phenomenon supports the picture of fireballs made up of hadronic matter and based on the theory of the finite degree of freedom. F.M.R.

N85-35960*# Academy of Sciences of the Uzbek SSR, Tashkent. Physical-Technical Inst.
A COMPARATIVE ANALYSIS OF GAMMA AND HADRON FAMILIES AT THE SUPERHIGH ENERGIES RECORDED IN EXPERIMENT PAMIR
S. A. Azimov, E. J. Mulladjanov, A. N. Nosov, H. Nuritdinov, D. A. Talipov, D. A. Halilov, and T. S. Yuldashbaev *In* NASA. Goddard Space Flight Center 19th Intern. Cosmic Ray Conf., Vol. 6 Aug. 1985 p 424-427 refs (For primary document see N85-35848 24-93)
(HE-3.7-1) Avail: NTIS HC as boxed set only $200/MF A01 per volume or E99 per entire set CSCL 03B

A comparative analysis of hadron and gamma families which have undergone the decascading procedure is made. Results are compared with different models of interactions. In hadron families with energies Summary E sub H sup gamma > 20 TeV as well

as in gamma families with energies Summary E sub gamma > 70 TeV, increasing azimuthal anisotropy is observed. Author

N85-35961*# Academy of Sciences of the Uzbek SSR, Tashkent. Physical-Technical Inst.
A STUDY OF GAMMA-FAMILIES GENERATED IN NUCLEON-NUCLEUS (NA) AND PION-NUCLEUS (PI A) INTERACTIONS
S. A. Azimov, E. J. Mulladjanov, H. Nuritdinov, and T. S. Yuldashbaev *In* NASA. Goddard Space Flight Center 19th Intern. Cosmic Ray Conf., Vol. 6 Aug. 1985 p 428-430 ref (For primary document see N85-35848 24-93)
(HE-3.7-2) Avail: NTIS HC as boxed set only $200/MF A01 per volume or E99 per entire set CSCL 03B

The separation of the gamma families generated in nucleon-nuclear and pion-nuclear (PI-A) interactions is realized from the analysis of simulated gamma families. Some characteristics of NA and PI families and the influence of the process of inelastic charge-exchange of charged pions neutral ones type of PI + or - A yields are studied. Author

N85-35962*# Lodz Univ. (Poland). Inst. of Physics.
HADRONS REGISTRATION IN EMULSION CHAMBER WITH CARBON BLOCK
A. Tomaszewski and Z. Wlodarczyk *In* NASA. Goddard Space Flight Center 19th Intern. Cosmic Ray Conf., Vol. 6 Aug. 1985 p 431-434 refs (For primary document see N85-35848 24-93)
(HE-3.7-3) Avail: NTIS HC as boxed set only $200/MF A01 per volume or E99 per entire set CSCL 03B

Nuclear-electro-magnetic cascade (NEC) in X-ray emulsion chambers with carbon block, which are usually used in the Pamir experiment, was Monte-Carlo simulated. Going over from optical density to Summary E sub gamma is discussed. The hole of NEC in the interpretation of energy spectra is analyzed. Author

N85-35963*# Hirosaki Univ. (Japan).
NEW ANALYSIS OF NUCLEAR INTERACTION OBSERVED BY MT. KANBARA EMULSION CHAMBER EXPERIMENT
H. Nanjo *In* NASA. Goddard Space Flight Center 19th Intern. Cosmic Ray Conf., Vol. 6 Aug. 1985 p 435-438 refs (For primary document see N85-35848 24-93)
(HE-3.7-4) Avail: NTIS HC as boxed set only $200/MF A01 per volume or E99 per entire set CSCL 03B

To date the analysis of the air cascade family has been performed using a full Monte Carlo simulation. It is difficult to draw a definite conclusion about the interaction mechanism by using only this kind of simulation. On the other hand, attempts to reproduce the original gamma ray at the interaction point, for example decascading, have also been made. This method makes it possible to observe the interaction directly and to analyze the data from various angles. All of these methods, however, assume a constant ER in the cascade shower, where E is energy and R is the distance from the center of the cascade shower. It is impossible to reproduce the exact interaction height and energy by these methods. A relative method in separating one cascade shower from others is adopted. This method makes it possible to estimate the interaction height and energy by using information about the lateral spread of the cascade shower. Author

N85-35964*# Academia Sinica, Beijing (China). Inst. of High Energy Physics.
INTENSITIES OF HIGH-ENERGY COSMIC RAYS AT MOUNT KANBALA
J. R. Ren, H. H. Kuang, A. X. Huo, S. L. Lu, S. Su, Y. X. Wang, Y. G. Xue, C. R. Wang (Shangdong Univ.), M. He (Shangdong Univ.), N. J. Zhang (Shangdong Univ.) et al *In* NASA. Goddard Space Flight Center 19th Intern. Cosmic Ray Conf., Vol. 6 Aug. 1985 p 439-442 refs Sponsored in part by Japanese Ministry of Education (For primary document see N85-35848 24-93)
(HE-3.7-5) Avail: NTIS HC as boxed set only $200/MF A01 per volume or E99 per entire set CSCL 03B

General features of family events with Summary E sub gamma > 200 TeV, observed by the emulsion chambers at Mt. Kanbala, are presented in comparison with the Monte Carlo simulation. The lateral and cluster structure, and the energy spectra of constituent gamma-rays and hadrons are shown to be consistent with the Monte Carlo results calculated under the assumption of heavy-enriched primary, scaling, QCD jets and increasing cross-section. Author

N85-35965*# Academy of Sciences of the Georgian SSR, Tbilisi (USSR). Inst. of Physics.
STRUCTURED EVENTS IN PAMIR CARBON X-RAY CHAMBERS
G. G. Leptukh *In* NASA. Goddard Space Flight Center 19th Intern. Cosmic Ray Conf., Vol. 6 Aug. 1985 p 443-446 refs (For primary document see N85-35848 24-93)
(HE-3.7-7) Avail: NTIS HC as boxed set only $200/MF A01 per volume or E99 per entire set CSCL 03B

Experimental and theoretical investigations of structured events or narrow groups of hadrons in the Pamir carbon chambers are presented. These events are formed by the usual fluctuations of in-chamber development of nuclear electromagnetic cascade (NEC) initiated by a single hadron from the atmosphere. Author

N85-35966*# Bordeaux 1 Univ., Gradignan (France). Lab. de Physique Theorique.
ULTRA HIGH ENERGY EVENTS IN ECHOS SERIES AND PRIMARY ENERGY SPECTRUM
J. N. Capdevielle, J. Iwai (Tokyo Univ.), and T. Ogata (Tokyo Univ.) *In* NASA. Goddard Space Flight Center 19th Intern. Cosmic Ray Conf., Vol. 6 Aug. 1985 p 447-450 refs (For primary document see N85-35848 24-93)
(HE-3.7-9) Avail: NTIS HC as boxed set only $200/MF A01 per volume or E99 per entire set CSCL 03B

The compilation of ultra high energy jets suggests at present the existence of a bump in primary energy spectrum (with the standard concept of high energy collisions). The pseudo-rapidity distribution exhibits some typical anomalies, more than the (P sub t) behavior, which are (may be) the fingerprints of quark gluon plasma transition. The next results of Emulsion Chamber on Supersonic (ECHOS) will be in both cases determinant to confirm those tendancies, as well as an important effort of the cosmic ray community to develop in that sense a flying emulsion chamber experiment. Author

N85-35967*# Academy of Sciences (USSR), Alma-Ata. High Energy Physics Inst.
PECULIARITIES OF GAMMA-QUANTA DISTRIBUTION AT 20 TeV ENERGY
P. M. Ermakov, A. A. Loktionov, Yu. T. Lukin, and T. Kh. Sadykov *In* NASA. Goddard Space Flight Center 19th Intern. Cosmic Ray Conf., Vol. 6 Aug. 1985 p 451-454 refs (For primary document see N85-35848 24-93)
(HE-3.7-10) Avail: NTIS HC as boxed set only $200/MF A01 per volume or E99 per entire set CSCL 03B

The angular distribution of protons from the fragmentational region is analyzed. The gamma-quanta families are generated in a dense target by cosmic ray particles at 20 Tev energy. Families were found which had dense groups (spikes) of gamma-quanta where the rapidity/density is 3 times more than the average value determined for all registered families. The experimental data is compared with the results of artificial families simulation. Author

N85-35968*# National Aeronautics and Space Administration. Goddard Space Flight Center, Greenbelt, Md.
NINETEENTH INTERNATIONAL COSMIC RAY CONFERENCE. HE SESSIONS, VOLUME 7
Frank C. Jones, comp. Washington Aug. 1985 398 p refs Conf. held in La Jolla, Calif., 11-23 Aug. 1985 8 Vol.
(NASA-CP-2376-Vol-7; NAS 1.55:2376-Vol-7) Avail: NTIS HC as boxed set only $200/MF A01 per volume or E99 per entire set CSCL 03B

Papers submitted for presentation at the 19th International Cosmic ray Conference are compiled. This volume contains papers which address various aspects of extensive air showers (EAS) produced by energetic particles and gamma rays. For individual titles, see N85-35969 through N85-36065.

N85-35969*# Maryland Univ., College Park. Dept. of Physics and Astronomy.
ELECTRONS, MUONS AND HADRONS IN EXTENSIVE AIR SHOWERS AND HOW DO THEY DEPEND ON NUCLEAR INTERACTION MODEL, PART 2
J. A. Wrotniak and G. B. Yodh *In* NASA. Goddard Space Flight Center 19th Intern. Cosmic Ray Conf., Vol. 7 Aug. 1985 p 1-4 (For primary document see N85-35968 24-93)
Avail: NTIS HC as boxed set only $200/MF A01 per volume or E99 per entire set CSCL 03B

Some of the results of Monte Carlo simulations of extensive air showers for nuclear interactions models are presented. The most significant part of scaling violation effect is generated by the inclusion of rising cross-section. Among the models considered the lowest value for Eo/N(max) is obtained when rapidly rising cross-section and charge exchange are both included (model R-F01). The value is still 1.38 GeV/electron. Except at the highest energies, the sensitivity to atomic mass of the primary is greater than to specific assumptions about multiple production. G.L.C.

N85-35970*# Tokyo Univ. (Japan). Inst. for Cosmic Ray Research.
ANALYSIS OF EQUI-INTENSITY CURVES AND NU DISTRIBUTION OF EAS
G. Tanahashi *In* NASA. Goddard Space Flight Center 19th Intern. Cosmic Ray Conf., Vol. 7 Aug. 1985 p 5-8 refs (For primary document see N85-35968 24-93)
Avail: NTIS HC as boxed set only $200/MF A01 per volume or E99 per entire set CSCL 03B

The distribution of the number of muons in extensive air showers (EAS) and the equi-intensity curves of EAS are analyzed on the basis of Monte Carlo simulation of various cosmic ray composition and the interaction models. Problems in the two best combined models are discussed. Author

N85-35971*# Bordeaux Univ. (France). Lab. de Physique Theorique.
ANALYSIS OF THE HADRON COMPONENT IN E.A.S.
J. Procureur, J. N. Stamenov (Bulgarian Academy of Science, Sofia), P. V. Stavrev (Bulgarian Academy of Sciences, Sofia), and S. Z. Ushev *In* NASA. Goddard Space Flight Center 19th Intern. Cosmic Ray Conf., Vol. 7 Aug. 1985 p 9-11 refs (For primary document see N85-35968 24-93)
Avail: NTIS HC as boxed set only $200/MF A01 per volume or E99 per entire set CSCL 03B

Hadrons in extensive air showers (E.A.S.) provide direct information about high energy interactions. As a rule the biases pertaining to different shower array arrangements have a relative large influence for the basic phenomenological characteristics of the E.A.S. hadron component. In this situation, the problem of the correct comparison between model calculated and experimental characteristics is of great importance for the reliability of the derived conclusions about the high energy interaction characteristics. G.L.C.

N85-35972*# Maryland Univ., College Park. Dept. of Physics and Astronomy.
ELECTRONS, MUONS AND HADRONS IN EXTENSIVE AIR SHOWERS AND HOW DO THEY DEPEND ON NUCLEAR INTERACTION MODEL, PART 1
J. A. Wrotniak and G. B. Yodh *In* NASA. Goddard Space Flight Center 19th Intern. Cosmic Ray Conf., Vol. 7 Aug. 1985 p 12-15 refs (For primary document see N85-35968 24-93)
(Grant NSF PHY-82-07425)
Avail: NTIS HC as boxed set only $200/MF A01 per volume or E99 per entire set CSCL 03B

Monte Carlo simulations of extensive air showers were performed using a couple of different nuclear interaction models and obtaining a variety of shower characteristics. The discussion of these shows that the sensitivity of observables to the primary mass spectrum is significantly stronger than to the interaction model, the latter being quite weak. Author

N85-35973*# Lodz Univ. (Poland). Inst. of Nuclear Studies.
SIMULATION OF EAS PROPERTIES ON THE BASIS OF HIGH ENERGY INTERACTION MODEL DEDUCED FROM THE ACCELERATOR DATA
G. Kubiak, J. Szabelski, J. Wdeyozyk, and A. W. Wolfendale (Durham Univ.) *In* NASA. Goddard Space Flight Center 19th Intern. Cosmic Ray Conf., Vol. 7 Aug. 1985 p 16-19 refs (For primary document see N85-35968 24-93)
Avail: NTIS HC as boxed set only $200/MF A01 per volume or E99 per entire set CSCL 03B

Calculations of extensive air showers in atmosphere were performed using formulae describing p-p and p-air nucleus interactions. The formulae fitted to the accelerator data were extrapolated taking the same trend up to 10 to the 16 eV. Above that energy it was assumed that the degree of scaling violating/ alpha-parameter/ is saturating or even decreasing. The latter assumption follows from earlier work where it was found that without this restriction shower maxima at the highest energies are located too high in the atmosphere. Results of calculations have been compared with experimental data. The comparison was made separately for the curves obtained from the so called equal intensity cuts and for the Cerenkov data. G.L.C.

N85-35974*# Bordeaux Univ. (France). Lab. de Physique Theorique.
NEW ASPECTS IN NUCLEON-NUCLEUS COLLISIONS AND EAS PROPERTIES AROUND 10(6) GeV
J. N. Capdevielle and J. Gawin (Lodz Univ.) *In* NASA. Goddard Space Flight Center 19th Intern. Cosmic Ray Conf., Vol. 7 Aug. 1985 p 20-23 refs (For primary document see N85-35968 24-93)
Avail: NTIS HC as boxed set only $200/MF A01 per volume or E99 per entire set CSCL 03B

At energies higher than 2 x 10 to the 5 GeV, very little information exists on detailed properties of nucleon-nucleon collision; the rare elements are coming from jets, and, as nondirect improvements from gamma-ray families. The results exhibit some conflicting features, or, at least, very large fluctuations like copious production of gamma-rays in opposition to Centauro-like events, sometimes suggest that phase transition to quark gluon plasma occurs in nucleus-nucleus collisions and even in nucleon-nucleus collision. The multicluster phenomenological model (MPM) extrapolated for extensive air showers EAS simulation up to 5 x 10 to the 6 GeV to put in evidence some significant deviation between experimental data and prediction. G.L.C.

N85-35975*# Bordeaux Univ. (France).
SMALL AIR SHOWERS AND COLLIDER PHYSICS
J. N. Capdevielle, J. Gawin (Institute of Nuclear Physics, Lodz, Poland), and B. Grochalska (Institute of Nuclear Physics, Lodz, Poland) *In* NASA. Goddard Space Flight Center 19th Intern. Cosmic Ray Conf., Vol. 7 Aug. 1985 p 24-27 refs (For primary document see N85-35968 24-93)
(HE-4.1-9) Avail: NTIS HC as boxed set only $200/MF A01 per volume or E99 per entire set CSCL 03B

At energies lower than 2.5 X 10 to the 5 GeV (in Lab. system), more accurate information on nucleon-nucleon collision (p-p collider and on primary composition now exist. The behavior of those both basic elements in cosmic ray phenomenology from ISR energy suggests some tendencies for reasonable extrapolation in the next decade 2.0x10 to the 5 to 2.0x10 to the 6 GeV. Small showers in altitude, recorded in the decade 2 X 10 to the 4 to 2 X 10 to the 5 GeV offers a good tool to testify the validity of all the Monte-Carlo simulation analysis and appreciate how nucleon-air collision are different from nucleon-nucleon collisions. G.L.C.

N85-35976*# Tata Inst. of Fundamental Research, Bombay (India).
HIGH ENERGY HADRONS IN EXTENSIVE AIR SHOWERS
S. C. Tonwar *In* NASA. Goddard Space Flight Center 19th Intern. Cosmic Ray Conf., Vol. 7 Aug. 1985 p 28-31 refs (For primary document see N85-35968 24-93)
Avail: NTIS HC as boxed set only $200/MF A01 per volume or E99 per entire set CSCL 03B

Experimental data on the high energy hadronic component in

extensive air showers of energies approx. 10 to the 14 to 10 to the 16 eV when compared with expectaticns from Monte Carlo simulations have shown the observed showers to be deficient in high energy hadrons relative to simulated showers. An attempt is made to understand these anomalous features with more accurate comparison of observations with expectations, taking into account the details of the experimental system. Results obtained from this analysis and their implications for the high energy physics of particle interactions at energy approx. 10 to the 15 eV are presented.
Author

N85-35977*# Academy of Sciences of the Armenian SSR, Erivan (USSR).
DEPENDENCE OF THE AVERAGE SPATIAL AND ENERGY CHARACTERISTICS OF THE HADRON-LEPTON CASCADE ON THE STRONG INTERACTION PARAMETERS AT SUPERHIGH ENERGIES
N. G. Boyadjian, P. Yu. Dallakyan, A. P. Garyaka, and E. A. Mamidjanian *In* NASA. Goddard Space Flight Center 19th Intern. Cosmic Ray Conf., Vol. 7 Aug. 1985 p 32-35 refs (For primary document see N85-35968 24-93)
Avail: NTIS HC as boxed set only $200/MF A01 per volume or E99 per entire set CSCL 03B

A method for calculating the average spatial and energy characteristics of hadron-lepton cascades in the atmosphere is described. The results of calculations for various strong interaction models of primary protons and nuclei are presented. The sensitivity of the experimentally observed extensive air showers (EAS) characteristics to variations of the elementary act parameters is analyzed.
Author

N85-35978*# Indian Statistical Inst., Calcutta.
HADRONIC COMPONENTS OF EAS BY RIGOROUS SADDLE POINT METHOD IN THE ENERGY RANGE BETWEEN 10(5) AND 10(8) GeV
Malabika Sinha and Sisir Roy *In* NASA. Goddard Space Flight Center 19th Intern. Cosmic Ray Conf., Vol. 7 Aug. 1985 p 36-39 refs (For primary document see N85-35968 24-93)
Avail: NTIS HC as boxed set only $200/MF A01 per volume or E99 per entire set CSCL 03B

The study of hadronic components in the high energy range between 10 to the 5 and 10 to the 8 Gev exhibits by far the strongest mass sensitivity since the primary energy spectrum as discussed by Linsley and measured by many air shower experimental groups indicates a change of slope from -1.7 to 2.0 in this energy range. This change of slope may be due to several reasons such as a genuine spectral feature of astrophysical origin, a confinement effect of galactic component or a rather rapid change of mass, a problem which we have attempted to study here in detail.
G.L.C.

N85-35979*# Academy of Sciences (USSR), Moscow.
ABOUT INCREASE OF THE LARGE TRANSVERE MOMENTUM PROCESSES FRACTION IN hA INTERACTIONS AT ENERGIES 5.10(14) - 10(16) eV ACCORDING TO THE DATA ON E.A.S. HADRONS
T. V. Danilova, A. G. Dubovy, A. D. Erlykin, N. M. Nesterova, and A. P. Chubenko *In* NASA. Goddard Space Flight Center 19th Intern. Cosmic Ray Conf., Vol. 7 Aug. 1985 p 40-43 refs (For primary document see N85-35968 24-93)
Avail: NTIS HC as boxed set only $200/MF A01 per volume or E99 per entire set CSCL 03B

The lateral distributions of extensive air showers (EAS) hadrons obtained at Tien-Shan array are compared with the simulations. The simulation data have been treated in the same way as experimental data, including the recording method. The comparison shows that the experimental hadron lateral distributions are wider than simulated ones. On the base of this result the conclusion is drawn that the fraction of processes with large p (perpendicular) increases in hadron-air interactions at energies 5 x 10 to the 14 to 10 to the 16 eV compared with accelerator data in p-p interactions at lower energies.
Author

N85-35980*# Moscow State Univ. (USSR). Inst. of Nuclear Physics.
PHENOMENOLOGY OF SOFT HADRON INTERACTIONS AND THE RELEVANT EAS DATA
N. N. Kalmykov, G. B. Khristiansen, and M. V. Motova *In* NASA. Goddard Space Flight Center 19th Intern. Cosmic Ray Conf., Vol. 7 Aug. 1984 p 44-47 refs (For primary document see N85-35968 24-93)
Avail: NTIS HC as boxed set only $200/MF A01 per volume or E99 per entire set CSCL 03B

The interpretation of the experimental data in superhigh energy cosmic rays requires the calculations using various models of elementary hadron interaction. One should prefer the models justified by accelerator data and giving definite predictions for superhigh energies. The model of quark-gluon pomeron strings (the QGPS models) satisfies this requirement.
G.L.C.

N85-35981*# Academy of Sciences (USSR), Yakutsk. Inst. of Cosmophysical Research and Aeronomy.
THE MAXIMUM DEPTH OF SHOWER WITH E SUB 0 LARGER THAN 10(17) eV ON AVERAGE CHARACTERISTICS OF EAS DIFFERENT COMPONENTS
A. V. Glushkov, N. N. Efimov, I. T. Makarov, M. I. Pravdin, and L. G. Dedenko (Scientific-Research Inst. of Nuclear Physics) *In* NASA. Goddard Space Flight Center 19th Intern. Cosmic Ray Conf., Vol. 7 Aug. 1985 p 48-51 refs (For primary document see N85-35968 24-93)
Avail: NTIS HC as boxed set only $200/MF A01 per volume or E99 per entire set CSCL 03B

The extensive air shower (EAS) development model independent method of the determination of a maximum depth of shower (X sub m) is considered. X sub m values obtained on various EAS parameters are in a good agreement.
Author

N85-35982*# Moscow State Univ. (USSR). Inst. of Nuclear Physics.
SENSITIVITY OF DEPTH OF MAXIMUM AND ABSORPTION DEPTH OF EAS TO HADRON PRODUCTION MECHANISM
R. A. Antonov, V. I. Galkin, L. A. Hein, I. P. Ivanenko, B. L. Kanevsky, and V. A. Kuzmin *In* NASA. Goddard Space Flight Center 19th Intern. Cosmic Ray Conf., Vol. 7 Aug. 1985 p 52-55 refs (For primary document see N85-35968 24-93)
Avail: NTIS HC as boxed set only $200/MF A01 per volume or E99 per entire set CSCL 03B

Comparison of experimental data on depth of extensive air showers (EAS) development maximum in the atmosphere, T sub M and path of absorption, lambda, in the lower atmosphere of EAS with fixed particle number in the energy region eV with the results of calculation show that these parameters are sensitive mainly to the inelastic interaction cross section and scaling violation in the fragmentation and pionization region. The data are explained in a unified manner within the framework of a model in which scaling is violated slightly in the fragmentation region and strongly in the pionization region at primary cosmic rays composition close to the normal one and a permanent increase of inelastic interaction cross section. It is shown that, while interpreting the experimental data, disregard of two methodical points causes a systematic shift in T sub M: (1) shower selection system; and (2) EAS electron lateral distribution when performing the calculations on basis of which the transfer is made from the Cerenkov pulse FWHM to the depth of shower maximum, T sub M.
G.L.C.

N85-35983*# University of North Bengal, Darjeeling (India). Dept. of Physics.
A CRITICAL ANALYSIS OF AIR SHOWER STRUCTURE FUNCTIONS AND SIZE SPECTRUM MEASUREMENTS WITH THE NBU AIR SHOWER ARRAY
N. Chaudhuri and D. K. Basak *In* NASA. Goddard Space Flight Center 19th Intern. Cosmic Ray Conf., Vol. 7 Aug. 1985 p 56-59 refs (For primary document see N85-35968 24-93)
Avail: NTIS HC as boxed set only $200/MF A01 per volume or E99 per entire set CSCL 03B

A total of 11,000 showers in the size range 10 to the 4 to 10

to the 6 particles so far detected by the NBU air shower array has been analyzed using five different structure functions. A comparison of structure functions in terms: (1) of shower size; and (2) electron density at various core distances has been discussed to indicate the present status of structure functions in air shower analysis. Author

N85-35984*# Chongqing Inst. of Architecture and Engineering (China).
MEASUREMENT OF THE LOCAL DENSITY SPECTRUM
Z. H. Liu, J. G. Liu, G. J. Li, G. Z. Bai, Q. X. Geng, J. Ling, W. E. Hazen (Michigan Univ., Ann Arbor), and E. S. Hazen (Michigan Univ., Ann Arbor) *In* NASA. Goddard Space Flight Center 19th Intern. Cosmic Ray Conf., Vol. 7 Aug. 1985 p 60-63 refs (For primary document see N85-35968 24-93)
Avail: NTIS HC as boxed set only $200/MF A01 per volume or E99 per entire set CSCL 03B

Since there is still disagreement among the results of various groups, a measurement of the local density spectrum with a close-packed array of four scintillators, each of area 0.14 sq cm was made. Data are taken with conventional electronics, supervised by an on-line microcomputer. The data are stored on audio cassettes and analyzed with the aid of another microcomputer. Since four independent samples for each shower are available, uncertainties inherent in results from many earlier experiments can be minimized. Author

N85-35985*# Kobe Women's Junior Coll. (Japan).
CHARACTER OF ENERGY FLOW IN AIR SHOWER CORE
K. Mizushima, K. Asakimori (Kobe Univ.), T. Maeda (Kobe Univ.), T. Kameda (Kobe Women's Univ.), and Y. Misaki (Osaka Univ.) *In* NASA. Goddard Space Flight Center 19th Intern. Cosmic Ray Conf., Vol. 7 Aug. 1985 p 64-67 refs (For primary document see N85-35968 24-93)
Avail: NTIS HC as boxed set only $200/MF A01 per volume or E99 per entire set CSCL 03B

Energy per charged particle near the core of air showers was measured by 9 energy flow detectors, which were the combination of Cerenkov counters and scintillators. Energy per particle of each detector was normalized to energy at 2m from the core. The following results were obtained as to the energy flow: (1) integral frequency distribution of mean energy per particle (averaged over 9 detectors) is composed of two groups separated distinctly; and (2) showers contained in one group show an anisotropy of arrival direction. Author

N85-35986*# Mesei Univ., Tokyo (Japan). Dept. of Physics.
OBSERVATION OF EAS USING A LARGE WATER TANK
K. Inoue, H. Sakuyama, N. Suzuki, and T. Suzuki *In* NASA. Goddard Space Flight Center 19th Intern. Cosmic Ray Conf., Vol. 7 Aug. 1985 p 68 (For primary document see N85-35968 24-93)
Avail: NTIS HC as boxed set only $200/MF A01 per volume or E99 per entire set CSCL 03B

Using a large water tank (30 m in diameter, 4.5 m in depth) transition of extensive air showers (EAS) was investigated at Taro (200 m above sea level). There are set 150,0.4 sq m proportional counters on the bottom of the water tank. A conventional EAS array of 25 plastic scintillation detectors was arranged within several tens meter from the water tank. A proportional counter (10x10x-200 cc x2) is made of a square shaped pipe of iron. Tungsten wire (100 mu m phi) is stretched tight in the center of the counter. A gas mixture of 90% argon and 10% methane is used at 760 mmHg. About 3000 EAS were obtained through 1 m of water since 1984. G.L.C.

N85-35987*# Aichi Women's Coll. (Japan).
THE DEVELOPMENT OF AIR SHOWER IN THE IRON ABSORBER
M. Hazama, S. Dake (Kobe Univ.), K. Harada (Kobe Univ.), M. Kawamoto (Kobe Univ.), M. Sakata, Y. Yamamoto (Konan Univ.), and T. Sugihara (Kobe Univ.) *In* NASA. Goddard Space Flight Center 19th Intern. Cosmic Ray Conf., Vol. 7 Aug. 1985 p 69-72 refs (For primary document see N85-35968 24-93)
Avail: NTIS HC as boxed set only $200/MF A01 per volume or E99 per entire set CSCL 03B

The iron open-sandwich experiments to observe one dimensional development of individual air showers were carried out at Akeno Observatory. One dimensional energy flow, incident energy and production height of shower is estimated using the data of size and age obtained from the above experiment and simple calculation. Author

N85-35988*# Konan Univ., Kobe (Japan). Dept. of Physics.
APPLICATION OF PHOTODIODES TO THE DETECTION OF ELECTROMAGNETIC BURSTS
Y. Fukushima, To. Saito, M. Sakata, M. Shima, and Y. Yamamoto *In* NASA. Goddard Space Flight Center 19th Intern. Cosmic Ray Conf., Vol. 7 Aug. 1985 p 73-76 refs (For primary document see N85-35968 24-93)
Avail: NTIS HC as boxed set only $200/MF A01 per volume or E99 per entire set CSCL 03B

A new type of photodiode + scintillator (1 m2 x 1 cm) detector is developed to detect the large electro-magnetic burst under an EX-chamber. The threshold burst size is found to be 4.3 x 10 the 5 particles at the center of the scintillator. Therefore a gamma-ray family of 10 TeV is detectable by it, when it is set under 14 r.l. of iron. In addition, a very fast (2.4 nsec width) and very bright (correspond to 10 to the 6 particles) scintillation pulse has become available for this study. Author

N85-35989*# Tokyo Univ. (Japan). Inst. for Cosmic Ray Research.
CORE STRUCTURE OF EAS IN 10(15) TO 10(17) eV
T. Hara, Y. Hatano, N. Hayashida, T. Kifune, M. Nagano, and G. Tanahashi *In* NASA. Goddard Space Flight Center 19th Intern. Cosmic Ray Conf., Vol. 7 Aug. 1985 p 77-80 refs (For primary document see N85-35968 24-93)
Avail: NTIS HC as boxed set only $200/MF A01 per volume or E99 per entire set CSCL 03B

With the use of Akeno calorimeter, the attenuation of particles in concrete is analyzed as the function of the shower size of 10 to the 5th power to 10 to the 7th power. The attenuation length does not depend much on the shower size but depends a little on the shower age. The average value is approx. 150 g/sq cm for s = 0.5 to 0.85 and approx. 40 g/sq cm for s = 0.85 to 1.15. These values and their fluctuations are consistent with the equi-intensity curves of extensive air showers (EAS). Author

N85-35990*# Leeds Univ. (England). Dept. of Physics.
PARTICLE DISTRIBUTIONS IN APPROXIMATELY 10(14) 10(16) eV AIR SHOWER CORES AT SEA LEVEL
A. L. Hodson, A. G. Ash, and R. M. Bull (Nottingham Univ.) *In* NASA. Goddard Space Flight Center 19th Intern. Cosmic Ray Conf., Vol. 7 Aug. 1985 p 81-84 refs (For primary document see N85-35968 24-93)
Avail: NTIS HC as boxed set only $200/MF A01 per volume or E99 per entire set CSCL 03B

Experimental evidence is reported for fixed distances (0, 1.0, 2.5 and 4.0 m) from the shower centers and for core flattening. The cores become flatter, on average, as the shower size (primary energy) increases. With improved statistics on 4192 cores, the previous results are exactly confirmed. B.W.

N85-35991*# Bulgarian Academy of Science, Sofia. Inst. of Nuclear Research and Nuclear Energy.
THEORETICAL STUDY OF EAS HADRONIC STRUCTURE
L. Popova *In* NASA. Goddard Space Flight Center 19th Intern. Cosmic Ray Conf., Vol. 7 Aug. 1985 p 85-88 refs (For primary document see N85-35968 24-93)
Avail: NTIS HC as boxed set only $200/MF A01 per volume or E99 per entire set CSCL 03B

The structure of extensive air showers (EAS) is determined mainly by the energetic hadrons. They are strongly collimated in the core of the shower and essential difficulties are encountered for resolution of individual hadrons. The properties for resolution

are different from the variety of hadron detectors used in EAS experiments. This is the main difficulty in obtaining a general agreement between actually registered data with different detectors. The most plausible source for disagreement is the uncertainty in determination of the energy of individual hadrons. This research demonstrates that a better agreement can be obtained with the average tendency of hadronic measurements if one assumes a larger coefficient of inelasticity and stronger energy increase of the total inelastic cross section in high energy pion interactions. EAS data above 10 to the 5th power GeV are revealing a faster development of hadronic cascades in the air then can be expected by extrapolating the parameters of hadron interactions obtained in accelerator measurements. B.W.

N85-35992*# Leeds Univ. (England). Dept. of Physics.
MONTE CARLO SIMULATIONS OF ELECTRON LATERAL DISTRIBUTIONS IN THE CORE REGION OF 10(13) - 10(16) eV AIR SHOWERS
A. G. Ash *In* NASA. Goddard Space Flight Center 19th Intern. Cosmic Ray Conf., Vol. 7 Aug. 1985 p 89-92 refs (For primary document see N85-35968 24-93)
Avail: NTIS HC as boxed set only $200/MF A01 per volume or E99 per entire set CSCL 03B

This paper contains details of computer models of shower development which have been used to investigate the experimental data on shower cores observed in the Leeds 35 sq m and Sacramento Peak (New Mexico) 20 sq m arrays of current limited spark (discharge) chambers. The simulations include predictions for primaries ranging from protons to iron nuclei (with heavy nuclei treated using both superposition and fragmentation models). Author

N85-35993*# Leeds Univ. (England). Dept. of Physics.
COMPARISON OF SIMULATION RESULTS WITH SEA-LEVEL EXPERIMENTAL DATA ON 10(14) - 10(16) AIR SHOWER CORES Abstract Only
A. G. Ash *In* NASA. Goddard Space Flight Center 19th Intern. Cosmic Ray Conf., Vol. 7 Aug. 1985 p 93 (For primary document see N85-35968 24-93)
Avail: NTIS HC as boxed set only $200/MF A01 per volume or E99 per entire set CSCL 03B

Simulation predictions for the Leeds 35 sq m horizontal discharge chamber array for proton primaries with a approx. E sup 2.7 spectrum extrapolated from balloon data to 10 to the 16th power eV give power law rho (r)-spectra with constant slope approx. -2 consistent with the experimental data up to the point at which they steepen but overshooting them at higher densities, and at high shower sizes predicted cores which are significantly steeper than those observed. Further comparisons with results for heavy nuclei primaries (up to A = 56) point to the inadequacy of changes in primary composition to account for the observed density spectra and core flattening, and the shower size spectrum together, and point, therefore, to the failure of the scaling interaction model at approx. 10 to the 15th power eV primary energy. Author

N85-35994*# Leeds Univ. (England). Dept. of Physics.
PARTICLE DISTRIBUTIONS IN APPROXIMATELY 10(13) - 10(16) eV AIR SHOWER CORES AT MOUNTAIN ALTITUDE AND COMPARISON WITH MONTE CARLO SIMULATIONS
A. G. Ash *In* NASA. Goddard Space Flight Center 19th Intern. Cosmic Ray Conf., Vol. 7 Aug. 1985 p 94-97 refs Sponsored in part by Science and Engineering Research Council (For primary document see N85-35968 24-93)
(HE-4.2-18) Avail: NTIS HC as boxed set only $200/MF A01 per volume or E99 per entire set CSCL 03B

Photographs of 521 shower cores in an array of current-limited spark (discharge) chambers at Sacramento Peak (2900m above sea level, 730 g /sq cm.), New Mexico, U.S.A., have been analyzed and the results compared with similar data from Leeds (80m above sea level, 1020 g sq cm.). It was found that the central density differential spectrum is consistent with a power law index of -2 up to approx. 1500/sq m where it steepens, and that shower cores become flatter on average with increasing size. Scaling model predictions for proton primaries with a approx E sup -2.71 energy spectrum account well for the altitude dependence of the data at lower densities. However, deviations at higher densities indicate a change in hadron interaction characteristics between approx few x 10 to the 14th power and 10 to the 15th power eV primary energy causing particles close to the shower axis to be spread further out. Author

N85-35995*# Academy of Sciences of the Georgian SSR, Tbilisi (USSR). Inst. of Physics.
TSKHRA-TSKARO COMPLEX INTENDED FOR THE INVESTIGATIONS OF EAS SPATIAL CHARACTERISTICS NEAR AXIS
O. L. Berdzenishvili, Yu. G. Verbetski, Yu. A. Gromov, D. M. Kotlyarevski, A. A. Novalov, I. V. Paziashvili, N. S. Rusishvili, L. Sh. Khachaturyan, P. V. Tsomaya, and Z. Sh. Sharvadze *In* NASA. Goddard Space Flight Center 19th Intern. Cosmic Ray Conf., Vol. 7 Aug. 1985 p 98-100 (For primary document see N85-35968 24-93)
Avail: NTIS HC as boxed set only $200/MF A01 per volume or E99 per entire set CSCL 03B

Tskhra-Tskaro EAS complex located at the height of 2500 m above sea level is intended for a correlated investigation of three main components of the extended atmospheric showers (EAS) - hadron, muon and electro-proton ones - near the shower axis. This complex is aimed at the investigation of proton and primary cosmic radiation nucleus interactions with the nuclei of air atoms within the energy range 10 to the 14th power to 10 to the 16th power eV. Research equipment design and installation are discussed. B.W.

N85-35996*# University of North Bengal, Darjeeling (India). Dept. of Physics.
A NEW STUDY OF SHOWER AGE DISTRIBUTION IN NEAR VERTICAL SHOWERS BY EAS AIR SHOWER ARRAY
N. Chaudhuri, D. K. Basak, G. C. Goswami, and B. Ghosh *In* NASA. Goddard Space Flight Center 19th Intern. Cosmic Ray Conf., Vol. 7 Aug. 1984 p 101-104 refs (For primary document see N85-35968 24-93)
Avail: NTIS HC as boxed set only $200/MF A01 per volume or E99 per entire set CSCL 03B

The air shower array has been developed since it started operation in 1931. The array covering an area of 900 sq m now incorporates 21 particle density sampling detectors around two muon magnetic spectrographs. The air showers are detected in the size range 10 to the 4th power to 10 to the 6th power particles. A total of 11000 showers has so far been detected. Average values of shower age have been obtained in various shower size ranges to study the dependence of shower age on shower size. The core distance dependence of shower age parameter has also been analyzed for presentation. Author

N85-35997*# University of North Bengal, Darjeeling (India). Dept. of Physics.
A NEW STUDY OF MUONS IN AIR SHOWERS BY NBU AIR SHOWER ARRAY
N. Chaudhuri, N. Mukherjee, S. Sarkar, D. K. Basak, and B. Ghosh *In* NASA. Goddard Space Flight Center 19th Intern. Cosmic Ray Conf., Vol. 7 Aug. 1985 p 105-106 refs (For primary document see N85-35968 24-93)
Avail: NTIS HC as boxed set only $200/MF A01 per volume or E99 per entire set CSCL 03B

The North Bengal University (NBU) air shower array has been in operation in conjunction with two muon magnetic spectrographs. The array incorporates 21 particle density sampling detectors around the magnetic spectrographs covering an area of 900 sq m. The layout of the array is based on the arrangement of detectors in a square symmetry. The array set up on the ground level is around a 10 m high magnetic spectrograph housing. This magnetic spectrograph housing limits the zenith angular acceptance of the incident showers to a few degrees. Three hundred muons in the fitted showers of size range 10 to the 4th power to 10 to the 5th power particles have so far been scanned and the momenta determined in the momentum range 2 - 440 GeV/c. More than

1500 recorded showers are now in the process of scanning and fitting. A lateral distribution of muons of energy greater than 300 MeV in the shower size range 10 to the 5th power to 7 x 10 to the 5th power has been obtained. B.W.

N85-35998*# Kobe Univ. (Japan). Dept. of Physics.
LATERAL DISTRIBUTION OF ELECTRONS OF AIR SHOWERS
K. Asakimori, T. Maeda, T. Kameda (Kobe Women's Univ.), K. Mizushima (Kobe Women's Junior Coll.), and Y. Misaki (Osaka Univ.) *In* NASA. Goddard Space Flight Center 19th Intern. Cosmic Ray Conf., Vol. 7 Aug. 1985 p 107-110 refs (For primary document see N85-35968 24-93)
Avail: NTIS HC as boxed set only $200/MF A01 per volume or E99 per entire set CSCL 03B

The lateral distribution of electrons (LDE) of the air showers of size 10 to the 5th power to 10 to the 6th power was studied within one MU. It was found that the LDE of the air showers observed is well represented by NKG function except for vicinity of the core. It was also found that LDE measured by thin scintillators does not differ from that measured by thick ones of 50mm thickness. Author

N85-35999*# Lodz Univ. (Poland). (Cosmic Ray Lab.)
DETAILED STUDIES OF THE ELECTRON LATERAL DISTRIBUTION IN EXTENSIVE AIR SHOWERS WITH ENERGIES AROUND 10(16) eV
T. Dzikowski, J. Gawin, and J. Wdowczyk *In* NASA. Goddard Space Flight Center 19th Intern. Cosmic Ray Conf., Vol. 7 Aug. 1984 p 111-113 refs (For primary document see N85-35968 24-93)
Avail: NTIS HC as boxed set only $200/MF A01 per volume or E99 per entire set CSCL 03B

Detailed studies have been performed of the electron lateral distribution in extensive air showers using the Lodz extensive air shower array. The showers were grouped according to their particle densities around 20 m from the core. The grouping was made in very narrow intervals of the densities. For every group of showers and for every distance interval /changing by 5 m/ histograms of the numbers of electron counters discharged have been obtained. The trays of G.M counters were located at following distances from the center of the triggering detectors array: 16 m, 76 m, 117 m, 137 m, 141 m and 147 m. B.W.

N85-36000*# Maryland Univ., College Park.
STUDY OF MUONS NEAR SHOWER CORES AT SEA LEVEL USING THE E594 NEUTRINO DETECTOR Abstract Only
J. A. Goodman, S. C. Gupta, H. Freudenreich, K. Sivaprasad, S. C. Tonwar (Tata Inst. of Fundamental Research), G. B. Yodh, R. W. Ellsworth (George Mason Univ.), M. C. Goodman (ANL), D. Bogert (Fermi National Lab.), and R. Burnstein (Illinois Inst. of Tech.) *In* NASA. Goddard Space Flight Center 19th Intern. Cosmic Ray Conf., Vol. 7 Aug. 1985 p 114 (For primary document see N85-35968 24-93)
Avail: NTIS HC as boxed set only $200/MF A01 per volume or E99 per entire set CSCL 03B

The E594 neutrino detector has been used to study the lateral distribution of muons of energy > 3 GeV near shower cores. The detector consists of a 340 ton fine grain calorimeter with 400, 000 cells of flash chamber and dimensions of 3.7 m x 20 m x 3.7 m (height). The average density in the calorimeter is 1.4 gm/sq cm, and the average Z is 21. The detector was triggered by four 0.6 sq m scintillators placed immediately on the top of the calorimeter. The trigger required at least two of these four counters. The accompanying extensive air showers (EAS) was sampled by 14 scintillation counters located up to 15 m from the calorimeter. Several off line cuts have been applied to the data. Demanding five particles in at least two of the trigger detectors, a total of 20 particles in all of them together, and an arrival angle for the shower < 450 deg reduced the data sample to 11053 events. Of these in 4869 cases, a computer algorithm found at least three muons in the calorimeter. B.W.

N85-36001*# Osaka City Univ. (Japan). Dept. of Physics.
CORRELATION OF HIGH ENERGY MUONS WITH PRIMARY COMPOSITION IN EXTENSIVE AIR SHOWER
C. Chou, S. Higashi, N. Hiraoka, S. Ozaki, T. Sato, T. Suwada, T. Takahasi, and H. Umeda *In* NASA. Goddard Space Flight Center 19th Intern. Cosmic Ray Conf., Vol. 7 Aug. 1985 p 115-118 refs (For primary document see N85-35968 24-93)
(HE-4.3-7) Avail: NTIS HC as boxed set only $200/MF A01 per volume or E99 per entire set CSCL 03B

An experimental investigation of high energy muons above 200 GeV in extensive air showers has been made for studying high energy interaction and primary composition of cosmic rays of energies in the range 10 to the 14th power approx. 10 to the 15th power eV. The muon energies are estimated from the burst sizes initiated by the muons in the rock, which are measured by four layers of proportional counters, each of area 5 x 2.6 sq m, placed at 30 m.w.e. deep, Funasaka tunnel vertically below the air shower array. These results are compared with Monte Carlo simulations based on the scaling model and the fireball model for two primary compositions, all proton and mixed. B.W.

N85-36002*# Tokyo Univ., Tanashi (Japan). Inst. for Cosmic Ray Research.
MEASUREMENT OF ENERGY MUONS IN EAS AT ENERGY REGION LARGER THEAN 10(17) eV
Y. Matsubara, T. Hara, N. Hayashida, K. Kamata, M. Nagano, H. Ohoka, G. Tanahasni, and T. Teshima (Kyoto Univ., Sakyo-Ku, Japan) *In* NASA. Goddard Space Flight Center 19th Intern. Cosmic Ray Conf., Vol. 7 Aug. 1985 p 119-122 refs (For primary document see N85-35968 24-93)
(HE-4.3-8) Avail: NTIS HC as boxed set only $200/MF A01 per volume or E99 per entire set CSCL 03B

A measurement of low energy muons in extensive air showers (EAS) (threshold energies are 0.25, 0.5, 0.75 and 1.38 GeV) was carried out. The density under the concrete shielding equivalent to 0.25 GeV at core distance less than 500 m and 0.5 GeV less than 150 m suffers contamination of electromagnetic components. Therefore the thickness of concrete shielding for muon detectors for the giant air shower array is determined to be 0.5 GeV equivalence. Effects of photoproduced muons are found to be negligible in the examined ranges of shower sizes and core distances. The fluctuation of the muon density in 90 sq m is at most 25% between 200 m and 600 m from the core around 10 to the 17th power eV. Author

N85-36003*# Nottingham Univ. (England).
MUON FLUCTUATION STUDIES OF EAS > 10(17) eV
P. R. Blake, M. Luksys, W. F. Nash, and A. J. Sephton *In* NASA. Goddard Space Flight Center 19th Intern. Cosmic Ray Conf., Vol. 7 Aug. 1985 p 123-126 refs (For primary document see N85-35968 24-93)
(HE-4.3-9) Avail: NTIS HC as boxed set only $200/MF A01 per volume or E99 per entire set CSCL 03B

Fluctuation studies need to compare a parameter which is sensitive to longitudinal fluctuations against a parameter which is insensitive. Cascade calculations indicate that the shower size parameter at Haverah Park, rho (500), and the muon density are insensitive while parameters that significantly reflect the longitudinal development of a particular extensive air shower (EAS) include the muon/water Cerenkov response ratio and the muon arrival time dispersion. This paper presents conclusions based on muon fluctuation studies of EAS measured between 1976 and 1981 at Haverah Park. Author

N85-36004*# Nottingham Univ. (England).
AVERAGE FEATURES OF THE MUON COMPONENT OF EAS > OR = 10(17) eV
P. R. Blake, M. Luksys, W. F. Nash, and A. J. Sephton *In* NASA. Goddard Space Flight Center 19th Intern. Cosmic Ray Conf., Vol. 7 Aug. 1985 p 127-130 refs (For primary document see N85-35968 24-93)
(HE-4.3-10) Avail: NTIS HC as boxed set only $200/MF A01 per volume or E99 per entire set CSCL 03B

Three 10 sq m liquid scintillators were situated at approximately 0 m, 150 m and 250 m from the center of the Haverah Park array. The detectors were shielded by lead/barytes giving muon detection thresholds of 317 MeV, 431 MeV and 488 MeV respectively. During part of the operational period the 431 MeV threshold was lowered to 313 MeV for comparison purposes. For risetime measurement fast phototubes were used and the 10% to 70% amplitude time interval was parameterized by T sub 70. A muon lateral density distribution of the form rho mu (R theta) = k[rho(500)]0.94 1/R(1 + R/490)-eta has been fitted to the data for 120 m R< 600 m and 0.27 < (500) < 2.55. The shower size parameter < (500) is the water Cerenkov response at 500 m from the core of the extensive air showers (EAS) and is relatable to the primary energy. The results show general consistency. B.W.

N85-36005*# Hong Kong Univ. Dept. of Physics.
MEASUREMENT OF SHOWER ELECTRONS AND MUONS USING A SMALL AIR SHOWER ARRAY
S. K. Chan and L. K. Ng *In* NASA. Goddard Space Flight Center 19th Intern. Cosmic Ray Conf., Vol. 7 Aug. 1985 p 131-134 refs (For primary document see N85-35968 24-93)
(HE-4.3-11) Avail: NTIS HC as boxed set only $200/MF A01 per volume or E99 per entire set CSCL 03B

A small air shower array has been used to measure the size spectrum of air showers at sea level in the size range 6.10 to the 3rd power to 10 to the 6th power. The result fitted with the power law gives an index 2.79 + or - 0.11 for the differential spectrum. Lateral distribution of electrons fitted with the well known NKG function results in an age parameter s = 1.35 for core distances less than 30m and s = 0.8 for longer core distances. Lateral distribution of muons follows the general shape of Greisen's relation but is much higher in intensity. Muon and electron densities at the same observation point are also compared. Author

N85-36006*# Hong Kong Univ. Dept. of Physics.
THE LONGITUDINAL DEVELOPMENT OF MUONS IN COSMIC RAY AIR SHOWERS AT ENERGIES 10(15) - 10(17) eV
In NASA. Goddard Space Flight Center 19th Intern. Cosmic Ray Conf., Vol. 7 Aug. 1985 p 135-138 refs (For primary document see N85-35968 24-93)
(HE-4.3-12) Avail: NTIS HC as boxed set only $200/MF A01 per volume or E99 per entire set CSCL 03B

The relationship between longitudinal development of muons and conventional equi-intensity cuts is carefully investigated. The development of muons in Extensive Air Showers (EAS) has been calculated using simulation with a scaling violation model at the highest energies and mixed primary composition. Profiles of equi-intensity cuts expected at observation altitudes of 550, 690 and 930/sq cm can fit the observed data very well. Author

N85-36007*# Bordeaux Univ. (France).
TOPOLOGICAL ASPECTS OF AGE PARAMETER
J. N. Capdevielle and J. Gawin (Institute of Nuclear Studies, Lodz, Poland) *In* NASA. Goddard Space Flight Center 19th Intern. Space Flight Center, Vol. 7 Aug. 1985 p 139-142 refs (For primary document see N85-35968 24-93)
(HE-4.3-13) Avail: NTIS HC as boxed set only $200/MF A01 per volume or E99 per entire set CSCL 03B

The well known NKG function is a very useful tool to describe the lateral extension of the electromagnetic component in Extensive Air Showers (EAS); however, in spite of non-negligible qualities (simplicity, normalization by beta function), it doesn't correspond exactly to the natural shape of the lateral electron distribution. Several bias may occur in size estimation if NKG is used without correction. It is shown that the longitudinal age parameter s sub t can be correlated with the information obtained from the lateral electron densities according to the conditions of use of the NKG function. Author

N85-36008*# Texas Univ. at Dallas, Richardson.
MONTE CARLO SIMULATION OF EAS GENERATED BY 10(14) - 10(16) eV PROTONS
E. J. Fenyves, B. C. Yunn, and Todor Stanev (Franklin Inst., Newark, Del.) *In* NASA. Goddard Space Flight Center 19th Intern. Cosmic Ray Conf., Vol. 7 Aug. 1985 p 143-146 refs Sponsored in part by NSF (For primary document see N85-35968 24-93)
(HE-4.3-14) Avail: NTIS HC as boxed set only $200/MF A01 per volume or E99 per entire set CSCL 03B

Detailed Monte Carlo simulations of extensive air showers to be detected by the Homestake Surface Underground Telescope and other similar detectors located at sea level and mountain altitudes have been performed for 10 to the 14th power to 10 to the 16th power eV primary energies. The results of these Monte Carlo calculations will provide an opportunity to compare the experimental data with different models for the composition and spectra of primaries and for the development of air showers. The results obtained for extensive air showers generated by 10 to the 14th power to 10 to the 16th power eV primary protons are reported. Author

N85-36009*# Moscow State Univ. (USSR). Inst. of Nuclear Physics.
LATERAL DISTRIBUTION ON CHARGED PARTICLES IN EAS
L. G. Dedenko, G. V. Kulikov, V. I. Solovjeva, and V. F. Sulakov *In* NASA. Goddard Space Flight Center 19th Intern. Cosmic Ray Conf., Vol. 7 Aug. 1985 p 147-150 refs (For primary document see N85-35968 24-93)
(HE-4.3-15) Avail: NTIS HC as boxed set only $200/MF A01 per volume or E99 per entire set CSCL 03B

Lateral distribution of charged particles which allow for the finiteness of energy gamma-quanta, the inhomogeneity of the atmosphere and the experimental selection of EAS are needed to interpret experimental data. The effects of finiteness of energy of gamma-quanta which produce the partial electron-photon cascades were considered by substituting K R sub m instead of R sub m in NKG approximation where K was found to be 0.56 from comparison with the experimental data. New results on the lateral distribution of electrons in the partial cascades from gamma-quanta were obtained. It is shown that the coefficient K can be regarded as a constant. The last approximation of K was found to be most adequate when compared with the experimental data. The inhomogeneity of the atmosphere, muons and experimental selection are considered. The calculation of Ne are extended from 100,000 to 10 million for sea level and for Akeno level. E.A.K.

N85-36010*# Moscow State Univ. (USSR). Inst. of Nuclear Physics.
LATERAL DISTRIBUTION OF HIGH ENERGY MUONS IN EAS OF SIZES Ne APPROXIMATELY EQUALS 10(5) AND Ne APPROXIMATELY EQUALS 10(6)
Yu. N. Bazhutov, G. G. Ermakov, G. G. Fomin, V. I. Isaev, Z. V. Jarochkina, N. N. Kalmykov, B. A. Khrenov, G. B. Khristiansen, G. V. Kulikov, M. V. Motova et al *In* NASA. Goddard Space Flight Center 19th Intern. Cosmic Ray Conf., Vol. 7 Aug. 1985 p 151-154 refs (For primary document see N85-35968 24-93)
(HE-4.3-16) Avail: NTIS HC as boxed set only $200/MF A01 per volume or E99 per entire set CSCL 03B

Muon energy spectra and muon lateral distribution in EAS were investigated with the underground magnetic spectrometer working as a part of the extensive air showers (EAS) array. For every registered muon the data on EAS are analyzed and the following EAS parameters are obtained, size N sub e, distance r from the shower axis to muon, age parameter s. The number of muons with energy over some threshold E associated to EAS of fixed parameters are measured, I sub reg. To obtain traditional characteristics, muon flux densities as a function of the distance r and muon energy E, muon lateral distribution and energy spectra are discussed for hadron-nucleus interaction model and composition of primary cosmic rays. E.A.K.

N85-36011*# Utah Univ., Salt Lake City. Dept. of Physics.
ENERGY CALIBRATION OF THE FLY'S EYE DETECTOR
R. M. Baltrusaitis, G. L. Cassiday, R. Cooper, J. W. Elbert, P. R. Gerhardy, S. Ko, E. C. Loh, Y. Mizumoto, P. Sokolsky, and D. Steck *In* NASA. Goddard Space Flight Center 19th Intern. Cosmic Ray Conf., Vol. 7 Aug. 1985 p 155-158 refs (For

primary document see N85-35968 24-93)
(Grant NSF PHY-82-01089)
(HE-4.4-1) Avail: NTIS HC as boxed set only $200/MF A01 per volume or E99 per entire set CSCL 03B

The methods used to calibrate the Fly's eye detector to evaluate the energy of EAS are discussed. The energy of extensive air showers (EAS) as seen by the Fly's Eye detector are obtained from track length integrals of observed shower development curves. The energy of the parent cosmic ray primary is estimated by applying corrections to account for undetected energy in the muon, neutrino and hadronic channels. Absolute values for E depend upon the measurement of shower sizes N sub e(x). The following items are necessary to convert apparent optical brightness into intrinsical optical brightness: (1) an assessment of those factors responsible for light production by the relativistic electrons in an EAS and the transmission of light thru the atmosphere, (2) calibration of the optical detection system, and (3) a knowledge of the trajectory of the shower. E.A.K.

N85-36012*# Utah Univ., Salt Lake City. Dept. of Physics.
THE STRUCTURE OF EAS AT E > 0.1 EeV
R. M. Baltrusaitis, G. L. Cassiday, R. Cooper, J. W. Elbert, P. R. Gerhardy, E. C. Loh, Y. Mizumoto, P. Sokolsky, and D. Steck *In* NASA. Goddard Space Flight Center 19th Intern. Cosmic Ray Conf., Vol. 7 Aug. 1985 p 159-162 refs (For primary document see N85-35968 24-93)
(Grant NSF PHY-82-01089)
(HE-4.4-2) Avail: NTIS HC as boxed set only $200/MF A01 per volume or E99 per entire set CSCL 03B

The ratio of extensive air showers (EAS) total shower energy in the electromagnetic channel (E em) to the size of the shower at maximum development (N max) from a direct measurement of shower longitudinal development using the air fluorescence technique was calculated. The values are not inconsistent with values based upon track length integrals of the Gaisser-Hillas formula for shower development or the known relation between shower energy and size at maximum for pure electromagnetic cascades. Using Linsley's estimates for undetected shower energy based on an analysis of a wide variety of cosmic ray data, the following relation for total shower energy E vs N max is obtained. The Gaisser Hillas implied undetected shower energy fractions. E.A.K.

N85-36013*# New Mexico Univ., Albuquerque. Dept. of Physics and Astronomy.
STANDARD VALUE FOR THE RADIATION LENGTH IN AIR
John Linsley *In* NASA. Goddard Space Flight Center 19th Intern. Cosmic Ray Conf., Vol. 7 Aug. 1985 p 163-166 refs (For primary document see N85-35968 24-93)
(HE-4.4-4) Avail: NTIS HC as boxed set only $200/MF A01 per volume or E99 per entire set CSCL 03B

The radiation length in air, was studied. Calculations were finished and give new values for t sub o in atomic oxygen and nitrogen which are entirely free of dependence on the Thomas-Fermi approximate model. With the usual small corrections for atmospheric A and CO2, these give t sub o air = 37.15 g cm/2, in close agreement with a value recommended, but in contrast to t sub o air = 36.66 g cm/2 obtained using the Thomas-Fermi approximation. E.A.K.

N85-36014*# New Mexico Univ., Albuquerque. Dept. of Physics and Astronomy.
LONGITUDINAL TRIAL FUNCTIONS AND THE COSMIC RAY ENERGY SCALE
John Linsley *In* NASA. Goddard Space Flight Center 19th Intern. Cosmic Ray Conf., Vol. 7 Aug. 1985 p 167-170 refs (For primary document see N85-35968 24-93)
Avail: NTIS HC as boxed set only $200/MF A01 per volume or E99 per entire set CSCL 03B

Formulae which were proposed to represent the longitudinal profiles of cosmic ray air showers are compared, and the physical interpretation of their parameters is examined. Applications to the problem of energy calibration are pointed out. Adoption of a certain especially simple formula is recommended, and its use is illustrated. E.A.K.

N85-36015*# Tokyo Univ. (Japan).
EAS DEVELOPMENT CURVE AT ENERGY OF 10(16) - 10(18) eV MEASURED BY OPTICAL CERENKOV LIGHT
T. Hara, M. Daigo (Wakayama Medical Coll., Japan), M. Honda, K. Kamata, T. Kifune, Y. Mizumoto (Fujitsu Ltd., Tokyo, Japan), M. Nagano, Y. Ohno, and G. Tanahasni *In* NASA. Goddard Space Flight Center 19th Intern. Cosmic Ray Conf., Vol. 7 Aug. 1985 p 171-174 refs (For primary document see N85-35968 24-93)
(HE-4.4-7) Avail: NTIS HC as boxed set only $200/MF A01 per volume or E99 per entire set CSCL 03B

The data of optical Cerenkov light from extensive air shower observed at the core distance more than 1 Km at Akeno are reexamined. Applying the new simulated results, the shower development curves for the individual events were constructed. For the showers of 10 to 17th power eV the average depth at the shower maximum is determined to be 660 + or - 40 gcm/2. The shower curve of average development is found to be well described by a Gaisser-Hillas shower development function with above shower maximum depth. E.A.K.

N85-36016*# Mansoura Univ. (Egypt). Dept. of Physics.
MISSING ENERGIES AT PAIR CREATION
Ahmed Abu El-Ela, Soad Hassan (Kiel Univ.), and Erich R. Bagge (Kiel Univ.) *In* NASA. Goddard Space Flight Center 19th Intern. Cosmic Ray Conf., Vol. 7 Aug. 1985 p 175-178 refs (For primary document see N85-35968 24-93)
(HE-4.4-8) Avail: NTIS HC as boxed set only $200/MF A01 per volume or E99 per entire set CSCL 03B

Wilson cloud chamber measurements of the separated spectra of positrons and electrons produced by gamma quanta of 6.14 MeV differ considerably from the theoretically predicted spectra by BETHE and HEITLER, but are in good agreement with those of a modified theory of pair creation. E.A.K.

N85-36017*# Kobe Univ. (Japan). Dept. of Physics.
TRANSITION EFFECT OF AIR SHOWER PARTICLES IN PLASTIC SCINTILLATORS
K. Asakimori, T. Maeda, T. Kameda (Kobe Women's Univ., Japan), K. Mizushima (Kobe Women's Junior Coll., Japan), and Y. Misaki (Osaka Univ.) *In* NASA. Goddard Space Flight Center 19th Intern. Cosmic Ray Conf., Vol. 7 Aug. 1985 p 179-182 refs (For primary document see N85-35968 24-93)
(HE-4.4-9) Avail: NTIS HC as boxed set only $200/MF A01 per volume or E99 per entire set CSCL 03B

The transition effect of air shower particles in the plastic scintillators near the core was measured by scintillators of various thickness. The air showers selected for the measurement were of > 10,000. Results obtained are as follows: (1) the multiplication of shower particles in the scintillators is less than 20% for that of 50 mm thickness; (2) dependence of the transition effect on age parameter is not recognized within the experimental errors. E.A.K.

N85-36018*# Academy of Sciences of the Armenian SSR, Erivan (USSR). Physics Inst.
THE SYSTEM OF EAS TIME ANALYSIS
A. Z. Khalafyan, V. M. Mkhitaryan, J. S. Oganezova, G. L. Bashindjaghayan (Moscow State Univ.), N. B. Sinev (Moscow State Univ.), and L. I. Sarycheva (Moscow State Univ.) *In* NASA. Goddard Space Flight Center 19th Intern. Cosmic Ray Conf., Vol. 7 Aug. 1985 p 183-186 (For primary document see N85-35968 24-93)
(HE-4.4-10) Avail: NTIS HC as boxed set only $200/MF A01 per volume or E99 per entire set CSCL 03B

The extensive air showers' (EAS) front shape, angle of incidence, disk thickness, particle distribution along the shower, on the delayed and EAS front advancing particles were determined. The suggested system of the EAS time analysis allows determination of the whole EAS longitudinal structure at the observation points. The information from the detectors is continuously recorded

in the memory with the memory cell switching in 5 ns, this enables fixation of the moment of pulse input from the detector with an accuracy to + or - 2.5 ns. Along with the fast memory, a slow memory with the cell switching in 1 micron s is introduced in the system, this permits observation of relatively large time intervals with respect to the trigger pulse with an appropriately lower accuracy. E.A.K.

N85-36019*# Samarkand Alisher Navoi State Univ. (USSR).
ON THE DETERMINATION OF THE DEPTH OF EAS DEVELOPMENT MAXIMUM USING THE LATERAL DISTRIBUTION OF CERENKOV LIGHT AT DISTANCES < 150 m FROM EAS AXIS
N. Aliev, T. Alimov, M. Kakhkharov, B. M. Makhmudov, N. Rakhimova, R. Tashpulatov, N. N. Kalmykov (Moscow State Univ.), G. B. Khristiansen (Moscow State Univ.), and V. V. Prosin (Moscow State Univ.) *In* NASA. Goddard Space Flight Center 19th Intern. Cosmic Ray Conf., Vol. 7 Aug. 1985 p 187-190 refs (For primary document see N85-35968 24-93)
(HE-4.4-13) Avail: NTIS HC as boxed set only $200/MF A01 per volume or E99 per entire unit CSCL 03B

The Samarkand extensive air showers (EAS) array was used to measure the mean and individual lateral distribution functions (LDF) of EAS Cerenkov light. The analysis of the individual parameters b showed that the mean depth of EAS maximum and the variance of the depth distribution of maxima of EAS with energies of approx. 2x10 to the 15th power eV can properly be described in terms of Kaidalov-Martirosyan quark-gluon string model (QGSM). E.A.K.

N85-36020*# Samarkand Alisher Navoi State Univ. (USSR).
STUDY OF THE ENERGY SPECTRUM OF PRIMARY COSMIC RAYS: EAS SIZE FLUCTUATIONS AT A FIXED PRIMARY ENERGY
N. Aliev, T. Alimov, N. Kakhharov, K. Khakimov, N. Rakhimova, R. Tashpulatov, and G. B. Khristiansen (Moscow State Univ.) *In* NASA Goddard Space Flight Center 19th Intern. Cosmic Ray Conf., Vol. 7 Aug. 1985 p 191-194 refs (For primary document see N85-35968 24-93)
(HE-4.4-14) Avail: NTIS HC as boxed set only $200/MF A01 per volume or E99 per entire set CSCL 03B

During the initial period of the Samarkand EAS array operations the showers were selected on the basis of charged-particle flux density, and during the subsequent periods the showers were selected on the basis of Cerenkov light flux density. This procedure made it possible to measure the shower energy, to estimate the EAS size fluctuations at a fixed primary energy, and to experimentally obtain the scaling factor K(Ne, Eo) from the EAS size spectrum to the primary energy spectrum. Six scintillators of area S = 2 sq m each were added to the array. The fluctuations of EAS sizes in the showers of fixed primary energies and the scaling factors K(Ne, Eo) were inferred from the data obtained. The showers with zenith angles < 30 deg were selected. The EAS axis positions were inferred from the amplitude data of the scintillators. The primary energy Eo was determined by the method of least squares for the known EAS axis position using the data of the Cerenkov detector located at 80 to 150 m EAS axis. It is shown that the Cerenkov light flux fluctuations at 100 m from EAS axis, q sub 100, do not exceed 10% at a fixed EAS energy, so the parameter q sub 100 may be used to estimate the EAS-generating primary particle-energy. E.A.K.

N85-36021*# Samarkand Alisher Navoi State Univ. (USSR).
STUDY OF THE SHOWER MAXIMUM DEPTH BY THE METHOD OF DETECTION OF THE EAS CERENKOV LIGHT PULSE SHAPE
N. Aliev, T. Alimov, M. Kakhkharov, N. Khakimov, B. M. Makhmudov, N. Rakhimova, R. Tashpulatov, G. B. Khristiansen (Moscow State Univ.), V. V. Prosin (Moscow State Univ.), and V. Yu. Zhukov (Moscow State Univ.) *In* NASA. Goddard Space Flight Center 19th Intern. Cosmic Ray Conf., Vol. 7 Aug. 1985 p 195-198 refs (For primary document see N85-35968 24-93)
(HE-4.4-15) Avail: NTIS HC as boxed set only $200/MF A01 per volume or E99 per entire set CSCL 03B

The results of processing the data on the shape of the EAS Cerenkov light pulses recorded by the extensive air showers (EAS) array are presented. The pulse FWHM is used to find the mean depth of EAS maximum. E.A.K.

N85-36022*# Adelaide Univ. (Australia). Dept. of Physics.
ANALYSIS OF CERENKOV PULSES RECORDED SIMULTANEOUSLY AT TWO SITES
D. F. Liebing and J. R. Patterson *In* NASA. Goddard Space Flight Center 19th Intern. Cosmic Ray Conf., Vol. 7 Aug. 1985 p 199-202 refs (For primary document see N85-35968 24-93)
(HE-4.4-16) Avail: NTIS HC as boxed set only $200/MF A01 per volume or E99 per entire set CSCL 03B

The agreement between measured distances to maximum for approx. 49 simultaneous Cerenkov pulse profiles from different sites is + or - approx. 0.1 km near 4.5 km and + or - 0.5 km near 7 km. Uncertainty in depths of maximum are approx. + or - 10 g sq and + or - 30 g cm/2 respectively. Usually the Hillas-Patterson simulation is able to fit both pulse shapes satisfactorily using a single N(x) profile. E.A.K.

N85-36023*# Crimean Astrophysical Observatory (USSR).
PRELIMINARY RESULTS OF THE CERENKOV EAS FLASHES THE CRIMEAN ASTROPHYSICAL OBSERVATORY
B. M. Vladimirsky, Yu. I. Zyskin, Yu. I. Nesphor, A. A. Stepanain, V. P. Fomin, and V. G. Shitov *In* NASA. Goddard Space Flight Center 19th Intern. Cosmic Ray Conf., Vol. 7 Aug. 1985 p 203-206 refs (For primary document see N85-35968 24-93)
(HE-4.4-17) Avail: NTIS HC as boxed set only $200/MF A01 per volume or E99 per entire set CSCL 03B

The facility designed for the study of angular resolution of light in the extensive air showers EAS flashes is described. The threshold energy of the facility is about 3 x 10 to the 12h power eV. The data on the angular distribution of light in a flash and the ratio of the flux in the UV and visual region as a function of the distance to the axis of a shower are given. Obtained results are compared to the published computations. E.A.K.

N85-36024*# Moscow State Univ. (USSR). Inst. of Nuclear Physics.
THE EXPERIMENTAL CASCADE CURVES OF EAS AT E SUB 0 > 10(17) eV OBTAINED BY THE METHOD OF DETECTION OF CHERENKOV PULSE SHAPE
Yu. A. Fomin, G. B. Kalmykov, M. V. Khristiansen, M. V. Motova, Yu. A. Nechin, V. V. Prosin, V. Yu. Zhukov, N. N. Efimov (Institute for Cosmophysical Research and Aeronomy), V. M. Grigoriev (Institute for Cosmophysical Research and Aeronomy), and E. S. Nikiforova (Institute for Cosmophysical Research and Aeronomy) *In* NASA. Goddard Space Flight Center 19th Intern. Cosmic Ray Conf., Vol. 7 Aug. 1985 p 207-210 refs (For primary document see N85-35968 24-93)
(HE-4.4-18) Avail: NTIS HC as boxed set only $200/MF A01 per volume or E99 per entire set CSCL 03B

The individual cascade curves of EAS with E sub 0 > 10 to the 17th power eV/I to 3/ were studied by detection of EAS Cherenkov light pulses. The scintillators located at the center of the Yakutsk EAS array within a 500-m radius circle were used to select the showers and to determine the main EAS parameters. The individual cascade curves N(t) were obtained using the EAS Cherenkov light pulses satisfying the following requirements: (1) the signal-to-noise ratio fm/delta sub n > 15, (2) the EAS axis-detector distance tau sub > 350 m, (3) the zenith angle theta < 30 deg, (4) the probability for EAS to be detected by scintillators W > 0.8. Condition (1) arises from the desire to reduce the amplitude distortion of Cherenkov pulses due to noise and determines the range of EAS sizes, N(t). The resolution times of the Cherenkov pulse shape detectors are tau sub 0 approx. 23 ns which results in distortion of a pulse during the process of the detection. The distortion of pulses due to the finiteness of tau sub 0 value was estimated. It is shown that the rise time of pulse becomes greater as tau sub 0.5/tau sub 0 ratio decreases. E.A.K.

N85-36025*# Moscow State Univ. (USSR). Inst. of Nuclear Physics.
LATERAL-ANGULAR AND TEMPORAL CHARACTERISTICS OF EAS OPTICAL RADIATION
T. A. Chuykova, V. I. Galkin, I. P. Ivanenko, and T. M. Roganova *In* NASA. Goddard Space Flight Center 19th Intern. Cosmic Ray Conf., Vol. 7 Aug. 1985 p 211-214 refs (For primary document see N85-35968 24-93)
(HE-4.4-19) Avail: NTIS HC as boxed set only $200/MF A01 per volume or E99 per entire set CSCL 03B

Characteristics of the direct and scattered components of electron-photon shower optical radiation for distances R > 500 m from the shower core to a detector, allowing for the Cerenkov and fluorescent mechanism of photon generation are presented. The results of calculations are employed to clarify the techniques for determination of the shower parameters detected by both installations registering fluorescent light and those recording Cerenkov light. E.A.K.

N85-36026*# Nottingham Univ. (England). Dept. of Physics.
THE IDENTIFICATION OF GAMMA RAY INDUCED EAS
P. R. Blake and W. F. Nash *In* NASA. Goddard Space Flight Center 19th Intern. Cosmic Ray Conf., Vol. 7 Aug. 1985 p 215-218 refs (For primary document see N85-35968 24-93)
(HE-4.5-1) Avail: NTIS HC as boxed set only $200/MF A01 per volume or E99 per entire set CSCL 03B

Some of the penetrating particles in gamma-induced EAS from Cygnus X-3 observed by a single layer of flash-bulbs under 880 g cm/2 concrete, may be punched through photons rather than muons. An analysis of the shielded flash-tube response detected from EAS is presented. The penetration of the electro-magnetic component through 20 cm of Pb is observed at core distances approx. < 10 m. E.A.K.

N85-36027*# Franklin Inst., Newark, Del.
MUONS IN GAMMA SHOWERS
Todor Stanev, Ch. P. Vankov, and Francis Halzen (Wisconsin Univ., Madison) *In* NASA. Goddard Space Flight Center 19th Intern. Cosmic Ray Conf., Vol. 7 Aug. 1985 p 219-222 refs Sponsored in part by US-Bulgarian Cooperative Research Program (For primary document see N85-35968 24-93)
(Contract DE-AC02-76ER-00881; Grant NSF PHY-84-10989)
(HE-4.5-3) Avail: NTIS HC as boxed set only $200/MF A01 per volume or E99 per entire set CSCL 03B

Muon production in gamma-induced air showers, accounting for all major processes. For muon energies in the GeV region the photoproduction is by far the most important process, while the contribution of micron + micron pair creation is not negligible for TeV muons. The total rate of muons in gamma showers is, however, very low. E.A.K.

N85-36028*# National Aeronautics and Space Administration. Goddard Space Flight Center, Greenbelt, Md.
MUON SPECTRUM IN AIR SHOWERS INITIATED BY GAMMA RAYS
S. A. Stephens (Tata Inst. of Fundamental Research, Bombay, India) and R. E. Streitmatter *In its* 19th Intern. Cosmic Ray Conf., Vol. 7 Aug. 1985 p 223-226 refs (For primary document see N85-35968 24-93)
(HE-4.5-4) Avail: NTIS HC as boxed set only $200/MF A01 per volume or E99 per entire set CSCL 03B

An analytic representation for the invariant cross-section for the production of charged pions in gamma P interactions was derived by using the available cross-sections. Using this the abundance of muons in a gamma ray initiated air shower is calculated. E.A.K.

N85-36029*# National Aeronautics and Space Administration. Goddard Space Flight Center, Greenbelt, Md.
DEVELOPMENT OF ELECTROMAGNETIC CASCADES IN THE ATMOSPHERE INCLUDING THE LANDAU-POMERANCHUK-MIGDAL EFFECT
R. E. Streitmatter and S. A. Stephens (Tata Inst. of Fundamental Research, Bombay, India) *In its* 19th Intern. Cosmic Ray Conf., Vol. 7 Aug. 1985 p 227-230 refs (For primary document see N85-35968 24-93)
(HE-4.5-5) Avail: NTIS HC as boxed set only $200/MF A01 per volume or E99 per entire set CSCL 03B

Numerical solutions have been obtained for the one-dimensional atmospheric electromagnetic cascade diffusion equations, including the Landau-Pomeranchuk-Migdal and screening effects. Spectra produced by primary gamma rays of various energies are given at a number of depths in the atmosphere. Author

N85-36030*# Leeds Univ. (England). Dept. of Physics.
ELECTROMAGNETIC AND MUONIC STRUCTURE OF SHOWERS INITIATED BY GAMMA-RAYS AND BY HADRONS
A. M. Hillas *In* NASA. Goddard Space Flight Center 19th Intern. Cosmic Ray Conf., Vol. 7 Aug. 1985 p 231-234 refs (For primary document see N85-35968 24-93)
(HE-4.5-6) Avail: NTIS HC as boxed set only $200/MF A01 per volume or E99 per entire set CSCL 03B

If photon cascades develop by the usual mechanisms, there should indeed be notable differences between the structure of showers due to photon and hadron primaries, as regards muon densities and lateral distributions of some detector signals. The muon content of showers from Cygnus X-3, observed at Kiel, cannot be understood in this way. One remedy is to postulate arbitrarily a strong hadronic interaction of photons in the TeV region. This would utterly change the nature of electromagnetic cascades, but surprisingly does not at first sight seem to be in conflict with air shower observations. Author

N85-36031*# Adelaide Univ. (Australia). Dept. of Physics.
THE MUON CONTENT OF GAMMA-RAY SHOWERS
P. G. Edwards and R. J. Protheroe *In* NASA. Goddard Space Flight Center 19th Intern. Cosmic Ray Conf., Vol. 7 Aug. 1985 p 235-238 refs Sponsored in part by Australian Research Grants Scheme and Commonwealth Postgraduate Research Award (For primary document see N85-35968 24-93)
(HE-4.5-7) Avail: NTIS HC as boxed set only $200/MF A01 per volume or E99 per entire set CSCL 03B

The result of a calculation of the expected number of muons in gamma ray initiated and cosmic ray initiated air showers using a realistic model of hadronic collisions in an effort to understand the available experimental results and to assess the feasibility of using the muon content of showers as a veto to reject cosmic ray initiated showers in ultra-high energy gamma ray astronomy are reported. The possibility of observing very-high energy gamma-ray sources by detecting narrow angle anisotropies in the high energy muon background radiation are considered. Author

N85-36032*# Tata Inst. of Fundamental Research, Bombay (India).
THE HUMP IN THE CERENKOV LATERAL DISTRIBUTION OF GAMMA RAY SHOWERS
S. Sinha and M. V. S. Sao *In* NASA. Goddard Space Flight Center 19th Intern. Cosmic Ray Conf., Vol. 7 Aug. 1985 p 239-242 refs (For primary document see N85-35968 24-93)
(HE-4.5-9) Avail: NTIS HC as boxed set only $200/MF A01 per volume or E99 per entire set CSCL 03B

The lateral distribution of atmospheric Cerenkov photons emitted by gamma ray showers of energy 100 GeV is calculated. The lateral distribution shows a characteristic hump at a distance of approx. 135 meter from the core. The hump is shown to be due to electrons of threshold energy 1 GeV, above which the mean scattering angle becomes smaller than the Cerenkov angle. Author

N85-36033*# Bulgarian Academy of Science, Sofia. Inst.for Nuclear Research and Nuclear Energy.
SIMULATION OF GAMMA-INITIATED SHOWERS
Yo. Stamenov, Kh. Vancov, and T. Vodenicharova *In* NASA. Goddard Space Flight Center 19th Intern. Cosmic Ray Conf., Vol. 7 Aug. 1985 p 243-246 refs (For primary document see N85-35968 24-93)

(HE-4.5-10) Avail: NTIS HC as boxed set only $200/MF A01 per volume or E99 per entire set CSCL 03B

The main average characteristics of muon, electron and hadron components of extensive air showers were calculate using a standard model of nuclear interaction. The obtained results are in good agreement with Tien Shan experimental data. Author

N85-36034*# Academy of Sciences (USSR), Moscow. Physical Inst.

PHENOMENOLOGICAL CHARACTERISTIC OF THE ELECTRON COMPONENT IN GAMMA-QUANTA INITIATED SHOWERS

S. I. Nikolsky, J. N. Stamenov, and S. Z. Ushev *In* NASA. Goddard Space Flight Center 19th Intern. Cosmic Ray Conf., Vol. 7 Aug. 1985 p 247-250 refs (For primary document see N85-35968 24-93)

(HE-4.5-11) Avail: NTIS HC as boxed set only $200/MF A01 per volume or E99 per entire set CSCL 03B

The phenomenological characteristics of the electron component in showers initiated by primary gamma-quanta were analyzed on the basis of the Tien Shan experimental data. It is shown that the lateral distribution of the electrons ion gamma-quanta initiated showers can be described with NKG - function with age parameters bar S equals 0, 76 plus or minus 0, 02, different from the same parameter for normal showers with the same size bar S equals 0, 85 plus or minus 0, 01. The lateral distribution of the correspondent electron energy flux in gamma-quanta initiated showers is steeper as in normal cosmic ray showers. Author

N85-36035*# Tokyo Univ. (Japan). Inst. for Cosmic Rays.

A THREE-DIMENSIONAL MONTE CARLO CALCULATION OF THE PHOTON INITIATED SHOWERS AND KIEL RESULT Abstract Only

A. Okada and Y. Muraki *In* NASA. Goddard Space Flight Center 19th Intern. Cosmic Ray Conf., Vol. 7 Aug. 1985 p 251 (For primary document see N85-35968 24-93)

(HE-4.5-13) Avail: NTIS HC as boxed set only $200/MF A01 per volume or E99 per entire set CSCL 03B

The Kiel experimental results indicate an existence of the ultra high-energy gamma-rays coming from Cyg. X-3. However the result indicates that the number of the muons included in the photon initiated shower is the same as the number included in the proton initiated showers. According to our Monte Carlo calculation as shown in the graph of underpart, the number of muons included in the photon initiated showers should be less than 1/15 of the photon's. The previous simulation was made under one dimensional approximation. This time the result of three dimensional calculation is reported. Author

N85-36036*# Hong Kong Univ. Dept. of Physics.

CONSTRUCTION OF A COSMIC RAY AIR SHOWER TELESCOPE

L. K. Ng and S. K. Chan *In* NASA. Goddard Space Flight Center 19th Intern. Cosmic Ray Conf., Vol. 7 Aug. 1985 p 252-255 refs (For primary document see N85-35968 24-93)

(HE-4.5-14) Avail: NTIS HC as boxed set only $200/MF A01 per volume or E99 per entire set CSCL 03B

The telescope under construction is mainly for the purpose of locating the arrival directions of energetic particles and quanta which generate air showers of sizes 10 to the 5th power to 10 to the 6th power. Both fast timing method and visual track method are incorporated in determining the arrival directions. The telescope is composed of four stations using scintillators and neon flash tubes as detectors. The system directional resolution is better than 1.5 deg. Author

N85-36037*# Hong Kong Univ. Dept. of Physics.

AN UNDERGROUND COSMIC RAY MUON TELESCOPE FOR OBSERVATION OF COSMIC RAY ANISOTROPY

Y. W. Lee and L. K. Ng *In* NASA. Goddard Space Flight Center 19th Intern. Cosmic Ray Conf., Vol. 7 Aug. 1985 p 256-259 refs (For primary document see N85-35968 24-93)

Avail: NTIS HC as boxed set only $200/MF A01 per volume or E99 per entire set CSCL 03B

A telescope housed in a tunnel laboratory has an overburden of 573 hg cm(-2) and is located under the center of a saddle-shaped landscape. It is composed of triple layers of proportional counters, each layer of area approx. 4m x 2m and their separation 0.5m. Events are selected by triple coincidence and software track identification. The telescope is in operation for over a year and the overall count rate is 1280 hr(-1). The structure and operation of the system is reported. Author

N85-36038*# Academy of Sciences (USSR), Moscow. Physical Inst.

NUCLEAR CASCADES IN ELECTROMAGNETIC SHOWERS PRODUCED BY PRIMARY GAMMA-QUANTA IN THE ATMOSPHERE

T. V. Danilova, A. D. Erlykin, A. V. Mironov, and E. I. Tukish *In* NASA. Goddard Space Flight Center 19th Intern. Cosmic Ray Conf., Vol. 7 Aug. 1985 p 260-263 refs (For primary document see N85-35968 24-93)

(HE-4.5-16) Avail: NTIS HC as boxed set only $200/MF A01 per volume or E99 per entire set CSCL 03B

Distributions were calculated for the number of electrons N sub e, number of muons with the energy above 5 GeV N sub mu and the energy of hadron component E sub h in electromagnetic showers, produced by primary gamma-quanta with energies theta approx. equals 30 deg and observed at the mountain level 700 g/square centimeters. The mean number of nuclear interactions of photos with the energy above 5 GeV is about 0.3 per each TeV of the primary energy and nuclear cascades take out in average about 2% of the total shower energy. The mean number of 5 GeV muons for the electromagnetic shower is (2 to 5)% from the number of muons in cosmic ray showers with the same number of electrons at the observation level. similar value for the total energy of hadron component is also (2 to 5)%. N sub mu and N sub e values as well as E sub h and n sub e don't correlate at the fixed primary energy E sug gamma (o). Between N sub mu and E sub h there is a positive correlation at the given E sub gamma. Author

N85-36039*# Academy of Sciences (USSR), Moscow. Inst. for Nuclear Research.

ON THE POSSIBILITIES OF LARGE-SCALE RADIO AND FIBER OPTICS DETECTORS IN COSMIC RAYS

G. A. Gusev, M. A. Markov, and I. M. Zheleznykh *In* NASA. Goddard Space Flight Center 19th Intern. Cosmic Ray Conf., Vol. 7 Aug. 1985 p 264-267 refs (For primary document see N85-35968 24-93)

(HE-4.6-2) Avail: NTIS HC as boxed set only $200/MF A01 per volume or E99 per entire set CSCL 03B

Different variants of radio and fiber optics detectors for registration of super high energy cascades in the atmosphere and in dense media are discussed. Particularly the possibilities for investigation of quasi horizontal cosmic ray showers (CRS) and simulated muons from these CRS with the help of radio detectors and fiber optics detectors located on the ice surface are considered. Author

N85-36040*# Tokyo Inst. of Tech. (Japan). Dept. of Physics.

RADIO SIGNALS FROM VERY LARGE SHOWERS

K. Suga, F. Kakimoto, and K. Nishi (Inst. of Physical and Chemical Research, Wako, Japan) *In* NASA. Goddard Space Flight Center 19th Intern. Cosmic Ray Conf., Vol. 7 Aug. 1985 p 268-271 refs (For primary document see N85-35968 24-93)

(HE-4.6-3) Avail: NTIS HC as boxed set only $200/MF A01 per volume or E99 per entire set CSCL 03B

Radio signals from air showers with electron sizes in the range 1 x 10 to the 7th power to 2 x 10 to the 9th power were detected at 50kHz, 170kHz, and 1,647kHz at large core distances in the Akeno square kilometers air-shower array. The field strength is higher than that expected from any mechanisms hitherto proposed. Author

N85-36041*# Gauhati Univ. (India). Dept. of Physics.

ON THE PRODUCTION MECHANISM OF RADIO-PULSES FROM

LARGE EXTENSIVE AIR SHOWERS
P. Datta and K. M. Pathak *In* NASA. Goddard Space Flight Center 19th Intern. Cosmic Ray Conf., Vol. 7 Aug. 1985 p 272-275 refs Sponsored by Dept. of Atomic Energy (BRNS), Government of India (For primary document see N85-35968 24-93)
(HE-4.6-4) Avail: NTIS HC as boxed set only $200/MF A01 per volume or E99 per entire set CSCL 03B

None of the theories put forward so far to explain the radio emission from cosmic ray showers, has been successful in giving a satisfactory explanation for all the experimental data obtained from various laboratories over the globe. It is apprehended that emission mechanism at low and high frequencies may be quite different. This calls for new theoretical look into the phenomenon. Theoretical as well as the experimental results indicate that the frequency spectrum is rather flat in the frequency range (40 to 60 MHz. Above 80 MHz, the radio emission can be explained with the help of geomagnetic mechanism. But at very low frequency (< 10 MHz), mechanisms other than geomagnetic are involved.
Author

N85-36042*# Gauhati Univ. (India). Dept. of Physics.
A NEW STUDY ON THE EMISSION OF EM WAVES FROM LARGE EAS
K. M. Pathak and G. K. D. Mazumdar *In* NASA. Goddard Space Flight Center 19th Intern. Cosmic Ray Conf., Vol. 7 Aug. 1985 p 276-279 refs Sponsored in part by Dept. of Atomic Energy (BRNS), Government of India, and the Inst. of Advance Studies in Science and Technology (Assam Science Society) (For primary document see N85-35968 24-93)
(HE-4.6-5) Avail: NTIS HC as boxed set only $200/MF A01 per volume or E99 per entire set CSCL 03B

A method used in locating the core of individual cosmic ray showers is described. Using a microprocessor-based detecting system, the density distribution and hence, energy of each detected shower was estimated.
R.J.F.

N85-36043*# Arizona Univ., Tucson. Dept. of Physics.
AIR FLUORESCENCE DETECTION OF LARGE AIR SHOWERS BELOW THE HORIZON
Peter Halverson and Theodore Bowen *In* NASA. Goddard Space Flight Center 19th Intern. Cosmic Ray Conf., Vol. 7 Aug. 1985 p 280-283 refs (For primary document see N85-35968 24-93)
(Grant NSF PHY-82-07697)
(HE-4.6-6) Avail: NTIS HC as boxed set only $200/MF A01 per volume or E99 per entire set CSCL 03B

In the interest of exploring the cosmic ray spectrum at energies greater than 10 to the 18th power eV, where flux rates at the Earth's surface drop below 100 yr(-1) km(-2) sr(-1), cosmic ray physicists have been forced to construct ever larger detectors in order to collect useful amounts of data in reasonable lengths of time. At present, the ultimate example of this trend is the Fly's Eye system in Utah, which uses the atmosphere around an array of skyward-looking photomultiplier tubes. The air acts as a scintillator to give detecting areas as large as 5000 square kilometers sr (for highest energy events). This experiment has revealed structure (and a possible cutoff) in the ultra-high energy region above 10 o the 19th power eV. The success of the Fly's Eye experiment provides impetus for continuing the development of larger detectors to make accessible even higher energies. However, due to the rapidly falling flux, a tenfold increase in observable energy would call for a hundredfold increase in the detecting area. But, the cost of expanding the Fly's Eye detecting area will approximately scale linearly with area. It is for these reasons that the authors have proposed a new approach to using the atmosphere as a scintillator; one which will require fewer photomultipliers, less hardware (thus being less extensive), yet will provide position and shower size information.
Author

N85-36044*# Turku Univ. (Finland). Wihuri Physical Lab.
INVESTIGATION OF COSMIC RAYS IN VERY SHORT TIME SCALES
J. Peltonen, E. Valtonen, J. J. Torsti, H. Arvela, M. Lumme, M. Nieminen, and E. Vainikka *In* NASA. Goddard Space Flight Center 19th Intern. Cosmic Ray Conf., Vol. 7 Aug. 1985 p 284-287 refs (For primary document see N85-35968 24-93)
(HE-4.6-7) Avail: NTIS HC as boxed set only $200/MF A01 per volume or E99 per entire set CSCL 03B

A fast databuffer system, where cosmic ray events in the Turku hadron spectrometer, including particle arrival times are recorded with time resolution of 100 ns was constructed. The databuffer can be read continuously by a microprocessor, which preanalyzes the data and transfers it to the main computer. The time span, that can be analyzed in every detail, is a few seconds. The high time resolution enables a study of time correlated groups of high energy particles. In addition the operational characteristics of the spectrometer can be monitored in detail.
Author

N85-36045*# Turku Univ. (Finland). Wilhuri Physical Lab.
A FACILITY FOR INVESTIGATION OF MULTIPLE HADRONS AT COSMIC-RAY ENERGIES
E. Valtonen, J. J. Torsti, H. Arvela, M. Lumme, M. Nieminen, J. Peltonen, and E. Vainikka *In* NASA. Goddard Space Flight Center 19th Intern. Cosmic Ray Conf., Vol. 7 Aug. 1985 p 288-291 refs (For primary document see N85-35968 24-93)
(HE-4.6-8) Avail: NTIS HC as boxed set only $200/MF A01 per volume or E99 per entire set CSCL 03B

An experimental arrangement for studying multiple hadrons produced in high-energy hadron-nucleus interactions is under construction at the university of Turku. The method of investigation is based on the detection of hadrons arriving simultaneously at sea level over an area of a few square meters. The apparatus consists of a hadron spectrometer with position-sensitive detectors in connection with a small air shower array. The position resolution using streamer tube detectors will be about 10 mm. Energy spectra of hadrons or groups of simultaneous hadrons produced at primary energies below 10 to the 16th power eV can be measured in the energy range 1 to 2000 GeV.
Author

N85-36046*# Maryland Univ., College Park. Dept. of Physics and Astronomy.
A POSSIBLE EAS ARRAY ABOVE THE SOUDAN 2 DETECTOR Abstract Only
K. Sivaprasad *In* NASA. Goddard Space Flight Center 19th Intern. Cosmic Ray Conf., Vol. 7 Aug. 1985 p 292 (For primary document see N85-35968 24-93)
(HE-4.6-9) Avail: NTIS HC as boxed set only $200/MF A01 per volume or E99 per entire set CSCL 03B

Multiple high energy muons, when studied with a large area detector, can be useful in the study of the composition of cosmic rays at energies approx. 10 14 eV. The Soudan II detector, primarily designed to detect nucleon decay, is located approx. 600 m deep underground and has dimensions of 16m x 8m x 5m (height), and is made up of drift tubes. The minimum muon energy needed to penetrate that depth is approximately 500 GeV. A set of simulated cosmic ray showers was set up to calculate the rate of muon associated events, using a trigger array with the number of detectors varying from 37 to 127 (the radius of acceptance varying from 50m to 100m). The number used in the calculations is given. The association rate is seen to be a strong function of the multiplicity of muons in the detector. The difference in the rates of association of proton and nuclei induced showers rises rapidly with multiplicity.
Author

N85-36047*# Kochi Univ., Akebono (Japan).
FAST SCINTILLATION COUNTER SYSTEM AND PERFORMANCE
H. Sasaki, A. Nishioka, N. Ohmori, M. Kusumose, T. Nakatsuka (Konan Univ.), T. Horiki (Inst. of Physical and Chemical Research), and Y. Hatano (Tokyo Univ., Tokyo) *In* NASA. Goddard Space Flight Center 19th Intern. Cosmic Ray Conf., Vol. 7 Aug. 1985 p 293-296 refs (For primary document see N85-35968 24-93)
(HE-4.6-10) Avail: NTIS HC as boxed set only $200/MF A01 per volume or E99 per entire set CSCL 03B

An experimental study of the fast scintillation counter (FS) system to observe a shower disk structure at Mt. Norikura is described, especially the system performance and a pulse

wave-form by a single charge particles. The photomultiplier tube (PT) pulse appears at the leading edge of the main pulse. To remove this PT-pulse from the main pulse, the frame of the scintillator vessel was changed. The fast triggering system was made to decrease the dead time which came from the use of the function of the self triggering of the storage oscilloscope (OSC). To provide a new field on the multi-parameter study of the cosmic ray showers, the system response of the FS system also improved as a result of many considerations. Author

N85-36048*# Durham Univ. (England). Dept. of Physics.
PERFORMANCE OF A LOCAL ELECTRON DENSITY TRIGGER TO SELECT EXTENSIVE AIR SHOWERS AT SEA LEVEL
T. Abbas, J. Madani, and F. Ashton *In* NASA. Goddard Space Flight Center 19th Intern. Cosmic Ray Conf., Vol. 7 Aug. 1985 p 297-300 refs (For primary document see N85-35968 24-93)
(HE-4.6-11) Avail: NTIS HC as boxed set only $200/MF A01 per volume or E99 per entire set CSCL 03B

Time coincident voltage pulses in the two closely space (1.6m) plastic scintillators were recorded. Most of the recorded events are expeted to be due to electrons in cosmic ray showers whose core fall at some distance from the detectors. This result is confirmed from a measurement of the frequency distribution of the recorded density ratios of the two scintillators. Author

N85-36049*# Gauhati Univ. (India). Dept. of Physics.
MICROPROCESSOR-BASED SINGLE PARTICLE CALIBRATION OF SCINTILLATION COUNTER
G. K. D. Mazumdar and K. M. Pathak *In* NASA. Goddard Space Flight Center 19th Intern. Cosmic Ray Conf., Vol. 7 Aug. 1985 p 301-303 refs Sponsored in part by Dept. of Atomic Energy (BRNS), Government of India, and Inst. of Advance Studies in Science and Technology (Assam Science Society) (For primary document see N85-35968 24-93)
(HE-4.6-13) Avail: NTIS HC as boxed set only $200/MF A01 per volume or E99 per entire set CSCL 03B

A microprocessor-base set-up is fabricated and tested for the single particle calibration of the plastic scintillator. The single particle response of the scintillator is digitized by an A/D converter, and a 8085 A based microprocessor stores the pulse heights. The digitized information is printed. Facilities for CRT display and cassette storing and recalling are also made available. Author

N85-36050*# Academy of Sciences (USSR), Troitsk. Inst. of Terrestrial Magnetism, Ionosphere and Radio Wave Propagation.
SAMARKAND COMPLEX SETUP FOR INVESTIGATION OF COSMIC RAY VARIATION IN THE ENERGY RANGE OF 7 10 (9) - 10 (15) eV
L. I. Dorman *In* NASA. Goddard Space Flight Center 19th Intern. Cosmic Ray Conf., Vol. 7 Aug. 1985 p 304-307 refs (For primary document see N85-35968 24-93)
(HE-4.6-14) Avail: NTIS HC as boxed set only $200/MF A01 per volume or E99 per entire set CSCL 03B

The Samarkand complex setup is aimed at the study of cosmic ray variations in a wide energy range from 7 billion eV (which corresponds to the geomagnetic threshold in the region of Samarkand) up to approx 10 to the 15th power to 10 to the 16th power eV. The setup consists of four 6-counter sections of neutron supermonitor with counters SNM-15 and 48 scintillator detectors (1 sq m each) placed under and above the supermonitor. The effective area of the setup for recording neutrons and muons is 24 sq m. The setup can register time variations of the following cosmic ray components: (1) the total neutron counting rate, (2) counting rates for neutrons of different multiplicity, (3) soft-muon fluxes, (4) hard-muon fluxes at various zenith and azimuth angles, (5) electron-photon component, (6) extensive air showers (EAS) induced by primary particles in a wide energy range and accompanied or not accompanied by muons and neutrons. Author

N85-36051*# Tokyo Univ. (Japan).
RADIO WAVE EMITTED BY AN EXTENSIVE AIR SHOWERS IN 10KHZ TO 1MHZ REGION
Jun Nichimura *In* NASA. Goddard Space Flight Center 19th Intern. Cosmic Ray Conf., Vol. 7 Aug. 1985 p 308-311 refs (For primary document see N85-35968 24-93)
(HE-4.6-15) Avail: NTIS HC as boxed set only $200/MF A01 per volume or E99 per entire set CSCL 03B

The importance of radio waves in a frequency range of less than 1MHz in an EAS shower is discussed. Estimates of radio intensities at 10KHz, 100KHz and 1MHz in EAS showers made on the basis of the Kahn-Lerche theory. Negative charge excess in a shower is the main source of low frequency radio emission, in spite of the importance of the contribution of transverse current in the geomagnetic field in a higher frequency range. An estimate is also made for radio intensity produced when the shower hits the ground. The contribution of this process seems to be important at a large distance, i.e., beyond 1km from the shower axis. Author

N85-36052*# Kochi Univ., Akebono (Japan).
THE STRUCTURE OF THE SHOWER DISK OBSERVED AT MT. NORIKURA
H. Sasaki, A. Nishioka, N. Ohmori, M. Kusumose, T. Nakatsuka (Konan Univ.), T. Horiki (Inst. of Physical and Chemical Research), and Y. Hatano (Tokyo Univ., Tokyo) *In* NASA. Goddard Space Flight Center 19th Intern. Cosmic Ray Conf., Vol. 7 Aug. 1985 p 312-315 refs (For primary document see N85-35968 24-93)
(HE-4.7-1) Avail: NTIS HC as boxed set only $200/MF A01 per volume or E99 per entire set CSCL 03B

The structure of the EAS shower disk, the arrival time distribution of charged particles at the core of the small or middle size shower, is measured at Mt. Norikura in Japan. Four fast scintillation counters with an area of 0.25 sq m and a fast trigger system are added to the Mt. Norikura EAS array for the study. F.M.R.

N85-36053*# Kobe Univ. (Japan). Graduate School of Science and Technology.
STRUCTURE OF AIR SHOWER DISC NEAR THE CORE
N. Inoue, M. Kawamoto, Y. Misaki, T. Maeda, T. Takeuchi, and Y. Toyoda *In* NASA. Goddard Space Flight Center 19th Intern. Cosmic Ray Conf., Vol. 7 Aug. 1985 p 316-319 refs (For primary document see N85-35968 24-93)
(HE-4.7-2) Avail: NTIS HC as boxed set only $200/MF A01 per volume or E99 per entire set CSCL 03B

The longitudinal structure of the air shower disk is studied by measuring the arrival time distributions of air shower particles for showers with electron size in the range 3.2 x 10 to the 5.5. power to 3.2 x 10 to the 7.5 power in the Akeno air-shower array (930 gcm squared atmospheric depth). The average FWHM as a parameter of thickness of air shower disk increases with core distances at less than 50m. AT the present stage, dependence on electron size, zenith angle and air shower age is not apparent. The average thickness of the air shower disk within a core distance of 50m could be determined by an electromagnetic cascade starting from the lower altitude. Author

N85-36054*# Tokyo Univ. (Japan). Inst. for Cosmic Research.
PROPERTIES OF 10 (18)-10 (19)eV EAS AT FAR CORE DISTANCE
M. Teshima (Kyoto Univ.), M. Nagano, T. Hara, Y. Hatano, N. Hayashida, C. X. He (Academia Sinica, Beijing), M. Honda, F. Ishikawa, K. Kamata, Y. Matsubara (Kyoto Univ.) et al *In* NASA. Goddard Space Flight Center 19th Intern. Cosmic Ray Conf., Vol. 7 Aug. 1985 p 320-323 refs (For primary document see N85-35968 24-93)
(HE-4.7-3) Avail: NTIS HC as boxed set only $200/MF A01 per volume or E99 per entire set CSCL 03B

The properties of 10 to the 18th power - 10 to the 19th power eV EAS showers such as the electron lateral distribution, the muon lateral distribution (> 1Gev), the ratio of muon density to a electron density, the shower front structure and the transition effects in scintillator of 5cm thickness are investigated with the Akeno 4 sq km/20sq km array at far core distances between 500m and 3000m. The fluctuation of densities and arrival time increase rapidly at core distances greater than 2km. Author

N85-36055*# Tokyo Inst. of Tech. (Japan). Dept. of Physics.
LONGITUDINAL DEVELOPMENT OF MUONS IN LARGE AIR SHOWERS STUDIES FROM THE ARRIVAL TIME DISTRIBUTIONS MEASURED AT 900m ABOVE SEA LEVEL
F. Kakimoto, I. Tsuchimoto, T. Enoki, K. Suga, and K. Nishi (Inst. of Physical and Chemical Research) *In* NASA. Goddard Space Flight Center 19th Intern. Cosmic Ray Conf., Vol. 7 Aug. 1985 p 324-327 refs (For primary document see N85-35968 24-93)
(HE-4.7-4) Avail: NTIS HC as boxed set only $200/MF A01 per volume or E99 per entire set CSCL 03B

The arrival time distributions of muons with energies above 1.0GeV and 0.5GeV have been measured in the Akeno air-shower array to study the longitudinal development of muons in air showers with primary energies in the range 10 to the 17th power to 10 to the 18th power ev. The average rise times of muons with energies above 1.0GeV at large core distances are consistent with those expected from very high multiplicity models and, on the contrary, with those expected from the low multiplicity models at small core distances. This implies that the longitudinal development at atmospheric depth smaller than 500 cm square is very fast and that at larger atmospheric depths is rather slow. Author

N85-36056*# Tokyo Inst. of Tech. (Japan). Dept. of Physics.
ARRIVAL TIME DISTRIBUTIONS OF ELECTRONS IN AIR SHOWERS WITH PRIMARY ENERGIES ABOVE 10 (18)eV OBSERVED AT 900m ABOVE SEA LEVEL
F. Kakimoto, I. Tsuchimoto, T. Enoki, K. Suga, and K. Nishi (Inst. of Physical and Chemical Research) *In* NASA. Goddard Space Flight Center 19th Intern. Cosmic Ray Conf., Vol. 7 Aug. 1985 p 328-331 refs (For primary document see N85-35968 24-93)
(HE-4.7-5) Avail: NTIS HC as boxed set only $200/MF A01 per volume or E99 per entire set CSCL 03B

Detection of air showers with primary energies above 10 to the 19th power eV with sufficient statistics is extremely important in an astrophysical aspect related to the Greisen cut off and the origin of such high energy cosmic rays. Recently, a method is proposed to observe such giant air showers by measuring the arrival time distributions of air-shower particles at large core distances with a mini array. Experiments to measure the arrival time distributions of muons were started in 1981 and those of electrons in early 1983 in the Akeno air-shower array (930 gcm cm squared atmospheric depth, 900m above sea level). During the time of observation, the detection area of the Akeno array was expanded from 1 sq km to sq km in 1982 and to 20 sq km in 1984. Now the arrival time distribution of electrons and muons can be measured for showers with primary energies above 1019eV at large core distances. Author

N85-36057*# Leeds Univ. (England). Dept. of Physics.
THE THICKNESS OF THE SHOWER DISC AS OBSERVED IN SHOWERS PRODUCED BY PRIMARIES ABOVE 10 (19)eV
M. A. Lawrence, A. A. Watson, and A. A. West *In* NASA. Goddard Space Flight Center 19th Intern. Cosmic Ray Conf., Vol. 7 Aug. 1985 p 332-335 refs Sponsored by the Science and Engineering Research Council (For primary document see N85-35968 24-93)
(HE-4.7-6) Avail: NTIS HC as boxed set only $200/MF A01 per volume or E99 per entire set CSCL 03B

The thickness of the shower disk has been measured in showers initiated by primaries of energy > to 10 the 19th power eV using the large area water Cerenkov detectors of the Haverah Park array. Results are presented which (1) provide supporting evidence for the accuracy of analysis procedures in giant showers, (2) offer an evaluation of the mini-array technique for the detection of giant showers and (3) extend earlier work on developmental fluctuations above 10 to the 19th power eV. Author

N85-36058*# Michigan Univ., Ann Arbor. Lab. of Physics.
METHODS FOR ROOF-TOP MINI-ARRAYS
Wayne E. Hazen and Eric S. Hazen (ETC Inc.) *In* NASA. Goddard Space Flight Center 19th Intern. Cosmic Ray Conf., Vol. 7 Aug. 1985 p 336-338 refs (For primary document see N85-35968 24-93)
(HE-4.7-7) Avail: NTIS HC as boxed set only $200/MF A01 per volume or E99 per entire set CSCL 03B

To test the idea of the Linsley effect mini array for the study of giant air showers, it is desirable to have a trigger that exploits the effect itself. In addition to the trigger, it is necessary to have a method for measuring the relative arrival times of the particle swarm selected by the trigger. Since the idea of mini arrays is likely to appeal to small research groups, it is desirable to try to design relatively simple and inexpensive methods, and methods that utilize existing detectors. Clusters of small detectors have been designed for operation in the local particle density realm where the probability of > or = 2 particles per detector is small. Consequently, this method can discriminate pulses from each detector and thenceforth deal mainly with logic pulses. Author

N85-36059*# Michigan Univ., Ann Arbor. Lab. of Physics.
EXPECTED RATES WITH MINI-ARRAYS FOR AIR SHOWERS
Wayne E. Hazen *In* NASA. Goddard Space Flight Center 19th Intern. Cosmic Ray Conf., Vol. 7 Aug. 1985 p 339-342 refs (For primary document see N85-35968 24-93)
(HE-4.7-8) Avail: NTIS HC as boxed set only $200/MF A01 per volume or E99 per entire set CSCL 03B

As a guide in the design of mini-arrays used to exploit the Linsley effect in the study of air showers, it is useful to calculate the expected rates. The results can aid in the choice of detectors and their placement or in predicting the utility of existing detector systems. Furthermore, the potential of the method can be appraised for the study of large showers. Specifically, we treat the case of a mini-array of dimensions small enough compared to the distance of axes of showers of interest so that it can be considered a point detector. The input information is taken from the many previous studies of air showers by other groups. The calculations will give: (1) the expected integral rate, F(sigma, rho), for disk thickness, sigma, or rise time, t sub 1/2, with local particle density, rho, as a parameter; (2) the effective detection area A(N) with sigma (min) and rho (min) and rho (min) as parameters; (3) the expected rate of collection of data F sub L (N) versus shower size, N. Author

N85-36060*# Hong Kong Univ. Dept. of Physics.
FAST SCINTILLATION COUNTER PREAMPLIFIER FOR THE OBSERVATION OF LINSLEY EFFECT
L. K. Ng *In* NASA. Goddard Space Flight Center 19th Intern. Cosmic Ray Conf., Vol. 7 Aug. 1985 p 343-346 (For primary document see N85-35968 24-93)
(HE-4.7-9) Avail: NTIS HC as boxed set only $200/MF A01 per volume or E99 per entire set CSCL 03B

A fast preamplifier circuit has been designed and thoroughly tested for the purpose of observing the air shower arrival directions including the Linsley effect. The circuit intends to eliminate the time jitter due to variation of scintillation counter signal amplitudes. It assumes that the output signals from one counter system have the same rise time. On this basis, error arising from time jitter is removed by voltage discrimination at about half signal amplitudes. Detailed description of the circuit is reported. Author

N85-36061*# Hong Kong Univ. Dept. of Physics.
A MINI-ARRAY FOR LARGE AIR SHOWERS
L. K. Ng, S. K. Chan, W. E. Hazen (Michigan Univ.), and E. S. Hazen (Michigan Univ.) *In* NASA. Goddard Space Flight Center 19th Intern. Cosmic Ray Conf., Vol. 7 Aug. 1985 p 347-350 refs (For primary document see N85-35968 24-93)
(HE-4.7-10) Avail: NTIS HC as boxed set only $200/MF A01 per volume or E99 per entire set CSCL 03B

A mini-array that utilizes the Linsley effect is proposed for the measurement of large air showers. An estimate of the detectable shower rates for various shower sizes is made. Details of the detection and data collection systems are also described. Author

N85-36062*# Potchefstroom Univ. for Christian Higher Education (South Africa). Cosmic Ray Research Unit.
A NOTE ON SOME STATISTICAL PROPERTIES OF RISE TIME PARAMETERS USED IN MUON ARRIVAL TIME MEASUREMENTS

D. J. vanderWalt and E. J. deVilliers *In* NASA. Goddard Space Flight Center 19th Intern. Cosmic Ray Conf., Vol. 7 Aug. 1985 p 351-354 refs (For primary document see N85-35968 24-93)
(HE-4.7-12) Avail: NTIS HC as boxed set only $200/MF A01 per volume or E99 per entire set CSCL 03B

Most investigations of the muon arrival time distribution in EAS during the past decade made use of parameters which can collectively be called rise time parameters. The rise time parameter T sub A/B is defined as the time taken for the integrated pulse from a detector to rise from A% to B% of its full amplitude. The use of these parameters are usually restricted to the determination of the radial dependence thereof. This radial dependence of the rise time parameters are usually taken as a signature of the particle interaction characteristics in the shower. As these parameters have a stochastic nature, it seems reasonable that one should also take notice of this aspect of the rise time parameters. A statistical approach to rise time parameters is presented. Author

N85-36063*# New Mexico Univ., Albuquerque. Dept. of Physics and Astronomy.
SUB-LUMINAL PULSES FROM COSMIC RAY AIR SHOWERS
John Linsley *In* NASA. Goddard Space Flight Center 19th Intern. Cosmic Ray Conf., Vol. 7 Aug. 1985 p 355-358 refs Sponsored in part by NSF (For primary document see N85-35968 24-93)
(HE-4.7-13) Avail: NTIS HC as boxed set only $200/MF A01 per volume or E99 per entire set CSCL 03B

Some of the signals produced by air showers in scintillators possess a distinctive feature, a sub-luminal pulse (SLP) following the normal one with a time delay of approximately 1.5 r/c. The average amplitude of the SLP corresponds to an energy deposit of about 50 MeV, three times as much as is deposited in a typical scintillator by vertical minimum ionizing muons. The SLP account for approximately 5% of the energy deposited in the atmosphere by IR showers with energy > 10 to the 10th power GeV at impact parameters > 1 km. Assuming that these pulses are due to neutrons travelling with a speed slightly less than c, they provide a unique means of estimating E sub h, the energy deposited by slow hadrons, in showers of this very high energy. On the other hand, if not allowed for properly, these pulses are liable to cause errors in estimating the impact parameters of large showers from pulse width observations. Author

N85-36064*# New Mexico Univ., Albuquerque. Dept. of Physics and Astronomy.
THICKNESS OF THE PARTICLE SWARM IN COSMIC RAY AIR SHOWERS
John Linsley *In* NASA. Goddard Space Flight Center 19th Intern. Cosmic Ray Conf., Vol. 7 Aug. 1985 p 359-362 refs (For primary document see N85-35968 24-93)
(HE-4.7-14) Avail: NTIS HC as boxed set only $200/MF A01 per volume or E99 per entire set CSCL 03B

The average dispersion in arrival time of air shower particles detected with a scintillator at an impact parameter r is described with accuracy 5-10% by the empirical formula < sigma > = Sigma sub to (1+r/r sub t) sup b, where Sigma sub to = 2.6 ns, r sub t = 30m and b = (1.94 + or - .08) (0.39 + or - .06) sec Theta, for r < 2 km, 10 to the 8th power < E < 10 to the 11th power GeV, and Theta < 60 deg. (E is the primary energy and theta is the zenith angle). The amount of fluctuation in sigma sub t due to fluctuations in the level of origin and shower development is less than 20%. These results provide a basis for estimating the impact parameters of very larger showers with data from very small detector arrays (mini-arrays). The energy of such showers can then be estimated from the local particle density. The formula also provides a basis for estimating the angular resolution of air shower array-telescopes. Author

N85-36065*# Moscow State Univ. (USSR). Inst. of Nuclear Physics.
STUDY OF THE TIME-DIFFERENTIATED PARTICLE FLUX DENSITY AT VARIOUS DISTANCES FROM EAS AXIS
V. G. Atrashkevich, R. J. Chernykh, Yu. A. Fomin, G. K. Garipov, G. B. Khristiansen, G. V. Kulikov, A. P. Lebedev, S. J. Matsenov, V. J. Nazarov, A. A. Silaev et al *In* NASA. Goddard Space Flight Center 19th Intern. Cosmic Ray Conf., Vol. 7 Aug. 1985 p 363-366 refs (For primary document see N85-35968 24-93)
(HE-4.7-15) Avail: NTIS HC as boxed set only $200/MF A01 per volume or E99 per entire set CSCL 03B

The EAS time structure is studied using the enlarged EAS array of the Moscow State University. The time measurements are made using 22 scintillators which form 13 rectanges of 180x190 sq m size covering the entire array area. The array is triggered by a signal of 4-fold coincidences of the pulses from the detectors forming each of the rectangles. The data were obtained during 2200 hours of the array operation in 1984. A total of 816 showers, to which at least 14 of 22 scintillator detectors responded, were selected among all those detected. The coordinates of the EAS axis in the observation plane and the EAS sizes were determined by the maximum likelihood method using a computer on the assumption that the electron LDF is the NKG form. A total of 492 shower s in the interval of EAS size Ne = 5x10 to the 6th power - 2x10 to the 8th power (N bar e = 1.7x 10 to the 7th power) with zenith angles theta < or = 45 deg and axes within the array are analyzed. Author

N85-36066*# National Aeronautics and Space Administration. Goddard Space Flight Center, Greenbelt, Md.
NINETEENTH INTERNATIONAL COSMIC RAY CONFERENCE. HE SESSIONS, VOLUME 8
Frank C. Jones, comp. Washington Aug. 1985 387 p refs Conf. held in La Jolla, Calif., 11-23 Aug. 1985 8 Vol.
(NASA-CP-2376-Vol-8; NAS 1.55:2376-Vol-8) Avail: NTIS HC as boxed set only $200/MF A01 per volume or E99 per entire set CSCL 03B

Papers submitted for presentation at the 19th International Cosmic Ray Conference are compiled. The present volume contains papers addressing high energy interactions and related phenomena. Specific topic areas include muons, neutrinos, magnetic monopoles, nucleon decay, searches for new particles, and acoustic and thermoluminescence detection techniques. For individual titles, see N85-36067 through N85-36162.

N85-36067*# Ecole Polytechnique, Palaiseau (France).
PRELIMINARY RESULTS ON UNDERGROUND MUON BUNDLES OBSERVED IN THE FREJUS PROTON-DECAY DETECTOR
B. Degrange *In* NASA. Goddard Space Flight Center 19th Intern. Cosmic Ray Conf., Vol. 8 Aug. 1985 p 1-3 refs Prepared in cooperation with Aachen-Orsay-Palaiseau-Saclay-Wuppertal Collaboration (For primary document see N85-36066 24-93)
(HE-5.1-1) Avail: NTIS HC as boxed set only $200/MF A01 per volume or E99 per entire set CSCL 03B

The proton-decay detector installed in the Modane Underground laboratory (4400 mwe) in the Frejus tunnel (French Alps) has recorded 80 880 single muon and 2 322 multi-muon events between March '84 and March '85 (6425 hours of active time). During this period, a part of this modular detector was running, while new modules were being mounted, so that the detector size has continuously increased. The final detector has been completed in May '85. Author

N85-36068*# Tata Inst. of Fundamental Research, Bombay (India).
MUON AND NEUTRINO RESULTS FROM KGF EXPERIMENT AT A DEPTH OF 7000 HG/SQUARE CM
M. R. Krishnaswamy, M. G. K. Menon, N. K. Mondal, V. S. Narasimham, B. V. Streekantan, Y. Hayashi (Osaka City Univ.), N. Ito (Osaka City Univ.), S. Kawakami (Osaka City Univ.), and S. Miyake (Tokyo Univ.) *In* NASA. Goddard Space Flight Center 19th Intern. Cosmic Ray Conf., Vol. 8 Aug. 1985 p 4-5 (For primary document see N85-36066 24-93)
(HE-5.1-2) Avail: NTIS HC as boxed set only $200/MF A01 per volume or E99 entire set CSCL 03B

The KGF nucleon decay experiment at a depth of 7000 hg/sq cm has provided valuable data on muons and neutrinos. The detector comprised of 34 crossed layers of proportional counters (cross section 10 x 10 sq cm; lengths 4m and 6m) sandwiched

between 1.2 cm thick iron plates can record tracks of charged particles to an accuracy of 1 deg from tracks that traverse the whole of the detector. A special two-fold coincidence system enables the detector to record charged particles that enter at very large zenith angles. In a live time of 3.6 years about 2600 events have been recorded. These events include atmospheric muons, neutrino induced muons for rock, stopping muons, showers and events which have their production vertex inside the detectors. The results on atmospheric muons and neutrino events are presented. Author

N85-36069*# Lodz Univ. (Poland). Inst. of Nuclear Science.
RELEVANCE OF MULTIPLE MUONS DETECTED UNDERGROUND TO THE MASS COMPOSITION OF PRIMARY COSMIC RAYS
J. Szabelski, J. Wdowczyk, and A. W. Wolfendale (Durham Univ.) *In* NASA. Goddard Space Flight Center 19th Intern. Cosmic Ray Conf., Vol. 8 Aug. 1985 p 6-7 refs (For primary document see N85-36066 24-93)
(HE-5.1-4) Avail: NTIS HC as boxed set only $200/MF A01 per volume or E99 per entire set CSCL 03B

Calculations have been made of the expected frequencies of multiple muons in the Soudan underground proton decay detector. It is concluded that the flux of heavy nuclei ($z > 10$) in the range 10 to the 15th power to 10 to the 16th power eV/nucleus is at most 25% of the total particle flux in the same range. Author

N85-36070*# National Aeronautics and Space Administration. Goddard Space Flight Center, Greenbelt, Md.
MULTIMUONS EVENTS AND PRIMARY COMPOSITION
B. S. Acharya and J. N. Capdevielle (Bordeaux Univ., Gradignan) *In its* 19th Intern. Cosmic Ray Conf., Vol. 8 Aug. 1985 p 8-11 refs (For primary document see N85-36066 24-93)
(HE-5.1-5) Avail: NTIS HC as boxed set only $200/MF A01 per volume or E99 per entire set CSCL 03B

Nucleon decay detectors at large depths offers now a total area larger than 1000 sq m to registrate muons of energy exceeding 1 TeV. Near complete high energy muon families are detected in those arrays. An extensive 3D Monte-Carlo simulation was conducted in view to understand the spatial distribution of those events and the possible link with elementary act or primary composition. As pion or kaon parents have a very small decay probability at so high energy, multimuon phenomena occurs at high altitude where the atmospheric density is small after the most energetic collisions. Author

N85-36071*# Academy of Sciences (USSR), Moscow. Inst. for Nuclear Research.
THE SPECTRUM OF COSMIC RAY MUONS OBTAINED WITH 100-TON SCINTILLATION DETECTOR UNDERGROUND AND THE ANALYSIS OF RECENT EXPERIMENTAL DATA
F. F. Khalchukov, E. V. Korolkova, V. A. Kudryavtsev, A. S. Malgin, O. G. Ryazhskaya, and G. T. Zatsepin *In its* 19th Intern. Cosmic Ray Conf., Vol. 8 Aug. 1985 p 12-15 refs (For primary document see N85-36066 24-93)
(HE-5.1-6) Avail: NTIS HC as boxed set only $200/MF A01 per volume or E99 per entire set CSCL 03B

The vertical muon spectrum up to 15 TeV obtained with the underground installation is presented. Recent experimental data dealing with horizontal and vertical cosmic ray muon spectra are analyzed and discussed. Author

N85-36072*# Aichi Women's Coll. (Japan). Dept. of Physics.
A LARGE AREA COSMIC MUON DETECTOR LOCATED AT OHYA STONE MINE
N. Nii, K. Mizutani (Saitama Univ.), T. Aoki (Tokyo Univ., Tanashi), T. Kitamura (Tokyo Univ., Tanashi), K. Mitsui (Tokyo Univ., Tanashi), S. Matsuno (Tokyo Univ., Tanashi), Y. Muraki (Tokyo Univ., Tanashi), Y. Ohashi (Tokyo Univ., Tanashi), A. Okada (Tokyo Univ., Tanashi), Y. Kamiya (Nagoya Univ.) et al *In* NASA. Goddard Space Flight Center 19th Intern. Cosmic Ray Conf., Vol. 8 Aug. 1985 p 16-19 refs (For primary document see N85-36066 24-93)
(HE-5.1-7) Avail: NTIS HC as boxed set only $200/MF A01 per volume or E99 per entire set CSCL 03B

The chemical composition of the primary cosmic rays between 10 to the 15th power eV and 10 to the 18th power eV were determined by a Large Area Cosmic Muon Detector located at Ohya stone mine. The experimental aims of Ohya project are; (1) search for the ultra high-energy gamma-rays; (2) search for the GUT monopole created by Big Bang; and (3) search for the muon bundle. A large number of muon chambers were installed at the shallow underground near Nikko (approx. 100 Km north of Tokyo, situated at Ohya-town, Utsunomiya-city). At the surface of the mine, very fast 100 channel scintillation counters were equipped in order to measure the direction of air showers. These air shower arrays were operated at the same time, together with the underground muon chamber. B.W.

N85-36073*# Case Western Reserve Univ., Cleveland, Ohio.
A NEW WORLD SURVEY EXPRESSION FOR COSMIC RAY VERTICAL INTENSITY VS. DEPTH IN STANDARD ROCK
Marshall Crouch *In* NASA. Goddard Space Flight Center 19th Intern. Cosmic Ray Conf., Vol. 8 Aug. 1985 p 20-23 refs (For primary document see N85-36066 24-93)
(HE-5.1-10) Avail: NTIS HC as boxed set only $200/MF A01 per volume or E99 per entire set CSCL 03B

The cosmic ray data on vertical intensity versus depth below 10 to the 5th power g sq cm is fitted to a 5 parameter empirical formula to give an analytical expression for interpretation of muon fluxes in underground measurements. This expression updates earlier published results and complements the more precise curves obtained by numerical integration or Monte Carlo techniques in which the fit is made to an energy spectrum at the top of the atmosphere. The expression is valid in the transitional region where neutrino induced muons begin to be important, as well as at great depths where this component becomes dominant. Author

N85-36074*# Academy of Sciences (USSR), Moscow. Inst. for Nuclear Research.
MUON GROUPS AND PRIMARY COMPOSITION AT 10 TO THE 13TH POWER TO 10 TO THE 15TH POWER eV
E. V. Budko, A. E. Chudakov, V. A. Dogujaev, A. R. Mihelev, V. A. Padey, V. A. Petkov, P. S. Striganov, O. V. Suvorova, and A. V. Voevodsky *In* NASA. Goddard Space Flight Center 19th Intern. Cosmic Ray Conf., Vol. 8 Aug. 1985 p 24-27 refs (For primary document see N85-36066 24-93)
(HE-5.1-12) Avail: NTIS HC as boxed set only $200/MF A01 per volume or E99 per entire set CSCL 03B

The data on muon groups observed at Baksan underground scintillation telescope is analyzed. In this analysis we compare the experimental data with calulations, based on a superposition model in order to obtain the effective atomic number of primary cosmic rays in the energy range 10 to the 13th power to 10 to the 15th power eV. Author

N85-36075*# Academy of Sciences (USSR), Moscow. Inst. for Nuclear Research.
PRIMARY CHEMICAL COMPOSITION FROM SIMULTANEOUS RECORDING OF MUONS INDUCED CASCADES AND ACCOMPANYING MUON GROUP UNDERGROUND
V. N. Bakatanov, S. N. Boziev, A. E. Chudakov, Yu. F. Novoseltsev, M. V. Novoseltseva, Yu. F. Stenkin, and A. V. Voevodsky *In* NASA. Goddard Space Flight Center 19th Intern. Cosmic Ray Conf., Vol. 8 Aug. 1985 p 28-31 refs (For primary document see N85-36066 24-93)
(HE-5.1-13) Avail: NTIS HC as boxed set only $200/MF A01 per volume or E99 entire set CSCL 03B

A new method to estimate the mean atomic number of primary cosmic rays in energy range 10 to the 3rd power to 10 to the 5th power Gev/nucleon is suggested. The Baksan underground scintillation telescope data are used for this analysis. The results of 7500 h run of this experiment are presented. Author

N85-36076*# Academy of Sciences (USSR), Moscow. Inst. for Nuclear Research.
ON MUON ENERGY SPECTRUM IN MUON GROUPS UNDER-

GROUND
V. N. Bakatanov, A. E. Chudakov, Yu. F. Novoseltsev, M. V. Novoseltseva, and Yu. V. Stenkin *In* NASA. Goddard Space Flight Center 19th Intern. Cosmic Ray Conf., Vol. 8 Aug. 1985 p 32-35 refs (For primary document see N85-36066 24-93)
(HE-5.1-14) Avail: NTIS HC as boxed set only $200/MF A01 per volume or E99 per entire set CSCL 03B

A method is described which was used to measure muon energy spectrum characteristics in muon groups underground using mu-e decays recording. The Baksan Telescope's experimental data on mu-e decays intensity in muon groups of various multiplicities are analyzed. The experimental data indicating very flat spectrum does not however represent the total spectrum in muon groups. Obviously the muon energy spectrum depends strongly on a distance from the group axis. The core attraction effect makes a significant distortion, making the spectrum flatter. After taking this into account and making corrections for this effect the integral total spectrum index in groups has a very small dependence on muon multiplicity and agrees well with expected one beta = beta (sub expected) = 1.75. Author

N85-36077*# Academy of Sciences (USSR), Moscow. Inst. for Nuclear Research.
ENERGY SPECTRUM OF CASCADES GENERATED BY MUONS IN BAKSAN UNDERGROUND SCINTILLATION TELESCOPE
V. N. Bakatanov, A. E. Chudakov, Yu. F. Novoseltsev, M. V. Novoseltseva, V. M. Achkasov, A. M. Semenov, and Yu. V. Stenkin *In* NASA. Goddard Space Flight Center 19th Intern. Cosmic Ray Conf., Vol. 8 Aug. 1985 p 36-38 refs (For primary document see N85-36066 24-93)
(HE-5.1-15) Avail: NTIS HC as boxed set only $200/MF A01 per volume or E99 per entire set CSCL 03B

Spectrum of cascades generated by cosmic ray muons underground is presented. The mean zenith angle of the muon arrival is theta=35 deg the depth approx. 1000 hg/sq cm. In cascades energy range > 700 GeV the measured spectrum is in agreement with the sea-level integral muon spectrum index gamma=3.0. Some decrease of this exponent has been found in the range > 4000 Gev. Author

N85-36078*# Academy of Sciences (USSR), Moscow. Physical Inst.
UNDERWATER MEASUREMENTS OF MUON INTENSITY
V. M. Fedorov, V. P. Pustovetov, Yu. A. Trubkin, and A. V. Kirilenkov *In* NASA. Goddard Space Flight Center 19th Intern. Cosmic Ray Conf., Vol. 8 Aug. 1985 p 39-42 refs (For primary document see N85-36066 24-93)
(HE-5.1-16) Avail: NTIS HC as boxed set only $200/MF A01 per volume or E99 per entire set CSCL 03B

Experimental measurements of cosmic ray muon intensity deep underwater aimed at determining a muon absorption curve are of considerable interest, as they allow to reproduce independently the muon energy spectrum at sea level. The comparison of the muon absorption curve in sea water with that in rock makes it possible to determine muon energy losses caused by nuclear interactions. The data available on muon absorption in water and that in rock are not equivalent. Underground measurements are numerous and have been carried out down to the depth of approx. 15km w.e., whereas underwater muon intensity have been measured twice and only down to approx. 3km deep. Author

N85-36079*# Indiana Univ., Bloomington.
MULTIPLE MUONS IN MACRO
R. Heinz *In* NASA. Goddard Space Flight Center 19th Intern. Cosmic Ray Conf., Vol. 8 Aug. 1985 p 43-46 refs Prepared in cooperation with MACRO Collaboration (For primary document see N85-36066 24-93)
(HE-5.2-1) Avail: NTIS HC as boxed set only $200/MF A01 per volume or E99 per entire set CSCL 03B

An analysis of the multiple muon events in the Monopole Astrophysics and Cosmic Ray Observatory detector was conducted to determine the cosmic ray composition. Particular emphasis is placed on the interesting primary cosmic ray energy region above 2000 TeV/nucleus. An extensive study of muon production in cosmic ray showers has been done. Results were used to parameterize the characteristics of muon penetration into the Earth to the location of a detector. B.W.

N85-36080*# Nagoya Univ. (Japan).
THE NAGOYA COSMIC-RAY MUON SPECTROMETER 3, PART 1: PRELIMINARY OBSERVATIONS
Y. Kamiya, S. Shibata, K. Iijima, and S. Iida (Toyohashi Univ. of Tech.) *In* NASA. Goddard Space Flight Center 19th Intern. Cosmic Ray Conf., Vol. 8 Aug. 1985 p 47-49 refs (For primary document see N85-36066 24-93)
(HE-5.2-2) Avail: NTIS HC as boxed set only $200/MF A01 per volume or E99 per entire set CSCL 03B

There are some discrepancies among the data of absolute muon intensities at large zenth angles. Through the analysis of the data obtained in the previous measurement by Nagoya Cosmic Ray Spectrometer, one of the sources of these discrepancies has been found to be the ambiguity induced by the selection criteria with which genuine muons are distinguished from the backgrounds. To remove the ambiguity of this kind, it is necessary to know the amount of the backgrounds and their characteristics in detail. Some features of the background events were reported from the observations by using this triggering system of Nagoya Cosmic Ray Spectrometer. In this paper, the results of extended observations using track detector together with this system are reported. Author

N85-36081*# Nagoya Univ. (Japan).
THE NAGOYA COSMIC-RAY MUON SPECTROMETER 3, PART 2: TRACK DETECTOR Abstract Only
S. Shibata, K. Iijima, Y. Kamiya, and S. Iida (Toyohashi Univ. of Tech.) *In* NASA. Goddard Space Flight Center 19th Intern. Cosmic Ray Conf., Vol. 8 Aug. 1985 p 50 refs (For primary document see N85-36066 24-93)
(HE-5.2-3) Avail: NTIS HC as boxed set only $200/MF A01 per volume or E99 entire set CSCL 03B

The twelve wide gap spark chambers were utilized as the track detectors of the Nagoya cosmic-ray muon spectrometer not only to obtain the precise locations of particles, but also to get some information about the correspondences between segments of trajectories. The area of each chamber is 150 x 70 sq cm and the width of a gap is 5 cm. The gas used is He at the atmospheric pressure. Each three pairs of them are placed on both sides of the deflection magnet. All images of sparks for each event are projected through the mirror system and recorded by two cameras stereoscopically. The mean detection efficiency of each chamber is 95 + or - 2% and the spacial resolution (jitter and drift) obtained from the prototype-experiment is 0.12 mm. Maximum detectable momentum of the spectrometer is estimated at about 10 TeV/c taking into account these characteristics together with the effects of the energy loss and multiple Coulomb scattering of muons in the iron magnet. B.W.

N85-36082*# Nagoya Univ. (Japan).
THE NAGOYA COSMIC-RAY MUON SPECTROMETER 3, PART 3: AUTOMATIC FILM SCANNING EQUIPMENT Abstract Only
S. Shibata, Y. Kamiya, K. Iijima, and S. Iida (Toyohashi Univ. of Tech.) *In* NASA. Goddard Space Flight Center 19th Intern. Cosmic Ray Conf., Vol. 8 Aug. 1985 p 51 ref (For primary document see N85-36066 24-93)
(HE-5.2-4) Avail: NTIS HC as boxed set only $200/MF A01 per volume or E99 entire set CSCL 03B

In the regular operation of the Nagoya cosmic-ray muon spectrometer, about 2000 events per day will be recorded on the photographic film. To derive the track locations from such a huge number of photographs with high accuracy in a short time, an automatic film scanning device has been developed. B.W.

N85-36083*# Nagoya Univ. (Japan).
THE NAGOYA COSMIC-RAY MUON SPECTROMETER 3, PART 4: TRACK RECONSTRUCTION METHOD Abstract Only
S. Shibata, Y. Kamiya, K. Iijima, and S. Iida (Toyohashi Univ. of

Tech.) *In* NASA. Goddard Space Flight Center 19th Intern. Cosmic Ray Conf., Vol. 8 Aug. 1985 p 52 ref (For primary document see N85-36066 24-93)
(HE-5.2-5) Avail: NTIS HC as boxed set only $200/MF A01 per volume or E99 per entire set CSCL 03B

One of the greatest problems in measuring particle trajectories with an optical or visual detector system, is the reconstruction of trajectories in real space from their recorded images. In the Nagoya cosmic-ray muon spectrometer, muon tracks are detected by wide gap spark chambers and their images are recorded on the photographic film through an optical system of 10 mirrors and two cameras. For the spatial reconstruction, 42 parameters of the optical system should be known to determine the configuration of this system. It is almost impossible to measure this many parameters directly with usual techniques. In order to solve this problem, the inverse transformation method was applied. In this method, all the optical parameters are determined from the locations of fiducial marks in real space and the locations of their images on the photographic film by the non-linear lesst square fitting. B.W.

N85-36084*# Tokyo Univ., Tanashi (Japan). Inst. for Cosmic Ray Research.
BACKGROUND LIGHT MEASUREMENTS AT THE DUMAND SITE
T. Aoki, T. Kitamura, S. Matsuno, K. Mitsui, Y. Ohashi, A. Okada, D. R. Cady (Hawaii Univ., Honolulu), J. G. Learned (Hawaii Univ., Honolulu), D. OConnor (Hawaii Univ., Honolulu), and M. McMurdo (Hawaii Univ., Honolulu) *In* NASA. Goddard Space Flight Center 19th Intern. Cosmic Ray Conf., Vol. 8 Aug. 1985 p 53-56 refs (For primary document see N85-36066 24-93)
(HE-5.2-7) Avail: NTIS HC as boxed set only $200/MF per volume or E99 per entire set CSCL 03B

Ambient light intensities at the DUMAND site, west of the island of Hawaii were measured around the one photoelectron level. Throughout the water column between 1,500m and 4,700m, a substantial amount of stimulateable bioluminescence is observed with a ship suspended detector. But non-stimulated bioluminescence level is comparable, or less than, K sup 40 background, when measured with a bottom tethered detector typical of a DUMAND optical module. Author

N85-36085*# Academy of Sciences (USSR), Moscow. Inst. for Nuclear Research.
MEASUREMENTS OF LIGHT BACKGROUND AT LARGE DEPTH IN THE OCEAN
A. E. Bannykh, V. I. Beresnev, V. A. Gaidash, O. M. Gulkhandanyan, V. I. Ivanov, M. A. Markov, V. T. Paka (Academy of Sciences, USSR, Kaliningrad), I. V. Shtranikh, N. M. Surin, A. N. Volkov et al *In* NASA. Goddard Space Flight Center 19th Intern. Cosmic Ray Conf., Vol. 8 Aug. 1985 p 57-60 refs (For primary document see N85-36066 24-93)
(HE-5.2-8) Avail: NTIS HC as boxed set only $200/MF per volume or E99 per entire set CSCL 03B

The mean intensity of Cerenkov emission from the products of K(40) decay and bioluminescence was measured at depths to 5 km. The intensity of ocean light background is found to depend upon depth and at the 5 km level is equal on averaged to 300 + or - 60 quanta/sq cms into spatial angle of 2 pi sterradian in transparency window. The amplitudes, duration and number of BL flashes were measured at various depths. The intensive flashes due to BL are shown to be observed rather seldom at depths over 4 km. Author

N85-36086*# Okayama Univ. (Japan).
HYBRID TLC-PAIR METER FOR THE SPHINX PROJECT
Tomonori Wada, Isao Yamamoto (Okayama Univ. of Science), Nobusuke Takahashi (Okayama Univ. of Science), and Akeo Misaki (Saitama Univ.) *In* NASA. Goddard Space Flight Center 19th Intern. Cosmic Ray Conf., Vol. 8 Aug. 1985 p 61-64 refs (For primary document see N85-36066 24-93)
(HE-5.2-10) Avail: NTIS HC as boxed set only $200/MF per volume or E99 per entire set CSCL 03B

The chief aims in THE SPHINX PROJECT are research of super lepton physics and new detector experiments. At the second phase of THE SPHINX PROJECT, a hybrid TLC-PAIR METER was designed for measuring high energy neutrino sources (E upsilon > * TeV), searching high energy muon sources (E mu > TeV) and measuring muon group (E mu > 1 TeV). The principle of PAIR METER has been already proposed. In this TLC-PAIR METER, electromagnetic shower induced by cosmic ray muons are detected using TL (Thermoluminescence) sheets with position counters. Author

N85-36087*# Osaka City Univ. (Japan). Dept. of Physics.
PROPORTIONAL DRIFT TUBES FOR LARGE AREA MUON DETECTORS
C. Cho, S. Higashi, N. Hiraoka, A. Maruyama, T. Okusawa, T. Sato, T. Suwada, T. Takahashi, and H. Umeda *In* NASA. Goddard Space Flight Center 19th Intern. Cosmic Ray Conf., Vol. 8 Aug. 1985 p 65-68 ref (For primary document see N85-36066 24-93)
(HE-5.2-11) Avail: NTIS HC as boxed set only $200/MF per volume or E99 per entire set CSCL 03B

A proportional drift chamber which consists of eight rectangular drift tubes with cross section of 10 cm x 5 cm, a sense wire of 100 micron phi gold-plated tungsten wire and the length of 6 m, was tested using cosmic ray muons. Spatial resolution (rms) is between 0.5 and 1 mm over drift space of 50 mm, depending on incident angle and distance from sense wire. E.A.K.

N85-36088*# Ehime Univ., Matsuyama (Japan). Inst. for Cosmic Ray Research.
AN UPPER LIMIT OF MUON FLUX OF ENERGIES ABOVE 100 TeV DETERMINED FROM HORIZONTAL AIR SHOWERS OBSERVED AT AKENO
M. Nagano, H. Yoshii (Ehime Univ.), T. Hara (Hirosaki Univ.), K. Kamata, S. Kawaguchi, and T. Kifune *In* NASA. Goddard Space Flight Center 19th Intern. Cosmic Ray Conf., Vol. 8 Aug. 1985 p 69-72 refs (For primary document see N85-36066 24-93)
(HE-5.2-12) Avail: NTIS HC as boxed set only $200/MF per volume or E99 per entire set CSCL 03B

Muon energy spectrum above 100 TeV was determined by observing the extensive air showers (EAS) from the horizontal direction (HAS). No definite muon originated shower of sizes above 100,000 and zenith angles above 60 deg was observed. The upper limits of HAS intensity is 5x10/12 m/2 s/1 sn/1 above 100,000. It is indicated that the upper limit of muon flux above 100 TeV is about 1.3x10/8 m/2 s/1 sr/1 and is in agreement with that expected from the primary spectrum with a knee assuming scaling in the fragmentation region and 40% protons in the primary beam. The critical energy at which muon flux from prompt processes take over that from the conventional process is higher than 100 Tev at horizontal direction. E.A.K.

N85-36089*# Osaka City Univ. (Japan). Dept. of Physics.
COMMENTS ON THE MEASUREMENTS OF MULTIPLE MUON PHENOMENA
T. Sato, T. Takahashi, and S. Higashi *In* NASA. Goddard Space Flight Center 19th Intern. Cosmic Ray Conf., Vol. 8 Aug. 1985 p 73-76 refs (For primary document see N85-36066 24-93)
(HE-5.2-13) Avail: NTIS HC as boxed set only $200/MF per volume or E99 per entire set CSCL 03B

The extensive air showers in the energy around 10 to the 15th power eV include those initiated by astrophysical primary gamma-rays. The observations need a precise measurement on the directions of primary particles. It is one of the methods to measure the directions of high-energy muons in air showers. The accuracy in measuring the direction, by calculating the cosmic-ray phenomena in the atmosphere at very high energy was investgated. The results calculated by Monte Carlo method suggest that one may determine the direction of primary cosmic-rays within errors of 10/3 rad in observing muons of above 100 GeV at sea level. E.A.K.

N85-36090*# Moscow Physical-Engineering Inst. (USSR).
ENERGY SPECTRUM OF CASCADE SHOWERS INDUCED BY COSMIC RAY MUONS IN THE RANGE FROM 50 GeV TO

5 TeV

V. D. Ashitkov, T. M. Kirina, A. P. Klimakov, R. P. Kokoulin, A. A. Petrukhin, and V. I. Yumatov *In* NASA. Goddard Space Flight Center 19th Intern. Cosmic Ray Conf., Vol. 8 Aug. 1985 p 77-80 refs (For primary document see N85-36066 24-93)

(HE-5.2-14) Avail: NTIS HC as boxed set only $200/MF per volume or E99 per entire set CSCL 03B

The energy spectrum of cascade showers induced by electromagnetic interactions of high energy muons of horizontal cosmic ray flux in iron absorber was measured. The total observation time exceeded 22,000 hours. Both the energy spectrum and angular distributions of cascade showers are fairly described in terms of the usual muon generation processes, with a single power index of the parent meson spectrum over the muon energy range from 150 GeV to 5 TeV. E.A.K.

N85-36091*# Chongqing Inst. of Architecture and Engineering (China).

MEASUREMENT OF MUON INTENSITY BY CERENKOV METHOD

Z. H. Liu, G. J. Li, G. Z. Bai, J. G. Liu, Q. X. Geng, and J. Ling *In* NASA. Goddard Space Flight Center 19th Intern. Cosmic Ray Conf., Vol. 8 Aug. 1985 p 81-82 refs (For primary document see N85-36066 24-93)

(HE-5.2-15) Avail: NTIS HC as boxed set only $200/MF per volume or E99 per entire set CSCL 03B

Optical detection is an important technique in studies and observations of air showers, muons and relevant phenomena. The muon intensity is measured in a proper energy range and to study some problems about Cerenkov radiation of cosmic rays are studied, by a muon-telescope operated with Cerenkov detector. It is found that the measured muon intensity agrees with the integral energy spectrum of cosmic ray muons. E.A.K.

N85-36092*# Kobe Univ. (Japan). Graduate School of Science and Tech.

ANALYTICAL CALCULATION OF MUON INTENSITIES UNDER DEEP SEA-WATER

H. Inazawa and K. Kobayakawa *In* NASA. Goddard Space Flight Center 19th Intern. Cosmic Ray Conf., Vol. 8 Aug. 1985 p 83-86 refs (For primary document see N85-36066 24-93)

(HE-5.2-16) Avail: NTIS HC as boxed set only $200/MF per volume or E99 per entire set CSCL 03B

The study of the energy loss of high energy muons through different materials, such as rock and sea-water can cast light on characteristics of lepton interactions. There are less ambiguities for the values of atomic number (Z) and mass number (A) in sea-water than in rock. Muon intensities should be measured as fundamental data and as background data for searching the fluxes of neutrino. The average range energy relation in sea-water is derived. The correction factors due to the range fluctuation is also computed. By applying these results, the intensities deep under sea are converted from a given muon energy spectra at sea-level. The spectra of conventional muons from eta, K decays have sec theta enhancement. The spectrum of prompt muons from charmed particles is almost isotropic. The effect of prompt muons is examined. E.A.K.

N85-36093*# Indian Statistical Inst., Calcutta. Electronics Unit.

PHOTO NUCLEAR ENERGY LOSS TERM FOR MUON-NUCLEUS INTERACTIONS BASED ON xi SCALING MODEL OF QCD

Rajkumar Roychoudhury *In* NASA. Goddard Space Flight Center 19th Intern. Cosmic Ray Conf., Vol. 8 Aug. 1985 p 87-89 refs (For primary document see N85-36066 24-93)

(HE-5.2-17) Avail: NTIS HC as boxed set only $200/MF per volume or E99 per entire set CSCL 03B

Extensive air showers (EMC) experiments discovered a significant deviation of the ratio of structure functions of iron and deuteron from unity. It was established that the quark parton distribution in nuclei are different from the corresponding distribution in the nucleus. It was examined whether these results have an effect on the calculation of photo nucleus energy loss term for muon-nucleus nuclear interaction. Though the EMC and SLAC data were restricted to rather large q sq region it is expected that the derivation would persist even in the low q sq domain. For the ratio of iron and deuteron structure function a rather naive least square fit of the form $R(x) = a + bx$ was taken and it is assumed that the formula is valid for the whole q sq region the absence of any knowledge of R(x) for small q sq. E.A.K.

N85-36094*# Academy of Sciences (USSR), Moscow. Inst. for Nuclear Research.

ON METHOD OF MUON SPECTRUM MEASUREMENTS BY THE SCINTILLATION DETECTORS OF A LARGE THICKNESS T<4T SUB O

O. G. Ryazhskaya *In* NASA. Goddard Space Flight Center 19th Intern. Cosmic Ray Conf., Vol. 8 Aug. 1985 p 90-93 refs (For primary document see N85-36066 24-93)

(HE-5.2-18) Avail: NTIS HC as boxed set only $200/MF per volume or E99 per entire set CSCL 03B

Various methods for the study of muon spectrum are presented. The direct ones include the muon energy measurements by magnetic spectrometers. The indirect ones deal with the reconstruction of the muon spectrum from the spectrum of secondary particles obtained by burst or calorimeter technique. The burst technique is based on the measurement of the number of cascade particles, mainly in the cascade maximum, by the detectors of small thickness T < sub 0. The calorimeter method consist in determination of the cascade energy with help of the cascade curve shape. The multilayer detectors are used for this purpose. They are usually comprised of proportional counters, X-ray emulsion chambers or scintillation counters with the target material placed between them. The scintillation detectors of a large thickness measures the total cascade energy directly and the detector works as a true calorimeter. When the total energy is detected, the cascade spectrum differs from the muon one. E.A.K.

N85-36095*# Kinki Univ., Osaka (Japan). Dept. of Physics.

RANGE FLUCTUATIONS OF HIGH ENERGY MUONS PASSING THROUGH MATTER

Y. Minorikawa and K. Mitsui (Tokyo Univ.) *In* NASA. Goddard Space Flight Center 19th Intern. Cosmic Ray Conf., Vol. 8 Aug. 1985 p 94-97 refs (For primary document see N85-36066 24-93)

(HE-5.2-19) Avail: NTIS HC as boxed set only $200/MF per volume or E99 per entire set CSCL 03B

The information about energy spectrum of sea level muons at high energies beyond magnetic spectrographs can be obtained from the underground intensity measurements if the fluctuations problems are solved. The correction factor R for the range fluctuations of high energy muons were calculated by analytical method of Zatsepin, where most probable energy loss parameter are used. It is shown that by using the R at great depth together with the slope, lambda, of the vertical depth-intensity (D-I) curve in the form of exp(-t/lambda), the spectral index, gamma, in the power law energy spectrum of muons at sea level can be obtained. E.A.K.

N85-36096*# Polytechnic of North London (England).

THE SPECTRUM OF NEUTRONS AT 60 HG M(-2)

J. C. Barton *In* NASA. Goddard Space Flight Center 19th Intern. Cosmic Ray Conf., Vol. 8 Aug. 1985 p 98-101 refs (For primary document see N85-36066 24-93)

(HE-5.2-20) Avail: NTIS HC as boxed set only $200/MF per volume or E99 per entire set CSCL 03B

The rate of neutron interactions was measured for the energy range 7.5 to 60 MeV, using a 3.85 kg cell of liquid scintillator. The neutrons are selected by pulse shape discrimination, with anticoincidence counters used to reduce interference from muons transversing the scintillator. The observed flux is interpreted in terms of neutrons produced from environmental uranium and thorium, those resulting from the capture of negative muons in nuclei and those from fast muon interactions. E.A.K.

N85-36097*# Adelaide Univ. (Australia). Physics Dept.

A TRANSIENT DIGITISER FOR FAST AIR SHOWER EVENTS

N. R. Wild and R. W. Clay *In* NASA. Goddard Space Flight

Center 19th Intern. Cosmic Ray Conf., Vol. 8 Aug. 1985 p 102-103 refs (For primary document see N85-36066 24-93)
(HE-5.2-21) Avail: NTIS HC as boxed set only $200/MF per volume or E99 per entire set CSCL 03B

Air shower structure are often measured on time scales of a few nanoseconds. Longitudinal disk structure near the core is of the order of meters in dimension, air Cerenkov pulses have full widths at half maximum of the order of tens of nanoseconds, and fast timing over typical arrays is usually measured to nanosecond accuracy. oscilloscopes can be used but have very limited dynamic range and are expensive if measurements down to a few nanoseconds are to be made. For the fast Cerenkov work, an instrument with better dynamic range than an oscilloscope and with a time resolution sufficient to allow measurements limited only by system risetime of a few nanoseconds is needed. A 16/32 channel, 8 bit, fast transient digitizer was designed and built which runs at sample intervals down to approx. 1 nanosecond per channel. E.A.K.

N85-36098*# Utah Univ., Salt Lake City. Dept. of Physics.
LIMITS ON DEEPLY PENETRATING PARTICLES IN THE < 10(17) eV COSMIC RAY FLUX
R. M. Baltrusaitis, G. L. Cassiday, R. Cooper, J. W. Elbert, J. W. Gerhardy, P. R. Loh, Y. Mizumoto, P. Sokolsky, P. Sommers, and D. Steck *In* NASA. Goddard Space Flight Center 19th Intern. Cosmic Ray Conf., Vol. 8 Aug. 1985 p 104-107 refs Sponsored by NSF (For primary document see N85-36066 24-93)
(HE-5.3-1) Avail: NTIS HC as boxed set only $200/MF A01 per volume or E99 per entire set CSCL 03B

Deeply penetrating particles in the < 10 to the 17th power eV cosmic ray flux were investigated. No such events were found in 8.2 x 10 to the 6th power sec of running time. Limits were set on the following: quark-matter in the primary cosmic ray flux; long-lived, weakly interacting particles produced in p-air collisions; the astrophysical neutrino flux. In particular, the neutrino flux limit at 10 to the 17th power eV implies that z, the red shift of maximum activity is < 10 in the model of Hill and Schramm. E.A.K.

N85-36099*# Consiglio Nazionale delle Ricerche, Turin (Italy). Ist. di Cosmogeofisica.
RESULTS OF LOW ENERGY BACKGROUND MEASUREMENTS WITH THE LIQUID SCINTILLATION DETECTOR (LSD) OF THE MONT BLANC LABORATORY
M. Aglietta, G. Badino (Turin Univ.), G. F. Bologna (Turin Univ.), C. Castagnoli (Turin Univ.), W. Fulgione (Turin Univ.), P. Galeotti (Turin Univ.), O. Saavedra (Turin Univ.), G. C. Trinchero (Turin Univ.), S. Vernetto (Turin Univ.), and V. L. Dadykin (Academy of Sciences (USSR), Moscow) *In* NASA. Goddard Space Flight Center 19th Intern. Cosmic Ray Conf., Vol. 8 Aug. 1985 p 108-111 ref (For primary document see N85-36066 24-93)
(HE-5.3-5) Avail: NTIS HC as boxed set only $200/MF A01 per volume or E99 per entire set CSCL 03B

The 90 tons liquid scintillation detector (LSD) is fully running since October 1984, at a depth of 5,200 hg/sq cm of standard rock underground. The main goal is to search for neutrino bursts from collapsing stars. The experiment is very sensitive to detect low energy particles and has a very good signature to gamma-rays from (n,p) reaction which follows the upsilon e + p yields n + e sup + neutrino capture. The analysis of data is presented and the preliminary results on low energy measurements are discussed. E.A.K.

N85-36100*# Academy of Sciences (USSR), Moscow. Inst. for Nuclear Research.
THE RESEARCH PROGRAM OF THE LIQUID SCINTILLATION DETECTOR (LSD) IN THE MONT BLANC LABORATORY
V. L. Dadykin, V. F. Yakushev, P. V. Korchagin, V. B. Korchagin, A. S. Malgin, F. G. Ryassny, O. G. Ryazhskaya, V. P. Talochkin, G. T. Zatsepin, G. Badino (Turin Univ.) et al *In* NASA. Goddard Space Flight Center 19th Intern. Cosmic Ray Conf., Vol. 8 Aug. 1985 p 112-115 refs (For primary document see N85-36066 24-93)
(HE-5.3-6) Avail: NTIS HC as boxed set only $200/MF A01 per volume or E99 per entire set CSCL 03B

A massive (90 tons) liquid scintillation detector (LSD) has been running since October 1984 in the Mont Blanc Laboratory at a depth of 5,200 hg/sq cm of standard rock. The research program of the experiment covers a variety of topics in particle physics and astrophysics. The performance of the detector, the main fields of research are presented and the preliminary results are discussed. E.A.K.

N85-36101*# California Inst. of Tech., Pasadena.
A STUDY OF ATMOSPHERIC NEUTRINOS WITH THE IMB DETECTOR
J. M. LoSecco, R. M. Bionta (Michigan Univ., Ann Arbor), G. Blewitt, C. B. Bratton (Cleveland State Univ.), D. Casper (Micigan Univ., Ann Arbor), P. Chrysicopoulou (Michigan Univ., Ann Arbor), R. Claus (Michigan Univ., Ann Arbor), B. G. Cortez, S. Errede (Michigan Univ., Ann Arbor), G. W. Foster (Michigan Univ., Ann Arbor) et al *In* NASA. Goddard Space Flight Center 19th Intern. Cosmic Ray Conf., Vol. 8 Aug. 1985 p 116-119 refs Sponsored in part by DOE (For primary document see N85-36066 24-93)
(HE-5.3-7) Avail: NTIS HC as boxed set only $200/MF A01 per volume or E99 per entire set CSCL 03B

A sample of 401 contained neutrino interactions collected in the 3300 metric ton fiducial mass IMB detector was used to study neutrino oscillations, geomagnetic modulation of the flux and to search for point sources. The majority of these events are attributed to neutrino interactions. For the most part, these neutrinos are believed to originate as tertiary products of cosmic ray interactions in the atmosphere. The neutrinos are a mixture of v sub e and v sub micron. E.A.K.

N85-36102*# Franklin Inst., Newark, Del.
ATMOSPHERIC NEUTRINOS OBSERVED IN UNDERGROUND DETECTORS
T. K. Gaisser and Todor Stanev *In* NASA. Goddard Space Flight Center 19th Intern. Cosmic Ray Conf., Vol. 8 Aug. 1985 p 120-123 refs (For primary document see N85-36066 24-93)
(Contract DE-AC02-76ER-05007; Grant NSF PHY-84-10989)
(HE-5.3-8) Avail: NTIS HC as boxed set only $200/MF A01 per volume or E99 entire set CSCL 03B

Atmospheric neutrinos are produced when the primary cosmic ray beam hits the atmosphere and initiates atmospheric cascades. Secondary mesons decay and give rise to neutrinos. The neutrino production was calculated and compared with the neutrino fluxes detected in underground detectors. Contained neutrino events are characterized by observation of an interaction within the fiducial volume of the detector when the incoming particle is not observed. Both the neutrino flux and the containment requirement restrict the energy of the neutrinos observed in contained interactions to less than several GeV. Neutrinos interact with the rock surrounding the detector but only muon neutrino interactions can be observed, as the electron energy is dissipated too fast in the rock. The direction of the neutrino is preserved in the interaction and at energies above 1 TeV the angular resolution is restricted by the scattering of the muon in the rock. The muon rate reflects the neutrino spectrum above some threshold energy, determined by the detector efficiency for muons. E.A.K.

N85-36103*# Wisconsin Univ., Madison. Dept. of Physics.
GEOPHYSICAL SEARCHES FOR THREE-NEUTRINO OSCILLATIONS
J. R. Cudell and T. K. Gaisser (Franklin Inst., Newark, Del.) *In* NASA. Goddard Space Flight Center 19th Intern. Cosmic Ray Conf., Vol. 8 Aug. 1985 p 124-127 refs (For primary document see N85-36066 24-93)
(HE-5.3-9) Avail: NTIS HC as boxed set only $200/MF A01 per volume or E99 entire set CSCL 03B

The possibilities of using cosmic ray induced neutrinos to detect oscillations in deep underground experiments were considered. The matter effects are nonnegligible in the two neutrino case, they reduce a mixing angle of 45 deg to 7.5 deg for 1 GeV neutrinos of squared mass difference 10/4 eV59 going through the Earth making the oscillation totally unobservable. They produce

a natural oscillation length of about 6000 km in the case of massless neutrinos. Adding a third neutrino flavor considerably modifies the oscillation pattern and suggests that scales down to 5 x 10/5 eV could be observed even when we take into account matter effects and the electron contribution to the incoming flux. The effect of matter on the probability curves for different cases are shown by varying the masses and the mixing matrix. The ratio upward upsilon + upsilon/downward upsilon + upsilon as a function of the zenith angle at Cleveland, neglecting angular smearing and energy threshold effects is predicted. E.A.K.

N85-36104*# Michigan Univ., Ann Arbor.
MEASUREMENT OF NEUTRINO OSCILLATIONS IN MACRO EXPERIMENT
J. Musser *In* NASA. Goddard Space Flight Center 19th Intern. Cosmic Ray Conf., Vol. 8 Aug. 1985 p 128-131 refs Prepared in cooperation with the MACRO Collaboration (For primary document see N85-36066 24-93)
(HE-5.3-10) Avail: NTIS HC as boxed set only $200/MF A01 per volume or E99 per entire set CSCL 03B

The possibility of investigating neutrino oscillations in the proposed MACRO experiment are considered. Its sensitivity taking into account the theoretical uncertainties coming from flux calculations, geomagnetic effects and propagation through matter, and the experimental limitations. E.A.K.

N85-36105*# Drexel Univ., Philadelphia, Pa. Dept. of Physics.
SEARCH FOR STELLAR COLLAPSE WITH THE MACRO DETECTOR AT GRAN SASSO
R. Steinberg *In* NASA. Goddard Space Flight Center 19th Intern. Cosmic Ray Conf., Vol. 8 Aug. 1985 p 132-135 refs Prepared in cooperation with the MACRO Collaboration (For primary document see N85-36066 24-93)
(HE-5.3-11) Avail: NTIS HC as boxed set only $200/MF A01 per volume or E99 er entire set CSCL 03B

It is viewed that in stellar evolution stars in the range of 8 to 12 solar masses evolve gradually as increasingly heavier nuclei are produced and then consumed in a series of exothermic thermonuclear processes ultimately leading to the formation of a core composed almost entirely of nickel and iron. When the mass of this hot iron-nickel core reaches the critical value of approximately 1.4 solar masses, electron degeneracy pressure is no longer able to support the outer layers of the star and a collapse process begins. Since the core has exhausted its thermonuclear fuel, further stages of thermonuclear burning cannot prevent a runaway collapse. As the density reaches 10 to the 10th power gm sub/cm at a temperature near 10 to the 10th power k, most of the heavy nuclei are dissociated into free nucleons and electron capture on free protons leads to a decrease in the degeneracy pressure and further acceleration of the collapse process. Although this general picture has received substantial confirmation over the past two decades with the discovery of radio pulsars (neutron stars), X-ray pulsars (accreting binary neutron stars) and Cyg X-1 (probably an accreting black hole), an actual neutrino burst is not yet convincingly detected. E.A.K.

N85-36106*# Istituto Nazionale di Fisica Nucleare, Rome (Italy).
HIGH ENERGY NEUTRINO ASTRONOMY WITH MACRO
G. Auriemma *In* NASA. Goddard Space Flight Center 19th Intern. Cosmic Ray Conf., Vol. 8 Aug. 1985 p 136-139 refs Prepared in cooperation with the MACRO Collaboration (For primary document see N85-36066 24-93)
(HE-5.3-12) Avail: NTIS HC as boxed set only $200/MF A01 per volume or E99 entire set CSCL 03B

A large area underground detector with accurate muon tracking and directionality can be used for the search of extraterrestrial sources of high energy neutrinos. The sensitivity of the MACRO detector to possible sources of neutrinos was evaluated with a Monte-Carlo simulation of the neutrino interaction in the rock and and of the detection in the real apparatus. Two categories of possible neutrino sources are discussed in comparison with the detector sensitivity. Promising candidate objects for this search appear to be the two binary X-ray sources in the southern key Vela X1 and LMC X4, which are known to emit gamma rays up to the 10,000 TeV region. E.A.K.

N85-36107*# Academy of Sciences (USSR), Moscow. Inst. for Nuclear Research.
THE CAPABILITY OF THE EXISTING NETWORK OF INSTALLATIONS FOR DETECTING THE ANTINEUTRINO BURST FROM COLLAPSING STARS
F. F. Khalchukov, V. G. Ryassny, O. G. Ryazhskaya, and G. T. Zatsepin *In* NASA. Goddard Space Flight Center 19th Intern. Cosmic Ray Conf., Vol. 8 Aug. 1985 p 140-143 refs (For primary document see N85-36066 24-93)
(HE-5.3-13) Avail: NTIS HC as boxed set only $200/MF A01 per volume or E99 per entire set CSCL 03B

As the neutrino fluxes can bring information from the internal layers of the collapsing star, the problem of the neutrino burst detection is of importance for both the direct registering of the collapse itself and the investigation of its dynamics. The main characteristics of the neutrino fluxes have been obtained by simulations. The total neutrino flux energy is estimated as 2.5 x 10 to the 53 to 1.4 x 10 to the 54 erg, the energy of NU sub E flux being 10 to the 53 erg. Predictions on neutrino energy spectra are quite different. Two models of the collapse will be used: the model by Bowers and Wilson, hereafter BW, and the model by Nadyozhin and Otroschenko (NO). The NU sub e spectrum in the BW-model reaches the maximum at E max sub NU = 8 MeV. Average energy of NU sub E E sub nu approx. = 10 MeV. The NO-model gives E max sub Nu = 10.5 MeV and E sub nu = 12.6 MeV. The NU sub E-burst duration is DELTA tau sub NU = 20s for the NO-model. As the black hole formation is the result of the star collapse in the BW-model, DELTA tau sub nu is taken to be 5s. G.L.C.

N85-36108*# Tokyo Univ. (Japan). Inst. for Cosmic Ray Research.
ENERGY SPECTRA OF HIGH ENERGY ATMOSPHERIC NEUTRINOS
K. Mitsui and Y. Minorikawa (Kinki Univ., Osaka, Japan) *In* NASA. Goddard Space Flight Center 19th Intern. Cosmic Ray Conf., Vol. 8 Aug. 1985 p 144-147 refs (For primary document see N85-36066 24-93)
(HE-5.3-14) Avail: NTIS HC as boxed set only $200/MF A01 per volume or E99 per entire set CSCL 03B

Focusing on high energy neutrinos (> or = 1 TeV), a new calculation of atmospheric neutrino intensities was carried out taking into account EMC effects observed in P-A collisions by accelerator, recent measurement of primary cosmic ray spectrum and results of cosmic ray muon spectrum and charge ratio. Other features of the present calculation are (1) taking into account kinematics of three body decays of kaons and charm particles in diffusion equations and (2) taking into account energy dependence of kaon production. G.L.C.

N85-36109*# Academy of Sciences (USSR), Moscow. Inst. of Nuclear Research.
A STANDARD SOURCE FOR HIGH ENERGY NEUTRINO ASTRONOMY
V. S. Berezinsky, C. Castagnoli (Turin Univ.), and P. Galeotti (Turin Univ.) *In* NASA. Goddard Space Flight Center 19th Intern. Cosmic Ray Conf., Vol. 8 Aug. 1985 p 148-151 refs (For primary document see N85-36066 24-93)
(HE-5.3-15) Avail: NTIS HC as boxed set only $200/MF A01 per volume or E99 per entire set CSCL 03B

A standard source of high energy neutrinos composed of a source of accelerated particles imbedded in a cloud of low density gas is described. The main mechanism of neutrino production in the source is pp-collision, and the main process of detection is through muons produced underground by the neutrions. The flux of neutrino-produced muons is computed for sources with different spectral index. Author

N85-36110*# Academy of Sciences (USSR), Moscow. Inst. of Nuclear Research.

A SEARCH FOR COSMIC SOURCES OF HIGH ENERGY NEUTRINOS WITH SMALL UNDERGROUND DETECTORS

V. S. Berezinsky, C. Castagnoli (Turin Univ.), and P. Galeotti (Turin Univ.) *In* NASA. Goddard Space Flight Center 19th Intern. Cosmic Ray Conf., Vol. 8 Aug. 1985 p 152-155 refs (For primary document see N85-36066 24-93)

(HE-5.3-16) Avail: NTIS HC as boxed set only $200/MF A01 per volume or E99 per entire set CSCL 03B

On the basis of standard source calculations of high energy neutrino fluxes, some models of astrophysical object (single stars and binary systems) are discussed from which a detectable muon flux is expected in small underground detectors. Author

N85-36111*# Franklin Inst., Newark, Del.

NEUTRINO ASTRONOMY AND THE ATMOSPHERIC BACKGROUND

T. K. Gaisser and Todor Stanev *In* NASA. Goddard Space Flight Center 19th Intern. Cosmic Ray Conf., Vol. 8 Aug. 1985 p 156-159 refs (For primary document see N85-36066 24-93)

(HE-5.3-17) Avail: NTIS HC as boxed set only $200/MF A01 per volume or E99 entire set CSCL 03B

Some aspects of neutrino astronomy are illustrated by calculating the neutrino-induced muon flux from Cygnus X-3 binary X-ray source. The signal depends primarily on the power in cosmic rays at the source and on the distance to the source, and only relatively little on details of the matter distribution in the neighborhood of the source. Author

N85-36112*# Max-Planck-Inst. fuer Astrophysik, Munich (West Germany).

HIGH-ENERGY NEUTRINOS FROM A LUNAR OBSERVATORY

Maurince M. Shapiro and Rein Silberberg (NRL, Washington, D.C.) *In* NASA. Goddard Space Flight Center 19th Intern. Cosmic Ray Conf., Vol. 8 Aug. 1985 p 160-163 refs (For primary document see N85-36066 24-93)

(HE-5.3-21) Avail: NTIS HC as boxed set only $200/MF A01 per volume or E99 per entire set CSCL 03B

The detection of high-energy (HE) cosmic and solar-flare neutrions near the lunar surface would be feasible at energies much lower than for a terrestrial observatory. At these lower energies (< 10 to the 9th eV), the neutrino background is drastically reduced below that generated by cosmic rays in the Earth's atmosphere. Because of the short mean free path (< 1m) of the progenitor pi and K mesons against nuclear interactions in lunar rocks, the neutrino background would be quite low. At 1 GeV, less than 1% of the pions would decay; at 10 GeV, 0.1%. Thus, if the neutrino flux to be observed is intense enough, and its spectrum is steep enough, then the signal-to-noise ratio is very favorable. The observation of HE neutrinos from solar flares would be dramatically enhanced, especially at lower energies, since the flare spectra are very steep. Detection of these neutrinos on Earth does not appear to be feasible. A remarkable feature of solar flares as viewed in HE neutrinos from a lunar base is that the entire surface of the Sun would be visible. Author

N85-36113*# Ohio State Univ., Columbus. Dept. of Physics.

CHARACTERISTICS OF SLOW PARTICLES EMITTED IN THE CHARGED CURRENT INTERACTIONS OF NEUTRINOS WITH EMULSION NUCLEI

N. W. Reay and A. El-Naghy (Cairo Univ., Giza, Egypt) *In* NASA. Goddard Space Flight Center 19th Intern. Cosmic Ray Conf., Vol. 8 Aug. 1985 p 164-167 refs Prepared in cooperation with the E-531 Collaboration (For primary document see N85-36066 24-93)

(HE-5.3-22) Avail: NTIS HC as boxed set only $200/MF A01 per volume or E99 per entire set CSCL 03B

Multiplicity, angular and energy distributions of secondary particles, produced in the charged current inelastic interactions of high energy neutrinos with emulsion nuclei, were investigated. Author

N85-36114*# Punjab Univ., Lahore (Pakistan). Centre for High Energy Physics.

QCD ANALYSIS OF NEUTRINO CHARGED CURRENT STRUCTURE FUNCTION F2 IN DEEP INELASTIC SCATTERING

Mohammad Saleem and Fazal Aleem *In* NASA. Goddard Space Flight Center 19th Intern. Cosmic Ray Conf., Vol. 8 Aug. 1985 p 168-170 refs (For primary document see N85-36066 24-93)

(HE-5.3-23) Avail: NTIS HC as boxed set only $200/MF A01 per volume or E99 per entire set CSCL 03B

An analytic expression for the neutrino charged current structure function F sub 2 (x, Q sup 2) in deep inelastic scattering, consistent with quantum chromodynamics, is proposed. The calculated results are in good agreement with experiment. Author

N85-36115*# Academy of Sciences (USSR), Moscow. Inst. for Nuclear Research.

ANGULAR DISTRIBUTION OF MUONS PRODUCED BY COSMIC RAY NEUTRINOS IN ROCK

M. M. Boliev, A. V. Buckevich, A. E. Chudakov, A. V. Leonov-Vendrovsky, S. P. Mikheyev, and V. N. Zakidyshev *In* NASA. Goddard Space Flight Center 19th Intern. Cosmic Ray Conf., Vol. 8 Aug. 1985 p 171-174 refs (For primary document see N85-36066 24-93)

(HE-5.3-24) Avail: NTIS HC as boxed set only $200/MF A01 per volume or E99 per entire set CSCL 03B

Measurement of the upgoing muons flux, produced by cosmic ray neutrinos is aiming at: (1) search for neutrino oscillation; (2); search for extraterrestrial neutrinos from local sources; and (3); search for any hypothetical neutral penetrating radiation different from neutrinos. Experimental data of the Baksan underground telescope on intensity of upward muons for three years of living time, was analyzed having in mind mainly neutrino oscillation. Author

N85-36116*# Tasmania Univ., Hobart (Australia). Dept. of Physics.

UNDERGROUND MEASUREMENTS ON SECONDARY COSMIC RAYS

C. W. Wilson, A. G. Fenton, and K. B. Fenton *In* NASA. Goddard Space Flight Center 19th Intern. Cosmic Ray Conf., Vol. 8 Aug. 1985 p 175-178 refs (For primary document see N85-36066 24-93)

(HE-5.4-1) Avail: NTIS HC as boxed set only $200/MF A01 per volume or E99 per entire set CSCL 03B

Measurements made at the Poatina cosmic ray station (41.8 S 149.9 E, 347 m.w.e.) from August 1983 to July 1984 are summarized. The cosmic ray primary particles responsible for events detected at the station have a median primary energy of 1.2 TeV. The motivation for part of this work came from the reported detection of narrow angle anisotropies in the arrival direction of cosmic rays. G.L.C.

N85-36117*# Bern Univ. (Switzerland). Physikalisches Inst.

MULTIPLE MUONS OF CONVENTIONAL AND EXOTIC ORIGIN IN DUMAND Abstract Only

K. F. Grieder *In* NASA. Goddard Space Flight Center 19th Intern. Cosmic Ray Conf., Vol. 8 Aug. 1985 p 179 (For primary document see N85-36066 24-93)

(HE-5.4-4) Avail: NTIS HC as boxed set only $200/MF A01 per volume or E99 per entire set CSCL 03B

A first summary of results from a theoretical analysis, based on hadron - muon cascade calculations, that yield relative intensities of very high energy multiple muons originating from ultra high energy interactions initiated by primary protons and iron nuclei in the atmosphere, under consideration of normal as well as direct and exotic production channels is presented. Lateral density distributions and target diagrams will be presented which show that only very large detectors, such as DUMAND, will be able to record multiple muons of conventional origin reliably. This, however, is a prerequisite for any primary mass determination based on multiple muon data. Author

N85-36118*# Trondheim Univ. (Norway).

ATMOSPHERIC MUONS AND NEUTRINOS, AND THE NEUTRINO-INDUCED MUON FLUX UNDERGROUND

A. Liland *In* NASA. Goddard Space Flight Center 19th Intern. Cosmic Ray Conf., Vol. 8 Aug. 1985 p 180-183 refs (For primary document see N85-36066 24-93)
(HE-5.4-7) Avail: NTIS HC as boxed set only $200/MF A01 per volume or E99 per entire set CSCL 03B

The diffusion equation for neutrino-induced cosmic ray muons underground was solved. The neutrino-induced muon flux and charge ratio underground have been calculated. The calculated horizontal neutrino-induced nuon flux in the energy range 0.1 - 10000 GeV is in agreement with the measured horizontal flux. The calculated vertical flux above 2 GeV is in agreement with the measured vertical flux. The average charge ratio of neutrino-induced muons underground was found to be mu+/mu- = 0.40. Author

N85-36119*# Bordeaux 1 Univ., Gradignan (France). Lab. de Physique.
ANALYSIS OF THE ELECTRON COMPONENT OF EAS AT OBSERVATIONAL LEVEL 700 g x cm(-2) WITH A SCALE BREAKING INTERACTION MODEL AND GAMMAISATION HYPOTHESIS
J. Procureur, J. N. Stamenov (Bulgarian Academy of Science), P. V. Stavrev (Bulgarian Academy of Science), and S. Z. Ushev (Bulgarian Academy of Science) *In* NASA. Goddard Space Flight Center 19th Intern. Cosmic Ray Conf., Vol. 8 Aug. 1985 p 184-187 refs (For primary document see N85-36066 24-93)
(HE-5.4-8) Avail: NTIS HC as boxed set only $200/MF A01 per volume or E99 per entire set CSCL 03B

Scale breaking model and gammaisation processes for high energies give a correct description of the longitudinal development of extensive air showers (E.A.S.). From the analysis of phenomenological characteristics of E.A.S. at Tien-Shan experiment, it follows that for energies near 10 to the 6 GeV the secondary particle multiplicity increases with energy faster than is predicted by the accepted scale breaking model. Author

N85-36120*# Academy of Sciences (USSR), Moscow. Physics Inst.
ANOMALIES IN COSMIC RAYS: NEW PARTICLES VERSUS CHARM?
G. L. Balayan, A. Yu. Khodjamirian, and A. G. Oganessian *In* NASA. Goddard Space Flight Center 19th Intern. Cosmic Ray Conf., Vol. 8 Aug. 1985 p 188-191 refs (For primary document see N85-36066 24-93)
(HE-5.4-9) Avail: NTIS HC as boxed set only $200/MF A01 per volume or E99 per entire set CSCL 03B

For a long time two anomalies are observed in cosmic rays at energies E approx. = 100 TeV: (1) the generation of long-flying cascades in the hadron calorimeter (the so-called Tien-Shan effect) and; (2) the enhancement of direct muon yield as compared with the accelerator energy region. The aim is to discuss the possibility that both anomalies have common origins arising from production and decays of the same particles. the main conclusions are the following: (1) direct muons cannot be generated by any new particles with mass exceeding 10+20 GeV; and (2) if both effects are originated from the charmed hadrons, then the needed charm hadroproduction cross section is unexpectedly large as compared with the quark-gluon model predictions. G.L.C.

N85-36121*# Ain Shams Univ., Cairo (Egypt). Dept. of Physics.
RELATIONSHIP OF SEA LEVEL MUON CHARGE RATIO TO PRIMARY COMPOSITION INCLUDING NUCLEAR TARGET EFFECTS
A. Goned, M. Shalaby, A. M. Salem, and M. Roushdy *In* NASA. Goddard Space Flight Center 19th Intern. Cosmic Ray Conf., Vol. 8 Aug. 1985 p 192-194 refs (For primary document see N85-36066 24-93)
(HE-5.4-10) Avail: NTIS HC as boxed set only $200/MF A01 per volume or E99 per entire set CSCL 03B

The discrepancy between the muon charge ratio observed at low energies and that calculated using pp data is removed by including nuclear target effects. Calculations at high energies show that the primary iron spectrum is expected to change slope from 2 to 2.2 to 2.4 to 2.5 for energies > approx. 4 x 10 to the 3 GeV/nucleon if scaling features continue to the highest energies. Author

N85-36122*# Academy of Sciences (USSR), Moscow. Inst. for Nuclear Research.
STUDY OF PHOTONUCLEAR MUON INTERACTIONS AT BAKSAN UNDERGROUND SCINTILLATION TELESCOPE
V. N. Bakatanov, a. E. Chudakov, V. L. Dadykin, Yu. F. Novoseltsev, V. M. Achkasov, A. M. Semenov, and Yu. V. Stenkin *In* NASA. Goddard Space Flight Center 19th Intern. Cosmic Ray Conf., Vol. 8 Aug. 1985 p 195-197 refs (For primary document see N85-36066 24-93)
(HE-5.4-10) Avail: NTIS HC as boxed set only $200/MF A01 per volume or E99 per entire set CSCL 03B

The method of pion-muon-electron decays recording was used to distinguish between purely electron-photon and hadronic cascades, induced by high energy muons underground. At energy approx. 1 Tev a ratio of the number of hadronic to electromagnetic cascades was found equal 0.11 + or - .03 in agreement with expectation. But, at an energy approx. 4 Tev a sharp increase of this ratio was indicated though not statistically sound (0.52 + or - .13). Author

N85-36123*# Academy of Sciences (USSR), Moscow. Physical Inst.
CALCULATION OF INTENSITY OF HIGH ENERGY MUON GROUPS OBSERVED DEEP UNDERGROUND
Yu. N. Vavilov and L. G. Dedenko (Moscow State Univ.) *In* NASA. Goddard Space Flight Center 19th Intern. Cosmic Ray Conf., Vol. 8 Aug. 1985 p 198-201 refs (For primary document see N85-36066 24-93)
(HE-5.4-13) Avail: NTIS HC as boxed set only $200/MF A01 per volume or E99 per entire set CSCL 03B

The intensity of narrow muon groups observed in Kolar Gold Field (KGF) at the depth of 3375 m.w.e. was calculated in terms of quark-gluon strings model for high energy hadron - air nuclei interactions by the method of direct modeling of nuclear cascade in the air and muon propagation in the ground for normal primary cosmic ray composition. The calculated intensity has been found to be approx. 10 to the 4 times less than one observed experimentally. Author

N85-36124*# Academy of Sciences (USSR), Moscow. Physical Inst.
COLLIMATED GROUPS OF PARTICLES AS POSSIBLE MANIFESTATION OF HEAVY MESON PRODUCTION
Yu. A. Smorodin *In* NASA. Goddard Space Flight Center 19th Intern. Cosmic Ray Conf., Vol. 8 Aug. 1985 p 202-205 refs (For primary document see N85-36066 24-93)
(HE-5.4-14) Avail: NTIS HC as boxed set only $200/MF A01 per volume or E99 per entire set CSCL 03B

The interpretation of miniclusters containing hadrons as well as gamma-quanta by the cascade decays of heavy mesons, in the first turn, of charmed D'-mesons is discussed. Author

N85-36125*# Moscow State Univ. (USSR). Inst. of Nuclear Physics.
MODULAR DETECTOR FOR DEEP UNDERWATER REGISTRATION OF MUONS AND MUON GROUPS
A. I. Demianov, L. I. Sarycheva, N. B. Sinyov, I. N. Varadanyan, and A. A. Yershov *In* NASA. Goddard Space Flight Center 19th Intern. Cosmic Ray Conf., Vol. 8 Aug. 1985 p 206-209 refs (For primary document see N85-36066 24-93)
(HE-5.4-15) Avail: NTIS HC as boxed set only $200/MF A01 per volume or E99 per entire set CSCL 03B

Registration and identification of muons and muon groups penetrating into the ocean depth, can be performed using a modular multilayer detector with high resolution bidimensional readout - deep underwater calorimeter (project NADIR). Laboratory testing of a prototype sensor cell with liquid scintillator in light-tight casing, testifies to the practicability of the full-scale experiment within reasonable expences. Author

N85-36126*# Moscow State Univ. (USSR). Inst. of Nuclear Physics.
RESULTS OF INVESTIGATION OF MUON FLUXES OF SUPER-HIGH ENERGY COSMIC RAYS WITH X-RAY EMULSION CHAMBERS
I. P. Ivanenko, M. A. Ivanova, L. A. Kuzmichev, N. P. Ilyina, K. V. Mandritskaya, E. A. Osipova, I. V. Rakobolskaya, and G. T. Zatsepin (Academy of Sciences (USSR), Moscow) *In* NASA. Goddard Space Flight Center 19th Intern. Cosmic Ray Conf., Vol. 8 Aug. 1985 p 210-213 refs (For primary document see N85-36066 24-93)
(HE-5.4-16) Avail: NTIS HC as boxed set only $200/MF A01 per volume or E99 per entire set CSCL 03B

The overall data from the investigation of the cosmic ray muon flux in the range of zenith angles (0-90) deg within the energy range (3.5 to 5.0) TeV is presented. The exposure of large X-ray emulsion chambers underground was 1200 tons. year. The data were processed using the method which was applied in the experiment Pamir and differred from the earlier applied one. The obtained value of a slope power index of the differential energy spectrum of the global muon flux is =3.7 that corresponds to the slope of the pion generation differential spectrum, gamma sub PI = 2.75 + or - .04. The analysis of the muon zenith-angular distribution showed that the contribution of rapid generation muons in the total muon flux agree the best with the value .2% and less with .7% at a 90% reliability level. G.L.C.

N85-36127*# Osaka Univ. (Japan). Dept. of Physics.
SEARCH FOR MAGNETIC MONOPOLES USING PROPORTIONAL COUNTERS FILLED WITH HELIUM GAS
C. Cho, S. Higashi, N. Hiraoka, A. Maruyama, S. Ozaki (Kinki Univ., Osaka, Japan), and K. Tsuji *In* NASA. Goddard Space Flight Center 19th Intern. Cosmic Ray Conf., Vol. 8 Aug. 1985 p 214-217 refs (For primary document see N85-36066 24-93)
(HE-6.1-1) Avail: NTIS HC as boxed set only $200/MF A01 per volume or E99 per entire set CSCL 03B

Slow magnetic monopoles in cosmic rays have been searched at sea level with the detector which consists of seven layers of proportional counters filled with a mixture of He + 20% CH4. The velocities and the energy losses of the incident particles are measured. The upper limit of flux for the monopoles in the velocity range of 1 x 0.001 < Beta < 4 x 0.001 is 2.78 x 10 to the minus 12th power square centimeters sr sec of 90% confidence level. Author

N85-36128*# Tokyo Univ., Tanashi (Japan). Inst. for Cosmic Ray Research.
MAGNETIC MONOPOLE SEARCH BY 130 m(2)sr He GAS PROPORTIONAL COUNTER
T. Hara, N. Hayashida, M. Honda, K. Kamata, M. Kobayashi (National Lab. for High Energy Physics, Tsukuba, Japan), T. Kondo (National Lab. for High Energy Physics, Tsukuba, Japan), Y. Matsubara (Kyoto Univ.), M. Mori (Kyoto Univ.), Y. Ohno, G. Tanahashi et al *In* NASA. Goddard Space Flight Center 19th Intern. Cosmic Ray Conf., Vol. 8 Aug. 1985 p 218-221 refs (For primary document see N85-36066 24-93)
(HE-6.1-2) Avail: NTIS HC as boxed set only $200/MF A01 per volume or E99 per entire set CSCL 03B

A search experiment for cosmic ray magnetic monopoles was performed by means of atomic induction mechanism by using He mixture gas proportional counters of the calorimeter (130 square meters sr) at the center of the Akeno air shower array. In 3,482 hours operation no monopole candidate was observed. The upper limit of the monopole flux is 1.44 x 10 to the minus 13th power cm-z, sec -1, sr-1 (90% C.L.) for the velocity faster than 7 x 0.0001 c. Author

N85-36129*# Moscow Physical-Engineering Inst. (USSR).
RESULTS OF A SEARCH FOR MONOPOLES AND TACHYONS IN HORIZONTAL COSMIC RAY FLUX
V. D. Ashitkov, T. M. Kirina, A. P. Klimakov, R. P. Kokoulin, and A. A. Petrukhin *In* NASA. Goddard Space Flight Center 19th Intern. Cosmic Ray Conf., Vol. 8 Aug. 1985 p 222-225 refs (For primary document see N85-36066 24-93)
(HE-6.1-3) Avail: NTIS HC as boxed set only $200/MF A01 per volume or E99 per entire set CSCL 03B

A search for monopoles and tachyons at ground level was carried out using an arrangement consisting of an ionization calorimeter and two hodoscope detectors. No clear evidence for these particles was obtained. The flux of monopoles with velocities beta approximately > 0.01 is found to be less than 5.1 x 10 to the minus 13th power square centimeters s(-1) sr(-1) (95% cl.). The upper limit on the tachyon flux density is set as a 6 x 10 the minus 9th power particle/square centimeter event. Author

N85-36130*# Bari Univ. (Italy).
MONOPOLE, ASTROPHYSICS AND COSMIC RAY OBSERVATORY AT GRAN SASSO
C. DeMarzo, O. Enriquez, N. Giglietto, F. Posa, M. Attolini (Bologna Univ., Italy), F. Baldetti (Bologna Univ., Italy), G. Giacomelli (Bologna Univ., Italy), F. Grianti (Bologna Univ., Italy), A. Margiotta (Bologna Univ., Italy), P. Serra (Bologna Univ., Italy) et al *In* NASA. Goddard Space Flight Center 19th Intern. Cosmic Ray Conf., Vol. 8 Aug. 1985 p 226-229 Prepared in cooperation with MACRO Collaboration (For primary document see N85-36066 24-93)
(HE-6.1-4) Avail: NTIS HC as boxed set only $200/MF A01 per volume or E99 per entire set CSCL 03B

A new large area detector, MACRO was approved for installation at the Gran Sasso Laboratory in Italy. The detector will be dedicated to the study of naturally penetrating radiation deep underground. It is designed with the general philosophy of covering the largest possible area with a detector having both sufficient built-in redundancy and use of complementary techniques to study very rare phenomena. The detector capabilities will include monopole investigations significantly below the Parker bound; astrophysics studies of very high energy gamma ray and neutrino point sources; cosmic ray measurements of single and multimuons; and the general observation of rare new forms of matter in the cosmic rays. Author

N85-36131*# Michigan Univ., Ann Arbor. Dept. of Physics.
MONOPOLE SEARCH BELOW THE PARKER LIMIT WITH THE MACRO DETECTOR AT GRAN SASSO
G. Tarle *In* NASA. Goddard Space Flight Center 19th Intern. Cosmic Ray Conf., Vol. 8 Aug. 1985 p 230-233 refs Prepared in cooperation with MACRO Collaboration (For primary document see N85-36066 24-93)
(HE-6.1-5) Avail: NTIS HC as boxed set only $200/MF A01 per volume or E99 per entire set CSCL 03B

The MACRO detector approved for the Gran Sasso Underground Laboratory in Italy will be the first capable of performing a definitive search for super-massive grand unified theory (GUT) monopoles at a level significantly below the Parker flux limit of 10 to the minus 15th power square centimeters Sr(-1) 5(-1). GUT monopoles will move at very low velocities (V approx. 0.001 c) relative to the Earth and a multifaceted detection technique is required to assume their unambiguous identification. Calculations of scintillator response to slow monopoles and measurements of scintillation efficiency for low energy protons have shown that bare monopoles and electrically charged monopoles moving at velocities as low as 5 x .0001 c will produce detectable scintillation signals. The time-of-flight between two thick (25 cm) liquid scintillation layers separated by 4.3m will be used in conjunction with waveform digitization of signals of extended duration in each thick scintillator to provide a redundant signature for slow penetrating particles. Limited streamer tubes filled with He and n-pentane will detect bare monopoles with velocities as low as 1 x 0.0001 c by exploiting monopole induced level mixing and the Penning effect. Author

N85-36132*# Tata Inst. of Fundamental Research, Bombay (India).
LIMITS ON MONOPOLE FLUXES FROM KFG EXPERIMENT
M. R. Krishnaswamy, M. G. K. Menon, N. K. Mondal, Y. Hayashi (Osaka City Univ.), N. Ito (Osaka City Univ.), S. Kawakami (Osaka City Univ.), and S. Miyake (Tokyo Univ.) *In* NASA. Goddard Space Flight Center 19th Intern. Cosmic Ray Conf., Vol. 8 Aug.

1985 p 234-237 refs (For primary document see N85-36066 24-93)
(HE-6.1-6) Avail: NTIS HC as boxed set only $200/MF A01 per volume or E99 per entire set CSCL 03B

The nucleon decay experiment at KGF at a depth of 2.3 Km is eminently suited for the search of Grand Unified theory (GUT) monopoles, whose velocities at the present epoch are predicted to be around 0.001C. At this depth the cosmic ray background is at a level 2/day in the detector of size 4m x 6m x 3.7m and one can look for monopoles traversing the detector in all directions, using three methods, i.e., (1) dE/dx (ionization); (2) time of flight and (3) catalysis of nucleon decay. The detector is composed of 34 layers of proportional counters arranged in horizontal planes one above the other in an orthogonal maxtrix. Each of the 1594 counters are instrumented to measure ionization in the gas (90% argon + 10% methane) as well as the time of arrival of particles. Author

N85-36133*# University Coll., Dublin (Ireland). Dept. of Physics.
AN EXPERIMENT TO DETECT GUT MONOPOLES
G. MacNeill and D. J. Fegan *In* NASA. Goddard Space Flight Center 19th Intern. Cosmic Ray Conf., Vol. 8 Aug. 1985 p 238-241 refs (For primary document see N85-36066 24-93)
(HE-6.1-7) Avail: NTIS HC as boxed set only $200/MF A01 per volume or E99 per entire set CSCL 03B

Recent advances in the development of Grand Unification Theories have led to several interesting predictions. One of these states that Grand Unification Monopoles (GUMs) exist as solutions in may nonabelian gauge theories. Another consequence of Unification is the possibility of baryon decay. The efficiency of the water tank detector in registering a Rubakov type decay will vary with both the interaction length and the GUM's velocity, expressed in terms of beta (> 0.01). The efficiency decreases at large values of because of the limited resolving time of the detector (approx. 50 ns). At lower values of Beta the time between interactions is such that the criterion of 4 events in 2 mu s can no longer be satisfied. The Rubakov experiment has now been in operation for almost 2 years with an estimated live time of 80%. During this time no candidate events have been observed leading to an estimated upper limit on the flux of 7.82 x 0.00001 m(-2) d(-1) Sr(-1). The ionization loss detection system has only recently come on line and as yet no results are available from this experiment. R.J.F.

N85-36134*# California Univ., Berkeley. Dept. of Physics.
SEARCH FOR SUPERMASSIVE MAGNETIC MONOPOLES USING MICA CRYSTALS
P. B. Price and M. H. Salamon *In* NASA. Goddard Space Flight Center 19th Intern. Cosmic Ray Conf., Vol. 8 Aug. 1985 p 242-245 refs (For primary document see N85-36066 24-93)
(Grant NSF PHY-84-03710)
(HE-6.1-8) Avail: NTIS HC as boxed set only $200/MF A01 per volume or E99 per entire set CSCL 03B

The survival of the Galactic magnetic field almost certainly sets an astrophysical upper bound of approx. 10 to the minus 15th power cm(-2) sr(-1) s(-1) on the flux of monopoles. To improve significantly upon this Parker limit with direct, real time searches would require a detector area of approx. 10,000 square meters and a collection time of years. Several such searches are being contemplated. A novel alternative scheme using large mica crystals capable of recording and storing tracks of slow monopoles over a time scale of approx. 10 to the 9th power years was proposed. Author

N85-36135*# Pennsylvania Univ., Philadelphia. Dept. of Physics.
THE HOMESTAKE SURFACE-UNDERGROUND SCINTILLATIONS: DESCRIPTION
M. L. Cherry, S. Corbato, T. Daily, E. J. Fenyves (Texas Univ., Dallas), D. Kieda, K. Lande, and C. K. Lee *In* NASA. Goddard Space Flight Center 19th Intern. Cosmic Ray Conf., Vol. 8 Aug. 1985 p 246-249 refs Sponsored by DOE (For primary document see N85-36066 24-93)
(HE-6.1-9) Avail: NTIS HC as boxed set only $200/MF A01 per volume or E99 per entire set CSCL 03B

Two new detectors are currently under construction at the Homestake Gold Mine a 140-ton Large Area Scintillation Detector (LASD) with an upper surface area of 130 square meters, a geometry factor (for an isotropic flux) of 1200 square meters, sr, and a depth of 4200 m.w.e.; and a surface air shower array consisting of 100 scintillator elements, each 3 square meters, spanning an area of approximately square kilometers. Underground, half of the LASD is currently running and collecting muon data; on the surface, the first section of the air shower array will begin operation in the spring of 1985. The detectors and their capabilities are described. Author

N85-36136*# Academy of Sciences (USSR), Moscow. Inst. for Nuclear Research.
UPPER LIMIT ON MAGNETIC MONOPOLE FLUX FROM BAKSAN EXPERIMENT
E. N. Alexeyev, M. M. Boliev, A. E. Chudakov, and S. P. Mikheyev *In* NASA. Goddard Space Flight Center 19th Intern. Cosmic Ray Conf., Vol. 8 Aug. 1985 p 250-252 refs (For primary document see N85-36066 24-93)
(HE-6.1-11) Avail: NTIS HC as boxed set only $200/MF A01 per volume or E99 per entire set CSCL 03B

No indication of slowly moving penetrating particles in cosmic radiation underground was found during two years observation. Particle velocity and pulse shape are main criteria for search. Probability of the imitation of slow particles (Beta < 0.1) by atmospheric muons is negligible. Our upper limit on superheavy magnetic monopole flux is now 1.86 x 10 to the minus 15th power cm(-2) sr(-1) s(-1) (90% c.l.) for velocity range 2 x 0.0001 < beta < 0.1. Author

N85-36137*# California Univ., San Diego, La Jolla. Dept. of Physics.
RESULTS FROM THE UCSD MAGNETIC MONOPOLE SEARCH
G. E. Masek, L. M. Knapp, E. Miller, J. P. Stronski, W. Vernon, and J. T. White *In* NASA. Goddard Space Flight Center 19th Intern. Cosmic Ray Conf., Vol. 8 Aug. 1985 p 253-256 refs (For primary document see N85-36066 24-93)
(HE-6.1-12) Avail: NTIS HC as boxed set only $200/MF A01 per volume or E99 per entire set CSCL 03B

The energy loss mechanism for slowly moving magnetic monopoles in helium provides a means of extending the search for such particles by ionization techniques to velocities approximately 3 X 1 million cm/sec (beta approximately equals 0.0001). Other gases (e.g., CH2 or CO2) mixed with helium will be ionized with high efficiency by collisions with excited helium atoms, thus allowing the use of large proportional chamber systems for the detection of the monopoles. The first reported results utilizing this mechanism was the experiment of Kajino, et al., using a detector with an area-solid angle product alpha time delta alpha of 24.7 square meters sr. They set a limit on the flux of monopoles of <7.2 x 10 to the 13th power cm(-2) sr(-1) sec(-1) at a 90% confidence level for beta > 3x 0.0001. Here, the results of a He:CH2 proportional tube array designed to extend the velocity limit down to beta approximately 0.0001 are reported. The detector which has been operating at the University of California, San Diego (UCSD) since last summer, is a prototype for a larger array currently under construction at UCSD. The data presented here is from 200 days of live time with the prototype detector. Author

N85-36138*# Technische Hochschule, Aachen (West Germany).
SEARCH FOR PROTON DECAY IN THE FREJUS EXPERIMENT
Ch. Berger, A. Hoffmann, F. Raupach, J. Tutas, G. Schmitz, B. Dudelzak (Lab. de l'Accelerateur Lineaire, Orsay, France), P. Eschstruth (Lab. de l'Accelerateur Lineaire, Orsay, France), G. Deuzet (Lab. de l'Accelerateur Lineaire, Orsay, France), S. Jullian (Lab. de l'Accelerateur Lineaire, Orsay, France), D. Lalanne (Lab. de l'Accelerateur Lineaire, Orsay, France) et al *In* NASA. Goddard Space Flight Center 19th Intern. Cosmic Ray Conf., Vol. 8 Aug. 1985 p 257-260 (For primary document see N85-36066 24-93)

(HE-6.2-2) Avail: NTIS HC as boxed set only $200/MF A01 per volume or E99 per entire set CSCL 03B

The status of the Frejus experiment and the preliminary results obtained in the search for nucleon decay are discussed. A modular, fine grain tracking calorimeter was installed in the Frejus laboratory in the period extending from October 1983 to May 1985. The 3300 cubic meter underground laboratory, located in the center of the Frejus tunnel in the Alps, is covered in the vertical direction by 1600 m of rocks (4400 m w.e.). The average number of atmospheric muons in the lab is 4.2 square meters per day. The 912 ton detector is made of 114 modules, each one including eight flash chamber and one Geiger vertical planes of (6 x 6) square meters dimensions. The flash chamber (and Geiger) planes are alternatively crossed to provide a 90 deg. stereo reconstruction. No candidate for the nucleon decay into charged lepton is found in the first sample of events. R.J.F.

N85-36139*# Tata Inst. of Fundamental Research, Bombay (India).
RESULTS ON NUCLEON LIFE-TIME FROM THE KOLAR GOLD FIELD EXPERIMENT
M. R. Krishnaswamy, M. G. K. Menon, N. K. Mondal, V. S. Narasimham, B. V. Sreekantan, Y. Hayashi (Osaka City Univ.), N. Ito (Osaka City Univ.), S. Kawakami (Osaka City Univ.), and S. Miyake (Tokyo Univ.) *In* NASA. Goddard Space Flight Center 19th Intern. Cosmic Ray Conf., Vol. 8 Aug. 1985 p 261-264 Sponsored in part by Japanese Ministry of Education (For primary document see N85-36066 24-93)
(HE-6.2-3) Avail: NTIS HC as boxed set only $200/MF A01 per volume or E99 per entire set CSCL 03B

The KGF nucleon decay experiment has been in operation since October 1980 with a 140 ton calorimetric detector at a depth of 2.3 Km underground. The detector comprises 34 layers of proportional counters arranged in an orthogonal geometry with 12 mm thick iron plates in between successive layers. The proportional counters are made up of square (10 x 10 square centimeters) iron plates of wall thickness 2.3 mm. Each of the 1600 counters is instrumented to provide data on ionization, DE/dx and arrival time. The visible energy of a particle is determined to an accuracy of approximately 20% from the ionization and range of its track. The end point ionization of a stopping track provides the direction of motion as well as the nature of the particle (mu/pi,k,p). Decay of mu is recorded with an overall efficiency of only 20% in view of the thickness of 13 g/square centimeters between successive layers. Author

N85-36140*# Tata Inst. of Fundamental Research, Bombay (India).
DATA ACQUISITION SYSTEM FOR PHASE-2 KGF PROTON DECAY EXPERIMENT
M. R. Krishnaswamy, M. G. K. Menon, N. K. Mondal, V. S. Narasimham, B. V. Sreekantan, Y. Hayashi (Osaka City Univ.), N. Ito (Osaka City Univ.), S. Kawakami (Osaka City Univ.), and S. Miyake (Tokyo Univ.) *In* NASA. Goddard Space Flight Center 19th Intern. Cosmic Ray Conf., Vol. 8 Aug. 1985 p 265-266 (For primary document see N85-36066 24-93)
(HE-6.2-4) Avail: NTIS HC as boxed set only $200/MF A01 per volume or E99 per entire set CSCL 03B

Phase-2 of KGF proton decay experiment using 4000 proportional counters will start operating from middle of 1985. The detection systems, in addition to measuring the time information to an accuracy of 200 n see, also records ionization in the hit counters. It also monitors different characteristics of the counters like pulse height spectrum, pulse width spectrum and counting rate. The acquisition system is discussed. Author

N85-36141*# Argonne National Lab., Ill.
CONSTRUCTION OF THE SOUDAN 2 DETECTOR
D. S. Ayres, W. L. Barrett, J. W. Dawson, T. H. Fields, M. C. Goodman, J. Hoftiezer, E. N. May, N. K. Mondal, L. E. Price, J. L. Schlereth et al *In* NASA. Goddard Space Flight Center 19th Intern. Cosmic Ray Conf., Vol. 8 Aug. 1985 p 267-270 refs (For primary document see N85-36066 24-93)
(HE-6.2-5) Avail: NTIS HC as boxed set only $200/MF A01 per volume or E99 per entire set CSCL 03B

Progress in the construction of the Soudan 2 nucleon decay detector which is being built at the Soudan iron mine in Minnesota is discussed. The expected event rate and characteristics of low energy neutrino events, muon events, multiple muon events, and other cosmic ray phenomena are discussed. Author

N85-36142*# Comitato Nazionale per l'Energia Nucleare, Frascati (Italy).
NUCLEON DECAY AND ATMOSPHERIC NEUTRINOS IN THE MONT BLANC EXPERIMENT
G. Battistoni, E. Bellotti (Milan Univ.), G. Bologne (CNR, Turin), P. Campana, C. Castagnoli (CNR, Turin), V. Chiarella, A. Ciocio (CNR, Turin), D. C. Cundy (CERN, Geneva), B. DEttorePiazzoli (CNR, Turin), E. Fiorini (Milan Univ.) et al *In* NASA. Goddard Space Flight Center 19th Intern. Cosmic Ray Conf., Vol. 8 Aug. 1985 p 271-274 refs (For primary document see N85-36066 24-93)
(HE-6.2-6) Avail: NTIS HC as boxed set only $200/MF A01 per volume or E99 per entire set CSCL 03B

In the NUSEX experiment, during 2.8 years of operation, 31 fully contained events have been collected; 3 among them are nucleon decay candidates, while the others have been attributed to upsilon interactions. Limits on nucleon lifetime and determinations of upsilon interaction rates are presented. Author

N85-36143*# Maryland Univ., College Park. Dept. of Physics and Astronomy.
A SEARCH FOR HEAVY LONG LIVED PARTICLES IN HIGH ENERGY COSMIC RAYS
A. Mincer, H. Freudenreich, J. A. Goodman, S. C. Tonwar, G. B. Yodh, R. W. Ellsworth (George Mason Univ, Fairfax, Va.), and D. Berley (NSF, Washington, D.C.) *In* NASA. Goddard Space Flight Center 19th Intern. Cosmic Ray Conf., Vol. 8 Aug. 1985 p 275-278 refs (For primary document see N85-36066 24-93)
(HE-6.2-7) Avail: NTIS HC as boxed set only $200/MF A01 per volume or E99 per entire set CSCL 03B

The results of an experimental search for energetic particles which arrive at sea level delayed with respect to the shower front, with an order of magnitude greater exposure than previous experiments are presented. The experiment was sensitive to showers from cosmic rays between 10 to the 5th power and 10 to the 7th power Gev per nucleus. No evidence for the existence of heavy long lived particles in air showers was found. An upper limit to the flux of these particles was set at the 90% confidence level of 1.4 x 10 to the minus 12th power cm(-2) sr(-1) s(-1). Author

N85-36144*# Mesei Univ., Tokyo (Japan). Dept. of Physics.
DELAYED PARTICLES IN EAS AT AKENO
H. Sakuyama, N. Suzuki, K. Watanabe, and K. Mizushima (Kobe Women's Junior Coll., Japan) *In* NASA. Goddard Space Flight Center 19th Intern. Cosmic Ray Conf., Vol. 8 Aug. 1985 p 279-282 refs (For primary document see N85-36066 24-93)
(HE-6.2-8) Avail: NTIS HC as boxed set only $200/MF A01 per volume or E99 per entire set CSCL 03B

Using two 2.25 square meter fast scintillation detectors, delayed particles in cosmic ray showers (CRS) have been observed at Akeno Observatory. These are set under 1 m concrete and 2.5 cm lead plates respectively. About 2500 CRS are analyzed. The lateral distribution of delayed particles for the CRS size > 10 to the 7th power is flatter than that for < to the 7th power. The lateral density of delayed particles is almost constant for the size range 2.2 X 10 to the 5th power approx. 10 to the 7th power and increases rapidly above 10 to the 7th power. These facts may suggest change of nuclear interaction at 10 to the 7th power and substantially the existence of heavy particles with long life. Author

N85-36145*# Okayama Univ. (Japan). Dept. of Physics.
ENERGETIC DELAYED HADRONS IN LARGE AIR SHOWERS OBSERVED AT 5200M ABOVE SEA LEVEL
T. Kaneko, K. Hagiwara (Inst. of Physical and Chemical Research, Saitama, Japan), H. Yoshii (Ehime Univ., Matsuyama, Japan), N. Martinic (Univ. Mayor de San Andres), L. Siles (Univ. Mayor de

San Andres), P. Miranda (Univ. Mayor de San Andres), F. Kakimoto (Tokyo Inst. of Tech.), I. Tsuchimoto (Tokyo Inst. of Tech.), N. Inoue (Tokyo Inst. of Tech.), and K. Suga (Tokyo Inst. of Tech.) *In* NASA. Goddard Space Flight Center 19th Intern. Cosmic Ray Conf., Vol. 8 Aug. 1985 p 283-286 refs (For primary document see N85-36066 24-93)
(HE-6.2-9) Avail: NTIS HC as boxed set only $200/MF A01 per volume or E99 per entire set CSCL 03B

Energetic delayed hadrons in air showers with electron sizes in the range 10 to the 6th power to 10 to the 9th power were studied by observing the delayed bursts produced in the shield of nine square meter scintillation detectors in the Chacaltaya air-shower array. The frequency of such delayed burst is presented as a function of electron size, core distance and sec theta. Author

N85-36146*# Kobe Univ. (Japan). School of Science and Technology.
SEARCH FOR LONG-LIVED MASSIVE PARTICLES IN EXTENSIVE AIR SHOWERS
M. Kawamoto, N. Inoue, Y. Misaki (Kobe Univ., Japan), O. Manabe (Kobe Univ., Japan), T. Takeuchi (Kobe Univ., Japan), and Y. Toyoda *In* NASA. Goddard Space Flight Center 19th Intern. Cosmic Ray Conf., Vol. 8 Aug. 1985 p 287-289 refs (For primary document see N85-36066 24-93)
(HE-6.2-10) Avail: NTIS HC as boxed set only $200/MF A01 per volume or E99 per entire set CSCL 03B

Air showers containing delayed sub-showers which may be produced by a long-lived massive particle have been investigated by using twelve detectors. Ten events have been selected out as the candidates. However, a definite conclusion cannot be reached at the present time. Author

N85-36147*# Institut d'Astrophysique, Paris (France).
HIGH ENERGY COSMIC RAY SIGNATURE OF QUARK NUGGETS
J. Audouze, R. Schaeffer (Lab. Rene Bernas, Orsay, France), and J. Silk (California Univ., Berkeley) *In* NASA. Goddard Space Flight Center 19th Intern. Cosmic Ray Conf., Vol. 8 Aug. 1985 p 290-293 refs (For primary document see N85-36066 24-93)
(HE-6.2-11) Avail: NTIS HC as boxed set only $200/MF A01 per volume or E99 per entire set CSCL 03B

It has been recently proposed that dark matter in the Universe might consist of nuggets of quarks which populate the nuclear desert between nucleons and neutron star matter. It is further suggested that the Centauro events which could be the signature of particles with atomic mass A approx. 100 and energy E approx. 10 to 15th power eV might also be related to debris produced in the encounter of two neutron stars. A further consequence of the former proposal is examined, and it is shown that the production of relativistic quark nuggets is accompanied by a substantial flux of potentially observable high energy neutrinos. Author

N85-36148*# Siegen Univ., (West Germany). Dept. of Physics.
SEARCH FOR ANOMALONS USING PLASTIC NUCLEAR TRACK DETECTORS
W. Heinrich, H. Drechsel, C. Brechtmann, and J. Dreute *In* NASA. Goddard Space Flight Center 19th Intern. Cosmic Ray Conf., Vol. 8 Aug. 1985 p 294-297 refs (For primary document see N85-36066 24-93)
(HE-6.2-12) Avail: NTIS HC as boxed set only $200/MF A01 per volume or E99 per entire set CSCL 03B

A stack of CR39 track detectors containing Ag foils was exposed to 1.7 GeV/nucleon Fe-56 beam and the anomalous mean free path effect investigated. Neither the whole set of 7517 nor a subset of 2542 interacting fragments produced probably in the Ag target show an effect. By combining the data of this and an earlier experiment we can also exclude an effect for 3219 interacting fragments produced in delta Z=1 collisions. Author

N85-36149*# Durham Univ. (England). Dept. of Physics.
SEARCH FOR TACHYONS ASSOCIATED WITH EXTENSIVE AIR SHOWERS IN THE GROUND LEVEL COSMIC RADIATION
H. F. Masjed and F. Ashton *In* NASA. Goddard Space Flight Center 19th Intern. Cosmic Ray Conf., Vol. 8 Aug. 1985 p 298-301 refs (For primary document see N85-36066 24-93)
(HE-6.2-13) Avail: NTIS HC as boxed set only $200/MF A01 per volume or E99 per entire set CSCL 03B

Events detected in a shielded plastic scintillation counter occurring in the 26 microsec preceding the arrival of an extensive air shower at ground level with local electron density > or = 20 m to the -2 power and the 240 microsec after its arrival have been studied. No significant excess of events (tachyons) arriving in the early time domain have been observed in a sample of 11,585 air shower triggers. Author

N85-36150*# Okayama Univ. (Japan).
CHARGE 4/3 LEPTONS IN COSMIC RAYS
Tomonori Wada, Yoshihiko Yamashita, Kuninisuke Imaeda (Okayama Univ.), and Isao Yamamoto (Okayama Univ.) *In* NASA. Goddard Space Flight Center 19th Intern. Cosmic Ray Conf., Vol. 8 Aug. 1985 p 302-305 refs (For primary document see N85-36066 24-93)
(HE-6.2-14) Avail: NTIS HC as boxed set only $200/MF A01 per volume or E99 per entire set CSCL 03B

A cosmic ray counter telescope has been operated at zenith angles of 0, 40, 44, and 60 degs in order to look for charge 4/3 particles. A few million clean single cosmic rays of each zenith angle are analyzed. Author

N85-36151*# Leeds Univ. (England). Dept. of Physics.
PROGRESS REPORT ON A NEW SEARCH FOR FREE e/3 QUARKS IN THE CORES OF 10(15) - 10(16) eV AIR SHOWERS
A. L. Hodson, R. M. Bull (Nottingham Univ.), R. S. Taylor, and C. H. Belford *In* NASA. Goddard Space Flight Center 19th Intern. Cosmic Ray Conf., Vol. 8 Aug. 1985 p 306-309 refs (For primary document see N85-36066 24-93)
(HE-6.2-15) Avail: NTIS HC as boxed set only $200/MF A01 per volume or E99 per entire set CSCL 03B

The Leeds 3 sq m Wilson cloud chamber is being used in a new search for free e/3 quarks close to the axes of 10 to the 15th power - 10 to the 16th power eV air showers. A ratio trigger circuit is used to detect the incidence of air shower cores; the position of the shower center and the axis direction are determined from photographs of current-limited spark chambers. It is thus possible, for the first time, to know where we have looked for quarks in air showers and to select for scanning only those cloud chamber photographs where we have good evidence that the shower axis was close to the chamber. 250 g/sq cm of lead/concrete absorber above the cloud chamber serve to reduce particle densities and make a quark search possible very close to the shower axes. The current status of the search is given. Author

N85-36152*# National Aeronautics and Space Administration. Goddard Space Flight Center, Greenbelt, Md.
OBSERVATION OF GENETIC RELATION AMONG NEW PHENOMENA GEMINION, CHIRON AND MINI-CENTAURO
In its 19th Intern. Cosmic Ray Conf., Vol. 8 Aug. 1985 p 310-313 refs Prepared in cooperation with Brasil-Japan Collaboration of Chacaltaya Emulsion Chamber Experiment (For primary document see N85-36066 24-93)
(HE-6.2-16) Avail: NTIS HC as boxed set only $200/MF A01 per volume or E99 per entire set CSCL 03B

The threshold energy problem of exotic type interactions is discussed on the basis of available information from the Chacaltaya emulsion chamber experiment. The genetic hypothesis is proposed as a working hypothesis to explain the discrepancy seen in cosmic ray study and CERN p bar -p collider experiments. Author

N85-36153*# Academy of Sciences (USSR), Moscow. Physical Inst.
TIEN-SHAN EFFECT AND CHARMED PARTICLES
I. M. Dremin, D. T. Madigozhin, V. A. Saakjan, A. D. Serdukov, V. I. Yakovlev, P. I. Golubnichy (Voroshilovgradski Mashinostroitelnyi Inst., USSR), L. A. Efimenko (Voroshilovgradski Mashinostroitelnyi

Inst., USSR), and R. T. Savchenko (Voroshilovgradski Mashinostroitelnyi Inst., USSR) *In* NASA. Goddard Space Flight Center 19th Intern. Cosmic Ray Conf., Vol. 8 Aug. 1985 p 314-317 refs (For primary document see N85-36066 24-93)
(HE-6.2-17) Avail: NTIS HC as boxed set only $200/MF A01 per volume or E99 per entire set CSCL 03B

It is shown that the Tien-Shan effect can be explained as a consequence of charmed particle production with a sufficiently high production cross-section (about 5 mb/nucleon at 100 TeV). Author

N85-36154*# Adelaide Univ. (Australia). Dept. of Physics.
MUON AND NEUTRINO FLUXES
P. G. Edwards and R. J. Protheroe *In* NASA. Goddard Space Flight Center 19th Intern. Cosmic Ray Conf., Vol. 8 Aug. 1985 p 318-321 refs (For primary document see N85-36066 24-93)
(HE-6.2-18) Avail: NTIS HC as boxed set only $200/MF A01 per volume or E99 per entire set CSCL 03B

The result of a new calculation of the atmospheric muon and neutrino fluxes and the energy spectrum of muon-neutrinos produced in individual extensive air showers (EAS) initiated by proton and gamma-ray primaries is reported. Also explained is the possibility of detecting atmospheric nu sub mu's due to gamma-rays from these sources. Author

N85-36155*# Arizona Univ., Tucson. Dept. of Physics.
SEARCH FOR ACOUSTIC SIGNALS FROM HIGH ENERGY CASCADES
Raymond Bell and Theodore Bowen *In* NASA. Goddard Space Flight Center 19th Intern. Cosmic Ray Conf., Vol. 8 Aug. 1985 p 322-324 refs (For primary document see N85-36066 24-93)
(HE-7.1-1) Avail: NTIS HC as boxed set only $200/MF A01 per volume or E99 per entire set CSCL 03B

High energy cosmic ray secondaries can be detected by means of the cascades they produce when they pass through matter. When the charged particles of these cascades ionize the matter they are traveling through, the heat produced and resulting thermal expansion causes a thermoacoustic wave. These sound waves travel at about one hundred-thousandth the speed of light, and should allow an array of acoustic transducers to resolve structure in the cascade to about 1 cm without high speed electronics or segmentation of the detector. Author

N85-36156*# Voroshilovgrad Machinery Building Inst., (USSR).
EXPERIMENTAL INVESTIGATION OF RADIATIVE-ACOUSTIC EFFECTS IN THE WATER BY THE THERMODYNAMICAL CONDITIONS OF DUMAND
P. I. Golubnichy, S. D. Korchikov, S. I. Nikolsky (Academy of Sciences (USSR), Moscow), and V. I. Yakovlev (Academy of Sciences (USSR), Moscow) *In* NASA. Goddard Space Flight Center 19th Intern. Cosmic Ray Conf., Vol. 8 Aug. 1985 p 325-328 refs (For primary document see N85-36066 24-93)
(HE-7.1-2) Avail: NTIS HC as boxed set only $200/MF A01 per volume or E99 per entire set CSCL 03B

The value of the sound pulse produced by a high energy neutrino, if the thermoacoustical mechanism of sound generation takes place, is proportional to the density of energy absorbed, the coefficient of thermal expansion, the sound velocity, and the specific heat all of which depend on temperature, pressure and the salt content of the water. Author

N85-36157*# Academia Sinica, Beijing (China). Inst. of High Energy Physics.
EXPLORING RESULTS OF THE POSSIBILITY ON DETECTING COSMIC RAY PARTICLES BY ACOUSTIC WAY
Yinlin Jiang, Yukui Yuan, Yanguo Li, Duonbao Chen, Rongting Zheng, and Jianning Song *In* NASA. Goddard Space Flight Center 19th Intern. Cosmic Ray Conf., Vol. 8 Aug. 1985 p 329-332 refs (For primary document see N85-36066 24-93)
(HE-7.1-3) Avail: NTIS HC as boxed set only $200/MF A01 per volume or E99 per entire set CSCL 03B

It has been demonstrated experimentally and theoretically that high energy particles produce detectable sounds in water. However, no one has been able to detect an acoustic signal generated by a high energy cosmic ray particle in water. Results show that transient ultrasonic signals in a large lake or reservoir are fairly complex and that the transient signals under water may arise mainly from sound radiation from microbubbles. This field is not explored in detail. Perhaps, the sounds created by cosmic ray particles hide in these ultrasonic signals. In order to develop the technique of acoustic detection, it is most important to make a thorough investigation of these ultrasonic signals in water. Author

N85-36158*# Yunnan Univ., Kunming (China). Dept. of Physics.
ACOUSTIC DETECTION OF AIR SHOWER CORES
Xiaoyu Gao, Yongyu Liu (Inst. of High Energy Physics, Peking), and Songlin Du *In* NASA. Goddard Space Flight Center 19th Intern. Cosmic Ray Conf., Vol. 8 Aug. 1985 p 333-336 refs (For primary document see N85-36066 24-93)
(HE-7.1-4) Avail: NTIS HC as boxed set only $200/MF A01 per volume or E99 per entire set CSCL 03B

At an altitude of 1890m, a pre-test with an Air shower (AS) core selector and a small acoustic array set up in an anechoic pool with a volume of 20x7x7 cu m was performed, beginning in Aug. 1984. In analyzing the waveforms recorded during the effective working time of 186 hrs, three acoustic signals which cannot be explained as from any source other than AS cores were obtained, and an estimation of related parameters was made. Author

N85-36159*# Osaka City Univ. (Japan).
DETECTION THRESHOLD ENERGY OF HIGH ENERGY CASCADE SHOWERS USING THERMOLUMINESCENCE PTFE-SHEET AND HOT-GAS READER
S. Kino, A. Nakanishi, S. Miono, T. Kitajima (Ashikaga Inst. of Tech., Japan), T. Yanagita, T. Nakatsuka (Konan Univ, Kobe, Japan), N. Ohmori (Kochi Univ., Japan), and M. Hazama (Aichi Women's Junior Coll., Japan) *In* NASA. Goddard Space Flight Center 19th Intern. Cosmic Ray Conf., Vol. 8 Aug. 1985 p 337-340 refs (For primary document see N85-36066 24-93)
(HE-7.1-5) Avail: NTIS HC as boxed set only $200/MF A01 per volume or E99 per entire set CSCL 03B

A new thermoluminescence (TL) sheet was developed as a detector for high energy components in air showers. For the investigation of detection threshold energy for a cascade shower, TL sheets were exposed at Mt. Fuji with X-ray films in emulsion chambers and were scanned by a hot-gas reader. It is concluded that if a gamma ray whose energy is more than 6 TeV enters vertically into lead chambers, the resulting cascade shower is readily detectable at maximum development. Author

N85-36160*# Hirosaki Univ. (Japan).
APPLICATION OF THERMOLUMINESCENCE FOR DETECTION OF CASCADE SHOWER 1: HARDWARE AND SOFTWARE OF READER SYSTEM
M. Akashi, S. Kawaguchi, Z. Watanabe, A. Misaki (Saitama Univ., Japan), M. Niwa (Saitama Univ., Japan), Y. Okamoto (Waseda Univ.), T. Fujinaga (Aoyamagakuin Univ., Tokyo), M. Ichimura (Aoyamagakuin Univ., Tokyo), T. Shibata (Aoyamagakuin Univ., Tokyo), S. Dake (Kobe Univ., Japan) et al *In* NASA. Goddard Space Flight Center 19th Intern. Cosmic Ray Conf., Vol. 8 Aug. 1985 p 341-344 refs (For primary document see N85-36066 24-93)
(HE-7.1-6) Avail: NTIS HC as boxed set only $200/MF A01 per volume or E99 per entire set CSCL 03B

A reader system for the detection of cascade showers via luminescence induced by heating sensitive material (BaSO4:Eu) is developed. The reader system is composed of following six instruments: (1) heater, (2) light guide, (3) image intensifier, (4) CCD camera, (5) image processor, (6) microcomputer. The efficiency of these apparatuses and software application for image analysis is reported. Author

N85-36161*# Okayama Univ. (Japan).
SPATIAL DISTRIBUTION READ-OUT SYSTEM FOR THERMOLUMINESCENCE SHEETS

I. Yamamoto, T. Tomiyama, K. Imaeda, K. Ninagawa, T. Wada (Okayama Univ.), Y. Yamashita (Okayama Univ.), and A. Misaki (Saitama Univ.) *In* NASA. Goddard Space Flight Center 19th Intern. Cosmic Ray Conf., Vol. 8 Aug. 1985 p 345-348 refs (For primary document see N85-36066 24-93)
(HE-7.1-7) Avail: NTIS HC as boxed set only $200/MF A01 per volume or E99 per entire set CSCL 03B

A spatial distribution read-out system of thermoluminescence (TL) sheets is developed. This system consists of high gain image intensifier, a CCD-TV camera, a video image processor and a host computer. This system has been applied to artificial TL sheets (BaSO4:Eu doped) for detecting high energy electromagnetic shower and heavy nuclei tracks. Author

N85-36162*# Hirosaki Univ. (Japan).
APPLICATION OF THERMOLUMINESCENCE FOR DETECTION OF CASCADE SHOWER 2: DETECTION OF COSMIC RAY CASCADE SHOWER AT MOUNT FUJI
M. Akashi, S. Kawaguchi, Z. Watanabe, A. Misaki (Saitama Univ.), M. Niwa (Saitama Univ.), Y. Okamoto (Waseda Univ.), T. Fujinaga (Aoyamagakuin Univ., Tokyo), M. Ichimura (Aoyamagakuin Univ., Tokyo), T. Shibata (Aoyamagakuin Univ., Tokyo), S. Dake (Kobe Univ.) et al *In* NASA. Goddard Space Flight Center 19th Intern. Cosmic Ray Conf., Vol. 8 Aug. 1985 p 349-352 refs (For primary document see N85-36066 24-93)
(HE-7.1-12) Avail: NTIS HC as boxed set only $200/MF A01 per volume or E99 per entire set CSCL 03B

The results of a thermoluminescence (TL) chamber exposed at Mt. Fuji during Aug. '83 - Aug. '84 are reported. The TL signal induced by cosmic ray shower is detected and compared with the spot darkness of X-ray film exposed at the same time. Author

99 GENERAL

No abstracts in this category.

SUBJECT INDEX

Typical Subject Index Listing

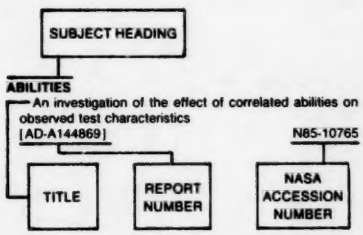

The subject heading is the key to the subject content of the document. Titles, report numbers, and accession numbers of pertinent documents are provided under each subject heading. When the title is insufficiently descriptive of the document content, a title extension has been added, separated from the title by three hyphens. The report number helps to indicate the type of document cited (e.g., NASA report, NASA translation, NASA contractor report). The NASA accession number is the number by which the document abstracts are arranged in this journal and by which the document is sold or requested. The titles, with title extensions if present, are arranged under each subject heading in ascending accession number order. The subject headings have been selected from the latest revision of the *NASA Thesaurus* (NASA SP-7051).

A

ABLATION
A study of the chemistry of alkali metals in the upper atmosphere
[AD-A156349] N85-35524

ABSORBENTS
Molecular and macromolecular sieving by asymmetric ultrafiltration membranes
[PB85-157766] N85-35266

ABSORPTION CROSS SECTIONS
Dissociative and double photoionization cross sections of NO from threshold to 120 A
[NASA-CR-176185] N85-35713

ABSORPTION SPECTRA
Dangling bonds and sub-gap optical absorption in silicon
[DE85-011752] N85-35302

ABSORPTIVITY
Underwater measurements of muon intensity
[HE-5.1-16] N85-36078

ABSTRACTS
Center for Electronics and Electrical Engineering technical progress bulletin covering center programs, July-September with 1985 CEEE events calendar
[PB85-191393] N85-35363

ACCELERATION (PHYSICS)
Matched filtering of visual evoked potentials to detect acceleration (+Gz) induced blackout
[AD-A155912] N85-35609

ACCELERATION STRESSES (PHYSIOLOGY)
The effect of +Gx acceleration on platelet activation as determined by plasma platelet factor 4 levels
[AD-A155881] N85-35608

ACCELERATION TOLERANCE
Matched filtering of visual evoked potentials to detect acceleration (+Gz) induced blackout
[AD-A155912] N85-35609

Simulation of high +Gz onset in the dynamic environment simulator
[AD-A155963] N85-35610

ACCESS CONTROL
Optimizing data access in the LAMPF control system
[DE85-012653] N85-35663

ACCIDENT PREVENTION
Transient three-phase three-component systems. Part 1: Formulation of the system of differential equations
[DE85-013267] N85-35384

ACCIDENT PRONENESS
Calculation of trajectories of detached wind turbine blades and prediction of site risk levels associated with failures of HAWT's N85-35475

ACCIDENTS
Computer code calculations of the TMI-2 accident: Initial and boundary conditions
[DE85-012613] N85-35666
Thermal hydraulic features of the TMI accident
[DE85-014569] N85-35747

ACCOUNTING
DOD Value Engineering Conference report. Value Engineering (VE): A tool that benefits line management held at Leesburg, Virginia on 1-2 November 1984. Part 1. Executive summary
[AD-A156067] N85-35810

ACCURACY
Determining an azimuth with a north seeking gyro
[AD-A155880] N85-35180
Accuracy and error analysis --- airborne instruments N85-35557

ACEE PROGRAM
Energy efficient engine, high pressure turbine thermal barrier coating. Support technology report
[NASA-CR-168037] N85-35199

ACETATES
Microbiological and biochemical studies towards optimization of substrate utilization by methanogenic bacteria
[PB85-188332] N85-35310

ACETYLENE
The photodissociation of acetylene at 193.3 NM
[AD-A155775] N85-35255

ACIDS
Origin of sedimentary humic acids, potential carriers of ore-forming elements N85-35443

ACOUSTIC EMISSION
Contribution to the properties of carbon fiber reinforced composites --- structural mechanics
[ESA-TT-849] N85-35246

ACOUSTIC MEASUREMENT
Search for acoustic signals from high energy cascades
[HE-7.1-1] N85-36155
Experimental investigation of radiative-acoustic effects in the water by the thermodynamical conditions of Dumand
[HE-7.1-2] N85-36156
Exploring results of the possibility on detecting cosmic ray particles by acoustic way
[HE-7.1-3] N85-36157
Acoustic detection of air shower cores
[HE-7.1-4] N85-36158

ACOUSTIC PROPERTIES
Acoustic scaling: The development of improved instrumentation
[BBC-RD-1985/7] N85-35694
Analysis of two-parameter constant background born inversion for acoustic synthetic data
[AD-A156394] N85-35698
Acoustic resonances in cylinder bundles oscillating in a compressible fluid
[DE85-004066] N85-35699

ACOUSTIC SCATTERING
Second Colloquim on the Scattering of Ultrasonic Waves
[AD-A156298] N85-35697

ACOUSTIC VELOCITY
Sound speed measurements in liquid oxygen-liquid nitrogen mixtures
[NASA-TP-2464] N85-35307

Experimental investigation of radiative-acoustic effects in the water by the thermodynamical conditions of Dumand
[HE-7.1-2] N85-36156

ACOUSTICS
Applications of the Kirchoff-Helmholtz integral to problems in body wave seismology N85-35515
Acoustic scaling: The development of improved instrumentation
[BBC-RD-1985/7] N85-35694

ACQUISITION
Second Colloquim on the Scattering of Ultrasonic Waves
[AD-A156298] N85-35697

ACTIVATION
The effect of +Gx acceleration on platelet activation as determined by plasma platelet factor 4 levels
[AD-A155881] N85-35608

ACTUATORS
Actuator rigging test set electromagnetic interference test (CE03)
[AD-A155819] N85-35327
Computer simulation of a cruise missile using brushless dc motor fin control
[AD-A155935] N85-35349

ADA (PROGRAMMING LANGUAGE)
Artificial intelligence in Ada (trademark): Pattern-directed processing
[AD-A156230] N85-35671

ADAPTIVE CONTROL
Recursive partitioning estimation N85-35670

ADSORPTION
Characterization of catalysts with metal-support effects and of the species adsorbed on their surfaces
[DE85-012254] N85-35394
Size and shape dependence of CO adsorption sites on sapphire supported Fe microcrystals
[NASA-CR-176171] N85-35794

AERIAL EXPLOSIONS
Study to assess the effects of magnetohydrodynamic electromagnetic pulse on electric power systems, phase 1, volume 3
[DE85-011301] N85-35771

AERODYNAMIC CONFIGURATIONS
Proceedings of the 14th Army Science Conference. Volume 2: Principal authors I through O
[AD-A149201] N85-35690

AERODYNAMIC DRAG
The influence of helicopter tail shape on drag: An aerodynamic study using a low speed wind tunnel
[AD-A156304] N85-35174

AERODYNAMIC HEAT TRANSFER
Mach 14 flow restrictor thermal stress analysis
[AD-A156215] N85-35208

AERODYNAMIC HEATING
SRB thermal protection systems materials test results in an arc-heated nitrogen environment
[NASA-CR-170881] N85-35236
Results of tests of weathered K5NA closeout material in the MSFC Hot Gas Facility
[NASA-CR-170893] N85-35239
Study of NSI and related cable performance during tests performed in the NASA Hot Gas Facility
[NASA-CR-170886] N85-35423

AERODYNAMIC NOISE
Optimally designed propellers constrained by noise N85-35196

AERODYNAMIC STABILITY
The physical and empirical basis for a specific clear-air turbulence risk index
[NASA-CR-178522] N85-35540

AERODYNAMICS
Aeronautical engineering: A continuing bibliography with indexes, supplement 190
[NASA-SP-7037(190)] N85-35152
Analysis of incompressible cascade flows using state-of-the-art computer programs
[AD-A155850] N85-35173

AEROELASTICITY
The application of bispectral analyses to aeroelastic phenomena N85-35157

Analysis of flexible aircraft longitudinal dynamics and handling qualities. Volume 1: Analysis methods
[NASA-CR-177943-VOL-1] N85-35202
Analysis of flexible aircraft longitudinal dynamics and handling qualities. Volume 2: Data
[NASA-CR-177943-VOL-2] N85-35203

AERONAUTICAL ENGINEERING
Aeronautical engineering: A continuing bibliography with indexes, supplement 190
[NASA-SP-7037(190)] N85-35152

AERONAUTICS
Aeronautical engineering: A continuing bibliography with indexes, supplement 190
[NASA-SP-7037(190)] N85-35152

AEROSOLS
System for the continuous generation of phosphorous aerosols from red phosphorus-butyl rubber
[DE85-013527] N85-35232
Experimental lithium system
[DE85-013252] N85-35382
Linear absorption and scattering of laser beams
[AD-A156167] N85-35401
Incorporating meteorological data into receptor analysis: RAPS (Regional Air Pollution Study) revisited
[PB85-188944] N85-35503
Literature search for new physical methods for biological aerosol detection
[AD-A155883] N85-35592
Calculation of the diffusion of light by aerosols: Description of the MIELOR software and results obtained
[REPT-80] N85-35638

AEROSPACE ENVIRONMENTS
Determination of characteristic values for fiber reinforced materials N85-35247

AEROSPACE INDUSTRY
Investment justification of robotic technology in aerospace manufacturing. User's manual
[AD-A156193] N85-35410

AEROSPACE MEDICINE
Proceedings of a Scientic Meeting on the Occasion of the Inauguration of New Buildings for the DFVLR Institute for Aerospace Medicine
[ESA-TT-857] N85-35595
The research programme of the Institute for Aerospace Medicine N85-35596
Simulation of high +Gz onset in the dynamic environment simulator
[AD-A155963] N85-35610

AEROSPACE SYSTEMS
Evaluation of nuclear detonation location capability under high attack scenario
[AD-A155761] N85-35729

AEROSPACE TECHNOLOGY TRANSFER
New technologies at the forefront of industrial developments N85-35168

AFTERBODIES
SRB TPS closeout materials characterization
[NASA-CR-170885] N85-35222
Study of NSI and related cable performance during tests performed in the NASA Hot Gas Facility
[NASA-CR-170886] N85-35423

AGING (MATERIALS)
Conduction and aging of piezoelectric PZT ceramics N85-35346
A kinetic model for predicting oxidative degradation rates in combined radiation-thermal environments
[TI85-002629] N85-35414

AGING (METALLURGY)
Effect of thermal ageing on the mechanical properties of PWR pressure vessel steels and weldments
[AERE-R-11460] N85-35275

AIR
Cerenkov radiation from periodic electron bunches for finite emission length in air
[AD-A156156] N85-35352
Proton-air and proton-proton cross sections from air shower data
[HE-1.1-1] N85-35849
Proton-air inelastic cross section at S(1/2) = 30 TeV
[HE-1.1-2] N85-35850

AIR CURRENTS
The physical and empirical basis for a specific clear-air turbulence risk index
[NASA-CR-178522] N85-35540

AIR FLOW
The influence of helicopter tail shape on drag: An aerodynamic study using a low speed wind tunnel
[AD-A156304] N85-35174
Experimental study of free and mixed convective flow of air in a heated cavity
[DE85-012538] N85-35380

AIR JETS
Jets in air-jet family
[HE-3.2-1] N85-35912

AIR LAND INTERACTIONS
An atmospheric boundary layer model forced by the operational ECMWV-model
[WSR-3] N85-35541

AIR POLLUTION
Basic research on pulse-combustion phenomena
[PB85-200228] N85-35265
Studies in photochemical smog chemistry. 1: Atmospheric chemistry of toulene. 2: Analysis of chemical reaction mechanisms for photochemical smog N85-35497
Incorporating meteorological data into receptor analysis: RAPS (Regional Air Pollution Study) revisited
[PB85-188944] N85-35503

AIR QUALITY
Review of US NOx abatement technology
[PB85-193522] N85-35501

AIR TO SURFACE MISSILES
Next generation gunship
[AD-A156361] N85-35193

AIR TRAFFIC
The contribution made by flight mechanics to civil aviation N85-35169

AIR TRAFFIC CONTROL
Introduction to European air traffic control
[AD-A156328] N85-35176
FAA requirements for model to support capacity, delay, noise and energy programs
[AD-A155815] N85-35179
Analogies of control mechanisms in flight guidance and medicine N85-35597

AIR TRAFFIC CONTROLLERS (PERSONNEL)
U.S. Civil airmen statistics for calendar year 1984
[AD-A156326] N85-35153

AIR TRANSPORTATION
The research programme of the Institute for Aerospace Medicine N85-35596

AIR WATER INTERACTIONS
Meteorological data from the OPTOMA (Ocean Prediction Through Observations, Modeling and Analysis) program OPTOMA 2, leg D2. 30 Jun. - 10 Jul. 1984
[AD-A156134] N85-35560
Mean cloudiness over the global tropics from satellite observations
[AD-A156188] N85-35561

AIRBORNE EQUIPMENT
The principles of wind measurement with the help of aircraft N85-35558

AIRBORNE/SPACEBORNE COMPUTERS
Development and operation of a measuring data acquisition system for use in light airplanes N85-35556

AIRCRAFT CONTROL
Energy management of three-dimensional minimum-time intercept
[NASA-CR-176174] N85-35186
Control variables in vertical wind determination using simple flight-mechanical equations N85-35546

AIRCRAFT DESIGN
A guide to USAF helicopter instrument flight procedures
[AD-A156102] N85-35182
Design and testing of an energy-absorbing crewseat for the F/FB-111 aircraft. Volume 2: Data from seat testing
[NASA-CR-3[illegible]7] N85-35184
Proceedings of the 14th Army Science Conference. Volume 2: Principal authors I through O
[AD-A149201] N85-35690
A research program to reduce the interior noise in general aviation aircraft, index and summary
[NASA-CR-176178] N85-35695

AIRCRAFT FUELS
Comparative analysis of operational forecasts versus actual weather conditions in airline flight planning, volume 1
[NASA-CR-167862] N85-35534
Comparative analysis of operational forecasts versus actual weather conditions in airline flight planning, volume 4
[NASA-CR-167865] N85-35537
Comparative analysis of operational forecasts versus actual weather conditions in airline flight planning: Summary report
[NASA-CR-167866] N85-35538

AIRCRAFT INDUSTRY
DOD Value Engineering Conference report. Value Engineering (VE): A tool that benefits line management held at Leesburg, Virginia on 1-2 November 1984. Part 2. Plenary session
[AD-A156068] N85-35811

AIRCRAFT LANDING
The integrated manual and automatic control of complex flight systems
[NASA-CR-176166] N85-35201

AIRCRAFT MANEUVERS
Control variables in vertical wind determination using simple flight-mechanical equations N85-35546

AIRCRAFT PERFORMANCE
Comparative analysis of operational forecasts versus actual weather conditions in airline flight planning, volume 1
[NASA-CR-167862] N85-35534

AIRCRAFT SAFETY
Investigation of experimental lightweight firewall materials for A/C engine bay applications
[AD-A155765] N85-35175

AIRCRAFT SPIN
Dual towline spin-recovery device
[NASA-CASE-LAR-13076-1] N85-35200

AIRCRAFT STRUCTURES
An automated technique for encasing specific payloads with low-drag fairings N85-35183
Fatigue lives of specimens representing critical locations in Mirage 3 spars under Australian and Swiss test spectra
[ARL-STRUC-R-415] N85-35187
Analysis of flexible aircraft longitudinal dynamics and handling qualities. Volume 1: Analysis methods
[NASA-CR-177943-VOL-1] N85-35202
Analysis of flexible aircraft longitudinal dynamics and handling qualities. Volume 2: Data
[NASA-CR-177943-VOL-2] N85-35203

AIRFOILS
A stream function approach to solving the conservative Euler equations for transonic flows N85-35156
Heat transfer characteristics for two-dimensional arrays of impinging jets with initial crossflow N85-35365

AIRSPACE
Introduction to European air traffic control
[AD-A156328] N85-35176

ALADIN 2 AIRCRAFT
Presentation of the acoustic and aerodynamic results of the Aladin 2 concept qualification testing
[NASA-TM-77883] N85-35161

ALANINE
Response of amino acids in hindlimb muscles to recovery from hypogravity and unloading by tail-cast suspension
[NASA-CR-176183] N85-35589
Response of rat hindlimb muscles to 12 hours recovery from tail-cast suspension
[NASA-CR-176182] N85-35590

ALASKA
Some geophysical guides to ore in southern and southwestern Alaska N85-35438

ALCOHOLS
Air university commander's and supervisor's guide on substance abuse
[AD-A156336] N85-35622

ALGEBRA
Stress analysis of axisymmetric sandwich shells of variable thickness N85-35419

ALGORITHMS
Energy management of three-dimensional minimum-time intercept
[NASA-CR-176174] N85-35186
Communication complexity of distributed shortest path algorithms
[AD-A156049] N85-35332
An evaluation of a class of practical optimization techniques for structural dynamics applications
[PB85-195766] N85-35434
Optimal estimation of a high degree gravity field from a global set of 1 deg x 1 deg anomalies to degree and order 250
[AD-A156008] N85-35519
Comparative analysis of operational forecasts versus actual weather conditions in airline flight planning, volume 2
[NASA-CR-167863] N85-35535
Reachable grasps on a polygon: The convex rope algorithm
[AD-A155913] N85-35647
L-step sequential decoding
[AD-A156121] N85-35649
Pruned error-trellis decoding of certain non-systematic convolutional codes
[AD-A156122] N85-35650
Three-dimensional finite deformation viscoelastic model accounting for damage effects
[DE85-012951] N85-35660
Recursive partitioning estimation N85-35670
Algorithmic approaches in sets of good answers in inverse problems
[PM/84/18] N85-35677
Smoothing surface data by spline functions
[AD-A155829] N85-35678

ALKALI METALS
A study of the chemistry of alkali metals in the upper atmosphere
[AD-A156349] N85-35524
ALLOCATIONS
Progress report on implementing the recommendations of the White House Science Council's Federal Laboratory Review Panel, volume 1
[PB85-185072] N85-35819
ALLOYS
Pitting corrosion of ferrous alloys
[AERE-R-11490] N85-35273
Fatigue damage detection in steels by optical correlation
[AD-A155830] N85-35277
X-ray fluorescence analysis of 304L stainless steel
[DE85-013254] N85-35288
ALPHA PARTICLES
Calculation of heavy-ion tracks in liquid water
[DE85-012101] N85-35725
Gamma-ray production cross sections for alpha-particle induced reactions on F-19 and Na-23
[DE85-012603] N85-35732
Some nuclear data needs in astrophysics
[DE85-012916] N85-35842
Determination of primary energy in nucleus-nucleus collisions and the high P(sub)T tail of alpha-particles N85-35875
ALTITUDE
Particle distributions in approximately 10(13) - 10(16) eV air shower cores at mountain altitude and comparison with Monte Carlo simulations
[HE-4.2-18] N85-35994
ALUMINUM
Elliptical X-ray analyzer spectrograph application to a laser-produced plasma
[DE85-013790] N85-35398
Few-particles generation channels in inelastic hadron-nuclear interactions at energy approximately equals 400 GeV
[HE-3.2-9] N85-35917
ALUMINUM ALLOYS
Fatigue lives of specimens representing critical locations in Mirage 3 spars under Australian and Swiss test spectra
[ARL-STRUC-R-415] N85-35187
Studies of the crystallization process of aluminum-silicon alloys using a high temperature microscope
[NASA-TM-77869] N85-35272
Development of a mathematical model for predicting the percentage fatigue life increase resulting from shot peened components
[AD-A155774] N85-35425
Prediction of plasticity characteristics for three-dimensional fracture specimens comparison with experiment
[AD-A156425] N85-35430
ALUMINUM COATINGS
Action of wear-inhibiting Al2O3-coatings when applied to hard metal cutting tools
[BLL-RISLEY-TR-5041-(9091.9F)] N85-35292
ALUMINUM OXIDES
Action of wear-inhibiting Al2O3-coatings when applied to hard metal cutting tools
[BLL-RISLEY-TR-5041-(9091.9F)] N85-35292
Noise in silver beta alumina ceramics
[AD-A156135] N85-35297
Size and shape dependence of CO adsorption sites on sapphire supported Fe microcrystals
[NASA-CR-176171] N85-35794
Noise in sodium beta alumina crystals
[AD-A156025] N85-35798
AMMUNITION
Laboratory vibration schedules
[AD-A155856] N85-35188
AMORPHOUS MATERIALS
Size and shape dependence of CO adsorption sites on sapphire supported Fe microcrystals
[NASA-CR-176171] N85-35794
AMPHIBIA
Report of Amphibian Development Group N85-35583
AMPLIFIERS
Solid state high power amplifier for driving the SLC injector klystron
[DE85-013063] N85-35356
AMPLITUDE MODULATION
A new description of combined trellis coding with asymmetric modulation
[NASA-CR-176197] N85-35323
AMPLITUDES
Applications of the Kirchoff-Helmholtz integral to problems in body wave seismology N85-35515
Average features of the muon component of EAS or = 10(17) eV
[HE-4.3-10] N85-36004
ANALOG CIRCUITS
Analog, still without fear
[AD-A155920] N85-35348
ANALOG TO DIGITAL CONVERTERS
Using an LSI-11/23 and RT-11 to digitize analog tapes
[DE85-012736] N85-35656
The structure of the shower disk observed at Mt. Norikura
[HE-4.7-1] N85-36052
Thickness of the particle swarm in cosmic ray air showers
[HE-4.7-14] N85-36064
Search for acoustic signals from high energy cascades
[HE-7.1-1] N85-36155
ANALOGIES
Analogies of control mechanisms in flight guidance and medicine N85-35597
ANALYSIS (MATHEMATICS)
Polylith: The early goals
[DE85-012534] N85-35658
ANALYTIC FUNCTIONS
Analysis of two-parameter constant background born inversion for acoustic synthetic data
[AD-A156394] N85-35698
ANECHOIC CHAMBERS
Acoustic detection of air shower cores
[HE-7.1-4] N85-36158
ANGLES (GEOMETRY)
Reachable grasps on a polygon: The convex rope algorithm
[AD-A155913] N85-35647
Geophysical searches for three-neutrino oscillations
[HE-5.3-9] N85-36103
ANGULAR DISTRIBUTION
Neutron production by Ne and Si ions on a thick Cu target at 670 MeV/A with application to radiation protection
[DE85-014526] N85-35746
1Single particle momentum and angular distributions in hadron-hadron collisions at ultrahigh energies
[HE-1.2-1] N85-35860
Angular distribution and multiplicity of backward hadrons in hFe interactions at 0.5-5.0 TeV energies (PION Experiment)
[HE-1.2-8] N85-35866
Anuglar distribution of shower particles produced in the collisions of 20-GeV/c and 300-GeV negative pions with emulsion nuclei N85-35868
Inclusive angular distribution of alpha and Li fragments produced in the Fe-C and Fe-Pb collisions at 1.88 GeV/u
[HE-1.4-11] N85-35898
Characteristics of anomalously high multiplicity cosmic ray interactions
[HE-3.3-1] N85-35920
Peculiarities of gamma-quanta distribution at 20 TeV energy
[HE-3.7-10] N85-35967
The thickness of the shower disc as observed in showers produced by primaries above 10 (19)eV
[HE-4.7-6] N85-36057
Thickness of the particle swarm in cosmic ray air showers
[HE-4.7-14] N85-36064
Measurement of neutrino oscillations in MACRO experiment
[HE-5.3-10] N85-36104
ANGULAR RESOLUTION
Preliminary results of the Cerenkov EAS flashes the Crimean Astrophysical Observatory
[HE-4.4-17] N85-36023
Thickness of the particle swarm in cosmic ray air showers
[HE-4.7-14] N85-36064
ANISOTROPY
A comparative analysis of gamma and hadron families at the superhigh energies recorded in experiment Pamir
[HE-3.7-1] N85-35960
Character of energy flow in air shower core N85-35985
An underground cosmic ray muon telescope for observation of cosmic ray anisotropy N85-36037
Underground measurements on secondary cosmic rays
[HE-5.4-1] N85-36116
ANNEALING
Decomposition of martensite in R6M5 and R6AM5 steels after direct immersion in liquid nitrogen
[BLL-M-36305] N85-35268
Advanced detectors and signal processing
[NASA-CR-176193] N85-35343
Size and shape dependence of CO adsorption sites on sapphire supported Fe microcrystals
[NASA-CR-176171] N85-35794
Laser and electron beam processing of semiconductors
[AD-A155914] N85-35796
ANNUAL VARIATIONS
Subseasonal variability in a two-level atmospheric general circulation model N85-35504
ANODES
Deposition of nickel-cobalt alloys by controlled-potential electrolysis
[PB85-198562] N85-35291
ANOMALIES
Search for anomalous C-jets in Chacaltaya emulsion chamber experiment
[HE-3.2-5] N85-35913
Anomalous correlation between hadron and electromagnetic particles in hadron and gamma-ray families
[HE-3.3-6] N85-35924
Anomalies in cosmic rays: New particles versus charm?
[HE-5.4-9] N85-36120
ANTENNA ARRAYS
A planar version of a 4.0 gigahertz reactively steered adaptive array
[AD-A156029] N85-35330
Signal space models for antenna arrays
[AD-A156063] N85-35335
Theory of mutual impedances and multiple reflections in an N-element array environment
[PB85-191419] N85-35364
ANTENNA DESIGN
Polarization diversity addition to the 10 centimeter Doppler weather radar
[AD-A156062] N85-35334
ANTENNA RADIATION PATTERNS
Characteristic modes for slots in a ground plane TE case
[AD-A155757] N85-35326
A planar version of a 4.0 gigahertz reactively steered adaptive array
[AD-A156029] N85-35330
Theory of mutual impedances and multiple reflections in an N-element array environment
[PB85-191419] N85-35364
ANTENNAS
Moment-method formulation of the cavity-probe aperture antenna
[DE85-013264] N85-35338
Center for Electronics and Electrical Engineering technical progress bulletin covering center programs, July-September with 1985 CEEE events calendar
[PB85-191393] N85-35363
ANTICLINES
Structural development of the west-central Grant Range, Nye County, Nevada N85-35508
ANTICYCLONES
Maintenance of blocking anticyclones in a general circulation model
[PB85-190866] N85-35567
ANTIGENS
Genetic and physiological control of protective antigen synthesis by bacillus anthracis
[AD-A156324] N85-35617
ANTIGRAVITY
Simulation of high +Gz onset in the dynamic environment simulator
[AD-A155963] N85-35610
ANTIMISSILE MISSILES
Arms control and The President's Strategic Defense Initiative
[AD-A156334] N85-35212
ANTINEUTRINOS
QCD analysis of neutrino charged current structure function F2 in deep inelastic scattering
[HE-5.3-23] N85-36114
ANTIPROTONS
Studies of relativistic heavy ion collisions
[DE85-014686] N85-35745
P(P bar)P elastic scattering and cosmic ray data
[HE-1.1-6] N85-35854
Some remarks about simulation of cosmic ray phenomena with use of nuclear interaction models based on the current SPS proton-antiproton data
[HE-1.2-6] N85-35864
A test of the Feynman scaling in the fragmentation region
[HE-1.2-9] N85-35867
APERTURES
Moment-method formulation of the cavity-probe aperture antenna
[DE85-013264] N85-35338
APPROACH CONTROL
The integrated manual and automatic control of complex flight systems
[NASA-CR-176166] N85-35201

APPROXIMATION
Finite analytic solutions of supersonic flows in two-dimensional non-symmetrical channels N85-35154
Prediction of turbulent internal recirculating flows with K-epsilon models N85-35366
Vibrations of free hollow circular cylindrical bodies N85-35418
An evaluation of a class of practical optimization techniques for structural dynamics applications [PB85-195766] N85-35434
A new theory for multistep discretizations of stiff ordinary differential equations: Stability with large step sizes [NASA-CR-177941] N85-35675
Model robust response surface designs: Scaling two-level factorials [AD-A156218] N85-35686
Applications and misapplications of the channel-capture formalism of direct neutron capture [DE85-013992] N85-35748
Optical receivers using rough reflectors [NASA-CR-176200] N85-35750
Study of the parameters affecting the collapse of a rotating protostellar cloud N85-35837

AQUICULTURE
Aquatic Invertebrate Development Working Group N85-35585

AQUIFERS
The geostatistical approach to the inverse problem in two-dimensional steady state groundwater modeling N85-35462
Hydrogeology of the lower Glen Rose Aquifer, south-central Texas N85-35466

ARCHITECTURE (COMPUTERS)
A methodology for the design of testable custom large-scale integrated circuits [AD-A156098] N85-35351
Design for MISP: A multiple instruction stream shared pipeline processor [AD-A156314] N85-35635
Distribution of computer functionality for accelerator control at the Brookhaven AGS [DE85-012520] N85-35669
Report on the SLC control system [DE85-013076] N85-35722

ARGON
Thermodynamics of the corrosion of chromium in molten carbonates [DE85-011407] N85-35282
Size and shape dependence of CO adsorption sites on sapphire supported Fe microcrystals [NASA-CR-176171] N85-35794

ARID LANDS
Remote sensing of hydrologic transport processes using spot simulation data [DE85-012412] N85-35467

ARMED FORCES (UNITED STATES)
U.S. Civil airmen statistics for calendar year 1984 [AD-A156326] N85-35153
Laboratory vibration schedules [AD-A155856] N85-35188
United States Army welding research and development topical and coordination meeting [AD-A155834] N85-35409
Solar pond technology for Navy applications [AD-A155877] N85-35488
Air university commander's and supervisor's guide on substance abuse [AD-A156336] N85-35622

ARRAYS
The ISAVF opto-mechanical test bed [NASA-TM-87505] N85-35206
Heat transfer characteristics for two-dimensional arrays of impinging jets with initial crossflow N85-35365
Measurement of shower electrons and muons using a small air shower array [HE-4.3-11] N85-36005

ARTIFICIAL INTELLIGENCE
Testbed for sensory control of intelligent machines [DE85-012355] N85-35412
Justified generalization: Acquiring procedures from examples [AD-A156408] N85-35626
Polylith: The early goals [DE85-012534] N85-35658
Artificial intelligence in Ada (trademark): Pattern-directed processing [AD-A156230] N85-35671

ASPARTATES
Response of rat hindlimb muscles to 12 hours recovery from tail-cast suspension [NASA-CR-176182] N85-35590

ASPECT RATIO
Generalized reduced fluid model with finite ion-gyroradius effects [DE85-013123] N85-35777

ASSEMBLY LANGUAGE
A quickly tested Pascal random number generator for microcomputers [AD-A156059] N85-35633

ASSESSMENTS
The role of regional subsurface geochemistry in resource assessment in the central United States N85-35440
Some recent deposit modeling efforts N85-35453

ASSIMILATION
Users guide for optimum interpolation method of global data assimilation [AD-A155929] N85-35648
Two methods of global data assimilation [AD-A155981] N85-35684

ASTEROIDS
The nature and origin of outer solar system asteroids from reflectance spectrophotometry N85-35838

ASTRO MISSIONS (STS)
The 1986 National Aeronautics and Space Administration authorization [GPO-47-635] N85-35829

ASTRONAUTS
The effect of +Gx acceleration on platelet activation as determined by plasma platelet factor 4 levels [AD-A155881] N85-35608

ASTRONOMICAL COORDINATES
Jets in air-jet family [HE-3.2-1] N85-35912

ASTRONOMICAL MAPS
Far-infrared observations of young clusters embedded in the R Coronae Austrinae and RHO Ophiuchi dark clouds [NASA-TM-86681] N85-35834

ASTRONOMICAL SPECTROSCOPY
Development of observational and instrumental techniques in hard X-ray and medium energy gamma-ray astronomy [NASA-CR-176172] N85-35841

ASTRONOMICAL TELESCOPES
High energy neutrino astronomy with MACRO [HE-5.3-12] N85-36106

ASTRONOMY
Neutrino astronomy and the atmospheric background [HE-5.3-17] N85-36111

ASTROPHYSICS
Pulsed-neutron-source models for the astrophysical s-process [DE85-012927] N85-35740
Development of observational and instrumental techniques in hard X-ray and medium energy gamma-ray astronomy [NASA-CR-176172] N85-35841
Some nuclear data needs in astrophysics [DE85-012916] N85-35842
The research program of the Liquid Scintillation Detector (LSD) in the Mont Blanc Laboratory [HE-5.3-6] N85-36100
A search for cosmic sources of high energy neutrinos with small underground detectors [HE-5.3-16] N85-36110
Monopole, astrophysics and cosmic ray observatory at Gran Sasso [HE-6.1-4] N85-36130

ASYMMETRY
A new description of combined trellis coding with asymmetric modulation [NASA-CR-176197] N85-35323

ASYMPTOTIC PROPERTIES
Error-correcting codes for computer memories N85-35636

ATLANTIC OCEAN
Marine phosphorite deposits model for exploration, with emphasis on deposits in the US Atlantic coastal plain N85-35439
Atlantic coast hindcast. Phase 2: Wave information, additional extremal estimates [AD-A156137] N85-35575

ATMOSPHERIC ATTENUATION
Linear absorption and scattering of laser beams [AD-A156167] N85-35401
Sensitivity of depth of maximum and absorption depth of EAS to hadron production mechanism N85-35982
EAS development curve at energy of 10(16) - 10(18) eV measured by optical Cerenkov light [HE-4.4-7] N85-36015

ATMOSPHERIC BOUNDARY LAYER
An atmospheric boundary layer model forced by the operational ECMWV-model [WSR-3] N85-35541
Measurements for the determination of the vertical structure of the convective boundary layer --- atmospheric boundary layer N85-35550
Partitioning of the vertical turbulent energy transport into positive and negative contributions --- meteorology N85-35551
Aircraft measurements during the Bonn Experiment (BONEX 1) --- meteorology N85-35552

ATMOSPHERIC CHEMISTRY
Elemental tracers of source regions of contaminants in precipitation [DE85-012858] N85-35499
Atmospheric nitrogen oxides: Their detection and chemistry [PB85-193910] N85-35502
Air chemistry measurements 2 [AD-A156041] N85-35520
A study of the chemistry of alkali metals in the upper atmosphere [AD-A156349] N85-35524
Time-dependent response of the climate to increasing atmospheric carbon dioxide N85-35532

ATMOSPHERIC CIRCULATION
Subseasonal variability in a two-level atmospheric general circulation model N85-35504
A strategy for calibrating atmospheric transport models [CSIRO-DAR-TP-9] N85-35518
The kinematic structure of cold frontal rainbands N85-35531
Case studies for flux measurements along a low-flying route to the south of Munich N85-35548
The determination of lee circulation during the foehn wind N85-35554
Maintenance of blocking anticyclones in a general circulation model [PB85-190866] N85-35567
Airborne Investigations of Mesoscale Convective Systems (AIMCS), 1984: Operational summary and data inventory [PB85-187904] N85-35571

ATMOSPHERIC DENSITY
Studies of the solar mesosphere explorer: Dynamics and horizon sensor performance. Part A: Spin axis precession and atmospheric drag. Part B: Clouds [NASA-CR-175308] N85-35213

ATMOSPHERIC EFFECTS
Determination of characteristic values for fiber reinforced materials N85-35247

ATMOSPHERIC ENERGY SOURCES
Comments on the measurements of multiple muon phenomena [HE-5.2-13] N85-36089

ATMOSPHERIC ENTRY
Results of tests of the SRB aft skirt heat shield curtain in the MSFC Hot Gas Facility [NASA-CR-170888] N85-35223

ATMOSPHERIC HEAT BUDGET
Partitioning of the vertical turbulent energy transport into positive and negative contributions --- meteorology N85-35551
Aircraft measurements during the Bonn Experiment (BONEX 1) --- meteorology N85-35552
Motor glider measurements during the Urban Atmosphere Energy Budget Experiment (EESA 1) N85-35553

ATMOSPHERIC LASERS
Linear absorption and scattering of laser beams [AD-A156167] N85-35401

ATMOSPHERIC MODELS
Millimeter-wave propagation in moist air: Model versus path data [AD-A156040] N85-35331
Application of a turbulent closure model to the parameterization of the vertical diffusion of heat, momentum, and humidity in the ECMWF model --- European Center for Medium Term Weather Forecasting (ECMWF) [MITT-41] N85-35387
Subseasonal variability in a two-level atmospheric general circulation model N85-35504
A strategy for calibrating atmospheric transport models [CSIRO-DAR-TP-9] N85-35518
Maintenance of blocking anticyclones in a general circulation model [PB85-190866] N85-35567

ATMOSPHERIC MOISTURE
Program for Regional Observing and Forecasting Services (PROFS) [PB85-188050] N85-35569

ATMOSPHERIC PHYSICS
Proceedings of Meteorological Motor Glider (MEMO) Workshop '84 [DFVLR-MITT-85-04] N85-35542
The measurement of nitrogen oxide (NO, NO2) exchange over plant/soil surfaces [CSIRO-DAR-TP-8] N85-35587

ATMOSPHERIC PRESSURE
Air chemistry measurements 2 [AD-A156041] N85-35520

Maintenance of blocking anticyclones in a general circulation model
[PB85-190866] N85-35567

ATMOSPHERIC RADIATION
Nucleon decay and atmospheric neutrinos in the Mont Blanc experiment
[HE-6.2-6] N85-36142

ATMOSPHERIC SCATTERING
Calculation of the diffusion of light by aerosols: Description of the MIELOR software and results obtained
[REPT-80] N85-35638
Atmospheric interactions detected in both the upper and the lower chambers at Chacaltaya
[HE-3.3-7] N85-35925

ATMOSPHERIC TEMPERATURE
Program for Regional Observing and Forecasting Services (PROFS)
[PB85-188050] N85-35569
Connection between variations of the atmosphere temperature profile and variations of the meson component intensity
[HE-3.1-12] N85-35910

ATMOSPHERIC TURBULENCE
Environmental-physical measurements and determination of atmospheric turbulence with the ASK-16 motor glider N85-35549

ATOMIC BEAMS
Cooling high intensity atomic hydrogen beams to liquid helium temperatures
[DE85-012515] N85-35718

ATOMIC COLLISIONS
Multiple vacancy production by high energy heavy ions
[DE85-004428] N85-35805

ATOMIC PHYSICS
The 2nd European Conference on Atomic and Molecular Physics
[AD-A155863] N85-35715

ATOMIC STRUCTURE
Standard value for the radiation length in air
[HE-4.4-4] N85-36013

ATOMS
High-resolution spectroscopy and dynamics of multiphoton processes in atoms and molecules
[AD-A155862] N85-35714
Exit channels of autoionization resonances in atoms
[DE85-012299] N85-35726

ATROPHY
Responses of skeletal muscle to unloading, a review
[NASA-CR-176177] N85-35594

ATTACKING (ASSAULTING)
Next generation gunship
[AD-A156361] N85-35193

ATTENUATION
Normal modes in an overmoded circular waveguide coated with lossy material
[NASA-CR-176186] N85-35320
Core structure of EAS in 10(15) to 10(17) eV N85-35989

ATTITUDE CONTROL
Computer simulation of a cruise missile using brushless dc motor fin control
[AD-A155935] N85-35349

ATTITUDE INDICATORS
Studies of the solar mesosphere explorer: Dynamics and horizon sensor performance. Part A: Spin axis precession and atmospheric drag. Part B: Clouds
[NASA-CR-175308] N85-35213

AUGER SPECTROSCOPY
Size and shape dependence of CO adsorption sites on sapphire supported Fe microcrystals
[NASA-CR-176171] N85-35794

AURORAL ARCS
Two-dimensional quasineutral description of particles and fields above discrete auroral arcs
[NASA-CR-176170] N85-35517

AURORAS
Two-dimensional quasineutral description of particles and fields above discrete auroral arcs
[NASA-CR-176170] N85-35517

AUSTENITE
Decomposition of martensite in R6M5 and R6AM5 steels after direct immersion in liquid nitrogen
[BLL-M-36305] N85-35268
Effect of prior warm rolling on the retained austenite content and hardening response of VIM-VAR (vacuum-induction melted-vacuum-arc remelted) AISI M-50 steel
[AD-A156145] N85-35281

AUSTENITIC STAINLESS STEELS
The use of austenitic stainless steel versus monel (Ni-cu) alloy in pressurized Gaseous Oxygen (GOX) life support systems
[AD-A156305] N85-35625

AUTOCLAVING
Chemoviscosity modeling for thermosetting resins, 2
[NASA-CR-177958] N85-35243

AUTOIONIZATION
Exit channels of autoionization resonances in atoms
[DE85-012299] N85-35726

AUTOMATA THEORY
TRICCS: A proposed teleoperator/robot integrated command and control system for space applications
[NASA-TM-87577] N85-35637

AUTOMATED GUIDEWAY TRANSIT VEHICLES
Network management simulation of automated guideway transit systems under vehicle-follower control
[PB85-188233] N85-35830

AUTOMATIC CONTROL
Space Missions for Automation and Robotics Technologies (SMART) Program
[NASA-TM-86820] N85-35210
Matched filtering of visual evoked potentials to detect acceleration (+Gz) induced blackout
[AD-A155912] N85-35609
Spreading the control complexity in decentralized control of interconnected systems
[BU-117] N85-35688

AUTOMATIC FLIGHT CONTROL
The integrated manual and automatic control of complex flight systems
[NASA-CR-176166] N85-35201
Analogies of control mechanisms in flight guidance and medicine N85-35597

AUTONOMOUS NAVIGATION
Visual position determination for autonomous vehicle navigation
[AD-A156007] N85-35181

AVAILABILITY
Solar pond technology for Navy applications
[AD-A155877] N85-35488

AXES OF ROTATION
Studies of the solar mesosphere explorer: Dynamics and horizon sensor performance. Part A: Spin axis precession and atmospheric drag. Part B: Clouds
[NASA-CR-175308] N85-35213

AXIAL FLOW
Wingtip vortex propeller
[NASA-CASE-LAR-13019-1] N85-35194

AXISYMMETRIC BODIES
Stress analysis of axisymmetric sandwich shells of variable thickness N85-35419

AXISYMMETRIC FLOW
Studies on effects of boundary conditions in confined turbulent flow predictions
[NASA-CR-3929] N85-35371

AZIMUTH
Jets in air-jet family
[HE-3.2-1] N85-35912
A comparative analysis of gamma and hadron families at the superhigh energies recorded in experiment Pamir
[HE-3.7-1] N85-35960

B

BACILLUS
Genetic and physiological control of protective antigen synthesis by bacillus anthracis
[AD-A156324] N85-35617

BACKGROUND RADIATION
The muon content of gamma-ray showers
[HE-4.5-7] N85-36031
The Nagoya cosmic-ray muon spectrometer 3, part 1: Preliminary observations
[HE-5.2-2] N85-36080

BACKSCATTERING
Quantitative non-destructive evaluation of composite materials based on ultrasonic wave propagation
[NASA-CR-176176] N85-35244

BACTERIA
Microbiological and biochemical studies towards optimization of substrate utilization by methanogenic bacteria
[PB85-188332] N85-35310

BAINITE
Development of a high strength isothermally heat-treated nodular iron road wheel arm
[AD-A155755] N85-35408

BALLOON SOUNDING
Environmental-physical measurements and determination of atmospheric turbulence with the ASK-16 motor glider N85-35549
Partitioning of the vertical turbulent energy transport into positive and negative contributions --- meteorology N85-35551
Aircraft measurements during the Bonn Experiment (BONEX 1) --- meteorology N85-35552

BALLOON-BORNE INSTRUMENTS
Some characteristic cosmic ray events and an attempt at their explanation
[HE-3.1-8] N85-35906

BALLOONS
Structure and properties of polyethylene films used in heavy lift balloons
[NASA-CR-176227] N85-35306

BANDWIDTH
Necessary bandwidth and spectral properties of digital modulation
[PB85-185387] N85-35340
Optical synthetic aperture techniques
[AD-A156151] N85-35752

BARIUM SULFIDES
Application of thermoluminescence for detection of cascade shower 1: Hardware and software of reader system
[HE-7.1-6] N85-36160
Spatial distribution read-out system for thermoluminescence sheets
[HE-7.1-7] N85-36161
Application of thermoluminescence for detection of cascade shower 2: Detection of cosmic ray cascade shower at Mount Fuji
[HE-7.1-12] N85-36162

BAROCLINIC WAVES
Subseasonal variability in a two-level atmospheric general circulation model N85-35504

BARYONS
On mini-cluster observed by Chacaltaya emulsion chamber experiment
[HE-3.6-12] N85-35959
An experiment to detect gut monopoles
[HE-6.1-7] N85-36133

BATCH PROCESSING
Optimize computer throughput using array processors
[AD-A155843] N85-35628

BAYES THEOREM
Model robust response surface designs: Scaling two-level factorials
[AD-A156218] N85-35686

BAYS (STRUCTURAL UNITS)
Investigation of experimental lightweight firewall materials for A/C engine bay applications
[AD-A155765] N85-35175

BEAM CURRENTS
ATA upgrade to 150 MeV
[DE85-013174] N85-35404
Robinson instability and beam loading
[DE85-013301] N85-35737
Beam intensity increases at the intense pulsed neutron source accelerator
[DE85-012377] N85-35764
High resolution beam profile monitors in the SLC
[DE85-013375] N85-35774
Recent advances in remote handling at LAMPF
[DE85-012725] N85-35775
Kinetic loss experiments on Mite
[DE85-012826] N85-35780
Numerical studies of high current beam compression in heavy ion fusion
[DE85-011874] N85-35783

BEAM INJECTION
Considerations on collective ion acceleration as an intense ion injector
[DE85-012706] N85-35757
Ion source development for the Los Alamos heavy ion fusion injector
[DE85-012682] N85-35766

BEAM INTERACTIONS
Report of working group on detectors for hadrons and event parameters at colliders N85-35705
A survey of multiplicities and rapidity densities from existing emission data on hadron-nucleus nucleus-nucleus collisions N85-35706

BEAM WAVEGUIDES
Beam potential measurement of an intense H(-) beam by use of the emissive probe technique
[DE85-012671] N85-35762
Beam intensity increases at the intense pulsed neutron source accelerator
[DE85-012377] N85-35764

BEAMS (RADIATION)
Width of nonlinear difference resonances
[DE85-013026] N85-35719
Use of a minimum-ellipse criterion in the study of ion-beam extraction systems
[DE85-012670] N85-35721
Time domain reflectometry for SLC BPM system
[DE85-012389] N85-35758
High resolution beam profile monitors in the SLC
[DE85-013375] N85-35774

BEAMS (SUPPORTS)
Design and behavior of coped beams N85-35417

User's guide: A computer program for strength analysis of non-hydraulic concrete structural elements. Report 1. Concrete General Strength Investigation (CGSI)
[AD-A156392] N85-35428
User's guide: A computer program for strength analysis of non-hydraulic concrete structural elements. Report 2. Strength design of reinforced concrete column sections (PCAUC)
[AD-A156393] N85-35429
Static and cyclic behavior of semi-rigid steel beam-column connections
[PB85-194363] N85-35433

BENDING
Stress-intensity factors for circumferential surface cracks in pipes and rods under tension and bending loads
[NASA-TM-87594] N85-35424
Major facility overhauls at LAMPF
[DE85-012724] N85-35765

BERYLLIUM
Beryllium production
[DE85-013360] N85-35716

BETA FACTOR
Confinement and heating of high beta plasmas with emphasis on compact toroids
[DE85-011459] N85-35761
Generalized reduced fluid model with finite ion-gyroradius effects
[DE85-013123] N85-35777

BETA PARTICLES
Pulsed-neutron-source models for the astrophysical s-process
[DE85-012927] N85-35740

BIBLIOGRAPHIES
Aeronautical engineering: A continuing bibliography with indexes, supplement 190
[NASA-SP-7037(190)] N85-35152
Technology for large space systems: A bibliography with indexes
[NASA-SP-7046(12)] N85-35209
Bibliography on tidal hydraulics. Report 2. Supplement 9: Supplementary material compiled from June 1980 - June 1983. Tidal flows in rivers and harbors
[AD-A155890] N85-35574
A research program to reduce the interior noise in general aviation aircraft, index and summary
[NASA-CR-176178] N85-35695
NASA patent abstracts bibliography, a continuing bibliography. Section 2: Indexes (supplement 27)
[NASA-SP-7039(27)-SECTION-2] N85-35820
Fire research publications, 1984
[PB85-206502] N85-35827

BIG BANG COSMOLOGY
Charge 4/3 leptons in cosmic rays
[HE-6.2-14] N85-36150

BINARY DATA
CRAYCDC
[NASA-CR-177374] N85-35639
CDCCRAY
[NASA-CR-177375] N85-35640

BIOASTRONAUTICS
Proceedings of a Scientic Meeting on the Occasion of the Inauguration of New Buildings for the DFVLR Institute for Aerospace Medicine
[ESA-TT-857] N85-35595
The research programme of the Institute for Aerospace Medicine N85-35596

BIOCHEMICAL OXYGEN DEMAND
The effect of an unphysiological oxygen supply on the organism N85-35605

BIOCHEMISTRY
Microbiological and biochemical studies towards optimization of substrate utilization by methanogenic bacteria
[PB85-188332] N85-35310

BIOCONVERSION
Microbiological and biochemical studies towards optimization of substrate utilization by methanogenic bacteria
[PB85-188332] N85-35310

BIODEGRADATION
Biodegradation of jet fuel by aquatic microbial communities
[PB85-191971] N85-35311

BIOLOGICAL EFFECTS
Electromagnetic compatibility conference features biological interactions
[AD-A155813] N85-35692

BIOLOGICAL EVOLUTION
NASA Developmental Biology Workshop: A summary
[NASA-TM-86756] N85-35578
Effects of microgravity and hypergravity on invertebrate development N85-35579
Vertebrate development in space: Gravity is a drag (and has been for eons and eons) N85-35580
Report of the NASA Mammalian Developmental Biology Working Group N85-35581
Report of the Avian Development Working Group N85-35582
Report of Amphibian Development Group N85-35583
Report of the Insect Development Group N85-35584
Aquatic Invertebrate Development Working Group N85-35585
Report of the Microbial Development Working Group N85-35586

BIOLOGICAL MODELS (MATHEMATICS)
Tritium hazard via the ingestion pathway
[DE85-012897] N85-35618

BIOLUMINESCENCE
Seasonal variability and spatial non-uniformity of bioluminescence in the Mediterranean Sea
[DRIC-T-7545] N85-35572
Background light measurements at the DUMAND site
[HE-5.2-7] N85-36084
Measurements of light background at large depth in the ocean
[HE-5.2-8] N85-36085

BIONICS
Tritium hazard via the ingestion pathway
[DE85-012897] N85-35618

BIOSYNTHESIS
Genetic and physiological control of protective antigen synthesis by bacillus anthracis
[AD-A156324] N85-35617

BIPOLARITY
Acoustic detection of air shower cores
[HE-7.1-4] N85-36158

BIRDS
Report of the Avian Development Working Group N85-35582

BIT ERROR RATE
Necessary bandwidth and spectral properties of digital modulation
[PB85-185387] N85-35340

BLACK BODY RADIATION
Self-study manual on optical radiation measurements. Part 1: Concepts. Chapter 12: Blackbodies, blackbody radiation, and temperature scales
[PB85-195303] N85-35754

BLACK HOLES (ASTRONOMY)
High energy cosmic ray signature of quark nuggets
[HE-6.2-11] N85-36147

BLACKOUT (PHYSIOLOGY)
Matched filtering of visual evoked potentials to detect acceleration (+Gz) induced blackout
[AD-A155912] N85-35609
Simulation of high +Gz onset in the dynamic environment simulator
[AD-A155963] N85-35610

BLADE TIPS
Optimally designed propellers constrained by noise N85-35196

BLAST DEFLECTORS
Results of tests of MTA-2 TPS on the SRB hold-down bolt blast container
[NASA-CR-170891] N85-35224

BLAST LOADS
Development of an NBS (National Bureau of Standards) polymer gage for dynamic soil stress measurement
[PB85-208494] N85-35526

BLOCKING
Maintenance of blocking anticyclones in a general circulation model
[PB85-190866] N85-35567

BLOOD
The effect of +Gx acceleration on platelet activation as determined by plasma platelet factor 4 levels
[AD-A155881] N85-35608

BLOOD VOLUME
Thirst and fluid intake following graded hypohydration levels in humans
[AD-A156201] N85-35615

BODY TEMPERATURE
Weight loss, rectal temperature and heart rates following the 1984 Boston Marathon
[AD-A155984] N85-35612

BODY VOLUME (BIOLOGY)
An analysis of aerobic capacity in a large United States population
[AD-A156200] N85-35614

BODY WEIGHT
Weight loss, rectal temperature and heart rates following the 1984 Boston Marathon
[AD-A155984] N85-35612
Thirst and fluid intake following graded hypohydration levels in humans
[AD-A156201] N85-35615

BOEING 737 AIRCRAFT
A preliminary evaluation of a failure detection filter for detecting and identifying control element failures in a transport aircraft
[NASA-TM-87576] N85-35204

BOILERS
Computer code calculations of the TMI-2 accident: Initial and boundary conditions
[DE85-012613] N85-35666

BOILING WATER REACTORS
Response of a BWR Mark 2 containment vessel head to loads beyond the design basis
[DE85-010524] N85-35432

BOLTS
Results of tests of MTA-2 TPS on the SRB hold-down bolt blast container
[NASA-CR-170891] N85-35224

BONDING
Dynamic compaction of a monosized spherical tungsten powder
[DE85-014808] N85-35289
Ionic crystals
[DE85-009482] N85-35809

BONES
Report of the NASA Mammalian Developmental Biology Working Group N85-35581

BOOLEAN FUNCTIONS
EPALIT: A data management system applied to the control and retrieval of technical reports
[PB85-193068] N85-35828

BOOSTER ROCKET ENGINES
Verification of the SRB motor case pin retainer band tips
[NASA-CR-170882] N85-35220
Results of tests of MTA-2 TPS on the SRB hold-down bolt blast container
[NASA-CR-170891] N85-35224
Evaluation of SRB phenolic TPS material made by an alternate vendor
[NASA-CR-170894] N85-35240
Space shuttle SRB TPS protective paint test and evaluation in NASA Hot Gas Facility and AEDC Tunnel C
[NASA-CR-170884] N85-35294
Results of tests of Insta-Foam Thermal Protection System (TPS) material for protection of equipment inside the SRB aft skirt
[NASA-CR-170892] N85-35295

BORON CARBIDES
Elliptical X-ray analyzer spectrograph application to a laser-produced plasma
[DE85-013790] N85-35398

BOSONS
Charge 4/3 leptons in cosmic rays
[HE-6.2-14] N85-36150

BOUNDARIES
Absorbing boundary conditions for exterior problems
[NASA-CR-177944] N85-35676

BOUNDARY LAYER FLOW
Adverse pressure gradient and separating turbulent boundary-layer flows: The effect of disequilibrium in initial conditions N85-35155
Studies on effects of boundary conditions in confined turbulent flow predictions
[NASA-CR-3929] N85-35371

BOUNDARY LAYER SEPARATION
Computation of three-dimensional shock wave and boundary-layer interactions
[NASA-TM-86780] N85-35372

BOUNDARY LAYERS
Unsteady flow in a supersonic cascade with two in-passage shocks
[NASA-CR-3925] N85-35158

BOUNDARY VALUE PROBLEMS
A new method for boundary value problems
[AD-A155934] N85-35683
Some rigorous results concerning spectral theory for ideal MHD
[DE85-013427] N85-35770

BOUSSINESQ APPROXIMATION
Two-point closure study of covariance budgets for turbulent Rayleigh-Benard convection
[PB85-189108] N85-35568

BRANCHING (PHYSICS)
Status of the zeta(8.3)
[DE85-013070] N85-35724

BREADBOARD MODELS
Noiseless coding for the Gamma Ray spectrometer
[NASA-CR-176201] N85-35219

BREAKING
The investigation of tethered satellite system dynamics
[NASA-CR-176180] N85-35215

BREATHING APPARATUS
Improved oxygen sources for breathing apparatus
[NASA-TM-86671] N85-35623

The use of austenitic stainless steel versus monel (Ni-cu) alloy in pressurized Gaseous Oxygen (GOX) life support systems
[AD-A156305] N85-35625

BREMSSTRAHLUNG
LPM effect and primary energy estimations
[HE-3.6-4] N85-35953
Result of Monte-Carlo simulation of electron-photon cascades in lead and layers of lead-scintillator
[HE-3.6-11] N85-35958

BRIGHTNESS DISTRIBUTION
Longitudinal trial functions and the cosmic ray energy scale N85-36014
Muon spectrum in air showers initiated by gamma rays
[HE-4.5-4] N85-36028

BRINES
Chemistry of ore-forming fluids N85-35436
Heat transfer and brine evolution in magma-hydrothermal systems N85-35441

BROADBAND
Cylindrical lens-array antenna for wideband electronic scanning
[AD-A156085] N85-35350
Scale separation closure and Alfven wave turbulence
[DE85-013124] N85-35385

BROWNIAN MOVEMENTS
Large deviations for the maxima of some random fields
[AD-A155909] N85-35681

BUBBLE CHAMBERS
Multidimensional analysis of data obtained in experiments with X-ray emulsion chambers and extensive air showers
[HE-3.6-2] N85-35951
Experimental basis for the models of cascade propagation in atmosphere
[HE-3.6-6] N85-35954
A comparative analysis of gamma and hadron families at the superhigh energies recorded in experiment Pamir
[HE-3.7-1] N85-35960
Hadrons registration in emulsion chamber with carbon block
[HE-3.7-3] N85-35962
New analysis of nuclear interaction observed by Mt. Kanbara emulsion chamber experiment
[HE-3.7-4] N85-35963
Intensities of high-energy cosmic rays at Mount Kanbala
[HE-3.7-5] N85-35964
Structured events in Pamir carbon X-ray chambers
[HE-3.7-7] N85-35965
Ultra high energy events in ECHOS series and primary energy spectrum
[HE-3.7-9] N85-35966
Search for anomalons using plastic nuclear track detectors
[HE-6.2-12] N85-36148

BUBBLE MEMORY DEVICES
Advanced detectors and signal processing
[NASA-CR-176193] N85-35343

BUBBLES
SU(2) x U(1) vacuum and the Centauro events N85-35885
Exploring results of the possibility on detecting cosmic ray particles by acoustic way
[HE-7.1-3] N85-36157

BUCKLING
Structural analysis of imperfect three-legged truss columns for large space structures applications N85-35416
Design and behavior of coped beams N85-35417

BUDGETING
The 1986 National Aeronautics and Space Administration authorization
[GPO-47-635] N85-35829

BUFFER STORAGE
Investigation of cosmic rays in very short time scales
[HE-4.6-7] N85-36044

BUNCHING
Synchronous timing of multi-energy fast beam extraction during a single AGS cycle
[DE85-011829] N85-35781

BUNDLES
Study of hadron bundles observed in Chacaltaya two-story emulsion chamber
[HE-3.3-4] N85-35922

BURSTS
DMSK: A practical 2400-bps receiver for the mobile satellite service: An MSAT-X Report
[NASA-CR-176194] N85-35324

BUS CONDUCTORS
Design of a microprogram control unit with concurrent error detection
[AD-A156447] N85-35655

BUTANES
Production of butanol by fermentation in the presence of cocultures of clostridium
[NASA-CASE-NPO-16203-1] N85-35227

BUTYRIC ACID
Production of butanol by fermentation in the presence of cocultures of clostridium
[NASA-CASE-NPO-16203-1] N85-35227

BYPASS RATIO
Energy Efficient Engine Program technology benefit/cost study, volume 1
[NASA-CR-174766-VOL-1] N85-35197
Energy Efficient Engine Program technology benefit/cost study, volume 2
[NASA-CR-174766-VOL-2] N85-35198

C

CABLES
Enhanced heat transfer computations for internally cooled cable superconductor
[DE85-011897] N85-35383

CABLES (ROPES)
Study of NSI and related cable performance during tests performed in the NASA Hot Gas Facility
[NASA-CR-170886] N85-35423

CADMIUM SULFIDES
Vectorial electron transfer on designed surfaces
[PB85-204600] N85-35263

CADMIUM TELLURIDES
HgCdTe surface and defect study program
[AD-A156079] N85-35799
Electron irradiation of N type cadmium telluride
[AD-A156117] N85-35801

CALCIUM OXIDES
Improved oxygen sources for breathing apparatus
[NASA-TM-86671] N85-35623

CALCULATORS
Development of NATOPS performance software for the SH-3D and SH-3H helicopters
[AD-A156140] N85-35192

CALCULUS OF VARIATIONS
Edge detection and geometric methods in computer vision
[AD-A155873] N85-35630

CALIBRATING
Calibrator for displacement gages used in the rock mechanics laboratory
[DE85-013257] N85-35393
Calibration of a high-level photon irradiation
[DE85-013044] N85-35738

CALIFORNIA
Simulated effects of increased recharge on the ground-water flow system of Yucca Mountain and vicinity, Nevada-California
[DE85-012985] N85-35469
Geology: Structural history and fluvial geomorphology of the southern Death Valley Fault Zone, Inyo and San Bernardino Counties, California N85-35506
Carbon fiber strainmeter studies in southern California
[PB85-196889] N85-35528
Sea surface and remotely sensed temperatures off Cape Mendocino, California
[NASA-TM-86712] N85-35573

CALORIMETERS
A lead glass tubing drift calorimeter N85-35711
X-ray film chamber with carbon target of Tien-Shan complex array N85-35915
Peculiarities of gamma-quanta distribution at 20 TeV energy
[HE-3.7-10] N85-35967
Study of muons near shower cores at sea level using the E594 neutrino detector N85-36000
Measurement of energy muons in EAS at energy region larger thean 10(17) eV
[HE-4.3-8] N85-36002
Magnetic monopole search by 130 m(2)sr He gas proportional counter
[HE-6.1-2] N85-36128
Results of a search for monopoles and tachyons in horizontal cosmic ray flux
[HE-6.1-3] N85-36129
Search for proton decay in the Frejus experiment
[HE-6.2-2] N85-36138
Results on nucleon life-time from the Kolar gold field experiment
[HE-6.2-3] N85-36139
Data acquisition system for phase-2 KGF proton decay experiment
[HE-6.2-4] N85-36140
Construction of the Soudan 2 detector
[HE-6.2-5] N85-36141
Tien-Shan effect and charmed particles
[HE-6.2-17] N85-36153
Search for acoustic signals from high energy cascades
[HE-7.1-1] N85-36155
Spatial distribution read-out system for thermoluminescence sheets
[HE-7.1-7] N85-36161
Application of thermoluminescence for detection of cascade shower 2: Detection of cosmic ray cascade shower at Mount Fuji
[HE-7.1-12] N85-36162

CAMERAS
Parametric stability of analytical close-range photogrammetry N85-35461
Application of thermoluminescence for detection of cascade shower 1: Hardware and software of reader system
[HE-7.1-6] N85-36160
Application of thermoluminescence for detection of cascade shower 2: Detection of cosmic ray cascade shower at Mount Fuji
[HE-7.1-12] N85-36162

CANARD CONFIGURATIONS
Vortex boundary-layer interactions
[NASA-CR-176192] N85-35373

CANTILEVER BEAMS
The application of bispectral analyses to aeroelastic phenomena N85-35157

CAPACITORS
Tuning system for capacitively loaded 1/4 accelerating cavity
[DE85-012516] N85-35358

CARBOHYDRATE METABOLISM
Possible mechanism for changes in glycogen metabolism in unloaded soleus muscle
[NASA-CR-176184] N85-35588
Muscle protein and glycogen responses to recovery from hypogravity and unloading by tail-cast suspension
[NASA-CR-176181] N85-35591

CARBON
Pressure measurements in a hydrogen combustion environment: Hydrogen-air combustion test series 1 and 2 in the FITS tank, volume 1
[TI85-009899] N85-35259
Development and characterization of carbon-bonded carbon fiber insulation for radioisotope space power systems
[DE85-013365] N85-35299
Excessive production of electron pairs by soft photons in low multiplicity ion interactions
[HE-1.4-6] N85-35894
The effect of the relative nuclear size on the nucleus-nucleus interactions
[HE-1.4-13] N85-35900
Japan - USSR joint emulsion chamber experiment at Pamir
[HE-3.1-1] N85-35901
Hadron intensity and energy spectrum at 4380 m above level
[HE-3.1-7] N85-35905
Scaling violation in fragmentation region at energies above 10-15 eV based on the data on cosmic ray hadron component
[HE-3.1-11] N85-35909
Hadrons registration in emulsion chamber with carbon block
[HE-3.7-3] N85-35962
Structured events in Pamir carbon X-ray chambers
[HE-3.7-7] N85-35965

CARBON CYCLE
Carbon dioxide and climate: A working glossary
[DE85-013535] N85-35562

CARBON DIOXIDE
Thermodynamics of the corrosion of chromium in molten carbonates
[DE85-011407] N85-35282
Microbiological and biochemical studies towards optimization of substrate utilization by methanogenic bacteria
[PB85-188332] N85-35310
Time-dependent response of the climate to increasing atmospheric carbon dioxide N85-35532
Carbon dioxide and climate: A working glossary
[DE85-013535] N85-35562
Far-infrared emission lines of CO and OH in the Orion-KL molecular shock
[NASA-TM-86721] N85-35832

CARBON DIOXIDE CONCENTRATION
Current inventory of anthropogenic carbon dioxide in the North Pacific Subarctic Gyre
[PB85-187938] N85-35570

CARBON FIBER REINFORCED PLASTICS
Ultrasonic inspection of carbon fiber reinforced plastic by means of sample-recognition methods
[NASA-TM-77806] N85-35245

Contribution to the properties of carbon fiber reinforced composites — structural mechanics
[ESA-TT-849] N85-35246
Methods for nondestructive tests of CFRP laminates N85-35248
Damage mechanisms in damaged CFRP laminates N85-35249

CARBON FIBERS
Crystallization of Polyetheretherketone (PEEK) in carbon fiber composites
[AD-A156316] N85-35252
Carbon fiber strainmeter studies in southern California
[PB85-196889] N85-35528

CARBON MONOXIDE
CO + H2 reaction over nitrogn-modified iron catalysts
[DE85-013791] N85-35231
Characterization of catalysts with metal-support effects and of the species adsorbed on their surfaces
[DE85-012254] N85-35394
Size and shape dependence of CO adsorption sites on sapphire supported Fe microcrystals
[NASA-CR-176171] N85-35794

CARBON STEELS
Effect of microstructure on the fatigue behavior of Fe-C-X alloys
[DE85-011749] N85-35285

CARBON-CARBON COMPOSITES
Oxidation resistant slurry coating for carbon-based materials
[NASA-CASE-LEW-13923-1] N85-35267

CARBONACEOUS MATERIALS
Fluidized bed desulfurization
[NASA-CASE-NPO-15924-1] N85-35253

CARBONATES
Thermodynamics of the corrosion of chromium in molten carbonates
[DE85-011407] N85-35282

CARDIOVASCULAR SYSTEM
Cardiovascular responses to orthostatism and weightlessness N85-35601

CARGO
Laboratory vibration schedules
[AD-A155856] N85-35188

CASCADE FLOW
Unsteady flow in a supersonic cascade with two in-passage shocks
[NASA-CR-3925] N85-35158
Analysis of incompressible cascade flows using state-of-the-art computer programs
[AD-A155850] N85-35173
Experimental basis for the models of cascade propagation in atmosphere
[HE-3.6-6] N85-35954
A comparative analysis of gamma and hadron families at the superhigh energies recorded in experiment Pamir
[HE-3.7-1] N85-35960
Hadrons registration in emulsion chamber with carbon block
[HE-3.7-3] N85-35962
Structured events in Pamir carbon X-ray chambers
[HE-3.7-7] N85-35965
Peculiarities of gamma-quanta distribution at 20 TeV energy
[HE-3.7-10] N85-35967

CASE BONDED PROPELLANTS
Dissected motors-propellants motor number STM-012. Phase 15: Surveillance report, stage 1
[AD-A156088] N85-35226

CASTING
Characterization of modified 9 r-1 Mo steel sand castings
[DE85-012057] N85-35287
Development of a high strength isothermally heat-treated nodular iron road wheel arm
[AD-A155755] N85-35408

CATALYSIS
Chemistry division report
[DE85-010586] N85-35228
Vectorial electron transfer on designed surfaces
[PB85-204600] N85-35263
Review of US NOx abatement technology
[PB85-193522] N85-35501

CATALYSTS
FTIR studies of hydrocarbon synthesis on Pd/ZSM5 catalysts
[DE85-012430] N85-35230
CO + H2 reaction over nitrogn-modified iron catalysts
[DE85-013791] N85-35231

CATHODES
Injector losses on Mite
[DE85-012356] N85-35355
Considerations on collective ion acceleration as an intense ion injector
[DE85-012706] N85-35757

CATIONS
Effect of temperature and ionic impurities at very low concentrations on stress corrosion cracking of Type 304 stainless steel
[TI85-003048] N85-35283

CAVITIES
Moment-method formulation of the cavity-probe aperture antenna
[DE85-013264] N85-35338
Experimental study of free and mixed convective flow of air in a heated cavity
[DE85-012538] N85-35380

CAVITY RESONATORS
Tuning system for capacitively loaded 1/4 accelerating cavity
[DE85-012516] N85-35358

CELESTIAL BODIES
Results of low energy background measurements with the Liquid Scintillation Detector (LSD) of the Mont Blanc Laboratory
[HE-5.3-5] N85-36099

CELLS (BIOLOGY)
Report of Amphibian Development Group N85-35583
Are living cells generally sensitive to gravity? N85-35602

CELLULOSE NITRATE
Oxidation resistant slurry coating for carbon-based materials
[NASA-CASE-LEW-13923-1] N85-35267

CENTRAL PROCESSING UNITS
Optimize computer throughput using array processors
[AD-A155843] N85-35628

CENTRIFUGES
Matched filtering of visual evoked potentials to detect acceleration (+Gz) induced blackout
[AD-A155912] N85-35609
Simulation of high +Gz onset in the dynamic environment simulator
[AD-A155963] N85-35610

CENTRIFUGING
Measurement of uranium enrichment for gaseous uranium at low pressure
[DE85-012697] N85-35733

CERAMICS
Method for measuring surface activity of silicon nitride powder
[NASA-TM-77906] N85-35242
Noise in silver beta alumina ceramics
[AD-A156135] N85-35297
Method of preparing thin porous sheets of ceramic material
[DE85-006399] N85-35300
High temperature corrosion of ceramics
[DE85-013481] N85-35303
Noise in sodium beta aiumina crystals
[AD-A156025] N85-35798

CERENKOV COUNTERS
The response of a scintillation counter below an emulsion chamber to heavy nucleus interactions in the chamber N85-35889
Study of the energy spectrum of primary cosmic rays: EAS size fluctuations at a fixed primary energy
[HE-4.4-14] N85-36020
The experimental cascade curves of EAS at E sub 0 10(17) eV obtained by the method of detection of Cherenkov pulse shape
[HE-4.4-18] N85-36024

CERENKOV RADIATION
Cerenkov radiation from periodic electron bunches for finite emission length in air
[AD-A156156] N85-35352
Simulation of EAS properties on the basis of high energy interaction model deduced from the accelerator data N85-35973
Sensitivity of depth of maximum and absorption depth of EAS to hadron production mechanism N85-35982
Muon fluctuation studies of EAS 10(17) eV
[HE-4.3-9] N85-36003
EAS development curve at energy of 10(16) - 10(18) eV measured by optical Cerenkov light
[HE-4.4-7] N85-36015
On the determination of the depth of EAS development maximum using the lateral distribution of Cerenkov light at distances 150 m from EAS axis
[HE-4.4-13] N85-36019
Study of the shower maximum depth by the method of detection of the EAS Cerenkov light pulse shape
[HE-4.4-15] N85-36021
Analysis of Cerenkov pulses recorded simultaneously at two sites
[HE-4.4-16] N85-36022
Preliminary results of the Cerenkov EAS flashes the Crimean Astrophysical Observatory
[HE-4.4-17] N85-36023
Lateral-angular and temporal characteristics of EAS optical radiation
[HE-4.4-19] N85-36025
The hump in the Cerenkov lateral distribution of gamma ray showers
[HE-4.5-9] N85-36032
A new study on the emission of EM waves from large EAS
[HE-4.6-5] N85-36042
Radio wave emitted by an extensive air showers in 10KHz to 1MHz region
[HE-4.6-15] N85-36051
Longitudinal development of muons in large air showers studies from the arrival time distributions measured at 900m above sea level
[HE-4.7-4] N85-36055
The thickness of the shower disc as observed in showers produced by primaries above 10 (19)eV
[HE-4.7-6] N85-36057
Measurements of light background at large depth in the ocean
[HE-5.2-8] N85-36085
Measurement of muon intensity by Cerenkov method
[HE-5.2-15] N85-36091
A transient digitiser for fast air shower events
[HE-5.2-21] N85-36097

CESIUM
Infrared generation and wave-mixing studies in cesium
[DE85-012883] N85-35304

CHANNEL FLOW
Finite analytic solutions of supersonic flows in two-dimensional non-symmetrical channels N85-35154

CHANNELS (DATA TRANSMISSION)
Operations considerations in designing a high speed multi-channel data acquisition system
[DE85-012840] N85-35756

CHARGE COUPLED DEVICES
The nature and origin of outer solar system asteroids from reflectance spectrophotometry N85-35838
Application of thermoluminescence for detection of cascade shower 1: Hardware and software of reader system
[HE-7.1-6] N85-36160
Spatial distribution read-out system for thermoluminescence sheets
[HE-7.1-7] N85-36161
Application of thermoluminescence for detection of cascade shower 2: Detection of cosmic ray cascade shower at Mount Fuji
[HE-7.1-12] N85-36162

CHARGE DISTRIBUTION
Lateral distribution on charged particles in EAS
[HE-4.3-15] N85-36009
Lateral distribution of high energy muons in EAS of sizes Ne approximately equals 10(5) and Ne approximately equals 10(6)
[HE-4.3-16] N85-36010
Properties of 10 (18)-10 (19)eV EAS at far core distance
[HE-4.7-3] N85-36054

CHARGE EFFICIENCY
Two-dimensional inversion of resistivity monitoring data from the Cerro Prieto geothermal field
[DE85-012554] N85-35494

CHARGE EXCHANGE
Noble metals as incipient transition metals
[DE85-013283] N85-35286
Is the inelastic charge-exchange contribution constant at the large X and superhigh energies? Qaut 01Kuchin, I. A. N85-35871
A study of gamma-families generated in nucleon-nucleus (NA) and pion-nucleus (pi A) interactions
[HE-3.7-2] N85-35961

CHARGED PARTICLES
The effect of the relative nuclear size on the nucleus-nucleus interactions
[HE-1.4-13] N85-35900
Experimental basis for the models of cascade propagation in atmosphere
[HE-3.6-6] N85-35954
The lateral distributions of charged particles of energy greater than 0.3 E sub crit in electron-photon cascades in lead and air
[HE-3.6-10] N85-35957
A study of gamma-families generated in nucleon-nucleus (NA) and pion-nucleus (pi A) interactions
[HE-3.7-2] N85-35961
Lateral distribution on charged particles in EAS
[HE-4.3-15] N85-36009
Muon spectrum in air showers initiated by gamma rays
[HE-4.5-4] N85-36028
High energy cosmic ray signature of quark nuggets
[HE-6.2-11] N85-36147

Experimental investigation of radiative-acoustic effects in the water by the thermodynamical conditions of Dumand
[HE-7.1-2] N85-36156

CHARM (PARTICLE PHYSICS)
Anomalies in cosmic rays: New particles versus charm?
[HE-5.4-9] N85-36120
Collimated groups of particles as possible manifestation of heavy meson production
[HE-5.4-14] N85-36124
Tien-Shan effect and charmed particles
[HE-6.2-17] N85-36153

CHECKOUT
International flight planning handbook
[AD-A156330] N85-35177

CHEMICAL ANALYSIS
Aspects of high-resolution gas chromatography as applied to the analysis of hydrocarbon fuels and other complex organic mixtures. Volume 1
[AD-A156154] N85-35257
Experimental technique for measuring the isentrope of hydrogen to several megabars
[DE85-014332] N85-35386
Measurement control for plutonium isotopic measurements using gamma-ray spectrometry
[DE85-013394] N85-35397

CHEMICAL BONDS
The photodissociation of acetylene at 193.3 NM
[AD-A155775] N85-35255
Dangling bonds and sub-gap optical absorption in silicon
[DE85-011752] N85-35302

CHEMICAL COMPOSITION
Ion composition measurements of the disturbed and quiet D-region in 1980 - 1981
[AD-A156055] N85-35521
Energy spectra of proton and nuclei of primary cosmic rays in energy region 10 TeV/particle
[HE-3.1-10] N85-35908
A comparative analysis of gamma and hadron families at the superhigh energies recorded in experiment Pamir
[HE-3.7-1] N85-35960
Correlation of high energy muons with primary composition in extensive air shower
[HE-4.3-7] N85-36001
A large area cosmic muon detector located at Ohya stone mine
[HE-5.1-7] N85-36072
On muon energy spectrum in muon groups underground
[HE-5.1-14] N85-36076
Multiple muons in MACRO
[HE-5.2-1] N85-36079

CHEMICAL EQUILIBRIUM
Aqueous volatile weak electrolyte equilibria to 300 C
[DE85-013840] N85-35261

CHEMICAL EXPLOSIONS
Friction, impact, and electrostatic discharge sensitivities of energetic materials
[DE85-013321] N85-35309

CHEMICAL PROPERTIES
Chemoviscosity modeling for thermosetting resins, 2
[NASA-CR-177958] N85-35243

CHEMICAL REACTIONS
CO + H2 reaction over nitrogn-modified iron catalysts
[DE85-013791] N85-35231

CHEMICAL WARFARE
The identification of compounds in mustard hydrolysate
[AD-A156381] N85-35258

CHEMILUMINESCENCE
Nitrogen analysis by chemiluminescence
[AD-A156197] N85-35308

CHLORINE
Fluidized bed desulfurization
[NASA-CASE-NPO-15924-1] N85-35253

CHLOROETHYLENE
Search for acoustic signals from high energy cascades
[HE-7.1-1] N85-36155

CHROMITES
Some recent deposit modeling efforts N85-35453

CHROMIUM
Thermodynamics of the corrosion of chromium in molten carbonates
[DE85-011407] N85-35282
X-ray fluorescence analysis of 304L stainless steel
[DE85-013254] N85-35288
Applications of the mineral resources data system and the international strategic minerals inventory in mineral-resource assessments by region and commodity N85-35451
The Conterminous United States Mineral Assessment Program N85-35458
The Alaska Mineral Resources Assessment Program N85-35460
Development of electrodes for the NASA iron/chromium
[NASA-CR-174724] N85-35471

CHROMIUM ALLOYS
Deposition of nickel-cobalt alloys by controlled-potential electrolysis
[PB85-198562] N85-35291

CHROMIUM STEELS
Characterization of modified 9 r-1 Mo steel sand castings
[DE85-012057] N85-35287

CIRCULAR CYLINDERS
Vibrations of free hollow circular cylindrical bodies N85-35418

CITIES
Motor glider measurements during the Urban Atmosphere Energy Budget Experiment (EESA 1) N85-35553

CIVIL AVIATION
U.S. Civil airmen statistics for calendar year 1984
[AD-A156326] N85-35153
The contribution made by flight mechanics to civil aviation N85-35169
Introduction to European air traffic control
[AD-A156328] N85-35176

CLASSIFICATIONS
Source hierarchy list. Volume 1: A through H
[AD-A156300] N85-35825

CLEAR AIR TURBULENCE
Millimeter-wave propagation in moist air: Model versus path data
[AD-A156040] N85-35331
The physical and empirical basis for a specific clear-air turbulence risk index
[NASA-CR-178522] N85-35540

CLIMATE
Simulated effects of increased recharge on the ground-water flow system of Yucca Mountain and vicinity, Nevada-California
[DE85-012985] N85-35469
Time-dependent response of the climate to increasing atmospheric carbon dioxide N85-35532
Carbon dioxide and climate: A working glossary
[DE85-013535] N85-35562

CLIMATOLOGY
Current inventory of anthropogenic carbon dioxide in the North Pacific Subarctic Gyre
[PB85-187938] N85-35570

CLINICAL MEDICINE
Analogies of control mechanisms in flight guidance and medicine N85-35597

CLOSTRIDIUM BOTULINUM
Production of butanol by fermentation in the presence of cocultures of clostridium
[NASA-CASE-NPO-16203-1] N85-35227

CLOSURE LAW
Application of a turbulent closure model to the parameterization of the vertical diffusion of heat, momentum, and humidity in the ECMWF model — European Center for Medium Term Weather Forecasting (ECMWF)
[MITT-41] N85-35387

CLOSURES
Scale separation closure and Alfven wave turbulence
[DE85-013124] N85-35385

CLOUD CHAMBERS
Missing energies at pair creation
[HE-4.4-8] N85-36016
Progress report on a new search for free e/3 quarks in the cores of 10(15) - 10(16) eV air showers
[HE-6.2-15] N85-36151

CLOUD COVER
Mean cloudiness over the global tropics from satellite observations
[AD-A156188] N85-35561

CLOUD PHYSICS
Study of the parameters affecting the collapse of a rotating protostellar cloud N85-35837

CLOUD SEEDING
Project Skywater, 1983-84 SCPP (Sierra Cooperative Pilot Project) data inventory
[PB85-187052] N85-35565

CLOUDS
Far-infrared observations of young clusters embedded in the R Coronae Austrinae and RHO Ophiuchi dark clouds
[NASA-TM-86681] N85-35834

CLOUDS (METEOROLOGY)
Mean cloudiness over the global tropics from satellite observations
[AD-A156188] N85-35561

CLUMPS
Cluster variation study of coherent ordering in FCC and BCC solid solutions
[AD-A156039] N85-35280

CMOS
Total integrated dose testing of solid-state scientific CD4011, CD4013, and CD4060 devices by irradiation with CO-60 gamma rays
[NASA-CR-176196] N85-35795

COAL
Fluidized bed desulfurization
[NASA-CASE-NPO-15924-1] N85-35253
Depositional systems and coal occurrence in the Fort Union Formation (Paleocene), Powder River Basin, Wyoming and Montana N85-35505

COAL UTILIZATION
Chemistry division report
[DE85-010586] N85-35228

COASTAL WATER
Sea surface and remotely sensed temperatures off Cape Mendocino, California
[NASA-TM-86712] N85-35573

COASTS
Marine phosphorite deposits model for exploration, with emphasis on deposits in the US Atlantic coastal plain N85-35439
USGS coastal research, studies and maps: A source of information for coastal decision making
[USGS-CIRC-883] N85-35465
Atlantic coast hindcast. Phase 2: Wave information, additional extremal estimates
[AD-A156137] N85-35575

COBALT
Cobalt-rich ferromanganese crusts in the oceans N85-35444
Applications of the mineral resources data system and the international strategic minerals inventory in mineral-resource assessments by region and commodity N85-35451
The Conterminous United States Mineral Assessment Program N85-35458
The Alaska Mineral Resources Assessment Program N85-35460

COBALT ALLOYS
Deposition of nickel-cobalt alloys by controlled-potential electrolysis
[PB85-198562] N85-35291

CODERS
Noiseless coding for the Gamma Ray spectrometer
[NASA-CR-176201] N85-35219

CODING
X-ray fluorescence analysis of 304L stainless steel
[DE85-013254] N85-35288

COEFFICIENT OF FRICTION
Action of wear-inhibiting Al2O3-coatings when applied to hard metal cutting tools
[BLL-RISLEY-TR-5041-(9091.9F)] N85-35292

COHERENT ACOUSTIC RADIATION
LANDSAT-4/5 image data quality analysis
[E85-10105] N85-35463

COHERENT ELECTROMAGNETIC RADIATION
The 2nd European Conference on Atomic and Molecular Physics
[AD-A155863] N85-35715

COLD DRAWING
A new drawing technique for nylon 6 by reversible plasticization with iodine
[AD-A156272] N85-35803

COLD FRONTS
The kinematic structure of cold frontal rainbands N85-35531

COLD PRESSING
Establishment of a Computer-Aided Design (CAD)-Computer-Aided Manufacturing (CAM) process for the production of cold forged gears
[AD-A155756] N85-35644

COLD WORKING
Wear-resistant coatings for tools intended for cold working
[BLL-RISLEY-TR-5040-(9091.9F)] N85-35293

COLLAPSE
The capability of the existing network of installations for detecting the antineutrino burst from collapsing stars
[HE-5.3-13] N85-36107

COLLISION PARAMETERS
Observations of accelerated high current low emittance beams in the SLC Linac
[DE85-013073] N85-35211
Relation between gamma-ray family and EAS core: Monte-Carlo simulation of EAS core
[HE-3.6-7] N85-35955
On mini-cluster observed by Chacaltaya emulsion chamber experiment
[HE-3.6-12] N85-35959

Observation of genetic relation among new phenomena Geminion, Chiron and mini-Centauro
[HE-6.2-16] N85-36152

COLLISIONLESS PLASMAS
Current interruption by density depression
[DE85-013120] N85-35846

COLOR
Radiation measurements on magnesium flames
[BLL-CE-TRANS-8110-(9022.09)] N85-35254
Edge information in color images based on histograms of differences
[AD-A156002] N85-35751

COLOR VISION
Edge information in color images based on histograms of differences
[AD-A156002] N85-35751

COLORADO
Aeromagnetic and gravity models of the pluton below the Lake City caldera, Colorado N85-35442

COLUMNS (SUPPORTS)
Structural analysis of imperfect three-legged truss columns for large space structures applications N85-35416
User's guide: A computer program for strength analysis of non-hydraulic concrete structural elements. Report 1. Concrete General Strength Investigation (CGSI)
[AD-A156392] N85-35428
Static and cyclic behavior of semi-rigid steel beam-column connections
[PB85-194363] N85-35433

COMBAT
Air university commander's and supervisor's guide on substance abuse
[AD-A156336] N85-35622

COMBUSTION
Pressure measurements in a hydrogen combustion environment: Hydrogen-air combustion test series 1 and 2 in the FITS tank, volume 1
[TI85-009899] N85-35259
Laser probes of natural gas ignition chemistry
[PB85-200210] N85-35264
An analytical and numerical model of radiation heat transfer in direct injection-type diesel combustion N85-35368
Review of US NOx abatement technology
[PB85-193522] N85-35501

COMBUSTION CHAMBERS
Flow modifying device
[NASA-CASE-LEW-13562-2] N85-35195
Basic research on pulse-combustion phenomena
[PB85-200228] N85-35265
Development of advanced high-temperature heat flux sensors. Phase 2: Verification testing
[NASA-CR-174973] N85-35391

COMBUSTION PRODUCTS
System for the continuous generation of phosphorous aerosols from red phosphorus-butyl rubber
[DE85-013527] N85-35232
Proceedings of the 7th Joint Panel Meeting of the UJNR Panel on Fire Research and Safety
[PB85-199545] N85-35317
Fire research publications, 1984
[PB85-208502] N85-35827

COMET TAILS
Comet Halley returns: A teachers' guide 1985-1986
[NASA-EP-197] N85-35839

COMETARY ATMOSPHERES
Comet Halley returns: A teachers' guide 1985-1986
[NASA-EP-197] N85-35839

COMMAND AND CONTROL
TRICCS: A proposed teleoperator/robot integrated command and control system for space applications
[NASA-TM-87577] N85-35637

COMMERCIAL AIRCRAFT
U.S. Civil airmen statistics for calendar year 1984
[AD-A156326] N85-35153

COMMUNICATION
A new description of combined trellis coding with asymmetric modulation
[NASA-CR-176197] N85-35323
DMSK: A practical 2400-bps receiver for the mobile satellite service: An MSAT-X Report
[NASA-CR-176194] N85-35324

COMMUNICATION NETWORKS
Communication complexity of distributed shortest path algorithms
[AD-A156049] N85-35332
A ray trace program for line-of-sight microwave communication links
[AD-A156168] N85-35336

COMMUNICATION SATELLITES
Second-generation mobile satellite system. A conceptual design and trade-off study
[NASA-CR-176195] N85-35325

COMPACTING
Dynamic compaction of a monosized spherical tungsten powder
[DE85-014808] N85-35289
Computational methods for the explosive and impact compaction of powders
[AD-A156219] N85-35653

COMPASSES
Determining an azimuth with a north seeking gyro
[AD-A155880] N85-35180

COMPENSATORS
Design of dynamic compensators of prescribed pattern
[BU-109] N85-35674

COMPLEXITY
Communication complexity of distributed shortest path algorithms
[AD-A156049] N85-35332

COMPOSITE MATERIALS
SRB TPS closeout materials characterization
[NASA-CR-170885] N85-35222

COMPRESSIBILITY
Characteristics of central collision events in Fe-nucleus interactions for 20 - 60 GeV/nucleon
[HE-1.4-3] N85-35891

COMPRESSIBILITY EFFECTS
Deceleration of a supersonic flow behind a curved shock wave with isentropic precompression
[NASA-TM-77920] N85-35164

COMPRESSIBLE FLOW
Calculation of compressible flow about three-dimensional inlets with auxiliary inlets, slats and vanes by means of a panel method
[NASA-CR-174975] N85-35162
Acoustic resonances in cylinder bundles oscillating in a compressible fluid
[DE85-004066] N85-35699

COMPRESSION LOADS
User's guide: A computer program for strength analysis of non-hydraulic concrete structural elements. Report 2. Strength design of reinforced concrete column sections (PCAUC)
[AD-A156393] N85-35429

COMPRESSION TESTS
System expectations for Pioneer 1 foil implosion experiments
[DE85-014129] N85-35359

COMPRESSOR BLADES
Unsteady flow in a supersonic cascade with two in-passage shocks
[NASA-CR-3925] N85-35158

COMPTON EFFECT
Breeding new light into old machines (and new)
[DE85-013055] N85-35763
Result of Monte-Carlo simulation of electron-photon cascades in lead and layers of lead-scintillator
[HE-3.6-11] N85-35958

COMPUTATION
Adaptive rezoner in a two-dimensional Lagrangian hydrodynamic code
[DE85-010108] N85-35381
DEPTH-CHARGE static and time-dependent perturbation/sensitivity system for nuclear reactor core analysis, revision 1
[DE85-013103] N85-35659

COMPUTATIONAL FLUID DYNAMICS
Studies on effects of boundary conditions in confined turbulent flow predictions
[NASA-CR-3929] N85-35371

COMPUTER AIDED DESIGN
Design and construction of an advanced power conditioning subsystem for small photovoltaic applications
[DE85-013940] N85-35495
VLSI (Very Large Scale Integrated) tutorials through the video-computer courseware implementation system
[AD-A155889] N85-35631
Establishment of a Computer-Aided Design (CAD)-Computer-Aided Manufacturing (CAM) process for the production of cold forged gears
[AD-A155756] N85-35644
Software maintenance relating to the input translator and z-80 realization volume of the computer systems design environment
[AD-A155849] N85-35646
Computer Aided Design (CAD) methods for very large scale integration systems
[BMFT-FB-T-85-029] N85-35668

COMPUTER AIDED MANUFACTURING
Establishment of a Computer-Aided Design (CAD)-Computer-Aided Manufacturing (CAM) process for the production of cold forged gears
[AD-A155756] N85-35644

COMPUTER ASSISTED INSTRUCTION
VLSI (Very Large Scale Integrated) tutorials through the video-computer courseware implementation system
[AD-A155889] N85-35631

COMPUTER DESIGN
A methodology for the design of testable custom large-scale integrated circuits
[AD-A156098] N85-35351

COMPUTER GRAPHICS
Raster functionality for a VDI
[DE85-006734] N85-35396
Edge detection and geometric methods in computer vision
[AD-A155873] N85-35630
An exploratory study of the effect of screen size and resolution on the legibility of graphics in automated job performance aids
[AD-A155989] N85-35632
Selected publications in image understanding and computer vision from 1974 to 1983
[AD-A156196] N85-35634
Master Fit users' guide, version 1.0
[DE85-014199] N85-35667

COMPUTER INFORMATION SECURITY
An approach to determining computer security requirements for Navy systems
[AD-A155750] N85-35627

COMPUTER PROGRAMMING
Development of NATOPS (Naval Air Training and Operating Procedure Standardization) performance software for the H-46D helicopter
[AD-A156089] N85-35190
AUTOSIM: An automated repetitive software testing tool
[NASA-CR-177930] N85-35643
Polylith: The early goals
[DE85-012534] N85-35658

COMPUTER PROGRAMS
General design method for 3-dimensional, potential flow fields. Part 2: Computer program DIN3D1 for simple, unbranched ducts
[NASA-CR-3926] N85-35159
Analysis of incompressible cascade flows using state-of-the-art computer programs
[AD-A155850] N85-35173
Development of NATOPS performance software for the SH-3D and SH-3H helicopters
[AD-A156140] N85-35192
The investigation of tethered satellite system dynamics
[NASA-CR-176180] N85-35215
Cluster variation study of coherent ordering in FCC and BCC solid solutions
[AD-A156039] N85-35280
X-ray fluorescence analysis of 304L stainless steel
[DE85-013254] N85-35288
Millimeter-wave propagation in moist air: Model versus path data
[AD-A156040] N85-35331
Solid state high power amplifier for driving the SLC injector klystron
[DE85-013063] N85-35356
Studies on effects of boundary conditions in confined turbulent flow predictions
[NASA-CR-3929] N85-35371
Design and behavior of coped beams N85-35417
Justified generalization: Acquiring procedures from examples
[AD-A156408] N85-35626
DSS/MIS (Decision Support Systems/Management Information Systems) design and implementation for LAMPS Mk 3 utilizing a microcomputer and a maintenance personnel assignment program
[AD-A155852] N85-35629
Users guide for optimum interpolation method of global data assimilation
[AD-A155929] N85-35648
Specifying and verifying concurrent programs
[AD-A156190] N85-35652
Using an LSI-11/23 and RT-11 to digitize analog tapes
[DE85-012736] N85-35656
SASSYS-1 computer code verification with EBR-2 test data
[DE85-012119] N85-35657
DEPTH-CHARGE static and time-dependent perturbation/sensitivity system for nuclear reactor core analysis, revision 1
[DE85-013103] N85-35659
RFQ modeling computer program
[DE85-012665] N85-35661
Error message recording and reporting in the SLC control system
[DE85-013057] N85-35664
Toolpack
[DE85-013135] N85-35665

Computer code calculations of the TMI-2 accident: Initial and boundary conditions
[DE85-012613] N85-35666
Master Fit users' guide, version 1.0
[DE85-014199] N85-35667

COMPUTER STORAGE DEVICES
L-step sequential decoding
[AD-A156121] N85-35649

COMPUTER SYSTEMS DESIGN
A Programmable Automatic Noise Data and Other Related parameter Acquisition system (PANDORA) --- wind energy converters N85-35479
Software maintenance relating to the input translator and z-80 realization volume of the computer systems design environment
[AD-A155849] N85-35646
Toolpack
[DE85-013135] N85-35665

COMPUTER SYSTEMS PERFORMANCE
Raster functionality for a VDI
[DE85-006734] N85-35396

COMPUTER SYSTEMS PROGRAMS
Calculation of the diffusion of light by aerosols: Description of the MIELOR software and results obtained
[REPT-80] N85-35638
AUTOSIM: An automated repetitive software testing tool
[NASA-CR-177930] N85-35643
Attacking software crisis: A macro approach
[AD-A155846] N85-35645
Software maintenance relating to the input translator and z-80 realization volume of the computer systems design environment
[AD-A155849] N85-35646

COMPUTER TECHNIQUES
Computational techniques for fiber reinforced components N85-35250
Wholebody radiation counting system
[AD-A155842] N85-35607
TRICCS: A proposed teleoperator/robot integrated command and control system for space applications
[NASA-TM-87577] N85-35637
Design of a microprogram control unit with concurrent error detection
[AD-A156447] N85-35655
Toolpack
[DE85-013135] N85-35665
Edge information in color images based on histograms of differences
[AD-A156002] N85-35751

COMPUTER VISION
Edge detection and geometric methods in computer vision
[AD-A155873] N85-35630
Selected publications in image understanding and computer vision from 1974 to 1983
[AD-A156196] N85-35634

COMPUTERIZED SIMULATION
Energy management of three-dimensional minimum-time intercept
[NASA-CR-176174] N85-35186
The investigation of tethered satellite system dynamics
[NASA-CR-176180] N85-35215
Actuator rigging test set electromagnetic interference test (CE03)
[AD-A155819] N85-35327
Investment justification of robotic technology in aerospace manufacturing. User's manual
[AD-A156193] N85-35410
Expert systems research in regional resource evaluation: Experiences in the application of microcomputer technologies N85-35450
The NORDA/FNOC (Naval Ocean Research and Development Activity's/Fleet Numerical Oceanography Center) Polar Ice Prediction System (PIPS)-Arctic: A technical description
[AD-A156332] N85-35577
Enhancement of the flexible spacecraft dynamics program for open spacecraft
[NASA-CR-175309] N85-35641
Benchmark evaluation of PC simscript
[AD-A156133] N85-35651
Computational methods for the explosive and impact compaction of powders
[AD-A156219] N85-35653
SASSYS-1 computer code verification with EBR-2 test data
[DE85-012119] N85-35657
RFQ modeling computer program
[DE85-012665] N85-35661
TOSCA calculations and measurements for the SLAC SLC damping ring dipole magnet
[DE85-014366] N85-35793
Investigations of the molecular beam epitaxial growth and characteristics of external excitation induced non-equilibrium phases of immiscible 3-5 compound semiconductors
[AD-A156325] N85-35804
Simulation of lattice damage due to dynamic loading
[DE85-008468] N85-35808
Network management simulation of automated guideway transit systems under vehicle-follower control
[PB85-188233] N85-35830
Preliminary results on underground muon bundles observed in the Frejus proton-decay detector
[HE-5.1-1] N85-36067
A transient digitiser for fast air shower events
[HE-5.2-21] N85-36097

CONCENTRATION (COMPOSITION)
The effect of +Gx acceleration on platelet activation as determined by plasma platelet factor 4 levels
[AD-A155881] N85-35608

CONCENTRATORS
Photovoltaics technology program summary
[DE85-013098] N85-35493

CONCENTRIC CYLINDERS
Couette flow of two fluids between concentric cylinders
[AD-A155827] N85-35376

CONCRETE STRUCTURES
Membrane reinforcement in concrete shells: Design versus nonlinear behavior N85-35312

CONCRETES
User's guide: A computer program for strength analysis of non-hydraulic concrete structural elements. Report 1. Concrete General Strength Investigation (CGSI)
[AD-A156392] N85-35428
User's guide: A computer program for strength analysis of non-hydraulic concrete structural elements. Report 2. Strength design of reinforced concrete column sections (PCAUC)
[AD-A156393] N85-35429

CONCURRENT PROCESSING
Specifying and verifying concurrent programs
[AD-A156190] N85-35652

CONDUCTIVE HEAT TRANSFER
Analytic solutions of inverse heat conduction problems N85-35367

CONFERENCES
Lectures of a Flight Mechanics Conference --- conferences
[ESA-TT-831] N85-35165
Proceedings of the 7th Joint Panel Meeting of the UJNR Panel on Fire Research and Safety
[PB85-199545] N85-35317
USGS research on mineral resources, 1985
[CIRC-949] N85-35435
Implementing agreement for cooperation in the development of large scale wind energy conversion systems
[JUEL-SPEZ-278] N85-35473
Land Disposal of Hazardous Waste
[PB85-196376] N85-35500
Workshop Proceedings: Interpretation of Seismic Wave Propagation in Laterally Heterogeneous Structures
[BMR-258] N85-35530
Proceedings of Meteorological Motor Glider (MEMO) Workshop '84
[DFVLR-MITT-85-04] N85-35542
Proceedings of a Scientic Meeting on the Occasion of the Inauguration of New Buildings for the DFVLR Institute for Aerospace Medicine
[ESA-TT-857] N85-35595
Proceedings of the 14th Army Science Conference. Volume 2: Principal authors I through O
[AD-A149201] N85-35690
Proceedings of the 14th Army Science Conference. Volume 3: Principal authors P through Z
[AD-A149202] N85-35691
Proceedings of the Workshop on Detectors for Relativistic Nuclear Collisions
[LBL-18225] N85-35700
The 2nd European Conference on Atomic and Molecular Physics
[AD-A155863] N85-35715
Nineteenth International Cosmic Ray Conference. HE Sessions, volume 6
[NASA-CP-2376-VOL-6] N85-35848
Nineteenth International Cosmic Ray Conference. HE Sessions, volume 7
[NASA-CP-2376-VOL-7] N85-35968
Nineteenth International Cosmic Ray Conference. HE sessions, volume 8
[NASA-CP-2376-VOL-8] N85-36066

CONFORMAL MAPPING
Adaptive rezoner in a two-dimensional Lagrangian hydrodynamic code
[DE85-010108] N85-35381

CONGRESSIONAL REPORTS
The 1986 National Aeronautics and Space Administration authorization
[GPO-47-635] N85-35829

CONNECTORS
Static and cyclic behavior of semi-rigid steel beam-column connections
[PB85-194363] N85-35433

CONSERVATION LAWS
Generalized reduced fluid model with finite ion-gyroradius effects
[DE85-013123] N85-35777
Phase space factors in multiparticle processes N85-35888

CONSTRAINTS
Design and testing of an energy-absorbing crewseat for the F/FB-111 aircraft. Volume 2: Data from seat testing
[NASA-CR-3917] N85-35184

CONSTRUCTION
Design and construction of an advanced power conditioning subsystem for small photovoltaic applications
[DE85-013940] N85-35495
Reachable grasps on a polygon: The convex rope algorithm
[AD-A155913] N85-35647
The 1986 National Aeronautics and Space Administration authorization
[GPO-47-635] N85-35829

CONTAINMENT
Fuel containment and damage tolerance for large composite primary aircraft structures. Phase 1: Testing
[NASA-CR-166091] N85-35241
Response of a BWR Mark 2 containment vessel head to loads beyond the design basis
[DE85-010524] N85-35432

CONTAMINATION
Radiation safety problems in handling highly active tritium targets
[DE85-014268] N85-35742

CONTINUOUS WAVE LASERS
Laser and electron beam processing of semiconductors
[AD-A155914] N85-35796

CONTOUR SENSORS
LANDSAT-4/5 image data quality analysis
[E85-10105] N85-35463

CONTOURS
Evaluation: Close-range photogrammetry for slope inventory and monitoring
[PB85-192755] N85-35470
Invariant tests and likelihood ratio tests for multivariate elliptically contoured distributions
[AD-A155844] N85-35679

CONTRACT MANAGEMENT
DoD Value Engineering conference report. Value Engineering (VE): A tool that benefits line management. Part 4, Workshop B: VE on spare parts
[AD-A156070] N85-35813
DoD Value Engineering conference report. Value Engineering (VE): A tool that benefits line management. Part 7, Workshop E: VE in construction and architect engineer contracts
[AD-A156073] N85-35816

CONTRACTION
On the convergence of an iterative formulation of the electromagnetic scattering from an infinite grating of thin wires N85-35319

CONTRACTS
Progress report on implementing the recommendations of the White House Science Council's Federal Laboratory Review Panel, volume 1
[PB85-185072] N85-35819

CONTROL
Solid state high power amplifier for driving the SLC injector klystron
[DE85-013063] N85-35356

CONTROL EQUIPMENT
The compliance of end effector force sensors for robot manipulator control N85-35406
On-line model driven control of the SLC electron Damping Ring
[DE85-013377] N85-35772

CONTROL SIMULATION
A preliminary evaluation of a failure detection filter for detecting and identifying control element failures in a transport aircraft
[NASA-TM-87576] N85-35204
Enhancement of the flexible spacecraft dynamics program for open spacecraft
[NASA-CR-175309] N85-35641
Network management simulation of automated guideway transit systems under vehicle-follower control
[PB85-188233] N85-35830

CONTROL SYSTEMS DESIGN
Report on the SLC control system
[DE85-013076] N85-35722
CONTROL THEORY
Analogies of control mechanisms in flight guidance and medicine N85-35597
Network management simulation of automated guideway transit systems under vehicle-follower control
[PB85-188233] N85-35830
CONTROLLABILITY
Analysis of flexible aircraft longitudinal dynamics and handling qualities. Volume 1: Analysis methods
[NASA-CR-177943-VOL-1] N85-35202
Analysis of flexible aircraft longitudinal dynamics and handling qualities. Volume 2: Data
[NASA-CR-177943-VOL-2] N85-35203
CONTROLLERS
State-of-the-art of solid-state motor controllers
[TI85-008674] N85-35806
CONVECTION
Experimental study of free and mixed convective flow of air in a heated cavity
[DE85-012538] N85-35380
Airborne Investigations of Mesoscale Convective Systems (AIMCS), 1984: Operational summary and data inventory
[PB85-187904] N85-35571
CONVECTION CURRENTS
Measurements for the determination of the vertical structure of the convective boundary layer — atmospheric boundary layer N85-35550
Two-point closure study of covariance budgets for turbulent Rayleigh-Benard convection
[PB85-189108] N85-35568
CONVERGENCE
On the convergence of an iterative formulation of the electromagnetic scattering from an infinite grating of thin wires N85-35319
Characterizations of generalized hyperexponential distributions
[AD-A155855] N85-35680
CONVEXITY
Reachable grasps on a polygon: The convex rope algorithm
[AD-A155913] N85-35647
COOLANTS
Computer code calculations of the TMI-2 accident: Initial and boundary conditions
[DE85-012613] N85-35666
COOLING
Enhanced heat transfer computations for internally cooled cable superconductor
[DE85-011897] N85-35383
COOLING SYSTEMS
A two-phase flow and heat transfer model for zero gravity
[AD-A156097] N85-35377
Transient three-phase three-component systems. Part 1: Formulation of the system of differential equations
[DE85-013267] N85-35384
COORDINATION
United States Army welding research and development topical and coordination meeting
[AD-A155834] N85-35409
COPLANARITY
Experiment Pamir-3. Coplanar emission of high energy gamma-quanta at interaction of hadrons with nuclei of air atoms at energies above 10 to the 7th power GeV
[HE-1.4-12] N85-35899
COPOLYMERS
Electrically conductive doped block copolymer of polyacetylene and polyisoprene
[DE85-006500] N85-35301
COPPER
Some recent deposit modeling efforts N85-35453
The Conterminous United States Mineral Assessment Program N85-35458
The Alaska Mineral Resources Assessment Program N85-35460
Ore genesis at the Monterrosas deposit in the Coastal Batholith, Ica, Peru N85-35510
Few-particles generation channels in inelastic hadron-nuclear interactions at energy approximately equals 400 GeV
[HE-3.2-9] N85-35917
CORES
Monte Carlo simulations of electron lateral distributions in the core region of 10(13) - 10(16) eV air showers N85-35992
A new study of shower age distribution in near vertical showers by EAS air shower array N85-35996
Lateral distribution of electrons of air showers N85-35998
Properties of 10 (18)-10 (19)eV EAS at far core distance
[HE-4.7-3] N85-36054
Longitudinal development of muons in large air showers studies from the arrival time distributions measured at 900m above sea level
[HE-4.7-4] N85-36055
Arrival time distributions of electrons in air showers with primary energies above 10 (18)eV observed at 900m above sea level
[HE-4.7-5] N85-36056
The thickness of the shower disc as observed in showers produced by primaries above 10 (19)eV
[HE-4.7-6] N85-36057
Sub-luminal pulses from cosmic ray air showers
[HE-4.7-13] N85-36063
Progress report on a new search for free e/3 quarks in the cores of 10(15) - 10(16) eV air showers
[HE-6.2-15] N85-36151
Acoustic detection of air shower cores
[HE-7.1-4] N85-36158
CORIOLIS EFFECT
Applications of the Galerkin formalism in the coupling of the earth's free oscillations N85-35514
CORK (MATERIALS)
Verification of the SRB motor case pin retainer band tips
[NASA-CR-170882] N85-35220
SRB TPS closeout materials characterization
[NASA-CR-170885] N85-35222
CORONAS
Far-infrared observations of young clusters embedded in the R Coronae Austrinae and RHO Ophiuchi dark clouds
[NASA-TM-86681] N85-35834
CORPUSCULAR RADIATION
Limits on deeply penetrating particles in the 10(17) eV cosmic ray flux
[HE-5.3-1] N85-36098
CORRELATION
A search for mini-clusters in Japan-USSR Joint Experiment at Pamir
[HE-3.5-2] N85-35941
Tskhra-Tskaro complex intended for the investigations of EAS spatial characteristics near axis N85-35995
Correlation of high energy muons with primary compositon in extensive air shower
[HE-4.3-7] N85-36001
CORRELATORS
Fatigue damage detection in steels by optical correlation
[AD-A155830] N85-35277
CORROSION
Thermodynamics of the corrosion of chromium in molten carbonates
[DE85-011407] N85-35282
Experimental lithium system
[DE85-013252] N85-35382
CORROSION RESISTANCE
Electrochemical method for investigation of the susceptibility of corrosion-resistant steels to intercrystalline corrosion
[BLL-CE-TRANS-8082-(9022.09)] N85-35269
X-ray fluorescence analysis of 304L stainless steel
[DE85-013254] N85-35288
Development of a mathematical model for predicting the percentage fatigue life increase resulting from shot peened components
[AD-A155774] N85-35425
COSMIC RAY SHOWERS
Proton-air and proton-proton cross sections from air shower data
[HE-1.1-1] N85-35849
Proton-air inelastic cross section at S(1/2) = 30 TeV
[HE-1.1-2] N85-35850
Hadron cross sections at ultra high energies and unitarity bounds on diffraction dissociation
[HE-1.1-3] N85-35851
P(P bar)P elastic scattering and cosmic ray data
[HE-1.1-6] N85-35854
Estimation of the total inelasticity coefficient in interaction of greater than or equal to 20 TeV hadrons with lead
[HE-1.1-9] N85-35857
The method for the study of the inelastic cross-section for high energy protons by means of shower arrays with the large calorimetric area
[HE-1.1-11] N85-35858
Multiplicity distributions in interaction models used for cascade simulations
[HE-1.2-5] N85-35863
Some remarks about simulation of cosmic ray phenomena with use of nuclear interaction models based on the current SPS proton-antiproton data
[HE-1.2-6] N85-35864
Anuglar distribution of shower particles produced in the collisions of 20-GeV/c and 300-GeV negative pions with emulsion nuclei N85-35868
Scaling violation in the fragmentation region of inclusive nucleon spektrum N85-35874
The response of a scintillation counter below an emulsion chamber to heavy nucleus interactions in the chamber N85-35889
Japan - USSR joint emulsion chamber experiment at Pamir
[HE-3.1-1] N85-35901
Energy spectra of proton and nuclei of primary cosmic rays in energy region 10 TeV/particle
[HE-3.1-10] N85-35908
Scaling violation in fragmentation region at energies above 10-15 eV based on the data on cosmic ray hadron component
[HE-3.1-11] N85-35909
High sensitive X-ray films to detect electron showers in 100 GeV region
[HE-3.1-13] N85-35911
Exotic interactions among C-jets and Pb-jets
[HE-3.2-6] N85-35914
X-ray film chamber with carbon target of Tien-Shan complex array N85-35915
Penetrative nature of high energy showers observed in Chacaltaya emulsion chamber
[HE-3.3-5] N85-35923
Anomalous correlation between hadron and electromagnetic particles in hadron and gamma-ray families
[HE-3.3-6] N85-35924
Atmospheric interactions detected in both the upper and the lower chambers at Chacaltaya
[HE-3.3-7] N85-35925
Lateral distribution of high energy hadrons and gamma ray in air shower cores observed with emulsion chambers
[HE-3.3-8] N85-35926
Size distributions of air showers accompanied with high energy gamma ray bundles observed at Mt. Chacaltaya
[HE-3.3-9] N85-35927
EAS accompanied by gamma-families at Mt. Norikura and comparison with Monte Carlo simulation
[HE-3.3-10] N85-35928
Comparison of absolute intensity between EAS with gamma-families and general EAS at Mount Norikura
[HE-3.3-11] N85-35929
Analytical-numerical methods of calculations of energy and three-dimensional particle distributions in electromagnetic cascades
[HE-3.5-13] N85-35950
Multidimensional analysis of data obtained in experiments with X-ray emulsion chambers and extensive air showers
[HE-3.6-2] N85-35951
LPM effect and primary energy estimations
[HE-3.6-4] N85-35953
Experimental basis for the models of cascade propagation in atmosphere
[HE-3.6-6] N85-35954
Relation between gamma-ray family and EAS core: Monte-Carlo simulation of EAS core
[HE-3.6-7] N85-35955
Comparison of big event with calculations of the air shower development
[HE-3.6-8] N85-35956
The lateral distributions of charged particles of energy greater than 0.3 E sub crit in electron-photon cascades in lead and air
[HE-3.6-10] N85-35957
Result of Monte-Carlo simulation of electron-photon cascades in lead and layers of lead-scintillator
[HE-3.6-11] N85-35958
On mini-cluster observed by Chacaltaya emulsion chamber experiment
[HE-3.6-12] N85-35959
A comparative analysis of gamma and hadron families at the superhigh energies recorded in experiment Pamir
[HE-3.7-1] N85-35960
A study of gamma-families generated in nucleon-nucleus (NA) and pion-nucleus (pi A) interactions
[HE-3.7-2] N85-35961
New analysis of nuclear interaction observed by Mt. Kanbara emulsion chamber experiment
[HE-3.7-4] N85-35963
Intensities of high-energy cosmic rays at Mount Kanbala
[HE-3.7-5] N85-35964
Structured events in Pamir carbon X-ray chambers
[HE-3.7-7] N85-35965
Ultra high energy events in ECHOS series and primary energy spectrum
[HE-3.7-9] N85-35966
Peculiarities of gamma-quanta distribution at 20 TeV energy
[HE-3.7-10] N85-35967

Nineteenth International Cosmic Ray Conference. HE Sessions, volume 7
[NASA-CP-2376-VOL-7] N85-35968
Electrons, muons and hadrons in extensive air showers and how do they depend on nuclear interaction model, part 2 N85-35969
Analysis of equi-intensity curves and NU distribution of EAS N85-35970
Analysis of the hadron component in E.A.S. N85-35971
Electrons, muons and hadrons in extensive air showers and how do they depend on nuclear interaction model, part 1 N85-35972
Simulation of EAS properties on the basis of high energy interaction model deduced from the accelerator data N85-35973
New aspects in nucleon-nucleus collisions and EAS properties around 10(6) GeV N85-35974
Small air showers and collider physics
[HE-4.1-9] N85-35975
High energy hadrons in extensive air showers N85-35976
Dependence of the average spatial and energy characteristics of the hadron-lepton cascade on the strong interaction parameters at superhigh energies N85-35977
Hadronic components of EAS by rigorous saddle point method in the energy range between 10(5) and 10(8) GeV N85-35978
About increase of the large transvere momentum processes fraction in hA interactions at energies 5.10(14) - 10(16) eV according to the data on E.A.S. hadrons N85-35979
Phenomenology of soft hadron interactions and the relevant EAS data N85-35980
The maximum depth of shower with E sub 0 larger than 10(17) eV on average characteristics of EAS different components N85-35981
Sensitivity of depth of maximum and absorption depth of EAS to hadron production mechanism N85-35982
A critical analysis of air shower structure functions and size spectrum measurements with the NBU air shower array N85-35983
Character of energy flow in air shower core N85-35985
Observation of EAS using a large water tank N85-35986
The development of air shower in the iron absorber N85-35987
Application of photodiodes to the detection of electromagnetic bursts N85-35988
Core structure of EAS in 10(15) to 10(17) eV N85-35989
Particle distributions in approximately 10(14) 10(16) eV air shower cores at sea level N85-35990
Theoretical study of EAS hadronic structure N85-35991
Monte Carlo simulations of electron lateral distributions in the core region of 10(13) - 10(16) eV air showers N85-35992
Comparison of simulation results with sea-level experimental data on 10(14) - 10(16) air shower cores N85-35993
Particle distributions in approximately 10(13) - 10(16) eV air shower cores at mountain altitude and comparison with Monte Carlo simulations
[HE-4.2-18] N85-35994
Tskhra-Tskaro complex intended for the investigations of EAS spatial characteristics near axis N85-35995
A new study of shower age distribution in near vertical showers by EAS air shower array N85-35996
A new study of muons in air showers by NBU air shower array N85-35997
Lateral distribution of electrons of air showers N85-35998
Detailed studies of the electron lateral distribution in extensive air showers with energies around 10(16) eV N85-35999
Study of muons near shower cores at sea level using the E594 neutrino detector N85-36000
Correlation of high energy muons with primary composition in extensive air shower
[HE-4.3-7] N85-36001
Measurement of energy muons in EAS at energy region larger thean 10(17) eV
[HE-4.3-8] N85-36002
Muon fluctuation studies of EAS 10(17) eV
[HE-4.3-9] N85-36003
Average features of the muon component of EAS or = 10(17) eV
[HE-4.3-10] N85-36004
Measurement of shower electrons and muons using a small air shower array
[HE-4.3-11] N85-36005
The longitudinal development of muons in cosmic ray air showers at energies 10(15) - 10(17) eV
[HE-4.3-12] N85-36006
Topological aspects of age parameter
[HE-4.3-13] N85-36007
Monte Carlo simulation of EAS generated by 10(14) - 10(16) eV protons
[HE-4.3-14] N85-36008
Lateral distribution on charged particles in EAS
[HE-4.3-15] N85-36009
Lateral distribution of high energy muons in EAS of sizes Ne approximately equals 10(5) and Ne approximately equals 10(6)
[HE-4.3-16] N85-36010
Energy calibration of the fly's eye detector
[HE-4.4-1] N85-36011
The structure of EAS at E 0.1 EeV
[HE-4.4-2] N85-36012
Standard value for the radiation length in air
[HE-4.4-4] N85-36013
Longitudinal trial functions and the cosmic ray energy scale N85-36014
EAS development curve at energy of 10(16) - 10(18) eV measured by optical Cerenkov light
[HE-4.4-7] N85-36015
Transition effect of air shower particles in plastic scintillators
[HE-4.4-9] N85-36017
The system of EAS time analysis
[HE-4.4-10] N85-36018
On the determination of the depth of EAS development maximum using the lateral distribution of Cerenkov light at distances 150 m from EAS axis
[HE-4.4-13] N85-36019
Study of the energy spectrum of primary cosmic rays: EAS size fluctuations at a fixed primary energy
[HE-4.4-14] N85-36020
Study of the shower maximum depth by the method of detection of the EAS Cerenkov light pulse shape
[HE-4.4-15] N85-36021
Analysis of Cerenkov pulses recorded simultaneously at two sites
[HE-4.4-16] N85-36022
Preliminary results of the Cerenkov EAS flashes the Crimean Astrophysical Observatory
[HE-4.4-17] N85-36023
The experimental cascade curves of EAS at E sub 0 10(17) eV obtained by the method of detection of Cherenkov pulse shape
[HE-4.4-18] N85-36024
Lateral-angular and temporal characteristics of EAS optical radiation
[HE-4.4-19] N85-36025
The identification of gamma ray induced EAS
[HE-4.5-1] N85-36026
Muons in gamma showers
[HE-4.5-3] N85-36027
Muon spectrum in air showers initiated by gamma rays
[HE-4.5-4] N85-36028
Electromagnetic and muonic structure of showers initiated by gamma-rays and by hadrons
[HE-4.5-6] N85-36030
The muon content of gamma-ray showers
[HE-4.5-7] N85-36031
Simulation of gamma-initiated showers
[HE-4.5-10] N85-36033
Phenomenological characteristic of the electron component in gamma-quanta initiated showers
[HE-4.5-11] N85-36034
A three-dimensional Monte Carlo calculation of the photon initiated showers and Kiel result
[HE-4.5-13] N85-36035
Construction of a cosmic ray air shower telescope
[HE-4.5-14] N85-36036
On the possibilities of large-scale radio and fiber optics detectors in cosmic rays
[HE-4.6-2] N85-36039
Radio signals from very large showers
[HE-4.6-3] N85-36040
On the production mechanism of radio-pulses from large extensive air showers
[HE-4.6-4] N85-36041
A new study on the emission of EM waves from large EAS
[HE-4.6-5] N85-36042
Air fluorescence detection of large air showers below the horizon
[HE-4.6-6] N85-36043
A facility for investigation of multiple hadrons at cosmic-ray energies
[HE-4.6-8] N85-36045
A possible EAS array above the Soudan 2 detector
[HE-4.6-9] N85-36046
Fast scintillation counter system and performance
[HE-4.6-10] N85-36047
Performance of a local electron density trigger to select extensive air showers at sea level
[HE-4.6-11] N85-36048
Microprocessor-based single particle calibration of scintillation counter
[HE-4.6-13] N85-36049
Samarkand complex setup for investigation of cosmic ray variation in the energy range of 7 10 (9) - 10 (15) eV
[HE-4.6-14] N85-36050
Radio wave emitted by an extensive air showers in 10KHz to 1MHz region
[HE-4.6-15] N85-36051
The structure of the shower disk observed at Mt. Norikura
[HE-4.7-1] N85-36052
Structure of air shower disc near the core
[HE-4.7-2] N85-36053
Properties of 10 (18)-10 (19)eV EAS at far core distance
[HE-4.7-3] N85-36054
Longitudinal development of muons in large air showers studies from the arrival time distributions measured at 900m above sea level
[HE-4.7-4] N85-36055
Arrival time distributions of electrons in air showers with primary energies above 10 (18)eV observed at 900m above sea level
[HE-4.7-5] N85-36056
The thickness of the shower disc as observed in showers produced by primaries above 10 (19)eV
[HE-4.7-6] N85-36057
Methods for roof-top mini-arrays
[HE-4.7-7] N85-36058
Expected rates with mini-arrays for air showers
[HE-4.7-8] N85-36059
Fast scintillation counter preamplifier for the observation of Linsley effect
[HE-4.7-9] N85-36060
A mini-array for large air showers
[HE-4.7-10] N85-36061
A note on some statistical properties of rise time parameters used in muon arrival time measurements
[HE-4.7-12] N85-36062
Sub-luminal pulses from cosmic ray air showers
[HE-4.7-13] N85-36063
Thickness of the particle swarm in cosmic ray air showers
[HE-4.7-14] N85-36064
Study of the time-differentiated particle flux density at various distances from EAS axis
[HE-4.7-15] N85-36065
Muon and neutrino results from KGF experiment at a depth of 7000 hg/square cm
[HE-5.1-2] N85-36066
A large area cosmic muon detector located at Ohya stone mine
[HE-5.1-7] N85-36072
The Nagoya cosmic-ray muon spectrometer 3, part 2: Track detector
[HE-5.2-3] N85-36081
An upper limit of muon flux of energies above 100 TeV determined from horizontal air showers observed at Akeno
[HE-5.2-12] N85-36088
Comments on the measurements of multiple muon phenomena
[HE-5.2-13] N85-36089
Energy spectrum of cascade showers induced by cosmic ray muons in the range from 50 GeV to 5 TeV
[HE-5.2-14] N85-36090
Measurement of muon intensity by Cerenkov method
[HE-5.2-15] N85-36091
Photo nuclear energy loss term for muon-nucleus interactions based on xi scaling model of QCD
[HE-5.2-17] N85-36093
On method of muon spectrum measurements by the scintillation detectors of a large thickness T4t sub o
[HE-5.2-18] N85-36094
A transient digitiser for fast air shower events
[HE-5.2-21] N85-36097
A study of atmospheric neutrinos with the IMB detector
[HE-5.3-7] N85-36101
Atmospheric neutrinos observed in underground detectors
[HE-5.3-8] N85-36102
Analysis of the electron component of EAS at observational level 700 g x cm(-2) with a scale breaking interaction model and gammaisation hypothesis
[HE-5.4-8] N85-36119
Calculation of intensity of high energy muon groups observed deep underground
[HE-5.4-13] N85-36123
A search for heavy long lived particles in high energy cosmic rays
[HE-6.2-7] N85-36143

Delayed particles in EAS at Akeno
[HE-6.2-8] N85-36144
Energetic delayed hadrons in large air showers observed at 5200m above sea level
[HE-6.2-9] N85-36145
Search for long-lived massive particles in extensive air showers
[HE-6.2-10] N85-36146
High energy cosmic ray signature of quark nuggets
[HE-6.2-11] N85-36147
Search for tachyons associated with extensive air showers in the ground level cosmic radiation
[HE-6.2-13] N85-36149
Charge 4/3 leptons in cosmic rays
[HE-6.2-14] N85-36150
Progress report on a new search for free e/3 quarks in the cores of 10(15) - 10(16) eV air showers
[HE-6.2-15] N85-36151
Observation of genetic relation among new phenomena Geminion, Chiron and mini-Centauro
[HE-6.2-16] N85-36152
Tian-Shan effect and charmed particles
[HE-6.2-17] N85-36153
Search for acoustic signals from high energy cascades
[HE-7.1-1] N85-36155
Experimental investigation of radiative-acoustic effects in the water by the thermodynamical conditions of Dumand
[HE-7.1-2] N85-36156
Exploring results of the possibility on detecting cosmic ray particles by acoustic way
[HE-7.1-3] N85-36157
Acoustic detection of air shower cores
[HE-7.1-4] N85-36158
Detection threshold energy of high energy cascade showers using thermoluminescence PTFE-sheet and hot-gas reader
[HE-7.1-5] N85-36159
Application of thermoluminescence for detection of cascade shower 1: Hardware and software of reader system
[HE-7.1-6] N85-36160
Spatial distribution read-out system for thermoluminescence sheets
[HE-7.1-7] N85-36161
Application of thermoluminescence for detection of cascade shower 2: Detection of cosmic ray cascade shower at Mount Fuji
[HE-7.1-12] N85-36162

COSMIC RAYS

Biophysical research in space --- radiation effects
N85-35603
Gamma-ray production cross sections for alpha-particle induced reactions on F-19 and Na-23
[DE85-012603] N85-35732
Nineteenth International Cosmic Ray Conference. HE Sessions, volume 6
[NASA-CP-2376-VOL-6] N85-35848
Measurement of interaction cross section of cosmic ray Fe nuclei (E4 GeV/N) with Al target
[HE-1.1-7] N85-35855
QCD-motivated description of very high energy particle interactions
[HE-1.2-2] N85-35861
Nucleon-nucleus interactions from JACEE
N85-35869
General consequences of the violated Feynman scaling N85-35872
Propagation of cosmic rays through the atmosphere in the quark-gluon strings model N85-35873
Determination of primary energy in nucleus-nucleus collisions and the high P(sub)T tail of alpha-particles
N85-35875
SU(2) x U(1) vacuum and the Centauro events
N85-35885
Ringlike inelastic events in cosmic rays and accelerators N85-35887
Heavy nucleus collisions between 20 and 60 GeV/nucleon
[HE-1.4-2] N85-35890
Characteristics of central collision events in Fe-nucleus interactions for 20 - 60 GeV/nucleon
[HE-1.4-3] N85-35891
Nucleus-nucleus interaction above several hundred GeV/n
[HE-1.4-4] N85-35892
Excessive production of electron pairs by soft photons in low multiplicity ion interactions
[HE-1.4-6] N85-35894
Forward particle production in inelastic Ne-22 inteVractions in emulsion at 4.1 A Ge/c
[HE-1.4-7] N85-35895
On the mechanism of anomalous nucleus-nucleus interactions at energies above 1 TeV/nucleon
[HE-1.4-8] N85-35896
Meson multiplicity in nucleus-nucleus collisions above 4 GeV/amu
[HE-1.4-10] N85-35897
Inclusive angular distribution of alpha and Li fragments produced in the Fe-C and Fe-Pb collisions at 1.88 GeV/u
[HE-1.4-11] N85-35898
The effect of the relative nuclear size on the nucleus-nucleus interactions
[HE-1.4-13] N85-35900
Intensities of high-energy cosmic rays at Mount Kanbala
[HE-3.1-2] N85-35902
On the characteristics of emulsion chamber family events produced in low heights
[HE-3.1-6] N85-35904
Hadron intensity and energy spectrum at 4380 m above level
[HE-3.1-7] N85-35905
The nucleon intensity in the atmosphere and the Pt distribution
[HE-3.1-9] N85-35907
Connection between variations of the atmosphere temperature profile and variations of the meson component intensity
[HE-3.1-12] N85-35910
Search for anomalous C-jets in Chacaltaya emulsion chamber experiment
[HE-3.2-5] N85-35913
Scaling violation in hadron-nucleus interaction
[HE-3.2-8] N85-35916
Few-particles generation channels in inelastic hadron-nuclear interactions at energy approximately equals 400 GeV
[HE-3.2-9] N85-35917
A cosmic ray super high multicore family event. 1: Experiment and general features
[HE-3.4-1] N85-35930
A cosmic ray super high energy multicore family event. 2: Structure and fragmentation characteristics of the jets
[HE-3.4-2] N85-35931
Observation of super high energy big family with large scale Fe emulsion chambers
[HE-3.4-3] N85-35932
A halo event created at 200 m above the Chacaltaya emulsion chamber
[HE-3.4-5] N85-35933
A binocular-type atmospheric interaction generating sequential exotic features
[HE-3.4-6] N85-35934
Gamma-hadron families and scaling violation
[HE-3.4-7] N85-35935
Super-family P2 C-96-125 observed by Japan-URSS Joint Emulsion Chamber Experiment
[HE-3.4-8] N85-35936
On the halo events observed by Mount Fuji and Mount Kanbala Emulsion Chamber Experiments
[HE-3.4-9] N85-35937
Experiment Pamir-2. Fianit: A giant super-family with halo (Epsilon sub 0 at approximately 10(17) eV)
[HE-3.4-10] N85-35938
Experiment Pamir-4: Analysis of superfamily with halo of electromagnetic nature detected in deep XEC
[HE-3.4-11] N85-35939
Particle interactions at energies over 1000 TeV inferred from gamma-families observed at Mount Fuji
[HE-3.5-1] N85-35940
A search for mini-clusters in Japan-USSR Joint Experiment at Pamir
[HE-3.5-2] N85-35941
Mini-clusters
[HE-3.5-3] N85-35942
Giant mini-clusters as possible origin of halo phenomena observed in super-families
[HE-3.5-4] N85-35943
Structure of super-families
[HE-3.5-7] N85-35944
Extremely high energy hadron and gamma-ray families(3). Core structure of the halo of superfamily
[HE-3.5-8] N85-35945
Numerical analysis of electromagnetic cascades in emulsion chambers
[HE-3.5-9] N85-35946
An experimental study of correlations in the development of the electron-photon cascades
[HE-3.5-10] N85-35947
The electromagnetic component of albedo from superhigh energy cascades in dense media
[HE-3.5-11] N85-35948
Integral functions of electron lateral distribution and their fluctuations in electron-photon cascades
[HE-3.5-12] N85-35949
Nineteenth International Cosmic Ray Conference. HE Sessions, volume 7
[NASA-CP-2376-VOL-7] N85-35968
Measurement of the local density spectrum
N85-35984
An underground cosmic ray muon telescope for observation of cosmic ray anisotropy N85-36037
Investigation of cosmic rays in very short time scales
[HE-4.6-7] N85-36044
Nineteenth International Cosmic Ray Conference. HE sessions, volume 8
[NASA-CP-2376-VOL-8] N85-36066
Preliminary results on underground muon bundles observed in the Frejus proton-decay detector
[HE-5.1-1] N85-36067
The spectrum of cosmic ray muons obtained with 100-ton scintillation detector underground and the analysis of recent experimental data
[HE-5.1-6] N85-36071
A new world survey expression for cosmic ray vertical intensity vs. depth in standard rock
[HE-5.1-10] N85-36073
On muon energy spectrum in muon groups underground
[HE-5.1-14] N85-36076
Energy spectrum of cascades generated by muons in Baksan underground scintillation telescope
[HE-5.1-15] N85-36077
Underwater measurements of muon intensity
[HE-5.1-16] N85-36078
The Nagoya cosmic-ray muon spectrometer 3, part 1: Preliminary observations
[HE-5.2-2] N85-36080
The Nagoya cosmic-ray muon spectrometer 3, part 3: Automatic film scanning equipment
[HE-5.2-4] N85-36082
The Nagoya cosmic-ray muon spectrometer 3, part 4: Track reconstruction method
[HE-5.2-5] N85-36083
Background light measurements at the DUMAND site
[HE-5.2-7] N85-36084
Measurements of light background at large depth in the ocean
[HE-5.2-8] N85-36085
Hybrid TLC-pair meter for the Sphinx Project
[HE-5.2-10] N85-36086
Proportional drift tubes for large area muon detectors
[HE-5.2-11] N85-36087
Analytical calculation of muon intensities under deep sea-water
[HE-5.2-16] N85-36092
The spectrum of neutrons at 60 hg m(-2)
[HE-5.2-20] N85-36096
Limits on deeply penetrating particles in the 10(17) eV cosmic ray flux
[HE-5.3-1] N85-36098
Results of low energy background measurements with the Liquid Scintillation Detector (LSD) of the Mont Blanc Laboratory
[HE-5.3-5] N85-36099
Geophysical searches for three-neutrino oscillations
[HE-5.3-9] N85-36103
Measurement of neutrino oscillations in MACRO experiment
[HE-5.3-10] N85-36104
Energy spectra of high energy atmospheric neutrinos
[HE-5.3-14] N85-36108
A search for cosmic sources of high energy neutrinos with small underground detectors
[HE-5.3-16] N85-36110
Neutrino astronomy and the atmospheric background
[HE-5.3-17] N85-36111
High-energy neutrinos from a lunar observatory
[HE-5.3-21] N85-36112
Angular distribution of muons produced by cosmic ray neutrinos in rock
[HE-5.3-24] N85-36115
Underground measurements on secondary cosmic rays
[HE-5.4-1] N85-36116
Atmospheric muons and neutrinos, and the neutrino-induced muon flux underground
[HE-5.4-7] N85-36118
Anomalies in cosmic rays: New particles versus charm?
[HE-5.4-9] N85-36120
Results of investigation of muon fluxes of superhigh energy cosmic rays with X-ray emulsion chambers
[HE-5.4-16] N85-36126
Search for magnetic monopoles using proportional counters filled with helium gas
[HE-6.1-1] N85-36127
Magnetic monopole search by 130 m(2)sr He gas proportional counter
[HE-6.1-2] N85-36128
Results of a search for monopoles and tachyons in horizontal cosmic ray flux
[HE-6.1-3] N85-36129

Monopole, astrophysics and cosmic ray observatory at Gran Sasso
[HE-6.1-4] N85-36130

COST ANALYSIS
Energy Efficient Engine Program technology benefit/cost study, volume 1
[NASA-CR-174766-VOL-1] N85-35197
Energy Efficient Engine Program technology benefit/cost study, volume 2
[NASA-CR-174766-VOL-2] N85-35198
Assessment of metal heating technologies for ferrous forging: A pilot study of the form value of natural gas
[PB85-204394] N85-35314
Investment justification of robotic technology in aerospace manufacturing. User's manual
[AD-A156193] N85-35410
DoD Value Engineering conference report. Value Engineering (VE): A tool that benefits line management. Part 3, Workshop A: VE in the program office
[AD-A156069] N85-35812
DoD Value Engineering conference report. Value Engineering (VE): A tool that benefits line management. Part 5, Workshop C: VEP/VECP administration, negotiation, and implementation
[AD-A156071] N85-35814
DoD Value Engineering conference report. Value Engineering (VE): A tool that benefits line management. Part 6, Workshop D: VE training-orientation
[AD-A156072] N85-35815

COST EFFECTIVENESS
Solar pond technology for Navy applications
[AD-A155877] N85-35488
Design for MISP: A multiple instruction stream shared pipeline processor
[AD-A156314] N85-35635

COST ESTIMATES
Attacking software crisis: A macro approach
[AD-A155846] N85-35645
Progress report on implementing the recommendations of the White House Science Council's Federal Laboratory Review Panel, volume 1
[PB85-185072] N85-35819

COST INCENTIVES
DoD Value Engineering conference report. Value Engineering (VE): A tool that benefits line management. Part 3, Workshop A: VE in the program office
[AD-A156069] N85-35812

COST REDUCTION
DoD Value Engineering conference report. Value Engineering (VE): A tool that benefits line management. Part 3, Workshop A: VE in the program office
[AD-A156069] N85-35812
DoD Value Engineering conference report. Value Engineering (VE): A tool that benefits line management. Part 5, Workshop C: VEP/VECP administration, negotiation, and implementation
[AD-A156071] N85-35814
DoD Value Engineering conference report. Value Engineering (VE): A tool that benefits line management. Part 6, Workshop D: VE training-orientation
[AD-A156072] N85-35815
DoD Value Engineering conference report. Value Engineering (VE): A tool that benefits line management. Part 7, Workshop E: VE in construction and architect engineer contracts
[AD-A156073] N85-35816

COUETTE FLOW
Couette flow of two fluids between concentric cylinders
[AD-A155827] N85-35376

COULOMB COLLISIONS
LPM effect and primary energy estimations
[HE-3.6-4] N85-35953
Result of Monte-Carlo simulation of electron-photon cascades in lead and layers of lead-scintillator
[HE-3.6-11] N85-35958
Structure of air shower disc near the core
[HE-4.7-2] N85-36053

COUPLING
Generation of stimulated emission in the soft X-ray range by nonlinear processes with excimer lasers
[DE85-012465] N85-35403
Applications of the Galerkin formalism in the coupling of the earth's free oscillations N85-35514
Study to assess the effects of magnetohydrodynamic electromagnetic pulse on electric power systems, phase 1, volume 3
[DE85-011301] N85-35771

COVARIANCE
Two-point closure study of covariance budgets for turbulent Rayleigh-Benard convection
[PB85-189108] N85-35568

CRAB NEBULA
High energy radiation from neutron stars
[DE85-014353] N85-35843

CRACK INITIATION
Computational techniques for fiber reinforced components N85-35250
Evaluation of the crack plane equilibrium model for predicting plastic fractures
[DE85-005558] N85-35431

CRACK PROPAGATION
Fatigue lives of specimens representing critical locations in Mirage 3 spars under Australian and Swiss test spectra
[ARL-STRUC-R-415] N85-35187
Effect of microstructure on the fatigue behavior of Fe-C-X alloys
[DE85-011749] N85-35285
Stress-intensity factors for circumferential surface cracks in pipes and rods under tension and bending loads
[NASA-TM-87594] N85-35424
On size effects in plane stress crack-growth resistance
[AD-A155926] N85-35426
Evaluation of the crack plane equilibrium model for predicting plastic fractures
[DE85-005558] N85-35431
Subcritical fracture propagation in rocks: An examination using the methods of fracture mechanics and non-destructive testing N85-35516

CRACKS
Damage induced stress redistribution in composite laminates N85-35235
On size effects in plane stress crack-growth resistance
[AD-A155926] N85-35426

CRASHWORTHINESS
Design and testing of an energy-absorbing crewseat for the F/FB-111 aircraft. Volume 2: Data from seat testing
[NASA-CR-3917] N85-35184

CROSS FLOW
Wingtip vortex propeller
[NASA-CASE-LAR-13019-1] N85-35194

CRUISE MISSILES
Computer simulation of a cruise missile using brushless dc motor fin control
[AD-A155935] N85-35349
Application of pulsed power in the simulation of severe natural lightning
[DE85-012866] N85-35564

CRUSHING
Single-point diamond crushing of Zerodur with in-situ polishing and metrology on a diamond turning machine
[DE85-012918] N85-35305

CRUSTAL FRACTURES
Subcritical fracture propagation in rocks: An examination using the methods of fracture mechanics and non-destructive testing N85-35516
Groundwater radon studies for earthquake precursors in southern California
[PB85-196871] N85-35529

CRUSTS
Cobalt-rich ferromanganese crusts in the oceans N85-35444

CRYOGENIC EQUIPMENT
Results of variable enthalpy tests of CPR-488 TIP panels in MSFC Hot Gas Facility
[NASA-CR-170889] N85-35237

CRYOGENICS
Cryogenic laser calorimetry for impurity analysis
[NASA-CR-176179] N85-35395
Solid neon sources for plasma and X-ray lasers
[DE85-011347] N85-35402

CRYSTAL DEFECTS
Simulation of lattice damage due to dynamic loading
[DE85-008468] N85-35808

CRYSTAL GROWTH
Crystallization of Polyetheretherketone (PEEK) in carbon fiber composites
[AD-A156316] N85-35252
Investigations of the molecular beam epitaxial growth and characteristics of external excitation induced non-equilibrium phases of immiscible 3-5 compound semiconductors
[AD-A156325] N85-35804

CRYSTAL LATTICES
Simulation of lattice damage due to dynamic loading
[DE85-008468] N85-35808

CRYSTAL STRUCTURE
Cluster variation study of coherent ordering in FCC and BCC solid solutions
[AD-A156039] N85-35280
Ionic crystals
[DE85-009482] N85-35809

CRYSTAL SURFACES
Characterization of catalysts with metal-support effects and of the species adsorbed on their surfaces
[DE85-012254] N85-35394

CRYSTALLIZATION
Crystallization of Polyetheretherketone (PEEK) in carbon fiber composites
[AD-A156316] N85-35252
High temperature corrosion of ceramics
[DE85-013481] N85-35303
A new drawing technique for nylon 6 by reversible plasticization with iodine
[AD-A156272] N85-35803

CRYSTALS
Characterization of catalysts with metal-support effects and of the species adsorbed on their surfaces
[DE85-012254] N85-35394
Search for supermassive magnetic monopoles using mica crystals
[HE-6.1-8] N85-36134

CULTURE TECHNIQUES
Production of butanol by fermentation in the presence of cocultures of clostridium
[NASA-CASE-NPO-16203-1] N85-35227

CUMULATIVE DAMAGE
Damage mechanisms in damaged CFRP laminates N85-35249

CURING
Chemoviscosity modeling for thermosetting resins, 2
[NASA-CR-177958] N85-35243

CURRENT AMPLIFIERS
Multi-channel pulser for the SLC thermionic electron source
[DE85-014222] N85-35792

CURRENT DENSITY
Electrochemical method for investigation of the susceptibility of corrosion-resistant steels to intercrystalline corrosion
[BLL-CE-TRANS-8082-(9022.09)] N85-35269
Effect of Cu4Ti compound formation on the characteristics of NbTi accelerator magnet wire
[DE85-014226] N85-35788
Current interruption by density depression
[DE85-013120] N85-35846

CURTAINS
Results of tests on a specimen of the SRB aft skirt heat shield curtain in the MSFC LRLF
[NASA-CR-170883] N85-35221
Results of tests of the SRB aft skirt heat shield curtain in the MSFC Hot Gas Facility
[NASA-CR-170888] N85-35223

CURVATURE
RF stabilization of interchange-ballooning modes
[DE85-012080] N85-35353

CURVE FITTING
A new world survey expression for cosmic ray vertical intensity vs. depth in standard rock
[HE-5.1-10] N85-36073

CUTTERS
Action of wear-inhibiting Al2O3-coatings when applied to hard metal cutting tools
[BLL-RISLEY-TR-5041-(9091.9F)] N85-35292

CYCLIC LOADS
Static and cyclic behavior of semi-rigid steel beam-column connections
[PB85-194363] N85-35433

CYCLOGENESIS
Surface cyclogenesis as indicated by satellite imagery
[PB85-191815] N85-35566

CYCLOTRON FREQUENCY
Generalized reduced fluid model with finite ion-gyroradius effects
[DE85-013123] N85-35777
Proposed FRX-D experiment
[DE85-012766] N85-35778

CYGNUS CONSTELLATION
The identification of gamma ray induced EAS
[HE-4.5-1] N85-36026

CYLINDRICAL ANTENNAS
Cylindrical lens-array antenna for wideband electronic scanning
[AD-A156085] N85-35350

CYLINDRICAL BODIES
Vibrations of free hollow circular cylindrical bodies N85-35418
A towed instrument vehicle for deep ocean sampling
[AD-A156322] N85-35576
Acoustic resonances in cylinder bundles oscillating in a compressible fluid
[DE85-004066] N85-35609

D

D REGION
Ion composition measurements of the disturbed and quiet D-region in 1980 - 1981
[AD-A156055] N85-35521

DAMAGE
Damage induced stress redistribution in composite laminates N85-35235
Fuel containment and damage tolerance for large composite primary aircraft structures. Phase 1: Testing [NASA-CR-166091] N85-35241
Fatigue damage detection in steels by optical correlation [AD-A155830] N85-35277
Static and cyclic behavior of semi-rigid steel beam-column connections [PB85-194363] N85-35433
Three-dimensional finite deformation viscoelastic model accounting for damage effects [DE85-012951] N85-35660
Thermal hydraulic features of the TMI accident [DE85-014569] N85-35747
DAMPING
A research program to reduce the interior noise in general aviation aircraft, index and summary [NASA-CR-176178] N85-35695
Accelerator physics measurements at the damping ring [DE85-013373] N85-35785
TOSCA calculations and measurements for the SLAC SLC damping ring dipole magnet [DE85-014366] N85-35793
DAMS
National program for inspection of non-federal dams. Woodward reservoir dam (VT 00209), Connecticut River Basin, Plymouth, Vermont. Phase 1 inspection report [AD-A156256] N85-35693
DATA ACQUISITION
Miniature infra-red data acquisition and telemetry system [NASA-CR-177953] N85-35390
Federal Mineral Land Information System N85-35459
A Programmable Automatic Noise Data and Other Related parameter Acquisition system (PANDORA) — wind energy converters N85-35479
Incorporating meteorological data into receptor analysis: RAPS (Regional Air Pollution Study) revisited [PB85-188944] N85-35503
Development and operation of a measuring data acquisition system for use in light airplanes N85-35556
Airborne Investigations of Mesoscale Convective Systems (AIMCS), 1984: Operational summary and data inventory [PB85-187904] N85-35571
Users guide for optimum interpolation method of global data assimilation [AD-A155929] N85-35648
Operations considerations in designing a high speed multi-channel data acquisition system [DE85-012840] N85-35756
Data acquisition system for phase-2 KGF proton decay experiment [HE-6.2-4] N85-36140
DATA BASE MANAGEMENT SYSTEMS
DSS/MIS (Decision Support Systems/Management Information Systems) design and implementation for LAMPS Mk 3 utilizing a microcomputer and a maintenance personnel assignment program [AD-A155852] N85-35629
Prototyping with data dictionaries for requirements analysis [AD-A156303] N85-35654
EPALIT: A data management system applied to the control and retrieval of technical reports [PB85-193068] N85-35828
DATA BASES
Applications of the mineral resources data system and the international strategic minerals inventory in mineral-resource assessments by region and commodity N85-35451
The NORDA/FNOC (Naval Ocean Research and Development Activity's/Fleet Numerical Oceanography Center) Polar Ice Prediction System (PIPS)-Arctic: A technical description [AD-A156332] N85-35577
LOCAT: A data retrieval program [AD-A156004] N85-35822
Source header list, supplement 3 [AD-A156100] N85-35824
DATA COMPRESSION
Noiseless coding for the Gamma Ray spectrometer [NASA-CR-176201] N85-35219
Raster functionality for a VDI [DE85-006734] N85-35396
DATA CONVERSION ROUTINES
CRAYCDC [NASA-CR-177374] N85-35639
CDCCRAY [NASA-CR-177375] N85-35640
Two methods of global data assimilation [AD-A155981] N85-35684
DATA PROCESSING
Aspects of input signal design for order and parameter estimation in linear dynamical systems [ER-83/05] N85-35362
Adaptive rezoner in a two-dimensional Lagrangian hydrodynamic code [DE85-010108] N85-35381
Federal Mineral Land Information System N85-35459
Gravity gradiometer survey data processing [AD-A156165] N85-35522
An approach to determining computer security requirements for Navy systems [AD-A155750] N85-35627
Optimize computer throughput using array processors [AD-A155843] N85-35628
Using an LSI-11/23 and RT-11 to digitize analog tapes [DE85-012736] N85-35656
Analysis of two-parameter constant background born inversion for acoustic synthetic data [AD-A156394] N85-35698
Data processing professionals and DP application users' perceptions and expectations of operational roles of persons working in a DP/application user interface group N85-35821
Investigation of cosmic rays in very short time scales [HE-4.6-7] N85-36044
DATA RECORDING
Error message recording and reporting in the SLC control system [DE85-013057] N85-35664
DATA REDUCTION
Three-dimensional gravity ideal body studies in rough terrain [DE85-014097] N85-35525
Users guide for optimum interpolation method of global data assimilation [AD-A155929] N85-35648
DATA RETRIEVAL
Federal Mineral Land Information System N85-35459
EPALIT: A data management system applied to the control and retrieval of technical reports [PB85-193068] N85-35828
DATA SMOOTHING
Smoothing surface data by spline functions [AD-A155829] N85-35678
Two methods of global data assimilation [AD-A155981] N85-35684
DATA TRANSMISSION
Optimizing data access in the LAMPF control system [DE85-012653] N85-35663
Investigation of cosmic rays in very short time scales [HE-4.6-7] N85-36044
DEATH VALLEY (CA)
Geology: Structural history and fluvial geomorphology of the southern Death Valley Fault Zone, Inyo and San Bernardino Counties, California N85-35506
DECAY
Pulsed-neutron-source models for the astrophysical s-process [DE85-012927] N85-35740
High energy physics at Tufts University [DOE/ER-40085/7] N85-35744
On mini-cluster observed by Chacaltaya emulsion chamber experiment [HE-3.6-12] N85-35959
A study of atmospheric neutrinos with the IMB detector [HE-5.3-7] N85-36101
Energy spectra of high energy atmospheric neutrinos [HE-5.3-14] N85-36108
A standard source for high energy neutrino astronomy [HE-5.3-15] N85-36109
DECAY RATES
Some nuclear data needs in astrophysics [DE85-012916] N85-35842
DECELERATION
Deceleration of a supersonic flow behind a curved shock wave with isentropic precompression [NASA-TM-77920] N85-35164
Applications of decelerated ions [DE85-011832] N85-35767
DECISION MAKING
Manual and computer-aided sequential diagnostic inference [AD-A156229] N85-35620
DSS/MIS (Decision Support Systems/Management Information Systems) design and implementation for LAMPS Mk 3 utilizing a microcomputer and a maintenance personnel assignment program [AD-A155852] N85-35629
DECODERS
Noiseless coding for the Gamma Ray spectrometer [NASA-CR-176201] N85-35219
DECODING
L-step sequential decoding [AD-A156121] N85-35649
Pruned error-trellis decoding of certain non-systematic convolutional codes [AD-A156122] N85-35650
DEFENSE PROGRAM
DoD Value Engineering conference report. Value Engineering (VE): A tool that benefits line management. Part 4, Workshop B: VE on spare parts [AD-A156070] N85-35813
DoD Value Engineering conference report. Value Engineering (VE): A tool that benefits line management. Part 7, Workshop E: VE in construction and architect engineer contracts [AD-A156073] N85-35816
DEFORMATION
Solid-state co-extrusion of nylon 6 gel [AD-A156187] N85-35298
Strain measurement using point recognition picture processing [DRIC-T-7407] N85-35421
Response of a BWR Mark 2 containment vessel head to loads beyond the design basis [DE85-010524] N85-35432
Geology: Structural history and fluvial geomorphology of the southern Death Valley Fault Zone, Inyo and San Bernardino Counties, California N85-35506
Structural development of the west-central Grant Range, Nye County, Nevada N85-35508
Three-dimensional finite deformation viscoelastic model accounting for damage effects [DE85-012951] N85-35660
DEGREES OF FREEDOM
Identification and control of structures in space [NASA-CR-176175] N85-35214
On mini-cluster observed by Chacaltaya emulsion chamber experiment [HE-3.6-12] N85-35959
DEHYDRATION
Thirst and fluid intake following graded hypohydration levels in humans [AD-A156201] N85-35615
DELAMINATING
Damage induced stress redistribution in composite laminates N85-35235
Damage mechanisms in damaged CFRP laminates N85-35249
Computational techniques for fiber reinforced components N85-35250
DELAY
FAA requirements for model to support capacity, delay, noise and energy programs [AD-A155815] N85-35179
DELTA WINGS
Vortex boundary-layer interactions [NASA-CR-176192] N85-35373
DELTAS
Depositional systems and coal occurrence in the Fort Union Formation (Paleocene), Powder River Basin, Wyoming and Montana N85-35505
DENMARK
Siting of large scale wind turbines in Denmark N85-35483
DENSIFICATION
Computational methods for the explosive and impact compaction of powders [AD-A156219] N85-35653
DENSITY DISTRIBUTION
Average features of the muon component of EAS or = 10(17) eV [HE-4.3-10] N85-36004
Transition effect of air shower particles in plastic scintillators [HE-4.4-9] N85-36017
DENSITY MEASUREMENT
The lateral distributions of charged particles of energy greater than 0.3 E sub crit in electron-photon cascades in lead and air [HE-3.6-10] N85-35957
Properties of 10 (18)-10 (19)eV EAS at far core distance [HE-4.7-3] N85-36054
DENTISTRY
Dental multi-purpose slowspeed handpieces test and evaluation [AD-A155764] N85-35606
DEOXYRIBONUCLEIC ACID
Molecular biology of environmental aromatic hydrocarbons [DE85-015036] N85-35593
DEPOSITION
Depositional systems and coal occurrence in the Fort Union Formation (Paleocene), Powder River Basin, Wyoming and Montana N85-35505

DEPTH MEASUREMENT
Analysis of Cerenkov pulses recorded simultaneously at two sites
[HE-4.4-16] N85-36022
DESIGN ANALYSIS
SLC arc transport system: Magnet design and construction
[DE85-014289] N85-35789
SLC Energy Upgrade Program at SLAC
[DE85-014290] N85-35790
DESIGN TO COST
A towed instrument vehicle for deep ocean sampling
[AD-A156322] N85-35576
DESORPTION
Method for measuring surface activity of silicon nitride powder
[NASA-TM-77906] N85-35242
Evaluation: Close-range photogrammetry for slope inventory and monitoring
[PB85-192755] N85-35470
DESULFURIZING
Fluidized bed desulfurization
[NASA-CASE-NPO-15924-1] N85-35253
DETECTION
A preliminary evaluation of a failure detection filter for detecting and identifying control element failures in a transport aircraft
[NASA-TM-87576] N85-35204
The detection and study of molecular species using time resolved laser spectroscopy
[AD-A155910] N85-35256
Fatigue damage detection in steels by optical correlation
[AD-A155830] N85-35277
LANDSAT-4/5 image data quality analysis
[E85-10105] N85-35463
Literature search for new physical methods for biological aerosol detection
[AD-A155883] N85-35592
Edge detection and geometric methods in computer vision
[AD-A155873] N85-35630
Proceedings of the Workshop on Detectors for Relativistic Nuclear Collisions
[LBL-18225] N85-35700
Detectors for relativistic nuclear collisions (report from the Fixed-Target Hadron Group) N85-35701
Event parameters: Fixed targets N85-35702
Working group on penetrating probes at fixed target facilities N85-35703
Summary of the working group on penetrating probes in collider experiments. 1: The collider environment N85-35704
Report of working group on detectors for hadrons and event parameters at colliders N85-35705
Detector requirements for intensity interferometry measurements N85-35709
A holographic streamer chamber for relativistic nucleus-nucleus collision experiments N85-35710
A lead glass tubing drift calorimeter N85-35711
X-ray fluorescence analysis of uranium concentrates
[DE85-013189] N85-35717
Observation of super high energy big family with large scale Fe emulsion chambers
[HE-3.4-3] N85-35932
A halo event created at 200 m above the Chacaltaya emulsion chamber
[HE-3.4-5] N85-35933
A critical analysis of air shower structure functions and size spectrum measurements with the NBU air shower array N85-35983
Measurement of the local density spectrum N85-35984
Character of energy flow in air shower core N85-35985
Observation of EAS using a large water tank N85-35986
The development of air shower in the iron absorber N85-35987
Application of photodiodes to the detection of electromagnetic bursts N85-35988
High-energy neutrinos from a lunar observatory
[HE-5.3-21] N85-36112
Underground measurements on secondary cosmic rays
[HE-5.4-1] N85-36116
Modular detector for deep underwater registration of muons and muon groups
[HE-5.4-15] N85-36125
Application of thermoluminescence for detection of cascade shower 2: Detection of cosmic ray cascade shower at Mount Fuji
[HE-7.1-12] N85-36162
DETECTORS
The ISAVF opto-mechanical test bed
[NASA-TM-87505] N85-35206
Preliminary results on underground muon bundles observed in the Frejus proton-decay detector
[HE-5.1-1] N85-36067
DETERIORATION
Dissected motors-propellants motor number STM-012. Phase 15: Surveillance report, stage 1
[AD-A156088] N85-35226
DETONATION
Investigation of the lightning vulnerability of nuclear explosive test systems at the Nevada Test Site
[DE85-011761] N85-35563
Evaluation of nuclear detonation location capability under high attack scenario
[AD-A155761] N85-35729
DIAMONDS
Single-point diamond crushing of Zerodur with in-situ polishing and metrology on a diamond turning machine
[DE85-012918] N85-35305
DIAPHRAGMS (MECHANICS)
Tuning system for capacitively loaded 1/4 accelerating cavity
[DE85-012516] N85-35358
Hadrons registration in emulsion chamber with carbon block
[HE-3.7-3] N85-35962
DIELECTRIC POLARIZATION
Transient analysis of electromagnetic reflection from dispersive materials
[PB85-200186] N85-35753
DIELECTRICS
An experimental study of dielectric rod antennas for millimeter-wave imaging applications
[AD-A155832] N85-35328
DIESEL ENGINES
An analytical and numerical model of radiation heat transfer in direct injection-type diesel combustion N85-35368
DIFFERENCES
Width of nonlinear difference resonances
[DE85-013026] N85-35719
DIFFERENTIAL EQUATIONS
The application of bispectral analyses to aeroelastic phenomena N85-35157
Identification and control of structures in space
[NASA-CR-176175] N85-35214
Noise-sustained structure, intermittency and the Ginzburg-Landau equation
[DE85-009626] N85-35379
A new theory for multistep discretizations of stiff ordinary differential equations: Stability with large step sizes
[NASA-CR-177941] N85-35675
A new method for boundary value problems
[AD-A155934] N85-35683
DIFFRACTION
Optical receivers using rough reflectors
[NASA-CR-176200] N85-35750
DIFFUSE RADIATION
Literature search for new physical methods for biological aerosol detection
[AD-A155883] N85-35592
DIFFUSION
Noise in sodium beta alumina crystals
[AD-A156025] N85-35798
The nucleon intensity in the atmosphere and the Pt distribution
[HE-3.1-9] N85-35907
Development of electromagnetic cascades in the atmosphere including the Landau-Pomeranchuk-Migdal effect
[HE-4.5-5] N85-36029
Search for tachyons associated with extensive air showers in the ground level cosmic radiation
[HE-6.2-13] N85-36149
DIGITAL SIMULATION
A preliminary evaluation of a failure detection filter for detecting and identifying control element failures in a transport aircraft
[NASA-TM-87576] N85-35204
Computer simulation of a cruise missile using brushless dc motor fin control
[AD-A155935] N85-35349
DIGITAL SYSTEMS
Microprocessor-based single particle calibration of scintillation counter
[HE-4.6-13] N85-36049
DIGITAL TECHNIQUES
Processing of LANDSAT imagery to map surface mineral alteration on the Alaska Peninsula, Alaska N85-35455
Remote sensing of hydrologic transport processes using spot simulation data
[DE85-012412] N85-35467
DIMENSIONAL ANALYSIS
Computation of three-dimensional shock wave and boundary-layer interactions
[NASA-TM-86780] N85-35372
DIODES
Power flow evaluations for HERMES 3
[DE85-013116] N85-35769
Surface discharges as intense photon sources in the extreme ultraviolet
[DE85-012593] N85-35782
DIRECT CURRENT
Computer simulation of a cruise missile using brushless dc motor fin control
[AD-A155935] N85-35349
DIRECTIVITY
Properties of 10 (18)-10 (19)eV EAS at far core distance
[HE-4.7-3] N85-36054
Fast scintillation counter preamplifier for the observation of Linsley effect
[HE-4.7-9] N85-36060
Acoustic detection of air shower cores
[HE-7.1-4] N85-36158
DISARMAMENT
Arms control and The President's Strategic Defense Initiative
[AD-A156334] N85-35212
DISCONTINUITY
Characterization of microstrip discontinuities in the time and frequency domains
[NASA-CR-176190] N85-35342
DISLOCATIONS (MATERIALS)
HgCdTe surface and defect study program
[AD-A156079] N85-35799
DISPLACEMENT
Calibrator for displacement gages used in the rock mechanics laboratory
[DE85-013257] N85-35393
DISPLAY DEVICES
Raster functionality for a VDI
[DE85-006734] N85-35396
The human engineering eye movement measurement research facility
[AD-A156099] N85-35613
An exploratory study of the effect of screen size and resolution on the legibility of graphics in automated job performance aids
[AD-A155989] N85-35632
DISPOSAL
Records Disposal: A guidebook for laboratory offices
[AD-A156064] N85-35823
DISTANCE
Particle distributions in approximately 10(14) 10(16) eV air shower cores at sea level N85-35990
DISTANCE MEASURING EQUIPMENT
Analysis of Cerenkov pulses recorded simultaneously at two sites
[HE-4.4-16] N85-36022
DISTILLATION
Nitrogen analysis by chemiluminescence
[AD-A156197] N85-35308
DISTRIBUTION
Limits on deeply penetrating particles in the 10(17) eV cosmic ray flux
[HE-5.3-1] N85-36096
DISTRIBUTION (PROPERTY)
Distribution of computer functionality for accelerator control at the Brookhaven AGS
[DE85-012520] N85-35669
Resonance localization in tokamaks excited with ICRF waves
[DE85-014559] N85-35791
Integral functions of electron lateral distribution and their fluctuations in electron-photon cascades
[HE-3.5-12] N85-35949
Analysis of equi-intensity curves and NU distribution of EAS N85-35970
About increase of the large transvere momentum processes fraction in hA interactions at energies 5.10(14) - 10(16) eV according to the data on E.A.S. hadrons N85-35979
DISTRIBUTION FUNCTIONS
On the determination of the depth of EAS development maximum using the lateral distribution of Cerenkov light at distances 150 m from EAS axis
[HE-4.4-13] N85-36019
DIVERTERS
Neutral pumping rates for a next step tokamak ignition device
[DE85-012780] N85-35776
DIVING (UNDERWATER)
Preliminary results of an ALVIN dive program on active hydrothermal vents at the southern Juan de Fuca Ridge N85-35454
The research programme of the Institute for Aerospace Medicine N85-35596
The deep diving simulator TITAN: Physiological problems associated with staying in great depths of water N85-35604

DOCUMENT STORAGE
Records Disposal: A guidebook for laboratory offices
[AD-A156064] N85-35823
DOCUMENTATION
EPALIT: A data management system applied to the control and retrieval of technical reports
[PB85-193068] N85-35828
DOPPLER EFFECT
DMSK: A practical 2400-bps receiver for the mobile satellite service: An MSAT-X Report
[NASA-CR-176194] N85-35324
DOPPLER RADAR
A multi-channel radar receiver
[AD-A156058] N85-35333
Polarization diversity addition to the 10 centimeter Doppler weather radar
[AD-A156062] N85-35334
DRAG REDUCTION
An automated technique for encasing specific payloads with low-drag fairings N85-35183
Wingtip vortex propeller
[NASA-CASE-LAR-13019-1] N85-35194
DRIFT RATE
Fractional charge resolution in music N85-35712
Proportional drift tubes for large area muon detectors
[HE-5.2-11] N85-36087
DRYING
Method of preparing thin porous sheets of ceramic material
[DE85-006398] N85-35300
DYE LASERS
Infrared generation and wave-mixing studies in cesium
[DE85-012883] N85-35304
DYNAMIC CHARACTERISTICS
Analysis of flexible aircraft longitudinal dynamics and handling qualities. Volume 1: Analysis methods
[NASA-CR-177943-VOL-1] N85-35202
Analysis of flexible aircraft longitudinal dynamics and handling qualities. Volume 2: Data
[NASA-CR-177943-VOL-2] N85-35203
A new drawing technique for nylon 6 by reversible plasticization with iodine
[AD-A156272] N85-35803
DYNAMIC CONTROL
Design of dynamic compensators of prescribed pattern
[BU-109] N85-35674
Spreading the control complexity in decentralized control of interconnected systems
[BU-117] N85-35688
Decentralized stabilization by high gain feedback
[BU-115] N85-35689
DYNAMIC RESPONSE
The investigation of tethered satellite system dynamics
[NASA-CR-176180] N85-35215
DYNAMIC STRUCTURAL ANALYSIS
Structural analysis of imperfect three-legged truss columns for large space structures applications N85-35416
An evaluation of a class of practical optimization techniques for structural dynamics applications
[PB85-195766] N85-35434
DYNAMICAL SYSTEMS
The investigation of tethered satellite system dynamics
[NASA-CR-176180] N85-35215
Aspects of input signal design for order and parameter estimation in linear dynamical systems
[ER-83/05] N85-35362

E

EARTH (PLANET)
Applications of the Galerkin formalism in the coupling of the earth's free oscillations N85-35514
EARTH ALBEDO
The electromagnetic component of albedo from superhigh energy cascades in dense media
[HE-3.5-11] N85-35948
EARTH ATMOSPHERE
Propagation of cosmic rays through the atmosphere in the quark-gluon strings model N85-35873
Experimental basis for the models of cascade propagation in atmosphere
[HE-3.6-6] N85-35954
The lateral distributions of charged particles of energy greater than 0.3 E sub crit in electron-photon cascades in lead and air
[HE-3.6-10] N85-35957
Longitudinal trial functions and the cosmic ray energy scale N85-36014
Nuclear cascades in electromagnetic showers produced by primary gamma-quanta in the atmosphere
[HE-4.5-16] N85-36038
Air fluorescence detection of large air showers below the horizon
[HE-4.6-6] N85-36043
EARTH CRUST
Crustal structure in southern California from array data N85-35512
Groundwater radon studies for earthquake precursors in southern California
[PB85-196871] N85-35529
EARTH MANTLE
A dynamic model of Venus's gravity field
[NASA-CR-176173] N85-35845
EARTH MOVEMENTS
Seismic stratigraphic analysis of the Mississippi Fan N85-35507
EARTH RADIATION BUDGET EXPERIMENT
Space Station Polar Platform: Integrating research and operational missions
[PB85-195279] N85-35218
The 1986 National Aeronautics and Space Administration authorization
[GPO-47-635] N85-35829
EARTH RESOURCES
Microwave properties of a quiet sea
[NASA-CR-176199] N85-35322
USGS coastal research, studies and maps: A source of information for coastal decision making
[USGS-CIRC-883] N85-35465
Remote sensing of hydrologic transport processes using spot simulation data
[DE85-012412] N85-35467
EARTH SURFACE
Gravity gradiometer survey data processing
[AD-A156165] N85-35522
EARTHQUAKES
Crustal structure in southern California from array data N85-35512
Attenuation properties of the Petatlan region, Mexico, and a local magnitude scale for microearthquakes in this area N85-35513
Simplified procedures for the evaluation of settlements in sands due to earthquake shaking
[PB85-197887] N85-35527
Carbon fiber strainmeter studies in southern California
[PB85-196889] N85-35528
Groundwater radon studies for earthquake precursors in southern California
[PB85-196871] N85-35529
ECONOMIC ANALYSIS
Investment justification of robotic technology in aerospace manufacturing. User's manual
[AD-A156193] N85-35410
Solar pond technology for Navy applications
[AD-A155877] N85-35488
EDDY CURRENTS
Development of contactless sensors for industrial and automative applications
[BMFT-FB-T-85-031] N85-35400
EDGES
Edge detection and geometric methods in computer vision
[AD-A155873] N85-35630
Edge information in color images based on histograms of differences
[AD-A156002] N85-35751
EDITING ROUTINES (COMPUTERS)
Procedure for editing the fluxgate magnetometer data of the AFGL (Air Force Geophysics Laboratory) magnetometer network
[AD-A156331] N85-35523
EDUCATION
Development of NATOPS (Naval Air Training and Operating Procedure Standardization) performance software for the H-46D helicopter
[AD-A156089] N85-35190
Benchmark evaluation of PC simscript
[AD-A156133] N85-35651
Comet Halley returns: A teachers' guide 1985-1986
[NASA-EP-197] N85-35839
EFFICIENCY
Development of a high-efficiency, gas-fired, heat pipe, warm-air heating system
[PB85-199636] N85-35318
The NORDA/FNOC (Naval Ocean Research and Development Activity's/Fleet Numerical Oceanography Center) Polar Ice Prediction System (PIPS)-Arctic: A technical description
[AD-A156332] N85-35577
EGGS
Report of Amphibian Development Group N85-35583
EGRESS
Fire research publications, 1984
[PB85-206502] N85-35827
EIGENVALUES
Vibrations of free hollow circular cylindrical bodies N85-35418
EJECTION SEATS
Design and testing of an energy-absorbing crewseat for the F/FB-111 aircraft. Volume 2: Data from seat testing
[NASA-CR-3917] N85-35184
ELASTIC CYLINDERS
Second Colloquim on the Scattering of Ultrasonic Waves
[AD-A156298] N85-35697
ELASTIC DEFORMATION
Identification and control of structures in space
[NASA-CR-176175] N85-35214
ELASTIC PROPERTIES
Analysis of the nonlinear equations describing the elastic, thermal, and electromagnetic behavior of solids: Existence of solutions of semi-inverse problems N85-35415
Vibrations of free hollow circular cylindrical bodies N85-35418
(NAT)Fe(n,n'x) spectra at 65.5 MeV
[AD-A155776] N85-35730
Ionic crystals
[DE85-009482] N85-35809
ELASTIC SCATTERING
P(P bar)P elastic scattering and cosmic ray data
[HE-1.1-6] N85-35854
General consequences of the violated Feynman scaling N85-35872
ELECTRIC BATTERIES
Development and evaluation of sulfonated polysulfone membranes for the zinc-ferricyanide battery
[DE85-009104] N85-35357
Cationic exchange membrane for the zinc-ferricyanide battery
[DE85-013152] N85-35489
ELECTRIC CHARGE
Friction, impact, and electrostatic discharge sensitivities of energetic materials
[DE85-013321] N85-35309
ELECTRIC CONDUCTORS
Feasibility study of radar-transmitting materials
[AD-A155839] N85-35329
ELECTRIC CONTACTS
Noise in silver beta alumina ceramics
[AD-A156135] N85-35297
Computer simulation of a cruise missile using brushless dc motor fin control
[AD-A155935] N85-35349
Development of contactless sensors for industrial and automative applications
[BMFT-FB-T-85-031] N85-35400
ELECTRIC CURRENT
System expectations for Pioneer 1 foil implosion experiments
[DE85-014129] N85-35359
Current interruption by density depression
[DE85-013120] N85-35846
ELECTRIC DISCHARGES
Surface discharges as intense photon sources in the extreme ultraviolet
[DE85-012593] N85-35782
ELECTRIC EQUIPMENT
High Temperature Heating System (HTHS)
[PB85-188340] N85-35316
ELECTRIC FIELDS
Moment-method formulation of the cavity-probe aperture antenna
[DE85-013264] N85-35338
Injector losses on Mite
[DE85-012356] N85-35355
A lead glass tubing drift calorimeter N85-35711
High energy plasma accelerators
[DE85-013121] N85-35760
ELECTRIC FURNACES
High Temperature Heating System (HTHS)
[PB85-188340] N85-35316
ELECTRIC GENERATORS
Study to assess the effects of magnetohydrodynamic electromagnetic pulse on electric power systems, phase 1, volume 3
[DE85-011301] N85-35771
ELECTRIC MOTORS
Computer simulation of a cruise missile using brushless dc motor fin control
[AD-A155935] N85-35349
ELECTRIC POTENTIAL
Statistical distribution of breakdown voltages in rep-rate spark gaps
[DE85-012813] N85-35354
System expectations for Pioneer 1 foil implosion experiments
[DE85-014129] N85-35359
ELECTRIC POWER SUPPLIES
Applicability of 100kWe-class of space reactor power systems to NASA manned space station missions
[NASA-CR-174696] N85-35728

ELECTRICAL ENGINEERING
Center for Electronics and Electrical Engineering technical progress bulletin covering center programs, July-September with 1985 CEEE events calendar
[PB85-191393] N85-35363
ELECTRICAL FAULTS
Statistical distribution of breakdown voltages in rep-rate spark gaps
[DE85-012813] N85-35354
ELECTRICAL PROPERTIES
Electronic structure and lattice dynamics of dimensionally constrained and disordered solids
[AD-A155927] N85-35797
ELECTRICAL RESISTIVITY
Electrically conductive doped block copolymer of polyacetylene and polyisoprene
[DE85-006500] N85-35301
Conduction and aging of piezoelectric PZT ceramics N85-35346
Two-dimensional inversion of resistivity monitoring data from the Cerro Prieto geothermal field
[DE85-012554] N85-35494
ELECTRIFICATION
Electronic information management and productivity
[DE85-013362] N85-35818
ELECTROCATALYSTS
Method of preparing thin porous sheets of ceramic material
[DE85-006399] N85-35300
ELECTROCHEMISTRY
Chemistry division report
[DE85-010586] N85-35228
Electrochemical method for investigation of the susceptibility of corrosion-resistant steels to intercrystalline corrosion
[BLL-CE-TRANS-8082-(9022.09)] N85-35269
ELECTRODES
Thermodynamics of the corrosion of chromium in molten carbonates
[DE85-011407] N85-35282
Method of preparing thin porous sheets of ceramic material
[DE85-006399] N85-35300
Development of electrodes for the NASA iron/chromium
[NASA-CR-174724] N85-35471
ELECTROLYSIS
Deposition of nickel-cobalt alloys by controlled-potential electrolysis
[PB85-198562] N85-35291
ELECTROLYTES
Aqueous volatile weak electrolyte equilibria to 300 C
[DE85-013840] N85-35261
ELECTROMAGNETIC ABSORPTION
Dangling bonds and sub-gap optical absorption in silicon
[DE85-011752] N85-35302
Muons in gamma showers
[HE-4.5-3] N85-36027
ELECTROMAGNETIC COMPATIBILITY
Electromagnetic compatibility conference features biological interactions
[AD-A155813] N85-35692
ELECTROMAGNETIC FIELDS
Theory of mutual impedances and multiple reflections in an N-element array environment
[PB85-191419] N85-35364
Electromagnetic compatibility conference features biological interactions
[AD-A155813] N85-35692
ELECTROMAGNETIC INTERFERENCE
Actuator rigging test set electromagnetic interference test (CE03)
[AD-A155819] N85-35327
Center for Electronics and Electrical Engineering technical progress bulletin covering center programs, July-September with 1985 CEEE events calendar
[PB85-191393] N85-35363
ELECTROMAGNETIC NOISE
Noise in silver beta alumina ceramics
[AD-A156135] N85-35297
ELECTROMAGNETIC PROPERTIES
Analysis of the nonlinear equations describing the elastic, thermal, and electromagnetic behavior of solids: Existence of solutions of semi-inverse problems N85-35415
ELECTROMAGNETIC PULSES
Study to assess the effects of magnetohydrodynamic electromagnetic pulse on electric power systems, phase 1, volume 3
[DE85-011301] N85-35771
ELECTROMAGNETIC RADIATION
RF stabilization of interchange-ballooning modes
[DE85-012080] N85-35353
Theory of mutual impedances and multiple reflections in an N-element array environment
[PB85-191419] N85-35364
High energy radiation from neutron stars
[DE85-014353] N85-35843
Analytical-numerical methods of calculations of energy and three-dimensional particle distributions in electromagnetic cascades
[HE-3.5-13] N85-35950
The lateral distributions of charged particles of energy greater than 0.3 E sub crit in electron-photon cascades in lead and air
[HE-3.6-10] N85-35957
Result of Monte-Carlo simulation of electron-photon cascades in lead and layers of lead-scintillator
[HE-3.6-11] N85-35958
On mini-cluster observed by Chacaltaya emulsion chamber experiment
[HE-3.6-12] N85-35959
A comparative analysis of gamma and hadron families at the superhigh energies recorded in experiment Pamir
[HE-3.7-1] N85-35960
Structured events in Pamir carbon X-ray chambers
[HE-3.7-7] N85-35965
Peculiarities of gamma-quanta distribution at 20 TeV energy
[HE-3.7-10] N85-35967
ELECTROMAGNETIC SCATTERING
On the convergence of an iterative formulation of the electromagnetic scattering from an infinite grating of thin wires N85-35319
Penetrative nature of high energy showers observed in Chacaltaya emulsion chamber
[HE-3.3-5] N85-35923
Anomalous correlation between hadron and electromagnetic particles in hadron and gamma-ray families
[HE-3.3-6] N85-35924
ELECTROMAGNETIC SHIELDING
Actuator rigging test set electromagnetic interference test (CE03)
[AD-A155819] N85-35327
ELECTROMAGNETIC SPECTRA
The ISAVF opto-mechanical test bed
[NASA-TM-87505] N85-35206
ELECTROMAGNETISM
Moment-method formulation of the cavity-probe aperture antenna
[DE85-013264] N85-35338
ELECTROMAGNETS
Major facility overhauls at LAMPF
[DE85-012724] N85-35765
ELECTROMECHANICS
Supersonic flow with feeding of energy
[NASA-TM-77912] N85-35163
ELECTRON ACCELERATORS
Four stage HELIA experiment
[DE85-012026] N85-35768
Power flow evaluations for HERMES 3
[DE85-013116] N85-35769
ELECTRON AVALANCHE
LPM effect and primary energy estimations
[HE-3.6-4] N85-35953
ELECTRON BEAMS
Observations of accelerated high current low emittance beams in the SLC Linac
[DE85-013073] N85-35211
Four stage HELIA experiment
[DE85-012026] N85-35768
Power flow evaluations for HERMES 3
[DE85-013116] N85-35769
Kinetic loss experiments on Mite
[DE85-012826] N85-35780
Laser and electron beam processing of semiconductors
[AD-A155914] N85-35796
ELECTRON BUNCHING
Cerenkov radiation from periodic electron bunches for finite emission length in air
[AD-A156156] N85-35352
ELECTRON CAPTURE
Search for stellar collapse with the MACRO detector at Gran Sasso
[HE-5.3-11] N85-36105
ELECTRON DENSITY (CONCENTRATION)
Cerenkov radiation from periodic electron bunches for finite emission length in air
[AD-A156156] N85-35352
Los Alamos free-electron laser
[DE85-012666] N85-35405
Structured events in Pamir carbon X-ray chambers
[HE-3.7-7] N85-35965
Performance of a local electron density trigger to select extensive air showers at sea level
[HE-4.6-11] N85-36048
ELECTRON DENSITY PROFILES
Relation between gamma-ray family and EAS core: Monte-Carlo simulation of EAS core
[HE-3.6-7] N85-35955
Hadrons registration in emulsion chamber with carbon block
[HE-3.7-3] N85-35962
ELECTRON DIFFRACTION
Size and shape dependence of CO adsorption sites on sapphire supported Fe microcrystals
[NASA-CR-176171] N85-35794
ELECTRON DISTRIBUTION
The lateral distributions of charged particles of energy greater than 0.3 E sub crit in electron-photon cascades in lead and air
[HE-3.6-10] N85-35957
Structured events in Pamir carbon X-ray chambers
[HE-3.7-7] N85-35965
A new study of shower age distribution in near vertical showers by EAS air shower array N85-35996
Lateral distribution of electrons of air showers N85-35998
Detailed studies of the electron lateral distribution in extensive air showers with energies around 10(16) eV N85-35999
Study of muons near shower cores at sea level using the E594 neutrino detector N85-36000
Measurement of shower electrons and muons using a small air shower array
[HE-4.3-11] N85-36005
Monte Carlo simulation of EAS generated by 10(14) - 10(16) eV protons
[HE-4.3-14] N85-36008
Properties of 10 (18)-10 (19)eV EAS at far core distance
[HE-4.7-3] N85-36054
ELECTRON ENERGY
High-resolution spectroscopy and dynamics of multiphoton processes in atoms and molecules
[AD-A155862] N85-35714
Proposed FRX-D experiment
[DE85-012766] N85-35778
ELECTRON GUNS
Multi-channel pulser for the SLC thermionic electron source
[DE85-014222] N85-35792
ELECTRON IRRADIATION
Electron irradiation of N type cadmium telluride
[AD-A156117] N85-35801
ELECTRON MICROSCOPY
The preparation of TEM specimens showing oxide scales in transverse cross-section
[AERE-R-11579] N85-35276
Size and shape dependence of CO adsorption sites on sapphire supported Fe microcrystals
[NASA-CR-176171] N85-35794
ELECTRON MOBILITY
Air chemistry measurements 2
[AD-A156041] N85-35520
ELECTRON PHOTON CASCADES
High sensitive X-ray films to detect electron showers in 100 GeV region
[HE-3.1-13] N85-35911
Comparison of big event with calculations of the air shower development
[HE-3.6-8] N85-35956
Result of Monte-Carlo simulation of electron-photon cascades in lead and layers of lead-scintillator
[HE-3.6-11] N85-35958
Theoretical study of EAS hadronic structure N85-35991
Tskhra-Tskaro complex intended for the investigations of EAS spatial characteristics near axis N85-35995
Topological aspects of age parameter
[HE-4.3-13] N85-36007
Lateral-angular and temporal characteristics of EAS optical radiation
[HE-4.4-19] N85-36025
Energy spectrum of cascades generated by muons in Baksan underground scintillation telescope
[HE-5.1-15] N85-36077
ELECTRON SCATTERING
Analytical-numerical methods of calculations of energy and three-dimensional particle distributions in electromagnetic cascades
[HE-3.5-13] N85-35950
ELECTRON SPECTROSCOPY
Size and shape dependence of CO adsorption sites on sapphire supported Fe microcrystals
[NASA-CR-176171] N85-35794
ELECTRON STATES
Optical properties of heterostructures and superlattices
[AD-A156243] N85-35802

ELECTRON TRANSFER
Vectorial electron transfer on designed surfaces
[PB85-204600] N85-35263
ELECTRON TUBES
Los Alamos free-electron laser
[DE85-012666] N85-35405
ELECTRON TUNNELING
Design considerations for personnel access penetrations for the superconducting super collider
[DE85-013027] N85-35807
ELECTRONIC AIRCRAFT
DOD Value Engineering Conference report. Value Engineering (VE): A tool that benefits line management held at Leesburg, Virginia on 1-2 November 1984. Part 2. Plenary session
[AD-A156068] N85-35811
ELECTRONIC EQUIPMENT
Electronic information management and productivity
[DE85-013962] N85-35818
ELECTRONIC EQUIPMENT TESTS
Testbed for sensory control of intelligent machines
[DE85-012355] N85-35412
ELECTRONIC TRANSDUCERS
Development of position sensors for microcomputer-oriented sensor systems
[BMFT-FB-T-85-021] N85-35361
Materials and process development for microcomputer-compatible pressure, temperature, and position sensors
[BMFT-FB-T-85-024] N85-35399
ELECTRONS
Pulsed-neutron-source models for the astrophysical s-process
[DE85-012927] N85-35740
Studies of relativistic heavy ion collisions
[DE85-014686] N85-35745
Mini-clusters
[HE-3.5-3] N85-35942
Structure of super-families
[HE-3.5-7] N85-35944
Extremely high energy hadron and gamma-ray families(3). Core structure of the halo of superfamily
[HE-3.5-8] N85-35945
Numerical analysis of electromagnetic cascades in emulsion chambers
[HE-3.5-9] N85-35946
An experimental study of correlations in the development of the electron-photon cascades
[HE-3.5-10] N85-35947
Integral functions of electron lateral distribution and their fluctuations in electron-photon cascades
[HE-3.5-12] N85-35949
Electrons, muons and hadrons in extensive air showers and how do they depend on nuclear interaction model, part 2
N85-35969
Electrons, muons and hadrons in extensive air showers and how do they depend on nuclear interaction model, part 1
N85-35972
Sensitivity of depth of maximum and absorption depth of EAS to hadron production mechanism N85-35982
A critical analysis of air shower structure functions and size spectrum measurements with the NBU air shower array N85-35983
Missing energies at pair creation
[HE-4.4-8] N85-36016
The hump in the Cerenkov lateral distribution of gamma ray showers
[HE-4.5-9] N85-36032
Simulation of gamma-initiated showers
[HE-4.5-10] N85-36033
Phenomenological characteristic of the electron component in gamma-quanta initiated showers
[HE-4.5-11] N85-36034
Nuclear cascades in electromagnetic showers produced by primary gamma-quanta in the atmosphere
[HE-4.5-16] N85-36038
Longitudinal development of muons in large air showers studies from the arrival time distributions measured at 900m above sea level
[HE-4.7-4] N85-36055
Arrival time distributions of electrons in air showers with primary energies above 10 (18)eV observed at 900m above sea level
[HE-4.7-5] N85-36056
Analysis of the electron component of EAS at observational level 700 g x cm(-2) with a scale breaking interaction model and gammaisation hypothesis
[HE-5.4-8] N85-36119
Study of photonuclear muon interactions at Baksan underground scintillation telescope
[HE-5.4-10] N85-36122
Collimated groups of particles as possible manifestation of heavy meson production
[HE-5.4-14] N85-36124
ELECTROSTATIC PRECIPITATORS
A study of the control of particulate emissions from turbine engine test cells N85-35205
ELECTROSTATICS
Friction, impact, and electrostatic discharge sensitivities of energetic materials
[DE85-013321] N85-35309
The effect of power law body forces on a thermally-driven flow between concentric rotating spheres
[NASA-TM-87596] N85-35374
Two-dimensional quasineutral description of particles and fields above discrete auroral arcs
[NASA-CR-176170] N85-35517
ELEMENTARY PARTICLE INTERACTIONS
Nucleon-nucleus interactions from JACEE
N85-35869
ELEMENTARY PARTICLES
The identification of gamma ray induced EAS
[HE-4.5-1] N85-36026
ELLIPSES
Use of a minimum-ellipse criterion in the study of ion-beam extraction systems
[DE85-012670] N85-35721
ELLIPTIC DIFFERENTIAL EQUATIONS
Absorbing boundary conditions for exterior problems
[NASA-CR-177944] N85-35676
ELLIPTICAL PLASMAS
Elliptical X-ray analyzer spectrograph application to a laser-produced plasma
[DE85-013790] N85-35398
EMERGENCIES
Fire service emergency management handbook
[AD-A155780] N85-35313
EMISSION
Results on nucleon life-time from the Kolar gold field experiment
[HE-6.2-3] N85-36139
EMISSION SPECTRA
The structure of Herbig-Haro object 43 and Orion dark cloud extinction
[NASA-TM-87503] N85-35831
The ionization structure of planetary nebulae. Part 4: NGC 7662
[NASA-CR-176151] N85-35844
EMITTANCE
Observations of accelerated high current low emittance beams in the SLC Linac
[DE85-013073] N85-35211
Beam potential measurement of an intense H(-) beam by use of the emissive probe technique
[DE85-012671] N85-35762
High resolution beam profile monitors in the SLC
[DE85-013375] N85-35774
Relation between field energy and RMS emittance in intense particle beams
[DE85-012655] N85-35784
EMPLOYEE RELATIONS
Data processing professionals and DP application users' perceptions and expectations of operational roles of persons working in a DP/application user interface group N85-35821
EMULSIONS
Multidimensional analysis of data obtained in experiments with X-ray emulsion chambers and extensive air showers
[HE-3.6-2] N85-35951
A new method of differential structural analysis of gamma-family basic parameters
[HE-3.6-3] N85-35952
Hadrons registration in emulsion chamber with carbon block
[HE-3.7-3] N85-35962
Structured events in Pamir carbon X-ray chambers
[HE-3.7-7] N85-35965
Ultra high energy events in ECHOS series and primary energy spectrum
[HE-3.7-9] N85-35966
Search for anomalons using plastic nuclear track detectors
[HE-6.2-12] N85-36148
Observation of genetic relation among new phenomena Geminion, Chiron and mini-Centauro
[HE-6.2-16] N85-36152
Detection threshold energy of high energy cascade showers using thermoluminescence PTFE-sheet and hot-gas reader
[HE-7.1-5] N85-36159
Application of thermoluminescence for detection of cascade shower 2: Detection of cosmic ray cascade shower at Mount Fuji
[HE-7.1-12] N85-36162
ENERGETIC PARTICLES
Multiple vacancy production by high energy heavy ions
[DE85-004428] N85-35805
A search for heavy long lived particles in high energy cosmic rays
[HE-6.2-7] N85-36143
ENERGY ABSORPTION
Design and testing of an energy-absorbing crewseat for the F/FB-111 aircraft. Volume 2: Data from seat testing
[NASA-CR-3917] N85-35184
ENERGY CONSERVATION
Energy Efficient Engine Program technology benefit/cost study, volume 2
[NASA-CR-174766-VOL-2] N85-35198
Comparative analysis of operational forecasts versus actual weather conditions in airline flight planning, volume 1
[NASA-CR-167862] N85-35534
Comparative analysis of operational forecasts versus actual weather conditions in airline flight planning, volume 2
[NASA-CR-167863] N85-35535
Comparative analysis of operational forecasts versus actual weather conditions in airline flight planning, volume 3
[NASA-CR-167864] N85-35536
Comparative analysis of operational forecasts versus actual weather conditions in airline flight planning, volume 4
[NASA-CR-167865] N85-35537
Comparative analysis of operational forecasts versus actual weather conditions in airline flight planning: Summary report
[NASA-CR-167866] N85-35538
Turbulent structure of stably stratified nocturnal slope flows
[AD-A155845] N85-35559
Phase space factors in multiparticle processes
N85-35888
ENERGY CONVERSION
Energy from low temperature differences
[DE85-008817] N85-35492
ENERGY CONVERSION EFFICIENCY
Energy Efficient Engine Program technology benefit/cost study, volume 1
[NASA-CR-174766-VOL-1] N85-35197
ENERGY DISSIPATION
Prediction of turbulent internal recirculating flows with K-epsilon models N85-35366
Turbulent structure of stably stratified nocturnal slope flows
[AD-A155845] N85-35559
Proposed FRX-D experiment
[DE85-012766] N85-35778
Experimental evidence of the decrease of kinetic energy of hadrons in passing through atomic nuclei
N85-35880
Analytical calculation of muon intensities under deep sea-water
[HE-5.2-16] N85-36092
Photo nuclear energy loss term for muon-nucleus interactions based on xi scaling model of QCD
[HE-5.2-17] N85-36093
Range fluctuations of high energy muons passing through matter
[HE-5.2-19] N85-36095
Results from the UCSD magnetic monopole search
[HE-6.1-12] N85-36137
ENERGY DISTRIBUTION
Status of the zeta(8.3)
[DE85-013070] N85-35724
Lateral distribution of high energy hadrons and gamma ray in air shower cores observed with emulsion chambers
[HE-3.3-8] N85-35926
Size distributions of air showers accompanied with high energy gamma ray bundles observed at Mt. Chacaltaya
[HE-3.3-9] N85-35927
Comparison of absolute intensity between EAS with gamma-families and general EAS at Mount Norikura
[HE-3.3-11] N85-35929
Analytical-numerical methods of calculations of energy and three-dimensional particle distributions in electromagnetic cascades
[HE-3.5-13] N85-35950
Comparison of big event with calculations of the air shower development
[HE-3.6-8] N85-35956
Character of energy flow in air shower core
N85-35985
The development of air shower in the iron absorber
N85-35987
Longitudinal trial functions and the cosmic ray energy scale N85-36014
Primary chemical composition from simultaneous recording of muons induced cascades and accompanying muon group underground
[HE-5.1-13] N85-36075

On method of muon spectrum measurements by the scintillation detectors of a large thickness T4t sub o
[HE-5.2-18] N85-36094
Characteristics of slow particles emitted in the charged current interactions of neutrinos with emulsion nuclei
[HE-5.3-22] N85-36113
Relationship of sea level muon charge ratio to primary composition including nuclear target effects
[HE-5.4-10] N85-36121

ENERGY LEVELS

Gamma-ray production cross sections for alpha-particle induced reactions on F-19 and Na-23
[DE85-012603] N85-35732
Standard value for the radiation length in air
[HE-4.4-4] N85-36013

ENERGY POLICY

Implementing agreement for cooperation in the development of large scale wind energy conversion systems
[JUEL-SPEZ-278] N85-35473
General environmental aspects of large scale wind energy utilization N85-35474
Environmental aspects of large-scale wind-power systems in the UK N85-35478
Visit to test facility Stoetten (West Germany) May 9, 1984, including the Voith Wind Energy Converter (WEC) 520 turbine. The annual production of various wind energy plants in selected locations N85-35487

ENERGY SOURCES

Atmospheric neutrinos observed in underground detectors
[HE-5.3-8] N85-36102
Geophysical searches for three-neutrino oscillations
[HE-5.3-9] N85-36103

ENERGY SPECTRA

Scale separation closure and Alfven wave turbulence
[DE85-013124] N85-35385
Los Alamos free-electron laser
[DE85-012666] N85-35405
(NAT)Fe(n,n'x) spectra at 65.5 MeV
[AD-A155776] N85-35730
Some rigorous results concerning spectral theory for ideal MHD
[DE85-013427] N85-35770
Proton-air and proton-proton cross sections from air shower data
[HE-1.1-1] N85-35849
Proton-air inelastic cross section at S(1/2) = 30 TeV
[HE-1.1-2] N85-35850
Hadron cross sections at ultra high energies and unitarity bounds on diffraction dissociation
[HE-1.1-3] N85-35851
On total cross sections and slopes at superhigh energies
[HE-1.1-4] N85-35852
On a possibility of inelasticity partial coefficient K sub gamma determination in pi C and pi Pb interactions at 10 to the 14th power eV (experiment PAMIR 1)
[HE-1.1-12] N85-35859
1Single particle momentum and angular distributions in hadron-hadron collisions at ultrahigh energies
[HE-1.2-1] N85-35860
Empirical description of the hadron-hadron and hadron-nucleus interaction at the accelerator energy range
[HE-1.2-4] N85-35862
Angular distribution and multiplicity of backward hadrons in hFe interactions at 0.5-5.0 TeV energies (PION Experiment)
[HE-1.2-8] N85-35866
Scaling violation in the fragmentation region of inclusive nucleon spektrum N85-35874
Intensities of high-energy cosmic rays at Mount Kanbala
[HE-3.1-2] N85-35902
High energy gamma-rays and hadrons at Mount Fuji
[HE-3.1-3] N85-35903
Hadron intensity and energy spectrum at 4380 m above level
[HE-3.1-7] N85-35905
The nucleon intensity in the atmosphere and the Pt distribution
[HE-3.1-9] N85-35907
Energy spectra of proton and nuclei of primary cosmic rays in energy region 10 TeV/particle
[HE-3.1-10] N85-35908
Atmospheric interactions detected in both the upper and the lower chambers at Chacaltaya
[HE-3.3-7] N85-35925
A cosmic ray super high multicore family event. 1: Experiment and general features
[HE-3.4-1] N85-35930
Observation of super high energy big family with large scale Fe emulsion chambers
[HE-3.4-3] N85-35932
Super-family P2 C-96-125 observed by Japan-URSS Joint Emulsion Chamber Experiment
[HE-3.4-8] N85-35936
Integral functions of electron lateral distribution and their fluctuations in electron-photon cascades
[HE-3.5-12] N85-35949
Comparison of big event with calculations of the air shower development
[HE-3.6-8] N85-35956
Hadrons registration in emulsion chamber with carbon block
[HE-3.7-3] N85-35962
Intensities of high-energy cosmic rays at Mount Kanbala
[HE-3.7-5] N85-35964
Ultra high energy events in ECHOS series and primary energy spectrum
[HE-3.7-9] N85-35966
The maximum depth of shower with E sub 0 larger than 10(17) eV on average characteristics of EAS different components N85-35981
Monte Carlo simulation of EAS generated by 10(14) - 10(16) eV protons
[HE-4.3-14] N85-36008
Lateral distribution of high energy muons in EAS of sizes Ne approximately equals 10(5) and Ne approximately equals 10(6)
[HE-4.3-16] N85-36010
Energy calibration of the fly's eye detector
[HE-4.4-1] N85-36011
The structure of EAS at E 0.1 EeV
[HE-4.4-2] N85-36012
Longitudinal trial functions and the cosmic ray energy scale N85-36014
EAS development curve at energy of 10(16) - 10(18) eV measured by optical Cerenkov light
[HE-4.4-7] N85-36015
Missing energies at pair creation
[HE-4.4-8] N85-36016
On the determination of the depth of EAS development maximum using the lateral distribution of Cerenkov light at distances 150 m from EAS axis
[HE-4.4-13] N85-36019
Study of the energy spectrum of primary cosmic rays: EAS size fluctuations at a fixed primary energy
[HE-4.4-14] N85-36020
Preliminary results of the Cerenkov EAS flashes the Crimean Astrophysical Observatory
[HE-4.4-17] N85-36023
The experimental cascade curves of EAS at E sub 0 10(17) eV obtained by the method of detection of Cherenkov pulse shape
[HE-4.4-18] N85-36024
Muons in gamma showers
[HE-4.5-3] N85-36027
Muon spectrum in air showers initiated by gamma rays
[HE-4.5-4] N85-36028
Expected rates with mini-arrays for air showers
[HE-4.7-8] N85-36059
The spectrum of cosmic ray muons obtained with 100-ton scintillation detector underground and the analysis of recent experimental data
[HE-5.1-6] N85-36071
A new world survey expression for cosmic ray vertical intensity vs. depth in standard rock
[HE-5.1-10] N85-36073
Muon groups and primary composition at 10 to the 13th power to 10 to the 15th power eV
[HE-5.1-12] N85-36074
On muon energy spectrum in muon groups underground
[HE-5.1-14] N85-36076
Underwater measurements of muon intensity
[HE-5.1-16] N85-36078
Hybrid TLC-pair meter for the Sphinx Project
[HE-5.2-10] N85-36086
An upper limit of muon flux of energies above 100 TeV determined from horizontal air showers observed at Akeno
[HE-5.2-12] N85-36088
Energy spectrum of cascade showers induced by cosmic ray muons in the range from 50 GeV to 5 TeV
[HE-5.2-14] N85-36090
Analytical calculation of muon intensities under deep sea-water
[HE-5.2-16] N85-36092
On method of muon spectrum measurements by the scintillation detectors of a large thickness T4t sub o
[HE-5.2-18] N85-36094
Range fluctuations of high energy muons passing through matter
[HE-5.2-19] N85-36095
The spectrum of neutrons at 60 hg m(-2)
[HE-5.2-20] N85-36096
A transient digitiser for fast air shower events
[HE-5.2-21] N85-36097
Results of low energy background measurements with the Liquid Scintillation Detector (LSD) of the Mont Blanc Laboratory
[HE-5.3-5] N85-36099
Measurement of neutrino oscillations in MACRO experiment
[HE-5.3-10] N85-36104
The capability of the existing network of installations for detecting the antineutrino burst from collapsing stars
[HE-5.3-13] N85-36107
Energy spectra of high energy atmospheric neutrinos
[HE-5.3-14] N85-36108
Relationship of sea level muon charge ratio to primary composition including nuclear target effects
[HE-5.4-10] N85-36121

ENERGY STORAGE

Solar pond technology for Navy applications
[AD-A155877] N85-35488
Strategic defense initiative
[DE85-012778] N85-35735
Analysis of a pulsed power system containing rotating machine
[DE85-014128] N85-35786

ENERGY TECHNOLOGY

New technologies at the forefront of industrial developments N85-35168
Chemistry division report
[DE85-010586] N85-35228
Photovoltaics technology program summary
[DE85-013098] N85-35493

ENERGY TRANSFER

Friction, impact, and electrostatic discharge sensitivities of energetic materials
[DE85-013321] N85-35309
Scaling violation in hadron-nucleus interaction
[HE-3.2-8] N85-35916
Few-particles generation channels in inelastic hadron-nuclear interactions at energy approximately equals 400 GeV
[HE-3.2-9] N85-35917
Sub-luminal pulses from cosmic ray air showers
[HE-4.7-13] N85-36063

ENGINE INLETS

Calculation of compressible flow about three-dimensional inlets with auxiliary inlets, slats and vanes by means of a panel method
[NASA-CR-174975] N85-35162

ENGINE TESTS

A study of the control of particulate emissions from turbine engine test cells N85-35205

ENGINEERING MANAGEMENT

DoD Value Engineering conference report. Value Engineering (VE): A tool that benefits line management. Part 4, Workshop B: VE on spare parts
[AD-A156070] N85-35813
DoD Value Engineering conference report. Value Engineering (VE): A tool that benefits line management. Part 7, Workshop E: VE in construction and architect engineer contracts
[AD-A156073] N85-35816

ENRICHMENT

Measurement of uranium enrichment for gaseous uranium at low pressure
[DE85-012697] N85-35733

ENTHALPY

Results of variable enthalpy tests of CPR-488 TIP panels in MSFC Hot Gas Facility
[NASA-CR-170889] N85-35237
Thermodynamics of the corrosion of chromium in molten carbonates
[DE85-011407] N85-35282

ENVIRONMENT EFFECTS

Contribution to the properties of carbon fiber reinforced composites — structural mechanics
[ESA-TT-849] N85-35246
Implementing agreement for cooperation in the development of large scale wind energy conversion systems
[JUEL-SPEZ-278] N85-35473
General environmental aspects of large scale wind energy utilization N85-35474
GROWIAN: First observations of the environmental impact at the GROWIAN site — wind energy converter N85-35476
Environmental aspects of large-scale wind-power systems in the UK N85-35478
Environmental Monitoring Burger Hill, Orkney wind turbine generator site and similar work at other UK WTG sites N85-35482
Environmental aspects of the Netherlands wind farm project N85-35485

ENVIRONMENT MANAGEMENT

A guide for new environmental coordinators
[AD-A156327] N85-35498
Land Disposal of Hazardous Waste
[PB85-196376] N85-35500

ENVIRONMENT PROTECTION
A guide for new environmental coordinators
[AD-A156327] N85-35498
ENVIRONMENT SIMULATION
The deep diving simulator TITAN: Physiological problems associated with staying in great depths of water N85-35604
ENVIRONMENTAL MONITORING
Environmental Monitoring Burger Hill, Orkney wind turbine generator site and similar work at other UK WTG sites N85-35482
Current inventory of anthropogenic carbon dioxide in the North Pacific Subarctic Gyre
[PB85-187938] N85-35570
ENVIRONMENTAL SURVEYS
Environmental-physical measurements and determination of atmospheric turbulence with the ASK-16 motor glider N85-35549
ENVIRONMENTS
International flight planning handbook
[AD-A156330] N85-35177
EPOXY COMPOUNDS
Molecular biology of environmental aromatic hydrocarbons
[DE85-015036] N85-35593
EQUATIONS OF MOTION
Identification and control of structures in space
[NASA-CR-176175] N85-35214
The compliance of end effector force sensors for robot manipulator control N85-35406
Time-dependent response of the climate to increasing atmospheric carbon dioxide N85-35532
EQUATIONS OF STATE
Equation of state study for polar fluids
[PB85-204345] N85-35262
Experimental technique for measuring the isentrope of hydrogen to several megabars
[DE85-014332] N85-35386
EQUILIBRIUM EQUATIONS
Analysis of the nonlinear equations describing the elastic, thermal, and electromagnetic behavior of solids: Existance of solutions of semi-inverse problems N85-35415
ERROR ANALYSIS
Gravity gradiometer survey data processing
[AD-A156165] N85-35522
A comparison between Falcon data and motor glider data N85-35547
Accuracy and error analysis --- airborne instruments N85-35557
Study of fault tolerant software technology for dynamic systems
[NASA-CR-172618] N85-35642
Specifying and verifying concurrent programs
[AD-A156190] N85-35652
ERROR CORRECTING CODES
Error-correcting codes for computer memories N85-35636
Pruned error-trellis decoding of certain non-systematic convolutional codes
[AD-A156122] N85-35650
ERROR DETECTION CODES
Study of fault tolerant software technology for dynamic systems
[NASA-CR-172618] N85-35642
AUTOSIM: An automated repetitive software testing tool
[NASA-CR-177930] N85-35643
Pruned error-trellis decoding of certain non-systematic convolutional codes
[AD-A156122] N85-35650
Design of a microprogram control unit with concurrent error detection
[AD-A156447] N85-35655
ERROR SIGNALS
LANDSAT-4/5 image data quality analysis
[E85-10105] N85-35463
ERRORS
Comparative analysis of operational forecasts versus actual weather conditions in airline flight planning, volume 4
[NASA-CR-167865] N85-35537
Comparative analysis of operational forecasts versus actual weather conditions in airline flight planning: Summary report
[NASA-CR-167866] N85-35538
Error message recording and reporting in the SLC control system
[DE85-013057] N85-35664
Multidimensional analysis of data obtained in experiments with X-ray emulsion chambers and extensive air showers
[HE-3.6-2] N85-35951
ESCAPE SYSTEMS
Design and testing of an energy-absorbing crewseat for the F/FB-111 aircraft. Volume 2: Data from seat testing
[NASA-CR-3917] N85-35184
ESTIMATES
Optimal estimation of a high degree gravity field from a global set of 1 deg x 1 deg anomalies to degree and order 250
[AD-A156008] N85-35519
Gravity gradiometer survey data processing
[AD-A156165] N85-35522
Atlantic coast hindcast. Phase 2: Wave information, additional extremal estimates
[AD-A156137] N85-35575
Error-correcting codes for computer memories N85-35636
ESTIMATING
Estimation of flight mechanical variables by means of Kalman filters N85-35171
LANDSAT-4/5 image data quality analysis
[E85-10105] N85-35463
EUCLIDEAN GEOMETRY
A new description of combined trellis coding with asymmetric modulation
[NASA-CR-176197] N85-35323
EULER EQUATIONS OF MOTION
A stream function approach to solving the conservative Euler equations for transonic flows N85-35156
Numerical studies of 2-dimensional flows
[NASA-CR-3930] N85-35160
EUROPE
Introduction to European air traffic control
[AD-A156328] N85-35176
EUTECTICS
Influence of yttrium on eutectoid transformation in irons
[BLL-M-35787-(5828.4)] N85-35270
EVALUATION
Expert systems research in regional resource evaluation: Experiences in the application of microcomputer technologies N85-35450
EVAPORATION
How are particle production, nucleon emission and target fragment evaporation processes interrelated in hadron-nucleus collisions? N85-35878
EVOKED RESPONSE (PSYCHOPHYSIOLOGY)
Matched filtering of visual evoked potentials to detect acceleration (+Gz) induced blackout
[AD-A155912] N85-35609
EVOLUTION (DEVELOPMENT)
Heat transfer and brine evolution in magma-hydrothermal systems N85-35441
Origin of sedimentary humic acids, potential carriers of ore-forming elements N85-35443
EXCIMER LASERS
Generation of stimulated emission in the soft X-ray range by nonlinear processes with excimer lasers
[DE85-012465] N85-35403
EXCITATION
Pressure cross spectra in turbulent boundary layers in water
[AD-A156153] N85-35378
Investigations of the molecular beam epitaxial growth and characteristics of external excitation induced non-equilibrium phases of immiscible 3-5 compound semiconductors
[AD-A156325] N85-35804
Observations of far-infrared transitions between excited states of OH
[NASA-TM-86722] N85-35833
EXCITONS
Optical properties of heterostructures and superlattices
[AD-A156243] N85-35802
EXERCISE PHYSIOLOGY
Weight loss, rectal temperature and heart rates following the 1984 Boston Marathon
[AD-A155984] N85-35612
Thirst and fluid intake following graded hypohydration levels in humans
[AD-A156201] N85-35615
EXHAUST EMISSION
A study of the control of particulate emissions from turbine engine test cells N85-35205
EXOBIOLOGY
NASA Developmental Biology Workshop: A summary
[NASA-TM-86756] N85-35578
Vertebrate development in space: Gravity is a drag (and has been for eons and eons) N85-35580
Report of the NASA Mammalian Developmental Biology Working Group N85-35581
Report of Amphibian Development Group N85-35583
Report of the Insect Development Group N85-35584
Aquatic Invertebrate Development Working Group N85-35585
Report of the Microbial Development Working Group N85-35586
EXPERIMENT DESIGN
Experimental lithium system
[DE85-013252] N85-35382
Model robust response surface designs: Scaling two-level factorials
[AD-A156218] N85-35686
EXPERIMENTAL BREEDER REACTOR 2
SASSYS-1 computer code verification with EBR-2 test data
[DE85-012119] N85-35657
EXPERIMENTATION
Experimental technique for measuring the isentrope of hydrogen to several megabars
[DE85-014332] N85-35386
EXPERT SYSTEMS
Expert systems research in regional resource evaluation: Experiences in the application of microcomputer technologies N85-35450
AUTOSIM: An automated repetitive software testing tool
[NASA-CR-177930] N85-35643
EXPLORATION
Some recent deposit modeling efforts N85-35453
EXPLOSIVE FORMING
Computational methods for the explosive and impact compaction of powders
[AD-A156219] N85-35653
EXPLOSIVES
Computational methods for the explosive and impact compaction of powders
[AD-A156219] N85-35653
EXTERNAL STORES
Results of variable enthalpy tests of CPR-488 TIP panels in MSFC Hot Gas Facility
[NASA-CR-170889] N85-35237
EXTRACTION
Use of a minimum-ellipse criterion in the study of ion-beam extraction systems
[DE85-012670] N85-35721
Measurement of uranium enrichment for gaseous uranium at low pressure
[DE85-012697] N85-35733
Synchronous timing of multi-energy fast beam extraction during a single AGS cycle
[DE85-011829] N85-35781
EXTRATERRESTRIAL RADIATION
Standard value for the radiation length in air
[HE-4.4-4] N85-36013
Samarkand complex setup for investigation of cosmic ray variation in the energy range of 7 10 (9) - 10 (15) eV
[HE-4.6-14] N85-36050
High energy neutrino astronomy with MACRO
[HE-5.3-12] N85-36106
EXTRATERRESTRIAL RADIO WAVES
High energy radiation from neutron stars
[DE85-014353] N85-35843
EXTREME ULTRAVIOLET EXPLORER SATELLITE
The 1986 National Aeronautics and Space Administration authorization
[GPO-47-635] N85-35829
EXTREMELY HIGH FREQUENCIES
An experimental study of dielectric rod antennas for millimeter-wave imaging applications
[AD-A155832] N85-35328
EXTREMUM VALUES
Master Fit users' guide, version 1.0
[DE85-014199] N85-35667
EXTRUDING
Solid-state co-extrusion of nylon 6 gel
[AD-A156187] N85-35298
Establishment of a Computer-Aided Design (CAD)-Computer-Aided Manufacturing (CAM) process for the production of cold forged gears
[AD-A155756] N85-35644
EYE MOVEMENTS
The human engineering eye movement measurement research facility
[AD-A156099] N85-35613

F

FABRICATION
Method of preparing thin porous sheets of ceramic material
[DE85-006399] N85-35300
Single-point diamond crushing of Zerodur with in-situ polishing and metrology on a diamond turning machine
[DE85-012918] N85-35305
SLC arc transport system: Magnet design and construction
[DE85-014289] N85-35789

FACTORIAL DESIGN
Model robust response surface designs: Scaling two-level factorials
[AD-A156218] N85-35686
FADING
DMSK: A practical 2400-bps receiver for the mobile satellite service: An MSAT-X Report
[NASA-CR-176194] N85-35324
FAILURE ANALYSIS
A preliminary evaluation of a failure detection filter for detecting and identifying control element failures in a transport aircraft
[NASA-TM-87576] N85-35204
Reliability prediction of the series system with spares subject to Weibull failure N85-35413
State-of-the-art of solid-state motor controllers
[TI85-008674] N85-35806
FAILURE MODES
Mechanical characterization and failure modes of fiber reinforced angle-ply composites N85-35234
Structure and properties of polyethylene films used in heavy lift balloons
[NASA-CR-176227] N85-35308
FAIRINGS
An automated technique for encasing specific payloads with low-drag fairings N85-35183
FAN BLADES
Energy Efficient Engine Program technology benefit/cost study, volume 1
[NASA-CR-174766-VOL-1] N85-35197
FAR INFRARED RADIATION
Far-infrared emission lines of CO and OH in the Orion-KL molecular shock
[NASA-TM-86721] N85-35832
Observations of far-infrared transitions between excited states of OH
[NASA-TM-86722] N85-35833
FAR ULTRAVIOLET RADIATION
Tuning system for capacitively loaded 1/4 accelerating cavity
[DE85-012516] N85-35358
FARADAY EFFECT
Injector losses on Mite
[DE85-012356] N85-35355
FAST FOURIER TRANSFORMATIONS
Matched filtering of visual evoked potentials to detect acceleration (+Gz) induced blackout
[AD-A155912] N85-35609
FAST NEUTRONS
Fast-neutron interaction with niobium
[DE85-011471] N85-35731
FATIGUE (BIOLOGY)
Physiological responses to unvarying (steady) and 2-2-1 shifts: Miami International Flight Service Station
[AD-A155751] N85-35619
FATIGUE (MATERIALS)
Fatigue damage detection in steels by optical correlation
[AD-A155830] N85-35277
Effect of microstructure on the fatigue behavior of Fe-C-X alloys
[DE85-011749] N85-35285
FATIGUE LIFE
The character of observed porosity and its possible effects on rolling contact fatigue life of M-50 steel
[AD-A155930] N85-35279
Effect of prior warm rolling on the retained austenite content and hardening response of VIM-VAR (vacuum-induction melted-vacuum-arc remelted) AISI M-50 steel
[AD-A156145] N85-35281
Development of a mathematical model for predicting the percentage fatigue life increase resulting from shot peened components
[AD-A155774] N85-35425
FATIGUE TESTS
Fatigue lives of specimens representing critical locations in Mirage 3 spars under Australian and Swiss test spectra
[ARL-STRUC-R-415] N85-35187
FAULT TOLERANCE
Study of fault tolerant software technology for dynamic systems
[NASA-CR-172618] N85-35642
FEASIBILITY ANALYSIS
Miniature infra-red data acquisition and telemetry system
[NASA-CR-177953] N85-35390
FEATHERING
Optimally designed propellers constrained by noise N85-35196
FEDERAL BUDGETS
Progress report on implementing the recommendations of the White House Science Council's Federal Laboratory Review Panel, volume 1
[PB85-185072] N85-35819
FEEDBACK CONTROL
A graph theoretic procedure for the design of feedback patterns
[REPT-110] N85-35673
Design of dynamic compensators of prescribed pattern
[BU-109] N85-35674
Spreading the control complexity in decentralized control of interconnected systems
[BU-117] N85-35688
Decentralized stabilization by high gain feedback
[BU-115] N85-35689
FERMENTATION
Production of butanol by fermentation in the presence of cocultures of clostridium
[NASA-CASE-NPO-16203-1] N85-35227
FERROELECTRICITY
Materials used by industry for the production of piezoelectric transducers. The state of the art of research work performed in the field of PZT ceramics and ferroelectric polymers
[ISL-CO-211/84] N85-35344
Ferroelectric homopolymer PVF2 and P (VDF-TrFe) copolymers N85-35347
FERROUS METALS
Pitting corrosion of ferrous alloys
[AERE-R-11490] N85-35273
Assessment of metal heating technologies for ferrous forging: A pilot study of the form value of natural gas
[PB85-204394] N85-35314
Cobalt-rich ferromanganese crusts in the oceans N85-35444
FEYNMAN DIAGRAMS
A test of the Feynman scaling in the fragmentation region
[HE-1.2-9] N85-35867
General consequences of the violated Feynman scaling N85-35872
FIBER OPTICS
Center for Electronics and Electrical Engineering technical progress bulletin covering center programs, July-September with 1985 CEEE events calendar
[PB85-191393] N85-35363
Optical synthetic aperture techniques
[AD-A156151] N85-35752
On the possibilities of large-scale radio and fiber optics detectors in cosmic rays
[HE-4.6-2] N85-36039
FIBER REINFORCED COMPOSITES
Mechanical characterization and failure modes of fiber reinforced angle-ply composites N85-35234
Quantitative non-destructive evaluation of composite materials based on ultrasonic wave propagation
[NASA-CR-176176] N85-35244
Determination of characteristic values for fiber reinforced materials N85-35247
Computational techniques for fiber reinforced components N85-35250
A research program to reduce the interior noise in general aviation aircraft, index and summary
[NASA-CR-176178] N85-35695
FIBERS
Development and characterization of carbon-bonded carbon fiber insulation for radioisotope space power systems
[DE85-013365] N85-35299
FIELD EFFECT TRANSISTORS
Two-dimensional numerical modeling of ion implanted GaAs MESFET devices N85-35341
FIELD THEORY (PHYSICS)
Monopole search below the Parker limit with the MACRO detector at Gran Sasso
[HE-6.1-5] N85-36131
Limits on monopole fluxes from KFG experiment
[HE-6.1-6] N85-36132
An experiment to detect gut monopoles
[HE-6.1-7] N85-36133
FIGHTER AIRCRAFT
Fatigue lives of specimens representing critical locations in Mirage 3 spars under Australian and Swiss test spectra
[ARL-STRUC-R-415] N85-35187
RAFTS: A T-38 replacement for the 21st century
[AD-A156103] N85-35191
FILLERS
Results of tests of weathered K5NA closeout material in the MSFC Hot Gas Facility
[NASA-CR-170893] N85-35239
FINITE DIFFERENCE THEORY
Finite analytic solutions of supersonic flows in two-dimensional non-symmetrical channels N85-35154
Numerical studies of 2-dimensional flows
[NASA-CR-3930] N85-35160
Two-dimensional numerical modeling of ion implanted GaAs MESFET devices N85-35341
Stress analysis of axisymmetric sandwich shells of variable thickness N85-35419
Thermal evolution of coastal California with implications for hydrocarbon maturation N85-35509
Three-dimensional finite deformation viscoelastic model accounting for damage effects
[DE85-012951] N85-35660
The finite element-difference method N85-35672
FINITE ELEMENT METHOD
Analysis of incompressible cascade flows using state-of-the-art computer programs
[AD-A155850] N85-35173
Design and behavior of coped beams N85-35417
Stress-intensity factors for circumferential surface cracks in pipes and rods under tension and bending loads
[NASA-TM-87594] N85-35424
Prediction of plasticity characteristics for three-dimensional fracture specimens comparison with experiment
[AD-A156425] N85-35430
The finite element-difference method N85-35672
A new method for boundary value problems
[AD-A155934] N85-35683
FINS
Computer simulation of a cruise missile using brushless dc motor fin control
[AD-A155935] N85-35349
FIRE FIGHTING
Fire research publications, 1984
[PB85-208502] N85-35827
FIRE PREVENTION
Investigation of experimental lightweight firewall materials for A/C engine bay applications
[AD-A155765] N85-35175
Proceedings of the 7th Joint Panel Meeting of the UJNR Panel on Fire Research and Safety
[PB85-199545] N85-35317
Fire research publications, 1984
[PB85-208502] N85-35827
FIREPROOFING
Investigation of experimental lightweight firewall materials for A/C engine bay applications
[AD-A155765] N85-35175
Fire research publications, 1984
[PB85-208502] N85-35827
FISCHER-TROPSCH PROCESS
CO + H2 reaction over nitrogn-modified iron catalysts
[DE85-013791] N85-35231
FLAME PROPAGATION
The use of austenitic stainless steel versus monel (Ni-cu) alloy in pressurized Gaseous Oxygen (GOX) life support systems
[AD-A156305] N85-35625
FLAME RETARDANTS
Investigation of experimental lightweight firewall materials for A/C engine bay applications
[AD-A155765] N85-35175
Fire research publications, 1984
[PB85-208502] N85-35827
FLAME SPRAYING
Thermal barrier coating system
[NASA-CASE-LEW-14057-1] N85-35233
FLAMES
Radiation measurements on magnesium flames
[BLL-CE-TRANS-8110-(9022.09)] N85-35254
FLAMMABILITY
The use of a laser Doppler velocimeter in a standard flammability tube
[NASA-CR-174960] N85-35389
FLAT PLATES
Vortex boundary-layer interactions
[NASA-CR-176192] N85-35373
FLEXIBLE BODIES
Analysis of flexible aircraft longitudinal dynamics and handling qualities. Volume 1: Analysis methods
[NASA-CR-177943-VOL-1] N85-35202
Analysis of flexible aircraft longitudinal dynamics and handling qualities. Volume 2: Data
[NASA-CR-177943-VOL-2] N85-35203
FLEXIBLE SPACECRAFT
Enhancement of the flexible spacecraft dynamics program for open spacecraft
[NASA-CR-175309] N85-35641
FLIGHT CHARACTERISTICS
Estimation of flight mechanical variables by means of Kalman filters N85-35171
FLIGHT CREWS
U.S. Civil airmen statistics for calendar year 1984
[AD-A156326] N85-35153
Introduction to European air traffic control
[AD-A156328] N85-35176
Models for assessing workload of aircrews on long distance flights N85-35599

FLIGHT INSTRUMENTS
A guide to USAF helicopter instrument flight procedures
[AD-A156102] N85-35182
Accuracy and error analysis — airborne instruments N85-35557

FLIGHT MECHANICS
Lectures of a Flight Mechanics Conference — conferences
[ESA-TT-831] N85-35165
Development of flight mechanics research in Brunswick N85-35166
The contribution made by flight mechanics to civil aviation N85-35169
The effect of instrumentation system parameters on the results of a flight mechanical system identification N85-35170
Estimation of flight mechanical variables by means of Kalman filters N85-35171
Gust simulation for flight mechanical wind tunnel tests N85-35172
Control variables in vertical wind determination using simple flight-mechanical equations N85-35546

FLIGHT PATHS
International flight planning handbook
[AD-A156330] N85-35177
Comparative analysis of operational forecasts versus actual weather conditions in airline flight planning, volume 2
[NASA-CR-167863] N85-35535
Comparative analysis of operational forecasts versus actual weather conditions in airline flight planning, volume 3
[NASA-CR-167864] N85-35536
Comparative analysis of operational forecasts versus actual weather conditions in airline flight planning, volume 4
[NASA-CR-167865] N85-35537
Comparative analysis of operational forecasts versus actual weather conditions in airline flight planning: Summary report
[NASA-CR-167866] N85-35538

FLIGHT PLANS
International flight planning handbook
[AD-A156330] N85-35177
Comparative analysis of operational forecasts versus actual weather conditions in airline flight planning, volume 1
[NASA-CR-167862] N85-35534
Comparative analysis of operational forecasts versus actual weather conditions in airline flight planning, volume 2
[NASA-CR-167863] N85-35535
Comparative analysis of operational forecasts versus actual weather conditions in airline flight planning: Summary report
[NASA-CR-167866] N85-35538

FLIGHT SIMULATION
Energy management of three-dimensional minimum-time intercept
[NASA-CR-176174] N85-35186
Comparative analysis of operational forecasts versus actual weather conditions in airline flight planning, volume 2
[NASA-CR-167863] N85-35535

FLIGHT TESTS
A comparison between Falcon data and motor glider data N85-35547

FLOW DISTRIBUTION
General design method for 3-dimensional, potential flow fields. Part 2: Computer program DIN3D1 for simple, unibranched ducts
[NASA-CR-3926] N85-35159
Calculation of compressible flow about three-dimensional inlets with auxiliary inlets, slats and vanes by means of a panel method
[NASA-CR-174975] N85-35162
The effect of power law body forces on a thermally-driven flow between concentric rotating spheres
[NASA-TM-87596] N85-35374
The kinematic structure of cold frontal rainbands N85-35531

FLOW REGULATORS
Fluidized bed desulfurization
[NASA-CASE-NPO-15924-1] N85-35253

FLOW STABILITY
Couette flow of two fluids between concentric cylinders
[AD-A155827] N85-35376

FLOW THEORY
Bibliography on tidal hydraulics. Report 2. Supplement 9: Supplementary material compiled from June 1980 - June 1983. Tidal flows in rivers and harbors
[AD-A155990] N85-35574

FLOW VELOCITY
Flow modifying device
[NASA-CASE-LEW-13562-2] N85-35195
The use of a laser Doppler velocimeter in a standard flammability tube
[NASA-CR-174960] N85-35389

FLOW VISUALIZATION
The influence of helicopter tail shape on drag: An aerodynamic study using a low speed wind tunnel
[AD-A156304] N85-35174

FLUCTUATION THEORY
Range fluctuations of high energy muons passing through matter
[HE-5.2-19] N85-36095

FLUID FILTERS
Molecular and macromolecular sieving by asymmetric ultrafiltration membranes
[PB85-157766] N85-35266

FLUID FLOW
Flow modifying device
[NASA-CASE-LEW-13562-2] N85-35195
The effect of power law body forces on a thermally-driven flow between concentric rotating spheres
[NASA-TM-87596] N85-35374
Noise-sustained structure, intermittency and the Ginzburg-Landau equation
[DE85-009626] N85-35379
Transient three-phase three-component systems. Part 1: Formulation of the system of differential equations
[DE85-013267] N85-35384

FLUID MECHANICS
Basic research on pulse-combustion phenomena
[PB85-200228] N85-35265

FLUIDIZED BED PROCESSORS
Fluidized bed desulfurization
[NASA-CASE-NPO-15924-1] N85-35253

FLUORESCENCE
Laser probes of natural gas ignition chemistry
[PB85-200210] N85-35264
Atmospheric nitrogen oxides: Their detection and chemistry
[PB85-193910] N85-35502
Lateral-angular and temporal characteristics of EAS optical radiation
[HE-4.4-19] N85-36025
Air fluorescence detection of large air showers below the horizon
[HE-4.6-6] N85-36043

FLUTTER
The application of bispectral analyses to aeroelastic phenomena N85-35157
Unsteady flow in a supersonic cascade with two in-passage shocks
[NASA-CR-3925] N85-35158

FLUX
Limits on deeply penetrating particles in the 10(17) eV cosmic ray flux
[HE-5.3-1] N85-36098
Atmospheric neutrinos observed in underground detectors
[HE-5.3-8] N85-36102

FLUX (RATE)
Limiter
[DE85-011620] N85-35736
Hadron intensity and energy spectrum at 4380 m above level
[HE-3.1-7] N85-35905
Scaling violation in fragmentation region at energies above 10-15 eV based on the data on cosmic ray hadron component
[HE-3.1-11] N85-35909
Monte Carlo simulations of electron lateral distributions in the core region of 10(13) - 10(16) eV air showers N85-35992
The Nagoya cosmic-ray muon spectrometer 3, part 1: Preliminary observations
[HE-5.2-2] N85-36080
Angular distribution of muons produced by cosmic ray neutrinos in rock
[HE-5.3-24] N85-36115
Muon and neutrino fluxes
[HE-6.2-18] N85-36154

FLUX DENSITY
Proton-air and proton-proton cross sections from air shower data
[HE-1.1-1] N85-35849
Multiplicity distributions in interaction models used for cascade simulations
[HE-1.2-5] N85-35863
Connection between variations of the atmosphere temperature profile and variations of the meson component intensity
[HE-3.1-12] N85-35910
The model of independent particles emission in the multiparticle production theory
[HE-3.2-10] N85-35918
A critical analysis of air shower structure functions and size spectrum measurements with the NBU air shower array N85-35983
Measurement of the local density spectrum N85-35984
Transition effect of air shower particles in plastic scintillators
[HE-4.4-9] N85-36017
On the determination of the depth of EAS development maximum using the lateral distribution of Cerenkov light at distances 150 m from EAS axis
[HE-4.4-13] N85-36019
An upper limit of muon flux of energies above 100 TeV determined from horizontal air showers observed at Akeno
[HE-5.2-12] N85-36088
Energy spectrum of cascade showers induced by cosmic ray muons in the range from 50 GeV to 5 TeV
[HE-5.2-14] N85-36090
Measurement of muon intensity by Cerenkov method
[HE-5.2-15] N85-36091
Analytical calculation of muon intensities under deep sea-water
[HE-5.2-16] N85-36092
The spectrum of neutrons at 60 hg m(-2)
[HE-5.2-20] N85-36096
Geophysical searches for three-neutrino oscillations
[HE-5.3-9] N85-36103
Angular distribution of muons produced by cosmic ray neutrinos in rock
[HE-5.3-24] N85-36115
Atmospheric muons and neutrinos, and the neutrino-induced muon flux underground
[HE-5.4-7] N85-36118
Results of investigation of muon fluxes of superhigh energy cosmic rays with X-ray emulsion chambers
[HE-5.4-16] N85-36126

FLYWHEELS
Strategic defense initiative
[DE85-012778] N85-35735

FOAMS
Results of variable enthalpy tests of CPR-488 TIP panels in MSFC Hot Gas Facility
[NASA-CR-170889] N85-35237
Results of tests of Insta-Foam Thermal Protection System (TPS) material for protection of equipment inside the SRB aft skirt
[NASA-CR-170892] N85-35295

FOCUSING
Parametric stability of analytical close-range photogrammetry N85-35461

FOILS (MATERIALS)
System expectations for Pioneer 1 foil implosion experiments
[DE85-014129] N85-35359
Diagnostics for Pioneer 1 imploding plasma experiments
[DE85-014120] N85-35787

FORECASTING
The NORDA/FNOC (Naval Ocean Research and Development Activity's/Fleet Numerical Oceanography Center) Polar Ice Prediction System (PIPS)-Arctic: A technical description
[AD-A156332] N85-35577

FORGING
Assessment of metal heating technologies for ferrous forging: A pilot study of the form value of natural gas
[PB85-204394] N85-35314
Establishment of a Computer-Aided Design (CAD)-Computer-Aided Manufacturing (CAM) process for the production of cold forged gears
[AD-A155756] N85-35644

FORTRAN
CRAYCDC
[NASA-CR-177374] N85-35639
CDCCRAY
[NASA-CR-177375] N85-35640

FOURIER SERIES
Stress analysis of axisymmetric sandwich shells of variable thickness N85-35419

FRACTURE MECHANICS
1983 review of experimental stress and strain analysis
[DRIC-T-7469] N85-35422
Subcritical fracture propagation in rocks: An examination using the methods of fracture mechanics and non-destructive testing N85-35516

FRACTURES (MATERIALS)
On size effects in plane stress crack-growth resistance
[AD-A155926] N85-35426

FRAGMENTATION
Experimental data for characterizing perforating impacts: Fragmentation processes
[AD-A156370] N85-35427

A test of the Feynman scaling in the fragmentation region
[HE-1.2-9] N85-35867
Scaling violation in fragmentation region at energies above 10-15 eV based on the data on cosmic ray hadron component
[HE-3.1-11] N85-35909
Peculiarities of gamma-quanta distribution at 20 TeV energy
[HE-3.7-10] N85-35967
FRAGMENTS
How are particle production, nucleon emission and target fragment evaporation processes interrelated in hadron-nucleus collisions? N85-35878
FREE ELECTRON LASERS
ATA upgrade to 150 MeV
[DE85-013174] N85-35404
Los Alamos free-electron laser
[DE85-012666] N85-35405
FREE FLIGHT TEST APPARATUS
The effect of instrumentation system parameters on the results of a flight mechanical system identification N85-35170
FREE FLOW
Experimental study of free and mixed convective flow of air in a heated cavity
[DE85-012538] N85-35380
FREE VIBRATION
Applications of the Galerkin formalism in the coupling of the earth's free oscillations N85-35514
FREQUENCY DISTRIBUTION
Performance of a local electron density trigger to select extensive air showers at sea level
[HE-4.6-11] N85-36048
FREQUENCY MEASUREMENT
Characterization of microstrip discontinuities in the time and frequency domains
[NASA-CR-176190] N85-35342
FREQUENCY SHIFT
DMSK: A practical 2400-bps receiver for the mobile satellite service: An MSAT-X Report
[NASA-CR-176194] N85-35324
Scale separation closure and Alfven wave turbulence
[DE85-013124] N85-35385
FREQUENCY STABILITY
RF stabilization of interchange-ballooning modes
[DE85-012080] N85-35353
FRICTION
Friction, impact, and electrostatic discharge sensitivities of energetic materials
[DE85-013321] N85-35309
The use of austenitic stainless steel versus monel (Ni-cu) alloy in pressurized Gaseous Oxygen (GOX) life support systems
[AD-A156305] N85-35625
FUEL CELLS
Thermodynamics of the corrosion of chromium in molten carbonates
[DE85-011407] N85-35282
FUEL COMBUSTION
Current inventory of anthropogenic carbon dioxide in the North Pacific Subarctic Gyre
[PB85-187938] N85-35570
FUEL CONSUMPTION
FAA requirements for model to support capacity, delay, noise and energy programs
[AD-A155815] N85-35179
Comparative analysis of operational forecasts versus actual weather conditions in airline flight planning, volume 1
[NASA-CR-167862] N85-35534
Comparative analysis of operational forecasts versus actual weather conditions in airline flight planning, volume 2
[NASA-CR-167863] N85-35535
Comparative analysis of operational forecasts versus actual weather conditions in airline flight planning, volume 3
[NASA-CR-167864] N85-35536
Comparative analysis of operational forecasts versus actual weather conditions in airline flight planning, volume 4
[NASA-CR-167865] N85-35537
FUEL CONTAMINATION
Sound speed measurements in liquid oxygen-liquid nitrogen mixtures
[NASA-TP-2464] N85-35307
FUEL TANKS
Fuel containment and damage tolerance for large composite primary aircraft structures. Phase 1: Testing
[NASA-CR-166091] N85-35241
FUEL-AIR RATIO
Flow modifying device
[NASA-CASE-LEW-13562-2] N85-35195
FUNCTIONS (MATHEMATICS)
Two methods of global data assimilation
[AD-A155981] N85-35684

G

GALACTIC RADIATION
A search for cosmic sources of high energy neutrinos with small underground detectors
[HE-5.3-16] N85-36110
GALACTIC STRUCTURE
High energy cosmic ray signature of quark nuggets
[HE-6.2-11] N85-36147
GALAXIES
Charge 4/3 leptons in cosmic rays
[HE-6.2-14] N85-36150
GALERKIN METHOD
Applications of the Galerkin formalism in the coupling of the earth's free oscillations N85-35514
GALILEO PROJECT
The 1986 National Aeronautics and Space Administration authorization
[GPO-47-635] N85-35829
GALLIUM ARSENIDES
Two-dimensional numerical modeling of ion implanted GaAs MESFET devices N85-35341
Center for Electronics and Electrical Engineering technical progress bulletin covering center programs, July-September with 1985 CEEE events calendar
[PB85-191393] N85-35363
GAMMA RAY BURSTS
Multidimensional analysis of data obtained in experiments with X-ray emulsion chambers and extensive air showers
[HE-3.6-2] N85-35951
A new method of differential structural analysis of gamma-family basic parameters
[HE-3.6-3] N85-35952
Relation between gamma-ray family and EAS core: Monte-Carlo simulation of EAS core
[HE-3.6-7] N85-35955
Comparison of big event with calculations of the air shower development
[HE-3.6-8] N85-35956
Result of Monte-Carlo simulation of electron-photon cascades in lead and layers of lead-scintillator
[HE-3.6-11] N85-35958
A study of gamma-families generated in nucleon-nucleus (NA) and pion-nucleus (pi A) interactions
[HE-3.7-2] N85-35961
New analysis of nuclear interaction observed by Mt. Kanbara emulsion chamber experiment
[HE-3.7-4] N85-35963
Intensities of high-energy cosmic rays at Mount Kanbala
[HE-3.7-5] N85-35964
Ultra high energy events in ECHOS series and primary energy spectrum
[HE-3.7-9] N85-35966
Peculiarities of gamma-quanta distribution at 20 TeV energy
[HE-3.7-10] N85-35967
Results of low energy background measurements with the Liquid Scintillation Detector (LSD) of the Mont Blanc Laboratory
[HE-5.3-5] N85-36099
The research program of the Liquid Scintillation Detector (LSD) in the Mont Blanc Laboratory
[HE-5.3-6] N85-36100
Muon and neutrino fluxes
[HE-6.2-18] N85-36154
Search for acoustic signals from high energy cascades
[HE-7.1-1] N85-36155
Exploring results of the possibility on detecting cosmic ray particles by acoustic way
[HE-7.1-3] N85-36157
GAMMA RAY SPECTRA
Measurement control for plutonium isotopic measurements using gamma-ray spectrometry
[DE85-013394] N85-35397
Gamma-ray production cross sections for alpha-particle induced reactions on F-19 and Na-23
[DE85-012603] N85-35732
GAMMA RAY SPECTROMETERS
Noiseless coding for the Gamma Ray spectrometer
[NASA-CR-176201] N85-35219
Measurement control for plutonium isotopic measurements using gamma-ray spectrometry
[DE85-013394] N85-35397
GAMMA RAY TELESCOPES
Construction of a cosmic ray air shower telescope
[HE-4.5-14] N85-36036
Thickness of the particle swarm in cosmic ray air showers
[HE-4.7-14] N85-36064
Charge 4/3 leptons in cosmic rays
[HE-6.2-14] N85-36150
GAMMA RAYS
Total integrated dose testing of solid-state scientific CD4011, CD4013, and CD4060 devices by irradiation with CO-60 gamma rays
[NASA-CR-176196] N85-35795
Experiment Pamir-3. Coplanar emission of high energy gamma-quanta at interaction of hadrons with nuclei of air atoms at energies above 10 to the 7th power GeV
[HE-1.4-12] N85-35899
High energy gamma-rays and hadrons at Mount Fuji
[HE-3.1-3] N85-35903
The multiplicity and the spectra of secondaries correlated with the leading particle energy
[HE-3.2-11] N85-35919
Study of hadron bundles observed in Chacaltaya two-story emulsion chamber
[HE-3.3-4] N85-35922
Lateral distribution of high energy hadrons and gamma ray in air shower cores observed with emulsion chambers
[HE-3.3-8] N85-35926
Size distributions of air showers accompanied with high energy gamma ray bundles observed at Mt. Chacaltaya
[HE-3.3-9] N85-35927
EAS accompanied by gamma-families at Mt. Norikura and comparison with Monte Carlo simulation
[HE-3.3-10] N85-35928
Comparison of absolute intensity between EAS with gamma-families and general EAS at Mount Norikura
[HE-3.3-11] N85-35929
A cosmic ray super high multicore family event. 1: Experiment and general features
[HE-3.4-1] N85-35930
A halo event created at 200 m above the Chacaltaya emulsion chamber
[HE-3.4-5] N85-35933
A binocular-type atmospheric interaction generating sequential exotic features
[HE-3.4-6] N85-35934
Gamma-hadron families and scaling violation
[HE-3.4-7] N85-35935
Super-family P2 C-96-125 observed by Japan-URSS Joint Emulsion Chamber Experiment
[HE-3.4-8] N85-35936
On the halo events observed by Mount Fuji and Mount Kanbala Emulsion Chamber Experiments
[HE-3.4-9] N85-35937
Experiment Pamir-2. Fianit: A giant super-family with halo (Epsilon sub 0 at approximately 10(17) eV)
[HE-3.4-10] N85-35938
Experiment Pamir-4: Analysis of superfamily with halo of electromagnetic nature detected in deep XEC
[HE-3.4-11] N85-35939
Particle interactions at energies over 1000 TeV inferred from gamma-families observed at Mount Fuji
[HE-3.5-1] N85-35940
A search for mini-clusters in Japan-USSR Joint Experiment at Pamir
[HE-3.5-2] N85-35941
Mini-clusters
[HE-3.5-3] N85-35942
Giant mini-clusters as possible origin of halo phenomena observed in super-families
[HE-3.5-4] N85-35943
The electromagnetic component of albedo from superhigh energy cascades in dense media
[HE-3.5-11] N85-35948
Integral functions of electron lateral distribution and their fluctuations in electron-photon cascades
[HE-3.5-12] N85-35949
A comparative analysis of gamma and hadron families at the superhigh energies recorded in experiment Pamir
[HE-3.7-1] N85-35960
Nineteenth International Cosmic Ray Conference. HE Sessions, volume 7
[NASA-CP-2376-VOL-7] N85-35968
New aspects in nucleon-nucleus collisions and EAS properties around 10(6) GeV N85-35974
Application of photodiodes to the detection of electromagnetic bursts N85-35988
Lateral distribution on charged particles in EAS
[HE-4.3-15] N85-36009
Longitudinal trial functions and the cosmic ray energy scale N85-36014
Missing energies at pair creation
[HE-4.4-8] N85-36016
The identification of gamma ray induced EAS
[HE-4.5-1] N85-36026
Muons in gamma showers
[HE-4.5-3] N85-36027

Muon spectrum in air showers initiated by gamma rays [HE-4.5-4] N85-36028
Development of electromagnetic cascades in the atmosphere including the Landau-Pomeranchuk-Migdal effect [HE-4.5-5] N85-36029
Electromagnetic and muonic structure of showers initiated by gamma-rays and by hadrons [HE-4.5-6] N85-36030
The muon content of gamma-ray showers [HE-4.5-7] N85-36031
The hump in the Cerenkov lateral distribution of gamma ray showers [HE-4.5-9] N85-36032
Simulation of gamma-initiated showers [HE-4.5-10] N85-36033
Phenomenological characteristic of the electron component in gamma-quanta initiated showers [HE-4.5-11] N85-36034
Construction of a cosmic ray air shower telescope [HE-4.5-14] N85-36036
Nuclear cascades in electromagnetic showers produced by primary gamma-quanta in the atmosphere [HE-4.5-16] N85-36038
Comments on the measurements of multiple muon phenomena [HE-5.2-13] N85-36089
High energy neutrino astronomy with MACRO [HE-5.3-12] N85-36106
Analysis of the electron component of EAS at observational level 700 g x cm(-2) with a scale breaking interaction model and gammaisation hypothesis [HE-5.4-8] N85-36119
Collimated groups of particles as possible manifestation of heavy meson production [HE-5.4-14] N85-36124

GAPS
SRB attach ring phenolic TPS fishtail seal evaluation tests [NASA-CR-170887] N85-35407

GARNETS
Advanced detectors and signal processing [NASA-CR-176193] N85-35343

GAS ANALYSIS
Gas analysis of ore-forming fluids N85-35447

GAS CHROMATOGRAPHY
Method for measuring surface activity of silicon nitride powder [NASA-TM-77906] N85-35242
Aspects of high-resolution gas chromatography as applied to the analysis of hydrocarbon fuels and other complex organic mixtures. Volume 1 [AD-A156154] N85-35257

GAS HEATING
High Temperature Heating System (HTHS) [PB85-188340] N85-35316

GAS TUNGSTEN ARC WELDING
Interaction of trace elements and welding parameters on GTA weld shape [DE85-004046] N85-35284

GAS TURBINE ENGINES
Energy Efficient Engine Program technology benefit/cost study, volume 2 [NASA-CR-174766-VOL-2] N85-35198
Energy efficient engine, high pressure turbine thermal barrier coating. Support technology report [NASA-CR-168037] N85-35199
Development of advanced high-temperature heat flux sensors. Phase 2: Verification testing [NASA-CR-174973] N85-35391

GAS TURBINES
Heat transfer characteristics for two-dimensional arrays of impinging jets with initial crossflow N85-35365

GASES
Measurement of uranium enrichment for gaseous uranium at low pressure [DE85-012697] N85-35733

GASKETS
Response of a BWR Mark 2 containment vessel head to loads beyond the design basis [DE85-010524] N85-35432

GAUSS EQUATION
Master Fit users' guide, version 1.0 [DE85-014199] N85-35667

GAUSS-MARKOV THEOREM
Nonlinear digital phase-locked loops with application to Loran-C receivers N85-35178

GEAR TEETH
Planetary-gear-support bearing test rig design [NASA-CR-174927] N85-35185

GEARS
Planetary-gear-support bearing test rig design [NASA-CR-174927] N85-35185
Establishment of a Computer-Aided Design (CAD)-Computer-Aided Manufacturing (CAM) process for the production of cold forged gears [AD-A155756] N85-35644

GELS
Solid-state co-extrusion of nylon 6 gel [AD-A156187] N85-35298

GENETICS
Genetic and physiological control of protective antigen synthesis by bacillus anthracis [AD-A156324] N85-35617

GEOCHEMISTRY
Chemistry division report [DE85-010586] N85-35228
The role of regional subsurface geochemistry in resource assessment in the central United States N85-35440
The development of assessment techniques program N85-35457
The Alaska Mineral Resources Assessment Program N85-35460

GEOCHRONOLOGY
Early and middle Cenozoic volcanic synthesis N85-35449
Hydrogeology of the lower Glen Rose Aquifer, south-central Texas N85-35466

GEODETIC SURVEYS
Carbon fiber strainmeter studies in southern California [PB85-196889] N85-35528

GEOIDS
A dynamic model of Venus's gravity field [NASA-CR-176173] N85-35845

GEOLOGICAL FAULTS
Geology: Structural history and fluvial geomorphology of the southern Death Valley Fault Zone, Inyo and San Bernardino Counties, California N85-35506
Structural development of the west-central Grant Range, Nye County, Nevada N85-35508

GEOLOGICAL SURVEYS
The development of assessment techniques program N85-35457
The Conterminous United States Mineral Assessment Program N85-35458
Federal Mineral Land Information System N85-35459
The Alaska Mineral Resources Assessment Program N85-35460
USGS coastal research, studies and maps: A source of information for coastal decision making [USGS-CIRC-883] N85-35465
Evaluation: Close-range photogrammetry for slope inventory and monitoring [PB85-192755] N85-35470

GEOMAGNETISM
Radio wave emitted by an extensive air showers in 10KHz to 1MHz region [HE-4.6-15] N85-36051
Measurement of neutrino oscillations in MACRO experiment [HE-5.3-10] N85-36104

GEOMETRIC RECTIFICATION (IMAGERY)
LANDSAT-4/5 image data quality analysis [E85-10105] N85-35463

GEOMETRICAL OPTICS
Edge detection and geometric methods in computer vision [AD-A155873] N85-35630

GEOMORPHOLOGY
Geology and geomorphology of the Roraima group, southeastern Venezuela N85-35511

GEOPHYSICS
Some geophysical guides to ore in southern and southwestern Alaska N85-35438
The development of assessment techniques program N85-35457
The Alaska Mineral Resources Assessment Program N85-35460
Procedure for editing the fluxgate magnetometer data of the AFGL (Air Force Geophysics Laboratory) magnetometer network [AD-A156331] N85-35523

GEOTHERMAL RESOURCES
Early and middle Cenozoic volcanic synthesis N85-35449
Evaluation of low-temperature geothermal potential in north-central Box Elder County, Utah [DE85-009541] N85-35490
Geothermal resources of the Washakie and Great Divide basins, Wyoming [DE85-013004] N85-35491

GETTERS
Vacuum system for the Argonne 6 GeV synchrotron light source [DE85-012286] N85-35773

GLASS
Single-point diamond crushing of Zerodur with in-situ polishing and metrology on a diamond turning machine [DE85-012918] N85-35305

GLIDERS
Proceedings of Meteorological Motor Glider (MEMO) Workshop '84 [DFVLR-MITT-85-04] N85-35542
Motor glider meteorology N85-35543
Typical and historical aspects of motor gliders as meteorological measuring aircraft N85-35544
A comparison between Falcon data and motor glider data N85-35547
Environmental-physical measurements and determination of atmospheric turbulence with the ASK-16 motor glider N85-35549
Partitioning of the vertical turbulent energy transport into positive and negative contributions --- meteorology N85-35551
Aircraft measurements during the Bonn Experiment (BONEX 1) --- meteorology N85-35552
Motor glider measurements during the Urban Atmosphere Energy Budget Experiment (EESA 1) N85-35553
Meteorological measurements with motor gliders in Poland N85-35555

GLUONS
Detectors for relativistic nuclear collisions (report from the Fixed-Target Hadron Group) N85-35701
Very high energy probes of the quark-gluon plasma N85-35708
Propagation of cosmic rays through the atmosphere in the quark-gluon strings model N85-35873
The phi-meson and Chiral-mass-meson production in heavy-ion collisions as potential probes of quark-gluon-plasma and Chiral symmetry transitions N85-35884
Heavy flavours production in quark-gluon plasma formed in high energy nuclear reactions N85-35886
A cosmic ray super high energy multicore family event. 2: Structure and fragmentation characteristics of the jets [HE-3.4-2] N85-35931
Peculiarities of gamma-quanta distribution at 20 TeV energy [HE-3.7-10] N85-35967
The maximum depth of shower with E sub 0 larger than 10(17) eV on average characteristics of EAS different components N85-35981
Calculation of intensity of high energy muon groups observed deep underground [HE-5.4-13] N85-36123

GLUTAMATES
Response of amino acids in hindlimb muscles to recovery from hypogravity and unloading by tail-cast suspension [NASA-CR-176183] N85-35589
Response of rat hindlimb muscles to 12 hours recovery from tail-cast suspension [NASA-CR-176182] N85-35590

GLUTAMINE
Response of amino acids in hindlimb muscles to recovery from hypogravity and unloading by tail-cast suspension [NASA-CR-176183] N85-35589
Response of rat hindlimb muscles to 12 hours recovery from tail-cast suspension [NASA-CR-176182] N85-35590

GLYCOGENS
Possible mechanism for changes in glycogen metabolism in unloaded soleus muscle [NASA-CR-176184] N85-35588
Muscle protein and glycogen responses to recovery from hypogravity and unloading by tail-cast suspension [NASA-CR-176181] N85-35591

GOLD
Elliptical X-ray analyzer spectrograph application to a laser-produced plasma [DE85-013790] N85-35398
Mineral deposit models: Theory and practice N85-35448
Some recent deposit modeling efforts N85-35453
The Conterminous United States Mineral Assessment Program N85-35458
Stopping relativistic Xe, Ho, Au and U nuclei in nuclear emulsions N85-35876

GOLD ALLOYS
Studies of the crystallization process of aluminum-silicon alloys using a high temperature microscope [NASA-TM-77869] N85-35272

GRAMMARS
Polylith: The early goals [DE85-012534] N85-35658

GRAPH THEORY
A graph theoretic procedure for the design of feedback patterns [REPT-110] N85-35673
Design of dynamic compensators of prescribed pattern [BU-109] N85-35674

GRAPHITE
Oxidation resistant slurry coating for carbon-based materials
[NASA-CASE-LEW-13923-1] N85-35267
Applications of the mineral resources data system and the international strategic minerals inventory in mineral-resource assessments by region and commodity N85-35451
GRAPHITE-EPOXY COMPOSITES
Damage induced stress redistribution in composite laminates N85-35235
Fuel containment and damage tolerance for large composite primary aircraft structures. Phase 1: Testing
[NASA-CR-166091] N85-35241
Quantitative non-destructive evaluation of composite materials based on ultrasonic wave propagation
[NASA-CR-176176] N85-35244
Effects of temperature on the tensile strength and elastic modulus of composite material
[AD-A156112] N85-35251
A normal incidence X-ray telescope sounding rocket payload
[NASA-CR-176169] N85-35749
GRASHOF NUMBER
Experimental study of free and mixed convective flow of air in a heated cavity
[DE85-012538] N85-35380
GRATINGS (SPECTRA)
On the convergence of an iterative formulation of the electromagnetic scattering from an infinite grating of thin wires N85-35319
Redefining the scratch standards
[PB85-194736] N85-35755
GRAVIRECEPTORS
Are living cells generally sensitive to gravity? N85-35602
GRAVITATION
The effect of power law body forces on a thermally-driven flow between concentric rotating spheres
[NASA-TM-87596] N85-35374
Aeromagnetic and gravity models of the pluton below the Lake City caldera, Colorado N85-35442
Three-dimensional gravity ideal body studies in rough terrain
[DE85-014097] N85-35525
GRAVITATIONAL EFFECTS
NASA Developmental Biology Workshop: A summary
[NASA-TM-86756] N85-35578
Effects of microgravity and hypergravity on invertebrate development N85-35579
Vertebrate development in space: Gravity is a drag (and has been for eons and eons) N85-35580
Report of the NASA Mammalian Developmental Biology Working Group N85-35581
Report of the Avian Development Working Group N85-35582
Report of Amphibian Development Group N85-35583
Report of the Insect Development Group N85-35584
Aquatic Invertebrate Development Working Group N85-35585
Report of the Microbial Development Working Group N85-35586
Cardiovascular responses to orthostatism and weightlessness N85-35601
Are living cells generally sensitive to gravity? N85-35602
Simulation of high +Gz onset in the dynamic environment simulator
[AD-A155963] N85-35610
GRAVITATIONAL FIELDS
The effect of power law body forces on a thermally-driven flow between concentric rotating spheres
[NASA-TM-87596] N85-35374
A dynamic model of Venus's gravity field
[NASA-CR-176173] N85-35845
GRAVITATIONAL WAVES
Some aspects of internal gravity waves in a multi-layered moving stratified flow N85-35369
GRAVITY ANOMALIES
Optimal estimation of a high degree gravity field from a global set of 1 deg x 1 deg anomalies to degree and order 250
[AD-A156008] N85-35519
Gravity gradiometer survey data processing
[AD-A156165] N85-35522
A dynamic model of Venus's gravity field
[NASA-CR-176173] N85-35845
GRAVITY GRADIOMETERS
Gravity gradiometer survey data processing
[AD-A156165] N85-35522
GREENHOUSE EFFECT
Carbon dioxide and climate: A working glossary
[DE85-013535] N85-35562
GRINDING (COMMINUTION)
Spectral characteristics of grinding sparks used for identification of scrap metals
[PB85-198570] N85-35290
GROUND BASED CONTROL
The development of assessment techniques program N85-35457
GROUND TRUTH
LANDSAT-4/5 image data quality analysis
[E85-10105] N85-35463
GROUND WATER
State-of-the-art construction technology for deep tunnels and shafts in rock
[AD-A156362] N85-35411
The geostatistical approach to the inverse problem in two-dimensional steady state groundwater modeling N85-35462
Simulated effects of increased recharge on the ground-water flow system of Yucca Mountain and vicinity, Nevada-California
[DE85-012985] N85-35469
Evaluation of low-temperature geothermal potential in north-central Box Elder County, Utah
[DE85-009541] N85-35490
Geothermal resources of the Washakie and Great Divide basins, Wyoming
[DE85-013004] N85-35491
Groundwater radon studies for earthquake precursors in southern California
[PB85-196871] N85-35529
GROUND WIND
The determination of lee circulation during the foehn wind N85-35554
Turbulent structure of stably stratified nocturnal slope flows
[AD-A155845] N85-35559
GUNS (ORDNANCE)
Next generation gunship
[AD-A156361] N85-35193
GUSTS
Lectures of a Flight Mechanics Conference — conferences
[ESA-TT-831] N85-35165
Gust simulation for flight mechanical wind tunnel tests N85-35172
GYRES
Current inventory of anthropogenic carbon dioxide in the North Pacific Subarctic Gyre
[PB85-187938] N85-35570
GYROSCOPES
Determining an azimuth with a north seeking gyro
[AD-A155880] N85-35180

H

HADRONS
Detector requirements for intensity interferometry measurements N85-35709
Status of the zeta(8.3)
[DE85-013070] N85-35724
Hadron cross sections at ultra high energies and unitarity bounds on diffraction dissociation
[HE-1.1-3] N85-35851
On total cross sections and slopes at superhigh energies
[HE-1.1-4] N85-35852
Hadron thermodynamics in relativistic nuclear collisions
[HE-1.1-8] N85-35856
Estimation of the total inelasticity coefficient in interaction of greater than or equal to 20 TeV hadrons with lead
[HE-1.1-9] N85-35857
1Single particle momentum and angular distributions in hadron-hadron collisions at ultrahigh energies
[HE-1.2-1] N85-35860
Empirical description of the hadron-hadron and hadron-nucleus interaction at the accelerator energy range
[HE-1.2-4] N85-35862
Low P sub T hadron-nucleus interactions
[HE-1.2-7] N85-35865
Angular distribution and multiplicity of backward hadrons in hFe interactions at 0.5-5.0 TeV energies (PION Experiment)
[HE-1.2-8] N85-35866
Nucleon-nucleus interactions from JACEE N85-35869
A unification of the interactions and the diffractive processes N85-35870
Is the inelastic charge-exchange contribution constant at the large X and superhigh energies? Qaut 01Kuchin, I. A. N85-35871
General consequences of the violated Feynman scaling N85-35872
Propagation of cosmic rays through the atmosphere in the quark-gluon strings model N85-35873
Scaling violation in the fragmentation region of inclusive nucleon spektrum N85-35874
Physical meaning of the multiplicities of emitted nucleons in hadron-nucleus collisions N85-35877
How are particle production, nucleon emission and target fragment evaporation processes interrelated in hadron-nucleus collisions? N85-35878
Experimental study of the space-time development of the particle production process in hadron-nucleon collisions, using massive target nucleus as a detector N85-35879
Experimental evidence of the decrease of kinetic energy of hadrons in passing through atomic nuclei N85-35880
Energy-range relations for hadrons in nuclear matter N85-35881
Scattering and stopping of hadrons in nuclear matter N85-35882
Measurements of hadron mean free path for the particle-producing collisions in nuclear matter N85-35883
The phi-meson and Chiral-mass-meson production in heavy-ion collisions as potential probes of quark-gluon-plasma and Chiral symmetry transitions N85-35884
Heavy flavours production in quark-gluon plasma formed in high energy nuclear reactions N85-35886
Observation of direct hadronic pairs in nucleus-nucleus collisions in JACEE emulsion chambers
[HE-1.4-5] N85-35893
Inclusive angular distribution of alpha and Li fragments produced in the Fe-C and Fe-Pb collisions at 1.88 GeV/u
[HE-1.4-11] N85-35898
Experiment Pamir-3. Coplanar emission of high energy gamma-quanta at interaction of hadrons with nuclei of air atoms at energies above 10 to the 7th power GeV
[HE-1.4-12] N85-35899
Japan - USSR joint emulsion chamber experiment at Pamir
[HE-3.1-1] N85-35901
Intensities of high-energy cosmic rays at Mount Kanbala
[HE-3.1-2] N85-35902
High energy gamma-rays and hadrons at Mount Fuji
[HE-3.1-3] N85-35903
Hadron intensity and energy spectrum at 4380 m above level
[HE-3.1-7] N85-35905
Some characteristic cosmic ray events and an attempt at their explanation
[HE-3.1-8] N85-35906
Scaling violation in fragmentation region at energies above 10-15 eV based on the data on cosmic ray hadron component
[HE-3.1-11] N85-35909
Jets in air-jet family
[HE-3.2-1] N85-35912
Scaling violation in hadron-nucleus interaction
[HE-3.2-8] N85-35916
Few-particles generation channels in inelastic hadron-nuclear interactions at energy approximately equals 400 GeV
[HE-3.2-9] N85-35917
Study of hadron bundles observed in Chacaltaya two-story emulsion chamber
[HE-3.3-4] N85-35922
Penetrative nature of high energy showers observed in Chacaltaya emulsion chamber
[HE-3.3-5] N85-35923
Anomalous correlation between hadron and electromagnetic particles in hadron and gamma-ray families
[HE-3.3-6] N85-35924
Atmospheric interactions detected in both the upper and the lower chambers at Chacaltaya
[HE-3.3-7] N85-35925
Lateral distribution of high energy hadrons and gamma ray in air shower cores observed with emulsion chambers
[HE-3.3-8] N85-35926
A cosmic ray super high energy multicore family event. 2: Structure and fragmentation characteristics of the jets
[HE-3.4-2] N85-35931
Observation of super high energy big family with large scale Fe emulsion chambers
[HE-3.4-3] N85-35932
A halo event created at 200 m above the Chacaltaya emulsion chamber
[HE-3.4-5] N85-35933
A binocular-type atmospheric interaction generating sequential exotic features
[HE-3.4-6] N85-35934

Gamma-hadron families and scaling violation
[HE-3.4-7] N85-35935
Super-family P2 C-96-125 observed by Japan-URSS Joint Emulsion Chamber Experiment
[HE-3.4-8] N85-35936
Experiment Pamir-2. Fianit: A giant super-family with halo (Epsilon sub 0 at approximately 10(17) eV)
[HE-3.4-10] N85-35938
Experiment Pamir-4: Analysis of superfamily with halo of electromagnetic nature detected in deep XEC
[HE-3.4-11] N85-35939
A search for mini-clusters in Japan-USSR Joint Experiment at Pamir
[HE-3.5-2] N85-35941
Mini-clusters
[HE-3.5-3] N85-35942
Giant mini-clusters as possible origin of halo phenomena observed in super-families
[HE-3.5-4] N85-35943
LPM effect and primary energy estimations
[HE-3.6-4] N85-35953
Experimental basis for the models of cascade propagation in atmosphere
[HE-3.6-6] N85-35954
Relation between gamma-ray family and EAS core: Monte-Carlo simulation of EAS core
[HE-3.6-7] N85-35955
Comparison of big event with calculations of the air shower development
[HE-3.6-8] N85-35956
On mini-cluster observed by Chacaltaya emulsion chamber experiment
[HE-3.6-12] N85-35959
A comparative analysis of gamma and hadron families at the superhigh energies recorded in experiment Pamir
[HE-3.7-1] N85-35960
Hadrons registration in emulsion chamber with carbon block
[HE-3.7-3] N85-35962
Intensities of high-energy cosmic rays at Mount Kanbala
[HE-3.7-5] N85-35964
Structured events in Pamir carbon X-ray chambers
[HE-3.7-7] N85-35965
Analysis of the hadron component in E.A.S.
N85-35971
Electrons, muons and hadrons in extensive air showers and how do they depend on nuclear interaction model, part 1
N85-35972
High energy hadrons in extensive air showers
N85-35976
Dependence of the average spatial and energy characteristics of the hadron-lepton cascade on the strong interaction parameters at superhigh energies
N85-35977
Hadronic components of EAS by rigorous saddle point method in the energy range between 10(5) and 10(8) GeV
N85-35978
About increase of the large transvere momentum processes fraction in hA interactions at energies 5.10(14) - 10(16) eV according to the data on E.A.S. hadrons
N85-35979
Phenomenology of soft hadron interactions and the relevant EAS data
N85-35980
The maximum depth of shower with E sub 0 larger than 10(17) eV on average characteristics of EAS different components
N85-35981
Sensitivity of depth of maximum and absorption depth of EAS to hadron production mechanism
N85-35982
Theoretical study of EAS hadronic structure
N85-35991
Muon spectrum in air showers initiated by gamma rays
[HE-4.5-4] N85-36028
Electromagnetic and muonic structure of showers initiated by gamma-rays and by hadrons
[HE-4.5-6] N85-36030
The muon content of gamma-ray showers
[HE-4.5-7] N85-36031
Simulation of gamma-initiated showers
[HE-4.5-10] N85-36033
Nuclear cascades in electromagnetic showers produced by primary gamma-quanta in the atmosphere
[HE-4.5-16] N85-36038
Investigation of cosmic rays in very short time scales
[HE-4.6-7] N85-36044
A facility for investigation of multiple hadrons at cosmic-ray energies
[HE-4.6-8] N85-36045
Sub-luminal pulses from cosmic ray air showers
[HE-4.7-13] N85-36063
Anomalies in cosmic rays: New particles versus charm?
[HE-5.4-9] N85-36120
Collimated groups of particles as possible manifestation of heavy meson production
[HE-5.4-14] N85-36124
Energetic delayed hadrons in large air showers observed at 5200m above sea level
[HE-6.2-9] N85-36145
Observation of genetic relation among new phenomena Geminion, Chiron and mini-Centauro
[HE-6.2-16] N85-36152
Tien-Shan effect and charmed particles
[HE-6.2-17] N85-36153

HALLEY'S COMET
The 1986 National Aeronautics and Space Administration authorization
[GPO-47-635] N85-35829
Comet Halley returns: A teachers' guide 1985-1986
[NASA-EP-197] N85-35839

HALOS
A cosmic ray super high multicore family event. 1: Experiment and general features
[HE-3.4-1] N85-35930
A halo event created at 200 m above the Chacaltaya emulsion chamber
[HE-3.4-5] N85-35933
On the halo events observed by Mount Fuji and Mount Kanbala Emulsion Chamber Experiments
[HE-3.4-9] N85-35937
Experiment Pamir-2. Fianit: A giant super-family with halo (Epsilon sub 0 at approximately 10(17) eV)
[HE-3.4-10] N85-35938
Experiment Pamir-4: Analysis of superfamily with halo of electromagnetic nature detected in deep XEC
[HE-3.4-11] N85-35939
Giant mini-clusters as possible origin of halo phenomena observed in super-families
[HE-3.5-4] N85-35943
Structure of super-families
[HE-3.5-7] N85-35944
Extremely high energy hadron and gamma-ray families(3). Core structure of the halo of superfamily
[HE-3.5-8] N85-35945
Numerical analysis of electromagnetic cascades in emulsion chambers
[HE-3.5-9] N85-35946

HAMILTONIAN FUNCTIONS
Width of nonlinear difference resonances
[DE85-013026] N85-35719

HANDBOOKS
International flight planning handbook
[AD-A156330] N85-35177
Fire service emergency management handbook
[AD-A155780] N85-35313
A guide for new environmental coordinators
[AD-A156327] N85-35498
Air university commander's and supervisor's guide on substance abuse
[AD-A156336] N85-35622
Recommendations for content revision and alternate delivery modes for the Human Engineering Guide to Equipment Design (HEGED)
[AD-A155781] N85-35624
Time domain reflectometry for SLC BPM system
[DE85-012389] N85-35758

HANDLING EQUIPMENT
Dental multi-purpose slowspeed handpieces test and evaluation
[AD-A155764] N85-35606

HARBORS
Bibliography on tidal hydraulics. Report 2. Supplement 9: Supplementary material compiled from June 1980 - June 1983. Tidal flows in rivers and harbors
[AD-A155990] N85-35574

HARDENING (MATERIALS)
Effect of prior warm rolling on the retained austenite content and hardening response of VIM-VAR (vacuum-induction melted-vacuum-arc remelted) AISI M-50 steel
[AD-A156145] N85-35281

HARDNESS
Tests on zirconium nitride coatings applied to SW 18 steel using the chemical vapor deposition method
N85-35271
Effect of thermal ageing on the mechanical properties of PWR pressure vessel steels and weldments
[AERE-R-11460] N85-35275

HARMONIC ANALYSIS
Optimal estimation of a high degree gravity field from a global set of 1 deg x 1 deg anomalies to degree and order 250
[AD-A156008] N85-35519

HARMONIC RADIATION
Cerenkov radiation from periodic electron bunches for finite emission length in air
[AD-A156156] N85-35352

HAZARDS
The investigation of tethered satellite system dynamics
[NASA-CR-176180] N85-35215
Fire service emergency management handbook
[AD-A155780] N85-35313
Investigation of the lightning vulnerability of nuclear explosive test systems at the Nevada Test Site
[DE85-011761] N85-35563
National program for inspection of non-federal dams. Woodward reservoir dam (VT 00209), Connecticut River Basin, Plymouth, Vermont. Phase 1 inspection report
[AD-A156256] N85-35693

HEALTH PHYSICS
Wholebody radiation counting system
[AD-A155842] N85-35607

HEART RATE
Weight loss, rectal temperature and heart rates following the 1984 Boston Marathon
[AD-A155984] N85-35612

HEAT
Advanced regenerative heat recovery system
[PB85-199602] N85-35315

HEAT BALANCE
Maintenance of blocking anticyclones in a general circulation model
[PB85-190866] N85-35567

HEAT EXCHANGERS
High Temperature Heating System (HTHS)
[PB85-188340] N85-35316
Experimental lithium system
[DE85-013252] N85-35382

HEAT FLUX
High Temperature Heating System (HTHS)
[PB85-188340] N85-35316
Development of advanced high-temperature heat flux sensors. Phase 2: Verification testing
[NASA-CR-174973] N85-35391
Case studies for flux measurements along a low-flying route to the south of Munich
N85-35548
Two-point closure study of covariance budgets for turbulent Rayleigh-Benard convection
[PB85-189108] N85-35568

HEAT MEASUREMENT
Cryogenic laser calorimetry for impurity analysis
[NASA-CR-176179] N85-35395
X-ray film chamber with carbon target of Tien-Shan complex array
N85-35915

HEAT OF FORMATION
Heats of formation of gas phase organosulfur molecules, radicals and ions measured by PEPICO and application of (17)O and (33)S NMR spectroscopy to structure determination of organosulfur compounds
[DE85-010558] N85-35229

HEAT PIPES
Infrared generation and wave-mixing studies in cesium
[DE85-012883] N85-35304
Development of a high-efficiency, gas-fired, heat pipe, warm-air heating system
[PB85-199636] N85-35318

HEAT RESISTANT ALLOYS
Microshrink, tensile properties, and the detection of microshrink
[AD-A155875] N85-35278

HEAT SHIELDING
Results of tests on a specimen of the SRB aft skirt heat shield curtain in the MSFC LRLF
[NASA-CR-170883] N85-35221
Results of tests of the SRB aft skirt heat shield curtain in the MSFC Hot Gas Facility
[NASA-CR-170888] N85-35223

HEAT SOURCES
Development and characterization of carbon-bonded carbon fiber insulation for radioisotope space power systems
[DE85-013365] N85-35299

HEAT TRANSFER
Advanced regenerative heat recovery system
[PB85-199602] N85-35315
High Temperature Heating System (HTHS)
[PB85-188340] N85-35316
Heat transfer characteristics for two-dimensional arrays of impinging jets with initial crossflow
N85-35365
A two-phase flow and heat transfer model for zero gravity
[AD-A156097] N85-35377
Experimental study of free and mixed convective flow of air in a heated cavity
[DE85-012538] N85-35380
Enhanced heat transfer computations for internally cooled cable superconductor
[DE85-011897] N85-35383
Transient three-phase three-component systems. Part 1: Formulation of the system of differential equations
[DE85-013267] N85-35384
Heat transfer and brine evolution in magma-hydrothermal systems
N85-35441
Computer code calculations of the TMI-2 accident: Initial and boundary conditions
[DE85-012613] N85-35666

Analysis of reactor material experiments investigating oxide fuel crust stability and heat transfer in jet impingement flow
[DE85-012097] N85-35739
HEAT TRANSFER COEFFICIENTS
Heat transfer coefficients for particles in liquid in axially rotating cans N85-35370
A two-phase flow and heat transfer model for zero gravity
[AD-A156097] N85-35377
HEAT TRANSMISSION
Advanced regenerative heat recovery system
[PB85-199602] N85-35315
Geothermal resources of the Washakie and Great Divide basins, Wyoming
[DE85-013004] N85-35491
HEAT TREATMENT
Studies of the crystallization process of aluminum-silicon alloys using a high temperature microscope
[NASA-TM-77869] N85-35272
The dynamic strain ageing of A533B class 1 nuclear pressure vessel steel
[AERE-R-11485] N85-35274
Effect of thermal ageing on the mechanical properties of PWR pressure vessel steels and weldments
[AERE-R-11460] N85-35275
The character of observed porosity and its possible effects on rolling contact fatigue life of M-50 steel
[AD-A155930] N85-35279
Development of a high strength isothermally heat-treated nodular iron road wheel arm
[AD-A155755] N85-35408
HEATING EQUIPMENT
Development of a high-efficiency, gas-fired, heat pipe, warm-air heating system
[PB85-199636] N85-35318
HEAVY ELEMENTS
Pulsed-neutron-source models for the astrophysical s-process
[DE85-012927] N85-35740
Some nuclear data needs in astrophysics
[DE85-012916] N85-35842
HEAVY IONS
Proceedings of the Workshop on Detectors for Relativistic Nuclear Collisions
[LBL-18225] N85-35700
Summary of the working group on penetrating probes in collider experiments. 1: The collider environment N85-35704
Fractional charge resolution in music N85-35712
Calculation of heavy-ion tracks in liquid water
[DE85-012101] N85-35725
Considerations on collective ion acceleration as an intense ion injector
[DE85-012706] N85-35757
Ion source development for the Los Alamos heavy ion fusion injector
[DE85-012682] N85-35766
Applications of decelerated ions
[DE85-011832] N85-35767
Numerical studies of high current beam compression in heavy ion fusion
[DE85-011874] N85-35783
Multiple vacancy production by high energy heavy ions
[DE85-004428] N85-35805
The phi-meson and Chiral-mass-meson production in heavy-ion collisions as potential probes of quark-gluon-plasma and Chiral symmetry transitions N85-35884
On the mechanism of anomalous nucleus-nucleus interactions at energies above 1 TeV/nucleon
[HE-1.4-8] N85-35896
Meson multiplicity in nucleus-nucleus collisions above 4 GeV/amu
[HE-1.4-10] N85-35897
Multidimensional analysis of data obtained in experiments with X-ray emulsion chambers and extensive air showers
[HE-3.6-2] N85-35951
HEAVY NUCLEI
The response of a scintillation counter below an emulsion chamber to heavy nucleus interactions in the chamber N85-35889
Heavy nucleus collisions between 20 and 60 GeV/nucleon
[HE-1.4-2] N85-35890
Characteristics of central collision events in Fe-nucleus interactions for 20 - 60 GeV/nucleon
[HE-1.4-3] N85-35891
Nucleus-nucleus interaction above several hundred GeV/n
[HE-1.4-4] N85-35892
Experiment Pamir-3. Coplanar emission of high energy gamma-quanta at interaction of hadrons with nuclei of air atoms at energies above 10 to the 7th power GeV
[HE-1.4-12] N85-35899
Intensities of high-energy cosmic rays at Mount Kanbala
[HE-3.1-2] N85-35902
Multidimensional analysis of data obtained in experiments with X-ray emulsion chambers and extensive air showers
[HE-3.6-2] N85-35951
On mini-cluster observed by Chacaltaya emulsion chamber experiment
[HE-3.6-12] N85-35959
Monte Carlo simulations of electron lateral distributions in the core region of 10(13) - 10(16) eV air showers N85-35992
Comparison of simulation results with sea-level experimental data on 10(14) - 10(16) air shower cores N85-35993
Relevance of multiple muons detected underground to the mass composition of primary cosmic rays
[HE-5.1-4] N85-36069
Search for stellar collapse with the MACRO detector at Gran Sasso
[HE-5.3-11] N85-36105
Spatial distribution read-out system for thermoluminescence sheets
[HE-7.1-7] N85-36161
HELICOPTER PERFORMANCE
The effects of parameter variation on helicopter performance
[AD-A156027] N85-35189
Development of NATOPS performance software for the SH-3D and SH-3H helicopters
[AD-A156140] N85-35192
HELICOPTERS
U.S. Civil airmen statistics for calendar year 1984
[AD-A156326] N85-35153
Laboratory vibration schedules
[AD-A155856] N85-35188
Development of NATOPS (Naval Air Training and Operating Procedure Standardization) performance software for the H-46D helicopter
[AD-A156089] N85-35190
Development of NATOPS performance software for the SH-3D and SH-3H helicopters
[AD-A156140] N85-35192
HELIOS 1
Parallel fast-forward shock within 1 AU: Helios-1 and 2 observations
[MPAE-W-79-84-27] N85-35847
HELIOS 2
Parallel fast-forward shock within 1 AU: Helios-1 and 2 observations
[MPAE-W-79-84-27] N85-35847
HELIUM
Experimental technique for measuring the isentrope of hydrogen to several megabars
[DE85-014332] N85-35386
Search for magnetic monopoles using proportional counters filled with helium gas
[HE-6.1-1] N85-36127
Magnetic monopole search by 130 m(2)sr He gas proportional counter
[HE-6.1-2] N85-36128
Results from the UCSD magnetic monopole search
[HE-6.1-12] N85-36137
HELMHOLTZ RESONATORS
A research program to reduce the interior noise in general aviation aircraft, index and summary
[NASA-CR-176178] N85-35695
HERBIG-HARO OBJECTS
The structure of Herbig-Haro object 43 and Orion dark cloud extinction
[NASA-TM-87503] N85-35831
HETEROJUNCTIONS
Optical properties of heterostructures and superlattices
[AD-A156243] N85-35802
HIERARCHIES
Source hierarchy list. Volume 1: A through H
[AD-A156300] N85-35825
Source hierarchy list. Volume 2: I through Z
[AD-A156301] N85-35826
HIGH CURRENT
Observations of accelerated high current low emittance beams in the SLC Linac
[DE85-013073] N85-35211
Numerical studies of high current beam compression in heavy ion fusion
[DE85-011874] N85-35783
HIGH ENERGY INTERACTIONS
A survey of multiplicities and rapidity densities from existing emission data on hadron-nucleus nucleus-nucleus collisions N85-35706
A simulation of ultra-relativistic nucleus-nucleus collisions N85-35707
Very high energy probes of the quark-gluon plasma N85-35708
Detector requirements for intensity interferometry measurements N85-35709
Forty-five years of e(+)e(-) annihilation physics: 1956 to 2001
[DE85-013052] N85-35723
Neutrino production of like sign dimuons
[DE85-013594] N85-35741
SLC Energy Upgrade Program at SLAC
[DE85-014290] N85-35790
Development of observational and instrumental techniques in hard X-ray and medium energy gamma-ray astronomy
[NASA-CR-176172] N85-35841
Nineteenth International Cosmic Ray Conference. HE Sessions, volume 6
[NASA-CP-2376-VOL-6] N85-35848
Estimation of the total inelasticity coefficient in interaction of greater than or equal to 20 TeV hadrons with lead
[HE-1.1-9] N85-35857
The method for the study of the inelastic cross-section for high energy protons by means of shower arrays with the large calorimetric area
[HE-1.1-11] N85-35858
On a possibility of inelasticity partial coefficient K sub gamma determination in pi C and pi Pb interactions at 10 to the 14th power eV (experiment PAMIR 1)
[HE-1.1-12] N85-35859
QCD-motivated description of very high energy particle interactions
[HE-1.2-2] N85-35861
Empirical description of the hadron-hadron and hadron-nucleus interaction at the accelerator energy range
[HE-1.2-4] N85-35862
Multiplicity distributions in interaction models used for cascade simulations
[HE-1.2-5] N85-35863
Transverse momentum distribution of pion deg in the fragmentation region of super high energy interactions N85-35921
Penetrative nature of high energy showers observed in Chacaltaya emulsion chamber
[HE-3.3-5] N85-35923
Lateral distribution of high energy hadrons and gamma ray in air shower cores observed with emulsion chambers
[HE-3.3-8] N85-35926
Size distributions of air showers accompanied with high energy gamma ray bundles observed at Mt. Chacaltaya
[HE-3.3-9] N85-35927
An experimental study of correlations in the development of the electron-photon cascades
[HE-3.5-10] N85-35947
A comparative analysis of gamma and hadron families at the superhigh energies recorded in experiment Pamir
[HE-3.7-1] N85-35960
Nineteenth International Cosmic Ray Conference. HE Sessions, volume 7
[NASA-CP-2376-VOL-7] N85-35968
Analysis of the hadron component in E.A.S. N85-35971
Electrons, muons and hadrons in extensive air showers and how do they depend on nuclear interaction model, part 1 N85-35972
Simulation of EAS properties on the basis of high energy interaction model deduced from the accelerator data N85-35973
High energy hadrons in extensive air showers N85-35976
Dependence of the average spatial and energy characteristics of the hadron-lepton cascade on the strong interaction parameters at superhigh energies N85-35977
Hadronic components of EAS by rigorous saddle point method in the energy range between 10(5) and 10(8) GeV N85-35978
Phenomenology of soft hadron interactions and the relevant EAS data N85-35980
Development of electromagnetic cascades in the atmosphere including the Landau-Pomeranchuk-Migdal effect
[HE-4.5-5] N85-36029
Nuclear cascades in electromagnetic showers produced by primary gamma-quanta in the atmosphere
[HE-4.5-16] N85-36038
Energy spectrum of cascade showers induced by cosmic ray muons in the range from 50 GeV to 5 TeV
[HE-5.2-14] N85-36090
Range fluctuations of high energy muons passing through matter
[HE-5.2-19] N85-36095
High energy neutrino astronomy with MACRO
[HE-5.3-12] N85-36106

The capability of the existing network of installations for detecting the antineutrino burst from collapsing stars [HE-5.3-13] N85-36107
Energy spectra of high energy atmospheric neutrinos [HE-5.3-14] N85-36108
A standard source for high energy neutrino astronomy [HE-5.3-15] N85-36109
A search for cosmic sources of high energy neutrinos with small underground detectors [HE-5.3-16] N85-36110
Characteristics of slow particles emitted in the charged current interactions of neutrinos with emulsion nuclei [HE-5.3-22] N85-36113
Multiple muons of conventional and exotic origin in DUMAND [HE-5.4-4] N85-36117
Study of photonuclear muon interactions at Baksan underground scintillation telescope [HE-5.4-10] N85-36122
Calculation of intensity of high energy muon groups observed deep underground [HE-5.4-13] N85-36123
Results of investigation of muon fluxes of superhigh energy cosmic rays with X-ray emulsion chambers [HE-5.4-16] N85-36126
High energy cosmic ray signature of quark nuggets [HE-6.2-11] N85-36147

HIGH GRAVITY ENVIRONMENTS
Effects of microgravity and hypergravity on invertebrate development N85-35579

HIGH PRESSURE
Experimental technique for measuring the isentrope of hydrogen to several megabars [DE85-014332] N85-35386

HIGH RESOLUTION
High-resolution spectroscopy and dynamics of multiphoton processes in atoms and molecules [AD-A155862] N85-35714
High resolution beam profile monitors in the SLC [DE85-013375] N85-35774

HIGH STRENGTH
Development of a high strength isothermally heat-treated nodular iron road wheel arm [AD-A155755] N85-35408

HIGH TEMPERATURE
Effects of temperature on the tensile strength and elastic modulus of composite material [AD-A156112] N85-35251

HIGH TEMPERATURE ENVIRONMENTS
Thermal barrier coating system [NASA-CASE-LEW-14057-1] N85-35233

HIGH TEMPERATURE GASES
Results of tests of weathered K5NA closeout material in the MSFC Hot Gas Facility [NASA-CR-170893] N85-35239
Study of NSI and related cable performance during tests performed in the NASA Hot Gas Facility [NASA-CR-170886] N85-35423

HIGH TEMPERATURE TESTS
Space shuttle SRB TPS protective paint test and evaluation in NASA Hot Gas Facility and AEDC Tunnel C [NASA-CR-170884] N85-35294

HIGH VOLTAGES
Photoconductive pulse power switches: A review [DE85-014125] N85-35360

HISTOGRAMS
Study of spectral/radiometric characteristics of the Thematic Mapper for land use applications [E85-10106] N85-35464
Edge information in color images based on histograms of differences [AD-A156002] N85-35751

HISTORIES
Development of flight mechanics research in Brunswick N85-35166
Typical and historical aspects of motor gliders as meteorological measuring aircraft N85-35544

HODOSCOPES
The response of a scintillation counter below an emulsion chamber to heavy nucleus interactions in the chamber N85-35889
Results of a search for monopoles and tachyons in horizontal cosmic ray flux [HE-6.1-3] N85-36129
Search for acoustic signals from high energy cascades [HE-7.1-1] N85-36155

HOLDERS
Results of tests of MTA-2 TPS on the SRB hold-down bolt blast container [NASA-CR-170891] N85-35224

HOLES (ELECTRON DEFICIENCIES)
Dangling bonds and sub-gap optical absorption in silicon [DE85-011752] N85-35302
Optical properties of heterostructures and superlattices [AD-A156243] N85-35802
Multiple vacancy production by high energy heavy ions [DE85-004428] N85-35805

HOLMIUM
Stopping relativistic Xe, Ho, Au and U nuclei in nuclear emulsions N85-35876

HOLOGRAPHY
Fatigue damage detection in steels by optical correlation [AD-A155830] N85-35277
Holoswitch [AD-A155841] N85-35392

HOMING
Determining an azimuth with a north seeking gyro [AD-A155880] N85-35180

HONEYCOMB CORES
Stress analysis of axisymmetric sandwich shells of variable thickness N85-35419

HONEYCOMB STRUCTURES
Computational methods for the explosive and impact compaction of powders [AD-A156219] N85-35653

HORIZON SCANNERS
Studies of the solar mesosphere explorer: Dynamics and horizon sensor performance. Part A: Spin axis precession and atmospheric drag. Part B: Clouds [NASA-CR-175308] N85-35213

HOT CORROSION
High temperature corrosion of ceramics [DE85-013481] N85-35303

HOT WORKING
Effect of prior warm rolling on the retained austenite content and hardening response of VIM-VAR (vacuum-induction melted-vacuum-arc remelted) AISI M-50 steel [AD-A156145] N85-35281

HUGONIOT EQUATION OF STATE
Dynamic compaction of a monosized spherical tungsten powder [DE85-014808] N85-35289

HUMAN BEINGS
Tritium hazard via the ingestion pathway [DE85-012897] N85-35618

HUMAN BODY
A mechanical model of the human body and its application N85-35598

HUMAN FACTORS ENGINEERING
Calculation of trajectories of detached wind turbine blades and prediction of site risk levels associated with failures of HAWT's N85-35475
The human engineering eye movement measurement research facility [AD-A156099] N85-35613
Recommendations for content revision and alternate delivery modes for the Human Engineering Guide to Equipment Design (HEGED) [AD-A155781] N85-35624
Attacking software crisis: A macro approach [AD-A155846] N85-35645

HUMAN PATHOLOGY
Analogies of control mechanisms in flight guidance and medicine N85-35597

HUMAN PERFORMANCE
The relationship between personality and performance N85-35600
The effect of an unphysiological oxygen supply on the organism N85-35605
An exploratory study of the effect of screen size and resolution on the legibility of graphics in automated job performance aids [AD-A155989] N85-35632

HUMIDITY
Millimeter-wave propagation in moist air: Model versus path data [AD-A156040] N85-35331

HURRICANES
Kinematic analysis of Hurricane Frederick (1979) using satellite, aircraft and rawinsonde data [NASA-CR-176167] N85-35533

HYDRAULICS
Computer code calculations of the TMI-2 accident: Initial and boundary conditions [DE85-012613] N85-35666

HYDROCARBON FUELS
Aspects of high-resolution gas chromatography as applied to the analysis of hydrocarbon fuels and other complex organic mixtures. Volume 1 [AD-A156154] N85-35257

HYDROCARBONS
FTIR studies of hydrocarbon synthesis on Pd/ZSM5 catalysts [DE85-012430] N85-35230
The Conterminous United States Mineral Assessment Program N85-35458
Thermal evolution of coastal California with implications for hydrocarbon maturation N85-35509
Molecular biology of environmental aromatic hydrocarbons [DE85-015036] N85-35593
Few-particles generation channels in inelastic hadron-nuclear interactions at energy approximately equals 400 GeV [HE-3.2-9] N85-35917

HYDROCHLORIC ACID
A study of the chemistry of alkali metals in the upper atmosphere [AD-A156349] N85-35524

HYDRODYNAMICS
Adaptive rezoner in a two-dimensional Lagrangian hydrodynamic code [DE85-010108] N85-35381

HYDROGEN
CO + H2 reaction over nitrogn-modified iron catalysts [DE85-013791] N85-35231
Fluidized bed desulfurization [NASA-CASE-NPO-15924-1] N85-35253
Pressure measurements in a hydrogen combustion environment: Hydrogen-air combustion test series 1 and 2 in the FITS tank, volume 1 [TI85-009899] N85-35259
Vectorial electron transfer on designed surfaces [PB85-204600] N85-35263
Effect of temperature and ionic impurities at very low concentrations on stress corrosion cracking of Type 304 stainless steel [TI85-003048] N85-35283
Experimental technique for measuring the isentrope of hydrogen to several megabars [DE85-014332] N85-35386
Characterization of catalysts with metal-support effects and of the species adsorbed on their surfaces [DE85-012254] N85-35394
Cooling high intensity atomic hydrogen beams to liquid helium temperatures [DE85-012515] N85-35718
Limiter [DE85-011620] N85-35736
Circumstellar shells of late-type stars: A study at millimeter and infrared wavelengths N85-35836
Some nuclear data needs in astrophysics [DE85-012916] N85-35842

HYDROGEN OXYGEN ENGINES
Status of advanced orbital transfer propulsion [NASA-TM-87069] N85-35225

HYDROGEN SULFIDE
The identification of compounds in mustard hydrolysate [AD-A156381] N85-35258

HYDROGEOLOGY
Hydrogeology of the lower Glen Rose Aquifer, south-central Texas N85-35466

HYDROGRAPHY
Federal Mineral Land Information System N85-35459

HYDROLOGY
USGS coastal research, studies and maps: A source of information for coastal decision making [USGS-CIRC-883] N85-35465
Two-dimensional inversion of resistivity monitoring data from the Cerro Prieto geothermal field [DE85-012554] N85-35494

HYDROLOGY MODELS
The development of assessment techniques program N85-35457

HYDROLYSIS
The identification of compounds in mustard hydrolysate [AD-A156381] N85-35258
Aqueous volatile weak electrolyte equilibria to 300 C [DE85-013840] N85-35261

HYDROTHERMAL SYSTEMS
Heat transfer and brine evolution in magma hydrothermal systems N85-35441
Massive sulfide deposits from the southern Juan de Fuca Ridge N85-35446
A comparison of LANDSAT thematic mapper, multispectral scanner and airborne sensors for mapping the distribution of alteration minerals: Examples from the southwestern United States N85-35452
Preliminary results of an ALVIN dive program on active hydrothermal vents at the southern Juan de Fuca Ridge N85-35454
Ore genesis at the Monterrosas deposit in the Coastal Batholith, Ica, Peru N85-35510

HYDROXYL EMISSION
Far-infrared emission lines of CO and OH in the Orion-KL molecular shock [NASA-TM-86721] N85-35832
Observations of far-infrared transitions between excited states of OH [NASA-TM-86722] N85-35833

HYPERBOLIC DIFFERENTIAL EQUATIONS
Absorbing boundary conditions for exterior problems
[NASA-CR-177944] N85-35676
HYPERSONIC FLOW
Mach 14 flow restrictor thermal stress analysis
[AD-A156215] N85-35208
HYPERSONIC WIND TUNNELS
Mach 14 flow restrictor thermal stress analysis
[AD-A156215] N85-35208
HYPERVELOCITY IMPACT
Experimental data for characterizing perforating impacts: Fragmentation processes
[AD-A156370] N85-35427
HYPERVELOCITY PROJECTILES
Experimental data for characterizing perforating impacts: Fragmentation processes
[AD-A156370] N85-35427
HYPOKINESIA
Possible mechanism for changes in glycogen metabolism in unloaded soleus muscle
[NASA-CR-176184] N85-35588
HYPOTHESES
Invariant tests and likelihood ratio tests for multivariate elliptically contoured distributions
[AD-A155844] N85-35679
HYPOXEMIA
The effect of an unphysiological oxygen supply on the organism N85-35605

I

ICE
Elemental tracers of source regions of contaminants in precipitation
[DE85-012858] N85-35499
ICE ENVIRONMENTS
The NORDA/FNOC (Naval Ocean Research and Development Activity's/Fleet Numerical Oceanography Center) Polar Ice Prediction System (PIPS)-Arctic: A technical description
[AD-A156332] N85-35577
IGNEOUS ROCKS
Aeromagnetic and gravity models of the pluton below the Lake City caldera, Colorado N85-35442
IGNITION
Laser probes of natural gas ignition chemistry
[PB85-200210] N85-35264
Neutral pumping rates for a next step tokamak ignition device
[DE85-012780] N85-35776
IGNITION LIMITS
The use of a laser Doppler velocimeter in a standard flammability tube
[NASA-CR-174960] N85-35389
ILLUMINANCE
Immediate visibility after red and white adaptation
[AD-A156271] N85-35616
IMAGE INTENSIFIERS
Application of thermoluminescence for detection of cascade shower 1: Hardware and software of reader system
[HE-7.1-6] N85-36160
Spatial distribution read-out system for thermoluminescence sheets
[HE-7.1-7] N85-36161
Application of thermoluminescence for detection of cascade shower 2: Detection of cosmic ray cascade shower at Mount Fuji
[HE-7.1-12] N85-36162
IMAGE PROCESSING
Raster functionality for a VDI
[DE85-006734] N85-35396
Strain measurement using point recognition picture processing
[DRIC-T-7407] N85-35421
Selected publications in image understanding and computer vision from 1974 to 1983
[AD-A156196] N85-35634
Edge information in color images based on histograms of differences
[AD-A156002] N85-35751
Application of thermoluminescence for detection of cascade shower 1: Hardware and software of reader system
[HE-7.1-6] N85-36160
Spatial distribution read-out system for thermoluminescence sheets
[HE-7.1-7] N85-36161
Application of thermoluminescence for detection of cascade shower 2: Detection of cosmic ray cascade shower at Mount Fuji
[HE-7.1-12] N85-36162
IMAGE RESOLUTION
An exploratory study of the effect of screen size and resolution on the legibility of graphics in automated job performance aids
[AD-A155989] N85-35632
IMAGERY
Selected publications in image understanding and computer vision from 1974 to 1983
[AD-A156196] N85-35634
IMAGES
Remote sensing of hydrologic transport processes using spot simulation data
[DE85-012412] N85-35467
Edge information in color images based on histograms of differences
[AD-A156002] N85-35751
IMAGING TECHNIQUES
An experimental study of dielectric rod antennas for millimeter-wave imaging applications
[AD-A155832] N85-35328
Strain measurement using point recognition picture processing
[DRIC-T-7407] N85-35421
Processing of LANDSAT imagery to map surface mineral alteration on the Alaska Peninsula, Alaska N85-35455
Selected publications in image understanding and computer vision from 1974 to 1983
[AD-A156196] N85-35634
Optical synthetic aperture techniques
[AD-A156151] N85-35752
IMPACT
Friction, impact, and electrostatic discharge sensitivities of energetic materials
[DE85-013321] N85-35309
IMPACT DAMAGE
Quantitative non-destructive evaluation of composite materials based on ultrasonic wave propagation
[NASA-CR-176176] N85-35244
IMPACT TESTS
Design and testing of an energy-absorbing crewseat for the F/FB-111 aircraft. Volume 2: Data from seat testing
[NASA-CR-3917] N85-35184
IMPACT TOLERANCES
Design and testing of an energy-absorbing crewseat for the F/FB-111 aircraft. Volume 2: Data from seat testing
[NASA-CR-3917] N85-35184
IMPEDANCE
Characterization of microstrip discontinuities in the time and frequency domains
[NASA-CR-176190] N85-35342
IMPINGEMENT
Computation of three-dimensional shock wave and boundary-layer interactions
[NASA-TM-86780] N85-35372
IMPLOSIONS
System expectations for Pioneer 1 foil implosion experiments
[DE85-014129] N85-35359
Diagnostics for Pioneer 1 imploding plasma experiments
[DE85-014120] N85-35787
IMPULSE GENERATORS
Application of pulsed power in the simulation of severe natural lightning
[DE85-012866] N85-35564
IMPURITIES
Effect of temperature and ionic impurities at very low concentrations on stress corrosion cracking of Type 304 stainless steel
[TI85-003048] N85-35283
Cryogenic laser calorimetry for impurity analysis
[NASA-CR-176179] N85-35395
X-ray fluorescence analysis of uranium concentrates
[DE85-013189] N85-35717
INCIDENCE
A normal incidence X-ray telescope sounding rocket payload
[NASA-CR-176169] N85-35749
INCOMPRESSIBLE FLOW
General design method for 3-dimensional, potential flow fields. Part 2: Computer program DIN3D1 for simple, unbranched ducts
[NASA-CR-3926] N85-35159
INDEPENDENT VARIABLES
The effects of parameter variation on helicopter performance
[AD-A156027] N85-35189
The NORDA/FNOC (Naval Ocean Research and Development Activity's/Fleet Numerical Oceanography Center) Polar Ice Prediction System (PIPS)-Arctic: A technical description
[AD-A156332] N85-35577
INDEXES (DOCUMENTATION)
A research program to reduce the interior noise in general aviation aircraft, index and summary
[NASA-CR-176178] N85-35695
Source hierarchy list. Volume 1: A through H
[AD-A156300] N85-35825
Source hierarchy list. Volume 2: I through Z
[AD-A156301] N85-35826
INDONESIA
Microwave propagation studies, measurements and education in Surabaya, Indonesia
[B8464633] N85-35339
INDUCTION MOTORS
State-of-the-art of solid-state motor controllers
[TI85-008674] N85-35806
INDUSTRIAL MANAGEMENT
DOD Value Engineering Conference report. Value Engineering (VE): A tool that benefits line management held at Leesburg, Virginia on 1-2 November 1984. Part 1. Executive summary
[AD-A156067] N85-35810
DOD Value Engineering Conference report. Value Engineering (VE): A tool that benefits line management held at Leesburg, Virginia on 1-2 November 1984. Part 2. Plenary session
[AD-A156068] N85-35811
INELASTIC COLLISIONS
On a possibility of inelasticity partial coefficient K sub gamma determination in pi C and pi Pb interactions at 10 to the 14th power eV (experiment PAMIR 1)
[HE-1.1-12] N85-35859
Determination of primary energy in nucleus-nucleus collisions and the high P(sub)T tail of alpha-particles N85-35875
INELASTIC SCATTERING
Calculation of heavy-ion tracks in liquid water
[DE85-012101] N85-35725
Fast-neutron interaction with niobium
[DE85-011471] N85-35731
Proton-air and proton-proton cross sections from air shower data
[HE-1.1-1] N85-35849
Proton-air inelastic cross section at S(1/2) = 30 TeV
[HE-1.1-2] N85-35850
Hadron cross sections at ultra high energies and unitarity bounds on diffraction dissociation
[HE-1.1-3] N85-35851
Determination of the cross section of the proton, pion and neutron inelastic interaction with lead and carbon nuclei at 0.5 - 5.0 TeV energies (PION experiment)
[HE-1.1-5] N85-35853
Estimation of the total inelasticity coefficient in interaction of greater than or equal to 20 TeV hadrons with lead
[HE-1.1-9] N85-35857
The method for the study of the inelastic cross-section for high energy protons by means of shower arrays with the large calorimetric area
[HE-1.1-11] N85-35858
Forward particle production in inelastic Ne-22 inteVractions in emulsion at 4.1 A Ge/c
[HE-1.4-7] N85-35895
Meson multiplicity in nucleus-nucleus collisions above 4 GeV/amu
[HE-1.4-10] N85-35897
On the characteristics of emulsion chamber family events produced in low heights
[HE-3.1-6] N85-35904
A study of gamma-families generated in nucleon-nucleus (NA) and pion-nucleus (pi A) interactions
[HE-3.7-2] N85-35961
QCD analysis of neutrino charged current structure function F2 in deep inelastic scattering
[HE-5.3-23] N85-36114
INELASTIC STRESS
Subcritical fracture propagation in rocks: An examination using the methods of fracture mechanics and non-destructive testing N85-35516
INERTIAL FUSION (REACTOR)
Ion source development for the Los Alamos heavy ion fusion injector
[DE85-012682] N85-35766
INFECTIOUS DISEASES
Molecular biology of environmental aromatic hydrocarbons
[DE85-015036] N85-35593
INFERENCE
Manual and computer-aided sequential diagnostic inference
[AD-A156229] N85-35620
INFINITY
On the convergence of an iterative formulation of the electromagnetic scattering from an infinite grating of thin wires N85-35319

INFORMATION DISSEMINATION
USGS coastal research, studies and maps: A source of information for coastal decision making
[USGS-CIRC-883] N85-35465
INFORMATION MANAGEMENT
Research report program of the US Army in Europe N85-35167
Electronic information management and productivity
[DE85-013362] N85-35818
Records Disposal: A guidebook for laboratory offices
[AD-A156064] N85-35823
INFORMATION RETRIEVAL
LOCAT: A data retrieval program
[AD-A156004] N85-35822
Source header list, supplement 3
[AD-A156100] N85-35824
Source hierarchy list. Volume 1: A through H
[AD-A156300] N85-35825
Source hierarchy list. Volume 2: I through Z
[AD-A156301] N85-35826
INFORMATION SYSTEMS
Procedure for editing the fluxgate magnetometer data of the AFGL (Air Force Geophysics Laboratory) magnetometer network
[AD-A156331] N85-35523
Electronic information management and productivity
[DE85-013362] N85-35818
INFRARED ASTRONOMY SATELLITE
The 1986 National Aeronautics and Space Administration authorization
[GPO-47-635] N85-35829
INFRARED IMAGERY
Surface cyclogenesis as indicated by satellite imagery
[PB85-191815] N85-35566
Far-infrared observations of young clusters embedded in the R Coronae Austrinae and RHO Ophiuchi dark clouds
[NASA-TM-86681] N85-35834
INFRARED RADIATION
Infrared generation and wave-mixing studies in cesium
[DE85-012883] N85-35304
Miniature infra-red data acquisition and telemetry system
[NASA-CR-177953] N85-35390
Electronic structure and lattice dynamics of dimensionally constrained and disordered solids
[AD-A155927] N85-35797
INFRARED REFLECTION
The nature and geometry of infrared reflection nebulae N85-35835
INFRARED SPECTRA
FTIR studies of hydrocarbon synthesis on Pd/ZSM5 catalysts
[DE85-012430] N85-35230
Infrared generation and wave-mixing studies in cesium
[DE85-012883] N85-35304
INFRARED TELESCOPES
The nature and geometry of infrared reflection nebulae N85-35835
INHIBITORS
Molecular biology of environmental aromatic hydrocarbons
[DE85-015036] N85-35593
INJECTORS
Solid state high power amplifier for driving the SLC injector klystron
[DE85-013063] N85-35356
INORGANIC PEROXIDES
Improved oxygen sources for breathing apparatus
[NASA-TM-86671] N85-35623
INPUT
Aspects of input signal design for order and parameter estimation in linear dynamical systems
[ER-83/05] N85-35362
Software maintenance relating to the input translator and z-80 realization volume of the computer systems design environment
[AD-A155849] N85-35646
INSECTS
Effects of microgravity and hypergravity on invertebrate development N85-35579
Report of the Insect Development Group N85-35584
INSPECTION
National program for inspection of non-federal dams. Woodward reservoir dam (VT 00209), Connecticut River Basin, Plymouth, Vermont. Phase 1 inspection report
[AD-A156256] N85-35693
INSTRUMENT FLIGHT RULES
A guide to USAF helicopter instrument flight procedures
[AD-A156102] N85-35182
INSULATION
Results of variable enthalpy tests of CPR-488 TIP panels in MSFC Hot Gas Facility
[NASA-CR-170889] N85-35237
Development and characterization of carbon-bonded carbon fiber insulation for radioisotope space power systems
[DE85-013365] N85-35299
Injector losses on Mite
[DE85-012356] N85-35355
Laser and electron beam processing of semiconductors
[AD-A155914] N85-35796
INSULATORS
Electronic structure and lattice dynamics of dimensionally constrained and disordered solids
[AD-A155927] N85-35797
INTAKE SYSTEMS
Calculation of compressible flow about three-dimensional inlets with auxiliary inlets, slats and vanes by means of a panel method
[NASA-CR-174975] N85-35162
INTEGRAL EQUATIONS
A new method of differential structural analysis of gamma-family basic parameters
[HE-3.6-3] N85-35952
INTEGRALS
Applications of the Kirchoff-Helmholtz integral to problems in body wave seismology N85-35515
INTEGRATED CIRCUITS
Analog, still without fear
[AD-A155920] N85-35348
A methodology for the design of testable custom large-scale integrated circuits
[AD-A156098] N85-35351
Monolithic photovoltaic series array for an energy coupler
[BMFT-FB-T-85-023] N85-35496
Computer Aided Design (CAD) methods for very large scale integration systems
[BMFT-FB-T-85-029] N85-35668
Laser and electron beam processing of semiconductors
[AD-A155914] N85-35796
INTELLECT
Manual and computer-aided sequential diagnostic inference
[AD-A156229] N85-35620
INTERFACES
Pluribus satellite IMP (Interface Message Processors) development mobile access terminal network
[AD-A155754] N85-35216
Raster functionality for a VDI
[DE85-006734] N85-35396
DSS/MIS (Decision Support Systems/Management Information Systems) design and implementation for LAMPS Mk 3 utilizing a microcomputer and a maintenance personnel assignment program
[AD-A155852] N85-35629
Research on GaSb/AlSb multi-quantum well superlattices
[AD-A156080] N85-35800
INTERFACIAL ENERGY
HgCdTe surface and defect study program
[AD-A156079] N85-35799
INTERFEROMETERS
Optical synthetic aperture techniques
[AD-A156151] N85-35752
INTERGRANULAR CORROSION
Electrochemical method for investigation of the susceptibility of corrosion-resistant steels to intercrystalline corrosion
[BLL-CE-TRANS-8082-(9022.09)] N85-35269
INTERMETALLICS
Oxidation resistant slurry coating for carbon-based materials
[NASA-CASE-LEW-13923-1] N85-35267
INTERMITTENCY
Noise-sustained structure, intermittency and the Ginzburg-Landau equation
[DE85-009626] N85-35379
INTERNAL WAVES
Some aspects of internal gravity waves in a multi-layered moving stratified flow N85-35369
INTERNATIONAL COOPERATION
Research report program of the US Army in Europe N85-35167
Microwave propagation studies, measurements and education in Surabaya, Indonesia
[B8464633] N85-35339
INTERPLANETARY MAGNETIC FIELDS
Parallel fast-forward shock within 1 AU: Helios-1 and 2 observations
[MPAE-W-79-84-27] N85-35847
INTERPOLATION
Users guide for optimum interpolation method of global data assimilation
[AD-A155929] N85-35648
Two methods of global data assimilation
[AD-A155981] N85-35684
INTERPROCESSOR COMMUNICATION
Interprocess communication
[AD-A156337] N85-35337
INTERRUPTION
Current interruption by density depression
[DE85-013120] N85-35846
INTERSTELLAR EXTINCTION
The structure of Herbig-Haro object 43 and Orion dark cloud extinction
[NASA-TM-87503] N85-35831
INTERSTELLAR GAS
The HEAO-2 Guest Investigator Program: Non-linear growth of instabilities in line-driven stellar winds
[NASA-CR-176168] N85-35840
INVARIANCE
A graph theoretic procedure for the design of feedback patterns
[REPT-110] N85-35673
INVERSE SCATTERING
Calculation of heavy-ion tracks in liquid water
[DE85-012101] N85-35725
INVERTEBRATES
Aquatic Invertebrate Development Working Group N85-35585
IODINE
Aqueous volatile weak electrolyte equilibria to 300 C
[DE85-013840] N85-35261
A new drawing technique for nylon 6 by reversible plasticization with iodine
[AD-A156272] N85-35803
ION ACCELERATORS
Considerations on collective ion aceleration as an intense ion injector
[DE85-012706] N85-35757
Applications of decelerated ions
[DE85-011832] N85-35767
Heavy nucleus collisions between 20 and 60 GeV/nucleon
[HE-1.4-2] N85-35890
Meson multiplicity in nucleus-nucleus collisions above 4 GeV/amu
[HE-1.4-10] N85-35897
ION ACOUSTIC WAVES
Current interruption by density depression
[DE85-013120] N85-35846
ION BEAMS
Use of a minimum-ellipse criterion in the study of ion-beam extraction systems
[DE85-012670] N85-35721
Neutron production by Ne and Si ions on a thick Cu target at 670 MeV/A with application to radiation protection
[DE85-014526] N85-35746
Ion source development for the Los Alamos heavy ion fusion injector
[DE85-012682] N85-35766
Applications of decelerated ions
[DE85-011832] N85-35767
ION CURRENTS
Feasibility study of radar-transmitting materials
[AD-A155839] N85-35329
Ion composition measurements of the disturbed and quiet D-region in 1980 - 1981
[AD-A156055] N85-35521
ION IMPACT
Air chemistry measurements 2
[AD-A156041] N85-35520
ION IMPLANTATION
Two-dimensional numerical modeling of ion implanted GaAs MESFET devices N85-35341
ION IRRADIATION
Size and shape dependence of CO adsorption sites on sapphire supported Fe microcrystals
[NASA-CR-176171] N85-35794
ION SOURCES
Beam intensity increases at the intense pulsed neutron source accelerator
[DE85-012377] N85-35764
IONIC COLLISIONS
Multiple vacancy production by high energy heavy ions
[DE85-004428] N85-35805
Heavy nucleus collisions between 20 and 60 GeV/nucleon
[HE-1.4-2] N85-35890
Nucleus-nucleus interaction above several hundred GeV/n
[HE-1.4-4] N85-35892
Observation of direct hadronic pairs in nucleus-nucleus collisions in JACEE emulsion chambers
[HE-1.4-5] N85-35893
Excessive production of electron pairs by soft photons in low multiplicity ion interactions
[HE-1.4-6] N85-35894
On the mechanism of anomalous nucleus-nucleus interactions at energies above 1 TeV/nucleon
[HE-1.4-8] N85-35896

Inclusive angular distribution of alpha and Li fragments produced in the Fe-C and Fe-Pb collisions at 1.88 GeV/u
[HE-1.4-11] N85-35898

IONIC CRYSTALS
Ionic crystals
[DE85-009482] N85-35809

IONIZATION
The detection and study of molecular species using time resolved laser spectroscopy
[AD-A155910] N85-35256
Aqueous volatile weak electrolyte equilibria to 300 C
[DE85-013840] N85-35261
Infrared generation and wave-mixing studies in cesium
[DE85-012883] N85-35304
The ionization structure of planetary nebulae. Part 4: NGC 7662
[NASA-CR-176151] N85-35844
Sub-luminal pulses from cosmic ray air showers
[HE-4.7-13] N85-36063
Search for acoustic signals from high energy cascades
[HE-7.1-1] N85-36155

IONIZATION CHAMBERS
Fractional charge resolution in music N85-35712
X-ray film chamber with carbon target of Tien-Shan complex array N85-35915
Peculiarities of gamma-quanta distribution at 20 TeV energy
[HE-3.7-10] N85-35967
Observation of genetic relation among new phenomena Geminion, Chiron and mini-Centauro
[HE-6.2-16] N85-36152

IONIZATION COEFFICIENTS
Air chemistry measurements 2
[AD-A156041] N85-35520

IONIZATION CROSS SECTIONS
EAS accompanied by gamma-families at Mt. Norikura and comparison with Monte Carlo simulation
[HE-3.3-10] N85-35928

IONOSPHERIC DISTURBANCES
Ion composition measurements of the disturbed and quiet D-region in 1980 - 1981
[AD-A156055] N85-35521

IONS
Ion composition measurements of the disturbed and quiet D-region in 1980 - 1981
[AD-A156055] N85-35521
Generalized reduced fluid model with finite ion-gyroradius effects
[DE85-013123] N85-35777
Noise in sodium beta alumina crystals
[AD-A156025] N85-35798

IRON
Influence of yttrium on eutectoid transformation in irons
[BLL-M-35787-(5828.4)] N85-35270
Development of a high strength isothermally heat-treated nodular iron road wheel arm
[AD-A155755] N85-35408
Development of electrodes for the NASA iron/chromium
[NASA-CR-174724] N85-35471
Ore genesis at the Monterrosas deposit in the Coastal Batholith, Ica, Peru N85-35510
Size and shape dependence of CO adsorption sites on sapphire supported Fe microcrystals
[NASA-CR-176171] N85-35794
Characteristics of central collision events in Fe-nucleus interactions for 20 - 60 GeV/nucleon
[HE-1.4-3] N85-35891
The electromagnetic component of albedo from superhigh energy cascades in dense media
[HE-3.5-11] N85-35948
The development of air shower in the iron absorber N85-35987
Monte Carlo simulations of electron lateral distributions in the core region of 10(13) - 10(16) eV air showers N85-35992
The longitudinal development of muons in cosmic ray air showers at energies 10(15) - 10(17) eV
[HE-4.3-12] N85-36006
Multiple muons in MACRO
[HE-5.2-1] N85-36079
The Nagoya cosmic-ray muon spectrometer 3, part 2: Track detector
[HE-5.2-3] N85-36081

IRON ALLOYS
Thermal barrier coating system
[NASA-CASE-LEW-14057-1] N85-35233

IRON CYANIDES
Development and evaluation of sulfonated polysulfone membranes for the zinc-ferricyanide battery
[DE85-009104] N85-35357
Cationic exchange membrane for the zinc-ferricyanide battery
[DE85-013152] N85-35489

IRRADIATION
Calibration of a high-level photon irradiation
[DE85-013044] N85-35738
Total integrated dose testing of solid-state scientific CD4011, CD4013, and CD4060 devices by irradiation with CO-60 gamma rays
[NASA-CR-176196] N85-35795

ISENTROPE
Experimental technique for measuring the isentrope of hydrogen to several megabars
[DE85-014332] N85-35386

ISOMERS
Noble metals as incipient transition metals
[DE85-013283] N85-35286

ISOTOPES
Stopping relativistic Xe, Ho, Au and U nuclei in nuclear emulsions N85-35876

ITERATION
Perturbation-iteration theory for analyzing microwave striplines
[NASA-CR-176189] N85-35321

ITERATIVE SOLUTION
On the convergence of an iterative formulation of the electromagnetic scattering from an infinite grating of thin wires N85-35319

J

JET ENGINE FUELS
Nitrogen analysis by chemiluminescence
[AD-A156197] N85-35308
Biodegradation of jet fuel by aquatic microbial communities
[PB85-191971] N85-35311

JET FLOW
Heat transfer characteristics for two-dimensional arrays of impinging jets with initial crossflow N85-35365
Meteorological data from the OPTOMA (Ocean Prediction Through Observations, Modeling and Analysis) program OPTOMA 2, leg D2. 30 Jun. - 10 Jul. 1984
[AD-A156134] N85-35560

JET IMPINGEMENT
Analysis of reactor material experiments investigating oxide fuel crust stability and heat transfer in jet impingement flow
[DE85-012097] N85-35739

JET STREAMS (METEOROLOGY)
A preliminary intercomparison between numerical upper wind forecasts and research aircraft measurements of jet streams
[NASA-CR-167884] N85-35539

JETS
Exotic interactions among C-jets and Pb-jets
[HE-3.2-6] N85-35914

JOINTS (JUNCTIONS)
Verification of the SRB motor case pin retainer band tips
[NASA-CR-170882] N85-35220

JUPITER (PLANET)
The 1986 National Aeronautics and Space Administration authorization
[GPO-47-635] N85-35829

K

KALMAN FILTERS
Lectures of a Flight Mechanics Conference — conferences
[ESA-TT-831] N85-35165
Estimation of flight mechanical variables by means of Kalman filters N85-35171
Recursive partitioning estimation N85-35670

KINEMATICS
The kinematic structure of cold frontal rainbands N85-35531
Kinematic analysis of Hurricane Frederick (1979) using satellite, aircraft and rawinsonde data
[NASA-CR-176167] N85-35533

KINETIC ENERGY
Prediction of turbulent internal recirculating flows with K-epsilon models N85-35366
Kinematic analysis of Hurricane Frederick (1979) using satellite, aircraft and rawinsonde data
[NASA-CR-176167] N85-35533
Turbulent structure of stably stratified nocturnal slope flows
[AD-A155845] N85-35559
Two-point closure study of covariance budgets for turbulent Rayleigh-Benard convection
[PB85-189108] N85-35568
Experimental evidence of the decrease of kinetic energy of hadrons in passing through atomic nuclei N85-35880

KIRCHHOFF LAW OF RADIATION
Applications of the Kirchoff-Helmholtz integral to problems in body wave seismology N85-35515

KLYSTRONS
Solid state high power amplifier for driving the SLC injector klystron
[DE85-013063] N85-35356
SLC Energy Upgrade Program at SLAC
[DE85-014290] N85-35790

L

LABORATORIES
Procedure for editing the fluxgate magnetometer data of the AFGL (Air Force Geophysics Laboratory) magnetometer network
[AD-A156331] N85-35523
Progress report on implementing the recommendations of the White House Science Council's Federal Laboratory Review Panel, volume 1
[PB85-185072] N85-35819
Search for proton decay in the Frejus experiment
[HE-6.2-2] N85-36138

LACQUERS
Oxidation resistant slurry coating for carbon-based materials
[NASA-CASE-LEW-13923-1] N85-35267

LAGRANGE COORDINATES
Adaptive rezoner in a two-dimensional Lagrangian hydrodynamic code
[DE85-010108] N85-35381

LAMINATES
Mechanical characterization and failure modes of fiber reinforced angle-ply composites N85-35234
Damage induced stress redistribution in composite laminates N85-35235
Methods for nondestructive tests of CFRP laminates N85-35248
Damage mechanisms in damaged CFRP laminates N85-35249

LAND USE
Land Disposal of Hazardous Waste
[PB85-196376] N85-35500

LANDAU FACTOR
Analytical-numerical methods of calculations of energy and three-dimensional particle distributions in electromagnetic cascades
[HE-3.5-13] N85-35950
Development of electromagnetic cascades in the atmosphere including the Landau-Pomeranchuk-Migdal effect
[HE-4.5-5] N85-36029

LANDFORMS
Massive sulfide deposits from the southern Juan de Fuca Ridge N85-35446

LANDSAT SATELLITES
A comparison of LANDSAT thematic mapper, multispectral scanner and airborne sensors for mapping the distribution of alteration minerals: Examples from the southwestern United States N85-35452
Processing of LANDSAT imagery to map surface mineral alteration on the Alaska Peninsula, Alaska N85-35455

LANDSAT 4
LANDSAT-4/5 image data quality analysis
[E85-10105] N85-35463
Study of spectral/radiometric characteristics of the Thematic Mapper for land use applications
[E85-10106] N85-35464

LANDSAT 5
LANDSAT-4/5 image data quality analysis
[E85-10105] N85-35463
Study of spectral/radiometric characteristics of the Thematic Mapper for land use applications
[E85-10106] N85-35464

LAPLACE TRANSFORMATION
Characterizations of generalized hyperexponential distributions
[AD-A155855] N85-35680

LARGE SCALE INTEGRATION
Laser and electron beam processing of semiconductors
[AD-A155914] N85-35796

LARGE SPACE STRUCTURES
Technology for large space systems: A bibliography with indexes
[NASA-SP-7046(12)] N85-35209
Identification and control of structures in space
[NASA-CR-176175] N85-35214
Structural analysis of imperfect three-legged truss columns for large space structures applications N85-35416

LASER DOPPLER VELOCIMETERS
The use of a laser Doppler velocimeter in a standard flammability tube
[NASA-CR-174960] N85-35389
LASER OUTPUTS
High energy plasma accelerators
[DE85-013121] N85-35760
Laser and electron beam processing of semiconductors
[AD-A155914] N85-35796
LASER PLASMAS
Elliptical X-ray analyzer spectrograph application to a laser-produced plasma
[DE85-013790] N85-35398
LASER SPECTROSCOPY
The detection and study of molecular species using time resolved laser spectroscopy
[AD-A155910] N85-35256
Infrared generation and wave-mixing studies in cesium
[DE85-012683] N85-35304
Cryogenic laser calorimetry for impurity analysis
[NASA-CR-176179] N85-35395
Atmospheric nitrogen oxides: Their detection and chemistry
[PB85-193910] N85-35502
LASER TARGETS
Solid neon sources for plasma and X-ray lasers
[DE85-011347] N85-35402
LASERS
Laser probes of natural gas ignition chemistry
[PB85-200210] N85-35264
Laser and electron beam processing of semiconductors
[AD-A155914] N85-35796
LATE STARS
Circumstellar shells of late-type stars: A study at millimeter and infrared wavelengths N85-35836
LATERAL STABILITY
The lateral distributions of charged particles of energy greater than 0.3 E sub crit in electron-photon cascades in lead and air
[HE-3.6-10] N85-35957
Properties of 10 (18)-10 (19)eV EAS at far core distance
[HE-4.7-3] N85-36054
LATTICE PARAMETERS
On-line model driven control of the SLC electron Damping Ring
[DE85-013377] N85-35772
Simulation of lattice damage due to dynamic loading
[DE85-008468] N85-35808
LAVA
Preliminary results of an ALVIN dive program on active hydrothermal vents at the southern Juan de Fuca Ridge N85-35454
LEAD (METAL)
The Conterminous United States Mineral Assessment Program N85-35458
Estimation of the total inelasticity coefficient in interaction of greater than or equal to 20 TeV hadrons with lead
[HE-1.1-9] N85-35857
LPM effect and primary energy estimations
[HE-3.6-4] N85-35953
The lateral distributions of charged particles of energy greater than 0.3 E sub crit in electron-photon cascades in lead and air
[HE-3.6-10] N85-35957
Result of Monte-Carlo simulation of electron-photon cascades in lead and layers of lead-scintillator
[HE-3.6-11] N85-35958
LEAD ZIRCONATE TITANATES
Materials used by industry for the production of piezoelectric transducers. The state of the art of research work performed in the field of PZT ceramics and ferroelectric polymers
[ISL-CO-211/84] N85-35344
Conduction and aging of piezoelectric PZT ceramics N85-35346
LEADING EDGE SLATS
Presentation of the acoustic and aerodynamic results of the Aladin 2 concept qualification testing
[NASA-TM-77883] N85-35161
LEARNING MACHINES
Justified generalization: Acquiring procedures from examples
[AD-A156408] N85-35626
LEAST SQUARES METHOD
Two-dimensional inversion of resistivity monitoring data from the Cerro Prieto geothermal field
[DE85-012554] N85-35494
LEE WAVES
The determination of lee circulation during the foehn wind N85-35554
LEG (ANATOMY)
The effect of +Gx acceleration on platelet activation as determined by plasma platelet factor 4 levels
[AD-A155881] N85-35608
LEGIBILITY
An exploratory study of the effect of screen size and resolution on the legibility of graphics in automated job performance aids
[AD-A155989] N85-35632
LENS ANTENNAS
Cylindrical lens-array antenna for wideband electronic scanning
[AD-A156085] N85-35350
LEPTONS
Dependence of the average spatial and energy characteristics of the hadron-lepton cascade on the strong interaction parameters at superhigh energies N85-35977
Charge 4/3 leptons in cosmic rays
[HE-6.2-14] N85-36150
LIBRARIES
Procedure for editing the fluxgate magnetometer data of the AFGL (Air Force Geophysics Laboratory) magnetometer network
[AD-A156331] N85-35523
Source header list, supplement 3
[AD-A156100] N85-35824
LIFE (DURABILITY)
Development of a high-efficiency, gas-fired, heat pipe, warm-air heating system
[PB85-199636] N85-35318
LIFE CYCLE COSTS
Development of a high-efficiency, gas-fired, heat pipe, warm-air heating system
[PB85-199636] N85-35318
LIFT AUGMENTATION
Presentation of the acoustic and aerodynamic results of the Aladin 2 concept qualification testing
[NASA-TM-77883] N85-35161
LIFT DRAG RATIO
The influence of helicopter tail shape on drag: An aerodynamic study using a low speed wind tunnel
[AD-A156304] N85-35174
LIGHT (VISIBLE RADIATION)
Self-study manual on optical radiation measurements. Part 1: Concepts. Chapter 12: Blackbodies, blackbody radiation, and temperature scales
[PB85-195303] N85-35754
Study of the shower maximum depth by the method of detection of the EAS Cerenkov light pulse shape
[HE-4.4-15] N85-36021
Preliminary results of the Cerenkov EAS flashes the Crimean Astrophysical Observatory
[HE-4.4-17] N85-36023
LIGHT AIRCRAFT
Development and operation of a measuring data acquisition system for use in light airplanes N85-35556
LIGHT CURVE
The experimental cascade curves of EAS at E sub 0 10(17) eV obtained by the method of detection of Cherenkov pulse shape
[HE-4.4-18] N85-36024
LIGHT IONS
Multidimensional analysis of data obtained in experiments with X-ray emulsion chambers and extensive air showers
[HE-3.6-2] N85-35951
LIGHT SCATTERING
Energy calibration of the fly's eye detector
[HE-4.4-1] N85-36011
LIGHT SOURCES
Vacuum system for the Argonne 6 GeV synchrotron light source
[DE85-012286] N85-35773
Background light measurements at the DUMAND site
[HE-5.2-7] N85-36084
LIGHT SPEED
Sub-luminal pulses from cosmic ray air showers
[HE-4.7-13] N85-36063
LIGHT TRANSMISSION
Energy calibration of the fly's eye detector
[HE-4.4-1] N85-36011
The structure of EAS at E 0.1 EeV
[HE-4.4-2] N85-36012
LIGHT WATER REACTORS
Pressure measurements in a hydrogen combustion environment: Hydrogen-air combustion test series 1 and 2 in the FITS tank, volume 1
[TI85-009899] N85-35259
LIGHTNING
Investigation of the lightning vulnerability of nuclear explosive test systems at the Nevada Test Site
[DE85-011761] N85-35563
Application of pulsed power in the simulation of severe natural lightning
[DE85-012866] N85-35564
LIMITERS (FUSION REACTORS)
Limiter
[DE85-011620] N85-35736
Neutral pumping rates for a next step tokamak ignition device
[DE85-012780] N85-35776
LIMONITE
A comparison of LANDSAT thematic mapper, multispectral scanner and airborne sensors for mapping the distribution of alteration minerals: Examples from the southwestern United States N85-35452
LINE OF SIGHT COMMUNICATION
A ray trace program for line-of-sight microwave communication links
[AD-A156168] N85-35336
Microwave propagation studies, measurements and education in Surabaya, Indonesia
[B8464633] N85-35339
LINE SPECTRA
Elliptical X-ray analyzer spectrograph application to a laser-produced plasma
[DE85-013790] N85-35398
Far-infrared emission lines of CO and OH in the Orion-KL molecular shock
[NASA-TM-86721] N85-35832
The HEAO-2 Guest Investigator Program: Non-linear growth of instabilities in line-driven stellar winds
[NASA-CR-176168] N85-35840
The ionization structure of planetary nebulae. Part 4: NGC 7662
[NASA-CR-176151] N85-35844
LINEAR ACCELERATORS
Observations of accelerated high current low emittance beams in the SLC Linac
[DE85-013073] N85-35211
Solid state high power amplifier for driving the SLC injector klystron
[DE85-013063] N85-35356
ATA upgrade to 150 MeV
[DE85-013174] N85-35404
Error message recording and reporting in the SLC control system
[DE85-013057] N85-35664
Time domain reflectometry for SLC BPM system
[DE85-012389] N85-35758
Four stage HELIA experiment
[DE85-012026] N85-35768
High resolution beam profile monitors in the SLC
[DE85-013375] N85-35774
Recent advances in remote handling at LAMPF
[DE85-012725] N85-35775
SLC Energy Upgrade Program at SLAC
[DE85-014290] N85-35790
Multi-channel pulser for the SLC thermionic electron source
[DE85-014222] N85-35792
TOSCA calculations and measurements for the SLAC SLC damping ring dipole magnet
[DE85-014366] N85-35793
LINEAR EQUATIONS
Stress analysis of axisymmetric sandwich shells of variable thickness N85-35419
A new method for boundary value problems
[AD-A155934] N85-35683
LINEAR SYSTEMS
A graph theoretic procedure for the design of feedback patterns
[REPT-110] N85-35673
A new theory for multistep discretizations of stiff ordinary differential equations: Stability with large step sizes
[NASA-CR-177941] N85-35675
Spreading the control complexity in decentralized control of interconnected systems
[BU-117] N85-35688
Decentralized stabilization by high gain feedback
[BU-115] N85-35689
LINEARITY
Scale separation closure and Alfven wave turbulence
[DE85-013124] N85-35385
The geostatistical approach to the inverse problem in two-dimensional steady state groundwater modeling N85-35462
LINGUISTICS
Artificial intelligence in Ada (trademark): Pattern-directed processing
[AD-A156230] N85-35671
LININGS
Development of advanced high-temperature heat flux sensors. Phase 2: Verification testing
[NASA-CR-174973] N85-35391
LIQUID COOLED REACTORS
Thermal hydraulic features of the TMI accident
[DE85-014569] N85-35747

LIQUID HELIUM
Cooling high intensity atomic hydrogen beams to liquid helium temperatures
[DE85-012515] N85-35718
LIQUID NITROGEN
Sound speed measurements in liquid oxygen-liquid nitrogen mixtures
[NASA-TP-2464] N85-35307
LIQUID OXYGEN
Sound speed measurements in liquid oxygen-liquid nitrogen mixtures
[NASA-TP-2464] N85-35307
LIQUID PHASES
Chemistry of ore-forming fluids N85-35436
LIQUID PROPELLANT ROCKET ENGINES
Sound speed measurements in liquid oxygen-liquid nitrogen mixtures
[NASA-TP-2464] N85-35307
LIQUID SLOSHING
Further studies on liquid sloshing
[PB85-198695] N85-35388
LIQUIDS
Gas analysis of ore-forming fluids N85-35447
Cationic exchange membrane for the zinc-ferricyanide battery
[DE85-013152] N85-35489
Calculation of heavy-ion tracks in liquid water
[DE85-012101] N85-35725
LITHIUM
Thermodynamics of the corrosion of chromium in molten carbonates
[DE85-011407] N85-35282
Experimental lithium system
[DE85-013252] N85-35382
The Conterminous United States Mineral Assessment Program N85-35458
LITHOLOGY
Some recent deposit modeling efforts N85-35453
Hydrogeology of the lower Glen Rose Aquifer, south-central Texas N85-35466
LITHOSPHERE
Workshop Proceedings: Interpretation of Seismic Wave Propagation in Laterally Heterogeneous Structures
[BMR-258] N85-35530
LOADS (FORCES)
Further studies on liquid sloshing
[PB85-198695] N85-35388
Stress-intensity factors for circumferential surface cracks in pipes and rods under tension and bending loads
[NASA-TM-87594] N85-35424
Prediction of plasticity characteristics for three-dimensional fracture specimens comparison with experiment
[AD-A156425] N85-35430
Evaluation of the crack plane equilibrium model for predicting plastic fractures
[DE85-005558] N85-35431
Response of a BWR Mark 2 containment vessel head to loads beyond the design basis
[DE85-010524] N85-35432
Simulation of lattice damage due to dynamic loading
[DE85-008468] N85-35808
LOGARITHMIC RECEIVERS
A multi-channel radar receiver
[AD-A156058] N85-35333
LOGISTICS MANAGEMENT
DoD Value Engineering conference report. Value Engineering (VE): A tool that benefits line management. Part 4, Workshop B: VE on spare parts
[AD-A156070] N85-35813
LONG TERM EFFECTS
High temperature corrosion of ceramics
[DE85-013481] N85-35303
LONGERONS
Fatigue lives of specimens representing critical locations in Mirage 3 spars under Australian and Swiss test spectra
[ARL-STRUC-R-415] N85-35187
LONGITUDE MEASUREMENT
The longitudinal development of muons in cosmic ray air showers at energies 10(15) - 10(17) eV
[HE-4.3-12] N85-36006
Longitudinal development of muons in large air showers studies from the arrival time distributions measured at 900m above sea level
[HE-4.7-4] N85-36055
LONGITUDINAL CONTROL
Analysis of flexible aircraft longitudinal dynamics and handling qualities. Volume 1: Analysis methods
[NASA-CR-177943-VOL-1] N85-35202
Analysis of flexible aircraft longitudinal dynamics and handling qualities. Volume 2: Data
[NASA-CR-177943-VOL-2] N85-35203
LORAN C
Nonlinear digital phase-locked loops with application to Loran-C receivers N85-35178
LORENTZ FORCE
On mini-cluster observed by Chacaltaya emulsion chamber experiment
[HE-3.6-12] N85-35959
LORENTZ TRANSFORMATIONS
Hadron thermodynamics in relativistic nuclear collisions
[HE-1.1-8] N85-35856
LOSSES
Kinetic loss experiments on Mite
[DE85-012826] N85-35780
LOSSY MEDIA
Normal modes in an overmoded circular waveguide coated with lossy material
[NASA-CR-176186] N85-35320
LOUDSPEAKERS
Acoustic scaling: The development of improved instrumentation
[BBC-RD-1985/7] N85-35694
LOW FREQUENCIES
RF stabilization of interchange-ballooning modes
[DE85-012080] N85-35353
LOW SPEED WIND TUNNELS
The influence of helicopter tail shape on drag: An aerodynamic study using a low speed wind tunnel
[AD-A156304] N85-35174
LOW TEMPERATURE
Decomposition of martensite in R6M5 and R6AM5 steels after direct immersion in liquid nitrogen
[BLL-M-36305] N85-35268
Evaluation of low-temperature geothermal potential in north-central Box Elder County, Utah
[DE85-009541] N85-35490
Energy from low temperature differences
[DE85-008817] N85-35492
LUMINANCE
Sub-luminal pulses from cosmic ray air showers
[HE-4.7-13] N85-36063
LUMINESCENCE
Optical properties of heterostructures and superlattices
[AD-A156243] N85-35802
LUMINOUS INTENSITY
Beam potential measurement of an intense H(-) beam by use of the emissive probe technique
[DE85-012671] N85-35762
Connection between variations of the atmosphere temperature profile and variations of the meson component intensity
[HE-3.1-12] N85-35910
LUNAR SURFACE
High-energy neutrinos from a lunar observatory
[HE-5.3-21] N85-36112

M

MACH NUMBER
Unsteady flow in a supersonic cascade with two in-passage shocks
[NASA-CR-3925] N85-35158
MACHINING
Single-point diamond crushing of Zerodur with in-situ polishing and metrology on a diamond turning machine
[DE85-012918] N85-35305
MAGMA
Heat transfer and brine evolution in magma-hydrothermal systems N85-35441
Ore genesis at the Monterrosas deposit in the Coastal Batholith, Ica, Peru N85-35510
MAGNESIUM
Radiation measurements on magnesium flames
[BLL-CE-TRANS-8110-(9022.09)] N85-35254
MAGNETIC COILS
Analysis of a pulsed power system containing rotating machine
[DE85-014128] N85-35786
Effect of Cu4Ti compound formation on the characteristics of NbTi accelerator magnet wire
[DE85-014226] N85-35788
MAGNETIC DIPOLES
Event parameters: Fixed targets N85-35702
High energy cosmic ray signature of quark nuggets
[HE-6.2-11] N85-36147
MAGNETIC EFFECTS
Injector losses on Mite
[DE85-012356] N85-35355
MAGNETIC FIELDS
Long-time asymptotics of a system for plasma diffusion
[NASA-CR-177947] N85-35375
Aeromagnetic and gravity models of the pluton below the Lake City caldera, Colorado N85-35442
SLC arc transport system: Magnet design and construction
[DE85-014289] N85-35789
TOSCA calculations and measurements for the SLAC SLC damping ring dipole magnet
[DE85-014366] N85-35793
A new study of muons in air showers by NBU air shower array N85-35997
Radio wave emitted by an extensive air showers in 10KHz to 1MHz region
[HE-4.6-15] N85-36051
MAGNETIC FLUX
System expectations for Pioneer 1 foil implosion experiments
[DE85-014129] N85-35359
Proposed FRX-D experiment
[DE85-012766] N85-35778
The structure of Herbig-Haro object 43 and Orion dark cloud extinction
[NASA-TM-87503] N85-35831
MAGNETIC FORMING
Major facility overhauls at LAMPF
[DE85-012724] N85-35765
MAGNETIC MIRRORS
RF stabilization of interchange-ballooning modes
[DE85-012080] N85-35353
Analysis of a pulsed power system containing rotating machine
[DE85-014128] N85-35786
MAGNETIC MONOPOLES
Nineteenth International Cosmic Ray Conference. HE sessions, volume 8
[NASA-CP-2376-VOL-8] N85-36066
Search for magnetic monopoles using proportional counters filled with helium gas
[HE-6.1-1] N85-36127
Magnetic monopole search by 130 m(2)sr He gas proportional counter
[HE-6.1-2] N85-36128
Results of a search for monopoles and tachyons in horizontal cosmic ray flux
[HE-6.1-3] N85-36129
Monopole, astrophysics and cosmic ray observatory at Gran Sasso
[HE-6.1-4] N85-36130
Monopole search below the Parker limit with the MACRO detector at Gran Sasso
[HE-6.1-5] N85-36131
Limits on monopole fluxes from KFG experiment
[HE-6.1-6] N85-36132
An experiment to detect gut monopoles
[HE-6.1-7] N85-36133
Search for supermassive magnetic monopoles using mica crystals
[HE-6.1-8] N85-36134
The homestake surface-underground scintillations: Description
[HE-6.1-9] N85-36135
Upper limit on magnetic monopole flux from Baksan experiment
[HE-6.1-11] N85-36136
Results from the UCSD magnetic monopole search
[HE-6.1-12] N85-36137
MAGNETIC PERMEABILITY
Advanced detectors and signal processing
[NASA-CR-176193] N85-35343
MAGNETIC PROPERTIES
ATA upgrade to 150 MeV
[DE85-013174] N85-35404
MAGNETIC SIGNATURES
Aeromagnetic and radiometric signatures of a possible porphyry system in the western Tushar Mountains, Utah N85-35437
MAGNETIC STARS
High energy cosmic ray signature of quark nuggets
[HE-6.2-11] N85-36147
MAGNETIC TAPES
Relaxation techniques
[AD-A156248] N85-35621
Using an LSI-11/23 and RT-11 to digitize analog tapes
[DE85-012736] N85-35656
Aeronautical Systems Division Manufacturing/Quality assurance orientation
[AD-A156128] N85-35817
MAGNETITE
Some recent deposit modeling efforts N85-35453
MAGNETOHYDRODYNAMIC GENERATORS
Study to assess the effects of magnetohydrodynamic electromagnetic pulse on electric power systems, phase 1, volume 3
[DE85-011301] N85-35771
MAGNETOHYDRODYNAMIC WAVES
Scale separation closure and Alfven wave turbulence
[DE85-013124] N85-35365

Parallel fast-forward shock within 1 AU: Helios-1 and 2 observations
[MPAE-W-79-84-27] N85-35847

MAGNETOHYDRODYNAMICS
Some rigorous results concerning spectral theory for ideal MHD
[DE85-013427] N85-35770

MAGNETOMETERS
Procedure for editing the fluxgate magnetometer data of the AFGL (Air Force Geophysics Laboratory) magnetometer network
[AD-A156331] N85-35523

MAGNETORESISTIVITY
Development of position sensors for microcomputer-oriented sensor systems
[BMFT-FB-T-85-021] N85-35361

MAGNETOSPHERE
Two-dimensional quasineutral description of particles and fields above discrete auroral arcs
[NASA-CR-176170] N85-35517
High energy radiation from neutron stars
[DE85-014353] N85-35843

MAGNETOSPHERIC INSTABILITY
Robinson instability and beam loading
[DE85-013301] N85-35737

MAGNETS
SLC arc transport system: Magnet design and construction
[DE85-014289] N85-35789

MAINTAINABILITY
Air university commander's and supervisor's guide on substance abuse
[AD-A156336] N85-35622

MAINTENANCE
Dissected motors-propellants motor number STM-012. Phase 15: Surveillance report, stage 1
[AD-A156088] N85-35226
Quality assurance considerations for the implementation of a pulsed power R and D project
[DE85-012357] N85-35720
Time domain reflectometry for SLC BPM system
[DE85-012389] N85-35758

MAMMALS
Vertebrate development in space: Gravity is a drag (and has been for eons and eons) N85-35580
Report of the NASA Mammalian Developmental Biology Working Group N85-35581

MAN MACHINE SYSTEMS
Development of NATOPS performance software for the SH-3D and SH-3H helicopters
[AD-A156140] N85-35192
The integrated manual and automatic control of complex flight systems
[NASA-CR-176166] N85-35201
An exploratory study of the effect of screen size and resolution on the legibility of graphics in automated job performance aids
[AD-A155989] N85-35632

MANAGEMENT
DOD Value Engineering Conference report. Value Engineering (VE): A tool that benefits line management held at Leesburg, Virginia on 1-2 November 1984. Part 1. Executive summary
[AD-A156067] N85-35810
DOD Value Engineering Conference report. Value Engineering (VE): A tool that benefits line management held at Leesburg, Virginia on 1-2 November 1984. Part 2. Plenary session
[AD-A156068] N85-35811
DoD Value Engineering conference report. Value Engineering (VE): A tool that benefits line management. Part 5, Workshop C: VEP/VECP administration, negotiation, and implementation
[AD-A156071] N85-35814

MANAGEMENT METHODS
Fire service emergency management handbook
[AD-A155780] N85-35313
DoD Value Engineering conference report. Value Engineering (VE): A tool that benefits line management. Part 6, Workshop D: VE training-orientation
[AD-A156072] N85-35815
Aeronautical Systems Division Manufacturing/Quality assurance orientation
[AD-A156128] N85-35817

MANAGEMENT PLANNING
Aeronautical Systems Division Manufacturing/Quality assurance orientation
[AD-A156128] N85-35817

MANAGEMENT SYSTEMS
DOD Value Engineering Conference report. Value Engineering (VE): A tool that benefits line management held at Leesburg, Virginia on 1-2 November 1984. Part 1. Executive summary
[AD-A156067] N85-35810
DOD Value Engineering Conference report. Value Engineering (VE): A tool that benefits line management held at Leesburg, Virginia on 1-2 November 1984. Part 2. Plenary session
[AD-A156068] N85-35811

MANGANESE
Cobalt-rich ferromanganese crusts in the oceans N85-35444
Applications of the mineral resources data system and the international strategic minerals inventory in mineral-resource assessments by region and commodity N85-35451

MANIPULATORS
The compliance of end effector force sensors for robot manipulator control N85-35406
Testbed for sensory control of intelligent machines
[DE85-012355] N85-35412

MANNED ORBITAL LABORATORIES
Space Station Polar Platform: Integrating research and operational missions
[PB85-195279] N85-35218

MANNED SPACE FLIGHT
Proceedings of a Scientic Meeting on the Occasion of the Inauguration of New Buildings for the DFVLR Institute for Aerospace Medicine
[ESA-TT-857] N85-35595
Biophysical research in space — radiation effects N85-35603

MANUAL CONTROL
The integrated manual and automatic control of complex flight systems
[NASA-CR-176166] N85-35201

MANUALS
Master Fit users' guide, version 1.0
[DE85-014199] N85-35667
Comet Halley returns: A teachers' guide 1985-1986
[NASA-EP-197] N85-35839

MAPPING
A comparison of LANDSAT thematic mapper, multispectral scanner and airborne sensors for mapping the distribution of alteration minerals: Examples from the southwestern United States N85-35452
Evaluation: Close-range photogrammetry for slope inventory and monitoring
[PB85-192755] N85-35470

MAPS
An experimental study of dielectric rod antennas for millimeter-wave imaging applications
[AD-A155832] N85-35328
New silver resource map of the United States: Potential for increased domestic silver production N85-35445
Early and middle Cenozoic volcanic synthesis N85-35449
Applications of the mineral resources data system and the international strategic minerals inventory in mineral-resource assessments by region and commodity N85-35451

MARTENSITE
Decomposition of martensite in R6M5 and R6AM5 steels after direct immersion in liquid nitrogen
[BLL-M-36305] N85-35268

MARTENSITIC TRANSFORMATION
Decomposition of martensite in R6M5 and R6AM5 steels after direct immersion in liquid nitrogen
[BLL-M-36305] N85-35268

MASS SPECTROMETERS
Ion composition measurements of the disturbed and quiet D-region in 1980 - 1981
[AD-A156055] N85-35521

MASS SPECTROSCOPY
Heats of formation of gas phase organosulfur molecules, radicals and ions measured by PEPICO and application of (17)O and (33)S NMR spectroscopy to structure determination of organosulfur compounds
[DE85-010558] N85-35229
Gas analysis of ore-forming fluids N85-35447
Ion composition measurements of the disturbed and quiet D-region in 1980 - 1981
[AD-A156055] N85-35521

MASS TRANSFER
Molecular and macromolecular sieving by asymmetric ultrafiltration membranes
[PB85-157766] N85-35266

MATCHED FILTERS
Matched filtering of visual evoked potentials to detect acceleration (+Gz) induced blackout
[AD-A155912] N85-35609

MATERIAL BALANCE
Measurement of uranium enrichment for gaseous uranium at low pressure
[DE85-012697] N85-35733

MATERIALS HANDLING
Laboratory vibration schedules
[AD-A155856] N85-35188
Radiation safety problems in handling highly active tritium targets
[DE85-014268] N85-35742

MATERIALS RECOVERY
Measurement of uranium enrichment for gaseous uranium at low pressure
[DE85-012697] N85-35733

MATHEMATICAL MODELS
Chemoviscosity modeling for thermosetting resins, 2
[NASA-CR-177958] N85-35243
An analytical and numerical model of radiation heat transfer in direct injection-type diesel combustion N85-35368
Studies on effects of boundary conditions in confined turbulent flow predictions
[NASA-CR-3929] N85-35371
Transient three-phase three-component systems. Part 1: Formulation of the system of differential equations
[DE85-013267] N85-35384
Development of a mathematical model for predicting the percentage fatigue life increase resulting from shot peened components
[AD-A155774] N85-35425
An atmospheric boundary layer model forced by the operational ECMWV-model
[WSR-3] N85-35541
A mechanical model of the human body and its application N85-35598
Benchmark evaluation of PC simscript
[AD-A156133] N85-35651
Algorithmic approaches in sets of good answers in inverse problems
[PM/84/18] N85-35677
Constrained stiffness matrix adjustment using mode data
[AD-A155988] N85-35685
Model robust response surface designs: Scaling two-level factorials
[AD-A156218] N85-35686
Acoustic resonances in cylinder bundles oscillating in a compressibile fluid
[DE85-004066] N85-35699
A lead glass tubing drift calorimeter N85-35711
Use of a minimum-ellipse criterion in the study of ion-beam extraction systems
[DE85-012670] N85-35721
Applications and misapplications of the channel-capture formalism of direct neutron capture
[DE85-013992] N85-35748
On-line model driven control of the SLC electron Damping Ring
[DE85-013377] N85-35772

MATRICES (MATHEMATICS)
Invariant tests and likelihood ratio tests for multivariate elliptically contoured distributions
[AD-A155844] N85-35679

MATTER (PHYSICS)
Characterization of the optical and thermal properties of matter by photothermal techniques
[DE85-012607] N85-35260

MAXIMA
Large deviations for the maxima of some random fields
[AD-A155909] N85-35681

MAXIMUM LIKELIHOOD ESTIMATES
Invariant tests and likelihood ratio tests for multivariate elliptically contoured distributions
[AD-A155844] N85-35679
A new method of differential structural analysis of gamma-family basic parameters
[HE-3.6-3] N85-35952
Study of the time-differentiated particle flux density at various distances from EAS axis
[HE-4.7-15] N85-36065

MAXWELL EQUATION
Analysis of the nonlinear equations describing the elastic, thermal, and electromagnetic behavior of solids: Existence of solutions of semi-inverse problems N85-35415
Relation between field energy and RMS emittance in intense particle beams
[DE85-012655] N85-35784

MEAN FREE PATH
Calculation of heavy-ion tracks in liquid water
[DE85-012101] N85-35725
Penetrative nature of high energy showers observed in Chacaltaya emulsion chamber
[HE-3.3-5] N85-35923
On mini-cluster observed by Chacaltaya emulsion chamber experiment
[HE-3.6-12] N85-35959
Search for anomalons using plastic nuclear track detectors
[HE-6.2-12] N85-36148

Search for acoustic signals from high energy cascades
[HE-7.1-1] N85-36155

MEASUREMENT
Measurement control for plutonium isotopic measurements using gamma-ray spectrometry
[DE85-013394] N85-35397

MEASURING INSTRUMENTS
Analyzer, flight line
[AD-A155777] N85-35207
Development of advanced high-temperature heat flux sensors. Phase 2: Verification testing
[NASA-CR-174973] N85-35391
Atmospheric nitrogen oxides: Their detection and chemistry
[PB85-193910] N85-35502
Development of an NBS (National Bureau of Standards) polymer gage for dynamic soil stress measurement
[PB85-208494] N85-35526

MECHANICAL DRIVES
State-of-the-art of solid-state motor controllers
[TI85-008674] N85-35806

MECHANICAL PROPERTIES
Contribution to the properties of carbon fiber reinforced composites --- structural mechanics
[ESA-TT-849] N85-35246
Interaction of trace elements and welding parameters on GTA weld shape
[DE85-004046] N85-35284
Development and characterization of carbon-bonded carbon fiber insulation for radioisotope space power systems
[DE85-013365] N85-35299
User's guide: A computer program for strength analysis of non-hydraulic concrete structural elements. Report 1. Concrete General Strength Investigation (CGSI)
[AD-A156392] N85-35428

MECHANICAL SHOCK
A mechanical model of the human body and its application N85-35598

MEDICAL EQUIPMENT
New technologies at the forefront of industrial developments N85-35168
Dental multi-purpose slowspeed handpieces test and evaluation
[AD-A155764] N85-35606

MEDICAL SCIENCE
Proceedings of the 14th Army Science Conference. Volume 2: Principal authors I through O
[AD-A149201] N85-35690

MEDITERRANEAN SEA
Seasonal variability and spatial non-uniformity of bioluminescence in the Mediterranean Sea
[DRIC-T-7545] N85-35572

MELTING
Dynamic compaction of a monosized spherical tungsten powder
[DE85-014808] N85-35289
Analysis of reactor material experiments investigating oxide fuel crust stability and heat transfer in jet impingement flow
[DE85-012097] N85-35739

MEMBRANES
Membrane reinforcement in concrete shells: Design versus nonlinear behavior N85-35312
Development and evaluation of sulfonated polysulfone membranes for the zinc-ferricyanide battery
[DE85-009104] N85-35357
Cationic exchange membrane for the zinc-ferricyanide battery
[DE85-013152] N85-35489

MEMORY (COMPUTERS)
Error-correcting codes for computer memories N85-35636

MENTAL PERFORMANCE
Manual and computer-aided sequential diagnostic inference
[AD-A156229] N85-35620

MERCURY CADMIUM TELLURIDES
HgCdTe surface and defect study program
[AD-A156079] N85-35799

MESH
Adaptive rezoner in a two-dimensional Lagrangian hydrodynamic code
[DE85-010108] N85-35381

MESONS
The phi-meson and Chiral-mass-meson production in heavy-ion collisions as potential probes of quark-gluon-plasma and Chiral symmetry transitions N85-35884
Forward particle production in inelastic Ne-22 inteVractions in emulsion at 4.1 A Ge/c
[HE-1.4-7] N85-35695
Meson multiplicity in nucleus-nucleus collisions above 4 GeV/amu
[HE-1.4-10] N85-35897
Connection between variations of the atmosphere temperature profile and variations of the meson component intensity
[HE-3.1-12] N85-35910

MESOSCALE PHENOMENA
Airborne Investigations of Mesoscale Convective Systems (AIMCS), 1984: Operational summary and data inventory
[PB85-187904] N85-35571

MESSAGE PROCESSING
Pluribus satellite IMP (Interface Message Processors) development mobile access terminal network
[AD-A155754] N85-35216

METABOLISM
Response of amino acids in hindlimb muscles to recovery from hypogravity and unloading by tail-cast suspension
[NASA-CR-176183] N85-35589

METAL COATINGS
Tests on zirconium nitride coatings applied to SW 18 steel using the chemical vapor deposition method N85-35271

METAL PARTICLES
Spectral characteristics of grinding sparks used for identification of scrap metals
[PB85-198570] N85-35290

METAL PLATES
Strain measurement using point recognition picture processing
[DRIC-T-7407] N85-35421

METAL SURFACES
Electronic structure and lattice dynamics of dimensionally constrained and disordered solids
[AD-A155927] N85-35797

METAL VAPOR LASERS
Infrared generation and wave-mixing studies in cesium
[DE85-012883] N85-35304

METALLOGRAPHY
Characterization of modified 9 r-1 Mo steel sand castings
[DE85-012057] N85-35287

METAMORPHISM (GEOLOGY)
Structural development of the west-central Grant Range, Nye County, Nevada N85-35508

METEOROIDS
A study of the chemistry of alkali metals in the upper atmosphere
[AD-A156349] N85-35524

METEOROLOGICAL FLIGHT
Proceedings of Meteorological Motor Glider (MEMO) Workshop '84
[DFVLR-MITT-85-04] N85-35542
Motor glider meteorology N85-35543
Typical and historical aspects of motor gliders as meteorological measuring aircraft N85-35544
Determination of vertical air velocity using measurements of the aircraft motion N85-35545
A comparison between Falcon data and motor glider data N85-35547
Case studies for flux measurements along a low-flying route to the south of Munich N85-35548
Environmental-physical measurements and determination of atmospheric turbulence with the ASK-16 motor glider N85-35549
Partitioning of the vertical turbulent energy transport into positive and negative contributions --- meteorology N85-35551
Aircraft measurements during the Bonn Experiment (BONEX 1) --- meteorology N85-35552
Meteorological measurements with motor gliders in Poland N85-35555
The principles of wind measurement with the help of aircraft N85-35558

METEOROLOGICAL PARAMETERS
Incorporating meteorological data into receptor analysis: RAPS (Regional Air Pollution Study) revisited
[PB85-188944] N85-35503
An atmospheric boundary layer model forced by the operational ECMWV-model
[WSR-3] N85-35541
Meteorological data from the OPTOMA (Ocean Prediction Through Observations, Modeling and Analysis) program OPTOMA 2, leg D2. 30 Jun. - 10 Jul. 1984
[AD-A156134] N85-35560

METEOROLOGICAL RADAR
A multi-channel radar receiver
[AD-A156058] N85-35333
Polarization diversity addition to the 10 centimeter Doppler weather radar
[AD-A156062] N85-35334

METEOROLOGICAL RESEARCH AIRCRAFT
A preliminary intercomparison between numerical upper wind forecasts and research aircraft measurements of jet streams
[NASA-CR-167884] N85-35539

METHANE
Microbiological and biochemical studies towards optimization of substrate utilization by methanogenic bacteria
[PB85-188332] N85-35310

MICA
Search for supermassive magnetic monopoles using mica crystals
[HE-6.1-8] N85-36134

MICROBIOLOGY
Microbiological and biochemical studies towards optimization of substrate utilization by methanogenic bacteria
[PB85-188332] N85-35310
Literature search for new physical methods for biological aerosol detection
[AD-A155883] N85-35592

MICROCOMPUTERS
Development of position sensors for microcomputer-oriented sensor systems
[BMFT-FB-T-85-021] N85-35361
Materials and process development for microcomputer-compatible pressure, temperature, and position sensors
[BMFT-FB-T-85-024] N85-35399
Expert systems research in regional resource evaluation: Experiences in the application of microcomputer technologies N85-35450
DSS/MIS (Decision Support Systems/Management Information Systems) design and implementation for LAMPS Mk 3 utilizing a microcomputer and a maintenance personnel assignment program
[AD-A155852] N85-35629
A quickly tested Pascal random number generator for microcomputers
[AD-A156059] N85-35633
A research program to reduce the interior noise in general aviation aircraft, index and summary
[NASA-CR-176178] N85-35695
Application of thermoluminescence for detection of cascade shower 1: Hardware and software of reader system
[HE-7.1-6] N85-36160
Spatial distribution read-out system for thermoluminescence sheets
[HE-7.1-7] N85-36161

MICROCRYSTALS
Size and shape dependence of CO adsorption sites on sapphire supported Fe microcrystals
[NASA-CR-176171] N85-35794

MICROORGANISMS
Production of butanol by fermentation in the presence of cocultures of clostridium
[NASA-CASE-NPO-16203-1] N85-35227
Biodegradation of jet fuel by aquatic microbial communities
[PB85-191971] N85-35311
Report of the Microbial Development Working Group N85-35586

MICROPHONES
Acoustic scaling: The development of improved instrumentation
[BBC-RD-1985/7] N85-35694

MICROPROCESSORS
New technologies at the forefront of industrial developments N85-35168
Design for MISP: A multiple instruction stream shared pipeline processor
[AD-A156314] N85-35635
Error message recording and reporting in the SLC control system
[DE85-013057] N85-35664
Report on the SLC control system
[DE85-013076] N85-35722
Investigation of cosmic rays in very short time scales
[HE-4.6-7] N85-36044
Microprocessor-based single particle calibration of scintillation counter
[HE-4.6-13] N85-36049
A mini-array for large air showers
[HE-4.7-10] N85-36061
Study of the time-differentiated particle flux density at various distances from EAS axis
[HE-4.7-15] N85-36065

MICROPROGRAMMING
Design of a microprogram control unit with concurrent error detection
[AD-A156447] N85-35655

MICROSTRIP TRANSMISSION LINES
Perturbation-iteration theory for analyzing microwave striplines
[NASA-CR-176189] N85-35321
Characterization of microstrip discontinuities in the time and frequency domains
[NASA-CR-176190] N85-35342

MICROSTRUCTURE
Effect of thermal ageing on the mechanical properties of PWR pressure vessel steels and weldments [AERE-R-11460] N85-35275
Effect of prior warm rolling on the retained austenite content and hardening response of VIM-VAR (vacuum-induction melted-vacuum-arc remelted) AISI M-50 steel [AD-A156145] N85-35281
Effect of microstructure on the fatigue behavior of Fe-C-X alloys [DE85-011749] N85-35285

MICROWAVE FREQUENCIES
Microwave properties of a quiet sea [NASA-CR-176199] N85-35322

MICROWAVE TRANSMISSION
Perturbation-iteration theory for analyzing microwave striplines [NASA-CR-176189] N85-35321
Microwave propagation studies, measurements and education in Surabaya, Indonesia [B8464633] N85-35339

MICROWAVES
Feasibility study of radar-transmitting materials [AD-A155839] N85-35329
A ray trace program for line-of-sight microwave communication links [AD-A156168] N85-35336
Literature search for new physical methods for biological aerosol detection [AD-A155883] N85-35592
Electromagnetic compatibility conference features biological interactions [AD-A155813] N85-35692

MIE SCATTERING
Calculation of the diffusion of light by aerosols: Description of the MIELOR software and results obtained [REPT-80] N85-35638

MILITARY AVIATION
Development of NATOPS (Naval Air Training and Operating Procedure Standardization) performance software for the H-46D helicopter [AD-A156089] N85-35190

MILITARY OPERATIONS
Introduction to European air traffic control [AD-A156328] N85-35176
A guide to USAF helicopter instrument flight procedures [AD-A156102] N85-35182
RAFTS: A T-38 replacement for the 21st century [AD-A156103] N85-35191
Next generation gunship [AD-A156361] N85-35193
Air university commander's and supervisor's guide on substance abuse [AD-A156336] N85-35622

MILITARY TECHNOLOGY
Proceedings of the 14th Army Science Conference. Volume 2: Principal authors I through O [AD-A149201] N85-35690
Proceedings of the 14th Army Science Conference. Volume 3: Principal authors P through Z [AD-A149202] N85-35691

MILLIMETER WAVES
An experimental study of dielectric rod antennas for millimeter-wave imaging applications [AD-A155832] N85-35328
Millimeter-wave propagation in moist air: Model versus path data [AD-A156040] N85-35331

MILLING (MACHINING)
Method for measuring surface activity of silicon nitride powder [NASA-TM-77906] N85-35242

MINERAL DEPOSITS
USGS research on mineral resources, 1985 [CIRC-949] N85-35435
Chemistry of ore-forming fluids N85-35436
Aeromagnetic and radiometric signatures of a possible porphyry system in the western Tushar Mountains, Utah N85-35437
Some geophysical guides to ore in southern and southwestern Alaska N85-35438
Marine phosphorite deposits model for exploration, with emphasis on deposits in the US Atlantic coastal plain N85-35439
The role of regional subsurface geochemistry in resource assessment in the central United States N85-35440
Aeromagnetic and gravity models of the pluton below the Lake City caldera, Colorado N85-35442
Origin of sedimentary humic acids, potential carriers of ore-forming elements N85-35443
Cobalt-rich ferromanganese crusts in the oceans N85-35444
New silver resource map of the United States: Potential for increased domestic silver production N85-35445
Massive sulfide deposits from the southern Juan de Fuca Ridge N85-35446
Gas analysis of ore-forming fluids N85-35447
Mineral deposit models: Theory and practice N85-35448
Expert systems research in regional resource evaluation: Experiences in the application of microcomputer technologies N85-35450
Applications of the mineral resources data system and the international strategic minerals inventory in mineral-resource assessments by region and commodity N85-35451
A comparison of LANDSAT thematic mapper, multispectral scanner and airborne sensors for mapping the distribution of alteration minerals: Examples from the southwestern United States N85-35452
Some recent deposit modeling efforts N85-35453
Processing of LANDSAT imagery to map surface mineral alteration on the Alaska Peninsula, Alaska N85-35455
Mineral resources programs N85-35456
The development of assessment techniques program N85-35457
The Conterminous United States Mineral Assessment Program N85-35458
Federal Mineral Land Information System N85-35459
The Alaska Mineral Resources Assessment Program N85-35460
Hydrogeology of the lower Glen Rose Aquifer, south-central Texas N85-35466
Ore genesis at the Monterrosas deposit in the Coastal Batholith, Ica, Peru N85-35510

MINERAL EXPLORATION
USGS research on mineral resources, 1985 [CIRC-949] N85-35435
Aeromagnetic and radiometric signatures of a possible porphyry system in the western Tushar Mountains, Utah N85-35437
Some geophysical guides to ore in southern and southwestern Alaska N85-35438
Marine phosphorite deposits model for exploration, with emphasis on deposits in the US Atlantic coastal plain N85-35439
The role of regional subsurface geochemistry in resource assessment in the central United States N85-35440
Aeromagnetic and gravity models of the pluton below the Lake City caldera, Colorado N85-35442
Massive sulfide deposits from the southern Juan de Fuca Ridge N85-35446
Gas analysis of ore-forming fluids N85-35447
Mineral deposit models: Theory and practice N85-35448
Early and middle Cenozoic volcanic synthesis N85-35449
Mineral resources programs N85-35456
The Conterminous United States Mineral Assessment Program N85-35458
Federal Mineral Land Information System N85-35459
The Alaska Mineral Resources Assessment Program N85-35460

MINERALS
Chemistry of ore-forming fluids N85-35436

MINES (EXCAVATIONS)
New silver resource map of the United States: Potential for increased domestic silver production N85-35445
Federal Mineral Land Information System N85-35459
The homestake surface-underground scintillations: Description [HE-6.1-9] N85-36135

MINIATURE ELECTRONIC EQUIPMENT
Miniature infra-red data acquisition and telemetry system [NASA-CR-177953] N85-35390

MINICOMPUTERS
Procedure for editing the fluxgate magnetometer data of the AFGL (Air Force Geophysics Laboratory) magnetometer network [AD-A156331] N85-35523
Optimize computer throughput using array processors [AD-A155843] N85-35628

MIRROR FUSION
Analysis of a pulsed power system containing rotating machine [DE85-014128] N85-35786

MIRRORS
Single-point diamond crushing of Zerodur with in-situ polishing and metrology on a diamond turning machine [DE85-012918] N85-35305
A normal incidence X-ray telescope sounding rocket payload [NASA-CR-176169] N85-35749

MISSILE CONTROL
Computer simulation of a cruise missile using brushless dc motor fin control [AD-A155935] N85-35349

MISSIONS
Search for proton decay in the Frejus experiment [HE-6.2-2] N85-36138
Data acquisition system for phase-2 KGF proton decay experiment [HE-6.2-4] N85-36140

MIXING
Holoswitch [AD-A155841] N85-35392

MIXTURES
Equation of state study for polar fluids [PB85-204345] N85-35262
Nitrogen analysis by chemiluminescence [AD-A156197] N85-35308

MOBILE COMMUNICATION SYSTEMS
Pluribus satellite IMP (Interface Message Processors) development mobile access terminal network [AD-A155754] N85-35216

MODELS
FAA requirements for model to support capacity, delay, noise and energy programs [AD-A155815] N85-35179
Elliptical X-ray analyzer spectrograph application to a laser-produced plasma [DE85-013790] N85-35398
Linear absorption and scattering of laser beams [AD-A156167] N85-35401
Investment justification of robotic technology in aerospace manufacturing. User's manual [AD-A156193] N85-35410
Expert systems research in regional resource evaluation: Experiences in the application of microcomputer technologies N85-35450
The development of assessment techniques program N85-35457
Comparative analysis of operational forecasts versus actual weather conditions in airline flight planning, volume 2 [NASA-CR-167863] N85-35535
Comparative analysis of operational forecasts versus actual weather conditions in airline flight planning: Summary report [NASA-CR-167866] N85-35538
On-line model driven control of the SLC electron Damping Ring [DE85-013377] N85-35772
Circumstellar shells of late-type stars: A study at millimeter and infrared wavelengths N85-35836
Gamma-hadron families and scaling violation [HE-3.4-7] N85-35935
On the halo events observed by Mount Fuji and Mount Kanbala Emulsion Chamber Experiments [HE-3.4-9] N85-35937
Multidimensional analysis of data obtained in experiments with X-ray emulsion chambers and extensive air showers [HE-3.6-2] N85-35951
Experimental basis for the models of cascade propagation in atmosphere [HE-3.6-6] N85-35954
Relation between gamma-ray family and EAS core: Monte-Carlo simulation of EAS core [HE-3.6-7] N85-35955
A comparative analysis of gamma and hadron families at the superhigh energies recorded in experiment Pamir [HE-3.7-1] N85-35960
Electrons, muons and hadrons in extensive air showers and how do they depend on nuclear interaction model, part 2 N85-35969
The maximum depth of shower with E sub 0 larger than 10(17) eV on average characteristics of EAS different components N85-35981
Sensitivity of depth of maximum and absorption depth of EAS to hadron production mechanism N85-35982
The capability of the existing network of installations for detecting the antineutrino burst from collapsing stars [HE-5.3-13] N85-36107
A search for cosmic sources of high energy neutrinos with small underground detectors [HE-5.3-16] N85-36110

MODULATORS
SLC Energy Upgrade Program at SLAC [DE85-014290] N85-35790

MODULUS OF ELASTICITY
Effects of temperature on the tensile strength and elastic modulus of composite material [AD-A156112] N85-35251

MOLECULAR BEAM EPITAXY
Investigations of the molecular beam epitaxial growth and characteristics of external excitation induced non-equilibrium phases of immiscible 3-5 compound semiconductors [AD-A156325] N85-35804

MOLECULAR BEAMS
High-resolution spectroscopy and dynamics of multiphoton processes in atoms and molecules
[AD-A155862] N85-35714
Investigations of the molecular beam epitaxial growth and characteristics of external excitation induced non-equilibrium phases of immiscible 3-5 compound semiconductors
[AD-A156325] N85-35804
MOLECULAR BIOLOGY
Molecular biology of environmental aromatic hydrocarbons
[DE85-015036] N85-35593
MOLECULAR CLOUDS
Far-infrared emission lines of CO and OH in the Orion-KL molecular shock
[NASA-TM-86721] N85-35832
MOLECULAR EXCITATION
The detection and study of molecular species using time resolved laser spectroscopy
[AD-A155910] N85-35256
High-resolution spectroscopy and dynamics of multiphoton processes in atoms and molecules
[AD-A155862] N85-35714
MOLECULAR GASES
Far-infrared observations of young clusters embedded in the R Coronae Austrinae and RHO Ophiuchi dark clouds
[NASA-TM-86681] N85-35834
MOLECULAR PHYSICS
The 2nd European Conference on Atomic and Molecular Physics
[AD-A155863] N85-35715
MOLECULAR STRUCTURE
The detection and study of molecular species using time resolved laser spectroscopy
[AD-A155910] N85-35256
MOLECULAR THEORY
Equation of state study for polar fluids
[PB85-204345] N85-35262
MOLECULAR WEIGHT
Molecular and macromolecular sieving by asymmetric ultrafiltration membranes
[PB85-157766] N85-35266
MOLTEN SALTS
Thermodynamics of the corrosion of chromium in molten carbonates
[DE85-011407] N85-35282
MOLYBDENUM
Some recent deposit modeling efforts N85-35453
The Conterminous United States Mineral Assessment Program N85-35458
MOLYBDENUM ALLOYS
Characterization of modified 9 r-1 Mo steel sand castings
[DE85-012057] N85-35287
MOMENT DISTRIBUTION
Moment-method formulation of the cavity-probe aperture antenna
[DE85-013264] N85-35338
MOMENTUM
1Single particle momentum and angular distributions in hadron-hadron collisions at ultrahigh energies
[HE-1.2-1] N85-35860
MOMENTUM THEORY
Phase space factors in multiparticle processes N85-35888
MOMENTUM TRANSFER
Transverse momentum distribution of pion deg in the fragmentation region of super high energy interactions N85-35921
MONEL (TRADEMARK)
The use of austenitic stainless steel versus monel (Ni-cu) alloy in pressurized Gaseous Oxygen (GOX) life support systems
[AD-A156305] N85-35625
MONITORS
Evaluation: Close-range photogrammetry for slope inventory and monitoring
[PB85-192755] N85-35470
MONTANA
Depositional systems and coal occurrence in the Fort Union Formation (Paleocene), Powder River Basin, Wyoming and Montana N85-35505
MONTE CARLO METHOD
Two-dimensional numerical modeling of ion implanted GaAs MESFET devices N85-35341
Calculation of heavy-ion tracks in liquid water
[DE85-012101] N85-35725
EAS accompanied by gamma-families at Mt. Norikura and comparison with Monte Carlo simulation
[HE-3.3-10] N85-35928
Relation between gamma-ray family and EAS core: Monte-Carlo simulation of EAS core
[HE-3.6-7] N85-35955
The lateral distributions of charged particles of energy greater than 0.3 E sub crit in electron-photon cascades in lead and air
[HE-3.6-10] N85-35957
Result of Monte-Carlo simulation of electron-photon cascades in lead and layers of lead-scintillator
[HE-3.6-11] N85-35958
Hadrons registration in emulsion chamber with carbon block
[HE-3.7-3] N85-35962
New analysis of nuclear interaction observed by Mt. Kanbara emulsion chamber experiment
[HE-3.7-4] N85-35963
Intensities of high-energy cosmic rays at Mount Kanbala
[HE-3.7-5] N85-35964
Ultra high energy events in ECHOS series and primary energy spectrum
[HE-3.7-9] N85-35966
Theoretical study of EAS hadronic structure N85-35991
Particle distributions in approximately 10(13) - 10(16) eV air shower cores at mountain altitude and comparison with Monte Carlo simulations
[HE-4.2-18] N85-35994
The longitudinal development of muons in cosmic ray air showers at energies 10(15) - 10(17) eV
[HE-4.3-12] N85-36006
Topological aspects of age parameter
[HE-4.3-13] N85-36007
Monte Carlo simulation of EAS generated by 10(14) - 10(16) eV protons
[HE-4.3-14] N85-36008
A three-dimensional Monte Carlo calculation of the photon initiated showers and Kiel result
[HE-4.5-13] N85-36035
Multimuons events and primary composition
[HE-5.1-5] N85-36070
The spectrum of cosmic ray muons obtained with 100-ton scintillation detector underground and the analysis of recent experimental data
[HE-5.1-6] N85-36071
A new world survey expression for cosmic ray vertical intensity vs. depth in standard rock
[HE-5.1-10] N85-36073
Muon groups and primary composition at 10 to the 13th power to 10 to the 15th power eV
[HE-5.1-12] N85-36074
MOSSBAUER EFFECT
Noble metals as incipient transition metals
[DE85-013283] N85-35286
MOTION SICKNESS
A review of motion sickness with special reference to simulator sickness
[AD-A155975] N85-35611
MOTIVATION
Air university commander's and supervisor's guide on substance abuse
[AD-A156336] N85-35622
MOUNTAINS
Aeromagnetic and radiometric signatures of a possible porphyry system in the western Tushar Mountains, Utah N85-35437
MSAT
Second-generation mobile satellite system. A conceptual design and trade-off study
[NASA-CR-176195] N85-35325
MULTIPATH TRANSMISSION
A comparison of multipath arrival structures observed in the presence of a surface duct with predictions obtained using classical ray techniques and the parabolic equation method
[AD-A156024] N85-35696
MULTIPHASE FLOW
Experimental study of free and mixed convective flow of air in a heated cavity
[DE85-012538] N85-35380
MULTIPHOTON ABSORPTION
Generation of stimulated emission in the soft X-ray range by nonlinear processes with excimer lasers
[DE85-012465] N85-35403
MULTISPECTRAL LINEAR ARRAYS
The application of bispectral analyses to aeroelastic phenomena N85-35157
MULTISPECTRAL RESOURCE SAMPLER
A comparison of LANDSAT thematic mapper, multispectral scanner and airborne sensors for mapping the distribution of alteration minerals: Examples from the southwestern United States N85-35452
MULTIVARIATE STATISTICAL ANALYSIS
Invariant tests and likelihood ratio tests for multivariate elliptically contoured distributions
[AD-A155844] N85-35679
MUON SPIN ROTATION
Proportional drift tubes for large area muon detectors
[HE-5.2-11] N85-36087
MUONS
Neutrino production of like sign dimuons
[DE85-013594] N85-35741
Electrons, muons and hadrons in extensive air showers and how do they depend on nuclear interaction model, part 2 N85-35969
Analysis of equi-intensity curves and NU distribution of EAS N85-35970
A new study of shower age distribution in near vertical showers by EAS air shower array N85-35996
A new study of muons in air showers by NBU air shower array N85-35997
Study of muons near shower cores at sea level using the E594 neutrino detector N85-36000
Correlation of high energy muons with primary composition in extensive air shower
[HE-4.3-7] N85-36001
Measurement of energy muons in EAS at energy region larger thean 10(17) eV
[HE-4.3-8] N85-36002
Muon fluctuation studies of EAS 10(17) eV
[HE-4.3-9] N85-36003
Average features of the muon component of EAS or = 10(17) eV
[HE-4.3-10] N85-36004
Measurement of shower electrons and muons using a small air shower array
[HE-4.3-11] N85-36005
The longitudinal development of muons in cosmic ray air showers at energies 10(15) - 10(17) eV
[HE-4.3-12] N85-36006
Lateral distribution of high energy muons in EAS of sizes Ne approximately equals 10(5) and Ne approximately equals 10(6)
[HE-4.3-16] N85-36010
The identification of gamma ray induced EAS
[HE-4.5-1] N85-36026
Muons in gamma showers
[HE-4.5-3] N85-36027
Muon spectrum in air showers initiated by gamma rays
[HE-4.5-4] N85-36028
Development of electromagnetic cascades in the atmosphere including the Landau-Pomeranchuk-Migdal effect
[HE-4.5-5] N85-36029
Electromagnetic and muonic structure of showers initiated by gamma-rays and by hadrons
[HE-4.5-6] N85-36030
The muon content of gamma-ray showers
[HE-4.5-7] N85-36031
Simulation of gamma-initiated showers
[HE-4.5-10] N85-36033
An underground cosmic ray muon telescope for observation of cosmic ray anisotropy N85-36037
Nuclear cascades in electromagnetic showers produced by primary gamma-quanta in the atmosphere
[HE-4.5-16] N85-36038
On the possibilities of large-scale radio and fiber optics detectors in cosmic rays
[HE-4.6-2] N85-36039
A possible EAS array above the Soudan 2 detector
[HE-4.6-9] N85-36046
Samarkand complex setup for investigation of cosmic ray variation in the energy range of 7 10 (9) - 10 (15) eV
[HE-4.6-14] N85-36050
Longitudinal development of muons in large air showers studies from the arrival time distributions measured at 900m above sea level
[HE-4.7-4] N85-36055
Arrival time distributions of electrons in air showers with primary energies above 10 (18)eV observed at 900m above sea level
[HE-4.7-5] N85-36056
A note on some statistical properties of rise time parameters used in muon arrival time measurements
[HE-4.7-12] N85-36062
Sub-luminal pulses from cosmic ray air showers
[HE-4.7-13] N85-36063
Nineteenth International Cosmic Ray Conference. HE sessions, volume 8
[NASA-CP-2376-VOL-8] N85-36066
Preliminary results on underground muon bundles observed in the Frejus proton-decay detector
[HE-5.1-1] N85-36067
Muon and neutrino results from KGF experiment at a depth of 7000 hg/square cm
[HE-5.1-2] N85-36068
Relevance of multiple muons detected underground to the mass composition of primary cosmic rays
[HE-5.1-4] N85-36069
Multimuons events and primary composition
[HE-5.1-5] N85-36070
The spectrum of cosmic ray muons obtained with 100-ton scintillation detector underground and the analysis of recent experimental data
[HE-5.1-6] N85-36071

A large area cosmic muon detector located at Ohya stone mine
[HE-5.1-7] N85-36072
A new world survey expression for cosmic ray vertical intensity vs. depth in standard rock
[HE-5.1-10] N85-36073
Muon groups and primary composition at 10 to the 13th power to 10 to the 15th power eV
[HE-5.1-12] N85-36074
On muon energy spectrum in muon groups underground
[HE-5.1-14] N85-36076
Energy spectrum of cascades generated by muons in Baksan underground scintillation telescope
[HE-5.1-15] N85-36077
Underwater measurements of muon intensity
[HE-5.1-16] N85-36078
Multiple muons in MACRO
[HE-5.2-1] N85-36079
The Nagoya cosmic-ray muon spectrometer 3, part 1: Preliminary observations
[HE-5.2-2] N85-36080
The Nagoya cosmic-ray muon spectrometer 3, part 2: Track detector
[HE-5.2-3] N85-36081
The Nagoya cosmic-ray muon spectrometer 3, part 3: Automatic film scanning equipment
[HE-5.2-4] N85-36082
The Nagoya cosmic-ray muon spectrometer 3, part 4: Track reconstruction method
[HE-5.2-5] N85-36083
Background light measurements at the DUMAND site
[HE-5.2-7] N85-36084
Hybrid TLC-pair meter for the Sphinx Project
[HE-5.2-10] N85-36086
Proportional drift tubes for large area muon detectors
[HE-5.2-11] N85-36087
An upper limit of muon flux of energies above 100 TeV determined from horizontal air showers observed at Akeno
[HE-5.2-12] N85-36088
Comments on the measurements of multiple muon phenomena
[HE-5.2-13] N85-36089
Energy spectrum of cascade showers induced by cosmic ray muons in the range from 50 GeV to 5 TeV
[HE-5.2-14] N85-36090
Measurement of muon intensity by Cerenkov method
[HE-5.2-15] N85-36091
Analytical calculation of muon intensities under deep sea-water
[HE-5.2-16] N85-36092
Photo nuclear energy loss term for muon-nucleus interactions based on xi scaling model of QCD
[HE-5.2-17] N85-36093
On method of muon spectrum measurements by the scintillation detectors of a large thickness T4t sub o
[HE-5.2-18] N85-36094
Range fluctuations of high energy muons passing through matter
[HE-5.2-19] N85-36095
The research program of the Liquid Scintillation Detector (LSD) in the Mont Blanc Laboratory
[HE-5.3-6] N85-36100
Atmospheric neutrinos observed in underground detectors
[HE-5.3-8] N85-36102
Measurement of neutrino oscillations in MACRO experiment
[HE-5.3-10] N85-36104
High energy neutrino astronomy with MACRO
[HE-5.3-12] N85-36106
Angular distribution of muons produced by cosmic ray neutrinos in rock
[HE-5.3-24] N85-36115
Multiple muons of conventional and exotic origin in DUMAND
[HE-5.4-4] N85-36117
Atmospheric muons and neutrinos, and the neutrino-induced muon flux underground
[HE-5.4-7] N85-36118
Analysis of the electron component of EAS at observational level 700 g x cm(-2) with a scale breaking interaction model and gammaisation hypothesis
[HE-5.4-8] N85-36119
Relationship of sea level muon charge ratio to primary composition including nuclear target effects
[HE-5.4-10] N85-36121
Study of photonuclear muon interactions at Baksan underground scintillation telescope
[HE-5.4-10] N85-36122
Calculation of intensity of high energy muon groups observed deep underground
[HE-5.4-13] N85-36123
Modular detector for deep underwater registration of muons and muon groups
[HE-5.4-15] N85-36125
Results of investigation of muon fluxes of superhigh energy cosmic rays with X-ray emulsion chambers
[HE-5.4-16] N85-36126
Energetic delayed hadrons in large air showers observed at 5200m above sea level
[HE-6.2-9] N85-36145
Muon and neutrino fluxes
[HE-6.2-18] N85-36154

MUSCLES
Response of amino acids in hindlimb muscles to recovery from hypogravity and unloading by tail-cast suspension
[NASA-CR-176183] N85-35589
Relaxation techniques
[AD-A156248] N85-35621

MUSCULAR FATIGUE
Responses of skeletal muscle to unloading, a review
[NASA-CR-176177] N85-35594

MUSCULAR FUNCTION
Muscle protein and glycogen responses to recovery from hypogravity and unloading by tail-cast suspension
[NASA-CR-176181] N85-35591

MUSCULAR STRENGTH
Responses of skeletal muscle to unloading, a review
[NASA-CR-176177] N85-35594

MUSCULOSKELETAL SYSTEM
Responses of skeletal muscle to unloading, a review
[NASA-CR-176177] N85-35594

N

NASA PROGRAMS
NASA patent abstracts bibliography, a continuing bibliography. Section 2: Indexes (supplement 27)
[NASA-SP-7039(27)-SECTION-2] N85-35820

NATURAL GAS
Laser probes of natural gas ignition chemistry
[PB85-200210] N85-35264
Assessment of metal heating technologies for ferrous forging: A pilot study of the form value of natural gas
[PB85-204394] N85-35314
High Temperature Heating System (HTHS)
[PB85-188340] N85-35316

NATURAL LANGUAGE (COMPUTERS)
EPALIT: A data management system applied to the control and retrieval of technical reports
[PB85-193068] N85-35828

NAVIGATION
Nonlinear digital phase-locked loops with application to Loran-C receivers N85-35178

NAVIGATORS
International flight planning handbook
[AD-A156330] N85-35177

NAVY
Development of NATOPS (Naval Air Training and Operating Procedure Standardization) performance software for the H-46D helicopter
[AD-A156089] N85-35190
Solar pond technology for Navy applications
[AD-A155877] N85-35488

NEAR INFRARED RADIATION
The ISAVF opto-mechanical test bed
[NASA-TM-87505] N85-35206

NEBULAE
Far-infrared observations of young clusters embedded in the R Coronae Austrinae and RHO Ophiuchi dark clouds
[NASA-TM-86681] N85-35834
The nature and geometry of infrared reflection nebulae N85-35835

NEODYMIUM LASERS
Infrared generation and wave-mixing studies in cesium
[DE85-012883] N85-35304
Elliptical X-ray analyzer spectrograph application to a laser-produced plasma
[DE85-013790] N85-35398

NEON ISOTOPES
Forward particle production in inelastic Ne-22 inteVractions in emulsion at 4.1 A Ge/c
[HE-1.4-7] N85-35895

NEPTUNE (PLANET)
The 1986 National Aeronautics and Space Administration authorization
[GPO-47-635] N85-35829

NETHERLANDS
Microwave propagation studies, measurements and education in Surabaya, Indonesia
[B8464633] N85-35339

NETWORKS
Procedure for editing the fluxgate magnetometer data of the AFGL (Air Force Geophysics Laboratory) magnetometer network
[AD-A156331] N85-35523

NEUTRAL BEAMS
Considerations on collective ion aceleration as an intense ion injector
[DE85-012706] N85-35757

NEUTRAL PARTICLES
Strategic defense initiative
[DE85-012778] N85-35735

NEUTRINOS
Neutrino production of like sign dimuons
[DE85-013594] N85-35741
High energy physics at Tufts University
[DOE/ER-40085/7] N85-35744
Nineteenth International Cosmic Ray Conference. HE sessions, volume 8
[NASA-CP-2376-VOL-8] N85-36066
Muon and neutrino results from KGF experiment at a depth of 7000 hg/square cm
[HE-5.1-2] N85-36068
Background light measurements at the DUMAND site
[HE-5.2-7] N85-36084
Hybrid TLC-pair meter for the Sphinx Project
[HE-5.2-10] N85-36086
A study of atmospheric neutrinos with the IMB detector
[HE-5.3-7] N85-36101
Atmospheric neutrinos observed in underground detectors
[HE-5.3-8] N85-36102
Geophysical searches for three-neutrino oscillations
[HE-5.3-9] N85-36103
Measurement of neutrino oscillations in MACRO experiment
[HE-5.3-10] N85-36104
The capability of the existing network of installations for detecting the antineutrino burst from collapsing stars
[HE-5.3-13] N85-36107
Energy spectra of high energy atmospheric neutrinos
[HE-5.3-14] N85-36108
A standard source for high energy neutrino astronomy
[HE-5.3-15] N85-36109
A search for cosmic sources of high energy neutrinos with small underground detectors
[HE-5.3-16] N85-36110
Neutrino astronomy and the atmospheric background
[HE-5.3-17] N85-36111
High-energy neutrinos from a lunar observatory
[HE-5.3-21] N85-36112
Characteristics of slow particles emitted in the charged current interactions of neutrinos with emulsion nuclei
[HE-5.3-22] N85-36113
QCD analysis of neutrino charged current structure function F2 in deep inelastic scattering
[HE-5.3-23] N85-36114
Angular distribution of muons produced by cosmic ray neutrinos in rock
[HE-5.3-24] N85-36115
Atmospheric muons and neutrinos, and the neutrino-induced muon flux underground
[HE-5.4-7] N85-36118
Nucleon decay and atmospheric neutrinos in the Mont Blanc experiment
[HE-6.2-6] N85-36142
Muon and neutrino fluxes
[HE-6.2-18] N85-36154
Experimental investigation of radiative-acoustic effects in the water by the thermodynamical conditions of Dumand
[HE-7.1-2] N85-36156

NEUTRON CROSS SECTIONS
(NAT)Fe(n,n'x) spectra at 65.5 MeV
[AD-A155776] N85-35730

NEUTRON EMISSION
Neutron production by Ne and Si ions on a thick Cu target at 670 MeV/A with application to radiation protection
[DE85-014526] N85-35746

NEUTRON FLUX DENSITY
Neutronic calculations for a new high flux reactor
[DE85-011551] N85-35734
Samarkand complex setup for investigation of cosmic ray variation in the energy range of 7 10 (9) - 10 (15) eV
[HE-4.6-14] N85-36050

NEUTRON SCATTERING
Some nuclear data needs in astrophysics
[DE85-012916] N85-35842

NEUTRON SOURCES
Pulsed-neutron-source models for the astrophysical s-process
[DE85-012927] N85-35740
Los Alamos high-current proton storage ring
[DE85-012664] N85-35779

NEUTRON STARS
High energy radiation from neutron stars
[DE85-014353] N85-35843
High energy cosmic ray signature of quark nuggets
[HE-6.2-11] N85-36147
NEUTRONS
(NAT)Fe(n,n'x) spectra at 65.5 MeV
[AD-A155776] N85-35730
Neutron production by Ne and Si ions on a thick Cu target at 670 MeV/A with application to radiation protection
[DE85-014526] N85-35746
Applications and misapplications of the channel-capture formalism of direct neutron capture
[DE85-013992] N85-35748
Los Alamos high-current proton storage ring
[DE85-012664] N85-35779
Some nuclear data needs in astrophysics
[DE85-012916] N85-35842
Determination of the cross section of the proton, pion and neutron inelastic interaction with lead and carbon nuclei at 0.5 - 5.0 TeV energies (PION experiment)
[HE-1.1-5] N85-35853
The spectrum of neutrons at 60 hg m(-2)
[HE-5.2-20] N85-36096
NEVADA
Simulated effects of increased recharge on the ground-water flow system of Yucca Mountain and vicinity, Nevada-California
[DE85-012985] N85-35469
NEW MEXICO
Remote sensing of hydrologic transport processes using spot simulation data
[DE85-012412] N85-35467
NICKEL
Oxidation resistant slurry coating for carbon-based materials
[NASA-CASE-LEW-13923-1] N85-35267
X-ray fluorescence analysis of 304L stainless steel
[DE85-013254] N85-35288
Applications of the mineral resources data system and the international strategic minerals inventory in mineral-resource assessments by region and commodity N85-35451
The Conterminous United States Mineral Assessment Program N85-35458
NICKEL ALLOYS
Microshrink, tensile properties, and the detection of microshrink
[AD-A155875] N85-35278
Deposition of nickel-cobalt alloys by controlled-potential electrolysis
[PB85-198562] N85-35291
NIGHT
Turbulent structure of stably stratified nocturnal slope flows
[AD-A155845] N85-35559
NIGHT VISION
Immediate visibility after red and white adaptation
[AD-A156271] N85-35616
NIOBIUM
Fast-neutron interaction with niobium
[DE85-011471] N85-35731
NITRIC OXIDE
Dissociative and double photoionization cross sections of NO from threshold to 120 A
[NASA-CR-176185] N85-35713
NITROGEN
Nitrogen analysis by chemiluminescence
[AD-A156197] N85-35308
Detection threshold energy of high energy cascade showers using thermoluminescence PTFE-sheet and hot-gas reader
[HE-7.1-5] N85-36159
NITROGEN OXIDES
Review of US NOx abatement technology
[PB85-193522] N85-35501
Atmospheric nitrogen oxides: Their detection and chemistry
[PB85-193910] N85-35502
The measurement of nitrogen oxide (NO, NO2) exchange over plant/soil surfaces
[CSIRO-DAR-TP-8] N85-35587
NITROUS OXIDES
Review of US NOx abatement technology
[PB85-193522] N85-35501
The measurement of nitrogen oxide (NO, NO2) exchange over plant/soil surfaces
[CSIRO-DAR-TP-8] N85-35587
NOBLE METALS
Noble metals as incipient transition metals
[DE85-013263] N85-35286
NOISE MEASUREMENT
A Programmable Automatic Noise Data and Other Related parameter Acquisition system (PANDORA) --- wind energy converters N85-35479
NOISE POLLUTION
GROWIAN: First observations of the environmental impact at the GROWIAN site --- wind energy converter N85-35476
NOISE PREDICTION
Wind turbine noise: Prediction tools and design parameter dependence N85-35477
NOISE PREDICTION (AIRCRAFT)
Optimally designed propellers constrained by noise N85-35196
NOISE REDUCTION
Optimally designed propellers constrained by noise N85-35196
A research program to reduce the interior noise in general aviation aircraft, index and summary
[NASA-CR-176178] N85-35695
NONDESTRUCTIVE TESTS
Quantitative non-destructive evaluation of composite materials based on ultrasonic wave propagation
[NASA-CR-176176] N85-35244
Ultrasonic inspection of carbon fiber reinforced plastic by means of sample-recognition methods
[NASA-TM-77896] N85-35245
Methods for nondestructive tests of CFRP laminates N85-35248
Fatigue damage detection in steels by optical correlation
[AD-A155830] N85-35277
Subcritical fracture propagation in rocks: An examination using the methods of fracture mechanics and non-destructive testing N85-35516
NONEQUILIBRIUM FLOW
Transient three-phase three-component systems. Part 1: Formulation of the system of differential equations
[DE85-013267] N85-35384
NONFLAMMABLE MATERIALS
Investigation of experimental lightweight firewall materials for A/C engine bay applications
[AD-A155765] N85-35175
NONLINEAR EQUATIONS
Identification and control of structures in space
[NASA-CR-176175] N85-35214
Long-time asymptotics of a system for plasma diffusion
[NASA-CR-177947] N85-35375
Analysis of the nonlinear equations describing the elastic, thermal, and electromagnetic behavior of solids: Existence of solutions of semi-inverse problems N85-35415
NONLINEAR OPTICS
Edge detection and geometric methods in computer vision
[AD-A155873] N85-35630
NONLINEAR SYSTEMS
The application of bispectral analyses to aeroelastic phenomena N85-35157
NONLINEARITY
Nonlinear digital phase-locked loops with application to Loran-C receivers N85-35178
Membrane reinforcement in concrete shells: Design versus nonlinear behavior N85-35312
Generation of stimulated emission in the soft X-ray range by nonlinear processes with excimer lasers
[DE85-012465] N85-35403
Analysis of the nonlinear equations describing the elastic, thermal, and electromagnetic behavior of solids: Existence of solutions of semi-inverse problems N85-35415
Width of nonlinear difference resonances
[DE85-013026] N85-35719
The HEAO-2 Guest Investigator Program: Non-linear growth of instabilities in line-driven stellar winds
[NASA-CR-176168] N85-35840
NONPARAMETRIC STATISTICS
Multidimensional analysis of data obtained in experiments with X-ray emulsion chambers and extensive air showers
[HE-3.6-2] N85-35951
NORMAL DENSITY FUNCTIONS
Large deviations for the maxima of some random fields
[AD-A155909] N85-35681
NORMAL SHOCK WAVES
Parallel fast-forward shock within 1 AU: Helios-1 and 2 observations
[MPAE-W-79-84-27] N85-35847
NOTCH STRENGTH
Damage mechanisms in damaged CFRP laminates N85-35249
NUCLEAR CAPTURE
Applications and misapplications of the channel-capture formalism of direct neutron capture
[DE85-013992] N85-35748
NUCLEAR EMULSIONS
A survey of multiplicities and rapidity densities from existing emission data on hadron-nucleus nucleus-nucleus collisions N85-35706
On a possibility of inelasticity partial coefficient K sub gamma determination in pi C and pi Pb interactions at 10 to the 14th power eV (experiment PAMIR 1)
[HE-1.1-12] N85-35859
Anuglar distribution of shower particles produced in the collisions of 20-GeV/c and 300-GeV negative pions with emulsion nuclei N85-35868
Stopping relativistic Xe, Ho, Au and U nuclei in nuclear emulsions N85-35876
Heavy nucleus collisions between 20 and 60 GeV/nucleon
[HE-1.4-2] N85-35890
Characteristics of central collision events in Fe-nucleus interactions for 20 - 60 GeV/nucleon
[HE-1.4-3] N85-35891
Nucleus-nucleus interaction above several hundred GeV/n
[HE-1.4-4] N85-35892
Observation of direct hadronic pairs in nucleus-nucleus collisions in JACEE emulsion chambers
[HE-1.4-5] N85-35893
Excessive production of electron pairs by soft photons in low multiplicity ion interactions
[HE-1.4-6] N85-35894
On the mechanism of anomalous nucleus-nucleus interactions at energies above 1 TeV/nucleon
[HE-1.4-8] N85-35896
Meson multiplicity in nucleus-nucleus collisions above 4 GeV/amu
[HE-1.4-10] N85-35897
Inclusive angular distribution of alpha and Li fragments produced in the Fe-C and Fe-Pb collisions at 1.88 GeV/u
[HE-1.4-11] N85-35898
Experiment Pamir-3. Coplanar emission of high energy gamma-quanta at interaction of hadrons with nuclei of air atoms at energies above 10 to the 7th power GeV
[HE-1.4-12] N85-35899
The effect of the relative nuclear size on the nucleus-nucleus interactions
[HE-1.4-13] N85-35900
Japan - USSR joint emulsion chamber experiment at Pamir
[HE-3.1-1] N85-35901
Intensities of high-energy cosmic rays at Mount Kanbala
[HE-3.1-2] N85-35902
High energy gamma-rays and hadrons at Mount Fuji
[HE-3.1-3] N85-35903
On the characteristics of emulsion chamber family events produced in low heights
[HE-3.1-6] N85-35904
Some characteristic cosmic ray events and an attempt at their explanation
[HE-3.1-8] N85-35906
Energy spectra of proton and nuclei of primary cosmic rays in energy region 10 TeV/particle
[HE-3.1-10] N85-35908
Jets in air-jet family
[HE-3.2-1] N85-35912
Search for anomalous C-jets in Chacaltaya emulsion chamber experiment
[HE-3.2-5] N85-35913
Exotic interactions among C-jets and Pb-jets
[HE-3.2-6] N85-35914
Characteristics of anomalously high multiplicity cosmic ray interactions
[HE-3.3-1] N85-35920
Transverse momentum distribution of pion deg in the fragmentation region of super high energy interactions N85-35921
Study of hadron bundles observed in Chacaltaya two-story emulsion chamber
[HE-3.3-4] N85-35922
Atmospheric interactions detected in both the upper and the lower chambers at Chacaltaya
[HE-3.3-7] N85-35925
NUCLEAR EXPLOSION EFFECT
Evaluation of nuclear detonation location capability under high attack scenario
[AD-A155761] N85-35729
NUCLEAR EXPLOSIONS
Investigation of the lightning vulnerability of nuclear explosive test systems at the Nevada Test Site
[DE85-011761] N85-35563
Evaluation of nuclear detonation location capability under high attack scenario
[AD-A155761] N85-35729
Ground motion measurements for the QUESO nuclear event
[DE85-014806] N85-35743

Heavy flavours production in quark-gluon plasma formed in high energy nuclear reactions N85-35886
NUCLEAR FISSION
Neutronic calculations for a new high flux reactor [DE85-011551] N85-35734
NUCLEAR FUEL ELEMENTS
Thermal hydraulic features of the TMI accident [DE85-014589] N85-35747
NUCLEAR FUEL REPROCESSING
Analytical methods in the purex process [BLL-DOUNREAY-TR-952(9091.9F)] N85-35727
NUCLEAR FUSION
Gamma-ray production cross sections for alpha-particle induced reactions on F-19 and Na-23 [DE85-012603] N85-35732
Operations considerations in designing a high speed multi-channel data acquisition system [DE85-012840] N85-35756
Some nuclear data needs in astrophysics [DE85-012916] N85-35842
NUCLEAR INTERACTIONS
Observations of accelerated high current low emittance beams in the SLC Linac [DE85-013073] N85-35211
Proceedings of the Workshop on Detectors for Relativistic Nuclear Collisions [LBL-18225] N85-35700
Detectors for relativistic nuclear collisions (report from the Fixed-Target Hadron Group) N85-35701
Event parameters: Fixed targets N85-35702
Working group on penetrating probes at fixed target facilities N85-35703
A survey of multiplicities and rapidity densities from existing emission data on hadron-nucleus nucleus-nucleus collisions N85-35706
A simulation of ultra-relativistic nucleus-nucleus collisions N85-35707
Some remarks about simulation of cosmic ray phenomena with use of nuclear interaction models based on the current SPS proton-antiproton data [HE-1.2-6] N85-35864
Low P sub T hadron-nucleus interactions [HE-1.2-7] N85-35865
The response of a scintillation counter below an emulsion chamber to heavy nucleus interactions in the chamber N85-35889
Characteristics of central collision events in Fe-nucleus interactions for 20 - 60 GeV/nucleon [HE-1.4-3] N85-35891
Nucleus-nucleus interaction above several hundred GeV/n [HE-1.4-4] N85-35892
Observation of direct hadronic pairs in nucleus-nucleus collisions in JACEE emulsion chambers [HE-1.4-5] N85-35893
Excessive production of electron pairs by soft photons in low multiplicity ion interactions [HE-1.4-6] N85-35894
Meson multiplicity in nucleus-nucleus collisions above 4 GeV/amu [HE-1.4-10] N85-35897
Inclusive angular distribution of alpha and Li fragments produced in the Fe-C and Fe-Pb collisions at 1.88 GeV/u [HE-1.4-11] N85-35898
The effect of the relative nuclear size on the nucleus-nucleus interactions [HE-1.4-13] N85-35900
Japan - USSR joint emulsion chamber experiment at Pamir [HE-3.1-1] N85-35901
On the characteristics of emulsion chamber family events produced in low heights [HE-3.1-6] N85-35904
Search for anomalous C-jets in Chacaltaya emulsion chamber experiment [HE-3.2-5] N85-35913
Exotic interactions among C-jets and Pb-jets [HE-3.2-6] N85-35914
Scaling violation in hadron-nucleus interaction [HE-3.2-8] N85-35916
The model of independent particles emission in the multiparticle production theory [HE-3.2-10] N85-35918
Study of hadron bundles observed in Chacaltaya two-story emulsion chamber [HE-3.3-4] N85-35922
Anomalous correlation between hadron and electromagnetic particles in hadron and gamma-ray families [HE-3.3-6] N85-35924
Atmospheric interactions detected in both the upper and the lower chambers at Chacaltaya [HE-3.3-7] N85-35925
Lateral distribution of high energy hadrons and gamma ray in air shower cores observed with emulsion chambers [HE-3.3-8] N85-35926
Size distributions of air showers accompanied with high energy gamma ray bundles observed at Mt. Chacaltaya [HE-3.3-9] N85-35927
A halo event created at 200 m above the Chacaltaya emulsion chamber [HE-3.4-5] N85-35933
A binocular-type atmospheric interaction generating sequential exotic features [HE-3.4-6] N85-35934
Gamma-hadron families and scaling violation [HE-3.4-7] N85-35935
Super-family P2 C-96-125 observed by Japan-URSS Joint Emulsion Chamber Experiment [HE-3.4-8] N85-35936
On the halo events observed by Mount Fuji and Mount Kanbala Emulsion Chamber Experiments [HE-3.4-9] N85-35937
Experiment Pamir-2. Fianit: A giant super-family with halo (Epsilon sub 0 at approximately 10(17) eV) [HE-3.4-10] N85-35938
Experiment Pamir-4: Analysis of superfamily with halo of electromagnetic nature detected in deep XEC [HE-3.4-11] N85-35939
Particle interactions at energies over 1000 TeV inferred from gamma-families observed at Mount Fuji [HE-3.5-1] N85-35940
A search for mini-clusters in Japan-USSR Joint Experiment at Pamir [HE-3.5-2] N85-35941
Mini-clusters [HE-3.5-3] N85-35942
Structure of super-families [HE-3.5-7] N85-35944
Extremely high energy hadron and gamma-ray families(3). Core structure of the halo of superfamily [HE-3.5-8] N85-35945
Numerical analysis of electromagnetic cascades in emulsion chambers [HE-3.5-9] N85-35946
New analysis of nuclear interaction observed by Mt. Kanbara emulsion chamber experiment [HE-3.7-4] N85-35963
Structured events in Pamir carbon X-ray chambers [HE-3.7-7] N85-35965
Electrons, muons and hadrons in extensive air showers and how do they depend on nuclear interaction model, part 2 N85-35969
Electrons, muons and hadrons in extensive air showers and how do they depend on nuclear interaction model, part 1 N85-35972
Tskhra-Tskaro complex intended for the investigations of EAS spatial characteristics near axis N85-35995
Correlation of high energy muons with primary composition in extensive air shower [HE-4.3-7] N85-36001
The longitudinal development of muons in cosmic ray air showers at energies 10(15) - 10(17) eV [HE-4.3-12] N85-36006
Simulation of gamma-initiated showers [HE-4.5-10] N85-36033
Delayed particles in EAS at Akeno [HE-6.2-8] N85-36144
NUCLEAR PHYSICS
Forty-five years of e(+)e(-) annihilation physics: 1956 to 2001 [DE85-013052] N85-35723
NUCLEAR POWER PLANTS
State-of-the-art of solid-state motor controllers [TI85-008674] N85-35806
NUCLEAR POWER REACTORS
Applicability of 100kWe-class of space reactor power systems to NASA manned space station missions [NASA-CR-174696] N85-35728
NUCLEAR REACTIONS
Some nuclear data needs in astrophysics [DE85-012916] N85-35842
Heavy flavours production in quark-gluon plasma formed in high energy nuclear reactions N85-35886
Preliminary results on underground muon bundles observed in the Frejus proton-decay detector [HE-5.1-1] N85-36067
NUCLEAR REACTORS
Neutronic calculations for a new high flux reactor [DE85-011551] N85-35734
NUCLEAR SCATTERING
A unification of the interactions and the diffractive processes N85-35870
On mini-cluster observed by Chacaltaya emulsion chamber experiment [HE-3.6-12] N85-35959
NUCLEAR WEAPONS
Evaluation of nuclear detonation location capability under high attack scenario [AD-A155761] N85-35729
NUCLEATION
Size and shape dependence of CO adsorption sites on sapphire supported Fe microcrystals [NASA-CR-176171] N85-35794
NUCLEI (NUCLEAR PHYSICS)
Nineteenth International Cosmic Ray Conference. HE Sessions, volume 6 [NASA-CP-2376-VOL-6] N85-35848
On total cross sections and slopes at superhigh energies [HE-1.1-4] N85-35852
Measurement of interaction cross section of cosmic ray Fe nuclei (E4 GeV/N) with Al target [HE-1.1-7] N85-35855
Empirical description of the hadron-hadron and hadron-nucleus interaction at the accelerator energy range [HE-1.2-4] N85-35862
Low P sub T hadron-nucleus interactions [HE-1.2-7] N85-35865
Anuglar distribution of shower particles produced in the collisions of 20-GeV/c and 300-GeV negative pions with emulsion nuclei N85-35868
Determination of primary energy in nucleus-nucleus collisions and the high P(sub)T tail of alpha-particles N85-35875
Stopping relativistic Xe, Ho, Au and U nuclei in nuclear emulsions N85-35876
Physical meaning of the multiplicities of emitted nucleons in hadron-nucleus collisions N85-35877
How are particle production, nucleon emission and target fragment evaporation processes interrelated in hadron-nucleus collisions? N85-35878
Experimental evidence of the decrease of kinetic energy of hadrons in passing through atomic nuclei N85-35880
Energy-range relations for hadrons in nuclear matter N85-35881
Scattering and stopping of hadrons in nuclear matter N85-35882
Measurements of hadron mean free path for the particle-producing collisions in nuclear matter N85-35883
The phi-meson and Chiral-mass-meson production in heavy-ion collisions as potential probes of quark-gluon-plasma and Chiral symmetry transitions N85-35884
Experimental basis for the models of cascade propagation in atmosphere [HE-3.6-6] N85-35954
A study of gamma-families generated in nucleon-nucleus (NA) and pion-nucleus (pi A) interactions [HE-3.7-2] N85-35961
Dependence of the average spatial and energy characteristics of the hadron-lepton cascade on the strong interaction parameters at superhigh energies N85-35977
A facility for investigation of multiple hadrons at cosmic-ray energies [HE-4.6-8] N85-36045
Photo nuclear energy loss term for muon-nucleus interactions based on xi scaling model of QCD [HE-5.2-17] N85-36093
NUCLEON-NUCLEON INTERACTIONS
The nucleon intensity in the atmosphere and the Pt distribution [HE-3.1-9] N85-35907
New aspects in nucleon-nucleus collisions and EAS properties around 10(6) GeV N85-35974
Small air showers and collider physics [HE-4.1-9] N85-35975
Primary chemical composition from simultaneous recording of muons induced cascades and accompanying muon group underground [HE-5.1-13] N85-36075
NUCLEON-NUCLEON SCATTERING
Comparison of big event with calculations of the air shower development [HE-3.6-8] N85-35956
NUCLEONS
Proceedings of the Workshop on Detectors for Relativistic Nuclear Collisions [LBL-18225] N85-35700
High energy physics at Tufts University [DOE/ER-40085/7] N85-35744
Nucleon-nucleus interactions from JACEE N85-35869
Is the inelastic charge-exchange contribution constant at the large X and superhigh energies? Qaut 01Kuchin, I. A. N85-35871
Propagation of cosmic rays through the atmosphere in the quark-gluon strings model N85-35873

Scaling violation in the fragmentation region of inclusive nucleon spektrum N85-35874
Physical meaning of the multiplicities of emitted nucleons in hadron-nucleus collisions N85-35877
How are particle production, nucleon emission and target fragment evaporation processes interrelated in hadron-nucleus collisions? N85-35878
Experimental study of the space-time development of the particle production process in hadron-nucleon collisions, using massive target nucleus as a detector N85-35879
Measurements of hadron mean free path for the particle-producing collisions in nuclear matter N85-35883
Ringlike inelastic events in cosmic rays and accelerators N85-35887
Experimental basis for the models of cascade propagation in atmosphere
[HE-3.6-6] N85-35954
On mini-cluster observed by Chacaltaya emulsion chamber experiment
[HE-3.6-12] N85-35959
A study of gamma-families generated in nucleon-nucleus (NA) and pion-nucleus (pi A) interactions
[HE-3.7-2] N85-35961
New aspects in nucleon-nucleus collisions and EAS properties around 10(6) GeV N85-35974
Small air showers and collider physics
[HE-4.1-9] N85-35975
Sub-luminal pulses from cosmic ray air showers
[HE-4.7-13] N85-36063
A study of atmospheric neutrinos with the IMB detector
[HE-5.3-7] N85-36101
Limits on monopole fluxes from KFG experiment
[HE-6.1-6] N85-36132
Search for proton decay in the Frejus experiment
[HE-6.2-2] N85-36138
Results on nucleon life-time from the Kolar gold field experiment
[HE-6.2-3] N85-36139
Construction of the Soudan 2 detector
[HE-6.2-5] N85-36141
Nucleon decay and atmospheric neutrinos in the Mont Blanc experiment
[HE-6.2-6] N85-36142
Energetic delayed hadrons in large air showers observed at 5200m above sea level
[HE-6.2-9] N85-36145

NUCLIDES
The detection and study of molecular species using time resolved laser spectroscopy
[AD-A155910] N85-35256

NULL ZONES
A planar version of a 4.0 gigahertz reactively steered adaptive array
[AD-A156029] N85-35330

NUMERICAL ANALYSIS
Algorithmic approaches in sets of good answers in inverse problems
[PM/84/18] N85-35677
Invariant tests and likelihood ratio tests for multivariate elliptically contoured distributions
[AD-A155844] N85-35679
Constrained stiffness matrix adjustment using mode data
[AD-A155988] N85-35685
Relation between field energy and RMS emittance in intense particle beams
[DE85-012655] N85-35784
Analytical-numerical methods of calculations of energy and three-dimensional particle distributions in electromagnetic cascades
[HE-3.5-13] N85-35950

NUMERICAL CONTROL
Design and construction of an advanced power conditioning subsystem for small photovoltaic applications
[DE85-013940] N85-35495
Optimizing data access in the LAMPF control system
[DE85-012653] N85-35663
Distribution of computer functionality for accelerator control at the Brookhaven AGS
[DE85-012520] N85-35669
On-line model driven control of the SLC electron Damping Ring
[DE85-013377] N85-35772

NUMERICAL INTEGRATION
Reliability prediction of the series system with spares subject to Weibull failure N85-35413

NYLON (TRADEMARK)
Solid-state co-extrusion of nylon 6 gel
[AD-A156187] N85-35296

O

OBSERVATION AIRCRAFT
Motor glider meteorology N85-35543

OBSERVATORIES
Monopole, astrophysics and cosmic ray observatory at Gran Sasso
[HE-6.1-4] N85-36130

OCEAN BOTTOM
Marine phosphorite deposits model for exploration, with emphasis on deposits in the US Atlantic coastal plain N85-35439
Massive sulfide deposits from the southern Juan de Fuca Ridge N85-35446
Background light measurements at the DUMAND site
[HE-5.2-7] N85-36084
Measurements of light background at large depth in the ocean
[HE-5.2-8] N85-36085

OCEAN CURRENTS
Meteorological data from the OPTOMA (Ocean Prediction Through Observations, Modeling and Analysis) program OPTOMA 2, leg D2. 30 Jun. - 10 Jul. 1984
[AD-A156134] N85-35560

OCEAN SURFACE
Microwave properties of a quiet sea
[NASA-CR-176199] N85-35322
Sea surface and remotely sensed temperatures off Cape Mendocino, California
[NASA-TM-86712] N85-35573

OCEAN THERMAL ENERGY CONVERSION
Energy from low temperature differences
[DE85-008817] N85-35492

OCEANOGRAPHY
Noiseless coding for the Gamma Ray spectrometer
[NASA-CR-176201] N85-35219
Microwave properties of a quiet sea
[NASA-CR-176199] N85-35322
Sea surface and remotely sensed temperatures off Cape Mendocino, California
[NASA-TM-86712] N85-35573

OCEANS
Cobalt-rich ferromanganese crusts in the oceans N85-35444

OIL FIELDS
Steamflood pilots in the O'Connell Ranch field and the T-4 Ranch field
[DE85-901363] N85-35468

OILS
Further studies on liquid sloshing
[PB85-198695] N85-35388
Steamflood pilots in the O'Connell Ranch field and the T-4 Ranch field
[DE85-901363] N85-35468

ON-LINE SYSTEMS
On-line model driven control of the SLC electron Damping Ring
[DE85-013377] N85-35772

ONE DIMENSIONAL FLOW
Unsteady flow in a supersonic cascade with two in-passage shocks
[NASA-CR-3925] N85-35158

ONTOGENY
NASA Developmental Biology Workshop: A summary
[NASA-TM-86756] N85-35578

OPERATOR PERFORMANCE
Manual and computer-aided sequential diagnostic inference
[AD-A156229] N85-35620

OPERATORS (MATHEMATICS)
Edge detection and geometric methods in computer vision
[AD-A155873] N85-35630
Some rigorous results concerning spectral theory for ideal MHD
[DE85-013427] N85-35770

OPTICAL COMMUNICATION
Optical receivers using rough reflectors
[NASA-CR-176200] N85-35750

OPTICAL DENSITY
Hadrons registration in emulsion chamber with carbon block
[HE-3.7-3] N85-35962
Structured events in Pamir carbon X-ray chambers
[HE-3.7-7] N85-35965

OPTICAL EQUIPMENT
Single-point diamond crushing of Zerodur with in-situ polishing and metrology on a diamond turning machine
[DE85-012918] N85-35305

OPTICAL MEASUREMENT
The ISAVF opto-mechanical test bed
[NASA-TM-87505] N85-35206
Self-study manual on optical radiation measurements. Part 1: Concepts. Chapter 12: Blackbodies, blackbody radiation, and temperature scales
[PB85-195303] N85-35754
Energy calibration of the fly's eye detector
[HE-4.4-1] N85-36011

OPTICAL MEASURING INSTRUMENTS
Redefining the scratch standards
[PB85-194736] N85-35755

OPTICAL PROPERTIES
Characterization of the optical and thermal properties of matter by photothermal techniques
[DE85-012607] N85-35260
Los Alamos free-electron laser
[DE85-012666] N85-35405
Optical properties of heterostructures and superlattices
[AD-A156243] N85-35802
Ionic crystals
[DE85-009482] N85-35809

OPTICAL PUMPING
Infrared generation and wave-mixing studies in cesium
[DE85-012883] N85-35304
Generation of stimulated emission in the soft X-ray range by nonlinear processes with excimer lasers
[DE85-012465] N85-35403

OPTIMIZATION
An automated technique for encasing specific payloads with low-drag fairings N85-35183
Energy management of three-dimensional minimum-time intercept
[NASA-CR-176174] N85-35186
An evaluation of a class of practical optimization techniques for structural dynamics applications
[PB85-195766] N85-35434
Optimizing data access in the LAMPF control system
[DE85-012653] N85-35663
Two methods of global data assimilation
[AD-A155981] N85-35684
Beryllium production
[DE85-013360] N85-35716

ORBIT TRANSFER VEHICLES
Status of advanced orbital transfer propulsion
[NASA-TM-87069] N85-35225

ORBITAL MANEUVERING VEHICLES
Status of advanced orbital transfer propulsion
[NASA-TM-87069] N85-35225

ORBITAL MECHANICS
Target observability for satellite-based sensors
[AD-A156139] N85-35217

ORBITAL SPACE STATIONS
Applicability of 100kWe-class of space reactor power systems to NASA manned space station missions
[NASA-CR-174696] N85-35728

ORDER-DISORDER TRANSFORMATIONS
Electronic structure and lattice dynamics of dimensionally constrained and disordered solids
[AD-A155927] N85-35797

ORGANIC CHEMISTRY
Studies in photochemical smog chemistry. 1: Atmospheric chemistry of toluene. 2: Analysis of chemical reaction mechanisms for photochemical smog N85-35497

ORGANIC COMPOUNDS
Aspects of high-resolution gas chromatography as applied to the analysis of hydrocarbon fuels and other complex organic mixtures. Volume 1
[AD-A156154] N85-35257

ORGANIC SULFUR COMPOUNDS
Heats of formation of gas phase organosulfur molecules, radicals and ions measured by PEPICO and application of (17)O and (33)S NMR spectroscopy to structure determination of organosulfur compounds
[DE85-010558] N85-35229

ORIENTATION
Parametric stability of analytical close-range photogrammetry N85-35461

ORION NEBULA
The structure of Herbig-Haro object 43 and Orion dark cloud extinction
[NASA-TM-87503] N85-35831
Far-infrared emission lines of CO and OH in the Orion-KL molecular shock
[NASA-TM-86721] N85-35832
Observations of far-infrared transitions between excited states of OH
[NASA-TM-86722] N85-35833

OROGRAPHY
Project Skywater, 1983-84 SCPP (Sierra Cooperative Pilot Project) data inventory
[PB85-187052] N85-35565

ORTHOSTATIC TOLERANCE
Cardiovascular responses to orthostatism and weightlessness N85-35601

ORTHOTROPIC SHELLS
Stress analysis of axisymmetric sandwich shells of variable thickness N85-35419
OSCILLATIONS
Robinson instability and beam loading [DE85-013301] N85-35737
Relation between field energy and RMS emittance in intense particle beams [DE85-012655] N85-35784
Geophysical searches for three-neutrino oscillations [HE-5.3-9] N85-36103
Measurement of neutrino oscillations in MACRO experiment [HE-5.3-10] N85-36104
OSCILLATORS
Los Alamos free-electron laser [DE85-012666] N85-35405
OSCILLOSCOPES
The structure of the shower disk observed at Mt. Norikura [HE-4.7-1] N85-36052
Sub-luminal pulses from cosmic ray air showers [HE-4.7-13] N85-36063
OUTPUT
Raster functionality for a VDI [DE85-006734] N85-35396
Optimize computer throughput using array processors [AD-A155843] N85-35626
Software maintenance relating to the input translator and z-80 realization volume of the computer systems design environment [AD-A155849] N85-35646
Beryllium production [DE85-013350] N85-35716
OXIDATION
The preparation of TEM specimens showing oxide scales in transverse cross-section [AERE-R-11579] N85-35276
High temperature corrosion of ceramics [DE85-013481] N85-35303
Development and evaluation of sulfonated polysulfone membranes for the zinc-ferricyanide battery [DE85-009104] N85-35357
OXIDATION RESISTANCE
Thermal barrier coating system [NASA-CASE-LEW-14057-1] N85-35233
OXIDATION-REDUCTION REACTIONS
A kinetic model for predicting oxidative degradation rates in combined radiation-thermal environments [TI85-002629] N85-35414
OXIDE FILMS
Thermal barrier coating system [NASA-CASE-LEW-14057-1] N85-35233
OXYGEN
Thermodynamics of the corrosion of chromium in molten carbonates [DE85-011407] N85-35282
OXYGEN CONSUMPTION
An analysis of aerobic capacity in a large United States population [AD-A156200] N85-35614
OXYGEN SUPPLY EQUIPMENT
Improved oxygen sources for breathing apparatus [NASA-TM-86671] N85-35623
OZONE
Space Station Polar Platform: Integrating research and operational missions [PB85-195279] N85-35218
A study of the chemistry of alkali metals in the upper atmosphere [AD-A156349] N85-35524

P

PACIFIC OCEAN
Meteorological data from the OPTOMA (Ocean Prediction Through Observations, Modeling and Analysis) program OPTOMA 2, leg D2. 30 Jun. - 10 Jul. 1984 [AD-A156134] N85-35560
PAINTS
Space shuttle SRB TPS protective paint test and evaluation in NASA Hot Gas Facility and AEDC Tunnel C [NASA-CR-170884] N85-35294
PAIR PRODUCTION
Observation of direct hadronic pairs in nucleus-nucleus collisions in JACEE emulsion chambers [HE-1.4-5] N85-35893
Excessive production of electron pairs by soft photons in low multiplicity ion interactions [HE-1.4-6] N85-35894
LPM effect and primary energy estimations [HE-3.6-4] N85-35953
Result of Monte-Carlo simulation of electron-photon cascades in lead and layers of lead-scintillator [HE-3.6-11] N85-35958
Missing energies at pair creation [HE-4.4-8] N85-36016
PALLADIUM
FTIR studies of hydrocarbon synthesis on Pd/ZSM5 catalysts [DE85-012430] N85-35230
Characterization of catalysts with metal-support effects and of the species adsorbed on their surfaces [DE85-012254] N85-35394
PANEL METHOD (FLUID DYNAMICS)
Calculation of compressible flow about three-dimensional inlets with auxiliary inlets, slats and vanes by means of a panel method [NASA-CR-174975] N85-35162
PANELS
A research program to reduce the interior noise in general aviation aircraft, index and summary [NASA-CR-176178] N85-35695
PARABOLIC DIFFERENTIAL EQUATIONS
Long-time asymptotics of a system for plasma diffusion [NASA-CR-177947] N85-35375
PARACHUTES
Dual towline spin-recovery device [NASA-CASE-LAR-13076-1] N85-35200
PARAMETER IDENTIFICATION
The effect of insirumentation system parameters on the results of a flight mechanical system identification N85-35170
Aspects of input signal design for order and parameter estimation in linear dynamical systems [ER-83/05] N85-35362
A strategy for calibrating atmospheric transport models [CSIRO-DAR-TP-9] N85-35518
Recursive partitioning estimation N85-35670
PARAMETERIZATION
Application of a turbulent closure model to the parameterization of the vertical diffusion of heat, momentum, and humidity in the ECMWF model — European Center for Medium Term Weather Forecasting (ECMWF) [MITT-41] N85-35387
A new method of differential structural analysis of gamma-family basic parameters [HE-3.6-3] N85-35952
Multiple muons in MACRO [HE-5.2-1] N85-36079
PARSING ALGORITHMS
Artificial intelligence in Ada (trademark): Pattern-directed processing [AD-A156230] N85-35671
PARTIAL DIFFERENTIAL EQUATIONS
Transient three-phase three-component systems. Part 1: Formulation of the system of differential equations [DE85-013267] N85-35384
Analysis of the nonlinear equations describing the elastic, thermal, and electromagnetic behavior of solids: Existence of solutions of semi-inverse problems N85-35415
Stress analysis of axisymmetric sandwich shells of variable thickness N85-35419
PARTIAL PRESSURE
Thermodynamics of the corrosion of chromium in molten carbonates [DE85-011407] N85-35282
PARTICLE ACCELERATOR TARGETS
Event parameters: Fixed targets N85-35702
Working group on penetrating probes at fixed target facilities N85-35703
Summary of the working group on penetrating probes in collider experiments. 1: The collider environment N85-35704
(NAT)Fe(n,n'x) spectra at 65.5 MeV [AD-A155776] N85-35730
Radiation safety problems in handling highly active tritium targets [DE85-014268] N85-35742
Neutron production by Ne and Si ions on a thick Cu target at 670 MeV/A with application to radiation protection [DE85-014526] N85-35746
Major facility overhauls at LAMPF [DE85-012724] N85-35765
Recent advances in remote handling at LAMPF [DE85-012725] N85-35775
How are particle production, nucleon emission and target fragment evaporation processes interrelated in hadron-nucleus collisions? N85-35878
PARTICLE ACCELERATORS
Distribution of computer functionality for accelerator control at the Brookhaven AGS [DE85-012520] N85-35669
Width of nonlinear difference resonances [DE85-013026] N85-35719
Quality assurance considerations for the implementation of a pulsed power R and D project [DE85-012357] N85-35720
Operations considerations in designing a high speed multi-channel data acquisition system [DE85-012840] N85-35756
High vacuum portable pumping station suitable for accelerator use [DE85-011840] N85-35759
Ion source development for the Los Alamos heavy ion fusion injector [DE85-012682] N85-35766
Surface discharges as intense photon sources in the extreme ultraviolet [DE85-012593] N85-35782
SLC arc transport system: Magnet design and construction [DE85-014289] N85-35789
PARTICLE BEAMS
Observations of accelerated high current low emittance beams in the SLC Linac [DE85-013073] N85-35211
Operations considerations in designing a high speed multi-channel data acquisition system [DE85-012840] N85-35756
Synchronous timing of multi-energy fast beam extraction during a single AGS cycle [DE85-011829] N85-35781
Relation between field energy and RMS emittance in intense particle beams [DE85-012655] N85-35784
Accelerator physics measurements at the damping ring [DE85-013373] N85-35785
PARTICLE COLLISIONS
The use of austenitic stainless steel versus monel (Ni-cu) alloy in pressurized Gaseous Oxygen (GOX) life support systems [AD-A156305] N85-35625
Working group on penetrating probes at fixed target facilities N85-35703
Summary of the working group on penetrating probes in collider experiments. 1: The collider environment N85-35704
Report of working group on detectors for hadrons and event parameters at colliders N85-35705
A survey of multiplicities and rapidity densities from existing emission data on hadron-nucleus nucleus-nucleus collisions N85-35706
A simulation of ultra-relativistic nucleus-nucleus collisions N85-35707
Very high energy probes of the quark-gluon plasma N85-35708
A holographic streamer chamber for relativistic nucleus-nucleus collision experiments N85-35710
SLC arc transport system: Magnet design and construction [DE85-014289] N85-35789
Design considerations for personnel access penetrations for the superconducting super collider [DE85-013027] N85-35807
Measurement of interaction cross section of cosmic ray Fe nuclei (E4 GeV/N) with Al target [HE-1.1-7] N85-35855
Hadron thermodynamics in relativistic nuclear collisions [HE-1.1-8] N85-35856
1Single particle momentum and angular distributions in hadron-hadron collisions at ultrahigh energies [HE-1.2-1] N85-35860
Low P sub T hadron-nucleus interactions [HE-1.2-7] N85-35865
A test of the Feynman scaling in the fragmentation region [HE-1.2-9] N85-35867
Anuglar distribution of shower particles produced in the collisions of 20-GeV/c and 300-GeV negative pions with emulsion nuclei N85-35868
Determination of primary energy in nucleus-nucleus collisions and the high P(sub)T tail of alpha-particles N85-35875
Physical meaning of the multiplicities of emitted nucleons in hadron-nucleus collisions N85-35877
How are particle production, nucleon emission and target fragment evaporation processes interrelated in hadron-nucleus collisions? N85-35878
Experimental study of the space-time development of the particle production process in hadron-nucleon collisions, using massive target nucleus as a detector N85-35879
Energy-range relations for hadrons in nuclear matter N85-35881
Scattering and stopping of hadrons in nuclear matter N85-35882

Measurements of hadron mean free path for the particle-producing collisions in nuclear matter
N85-35883
SU(2) x U(1) vacuum and the Centauro events
N85-35885
The multiplicity and the spectra of secondaries correlated with the leading particle energy
[HE-3.2-11] N85-35919
A study of gamma-families generated in nucleon-nucleus (NA) and pion-nucleus (pi A) interactions
[HE-3.7-2] N85-35961
The muon content of gamma-ray showers
[HE-4.5-7] N85-36031
Fast scintillation counter preamplifier for the observation of Linsley effect
[HE-4.7-9] N85-36060
A mini-array for large air showers
[HE-4.7-10] N85-36061
A note on some statistical properties of rise time parameters used in muon arrival time measurements
[HE-4.7-12] N85-36062

PARTICLE DENSITY (CONCENTRATION)

Hadrons registration in emulsion chamber with carbon block
[HE-3.7-3] N85-35962
Peculiarities of gamma-quanta distribution at 20 TeV energy
[HE-3.7-10] N85-35967
Core structure of EAS in 10(15) to 10(17) eV
N85-35989
Particle distributions in approximately 10(14) 10(16) eV air shower cores at sea level N85-35990
Monte Carlo simulations of electron lateral distributions in the core region of 10(13) - 10(16) eV air showers
N85-35992
Comparison of simulation results with sea-level experimental data on 10(14) - 10(16) air shower cores
N85-35993
A new study of shower age distribution in near vertical showers by EAS air shower array N85-35996
A new study of muons in air showers by NBU air shower array N85-35997
Lateral distribution of electrons of air showers
N85-35998
Detailed studies of the electron lateral distribution in extensive air showers with energies around 10(16) eV
N85-35999
Measurement of energy muons in EAS at energy region larger thean 10(17) eV
[HE-4.3-8] N85-36002
Muon fluctuation studies of EAS 10(17) eV
[HE-4.3-9] N85-36003
Measurement of shower electrons and muons using a small air shower array
[HE-4.3-11] N85-36005
The system of EAS time analysis
[HE-4.4-10] N85-36018
Properties of 10 (18)-10 (19)eV EAS at far core distance
[HE-4.7-3] N85-36054
The thickness of the shower disc as observed in showers produced by primaries above 10 (19)eV
[HE-4.7-6] N85-36057
Expected rates with mini-arrays for air showers
[HE-4.7-8] N85-36059
Thickness of the particle swarm in cosmic ray air showers
[HE-4.7-14] N85-36064
Progress report on a new search for free e/3 quarks in the cores of 10(15) - 10(16) eV air showers
[HE-6.2-15] N85-36151

PARTICLE DIFFUSION

Calculation of the diffusion of light by aerosols: Description of the MIELOR software and results obtained
[REPT-80] N85-35638
Atmospheric muons and neutrinos, and the neutrino-induced muon flux underground
[HE-5.4-7] N85-36118

PARTICLE EMISSION

Physical meaning of the multiplicities of emitted nucleons in hadron-nucleus collisions N85-35877
How are particle production, nucleon emission and target fragment evaporation processes interrelated in hadron-nucleus collisions? N85-35878
Experimental evidence of the decrease of kinetic energy of hadrons in passing through atomic nuclei
N85-35880
Energy-range relations for hadrons in nuclear matter
N85-35881
The model of independent particles emission in the multiparticle production theory
[HE-3.2-10] N85-35918
A study of atmospheric neutrinos with the IMB detector
[HE-5.3-7] N85-36101
Study of photonuclear muon interactions at Baksan underground scintillation telescope
[HE-5.4-10] N85-36122
Collimated groups of particles as possible manifestation of heavy meson production
[HE-5.4-14] N85-36124
Limits on monopole fluxes from KFG experiment
[HE-6.1-6] N85-36132
An experiment to detect gut monopoles
[HE-6.1-7] N85-36133
Construction of the Soudan 2 detector
[HE-6.2-5] N85-36141
Nucleon decay and atmospheric neutrinos in the Mont Blanc experiment
[HE-6.2-8] N85-36142

PARTICLE ENERGY

The model of independent particles emission in the multiparticle production theory
[HE-3.2-10] N85-35918
The multiplicity and the spectra of secondaries correlated with the leading particle energy
[HE-3.2-11] N85-35919

PARTICLE FLUX DENSITY

A mini-array for large air showers
[HE-4.7-10] N85-36061
A note on some statistical properties of rise time parameters used in muon arrival time measurements
[HE-4.7-12] N85-36062
Study of the time-differentiated particle flux density at various distances from EAS axis
[HE-4.7-15] N85-36065
The capability of the existing network of installations for detecting the antineutrino burst from collapsing stars
[HE-5.3-13] N85-36107

PARTICLE INTERACTIONS

Detector requirements for intensity interferometry measurements N85-35709
A holographic streamer chamber for relativistic nucleus-nucleus collision experiments N85-35710
Fractional charge resolution in music N85-35712
Neutrino production of like sign dimuons
[DE85-013594] N85-35741
High energy physics at Tufts University
[DOE/ER-40085/7] N85-35744
Studies of relativistic heavy ion collisions
[DE85-014686] N85-35745
Resonance localization in tokamaks excited with ICRF waves
[DE85-014559] N85-35791
Some nuclear data needs in astrophysics
[DE85-012916] N85-35842
Nineteenth International Cosmic Ray Conference. HE Sessions, volume 6
[NASA-CP-2376-VOL-6] N85-35848
On total cross sections and slopes at superhigh energies
[HE-1.1-4] N85-35852
Determination of the cross section of the proton, pion and neutron inelastic interaction with lead and carbon nuclei at 0.5 - 5.0 TeV energies (PION experiment)
[HE-1.1-5] N85-35853
Measurement of interaction cross section of cosmic ray Fe nuclei (E4 GeV/N) with Al target
[HE-1.1-7] N85-35855
QCD-motivated description of very high energy particle interactions
[HE-1.2-2] N85-35861
Empirical description of the hadron-hadron and hadron-nucleus interaction at the accelerator energy range
[HE-1.2-4] N85-35862
Low P sub T hadron-nucleus interactions
[HE-1.2-7] N85-35865
Angular distribution and multiplicity of backward hadrons in hFe interactions at 0.5-5.0 TeV energies (PION Experiment)
[HE-1.2-8] N85-35866
A test of the Feynman scaling in the fragmentation region
[HE-1.2-9] N85-35867
A unification of the interactions and the diffractive processes N85-35870
Propagation of cosmic rays through the atmosphere in the quark-gluon strings model N85-35873
Experimental evidence of the decrease of kinetic energy of hadrons in passing through atomic nuclei
N85-35880
The phi-meson and Chiral-mass-meson production in heavy-ion collisions as potential probes of quark-gluon-plasma and Chiral symmetry transitions
N85-35884
Ringlike inelastic events in cosmic rays and accelerators N85-35887
Few-particles generation channels in inelastic hadron-nuclear interactions at energy approximately equals 400 GeV
[HE-3.2-9] N85-35917
The multiplicity and the spectra of secondaries correlated with the leading particle energy
[HE-3.2-11] N85-35919
Characteristics of anomalously high multiplicity cosmic ray interactions
[HE-3.3-1] N85-35920
Analytical-numerical methods of calculations of energy and three-dimensional particle distributions in electromagnetic cascades
[HE-3.5-13] N85-35950
Relation between gamma-ray family and EAS core: Monte-Carlo simulation of EAS core
[HE-3.6-7] N85-35955
A study of gamma-families generated in nucleon-nucleus (NA) and pion-nucleus (pi A) interactions
[HE-3.7-2] N85-35961
High energy hadrons in extensive air showers
N85-35976
Electromagnetic and muonic structure of showers initiated by gamma-rays and by hadrons
[HE-4.5-6] N85-36030
A facility for investigation of multiple hadrons at cosmic-ray energies
[HE-4.6-8] N85-36045
Arrival time distributions of electrons in air showers with primary energies above 10 (18)eV observed at 900m above sea level
[HE-4.7-5] N85-36056
Methods for roof-top mini-arrays
[HE-4.7-7] N85-36058
Photo nuclear energy loss term for muon-nucleus interactions based on xi scaling model of QCD
[HE-5.2-17] N85-36093
The spectrum of neutrons at 60 hg m(-2)
[HE-5.2-20] N85-36096
Limits on deeply penetrating particles in the 10(17) eV cosmic ray flux
[HE-5.3-1] N85-36098
A study of atmospheric neutrinos with the IMB detector
[HE-5.3-7] N85-36101
Atmospheric neutrinos observed in underground detectors
[HE-5.3-8] N85-36102
High energy neutrino astronomy with MACRO
[HE-5.3-12] N85-36106
Characteristics of slow particles emitted in the charged current interactions of neutrinos with emulsion nuclei
[HE-5.3-22] N85-36113
Nucleon decay and atmospheric neutrinos in the Mont Blanc experiment
[HE-6.2-6] N85-36142
Energetic delayed hadrons in large air showers observed at 5200m above sea level
[HE-6.2-9] N85-36145
Search for long-lived massive particles in extensive air showers
[HE-6.2-10] N85-36146
Search for anomalons using plastic nuclear track detectors
[HE-6.2-12] N85-36148
Observation of genetic relation among new phenomena Geminion, Chiron and mini-Centauro
[HE-6.2-16] N85-36152
Tien-Shan effect and charmed particles
[HE-6.2-17] N85-36153
Muon and neutrino fluxes
[HE-6.2-18] N85-36154

PARTICLE LADEN JETS

Jets in air-jet family
[HE-3.2-1] N85-35912
Search for anomalous C-jets in Chacaltaya emulsion chamber experiment
[HE-3.2-5] N85-35913
Exotic interactions among C-jets and Pb-jets
[HE-3.2-6] N85-35914

PARTICLE MOTION

Two-dimensional quasineutral description of particles and fields above discrete auroral arcs
[NASA-CR-176170] N85-35517
Peculiarities of gamma-quanta distribution at 20 TeV energy
[HE-3.7-10] N85-35967

PARTICLE PRODUCTION

High energy physics at Tufts University
[DOE/ER-40085/7] N85-35744
Studies of relativistic heavy ion collisions
[DE85-014686] N85-35745
Nineteenth International Cosmic Ray Conference. HE Sessions, volume 6
[NASA-CP-2376-VOL-6] N85-35848

QCD-motivated description of very high energy particle interactions
[HE-1.2-2] N85-35861
Multiplicity distributions in interaction models used for cascade simulations
[HE-1.2-5] N85-35863
Is the inelastic charge-exchange contribution constant at the large X and superhigh energies? Qaut 01Kuchin, I. A. N85-35871
General consequences of the violated Feynman scaling N85-35872
How are particle production, nucleon emission and target fragment evaporation processes interrelated in hadron-nucleus collisions? N85-35878
Experimental study of the space-time development of the particle production process in hadron-nucleon collisions, using massive target nucleus as a detector N85-35879
Energy-range relations for hadrons in nuclear matter N85-35881
Scattering and stopping of hadrons in nuclear matter N85-35882
Measurements of hadron mean free path for the particle-producing collisions in nuclear matter N85-35883
The phi-meson and Chiral-mass-meson production in heavy-ion collisions as potential probes of quark-gluon-plasma and Chiral symmetry transitions N85-35884
Heavy flavours production in quark-gluon plasma formed in high energy nuclear reactions N85-35886
Forward particle production in inelastic Ne-22 inteVractions in emulsion at 4.1 A Ge/c
[HE-1.4-7] N85-35895
High energy gamma-rays and hadrons at Mount Fuji
[HE-3.1-3] N85-35903
Some characteristic cosmic ray events and an attempt at their explanation
[HE-3.1-8] N85-35906
The model of independent particles emission in the multiparticle production theory
[HE-3.2-10] N85-35918
Experimental basis for the models of cascade propagation in atmosphere
[HE-3.6-6] N85-35954
Atmospheric neutrinos observed in underground detectors
[HE-5.3-8] N85-36102
Collimated groups of particles as possible manifestation of heavy meson production
[HE-5.4-14] N85-36124

PARTICLE SIZE DISTRIBUTION
Size distributions of air showers accompanied with high energy gamma ray bundles observed at Mt. Chacaltaya
[HE-3.3-9] N85-35927
Comparison of absolute intensity between EAS with gamma-families and general EAS at Mount Norikura
[HE-3.3-11] N85-35929
Photo nuclear energy loss term for muon-nucleus interactions based on xi scaling model of QCD
[HE-5.2-17] N85-36093

PARTICLE SPIN
Cooling high intensity atomic hydrogen beams to liquid helium temperatures
[DE85-012515] N85-35718

PARTICLE TELESCOPES
An underground cosmic ray muon telescope for observation of cosmic ray anisotropy N85-36037

PARTICLE TRACKS
Elemental tracers of source regions of contaminants in precipitation
[DE85-012858] N85-35499
Calculation of heavy-ion tracks in liquid water
[DE85-012101] N85-35725
Experimental basis for the models of cascade propagation in atmosphere
[HE-3.6-6] N85-35954
Search for supermassive magnetic monopoles using mica crystals
[HE-6.1-8] N85-36134
Spatial distribution read-out system for thermoluminescence sheets
[HE-7.1-7] N85-36151

PARTICLE TRAJECTORIES
Strategic defense initiative
[DE85-012778] N85-35735
The structure of EAS at E 0.1 EeV
[HE-4.4-2] N85-36012
Transition effect of air shower particles in plastic scintillators
[HE-4.4-9] N85-36017
The Nagoya cosmic-ray muon spectrometer 3, part 4: Track reconstruction method
[HE-5.2-5] N85-36083
Comments on the measurements of multiple muon phenomena
[HE-5.2-13] N85-36089

PARTICLES
Search for proton decay in the Frejus experiment
[HE-6.2-2] N85-36138
Results on nucleon life-time from the Kolar gold field experiment
[HE-6.2-3] N85-36139
Data acquisition system for phase-2 KGF proton decay experiment
[HE-6.2-4] N85-36140
Search for long-lived massive particles in extensive air showers
[HE-6.2-10] N85-36146

PARTICULATE SAMPLING
A study of the control of particulate emissions from turbine engine test cells N85-35205

PASCAL (PROGRAMMING LANGUAGE)
A quickly tested Pascal random number generator for microcomputers
[AD-A156059] N85-35633

PATENT POLICY
NASA patent abstracts bibliography, a continuing bibliography. Section 2: Indexes (supplement 27)
[NASA-SP-7039(27)-SECTION-2] N85-35820

PATTERN RECOGNITION
Artificial intelligence in Ada (trademark): Pattern-directed processing
[AD-A156230] N85-35671
A holographic streamer chamber for relativistic nucleus-nucleus collision experiments N85-35710

PAYLOAD CONTROL
A normal incidence X-ray telescope sounding rocket payload
[NASA-CR-176169] N85-35749

PAYLOADS
An automated technique for encasing specific payloads with low-drag fairings N85-35183

PENETRATION
Experimental data for characterizing perforating impacts: Fragmentation processes
[AD-A156370] N85-35427

PENNSYLVANIA
Remote sensing of hydrologic transport processes using spot simulation data
[DE85-012412] N85-35467

PERFORMANCE PREDICTION
Assessment of metal heating technologies for ferrous forging: A pilot study of the form value of natural gas
[PB85-204394] N85-35314
Wind turbine noise: Prediction tools and design parameter dependence N85-35477

PERFORMANCE TESTS
Planetary-gear-support bearing test rig design
[NASA-CR-174927] N85-35185
Development of NATOPS (Naval Air Training and Operating Procedure Standardization) performance software for the H-46D helicopter
[AD-A156089] N85-35190
Dissected motors-propellants motor number STM-012. Phase 15: Surveillance report, stage 1
[AD-A156088] N85-35226
Solid state high power amplifier for driving the SLC injector klystron
[DE85-013063] N85-35356
Dental multi-purpose slowspeed handpieces test and evaluation
[AD-A155764] N85-35606
Four stage HELIA experiment
[DE85-012026] N85-35768

PERIODIC FUNCTIONS
On the convergence of an iterative formulation of the electromagnetic scattering from an infinite grating of thin wires N85-35319

PERISCOPES
Immediate visibility after red and white adaptation
[AD-A156271] N85-35616

PERMEABILITY
Development and evaluation of sulfonated polysulfone membranes for the zinc-ferricyanide battery
[DE85-009104] N85-35357

PERSONAL COMPUTERS
Benchmark evaluation of PC simscript
[AD-A156133] N85-35651

PERSONALITY
The relationship between personality and performance N85-35600

PERSONNEL
U.S. Civil airmen statistics for calendar year 1984
[AD-A156326] N85-35153
Data processing professionals and DP application users' perceptions and expectations of operational roles of persons working in a DP/application user interface group N85-35821

PERTURBATION
DEPTH-CHARGE static and time-dependent perturbation/sensitivity system for nuclear reactor core analysis, revision 1
[DE85-013103] N85-35659
Acoustic resonances in cylinder bundles oscillating in a compressibile fluid
[DE85-004066] N85-35699

PERTURBATION THEORY
Identification and control of structures in space
[NASA-CR-176175] N85-35214
Perturbation-iteration theory for analyzing microwave striplines
[NASA-CR-176189] N85-35321
Two-point closure study of covariance budgets for turbulent Rayleigh-Benard convection
[PB85-189108] N85-35568
Multiple vacancy production by high energy heavy ions
[DE85-004428] N85-35805

PETN
Friction, impact, and electrostatic discharge sensitivities of energetic materials
[DE85-013321] N85-35309

PETROGRAPHY
Chemistry of ore-forming fluids N85-35436

PETROLEUM PRODUCTS
Biodegradation of jet fuel by aquatic microbial communities
[PB85-191971] N85-35311

PHASE DIAGRAMS
Cluster variation study of coherent ordering in FCC and BCC solid solutions
[AD-A156039] N85-35280

PHASE LOCKED SYSTEMS
Nonlinear digital phase-locked loops with application to Loran-C receivers N85-35178

PHASE MODULATION
A new description of combined trellis coding with asymmetric modulation
[NASA-CR-176197] N85-35323

PHASE SHIFT
Solid state high power amplifier for driving the SLC injector klystron
[DE85-013063] N85-35356
Analysis of two-parameter constant background born inversion for acoustic synthetic data
[AD-A156394] N85-35698

PHASE SHIFT KEYING
A new description of combined trellis coding with asymmetric modulation
[NASA-CR-176197] N85-35323
DMSK: A practical 2400-bps receiver for the mobile satellite service: An MSAT-X Report
[NASA-CR-176194] N85-35324
Necessary bandwidth and spectral properties of digital modulation
[PB85-185387] N85-35340

PHASE TRANSFORMATIONS
Transient three-phase three-component systems. Part 1: Formulation of the system of differential equations
[DE85-013267] N85-35384

PHASE-SPACE INTEGRAL
Phase space factors in multiparticle processes N85-35888

PHENOLS
SRB attach ring phenolic TPS fishtail seal evaluation tests
[NASA-CR-170887] N85-35407

PHOSPHATES
Applications of the mineral resources data system and the international strategic minerals inventory in mineral-resource assessments by region and commodity N85-35451

PHOSPHORIC ACID
System for the continuous generation of phosphorous aerosols from red phosphorus-butyl rubber
[DE85-013527] N85-35232

PHOSPHORUS
Marine phosphorite deposits model for exploration, with emphasis on deposits in the US Atlantic coastal plain N85-35439

PHOTOABSORPTION
High-resolution spectroscopy and dynamics of multiphoton processes in atoms and molecules
[AD-A155862] N85-35714

PHOTOCATHODES
On the possibilities of large-scale radio and fiber optics detectors in cosmic rays
[HE-4.6-2] N85-36039

PHOTOCHEMICAL REACTIONS
The photodissociation of acetylene at 193.3 NM
[AD-A155775] N85-35255
Vectorial electron transfer on designed surfaces
[PB85-204600] N85-35263

Studies in photochemical smog chemistry. 1: Atmospheric chemistry of toulene. 2: Analysis of chemical reaction mechanisms for photochemical smog
N85-35497

PHOTOCONDUCTIVITY
Electron irradiation of N type cadmium telluride
[AD-A156117] N85-35801

PHOTOCONDUCTORS
Photoconductive pulse power switches: A review
[DE85-014125] N85-35360

PHOTODECOMPOSITION
The detection and study of molecular species using time resolved laser spectroscopy
[AD-A155910] N85-35256

PHOTODIODES
Application of photodiodes to the detection of electromagnetic bursts N85-35988

PHOTODISSOCIATION
The photodissociation of acetylene at 193.3 NM
[AD-A155775] N85-35255
High-resolution spectroscopy and dynamics of multiphoton processes in atoms and molecules
[AD-A155862] N85-35714

PHOTOELECTRIC EMISSION
Noble metals as incipient transition metals
[DE85-013283] N85-35286
Exit channels of autoionization resonances in atoms
[DE85-012299] N85-35726
Ionic crystals
[DE85-009482] N85-35809

PHOTOELECTRIC MATERIALS
Practical aspects of photovoltaic technology, applications and cost (revised)
[NASA-CR-174963] N85-35472

PHOTOELECTRON SPECTROSCOPY
Heats of formation of gas phase organosulfur molecules, radicals and ions measured by PEPICO and application of (17)O and (33)S NMR spectroscopy to structure determination of organosulfur compounds
[DE85-010558] N85-35229

PHOTOGEOLOGY
Geology and geomorphology of the Roraima group, southeastern Venezuela N85-35511

PHOTOGRAMMETRY
Parametric stability of analytical close-range photogrammetry N85-35461
Evaluation: Close-range photogrammetry for slope inventory and monitoring
[PB85-192755] N85-35470

PHOTOGRAPHIC FILM
High sensitive X-ray films to detect electron showers in 100 GeV region
[HE-3.1-13] N85-35911
X-ray film chamber with carbon target of Tien-Shan complex array N85-35915
The Nagoya cosmic-ray muon spectrometer 3, part 3: Automatic film scanning equipment
[HE-5.2-4] N85-36082

PHOTOIONIZATION
Heats of formation of gas phase organosulfur molecules, radicals and ions measured by PEPICO and application of (17)O and (33)S NMR spectroscopy to structure determination of organosulfur compounds
[DE85-010558] N85-35229
Dissociative and double photoionization cross sections of NO from threshold to 120 A
[NASA-CR-176185] N85-35713
High-resolution spectroscopy and dynamics of multiphoton processes in atoms and molecules
[AD-A155862] N85-35714
Exit channels of autoionization resonances in atoms
[DE85-012299] N85-35726

PHOTOMETERS
Hadrons registration in emulsion chamber with carbon block
[HE-3.7-3] N85-35962

PHOTOMETRY
A cosmic ray super high multicore family event. 1: Experiment and general features
[HE-3.4-1] N85-35930

PHOTOMULTIPLIER TUBES
Air fluorescence detection of large air showers below the horizon
[HE-4.6-6] N85-36043
The structure of the shower disk observed at Mt. Norikura
[HE-4.7-1] N85-36052
Structure of air shower disc near the core
[HE-4.7-2] N85-36053
Arrival time distributions of electrons in air showers with primary energies above 10 (18)eV observed at 900m above sea level
[HE-4.7-5] N85-36056
Methods for roof-top mini-arrays
[HE-4.7-7] N85-36058
Fast scintillation counter preamplifier for the observation of Linsley effect
[HE-4.7-9] N85-36060
A mini-array for large air showers
[HE-4.7-10] N85-36061
Detection threshold energy of high energy cascade showers using thermoluminescence PTFE-sheet and hot-gas reader
[HE-7.1-5] N85-36159

PHOTON BEAMS
Breeding new light into old machines (and new)
[DE85-013055] N85-35763

PHOTON-ELECTRON INTERACTION
A new method of differential structural analysis of gamma-family basic parameters
[HE-3.6-3] N85-35952
Samarkand complex setup for investigation of cosmic ray variation in the energy range of 7 10 (9) - 10 (15) eV
[HE-4.6-14] N85-36050

PHOTONS
Generation of stimulated emission in the soft X-ray range by nonlinear processes with excimer lasers
[DE85-012465] N85-35403
Status of the zeta(8.3)
[DE85-013070] N85-35724
Calibration of a high-level photon irradiation
[DE85-013044] N85-35738
Surface discharges as intense photon sources in the extreme ultraviolet
[DE85-012593] N85-35782
Circumstellar shells of late-type stars: A study at millimeter and infrared wavelengths N85-35836
Nucleon-nucleus interactions from JACEE
N85-35869
An experimental study of correlations in the development of the electron-photon cascades
[HE-3.5-10] N85-35947
Electrons, muons and hadrons in extensive air showers and how do they depend on nuclear interaction model, part 1 N85-35972
The identification of gamma ray induced EAS
[HE-4.5-1] N85-36026
Electromagnetic and muonic structure of showers initiated by gamma-rays and by hadrons
[HE-4.5-6] N85-36030
The hump in the Cerenkov lateral distribution of gamma ray showers
[HE-4.5-9] N85-36032
A three-dimensional Monte Carlo calculation of the photon initiated showers and Kiel result
[HE-4.5-13] N85-36035
Study of photonuclear muon interactions at Baksan underground scintillation telescope
[HE-5.4-10] N85-36122

PHOTONUCLEAR REACTIONS
Longitudinal development of muons in large air showers studies from the arrival time distributions measured at 900m above sea level
[HE-4.7-4] N85-36055
Study of the time-differentiated particle flux density at various distances from EAS axis
[HE-4.7-15] N85-36065

PHOTOOXIDATION
Atmospheric nitrogen oxides: Their detection and chemistry
[PB85-193910] N85-35502

PHOTOPRODUCTION
Muons in gamma showers
[HE-4.5-3] N85-36027

PHOTOSENSITIVITY
High sensitive X-ray films to detect electron showers in 100 GeV region
[HE-3.1-13] N85-35911

PHOTOSPHERE
The HEAO-2 Guest Investigator Program: Non-linear growth of instabilities in line-driven stellar winds
[NASA-CR-176168] N85-35840

PHOTOTHERMAL CONVERSION
Characterization of the optical and thermal properties of matter by photothermal techniques
[DE85-012607] N85-35260

PHOTOVOLTAIC CELLS
Practical aspects of photovoltaic technology, applications and cost (revised)
[NASA-CR-174963] N85-35472
Monolithic photovoltaic series array for an energy coupler
[BMFT-FB-T-85-023] N85-35496

PHOTOVOLTAIC CONVERSION
Photovoltaics technology program summary
[DE85-013098] N85-35493
Design and construction of an advanced power conditioning subsystem for small photovoltaic applications
[DE85-013940] N85-35495

PHYSICAL CHEMISTRY
Chemistry division report
[DE85-010586] N85-35228

PHYSICAL FITNESS
An analysis of aerobic capacity in a large United States population
[AD-A156200] N85-35614
Relaxation techniques
[AD-A156248] N85-35621

PHYSIOCHEMISTRY
Tests on zirconium nitride costings applied to SW 18 steel using the chemical vapor deposition method
N85-35271

PHYSIOLOGICAL EFFECTS
Proceedings of a Scientic Meeting on the Occasion of the Inauguration of New Buildings for the DFVLR Institute for Aerospace Medicine
[ESA-TT-857] N85-35595
The deep diving simulator TITAN: Physiological problems associated with staying in great depths of water N85-35604
Genetic and physiological control of protective antigen synthesis by bacillus anthracis
[AD-A156324] N85-35617

PHYSIOLOGICAL RESPONSES
Cardiovascular responses to orthostatism and weightlessness N85-35601
Physiological responses to unvarying (steady) and 2-2-1 shifts: Miami International Flight Service Station
[AD-A155751] N85-35619

PIEZOELECTRIC CERAMICS
Materials used by industry for the production of piezoelectric transducers. The state of the art of research work performed in the field of PZT ceramics and ferroelectric polymers
[ISL-CO-211/84] N85-35344
Piezoelectric transducers, state of research
N85-35345
Conduction and aging of piezoelectric PZT ceramics
N85-35348

PIEZOELECTRIC CRYSTALS
Materials used by industry for the production of piezoelectric transducers. The state of the art of research work performed in the field of PZT ceramics and ferroelectric polymers
[ISL-CO-211/84] N85-35344

PIEZOELECTRIC TRANSDUCERS
Materials used by industry for the production of piezoelectric transducers. The state of the art of research work performed in the field of PZT ceramics and ferroelectric polymers
[ISL-CO-211/84] N85-35344
Piezoelectric transducers, state of research
N85-35345
Ferroelectric homopolymer PVF2 and P (VDF-TrFe) copolymers N85-35347

PILOT TRAINING
RAFTS: A T-38 replacement for the 21st century
[AD-A156103] N85-35191

PILOTS (PERSONNEL)
U.S. Civil airmen statistics for calendar year 1984
[AD-A156326] N85-35153
International flight planning handbook
[AD-A156330] N85-35177

PINS
Verification of the SRB motor case pin retainer band tips
[NASA-CR-170682] N85-35220

PION BEAMS
Study of hadron bundles observed in Chacaltaya two-story emulsion chamber
[HE-3.3-4] N85-35922
Experimental basis for the models of cascade propagation in atmosphere
[HE-3.6-6] N85-35954

PIONS
Determination of the cross section of the proton, pion and neutron inelastic interaction with lead and carbon nuclei at 0.5 - 5.0 TeV energies (PION experiment)
[HE-1.1-5] N85-35853
Angular distribution and multiplicity of backward hadrons in hFe interactions at 0.5-5.0 TeV energies (PION Experiment)
[HE-1.2-8] N85-35866
Anuglar distribution of shower particles produced in the collisions of 20-GeV/c and 300-GeV negative pions with emulsion nuclei N85-35868
Is the inelastic charge-exchange contribution constant at the large X and superhigh energies? Qaut 01Kuchin, I. A. N85-35871
Energy-range relations for hadrons in nuclear matter
N85-35881
Measurements of hadron mean free path for the particle-producing collisions in nuclear matter
N85-35883

On mini-cluster observed by Chacaltaya emulsion chamber experiment
[HE-3.6-12] N85-35959
A study of gamma-families generated in nucleon-nucleus (NA) and pion-nucleus (pi A) interactions
[HE-3.7-2] N85-35961
Study of photonuclear muon interactions at Baksan underground scintillation telescope
[HE-5.4-10] N85-36122
Observation of genetic relation among new phenomena Geminion, Chiron and mini-Centauro
[HE-6.2-16] N85-36152
Tien-Shan effect and charmed particles
[HE-6.2-17] N85-36153

PIPES (TUBES)
Stress-intensity factors for circumferential surface cracks in pipes and rods under tension and bending loads
[NASA-TM-87594] N85-35424
Evaluation of the crack plane equilibrium model for predicting plastic fractures
[DE85-005558] N85-35431

PITTING
Pitting corrosion of ferrous alloys
[AERE-R-11490] N85-35273

PLANAR STRUCTURES
A planar version of a 4.0 gigahertz reactively steered adaptive array
[AD-A156029] N85-35330

PLANE WAVES
Transient analysis of electromagnetic reflection from dispersive materials
[PB85-200186] N85-35753

PLANETARY BOUNDARY LAYER
Application of a turbulent closure model to the parameterization of the vertical diffusion of heat, momentum, and humidity in the ECMWF model — European Center for Medium Term Weather Forecasting (ECMWF)
[MITT-41] N85-35387

PLANETARY EVOLUTION
Thermal evolution of coastal California with implications for hydrocarbon maturation N85-35509
The ionization structure of planetary nebulae. Part 4: NGC 7662
[NASA-CR-176151] N85-35844

PLANETARY NEBULAE
The ionization structure of planetary nebulae. Part 4: NGC 7662
[NASA-CR-176151] N85-35844

PLANETARY STRUCTURE
Applications of the Galerkin formalism in the coupling of the earth's free oscillations N85-35514

PLANKTON
Seasonal variability and spatial non-uniformity of bioluminescence in the Mediterranean Sea
[DRIC-T-7545] N85-35572

PLANNING
Quality assurance considerations for the implementation of a pulsed power R and D project
[DE85-012357] N85-35720

PLANTS (BOTANY)
Mineral deposit models: Theory and practice N85-35448
The measurement of nitrogen oxide (NO, NO2) exchange over plant/soil surfaces
[CSIRO-DAR-TP-8] N85-35587

PLASMA ACCELERATION
High energy plasma accelerators
[DE85-013121] N85-35760

PLASMA ACCELERATORS
High energy plasma accelerators
[DE85-013121] N85-35760

PLASMA COMPRESSION
Numerical studies of high current beam compression in heavy ion fusion
[DE85-011874] N85-35783

PLASMA CONTROL
Limiter
[DE85-011620] N85-35736
Confinement and heating of high beta plasmas with emphasis on compact toroids
[DE85-011459] N85-35761
Analysis of a pulsed power system containing rotating machine
[DE85-014128] N85-35786
Diagnostics for Pioneer 1 imploding plasma experiments
[DE85-014120] N85-35787

PLASMA DENSITY
Current interruption by density depression
[DE85-013120] N85-35846

PLASMA DIAGNOSTICS
Diagnostics for Pioneer 1 imploding plasma experiments
[DE85-014120] N85-35787

PLASMA DIFFUSION
Long-time asymptotics of a system for plasma diffusion
[NASA-CR-177947] N85-35375

PLASMA FLUX MEASUREMENT
Confinement and heating of high beta plasmas with emphasis on compact toroids
[DE85-011459] N85-35761

PLASMA HEATING
Scale separation closure and Alfven wave turbulence
[DE85-013124] N85-35385
Confinement and heating of high beta plasmas with emphasis on compact toroids
[DE85-011459] N85-35761
Proposed FRX-D experiment
[DE85-012766] N85-35778

PLASMA INTERACTIONS
Beam potential measurement of an intense H(-) beam by use of the emissive probe technique
[DE85-012671] N85-35762

PLASMA JETS
Jets in air-jet family
[HE-3.2-1] N85-35912
Search for anomalous C-jets in Chacaltaya emulsion chamber experiment
[HE-3.2-5] N85-35913

PLASMA OSCILLATIONS
High energy plasma accelerators
[DE85-013121] N85-35760

PLASMA RADIATION
Beam potential measurement of an intense H(-) beam by use of the emissive probe technique
[DE85-012671] N85-35762

PLASMA SPRAYING
Thermal barrier coating system
[NASA-CASE-LEW-14057-1] N85-35233

PLASMAS (PHYSICS)
Very high energy probes of the quark-gluon plasma N85-35708
Kinetic loss experiments on Mite
[DE85-012826] N85-35780
The phi-meson and Chiral-mass-meson production in heavy-ion collisions as potential probes of quark-gluon-plasma and Chiral symmetry transitions N85-35884
Heavy flavours production in quark-gluon plasma formed in high energy nuclear reactions N85-35886
The maximum depth of shower with E sub 0 larger than 10(17) eV on average characteristics of EAS different components N85-35981

PLASTIC DEFORMATION
Prediction of plasticity characteristics for three-dimensional fracture specimens comparison with experiment
[AD-A156425] N85-35430

PLASTICIZERS
A new drawing technique for nylon 6 by reversible plasticization with iodine
[AD-A156272] N85-35803

PLATELETS
The effect of +Gx acceleration on platelet activation as determined by plasma platelet factor 4 levels
[AD-A155881] N85-35608

PLATES (TECTONICS)
Thermal evolution of coastal California with implications for hydrocarbon maturation N85-35509
A dynamic model of Venus's gravity field
[NASA-CR-176173] N85-35845

PLATINUM
Characterization of catalysts with metal-support effects and of the species adsorbed on their surfaces
[DE85-012254] N85-35394
Applications of the mineral resources data system and the international strategic minerals inventory in mineral-resource assessments by region and commodity N85-35451

PLUMES
A dynamic model of Venus's gravity field
[NASA-CR-176173] N85-35845

PLUTONIUM
Measurement control for plutonium isotopic measurements using gamma-ray spectrometry
[DE85-013394] N85-35397

POINT SOURCES
Expected rates with mini-arrays for air showers
[HE-4.7-8] N85-36059
A large area cosmic muon detector located at Ohya stone mine
[HE-5.1-7] N85-36072
A study of atmospheric neutrinos with the IMB detector
[HE-5.3-7] N85-36101

POLAND
Meteorological measurements with motor gliders in Poland N85-35555

POLAR GASES
Equation of state study for polar fluids
[PB85-204345] N85-35262

POLAR ORBITS
Space Station Polar Platform: Integrating research and operational missions
[PB85-195279] N85-35218

POLAR REGIONS
The NORDA/FNOC (Naval Ocean Research and Development Activity's/Fleet Numerical Oceanography Center) Polar Ice Prediction System (PIPS)-Arctic: A technical description
[AD-A156332] N85-35577

POLARIMETRY
The nature and geometry of infrared reflection nebulae N85-35835

POLARIZATION (CHARGE SEPARATION)
Equation of state study for polar fluids
[PB85-204345] N85-35262

POLARIZATION (WAVES)
Transient analysis of electromagnetic reflection from dispersive materials
[PB85-200186] N85-35753

POLARIZERS
Polarization diversity addition to the 10 centimeter Doppler weather radar
[AD-A156062] N85-35334

POLICIES
A guide for new environmental coordinators
[AD-A156327] N85-35498

POLLUTION CONTROL
A guide for new environmental coordinators
[AD-A156327] N85-35498
Review of US NOx abatement technology
[PB85-193522] N85-35501

POLYACETYLENE
Electrically conductive doped block copolymer of polyacetylene and polyisoprene
[DE85-006500] N85-35301

POLYAMIDE RESINS
Determination of the viscosity number of thermoplastics in dilute solution; polyamides (PA)
[NASA-TM-77673] N85-35296

POLYCRYSTALS
Noise in sodium beta alumina crystals
[AD-A156025] N85-35798

POLYETHYLENES
Structure and properties of polyethylene films used in heavy lift balloons
[NASA-CR-176227] N85-35306

POLYGONS
Reachable grasps on a polygon: The convex rope algorithm
[AD-A155913] N85-35647

POLYMERIC FILMS
Structure and properties of polyethylene films used in heavy lift balloons
[NASA-CR-176227] N85-35306

POLYMERS
Development of an NBS (National Bureau of Standards) polymer gage for dynamic soil stress measurement
[PB85-208494] N85-35526

POLYTETRAFLUOROETHYLENE
Detection threshold energy of high energy cascade showers using thermoluminescence PTFE-sheet and hot-gas reader
[HE-7.1-5] N85-36159

POLYVINYL FLUORIDE
Ferroelectric homopolymer PVF2 and P (VDF-TrFe) copolymers N85-35347

PONDS
Solar pond technology for Navy applications
[AD-A155877] N85-35488

POROSITY
The character of observed porosity and its possible effects on rolling contact fatigue life of M-50 steel
[AD-A155930] N85-35279
Development and evaluation of sulfonated polysulfone membranes for the zinc-ferricyanide battery
[DE85-009104] N85-35357
Simplified procedures for the evaluation of settlements in sands due to earthquake shaking
[PB85-197887] N85-35527

POROUS MATERIALS
Method of preparing thin porous sheets of ceramic material
[DE85-006399] N85-35300

POSITION (LOCATION)
Visual position determination for autonomous vehicle navigation
[AD-A156007] N85-35181
Development of position sensors for microcomputer-oriented sensor systems
[BMFT-FB-T-85-021] N85-35361

Materials and process development for microcomputer-compatible pressure, temperature, and position sensors
[BMFT-FB-T-85-024] N85-35399
Evaluation of nuclear detonation location capability under high attack scenario
[AD-A155761] N85-35729

POSITIONING
Time domain reflectometry for SLC BPM system
[DE85-012389] N85-35758

POSITRON ANNIHILATION
Forty-five years of e(+)e(-) annihilation physics: 1956 to 2001
[DE85-013052] N85-35723

POSITRONS
Pulsed-neutron-source models for the astrophysical s-process
[DE85-012927] N85-35740
Vacuum system for the Argonne 6 GeV synchrotron light source
[DE85-012286] N85-35773
Missing energies at pair creation
[HE-4.4-8] N85-36016

POTASSIUM
Thermodynamics of the corrosion of chromium in molten carbonates
[DE85-011407] N85-35282

POTASSIUM OXIDES
Improved oxygen sources for breathing apparatus
[NASA-TM-86671] N85-35623

POTASSIUM PERCHLORATES
Friction, impact, and electrostatic discharge sensitivities of energetic materials
[DE85-013321] N85-35309

POTENTIAL FLOW
Calculation of compressible flow about three-dimensional inlets with auxiliary inlets, slats and vanes by means of a panel method
[NASA-CR-174975] N85-35162

POWDER (PARTICLES)
Dynamic compaction of a monosized spherical tungsten powder
[DE85-014808] N85-35289
Computational methods for the explosive and impact compaction of powders
[AD-A156219] N85-35653

POWDER METALLURGY
Method for measuring surface activity of silicon nitride powder
[NASA-TM-77906] N85-35242
Oxidation resistant slurry coating for carbon-based materials
[NASA-CASE-LEW-13923-1] N85-35267

POWER CONDITIONING
Design and construction of an advanced power conditioning subsystem for small photovoltaic applications
[DE85-013940] N85-35495

POWER EFFICIENCY
Wingtip vortex propeller
[NASA-CASE-LAR-13019-1] N85-35194

POWER LINES
Injector losses on Mite
[DE85-012356] N85-35355
RFQ modeling computer program
[DE85-012665] N85-35661

POWER REACTORS
Transient three-phase three-component systems. Part 1: Formulation of the system of differential equations
[DE85-013267] N85-35384
DEPTH-CHARGE static and time-dependent perturbation/sensitivity system for nuclear reactor core analysis, revision 1
[DE85-013103] N85-35659
Applicability of 100kWe-class of space reactor power systems to NASA manned space station missions
[NASA-CR-174696] N85-35728

POWER SPECTRA
Pressure cross spectra in turbulent boundary layers in water
[AD-A156153] N85-35378
Noise in sodium beta alumina crystals
[AD-A156025] N85-35798

PREAMPLIFIERS
Fast scintillation counter preamplifier for the observation of Linsley effect
[HE-4.7-9] N85-36060
A mini-array for large air showers
[HE-4.7-10] N85-36061

PRECIPITATION HARDENING
The dynamic strain ageing of A533B class 1 nuclear pressure vessel steel
[AERE-R-11485] N85-35274

PRECISION
Analyzer, flight line
[AD-A155777] N85-35207

PREDICTION ANALYSIS TECHNIQUES
Cerenkov radiation from periodic electron bunches for finite emission length in air
[AD-A156156] N85-35352
Development and application of a unified viscoelastic constitutive model for the prediction of material response under thermomechanical loading N85-35420
Development of a mathematical model for predicting the percentage fatigue life increase resulting from shot peened components
[AD-A155774] N85-35425
Evaluation of the crack plane equilibrium model for predicting plastic fractures
[DE85-005558] N85-35431
Meteorological data from the OPTOMA (Ocean Prediction Through Observations, Modeling and Analysis) program OPTOMA 2, leg D2. 30 Jun. - 10 Jul. 1984
[AD-A156134] N85-35560
The NORDA/FNOC (Naval Ocean Research and Development Activity's/Fleet Numerical Oceanography Center) Polar Ice Prediction System (PIPS)-Arctic: A technical description
[AD-A156332] N85-35577
Models for assessing workload of aircrews on long distance flights N85-35599
SASSYS-1 computer code verification with EBR-2 test data
[DE85-012119] N85-35657
A comparison of multipath arrival structures observed in the presence of a surface duct with predictions obtained using classical ray techniques and the parabolic equation method
[AD-A156024] N85-35696

PREDICTIONS
System expectations for Pioneer 1 foil implosion experiments
[DE85-014129] N85-35359
Calculation of trajectories of detached wind turbine blades and prediction of site risk levels associated with failures of HAWT's N85-35475

PRELAUNCH PROBLEMS
Results of tests of K5NA and a revised formulation of EPDM/cork patch material in MSFC Hot Gas Facility
[NASA-CR-170890] N85-35238

PRESSURE DISTRIBUTION
Pressure cross spectra in turbulent boundary layers in water
[AD-A156153] N85-35378

PRESSURE GRADIENTS
Adverse pressure gradient and separating turbulent boundary-layer flows: The effect of disequilibrium in initial conditions N85-35155
Computer code calculations of the TMI-2 accident: Initial and boundary conditions
[DE85-012613] N85-35666

PRESSURE SENSORS
Materials and process development for microcomputer-compatible pressure, temperature, and position sensors
[BMFT-FB-T-85-024] N85-35399

PRESSURE SUITS
Simulation of high +Gz onset in the dynamic environment simulator
[AD-A155963] N85-35610

PRESSURE VESSELS
The dynamic strain ageing of A533B class 1 nuclear pressure vessel steel
[AERE-R-11485] N85-35274

PRIMARY COSMIC RAYS
Energy spectra of proton and nuclei of primary cosmic rays in energy region 10 TeV/particle
[HE-3.1-10] N85-35908
Size distributions of air showers accompanied with high energy gamma ray bundles observed at Mt. Chacaltaya
[HE-3.3-9] N85-35927
Multidimensional analysis of data obtained in experiments with X-ray emulsion chambers and extensive air showers
[HE-3.6-2] N85-35951
LPM effect and primary energy estimations
[HE-3.6-4] N85-35953
The lateral distributions of charged particles of energy greater than 0.3 E sub crit in electron-photon cascades in lead and air
[HE-3.6-10] N85-35957
Result of Monte-Carlo simulation of electron-photon cascades in lead and layers of lead-scintillator
[HE-3.6-11] N85-35958
Intensities of high-energy cosmic rays at Mount Kanbala
[HE-3.7-5] N85-35964
Ultra high energy events in ECHOS series and primary energy spectrum
[HE-3.7-9] N85-35966
Study of the energy spectrum of primary cosmic rays: EAS size fluctuations at a fixed primary energy
[HE-4.4-14] N85-36020
Thickness of the particle swarm in cosmic ray air showers
[HE-4.7-14] N85-36064
Relevance of multiple muons detected underground to the mass composition of primary cosmic rays
[HE-5.1-4] N85-36069
Multimuons events and primary composition
[HE-5.1-5] N85-36070
Muon groups and primary composition at 10 to the 13th power to 10 to the 15th power eV
[HE-5.1-12] N85-36074
Primary chemical composition from simultaneous recording of muons induced cascades and accompanying muon group underground
[HE-5.1-13] N85-36075
Multiple muons in MACRO
[HE-5.2-1] N85-36079
Search for tachyons associated with extensive air showers in the ground level cosmic radiation
[HE-6.2-13] N85-36149
Observation of genetic relation among new phenomena Geminion, Chiron and mini-Centauro
[HE-6.2-16] N85-36152
Muon and neutrino fluxes
[HE-6.2-18] N85-36154

PRIMERS (COATINGS)
Results of tests of weathered K5NA closeout material in the MSFC Hot Gas Facility
[NASA-CR-170893] N85-35239

PROBABILITY DENSITY FUNCTIONS
Relaxation phenomena and stability of probability densities
[AD-A155923] N85-35682

PROBABILITY DISTRIBUTION FUNCTIONS
Characterizations of generalized hyperexponential distributions
[AD-A155855] N85-35680

PROBABILITY THEORY
Large deviations for the maxima of some random fields
[AD-A155909] N85-35681
Relaxation phenomena and stability of probability densities
[AD-A155923] N85-35682

PROBLEM SOLVING
Analytic solutions of inverse heat conduction problems N85-35367
Algorithmic approaches in sets of good answers in inverse problems
[PM/84/18] N85-35677

PROCEDURES
Procedure for editing the fluxgate magnetometer data of the AFGL (Air Force Geophysics Laboratory) magnetometer network
[AD-A156331] N85-35523

PROCESS CONTROL (INDUSTRY)
Electrically conductive doped block copolymer of polyacetylene and polyisoprene
[DE85-006500] N85-35301

PROCUREMENT MANAGEMENT
Progress report on implementing the recommendations of the White House Science Council's Federal Laboratory Review Panel, volume 1
[PB85-185072] N85-35819

PRODUCT DEVELOPMENT
New technologies at the forefront of industrial developments N85-35168
Development of position sensors for microcomputer-oriented sensor systems
[BMFT-FB-T-85-021] N85-35361
Development of contactless sensors for industrial and automative applications
[BMFT-FB-T-85-031] N85-35400
Monolithic photovoltaic series array for an energy coupler
[BMFT-FB-T-85-023] N85-35496
Development and operation of a measuring data acquisition system for use in light airplanes N85-35556

PRODUCTIVITY
Electronic information management and productivity
[DE85-013362] N85-35818

PROGRAM VERIFICATION (COMPUTERS)
Specifying and verifying concurrent programs
[AD-A156190] N85-35652

PROGRAMMERS
Data processing professionals and DP application users' perceptions and expectations of operational roles of persons working in a DP/application user interface group N85-35821

PROGRAMMING LANGUAGES
Software maintenance relating to the input translator and z-80 realization volume of the computer systems design environment
[AD-A155849] N85-35646
Benchmark evaluation of PC simscript
[AD-A156133] N85-35651
Polylith: The early goals
[DE85-012534] N85-35658
Artificial intelligence in Ada (trademark): Pattern-directed processing
[AD-A156230] N85-35671
PROPAGATION MODES
Advanced detectors and signal processing.
[NASA-CR-176193] N85-35343
PROPELLANT TESTS
Dissected motors-propellants motor number STM-012. Phase 15: Surveillance report, stage 1
[AD-A156086] N85-35226
PROPELLER BLADES
Optimally designed propellers constrained by noise
N85-35196
PROPELLER EFFICIENCY
Optimally designed propellers constrained by noise
N85-35196
PROPELLERS
Wingtip vortex propeller
[NASA-CASE-LAR-13019-1] N85-35194
PROPORTIONAL COUNTERS
Search for magnetic monopoles using proportional counters filled with helium gas
[HE-6.1-1] N85-36127
Magnetic monopole search by 130 m(2)sr He gas proportional counter
[HE-6.1-2] N85-36128
Limits on monopole fluxes from KFG experiment
[HE-6.1-6] N85-36132
Results from the UCSD magnetic monopole search
[HE-6.1-12] N85-36137
Results on nucleon life-time from the Kolar gold field experiment
[HE-6.2-3] N85-36139
Data acquisition system for phase-2 KGF proton decay experiment
[HE-6.2-4] N85-36140
PROPULSION
Status of advanced orbital transfer propulsion
[NASA-TM-87069] N85-35225
PROPULSION SYSTEM CONFIGURATIONS
Presentation of the acoustic and aerodynamic results of the Aladin 2 concept qualification testing
[NASA-TM-77883] N85-35161
PROTECTIVE COATINGS
Wear-resistant coatings for tools intended for cold working
[BLL-RISLEY-TR-5040-(9091.9F)] N85-35293
Space shuttle SRB TPS protective paint test and evaluation in NASA Hot Gas Facility and AEDC Tunnel C
[NASA-CR-170884] N85-35294
PROTECTORS
Results of tests of MTA-2 TPS on the SRB hold-down bolt blast container
[NASA-CR-170891] N85-35224
PROTEINS
Muscle protein and glycogen responses to recovery from hypogravity and unloading by tail-cast suspension
[NASA-CR-176181] N85-35591
PROTON BEAMS
Major facility overhauls at LAMPF
[DE85-012724] N85-35765
Los Alamos high-current proton storage ring
[DE85-012664] N85-35779
Hadrons registration in emulsion chamber with carbon block
[HE-3.7-3] N85-35962
Intensities of high-energy cosmic rays at Mount Kanbala
[HE-3.7-5] N85-35964
Muon and neutrino fluxes
[HE-6.2-18] N85-36154
Acoustic detection of air shower cores
[HE-7.1-4] N85-36158
PROTON SCATTERING
Some nuclear data needs in astrophysics
[DE85-012916] N85-35842
PROTON-PROTON REACTIONS
Small air showers and collider physics
[HE-4.1-9] N85-35975
A standard source for high energy neutrino astronomy
[HE-5.3-15] N85-36109
Relationship of sea level muon charge ratio to primary composition including nuclear target effects
[HE-5.4-10] N85-36121
PROTONS
Calculation of heavy-ion tracks in liquid water
[DE85-012101] N85-35725
Studies of relativistic heavy ion collisions
[DE85-014686] N85-35745
Proton-air and proton-proton cross sections from air shower data
[HE-1.1-1] N85-35849
Proton-air inelastic cross section at S(1/2) = 30 TeV
[HE-1.1-2] N85-35850
Determination of the cross section of the proton, pion and neutron inelastic interaction with lead and carbon nuclei at 0.5 - 5.0 TeV energies (PION experiment)
[HE-1.1-5] N85-35853
P(P bar)P elastic scattering and cosmic ray data
[HE-1.1-6] N85-35854
The method for the study of the inelastic cross-section for high energy protons by means of shower arrays with the large calorimetric area
[HE-1.1-11] N85-35858
A test of the Feynman scaling in the fragmentation region
[HE-1.2-9] N85-35867
Nucleon-nucleus interactions from JACEE
N85-35869
Determination of primary energy in nucleus-nucleus collisions and the high P(sub)T tail of alpha-particles
N85-35875
Ringlike inelastic events in cosmic rays and accelerators N85-35887
On the halo events observed by Mount Fuji and Mount Kanbala Emulsion Chamber Experiments
[HE-3.4-9] N85-35937
Particle interactions at energies over 1000 TeV inferred from gamma-families observed at Mount Fuji
[HE-3.5-1] N85-35940
Giant mini-clusters as possible origin of halo phenomena observed in super-families
[HE-3.5-4] N85-35943
The electromagnetic component of albedo from superhigh energy cascades in dense media
[HE-3.5-11] N85-35948
Peculiarities of gamma-quanta distribution at 20 TeV energy
[HE-3.7-10] N85-35967
Electrons, muons and hadrons in extensive air showers and how do they depend on nuclear interaction model, part 2 N85-35969
Analysis of the hadron component in E.A.S.
N85-35971
Small air showers and collider physics
[HE-4.1-9] N85-35975
Dependence of the average spatial and energy characteristics of the hadron-lepton cascade on the strong interaction parameters at superhigh energies
N85-35977
Preliminary results on underground muon bundles observed in the Frejus proton-decay detector
[HE-5.1-1] N85-36067
Neutrino astronomy and the atmospheric background
[HE-5.3-17] N85-36111
Multiple muons of conventional and exotic origin in DUMAND
[HE-5.4-4] N85-36117
An experiment to detect gut monopoles
[HE-6.1-7] N85-36133
Data acquisition system for phase-2 KGF proton decay experiment
[HE-6.2-4] N85-36140
PROTOPLANETS
Study of the parameters affecting the collapse of a rotating protostellar cloud N85-35837
PROTOTYPES
Prototyping with data dictionaries for requirements analysis
[AD-A156303] N85-35654
PULSARS
High energy radiation from neutron stars
[DE85-014353] N85-35843
PULSE AMPLITUDE
Study of the shower maximum depth by the method of detection of the EAS Cerenkov light pulse shape
[HE-4.4-15] N85-36021
Analysis of Cerenkov pulses recorded simultaneously at two sites
[HE-4.4-16] N85-36022
Microprocessor-based single particle calibration of scintillation counter
[HE-4.6-13] N85-36049
Samarkand complex setup for investigation of cosmic ray variation in the energy range of 7 10 (9) - 10 (15) eV
[HE-4.6-14] N85-36050
The structure of the shower disk observed at Mt. Norikura
[HE-4.7-1] N85-36052
PULSE COMMUNICATION
Necessary bandwidth and spectral properties of digital modulation
[PB85-185387] N85-35340
PULSE DURATION
Sub-luminal pulses from cosmic ray air showers
[HE-4.7-13] N85-36063
PULSE GENERATORS
Photoconductive pulse power switches: A review
[DE85-014125] N85-35360
Quality assurance considerations for the implementation of a pulsed power R and D project
[DE85-012357] N85-35720
Beam intensity increases at the intense pulsed neutron source accelerator
[DE85-012377] N85-35764
Power flow evaluations for HERMES 3
[DE85-013116] N85-35769
PULSE RADAR
Signal space models for antenna arrays
[AD-A156063] N85-35335
PULSED LASERS
ATA upgrade to 150 MeV
[DE85-013174] N85-35404
PULSED RADIATION
Study of the shower maximum depth by the method of detection of the EAS Cerenkov light pulse shape
[HE-4.4-15] N85-36021
Analysis of Cerenkov pulses recorded simultaneously at two sites
[HE-4.4-16] N85-36022
The experimental cascade curves of EAS at E sub 0 10(17) eV obtained by the method of detection of Cherenkov pulse shape
[HE-4.4-18] N85-36024
PUMPS
Experimental lithium system
[DE85-013252] N85-35382

Q

Q DEVICES
Confinement and heating of high beta plasmas with emphasis on compact toroids
[DE85-011459] N85-35761
QUADRUPOLE NETWORKS
RFQ modeling computer program
[DE85-012665] N85-35661
QUALITY
Acoustic scaling: The development of improved instrumentation
[BBC-RD-1985/7] N85-35694
QUALITY CONTROL
Quality assurance considerations for the implementation of a pulsed power R and D project
[DE85-012357] N85-35720
Aeronautical Systems Division Manufacturing/Quality assurance orientation
[AD-A156128] N85-35817
QUANTUM CHROMODYNAMICS
Very high energy probes of the quark-gluon plasma
N85-35708
High energy physics at Tufts University
[DOE/ER-40085/7] N85-35744
QCD-motivated description of very high energy particle interactions
[HE-1.2-2] N85-35861
A cosmic ray super high energy multicore family event. 2: Structure and fragmentation characteristics of the jets
[HE-3.4-2] N85-35931
QCD analysis of neutrino charged current structure function F2 in deep inelastic scattering
[HE-5.3-23] N85-36114
QUANTUM COUNTERS
Lateral distribution on charged particles in EAS
[HE-4.3-15] N85-36009
QUANTUM WELLS
Optical properties of heterostructures and superlattices
[AD-A156243] N85-35802
QUARKS
Detectors for relativistic nuclear collisions (report from the Fixed-Target Hadron Group) N85-35701
Very high energy probes of the quark-gluon plasma
N85-35708
Propagation of cosmic rays through the atmosphere in the quark-gluon strings model N85-35873
The phi-meson and Chiral-mass-meson production in heavy-ion collisions as potential probes of quark-gluon-plasma and Chiral symmetry transitions
N85-35884
Heavy flavours production in quark-gluon plasma formed in high energy nuclear reactions N85-35886

A cosmic ray super high energy multicore family event. 2: Structure and fragmentation characteristics of the jets
[HE-3.4-2] N85-35931
On mini-cluster observed by Chacaltaya emulsion chamber experiment
[HE-3.6-12] N85-35959
The maximum depth of shower with E sub 0 larger than 10(17) eV on average characteristics of EAS different components N85-35961
Calculation of intensity of high energy muon groups observed deep underground
[HE-5.4-13] N85-36123
High energy cosmic ray signature of quark nuggets
[HE-6.2-11] N85-36147
Progress report on a new search for free e/3 quarks in the cores of 10(15) - 10(16) eV air showers
[HE-6.2-15] N85-36151
Tien-Shan effect and charmed particles
[HE-6.2-17] N85-36153

R

RADAR
A planar version of a 4.0 gigahertz reactively steered adaptive array
[AD-A156029] N85-35330
RADAR ANTENNAS
Signal space models for antenna arrays
[AD-A156063] N85-35335
RADAR CROSS SECTIONS
Normal modes in an overmoded circular waveguide coated with lossy material
[NASA-CR-176186] N85-35320
RADAR IMAGERY
An experimental study of dielectric rod antennas for millimeter-wave imaging applications
[AD-A155832] N85-35328
Surface cyclogenesis as indicated by satellite imagery
[PB85-191815] N85-35566
Optical synthetic aperture techniques
[AD-A156151] N85-35752
RADAR MAPS
Geology and geomorphology of the Roraima group, southeastern Venezuela N85-35511
RADAR RECEIVERS
A multi-channel radar receiver
[AD-A156058] N85-35333
RADAR TRANSMISSION
Feasibility study of radar-transmitting materials
[AD-A155839] N85-35329
RADIAL DISTRIBUTION
A note on some statistical properties of rise time parameters used in muon arrival time measurements
[HE-4.7-12] N85-36062
RADIANT FLUX DENSITY
The structure of Herbig-Haro object 43 and Orion dark cloud extinction
[NASA-TM-87503] N85-35831
Measurement of interaction cross section of cosmic ray Fe nuclei (E4 GeV/N) with Al target
[HE-1.1-7] N85-35855
RADIANT HEATING
Characterization of the optical and thermal properties of matter by photothermal techniques
[DE85-012607] N85-35260
Development of advanced high-temperature heat flux sensors. Phase 2: Verification testing
[NASA-CR-174973] N85-35391
RADIATION
The identification of gamma ray induced EAS
[HE-4.5-1] N85-36026
RADIATION ABSORPTION
Linear absorption and scattering of laser beams
[AD-A156167] N85-35401
Some nuclear data needs in astrophysics
[DE85-012916] N85-35842
RADIATION COUNTERS
Working group on penetrating probes at fixed target facilities N85-35703
Microprocessor-based single particle calibration of scintillation counter
[HE-4.6-13] N85-36049
The thickness of the shower disc as observed in showers produced by primaries above 10 (19)eV
[HE-4.7-6] N85-36057
Search for anomalons using plastic nuclear track detectors
[HE-6.2-12] N85-36148
RADIATION DETECTORS
High resolution beam profile monitors in the SLC
[DE85-013375] N85-35774
The structure of EAS at E 0.1 EeV
[HE-4.4-2] N85-36012
Expected rates with mini-arrays for air showers
[HE-4.7-8] N85-36059
A note on some statistical properties of rise time parameters used in muon arrival time measurements
[HE-4.7-12] N85-36062
Multimuons events and primary composition
[HE-5.1-5] N85-36070
RADIATION DISTRIBUTION
A kinetic model for predicting oxidative degradation rates in combined radiation-thermal environments
[TI85-002629] N85-35414
Multiplicity distributions in interaction models used for cascade simulations
[HE-1.2-5] N85-35863
Angular distribution and multiplicity of backward hadrons in hFe interactions at 0.5-5.0 TeV energies (PION Experiment)
[HE-1.2-8] N85-35866
Measurement of the local density spectrum N85-35984
RADIATION DOSAGE
A kinetic model for predicting oxidative degradation rates in combined radiation-thermal environments
[TI85-002629] N85-35414
Wholebody radiation counting system
[AD-A155842] N85-35607
Tritium hazard via the ingestion pathway
[DE85-012897] N85-35618
Calibration of a high-level photon irradiation
[DE85-013044] N85-35738
Recent advances in remote handling at LAMPF
[DE85-012725] N85-35775
Total integrated dose testing of solid-state scientific CD4011, CD4013, and CD4060 devices by irradiation with CO-60 gamma rays
[NASA-CR-176196] N85-35795
RADIATION EFFECTS
System expectations for Pioneer 1 foil implosion experiments
[DE85-014129] N85-35359
A kinetic model for predicting oxidative degradation rates in combined radiation-thermal environments
[TI85-002629] N85-35414
Biophysical research in space --- radiation effects N85-35603
Total integrated dose testing of solid-state scientific CD4011, CD4013, and CD4060 devices by irradiation with CO-60 gamma rays
[NASA-CR-176196] N85-35795
Electron irradiation of N type cadmium telluride
[AD-A156117] N85-35801
RADIATION HAZARDS
Biophysical research in space --- radiation effects N85-35603
Computer code calculations of the TMI-2 accident: Initial and boundary conditions
[DE85-012613] N85-35666
RADIATION MEASUREMENT
Radiation measurements on magnesium flames
[BLL-CE-TRANS-8110-(9022.09)] N85-35254
Study of hadron bundles observed in Chacaltaya two-story emulsion chamber
[HE-3.3-4] N85-35922
RADIATION MEASURING INSTRUMENTS
Wholebody radiation counting system
[AD-A155842] N85-35607
Monopole, astrophysics and cosmic ray observatory at Gran Sasso
[HE-6.1-4] N85-36130
Monopole search below the Parker limit with the MACRO detector at Gran Sasso
[HE-6.1-5] N85-36131
Upper limit on magnetic monopole flux from Baksan experiment
[HE-6.1-11] N85-36136
RADIATION PROTECTION
Design considerations for personnel access penetrations for the superconducting super collider
[DE85-013027] N85-35807
RADIATION SHIELDING
Applicability of 100kWe-class of space reactor power systems to NASA manned space station missions
[NASA-CR-174696] N85-35728
RADIATION SOURCES
Cooling high intensity atomic hydrogen beams to liquid helium temperatures
[DE85-012515] N85-35718
Calibration of a high-level photon irradiation
[DE85-013044] N85-35738
RADIATION SPECTRA
Standard value for the radiation length in air
[HE-4.4-4] N85-36013
Lateral-angular and temporal characteristics of EAS optical radiation
[HE-4.4-19] N85-36025
RADIATION TRANSPORT
Numerical studies of high current beam compression in heavy ion fusion
[DE85-011874] N85-35783
RADIATIVE HEAT TRANSFER
An analytical and numerical model of radiation heat transfer in direct injection-type diesel combustion N85-35368
RADIO ANTENNAS
On the possibilities of large-scale radio and fiber optics detectors in cosmic rays
[HE-4.6-2] N85-36039
RADIO ELECTRONICS
Center for Electronics and Electrical Engineering technical progress bulletin covering center programs, July-September with 1985 CEEE events calendar
[PB85-191393] N85-35363
RADIO EMISSION
On the possibilities of large-scale radio and fiber optics detectors in cosmic rays
[HE-4.6-2] N85-36039
On the production mechanism of radio-pulses from large extensive air showers
[HE-4.6-4] N85-36041
RADIO FREQUENCIES
Analyzer, flight line
[AD-A155777] N85-35207
RF stabilization of interchange-ballooning modes
[DE85-012080] N85-35353
Robinson instability and beam loading
[DE85-013301] N85-35737
A new study on the emission of EM waves from large EAS
[HE-4.6-5] N85-36042
Radio wave emitted by an extensive air showers in 10KHz to 1MHz region
[HE-4.6-15] N85-36051
RADIO FREQUENCY INTERFERENCE
Television interference at the Maglarp (Sweden) wind turbine N85-35480
Television interference measurement at Kalkugnen (Sweden) test windmill N85-35481
RADIO SIGNALS
Radio signals from very large showers
[HE-4.6-3] N85-36040
RADIOACTIVE DECAY
Preliminary results on underground muon bundles observed in the Frejus proton-decay detector
[HE-5.1-1] N85-36067
Muon and neutrino results from KGF experiment at a depth of 7000 hg/square cm
[HE-5.1-2] N85-36068
Relevance of multiple muons detected underground to the mass composition of primary cosmic rays
[HE-5.1-4] N85-36069
On muon energy spectrum in muon groups underground
[HE-5.1-14] N85-36076
RADIOACTIVE ISOTOPES
Wholebody radiation counting system
[AD-A155842] N85-35607
Tritium hazard via the ingestion pathway
[DE85-012897] N85-35618
RADIOACTIVE MATERIALS
Radiation safety problems in handling highly active tritium targets
[DE85-014268] N85-35742
RADIOACTIVE WASTES
Simulated effects of increased recharge on the ground-water flow system of Yucca Mountain and vicinity, Nevada-California
[DE85-012985] N85-35469
RADIOBIOLOGY
Biophysical research in space --- radiation effects N85-35603
RADIOMETERS
Analyzer, flight line
[AD-A155777] N85-35207
Development of advanced high-temperature heat flux sensors. Phase 2: Verification testing
[NASA-CR-174973] N85-35391
Aeromagnetic and radiometric signatures of a possible porphyry system in the western Tushar Mountains, Utah N85-35437
RADIOMETRIC CORRECTION
LANDSAT-4/5 image data quality analysis
[E85-10105] N85-35483
RADIOMETRIC RESOLUTION
Study of spectral/radiometric characteristics of the Thematic Mapper for land use applications
[E85-10106] N85-35484
RADIOSONDES
Meteorological data from the OPTOMA (Ocean Prediction Through Observations, Modeling and Analysis) program OPTOMA 2, leg D2. 30 Jun. - 10 Jul. 1984
[AD-A156134] N85-35560

RADON
Groundwater radon studies for earthquake precursors in southern California
[PB85-196871] N85-35529
RAIN
Elemental tracers of source regions of contaminants in precipitation
[DE85-012858] N85-35499
The kinematic structure of cold frontal rainbands N85-35531
RAMAN SPECTRA
Electronic structure and lattice dynamics of dimensionally constrained and disordered solids
[AD-A155927] N85-35797
RANDOM NOISE
A new description of combined trellis coding with asymmetric modulation
[NASA-CR-176197] N85-35323
RANDOM NUMBERS
A quickly tested Pascal random number generator for microcomputers
[AD-A156059] N85-35633
RANGE (EXTREMES)
Evaluation: Close-range photogrammetry for slope inventory and monitoring
[PB85-192755] N85-35470
RARE GASES
Fluidized bed desulfurization
[NASA-CASE-NPO-15924-1] N85-35253
Groundwater radon studies for earthquake precursors in southern California
[PB85-196871] N85-35529
RATES (PER TIME)
The application of bispectral analyses to aeroelastic phenomena N85-35157
The structure of the shower disk observed at Mt. Norikura
[HE-4.7-1] N85-36052
Methods for roof-top mini-arrays
[HE-4.7-7] N85-36058
Fast scintillation counter preamplifier for the observation of Linsley effect
[HE-4.7-9] N85-36060
RATS
Response of amino acids in hindlimb muscles to recovery from hypogravity and unloading by tail-cast suspension
[NASA-CR-176183] N85-35589
Response of rat hindlimb muscles to 12 hours recovery from tail-cast suspension
[NASA-CR-176182] N85-35590
RAY TRACING
A ray trace program for line-of-sight microwave communication links
[AD-A156168] N85-35336
REACTION KINETICS
FTIR studies of hydrocarbon synthesis on Pd/ZSM5 catalysts
[DE85-012430] N85-35230
Basic research on pulse-combustion phenomena
[PB85-200228] N85-35265
A study of the chemistry of alkali metals in the upper atmosphere
[AD-A156349] N85-35524
REACTOR CORES
DEPTH-CHARGE static and time-dependent perturbation/sensitivity system for nuclear reactor core analysis, revision 1
[DE85-013103] N85-35659
Neutronic calculations for a new high flux reactor
[DE85-011551] N85-35734
Thermal hydraulic features of the TMI accident
[DE85-014569] N85-35747
REACTOR MATERIALS
The dynamic strain ageing of A533B class 1 nuclear pressure vessel steel
[AERE-R-11485] N85-35274
Analysis of reactor material experiments investigating oxide fuel crust stability and heat transfer in jet impingement flow
[DE85-012097] N85-35739
REACTOR SAFETY
Transient three-phase three-component systems. Part 1: Formulation of the system of differential equations
[DE85-013267] N85-35384
READOUT
Spatial distribution read-out system for thermoluminescence sheets
[HE-7.1-7] N85-36161
REAL TIME OPERATION
Space Missions for Automation and Robotics Technologies (SMART) Program
[NASA-TM-86820] N85-35210
Holoswitch
[AD-A155841] N85-35392
Optimize computer throughput using array processors
[AD-A155843] N85-35628
RECEPTION DIVERSITY
Polarization diversity addition to the 10 centimeter Doppler weather radar
[AD-A156062] N85-35334
RECESSION
Results of variable enthalpy tests of CPR-488 TIP panels in MSFC Hot Gas Facility
[NASA-CR-170889] N85-35237
RECOMBINATION COEFFICIENT
Photoconductive pulse power switches: A review
[DE85-014125] N85-35360
RECOMMENDATIONS
Recommendations for content revision and alternate delivery modes for the Human Engineering Guide to Equipment Design (HEGED)
[AD-A155781] N85-35624
RECONNAISSANCE SPACECRAFT
Target observability for satellite-based sensors
[AD-A156139] N85-35217
RECORDING INSTRUMENTS
Acoustic scaling: The development of improved instrumentation
[BBC-RD-1985/7] N85-35694
RECORDS
Records Disposal: A guidebook for laboratory offices
[AD-A156064] N85-35823
RECRYSTALLIZATION
Crystallization of Polyetheretherketone (PEEK) in carbon fiber composites
[AD-A156316] N85-35252
RECTUM
Weight loss, rectal temperature and heart rates following the 1984 Boston Marathon
[AD-A155984] N85-35612
RECURSIVE FUNCTIONS
Reliability prediction of the series system with spares subject to Weibull failure N85-35413
Recursive partitioning estimation N85-35670
RECYCLING
Neutral pumping rates for a next step tokamak ignition device
[DE85-012780] N85-35776
REDOX CELLS
Development of electrodes for the NASA iron/chromium
[NASA-CR-174724] N85-35471
REDUCED GRAVITY
NASA Developmental Biology Workshop: A summary
[NASA-TM-86756] N85-35578
Effects of microgravity and hypergravity on invertebrate development N85-35579
REFLECTION
Radiation measurements on magnesium flames
[BLL-CE-TRANS-8110-(9022.09)] N85-35254
Literature search for new physical methods for biological aerosol detection
[AD-A155883] N85-35592
REFLECTORS
Optical receivers using rough reflectors
[NASA-CR-176200] N85-35750
REFRACTION
Crustal structure in southern California from array data N85-35512
REFRACTIVITY
The use of a laser Doppler velocimeter in a standard flammability tube
[NASA-CR-174960] N85-35389
REGGE POLES
Is the inelastic charge-exchange contribution constant at the large X and superhigh energies? Qaut 01Kuchin, I. A. N85-35871
REGISTERS (COMPUTERS)
Interprocess communication
[AD-A156337] N85-35337
REGRESSION ANALYSIS
Development of NATOPS performance software for the SH-3D and SH-3H helicopters
[AD-A156140] N85-35192
REINFORCEMENT (STRUCTURES)
Membrane reinforcement in concrete shells: Design versus nonlinear behavior N85-35312
User's guide: A computer program for strength analysis of non-hydraulic concrete structural elements. Report 2. Strength design of reinforced concrete column sections (PCAUC)
[AD-A156393] N85-35429
RELATIVISTIC PARTICLES
Proceedings of the Workshop on Detectors for Relativistic Nuclear Collisions
[LBL-18225] N85-35700
Report of working group on detectors for hadrons and event parameters at colliders N85-35705
A simulation of ultra-relativistic nucleus-nucleus collisions N85-35707
A holographic streamer chamber for relativistic nucleus-nucleus collision experiments N85-35710
Fractional charge resolution in music N85-35712
Hadron thermodynamics in relativistic nuclear collisions
[HE-1.1-8] N85-35856
Structure of air shower disc near the core
[HE-4.7-2] N85-36053
High energy cosmic ray signature of quark nuggets
[HE-6.2-11] N85-36147
Search for anomalons using plastic nuclear track detectors
[HE-6.2-12] N85-36148
RELATIVISTIC PLASMAS
Detectors for relativistic nuclear collisions (report from the Fixed-Target Hadron Group) N85-35701
RELAXATION (PHYSIOLOGY)
Responses of skeletal muscle to unloading, a review
[NASA-CR-176177] N85-35594
Relaxation techniques
[AD-A156248] N85-35621
RELAXATION METHOD (MATHEMATICS)
Relaxation phenomena and stability of probability densities
[AD-A155923] N85-35682
RELIABILITY
Development of an NBS (National Bureau of Standards) polymer gage for dynamic soil stress measurement
[PB85-208494] N85-35526
RELIABILITY ANALYSIS
Reliability prediction of the series system with spares subject to Weibull failure N85-35413
REMOTE HANDLING
Recent advances in remote handling at LAMPF
[DE85-012725] N85-35775
REMOTE SENSING
Microwave properties of a quiet sea
[NASA-CR-176199] N85-35322
Processing of LANDSAT imagery to map surface mineral alteration on the Alaska Peninsula, Alaska N85-35455
The development of assessment techniques program N85-35457
Remote sensing of hydrologic transport processes using spot simulation data
[DE85-012412] N85-35467
Kinematic analysis of Hurricane Frederick (1979) using satellite, aircraft and rawinsonde data
[NASA-CR-176167] N85-35533
Sea surface and remotely sensed temperatures off Cape Mendocino, California
[NASA-TM-86712] N85-35573
REMOTE SENSORS
Target observability for satellite-based sensors
[AD-A156139] N85-35217
REPRODUCTION (BIOLOGY)
Vertebrate development in space: Gravity is a drag (and has been for eons and eons) N85-35580
REQUIREMENTS
Proceedings of the Workshop on Detectors for Relativistic Nuclear Collisions
[LBL-18225] N85-35700
RESEARCH AND DEVELOPMENT
Development of flight mechanics research in Brunswick N85-35166
Piezoelectric transducers, state of research N85-35345
Development and evaluation of sulfonated polysulfone membranes for the zinc-ferricyanide battery
[DE85-009104] N85-35357
United States Army welding research and development topical and coordination meeting
[AD-A155834] N85-35409
Quality assurance considerations for the implementation of a pulsed power R and D project
[DE85-012357] N85-35720
The 1986 National Aeronautics and Space Administration authorization
[GPO-47-635] N85-35829
RESEARCH FACILITIES
United States Army welding research and development topical and coordination meeting
[AD-A155834] N85-35409
RESEARCH MANAGEMENT
Research report program of the US Army in Europe N85-35167
DoD Value Engineering conference report. Value Engineering (VE): A tool that benefits line management. Part 3, Workshop A: VE in the program office
[AD-A156069] N85-35812
RESEARCH VEHICLES
Preliminary results of an ALVIN dive program on active hydrothermal vents at the southern Juan de Fuca Ridge N85-35454

RESERVOIRS
National program for inspection of non-federal dams. Woodward reservoir dam (VT 00209), Connecticut River Basin, Plymouth, Vermont. Phase 1 inspection report
[AD-A156256] N85-35693
RESIDENTIAL ENERGY
Design and construction of an advanced power conditioning subsystem for small photovoltaic applications
[DE85-013940] N85-35495
RESIDUAL STRESS
Development of a mathematical model for predicting the percentage fatigue life increase resulting from shot peened components
[AD-A155774] N85-35425
RESISTANCE HEATING
High Temperature Heating System (HTHS)
[PB85-188340] N85-35316
RESOLUTION
Single-point diamond crushing of Zerodur with in-situ polishing and metrology on a diamond turning machine
[DE85-012918] N85-35305
LANDSAT-4/5 image data quality analysis
[E85-10105] N85-35463
RESONANCE
Some aspects of internal gravity waves in a multi-layered moving stratified flow N85-35369
Width of nonlinear difference resonances
[DE85-013026] N85-35719
Exit channels of autoionization resonances in atoms
[DE85-012299] N85-35726
Resonance localization in tokamaks excited with ICRF waves
[DE85-014559] N85-35791
RESONANCE SCATTERING
Circumstellar shells of late-type stars: A study at millimeter and infrared wavelengths N85-35836
RESONANT VIBRATION
Acoustic resonances in cylinder bundles oscillating in a compressibile fluid
[DE85-004066] N85-35699
RESOURCES
Expert systems research in regional resource evaluation: Experiences in the application of microcomputer technologies N85-35450
Applications of the mineral resources data system and the international strategic minerals inventory in mineral-resource assessments by region and commodity N85-35451
RESOURCES MANAGEMENT
Some recent deposit modeling efforts N85-35453
Mineral resources programs N85-35456
Federal Mineral Land Information System N85-35459
USGS coastal research, studies and maps: A source of information for coastal decision making
[USGS-CIRC-883] N85-35465
RESPIRATION
An analysis of aerobic capacity in a large United States population
[AD-A156200] N85-35614
RESPONSES
Relaxation phenomena and stability of probability densities
[AD-A155923] N85-35682
RETRAINING
Data processing professionals and DP application users' perceptions and expectations of operational roles of persons working in a DP/application user interface group N85-35821
REVERSE FIELD PINCH
Proposed FRX-D experiment
[DE85-012766] N85-35778
REVERSING
A new drawing technique for nylon 6 by reversible plasticization with iodine
[AD-A156272] N85-35803
RIGGING
Actuator rigging test set electromagnetic interference test (CE03)
[AD-A155819] N85-35327
RIGID STRUCTURES
Identification and control of structures in space
[NASA-CR-176175] N85-35214
RING STRUCTURES
SRB attach ring phenolic TPS fishtail seal evaluation tests
[NASA-CR-170887] N85-35407
RISK
Fire service emergency management handbook
[AD-A155780] N85-35313
Calculation of trajectories of detached wind turbine blades and prediction of site risk levels associated with failures of HAWT's N85-35475
The physical and empirical basis for a specific clear-air turbulence risk index
[NASA-CR-178522] N85-35540
Risk analysis and sensitivity: Antithesis or synthesis
[B8562444] N85-35687
RIVERS
Depositional systems and coal occurrence in the Fort Union Formation (Paleocene), Powder River Basin, Wyoming and Montana N85-35505
Bibliography on tidal hydraulics. Report 2. Supplement 9: Supplementary material compiled from June 1980 - June 1983. Tidal flows in rivers and harbors
[AD-A155990] N85-35574
ROBOTICS
Space Missions for Automation and Robotics Technologies (SMART) Program
[NASA-TM-86820] N85-35210
Investment justification of robotic technology in aerospace manufacturing. User's manual
[AD-A156193] N85-35410
TRICCS: A proposed teleoperator/robot integrated command and control system for space applications
[NASA-TM-87577] N85-35637
ROBOTS
The compliance of end effector force sensors for robot manipulator control N85-35406
Testbed for sensory control of intelligent machines
[DE85-012355] N85-35412
ROBUSTNESS (MATHEMATICS)
Decentralized stabilization by high gain feedback
[BU-115] N85-35689
ROCK INTRUSIONS
Three-dimensional gravity ideal body studies in rough terrain
[DE85-014097] N85-35525
ROCK MECHANICS
Calibrator for displacement gages used in the rock mechanics laboratory
[DE85-013257] N85-35393
Seismic stratigraphic analysis of the Mississippi Fan N85-35507
Crustal structure in southern California from array data N85-35512
ROCKET ENGINE CASES
Verification of the SRB motor case pin retainer band tips
[NASA-CR-170882] N85-35220
ROCKET ENGINES
SRB attach ring phenolic TPS fishtail seal evaluation tests
[NASA-CR-170887] N85-35407
ROCKS
Subcritical fracture propagation in rocks: An examination using the methods of fracture mechanics and non-destructive testing N85-35516
Underwater measurements of muon intensity
[HE-5.1-16] N85-36078
Results of low energy background measurements with the Liquid Scintillation Detector (LSD) of the Mont Blanc Laboratory
[HE-5.3-5] N85-36099
The research program of the Liquid Scintillation Detector (LSD) in the Mont Blanc Laboratory
[HE-5.3-6] N85-36100
RODS
Stress-intensity factors for circumferential surface cracks in pipes and rods under tension and bending loads
[NASA-TM-87594] N85-35424
ROLL FORMING
The character of observed porosity and its possible effects on rolling contact fatigue life of M-50 steel
[AD-A155930] N85-35279
Effect of prior warm rolling on the retained austenite content and hardening response of VIM-VAR (vacuum-induction melted-vacuum-arc remelted) AISI M-50 steel
[AD-A156145] N85-35281
ROLLER BEARINGS
Planetary-gear-support bearing test rig design
[NASA-CR-174927] N85-35185
ROOT-MEAN-SQUARE ERRORS
Comparative analysis of operational forecasts versus actual weather conditions in airline flight planning, volume 3
[NASA-CR-167864] N85-35536
Study of the time-differentiated particle flux density at various distances from EAS axis
[HE-4.7-15] N85-36065
ROTARY WINGS
The effects of parameter variation on helicopter performance
[AD-A156027] N85-35189
ROTATING SPHERES
The effect of power law body forces on a thermally-driven flow between concentric rotating spheres
[NASA-TM-87596] N85-35374
ROTATION
Optimally designed propellers constrained by noise N85-35196
ROTONS
Scaling violation in the fragmentation region of inclusive nucleon spektrum N85-35874
RUNNING
Weight loss, rectal temperature and heart rates following the 1984 Boston Marathon
[AD-A155984] N85-35612
RURAL AREAS
Motor glider measurements during the Urban Atmosphere Energy Budget Experiment (EESA 1) N85-35553

S

S WAVES
Scale separation closure and Alfven wave turbulence
[DE85-013124] N85-35385
SAFETY
Experimental lithium system
[DE85-013252] N85-35382
SAMPLING
Ultrasonic inspection of carbon fiber reinforced plastic by means of sample-recognition methods
[NASA-TM-77896] N85-35245
SAN ANDREAS FAULT
Carbon fiber strainmeter studies in southern California
[PB85-196889] N85-35528
SANDS
Steamflood pilots in the O'Connell Ranch field and the T-4 Ranch field
[DE85-901363] N85-35468
Simplified procedures for the evaluation of settlements in sands due to earthquake shaking
[PB85-197887] N85-35527
SANDSTONES
Steamflood pilots in the O'Connell Ranch field and the T-4 Ranch field
[DE85-901363] N85-35468
SAPPHIRE
Size and shape dependence of CO adsorption sites on sapphire supported Fe microcrystals
[NASA-CR-176171] N85-35794
SARSAT
LOCAT: A data retrieval program
[AD-A156004] N85-35822
SATELLITE DESIGN
Second-generation mobile satellite system. A conceptual design and trade-off study
[NASA-CR-176195] N85-35325
SATELLITE NETWORKS
Pluribus satellite IMP (Interface Message Processors) development mobile access terminal network
[AD-A155754] N85-35216
Second-generation mobile satellite system. A conceptual design and trade-off study
[NASA-CR-176195] N85-35325
SATELLITE OBSERVATION
Target observability for satellite-based sensors
[AD-A156139] N85-35217
Remote sensing of hydrologic transport processes using spot simulation data
[DE85-012412] N85-35467
Two-dimensional quasineutral description of particles and fields above discrete auroral arcs
[NASA-CR-176170] N85-35517
Mean cloudiness over the global tropics from satellite observations
[AD-A156188] N85-35561
SATELLITE-BORNE PHOTOGRAPHY
Surface cyclogenesis as indicated by satellite imagery
[PB85-191815] N85-35566
SCALARS
Three-dimensional gravity ideal body studies in rough terrain
[DE85-014097] N85-35525
SCALE (CORROSION)
The preparation of TEM specimens showing oxide scales in transverse cross-section
[AERE-R-11579] N85-35276
SCALE (RATIO)
Scaling violation in the fragmentation region of inclusive nucleon spektrum N85-35874
SCALE EFFECT
Scale separation closure and Alfven wave turbulence
[DE85-013124] N85-35385
SCALING LAWS
Model robust response surface designs: Scaling two-level factorials
[AD-A156218] N85-35686
Scaling violation in hadron-nucleus interaction
[HE-3.2-8] N85-35916

Particle interactions at energies over 1000 TeV inferred from gamma-families observed at Mount Fuji
[HE-3.5-1] N85-35940
Multidimensional analysis of data obtained in experiments with X-ray emulsion chambers and extensive air showers
[HE-3.6-2] N85-35951
Hadrons registration in emulsion chamber with carbon block
[HE-3.7-3] N85-35962
Intensities of high-energy cosmic rays at Mount Kanbala
[HE-3.7-5] N85-35964
Simulation of EAS properties on the basis of high energy interaction model deduced from the accelerator data N85-35973

SCANNERS
Cylindrical lens-array antenna for wideband electronic scanning
[AD-A156085] N85-35350

SCANNING
LANDSAT-4/5 image data quality analysis
[E85-10105] N85-35463

SCATTER PROPAGATION
Linear absorption and scattering of laser beams
[AD-A156167] N85-35401

SCATTERING
The HEAO-2 Guest Investigator Program: Non-linear growth of instabilities in line-driven stellar winds
[NASA-CR-176168] N85-35840
Scattering and stopping of hadrons in nuclear matter N85-35882
The hump in the Cerenkov lateral distribution of gamma ray showers
[HE-4.5-9] N85-36032
Search for tachyons associated with extensive air showers in the ground level cosmic radiation
[HE-6.2-13] N85-36149

SCATTERING CROSS SECTIONS
Proton-air and proton-proton cross sections from air shower data
[HE-1.1-1] N85-35849
Proton-air inelastic cross section at S(1/2) = 30 TeV
[HE-1.1-2] N85-35850
Hadron cross sections at ultra high energies and unitarity bounds on diffraction dissociation
[HE-1.1-3] N85-35851
On total cross sections and slopes at superhigh energies
[HE-1.1-4] N85-35852
Determination of the cross section of the proton, pion and neutron inelastic interaction with lead and carbon nuclei at 0.5 - 5.0 TeV energies (PION experiment)
[HE-1.1-5] N85-35853
P(P bar)P elastic scattering and cosmic ray data
[HE-1.1-6] N85-35854
Measurement of interaction cross section of cosmic ray Fe nuclei (E4 GeV/N) with Al target
[HE-1.1-7] N85-35855
Hadron thermodynamics in relativistic nuclear collisions
[HE-1.1-8] N85-35856
The method for the study of the inelastic cross-section for high energy protons by means of shower arrays with the large calorimetric area
[HE-1.1-11] N85-35858
QCD-motivated description of very high energy particle interactions
[HE-1.2-2] N85-35861
Is the inelastic charge-exchange contribution constant at the large X and superhigh energies? Qaut 01Kuchin, I. A. N85-35871
General consequences of the violated Feynman scaling N85-35872
Intensities of high-energy cosmic rays at Mount Kanbala
[HE-3.7-5] N85-35964

SCINTILLATION
Air fluorescence detection of large air showers below the horizon
[HE-4.6-6] N85-36043

SCINTILLATION COUNTERS
Wholebody radiation counting system
[AD-A155842] N85-35607
A lead glass tubing drift calorimeter N85-35711
The response of a scintillation counter below an emulsion chamber to heavy nucleus interactions in the chamber N85-35889
Result of Monte-Carlo simulation of electron-photon cascades in lead and layers of lead-scintillator
[HE-3.6-11] N85-35958
Application of photodiodes to the detection of electromagnetic bursts N85-35988
Study of muons near shower cores at sea level using the E594 neutrino detector N85-36000
Average features of the muon component of EAS or = 10(17) eV
[HE-4.3-10] N85-36004
Transition effect of air shower particles in plastic scintillators
[HE-4.4-9] N85-36017
A new study on the emission of EM waves from large EAS
[HE-4.6-5] N85-36042
Fast scintillation counter system and performance
[HE-4.6-10] N85-36047
Performance of a local electron density trigger to select extensive air showers at sea level
[HE-4.6-11] N85-36048
Microprocessor-based single particle calibration of scintillation counter
[HE-4.6-13] N85-36049
Samarkand complex setup for investigation of cosmic ray variation in the energy range of 7 10 (9) - 10 (15) eV
[HE-4.6-14] N85-36050
The structure of the shower disk observed at Mt. Norikura
[HE-4.7-1] N85-36052
Arrival time distributions of electrons in air showers with primary energies above 10 (18)eV observed at 900m above sea level
[HE-4.7-5] N85-36056
Methods for roof-top mini-arrays
[HE-4.7-7] N85-36058
Fast scintillation counter preamplifier for the observation of Linsley effect
[HE-4.7-9] N85-36060
A mini-array for large air showers
[HE-4.7-10] N85-36061
Sub-luminal pulses from cosmic ray air showers
[HE-4.7-13] N85-36063
Thickness of the particle swarm in cosmic ray air showers
[HE-4.7-14] N85-36064
Study of the time-differentiated particle flux density at various distances from EAS axis
[HE-4.7-15] N85-36065
On method of muon spectrum measurements by the scintillation detectors of a large thickness T4t sub o
[HE-5.2-18] N85-36094
Results of low energy background measurements with the Liquid Scintillation Detector (LSD) of the Mont Blanc Laboratory
[HE-5.3-5] N85-36099
The research program of the Liquid Scintillation Detector (LSD) in the Mont Blanc Laboratory
[HE-5.3-6] N85-36100
Search for stellar collapse with the MACRO detector at Gran Sasso
[HE-5.3-11] N85-36105
The homestake surface-underground scintillations: Description
[HE-6.1-9] N85-36135
A search for heavy long lived particles in high energy cosmic rays
[HE-6.2-7] N85-36143
Delayed particles in EAS at Akeno
[HE-6.2-8] N85-36144
Energetic delayed hadrons in large air showers observed at 5200m above sea level
[HE-6.2-9] N85-36145
Search for long-lived massive particles in extensive air showers
[HE-6.2-10] N85-36146
Search for tachyons associated with extensive air showers in the ground level cosmic radiation
[HE-6.2-13] N85-36149
Progress report on a new search for free e/3 quarks in the cores of 10(15) - 10(16) eV air showers
[HE-6.2-15] N85-36151
Exploring results of the possibility on detecting cosmic ray particles by acoustic way
[HE-7.1-3] N85-36157

SCRAP
Spectral characteristics of grinding sparks used for identification of scrap metals
[PB85-198570] N85-35290
Deposition of nickel-cobalt alloys by controlled-potential electrolysis
[PB85-198562] N85-35291

SCRUBBERS
A study of the control of particulate emissions from turbine engine test cells N85-35205

SEA ICE
The NORDA/FNOC (Naval Ocean Research and Development Activity's/Fleet Numerical Oceanography Center) Polar Ice Prediction System (PIPS)-Arctic: A technical description
[AD-A156332] N85-35577

SEA LEVEL
Particle distributions in approximately 10(14) 10(16) eV air shower cores at sea level N85-35990
Comparison of simulation results with sea-level experimental data on 10(14) - 10(16) air shower cores N85-35993
Particle distributions in approximately 10(13) - 10(16) eV air shower cores at mountain altitude and comparison with Monte Carlo simulations
[HE-4.2-18] N85-35994
Energy spectrum of cascades generated by muons in Baksan underground scintillation telescope
[HE-5.1-15] N85-36077
Range fluctuations of high energy muons passing through matter
[HE-5.2-19] N85-36095

SEA SURFACE TEMPERATURE
Sea surface and remotely sensed temperatures off Cape Mendocino, California
[NASA-TM-86712] N85-35573

SEA WATER
Microwave properties of a quiet sea
[NASA-CR-176199] N85-35322
Underwater measurements of muon intensity
[HE-5.1-16] N85-36078
Background light measurements at the DUMAND site
[HE-5.2-7] N85-36084
Measurements of light background at large depth in the ocean
[HE-5.2-8] N85-36085
Analytical calculation of muon intensities under deep sea-water
[HE-5.2-16] N85-36092
Modular detector for deep underwater registration of muons and muon groups
[HE-5.4-15] N85-36125

SEALS (STOPPERS)
SRB attach ring phenolic TPS fishtail seal evaluation tests
[NASA-CR-170887] N85-35407

SECONDARY COSMIC RAYS
The multiplicity and the spectra of secondaries correlated with the leading particle energy
[HE-3.2-11] N85-35919
Characteristics of anomalously high multiplicity cosmic ray interactions
[HE-3.3-1] N85-35920
Peculiarities of gamma-quanta distribution at 20 TeV energy
[HE-3.7-10] N85-35967

SECONDARY EMISSION
Characteristics of slow particles emitted in the charged current interactions of neutrinos with emulsion nuclei
[HE-5.3-22] N85-36113
Underground measurements on secondary cosmic rays
[HE-5.4-1] N85-36116
Analysis of the electron component of EAS at observational level 700 g x cm(-2) with a scale breaking interaction model and gammaisation hypothesis
[HE-5.4-8] N85-36119

SEDIMENTARY ROCKS
Marine phosphorite deposits model for exploration, with emphasis on deposits in the US Atlantic coastal plain N85-35439
Seismic stratigraphic analysis of the Mississippi Fan N85-35507
Geology and geomorphology of the Roraima group, southeastern Venezuela N85-35511

SEDIMENTS
Origin of sedimentary humic acids, potential carriers of ore-forming elements N85-35443
Depositional systems and coal occurrence in the Fort Union Formation (Paleocene), Powder River Basin, Wyoming and Montana N85-35505
Bibliography on tidal hydraulics. Report 2. Supplement 9: Supplementary material compiled from June 1980 - June 1983. Tidal flows in rivers and harbors
[AD-A155990] N85-35574

SEISMIC WAVES
Attenuation properties of the Petatlan region, Mexico, and a local magnitude scale for microearthquakes in this area N85-35513
Applications of the Kirchoff-Helmholtz integral to problems in body wave seismology N85-35515
Workshop Proceedings: Interpretation of Seismic Wave Propagation in Laterally Heterogeneous Structures
[BMR-258] N85-35530

SEISMOLOGY
Seismic stratigraphic analysis of the Mississippi Fan N85-35507
Attenuation properties of the Petatlan region, Mexico, and a local magnitude scale for microearthquakes in this area N85-35513
Applications of the Kirchoff-Helmholtz integral to problems in body wave seismology N85-35515

SELECTIVE DISSEMINATION OF INFORMATION
Source header list, supplement 3
[AD-A156100] N85-35824
Source hierarchy list. Volume 2: I through Z
[AD-A156301] N85-35826
SEMICONDUCTOR DEVICES
Error-correcting codes for computer memories N85-35636
Electron irradiation of N type cadmium telluride
[AD-A156117] N85-35801
Optical properties of heterostructures and superlattices
[AD-A156243] N85-35802
SEMICONDUCTOR JUNCTIONS
HgCdTe surface and defect study program
[AD-A156079] N85-35799
SEMICONDUCTOR LASERS
Optical properties of heterostructures and superlattices
[AD-A156243] N85-35802
SEMICONDUCTORS (MATERIALS)
Electronic structure and lattice dynamics of dimensionally constrained and disordered solids
[AD-A155927] N85-35797
Investigations of the molecular beam epitaxial growth and characteristics of external excitation induced non-equilibrium phases of immiscible 3-5 compound semiconductors
[AD-A156325] N85-35804
SENSITIVITY
Friction, impact, and electrostatic discharge sensitivities of energetic materials
[DE85-013321] N85-35309
Assessment of metal heating technologies for ferrous forging: A pilot study of the form value of natural gas
[PB85-204394] N85-35314
Reliability prediction of the series system with spares subject to Weibull failure N85-35413
Risk analysis and sensitivity: Antithesis or synthesis
[B8562444] N85-35687
Measurement of uranium enrichment for gaseous uranium at low pressure
[DE85-012697] N85-35733
SENSORS
Atmospheric nitrogen oxides: Their detection and chemistry
[PB85-193910] N85-35502
SENSORY PERCEPTION
Testbed for sensory control of intelligent machines
[DE85-012355] N85-35412
A review of motion sickness with special reference to simulator sickness
[AD-A155975] N85-35611
Thirst and fluid intake following graded hypohydration levels in humans
[AD-A156201] N85-35615
SEPARATORS
Cationic exchange membrane for the zinc-ferricyanide battery
[DE85-013152] N85-35489
SERVOMOTORS
Computer simulation of a cruise missile using brushless dc motor fin control
[AD-A155935] N85-35349
SHALE OIL
Aspects of high-resolution gas chromatography as applied to the analysis of hydrocarbon fuels and other complex organic mixtures. Volume 1
[AD-A156154] N85-35257
SHEAR STRESS
Stress analysis of axisymmetric sandwich shells of variable thickness N85-35419
SHELL STABILITY
Stress analysis of axisymmetric sandwich shells of variable thickness N85-35419
SHELLS (STRUCTURAL FORMS)
Membrane reinforcement in concrete shells: Design versus nonlinear behavior N85-35312
Response of a BWR Mark 2 containment vessel head to loads beyond the design basis
[DE85-010524] N85-35432
SHIELDING
Design considerations for personnel access penetrations for the superconducting super collider
[DE85-013027] N85-35807
SHOCK FRONTS
Properties of 10 (18)-10 (19)eV EAS at far core distance
[HE-4.7-3] N85-36054
A note on some statistical properties of rise time parameters used in muon arrival time measurements
[HE-4.7-12] N85-36062
SHOCK WAVE ATTENUATION
Supersonic flow with feeding of energy
[NASA-TM-77912] N85-35163
Attenuation properties of the Petatlan region, Mexico, and a local magnitude scale for microearthquakes in this area N85-35513
SHOCK WAVE PROFILES
Deceleration of a supersonic flow behind a curved shock wave with isentropic precompression
[NASA-TM-77920] N85-35164
Ground motion measurements for the QUESO nuclear event
[DE85-014806] N85-35743
SHOCK WAVE PROPAGATION
Ground motion measurements for the QUESO nuclear event
[DE85-014806] N85-35743
SHOCK WAVES
Finite analytic solutions of supersonic flows in two-dimensional non-symmetrical channels N85-35154
Unsteady flow in a supersonic cascade with two in-passage shocks
[NASA-CR-3925] N85-35158
Numerical studies of 2-dimensional flows
[NASA-CR-3930] N85-35160
Computation of three-dimensional shock wave and boundary-layer interactions
[NASA-TM-86780] N85-35372
SHORT TAKEOFF AIRCRAFT
Presentation of the acoustic and aerodynamic results of the Aladin 2 concept qualification testing
[NASA-TM-77883] N85-35161
SHOT PEENING
Development of a mathematical model for predicting the percentage fatigue life increase resulting from shot peened components
[AD-A155774] N85-35425
SHRINKAGE
Microshrink, tensile properties, and the detection of microshrink
[AD-A155875] N85-35278
SIEVES
Molecular and macromolecular sieving by asymmetric ultrafiltration membranes
[PB85-157766] N85-35266
SIGNAL DETECTION
Manual and computer-aided sequential diagnostic inference
[AD-A156229] N85-35620
SIGNAL DETECTORS
Advanced detectors and signal processing
[NASA-CR-176193] N85-35343
SIGNAL PROCESSING
Nonlinear digital phase-locked loops with application to Loran-C receivers N85-35178
Advanced detectors and signal processing
[NASA-CR-176193] N85-35343
Aspects of input signal design for order and parameter estimation in linear dynamical systems
[ER-83/05] N85-35362
SIG: A general-purpose signal processing program. User's manual: Revision 1
[DE85-013035] N85-35662
SIGNAL TO NOISE RATIOS
Search for acoustic signals from high energy cascades
[HE-7.1-1] N85-36155
Acoustic detection of air shower cores
[HE-7.1-4] N85-36158
SIGNAL TRANSMISSION
Signal space models for antenna arrays
[AD-A156063] N85-35335
SIGNS AND SYMPTOMS
A review of motion sickness with special reference to simulator sickness
[AD-A155975] N85-35611
SILICON
Oxidation resistant slurry coating for carbon-based materials
[NASA-CASE-LEW-13923-1] N85-35267
Dangling bonds and sub-gap optical absorption in silicon
[DE85-011752] N85-35302
Advanced detectors and signal processing
[NASA-CR-176193] N85-35343
Photoconductive pulse power switches: A review
[DE85-014125] N85-35360
Cryogenic laser calorimetry for impurity analysis
[NASA-CR-176179] N85-35395
Electronic structure and lattice dynamics of dimensionally constrained and disordered solids
[AD-A155927] N85-35797
SILICON ALLOYS
Studies of the crystallization process of aluminum-silicon alloys using a high temperature microscope
[NASA-TM-77869] N85-35272
SILICON CARBIDES
Oxidation resistant slurry coating for carbon-based materials
[NASA-CASE-LEW-13923-1] N85-35267
SILICON COMPOUNDS
Center for Electronics and Electrical Engineering technical progress bulletin covering center programs, July-September with 1985 CEEE events calendar
[PB85-191393] N85-35383
Circumstellar shells of late-type stars: A study at millimeter and infrared wavelengths N85-35836
SILICON DIOXIDE
Characterization of catalysts with metal-support effects and of the species adsorbed on their surfaces
[DE85-012254] N85-35394
SILICON NITRIDES
Method for measuring surface activity of silicon nitride powder
[NASA-TM-77906] N85-35242
SILICONIZING
Studies of the crystallization process of aluminum-silicon alloys using a high temperature microscope
[NASA-TM-77869] N85-35272
SILVER
Noise in silver beta alumina ceramics
[AD-A156135] N85-35297
New silver resource map of the United States: Potential for increased domestic silver production N85-35445
SILVER ALLOYS
Studies of the crystallization process of aluminum-silicon alloys using a high temperature microscope
[NASA-TM-77869] N85-35272
SIMULATION
Simulated effects of increased recharge on the ground-water flow system of Yucca Mountain and vicinity, Nevada-California
[DE85-012985] N85-35469
Application of pulsed power in the simulation of severe natural lightning
[DE85-012666] N85-35584
Simulation of high +Gz onset in the dynamic environment simulator
[AD-A155963] N85-35610
Constrained stiffness matrix adjustment using mode data
[AD-A155988] N85-35685
A simulation of ultra-relativistic nucleus-nucleus collisions N85-35707
Detector requirements for intensity interferometry measurements N85-35709
A lead glass tubing drift calorimeter N85-35711
Pulsed-neutron-source models for the astrophysical s-process
[DE85-012927] N85-35740
Numerical studies of high current beam compression in heavy ion fusion
[DE85-011874] N85-35783
Multiplicity distributions in interaction models used for cascade simulations
[HE-1.2-5] N85-35883
Some remarks about simulation of cosmic ray phenomena with use of nuclear interaction models based on the current SPS proton-antiproton data
[HE-1.2-6] N85-35884
Relation between gamma-ray family and EAS core: Monte-Carlo simulation of EAS core
[HE-3.6-7] N85-35955
The lateral distributions of charged particles of energy greater than 0.3 E sub crit in electron-photon cascades in lead and air
[HE-3.6-10] N85-35957
Result of Monte-Carlo simulation of electron-photon cascades in lead and layers of lead-scintillator
[HE-3.6-11] N85-35958
A study of gamma-families generated in nucleon-nucleus (NA) and pion-nucleus (pi A) interactions
[HE-3.7-2] N85-35961
Hadrons registration in emulsion chamber with carbon block
[HE-3.7-3] N85-35962
New analysis of nuclear interaction observed by Mt. Kanbara emulsion chamber experiment
[HE-3.7-4] N85-35963
Intensities of high-energy cosmic rays at Mount Kanbala
[HE-3.7-5] N85-35964
Structured events in Pamir carbon X-ray chambers
[HE-3.7-7] N85-35965
Ultra high energy events in ECHOS series and primary energy spectrum
[HE-3.7-9] N85-35966
Peculiarities of gamma-quanta distribution at 20 TeV energy
[HE-3.7-10] N85-35967
Analysis of equi-intensity curves and NU distribution of EAS N85-35970

Electrons, muons and hadrons in extensive air showers and how do they depend on nuclear interaction model, part 1 N85-35972
Simulation of EAS properties on the basis of high energy interaction model deduced from the accelerator data N85-35973
New aspects in nucleon-nucleus collisions and EAS properties around 10(6) GeV N85-35974
Small air showers and collider physics [HE-4.1-9] N85-35975
High energy hadrons in extensive air showers N85-35976
Hadronic components of EAS by rigorous saddle point method in the energy range between 10(5) and 10(8) GeV N85-35978
About increase of the large transvere momentum processes fraction in hA interactions at energies 5.10(14) - 10(16) eV according to the data on E.A.S. hadrons N85-35979
Phenomenology of soft hadron interactions and the relevant EAS data N85-35980
Theoretical study of EAS hadronic structure N85-35991
Comparison of simulation results with sea-level experimental data on 10(14) - 10(16) air shower cores N85-35993
Particle distributions in approximately 10(13) - 10(16) eV air shower cores at mountain altitude and comparison with Monte Carlo simulations [HE-4.2-18] N85-35994
The longitudinal development of muons in cosmic ray air showers at energies 10(15) - 10(17) eV [HE-4.3-12] N85-36006
Topological aspects of age parameter [HE-4.3-13] N85-36007
Monte Carlo simulation of EAS generated by 10(14) - 10(16) eV protons [HE-4.3-14] N85-36008
Hybrid TLC-pair meter for the Sphinx Project [HE-5.2-10] N85-36086

SIMULATORS
Gust simulation for flight mechanical wind tunnel tests N85-35172
A review of motion sickness with special reference to simulator sickness [AD-A155975] N85-35611

SINGLE CRYSTALS
Wholebody radiation counting system [AD-A155842] N85-35607

SITE SELECTION
Simulated effects of increased recharge on the ground-water flow system of Yucca Mountain and vicinity, Nevada-California [DE85-012985] N85-35469
Siting of large scale wind turbines in Denmark N85-35483
Special questions of siting wind turbine arrays and networks — West Germany N85-35484
Environmental aspects of the Netherlands wind farm project N85-35485
Visual impact of GROWIAN and resulting recommendations for siting of large wind energy converters N85-35486

SIZE (DIMENSIONS)
An exploratory study of the effect of screen size and resolution on the legibility of graphics in automated job performance aids [AD-A155989] N85-35632

SIZE DISTRIBUTION
Atmospheric neutrinos observed in underground detectors [HE-5.3-8] N85-36102

SKIN (STRUCTURAL MEMBER)
A normal incidence X-ray telescope sounding rocket payload [NASA-CR-176169] N85-35749

SKIRTS
Results of tests on a specimen of the SRB aft skirt heat shield curtain in the MSFC LRLF [NASA-CR-170883] N85-35221
SRB TPS closeout materials characterization [NASA-CR-170885] N85-35222
Study of NSI and related cable performance during tests performed in the NASA Hot Gas Facility [NASA-CR-170886] N85-35423

SLEDS
Design and testing of an energy-absorbing crewseat for the F/FB-111 aircraft. Volume 2: Data from seat testing [NASA-CR-3917] N85-35184

SLOPES
Evaluation: Close-range photogrammetry for slope inventory and monitoring [PB85-192755] N85-35470
Turbulent structure of stably stratified nocturnal slope flows [AD-A155845] N85-35559

SLOT ANTENNAS
Characteristic modes for slots in a ground plane TE case [AD-A155757] N85-35326

SLURRIES
Method of preparing thin porous sheets of ceramic material [DE85-006399] N85-35300

SMELTING
Assessment of metal heating technologies for ferrous forging: A pilot study of the form value of natural gas [PB85-204394] N85-35314

SMOG
Studies in photochemical smog chemistry. 1: Atmospheric chemistry of toulene. 2: Analysis of chemical reaction mechanisms for photochemical smog N85-35497

SNOW
Elemental tracers of source regions of contaminants in precipitation [DE85-012858] N85-35499

SODIUM
Effect of temperature and ionic impurities at very low concentrations on stress corrosion cracking of Type 304 stainless steel [TI85-003048] N85-35283
Development and evaluation of sulfonated polysulfone membranes for the zinc-ferricyanide battery [DE85-009104] N85-35357
A study of the chemistry of alkali metals in the upper atmosphere [AD-A156349] N85-35524
Noise in sodium beta alumina crystals [AD-A156025] N85-35798
A new drawing technique for nylon 6 by reversible plasticization with iodine [AD-A156272] N85-35803

SODIUM CHLORIDES
Experimental investigation of radiative-acoustic effects in the water by the thermodynamical conditions of Dumand [HE-7.1-2] N85-36156

SOFTWARE ENGINEERING
Calculation of the diffusion of light by aerosols: Description of the MIELOR software and results obtained [REPT-80] N85-35638
CRAYCDC [NASA-CR-177374] N85-35639
CDCCRAY [NASA-CR-177375] N85-35640
Study of fault tolerant software technology for dynamic systems [NASA-CR-172618] N85-35642
Attacking software crisis: A macro approach [AD-A155846] N85-35645
Prototyping with data dictionaries for requirements analysis [AD-A156303] N85-35654
Toolpack [DE85-013135] N85-35665

SOFTWARE TOOLS
Study of fault tolerant software technology for dynamic systems [NASA-CR-172618] N85-35642
Attacking software crisis: A macro approach [AD-A155846] N85-35645
Error message recording and reporting in the SLC control system [DE85-013057] N85-35664

SOILS
Mineral deposit models: Theory and practice N85-35448
Development of an NBS (National Bureau of Standards) polymer gage for dynamic soil stress measurement [PB85-208494] N85-35526
The measurement of nitrogen oxide (NO, NO2) exchange over plant/soil surfaces [CSIRO-DAR-TP-8] N85-35587

SOLAR CELLS
Practical aspects of photovoltaic technology, applications and cost (revised) [NASA-CR-174963] N85-35472
Photovoltaics technology program summary [DE85-013098] N85-35493
Design and construction of an advanced power conditioning subsystem for small photovoltaic applications [DE85-013940] N85-35495

SOLAR COLLECTORS
Solar pond technology for Navy applications [AD-A155877] N85-35488

SOLAR ENERGY CONVERSION
Practical aspects of photovoltaic technology, applications and cost (revised) [NASA-CR-174963] N85-35472

SOLAR FLARES
Preliminary results of the Cerenkov EAS flashes the Crimean Astrophysical Observatory [HE-4.4-17] N85-36023
High-energy neutrinos from a lunar observatory [HE-5.3-21] N85-36112

SOLAR HEATING
Solar pond technology for Navy applications [AD-A155877] N85-35488

SOLAR MAXIMUM MISSION
The 1986 National Aeronautics and Space Administration authori. tion [GPO-47-635] N85-35829

SOLAR NEUTRINOS
The research program of the Liquid Scintillation Detector (LSD) in the Mont Blanc Laboratory [HE-5.3-6] N85-36100
High energy neutrino astronomy with MACRO [HE-5.3-12] N85-36106

SOLAR OBSERVATORIES
Development of observational and instrumental techniques in hard X-ray and medium energy gamma-ray astronomy [NASA-CR-176172] N85-3[illegible]41

SOLAR ORBITS
Development of observational and instrumental techniques in hard X-ray and medium energy gamma-ray astronomy [NASA-CR-176172] N85-35841

SOLAR PONDS (HEAT STORAGE)
Solar pond technology for Navy applications [AD-A155877] N85-35488
Energy from low temperature differences [DE85-008817] N85-35492

SOLAR RADIATION
Space Station Polar Platform: Integrating research and operational missions [PB85-195279] N85-35218

SOLAR SYSTEM
The nature and origin of outer solar system asteroids from reflectance spectrophotometry N85-35838

SOLAR TERRESTRIAL INTERACTIONS
Space Station Polar Platform: Integrating research and operational missions [PB85-195279] N85-35218

SOLAR WIND
Parallel fast-forward shock within 1 AU: Helios-1 and 2 observations [MPAE-W-79-84-27] N85-35847

SOLID PROPELLANT ROCKET ENGINES
Verification of the SRB motor case pin retainer band tips [NASA-CR-170882] N85-35220
Results of tests on a specimen of the SRB aft skirt heat shield curtain in the MSFC LRLF [NASA-CR-170883] N85-35221
Dissected motors-propellants motor number STM-012. Phase 15: Surveillance report, stage 1 [AD-A156088] N85-35226
Results of tests of K5NA and a revised formulation of EPDM/cork patch material in MSFC Hot Gas Facility [NASA-CR-170890] N85-35238
Evaluation of SRB phenolic TPS material made by an alternate vendor [NASA-CR-170894] N85-35240
Space shuttle SRB TPS protective paint test and evaluation in NASA Hot Gas Facility and AEDC Tunnel C [NASA-CR-170884] N85-35294
Results of tests of Insta-Foam Thermal Protection System (TPS) material for protection of equipment inside the SRB aft skirt [NASA-CR-170892] N85-35295

SOLID SOLUTIONS
Cluster variation study of coherent ordering in FCC and BCC solid solutions [AD-A156039] N85-35280

SOLID STATE
Solid state high power amplifier for driving the SLC injector klystron [DE85-013063] N85-35356
State-of-the-art of solid-state motor controllers [TI85-008674] N85-35806
Ionic crystals [DE85-009482] N85-35809

SOLIDS
Experimental technique for measuring the isentrope of hydrogen to several megabars [DE85-014332] N85-35386

Analysis of the nonlinear equations describing the elastic, thermal, and electromagnetic behavior of solids: Existence of solutions of semi-inverse problems N85-35415

SOLVENTS
Production of butanol by fermentation in the presence of cocultures of clostridium
[NASA-CASE-NPO-16203-1] N85-35227

SOOT
An analytical and numerical model of radiation heat transfer in direct injection-type diesel combustion N85-35368

SORPTION
Biodegradation of jet fuel by aquatic microbial communities
[PB85-191971] N85-35311

SOUND WAVES
A comparison of multipath arrival structures observed in the presence of a surface duct with predictions obtained using classical ray techniques and the parabolic equation method
[AD-A156024] N85-35696
Search for acoustic signals from high energy cascades
[HE-7.1-1] N85-36155
Experimental investigation of radiative-acoustic effects in the water by the thermodynamical conditions of Dumand
[HE-7.1-2] N85-36156
Acoustic detection of air shower cores
[HE-7.1-4] N85-36158

SOUNDING ROCKETS
A normal incidence X-ray telescope sounding rocket payload
[NASA-CR-176169] N85-35749

SPACE CHARGE
Numerical studies of high current beam compression in heavy ion fusion
[DE85-011874] N85-35783
Relation between field energy and RMS emittance in intense particle beams
[DE85-012655] N85-35784

SPACE ENVIRONMENT SIMULATION
DMSK: A practical 2400-bps receiver for the mobile satellite service: An MSAT-X Report
[NASA-CR-176194] N85-35324

SPACE MANUFACTURING
Investment justification of robotic technology in aerospace manufacturing. User's manual
[AD-A156193] N85-35410

SPACE MISSIONS
Space Missions for Automation and Robotics Technologies (SMART) Program
[NASA-TM-86820] N85-35210

SPACE POWER REACTORS
Strategic defense initiative
[DE85-012778] N85-35735

SPACE SHUTTLE BOOSTERS
SRB TPS closeout materials characterization
[NASA-CR-170885] N85-35222
SRB thermal protection systems materials test results in an arc-heated nitrogen environment
[NASA-CR-170881] N85-35236
Study of NSI and related cable performance during tests performed in the NASA Hot Gas Facility
[NASA-CR-170866] N85-35423

SPACE SHUTTLE MAIN ENGINE
SRB thermal protection systems materials test results in an arc-heated nitrogen environment
[NASA-CR-170881] N85-35236

SPACE SHUTTLES
Space Missions for Automation and Robotics Technologies (SMART) Program
[NASA-TM-86820] N85-35210
Results of tests of the SRB aft skirt heat shield curtain in the MSFC Hot Gas Facility
[NASA-CR-170888] N85-35223
Evaluation of SRB phenolic TPS material made by an alternate vendor
[NASA-CR-170894] N85-35240
Space shuttle SRB TPS protective paint test and evaluation in NASA Hot Gas Facility and AEDC Tunnel C
[NASA-CR-170884] N85-35294
Results of tests of Insta-Foam Thermal Protection System (TPS) material for protection of equipment inside the SRB aft skirt
[NASA-CR-170892] N85-35295
The 1986 National Aeronautics and Space Administration authorization
[GPO-47-635] N85-35829

SPACE STATIONS
Technology for large space systems: A bibliography with indexes
[NASA-SP-7046(12)] N85-35209
Space Missions for Automation and Robotics Technologies (SMART) Program
[NASA-TM-86820] N85-35210
Space Station Polar Platform: Integrating research and operational missions
[PB85-195279] N85-35218
The 1986 National Aeronautics and Space Administration authorization
[GPO-47-635] N85-35829

SPACE WEAPONS
Strategic defense initiative
[DE85-012778] N85-35735

SPACEBORNE EXPERIMENTS
NASA Developmental Biology Workshop: A summary
[NASA-TM-86756] N85-35578

SPACECRAFT COMMUNICATION
Second-generation mobile satellite system. A conceptual design and trade-off study
[NASA-CR-176195] N85-35325

SPACECRAFT CONTROL
Identification and control of structures in space
[NASA-CR-176175] N85-35214
TRICCS: A proposed teleoperator/robot integrated command and control system for space applications
[NASA-TM-87577] N85-35637
Enhancement of the flexible spacecraft dynamics program for open spacecraft
[NASA-CR-175309] N85-35641

SPACECRAFT MANEUVERS
Identification and control of structures in space
[NASA-CR-176175] N85-35214

SPACECRAFT POWER SUPPLIES
Development and characterization of carbon-bonded carbon fiber insulation for radioisotope space power systems
[DE85-013365] N85-35299

SPACECRAFT TRACKING
Optical receivers using rough reflectors
[NASA-CR-176200] N85-35750

SPACELAB
The 1986 National Aeronautics and Space Administration authorization
[GPO-47-635] N85-35829

SPALLATION
Los Alamos high-current proton storage ring
[DE85-012664] N85-35779

SPALLING
High temperature corrosion of ceramics
[DE85-013481] N85-35303

SPARE PARTS
Reliability prediction of the series system with spares subject to Weibull failure N85-35413
DoD Value Engineering conference report. Value Engineering (VE): A tool that benefits line management. Part 4, Workshop B: VE on spare parts
[AD-A156070] N85-35813

SPARK CHAMBERS
Relation between gamma-ray family and EAS core: Monte-Carlo simulation of EAS core
[HE-3.6-7] N85-35955
The Nagoya cosmic-ray muon spectrometer 3, part 2: Track detector
[HE-5.2-3] N85-36081

SPARK GAPS
Statistical distribution of breakdown voltages in rep-rate spark gaps
[DE85-012813] N85-35354

SPARKS
Spectral characteristics of grinding sparks used for identification of scrap metals
[PB85-198570] N85-35290

SPATIAL DISTRIBUTION
Noise-sustained structure, intermittency and the Ginzburg-Landau equation
[DE85-009626] N85-35379
Use of a minimum-ellipse criterion in the study of ion-beam extraction systems
[DE85-012670] N85-35721
Tskhra-Tskaro complex intended for the investigations of EAS spatial characteristics near axis N85-35995
Hybrid TLC-pair meter for the Sphinx Project
[HE-5.2-10] N85-36086
Spatial distribution read-out system for thermoluminescence sheets
[HE-7.1-7] N85-36161

SPATIAL RESOLUTION
Adaptive rezoner in a two-dimensional Lagrangian hydrodynamic code
[DE85-010108] N85-35381
Proportional drift tubes for large area muon detectors
[HE-5.2-11] N85-36087

SPECIFIC HEAT
Experimental investigation of radiative-acoustic effects in the water by the thermodynamical conditions of Dumand
[HE-7.1-2] N85-36156

SPECIFICATIONS
Specifying and verifying concurrent programs
[AD-A156190] N85-35652
SLC arc transport system: Magnet design and construction
[DE85-014289] N85-35789

SPECIMENS
The preparation of TEM specimens showing oxide scales in transverse cross-section
[AERE-R-11579] N85-35276

SPECTRA
Master Fit users' guide, version 1.0
[DE85-014199] N85-35667

SPECTRAL EMISSION
A comparison of LANDSAT thematic mapper, multispectral scanner and airborne sensors for mapping the distribution of alteration minerals: Examples from the southwestern United States N85-35452
Observations of far-infrared transitions between excited states of OH
[NASA-TM-86722] N85-35833

SPECTRAL ENERGY DISTRIBUTION
Some rigorous results concerning spectral theory for ideal MHD
[DE85-013427] N85-35770
The structure of the shower disk observed at Mt. Norikura
[HE-4.7-1] N85-36052
Structure of air shower disc near the core
[HE-4.7-2] N85-36053
A mini-array for large air showers
[HE-4.7-10] N85-36061
A note on some statistical properties of rise time parameters used in muon arrival time measurements
[HE-4.7-12] N85-36062

SPECTRAL METHODS
Study of spectral/radiometric characteristics of the Thematic Mapper for land use applications
[E85-10106] N85-35464

SPECTRAL REFLECTANCE
Processing of LANDSAT imagery to map surface mineral alteration on the Alaska Peninsula, Alaska N85-35455

SPECTRAL THEORY
Some rigorous results concerning spectral theory for ideal MHD
[DE85-013427] N85-35770

SPECTROGRAPHS
A new study of muons in air showers by NBU air shower array N85-35997

SPECTROMETERS
Investigation of cosmic rays in very short time scales
[HE-4.6-7] N85-36044
A facility for investigation of multiple hadrons at cosmic-ray energies
[HE-4.6-8] N85-36045
Fast scintillation counter system and performance
[HE-4.6-10] N85-36047

SPECTROPHOTOMETRY
The nature and origin of outer solar system asteroids from reflectance spectrophotometry N85-35838

SPECTRORADIOMETERS
A comparison of LANDSAT thematic mapper, multispectral scanner and airborne sensors for mapping the distribution of alteration minerals: Examples from the southwestern United States N85-35452

SPECTROSCOPY
Literature search for new physical methods for biological aerosol detection
[AD-A155883] N85-35592
High-resolution spectroscopy and dynamics of multiphoton processes in atoms and molecules
[AD-A155862] N85-35714

SPECTRUM ANALYSIS
The application of bispectral analyses to aeroelastic phenomena N85-35157
The spectrum of cosmic ray muons obtained with 100-ton scintillation detector underground and the analysis of recent experimental data
[HE-5.1-6] N85-36071

SPECULAR REFLECTION
Signal space models for antenna arrays
[AD-A156063] N85-35335

SPEED INDICATORS
Development of contactless sensors for industrial and automative applications
[BMFT-FB-T-85-031] N85-35400

SPENT FUELS
Analytical methods in the purex process
[BLL-DOUNREAY-TR-952(9091.9F)] N85-35727

SPHERICAL SHELLS
The effect of power law body forces on a thermally-driven flow between concentric rotating spheres
[NASA-TM-87596] N85-35374

SPIN DYNAMICS
Dual towline spin-recovery device
[NASA-CASE-LAR-13076-1] N85-35200

Studies of the solar mesosphere explorer: Dynamics and horizon sensor performance. Part A: Spin axis precession and atmospheric drag. Part B: Clouds
[NASA-CR-175308] N85-35213
The NORDA/FNOC (Naval Ocean Research and Development Activity's/Fleet Numerical Oceanography Center) Polar Ice Prediction System (PIPS)-Arctic: A technical description
[AD-A156332] N85-35577

SPIN RESONANCE
Dangling bonds and sub-gap optical absorption in silicon
[DE85-011752] N85-35302

SPLINE FUNCTIONS
Smoothing surface data by spline functions
[AD-A155829] N85-35678

STABILITY
Parametric stability of analytical close-range photogrammetry N85-35461
Relaxation phenomena and stability of probability densities
[AD-A155923] N85-35682
Analysis of reactor material experiments investigating oxide fuel crust stability and heat transfer in jet impingement flow
[DE85-012097] N85-35739

STABILIZATION
Design of dynamic compensators of prescribed pattern
[BU-109] N85-35674
Spreading the control complexity in decentralized control of interconnected systems
[BU-117] N85-35688
Decentralized stabilization by high gain feedback
[BU-115] N85-35689

STABILIZERS (FLUID DYNAMICS)
A towed instrument vehicle for deep ocean sampling
[AD-A156322] N85-35576

STAINING
Processing of LANDSAT imagery to map surface mineral alteration on the Alaska Peninsula, Alaska N85-35455

STAINLESS STEELS
Electrochemical method for investigation of the susceptibility of corrosion-resistant steels to intercrystalline corrosion
[BLL-CE-TRANS-8082-(9022.09)] N85-35269
Effect of temperature and ionic impurities at very low concentrations on stress corrosion cracking of Type 304 stainless steel
[TI85-003048] N85-35283
X-ray fluorescence analysis of 304L stainless steel
[DE85-013254] N85-35288
Spectral characteristics of grinding sparks used for identification of scrap metals
[PB85-198570] N85-35290
Analysis of reactor material experiments investigating oxide fuel crust stability and heat transfer in jet impingement flow
[DE85-012097] N85-35739

STANDARD DEVIATION
Large deviations for the maxima of some random fields
[AD-A155909] N85-35681

STANDARDIZATION
Development of NATOPS (Naval Air Training and Operating Procedure Standardization) performance software for the H-46D helicopter
[AD-A156089] N85-35190
Necessary bandwidth and spectral properties of digital modulation
[PB85-185387] N85-35340
Redefining the scratch standards
[PB85-194736] N85-35755

STANDARDS
Redefining the scratch standards
[PB85-194736] N85-35755

STAR CLUSTERS
Far-infrared observations of young clusters embedded in the R Coronae Austrinae and RHO Ophiuchi dark clouds
[NASA-TM-86681] N85-35834

STARS
The capability of the existing network of installations for detecting the antineutrino burst from collapsing stars
[HE-5.3-13] N85-36107

STATIC LOADS
Static and cyclic behavior of semi-rigid steel beam-column connections
[PB85-194363] N85-35433

STATIC TESTS
Static and cyclic behavior of semi-rigid steel beam-column connections
[PB85-194363] N85-35433

STATISTICAL ANALYSIS
Statistical distribution of breakdown voltages in rep-rate spark gaps
[DE85-012813] N85-35354
Users guide for optimum interpolation method of global data assimilation
[AD-A155929] N85-35648
Risk analysis and sensitivity: Antithesis or synthesis
[B8562444] N85-35687

STATISTICAL CORRELATION
The relationship between personality and performance N85-35600

STATISTICAL DISTRIBUTIONS
Statistical distribution of breakdown voltages in rep-rate spark gaps
[DE85-012813] N85-35354
Large deviations for the maxima of some random fields
[AD-A155909] N85-35681
The model of independent particles emission in the multiparticle production theory
[HE-3.2-10] N85-35918

STATISTICAL MECHANICS
Cluster variation study of coherent ordering in FCC and BCC solid solutions
[AD-A156039] N85-35280

STATISTICAL WEATHER FORECASTING
An atmospheric boundary layer model forced by the operational ECMWV-model
[WSR-3] N85-35541
Users guide for optimum interpolation method of global data assimilation
[AD-A155929] N85-35648
Two methods of global data assimilation
[AD-A155981] N85-35684

STEADY STATE
The geostatistical approach to the inverse problem in two-dimensional steady state groundwater modeling N85-35462

STEAM
Pressure measurements in a hydrogen combustion environment: Hydrogen-air combustion test series 1 and 2 in the FITS tank, volume 1
[TI85-009899] N85-35259
Heat transfer coefficients for particles in liquid in axially rotating cans N85-35370
Steamflood pilots in the O'Connell Ranch field and the T-4 Ranch field
[DE85-901363] N85-35468

STEAM TURBINES
Computer code calculations of the TMI-2 accident: Initial and boundary conditions
[DE85-012613] N85-35666

STEELS
Decomposition of martensite in R6M5 and R6AM5 steels after direct immersion in liquid nitrogen
[BLL-M-36305] N85-35268
Tests on zirconium nitride coatings applied to SW 18 steel using the chemical vapor deposition method N85-35271
The dynamic strain ageing of A533B class 1 nuclear pressure vessel steel
[AERE-R-11485] N85-35274
The character of observed porosity and its possible effects on rolling contact fatigue life of M-50 steel
[AD-A155930] N85-35279
Effect of prior warm rolling on the retained austenite content and hardening response of VIM-VAR (vacuum-induction melted-vacuum-arc remelted) AISI M-50 steel
[AD-A156145] N85-35281

STEERABLE ANTENNAS
A planar version of a 4.0 gigahertz reactively steered adaptive array
[AD-A156029] N85-35330

STELLAR ACTIVITY
Search for stellar collapse with the MACRO detector at Gran Sasso
[HE-5.3-11] N85-36105

STELLAR ATMOSPHERES
The HEAO-2 Guest Investigator Program: Non-linear growth of instabilities in line-driven stellar winds
[NASA-CR-176168] N85-35840

STELLAR COMPOSITION
Search for stellar collapse with the MACRO detector at Gran Sasso
[HE-5.3-11] N85-36105

STELLAR EVOLUTION
Search for stellar collapse with the MACRO detector at Gran Sasso
[HE-5.3-11] N85-36105

STELLAR ROTATION
Study of the parameters affecting the collapse of a rotating protostellar cloud N85-35837

STELLAR SPECTRA
The HEAO-2 Guest Investigator Program: Non-linear growth of instabilities in line-driven stellar winds
[NASA-CR-176168] N85-35840

STELLAR WINDS
The HEAO-2 Guest Investigator Program: Non-linear growth of instabilities in line-driven stellar winds
[NASA-CR-176168] N85-35840

STELLARATORS
Confinement and heating of high beta plasmas with emphasis on compact toroids
[DE85-011459] N85-35761

STEREOPHOTOGRAPHY
Progress report on a new search for free e/3 quarks in the cores of 10(15) - 10(16) eV air showers
[HE-6.2-15] N85-36151

STIFFNESS MATRIX
Constrained stiffness matrix adjustment using mode data
[AD-A155988] N85-35685

STOICHIOMETRY
CO + H2 reaction over nitrogn-modified iron catalysts
[DE85-013791] N85-35231
Size and shape dependence of CO adsorption sites on sapphire supported Fe microcrystals
[NASA-CR-176171] N85-35794

STORAGE RINGS (PARTICLE ACCELERATORS)
Forty-five years of e(+)e(-) annihilation physics: 1956 to 2001
[DE85-013052] N85-35723
Breeding new light into old machines (and new)
[DE85-013055] N85-35763
Vacuum system for the Argonne 6 GeV synchrotron light source
[DE85-012286] N85-35773
Los Alamos high-current proton storage ring
[DE85-012664] N85-35779
Accelerator physics measurements at the damping ring
[DE85-013373] N85-35785
TOSCA calculations and measurements for the SLAC SLC damping ring dipole magnet
[DE85-014366] N85-35793

STORAGE STABILITY
Dissected motors-propellants motor number STM-012. Phase 15: Surveillance report, stage 1
[AD-A156088] N85-35226

STORAGE TANKS
Results of variable enthalpy tests of CPR-488 TIP panels in MSFC Hot Gas Facility
[NASA-CR-170889] N85-35237

STRAIN GAGES
The compliance of end effector force sensors for robot manipulator control N85-35406
Carbon fiber strainmeter studies in southern California
[PB85-196889] N85-35528

STRAIN MEASUREMENT
Strain measurement using point recognition picture processing
[DRIC-T-7407] N85-35421
1983 review of experimental stress and strain analysis
[DRIC-T-7469] N85-35422

STRAIN RATE
Carbon fiber strainmeter studies in southern California
[PB85-196889] N85-35528
Simulation of lattice damage due to dynamic loading
[DE85-008468] N85-35808

STRANGENESS
A holographic streamer chamber for relativistic nucleus-nucleus collision experiments N85-35710

STRAPS
Verification of the SRB motor case pin retainer band tips
[NASA-CR-170882] N85-35220

STRATEGIC MATERIALS
Applications of the mineral resources data system and the international strategic minerals inventory in mineral-resource assessments by region and commodity N85-35451
Mineral resources programs N85-35456
The Conterminous United States Mineral Assessment Program N85-35458

STRATEGY
Arms control and The President's Strategic Defense Initiative
[AD-A156334] N85-35212

STRATIFICATION
Turbulent structure of stably stratified nocturnal slope flows
[AD-A155845] N85-35559
Analysis of two-parameter constant background born inversion for acoustic synthetic data
[AD-A156394] N85-35698

STRATIFIED FLOW
Some aspects of internal gravity waves in a multi-layered moving stratified flow N85-35369

STRATIGRAPHY
Seismic stratigraphic analysis of the Mississippi Fan N85-35507
STREAM FUNCTIONS (FLUIDS)
A stream function approach to solving the conservative Euler equations for transonic flows N85-35156
STRESS (PHYSIOLOGY)
Report of Amphibian Development Group N85-35583
Weight loss, rectal temperature and heart rates following the 1984 Boston Marathon
[AD-A155984] N85-35612
STRESS ANALYSIS
Damage induced stress redistribution in composite laminates N85-35235
Development of a high strength isothermally heat-treated nodular iron road wheel arm
[AD-A155755] N85-35406
Stress analysis of axisymmetric sandwich shells of variable thickness N85-35419
1983 review of experimental stress and strain analysis
[DRIC-T-7469] N85-35422
On size effects in plane stress crack-growth resistance
[AD-A155926] N85-35426
Simplified procedures for the evaluation of settlements in sands due to earthquake shaking
[PB85-197887] N85-35527
Establishment of a Computer-Aided Design (CAD)-Computer-Aided Manufacturing (CAM) process for the production of cold forged gears
[AD-A155756] N85-35644
The finite element-difference method N85-35672
STRESS CONCENTRATION
Damage induced stress redistribution in composite laminates N85-35235
Static and cyclic behavior of semi-rigid steel beam-column connections
[PB85-194363] N85-35433
The finite element-difference method N85-35672
STRESS CORROSION CRACKING
Effect of temperature and ionic impurities at very low concentrations on stress corrosion cracking of Type 304 stainless steel
[TI85-003048] N85-35283
STRESS CYCLES
Simplified procedures for the evaluation of settlements in sands due to earthquake shaking
[PB85-197887] N85-35527
STRESS INTENSITY FACTORS
Stress-intensity factors for circumferential surface cracks in pipes and rods under tension and bending loads
[NASA-TM-87594] N85-35424
STRESS MEASUREMENT
Development of an NBS (National Bureau of Standards) polymer gage for dynamic soil stress measurement
[PB85-208494] N85-35526
STRESS TENSORS
Analysis of the nonlinear equations describing the elastic, thermal, and electromagnetic behavior of solids: Existence of solutions of semi-inverse problems N85-35415
STRESS-STRAIN RELATIONSHIPS
Development and application of a unified viscoelastic constitutive model for the prediction of material response under thermomechanical loading N85-35420
1983 review of experimental stress and strain analysis
[DRIC-T-7469] N85-35422
STRESSES
Damage induced stress redistribution in composite laminates N85-35235
STRIP TRANSMISSION LINES
Power flow evaluations for HERMES 3
[DE85-013116] N85-35769
STRONG INTERACTIONS (FIELD THEORY)
Dependence of the average spatial and energy characteristics of the hadron-lepton cascade on the strong interaction parameters at superhigh energies N85-35977
STRUCTURAL ANALYSIS
Kinematic analysis of Hurricane Frederick (1979) using satellite, aircraft and rawinsonde data
[NASA-CR-176167] N85-35533
A new method of differential structural analysis of gamma-family basic parameters
[HE-3.6-3] N85-35952
STRUCTURAL BASINS
Geothermal resources of the Washakie and Great Divide basins, Wyoming
[DE85-013004] N85-35491
Depositional systems and coal occurrence in the Fort Union Formation (Paleocene), Powder River Basin, Wyoming and Montana N85-35505
Geology: Structural history and fluvial geomorphology of the southern Death Valley Fault Zone, Inyo and San Bernardino Counties, California N85-35506
STRUCTURAL MEMBERS
User's guide: A computer program for strength analysis of non-hydraulic concrete structural elements. Report 2. Strength design of reinforced concrete column sections (PCAUC)
[AD-A156393] N85-35429
STRUCTURAL PROPERTIES (GEOLOGY)
Structural development of the west-central Grant Range, Nye County, Nevada N85-35508
Crustal structure in southern California from array data N85-35512
SUBARCTIC REGIONS
Current inventory of anthropogenic carbon dioxide in the North Pacific Subarctic Gyre
[PB85-187938] N85-35570
SUBDUCTION (GEOLOGY)
Thermal evolution of coastal California with implications for hydrocarbon maturation N85-35509
A dynamic model of Venus's gravity field
[NASA-CR-176173] N85-35845
SUBMARINES
Preliminary results of an ALVIN dive program on active hydrothermal vents at the southern Juan de Fuca Ridge N85-35454
SUBROUTINES
A quickly tested Pascal random number generator for microcomputers
[AD-A156059] N85-35633
CRAYCDC
[NASA-CR-177374] N85-35639
CDCCRAY
[NASA-CR-177375] N85-35640
SUBSTRATES
Thermal barrier coating system
[NASA-CASE-LEW-14057-1] N85-35233
Oxidation resistant slurry coating for carbon-based materials
[NASA-CASE-LEW-13923-1] N85-35267
Wear-resistant coatings for tools intended for cold working
[BLL-RISLEY-TR-5040-(9091.9F)] N85-35293
Advanced detectors and signal processing
[NASA-CR-176193] N85-35343
Solid neon sources for plasma and X-ray lasers
[DE85-011347] N85-35402
SUGARS
Production of butanol by fermentation in the presence of cocultures of clostridium
[NASA-CASE-NPO-16203-1] N85-35227
SULFATES
Incorporating meteorological data into receptor analysis: RAPS (Regional Air Pollution Study) revisited
[PB85-188944] N85-35503
A new drawing technique for nylon 6 by reversible plasticization with iodine
[AD-A156272] N85-35803
SULFIDES
Some geophysical guides to ore in southern and southwestern Alaska N85-35438
Massive sulfide deposits from the southern Juan de Fuca Ridge N85-35446
SULFONATES
Development and evaluation of sulfonated polysulfone membranes for the zinc-ferricyanide battery
[DE85-009104] N85-35357
SULFUR
Circumstellar shells of late-type stars: A study at millimeter and infrared wavelengths N85-35836
SULFURIC ACID
Determination of the viscosity number of thermoplastics in dilute solution; polyamides (PA)
[NASA-TM-77673] N85-35296
SUMMARIES
A research program to reduce the interior noise in general aviation aircraft, index and summary
[NASA-CR-176178] N85-35695
SUPERCONDUCTING MAGNETS
Enhanced heat transfer computations for internally cooled cable superconductor
[DE85-011897] N85-35383
Effect of Cu4Ti compound formation on the characteristics of NbTi accelerator magnet wire
[DE85-014226] N85-35788
SUPERCONDUCTIVITY
Design considerations for personnel access penetrations for the superconducting super collider
[DE85-013027] N85-35807
SUPERCONDUCTORS
Center for Electronics and Electrical Engineering technical progress bulletin covering center programs, July-September with 1985 CEEE events calendar
[PB85-191393] N85-35363
SUPERHIGH FREQUENCIES
On total cross sections and slopes at superhigh energies
[HE-1.1-4] N85-35852
SUPERLATTICES
Optical properties of heterostructures and superlattices
[AD-A156243] N85-35802
SUPERSONIC FLOW
Finite analytic solutions of supersonic flows in two-dimensional non-symmetrical channels N85-35154
Unsteady flow in a supersonic cascade with two in-passage shocks
[NASA-CR-3925] N85-35158
Supersonic flow with feeding of energy
[NASA-TM-77912] N85-35163
Deceleration of a supersonic flow behind a curved shock wave with isentropic precompression
[NASA-TM-77920] N85-35164
SUPERSONIC WIND TUNNELS
Supersonic flow with feeding of energy
[NASA-TM-77912] N85-35163
SURFACE DEFECTS
Redefining the scratch standards
[PB85-194736] N85-35755
SURFACE FINISHING
Results of tests of weathered K5NA closeout material in the MSFC Hot Gas Facility
[NASA-CR-170893] N85-35239
Wear-resistant coatings for tools intended for cold working
[BLL-RISLEY-TR-5040-(9091.9F)] N85-35293
Size and shape dependence of CO adsorption sites on sapphire supported Fe microcrystals
[NASA-CR-176171] N85-35794
SURFACE PROPERTIES
Redefining the scratch standards
[PB85-194736] N85-35755
Size and shape dependence of CO adsorption sites on sapphire supported Fe microcrystals
[NASA-CR-176171] N85-35794
Electronic structure and lattice dynamics of dimensionally constrained and disordered solids
[AD-A155927] N85-35797
SURFACE REACTIONS
Method for measuring surface activity of silicon nitride powder
[NASA-TM-77906] N85-35242
Prediction of plasticity characteristics for three-dimensional fracture specimens comparison with experiment
[AD-A156425] N85-35430
SURFACE TO SURFACE MISSILES
Dissected motors-propellants motor number STM-012. Phase 15: Surveillance report, stage 1
[AD-A156088] N85-35226
SURFACE VEHICLES
Visual position determination for autonomous vehicle navigation
[AD-A156007] N85-35181
SURFACE WAVES
Second Colloquim on the Scattering of Ultrasonic Waves
[AD-A156298] N85-35697
SURGES
Exploring results of the possibility on detecting cosmic ray particles by acoustic way
[HE-7.1-3] N85-35157
SURVEILLANCE
Evaluation of nuclear detonation location capability under high attack scenario
[AD-A155761] N85-35729
SWALLOWING
Tritium hazard via the ingestion pathway
[DE85-012897] N85-35618
SWIRLING
Flow modifying device
[NASA-CASE-LEW-13562-2] N85-35195
SWITCHES
Photoconductive pulse power switches: A review
[DE85-014125] N85-35360
SYNCHROTRON RADIATION
Dissociative and double photoionization cross sections of NO from threshold to 120 A
[NASA-CR-176185] N85-35713
Exit channels of autoionization resonances in atoms
[DE85-012299] N85-35726
Breeding new light into old machines (and new)
[DE85-013055] N85-35763
Accelerator physics measurements at the damping ring
[DE85-013373] N85-35785
SYNCHROTRONS
Robinson instability and beam loading
[DE85-013301] N85-35737
Vacuum system for the Argonne 6 GeV synchrotron light source
[DE85-012286] N85-35773

SYNTHESIS (CHEMISTRY)
FTIR studies of hydrocarbon synthesis on Pd/ZSM5 catalysts
[DE85-012430] N85-35230
System for the continuous generation of phosphorous aerosols from red phosphorus-butyl rubber
[DE85-013527] N85-35232
SYNTHETIC APERTURES
Optical synthetic aperture techniques
[AD-A156151] N85-35752
SYNTHETIC FUELS
Aspects of high-resolution gas chromatography as applied to the analysis of hydrocarbon fuels and other complex organic mixtures. Volume 1
[AD-A156154] N85-35257
SYNTHETIC RUBBERS
System for the continuous generation of phosphorous aerosols from red phosphorus-butyl rubber
[DE85-013527] N85-35232
SYSTEM IDENTIFICATION
Lectures of a Flight Mechanics Conference --- conferences
[ESA-TT-831] N85-35165
The effect of instrumentation system parameters on the results of a flight mechanical system identification N85-35170
SYSTEMS ANALYSIS
An evaluation of a class of practical optimization techniques for structural dynamics applications
[PB85-195766] N85-35434
Prototyping with data dictionaries for requirements analysis
[AD-A156303] N85-35654
SYSTEMS ENGINEERING
A methodology for the design of testable custom large-scale integrated circuits
[AD-A156098] N85-35351
Wind turbine noise: Prediction tools and design parameter dependence N85-35477
Recommendations for content revision and alternate delivery modes for the Human Engineering Guide to Equipment Design (HEGED)
[AD-A155781] N85-35624
An approach to determining computer security requirements for Navy systems
[AD-A155750] N85-35627
SYSTEMS INTEGRATION
The integrated manual and automatic control of complex flight systems
[NASA-CR-176166] N85-35201
Analog, still without fear
[AD-A155920] N85-35348

T

TABULATION PROCESSES
(NAT)Fe(n,n'x) spectra at 65.5 MeV
[AD-A155776] N85-35730
TACHYONS
Results of a search for monopoles and tachyons in horizontal cosmic ray flux
[HE-6.1-3] N85-36129
Search for tachyons associated with extensive air showers in the ground level cosmic radiation
[HE-6.2-13] N85-36149
TAIL ASSEMBLIES
The influence of helicopter tail shape on drag: An aerodynamic study using a low speed wind tunnel
[AD-A156304] N85-35174
TANKER SHIPS
Further studies on liquid sloshing
[PB85-198695] N85-35388
TARGETS
Target observability for satellite-based sensors
[AD-A156139] N85-35217
TATB
Friction, impact, and electrostatic discharge sensitivities of energetic materials
[DE85-013321] N85-35309
TEARING
On size effects in plane stress crack-growth resistance
[AD-A155926] N85-35426
TECHNOLOGIES
EPALIT: A data management system applied to the control and retrieval of technical reports
[PB85-193068] N85-35828
TECHNOLOGY ASSESSMENT
Analysis of incompressible cascade flows using state-of-the-art computer programs
[AD-A155850] N85-35173
Energy Efficient Engine Program technology benefit/cost study, volume 2
[NASA-CR-174766-VOL-2] N85-35198
Technology for large space systems: A bibliography with indexes
[NASA-SP-7046(12)] N85-35209
State-of-the-art construction technology for deep tunnels and shafts in rock
[AD-A153362] N85-35411
Practical aspects of photovoltaic technology, applications and cost (revised)
[NASA-CR-174963] N85-35472
A Programmable Automatic Noise Data and Other Related parameter Acquisition system (PANDORA) --- wind energy converters N85-35479
Visit to test facility Stoetten (West Germany) May 9, 1984, including the Voith Wind Energy Converter (WEC) 520 turbine. The annual production of various wind energy plants in selected locations N85-35487
TECHNOLOGY TRANSFER
Proceedings of the 14th Army Science Conference. Volume 3: Principal authors P through Z
[AD-A149202] N85-35691
Electronic information management and productivity
[DE85-013362] N85-35818
TECHNOLOGY UTILIZATION
Energy Efficient Engine Program technology benefit/cost study, volume 1
[NASA-CR-174766-VOL-1] N85-35197
Motor glider meteorology N85-35543
TECTONICS
Some recent deposit modeling efforts N85-35453
Seismic stratigraphic analysis of the Mississippi Fan N85-35507
A dynamic model of Venus's gravity field
[NASA-CR-176173] N85-35845
TEFLON (TRADEMARK)
Elliptical X-ray analyzer spectrograph application to a laser-produced plasma
[DE85-013790] N85-35398
TELECOMMUNICATION
Interprocess communication
[AD-A156337] N85-35337
Proceedings of the 14th Army Science Conference. Volume 3: Principal authors P through Z
[AD-A149202] N85-35691
TELEMETRY
Miniature infra-red data acquisition and telemetry system
[NASA-CR-177953] N85-35390
TELEOPERATORS
Space Missions for Automation and Robotics Technologies (SMART) Program
[NASA-TM-86820] N85-35210
TELESCOPES
Upper limit on magnetic monopole flux from Baksan experiment
[HE-6.1-11] N85-36136
TELEVISION CAMERAS
Spatial distribution read-out system for thermoluminescence sheets
[HE-7.1-7] N85-36161
TELEVISION RECEPTION
GROWIAN: First observations of the environmental impact at the GROWIAN site --- wind energy converter N85-35476
Television interference at the Maglarp (Sweden) wind turbine N85-35480
Television interference measurement at Kalkugnen (Sweden) test windmill N85-35481
TEMPERATURE DEPENDENCE
Aqueous volatile weak electrolyte equilibria to 300 C
[DE85-013840] N85-35261
TEMPERATURE DISTRIBUTION
Interaction of trace elements and welding parameters on GTA weld shape
[DE85-004046] N85-35284
Heat transfer coefficients for particles in liquid in axially rotating cans N85-35370
A two-phase flow and heat transfer model for zero gravity
[AD-A156097] N85-35377
Response of a BWR Mark 2 containment vessel head to loads beyond the design basis
[DE85-010524] N85-35432
TEMPERATURE EFFECTS
Pressure measurements in a hydrogen combustion environment: Hydrogen-air combustion test series 1 and 2 in the FITS tank, volume 1
[TI85-009899] N85-35259
Effect of temperature and ionic impurities at very low concentrations on stress corrosion cracking of Type 304 stainless steel
[TI85-003048] N85-35283
Search for acoustic signals from high energy cascades
[HE-7.1-1] N85-36155
Experimental investigation of radiative-acoustic effects in the water by the thermodynamical conditions of Dumand
[HE-7.1-2] N85-36156
TEMPERATURE GRADIENTS
Evaluation of low-temperature geothermal potential in north-central Box Elder County, Utah
[DE85-009541] N85-35490
Comparative analysis of operational forecasts versus actual weather conditions in airline flight planning, volume 4
[NASA-CR-167865] N85-35537
TEMPERATURE INVERSIONS
Analytic solutions of inverse heat conduction problems N85-35367
TEMPERATURE MEASUREMENT
Electron irradiation of N type cadmium telluride
[AD-A156117] N85-35801
TEMPERATURE PROFILES
Turbulent structure of stably stratified nocturnal slope flows
[AD-A155845] N85-35559
TEMPERATURE SCALES
Self-study manual on optical radiation measurements. Part 1: Concepts. Chapter 12: Blackbodies, blackbody radiation, and temperature scales
[PB85-195303] N85-35754
TEMPERATURE SENSORS
Materials and process development for microcomputer-compatible pressure, temperature, and position sensors
[BMFT-FB-T-85-024] N85-35399
TENSILE PROPERTIES
Effect of thermal ageing on the mechanical properties of PWR pressure vessel steels and weldments
[AERE-R-11460] N85-35275
Microshrink, tensile properties, and the detection of microshrink
[AD-A155875] N85-35278
TENSILE STRENGTH
Effects of temperature on the tensile strength and elastic modulus of composite material
[AD-A156112] N85-35251
Crystallization of Polyetheretherketone (PEEK) in carbon fiber composites
[AD-A156316] N85-35252
Effect of microstructure on the fatigue behavior of Fe-C-X alloys
[DE85-011749] N85-35285
TENSILE TESTS
Effect of temperature and ionic impurities at very low concentrations on stress corrosion cracking of Type 304 stainless steel
[TI85-003048] N85-35283
TERMINAL BALLISTICS
Experimental data for characterizing perforating impacts: Fragmentation processes
[AD-A156370] N85-35427
TERRAIN
Three-dimensional gravity ideal body studies in rough terrain
[DE85-014097] N85-35525
Turbulent structure of stably stratified nocturnal slope flows
[AD-A155845] N85-35559
TEST CHAMBERS
Multidimensional analysis of data obtained in experiments with X-ray emulsion chambers and extensive air showers
[HE-3.6-2] N85-35951
TEST FACILITIES
Design and testing of an energy-absorbing crewseat for the F/FB-111 aircraft. Volume 2: Data from seat testing
[NASA-CR-3917] N85-35184
A study of the control of particulate emissions from turbine engine test cells N85-35205
TETHERED SATELLITES
The investigation of tethered satellite system dynamics
[NASA-CR-176180] N85-35215
THEMATIC MAPPING
LANDSAT-4/5 image data quality analysis
[E85-10105] N85-35463
Study of spectral/radiometric characteristics of the Thematic Mapper for land use applications
[E85-10106] N85-35464
Geology and geomorphology of the Roraima group, southeastern Venezuela N85-35511
THERMAL CONTROL COATINGS
Energy efficient engine, high pressure turbine thermal barrier coating. Support technology report
[NASA-CR-168037] N85-35199

THERMAL DIFFUSIVITY
Characterization of the optical and thermal properties of matter by photothermal techniques
[DE85-012607] N85-35260
THERMAL ENERGY
Heat transfer coefficients for particles in liquid in axially rotating cans N85-35370
THERMAL ENVIRONMENTS
A kinetic model for predicting oxidative degradation rates in combined radiation-thermal environments
[TI85-002629] N85-35414
THERMAL EXPANSION
Search for acoustic signals from high energy cascades
[HE-7.1-1] N85-36155
Experimental investigation of radiative-acoustic effects in the water by the thermodynamical conditions of Dumand
[HE-7.1-2] N85-36156
Acoustic detection of air shower cores
[HE-7.1-4] N85-36158
THERMAL INSULATION
SRB attach ring phenolic TPS fishtail seal evaluation tests
[NASA-CR-170887] N85-35407
Study of NSI and related cable performance during tests performed in the NASA Hot Gas Facility
[NASA-CR-170886] N85-35423
THERMAL NEUTRONS
Properties of 10 (18)-10 (19)eV EAS at far core distance
[HE-4.7-3] N85-36054
THERMAL PROTECTION
Investigation of experimental lightweight firewall materials for A/C engine bay applications
[AD-A155765] N85-35175
Verification of the SRB motor case pin retainer band tips
[NASA-CR-170882] N85-35220
SRB TPS closeout materials characterization
[NASA-CR-170885] N85-35222
Results of tests of the SRB aft skirt heat shield curtain in the MSFC Hot Gas Facility
[NASA-CR-170888] N85-35223
Results of tests of MTA-2 TPS on the SRB hold-down bolt blast container
[NASA-CR-170891] N85-35224
SRB thermal protection systems materials test results in an arc-heated nitrogen environment
[NASA-CR-170881] N85-35236
Results of tests of K5NA and a revised formulation of EPDM/cork patch material in MSFC Hot Gas Facility
[NASA-CR-170890] N85-35238
Results of tests of weathered K5NA closeout material in the MSFC Hot Gas Facility
[NASA-CR-170893] N85-35239
Evaluation of SRB phenolic TPS material made by an alternate vendor
[NASA-CR-170894] N85-35240
Space shuttle SRB TPS protective paint test and evaluation in NASA Hot Gas Facility and AEDC Tunnel C
[NASA-CR-170884] N85-35294
Results of tests of Insta-Foam Thermal Protection System (TPS) material for protection of equipment inside the SRB aft skirt
[NASA-CR-170892] N85-35295
THERMAL RADIATION
Fire research publications, 1984
[PB85-208502] N85-35827
THERMAL RESISTANCE
Investigation of experimental lightweight firewall materials for A/C engine bay applications
[AD-A155765] N85-35175
THERMAL STRESSES
Mach 14 flow restrictor thermal stress analysis
[AD-A156215] N85-35208
THERMIONIC EMITTERS
Multi-channel pulser for the SLC thermionic electron source
[DE85-014222] N85-35792
THERMOCHEMISTRY
Thermodynamics of the corrosion of chromium in molten carbonates
[DE85-011407] N85-35282
THERMOCLINES
Thermal evolution of coastal California with implications for hydrocarbon maturation N85-35509
THERMODYNAMIC PROPERTIES
Characterization of the optical and thermal properties of matter by photothermal techniques
[DE85-012607] N85-35260
Analysis of the nonlinear equations describing the elastic, thermal, and electromagnetic behavior of solids: Existence of solutions of semi-inverse problems N85-35415
THERMODYNAMICS
Thermodynamics of the corrosion of chromium in molten carbonates
[DE85-011407] N85-35282
Hadron thermodynamics in relativistic nuclear collisions
[HE-1.1-8] N85-35856
THERMOLUMINESCENCE
Detection threshold energy of high energy cascade showers using thermoluminescence PTFE-sheet and hot-gas reader
[HE-7.1-5] N85-36159
Application of thermoluminescence for detection of cascade shower 1: Hardware and software of reader system
[HE-7.1-6] N85-36160
Spatial distribution read-out system for thermoluminescence sheets
[HE-7.1-7] N85-36161
Application of thermoluminescence for detection of cascade shower 2: Detection of cosmic ray cascade shower at Mount Fuji
[HE-7.1-12] N85-36162
THERMOMECHANICAL TREATMENT
Development and application of a unified viscoelastic constitutive model for the prediction of material response under thermomechanical loading N85-35420
THERMOPLASTIC RESINS
Determination of the viscosity number of thermoplastics in dilute solution; polyamides (PA)
[NASA-TM-77673] N85-35296
THERMOPLASTICITY
Chemoviscosity modeling for thermosetting resins, 2
[NASA-CR-177958] N85-35243
THERMOSETTING RESINS
Chemoviscosity modeling for thermosetting resins, 2
[NASA-CR-177958] N85-35243
THICKNESS
Solid neon sources for plasma and X-ray lasers
[DE85-011347] N85-35402
THIN PLATES
Method of preparing thin porous sheets of ceramic material
[DE85-006399] N85-35300
THREE DIMENSIONAL FLOW
Unsteady flow in a supersonic cascade with two in-passage shocks
[NASA-CR-3925] N85-35158
General design method for 3-dimensional, potential flow fields. Part 2: Computer program DIN3D1 for simple, unbranched ducts
[NASA-CR-3926] N85-35159
The lateral distributions of charged particles of energy greater than 0.3 E sub crit in electron-photon cascades in lead and air
[HE-3.6-10] N85-35957
THREE DIMENSIONAL MOTION
Computation of three-dimensional shock wave and boundary-layer interactions
[NASA-TM-86780] N85-35372
Analytical-numerical methods of calculations of energy and three-dimensional particle distributions in electromagnetic cascades
[HE-3.5-13] N85-35950
On mini-cluster observed by Chacaltaya emulsion chamber experiment
[HE-3.6-12] N85-35959
Peculiarities of gamma-quanta distribution at 20 TeV energy
[HE-3.7-10] N85-35967
THRESHOLD DETECTORS (DOSIMETERS)
Search for anomalous C-jets in Chacaltaya emulsion chamber experiment
[HE-3.2-5] N85-35913
Exotic interactions among C-jets and Pb-jets
[HE-3.2-6] N85-35914
Detection threshold energy of high energy cascade showers using thermoluminescence PTFE-sheet and hot-gas reader
[HE-7.1-5] N85-36159
TIDES
Bibliography on tidal hydraulics. Report 2. Supplement 9: Supplementary material compiled from June 1980 - June 1983. Tidal flows in rivers and harbors
[AD-A155990] N85-35574
TIME DEPENDENCE
Identification and control of structures in space
[NASA-CR-176175] N85-35214
Subcritical fracture propagation in rocks: An examination using the methods of fracture mechanics and non-destructive testing N85-35516
Time-dependent response of the climate to increasing atmospheric carbon dioxide N85-35532
DEPTH-CHARGE static and time-dependent perturbation/sensitivity system for nuclear reactor core analysis, revision 1
[DE85-013103] N85-35659
A graph theoretic procedure for the design of feedback patterns
[REPT-110] N85-35673
Decentralized stabilization by high gain feedback
[BU-115] N85-35689
Structure of air shower disc near the core
[HE-4.7-2] N85-36053
Longitudinal development of muons in large air showers studies from the arrival time distributions measured at 900m above sea level
[HE-4.7-4] N85-36055
Arrival time distributions of electrons in air showers with primary energies above 10 (18)eV observed at 900m above sea level
[HE-4.7-5] N85-36056
A note on some statistical properties of rise time parameters used in muon arrival time measurements
[HE-4.7-12] N85-36062
Study of the time-differentiated particle flux density at various distances from EAS axis
[HE-4.7-15] N85-36065
TIME FUNCTIONS
SIG: A general-purpose signal processing program. User's manual: Revision 1
[DE85-013035] N85-35662
TIME LAG
Sub-luminal pulses from cosmic ray air showers
[HE-4.7-13] N85-36063
TIME MEASUREMENT
Characterization of microstrip discontinuities in the time and frequency domains
[NASA-CR-176190] N85-35342
The system of EAS time analysis
[HE-4.4-10] N85-36018
TIME OF FLIGHT SPECTROMETERS
The Nagoya cosmic-ray muon spectrometer 3, part 1: Preliminary observations
[HE-5.2-2] N85-36080
The Nagoya cosmic-ray muon spectrometer 3, part 2: Track detector
[HE-5.2-3] N85-36081
The Nagoya cosmic-ray muon spectrometer 3, part 3: Automatic film scanning equipment
[HE-5.2-4] N85-36082
The Nagoya cosmic-ray muon spectrometer 3, part 4: Track reconstruction method
[HE-5.2-5] N85-36083
TIME SERIES ANALYSIS
Signal space models for antenna arrays
[AD-A156063] N85-35335
TIN
The Conterminous United States Mineral Assessment Program N85-35458
The Alaska Mineral Resources Assessment Program N85-35460
TITANIUM
Applications of the mineral resources data system and the international strategic minerals inventory in mineral-resource assessments by region and commodity N85-35451
TITANIUM OXIDES
Characterization of catalysts with metal-support effects and of the species adsorbed on their surfaces
[DE85-012254] N85-35394
TOKAMAK DEVICES
Neutral pumping rates for a next step tokamak ignition device
[DE85-012780] N85-35776
Generalized reduced fluid model with finite ion-gyroradius effects
[DE85-013123] N85-35777
Resonance localization in tokamaks excited with ICRF waves
[DE85-014559] N85-35791
TOLUENE
Studies in photochemical smog chemistry. 1: Atmospheric chemistry of toulene. 2: Analysis of chemical reaction mechanisms for photochemical smog N85-35497
TOOLS
Action of wear-inhibiting Al2O3-coatings when applied to hard metal cutting tools
[BLL-RISLEY-TR-5041-(9091.9F)] N85-35292
Wear-resistant coatings for tools intended for cold working
[BLL-RISLEY-TR-5040-(9091.9F)] N85-35293
TOPOGRAPHY
Evaluation: Close-range photogrammetry for slope inventory and monitoring
[PB85-192755] N85-35470

Three-dimensional gravity ideal body studies in rough terrain
[DE85-014097] N85-35525

TOPOLOGY
Edge detection and geometric methods in computer vision
[AD-A155873] N85-35630

TOROIDAL PLASMAS
Proposed FRX-D experiment
[DE85-012766] N85-35778

TORQUE
Dual towline spin-recovery device
[NASA-CASE-LAR-13076-1] N85-35200

TORQUEMETERS
Development of contactless sensors for industrial and automative applications
[BMFT-FB-T-85-031] N85-35400

TOUGHNESS
Development of a high strength isothermally heat-treated nodular iron road wheel arm
[AD-A155755] N85-35408

TOWED BODIES
A towed instrument vehicle for deep ocean sampling
[AD-A156322] N85-35576

TOXIC HAZARDS
Proceedings of the 7th Joint Panel Meeting of the UJNR Panel on Fire Research and Safety
[PB85-199545] N85-35317
Land Disposal of Hazardous Waste
[PB85-196376] N85-35500

TRACE CONTAMINANTS
X-ray fluorescence analysis of uranium concentrates
[DE85-013189] N85-35717

TRACE ELEMENTS
The identification of compounds in mustard hydrolysate
[AD-A156381] N85-35258
Interaction of trace elements and welding parameters on GTA weld shape
[DE85-004046] N85-35284
Elemental tracers of source regions of contaminants in precipitation
[DE85-012858] N85-35499

TRACERS
A strategy for calibrating atmospheric transport models
[CSIRO-DAR-TP-9] N85-35518

TRACKING (POSITION)
Comparative analysis of operational forecasts versus actual weather conditions in airline flight planning, volume 1
[NASA-CR-167862] N85-35534
Comparative analysis of operational forecasts versus actual weather conditions in airline flight planning, volume 2
[NASA-CR-167863] N85-35535

TRAINING AIRCRAFT
RAFTS: A T-38 replacement for the 21st century
[AD-A156103] N85-35191

TRAJECTORIES
Use of a minimum-ellipse criterion in the study of ion-beam extraction systems
[DE85-012670] N85-35721

TRAJECTORY ANALYSIS
Calculation of trajectories of detached wind turbine blades and prediction of site risk levels associated with failures of HAWT's N85-35475

TRANSITION METALS
Noble metals as incipient transition metals
[DE85-013283] N85-35286

TRANSMISSION LINES
Injector losses on Mite
[DE85-012356] N85-35355
RFQ modeling computer program
[DE85-012665] N85-35661

TRANSMISSIVITY
The geostatistical approach to the inverse problem in two-dimensional steady state groundwater modeling N85-35462

TRANSMITTANCE
Characteristic modes for slots in a ground plane TE case
[AD-A155757] N85-35326
Feasibility study of radar-transmitting materials
[AD-A155839] N85-35329
Linear absorption and scattering of laser beams
[AD-A156167] N85-35401

TRANSONIC FLOW
A stream function approach to solving the conservative Euler equations for transonic flows N85-35156
Numerical studies of 2-dimensional flows
[NASA-CR-3930] N85-35160

TRANSPORT PROPERTIES
Subseasonal variability in a two-level atmospheric general circulation model N85-35504
A strategy for calibrating atmospheric transport models
[CSIRO-DAR-TP-9] N85-35518
Calculation of heavy-ion tracks in liquid water
[DE85-012101] N85-35725
Beam intensity increases at the intense pulsed neutron source accelerator
[DE85-012377] N85-35764
Neutral pumping rates for a next step tokamak ignition device
[DE85-012780] N85-35776

TRANSVERSE ACCELERATION
Relation between gamma-ray family and EAS core: Monte-Carlo simulation of EAS core
[HE-3.6-7] N85-35955
Structured events in Pamir carbon X-ray chambers
[HE-3.7-7] N85-35965
Structure of air shower disc near the core
[HE-4.7-2] N85-36053

TRANSVERSE WAVES
Transverse momentum distribution of pion deg in the fragmentation region of super high energy interactions N85-35921
Radio wave emitted by an extensive air showers in 10KHz to 1MHz region
[HE-4.6-15] N85-36051

TRAPPED PARTICLES
HgCdTe surface and defect study program
[AD-A156079] N85-35799

TRIGGER CIRCUITS
Synchronous timing of multi-energy fast beam extraction during a single AGS cycle
[DE85-011829] N85-35781
Arrival time distributions of electrons in air showers with primary energies above 10 (18)eV observed at 900m above sea level
[HE-4.7-5] N85-36056
Methods for roof-top mini-arrays
[HE-4.7-7] N85-36058
Progress report on a new search for free e/3 quarks in the cores of 10(15) - 10(16) eV air showers
[HE-6.2-15] N85-36151

TRIODES
Multi-channel pulser for the SLC thermionic electron source
[DE85-014222] N85-35792

TRITIUM
Tritium hazard via the ingestion pathway
[DE85-012897] N85-35618

TROPICAL REGIONS
Mean cloudiness over the global tropics from satellite observations
[AD-A156188] N85-35561

TROPOSPHERIC SCATTERING
Microwave propagation studies, measurements and education in Surabaya, Indonesia
[B8464633] N85-35339

TUNABLE LASERS
High-resolution spectroscopy and dynamics of multiphoton processes in atoms and molecules
[AD-A155862] N85-35714

TUNGSTATES
Electronic structure and lattice dynamics of dimensionally constrained and disordered solids
[AD-A155927] N85-35797

TUNGSTEN
Dynamic compaction of a monosized spherical tungsten powder
[DE85-014808] N85-35289
Applications of the mineral resources data system and the international strategic minerals inventory in mineral-resource assessments by region and commodity N85-35451
The Conterminous United States Mineral Assessment Program N85-35458

TUNING
Tuning system for capacitively loaded 1/4 accelerating cavity
[DE85-012516] N85-35358

TURBINE BLADES
Calculation of trajectories of detached wind turbine blades and prediction of site risk levels associated with failures of HAWT's N85-35475

TURBINE ENGINES
Energy efficient engine, high pressure turbine thermal barrier coating. Support technology report
[NASA-CR-168037] N85-35199
A study of the control of particulate emissions from turbine engine test cells N85-35205

TURBOFAN ENGINES
Energy Efficient Engine Program technology benefit/cost study, volume 1
[NASA-CR-174766-VOL-1] N85-35197
Energy Efficient Engine Program technology benefit/cost study, volume 2
[NASA-CR-174766-VOL-2] N85-35198

TURBULENCE
Noise-sustained structure, intermittency and the Ginzburg-Landau equation
[DE85-009626] N85-35379
Study of the parameters affecting the collapse of a rotating protostellar cloud N85-35837

TURBULENCE EFFECTS
The physical and empirical basis for a specific clear-air turbulence risk index
[NASA-CR-178522] N85-35540

TURBULENT BOUNDARY LAYER
Adverse pressure gradient and separating turbulent boundary-layer flows: The effect of disequilibrium in initial conditions N85-35155
Vortex boundary-layer interactions
[NASA-CR-176192] N85-35373
Pressure cross spectra in turbulent boundary layers in water
[AD-A156153] N85-35378

TURBULENT DIFFUSION
Application of a turbulent closure model to the parameterization of the vertical diffusion of heat, momentum, and humidity in the ECMWF model --- European Center for Medium Term Weather Forecasting (ECMWF)
[MITT-41] N85-35387

TURBULENT FLOW
Adverse pressure gradient and separating turbulent boundary-layer flows: The effect of disequilibrium in initial conditions N85-35155
Prediction of turbulent internal recirculating flows with K-epsilon models N85-35366
Studies on effects of boundary conditions in confined turbulent flow predictions
[NASA-CR-3929] N85-35371
Turbulent structure of stably stratified nocturnal slope flows
[AD-A155845] N85-35559
Two-point closure study of covariance budgets for turbulent Rayleigh-Benard convection
[PB85-189108] N85-35568

TURBULENT HEAT TRANSFER
Scale separation closure and Alfven wave turbulence
[DE85-013124] N85-35385

TWO DIMENSIONAL BODIES
Adaptive rezoner in a two-dimensional Lagrangian hydrodynamic code
[DE85-010108] N85-35381
Use of a minimum-ellipse criterion in the study of ion-beam extraction systems
[DE85-012670] N85-35721

TWO DIMENSIONAL FLOW
Unsteady flow in a supersonic cascade with two in-passage shocks
[NASA-CR-3925] N85-35158
Numerical studies of 2-dimensional flows
[NASA-CR-3930] N85-35160

TWO PHASE FLOW
A two-phase flow and heat transfer model for zero gravity
[AD-A156097] N85-35377

U

ULTRAHIGH FREQUENCIES
Hadron cross sections at ultra high energies and unitarity bounds on diffraction dissociation
[HE-1.1-3] N85-35851
1Single particle momentum and angular distributions in hadron-hadron collisions at ultrahigh energies
[HE-1.2-1] N85-35860

ULTRASONIC FLAW DETECTION
Ultrasonic inspection of carbon fiber reinforced plastic by means of sample-recognition methods
[NASA-TM-77896] N85-35245

ULTRASONIC RADIATION
Second Colloquim on the Scattering of Ultrasonic Waves
[AD-A156298] N85-35697
Exploring results of the possibility on detecting cosmic ray particles by acoustic way
[HE-7.1-3] N85-36157

ULTRASONIC SPECTROSCOPY
Second Colloquim on the Scattering of Ultrasonic Waves
[AD-A156298] N85-35697

ULTRASONIC TESTS
Quantitative non-destructive evaluation of composite materials based on ultrasonic wave propagation
[NASA-CR-176176] N85-35244

ULTRASONICS
Sound speed measurements in liquid oxygen-liquid nitrogen mixtures
[NASA-TP-2464] N85-35307

ULTRAVIOLET RADIATION
The 2nd European Conference on Atomic and Molecular Physics
[AD-A155863] N85-35715
Surface discharges as intense photon sources in the extreme ultraviolet
[DE85-012593] N85-35782
ULTRAVIOLET SPECTROSCOPY
The 2nd European Conference on Atomic and Molecular Physics
[AD-A155863] N85-35715
UNDERGROUND EXPLOSIONS
Investigation of the lightning vulnerability of nuclear explosive test systems at the Nevada Test Site
[DE85-011761] N85-35563
Ground motion measurements for the QUESO nuclear event
[DE85-014806] N85-35743
UNDERGROUND STRUCTURES
An underground cosmic ray muon telescope for observation of cosmic ray anisotropy N85-36037
A possible EAS array above the Soudan 2 detector
[HE-4.6-9] N85-36046
Upper limit on magnetic monopole flux from Baksan experiment
[HE-6.1-11] N85-36136
UNDERWATER ACOUSTICS
Pressure cross spectra in turbulent boundary layers in water
[AD-A156153] N85-35378
A comparison of multipath arrival structures observed in the presence of a surface duct with predictions obtained using classical ray techniques and the parabolic equation method
[AD-A156024] N85-35696
UNDERWATER BREATHING APPARATUS
The use of austenitic stainless steel versus monel (Ni-cu) alloy in pressurized Gaseous Oxygen (GOX) life support systems
[AD-A156305] N85-35625
UNDERWATER RESEARCH LABORATORIES
Preliminary results of an ALVIN dive program on active hydrothermal vents at the southern Juan de Fuca Ridge N85-35454
UNDERWATER RESOURCES
Massive sulfide deposits from the southern Juan de Fuca Ridge N85-35446
UNDERWATER TESTS
Modular detector for deep underwater registration of muons and muon groups
[HE-5.4-15] N85-36125
UNDERWATER VEHICLES
A towed instrument vehicle for deep ocean sampling
[AD-A156322] N85-35576
UNIFIED FIELD THEORY
Charge 4/3 leptons in cosmic rays
[HE-6.2-14] N85-36150
UNITED KINGDOM
Environmental aspects of large-scale wind-power systems in the UK N85-35478
UNITED STATES
The role of regional subsurface geochemistry in resource assessment in the central United States N85-35440
New silver resource map of the United States: Potential for increased domestic silver production N85-35445
Early and middle Cenozoic volcanic synthesis N85-35449
UNLOADING
Responses of skeletal muscle to unloading, a review
[NASA-CR-176177] N85-35594
UNMANNED SPACECRAFT
Noiseless coding for the Gamma Ray spectrometer
[NASA-CR-176201] N85-35219
UNSTEADY FLOW
Unsteady flow in a supersonic cascade with two in-passage shocks
[NASA-CR-3925] N85-35158
UPPER ATMOSPHERE
Space Station Polar Platform: Integrating research and operational missions
[PB85-195279] N85-35218
URANIUM
X-ray fluorescence analysis of uranium concentrates
[DE85-013189] N85-35717
Measurement of uranium enrichment for gaseous uranium at low pressure
[DE85-012697] N85-35733
Stopping relativistic Xe, Ho, Au and U nuclei in nuclear emulsions N85-35876
URANIUM COMPOUNDS
Measurement of uranium enrichment for gaseous uranium at low pressure
[DE85-012697] N85-35733
URANIUM 235
Measurement of uranium enrichment for gaseous uranium at low pressure
[DE85-012697] N85-35733
USER MANUALS (COMPUTER PROGRAMS)
Development of NATOPS performance software for the SH-3D and SH-3H helicopters
[AD-A156140] N85-35192
User's guide: A computer program for strength analysis of non-hydraulic concrete structural elements. Report 2. Strength design of reinforced concrete column sections (PCAUC)
[AD-A156393] N85-35429
Users guide for optimum interpolation method of global data assimilation
[AD-A155929] N85-35648
SIG: A general-purpose signal processing program. User's manual: Revision 1
[DE85-013035] N85-35862
LOCAT: A data retrieval program
[AD-A156004] N85-35822
UTAH
Aeromagnetic and radiometric signatures of a possible porphyry system in the western Tushar Mountains, Utah N85-35437
Evaluation of low-temperature geothermal potential in north-central Box Elder County, Utah
[DE85-009541] N85-35490

V

VACCINES
Genetic and physiological control of protective antigen synthesis by bacillus anthracis
[AD-A156324] N85-35617
VACUUM
The 2nd European Conference on Atomic and Molecular Physics
[AD-A155863] N85-35715
SU(2) x U(1) vacuum and the Centauro events N85-35885
VACUUM MELTING
Effect of prior warm rolling on the retained austenite content and hardening response of VIM-VAR (vacuum-induction melted-vacuum-arc remelted) AISI M-50 steel
[AD-A156145] N85-35281
X-ray fluorescence analysis of 304L stainless steel
[DE85-013254] N85-35288
VACUUM SYSTEMS
Experimental lithium system
[DE85-013252] N85-35382
High vacuum portable pumping station suitable for accelerator use
[DE85-011840] N85-35759
Vacuum system for the Argonne 6 GeV synchrotron light source
[DE85-012286] N85-35773
Neutral pumping rates for a next step tokamak ignition device
[DE85-012780] N85-35776
VALUE ENGINEERING
DOD Value Engineering Conference report. Value Engineering (VE): A tool that benefits line management held at Leesburg, Virginia on 1-2 November 1984. Part 1. Executive summary
[AD-A156067] N85-35810
DOD Value Engineering Conference report. Value Engineering (VE): A tool that benefits line management held at Leesburg, Virginia on 1-2 November 1984. Part 2. Plenary session
[AD-A156068] N85-35811
DoD Value Engineering conference report. Value Engineering (VE): A tool that benefits line management. Part 3, Workshop A: VE in the program office
[AD-A156069] N85-35812
DoD Value Engineering conference report. Value Engineering (VE): A tool that benefits line management. Part 4, Workshop B: VE on spare parts
[AD-A156070] N85-35813
DoD Value Engineering conference report. Value Engineering (VE): A tool that benefits line management. Part 5, Workshop C: VEP/VECP administration, negotiation, and implementation
[AD-A156071] N85-35814
DoD Value Engineering conference report. Value Engineering (VE): A tool that benefits line management. Part 6, Workshop D: VE training-orientation
[AD-A156072] N85-35815
DoD Value Engineering conference report. Value Engineering (VE): A tool that benefits line management. Part 7, Workshop E: VE in construction and architect engineer contracts
[AD-A156073] N85-35816
VANADIUM
Applications of the mineral resources data system and the international strategic minerals inventory in mineral-resource assessments by region and commodity N85-35451
VAPOR DEPOSITION
Tests on zirconium nitride coatings applied to SW 18 steel using the chemical vapor deposition method N85-35271
VAPOR PHASES
Heats of formation of gas phase organosulfur molecules, radicals and ions measured by PEPICO and application of (17)O and (33)S NMR spectroscopy to structure determination of organosulfur compounds
[DE85-010558] N85-35229
VARIATIONS
The effects of parameter variation on helicopter performance
[AD-A156027] N85-35189
Cluster variation study of coherent ordering in FCC and BCC solid solutions
[AD-A156039] N85-35280
The measurement of nitrogen oxide (NO, NO2) exchange over plant/soil surfaces
[CSIRO-DAR-TP-8] N85-35587
Muon fluctuation studies of EAS 10(17) eV
[HE-4.3-9] N85-36003
VAX COMPUTERS
Report on the SLC control system
[DE85-013076] N85-35722
VECTOR ANALYSIS
Invariant tests and likelihood ratio tests for multivariate elliptically contoured distributions
[AD-A155844] N85-35679
VECTOR SPACES
On the convergence of an iterative formulation of the electromagnetic scattering from an infinite grating of thin wires N85-35319
VECTORS (MATHEMATICS)
Optimizing data access in the LAMPF control system
[DE85-012653] N85-35663
VELOCITY
Crustal structure in southern California from array data N85-35512
VELOCITY DISTRIBUTION
Workshop Proceedings: Interpretation of Seismic Wave Propagation in Laterally Heterogeneous Structures
[BMR-258] N85-35530
Analysis of two-parameter constant background born inversion for acoustic synthetic data
[AD-A156394] N85-35698
VELOCITY MEASUREMENT
Noise-sustained structure, intermittency and the Ginzburg-Landau equation
[DE85-009626] N85-35379
Determination of vertical air velocity using measurements of the aircraft motion N85-35545
VENTS
Preliminary results of an ALVIN dive program on active hydrothermal vents at the southern Juan de Fuca Ridge N85-35454
VENUS (PLANET)
A dynamic model of Venus's gravity field
[NASA-CR-176173] N85-35845
VERTICAL AIR CURRENTS
Determination of vertical air velocity using measurements of the aircraft motion N85-35545
Measurements for the determination of the vertical structure of the convective boundary layer — atmospheric boundary layer N85-35550
VERTICAL DISTRIBUTION
Partitioning of the vertical turbulent energy transport into positive and negative contributions — meteorology N85-35551
Aircraft measurements during the Bonn Experiment (BONEX 1) — meteorology N85-35552
VERY LARGE SCALE INTEGRATION
VLSI (Very Large Scale Integrated) tutorials through the video-computer courseware implementation system
[AD-A155889] N85-35831
Computer Aided Design (CAD) methods for very large scale integration systems
[BMFT-FB-T-85-029] N85-35668
VIBRATION
Laboratory vibration schedules
[AD-A155856] N85-35188
Vibrations of free hollow circular cylindrical bodies N85-35418
A normal incidence X-ray telescope sounding rocket payload
[NASA-CR-176169] N85-35749
VIBRATION EFFECTS
A mechanical model of the human body and its application N85-35596

VIBRATION ISOLATORS
Fast scintillation counter preamplifier for the observation of Linsley effect
[HE-4.7-9] N85-36060
A mini-array for large air showers
[HE-4.7-10] N85-36061
VIBRATIONAL SPECTRA
The photodissociation of acetylene at 193.3 NM
[AD-A155775] N85-35255
Circumstellar shells of late-type stars: A study at millimeter and infrared wavelengths N85-35836
VIDEO DATA
Relaxation techniques
[AD-A156248] N85-35621
Aeronautical Systems Division Manufacturing/Quality assurance orientation
[AD-A156128] N85-35817
VINYL COPOLYMERS
Ferroelectric homopolymer PVF2 and P (VDF-TrFe) copolymers N85-35347
VISCOELASTICITY
Three-dimensional finite deformation viscoelastic model accounting for damage effects
[DE85-012951] N85-35660
VISCOPLASTICITY
Development and application of a unified viscoelastic constitutive model for the prediction of material response under thermomechanical loading N85-35420
VISCOSITY
Chemoviscosity modeling for thermosetting resins, 2
[NASA-CR-177958] N85-35243
Determination of the viscosity number of thermoplastics in dilute solution; polyamides (PA)
[NASA-TM-77673] N85-35296
Study of the parameters affecting the collapse of a rotating protostellar cloud N85-35837
VISCOUS FLOW
Cooling high intensity atomic hydrogen beams to liquid helium temperatures
[DE85-012515] N85-35718
VISCOUS FLUIDS
Couette flow of two fluids between concentric cylinders
[AD-A155827] N85-35376
VISIBILITY
Immediate visibility after red and white adaptation
[AD-A156271] N85-35616
VISIBLE SPECTRUM
The ISAVF opto-mechanical test bed
[NASA-TM-87505] N85-35206
VISUAL ACUITY
Immediate visibility after red and white adaptation
[AD-A156271] N85-35616
VISUAL PERCEPTION
Visual impact of GROWIAN and resulting recommendations for siting of large wind energy converters N85-35486
Matched filtering of visual evoked potentials to detect acceleration (+Gz) induced blackout
[AD-A155912] N85-35609
The human engineering eye movement measurement research facility
[AD-A156099] N85-35613
Immediate visibility after red and white adaptation
[AD-A156271] N85-35616
VOLCANOES
Early and middle Cenozoic volcanic synthesis N85-35449
Preliminary results of an ALVIN dive program on active hydrothermal vents at the southern Juan de Fuca Ridge N85-35454
VOLUMETRIC ANALYSIS
Chemistry of ore-forming fluids N85-35436
VORTEX GENERATORS
Wingtip vortex propeller
[NASA-CASE-LAR-13019-1] N85-35194
Vortex boundary-layer interactions
[NASA-CR-176192] N85-35373
VORTICITY
Maintenance of blocking anticyclones in a general circulation model
[PB85-190666] N85-35567
VULNERABILITY
Investigation of the lightning vulnerability of nuclear explosive test systems at the Nevada Test Site
[DE85-011761] N85-35563

W

WARFARE
Arms control and The President's Strategic Defense Initiative
[AD-A156334] N85-35212
WARNING SYSTEMS
An approach to determining computer security requirements for Navy systems
[AD-A155750] N85-35627
WASTE DISPOSAL
Simulated effects of increased recharge on the ground-water flow system of Yucca Mountain and vicinity, Nevada-California
[DE85-012985] N85-35469
Land Disposal of Hazardous Waste
[PB85-196376] N85-35500
WASTE ENERGY UTILIZATION
Advanced regenerative heat recovery system
[PB85-199602] N85-35315
WASTE HEAT
Energy from low temperature differences
[DE85-008817] N85-35492
WATER
Pressure cross spectra in turbulent boundary layers in water
[AD-A156153] N85-35378
Calculation of heavy-ion tracks in liquid water
[DE85-012101] N85-35725
Observation of EAS using a large water tank N85-35986
An experiment to detect gut monopoles
[HE-6.1-7] N85-36133
WATER FLOW
National program for inspection of non-federal dams. Woodward reservoir dam (VT 00209), Connecticut River Basin, Plymouth, Vermont. Phase 1 inspection report
[AD-A156256] N85-35693
WATER INJECTION
Steamflood pilots in the O'Connell Ranch field and the T-4 Ranch field
[DE85-901363] N85-35468
WATER TEMPERATURE
Geothermal resources of the Washakie and Great Divide basins, Wyoming
[DE85-013004] N85-35491
WATER VAPOR
Millimeter-wave propagation in moist air: Model versus path data
[AD-A156040] N85-35331
Air chemistry measurements 2
[AD-A156041] N85-35520
WATER WAVES
Atlantic coast hindcast. Phase 2: Wave information, additional extremal estimates
[AD-A156137] N85-35575
WAVE DIFFRACTION
Holoswitch
[AD-A155841] N85-35392
WAVE DISPERSION
Transient analysis of electromagnetic reflection from dispersive materials
[PB85-200186] N85-35753
WAVE EQUATIONS
Absorbing boundary conditions for exterior problems
[NASA-CR-177944] N85-35676
WAVE INTERACTION
Computation of three-dimensional shock wave and boundary-layer interactions
[NASA-TM-86780] N85-35372
Resonance localization in tokamaks excited with ICRF waves
[DE85-014559] N85-35791
WAVE PROPAGATION
Perturbation-iteration theory for analyzing microwave striplines
[NASA-CR-176189] N85-35321
Millimeter-wave propagation in moist air: Model versus path data
[AD-A156040] N85-35331
Workshop Proceedings: Interpretation of Seismic Wave Propagation in Laterally Heterogeneous Structures
[BMR-258] N85-35530
A comparison of multipath arrival structures observed in the presence of a surface duct with predictions obtained using classical ray techniques and the parabolic equation method
[AD-A156024] N85-35696
Propagation of cosmic rays through the atmosphere in the quark-gluon strings model N85-35873
WAVE REFLECTION
Transient analysis of electromagnetic reflection from dispersive materials
[PB85-200186] N85-35753
WAVE SCATTERING
Attenuation properties of the Petatlan region, Mexico, and a local magnitude scale for microearthquakes in this area N85-35513
Second Colloquim on the Scattering of Ultrasonic Waves
[AD-A156298] N85-35697
WAVEFORMS
Fast scintillation counter system and performance
[HE-4.6-10] N85-36047
Search for acoustic signals from high energy cascades
[HE-7.1-1] N85-36155
WAVEGUIDES
Normal modes in an overmoded circular waveguide coated with lossy material
[NASA-CR-176186] N85-35320
WEAPON SYSTEMS
Next generation gunship
[AD-A156361] N85-35193
Proceedings of the 14th Army Science Conference. Volume 3: Principal authors P through Z
[AD-A149202] N85-35691
WEAR INHIBITORS
Action of wear-inhibiting Al2O3-coatings when applied to hard metal cutting tools
[BLL-RISLEY-TR-5041-(9091.9F)] N85-35292
Wear-resistant coatings for tools intended for cold working
[BLL-RISLEY-TR-5040-(9091.9F)] N85-35293
WEATHER FORECASTING
Application of a turbulent closure model to the parameterization of the vertical diffusion of heat, momentum, and humidity in the ECMWF model — European Center for Medium Term Weather Forecasting (ECMWF)
[MITT-41] N85-35387
Comparative analysis of operational forecasts versus actual weather conditions in airline flight planning, volume 1
[NASA-CR-167862] N85-35534
Comparative analysis of operational forecasts versus actual weather conditions in airline flight planning, volume 2
[NASA-CR-167863] N85-35535
Comparative analysis of operational forecasts versus actual weather conditions in airline flight planning, volume 3
[NASA-CR-167864] N85-35536
Comparative analysis of operational forecasts versus actual weather conditions in airline flight planning, volume 4
[NASA-CR-167865] N85-35537
Comparative analysis of operational forecasts versus actual weather conditions in airline flight planning: Summary report
[NASA-CR-167866] N85-35538
A preliminary intercomparison between numerical upper wind forecasts and research aircraft measurements of jet streams
[NASA-CR-167884] N85-35539
The physical and empirical basis for a specific clear-air turbulence risk index
[NASA-CR-178522] N85-35540
Project Skywater, 1983-84 SCPP (Sierra Cooperative Pilot Project) data inventory
[PB85-187052] N85-35565
Surface cyclogenesis as indicated by satellite imagery
[PB85-191815] N85-35566
Program for Regional Observing and Forecasting Services (PROFS)
[PB85-188050] N85-35569
WEATHER MODIFICATION
Project Skywater, 1983-84 SCPP (Sierra Cooperative Pilot Project) data inventory
[PB85-187052] N85-35565
WEIBEL INSTABILITY
Reliability prediction of the series system with spares subject to Weibull failure N85-35413
WEIGHTLESSNESS
A two-phase flow and heat transfer model for zero gravity
[AD-A156097] N85-35377
The use of a laser Doppler velocimeter in a standard flammability tube
[NASA-CR-174960] N85-35389
Possible mechanism for changes in glycogen metabolism in unloaded soleus muscle
[NASA-CR-176184] N85-35588
Response of amino acids in hindlimb muscles to recovery from hypogravity and unloading by tail-cast suspension
[NASA-CR-176183] N85-35589
Muscle protein and glycogen responses to recovery from hypogravity and unloading by tail-cast suspension
[NASA-CR-176181] N85-35591
Cardiovascular responses to orthostatism and weightlessness N85-35601
WELDED JOINTS
X-ray fluorescence analysis of 304L stainless steel
[DE85-013254] N85-35288

WELDING
United States Army welding research and development topical and coordination meeting
[AD-A155834] N85-35409
WELLS
Evaluation of low-temperature geothermal potential in north-central Box Elder County, Utah
[DE85-009541] N85-35490
WEST GERMANY
Special questions of siting wind turbine arrays and networks --- West Germany N85-35484
WHEELS
Development of a high strength isothermally heat-treated nodular iron road wheel arm
[AD-A155755] N85-35408
WIGGLER MAGNETS
Breeding new light into old machines (and new)
[DE85-013055] N85-35763
WIND (METEOROLOGY)
Program for Regional Observing and Forecasting Services (PROFS)
[PB85-188050] N85-35569
WIND EFFECTS
Comparative analysis of operational forecasts versus actual weather conditions in airline flight planning, volume 4
[NASA-CR-167865] N85-35537
WIND PROFILES
Determination of vertical air velocity using measurements of the aircraft motion N85-35545
Control variables in vertical wind determination using simple flight-mechanical equations N85-35546
WIND TUNNEL APPARATUS
Gust simulation for flight mechanical wind tunnel tests N85-35172
WIND TUNNEL TESTS
Presentation of the acoustic and aerodynamic results of the Aladin 2 concept qualification testing
[NASA-TM-77883] N85-35161
Gust simulation for flight mechanical wind tunnel tests N85-35172
The influence of helicopter tail shape on drag: An aerodynamic study using a low speed wind tunnel
[AD-A156304] N85-35174
Miniature infra-red data acquisition and telemetry system
[NASA-CR-177953] N85-35390
WIND TURBINES
General environmental aspects of large scale wind energy utilization N85-35474
Calculation of trajectories of detached wind turbine blades and prediction of site risk levels associated with failures of HAWT's N85-35475
GROWIAN: First observations of the environmental impact at the GROWIAN site --- wind energy converter N85-35476
Wind turbine noise: Prediction tools and design parameter dependence N85-35477
Environmental Monitoring Burger Hill, Orkney wind turbine generator site and similar work at other UK WTG sites N85-35482
Siting of large scale wind turbines in Denmark N85-35483
Special questions of siting wind turbine arrays and networks --- West Germany N85-35484
Environmental aspects of the Netherlands wind farm project N85-35485
Visit to test facility Stoetten (West Germany) May 9, 1984, including the Voith Wind Energy Converter (WEC) 520 turbine. The annual production of various wind energy plants in selected locations N85-35487
WIND VELOCITY
Comparative analysis of operational forecasts versus actual weather conditions in airline flight planning, volume 1
[NASA-CR-167862] N85-35534
Comparative analysis of operational forecasts versus actual weather conditions in airline flight planning, volume 2
[NASA-CR-167863] N85-35535
Comparative analysis of operational forecasts versus actual weather conditions in airline flight planning, volume 3
[NASA-CR-167864] N85-35536
Comparative analysis of operational forecasts versus actual weather conditions in airline flight planning, volume 4
[NASA-CR-167865] N85-35537
Comparative analysis of operational forecasts versus actual weather conditions in airline flight planning: Summary report
[NASA-CR-167866] N85-35538
WIND VELOCITY MEASUREMENT
Kinematic analysis of Hurricane Frederick (1979) using satellite, aircraft and rawinsonde data
[NASA-CR-176167] N85-35533
Control variables in vertical wind determination using simple flight-mechanical equations N85-35546
The principles of wind measurement with the help of aircraft N85-35558
WINDMILLS (WINDPOWERED MACHINES)
Television interference measurement at Kalkugnen (Sweden) test windmill N85-35481
WINDPOWER UTILIZATION
Implementing agreement for cooperation in the development of large scale wind energy conversion systems
[JUEL-SPEZ-278] N85-35473
General environmental aspects of large scale wind energy utilization N85-35474
GROWIAN: First observations of the environmental impact at the GROWIAN site --- wind energy converter N85-35476
Environmental aspects of large-scale wind-power systems in the UK N85-35478
Environmental Monitoring Burger Hill, Orkney wind turbine generator site and similar work at other UK WTG sites N85-35482
Visit to test facility Stoetten (West Germany) May 9, 1984, including the Voith Wind Energy Converter (WEC) 520 turbine. The annual production of various wind energy plants in selected locations N85-35487
WINDPOWERED GENERATORS
Implementing agreement for cooperation in the development of large scale wind energy conversion systems
[JUEL-SPEZ-278] N85-35473
General environmental aspects of large scale wind energy utilization N85-35474
Calculation of trajectories of detached wind turbine blades and prediction of site risk levels associated with failures of HAWT's N85-35475
GROWIAN: First observations of the environmental impact at the GROWIAN site --- wind energy converter N85-35476
Wind turbine noise: Prediction tools and design parameter dependence N85-35477
Environmental aspects of large-scale wind-power systems in the UK N85-35478
A Programmable Automatic Noise Data and Other Related parameter Acquisition system (PANDORA) --- wind energy converters N85-35479
Television interference at the Maglarp (Sweden) wind turbine N85-35480
Environmental Monitoring Burger Hill, Orkney wind turbine generator site and similar work at other UK WTG sites N85-35482
Special questions of siting wind turbine arrays and networks --- West Germany N85-35484
Environmental aspects of the Netherlands wind farm project N85-35485
Visual impact of GROWIAN and resulting recommendations for siting of large wind energy converters N85-35486
Visit to test facility Stoetten (West Germany) May 9, 1984, including the Voith Wind Energy Converter (WEC) 520 turbine. The annual production of various wind energy plants in selected locations N85-35487
WING TIPS
Wingtip vortex propeller
[NASA-CASE-LAR-13019-1] N85-35194
WINGS
Fuel containment and damage tolerance for large composite primary aircraft structures. Phase 1: Testing
[NASA-CR-166091] N85-35241
WINTER
Project Skywater, 1983-84 SCPP (Sierra Cooperative Pilot Project) data inventory
[PB85-187052] N85-35565
WIRE
Effect of Cu4Ti compound formation on the characteristics of NbTi accelerator magnet wire
[DE85-014226] N85-35788
WORK CAPACITY
Responses of skeletal muscle to unloading, a review
[NASA-CR-173177] N85-35594
Physiological responses to unvarying (steady) and 2-2-1 shifts: Miami International Flight Service Station
[AD-A155751] N85-35619
WORK-REST CYCLE
Physiological responses to unvarying (steady) and 2-2-1 shifts: Miami International Flight Service Station
[AD-A155751] N85-35619
WORKLOADS (PSYCHOPHYSIOLOGY)
Models for assessing workload of aircrews on long distance flights N85-35599
Physiological responses to unvarying (steady) and 2-2-1 shifts: Miami International Flight Service Station
[AD-A155751] N85-35619
WRIST
The compliance of end effector force sensors for robot manipulator control N85-35406
WROUGHT ALLOYS
Characterization of modified 9 r-1 Mo steel sand castings
[DE85-012057] N85-35287
WYOMING
Depositional systems and coal occurrence in the Fort Union Formation (Paleocene), Powder River Basin, Wyoming and Montana N85-35505

X

X RAY ANALYSIS
X-ray fluorescence analysis of 304L stainless steel
[DE85-013254] N85-35288
Detection threshold energy of high energy cascade showers using thermoluminescence PTFE-sheet and hot-gas reader
[HE-7.1-5] N85-36159
Application of thermoluminescence for detection of cascade shower 2: Detection of cosmic ray cascade shower at Mount Fuji
[HE-7.1-12] N85-36162
X RAY FLUORESCENCE
X-ray fluorescence analysis of 304L stainless steel
[DE85-013254] N85-35288
Measurement of uranium enrichment for gaseous uranium at low pressure
[DE85-012697] N85-35733
X RAY IMAGERY
Development of observational and instrumental techniques in hard X-ray and medium energy gamma-ray astronomy
[NASA-CR-176172] N85-35841
High sensitive X-ray films to detect electron showers in 100 GeV region
[HE-3.1-13] N85-35911
X-ray film chamber with carbon target of Tien-Shan complex array N85-35915
A new method of differential structural analysis of gamma-family basic parameters
[HE-3.6-3] N85-35952
X RAY IRRADIATION
Neutrino astronomy and the atmospheric background
[HE-5.3-17] N85-36111
X RAY LASERS
Solid neon sources for plasma and X-ray lasers
[DE85-011347] N85-35402
X RAY SPECTRA
Multidimensional analysis of data obtained in experiments with X-ray emulsion chambers and extensive air showers
[HE-3.6-2] N85-35951
X RAY SPECTROSCOPY
Elliptical X-ray analyzer spectrograph application to a laser-produced plasma
[DE85-013790] N85-35398
Size and shape dependence of CO adsorption sites on sapphire supported Fe microcrystals
[NASA-CR-176171] N85-35794
X RAY TELESCOPES
A normal incidence X-ray telescope sounding rocket payload
[NASA-CR-176169] N85-35749
X RAYS
Generation of stimulated emission in the soft X-ray range by nonlinear processes with excimer lasers
[DE85-012465] N85-35403
On a possibility of inelasticity partial coefficient K sub gamma determination in pi C and pi Pb interactions at 10 to the 14th power eV (experiment PAMIR 1)
[HE-1.1-12] N85-35859
Experiment Pamir-3. Coplanar emission of high energy gamma-quanta at interaction of hadrons with nuclei of air atoms at energies above 10 to the 7th power GeV
[HE-1.4-12] N85-35899
Hadrons registration in emulsion chamber with carbon block
[HE-3.7-3] N85-35962
Structured events in Pamir carbon X-ray chambers
[HE-3.7-7] N85-35965
Ultra high energy events in ECHOS series and primary energy spectrum
[HE-3.7-9] N85-35966
XENON
Stopping relativistic Xe, Ho, Au and U nuclei in nuclear emulsions N85-35876
Experimental basis for the models of cascade propagation in atmosphere
[HE-3.6-6] N85-35954

Y

YIELD POINT
Fuel containment and damage tolerance for large composite primary aircraft structures. Phase 1: Testing
[NASA-CR-166091] N85-35241
YTTERBIUM
Thermal barrier coating system
[NASA-CASE-LEW-14057-1] N85-35233
YTTRIUM
Influence of yttrium on eutectoid transformation in irons
[BLL-M-35787-(5828.4)] N85-35270

Z

ZENITH
The thickness of the shower disc as observed in showers produced by primaries above 10 (19)eV
[HE-4.7-6] N85-36057
Thickness of the particle swarm in cosmic ray air showers
[HE-4.7-14] N85-36064
Energy spectrum of cascades generated by muons in Baksan underground scintillation telescope
[HE-5.1-15] N85-36077
Geophysical searches for three-neutrino oscillations
[HE-5.3-9] N85-36103
ZEOLITES
FTIR studies of hydrocarbon synthesis on Pd/ZSM5 catalysts
[DE85-012430] N85-35230
ZINC
The Conterminous United States Mineral Assessment Program N85-35458
ZINC OXIDES
Development and evaluation of sulfonated polysulfone membranes for the zinc-ferricyanide battery
[DE85-009104] N85-35357
ZINC SULFIDES
Vectorial electron transfer on designed surfaces
[PB85-204600] N85-35263
ZIRCONIUM
Thermal barrier coating system
[NASA-CASE-LEW-14057-1] N85-35233
ZIRCONIUM NITRIDES
Tests on zirconium nitride coatings applied to SW 18 steel using the chemical vapor deposition method
N85-35271

PERSONAL AUTHOR INDEX

Typical Personal Author Index Listing

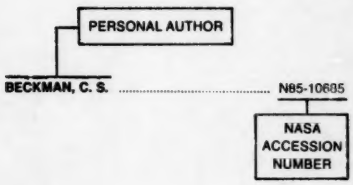

Listings in this index are arranged alphabetically by personal author. The NASA accession number denotes the number by which the citation is identified.

A

ABBAS, T. N85-36048
ABDOLLAHIAN, D. N85-35377
ABI-SAMRA, N. C. N85-35771
ABUSAID, M. F. N85-35341
ACHARYA, B. S. N85-36070
ACHKASOV, V. M. N85-36077
N85-36122
ADLER, U. N85-35638
AGARWAL, P. N85-35199
AGLIETTA, M. N85-36099
AGRELL, M. N85-35480
AIZU, H. N85-35911
AKASHI, M. N85-36160
N85-36162
AKASOFU, S. I. N85-35846
AKBAR, H. N85-35312
AL-NAJEM, N. M. N85-35367
ALBERY, W. B. N85-35610
ALDISSI, M. N85-35301
ALEEM, F. N85-36114
ALEKSOFF, C. C. N85-35752
ALEXEYEV, E. N. N85-36136
ALIEV, N. N85-36019
N85-36021
ALIMOV, T. N85-36019
N85-36020
N85-36021
ALLEN, K. C. N85-35331
ALLEN, M. A. N85-35785
N85-35790
ALLEV, N. N85-36020
ALLISON, P. N85-35721
N85-35762
ALMOQ, I. N85-35772
ALTAN, T. N85-35644
AMATO, N. M. N85-35925
N85-35933
N85-35934
AMEEV, S. S. N85-35896
AMENOMORI, M. N85-35903
N85-35940
AMER, N. M. N85-35260
AMMIRAJU, P. N85-35856
ANDER, M. E. N85-35525
ANDERSON, B. D. O. N85-35688
ANDERSON, M. N85-35789
ANDERSON, T. W. N85-35679
ANDO, Y. N85-35421
ANDREAE, P. M. N85-35626
ANDRESEN, F. P. N85-35181
ANIKIN, A. A. N85-35270
ANSORGE, J. N85-35530
ANTONOV, R. A. N85-35982
ANUTA, P. E. N85-35463
AOKI, H. N85-35922
AOKI, T. N85-36072
N85-36084
AQUIRRE, C. N85-35926
N85-35927
ARATA, N. N85-35925
N85-35933
N85-35934
ARLTON, P. E. N85-35213
ARMSTRONG, W. T. N85-35778
ARNOLD, C., JR. N85-35357
ARVELA, H. N85-36044
N85-36045
ARVESEN, J. C. N85-35573
ASAKIMORI, K. N85-35985
N85-35998
N85-36017
ASATIANI, T. L. N85-35899
ASAY, J. R. N85-35386
ASH, A. G. N85-35990
N85-35992
N85-35993
N85-35994
ASH, J. E. N85-35432
ASHITKOV, V. D. N85-36090
N85-36129
ASHTON, F. N85-36048
N85-36149
ASSINK, R. A. N85-35357
ATKINS, H. L. N85-35158
ATKINSON, W. H. N85-35391
ATRASHKEVICH, V. G. N85-36065
ATTOLINI, M. N85-36130
ATWATER, H. F. N85-35733
ATWATER, T. W. N85-35875
N85-35897
AUCHINCLOSS, P. N85-35741
AUDA, H. A. N85-35326
AUDOUZE, J. N85-36147
AURIEMMA, G. N85-36106
AVAKIAN, V. V. N85-35853
N85-35866
AWERBUCH, B. N85-35332
AYERS, W. B., JR. N85-35505
AYRES, D. S. N85-36141
AZARIAN, M. O. N85-35866
AZEVEDO, S. N85-35662
AZIMOV, S. A. N85-35960
N85-35961
AZIZINAMINI, A. N85-35433

B

BACKMAN, M. E. N85-35427
BADINO, G. N85-36099
N85-36100
BAE, H. R. N85-35251
BAECHLE, A. N85-35668
BAER, T. N85-35229
BAGGE, E. R. N85-36016
BAI, G. Z. N85-35984
N85-36091
BAILEY, A. D. N85-35521
BAISCH, F. N85-35601
BAKATANOV, V. N. N85-36075
N85-36076
N85-36077
N85-36122
BALASUBRAHMANYAN, V. K. N85-35885
BALAYAN, G. L. N85-36120
BALDETTI, F. N85-36130
BALTRUSAITIS, R. M. N85-35850
N85-36011
N85-36012
N85-36096
BANE, K. N85-35785
BANNYKH, A. E. N85-36085
BANZHAF, H. U. N85-35487
BARASCH, E. N85-35712
BARD, A. J. N85-35263
BARKER, L. M. N85-35386
BARKER, T. N85-35844
BARR, G. W. N85-35720
BARRER, J. N. N85-35179
BARRETT, W. L. N85-36141
BARTOLUCCI, L. A. N85-35463
BARTON, J. C. N85-36096
BARTON, P. N85-35448
BASAK, D. K. N85-35983
N85-35996
N85-35997
BASHINDJAGHAYAN, G. L. N85-36018
BASSETT, H. L. N85-35334
BATTERMAN, S. A. N85-35503
BATTISTONI, G. N85-36142
BAUER, C. P., JR. N85-35801
BAUER, F. N85-35344
N85-35345
N85-35346
N85-35347
BAUER, R. W. N85-35842
BAUMER, G. M. N85-35467
BAYOR, A. N85-35717
BAZHUTOV, Y. N. N85-36010
BEATON, B. N85-35499
BEAVIS, D. N85-35705
BECKER, E. J. N85-35208
BECKER, F. N85-35318
BECKER, R. L. N85-35805
BEHLING, S. R. N85-35666
BEITZELL, J. N85-35825
N85-35826
BELFORD, C. H. N85-36151
BELL, R. N85-36155
BELLANDIFILHO, J. N85-35942
BELLAZZINI, R. N85-35711
BELLOTTI, E. N85-36142
BENCK, R. F. N85-35653
BENJAMIN, R. F. N85-35787
BENKE, B. L. N85-35398
BENNETT, L. H. N85-35286
BENNETT, R. D. N85-35411
BERDZENISHVILI, O. L. N85-35995
BERESNEV, V. I. N85-36085
BEREZINSKY, V. S. N85-36109
N85-36110
BERG, J. D. N85-35382
BERGER, C. N85-36138
BERGSTROM, S. L. N85-35227
BERLEY, D. N85-36143
BERNIER, R. N85-35636
BEYER, D. N85-35742
BHATTACHARYYA, S. N85-35906
BILGRAM, R. N85-35245
BILLS, B. G. N85-35845
BINDER, J. N85-35399
BIONTA, R. M. N85-36101
BIRX, D. L. N85-35404
BISCHOFF, J. L. N85-35446
N85-35454
BISHOP, A. W. N85-35333
BISOGNANO, J. N85-35783
BITYUKOV, E. P. N85-35572
BLACHERE, J. R. N85-35303
BLAIR, R. N85-35741
BLAKE, P. R. N85-36003
N85-36004
N85-36026
BLASSER, I. N85-35668
BLAUM, M. N85-35636
BLEWITT, G. N85-36101
BLICHER, A. P. N85-35630
BLOCK, J. N85-35248
BLOKH, Y. L. N85-35910
BLOOM, S. D. N85-35842
BLUMENTHAL, S. N85-35216
BODEK, A. N85-35741
BODNAR, R. J. N85-35436
BOGART, J. N85-35664
BOGERT, D. N85-36000
BOLIEV, M. M. N85-36115
N85-36136
BOLOGNA, G. F. N85-36099
BOLOGNE, G. N85-36142
BON, J. J. N85-35212
BOND, R. E. L. N85-35217
BONDURANT, R. L. N85-35839
BOOKER, H. E. N85-35622
BORCHERDING, F. N85-35741
BORENSTEIN, S. N85-35702
BORISOV, A. S. N85-35859
BOSE, B. K. N85-35495

BOTTA, R. F. N85-35680
BOTZ, L. H. N85-35306
BOUCHIER, F. A. N85-35756
BOURDEAU, M. F. N85-35953
BOWEN, T. N85-36043
N85-36155
BOYADJIAN, N. G. N85-35977
BOYER, K. N85-35403
BOZIEV, S. N. N85-36075
BRADBURN, J. H. N85-35433
BRADSHAW, P. N85-35373
BRADY, F. P. N85-35712
BRAND, J. C. N85-35319
BRATTON, C. B. N85-36101
BRAUN, W. H. N85-35158
BRAUNSTEIN, R. N85-35797
BREAKER, L. C. N85-35573
BRECHTMANN, C. N85-36148
BRETT, R. N85-35454
BRIEGLEB, W. N85-35602
BRIGGS, J. N85-35759
BRODSKY, S. J. N85-35763
BROPHY, J. J. N85-35297
N85-35798
BROWER, K. L. N85-35302
BROWNE, M. J. N85-35792
BROWNELL, J. H. N85-35359
N85-35787
BRUMWELL, F. N85-35764
BRUZA, I. V. N85-35339
BRYAN, J. B. N85-35305
BUCKEVICH, A. V. N85-36115
BUDIANSKY, B. N85-35426
BUDKO, E. V. N85-36074
BUECKER, H. N85-35603
BUELOW, K. L. N85-35491
BULL, R. M. N85-35990
N85-36151
BUNDICK, W. T. N85-35204
BUR, A. J. N85-35526
BURGARDT, P. N85-35284
BURNETT, T. H. N85-35869
N85-35889
N85-35890
N85-35891
N85-35892
N85-35893
N85-35894
BURNSTEIN, R. N85-36000
BURRELL, J. P. N85-35824
BURT, M. R. N85-35479
BUTLER, P. R. N85-35506
BUTLER, T. A. N85-35431
BUTTON, A. N85-35785
BUTTRAM, M. T. N85-35354
BYERS, R. N85-35789

C

CADY, D. R. N85-36084
CAGLAYAN, A. K. N85-35642
CAHARISHNIKOV, S. A. N85-35947
CAIRD, R. S. N85-35359
CALLISON, P. M. N85-35606
CAMERINO, N. H., JR. N85-35281
CAMMAROTA, J. P. N85-35609
CAMPANA, P. N85-36142
CAMPBELL, D. L. N85-35437
CAMPION, A. N85-35263
CANANOV, S. D. N85-35905
CAPDEVIELLE, J. N. N85-35953
N85-35966
N85-35974
N85-35975
N85-36007
N85-36070
CARAM, J. M. N85-35190
CAREY, G. P. N85-35799
CARMONY, D. N85-35705
CARRITHERS, W. N85-35705
CARROLL, D. N85-35381
CARROLL, J. N85-35703
CARTER, D. L. N85-35305
CARTER, G. L. N85-35738
CASPER, D. N85-36101
CASSEL, R. L. N85-35790
CASSIDAY, G. L. N85-35850
N85-36011
N85-36012
N85-36098
CASTAGNOLI, C. N85-36099
N85-36109
N85-36110
N85-36142
CASTANEDA, C. M. N85-35712
CASTELAZ, M. W. N85-35835
CATHCART, J. B. N85-35439
CAULFIELD, H. J. N85-35392
CHADRANYAN, E. K. N85-35905
CHAE, I. K. N85-35898
CHAN, S. K. N85-36005
N85-36036
N85-36061
CHANG, J. H. N85-35157
CHANG, S. L. N85-35368
CHANG, S. M. N85-35366
CHANTRY, P. J. N85-35520
CHAPMAN, R. C., JR. N85-35191
CHAPMAN, R. D. N85-35839
CHASNIKOV, I. Y. N85-35920
CHAUDHURI, N. N85-35983
N85-35996
N85-35997
CHEN, C. P. N85-35371
CHEN, C. Y. N85-35385
CHEN, D. N85-36157
CHEN, K. S. N85-35380
CHEN, M. Y. N85-35855
CHEN, N. Y. N85-35860
CHEN, W. C. N85-35154
CHENG, J. J. N85-35417
CHERDYNTSEVA, K. V. N85-35859
N85-35915
CHERNYKH, R. J. N85-36065
CHERRY, M. L. N85-36135
CHIARELLA, V. N85-36142
CHILINGARYAN, A. A. N85-35951
CHINELLATO, J. A. N85-35942
N85-35944
N85-35945
CHIU, H. Y. N85-35830
CHIU, Y. T. N85-35517
CHNUMA, S. N85-35719
CHO, C. N85-36087
N85-36127
CHOU, C. N85-36001
CHOU, I. M. N85-35436
CHOU, T. T. N85-35860
CHOWDHURI, P. N85-35786
CHRIEN, R. E. N85-35778
CHRISTIAN, W. N85-35304
CHRISTIE, B. N85-35712
CHRYSICOPOULOU, P. N85-36101
CHUAH, H. H. N85-35298
N85-35803
CHUANG, S. L. N85-35320
CHUBENKO, A. P. N85-35874
N85-35915
N85-35979
CHUDAKOV, A. E. N85-36074
N85-36075
N85-36076
N85-36077
N85-36115
N85-36122
N85-36136
CHUNG, R. M. N85-35526
CHUNG, T. H. N85-35262
CHUPP, T. E. N85-35732
CHUYKOVA, T. A. N85-36025
CIHAL, V. N85-35269
CIOCIO, A. N85-36142
CLAGUE, D. A. N85-35446
CLARK, A. S. N85-35574
CLARK, R. W. N85-35162
CLAUS, R. N85-36101
CLAY, R. W. N85-36097
CLELAND, W. N85-35703
CLENDENIN, J. E. N85-35356
N85-35792
CLIFF, E. M. N85-35186
CLIFFONE, D. L. N85-35210
CLIFFORD, T. N85-35669
CLINE, J. D. N85-35570
CLOSE, D. A. N85-35733
CLOUGH, R. L. N85-35414
CLOUGH, S. A. N85-35401
CLOUT, P. N. N85-35779
COBB, J. K. N85-35793
COHEN, D. J. N85-35340
COHEN, M. N85-35831
COHEN, S. A. N85-35736
COLLARD, M. N85-35161
COLLINS, W. E. N85-35452
COLSON, S. D. N85-35256
COLTON, M. C. N85-35560
COLWELL, C. J. N85-35633
COMPTON, R. N. N85-35304
CONNORS, K. F. N85-35467
COOK, K. H. N85-35532
COOK, P. H. N85-35589
N85-35591
COOPER, L. P. N85-35225
COOPER, R. N85-35850
N85-36011
N85-36012
N85-36098
CORBATO, S. N85-36135
CORK, B. N85-35703
CORLEY, J. K. N85-35663
CORLEY, J. P. N85-35768
N85-35769
CORLISS, J. M. N85-35265
CORNWALL, J. M. N85-35517
CORREDOURA, P. I. N85-35792
CORSON, W. D. N85-35575
CORTEZ, B. G. N85-36101
COSS, J. R. N85-35795
COSSAIRT, J. D. N85-35807
COTTON, V. A. N85-35799
COWLEY, J. R., JR. N85-35213
COX, D. P. N85-35453
CRAFT, B. C., III N85-35737
CRAMER, F. S. N85-35608
CRANDALL, K. R. N85-35784
CRAWFORD, H. J. N85-35712
CRISSMAN, J. M. N85-35306
CROSLEY, D. R. N85-35264
CROUCH, M. N85-36073
CUDELL, J. R. N85-36103
CUNDY, D. C. N85-36142
CUNNINGHAM, C. G. N85-35437
N85-35457
CUPPEN, H. J. J. N85-35339
CURTIN, G. C. N85-35458
CURTIS, J. T. N85-35192
CUTLER, A. D. N85-35155
CYR, M. A. N85-35391
CZARNECKI, J. B. N85-35469

D

DADYKIN, V. L. N85-36099
N85-36100
N85-36122
DAGOSTINO, P. A. N85-35258
DAIGO, M. N85-36015
DAILY, T. N85-36135
DAKE, S. N85-35869
N85-35889
N85-35890
N85-35892
N85-35893
N85-35894
N85-35929
N85-35987
N85-36160
N85-36162
DALLAKYAN, P. Y. N85-35977
DANIELS, W. L. N85-35612
N85-35614
DANILOVA, T. V. N85-35858
N85-35979
N85-36038
DANNEVIK, W. P. N85-35568
DANTAS, A. R. V. N85-35795
DATTA, P. N85-36041
DAVARIAN, F. N85-35324
DAVIES, D. K. N85-35520
DAVIS, D. N85-35502
DAVIS, K. N85-35317
DAVIS, L. S. N85-35181
DAVIS, M. C. N85-35490
DAVISTER, M. D. N85-35428
DAWSON, J. W. N85-36141
DEAN, N. R. N85-35790
DEAN, W. G. N85-35221
N85-35223
N85-35224
N85-35237
N85-35238
N85-35239
N85-35295
DEBOER, W. N85-35759
DECKERT, A. A., JR. N85-35651
DEDENKO, L. G. N85-35981
N85-36009
N85-36123
DEENEN, R. J. N85-35339
DEFACCIO, M. A. N85-35732
DEFONTAINE, D. N85-35280
DEGRANGE, B. N85-36067
DEHMER, J. L. N85-35714
DEHMER, P. M. N85-35714
DEISSLER, R. J. N85-35379
DELAGRANGE, A. D. N85-35348
DELAHAYE, J. P. N85-35785

DELGASS, W. N. N85-35231
DELGUERRA, A. N85-35711
DEMARZO, C. N85-36130
DEMIANOV, A. I. N85-36125
DEMPSEY, M. D. N85-35489
DENISOVA, V. G. N85-35859
DERRICKSON, J. H. N85-35889
N85-35891
DESAI, T. M. N85-35314
DETTOREPIAZZOLI, B. N85-36142
DEUZET, G. N85-36138
DEVAN, J. H. N85-35282
DEVILLIERS, E. J. N85-36062
DEVITO, B. N85-35718
DEYOUNG, J. H., JR. N85-35451
DIAZ-GUERRA, J. P. N85-35717
DIFILIPPO, F. C. N85-35734
DIJK, J. N85-35339
DING, L. N85-35904
DINGER, R. J. N85-35330
DIPPOLITO, D. A. N85-35353
DIXON, R. H. N85-35402
DOBBERN, U. N85-35361
DOBRIGKEIT, C. N85-35942
DODHY, A. N85-35304
DODSON, B. W. N85-35808
DOGUJAEV, V. A. N85-36074
DOKE, T. N85-35867
DOLENTI, J. E. N85-35629
DONOHOE, G. W. N85-35412
DOPITA, M. A. N85-35831
DORAN, J. C. N85-35559
DORAN, S. H. N85-35328
DORMAN, L. I. N85-36050
DOYOTTE, C. N85-35161
DRAKE, S. N85-35891
DRAMSTAD, R. A. N85-35633
DRECHSEL, H. N85-36148
DREMIN, I. M. N85-35867
N85-36153
DREUTE, J. N85-36148
DROLET, L. N85-35615
DRUCE, S. G. N85-35275
DRUMMOND, J. N85-35712
DU, S. N85-36158
DUBOVY, A. G. N85-35915
N85-35979
DUDELZAK, B. N85-36138
DUDERSTADT, E. C. N85-35199
DUEMENIL, L. N85-35387
DUFFY, P. B. N85-35833
DULOV, V. G. N85-35164
DUNAEVSKY, A. M. N85-35859
N85-35951
DUNHAM, J. R. N85-35643
DUNN, F. E. N85-35657
DUNNING, B. W. N85-35290
DUVAL, J. S. N85-35437
DWYER, D. J. N85-35632
DZIKOWSKI, T. N85-35999

E

EARLY, R. A. N85-35793
EBY, P. B. N85-35884
ECKARDT, V. N85-35710
EDWARDS, P. G. N85-36031
N85-36154
EFIMENKO, L. A. N85-36153
EFIMOV, N. N. N85-35981
N85-36024
EGGERS, H. N85-35250
EGIYAN, K. S. N85-35866
EL-AZHARI, S. A. N85-35418
EL-ELA, A. A. N85-36016
EL-NAGHY, A. N85-36113
ELBERT, J. W. N85-35850
N85-36011
N85-36012
N85-36098
ELKINS, M. A. N85-35234
ELLROD, G. P. N85-35566
ELLSWORTH, R. W. N85-35863
N85-36000
N85-36143
ELSWORTH, C. M. N85-35587
ELTON, R. C. N85-35402
ELYADA, D. N85-35416
ENG, C. N85-35694
ENGELHARDT, L. S. N85-35766
ENGELL, D. B. N85-35615
ENGSTROEM, S. N85-35474
ENOKI, T. N85-36055
N85-36056
ENRIQUEZ, O. N85-36130
ENTING, I. G. N85-35518
EREMENKO, Y. A. N85-35920
ERICKSON, D. J. N85-35359
N85-35787
ERICKSON, E. F. N85-35833
ERICKSON, M. S. N85-35440
ERICKSON, R. L. N85-35440
ERLYKIN, A. D. N85-35858
N85-35873
N85-35979
N85-36038
ERMAKOV, G. G. N85-36010
ERMAKOV, P. M. N85-35967
ERNST, H. N85-35484
EROFEEVA, I. N. N85-35900
ERREDE, S. N85-36101
ERTEL, D. N85-35727
ESCHSTRUTH, P. N85-36138
ESPELAND, R. H. N85-35331
EVANS, S. A., JR. N85-35229
EYKHOFF, P. N85-35362
EYRAUD, L. N85-35344
N85-35345
N85-35346
N85-35347
EYRAUD, P. N85-35344
N85-35345
N85-35346

F

FAEHL, R. J. N85-35757
FALLON, J. F. N85-35582
FANCONI, B. M. N85-35306
FAY, J. A. N85-35503
FAZAL-E-ALEEM N85-35854
FECHTER, G. M. N85-35607
FEDERICO, G. S. N85-35521
FEDOROV, V. M. N85-36078
FEELEY, M. H. N85-35507
FEELY, R. A. N85-35570
FEGAN, D. J. N85-36133
FELDMAN, S. N85-35318
FELDMAN, U. N85-35342
FENN, R. W. N85-35401
FENTON, A. G. N85-36116
FENTON, K. B. N85-36116
FENYVES, E. J. N85-36008
N85-36135
FERRY, J. G. N85-35310
FIEGUTH, T. N85-35785
FIELDS, T. H. N85-36141
FINLAYSON, D. M. N85-35530
FINNEGAN, S. A. N85-35427
FIORINI, E. N85-36142
FISCHER, G. E. N85-35789
FITZGERALD, P. I. N85-35612
FIXSEN, D. J. N85-35876
FLEISSNER, J. G. N85-35397
FLYNN, E. M. N85-35369
FOLEY, K. N85-35702
FOMIN, G. G. N85-36010
FOMIN, V. P. N85-36023
FOMIN, Y. A. N85-36024
N85-36065
FORD, A. L. N85-35805
FORD, J. L. N85-35402
FOSDICK, L. D. N85-35665
FOSTER, C. D. N85-35606
FOSTER, G. W. N85-36101
FOUNTAIN, W. N85-35891
FOUNTAIN, W. F. N85-35889
FOURNIER, R. O. N85-35441
FOUTCH, G. L. N85-35227
FOX, M. A. N85-35263
FOX, R. A. N85-35738
FOX, S. R. N85-35183
FRANCESCONI, R. N. N85-35615
FRANK, G. N85-35810
N85-35811
N85-35812
N85-35813
N85-35814
N85-35815
N85-35816
FRANK, L. H. N85-35611
FRANK, W. M. N85-35533
FRANKEL, B. N85-35669
FRANKLIN, G. C. N85-35349
FRAZIER, J. N85-35610
FREESE, H. A. N85-35696
FREIER, P. S. N85-35875
N85-35876
N85-35897
FREUDENREICH, H. N85-36000
N85-36143
FRIEDMAN, D. M. N85-35182
FRIEDRICH, W. N85-35742
FRYDENLUND, D. N85-35573
FRYXELL, J. E. N85-35508
FUJII, M. N85-35911
FUJINAGA, T. N85-36160
N85-36162
FUJIYOSHI, T. N85-35422
FUKI, M. N85-35889
N85-35889
N85-35890
N85-35891
N85-35892
N85-35893
N85-35894
FUKUSHIMA, Y. N85-35988
FULGIONE, W. N85-36099
FUNAYAMA, Y. N85-35923
FURAUS, J. P. N85-35720
FURYCHOVA, J. N85-35269
FUST, H. D. N85-35604

G

GABUSI, J. N85-35781
GAEDKE, M. N85-35247
GAGE, G. N85-35275
GAIDASH, V. A. N85-36085
GAISSER, T. K. N85-35851
N85-35861
N85-35863
N85-35935
N85-36102
N85-36103
N85-36111
GALAMBOS, J. D. N85-35776
GALBALLY, I. E. N85-35587
GALEOTTI, P. N85-36099
N85-36109
N85-36110
GALFAYAN, S. K. N85-35951
GALKIN, V. I. N85-35982
N85-36025
GALLAGER, R. G. N85-35332
GALYEAN, W. E. N85-35429
GAO, X. N85-36158
GARBER, M. N85-35788
GARDNER, T. W. N85-35467
GARDNER, W. B. N85-35197
N85-35198
GARIPOV, G. K. N85-36085
GARSEVANISHVILI, L. P. N85-35916
GARVIN, H. J. N85-35177
GARYAKA, A. P. N85-35977
GAU, C. F. N85-35670
GAUTHIER, M. K. N85-35795
GAWIN, J. N85-35974
N85-35975
N85-35999
N85-36007
GAYLE, T. M. N85-35232
GAYNOR, E. S. N85-35392
GEER, L. N85-35408
GENDRON, J. F. N85-35570
GENG, Q. X. N85-35984
N85-36091
GENINA, L. E. N85-35899
GENSKOW, P. E. N85-35173
GENZEL, R. N85-35832
GEORGE, M. E. N85-35428
GERHARDY, J. W. N85-36098
GERHARDY, P. R. N85-35850
N85-36011
N85-36012
GHOSH, B. N85-35996
N85-35997
GIACOMELLI, G. N85-36130
GIBBONS, J. F. N85-35798
GIGLIETTO, N. N85-36130
GILLEN, K. T. N85-35414
GIOKARIS, N. N85-35741
GLENN, H. D. N85-35743
GLUCKSTERN, R. L. N85-35719
GLUSHKOV, A. V. N85-35981
GOFORTH, J. H. N85-35359
N85-35787
GOLDBERG, M. N85-35703
GOLDSTEIN, J. D. N85-35522
GOLDSTEIN, N. E. N85-35494
GOLOMB, D. N85-35503
GOLUB, L. N85-35749
GOLUBNICHY, P. I. N85-36153
N85-36156
GOLYNSKAYA, R. M. N85-35948
GONED, A. N85-36121

GOODMAN, J. A. N85-36000
N85-36143
GOODMAN, M. C. N85-36000
N85-36141
GORDON, S. E. N85-35620
GOSWAMI, G. C. N85-35996
GOULD, R. J. N85-35888
GOURDIN, W. H. N85-35289
GRANT, D. J. N85-35206
GRAUCH, V. J. S. N85-35442
GRAY, D. E. N85-35197
N85-35198
GREENE, A. E. N85-35359
N85-35787
GREGORY, J. C. N85-35869
N85-35889
N85-35890
N85-35891
N85-35892
N85-35893
N85-35894
GREINER, D. E. N85-35705
GREVE, D. W. N85-35343
GRIANTI, F. N85-36130
GRIEDER, K. F. N85-36117
GRIGORIEV, V. M. N85-36024
GRISHAM, D. L. N85-35765
N85-35775
GROCHALSKA, B. N85-35975
GROMOV, Y. A. N85-35995
GRUHN, C. N85-35701
GUENTHER, P. T. N85-35731
GUEST, C. J. N85-35639
N85-35640
GULKHANDANYAN, O. M. N85-36085
GUPTA, S. C. N85-36000
GUSEV, G. A. N85-36039
GUSEVA, Z. M. N85-35859
GUSTAFSSON, A. N85-35474

H

HAAS, M. R. N85-35833
HABER, C. N85-35741
HACKER, J. M. N85-35551
N85-35553
HAGER, B. H. N85-35845
HAGIWARA, K. N85-36145
HAHN, K. U. N85-35546
HAIGHT, R. C. N85-35842
HAJELA, D. P. N85-35519
HALBACH, K. N85-35789
HALBERSTAM, I. N85-35684
HALILOV, D. A. N85-35960
HALL, G. F. N85-35309
HALL, R. B. N85-35445
HALSTEAD, T. W. N85-35578
HALVERSON, P. N85-36043
HALZEN, F. N85-35861
N85-36027
HAMBY, C. C. N85-35429
HAMEL, P. N85-35169
HAMILTON, M. A. N85-35730
HAMM, R. N. N85-35725
HAMMOND, W. W., JR. N85-35466
HAND, G. R. N85-35331
HARA, T. N85-35989
N85-36002
N85-36015
N85-36054
N85-36088
N85-36128
HARADA, K. N85-35987
HARDEKOPF, R. A. N85-35779
HARIHARAN, S. I. N85-35676
HARRINGTON, R. F. N85-35326
HARRIS, C. M. N85-35680
HARVEY, P. M. N85-35834
HARWIT, M. N85-35833
HARWOOD, D. N85-35751
HASBROUCK, R. T. N85-35563
HASHIMOTO, K. N85-35926
N85-35927
HASSAN, B. H. N85-35370
HASSAN, S. N85-36016
HASTI, D. E. N85-35768
N85-35769
HATANO, Y. N85-35989
N85-36047
N85-36052
N85-36054
HATCHER, P. G. N85-35443
HAWKINS, S. A. N85-35404
HAWORTH, W. L. N85-35277
HAYASHI, T. N85-35869
N85-35889
N85-35890
N85-35891
N85-35891
N85-35892
N85-35893
N85-35893
N85-35894
HAYASHI, Y. N85-36068
N85-36132
N85-36139
N85-36140
HAYASHIDA, N. N85-35989
N85-36002
N85-36054
N85-36128
HAYES, I. J. N85-35176
HAZAMA, M. N85-35987
N85-36159
HAZELTINE, R. D. N85-35777
HAZEN, E. S. N85-35984
N85-36058
N85-36061
HAZEN, W. E. N85-35984
N85-36058
N85-36059
N85-36061
HE, C. X. N85-36054
HE, M. N85-35902
N85-35921
N85-35930
N85-35937
N85-35964
HEARN, T. M. N85-35512
HEASLER, H. P. N85-35491
N85-35509
HEIDLER, E. A. N85-35400
HEIFETZ, D. N85-35776
HEIN, J. R. N85-35444
HEIN, L. A. N85-35948
N85-35982
HEINEMANN, K. N85-35794
HEINRICH, W. N85-36148
HEINZ, R. N85-36079
HEIPLE, C. R. N85-35284
HENDRIE, D. N85-35703
HENKE, L. N85-35484
HENRIKSEN, E. J. N85-35588
N85-35589
N85-35590
N85-35591
N85-35594
HENYEY, T. L. N85-35526
HEREDIA, N. F. N85-35683
HERSHCOVITCH, A. N85-35718
HESS, J. L. N85-35162
HEYL, A. V. N85-35445
HIGASHI, S. N85-36001
N85-36087
N85-36089
N85-36127
HIGHSMITH, A. L. N85-35235
HIGNETT, H. J. N85-35411
HILLAS, A. M. N85-36030
HIRAOKA, N. N85-36001
N85-36087
N85-36127
HIRAYAMA, H. N85-35711
HODSON, A. L. N85-35990
N85-36151
HOEKSEMA, R. J. N85-35462
HOFFMANN, A. N85-36138
HOFMANN, A. N85-35785
HOFTIEZER, J. N85-36141
HOGAN, M. L. N85-35681
HOGAN, R. T. N85-35738
HOINKA, K. P. N85-35554
HOLCOMB, R. T. N85-35454
HOLLOWAY, W. F. N85-35193
HOLMAN, J. L. N85-35291
HOLMBERG, R. W. N85-35232
HOLYNSKI, R. N85-35865
N85-35869
N85-35889
N85-35890
N85-35891
N85-35892
N85-35893
N85-35894
HONDA, K. N85-35926
N85-35927
HONDA, M. N85-36015
N85-36054
N85-36128
HOOKER, C. D. N85-35738
HOOKS, B. N85-35327
HORI, A. N85-35561
HORIKI, T. N85-36047
N85-36052
HORN, G. N85-35727
HORST, T. W. N85-35559
HOSEA, J. C. N85-35736
HOTTA, N. N85-35903
N85-35928
N85-35940
HOU, T. H. N85-35243
HOWARD, W. M. N85-35740
N85-35842
HOWELL, L. L. N85-35608
HOWERTON, R. J. N85-35731
HREBIEN, L. N85-35609
HSIEH, B. J. N85-35432
HSIEH, K. C. N85-35847
HSU, C. T. N85-35777
HSU, H. N85-35679
HSU, H. S. N85-35282
HUANG, L. C. P. N85-35488
HUANG, R. Q. N85-35855
HUANG, X. N85-35672
HUBER, P. N85-35556
HUDSON, J. A. N85-35274
N85-35275
HUEBNER, S. R. N85-35316
HUESTIS, S. P. N85-35525
HUGRASS, W. N. N85-35778
HUMPHREY, J. A. C. N85-35380
HUMPHRIES, S., JR. N85-35766
HUNG, C. M. N85-35372
HUO, A. X. N85-35902
N85-35921
N85-35930
N85-35937
N85-35964
HUTTER, M. N85-35545
N85-35549
HYLAND, A. R. N85-35834

I

ICHIMURA, M. N85-36160
N85-36162
IGO, G. N85-35703
IIDA, S. N85-36080
N85-36081
N85-36082
N85-36083
IIJIMA, K. N85-36080
N85-36081
N85-36082
N85-36083
ILYINA, N. P. N85-36126
IMAEDA, K. N85-36150
N85-36161
IMAI, H. N85-35242
INAZAWA, H. N85-36092
INNOCENTE, V. N85-35867
INOUE, K. N85-35986
INOUE, N. N85-36053
N85-36145
N85-36146
INTERHOFF, H. N85-35400
ISAEV, V. I. N85-36010
ISHIKAWA, F. N85-36054
ITO, N. N85-36068
N85-36132
N85-36139
N85-36140
IVANENKO, I. P. N85-35949
N85-35950
N85-35982
N85-36025
N85-36126
IVANOV, V. I. N85-36085
IVANOVA, M. A. N85-36126
IWAI, J. N85-35869
N85-35889
N85-35890
N85-35891
N85-35892
N85-35893
N85-35894
N85-35966

J

JACKSON, K. N85-35695
JACOB, S. N85-35589
N85-35590
N85-35591
N85-35594

JAEGER, J. N85-35772
JALAN, V. N85-35471
JAREM, J. M. N85-35338
JAROCHKINA, Z. V. N85-36010
JAROSS, R. A. N85-35806
JASON, A. J. N85-35779
JASON, N. H. N85-35317
N85-35827
JASPERS, S. R. N85-35590
N85-35594
JATA, K. V. N85-35285
JENNINGS, T. N85-35610
JENNINGS, T. J. N85-35608
JIANG, Y. N85-36157
JIN, C. J. N85-35546
JING, C. N85-35904
JING, G. N85-35904
JOBE, R. K. N85-35774
N85-35792
JOCHUM, A. M. N85-35550
JOHANN, U. N85-35403
JOHANSSON, S. N85-35411
JOHNSON, B. M. N85-35767
JOHNSON, B. W. N85-35531
JOHNSON, C. N85-35684
JOHNSON, E. G. N85-35755
JONES, B. H. N85-35612
JONES, F. C. N85-35848
N85-35968
N85-36066
JONES, G. D. N85-35501
JONES, O. D. N85-35452
JONES, T. C., II N85-35629
JONES, T. J. N85-35834
JONES, W. V. N85-35869
N85-35890
N85-35892
N85-35893
N85-35894
JORDAN, G. R. N85-35275
JOSEPH, D. D. N85-35376
JOY, M. N85-35834
JUDKINS, J. G. N85-35356
JULLIAN, S. N85-36138
JURAK, A. N85-35869
N85-35890
N85-35892
N85-35893
N85-35894
JUSTI, S. N85-35272

K

KABALAN, K. Y. N85-35326
KABE, A. M. N85-35685
KAKHHAROV, N. N85-36020
KAKHKHAROV, M. N85-36019
N85-36021
KAKIMOTO, F. N85-36040
N85-36055
N85-36056
N85-36145
KALINOWSKI, J. A. N85-35743
KALLVINSKAS, J. J. N85-35253
KALMYKOV, G. B. N85-36024
KALMYKOV, N. N. N85-35980
N85-36010
N85-36019
KAMATA, K. N85-36002
N85-36015
N85-36054
N85-36088
N85-36128
KAMBEROV, G. N85-35872
KAMEDA, T. N85-35985
N85-35998
N85-36017
KAMIYA, Y. N85-36072
N85-36080
N85-36081
N85-36082
N85-36083
KANBACH, H. N85-35400
KANEKO, T. N85-36145
KANEVSKAYA, E. A. N85-35859
KANEVSKY, B. L. N85-35857
N85-35949
N85-35950
N85-35982
KANNO, Y. N85-35242
KAPPEL, E. S. N85-35454
KARAGJOZIAN, G. V. N85-35853
KARASEK, J. F. N85-35498
KARU, Z. S. N85-35220
N85-35222
N85-35240
N85-35294
N85-35407
N85-35423
KASAHARA, K. N85-35867
N85-35903
N85-35928
N85-35940
KASHIWAGI, T. N85-35867
KASPER, E. N85-35668
KASSNER, T. F. N85-35283
KAWAGUCHI, S. N85-36088
N85-36160
N85-36162
KAWAKAMI, S. N85-36068
N85-36132
N85-36139
N85-36140
KAWAMOTO, M. N85-35929
N85-35987
N85-36053
N85-36146
KAWASUMI, N. N85-35926
N85-35927
KAZANAS, D. N85-35885
KAZUNO, M. N85-35911
KEANE, D. N85-35702
KEEFE, J. R. N85-35580
N85-35581
KEITZ, J. F. N85-35534
N85-35535
N85-35536
N85-35537
N85-35538
KELLER, J. L. N85-35540
KELLER, R. N85-35721
KELLEY, H. J. N85-35186
KELLY-HANSON, K. N85-35570
KELM, J. S. N85-35195
KEMPA, J. N85-35862
KENNEDY, J. M. N85-35432
KENNEDY, K. M. N85-35574
KENNEDY, R. S. N85-35611
KERBEL, G. D. N85-35791
KEROPIAN, M. I. N85-35853
KERSHNER, D. L. N85-35830
KESPE, V. N85-35552
KETZMAN, M. P. N85-35897
KHACHATURYAN, L. S. N85-35995
KHAKIMOV, K. N85-36020
KHAKIMOV, N. N85-36021
KHALAF, A. Z. N85-35461
KHALAFYAN, A. Z. N85-36018
KHALCHUKOV, F. F. N85-36071
N85-36107
KHIZANISHVILI, L. A. N85-35905
KHODJAMIRIAN, A. Y. N85-36120
KHOURY, F. N85-35306
KHRENOV, B. A. N85-36010
KHRISTIANSEN, G. B. N85-35980
N85-36010
N85-36019
N85-36020
N85-36021
N85-36065
KHRISTIANSEN, M. V. N85-36024
KIEDA, D. N85-36135
KIEFER, W. S. N85-35845
KIFUNE, T. N85-35989
N85-36015
N85-36088
KIKUCHI, J. N85-35867
KILLIAN, J. N85-35668
KILONSKY, B. N85-35561
KIM, C. K. N85-35189
KIM, C. O. N85-35868
N85-35898
KIM, D. H. N85-35896
KIM, S. N. N85-35868
N85-35898
KINO, S. N85-36159
KIRILENKOV, A. V. N85-36078
KIRILLOV, A. A. N85-35949
KIRINA, T. M. N85-36090
N85-36129
KIRSCHKE, L. N85-35249
KITAJIMA, T. N85-36159
KITAMURA, T. N85-36072
N85-36084
KLECKNER, R. L. N85-35459
KLEIJNEN, J. P. C. N85-35687
KLEIN, K. E. N85-35596
KLIMAKOV, A. P. N85-36090
N85-36129
KLOSKINSKI, J. N85-35886
KLUBERG, L. N85-35703
KNAPP, L. M. N85-36137
KNEIZYS, F. X. N85-35401
KNIEPER, J. N85-35742
KO, S. N85-35850
N85-36011
KOBAYAKAWA, K. N85-36092
KOBAYASHI, M. N85-36126
KOBAYASHI, T. N85-35903
N85-35940
KOBUS, D. A. N85-35616
KOEHL, E. R. N85-35806
KOERBER, F. N85-35476
KOKOULIN, R. P. N85-36090
N85-36129
KOLB, C. E. N85-35524
KOLESAR, P. T. N85-35490
KOLEV, N. I. N85-35384
KOLOWITH, R. N85-35382
KONDO, T. N85-36128
KONISHI, E. N85-35903
N85-35940
KONRAD, G. T. N85-35790
KOONTZ, R. F. N85-35790
N85-35792
KORCHAGIN, P. V. N85-36100
KORCHAGIN, V. B. N85-36100
KORCHIKOV, S. D. N85-36156
KOROLKOVA, E. V. N85-36071
KOSKI, R. A. N85-35446
N85-35454
KOSLOW, M. H. N85-35452
KOTLYAREVSKI, D. M. N85-35916
N85-35995
KOVARIK, V. N85-35718
KPONOU, A. N85-35718
KRAFFT, K. N85-35435
KRAG, B. N85-35172
KRASIJ, M. N85-35300
KRATENKO, Y. P. N85-35947
KRAUS, H. N85-35543
KRAUSE, M. C. N85-35726
KRETCH, B. E. N85-35321
KREUTER, J. N85-35671
KRISHNASWAMY, M. R. N85-36068
N85-36132
N85-36139
N85-36140
KROEMER, H. N85-35800
KROLIKOWSKI, A. N85-35362
KRUGLOV, N. A. N85-35919
KRUTIKOVA, N. P. N85-35873
N85-35915
KRYDER, M. H. N85-35343
KRYS, E. N85-35957
N85-35958
KUANG, H. H. N85-35902
N85-35921
N85-35930
N85-35937
N85-35964
KUBELKA, J. N85-35269
KUBIAK, G. N85-35862
N85-35973
KUCHIN, I. A. N85-35870
KUDRYAVTSEV, V. A. N85-36071
KUEBERT, M. N85-35293
KUHLMANN, D. J. N85-35644
KUHLMANN, W. N85-35496
KUIPERS, J. A. N85-35485
KUISL, M. N85-35668
KULAK, R. F. N85-35432
KULIKOV, G. V. N85-36009
N85-36010
N85-36065
KUMANO, H. N85-35913
KUSHNIR, Y. N85-35504
KUSUMOSE, M. N85-35929
N85-36047
N85-36052
KUZMICHEV, L. A. N85-36126
KUZMIN, V. A. N85-35982

L

LADARIA, N. K. N85-35905
N85-35916
LAESSIG, W. F. N85-35817
LAGER, D. N85-35982
LAIRD, A. N85-35817
LALANNE, D. N85-36138
LAMBERT, J. E. N85-35765
N85-35775
LAMPORT, L. N85-35337
N85-35652
LANDE, K. N85-36135
LANDIS, G. P. N85-35447

LANDWEHR, C. E. N85-35627
LANG, K. N85-35741
LANSDOWNE, K. F. L. N85-35694
LANTZ, L. L. N85-35288
LANZANO, S. N85-35867
LAPLANT, P. R. N85-35746
LATTES, C. M. G. N85-35942
LAURENCE, P. N85-35770
LAVOIE, D. M. N85-35576
LAWRENCE, G. M. N85-35213
LAWRENCE, G. P. N85-35779
LAWRENCE, M. A. N85-36057
LAX, B. N85-35902
LEARNED, J. G. N85-36084
LEARY, P. C. N85-35528
LEBACQZ, J. V. N85-35790
LEBEDEV, A. P. N85-36065
LEE, C. K. N85-35388
N85-36135
LEE, C. S. N85-35320
LEE, E. P. N85-35783
LEE, J. J. N85-35219
LEE, L. L. N85-35262
LEE, M. N85-35772
N85-35785
LEE, P. H. Y. N85-35787
LEE, S. W. N85-35320
LEE, T. N. N85-35402
LEE, Y. C. N85-35252
LEE, Y. T. N85-35255
LEE, Y. W. N85-36037
LEGRO, J. R. N85-35771
LEHNIGK, S. H. N85-35167
LENAHAN, P. M. N85-35302
LEONE, J. A. N85-35497
LEONOV-VENDROVSKY, A. V. N85-36115
LEPTUKH, G. G. N85-35965
LESKO, K. T. N85-35732
LEVY, S. N85-35377
LI, G. J. N85-35984
N85-36091
LI, M. H. N85-35262
LI, Y. N85-36157
LIEBE, H. J. N85-35331
LIEBERMAN, A. G. N85-35753
LIEBING, D. F. N85-36022
LIEBOWITZ, H. N85-35430
LILAND, A. N85-35907
N85-36118
LIN, W. H. N85-35699
LINDE, I. A. N85-35949
LINDEMUTH, I. R. N85-35359
LINEBARGER, W. N85-35785
LINFORD, R. K. N85-35778
LING, J. N85-35984
N85-36091
LINNEMANN, A. N85-35673
N85-35674
N85-35688
N85-35689
LINSLEY, J. N85-35849
N85-36013
N85-36014
N85-36063
N85-36064
LITTLE, E. A. N85-35274
LITVINOV, V. A. N85-35918
LIU, J. G. N85-35984
N85-36091
LIU, Y. N85-36158
LIU, Z. H. N85-35984
N85-36091
LOEW, G. A. N85-35790
LOGAN, K. P. N85-35180
LOH, E. C. N85-35850
N85-36011
N85-36012
LOH, P. R. N85-36098
LOKTIONOV, A. A. N85-35967
LOPEZ, M. E. N85-35633
LORD, J. J. N85-35869
N85-35890
N85-35892
N85-35894
LORENZINI, E. N85-35215
LOSECCO, J. M. N85-36101
LOU, Y. K. N85-35388
LOVE, W. N85-35702
LOWE, S. T. N85-35724
LOZANO, D. F. N85-35463
LU, S. L. N85-35902
N85-35921
N85-35930
N85-35937
N85-35964
LUBBES, H. O. N85-35627
LUDEWIGT, B. N85-35702
LUDINGTON, S. N85-35448
LUDLAM, T. N85-35704
N85-35708
LUEDKE, R. G. N85-35449
LUK, T. S. N85-35403
LUKIN, Y. T. N85-35967
LUKSYS, M. N85-36003
N85-36004
LUM, H., JR. N85-35210
LUMME, M. N85-36044
N85-36045
LURIA, S. M. N85-35616
LUX, B. N85-35292
LYNN, J. E. N85-35748
LYUTOV, Y. G. N85-35949

M

MAARTENSE, P. F. N85-35339
MACARAEG, M. G. N85-35374
MACHAVARIANI, S. K. N85-35874
MACHIDA, M. N85-35926
N85-35927
MACNEILL, G. N85-36133
MADANI, J. N85-36048
MADANSKY, I. N85-35745
MADANSKY, L. N85-35708
MADHUKAR, A. N85-35804
MADIGOZHIN, D. T. N85-35920
N85-36153
MAEDA, T. N85-35985
N85-35998
N85-36017
N85-36053
MAENCHEN, J. E. N85-35782
MAHAJAN, S. M. N85-35385
MAHAN, G. D. N85-35809
MAHDYIAR, M. N85-35513
MAJDA, G. N85-35675
MAJOR, W. R. N85-35488
MAKAROV, I. T. N85-35981
MAKHMUDOV, B. M. N85-36019
N85-36021
MALACINSKI, G. N85-35583
MALANIFY, J. J. N85-35733
MALARET, E. N85-35463
MALDONADO, R. H. C. N85-35925
N85-35933
N85-35934
MALGIN, A. S. N85-36071
N85-36100
MALILA, W. A. N85-35464
MALINOWSKI, S. P. N85-35555
MALLER, O. N85-35615
MAMIDJANIAN, E. A. N85-35853
N85-35866
N85-35977
MANABE, O. N85-36146
MANDRITSKAYA, K. V. N85-35908
N85-36126
MANHEIM, F. T. N85-35444
MANK, O. N85-35668
MANN, J. Y. N85-35187
MAO, R. N85-35419
MARCHAND, M. N85-35170
MARCONI-DOOLEY, R. N85-35621
MARGIOTTA, A. N85-36130
MARIS, H. N85-35703
MARK, J. W. K. N85-35783
MARKOV, M. A. N85-36039
N85-36085
MARSH, B. N85-35625
MARTIN, D. K. N85-35429
MARTIN, F. D. N85-35468
MARTINIC, N. N85-35927
N85-36145
MARTIROSOV, R. M. N85-35853
MARUYAMA, A. N85-36087
N85-36127
MASEK, G. E. N85-36137
MASJED, H. F. N85-36149
MASRI, S. F. N85-35434
MASSAI, M. M. N85-35711
MASUDA, K. N85-35867
MASUOKA, T. N85-35713
MATANO, T. N85-35926
N85-35927
N85-35956
MATHERS, C. D. N85-35694
MATHEWS, G. J. N85-35740
N85-35842
MATINIC, N. N85-35926
MATSENOV, S. J. N85-36065
MATSUBARA, Y. N85-36002
N85-36054
N85-36128
MATSUNO, S. N85-36072
N85-36084
MATSUURA, S. N85-35421
MATTHEW, W. T. N85-35612
MATTSON, C. R. N85-35756
MAUTZ, J. R. N85-35326
MAXIMENKO, V. M. N85-35859
MAY-WELLS, J. F. N85-35363
MAY, E. N. N85-36141
MAZEL, D. S. N85-35307
MAZUMDAR, G. K. D. N85-36042
N85-36049
MAZURCZAK, J. N85-35613
MCBRIDE, S. E. N85-35643
MCCAIN, W. B. N85-35178
MCCAMMON, R. B. N85-35450
MCCASLIN, J. B. N85-35746
MCCOY, M. G. N85-35791
MCDONALD, G. A. N85-35608
MCELROY, J. H. N85-35218
MCEVADDY, P. J. N85-35830
MCGILLEM, C. D. N85-35463
MCGURN, J. S. N85-35787
MCKAY, P. F. N85-35782
MCKENNA, K. F. N85-35778
MCKENZIE-WILSON, R. B. N85-35358
MCMURDO, M. N85-36084
MCNAMEE, M. J. N85-35393
MEANS, S. M. N85-35828
MEDLIN, A. L. N85-35451
MEIER, R. N85-35718
MEIJER, S. N85-35477
MEIROVITCH, L. N85-35214
MELKUMIAN, L. G. N85-35952
MELLO, R. P. N85-35614
MELTON, C. E. N85-35619
MENON, M. G. K. N85-36068
N85-36132
N85-36139
N85-36140
MENON, M. J. N85-35942
METCALF, J. I. N85-35333
METZLER, M. D. N85-35464
MEYER, E. A. N85-35766
MEYERS, D. N85-35585
MIHELEV, A. R. N85-36074
MIKAWA, R. E. N85-35302
MIKHAILOVA, I. A. N85-35857
MIKHEYEV, S. P. N85-36115
N85-36136
MIKUMO, E. N85-35903
N85-35940
MILLER, C. J. N85-35196
MILLER, E. N85-36137
MILLER, J. G. N85-35244
MILLER, W. C. N85-35382
MILLS, R. S. N85-35784
MILORAD, V. N85-35352
MINCER, A. N85-36143
MINORIKAWA, Y. N85-36095
N85-36108
MIONO, S. N85-36159
MIQUEL, J. N85-35579
MIRANDA, P. N85-36145
MIRONOV, A. V. N85-36038
MISAKI, A. N85-35956
N85-36086
N85-36160
N85-36161
N85-36162
MISAKI, Y. N85-35985
N85-35998
N85-36017
N85-36053
N85-36146
MISHRA, S. N85-35741
MITSUI, K. N85-36072
N85-36084
N85-36095
N85-36108
MITSUMUNE, T. N85-35929
MITTRA, R. N85-35328
N85-35342
MIYAKE, S. N85-36068
N85-36132
N85-36139
N85-36140
MIZUMOTO, Y. N85-35850
N85-36011
N85-36012
N85-36015
N85-36098
MIZUSHIMA, K. N85-35985
N85-35998
N85-36017
N85-36144

MIZUTANI, K. N85-35903
N85-35940
N85-36072
MKHITARYAN, V. M. N85-36018
MOAKLER, M. W., JR. N85-35628
MOBLEY, J. D. N85-35501
MOENICH, J. N85-35773
MONDAL, N. K. N85-36068
N85-36132
N85-36139
N85-36140
N85-36141
MONEYHUN, J. H. N85-35232
MOOERS, C. N. K. N85-35560
MOON, D. P. N85-35276
MOORE, A. R. N85-35408
MORENO, V., JR. N85-35420
MORETTI, G. N85-35160
MORGAN, L. N85-35695
MORI, M. N85-36128
MORRISON, P. J. N85-35777
MORRISSEY, J. F. N85-35336
MORTON, J. L. N85-35454
MOSIER, E. L. N85-35440
MOTOVA, M. V. N85-35980
N85-36010
N85-36024
MOYER, E. T., JR. N85-35430
MOYER, J. J. N85-35175
MUESSIG, H. N85-35470
MUKHERJEE, N. N85-35997
MULCAHEY, T. P. N85-35806
MULERA, T. N85-35703
MULERA, T. A. N85-35711
MULLADJANOV, E. J. N85-35960
N85-35961
MULLEN, S. L. N85-35567
MURAKAMI, H. N85-35867
MURAKI, Y. N85-35867
N85-36035
N85-36072
MURZIN, V. S. N85-35900
MUSSER, J. N85-36104
MUTH, L. A. N85-35364
MUTH, L. R. N85-35631
MYERS, J. S. N85-35573
MYERS, W. N85-35705
MYRA, J. R. N85-35353

N

NAASE, S. N85-35781
NAESER, C. W. N85-35437
NAGANO, M. N85-35989
N85-36002
N85-36015
N85-36054
N85-36088
NAIRNE, P. J. N85-35479
NAKADA, T. N85-35867
NAKANISHI, A. N85-36159
NAKATSUKA, T. N85-35929
N85-36047
N85-36052
N85-36159
NALLASAMY, M. N85-35371
NAM, R. A. N85-35859
NANJO, H. N85-35903
N85-35940
N85-35963
NARASIMHAM, V. S. N85-36063
N85-36139
N85-36140
NARAYAN, N. N85-35378
NASH, W. F. N85-36003
N85-36004
N85-36026
NAVIA, C. E. N85-35912
N85-35926
N85-35927
N85-35942
NAZAROV, V. J. N85-36065
NECHIN, Y. A. N85-36024
NELSON, G. N85-35586
NELSON, J. G. N85-35609
NELSON, W. R. N85-35711
NESPHOR, Y. I. N85-36023
NESTEROVA, N. M. N85-35915
N85-35979
NEUBAUER, F. M. N85-35847
NEUMEIER, L. A. N85-35291
NEWMAN, A. L. N85-35517
NEWMAN, E. M. N85-35350
NEWMAN, J. C., JR. N85-35424
NG, L. K. N85-36005
N85-36036
N85-36037
N85-36060
N85-36061
NGAI, K. L. N85-35682
NICHIMURA, J. N85-36051
NICHOLS, J. P. N85-35735
NICKOLS, R. C. N85-35300
NICODEMUS, F. E. N85-35754
NIELAND, M. E. N85-35667
NIELSEN, K. E. N85-35768
NIEMINEN, M. N85-36044
N85-36045
NII, N. N85-36072
NIKIFOROVA, E. S. N85-36024
NIKOLSKAJA, N. M. N85-35915
NIKOLSKY, S. I. N85-35874
N85-35915
N85-36034
N85-36156
NINAGAWA, K. N85-36161
NISHI, K. N85-36040
N85-36055
N85-36056
NISHIKAWA, K. N85-35929
NISHIMOTO, H. N. N85-35768
NISHIMURA, J. N85-35911
NISHIOKA, A. N85-36047
N85-36052
NIWA, M. N85-35956
N85-36160
N85-36162
NIXON, K. V. N85-35733
NOEL, A. F. N85-35654
NOMURA, Y. N85-35911
NOREM, J. N85-35764
NORMAN, E. B. N85-35732
NORMARK, W. R. N85-35454
NORQUIST, D. C. N85-35648
N85-35684
NOSOV, A. N. N85-35960
NOVALOV, A. A. N85-35995
NOVOSELTSEV, Y. F. N85-36075
N85-36076
N85-36077
N85-36122
NOVOSELTSEVA, M. V. N85-36075
N85-36076
N85-36077
NOWACKI, J. N85-35271
NUNNALLY, W. C. N85-35360
NURITDINOV, H. N85-35960
N85-35961

O

OCONNOR, D. N85-36084
ODA, L. N85-35561
OGANESSIAN, A. G. N85-36120
OGANEZOVA, J. S. N85-36018
OGATA, T. N85-35966
OHANIAN, G. Z. N85-35866
OHASHI, Y. N85-36072
N85-36084
OHMORI, N. N85-36047
N85-36052
N85-36159
OHNO, Y. N85-36015
N85-36128
OHOKA, H. N85-36002
OHSAWA, A. N85-35944
N85-35945
OKADA, A. N85-36035
N85-36072
N85-36084
OKAMOTO, Y. N85-36160
N85-36162
OKUSAWA, T. N85-36087
OLIPHANT, T. A. N85-35359
OLSON, C. T. N85-35606
OLSON, D. L. N85-35409
OONA, H. N85-35766
N85-35787
ORLOV, A. M. N85-35887
OSIPOVA, E. A. N85-36126
OSTERWEIL, L. J. N85-35665
OTTEN, A. A. J. N85-35339
OTTERLUND, I. N85-35701
N85-35706
N85-35707
OVSEPIAN, G. G. N85-35853
OZAKI, S. N85-36001
N85-36127

P

PABOOJIAN, A. J. N85-35523
PADEY, V. A. N85-36074
PAIGE, F. N85-35708
PAKA, V. T. N85-36085
PALMER, M. A. N85-35398
PAMILAJU, A. N85-35942
PAN, J. N. N85-35413
PAPAGEORGOPOULOS, C. N85-35794
PAREEK, P. N. N85-35713
PARK, I. G. N85-35868
PARK, J. J. N85-35514
PARK, Y. H. N85-35325
PARSONS, B. K. N85-35492
PASHKOV, S. V. N85-35859
PATHAK, K. M. N85-36041
N85-36042
N85-36049
PATRICK, D. M. N85-35411
PATTERSON, J. C., JR. N85-35194
PATTERSON, J. R. N85-36022
PATTON, J. F. N85-35614
PAULSON, L. N85-35810
N85-35811
N85-35812
N85-35813
N85-35814
N85-35815
N85-35816
PAVLAKOS, C. N85-35398
PAZIASHVILI, I. V. N85-35995
PECOS, J. F. N85-35787
PEDERSEN, L. M. N85-35635
PELLING, M. N85-35841
PELTONEN, J. N85-36044
N85-36045
PEMSLER, J. P. N85-35489
PENG, Y. K. M. N85-35776
PEREZ-MENDEZ, V. N85-35711
PERRY, J. L. N85-35279
PESHKIN, M. A. N85-35647
PETER, W. K. N85-35757
PETERSEN, G. W. N85-35467
PETKOV, V. A. N85-36074
PETRUKHIN, A. A. N85-36090
N85-36129
PETTIT, F. S. N85-35303
PHILLIPS, S. I. N85-35261
PHINNEY, N. N85-35664
N85-35722
PIETIKAINEN, M. N85-35751
PILLALAMARRI, R. S. N85-35613
PILON, D. N85-35638
PIOTROWSKA, A. N85-35862
PITKIN, J. A. N85-35437
PITTS, J. A. S. N85-35823
PLAETSCHKE, E. N85-35171
PLASIL, F. N85-35702
PLATNER, E. N85-35702
PLUNKETT, R. N85-35378
PLYASHESHNIKOV, A. V. N85-35946
N85-35948
PODWYSOCKI, M. H. N85-35452
POENITZ, W. P. N85-35731
POOR, S. E. N85-35404
POPANDOPULO, A. N. N85-35268
POPOVA, L. N85-35872
N85-35991
POPPINGER, M. N85-35399
PORTER, R. S. N85-35252
N85-35298
N85-35803
POSA, F. N85-36130
POSKANZER, A. N85-35702
POTTER, J. M. N85-35661
POTTS, C. N85-35764
POUKEY, J. W. N85-35768
POULOSE, P. K. N85-35430
POWER, M. S. N85-35452
PRATT, J. C. N85-35733
PRAVDIN, M. I. N85-35981
PRELLER, R. N85-35577
PRESTWICH, K. R. N85-35788
PRICE, L. E. N85-36141
PRICE, P. B. N85-36134
PRICE, R. H. N85-35787
PRICE, W. A., III N85-35428
PROCUREUR, J. N85-35971
N85-36119
PROSIN, V. V. N85-36019
N85-36021
N85-36024
PROSKURYAKOV, A. S. N85-35919
PROTHEROE, R. J. N85-36031
N85-36154

PROVOST, L. R. N85-35258
PUCHKOV, V. S. N85-35859
PURNOMO, A. N85-35339
PURTILO, J. M. N85-35658
PUSTOVETOV, V. P. N85-36078
PUTNAM, A. A. N85-35265
PYUN, J. J. N85-35381

Q

QURESHI, T. N. N85-35645

R

RABICH, H. A. N85-35587
RADZIMINSKI, J. B. N85-35433
RAGHUPATHI, P. S. N85-35644
RAHN, K. A. N85-35499
RAJAGOPAL, A. K. N85-35682
RAJU, I. S. N85-35424
RAKHIMOVA, N. N85-36019
N85-36020
N85-36021
RAKOBOLSKAYA, I. V. N85-35857
N85-36126
RAMAN, S. N85-35748
RAMIREZ, J. J. N85-35768
N85-35769
RAPTIS, A. C. N85-35699
RASKY, P. H. L. N85-35343
RASMUSSEN, S. N85-35483
RATINO, D. N85-35610
RAUCHAS, A. N85-35764
RAUPACH, F. N85-36138
RAVINDRAM, M. N85-35253
READING, J. F. N85-35805
REASNER, E. N85-35526
REAY, N. W. N85-36113
REED, I. S. N85-35649
N85-35650
REEKER, L. H. N85-35671
REGINATO, L. L. N85-35404
REIN, C. R. N85-35576
REINHARDT, M. E. N85-35544
N85-35548
REISER, M. N85-35784
REJ, D. J. N85-35778
REN, G. X. N85-35855
REN, J. R. N85-35902
N85-35921
N85-35930
N85-35937
N85-35964
RENARDY, Y. N85-35376
RENTZEPIS, P. M. N85-35256
REVILL, G. W. N85-35187
RHODES, C. K. N85-35403
RIBE, F. I. N85-35761
RICE, R. N85-35219
RICHARDS, M. A. N85-35845
RICHMOND, J. C. N85-35754
RICHTER, A. K. N85-35847
RICHTER, B. N85-35723
RICKER, T. N85-35668
RILEY, W. D. N85-35290
RINDERLE, H. N85-35668
RINEHART, L. F. N85-35354
RITCHIE, R. H. N85-35725
RITTER, H. G. N85-35702
RIVKIN, L. N85-35785
ROARK, M. N85-35610
ROBBINS, J. M. N85-35299
ROBERSON, P. L. N85-35738
ROBERTS, R. K. N85-35406
ROBERTSON, C. N85-35728
ROBERTSON, C. R. N85-35266
ROBSON, A. N85-35478
ROCA, M. N85-35717
ROCHE, G. N85-35703
ROCKSTEIN, M. N85-35584
ROEDDER, E. N85-35436
ROESSLER, F. N85-35254
ROGANOVA, T. M. N85-35950
N85-36025
ROGERS, J. D. N85-35383
ROGERS, R. C. N85-35415
ROGOVAYA, S. I. N85-35910
ROGNISHVILI, N. N. N85-35905
ROLLER, S. F. N85-35259
ROMAN, P. N85-35715
ROMERO, J. L. N85-35712
ROSE, P. A. N85-35663
ROSENAU, P. N85-35375
ROSENBAUER, H. N85-35847
ROSENBLUM, L. N85-35472
ROSENLIEB, J. W. N85-35185
ROSKA, R. N85-35293
ROSKAM, J. N85-35695
ROSS, M. C. N85-35211
N85-35774
ROSS, S. L. N85-35454
ROSSI, R. N85-35521
ROUSHDY, M. N85-36121
ROY, C. R. N85-35587
ROY, S. N85-35978
ROYCHOUDHURY, R. N85-36093
ROYER, A. N85-35638
ROZZELL, T. C. N85-35692
RUBEY, W. A. N85-35257
RUDERMAN, M. N85-35843
RUIZ, M. N85-35741
RUSISHVILI, N. S. N85-35995
RUSKOWSKI, C. M. N85-35350
RUTHER, W. E. N85-35283
RUTKOWSKI, H. L. N85-35766
RYASSNY, F. G. N85-36100
RYASSNY, V. G. N85-36107
RYAZHSKAYA, O. G. N85-36071
N85-36094
N85-36100
N85-36107
RYBICKI, G. B. N85-35840
RYBICKI, G. C. N85-35267

S

SAAKJAN, V. A. N85-36153
SAAVEDRA, O. N85-36099
SABATIER, P. C. N35-35677
SABATINI, R. L. N85-35788
SADLER, J. C. N85-35561
SADYKOV, T. K. N85-35920
N85-35967
SAGNER, M. N85-35161
SAHAI, R. S. N85-35836
SAITO, T. N85-35928
N85-35929
N85-35988
SAKATA, M. N85-35928
N85-35929
N85-35987
N85-35988
SAKUYAMA, H. N85-35986
N85-36144
SALAMA, S. Y. N85-35314
SALAMON, M. H. N85-36134
SALEEM, M. N85-35854
N85-36114
SALEM, A. M. N85-36121
SALTZMAN, J. S. N85-35381
SAMPSON, W. B. N85-35788
SAMSON, J. A. R. N85-35713
SANDERSON, A. C. N85-35647
SANDIFER, J. P. N85-35241
SANDLER, S. S. N85-35335
SAO, M. V. S. N85-36032
SARGENT, C. L. N85-35174
SARKAR, S. N85-35997
SARYCHEVA, L. I. N85-35919
N85-36018
N85-36125
SASAKI, H. N85-36047
N85-36052
SASAKI, Y. N85-35494
SASS, B. H. N85-35541
SATO, K. N85-35903
N85-35940
SATO, T. N85-36001
N85-36087
N85-36089
SATROM, K. D. N85-35606
SAUERMANN, H. N85-35361
SAUERMANN, P. F. N85-35742
SAVCHENKO, R. T. N85-36153
SAWAYANAGI, K. N85-35912
N85-35942
SAWKA, M. N. N85-35615
SAWYER, G. A. N85-35779
SAZHINA, G. P. N85-35908
SCANNAPIECO, A. J. N85-35381
SCHACHNER, H. N85-35292
SCHAEFER, G. N85-35605
SCHAEFFER, R. N85-36147
SCHALLER, S. C. N85-35663
SCHINDEL, U. G. N85-35668
SCHLERETH, J. L. N85-36141
SCHLITT, L. G. N85-35768
SCHMIDT, D. K. N85-35201
N85-35203
SCHMIDT, D. S. N85-35202
SCHMITZ, G. N85-36138
SCHNEIDER, S. R. N85-35218
SCHROEDER, L. S. N85-35705
SCHULZ, W. N85-35166
SCHWALBACH, P. N85-35732
SCHWARTZ, R. D. N85-35831
SCHWARZ, H. D. N85-35356
SCHWARZENBACH, A. P. N85-35403
SCHWARZMEIER, J. L. N85-35778
SCOTT, P. F. N85-35515
SEAGER, C. H. N85-35302
SEED, H. B. N85-35527
SEEMAN, J. T. N85-35211
N85-35774
SEMENOV, A. M. N85-36077
N85-36122
SEPHTON, A. J. N85-36003
N85-36004
SERDUKOV, A. D. N85-36153
SERRA, P. N85-36130
SHABELSKI, Y. M. N85-35873
N85-35916
SHALABY, M. N85-36121
SHANE, S. J. N85-35184
SHANG, P. C. N85-35369
SHANKS, W. C., III N85-35454
SHAPIRO, L. N85-35592
SHAPIRO, M. A. N85-35539
SHAPIRO, M. M. N85-36112
SHARVADZE, Z. S. N85-35995
SHCHEPANOVSKIY, V. A. N85-35164
SHEPPARD, J. C. N85-35211
N85-35774
SHERER, N. I. N85-35916
SHERMAN, F. S. N85-35380
SHERMAN, J. D. N85-35721
N85-35762
SHETTLE, E. P. N85-35401
SHIBATA, S. N85-36080
N85-36081
N85-36082
N85-36083
SHIBATA, T. N85-36160
N85-36162
SHIBUYA, E. H. N85-35936
N85-35942
N85-35945
SHIFLET, G. J. N85-35285
SHIH, C. K. N85-35799
SHIMA, M. N85-35928
N85-35929
N85-35988
SHIRAI, T. N85-35911
SHIRLEY, C. G. N85-35720
SHITOV, V. G. N85-36023
SHMONIN, V. L. N85-35896
SHORT, K. N85-35573
SHTRANIKH, I. V. N85-36085
SHURTER, R. P. N85-35766
SIDDER, G. B. N85-35510
SIEGMUND, D. N85-35681
SIEMON, R. E. N85-35778
SIENICKI, J. J. N85-35739
SIGMON, E. B. N85-35818
SIKKA, V. K. N85-35287
SILAEV, A. A. N85-36065
SILBERBERG, R. N85-36112
SILBERMAN, J. A. N85-35799
SILES, L. N85-36145
SILK, J. N85-36147
SILVER, J. A. N85-35524
SILVERMAN, S. W. N85-35728
SIMO, J. C. N85-35660
SIMON, M. K. N85-35323
N85-35324
SIMPSON, J. A. N85-35410
SIMPSON, R. S. N85-35425
SINEV, N. B. N85-36018
SINGER, D. A. N85-35453
SINHA, M. N85-35978
SINHA, S. N85-36032
SINYOV, N. B. N85-36125
SIVAPRASAD, K. N85-36000
N85-36046
SIVOKLOKOV, S. Y. N85-35900
SIZOV, V. V. N85-35950
SKELTON, R. N85-35759
SKUDRIDAKIS, J. N85-35557
SLACK, J. F. N85-35454
SLINN, S. Y. N85-35822
SLUYTERS, T. N85-35718
SMIALEK, J. L. N85-35267
SMIGIELSKI, F. J. N85-35566
SMIRNOVA, L. N. N85-35900
N85-35919

SMITH, A. B. N85-35731
SMITH, A. R. N85-35746
SMITH, D. L. N85-35731
N85-35769
SMITH, F. W. N85-35431
SMITH, H. V., JR. N85-35762
SMITH, I. D. N85-35768
SMITH, M. W. N85-35404
SMITH, S. W. N85-35297
N85-35798
SMOOT, P. R. N85-35278
SMORODIN, Y. A. N85-35952
N85-36124
SO, C. K. N85-35262
SOBOROFF, D. M. N85-35290
SODJA, J. N85-35792
SOERENSEN, J. N. N85-35475
SOKHOYAN, S. O. N85-35853
SOKOLSKAYA, N. V. N85-35908
SOKOLSKY, P. N85-35850
N85-36011
N85-36012
N85-36098
SOLOVJEVA, V. I. N85-36009
SOMMER, W. F., JR. N85-35765
SOMMERS, P. N85-36098
SOMMERVILLE, C. C. N85-35311
SONG, J. N85-36157
SOPPER, W. K. N85-35283
SOUZA, K. A. N85-35578
SPAIN, J. C. N85-35311
SPARKS, M. N85-35329
SPARN, T. P. N85-35213
SPEIR, L. G. N85-35733
SPENCE, P. W. N85-35768
SPENCER, B. W. N85-35739
SPENCER, J. E. N85-35763
SPENCER, N. N85-35664
SREEKANTAN, B. V. N85-36139
N85-36140
STACEY, G. J. N85-35833
STACEY, J. N85-35322
STAMENOV, J. N. N85-35971
N85-36034
N85-36119
STAMENOV, Y. N85-36033
STANEV, T. N85-35863
N85-35935
N85-36008
N85-36027
N85-36102
N85-36111
STANITZ, J. D. N85-35159
STARKE, B. A., JR. N85-35285
STARLING, K. E. N85-35262
STATTEL, P. N85-35759
STAVREV, P. V. N85-35971
N85-36119
STECK, D. N85-35850
N85-36011
N85-36012
N85-36098
STECURA, S. N85-35233
STEIGERWALD, R. I. N85-35495
STEIN, P. C. N85-35678
STEINBERG, D. M. N85-35686
STEINBERG, R. N85-36105
STEINER, H. N85-35705
STEININGER, K. N85-35600
STEMANETYAN, G. Z. N85-35916
STENDAHL, L. O. N85-35182
STENKIN, Y. F. N85-36075
STENKIN, Y. V. N85-36076
N85-36077
N85-36122
STENLUND, E. N85-35707
STEPANAIN, A. A. N85-36023
STEPHENS, S. A. N85-36028
N85-36029
STEVEN, T. A. N85-35437
STEVENS, A. N85-35669
STEVENS, J. E., JR. N85-35205
STEVENSON, W. G. N85-35482
STEWART, J. N. N85-35656
STIENING, R. F. N85-35211
N85-35774
STINNETT, R. W. N85-35355
N85-35780
STIPP, V. N85-35764
STOCKDALE, I. R. N85-35741
STOCKDALE, J. A. D. N85-35304
STOCKMAN, T. D. N85-35606
STOKES, J. H. N85-35390
STOREY, J. M. Y. N85-35832
STRANGE, R. R. N85-35391
STREEKANTAN, B. V. N85-36068
STREHLOW, R. A. N85-35389
STREITMATTER, R. E. N85-35885
N85-36028
N85-36029
STRIEBICH, R. C. N85-35308
STRIGANOV, P. S. N85-36074
STRONSKI, J. P. N85-36137
STRUGALSKI, Z. N85-35877
N85-35878
N85-35879
N85-35880
N85-35881
N85-35882
N85-35883
N85-35954
STUBBS, T. F. N85-35743
SU, C. C. J. N85-35365
SU, S. N85-35902
N85-35921
N85-35930
N85-35937
N85-35964
SUE, M. K. N85-35325
SUENAGA, M. N85-35788
SUGA, K. N85-36040
N85-36055
N85-36056
N85-36145
SUGIHARA, T. N85-35987
SUGONDO, P. N85-35339
SULAKOV, V. F. N85-36009
SUMIDA, J. N85-35324
SUMNER, E. E., JR. N85-35426
SUN, J. T. N85-35465
SURIN, N. M. N85-36085
SUTPHIN, D. M. N85-35451
SUVOROVA, O. V. N85-36074
SUWADA, T. N85-36001
N85-36087
SUZUKI, N. N85-35986
N85-36144
SUZUKI, T. N85-35986
SVESHNIKOVA, L. G. N85-35857
SWANSON, P. L. N85-35516
SWANSON, W. P. N85-35746
SWARR, T. E. N85-35300
SWETTE, L. N85-35471
SWIDER, W. N85-35521
SWIMM, R. T. N85-35395
SYMONS, T. J. M. N85-35705
SZABELSKI, J. N85-35862
N85-35973
N85-36069
SZCZESNY, P. M. N85-35495
SZLYK, P. N85-35612

T

TAIRA, T. N85-35911
TAJIMA, T. N85-35760
N85-35846
TAKAHASHI, K. N85-35740
N85-35842
TAKAHASHI, N. N85-36086
TAKAHASHI, T. N85-36087
N85-36089
TAKAHASHI, Y. N85-35884
TAKAHASI, T. N85-36001
TAKEUCHI, T. N85-36053
N85-36146
TALIPOV, D. A. N85-35960
TALOCHKIN, V. P. N85-36100
TAMADA, M. N85-35923
N85-35924
TANAHASHI, G. N85-35970
N85-35989
N85-36128
TANAHASNI, G. N85-36002
N85-36015
TANAKA, T. J. N85-35398
TARLE, G. N85-36131
TASHPULATOV, R. N85-36019
N85-36020
N85-36021
TATALASHVILI, N. G. N85-35916
TATEYAMA, N. N85-35911
TATI, T. N85-35959
TAYLOR, J. R. N85-35195
TAYLOR, P. A. N85-35411
TAYLOR, R. A. N85-35808
TAYLOR, R. L. N85-35660
TAYLOR, R. S. N85-36151
TEGHT, U. N85-35480
TEGTH, U. N85-35481
TEITLER, S. N85-35682
TENG, T. N85-35529
TER-ANTONIAN, S. V. N85-35866
N85-35952
TESCHE, F. M. N85-35771
TESHIMA, M. N85-36054
TESHIMA, T. N85-36002
THOMAS, F. N85-35597
THOMAS, R. H. N85-35746
THOMPSON, D. R. N85-35758
THOMPSON, J. A. N85-35226
THOMPSON, K. N85-35664
THORNE, C. B. N85-35617
TIMBERLAKE, J. R. N85-35736
TISCHLER, M. E. N85-35588
N85-35589
N85-35590
N85-35591
N85-35594
TOBISKA, W. K. N85-35213
TOKIMATSU, K. N85-35527
TOLMAN, B. N85-35747
TOMASZEWSKI, A. N85-35962
TOMIYAMA, T. N85-36161
TONWAR, S. C. N85-35976
N85-36000
N85-36143
TORII, S. N85-35911
N85-35928
TORSTI, J. J. N85-36044
N85-36045
TOWNES, C. H. N85-35832
TOYODA, Y. N85-36053
N85-36146
TRACY, B. A. N85-35575
TRAVIS, C. C. N85-35618
TRETYAKOVA, M. I. N85-35887
TRINCHERO, G. C. N85-36099
TRIPHONOVA, S. V. N85-35950
TRUBKIN, Y. A. N85-36078
TRUNCANO, T. G. N85-35386
TSOMAYA, P. V. N85-35916
N85-35917
N85-35995
TSUCHIMA, I. N85-35927
TSUCHIMOTO, I. N85-36055
N85-36056
N85-36145
TSUJI, K. N85-36127
TSUSHIMA, I. N85-35926
TUKISH, E. I. N85-35915
N85-36038
TULL, C. N85-35712
TUNG, S. L. N85-35684
TURKEL, E. N85-35375
TURNER, J. E. N85-35725
TURTELLI, A., JR. N85-35942
TUSZEWSKI, M. N85-35778
TUTAS, J. N85-36138

U

UBERALL, H. N85-35697
UCHAIKIN, V. V. N85-35918
ULKE, H. N85-35168
UMEDA, H. N85-36001
N85-36087
USHEV, S. Z. N85-35971
N85-36034
N85-36119
USSAILIS, J. S. N85-35334

V

VAINIKKA, E. N85-36044
N85-36045
VALTONEN, E. N85-36044
N85-36045
VANAJAKSHI, C. T. N85-35837
VANCOV, K. N85-36033
VANDALEN, G. N85-35705
VANDERWALT, D. J. N85-36062
VANKOV, C. P. N85-36027
VANNICE, M. A. N85-35394
VARADANYAN, I. N. N85-36125
VARKOVITSKAYA, A. Y. N85-35908
VAVILOV, Y. N. N85-36123
VERBETSKI, Y. G. N85-35916
N85-35995
VERLY, J. G. N85-35634
VERNETTO, S. N85-36099
VERNON, W. N85-36137
VICKERS, E. C. N85-35195
VIETS, J. G. N85-35440
VILAS, F. N85-35838

VILDANOV, N. G. N85-35915
VILNROTTER, V. A. N85-35750
VINCENT, F. J. M. N85-35339
VIOLETTE, E. J. N85-35331
VIOLETTE, P. B. N85-35698
VISCUSO, P. J. N85-35833
VISSER, H. G. N85-35186
VLADIMIRSKY, B. M. N85-36023
VODENICHAROVA, T. N85-36033
VOERSMANN, P. N85-35558
VOEVODSKY, A. V. N85-36074
N85-36075
VOGEL, J. A. N85-35614
VOGEL, R. R. N85-35646
VOGT, H. L. N85-35598
VOINOV, V. G. N85-35920
VOLK, G. N85-35764
VOLKOV, A. N. N85-36005
VONDY, D. R. N85-35734
VOROBYEV, K. V. N85-35946
N85-35948

W

WADA, T. N85-36086
N85-36150
N85-36161
WADDINGTON, C. J. N85-35876
WAGNER, H. L. N85-35306
WAGNER, J. S. N85-35846
WANG, C. R. N85-35902
N85-35921
N85-35930
N85-35937
N85-35964
WANG, P. S. N85-35309
WANG, Y. X. N85-35902
N85-35921
N85-35930
N85-35937
N85-35964
WANGLER, T. P. N85-35784
WARD, R. A. N85-35740
N85-35842
WARD, S. M. N85-35390
WARINNER, D. K. N85-35657
WASILEWSKI, A. N85-35957
N85-35958
WASZAK, M. R. N85-35202
N85-35203
WATANABE, K. N85-36144
WATANABE, Z. N85-36160
N85-36162
WATSON, A. A. N85-36057
WATSON, D. M. N85-35832
WATSON, J. M. N85-35405
WATSON, R. E. N85-35286
WAUCHOPE, K. N85-35671
WDEYOZYK, J. N85-35973
WDOWCZYK, J. N85-35862
N85-35999
N85-36069
WEBB, M. L. N85-35712
WEBBER, S. E. N85-35263
WEBER, W. N85-35487
WEGMANN, H. M. N85-35599
WEHRLE, R. N85-35773
WEI, G. C. N85-35299
WEINLAND, S. L. N85-35289
WEISS, D. L. N85-35359
WEISS, S. B. N85-35593
WEISS, W. E. N85-35179
WERNER, S. D. N85-35434
WEST, A. A. N85-36057
WESTCOTT, C. N85-35273
WHALEN, J. F. N85-35731
WHITBECK, R. G. N85-35315
WHITE, J. M. N85-35263
WHITE, J. R. N85-35659
WHITE, J. T. N85-36137
WHITE, J. V. N85-35522
WHITE, R. A. N85-35564
WHITE, W. L. N85-35200
N85-35678
WIESENBURG, D. A. N85-35576
WIJDEMANS, L. J. M. N85-35339
WILD, N. R. N85-36097
WILKING, B. A. N85-35834
WILL, R. W. N85-35637
WILLE, K. N85-35785
WILLEKE, H. N85-35547
WILLENBERG, H. J. N85-35728
WILLIAMS, J. J. N85-35195
WILSON, C. W. N85-36116
WILSON, F. H. N85-35455
WILSON, J. A. N85-35799
WILT, M. J. N85-35494
WINKLER, G. R. N85-35460
WISE, J. I. N85-35386
WISEGARVER, D. P. N85-35570
WLODARCZYK, Z. N85-35962
WLODYKA, L. N85-35521
WODTKE, A. M. N85-35255
WOJCIECHOWSKI, C. J. N85-35236
WOLF, E. E. N85-35230
WOLF, M. K. N85-35821
WOLFENDALE, A. W. N85-35973
N85-36069
WOLFF, D. N85-35668
WOOD, P. C. N85-35623
WOODALL, H. N. N85-35355
N85-35780
WOODLEY, M. N85-35772
WOODWORTH, J. R. N85-35782
WORLEY, B. A. N85-35734
WOZNIAK, K. N85-35865
WRIGHT, H. A. N85-35725
WROTNIAK, J. A. N85-35864
N85-35935
N85-35969
N85-35972
WU, M. C. N85-35388
WYDEVEN, T. N85-35623

X

XUE, Y. G. N85-35902
N85-35921
N85-35930
N85-35937
N85-35964

Y

YAGAWA, G. N85-35421
YAKOVLEV, V. I. N85-36153
N85-36156
YAKOVLEVA, T. I. N85-35915
YAKUSHEV, V. F. N85-36100
YAMAMOTO, I. N85-36086
N85-36150
N85-36161
YAMAMOTO, Y. N85-35928
N85-35929
N85-35987
N85-35988
YAMASHITA, S. N85-35944
N85-35945
YAMASHITA, Y. N85-36150
N85-36161
YANAGITA, T. N85-35955
N85-36159
YANEZPINTADO, G. N85-35511
YEN, M. M. N85-35655
YEREMIAN, S. S. N85-35852
YERSHOV, A. A. N85-36125
YODH, G. B. N85-35851
N85-35864
N85-35969
N85-35972
N85-36000
N85-36143
YOON, C. S. N85-35868
YORK, J. E. N85-35455
YOSHIDA, A. N85-35911
YOSHII, H. N85-36088
N85-36145
YOUNG, G. N85-35705
YOUNG, J. C. N85-35712
YOUNG, M. N85-35755
YUAN, Y. N85-36157
YUDA, T. N85-35903
N85-35928
N85-35940
YULDASHBAEV, T. S. N85-35960
N85-35961
YUMATOV, V. I. N85-36090
YUNN, B. C. N85-36008

Z

ZACHARIAS, G. L. N85-35642
ZAJC, W. N85-35709
ZAKIDYSHEV, V. N. N85-36115
ZAMCHALOVA, E. A. N85-35908
ZAPATA, J. N85-35927
ZAREMBA, W. N85-35163
ZATSEPIN, G. T. N85-35899
N85-35938
N85-35939
N85-36071
N85-36100
N85-36107
N85-36126
ZATSEPIN, V. I. N85-35908
ZAWADA, F. A. N85-35729
ZAZYAN, M. Z. N85-35951
ZHAMKOCHIAN, V. M. N85-35852
ZHANG, N. J. N85-35902
N85-35921
N85-35930
N85-35937
N85-35964
ZHELEZNYKH, I. M. N85-36039
ZHENG, R. N85-36157
ZHOU, Y. Z. N85-35855
ZHU, Q. N85-35904
ZHUKOV, V. Y. N85-36021
N85-36024
ZHUKOVA, L. T. N85-35268
ZIERENBERG, R. A. N85-35446
ZUCKERWAR, A. J. N85-35307
ZWAHR, H. N85-35486
ZYSKIN, Y. I. N85-36023

CORPORATE SOURCE INDEX

Typical Corporate Source Index Listing

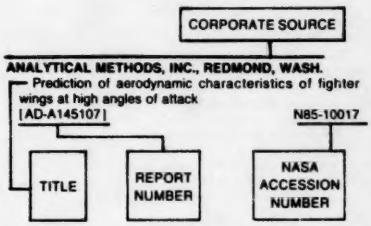

Listings in this index are arranged alphabetically by corporate source. The title of the document provides the user with a brief description of the subject matter. The report number helps to indicate the type of document cited (e.g., NASA report, translation, NASA contractor report). The NASA accession number denotes the number by which the citation is identified. The titles are arranged under each corporate source in ascending accession number order.

A

ACADEMIA SINICA, BEIJING (CHINA).
Measurement of interaction cross section of cosmic ray Fe nuclei (E4 GeV/N) with Al target
[HE-1.1-7] N85-35855
Intensities of high-energy cosmic rays at Mount Kanbala
[HE-3.1-2] N85-35902
On the characteristics of emulsion chamber family events produced in low heights
[HE-3.1-8] N85-35904
Transverse momentum distribution of pion deg in the fragmentation region of super high energy interactions N85-35921
A cosmic ray super high multicore family event. 1: Experiment and general features
[HE-3.4-1] N85-35930
Observation of super high energy big family with large scale Fe emulsion chambers
[HE-3.4-3] N85-35932
On the halo events observed by Mount Fuji and Mount Kanbala Emulsion Chamber Experiments
[HE-3.4-9] N85-35937
Intensities of high-energy cosmic rays at Mount Kanbala
[HE-3.7-5] N85-35964
Exploring results of the possibility on detecting cosmic ray particles by acoustic way
[HE-7.1-3] N85-36157

ACADEMY OF SCIENCES OF THE ARMENIAN SSR, ERIVAN (USSR).
On total cross sections and slopes at superhigh energies
[HE-1.1-4] N85-35852
Determination of the cross section of the proton, pion and neutron inelastic interaction with lead and carbon nuclei at 0.5 - 5.0 TeV energies (PION experiment)
[HE-1.1-5] N85-35853
Angular distribution and multiplicity of backward hadrons in hFe interactions at 0.5-5.0 TeV energies (PION Experiment)
[HE-1.2-8] N85-35866
Experiment Pamir-3. Coplanar emission of high energy gamma-quanta at interaction of hadrons with nuclei of air atoms at energies above 10 to the 7th power GeV
[HE-1.4-12] N85-35899
Multidimensional analysis of data obtained in experiments with X-ray emulsion chambers and extensive air showers
[HE-3.6-2] N85-35951
A new method of differential structural analysis of gamma-family basic parameters
[HE-3.6-3] N85-35952
Dependence of the average spatial and energy characteristics of the hadron-lepton cascade on the strong interaction parameters at superhigh energies N85-35977
The system of EAS time analysis
[HE-4.4-10] N85-36018

ACADEMY OF SCIENCES OF THE GEORGIAN SSR, TBILISI (USSR).
Hadron intensity and energy spectrum at 4380 m above level
[HE-3.1-7] N85-35905
Scaling violation in hadron-nucleus interaction
[HE-3.2-8] N85-35916
Few-particles generation channels in inelastic hadron-nuclear interactions at energy approximately equals 400 GeV
[HE-3.2-9] N85-35917
Structured events in Pamir carbon X-ray chambers
[HE-3.7-7] N85-35965
Tskhra-Tskaro complex intended for the investigations of EAS spatial characteristics near axis N85-35995

ACADEMY OF SCIENCES OF THE UZBEK SSR, TASHKENT.
A comparative analysis of gamma and hadron families at the superhigh energies recorded in experiment Pamir
[HE-3.7-1] N85-35960
A study of gamma-families generated in nucleon-nucleus (NA) and pion-nucleus (pi A) interactions
[HE-3.7-2] N85-35961

ACADEMY OF SCIENCES (USSR), ALMA-ATA.
A unification of the interactions and the diffractive processes N85-35870
Is the inelastic charge-exchange contribution constant at the large X and superhigh energies? Qaut 01Kuchin, I. A. N85-35871
On the mechanism of anomalous nucleus-nucleus interactions at energies above 1 TeV/nucleon
[HE-1.4-8] N85-35896
Characteristics of anomalously high multiplicity cosmic ray interactions
[HE-3.3-1] N85-35920
Peculiarities of gamma-quanta distribution at 20 TeV energy
[HE-3.7-10] N85-35967

ACADEMY OF SCIENCES (USSR), MOSCOW.
The method for the study of the inelastic cross-section for high energy protons by means of shower arrays with the large calorimetric area
[HE-1.1-11] N85-35858
On a possibility of inelasticity partial coefficient K sub gamma determination in pi C and pi Pb interactions at 10 to the 14th power eV (experiment PAMIR 1)
[HE-1.1-12] N85-35859
Propagation of cosmic rays through the atmosphere in the quark-gluon strings model N85-35873
Scaling violation in the fragmentation region of inclusive nucleon spektrum N85-35874
Ringlike inelastic events in cosmic rays and accelerators N85-35887
X-ray film chamber with carbon target of Tien-Shan complex array N85-35915
Experiment Pamir-2. Fianit: A giant super-family with halo (Epsilon sub 0 at approximately 10(17) eV)
[HE-3.4-10] N85-35938
Experiment Pamir-4: Analysis of superfamily with halo of electromagnetic nature detected in deep XEC
[HE-3.4-11] N85-35939
About increase of the large transvere momentum processes fraction in hA interactions at energies 5.10(14) - 10(16) eV according to the data on E.A.S. hadrons N85-35979
Phenomenological characteristic of the electron component in gamma-quanta initiated showers
[HE-4.5-11] N85-36034
Nuclear cascades in electromagnetic showers produced by primary gamma-quanta in the atmosphere
[HE-4.5-16] N85-36038
On the possibilities of large-scale radio and fiber optics detectors in cosmic rays
[HE-4.6-2] N85-36039
The spectrum of cosmic ray muons obtained with 100-ton scintillation detector underground and the analysis of recent experimental data
[HE-5.1-6] N85-36071
Muon groups and primary composition at 10 to the 13th power to 10 to the 15th power eV
[HE-5.1-12] N85-36074
Primary chemical composition from simultaneous recording of muons induced cascades and accompanying muon group underground
[HE-5.1-13] N85-36075
On muon energy spectrum in muon groups underground
[HE-5.1-14] N85-36076
Energy spectrum of cascades generated by muons in Baksan underground scintillation telescope
[HE-5.1-15] N85-36077
Underwater measurements of muon intensity
[HE-5.1-16] N85-36078
Measurements of light background at large depth in the ocean
[HE-5.2-8] N85-36085
On method of muon spectrum measurements by the scintillation detectors of a large thickness T4t sub o
[HE-5.2-18] N85-36094
The research program of the Liquid Scintillation Detector (LSD) in the Mont Blanc Laboratory
[HE-5.3-6] N85-36100
The capability of the existing network of installations for detecting the antineutrino burst from collapsing stars
[HE-5.3-13] N85-36107
A standard source for high energy neutrino astronomy
[HE-5.3-15] N85-36109
A search for cosmic sources of high energy neutrinos with small underground detectors
[HE-5.3-16] N85-36110
Angular distribution of muons produced by cosmic ray neutrinos in rock
[HE-5.3-24] N85-36115
Anomalies in cosmic rays: New particles versus charm?
[HE-5.4-9] N85-36120
Study of photonuclear muon interactions at Baksan underground scintillation telescope
[HE-5.4-10] N85-36122
Calculation of intensity of high energy muon groups observed deep underground
[HE-5.4-13] N85-36123
Collimated groups of particles as possible manifestation of heavy meson production
[HE-5.4-14] N85-36124
Upper limit on magnetic monopole flux from Baksan experiment
[HE-6.1-11] N85-36136
Tien-Shan effect and charmed particles
[HE-6.2-17] N85-36153

ACADEMY OF SCIENCES (USSR), TROITSK.
Connection between variations of the atmosphere temperature profile and variations of the meson component intensity
[HE-3.1-12] N85-35910
Samarkand complex setup for investigation of cosmic ray variation in the energy range of 7 10 (9) - 10 (15) eV
[HE-4.6-14] N85-36050

ACADEMY OF SCIENCES (USSR), YAKUTSK.
The maximum depth of shower with E sub 0 larger than 10(17) eV on average characteristics of EAS different components N85-35981

ADAPTIVE SENSORS, INC., SANTA MONICA, CALIF.
L-step sequential decoding
[AD-A156121] N85-35649
Pruned error-trellis decoding of certain non-systematic convolutional codes
[AD-A156122] N85-35650

ADELAIDE UNIV. (AUSTRALIA).
Analysis of Cerenkov pulses recorded simultaneously at two sites
[HE-4.4-16] N85-36022
The muon content of gamma-ray showers
[HE-4.5-7] N85-36031
A transient digitiser for fast air shower events
[HE-5.2-21] N85-36097

Muon and neutrino fluxes
[HE-6.2-18] N85-36154

AEG-TELEFUNKEN, FRANKFURT AM MAIN (WEST GERMANY).
Development of contactless sensors for industrial and automative applications
[BMFT-FB-T-85-031] N85-35400

AERODYNE RESEARCH, INC., BILLERICA, MASS.
Holoswitch
[AD-A155841] N85-35392
A study of the chemistry of alkali metals in the upper atmosphere
[AD-A156349] N85-35524

AERONAUTICAL RESEARCH INST. OF SWEDEN, STOCKHOLM.
General environmental aspects of large scale wind energy utilization N85-35474
Wind turbine noise: Prediction tools and design parameter dependence N85-35477

AERONAUTICAL RESEARCH LABS., MELBOURNE (AUSTRALIA).
Fatigue lives of specimens representing critical locations in Mirage 3 spars under Australian and Swiss test spectra
[ARL-STRUC-R-415] N85-35187

AEROSPACE CORP., EL SEGUNDO, CALIF.
A methodology for the design of testable custom large-scale integrated circuits
[AD-A156098] N85-35351
Two-dimensional quasineutral description of particles and fields above discrete auroral arcs
[NASA-CR-176170] N85-35517
Constrained stiffness matrix adjustment using mode data
[AD-A155988] N85-35685

AEROSPACE MEDICAL RESEARCH LABS., WRIGHT-PATTERSON AFB, OHIO.
The effect of +Gx acceleration on platelet activation as determined by plasma platelet factor 4 levels
[AD-A155861] N85-35608
Simulation of high +Gz onset in the dynamic environment simulator
[AD-A155963] N85-35610

AGBABIAN ASSOCIATES, EL SEGUNDO, CALIF.
An evaluation of a class of practical optimization techniques for structural dynamics applications
[PB85-195766] N85-35434

AICHI WOMEN'S COLL. (JAPAN).
The development of air shower in the iron absorber N85-35987
A large area cosmic muon detector located at Ohya stone mine
[HE-5.1-7] N85-36072

AIN SHAMS UNIV., CAIRO (EGYPT).
Relationship of sea level muon charge ratio to primary composition including nuclear target effects
[HE-5.4-10] N85-36121

AIR COMMAND AND STAFF COLL., MAXWELL AFB, ALA.
Introduction to European air traffic control
[AD-A156328] N85-35176
International flight planning handbook
[AD-A156330] N85-35177
A guide to USAF helicopter instrument flight procedures
[AD-A156102] N85-35182
RAFTS: A T-38 replacement for the 21st century
[AD-A156103] N85-35191
Next generation gunship
[AD-A156361] N85-35193
Arms control and The President's Strategic Defense Initiative
[AD-A156334] N85-35212
A guide for new environmental coordinators
[AD-A156327] N85-35498
Relaxation techniques
[AD-A156248] N85-35621
Air university commander's and supervisor's guide on substance abuse
[AD-A156336] N85-35622
Aeronautical Systems Division Manufacturing/Quality assurance orientation
[AD-A156128] N85-35817

AIR FORCE GEOPHYSICS LAB., HANSCOM AFB, MASS.
A multi-channel radar receiver
[AD-A156058] N85-35333
A ray trace program for line-of-sight microwave communication links
[AD-A156168] N85-35336
Linear absorption and scattering of laser beams
[AD-A156167] N85-35401
Optimal estimation of a high degree gravity field from a global set of 1 deg x 1 deg anomalies to degree and order 250
[AD-A156008] N85-35519
Ion composition measurements of the disturbed and quiet D-region in 1980 - 1981
[AD-A156055] N85-35521

AIR FORCE HUMAN RESOURCES LAB., BROOKS AFB, TEX.
An exploratory study of the effect of screen size and resolution on the legibility of graphics in automated job performance aids
[AD-A155969] N85-35632

AIR FORCE INST. OF TECH., WRIGHT-PATTERSON AFB, OHIO.
Investigation of experimental lightweight firewall materials for A/C engine bay applications
[AD-A155765] N85-35175
Evaluation of nuclear detonation location capability under high attack scenario
[AD-A155761] N85-35729

AIR FORCE WRIGHT AERONAUTICAL LABS., WRIGHT-PATTERSON AFB, OHIO.
Nitrogen analysis by chemiluminescence
[AD-A156197] N85-35308

AIRTECH PRECISION SHOT PEENING, LIVONIA, MICH.
Development of a mathematical model for predicting the percentage fatigue life increase resulting from shot peened components
[AD-A155774] N85-35425

ALLIED BENDIX AEROSPACE, KANSAS CITY, MO.
X-ray fluorescence analysis of 304L stainless steel
[DE85-013254] N85-35288

ALTAI STATE UNIV., BARNAUL (USSR).
The model of independent particles emission in the multiparticle production theory
[HE-3.2-10] N85-35918
Numerical analysis of electromagnetic cascades in emulsion chambers
[HE-3.5-9] N85-35946

AMES LAB., IOWA.
Master Fit users' guide, version 1.0
[DE85-014199] N85-35667

ANALYTIC SCIENCES CORP., READING, MASS.
Gravity gradiometer survey data processing
[AD-A156165] N85-35522

APPLIED CONCEPTS CORP., WOODSTOCK, VA.
Investment justification of robotic technology in aerospace manufacturing. User's manual
[AD-A156193] N85-35410

APPLIED PHYSICS LAB., JOHNS HOPKINS UNIV., LAUREL, MD.
Network management simulation of automated guideway transit systems under vehicle-follower control
[PB85-188233] N85-35830

ARGONNE NATIONAL LAB., ILL.
Effect of temperature and ionic impurities at very low concentrations on stress corrosion cracking of Type 304 stainless steel
[TI85-003048] N85-35283
Response of a BWR Mark 2 containment vessel head to loads beyond the design basis
[DE85-010524] N85-35432
SASSYS-1 computer code verification with EBR-2 test data
[DE85-012119] N85-35657
Acoustic resonances in cylinder bundles oscillating in a compressible fluid
[DE85-004066] N85-35699
High-resolution spectroscopy and dynamics of multiphoton processes in atoms and molecules
[AD-A155862] N85-35714
Fast-neutron interaction with niobium
[DE85-011471] N85-35731
Analysis of reactor material experiments investigating oxide fuel crust stability and heat transfer in jet impingement flow
[DE85-012097] N85-35739
Beam intensity increases at the intense pulsed neutron source accelerator
[DE85-012377] N85-35764
Vacuum system for the Argonne 6 GeV synchrotron light source
[DE85-012286] N85-35773
State-of-the-art of solid-state motor controllers
[TI85-008674] N85-35806
Construction of the Soudan 2 detector
[HE-6.2-5] N85-36141

ARIZONA STATE UNIV., TEMPE.
Heat transfer characteristics for two-dimensional arrays of impinging jets with initial crossflow N85-35365

ARIZONA UNIV., TUCSON.
Possible mechanism for changes in glycogen metabolism in unloaded soleus muscle
[NASA-CR-176184] N85-35588
Response of amino acids in hindlimb muscles to recovery from hypogravity and unloading by tail-cast suspension
[NASA-CR-176183] N85-35589
Response of rat hindlimb muscles to 12 hours recovery from tail-cast suspension
[NASA-CR-176182] N85-35590
Muscle protein and glycogen responses to recovery from hypogravity and unloading by tail-cast suspension
[NASA-CR-176181] N85-35591
Responses of skeletal muscle to unloading, a review
[NASA-CR-176177] N85-35594
The nature and origin of outer solar system asteroids from reflectance spectrophotometry N85-35838
Air fluorescence detection of large air showers below the horizon
[HE-4.6-6] N85-36043
Search for acoustic signals from high energy cascades
[HE-7.1-1] N85-36155

ARMY ENGINEER TOPOGRAPHIC LABS., FORT BELVOIR, VA.
Determining an azimuth with a north seeking gyro
[AD-A155880] N85-35180

ARMY ENGINEER WATERWAYS EXPERIMENT STATION, VICKSBURG, MISS.
State-of-the-art construction technology for deep tunnels and shafts in rock
[AD-A156362] N85-35411
User's guide: A computer program for strength analysis of non-hydraulic concrete structural elements. Report 1. Concrete General Strength Investigation (CGSI)
[AD-A156392] N85-35428
User's guide: A computer program for strength analysis of non-hydraulic concrete structural elements. Report 2. Strength design of reinforced concrete column sections (PCAUC)
[AD-A156393] N85-35429

ARMY MATERIALS AND MECHANICS RESEARCH CENTER, WATERTOWN, MASS.
Microshrink, tensile properties, and the detection of microshrink
[AD-A155875] N85-35278

ARMY MILITARY PERSONNEL CENTER, ALEXANDRIA, VA.
Wholebody radiation counting system
[AD-A155842] N85-35607
Optimize computer throughput using array processors
[AD-A155843] N85-35628
(NAT)Fe(n,n'x) spectra at 65.5 MeV
[AD-A155776] N85-35730

ARMY MISSILE COMMAND, REDSTONE ARSENAL, ALA.
Actuator rigging test set electromagnetic interference test (CE03)
[AD-A155819] N85-35327

ARMY RESEARCH INST. OF ENVIRONMENTAL MEDICINE, NATICK, MASS.
Weight loss, rectal temperature and heart rates following the 1984 Boston Marathon
[AD-A155984] N85-35612
An analysis of aerobic capacity in a large United States population
[AD-A156200] N85-35614
Thirst and fluid intake following graded hypohydration levels in humans
[AD-A156201] N85-35615

ARMY TEST AND EVALUATION COMMAND, ABERDEEN PROVING GROUND, MD.
Laboratory vibration schedules
[AD-A155856] N85-35188
Analyzer, flight line
[AD-A155777] N85-35207

AVCO SYSTEMS DIV., WILMINGTON, MASS.
Enhancement of the flexible spacecraft dynamics program for open spacecraft
[NASA-CR-175309] N85-35641

B

BALLISTIC RESEARCH LABS., ABERDEEN PROVING GROUND, MD.
Computational methods for the explosive and impact compaction of powders
[AD-A156219] N85-35653

BARI UNIV. (ITALY).
Monopole, astrophysics and cosmic ray observatory at Gran Sasso
[HE-6.1-4] N85-36130

BATTELLE COLUMBUS LABS., OHIO.
Basic research on pulse-combustion phenomena
[PB85-200228] N85-35265
Establishment of a Computer-Aided Design (CAD)-Computer-Aided Manufacturing (CAM) process for the production of cold forged gears
[AD-A155756] N85-35644

BATTELLE PACIFIC NORTHWEST LABS., RICHLAND, WASH.
Turbulent structure of stably stratified nocturnal slope flows
[AD-A155845] N85-35559
BERN UNIV. (SWITZERLAND).
Multiple muons of conventional and exotic origin in DUMAND
[HE-5.4-4] N85-36117
BOEING AEROSPACE CO., SEATTLE, WASH.
Applicability of 100kWe-class of space reactor power systems to NASA manned space station missions
[NASA-CR-174696] N85-35728
BOLT, BERANEK, AND NEWMAN, INC., CAMBRIDGE, MASS.
Pluribus satellite IMP (Interface Message Processors) development mobile access terminal network
[AD-A155754] N85-35216
BONN UNIV. (WEST GERMANY).
Motor glider meteorology N85-35543
Partitioning of the vertical turbulent energy transport into positive and negative contributions N85-35551
Aircraft measurements during the Bonn Experiment (BONEX 1) N85-35552
Motor glider measurements during the Urban Atmosphere Energy Budget Experiment (EESA 1) N85-35553
BORDEAUX UNIV. (FRANCE).
Analysis of the hadron component in E.A.S. N85-35971
New aspects in nucleon-nucleus collisions and EAS properties around 10(6) GeV N85-35974
Small air showers and collider physics
[HE-4.1-9] N85-35975
Topological aspects of age parameter
[HE-4.3-13] N85-36007
BORDEAUX 1 UNIV., GRADIGNAN (FRANCE).
LPM effect and primary energy estimations
[HE-3.6-4] N85-35953
Ultra high energy events in ECHOS series and primary energy spectrum
[HE-3.7-9] N85-35966
Analysis of the electron component of EAS at observational level 700 g x cm(-2) with a scale breaking interaction model and gammaisation hypothesis
[HE-5.4-8] N85-36119
BRAUN (WILLIS H.), BEREA, OHIO.
Unsteady flow in a supersonic cascade with two in-passage shocks
[NASA-CR-3925] N85-35158
BREMEN UNIV., (WEST GERMANY).
A graph theoretic procedure for the design of feedback patterns
[REPT-110] N85-35673
Design of dynamic compensators of prescribed pattern
[BU-109] N85-35674
Spreading the control complexity in decentralized control of interconnected systems
[BU-117] N85-35688
Decentralized stabilization by high gain feedback
[BU-115] N85-35689
BRITISH BROADCASTING CORP., KINGSWOOD (ENGLAND).
Acoustic scaling: The development of improved instrumentation
[BBC-RD-1985/7] N85-35694
BRITISH LIBRARY LENDING DIV., BOSTON SPA (ENGLAND).
Decomposition of martensite in R6M5 and R6AM5 steels after direct immersion in liquid nitrogen
[BLL-M-36305] N85-35268
Influence of yttrium on eutectoid transformation in irons
[BLL-M-35787-(5828.4)] N85-35270
BROOKHAVEN NATIONAL LAB., UPTON, N. Y.
Noble metals as incipient transition metals
[DE85-013283] N85-35286
Tuning system for capacitively loaded 1/4 accelerating cavity
[DE85-012516] N85-35358
Distribution of computer functionality for accelerator control at the Brookhaven AGS
[DE85-012520] N85-35669
Summary of the working group on penetrating probes in collider experiments. 1: The collider environment N85-35704
Very high energy probes of the quark-gluon plasma N85-35708
Cooling high intensity atomic hydrogen beams to liquid helium temperatures
[DE85-012515] N85-35718
Robinson instability and beam loading
[DE85-013301] N85-35737
High vacuum portable pumping station suitable for accelerator use
[DE85-011840] N85-35759
Applications of decelerated ions
[DE85-011832] N85-35767
Synchronous timing of multi-energy fast beam extraction during a single AGS cycle
[DE85-011829] N85-35781
Effect of Cu4Ti compound formation on the characteristics of NbTi accelerator magnet wire
[DE85-014226] N85-35788
BRUSH WELLMAN, INC., CLEVELAND, OHIO.
Beryllium production
[DE85-013360] N85-35716
BULGARIAN ACADEMY OF SCIENCE, SOFIA.
Theoretical study of EAS hadronic structure N85-35991
Simulation of gamma-initiated showers
[HE-4.5-10] N85-36033
BUREAU OF MINERAL RESOURCES, GEOLOGY AND GEOPHYSICS, CANBERRA (AUSTRALIA).
Workshop Proceedings: Interpretation of Seismic Wave Propagation in Laterally Heterogeneous Structures
[BMR-258] N85-35530
BUREAU OF MINES, AVONDALE, MD.
Spectral characteristics of grinding sparks used for identification of scrap metals
[PB85-198570] N85-35290
BUREAU OF MINES, ROLLA, MO.
Deposition of nickel-cobalt alloys by controlled-potential electrolysis
[PB85-198562] N85-35291
BUREAU OF RECLAMATION, DENVER, COLO.
Project Skywater, 1983-84 SCPP (Sierra Cooperative Pilot Project) data inventory
[PB85-187052] N85-35565

C

CALIFORNIA INST. OF TECH., PASADENA.
Structural analysis of imperfect three-legged truss columns for large space structures applications N85-35416
Studies in photochemical smog chemistry. 1: Atmospheric chemistry of toulene. 2: Analysis of chemical reaction mechanisms for photochemical smog N85-35497
Crustal structure in southern California from array data N85-35512
Applications of the Kirchoff-Helmholtz integral to problems in body wave seismology N85-35515
Error-correcting codes for computer memories N85-35636
Neutrino production of like sign dimuons
[DE85-013594] N85-35741
Accelerator physics measurements at the damping ring
[DE85-013373] N85-35785
Circumstellar shells of late-type stars: A study at millimeter and infrared wavelengths N85-35836
A dynamic model of Venus's gravity field
[NASA-CR-176173] N85-35845
A study of atmospheric neutrinos with the IMB detector
[HE-5.3-7] N85-36101
CALIFORNIA UNIV., BERKELEY.
The photodissociation of acetylene at 193.3 NM
[AD-A155775] N85-35255
Cluster variation study of coherent ordering in FCC and BCC solid solutions
[AD-A156039] N85-35280
Experimental study of free and mixed convective flow of air in a heated cavity
[DE85-012538] N85-35380
Three-dimensional finite deformation viscoelastic model accounting for damage effects
[DE85-012951] N85-35660
Search for supermassive magnetic monopoles using mica crystals
[HE-6.1-8] N85-36134
CALIFORNIA UNIV., BERKELEY. LAWRENCE BERKELEY LAB.
Characterization of the optical and thermal properties of matter by photothermal techniques
[DE85-012607] N85-35260
Aqueous volatile weak electrolyte equilibria to 300 C
[DE85-013840] N85-35261
Two-dimensional inversion of resistivity monitoring data from the Cerro Prieto geothermal field
[DE85-012554] N85-35494
Proceedings of the Workshop on Detectors for Relativistic Nuclear Collisions
[LBL-18225] N85-35700
Event parameters: Fixed targets N85-35702
Report of working group on detectors for hadrons and event parameters at colliders N85-35705
A lead glass tubing drift calorimeter N85-35711
Gamma-ray production cross sections for alpha-particle induced reactions on F-19 and Na-23
[DE85-012603] N85-35732
Neutron production by Ne and Si ions on a thick Cu target at 670 MeV/A with application to radiation protection
[DE85-014526] N85-35746
Numerical studies of high current beam compression in heavy ion fusion
[DE85-011874] N85-35783
CALIFORNIA UNIV., DAVIS.
Heat transfer coefficients for particles in liquid in axially rotating cans N85-35370
Vibrations of free hollow circular cylindrical bodies N85-35418
Geology: Structural history and fluvial geomorphology of the southern Death Valley Fault Zone, Inyo and San Bernardino Counties, California N85-35506
Fractional charge resolution in music N85-35712
CALIFORNIA UNIV., LA JOLLA.
Phase space factors in multiparticle processes N85-35888
CALIFORNIA UNIV., LIVERMORE. LAWRENCE LIVERMORE LAB.
Dynamic compaction of a monosized spherical tungsten powder
[DE85-014808] N85-35289
Single-point diamond crushing of Zerodur with in-situ polishing and metrology on a diamond turning machine
[DE85-012918] N85-35305
ATA upgrade to 150 MeV
[DE85-013174] N85-35404
Investigation of the lightning vulnerability of nuclear explosive test systems at the Nevada Test Site
[DE85-011761] N85-35563
SIG: A general-purpose signal processing program. User's manual: Revision 1
[DE85-013035] N85-35662
Pulsed-neutron-source models for the astrophysical s-process
[DE85-012927] N85-35740
Ground motion measurements for the QUESO nuclear event
[DE85-014806] N85-35743
Numerical studies of high current beam compression in heavy ion fusion
[DE85-011874] N85-35783
Resonance localization in tokamaks excited with ICRF waves
[DE85-014559] N85-35791
Some nuclear data needs in astrophysics
[DE85-012916] N85-35842
CALIFORNIA UNIV., LOS ANGELES.
Working group on penetrating probes at fixed target facilities N85-35703
Electronic structure and lattice dynamics of dimensionally constrained and disordered solids
[AD-A155927] N85-35797
CALIFORNIA UNIV., RICHMOND.
Simplified procedures for the evaluation of settlements in sands due to earthquake shaking
[PB85-197887] N85-35527
CALIFORNIA UNIV., SAN DIEGO.
Applications of the Galerkin formalism in the coupling of the earth's free oscillations N85-35514
CALIFORNIA UNIV., SAN DIEGO, LA JOLLA.
Development of observational and instrumental techniques in hard X-ray and medium energy gamma-ray astronomy
[NASA-CR-176172] N85-35841
Results from the UCSD magnetic monopole search
[HE-6.1-12] N85-36137
CALIFORNIA UNIV., SANTA BARBARA.
Research on GaSb/AlSb multi-quantum well superlattices
[AD-A156080] N85-35800
CANYON RESEARCH GROUP, INC., WESTLAKE VILLAGE, CALIF.
A review of motion sickness with special reference to simulator sickness
[AD-A155975] N85-35611
CARNEGIE-MELLON INST. OF RESEARCH, PITTSBURGH, PA.
Reachable grasps on a polygon: The convex rope algorithm
[AD-A155913] N85-35647
CARNEGIE-MELLON UNIV., PITTSBURGH, PA.
Advanced detectors and signal processing
[NASA-CR-176193] N85-35343
CASE WESTERN RESERVE UNIV., CLEVELAND, OHIO.
Perturbation-iteration theory for analyzing microwave striplines
[NASA-CR-176189] N85-35321

Vertebrate development in space: Gravity is a drag (and has been for eons and eons) N85-35580
Report of the NASA Mammalian Developmental Biology Working Group N85-35581
A new world survey expression for cosmic ray vertical intensity vs. depth in standard rock
[HE-5.1-10] N85-36073

CASTLE TECHNOLOGY CORP., WOBURN, MASS.
Cationic exchange membrane for the zinc-ferricyanide battery
[DE85-013152] N85-35489

CATHOLIC UNIV. OF AMERICA, WASHINGTON, D.C.
Second Colloquim on the Scattering of Ultrasonic Waves
[AD-A156298] N85-35697

CENTRAL ELECTRICITY GENERATING BOARD, LONDON (ENGLAND).
Radiation measurements on magnesium flames
[BLL-CE-TRANS-8110-(9022.09)] N85-35254
Electrochemical method for investigation of the susceptibility of corrosion-resistant steels to intercrystalline corrosion
[BLL-CE-TRANS-8082-(9022.09)] N85-35269
Environmental aspects of large-scale wind-power systems in the UK N85-35478
A Programmable Automatic Noise Data and Other Related parameter Acquisition system (PANDORA) N85-35479

CENTRO BRASILEIRO DE PESQUISAS FISICAS, RIO DE JANEIRO.
Atmospheric interactions detected in both the upper and the lower chambers at Chacaltaya
[HE-3.3-7] N85-35925
A halo event created at 200 m above the Chacaltaya emulsion chamber
[HE-3.4-5] N85-35933
A binocular-type atmospheric interaction generating sequential exotic features
[HE-3.4-6] N85-35934

CHARLES RIVER ANALYTICS, INC., CAMBRIDGE, MASS.
Study of fault tolerant software technology for dynamic systems
[NASA-CR-172618] N85-35642

CHEVRON OIL FIELD RESEARCH CO., LA HABRA, CALIF.
Chemistry of ore-forming fluids N85-35436

CHICAGO UNIV., ILL.
Molecular biology of environmental aromatic hydrocarbons
[DE85-015036] N85-35593
Neutrino production of like sign dimuons
[DE85-013594] N85-35741

CHONGQING INST. OF ARCHITECTURE AND ENGINEERING (CHINA).
Measurement of the local density spectrum N85-35984
Measurement of muon intensity by Cerenkov method
[HE-5.2-15] N85-36091

COASTAL ENGINEERING RESEARCH CENTER, VICKSBURG, MISS.
Atlantic coast hindcast. Phase 2: Wave information, additional extremal estimates
[AD-A156137] N85-35575

COLOGNE UNIV. (WEST GERMANY).
Application of a turbulent closure model to the parameterization of the vertical diffusion of heat, momentum, and humidity in the ECMWF model
[MITT-41] N85-35387

COLORADO SCHOOL OF MINES, GOLDEN.
United States Army welding research and development topical and coordination meeting
[AD-A155834] N85-35409
Analysis of two-parameter constant background born inversion for acoustic synthetic data
[AD-A156394] N85-35698

COLORADO UNIV., BOULDER.
Studies of the solar mesosphere explorer: Dynamics and horizon sensor performance. Part A: Spin axis precession and atmospheric drag. Part B: Clouds
[NASA-CR-175306] N85-35213
Subcritical fracture propagation in rocks: An examination using the methods of fracture mechanics and non-destructive testing N85-35516
Toolpack
[DE85-013135] N85-35665

COLUMBIA UNIV., NEW YORK.
Neutrino production of like sign dimuons
[DE85-013594] N85-35741
High energy radiation from neutron stars
[DE85-014353] N85-35843

COMITATO NAZIONALE PER L'ENERGIA NUCLEARE, FRASCATI (ITALY).
Nucleon decay and atmospheric neutrinos in the Mont Blanc experiment
[HE-6.2-6] N85-36142

COMMITTEE ON SCIENCE AND TECHNOLOGY (U. S. HOUSE).
The 1986 National Aeronautics and Space Administration authorization
[GPO-47-635] N85-35829

COMMITTEE ON TIDAL HYDRAULICS (ARMY), WASHINGTON, D.C.
Bibliography on tidal hydraulics. Report 2. Supplement 9: Supplementary material compiled from June 1980 - June 1983. Tidal flows in rivers and harbors
[AD-A155990] N85-35574

COMMONWEALTH SCIENTIFIC AND INDUSTRIAL RESEARCH ORGANIZATION, ASPENDALE (AUSTRALIA).
The measurement of nitrogen oxide (NO, NO2) exchange over plant/soil surfaces
[CSIRO-DAR-TP-8] N85-35587

COMMONWEALTH SCIENTIFIC AND INDUSTRIAL RESEARCH ORGANIZATION, MORDIALOC (AUSTRALIA).
A strategy for calibrating atmospheric transport models
[CSIRO-DAR-TP-9] N85-35518

COMPUTER SCIENCES CORP., GULF BREEZE, FLA.
EPALIT: A data management system applied to the control and retrieval of technical reports
[PB85-193068] N85-35828

CONNECTICUT UNIV., STORRS.
Development and application of a unified viscoelastic constitutive model for the prediction of material response under thermomechanical loading N85-35420

CONSERVATION AND RENEWABLE ENERGY INQUIRY AND REFERRAL SERVICE, SILVER SPRING, MD.
Photovoltaics technology program summary
[DE85-013096] N85-35493

CONSIGLIO NAZIONALE DELLE RICERCHE, TURIN (ITALY).
Results of low energy background measurements with the Liquid Scintillation Detector (LSD) of the Mont Blanc Laboratory
[HE-5.3-5] N85-36099

CRIMEAN ASTROPHYSICAL OBSERVATORY (USSR).
Preliminary results of the Cerenkov EAS flashes the Crimean Astrophysical Observatory
[HE-4.4-17] N85-36023

D

DANISH METEOROLOGICAL INST., COPENHAGEN.
An atmospheric boundary layer model forced by the operational ECMWV-model
[WSR-3] N85-35541

DAVIDSON COLL., N.C.
Infrared generation and wave-mixing studies in cesium
[DE85-012883] N85-35304

DAYTON UNIV., OHIO.
Aspects of high-resolution gas chromatography as applied to the analysis of hydrocarbon fuels and other complex organic mixtures. Volume 1
[AD-A156154] N85-35257
The physical and empirical basis for a specific clear-air turbulence risk index
[NASA-CR-178522] N85-35540

DEFENCE RESEARCH ESTABLISHMENT, OTTAWA. (ONTARIO).
LOCAT: A data retrieval program
[AD-A156004] N85-35822

DEFENCE RESEARCH ESTABLISHMENT SUFFIELD, RALSTON (ALBERTA).
The identification of compounds in mustard hydrolysate
[AD-A156381] N85-35258

DEFENCE RESEARCH INFORMATION CENTRE, ORPINGTON (ENGLAND).
Strain measurement using point recognition picture processing
[DRIC-T-7407] N85-35421
1983 review of experimental stress and strain analysis
[DRIC-T-7469] N85-35422
Seasonal variability and spatial non-uniformity of bioluminescence in the Mediterranean Sea
[DRIC-T-7545] N85-35572

DEFENSE TECHNICAL INFORMATION CENTER, ALEXANDRIA, VA.
Source header list, supplement 3
[AD-A156100] N85-35824
Source hierarchy list. Volume 1: A through H
[AD-A156300] N85-35825
Source hierarchy list. Volume 2: I through Z
[AD-A156301] N85-35826

DENNETT, MUESSING, RYAN AND ASSOCIATES LTD., IOWA CITY, IOWA.
Evaluation: Close-range photogrammetry for slope inventory and monitoring
[PB85-192755] N85-35470

DEPARTMENT OF ENERGY, WASHINGTON, D. C.
Method of preparing thin porous sheets of ceramic material
[DE85-006399] N85-35300
Electrically conductive doped block copolymer of polyacetylene and polyisoprene
[DE85-006500] N85-35301
Limiter
[DE85-011620] N85-35736

DEPUTY CHIEF OF STAFF FOR RESEARCH DEVELOPMENT AND ACQUISITION (ARMY), WASHINGTON, D.C.
Proceedings of the 14th Army Science Conference. Volume 2: Principal authors I through O
[AD-A149201] N85-35690
Proceedings of the 14th Army Science Conference. Volume 3: Principal authors P through Z
[AD-A149202] N85-35691

DEUTSCHE FORSCHUNGS- UND VERSUCHSANSTALT FUER LUFT- UND RAUMFAHRT, OBERPFAFFENHOFEN (WEST GERMANY).
Proceedings of Meteorological Motor Glider (MEMO) Workshop '84
[DFVLR-MITT-85-04] N85-35542
Typical and historical aspects of motor gliders as meteorological measuring aircraft N85-35544
A comparison between Falcon data and motor glider data N85-35547
Case studies for flux measurements along a low-flying route to the south of Munich N85-35548
Measurements for the determination of the vertical structure of the convective boundary layer N85-35550
The determination of lee circulation during the foehn wind N85-35554
Accuracy and error analysis N85-35557

DEUTSCHES ELEKTRONEN-SYNCHROTRON, HAMBURG (WEST GERMANY).
Accelerator physics measurements at the damping ring
[DE85-013373] N85-35785

DIKEWOOD CORP., ALBUQUERQUE, N. MEX.
Air chemistry measurements 2
[AD-A156041] N85-35520

DOD PRODUCT ENGINEERING SERVICES OFFICE, ALEXANDRIA, VA.
DOD Value Engineering Conference report. Value Engineering (VE): A tool that benefits line management held at Leesburg, Virginia on 1-2 November 1984. Part 1. Executive summary
[AD-A156067] N85-35810
DOD Value Engineering Conference report. Value Engineering (VE): A tool that benefits line management held at Leesburg, Virginia on 1-2 November 1984. Part 2. Plenary session
[AD-A156068] N85-35811
DoD Value Engineering conference report. Value Engineering (VE): A tool that benefits line management. Part 3, Workshop A: VE in the program office
[AD-A155069] N85-35812
DoD Value Engineering conference report. Value Engineering (VE): A tool that benefits line management. Part 4, Workshop B: VE on spare parts
[AD-A156070] N85-35813
DoD Value Engineering conference report. Value Engineering (VE): A tool that benefits line management. Part 5, Workshop C: VEP/VECP administration, negotiation, and implementation
[AD-A156071] N85-35814
DoD Value Engineering conference report. Value Engineering (VE): A tool that benefits line management. Part 6, Workshop D: VE training-orientation
[AD-A156072] N85-35815
DoD Value Engineering conference report. Value Engineering (VE): A tool that benefits line management. Part 7, Workshop E: VE in construction and architect engineer contracts
[AD-A156073] N85-35816

DOUGLAS AIRCRAFT CO., INC., LONG BEACH, CALIF.
Calculation of compressible flow about three-dimensional inlets with auxiliary inlets, slats and vanes by means of a panel method
[NASA-CR-174975] N85-35162

DREXEL UNIV., PHILADELPHIA, PA.
Search for stellar collapse with the MACRO detector at Gran Sasso
[HE-5.3-11] N85-36105

DU PONT DE NEMOURS (E. I.) AND CO., AIKEN, S.C.
Radiation safety problems in handling highly active tritium targets
[DE85-014268] N85-35742

DURHAM UNIV. (ENGLAND).
Performance of a local electron density trigger to select extensive air showers at sea level
[HE-4.6-11] N85-36048

Search for tachyons associated with extensive air showers in the ground level cosmic radiation
[HE-6.2-13] N85-36149

E

EATON CORP., WILLOUGHBY HILLS, OHIO.
Establishment of a Computer-Aided Design (CAD)-Computer-Aided Manufacturing (CAM) process for the production of cold forged gears
[AD-A155756] N85-35644
ECOLE POLYTECHNIQUE, PALAISEAU (FRANCE).
Preliminary results on underground muon bundles observed in the Frejus proton-decay detector
[HE-5.1-1] N85-36067
EDGERTON, GERMESHAUSEN AND GRIER, INC., IDAHO FALLS, IDAHO.
Computer code calculations of the TMI-2 accident: Initial and boundary conditions
[DE85-012613] N85-35666
EDGERTON, GERMESHAUSEN AND GRIER, INC., SAN RAMON, CALIF.
Ground motion measurements for the QUESO nuclear event
[DE85-014806] N85-35743
EHIME UNIV., MATSUYAMA (JAPAN).
An upper limit of muon flux of energies above 100 TeV determined from horizontal air showers observed at Akeno
[HE-5.2-12] N85-36088
EIDGENOESSISCHES INST. FUER REAKTORFORSCHUNG, WUERENLINGEN (SWITZERLAND).
Determination of vertical air velocity using measurements of the aircraft motion N85-35545
Environmental-physical measurements and determination of atmospheric turbulence with the ASK-16 motor glider N85-35549
ELORET CORP., SUNNYVALE, CALIF.
Size and shape dependence of CO adsorption sites on sapphire supported Fe microcrystals
[NASA-CR-176171] N85-35794
ENERGY AND ENVIRONMENTAL ANALYSIS, INC., ARLINGTON, VA.
Assessment of metal heating technologies for ferrous forging: A pilot study of the form value of natural gas
[PB85-204394] N85-35314
ENERGY OPTICS, INC., LAS CRUCES, N. MEX.
Miniature infra-red data acquisition and telemetry system
[NASA-CR-177953] N85-35390
ENVIRONMENTAL RESEARCH INST. OF MICHIGAN, ANN ARBOR.
Study of spectral/radiometric characteristics of the Thematic Mapper for land use applications
[E85-10106] N85-35464
Optical synthetic aperture techniques
[AD-A156151] N85-35752
EUROPEAN ORGANIZATION FOR NUCLEAR RESEARCH, GENEVA (SWITZERLAND).
Detectors for relativistic nuclear collisions (report from the Fixed-Target Hadron Group) N85-35701
Accelerator physics measurements at the damping ring
[DE85-013373] N85-35785
EUROPEAN SPACE AGENCY, PARIS (FRANCE).
Lectures of a Flight Mechanics Conference
[ESA-TT-831] N85-35165
Development of flight mechanics research in Brunswick N85-35166
Research report program of the US Army in Europe N85-35167
New technologies at the forefront of industrial developments N85-35168
The contribution made by flight mechanics to civil aviation N85-35169
The effect of instrumentation system parameters on the results of a flight mechanical system identification N85-35170
Estimation of flight mechanical variables by means of Kalman filters N85-35171
Gust simulation for flight mechanical wind tunnel tests N85-35172
Contribution to the properties of carbon fiber reinforced composites
[ESA-TT-849] N85-35246
Determination of characteristic values for fiber reinforced materials N85-35247
Methods for nondestructive tests of CFRP laminates N85-35248
Damage mechanisms in damaged CFRP laminates N85-35249
Computational techniques for fiber reinforced components N85-35250
Proceedings of a Scientic Meeting on the Occasion of the Inauguration of New Buildings for the DFVLR Institute for Aerospace Medicine
[ESA-TT-857] N85-35595
The research programme of the Institute for Aerospace Medicine N85-35596
Analogies of control mechanisms in flight guidance and medicine N85-35597
A mechanical model of the human body and its application N85-35598
Models for assessing workload of aircrews on long distance flights N85-35599
The relationship between personality and performance N85-35600
Cardiovascular responses to orthostatism and weightlessness N85-35601
Are living cells generally sensitive to gravity? N85-35602
Biophysical research in space N85-35603
The deep diving simulator TITAN: Physiological problems associated with staying in great depths of water N85-35604
The effect of an unphysiological oxygen supply on the organism N85-35605

F

FEDERAL AVIATION AGENCY, WASHINGTON, D.C.
U.S. Civil airmen statistics for calendar year 1984
[AD-A156326] N85-35153
Physiological responses to unvarying (steady) and 2-2-1 shifts: Miami International Flight Service Station
[AD-A155751] N85-35619
FERMI NATIONAL ACCELERATOR LAB., BATAVIA, ILL.
Width of nonlinear difference resonances
[DE85-013026] N85-35719
Neutrino production of like sign dimuons
[DE85-013594] N85-35741
Design considerations for personnel access penetrations for the superconducting super collider
[DE85-013027] N85-35807
FRANKLIN INST., NEWARK, DEL.
QCD-motivated description of very high energy particle interactions
[HE-1.2-2] N85-35861
Gamma-hadron families and scaling violation
[HE-3.4-7] N85-35935
Muons in gamma showers
[HE-4.5-3] N85-36027
Atmospheric neutrinos observed in underground detectors
[HE-5.3-8] N85-36102
Neutrino astronomy and the atmospheric background
[HE-5.3-17] N85-36111

G

GAUHATI UNIV. (INDIA).
On the production mechanism of radio-pulses from large extensive air showers
[HE-4.6-4] N85-36041
A new study on the emission of EM waves from large EAS
[HE-4.6-5] N85-36042
Microprocessor-based single particle calibration of scintillation counter
[HE-4.6-13] N85-36049
GENERAL ELECTRIC CO., CINCINNATI, OHIO.
Flow modifying device
[NASA-CASE-LEW-13562-2] N85-35195
Energy efficient engine, high pressure turbine thermal barrier coating. Support technology report
[NASA-CR-168037] N85-35199
GENERAL ELECTRIC CO., SCHENECTADY, N. Y.
Design and construction of an advanced power conditioning subsystem for small photovoltaic applications
[DE85-013940] N85-35495
GEOLOGICAL SURVEY, ALEXANDRIA, VA.
USGS research on mineral resources, 1985
[CIRC-949] N85-35435
Aeromagnetic and radiometric signatures of a possible porphyry system in the western Tushar Mountains, Utah N85-35437
Some geophysical guides to ore in southern and southwestern Alaska N85-35438
Marine phosphorite deposits model for exploration, with emphasis on deposits in the US Atlantic coastal plain N85-35439
The role of regional subsurface geochemistry in resource assessment in the central United States N85-35440
Heat transfer and brine evolution in magma-hydrothermal systems N85-35441
Aeromagnetic and gravity models of the pluton below the Lake City caldera, Colorado N85-35442
Origin of sedimentary humic acids, potential carriers of ore-forming elements N85-35443
Cobalt-rich ferromanganese crusts in the oceans N85-35444
New silver resource map of the United States: Potential for increased domestic silver production N85-35445
Massive sulfide deposits from the southern Juan de Fuca Ridge N85-35446
Gas analysis of ore-forming fluids N85-35447
Mineral deposit models: Theory and practice N85-35448
Early and middle Cenozoic volcanic synthesis N85-35449
Expert systems research in regional resource evaluation: Experiences in the application of microcomputer technologies N85-35450
Applications of the mineral resources data system and the international strategic minerals inventory in mineral-resource assessments by region and commodity N85-35451
A comparison of LANDSAT thematic mapper, multispectral scanner and airborne sensors for mapping the distribution of alteration minerals: Examples from the southwestern United States N85-35452
Some recent deposit modeling efforts N85-35453
Preliminary results of an ALVIN dive program on active hydrothermal vents at the southern Juan de Fuca Ridge N85-35454
Processing of LANDSAT imagery to map surface mineral alteration on the Alaska Peninsula, Alaska N85-35455
Mineral resources programs N85-35456
The development of assessment techniques program N85-35457
The Conterminous United States Mineral Assessment Program N85-35458
Federal Mineral Land Information System N85-35459
The Alaska Mineral Resources Assessment Program N85-35460
GEOLOGICAL SURVEY, DENVER, COLO.
Simulated effects of increased recharge on the ground-water flow system of Yucca Mountain and vicinity, Nevada-California
[DE85-012985] N85-35489
GEOLOGICAL SURVEY, WASHINGTON, D.C.
USGS coastal research, studies and maps: A source of information for coastal decision making
[USGS-CIRC-883] N85-35485
GEORGE MASON UNIV., FAIRFAX, VA.
Multiplicity distributions in interaction models used for cascade simulations
[HE-1.2-5] N85-35863
GEORGE WASHINGTON UNIV., WASHINGTON, D.C.
Prediction of plasticity characteristics for three-dimensional fracture specimens comparison with experiment
[AD-A156425] N85-35430
Data processing professionals and DP application users' perceptions and expectations of operational roles of persons working in a DP/application user interface group N85-35821
GEORGIA INST. OF TECH., ATLANTA.
Atmospheric nitrogen oxides: Their detection and chemistry
[PB85-193910] N85-35502
GEORGIA STATE UNIV., ATLANTA.
Biodegradation of jet fuel by aquatic microbial communities
[PB85-191971] N85-35311
GEORGIA TECH RESEARCH INST., ATLANTA.
Polarization diversity addition to the 10 centimeter Doppler weather radar
[AD-A156062] N85-35334
GEORGIA UNIV., ATHENS.
1Single particle momentum and angular distributions in hadron-hadron collisions at ultrahigh energies
[HE-1.2-1] N85-35860
GINER, INC., WALTHAM, MASS.
Development of electrodes for the NASA iron/chromium
[NASA-CR-174724] N85-35471
GMAF, INC., FREEPORT, N.Y.
Numerical studies of 2-dimensional flows
[NASA-CR-3930] N85-35160
GROWIAN CO. (WEST GERMANY).
Visual impact of GROWIAN and resulting recommendations for siting of large wind energy converters N85-35486
GTE LABS., INC., WALTHAM, MASS.
National program for inspection of non-federal dams. Woodward reservoir dam (VT 00209), Connecticut River Basin, Plymouth, Vermont. Phase 1 inspection report
[AD-A156258] N85-35693

H

HANFORD ENVIRONMENTAL HEALTH FOUNDATION, RICHLAND, WASH.
Experimental lithium system
[DE85-013252] N85-35382
HARVARD UNIV., CAMBRIDGE, MASS.
On size effects in plane stress crack-growth resistance
[AD-A155926] N85-35426
HAWAII UNIV., HONOLULU.
Elliptical X-ray analyzer spectrograph application to a laser-produced plasma
[DE85-013790] N85-35398
Mean cloudiness over the global tropics from satellite observations
[AD-A156168] N85-35561
HAYES-ALBION CORP., MICH.
Development of a high strength isothermally heat-treated nodular iron road wheel arm
[AD-A155755] N85-35408
HAZELTINE CORP., GREENLAWN, N. Y.
Cylindrical lens-array antenna for wideband electronic scanning
[AD-A156085] N85-35350
HIROSAKI UNIV. (JAPAN).
High energy gamma-rays and hadrons at Mount Fuji
[HE-3.1-3] N85-35903
Particle interactions at energies over 1000 TeV inferred from gamma-families observed at Mount Fuji
[HE-3.5-1] N85-35940
New analysis of nuclear interaction observed by Mt. Kanbara emulsion chamber experiment
[HE-3.7-4] N85-35963
Application of thermoluminescence for detection of cascade shower 1: Hardware and software of reader system
[HE-7.1-6] N85-36160
Application of thermoluminescence for detection of cascade shower 2: Detection of cosmic ray cascade shower at Mount Fuji
[HE-7.1-12] N85-36162
HIROSHIMA UNIV. (JAPAN).
On mini-cluster observed by Chacaltaya emulsion chamber experiment
[HE-3.6-12] N85-35959
HONG KONG UNIV.
Measurement of shower electrons and muons using a small air shower array
[HE-4.3-11] N85-36005
The longitudinal development of muons in cosmic ray air showers at energies 10(15) - 10(17) eV
[HE-4.3-12] N85-36006
Construction of a cosmic ray air shower telescope
[HE-4.5-14] N85-36036
An underground cosmic ray muon telescope for observation of cosmic ray anisotropy N85-36037
Fast scintillation counter preamplifier for the observation of Linsley effect
[HE-4.7-9] N85-36060
A mini-array for large air showers
[HE-4.7-10] N85-36061
HUMAN ENGINEERING LABS., ABERDEEN PROVING GROUND, MD.
The human engineering eye movement measurement research facility
[AD-A156099] N85-35613

I

IDAHO NATIONAL ENGINEERING LAB., IDAHO FALLS.
Thermal hydraulic features of the TMI accident
[DE85-014569] N85-35747
IDAHO UNIV., MOSCOW.
Manual and computer-aided sequential diagnostic inference
[AD-A156229] N85-35620
ILLINOIS UNIV. AT URBANA-CHAMPAIGN, SAVOY.
Design of a microprogram control unit with concurrent error detection
[AD-A156447] N85-35655
ILLINOIS UNIV., CHICAGO.
Generation of stimulated emission in the soft X-ray range by nonlinear processes with excimer lasers
[DE85-012465] N85-35403
ILLINOIS UNIV., URBANA.
Normal modes in an overmoded circular waveguide coated with lossy material
[NASA-CR-176186] N85-35320
An experimental study of dielectric rod antennas for millimeter-wave imaging applications
[AD-A155832] N85-35328
Characterization of microstrip discontinuities in the time and frequency domains
[NASA-CR-176190] N85-35342
The use of a laser Doppler velocimeter in a standard flammability tube
[NASA-CR-174960] N85-35389
Design for MISP: A multiple instruction stream shared pipeline processor
[AD-A156314] N85-35635
Polylith: The early goals
[DE85-012534] N85-35658
IMPERIAL COLL. OF SCIENCE AND TECHNOLOGY, LONDON (ENGLAND).
Vortex boundary-layer interactions
[NASA-CR-176192] N85-35373
INDIAN STATISTICAL INST., CALCUTTA.
Some characteristic cosmic ray events and an attempt at their explanation
[HE-3.1-8] N85-35906
Hadronic components of EAS by rigorous saddle point method in the energy range between 10(5) and 10(8) GeV N85-35978
Photo nuclear energy loss term for muon-nucleus interactions based on xi scaling model of QCD
[HE-5.2-17] N85-36093
INDIANA UNIV., BLOOMINGTON.
Report of Amphibian Development Group N85-35583
Multiple muons in MACRO
[HE-5.2-1] N85-36079
INFORMATICS-PMI, INC., PALO ALTO, CALIF.
CRAYCDC
[NASA-CR-177374] N85-35639
CDCCRAY
[NASA-CR-177375] N85-35640
INSTITUT D'ASTROPHYSIQUE, PARIS (FRANCE).
High energy cosmic ray signature of quark nuggets
[HE-6.2-11] N85-36147
INSTITUT FRANCO-ALLEMAND DE RECHERCHES, ST. LOUIS (FRANCE).
Materials used by industry for the production of piezoelectric transducers. The state of the art of research work performed in the field of PZT ceramics and ferroelectric polymers
[ISL-CO-211/84] N85-35344
Piezoelectric transducers, state of research N85-35345
Conduction and aging of piezoelectric PZT ceramics N85-35346
Ferroelectric homopolymer PVF2 and P (VDF-TrFe) copolymers N85-35347
INSTITUTE OF NUCLEAR PHYSICS, KRAKOW (POLAND).
Low P sub T hadron-nucleus interactions
[HE-1.2-7] N85-35865
Forward particle production in inelastic Ne-22 inteVractions in emulsion at 4.1 A Ge/c
[HE-1.4-7] N85-35895
INTERNATIONAL ASSOCIATION OF FIRE CHIEFS, WASHINGTON, D.C.
Fire service emergency management handbook
[AD-A155780] N85-35313
IOWA UNIV., IOWA CITY.
Finite analytic solutions of supersonic flows in two-dimensional non-symmetrical channels N85-35154
Prediction of turbulent internal recirculating flows with K-epsilon models N85-35366
The geostatistical approach to the inverse problem in two-dimensional steady state groundwater modeling N85-35462
ISTITUTO NAZIONALE DI FISICA NUCLEARE, ROME (ITALY).
High energy neutrino astronomy with MACRO
[HE-5.3-12] N85-36106

J

JACA CORP., FORT WASHINGTON, PA.
Land Disposal of Hazardous Waste
[PB85-196376] N85-35500
JACKSON STATE UNIV., MISS.
Smoothing surface data by spline functions
[AD-A155829] N85-35678
JET PROPULSION LAB., CALIFORNIA INST. OF TECH., PASADENA.
Noiseless coding for the Gamma Ray spectrometer
[NASA-CR-176201] N85-35219
Production of butanol by fermentation in the presence of cocultures of clostridium
[NASA-CASE-NPO-16203-1] N85-35227
Fluidized bed desulfurization
[NASA-CASE-NPO-15924-1] N85-35253
Microwave properties of a quiet sea
[NASA-CR-176199] N85-35322
A new description of combined trellis coding with asymmetric modulation
[NASA-CR-176197] N85-35323
DMSK: A practical 2400-bps receiver for the mobile satellite service: An MSAT-X Report
[NASA-CR-176194] N85-35324
Second-generation mobile satellite system. A conceptual design and trade-off study
[NASA-CR-176195] N85-35325
Report of the Microbial Development Working Group N85-35586
Optical receivers using rough reflectors
[NASA-CR-176200] N85-35750
Total integrated dose testing of solid-state scientific CD4011, CD4013, and CD4060 devices by irradiation with CO-60 gamma rays
[NASA-CR-176196] N85-35795
JOHNS HOPKINS UNIV., BALTIMORE, MD.
Studies of relativistic heavy ion collisions
[DE85-014686] N85-35745

K

KANAGAWA UNIV. (JAPAN).
High sensitive X-ray films to detect electron showers in 100 GeV region
[HE-3.1-13] N85-35911
KANNER (LEO) ASSOCIATES, REDWOOD CITY, CALIF.
Transient three-phase three-component systems. Part 1: Formulation of the system of differential equations
[DE85-013267] N85-35384
X-ray fluorescence analysis of uranium concentrates
[DE85-013189] N85-35717
KANSAS UNIV. CENTER FOR RESEARCH, INC., LAWRENCE.
A research program to reduce the interior noise in general aviation aircraft, index and summary
[NASA-CR-176178] N85-35695
KEMA (N. V.), ARNHEM (NETHERLANDS).
Environmental aspects of the Netherlands wind farm project N85-35485
KERNFORSCHUNGSANLAGE, JUELICH (WEST GERMANY).
Implementing agreement for cooperation in the development of large scale wind energy conversion systems
[JUEL-SPEZ-278] N85-35473
Radiation safety problems in handling highly active tritium targets
[DE85-014268] N85-35742
KINKI UNIV., OSAKA (JAPAN).
Range fluctuations of high energy muons passing through matter
[HE-5.2-19] N85-36095
KOBE UNIV. (JAPAN).
Lateral distribution of electrons of air showers N85-35998
Transition effect of air shower particles in plastic scintillators
[HE-4.4-9] N85-36017
Structure of air shower disc near the core
[HE-4.7-2] N85-36053
Analytical calculation of muon intensities under deep sea-water
[HE-5.2-16] N85-36092
Search for long-lived massive particles in extensive air showers
[HE-6.2-10] N85-36146
KOBE WOMEN'S JUNIOR COLL. (JAPAN).
Character of energy flow in air shower core N85-35985
KOCHI UNIV., AKEBONO (JAPAN).
Fast scintillation counter system and performance
[HE-4.6-10] N85-36047
The structure of the shower disk observed at Mt. Norikura
[HE-4.7-1] N85-36052
KONAN UNIV., KOBE (JAPAN).
EAS accompanied by gamma-families at Mt. Norikura and comparison with Monte Carlo simulation
[HE-3.3-10] N85-35928
Comparison of absolute intensity between EAS with gamma-families and general EAS at Mount Norikura
[HE-3.3-11] N85-35929
Application of photodiodes to the detection of electromagnetic bursts N85-35988
KOREA UNIV., SEOUL.
Anuglar distribution of shower particles produced in the collisions of 20-GeV/c and 300-GeV negative pions with emulsion nuclei N85-35868
Inclusive angular distribution of alpha and Li fragments produced in the Fe-C and Fe-Pb collisions at 1.88 GeV/u
[HE-1.4-11] N85-35898

L

LAHMEYER INTERNATIONAL (WEST GERMANY).
Special questions of siting wind turbine arrays and networks N85-35484

LEEDS UNIV. (ENGLAND).
Particle distributions in approximately 10(14) 10(16) eV air shower cores at sea level N85-35990
Monte Carlo simulations of electron lateral distributions in the core region of 10(13) - 10(16) eV air showers N85-35992
Comparison of simulation results with sea-level experimental data on 10(14) - 10(16) air shower cores N85-35993
Particle distributions in approximately 10(13) - 10(16) eV air shower cores at mountain altitude and comparison with Monte Carlo simulations
[HE-4.2-18] N85-35994
Electromagnetic and muonic structure of showers initiated by gamma-rays and by hadrons
[HE-4.5-6] N85-36030
The thickness of the shower disc as observed in showers produced by primaries above 10 (19)eV
[HE-4.7-6] N85-36057
Progress report on a new search for free e/3 quarks in the cores of 10(15) - 10(16) eV air showers
[HE-6.2-15] N85-36151

LEVY (SALOMON), INC., CAMPBELL, CALIF.
A two-phase flow and heat transfer model for zero gravity
[AD-A156097] N85-35377

LINCOLN LAB., MASS. INST. OF TECH., LEXINGTON.
Selected publications in image understanding and computer vision from 1974 to 1983
[AD-A156196] N85-35634

LOCKHEED-CALIFORNIA CO., BURBANK.
Fuel containment and damage tolerance for large composite primary aircraft structures. Phase 1: Testing
[NASA-CR-166091] N85-35241

LOCKHEED MISSILES AND SPACE CO., HUNTSVILLE, ALA.
Verification of the SRB motor case pin retainer band tips
[NASA-CR-170882] N85-35220
Results of tests on a specimen of the SRB aft skirt heat shield curtain in the MSFC LRLF
[NASA-CR-170883] N85-35221
SRB TPS closeout materials characterization
[NASA-CR-170885] N85-35222
Results of tests of the SRB aft skirt heat shield curtain in the MSFC Hot Gas Facility
[NASA-CR-170888] N85-35223
Results of tests of MTA-2 TPS on the SRB hold-down bolt blast container
[NASA-CR-170891] N85-35224
SRB thermal protection systems materials test results in an arc-heated nitrogen environment
[NASA-CR-170881] N85-35236
Results of variable enthalpy tests of CPR-488 TIP panels in MSFC Hot Gas Facility
[NASA-CR-170889] N85-35237
Results of tests of K5NA and a revised formulation of EPDM/cork patch material in MSFC Hot Gas Facility
[NASA-CR-170890] N85-35238
Results of tests of weathered K5NA closeout material in the MSFC Hot Gas Facility
[NASA-CR-170893] N85-35239
Evaluation of SRB phenolic TPS material made by an alternate vendor
[NASA-CR-170894] N85-35240
Space shuttle SRB TPS protective paint test and evaluation in NASA Hot Gas Facility and AEDC Tunnel C
[NASA-CR-170884] N85-35294
Results of tests of Insta-Foam Thermal Protection System (TPS) material for protection of equipment inside the SRB aft skirt
[NASA-CR-170892] N85-35295
SRB attach ring phenolic TPS fishtail seal evaluation tests
[NASA-CR-170887] N85-35407
Study of NSI and related cable performance during tests performed in the NASA Hot Gas Facility
[NASA-CR-170886] N85-35423

LODZ UNIV. (POLAND).
Empirical description of the hadron-hadron and hadron-nucleus interaction at the accelerator energy range
[HE-1.2-4] N85-35862
The lateral distributions of charged particles of energy greater than 0.3 E sub crit in electron-photon cascades in lead and air
[HE-3.6-10] N85-35957
Result of Monte-Carlo simulation of electron-photon cascades in lead and layers of lead-scintillator
[HE-3.6-11] N85-35958
Hadrons registration in emulsion chamber with carbon block
[HE-3.7-3] N85-35962
Simulation of EAS properties on the basis of high energy interaction model deduced from the accelerator data N85-35973
Detailed studies of the electron lateral distribution in extensive air showers with energies around 10(16) eV N85-35999
Relevance of multiple muons detected underground to the mass composition of primary cosmic rays
[HE-5.1-4] N85-36069

LOS ALAMOS NATIONAL LAB., N. MEX.
Los Alamos free-electron laser
[DE85-012666] N85-35405
Evaluation of the crack plane equilibrium model for predicting plastic fractures
[DE85-005558] N85-35431
Use of a minimum-ellipse criterion in the study of ion-beam extraction systems
[DE85-012670] N85-35721
Considerations on collective ion aceleration as an intense ion injector
[DE85-012706] N85-35757

LOS ALAMOS SCIENTIFIC LAB., N. MEX.
System expectations for Pioneer 1 foil implosion experiments
[DE85-014129] N85-35359
Photoconductive pulse power switches: A review
[DE85-014125] N85-35360
Noise-sustained structure, intermittency and the Ginzburg-Landau equation
[DE85-009626] N85-35379
Adaptive rezoner in a two-dimensional Lagrangian hydrodynamic code
[DE85-010108] N85-35381
Enhanced heat transfer computations for internally cooled cable superconductor
[DE85-011897] N85-35383
Three-dimensional gravity ideal body studies in rough terrain
[DE85-014097] N85-35525
Using an LSI-11/23 and RT-11 to digitize analog tapes
[DE85-012736] N85-35656
RFQ modeling computer program
[DE85-012665] N85-35661
Optimizing data access in the LAMPF control system
[DE85-012653] N85-35663
X-ray fluorescence analysis of uranium concentrates
[DE85-013189] N85-35717
Measurement of uranium enrichment for gaseous uranium at low pressure
[DE85-012697] N85-35733
Beam potential measurement of an intense H(-) beam by use of the emissive probe technique
[DE85-012671] N85-35762
Major facility overhauls at LAMPF
[DE85-012724] N85-35765
Ion source development for the Los Alamos heavy ion fusion injector
[DE85-012682] N85-35766
Recent advances in remote handling at LAMPF
[DE85-012725] N85-35775
Proposed FRX-D experiment
[DE85-012766] N85-35778
Los Alamos high-current proton storage ring
[DE85-012664] N85-35779
Relation between field energy and RMS emittance in intense particle beams
[DE85-012655] N85-35784
Analysis of a pulsed power system containing rotating machine
[DE85-014128] N85-35786
Diagnostics for Pioneer 1 imploding plasma experiments
[DE85-014120] N85-35787

LUND UNIV. (SWEDEN).
A survey of multiplicities and rapidity densities from existing emission data on hadron-nucleus nucleus-nucleus collisions N85-35706
A simulation of ultra-relativistic nucleus-nucleus collisions N85-35707

M

MANSOURA UNIV. (EGYPT).
Missing energies at pair creation
[HE-4.4-8] N85-36016

MARTIN MARIETTA ENERGY SYSTEMS, INC., OAK RIDGE, TENN.
Strategic defense initiative
[DE85-012778] N85-35735

MARYLAND UNIV., COLLEGE PARK.
Visual position determination for autonomous vehicle navigation
[AD-A156007] N85-35181
Analysis of the nonlinear equations describing the elastic, thermal, and electromagnetic behavior of solids: Existence of solutions of semi-inverse problems N85-35415
Width of nonlinear difference resonances
[DE85-013026] N85-35719
Edge information in color images based on histograms of differences
[AD-A156002] N85-35751
Relation between field energy and RMS emittance in intense particle beams
[DE85-012655] N85-35784
Hadron cross sections at ultra high energies and unitarity bounds on diffraction dissociation
[HE-1.1-3] N85-35851
Some remarks about simulation of cosmic ray phenomena with use of nuclear interaction models based on the current SPS proton-antiproton data
[HE-1.2-6] N85-35864
Electrons, muons and hadrons in extensive air showers and how do they depend on nuclear interaction model, part 2 N85-35969
Electrons, muons and hadrons in extensive air showers and how do they depend on nuclear interaction model, part 1 N85-35972
Study of muons near shower cores at sea level using the E594 neutrino detector N85-36000
A possible EAS array above the Soudan 2 detector
[HE-4.6-9] N85-36046
A search for heavy long lived particles in high energy cosmic rays
[HE-6.2-7] N85-36143

MASCHINENFABRIK AUGSBURG-NUERNBERG A.G., MUNICH (WEST GERMANY).
GROWIAN: First observations of the environmental impact at the GROWIAN site N85-35476

MASSACHUSETTS INST. OF TECH., CAMBRIDGE.
Communication complexity of distributed shortest path algorithms
[AD-A156049] N85-35332
Incorporating meteorological data into receptor analysis: RAPS (Regional Air Pollution Study) revisited
[PB85-188944] N85-35503
Justified generalization: Acquiring procedures from examples
[AD-A156408] N85-35626
Optical properties of heterostructures and superlattices
[AD-A156243] N85-35802

MASSACHUSETTS UNIV., AMHERST.
Crystallization of Polyetheretherketone (PEEK) in carbon fiber composites
[AD-A156316] N85-35252
Solid-state co-extrusion of nylon 6 gel
[AD-A156187] N85-35298
Genetic and physiological control of protective antigen synthesis by bacillus anthracis
[AD-A156324] N85-35617
A new drawing technique for nylon 6 by reversible plasticization with iodine
[AD-A156272] N85-35803

MAX-PLANCK-INST. FUER AERONOMIE, KATLENBURG-LINDAU (WEST GERMANY).
Parallel fast-forward shock within 1 AU: Helios-1 and 2 observations
[MPAE-W-?9-84-27] N85-35847

MAX-PLANCK-INST. FUER ASTROPHYSIK, MUNICH (WEST GERMANY).
A holographic streamer chamber for relativistic nucleus-nucleus collision experiments N85-35710
High-energy neutrinos from a lunar observatory
[HE-5.3-21] N85-36112

MESEI UNIV., TOKYO (JAPAN).
Observation of EAS using a large water tank N85-35986
Delayed particles in EAS at Akeno
[HE-6.2-8] N85-36144

MICHIGAN UNIV., ANN ARBOR.
Practical aspects of photovoltaic technology, applications and cost (revised)
[NASA-CR-174983] N85-35472
Methods for roof-top mini-arrays
[HE-4.7-7] N85-36058
Expected rates with mini-arrays for air showers
[HE-4.7-8] N85-36059
Measurement of neutrino oscillations in MACRO experiment
[HE-5.3-10] N85-36104

Monopole search below the Parker limit with the MACRO detector at Gran Sasso
[HE-6.1-5] N85-36131

MIDLAND-ROSS CORP., TOLEDO, OHIO.
Advanced regenerative heat recovery system
[PB85-199802] N85-35315
High Temperature Heating System (HTHS)
[PB85-186340] N85-35316

MIDWEST RESEARCH INST., GOLDEN, COLO.
Energy from low temperature differences
[DE85-008817] N85-35492

MILLSAPS COLL., JACKSON, MISS.
Aquatic Invertebrate Development Working Group
N85-35585

MINNESOTA UNIV., MINNEAPOLIS.
Pressure cross spectra in turbulent boundary layers in water
[AD-A156153] N85-35378
Determination of primary energy in nucleus-nucleus collisions and the high P(sub)T tail of alpha-particles
N85-35875
Stopping relativistic Xe, Ho, Au and U nuclei in nuclear emulsions N85-35876
Meson multiplicity in nucleus-nucleus collisions above 4 GeV/amu
[HE-1.4-10] N85-35897

MITRE CORP., BEDFORD, MASS.
A quickly tested Pascal random number generator for microcomputers
[AD-A156059] N85-35633

MITRE CORP., MCLEAN, VA.
FAA requirements for model to support capacity, delay, noise and energy programs
[AD-A155815] N85-35179

MONTREAL UNIV. (QUEBEC).
Algorithmic approaches in sets of good answers in inverse problems
[PM/84/18] N85-35677

MOSCOW PHYSICAL-ENGINEERING INST. (USSR).
Energy spectrum of cascade showers induced by cosmic ray muons in the range from 50 GeV to 5 TeV
[HE-5.2-14] N85-36090
Results of a search for monopoles and tachyons in horizontal cosmic ray flux
[HE-6.1-3] N85-36129

MOSCOW STATE UNIV. (USSR).
Estimation of the total inelasticity coefficient in interaction of greater than or equal to 20 TeV hadrons with lead
[HE-1.1-9] N85-35857
The effect of the relative nuclear size on the nucleus-nucleus interactions
[HE-1.4-13] N85-35900
Energy spectra of proton and nuclei of primary cosmic rays in energy region 10 TeV/particle
[HE-3.1-10] N85-35908
The multiplicity and the spectra of secondaries correlated with the leading particle energy
[HE-3.2-11] N85-35919
The electromagnetic component of albedo from superhigh energy cascades in dense media
[HE-3.5-11] N85-35948
Integral functions of electron lateral distribution and their fluctuations in electron-photon cascades
[HE-3.5-12] N85-35949
Analytical-numerical methods of calculations of energy and three-dimensional particle distributions in electromagnetic cascades
[HE-3.5-13] N85-35950
Phenomenology of soft hadron interactions and the relevant EAS data N85-35980
Sensitivity of depth of maximum and absorption depth of EAS to hadron production mechanism N85-35982
Lateral distribution on charged particles in EAS
[HE-4.3-15] N85-36009
Lateral distribution of high energy muons in EAS of sizes Ne approximately equals 10(5) and Ne approximately equals 10(6)
[HE-4.3-16] N85-36010
The experimental cascade curves of EAS at E sub 0 10(17) eV obtained by the method of detection of Cherenkov pulse shape
[HE-4.4-18] N85-36024
Lateral-angular and temporal characteristics of EAS optical radiation
[HE-4.4-19] N85-36025
Study of the time-differentiated particle flux density at various distances from EAS axis
[HE-4.7-15] N85-36065
Modular detector for deep underwater registration of muons and muon groups
[HE-5.4-15] N85-36125
Results of investigation of muon fluxes of superhigh energy cosmic rays with X-ray emulsion chambers
[HE-5.4-16] N85-36126

MOUND LAB., MIAMISBURG, OHIO.
Friction, impact, and electrostatic discharge sensitivities of energetic materials
[DE85-013321] N85-35309

N

NAGOYA UNIV. (JAPAN).
The Nagoya cosmic-ray muon spectrometer 3, part 1: Preliminary observations
[HE-5.2-2] N85-36080
The Nagoya cosmic-ray muon spectrometer 3, part 2: Track detector
[HE-5.2-3] N85-36081
The Nagoya cosmic-ray muon spectrometer 3, part 3: Automatic film scanning equipment
[HE-5.2-4] N85-36082
The Nagoya cosmic-ray muon spectrometer 3, part 4: Track reconstruction method
[HE-5.2-5] N85-36083

NATIONAL AERONAUTICS AND SPACE ADMINISTRATION, WASHINGTON, D. C.
Aeronautical engineering: A continuing bibliography with indexes, supplement 190
[NASA-SP-7037(190)] N85-35152
Presentation of the acoustic and aerodynamic results of the Aladin 2 concept qualification testing
[NASA-TM-77883] N85-35161
Supersonic flow with feeding of energy
[NASA-TM-77912] N85-35163
Deceleration of a supersonic flow behind a curved shock wave with isentropic precompression
[NASA-TM-77920] N85-35164
Technology for large space systems: A bibliography with indexes
[NASA-SP-7046(12)] N85-35209
Method for measuring surface activity of silicon nitride powder
[NASA-TM-77906] N85-35242
Ultrasonic inspection of carbon fiber reinforced plastic by means of sample-recognition methods
[NASA-TM-77896] N85-35245
Studies of the crystallization process of aluminum-silicon alloys using a high temperature microscope
[NASA-TM-77869] N85-35272
Determination of the viscosity number of thermoplastics in dilute solution; polyamides (PA)
[NASA-TM-77673] N85-35296
NASA patent abstracts bibliography, a continuing bibliography. Section 2: Indexes (supplement 27)
[NASA-SP-7039(27)-SECTION-2] N85-35820

NATIONAL AERONAUTICS AND SPACE ADMINISTRATION. AMES RESEARCH CENTER, MOFFETT FIELD, CALIF.
Space Missions for Automation and Robotics Technologies (SMART) Program
[NASA-TM-86820] N85-35210
Computation of three-dimensional shock wave and boundary-layer interactions
[NASA-TM-86780] N85-35372
Sea surface and remotely sensed temperatures off Cape Mendocino, California
[NASA-TM-86712] N85-35573
NASA Developmental Biology Workshop: A summary
[NASA-TM-86756] N85-35578
Effects of microgravity and hypergravity on invertebrate development N85-35579
Improved oxygen sources for breathing apparatus
[NASA-TM-86671] N85-35623
The structure of Herbig-Haro object 43 and Orion dark cloud extinction
[NASA-TM-87503] N85-35831
Far-infrared emission lines of CO and OH in the Orion-KL molecular shock
[NASA-TM-86721] N85-35832
Observations of far-infrared transitions between excited states of OH
[NASA-TM-86722] N85-35833
Far-infrared observations of young clusters embedded in the R Coronae Austrinae and RHO Ophiuchi dark clouds
[NASA-TM-86681] N85-35834

NATIONAL AERONAUTICS AND SPACE ADMINISTRATION. GODDARD SPACE FLIGHT CENTER, GREENBELT, MD.
The ISAVF opto-mechanical test bed
[NASA-TM-87505] N85-35206
Comet Halley returns: A teachers' guide 1985-1986
[NASA-EP-197] N85-35839
Nineteenth International Cosmic Ray Conference. HE Sessions, volume 6
[NASA-CP-2376-VOL-6] N85-35848
SU(2) x U(1) vacuum and the Centauro events
N85-35885
Japan - USSR joint emulsion chamber experiment at Pamir
[HE-3.1-1] N85-35901
Scaling violation in fragmentation region at energies above 10-15 eV based on the data on cosmic ray hadron component
[HE-3.1-11] N85-35909
Exotic interactions among C-jets and Pb-jets
[HE-3.2-6] N85-35914
A cosmic ray super high energy multicore family event. 2: Structure and fragmentation characteristics of the jets
[HE-3.4-2] N85-35931
Nineteenth International Cosmic Ray Conference. HE Sessions, volume 7
[NASA-CP-2376-VOL-7] N85-35968
Muon spectrum in air showers initiated by gamma rays
[HE-4.5-4] N85-36028
Development of electromagnetic cascades in the atmosphere including the Landau-Pomeranchuk-Migdal effect
[HE-4.5-5] N85-36029
Nineteenth International Cosmic Ray Conference. HE sessions, volume 8
[NASA-CP-2376-VOL-8] N85-36066
Multimuons events and primary composition
[HE-5.1-5] N85-36070
Observation of genetic relation among new phenomena Geminion, Chiron and mini-Centauro
[HE-6.2-16] N85-36152

NATIONAL AERONAUTICS AND SPACE ADMINISTRATION. LANGLEY RESEARCH CENTER, HAMPTON, VA.
Wingtip vortex propeller
[NASA-CASE-LAR-13019-1] N85-35194
Dual towline spin-recovery device
[NASA-CASE-LAR-13076-1] N85-35200
A preliminary evaluation of a failure detection filter for detecting and identifying control element failures in a transport aircraft
[NASA-TM-87576] N85-35204
Sound speed measurements in liquid oxygen-liquid nitrogen mixtures
[NASA-TP-2464] N85-35307
The effect of power law body forces on a thermally-driven flow between concentric rotating spheres
[NASA-TM-87596] N85-35374
Long-time asymptotics of a system for plasma diffusion
[NASA-CR-177947] N85-35375
Stress-intensity factors for circumferential surface cracks in pipes and rods under tension and bending loads
[NASA-TM-87594] N85-35424
TRICCS: A proposed teleoperator/robot integrated command and control system for space applications
[NASA-TM-87577] N85-35637
A new theory for multistep discretizations of stiff ordinary differential equations: Stability with large step sizes
[NASA-CR-177941] N85-35675
Absorbing boundary conditions for exterior problems
[NASA-CR-177944] N85-35676

NATIONAL AERONAUTICS AND SPACE ADMINISTRATION. LEWIS RESEARCH CENTER, CLEVELAND, OHIO.
Flow modifying device
[NASA-CASE-LEW-13562-2] N85-35195
Status of advanced orbital transfer propulsion
[NASA-TM-87069] N85-35225
Thermal barrier coating system
[NASA-CASE-LEW-14057-1] N85-35233
Oxidation resistant slurry coating for carbon-based materials
[NASA-CASE-LEW-13923-1] N85-35267

NATIONAL AERONAUTICS AND SPACE ADMINISTRATION. MARSHALL SPACE FLIGHT CENTER, HUNTSVILLE, ALA.
Nucleon-nucleus interactions from JACEE
N85-35869
The phi-meson and Chiral-mass-meson production in heavy-ion collisions as potential probes of quark-gluon-plasma and Chiral symmetry transitions
N85-35884
The response of a scintillation counter below an emulsion chamber to heavy nucleus interactions in the chamber N85-35889
Characteristics of central collision events in Fe-nucleus interactions for 20 - 60 GeV/nucleon
[HE-1.4-3] N85-35891
Nucleus-nucleus interaction above several hundred GeV/n
[HE-1.4-4] N85-35892
Observation of direct hadronic pairs in nucleus-nucleus collisions in JACEE emulsion chambers
[HE-1.4-5] N85-35893

Excessive production of electron pairs by soft photons in low multiplicity ion interactions
[HE-1.4-6] N85-35604

NATIONAL AERONAUTICS AND SPACE ADMINISTRATION. PASADENA OFFICE, CALIF.
Production of butanol by fermentation in the presence of cocultures of clostridium
[NASA-CASE-NPO-16203-1] N85-35227
Fluidized bed desulfurization
[NASA-CASE-NPO-15924-1] N85-35253

NATIONAL AGENCY FOR PHYSICAL PLANNING (DENMARK).
Siting of large scale wind turbines in Denmark N85-35483

NATIONAL BUREAU OF STANDARDS, BOULDER, COLO.
Theory of mutual impedances and multiple reflections in an N-element array environment
[PB85-191419] N85-35364

NATIONAL BUREAU OF STANDARDS, GAITHERSBURG, MD.
Structure and properties of polyethylene films used in heavy lift balloons
[NASA-CR-176227] N85-35306
Proceedings of the 7th Joint Panel Meeting of the UJNR Panel on Fire Research and Safety
[PB85-199545] N85-35317
Center for Electronics and Electrical Engineering technical progress bulletin covering center programs, July-September with 1985 CEEE events calendar
[PB85-191393] N85-35363
Development of an NBS (National Bureau of Standards) polymer gage for dynamic soil stress measurement
[PB85-208494] N85-35526
Transient analysis of electromagnetic reflection from dispersive materials
[PB85-200186] N85-35753
Self-study manual on optical radiation measurements. Part 1: Concepts. Chapter 12: Blackbodies, blackbody radiation, and temperature scales
[PB85-195303] N85-35754
Fire research publications, 1984
[PB85-208502] N85-35827

NATIONAL BUREAU OF STANDARDS, WASHINGTON, D.C.
Noble metals as incipient transition metals
[DE85-013283] N85-35286
Redefining the scratch standards
[PB85-194736] N85-35755

NATIONAL CENTER FOR ATMOSPHERIC RESEARCH, BOULDER, COLO.
Maintenance of blocking anticyclones in a general circulation model
[PB85-190666] N85-35567
Two-point closure study of covariance budgets for turbulent Rayleigh-Benard convection
[PB85-189108] N85-35568

NATIONAL ENVIRONMENTAL SATELLITE SERVICE, WASHINGTON, D. C.
Space Station Polar Platform: Integrating research and operational missions
[PB85-195279] N85-35218

NATIONAL OCEANIC AND ATMOSPHERIC ADMINISTRATION, BOULDER, COLO.
Airborne Investigations of Mesoscale Convective Systems (AIMCS), 1984: Operational summary and data inventory
[PB85-187904] N85-35571

NATIONAL OCEANIC AND ATMOSPHERIC ADMINISTRATION, SEATTLE, WASH.
Current inventory of anthropogenic carbon dioxide in the North Pacific Subarctic Gyre
[PB85-187938] N85-35570

NATIONAL OCEANIC AND ATMOSPHERIC ADMINISTRATION, WASHINGTON, D. C.
Surface cyclogenesis as indicated by satellite imagery
[PB85-191815] N85-35566
Program for Regional Observing and Forecasting Services (PROFS)
[PB85-188050] N85-35569

NATIONAL RESOURCE ANALYSIS CENTER, WASHINGTON, D. C.
Recommendations for content revision and alternate delivery modes for the Human Engineering Guide to Equipment Design (HEGED)
[AD-A155781] N85-35624

NATIONAL TELECOMMUNICATIONS AND INFORMATION ADMINISTRATION, ANNAPOLIS, MD.
Necessary bandwidth and spectral properties of digital modulation
[PB85-185387] N85-35340

NATIONAL TELECOMMUNICATIONS AND INFORMATION ADMINISTRATION, BOULDER, COLO.
Millimeter-wave propagation in moist air: Model versus path data
[AD-A156040] N85-35331

NAVAL AIR DEVELOPMENT CENTER, WARMINSTER, PA.
Matched filtering of visual evoked potentials to detect acceleration (+Gz) induced blackout
[AD-A155912] N85-35609

NAVAL CIVIL ENGINEERING LAB., PORT HUENEME, CALIF.
Solar pond technology for Navy applications
[AD-A155877] N85-35488

NAVAL OCEAN RESEARCH AND DEVELOPMENT ACTIVITY, BAY ST. LOUIS, MISS.
A towed instrument vehicle for deep ocean sampling
[AD-A156322] N85-35576
The NORDA/FNOC (Naval Ocean Research and Development Activity's/Fleet Numerical Oceanography Center) Polar Ice Prediction System (PIPS)-Arctic: A technical description
[AD-A156332] N85-35577

NAVAL POSTGRADUATE SCHOOL, MONTEREY, CALIF.
Analysis of incompressible cascade flows using state-of-the-art computer programs
[AD-A155850] N85-35173
The influence of helicopter tail shape on drag: An aerodynamic study using a low speed wind tunnel
[AD-A156304] N85-35174
The effects of parameter variation on helicopter performance
[AD-A156027] N85-35189
Development of NATOPS (Naval Air Training and Operating Procedure Standardization) performance software for the H-46D helicopter
[AD-A156089] N85-35190
Development of NATOPS performance software for the SH-3D and SH-3H helicopters
[AD-A156140] N85-35192
Target observability for satellite-based sensors
[AD-A156139] N85-35217
Effects of temperature on the tensile strength and elastic modulus of composite material
[AD-A156112] N85-35251
The character of observed porosity and its possible effects on rolling contact fatigue life of M-50 steel
[AD-A155930] N85-35279
Effect of prior warm rolling on the retained austenite content and hardening response of VIM-VAR (vacuum-induction melted-vacuum-arc remelted) AISI M-50 steel
[AD-A156145] N85-35281
Computer simulation of a cruise missile using brushless dc motor fin control
[AD-A155935] N85-35349
Cerenkov radiation from periodic electron bunches for finite emission length in air
[AD-A156156] N85-35352
Meteorological data from the OPTOMA (Ocean Prediction Through Observations, Modeling and Analysis) program OPTOMA 2, leg D2. 30 Jun. - 10 Jul. 1984
[AD-A156134] N85-35560
The use of austenitic stainless steel versus monel (Ni-cu) alloy in pressurized Gaseous Oxygen (GOX) life support systems
[AD-A156305] N85-35625
DSS/MIS (Decision Support Systems/Management Information Systems) design and implementation for LAMPS Mk 3 utilizing a microcomputer and a maintenance personnel assignment program
[AD-A155852] N85-35629
VLSI (Very Large Scale Integrated) tutorials through the video-computer courseware implementation system
[AD-A155889] N85-35631
Attacking software crisis: A macro approach
[AD-A155846] N85-35645
Software maintenance relating to the input translator and z-80 realization volume of the computer systems design environment
[AD-A155849] N85-35646
Benchmark evaluation of PC simscript
[AD-A156133] N85-35651
Prototyping with data dictionaries for requirements analysis
[AD-A156303] N85-35654
A new method for boundary value problems
[AD-A155934] N85-35683
Electron irradiation of N type cadmium telluride
[AD-A156117] N85-35801

NAVAL RESEARCH LAB., WASHINGTON, D. C.
Solid neon sources for plasma and X-ray lasers
[DE85-011347] N85-35402
An approach to determining computer security requirements for Navy systems
[AD-A155750] N85-35627
Relaxation phenomena and stability of probability densities
[AD-A155923] N85-35682
Records Disposal: A guidebook for laboratory offices
[AD-A156064] N85-35823

NAVAL SUBMARINE MEDICAL RESEARCH LAB., GROTON, CONN.
Immediate visibility after red and white adaptation
[AD-A156271] N85-35616

NAVAL SURFACE WEAPONS CENTER, WHITE OAK, MD.
Mach 14 flow restrictor thermal stress analysis
[AD-A156215] N85-35208
Analog, still without fear
[AD-A155920] N85-35348

NAVAL TRAINING EQUIPMENT CENTER, ORLANDO, FLA.
An exploratory study of the effect of screen size and resolution on the legibility of graphics in automated job performance aids
[AD-A155989] N85-35632

NAVAL UNDERWATER SYSTEMS CENTER, NEW LONDON, CONN.
A comparison of multipath arrival structures observed in the presence of a surface duct with predictions obtained using classical ray techniques and the parabolic equation method
[AD-A156024] N85-35696

NAVAL WEAPONS CENTER, CHINA LAKE, CALIF.
A planar version of a 4.0 gigahertz reactively steered adaptive array
[AD-A156029] N85-35330
Experimental data for characterizing perforating impacts: Fragmentation processes
[AD-A156370] N85-35427

NEBRASKA UNIV., LINCOLN.
Dissociative and double photoionization cross sections of NO from threshold to 120 A
[NASA-CR-176185] N85-35713

NEW MEXICO INST. OF MINING AND TECHNOLOGY, SOCORRO.
Steamflood pilots in the O'Connell Ranch field and the T-4 Ranch field
[DE85-901363] N85-35468

NEW MEXICO UNIV., ALBUQUERQUE.
Three-dimensional gravity ideal body studies in rough terrain
[DE85-014097] N85-35525
Proton-air and proton-proton cross sections from air shower data
[HE-1.1-1] N85-35849
Standard value for the radiation length in air
[HE-4.4-4] N85-36013
Longitudinal trial functions and the cosmic ray energy scale N85-36014
Sub-luminal pulses from cosmic ray air showers
[HE-4.7-13] N85-36063
Thickness of the particle swarm in cosmic ray air showers
[HE-4.7-14] N85-36064

NEW YORK UNIV., NEW YORK.
Some rigorous results concerning spectral theory for ideal MHD
[DE85-013427] N85-35770

NORTH CAROLINA STATE UNIV., RALEIGH.
A stream function approach to solving the conservative Euler equations for transonic flows N85-35156
An automated technique for encasing specific payloads with low-drag fairings N85-35183
Mechanical characterization and failure modes of fiber reinforced angle-ply composites N85-35234
Membrane reinforcement in concrete shells: Design versus nonlinear behavior N85-35312
On the convergence of an iterative formulation of the electromagnetic scattering from an infinite grating of thin wires N85-35319
Two-dimensional numerical modeling of ion implanted GaAs MESFET devices N85-35341
Analytic solutions of inverse heat conduction problems N85-35367
Time-dependent response of the climate to increasing atmospheric carbon dioxide N85-35532
Study of the parameters affecting the collapse of a rotating protostellar cloud N85-35837

NORTH CAROLINA UNIV., CHAPEL HILL.
Heats of formation of gas phase organosulfur molecules, radicals and ions measured by PEPICO and application of (17)O and (33)S NMR spectroscopy to structure determination of organosulfur compounds
[DE85-010558] N85-35229
Structural development of the west-central Grant Range, Nye County, Nevada N85-35508

NORTH OF SCOTLAND HYDRO-ELECTRIC BOARD.
Environmental Monitoring Burger Hill, Orkney wind turbine generator site and similar work at other UK WTG sites N85-35482

NOTRE DAME UNIV., IND.
FTIR studies of hydrocarbon synthesis on Pd/ZSM5 catalysts
[DE85-012430] N85-35230
NOTTINGHAM UNIV. (ENGLAND).
Muon fluctuation studies of EAS 10(17) eV
[HE-4.3-9] N85-36003
Average features of the muon component of EAS or = 10(17) eV
[HE-4.3-10] N85-36004
The identification of gamma ray induced EAS
[HE-4.5-1] N85-36026

O

OAK RIDGE ASSOCIATED UNIVERSITIES, TENN.
Electronic information management and productivity
[DE85-013362] N85-35818
OAK RIDGE NATIONAL LAB., TENN.
Chemistry division report
[DE85-010586] N85-35228
System for the continuous generation of phosphorous aerosols from red phosphorus-butyl rubber
[DE85-013527] N85-35232
Thermodynamics of the corrosion of chromium in molten carbonates
[DE85-011407] N85-35282
Characterization of modified 9 r-1 Mo steel sand castings
[DE85-012057] N85-35287
Development and characterization of carbon-bonded carbon fiber insulation for radioisotope space power systems
[DE85-013365] N85-35299
Infrared generation and wave-mixing studies in cesium
[DE85-012883] N85-35304
Carbon dioxide and climate: A working glossary
[DE85-013535] N85-35562
Tritium hazard via the ingestion pathway
[DE85-012897] N85-35618
DEPTH-CHARGE static and time-dependent perturbation/sensitivity system for nuclear reactor core analysis, revision 1
[DE85-013103] N85-35659
Calculation of heavy-ion tracks in liquid water
[DE85-012101] N85-35725
Exit channels of autoionization resonances in atoms
[DE85-012299] N85-35726
Neutronic calculations for a new high flux reactor
[DE85-011551] N85-35734
Applications and misapplications of the channel-capture formalism of direct neutron capture
[DE85-013992] N85-35748
Neutral pumping rates for a next step tokamak ignition device
[DE85-012780] N85-35776
Multiple vacancy production by high energy heavy ions
[DE85-004426] N85-35805
Ionic crystals
[DE85-009482] N85-35809
OFFICE OF NAVAL RESEARCH, LONDON (ENGLAND).
Electromagnetic compatibility conference features biological interactions
[AD-A155313] N85-35692
The 2nd European Conference on Atomic and Molecular Physics
[AD-A155863] N85-35715
OFFICE OF SCIENCE AND TECHNOLOGY, WASHINGTON, D. C.
Progress report on implementing the recommendations of the White House Science Council's Federal Laboratory Review Panel, volume 1
[PB85-185072] N85-35819
OGDEN AIR LOGISTICS CENTER, HILL AFB, UTAH.
Dissected motors-propellants motor number STM-012. Phase 15: Surveillance report, stage 1
[AD-A156088] N85-35226
OHIO STATE UNIV., COLUMBUS.
Optimal estimation of a high degree gravity field from a global set of 1 deg x 1 deg anomalies to degree and order 250
[AD-A156008] N85-35519
Characteristics of slow particles emitted in the charged current interactions of neutrinos with emulsion nuclei
[HE-5.3-22] N85-36113
OKAYAMA UNIV. (JAPAN).
Hybrid TLC-pair meter for the Sphinx Project
[HE-5.2-10] N85-36086
Energetic delayed hadrons in large air showers observed at 5200m above sea level
[HE-6.2-9] N85-36145
Charge 4/3 leptons in cosmic rays
[HE-6.2-14] N85-36150
Spatial distribution read-out system for thermoluminescence sheets
[HE-7.1-7] N85-36161
OKLAHOMA UNIV., NORMAN.
Equation of state study for polar fluids
[PB85-204345] N85-35262
OREGON STATE UNIV., CORVALLIS.
Subseasonal variability in a two-level atmospheric general circulation model N85-35504
Ore genesis at the Monterrosas deposit in the Coastal Batholith, Ica, Peru N85-35510
OSAKA CITY UNIV. (JAPAN).
Correlation of high energy muons with primary composition in extensive air shower
[HE-4.3-7] N85-36001
Proportional drift tubes for large area muon detectors
[HE-5.2-11] N85-36087
Comments on the measurements of multiple muon phenomena
[HE-5.2-13] N85-36089
Detection threshold energy of high energy cascade showers using thermoluminescence PTFE-sheet and hot-gas reader
[HE-7.1-5] N85-36159
OSAKA UNIV. (JAPAN).
Search for magnetic monopoles using proportional counters filled with helium gas
[HE-6.1-1] N85-36127

P

PACIFIC NORTHWEST LAB., RICHLAND, WASH.
Calibration of a high-level photon irradiation
[DE85-013044] N85-35738
PENNSYLVANIA STATE UNIV., UNIVERSITY PARK.
Characterization of catalysts with metal-support effects and of the species adsorbed on their surfaces
[DE85-012254] N85-35394
Remote sensing of hydrologic transport processes using spot simulation data
[DE85-012412] N85-35467
Kinematic analysis of Hurricane Frederick (1979) using satellite, aircraft and rawinsonde data
[NASA-CR-176167] N85-35533
PENNSYLVANIA UNIV., PHILADELPHIA.
Detector requirements for inwnsity interferometry measurements N85-35709
The homestake surface-underground scintillations: Description
[HE-6.1-9] N85-36135
PITTSBURGH UNIV., PA.
High temperature corrosion of ceramics
[DE85-013481] N85-35303
POLYTECHNIC OF NORTH LONDON (ENGLAND).
The spectrum of neutrons at 60 hg m(-2)
[HE-5.2-20] N85-36096
POTCHEFSTROOM UNIV. FOR CHRISTIAN HIGHER EDUCATION (SOUTH AFRICA).
A note on some statistical properties of rise time parameters used in muon arrival time measurements
[HE-4.7-12] N85-36062
PRATT AND WHITNEY AIRCRAFT, EAST HARTFORD, CONN.
Energy Efficient Engine Program technology benefit/cost study, volume 1
[NASA-CR-174766-VOL-1] N85-35197
Energy Efficient Engine Program technology benefit/cost study, volume 2
[NASA-CR-174766-VOL-2] N85-35198
Development of advanced high-temperature heat flux sensors. Phase 2: Verification testing
[NASA-CR-174973] N85-35391
PRC KENTRON, INC., HAMPTON, VA.
Chemoviscosity modeling for thermosetting resins, 2
[NASA-CR-177958] N85-35243
PRC PLANNING AND ECONOMICS, INC., LAKE SUCCESS, N.Y.
Comparative analysis of operational forecasts versus actual weather conditions in airline flight planning, volume 1
[NASA-CR-167862] N85-35534
Comparative analysis of operational forecasts versus actual weather conditions in airline flight planning, volume 2
[NASA-CR-167863] N85-35535
Comparative analysis of operational forecasts versus actual weather conditions in airline flight planning, volume 3
[NASA-CR-167864] N85-35536
Comparative analysis of operational forecasts versus actual weather conditions in airline flight planning, volume 4
[NASA-CR-167865] N85-35537
Comparative analysis of operational forecasts versus actual weather conditions in airline flight planning: Summary report
[NASA-CR-167866] N85-35538
PRINCETON UNIV., N. J.
Limiter
[DE85-011620] N85-35736
Neutral pumping rates for a next step tokamak ignition device
[DE85-012780] N85-35776
PULSE SCIENCES, INC., SAN LEANDRO, CALIF.
Four stage HELIA experiment
[DE85-012026] N85-35768
PUNJAB UNIV., LAHORE (PAKISTAN).
P(P bar)P elastic scattering and cosmic ray data
[HE-1.1-6] N85-35854
QCD analysis of neutrino charged current structure function F2 in deep inelastic scattering
[HE-5.3-23] N85-36114
PURDUE UNIV., LAFAYETTE, IND.
Nonlinear digital phase-locked loops with application to Loran-C receivers N85-35178
Optimally designed propellers constrained by noise N85-35196
The integrated manual and automatic control of complex flight systems
[NASA-CR-176166] N85-35201
Analysis of flexible aircraft longitudinal dynamics and handling qualities. Volume 1: Analysis methods
[NASA-CR-177943-VOL-1] N85-35202
Analysis of flexible aircraft longitudinal dynamics and handling qualities. Volume 2: Data
[NASA-CR-177943-VOL-2] N85-35203
CO + H2 reaction over nitrogn-modified iron catalysts
[DE85-013791] N85-35231
The compliance of end effector force sensors for robot manipulator control N85-35406
LANDSAT-4/5 image data quality analysis
[E85-10105] N85-35463
Geology and geomorphology of the Roraima group, southeastern Venezuela N85-35511
Recursive partitioning estimation N85-35670

R

RADIAN CORP., RESEARCH TRIANGLE PARK, N.C.
Review of US NOx abatement technology
[PB85-193522] N85-35501
RESEARCH TRIANGLE INST., RESEARCH TRIANGLE PARK, N.C.
AUTOSIM: An automated repetitive software testing tool
[NASA-CR-177930] N85-35643
RHODE ISLAND UNIV., NARRAGANSETT.
Elemental tracers of source regions of contaminants in precipitation
[DE85-012858] N85-35499
RIVERS STATE UNIV. OF SCIENCE AND TECHNOLOGY, PORT HARCOURT (NIGERIA).
Heavy flavours production in quark-gluon plasma formed in high energy nuclear reactions N85-35886
ROCHESTER UNIV., N. Y.
Neutrino production of like sign dimuons
[DE85-013594] N85-35741
ROCKSTEIN (MORRIS), CORAL GABLES, FLA.
Report of the Insect Development Group N85-35584
ROCKWELL INTERNATIONAL CORP., GOLDEN, COLO.
Interaction of trace elements and welding parameters on GTA weld shape
[DE85-004046] N85-35284
Measurement control for plutonium isotopic measurements using gamma-ray spectrometry
[DE85-013394] N85-35397
RUTGERS - THE STATE UNIV., NEW BRUNSWICK, N. J.
An analytical and numerical model of radiation heat transfer in direct injection-type diesel combustion N85-35368
Some aspects of internal gravity waves in a multi-layered moving stratified flow N85-35369

S

SAINT LOUIS UNIV., MO.
Two-point closure study of covariance budgets for turbulent Rayleigh-Benard convection
[PB85-189108] N85-35568
SAITAMA UNIV., URAWA (JAPAN).
Lateral distribution of high energy hadrons and gamma ray in air shower cores observed with emulsion chambers
[HE-3.3-8] N85-35926
Size distributions of air showers accompanied with high energy gamma ray bundles observed at Mt. Chacaltaya
[HE-3.3-9] N85-35927

Comparison of big event with calculations of the air shower development
[HE-3.6-8] N85-35956

SAMARKAND ALISHER NAVOI STATE UNIV. (USSR).
On the determination of the depth of EAS development maximum using the lateral distribution of Cerenkov light at distances 150 m from EAS axis
[HE-4.4-13] N85-36019
Study of the energy spectrum of primary cosmic rays: EAS size fluctuations at a fixed primary energy
[HE-4.4-14] N85-36020
Study of the shower maximum depth by the method of detection of the EAS Cerenkov light pulse shape
[HE-4.4-15] N85-36021

SANDIA LABS., ALBUQUERQUE, N. MEX.
Pressure measurements in a hydrogen combustion environment: Hydrogen-air combustion test series 1 and 2 in the FITS tank, volume 1
[TI85-009899] N85-35259
Dangling bonds and sub-gap optical absorption in silicon
[DE85-011752] N85-35302
Moment-method formulation of the cavity-probe aperture antenna
[DE85-013264] N85-35338
Statistical distribution of breakdown voltages in rep-rate spark gaps
[DE85-012813] N85-35354
Injector losses on Mite
[DE85-012356] N85-35355
Development and evaluation of sulfonated polysulfone membranes for the zinc-ferricyanide battery
[DE85-009104] N85-35357
Experimental technique for measuring the isentrope of hydrogen to several megabars
[DE85-014332] N85-35386
Calibrator for displacement gages used in the rock mechanics laboratory
[DE85-013257] N85-35393
Raster functionality for a VDI
[DE85-006734] N85-35396
Elliptical X-ray analyzer spectrograph application to a laser-produced plasma
[DE85-013790] N85-35398
Testbed for sensory control of intelligent machines
[DE85-012355] N85-35412
A kinetic model for predicting oxidative degradation rates in combined radiation-thermal environments
[TI85-002629] N85-35414
Design and construction of an advanced power conditioning subsystem for small photovoltaic applications
[DE85-013940] N85-35495
Application of pulsed power in the simulation of severe natural lightning
[DE85-012866] N85-35564
Quality assurance considerations for the implementation of a pulsed power R and D project
[DE85-012357] N85-35720
Operations considerations in designing a high speed multi-channel data acquisition system
[DE85-012840] N85-35756
Four stage HELIA experiment
[DE85-012026] N85-35768
Power flow evaluations for HERMES 3
[DE85-013116] N85-35769
Kinetic loss experiments on Mite
[DE85-012826] N85-35780
Surface discharges as intense photon sources in the extreme ultraviolet
[DE85-012593] N85-35782
Simulation of lattice damage due to dynamic loading
[DE85-008468] N85-35808

SANTA BARBARA RESEARCH CENTER, CALIF.
HgCdTe surface and defect study program
[AD-A156079] N85-35799

SCHOOL OF AEROSPACE MEDICINE, BROOKS AFB, TEX.
Dental multi-purpose slowspeed handpieces test and evaluation
[AD-A155764] N85-35606

SCIENCE APPLICATIONS INTERNATIONAL CORP., BOULDER, COLO.
RF stabilization of interchange-ballooning modes
[DE85-012080] N85-35353

SCIENTIFIC RESEARCH CENTER, LOS ANGELES, CALIF.
Feasibility study of radar-transmitting materials
[AD-A155839] N85-35329

SHERBROOKE UNIV. (QUEBEC).
Calculation of the diffusion of light by aerosols: Description of the MIELOR software and results obtained
[REPT-80] N85-35638

SIEGEN UNIV., (WEST GERMANY).
Search for anomalons using plastic nuclear track detectors
[HE-6.2-12] N85-36148

SIEMENS A.G., MUNICH (WEST GERMANY).
Materials and process development for microcomputer-compatible pressure, temperature, and position sensors
[BMFT-FB-T-85-024] N85-35399
Monolithic photovoltaic series array for an energy coupler
[BMFT-FB-T-85-023] N85-35496

SIMULA, INC., PHOENIX, ARIZ.
Design and testing of an energy-absorbing crewseat for the F/FB-111 aircraft. Volume 2: Data from seat testing
[NASA-CR-3917] N85-35184

SKF INDUSTRIES, INC., KING OF PRUSSIA, PA.
Planetary-gear-support bearing test rig design
[NASA-CR-174927] N85-35185

SMITHSONIAN ASTROPHYSICAL OBSERVATORY, CAMBRIDGE, MASS.
The investigation of tethered satellite system dynamics
[NASA-CR-176180] N85-35215
A normal incidence X-ray telescope sounding rocket payload
[NASA-CR-176169] N85-35749
The HEAO-2 Guest Investigator Program: Non-linear growth of instabilities in line-driven stellar winds
[NASA-CR-176168] N85-35840

SOFIA UNIV. (BULGARIA).
General consequences of the violated Feynman scaling N85-35872

SOUTH CAROLINA UNIV., COLUMBIA.
Static and cyclic behavior of semi-rigid steel beam-column connections
[PB85-194363] N85-35433

SRI INTERNATIONAL CORP., MENLO PARK, CALIF.
Laser probes of natural gas ignition chemistry
[PB85-200210] N85-35264
Interprocess communication
[AD-A156337] N85-35337
Specifying and verifying concurrent programs
[AD-A156190] N85-35652

STANFORD LINEAR ACCELERATOR CENTER, CALIF.
Observations of accelerated high current low emittance beams in the SLC Linac
[DE85-013073] N85-35211
Solid state high power amplifier for driving the SLC injector klystron
[DE85-013063] N85-35356
Error message recording and reporting in the SLC control system
[DE85-013057] N85-35664
Report on the SLC control system
[DE85-013076] N85-35722
Forty-five years of e(+)e(-) annihilation physics: 1956 to 2001
[DE85-013052] N85-35723
Status of the zeta(8.3)
[DE85-013070] N85-35724
Time domain reflectometry for SLC BPM system
[DE85-012389] N85-35758
Breeding new light into old machines (and new)
[DE85-013055] N85-35763
On-line model driven control of the SLC electron Damping Ring
[DE85-013077] N85-35772
High resolution beam profile monitors in the SLC
[DE85-013075] N85-35774
Accelerator physics measurements at the damping ring
[DE85-013073] N85-35785
SLC arc transport system: Magnet design and construction
[DE85-014289] N85-35789
SLC Energy Upgrade Program at SLAC
[DE85-014290] N85-35790
Multi-channel pulser for the SLC thermionic electron source
[DE85-014222] N85-35792
TOSCA calculations and measurements for the SLAC SLC damping ring dipole magnet
[DE85-014366] N85-35793
High energy radiation from neutron stars
[DE85-014353] N85-35843

STANFORD UNIV., CALIF.
Adverse pressure gradient and separating turbulent boundary-layer flows: The effect of disequilibrium in initial conditions N85-35155
Molecular and macromolecular sieving by asymmetric ultrafiltration membranes
[PB85-157766] N85-35266
Edge detection and geometric methods in computer vision
[AD-A155873] N85-35630
Invariant tests and likelihood ratio tests for multivariate elliptically contoured distributions
[AD-A155844] N85-35679
Large deviations for the maxima of some random fields
[AD-A155909] N85-35681
Model robust response surface designs: Scaling two-level factorials
[AD-A156218] N85-35686
Laser and electron beam processing of semiconductors
[AD-A155914] N85-35796

STANITZ (JOHN D.), UNIVERSITY HEIGHTS, OHIO.
General design method for 3-dimensional, potential flow fields. Part 2: Computer program DIN3D1 for simple, unbranched ducts
[NASA-CR-3926] N85-35159

SURABAYA INST. OF TECH., INDONESIA.
Microwave propagation studies, measurements and education in Surabaya, Indonesia
[B8464633] N85-35339

SWEDISH TELECOMMUNICATIONS ADMINISTRATION, FARSTA.
Television interference measurement at Kalkugnen (Sweden) test windmill N85-35481

SYDKRAFT AB (SYDSVENSKA KRAFT- OCH VAERME AKTIEBOLAGET), MALMOE (SWEDEN).
Television interference at the Maglarp (Sweden) wind turbine N85-35480

SYRACUSE UNIV., N. Y.
Characteristic modes for slots in a ground plane TE case
[AD-A155757] N85-35326
Signal space models for antenna arrays
[AD-A156063] N85-35335
Stress analysis of axisymmetric sandwich shells of variable thickness N85-35419

SYSTEMS AND APPLIED SCIENCES CORP., HYATTSVILLE, MD.
Literature search for new physical methods for biological aerosol detection
[AD-A155883] N85-35592

SYSTEMS AND APPLIED SCIENCES CORP., VIENNA, VA.
Users guide for optimum interpolation method of global data assimilation
[AD-A155929] N85-35648
Two methods of global data assimilation
[AD-A155981] N85-35664

T

TASHKENT V. I. LENIN STATE UNIV., VUZGORODOK (USSR).
An experimental study of correlations in the development of the electron-photon cascades
[HE-3.5-10] N85-35947

TASMANIA UNIV., HOBART (AUSTRALIA).
Underground measurements on secondary cosmic rays
[HE-5.4-1] N85-36116

TATA INST. OF FUNDAMENTAL RESEARCH, BOMBAY (INDIA).
High energy hadrons in extensive air showers N85-35976
The hump in the Cerenkov lateral distribution of gamma ray showers
[HE-4.5-9] N85-36032
Muon and neutrino results from KGF experiment at a depth of 7000 hg/square cm
[HE-5.1-2] N85-36068
Limits on monopole fluxes from KFG experiment
[HE-6.1-6] N85-36132
Results on nucleon life-time from the Kolar gold field experiment
[HE-6.2-3] N85-36139
Data acquisition system for phase-2 KGF proton decay experiment
[HE-6.2-4] N85-36140

TECHNICAL UNIV. OF DENMARK, LYNGBY.
Calculation of trajectories of detached wind turbine blades and prediction of site risk levels associated with failures of HAWT's N85-35475

TECHNISCHE HOCHSCHULE, AACHEN (WEST GERMANY).
Search for proton decay in the Frejus experiment
[HE-6.2-2] N85-36138

TECHNISCHE HOGESCHOOL, EINDHOVEN (NETHERLANDS).
Microwave propagation studies, measurements and education in Surabaya, Indonesia
[B8464633] N85-35339

Aspects of input signal design for order and parameter estimation in linear dynamical systems
[ER-83/05] N85-35362

TECHNISCHE UNIV., BRUNSWICK (WEST GERMANY).
Control variables in vertical wind determination using simple flight-mechanical equations N85-35546
The principles of wind measurement with the help of aircraft N85-35558

TECHNISCHE UNIV., MUNICH (WEST GERMANY).
Development and operation of a measuring data acquisition system for use in light airplanes N85-35556

TELEFUNKEN ELECTRONIC G.M.B.H., HEILBRONN (WEST GERMANY).
Computer Aided Design (CAD) methods for very large scale integration systems
[BMFT-FB-T-85-029] N85-35668

TEXAS A&M UNIV., COLLEGE STATION.
Seismic stratigraphic analysis of the Mississippi Fan N85-35507

TEXAS TECHNOLOGICAL UNIV., LUBBOCK.
Reliability prediction of the series system with spares subject to Weibull failure N85-35413

TEXAS UNIV., AUSTIN.
The application of bispectral analyses to aeroelastic phenomena N85-35157
A study of the control of particulate emissions from turbine engine test cells N85-35205
Vectorial electron transfer on designed surfaces
[PB85-204600] N85-35263
Scale separation closure and Alfven wave turbulence
[DE85-013124] N85-35385
Further studies on liquid sloshing
[PB85-198695] N85-35388
Design and behavior of coped beams N85-35417
Hydrogeology of the lower Glen Rose Aquifer, south-central Texas N85-35466
Depositional systems and coal occurrence in the Fort Union Formation (Paleocene), Powder River Basin, Wyoming and Montana N85-35505
High energy plasma accelerators
[DE85-013121] N85-35760
Generalized reduced fluid model with finite ion-gyroradius effects
[DE85-013123] N85-35777
Current interruption by density depression
[DE85-013120] N85-35846

TEXAS UNIV. AT DALLAS, RICHARDSON.
Monte Carlo simulation of EAS generated by 10(14) - 10(16) eV protons
[HE-4.3-14] N85-36008

THERMO ELECTRON CORP., WALTHAM, MASS.
Development of a high-efficiency, gas-fired, heat pipe, warm-air heating system
[PB85-199636] N85-35318

TILBURG UNIV. (NETHERLANDS).
Risk analysis and sensitivity: Antithesis or synthesis
[B8562444] N85-35687

TOKYO INST. OF TECH. (JAPAN).
Radio signals from very large showers
[HE-4.6-3] N85-36040
Longitudinal development of muons in large air showers studies from the arrival time distributions measured at 900m above sea level
[HE-4.7-4] N85-36055
Arrival time distributions of electrons in air showers with primary energies above 10 (16)eV observed at 900m above sea level
[HE-4.7-5] N85-36056

TOKYO UNIV. (JAPAN).
Heavy nucleus collisions between 20 and 60 GeV/nucleon
[HE-1.4-2] N85-35890
Super-family P2 C-96-125 observed by Japan-URSS Joint Emulsion Chamber Experiment
[HE-3.4-8] N85-35936
Analysis of equi-intensity curves and NU distribution of EAS N85-35970
Core structure of EAS in 10(15) to 10(17) eV N85-35989
EAS development curve at energy of 10(16) - 10(18) eV measured by optical Cerenkov light
[HE-4.4-7] N85-36015
A three-dimensional Monte Carlo calculation of the photon initiated showers and Kiel result
[HE-4.5-13] N85-36035
Radio wave emitted by an extensive air showers in 10KHz to 1MHz region
[HE-4.6-15] N85-36051
Properties of 10 (18)-10 (19)eV EAS at far core distance
[HE-4.7-3] N85-36054
Energy spectra of high energy atmospheric neutrinos
[HE-5.3-14] N85-36108

TOKYO UNIV., TANASHI (JAPAN).
Measurement of energy muons in EAS at energy region larger thean 10(17) eV
[HE-4.3-8] N85-36002
Background light measurements at the DUMAND site
[HE-5.2-7] N85-36084
Magnetic monopole search by 130 m(2)sr He gas proportional counter
[HE-6.1-2] N85-36128

TRONDHEIM UNIV. (NORWAY).
The nucleon intensity in the atmosphere and the Pt distribution
[HE-3.1-9] N85-35907
Atmospheric muons and neutrinos, and the neutrino-induced muon flux underground
[HE-5.4-7] N85-36118

TUFTS UNIV., MEDFORD, MASS.
High energy physics at Tufts University
[DOE/ER-40085/7] N85-35744

TULANE UNIV., NEW ORLEANS, LA.
Artificial intelligence in Ada (trademark): Pattern-directed processing
[AD-A156230] N85-35671

TURKU UNIV. (FINLAND).
Investigation of cosmic rays in very short time scales
[HE-4.6-7] N85-36044
A facility for investigation of multiple hadrons at cosmic-ray energies
[HE-4.6-8] N85-36045

U

UNITED KINGDOM ATOMIC ENERGY AUTHORITY, DOUNREAY (SCOTLAND).
Analytical methods in the purex process
[BLL-DOUNREAY-TR-952(9091.9F)] N85-35727

UNITED KINGDOM ATOMIC ENERGY AUTHORITY, HARWELL (ENGLAND).
Pitting corrosion of ferrous alloys
[AERE-R-11490] N85-35273
The dynamic strain ageing of A533B class 1 nuclear pressure vessel steel
[AERE-R-11485] N85-35274
Effect of thermal ageing on the mechanical properties of PWR pressure vessel steels and weldments
[AERE-R-11460] N85-35275
The preparation of TEM specimens showing oxide scales in transverse cross-section
[AERE-R-11579] N85-35276
Applications and misapplications of the channel-capture formalism of direct neutron capture
[DE85-013992] N85-35748

UNITED KINGDOM ATOMIC ENERGY AUTHORITY, RISLEY (ENGLAND).
Tests on zirconium nitride coatings applied to SW 18 steel using the chemical vapor deposition method N85-35271
Action of wear-inhibiting Al2O3-coatings when applied to hard metal cutting tools
[BLL-RISLEY-TR-5041-(9091.9F)] N85-35292
Wear-resistant coatings for tools intended for cold working
[BLL-RISLEY-TR-5040-(9091.9F)] N85-35293

UNIVERSIDADE ESTADUAL DE CAMPINAS (BRAZIL).
Hadron thermodynamics in relativistic nuclear collisions
[HE-1.1-8] N85-35856
Jets in air-jet family
[HE-3.2-1] N85-35912
Mini-clusters
[HE-3.5-3] N85-35942
Giant mini-clusters as possible origin of halo phenomena observed in super-families
[HE-3.5-4] N85-35943

UNIVERSITIES SPACE RESEARCH ASSOCIATION, COLUMBIA, MD.
Studies on effects of boundary conditions in confined turbulent flow predictions
[NASA-CR-3929] N85-35371

UNIVERSITY COLL., DUBLIN (IRELAND).
An experiment to detect gut monopoles
[HE-6.1-7] N85-36133

UNIVERSITY CORP. FOR ATMOSPHERIC RESEARCH, BOULDER, COLO.
A preliminary intercomparison between numerical upper wind forecasts and research aircraft measurements of jet streams
[NASA-CR-167884] N85-35539

UNIVERSITY OF NORTH BENGAL, DARJEELING (INDIA).
A critical analysis of air shower structure functions and size spectrum measurements with the NBU air shower array N85-35983
A new study of shower age distribution in near vertical showers by EAS air shower array N85-35996
A new study of muons in air showers by NBU air shower array N85-35997

UNIVERSITY OF SOUTHERN CALIFORNIA, LOS ANGELES.
Cryogenic laser calorimetry for impurity analysis
[NASA-CR-176179] N85-35395
Carbon fiber strainmeter studies in southern California
[PB85-196889] N85-35528
Groundwater radon studies for earthquake precursors in southern California
[PB85-196871] N85-35529
Investigations of the molecular beam epitaxial growth and characteristics of external excitation induced non-equilibrium phases of immiscible 3-5 compound semiconductors
[AD-A156325] N85-35804

UTAH GEOLOGICAL AND MINERALOGICAL SURVEY, SALT LAKE CITY.
Evaluation of low-temperature geothermal potential in north-central Box Elder County, Utah
[DE85-009541] N85-35490

UTAH UNIV., SALT LAKE CITY.
Noise in silver beta alumina ceramics
[AD-A156135] N85-35297
Noise in sodium beta alumina crystals
[AD-A156025] N85-35798
Proton-air inelastic cross section at S(1/2) = 30 TeV
[HE-1.1-2] N85-35850
Energy calibration of the fly's eye detector
[HE-4.4-1] N85-36011
The structure of EAS at E 0.1 EeV
[HE-4.4-2] N85-36012
Limits on deeply penetrating particles in the 10(17) eV cosmic ray flux
[HE-5.3-1] N85-36098

V

VALVO ROEHREN- UND HALBLEITERWERKE DER PHILIPS G.M.B.H., HAMBURG (WEST GERMANY).
Development of position sensors for microcomputer-oriented sensor systems
[BMFT-FB-T-85-021] N85-35361

VIRGINIA POLYTECHNIC INST. AND STATE UNIV., BLACKSBURG.
Energy management of three-dimensional minimum-time intercept
[NASA-CR-176174] N85-35186
Identification and control of structures in space
[NASA-CR-176175] N85-35214
Damage induced stress redistribution in composite laminates N85-35235
Microbiological and biochemical studies towards optimization of substrate utilization by methanogenic bacteria
[PB85-188332] N85-35310

VIRGINIA UNIV., CHARLOTTESVILLE.
Effect of microstructure on the fatigue behavior of Fe-C-X alloys
[DE85-011749] N85-35285
Characterizations of generalized hyperexponential distributions
[AD-A155855] N85-35680

VOITH (J. M.) G.M.B.H., HERDENHERN (WEST GERMANY).
Visit to test facility Stoetten (West Germany) May 9, 1984, including the Voith Wind Energy Converter (WEC) 520 turbine. The annual production of various wind energy plants in selected locations N85-35467

VOROSHILOVGRAD MACHINERY BUILDING INST., (USSR).
Experimental investigation of radiative-acoustic effects in the water by the thermodynamical conditions of Dumand
[HE-7.1-2] N85-36156

W

WARSAW TECHNICAL UNIV. (POLAND).
Physical meaning of the multiplicities of emitted nucleons in hadron-nucleus collisions N85-35877
How are particle production, nucleon emission and target fragment evaporation processes interrelated in hadron-nucleus collisions? N85-35878
Experimental study of the space-time development of the particle production process in hadron-nucleon collisions, using massive target nucleus as a detector N85-35879
Experimental evidence of the decrease of kinetic energy of hadrons in passing through atomic nuclei N85-35880
Energy-range relations for hadrons in nuclear matter N85-35881

Scattering and stopping of hadrons in nuclear matter N85-35882
Measurements of hadron mean free path for the particle-producing collisions in nuclear matter N85-35883
Experimental basis for the models of cascade propagation in atmosphere
[HE-3.6-6] N85-35954

WARSAW UNIV. (POLAND).
Meteorological measurements with motor gliders in Poland N85-35555

WASEDA UNIV., TOKYO (JAPAN).
A test of the Feynman scaling in the fragmentation region
[HE-1.2-9] N85-35867
Search for anomalous C-jets in Chacaltaya emulsion chamber experiment
[HE-3.2-5] N85-35913
Study of hadron bundles observed in Chacaltaya two-story emulsion chamber
[HE-3.3-4] N85-35922
Penetrative nature of high energy showers observed in Chacaltaya emulsion chamber
[HE-3.3-5] N85-35923
Anomalous correlation between hadron and electromagnetic particles in hadron and gamma-ray families
[HE-3.3-6] N85-35924
A search for mini-clusters in Japan-USSR Joint Experiment at Pamir
[HE-3.5-2] N85-35941
Structure of super-families
[HE-3.5-7] N85-35944
Extremely high energy hadron and gamma-ray families(3). Core structure of the halo of superfamily
[HE-3.5-8] N85-35945

WASHINGTON UNIV., SEATTLE.
Parametric stability of analytical close-range photogrammetry N85-35461
Confinement and heating of high beta plasmas with emphasis on compact toroids
[DE85-011459] N85-35761

WASHINGTON UNIV., ST. LOUIS, MO.
Quantitative non-destructive evaluation of composite materials based on ultrasonic wave propagation
[NASA-CR-176176] N85-35244

WAYNE STATE UNIV., DETROIT, MICH.
Fatigue damage detection in steels by optical correlation
[AD-A155830] N85-35277

WESTINGHOUSE ELECTRIC CORP., PITTSBURGH, PA.
Study to assess the effects of magnetohydrodynamic electromagnetic pulse on electric power systems, phase 1, volume 3
[DE85-011301] N85-35771

WESTON OBSERVATORY, MASS.
Procedure for editing the fluxgate magnetometer data of the AFGL (Air Force Geophysics Laboratory) magnetometer network
[AD-A156331] N85-35523

WHEATON COLL., NORTON, MASS.
The ionization structure of planetary nebulae. Part 4: NGC 7662
[NASA-CR-176151] N85-35844

WISCONSIN UNIV., MADISON.
Couette flow of two fluids between concentric cylinders
[AD-A155827] N85-35376
Attenuation properties of the Petatlan region, Mexico, and a local magnitude scale for microearthquakes in this area N85-35513
Report of the Avian Development Working Group N85-35582
The finite element-difference method N85-35672
Geophysical searches for three-neutrino oscillations
[HE-5.3-9] N85-36103

WYOMING UNIV., LARAMIE.
Geothermal resources of the Washakie and Great Divide basins, Wyoming
[DE85-013004] N85-35491
Thermal evolution of coastal California with implications for hydrocarbon maturation N85-35509
The kinematic structure of cold frontal rainbands N85-35531
The nature and geometry of infrared reflection nebulae N85-35835

Y

YALE UNIV. OBSERVATORY, NEW HAVEN, CONN.
The detection and study of molecular species using time resolved laser spectroscopy
[AD-A155910] N85-35256

YANAGITA (TOMOTAKE), TAKAKURA (JAPAN).
Relation between gamma-ray family and EAS core: Monte-Carlo simulation of EAS core
[HE-3.6-7] N85-35955

YUNNAN UNIV., KUNMING (CHINA).
Acoustic detection of air shower cores
[HE-7.1-4] N85-36158

CONTRACT NUMBER INDEX

Typical Contract Number Index Listing

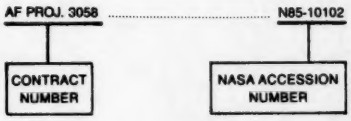

Listings in this index are arranged alphanumerically by contract number. Under each contract number the NASA accession numbers denoting documents that have been produced as a result of research done under that contract are arranged in ascending order. The NASA accession number denotes the number by which the citation is identified.

AF PROJ. 7231 ..... N85-35608
N85-35610
AF PROJ. 7670 ..... N85-35401
ARPA ORDER 4881 ..... N85-35634
DA PROJ. WR0-4101 ..... N85-35609
DA PROJ. 1L1-62618-AH-80 ..... N85-35653
DA PROJ. 3M1-61102-BS-12 ..... N85-35617
DA PROJ. 236-2 ..... N85-35632
DAAE07-82-C-4063 ..... N85-35644
DAAE07-83-C-R051 ..... N85-35408
DAAG29-80-C-0041 ..... N85-35376
DAAG29-80-K-0008 ..... N85-35752
DAAG29-80-K-0044 ..... N85-35280
DAAG29-81-K-0114 ..... N85-35277
DAAG29-81-K-0164 ..... N85-35797
DAAG29-82-G-0002 ..... N85-35678
DAAG29-82-K-0084 ..... N85-35328
DAAG29-82-K-0156 ..... N85-35679
DAAG29-83-K-0032 ..... N85-35256
DAAG29-83-K-0052 ..... N85-35559
DAAG29-83-K-0119 ..... N85-35652
DAAG29-85-M-0101 ..... N85-35409
DAAK11-82-C-0113 ..... N85-35592
DAAK70-83-K-0018 ..... N85-35181
N85-35751
DAMD17-80-C-0099 ..... N85-35617
DARPA ORDER 3045 ..... N85-35332
DARPA ORDER 3206 ..... N85-35181
N85-35751
DARPA ORDER 4941 ..... N85-35392
DE-AC03-76SF-00515 ..... N85-35772
DE-AC01-83CE-30780 ..... N85-35493
DE-AC02-76CH-00016 ..... N85-35286
N85-35358
N85-35669
N85-35718
N85-35737
N85-35759
N85-35767
N85-35788
DE-AC02-76CH-03000 ..... N85-35719
N85-35807
DE-AC02-76CH-03073 ..... N85-35736
DE-AC02-76ER-00881 ..... N85-36027
DE-AC02-76ER-02383 ..... N85-35658
DE-AC02-76ER-03077 ..... N85-35770
DE-AC02-76ER-03274 ..... N85-35745
DE-AC02-76ER-05007 ..... N85-35935
N85-36102
DE-AC02-76ER-13065 ..... N85-35741
DE-AC02-80ER-10718 ..... N85-35665
DE-AC02-80EV-10328 ..... N85-35593
DE-AC02-83CH-10093 ..... N85-35492
DE-AC02-83ER-13137 ..... N85-35403
DE-AC02-83ER-40085 ..... N85-35744
DE-AC02-83ER-60182 ..... N85-35467
DE-AC03-76ET-53057 ..... N85-35353
DE-AC03-76SF-00098 ..... N85-35260
N85-35261
N85-35494
N85-35700
N85-35711
N85-35712
N85-35746
DE-AC03-76SF-00515 ..... N85-35356
N85-35664
N85-35711
N85-35722
N85-35723
N85-35724
N85-35758
N85-35763
N85-35774
N85-35785
N85-35789
N85-35790
N85-35792
N85-35793
N85-35843
DE-AC03-81ER-40050 ..... N85-35785
DE-AC04-76DP-0789 ..... N85-35782
DE-AC04-76DP-00053 ..... N85-35309
DE-AC04-76DP-00613 ..... N85-35288
DE-AC04-76DP-00789 ..... N85-35302
N85-35338
N85-35354
N85-35355
N85-35357
N85-35386
N85-35393
N85-35396
N85-35398
N85-35412
N85-35489
N85-35495
N85-35564
N85-35720
N85-35756
N85-35768
N85-35769
N85-35780
N85-35808
DE-AC04-76DP-03533 ..... N85-35284
N85-35397
DE-AC04-76DR-00789 ..... N85-35380
DE-AC04-82AL-18071 ..... N85-35716
DE-AC05-76OR-00033 ..... N85-35818
DE-AC05-84OR-21400 ..... N85-35228
N85-35232
N85-35282
N85-35287
N85-35299
N85-35304
N85-35562
N85-35618
N85-35659
N85-35725
N85-35726
N85-35734
N85-35735
N85-35748
N85-35771
N85-35776
N85-35809
DE-AC06-76FF-02170 ..... N85-35382
DE-AC06-76RL-01830 ..... N85-35738
DE-AC07-76ID-01570 ..... N85-35666
N85-35747
DE-AC09-76SF-00001 ..... N85-35742
DE-AC21-79ET-15440 ..... N85-35300
DE-AI04-80AL-12726 ..... N85-35471
DE-AI08-78ET-44802 ..... N85-35469
DE-AI08-79DP-40092 ..... N85-35402
DE-AS05-80ER-10641 ..... N85-35229
DE-AS05-83ER-45035 ..... N85-35285
DE-AS07-77ET-28393 ..... N85-35490
DE-AT06-72ET-53047 ..... N85-35761
DE-FC07-79ID-12026 ..... N85-35491
DE-FG02-84ER-13276 ..... N85-35394
DE-FG02-84ER-45117 ..... N85-35303
DE-FG05-80ET-53088 ..... N85-35385
N85-35760
N85-35846
DE-FG09-84ER-40160 ..... N85-35861
DE-FG22-82PC-50804 ..... N85-35231
DE-FG22-84PC-70788 ..... N85-35230
DE-FG22-84PC-71253 ..... N85-35499
DEN3-262 ..... N85-35471
DI-14-08-0001-21193 ..... N85-35529
DI-14-08-0001-21240 ..... N85-35528
DI-14-34-0001-8548 ..... N85-35266
DOT-UT-90042 ..... N85-35830
DTFA01-84-C-00001 ..... N85-35179
DTMA91-82-C-20036 ..... N85-35388
EMW-C-0743 ..... N85-35313
EPA-R-809370 ..... N85-35311
EPA-R-811534 ..... N85-35503
EPA-68-01-6639-236 ..... N85-35828
EPA-68-02-3994 ..... N85-35501
EPA-68-03-3131 ..... N85-35500
FG05-80ET-53088 ..... N85-35777
F04701-83-C-0084 ..... N85-35351
N85-35685
F08606-73-C-0027 ..... N85-35216
F08606-75-C-0032 ..... N85-35216
F19628-80-C-0110 ..... N85-35350
F19628-82-C-0023 ..... N85-35684
F19628-82-K-0022 ..... N85-35519
F19628-82-K-0038 ..... N85-35334
F19628-82-K-0040 ..... N85-35523
F19628-83-C-0010 ..... N85-35524
F19628-83-C-0053 ..... N85-35522
F19628-84-C-0001 ..... N85-35633
F19628-85-C-0002 ..... N85-35634
F29601-81-C-0044 ..... N85-35520
F30602-81-C-0169 ..... N85-35335
F33615-77-C-2004 ..... N85-35257
F33615-83-C-3252 ..... N85-35425
F33615-83-C-5080 ..... N85-35410
F33615-84-C-3412 ..... N85-35377
F49620-82-C-0035 ..... N85-35671
GRI-5082-260-0756 ..... N85-35263
MDA903-80-C-0102 ..... N85-35630
MDA903-80-C-0353 ..... N85-35216
MDA903-81-C-0294 ..... N85-35796
MDA903-83-C-0108 ..... N85-35799
MIPR-ARO-111-85 ..... N85-35331
NAGW-227 ..... N85-35588
N85-35589
N85-35590
N85-35591
N85-35594
NAGW-581 ..... N85-35373
NAG1-203 ..... N85-35186
NAG1-225 ..... N85-35214
NAG1-254 ..... N85-35202
N85-35203
NAG1-395 ..... N85-35343
NAG1-527 ..... N85-35676
NAG3-185 ..... N85-35472
NAG3-475 ..... N85-35320
NAG4-1 ..... N85-35201
NAG5-102 ..... N85-35533
NAG5-315 ..... N85-35845
NAG5-626 ..... N85-35749
NAG8-463 ..... N85-35840
NAG8-500 ..... N85-35876
NASA ORDER-501834D N85-35306
NASW-3389 ..... N85-35845
NASW-3839 ..... N85-35517
NASW-4004 ..... N85-35161
N85-35242
N85-35272
NASW-4005 ..... N85-35245
NASW-4006 ..... N85-35163
N85-35164
NASW-4070 ..... N85-35296
NAS1-16489 ..... N85-35643
NAS1-16856 ..... N85-35241
NAS1-17070 ..... N85-35375
N85-35675
N85-35676
NAS1-17262 ..... N85-35160
NAS1-17387 ..... N85-35184
NAS1-17705 ..... N85-35642
NAS1-17944 ..... N85-35390
NAS1-18000 ..... N85-35243

NAS2-11555 ..... N85-35639
N85-35640
NAS3-2266C N85-35389
NAS3-20643 ..... N85-35199
NAS3-20646 ..... N85-35197
N85-35198
NAS3-21991 ..... N85-35159
NAS3-22133 ..... N85-35391
NAS3-22250 ..... N85-35162
NAS3-22748 ..... N85-35534
N85-35535
N85-35536
N85-35537
N85-35538
NAS3-23702 ..... N85-35185
NAS3-23865 ..... N85-35728
NAS3-24100 ..... N85-35158
NAS5-26859 ..... N85-35463
NAS5-27346 ..... N85-35464
NAS5-28037 ..... N85-35213
NAS5-28128 ..... N85-35641
NAS7-100 ..... N85-35395
NAS7-918 ..... N85-35219
N85-35322
N85-35323
N85-35324
N85-35325
N85-35750
N85-35795
NAS8-32962 ..... N85-35220
N85-35221
N85-35222
N85-35223
N85-35224
N85-35236
N85-35237
N85-35238
N85-35239
N85-35240
N85-35294
N85-35295
N85-35407
N85-35423
NAS8-34678 ..... N85-35540
NAS8-35918 ..... N85-35371
NAS8-36160 ..... N85-35215
NCC2-323 ..... N85-35794
NCC3-29 ..... N85-35321
NCC3-38 ..... N85-35342
NGL-05-005-003 ..... N85-35841
NGR-05-005-004 ..... N85-35888
NGR-24-005-050 ..... N85-35875
N85-35876
N85-35897
NGR-28-002-01 ..... N85-35713
NR PROJ. F59-553 ..... N85-35561
NR PROJ. M01-00 ..... N85-35616
NR PROJ. R01-103 ..... N85-35714
NR PROJ. Z03-71 ..... N85-35488
NR PROJ. 384-914 ..... N85-35697
NSF CEE-81-10734 ..... N85-35527
NSF CEE-81-11964 ..... N85-35434
NSF CEE-81-15014 ..... N85-35433
NSF INT-82-05325 ..... N85-35847
NSF MCS-80-24649 ..... N85-35681
NSF MEA-82-13925 ..... N85-35426
NSF PHY-81-09110-A01 ..... N85-35861
NSF PHY-82-01089 ..... N85-35850
N85-36011
N85-36012
NSF PHY-82-07425 ..... N85-35864
N85-35972
NSF PHY-82-07697 ..... N85-36043
NSF PHY-84-03710 ..... N85-36134
NSF PHY-84-05852 ..... N85-35875
N85-35876
N85-35897
NSF PHY-84-10989 ..... N85-35935
N85-36027
N85-36102
NSG-1301 ..... N85-35695
NSG-1601 ..... N85-35244
NSG-5376 ..... N85-35844
N00014-76-C-0430 ..... N85-35697
N00014-76-C-0475 ..... N85-35686
N00014-76-C-1044 ..... N85-35800
N00014-77-C-0306 ..... N85-35681
N00014-77-C-1234 ..... N85-35252
N00014-80-C-0505 ..... N85-35626
N00014-82-K-0603 ..... N85-35297
N85-35798
N00014-83-K-0050 ..... N85-35804
N00014-83-K-0069 ..... N85-35255
N00014-83-K-0145 ..... N85-35378
N00014-83-K-0228 ..... N85-35252
N85-35298
N85-35803
N00014-83-K-0496 ..... N85-35561
N00014-83-K-0624 ..... N85-35680
N00014-84-C-0621 ..... N85-35337
N00014-84-C-0720 ..... N85-35649
N85-35650
N00014-84-C-0727 ..... N85-35392
N00014-84-K-0027 ..... N85-35430
N00014-84-K-0049 ..... N85-35698
N00014-84-K-0357 ..... N85-35332
N00014-84-K-0431 ..... N85-35802
N00014-84-K-0510 ..... N85-35426
N00014-85-F-0015 ..... N85-35714
N00014-85-G-0093 ..... N85-35624
N00014-85-K-0082 ..... N85-35326
N00019-84-C-0356 ..... N85-35329
N00039-80-C-0556 ..... N85-35635
N85-35655
N00039-81-C-0408 ..... N85-35216
N00039-82-C-0250 ..... N85-35630
N61339-81-C-0105 ..... N85-35611
P-PU/PHYS(11/2) N85-35854
RR0-1108 ..... N85-35697
W-31-109-ENG-38 ..... N85-35283
N85-35657
N85-35699
N85-35731
N85-35739
N85-35764
N85-35773
W-7405-ENG-36 ..... N85-35301
N85-35359
N85-35360
N85-35379
N85-35381
N85-35383
N85-35384
N85-35405
N85-35525
N85-35656
N85-35661
N85-35717
N85-35721
N85-35733
N85-35757
N85-35762
N85-35765
N85-35766
N85-35775
N85-35778
N85-35779
N85-35784
N85-35786
N85-35787
W-7405-ENG-48 ..... N85-35289
N85-35305
N85-35404
N85-35563
N85-35660
N85-35662
N85-35740
N85-35743
N85-35783
N85-35791
N85-35842
W-7405-ENG-82 ..... N85-35667
W-7503-ENG-36 ..... N85-35663
W-31109-ENG-38 ..... N85-35432
ZR0-0001 ..... N85-35427
199-40-22 ..... N85-35578
310-20-67-55-00 ..... N85-35750
323-51-45-00-02 ..... N85-35795
324-01-00 ..... N85-35390
351-02-03 ..... N85-35834
352-02-03 ..... N85-35832
N85-35833
505-31-01 ..... N85-35372
505-31-03-02 ..... N85-35160
505-31-83-01 ..... N85-35375
505-33-23 ..... N85-35424
505-33-33 ..... N85-35243
505-33-53-14 ..... N85-35307
505-33-83-01 ..... N85-35675
505-34-03 ..... N85-35204
505-34-03-03 ..... N85-35202
N85-35203
505-34-13 ..... N85-35643
505-37-13 ..... N85-35642
505-90-22 ..... N85-35158
506-53-33-04 ..... N85-35374
506-54-61 ..... N85-35210
506-54-63 ..... N85-35637
506-60-42 ..... N85-35225
650-60-15-01-00 ..... N85-35324
776-54-01 ..... N85-35472
838-10-04-54-00 ..... N85-35219
999-53-02 ..... N85-35639
N85-35640

REPORT / ACCESSION NUMBER INDEX

Typical Report / Accession Number Index Listing

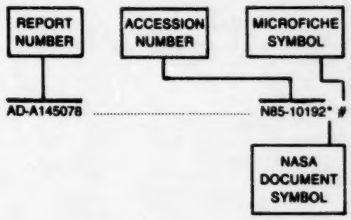

Listings in this index are arranged alphanumerically by report number. The NASA accession number denotes the number by which the citation is identified. An asterisk (*) indicates that the item is a NASA report. A pound sign (#) indicates that the item is available on microfiche.

A-3226 ..... N85-35334 #

AA-R-8222-5817 ..... N85-35434 #

ACSC-85-0240 ..... N85-35212 #
ACSC-85-0245 ..... N85-35622 #
ACSC-85-0435 ..... N85-35191 #
ACSC-85-0915 ..... N85-35177 #
ACSC-85-1095 ..... N85-35176 #
ACSC-85-1235 ..... N85-35193 #
ACSC-85-1405 ..... N85-35498 #
ACSC-85-1535 ..... N85-35817 #
ACSC-85-1725 ..... N85-35621 #
ACSC-85-2610 ..... N85-35182 #

AD-A149201 ..... N85-35690 #
AD-A149202 ..... N85-35691 #
AD-A155750 ..... N85-35627 #
AD-A155751 ..... N85-35619 #
AD-A155754 ..... N85-35216 #
AD-A155755 ..... N85-35408 #
AD-A155756 ..... N85-35644 #
AD-A155757 ..... N85-35326 #
AD-A155761 ..... N85-35729 #
AD-A155764 ..... N85-35606 #
AD-A155765 ..... N85-35175 #
AD-A155774 ..... N85-35425 #
AD-A155775 ..... N85-35255 #
AD-A155776 ..... N85-35730 #
AD-A155777 ..... N85-35207 #
AD-A155780 ..... N85-35313 #
AD-A155781 ..... N85-35624 #
AD-A155813 ..... N85-35692 #
AD-A155815 ..... N85-35179 #
AD-A155819 ..... N85-35327 #
AD-A155827 ..... N85-35376 #
AD-A155829 ..... N85-35678 #
AD-A155830 ..... N85-35277 #
AD-A155832 ..... N85-35328 #
AD-A155834 ..... N85-35409 #
AD-A155839 ..... N85-35329 #
AD-A155841 ..... N85-35392 #
AD-A155842 ..... N85-35607 #
AD-A155843 ..... N85-35628 #
AD-A155844 ..... N85-35679 #
AD-A155845 ..... N85-35559 #
AD-A155846 ..... N85-35645 #
AD-A155849 ..... N85-35646 #
AD-A155850 ..... N85-35173 #
AD-A155852 ..... N85-35629 #
AD-A155855 ..... N85-35680 #
AD-A155856 ..... N85-35188 #
AD-A155862 ..... N85-35714 #
AD-A155863 ..... N85-35715 #
AD-A155873 ..... N85-35630 #
AD-A155875 ..... N85-35278 #
AD-A155877 ..... N85-35488 #
AD-A155880 ..... N85-35180 #
AD-A155881 ..... N85-35608 #
AD-A155883 ..... N85-35592 #
AD-A155889 ..... N85-35631 #
AD-A155909 ..... N85-35681 #
AD-A155910 ..... N85-35256 #
AD-A155912 ..... N85-35609 #
AD-A155913 ..... N85-35647 #
AD-A155914 ..... N85-35796 #
AD-A155920 ..... N85-35348 #
AD-A155923 ..... N85-35682 #
AD-A155926 ..... N85-35426 #
AD-A155927 ..... N85-35797 #
AD-A155929 ..... N85-35648 #
AD-A155930 ..... N85-35279 #
AD-A155934 ..... N85-35683 #
AD-A155935 ..... N85-35349 #
AD-A155963 ..... N85-35610 #
AD-A155975 ..... N85-35611 #
AD-A155981 ..... N85-35684 #
AD-A155984 ..... N85-35612 #
AD-A155988 ..... N85-35685 #
AD-A155989 ..... N85-35632 #
AD-A155990 ..... N85-35574 #
AD-A156002 ..... N85-35751 #
AD-A156004 ..... N85-35822 #
AD-A156007 ..... N85-35181 #
AD-A156008 ..... N85-35519 #
AD-A156024 ..... N85-35696 #
AD-A156025 ..... N85-35798 #
AD-A156027 ..... N85-35189 #
AD-A156029 ..... N85-35330 #
AD-A156039 ..... N85-35280 #
AD-A156040 ..... N85-35331 #
AD-A156041 ..... N85-35520 #
AD-A156049 ..... N85-35332 #
AD-A156055 ..... N85-35521 #
AD-A156058 ..... N85-35333 #
AD-A156059 ..... N85-35633 #
AD-A156062 ..... N85-35334 #
AD-A156063 ..... N85-35335 #
AD-A156064 ..... N85-35823 #
AD-A156067 ..... N85-35810 #
AD-A156068 ..... N85-35811 #
AD-A156069 ..... N85-35812 #
AD-A156070 ..... N85-35813 #
AD-A156071 ..... N85-35814 #
AD-A156072 ..... N85-35815 #
AD-A156073 ..... N85-35816 #
AD-A156079 ..... N85-35799 #
AD-A156080 ..... N85-35800 #
AD-A156085 ..... N85-35350 #
AD-A156088 ..... N85-35226 #
AD-A156089 ..... N85-35190 #
AD-A156097 ..... N85-35377 #
AD-A156098 ..... N85-35351 #
AD-A156099 ..... N85-35613 #
AD-A156100 ..... N85-35824 #
AD-A156102 ..... N85-35182 #
AD-A156103 ..... N85-35191 #
AD-A156112 ..... N85-35251 #
AD-A156117 ..... N85-35801 #
AD-A156121 ..... N85-35649 #
AD-A156122 ..... N85-35650 #
AD-A156128 ..... N85-35817 #
AD-A156133 ..... N85-35651 #
AD-A156134 ..... N85-35560 #
AD-A156135 ..... N85-35297 #
AD-A156137 ..... N85-35575 #
AD-A156139 ..... N85-35217 #
AD-A156140 ..... N85-35192 #
AD-A156145 ..... N85-35281 #
AD-A156151 ..... N85-35752 #
AD-A156153 ..... N85-35378 #
AD-A156154 ..... N85-35257 #
AD-A156156 ..... N85-35352 #
AD-A156165 ..... N85-35522 #
AD-A156167 ..... N85-35401 #
AD-A156168 ..... N85-35336 #
AD-A156187 ..... N85-35298 #
AD-A156188 ..... N85-35561 #
AD-A156190 ..... N85-35652 #
AD-A156193 ..... N85-35410 #
AD-A156196 ..... N85-35634 #
AD-A156197 ..... N85-35308 #
AD-A156200 ..... N85-35614 #
AD-A156201 ..... N85-35615 #
AD-A156215 ..... N85-35208 #
AD-A156218 ..... N85-35686 #
AD-A156219 ..... N85-35653 #
AD-A156229 ..... N85-35620 #
AD-A156230 ..... N85-35671 #
AD-A156243 ..... N85-35802 #
AD-A156248 ..... N85-35621 #
AD-A156256 ..... N85-35693 #
AD-A156271 ..... N85-35616 #
AD-A156272 ..... N85-35803 #
AD-A156298 ..... N85-35697 #
AD-A156300 ..... N85-35825 #
AD-A156301 ..... N85-35826 #
AD-A156303 ..... N85-35654 #
AD-A156304 ..... N85-35174 #
AD-A156305 ..... N85-35625 #
AD-A156314 ..... N85-35635 #
AD-A156316 ..... N85-35252 #
AD-A156322 ..... N85-35576 #
AD-A156324 ..... N85-35617 #
AD-A156325 ..... N85-35804 #
AD-A156326 ..... N85-35153 #
AD-A156327 ..... N85-35498 #
AD-A156328 ..... N85-35176 #
AD-A156330 ..... N85-35177 #
AD-A156331 ..... N85-35523 #
AD-A156332 ..... N85-35577 #
AD-A156334 ..... N85-35212 #
AD-A156336 ..... N85-35622 #
AD-A156337 ..... N85-35337 #
AD-A156349 ..... N85-35524 #
AD-A156361 ..... N85-35193 #
AD-A156362 ..... N85-35411 #
AD-A156370 ..... N85-35427 #
AD-A156381 ..... N85-35258 #
AD-A156392 ..... N85-35428 #
AD-A156393 ..... N85-35429 #
AD-A156394 ..... N85-35698 #
AD-A156408 ..... N85-35626 #
AD-A156425 ..... N85-35430 #
AD-A156447 ..... N85-35655 #

AD-E301677 ..... N85-35823 #
AD-E301698 ..... N85-35610 #
AD-E440284 ..... N85-35336 #
AD-E440284 ..... N85-35401 #
AD-E900451 ..... N85-35189 #
AD-E900451 ..... N85-35330 #
AD-E900451 ..... N85-35696 #
AD-E900451 ..... N85-35798 #
AD-E900463 ..... N85-35193 #
AD-E900463 ..... N85-35411 #
AD-E900463 ..... N85-35427 #
AD-E950713 ..... N85-35327 #

AD-F630668 ..... N85-35616 #
AD-F630668 ..... N85-35803 #

AEM-85-1-RP ..... N85-35378 #

AERE-R-11460 ..... N85-35275 #
AERE-R-11485 ..... N85-35274 #
AERE-R-11490 ..... N85-35273 #
AERE-R-11579 ..... N85-35276 #

AFAMRL-TR-85-030 ..... N85-35610 #
AFAMRL-TR-85-038 ..... N85-35606 #

AFGL-ERP-889 ..... N85-35401 #
AFGL-ERP-893 ..... N85-35336 #
AFGL-ERP-901 ..... N85-35521 #

AFGL-IP-328 ..... N85-35333 #

AFGL-TR-84-0198 ..... N85-35522 #
AFGL-TR-84-0239 ..... N85-35334 #
AFGL-TR-84-0260 ..... N85-35684 #
AFGL-TR-84-0263 ..... N85-35519 #
AFGL-TR-84-0265 ..... N85-35401 #
AFGL-TR-84-0275 ..... N85-35523 #
AFGL-TR-84-0290 ..... N85-35648 #
AFGL-TR-84-0293 ..... N85-35336 #
AFGL-TR-84-0316 ..... N85-35521 #

AFGL-TR-85-0006 ..... N85-35333 #
AFGL-TR-85-0006 ..... N85-35524 #

AFHRL-TP-84-51 ..... N85-35620 #

AFHRL-TR-84-55 ..... N85-35632 #
AFHRL-TR-85-12 ..... N85-35671 #

AFIT/OS/GST/85M-16 ..... N85-35729 #

AFWAL-TR-84-2082 ..... N85-35175 #
AFWAL-TR-84-2089 ..... N85-35306 #
AFWAL-TR-84-2096-VOL-1 ..... N85-35257 #
AFWAL-TR-84-3116 ..... N85-35425 #
AFWAL-TR-85-3014 ..... N85-35377 #

AFWL-TR-84-130 ..... N85-35520 #

AI-TR-834 ..... N85-35626 #

AMMRC-TR-84-43 ..... N85-35278 #

AMSMI/RT-85-7-TR ..... N85-35327 #

APR-5 ..... N85-35617 #

AR-003-998 ..... N85-35187 #

ARI-RR-441 ..... N85-35524 #
ARI-RR-447 ..... N85-35392 #

ARL-STRUC-R-415 ..... N85-35187 #

ARO-16415.735-MA ..... N85-35376 #
ARO-16964.8-MS ..... N85-35280 #
ARO-17826.19-PH ..... N85-35797 #
ARO-17870.6-MS ..... N85-35277 #
ARO-18054.14-EL ..... N85-35328 #
ARO-18612.1-MA-H ..... N85-35678 #
ARO-19065.14-MA ..... N85-35679 #
ARO-19748.2-CH ..... N85-35256 #
ARO-19862.2-GS ..... N85-35559 #
ARO-20628.5-EL ..... N85-35652 #
ARO-21677.1-GS ..... N85-35331 #
ARO-22674.1-MS-CF ..... N85-35409 #

ATR-85(7083)-8 ..... N85-35517* #

AT85T004 ..... N85-35185* #

BBC-RD-1985/7 ..... N85-35694

BBN-5977 ..... N85-35216 #

BDX-613-3260 ..... N85-35288 #

BLL-CE-TRANS-8082-(9022.09) N85-35269
BLL-CE-TRANS-8110-(9022.09) N85-35254

BLL-DOUNREAY-TR-952(9091.9F) N85-35727

BLL-M-35787-(5828.4) N85-35270
BLL-M-35305 ..... N85-35268

BLL-RISLEY-TR-5040-(9091.9F) N85-35293
BLL-RISLEY-TR-5041-(9091.9F) N85-35292

BM-RI-8931 ..... N85-35291 #
BM-RI-8932 ..... N85-35290 #

BMFT-FB-T-85-021 ..... N85-35361 #
BMFT-FB-T-85-023 ..... N85-35496 #
BMFT-FB-T-85-024 ..... N85-35399 #
BMFT-FB-T-85-029 ..... N85-35668 #
BMFT-FB-T-85-031 ..... N85-35400 #

BMR-258 ..... N85-35530 #

BNI-36479 ..... N85-35358 #

BNL-36391 ..... N85-35781 #
BNL-36393 ..... N85-35669 #
BNL-36417 ..... N85-35767 #
BNL-36454 ..... N85-35759 #
BNL-36462 ..... N85-35737 #
BNL-36483 ..... N85-35718 #
BNL-36570 ..... N85-35286 #
BNL-36632 ..... N85-35788 #

BRL-MR-3448 ..... N85-35653 #

BRMC-83-5080-3 ..... N85-35410 #

BR94271 ..... N85-35421
BR94501 ..... N85-35422
BR98067 ..... N85-35572 #

BU-REC-C-80292-S(1) ..... N85-35266 #

BU-109 ..... N85-35674 #
BU-115 ..... N85-35689 #
BU-117 ..... N85-35688 #

B8464633 ..... N85-35339 #
B8562444 ..... N85-35687 #

CAR-TR-100 ..... N85-35181 #
CAR-TR-112 ..... N85-35751 #

CIDC-949 ..... N85-35435 #

CMU-RI-TR-85-6 ..... N85-35647 #

COE-277 ..... N85-35388 #

CONF-050560-4 ..... N85-35726 #
CONF-841121-22 ..... N85-35261 #
CONF-850165-3 ..... N85-35379 #
CONF-850211-9 ..... N85-35286 #
CONF-850310-101 ..... N85-35776 #
CONF-850311-1 ..... N85-35283 #
CONF-850311-14-DRAFT ..... N85-35282 #
CONF-850357-7 ..... N85-35357 #
CONF-850375-2 ..... N85-35724 #
CONF-850375-6 ..... N85-35740 #
CONF-850375-8 ..... N85-35741 #
CONF-850405-9 ..... N85-35618 #
CONF-850410-46 ..... N85-35657 #
CONF-850410-50 ..... N85-35739 #
CONF-850421-5 ..... N85-35302 #
CONF-850504-31 ..... N85-35781 #
CONF-850504-35 ..... N85-35759 #
CONF-850504-40 ..... N85-35783 #
CONF-850504-43 ..... N85-35773 #
CONF-850504-49 ..... N85-35405 #
CONF-850504-50 ..... N85-35661 #
CONF-850504-51 ..... N85-35779 #
CONF-850504-55 ..... N85-35663 #
CONF-850504-58 ..... N85-35784 #
CONF-850504-65 ..... N85-35762 #
CONF-850504-66 ..... N85-35774 #
CONF-850504-73 ..... N85-35772 #
CONF-850504-78 ..... N85-35763 #
CONF-850504-81 ..... N85-35358 #
CONF-850504-84 ..... N85-35664 #
CONF-850504-85 ..... N85-35211 #
CONF-850504-90 ..... N85-35757 #
CONF-850504-95 ..... N85-35721 #
CONF-850504-97 ..... N85-35719 #
CONF-850504-107 ..... N85-35775 #
CONF-850504-112 ..... N85-35765 #
CONF-850504-115 ..... N85-35764 #
CONF-850504-122 ..... N85-35718 #
CONF-850504-127 ..... N85-35356 #
CONF-850504-137 ..... N85-35722 #
CONF-850504-141 ..... N85-35669 #
CONF-850504-149 ..... N85-35737 #
CONF-850504-151 ..... N85-35785 #
CONF-850504-152 ..... N85-35766 #
CONF-850504-188 ..... N85-35793 #
CONF-850504-197 ..... N85-35788 #
CONF-850504-199 ..... N85-35790 #
CONF-850504-200 ..... N85-35789 #
CONF-850504-202 ..... N85-35792 #
CONF-850504-208 ..... N85-35746 #
CONF-850507-14 ..... N85-35734 #
CONF-850507-15 ..... N85-35731 #
CONF-850507-16 ..... N85-35732 #
CONF-850507-20 ..... N85-35842 #
CONF-850556-5 ..... N85-35733 #
CONF-850558-2 ..... N85-35304 #
CONF-850616-2 ..... N85-35768 #
CONF-850616-3 ..... N85-35720 #
CONF-850616-4 ..... N85-35355 #
CONF-850616-6 ..... N85-35354 #
CONF-850616-7 ..... N85-35780 #
CONF-850616-13 ..... N85-35564 #
CONF-850616-22 ..... N85-35759 #
CONF-850616-26 ..... N85-35782 #
CONF-850616-27 ..... N85-35756 #
CONF-850616-55 ..... N85-35359 #
CONF-850616-56 ..... N85-35786 #
CONF-850616-57 ..... N85-35787 #
CONF-850616-65 ..... N85-35360 #
CONF-850635-1 ..... N85-35748 #
CONF-850648-1 ..... N85-35699 #
CONF-850670-1 ..... N85-35431 #
CONF-850727-1 ..... N85-35396 #
CONF-850736-1 ..... N85-35808 #
CONF-850736-17 ..... N85-35386 #
CONF-850736-22 ..... N85-35289 #
CONF-850736-26 ..... N85-35743 #
CONF-850745-1 ..... N85-35361 #

CONF-850763-1 ..... N85-35525 #
CONF-850801-39 ..... N85-35494 #
CONF-850809-55 ..... N85-35432 #
CONF-850867-2 ..... N85-35398 #
CONF-8403137 ..... N85-35700 #
CONF-8407112-9 ..... N85-35723 #
CONF-8408110-3 ..... N85-35805 #
CONF-8409243-1 ..... N85-35260 #
CONF-8410172-10 ..... N85-35767 #
CONF-8503145-2 ..... N85-35843 #
CONF-8504137-1 ..... N85-35492 #
CONF-8504139-1 ..... N85-35305 #
CONF-8505100-8 ..... N85-35778 #
CONF-8505103-2 ..... N85-35738 #
CONF-8505113-1 ..... N85-35725 #
CONF-8505122-1 ..... N85-35412 #
CONF-8505130-7 ..... N85-35791 #
CONF-8505131-4 ..... N85-35656 #
CONF-8505179-1 ..... N85-35747 #
CONF-8506121-1 ..... N85-35563 #

CP-143 ..... N85-35161* #

CRC-APRAC-CAPA-83-01 ..... N85-35502 #

CRDC-CR-84132 ..... N85-35592 #

CS-TR-1479 ..... N85-35751 #

CSC-TR-1458 ..... N85-35181 #

CSG-30 ..... N85-35655 #
CSG-37 ..... N85-35635 #

CSIRO-DAR-TP-8 ..... N85-35587 #
CSIRO-DAR-TP-9 ..... N85-35518 #

CWP-029 ..... N85-35698 #

DC-TN-2030.308-2 ..... N85-35520 #

DE85-004046 ..... N85-35284 #
DE85-004066 ..... N85-35699 #
DE85-004428 ..... N85-35805 #
DE85-005558 ..... N85-35431 #
DE85-006399 ..... N85-35300 #
DE85-006500 ..... N85-35301 #
DE85-006734 ..... N85-35396 #
DE85-008468 ..... N85-35808 #
DE85-008117 ..... N85-35432 #
DE85-009104 ..... N85-35357 #
DE85-009482 ..... N85-35809 #
DE85-009541 ..... N85-35490 #
DE85-009626 ..... N85-35379 #
DE85-010108 ..... N85-35381 #
DE85-010524 ..... N85-35432 #
DE85-010558 ..... N85-35229 #
DE85-010586 ..... N85-35228 #
DE85-011301 ..... N85-35771 #
DE85-011347 ..... N85-35402 #
DE85-011407 ..... N85-35282 #
DE85-011459 ..... N85-35761 #
DE85-011471 ..... N85-35731 #
DE85-011551 ..... N85-35734 #
DE85-011620 ..... N85-35736 #
DE85-011749 ..... N85-35285 #
DE85-011752 ..... N85-35302 #
DE85-011761 ..... N85-35563 #
DE85-011829 ..... N85-35781 #
DE85-011832 ..... N85-35767 #
DE85-011840 ..... N85-35759 #
DE85-011874 ..... N85-35783 #
DE85-011897 ..... N85-35383 #
DE85-012026 ..... N85-35768 #
DE85-012057 ..... N85-35287 #
DE85-012080 ..... N85-35353 #
DE85-012097 ..... N85-35739 #
DE85-012101 ..... N85-35725 #
DE85-012119 ..... N85-35657 #
DE85-012254 ..... N85-35394 #
DE85-012286 ..... N85-35773 #
DE85-012299 ..... N85-35726 #
DE85-012355 ..... N85-35412 #
DE85-012356 ..... N85-35355 #
DE85-012357 ..... N85-35720 #
DE85-012377 ..... N85-35764 #
DE85-012389 ..... N85-35758 #
DE85-012412 ..... N85-35467 #
DE85-012430 ..... N85-35230 #
DE85-012465 ..... N85-35403 #
DE85-012515 ..... N85-35718 #
DE85-012516 ..... N85-35358 #
DE85-012520 ..... N85-35669 #
DE85-012534 ..... N85-35658 #
DE85-012538 ..... N85-35380 #
DE85-012554 ..... N85-35494 #

DE85-012593 ..... N85-35782 #
DE85-012603 ..... N85-35732 #
DE85-012607 ..... N85-35260 #
DE85-012613 ..... N85-35666 #
DE85-012653 ..... N85-35663 #
DE85-012655 ..... N85-35784 #
DE85-012664 ..... N85-35779 #
DE85-012665 ..... N85-35661 #
DE85-012666 ..... N85-35405 #
DE85-012670 ..... N85-35721 #
DE85-012671 ..... N85-35762 #
DE85-012682 ..... N85-35766 #
DE85-012697 ..... N85-35733 #
DE85-012706 ..... N85-35757 #
DE85-012724 ..... N85-35765 #
DE85-012725 ..... N85-35775 #
DE85-012736 ..... N85-35656 #
DE85-012766 ..... N85-35778 #
DE85-012778 ..... N85-35735 #
DE85-012780 ..... N85-35776 #
DE85-012793 ..... N85-35395* #
DE85-012813 ..... N85-35354 #
DE85-012826 ..... N85-35780 #
DE85-012840 ..... N85-35756 #
DE85-012858 ..... N85-35499 #
DE85-012866 ..... N85-35564 #
DE85-012883 ..... N85-35304 #
DE85-012897 ..... N85-35618 #
DE85-012916 ..... N85-35842 #
DE85-012918 ..... N85-35305 #
DE85-012927 ..... N85-35740 #
DE85-012951 ..... N85-35660 #
DE85-012985 ..... N85-35469 #
DE85-013004 ..... N85-35491 #
DE85-013026 ..... N85-35719 #
DE85-013027 ..... N85-35807 #
DE85-013035 ..... N85-35662 #
DE85-013044 ..... N85-35738 #
DE85-013052 ..... N85-35723 #
DE85-013055 ..... N85-35763 #
DE85-013057 ..... N85-35664 #
DE85-013063 ..... N85-35356 #
DE85-013070 ..... N85-35724 #
DE85-013073 ..... N85-35211 #
DE85-013076 ..... N85-35722 #
DE85-013096 ..... N85-35493 #
DE85-013103 ..... N85-35659 #
DE85-013116 ..... N85-35769 #
DE85-013120 ..... N85-35846 #
DE85-013121 ..... N85-35760 #
DE85-013123 ..... N85-35777 #
DE85-013124 ..... N85-35385 #
DE85-013135 ..... N85-35665 #
DE85-013152 ..... N85-35489 #
DE85-013174 ..... N85-35404 #
DE85-013189 ..... N85-35717 #
DE85-013252 ..... N85-35382 #
DE85-013254 ..... N85-35288 #
DE85-013257 ..... N85-35393 #
DE85-013264 ..... N85-35338 #
DE85-013267 ..... N85-35384 #
DE85-013283 ..... N85-35286 #
DE85-013301 ..... N85-35737 #
DE85-013321 ..... N85-35309 #
DE85-013360 ..... N85-35716 #
DE85-013362 ..... N85-35818 #
DE85-013365 ..... N85-35299 #
DE85-013373 ..... N85-35785 #
DE85-013375 ..... N85-35774 #
DE85-013377 ..... N85-35772 #
DE85-013394 ..... N85-35397 #
DE85-013427 ..... N85-35770 #
DE85-013481 ..... N85-35303 #
DE85-013527 ..... N85-35232 #
DE85-013535 ..... N85-35562 #
DE85-013594 ..... N85-35741 #
DE85-013790 ..... N85-35398 #
DE85-013791 ..... N85-35231 #
DE85-013840 ..... N85-35261 #
DE85-013940 ..... N85-35495 #
DE85-013992 ..... N85-35748 #
DE85-014097 ..... N85-35525 #
DE85-014120 ..... N85-35787 #
DE85-014125 ..... N85-35360 #
DE85-014128 ..... N85-35786 #
DE85-014129 ..... N85-35359 #
DE85-014199 ..... N85-35667 #
DE85-014222 ..... N85-35792 #
DE85-014226 ..... N85-35788 #
DE85-014268 ..... N85-35742 #
DE85-014289 ..... N85-35789 #
DE85-014290 ..... N85-35790 #
DE85-014332 ..... N85-35386 #
DE85-014353 ..... N85-35843 #
DE85-014366 ..... N85-35793 #
DE85-014526 ..... N85-35746 #

DE85-014559 ..... N85-35791 #
DE85-014569 ..... N85-35747 #
DE85-014686 ..... N85-35745 #
DE85-014806 ..... N85-35743 #
DE85-014808 ..... N85-35289 #
DE85-015036 ..... N85-35593 #
DE85-901363 ..... N85-35468 #

DFVLR-MITT-83-05 ..... N85-35165 #
DFVLR-MITT-83-16 ..... N85-35246 #
DFVLR-MITT-83-19 ..... N85-35595 #
DFVLR-MITT-85-04 ..... N85-35542 #

DOE/AL-18071/T5 ..... N85-35716 #

DOE/CE-0106 ..... N85-35493 #

DOE/ER-02383/0108 ..... N85-35658 #
DOE/ER-03077/245 ..... N85-35770 #
DOE/ER-03275/6 ..... N85-35745 #
DOE/ER-10841/T1 ..... N85-35229 #
DOE/ER-10718/5 ..... N85-35665 #
DOE/ER-13065/415 ..... N85-35741 #
DOE/ER-13137/T1 ..... N85-35403 #
DOE/ER-13276/1 ..... N85-35394 #
DOE/ER-40085/7 ..... N85-35744 #
DOE/ER-45035/1 ..... N85-35285 #
DOE/ER-45117/1 ..... N85-35303 #
DOE/ER-60182/1 ..... N85-35467 #

DOE/ET-28393/T8 ..... N85-35490 #
DOE/ET-53047/21 ..... N85-35761 #
DOE/ET-53088/171 ..... N85-35777 #
DOE/ET-53088/179 ..... N85-35385 #
DOE/ET-53088/187 ..... N85-35846 #
DOE/ET-53088/190 ..... N85-35760 #

DOE/EV-10328/4 ..... N85-35593 #

DOE/ID-12026/T11 ..... N85-35491 #

DOE/JPL-956613-85/1 ..... N85-35395* #

DOE/NASA/0262-1 ..... N85-35471* #

DOE/OR-21400/T124 ..... N85-35735 #
DOE/OR-21400/T147 ..... N85-35809 #

DOE/PC-50804/9 ..... N85-35231 #
DOE/PC-70788/T1 ..... N85-35230 #
DOE/PC-71253/2 ..... N85-35499 #

DP-TR-80 ..... N85-35742 #

DREO-TN-84-30 ..... N85-35822 #

DRES-412 ..... N85-35258 #

DRIC-T-7407 ..... N85-35421
DRIC-T-7469 ..... N85-35422
DRIC-T-7545 ..... N85-35572 #

DTIC/TR-85/5 ..... N85-35824 #
DTIC/TR-85/7-VOL-1 ..... N85-35825 #
DTIC/TR-85/7-VOL-2 ..... N85-35826 #

D180-28461-1 ..... N85-35728* #

E-2129 ..... N85-35158* #
E-2388 ..... N85-35159* #
E-2638 ..... N85-35225* #

EC-85-3 ..... N85-35328 #

EERC-84/16 ..... N85-35527 #

EGG-M-12085 ..... N85-35747 #

EGG-TMI-6859 ..... N85-35666 #

EI85-0923 ..... N85-35794* #

EPA-600/D-85-061 ..... N85-35503 #
EPA-600/D-85-084 ..... N85-35311 #
EPA-600/D-85-085 ..... N85-35828 #
EPA-600/D-85-105 ..... N85-35501 #
EPA-600/9-85-013 ..... N85-35500 #

ER-83/05 ..... N85-35362 #

ERIM-151200-17-F ..... N85-35752 #
ERIM-164000-18-P ..... N85-35464* #

ESA-TT-831 ..... N85-35165 #
ESA-TT-849 ..... N85-35246 #
ESA-TT-857 ..... N85-35595 #

ESD-TR-84-202 ..... N85-35633 #
ESD-TR-85-180 ..... N85-35634 #

ETL-R-070 ..... N85-35180 #

E85-10105 ..... N85-35483* #
E85-10106 ..... N85-35484* #

FAA-AM-85-2 ..... N85-35619 #

FAA-DL5-85-1 ..... N85-35179 #

FHWA/PA-84-012 ..... N85-35470 #

FNAL-TM-1307 ..... N85-35807 #
FNAL-TM-1311 ..... N85-35719 #

GPO-47-635 ..... N85-35829 #

GRI-85/0002 ..... N85-35262 #
GRI-85/0004 ..... N85-35310 #
GRI-85/0014 ..... N85-35316 #
GRI-85/0019 ..... N85-35314 #
GRI-85/0022 ..... N85-35315 #
GRI-85/0025 ..... N85-35264 #
GRI-85/0029 ..... N85-35265 #
GRI-85/0053 ..... N85-35263 #
GRI-85/0062 ..... N85-35318 #

HE-1.1-1 ..... N85-35849* #
HE-1.1-2 ..... N85-35850* #
HE-1.1-3 ..... N85-35851* #
HE-1.1-4 ..... N85-35852* #
HE-1.1-5 ..... N85-35853* #
HE-1.1-6 ..... N85-35854* #
HE-1.1-7 ..... N85-35855* #
HE-1.1-8 ..... N85-35856* #
HE-1.1-9 ..... N85-35857* #
HE-1.1-11 ..... N85-35858* #
HE-1.1-12 ..... N85-35859* #
HE-1.2-1 ..... N85-35860* #
HE-1.2-2 ..... N85-35861* #
HE-1.2-4 ..... N85-35862* #
HE-1.2-5 ..... N85-35863* #
HE-1.2-6 ..... N85-35864* #
HE-1.2-7 ..... N85-35865* #
HE-1.2-8 ..... N85-35866* #
HE-1.2-9 ..... N85-35867* #
HE-1.4-2 ..... N85-35890* #
HE-1.4-3 ..... N85-35891* #
HE-1.4-4 ..... N85-35892* #
HE-1.4-5 ..... N85-35893* #
HE-1.4-6 ..... N85-35894* #
HE-1.4-7 ..... N85-35895* #
HE-1.4-8 ..... N85-35896* #
HE-1.4-10 ..... N85-35897* #
HE-1.4-11 ..... N85-35898* #
HE-1.4-12 ..... N85-35899* #
HE-1.4-13 ..... N85-35900* #
HE-3.1-1 ..... N85-35901* #
HE-3.1-2 ..... N85-35902* #
HE-3.1-3 ..... N85-35903* #
HE-3.1-6 ..... N85-35904* #
HE-3.1-7 ..... N85-35905* #
HE-3.1-8 ..... N85-35906* #
HE-3.1-9 ..... N85-35907* #
HE-3.1-10 ..... N85-35908* #
HE-3.1-11 ..... N85-35909* #
HE-3.1-12 ..... N85-35910* #
HE-3.1-13 ..... N85-35911* #
HE-3.2-1 ..... N85-35912* #
HE-3.2-5 ..... N85-35913* #
HE-3.2-6 ..... N85-35914* #
HE-3.2-8 ..... N85-35916* #
HE-3.2-9 ..... N85-35917* #
HE-3.2-10 ..... N85-35918* #
HE-3.2-11 ..... N85-35919* #
HE-3.3-1 ..... N85-35920* #
HE-3.3-4 ..... N85-35922* #
HE-3.3-5 ..... N85-35923* #
HE-3.3-6 ..... N85-35924* #
HE-3.3-7 ..... N85-35925* #
HE-3.3-8 ..... N85-35926* #
HE-3.3-9 ..... N85-35927* #
HE-3.3-10 ..... N85-35928* #
HE-3.3-11 ..... N85-35929* #
HE-3.4-1 ..... N85-35930* #
HE-3.4-2 ..... N85-35931* #
HE-3.4-3 ..... N85-35932* #
HE-3.4-5 ..... N85-35933* #
HE-3.4-6 ..... N85-35934* #
HE-3.4-7 ..... N85-35935* #
HE-3.4-8 ..... N85-35936* #
HE-3.4-9 ..... N85-35937* #
HE-3.4-10 ..... N85-35938* #
HE-3.4-11 ..... N85-35939* #

HE-3.5-1 ..... N85-35940* #
HE-3.5-2 ..... N85-35941* #
HE-3.5-3 ..... N85-35942* #
HE-3.5-4 ..... N85-35943* #
HE-3.5-7 ..... N85-35944* #
HE-3.5-8 ..... N85-35945* #
HE-3.5-9 ..... N85-35946* #
HE-3.5-10 ..... N85-35947* #
HE-3.5-11 ..... N85-35948* #
HE-3.5-12 ..... N85-35949* #
HE-3.5-13 ..... N85-35950* #
HE-3.6-2 ..... N85-35951* #
HE-3.6-3 ..... N85-35952* #
HE-3.6-4 ..... N85-35953* #
HE-3.6-6 ..... N85-35954* #
HE-3.6-7 ..... N85-35955* #
HE-3.6-8 ..... N85-35956* #
HE-3.6-10 ..... N85-35957* #
HE-3.6-11 ..... N85-35958* #
HE-3.6-12 ..... N85-35959* #
HE-3.7-1 ..... N85-35960* #
HE-3.7-2 ..... N85-35961* #
HE-3.7-3 ..... N85-35962* #
HE-3.7-4 ..... N85-35963* #
HE-3.7-5 ..... N85-35964* #
HE-3.7-7 ..... N85-35965* #
HE-3.7-9 ..... N85-35966* #
HE-3.7-10 ..... N85-35967* #
HE-4.1-9 ..... N85-35975* #
HE-4.2-18 ..... N85-35994* #
HE-4.3-7 ..... N85-36001* #
HE-4.3-8 ..... N85-36002* #
HE-4.3-9 ..... N85-36003* #
HE-4.3-10 ..... N85-36004* #
HE-4.3-11 ..... N85-36005* #
HE-4.3-12 ..... N85-36006* #
HE-4.3-13 ..... N85-36007* #
HE-4.3-14 ..... N85-36008* #
HE-4.3-15 ..... N85-36009* #
HE-4.3-16 ..... N85-36010* #
HE-4.4-1 ..... N85-36011* #
HE-4.4-2 ..... N85-36012* #
HE-4.4-4 ..... N85-36013* #
HE-4.4-7 ..... N85-36015* #
HE-4.4-8 ..... N85-36016* #
HE-4.4-9 ..... N85-36017* #
HE-4.4-10 ..... N85-36018* #
HE-4.4-13 ..... N85-36019* #
HE-4.4-14 ..... N85-36020* #
HE-4.4-15 ..... N85-36021* #
HE-4.4-16 ..... N85-36022* #
HE 4.4-17 ..... N85-36023* #
HE-4.4-18 ..... N85-36024* #
HE-4.4-19 ..... N85-36025* #
HE-4.5-1 ..... N85-36026* #
HE-4.5-3 ..... N85-36027* #
HE-4.5-4 ..... N85-36028* #
HE-4.5-5 ..... N85-36029* #
HE-4.5-6 ..... N85-36030* #
HE-4.5-7 ..... N85-36031* #
HE-4.5-9 ..... N85-36032* #
HE-4.5-10 ..... N85-36033* #
HE-4.5-11 ..... N85-36034* #
HE-4.5-13 ..... N85-36035* #
HE-4.5-14 ..... N85-36036* #
HE-4.5-16 ..... N85-36038* #
HE-4.6-2 ..... N85-36039* #
HE-4.6-3 ..... N85-36040* #
HE-4.6-4 ..... N85-36041* #
HE-4.6-5 ..... N85-36042* #
HE-4.6-6 ..... N85-36043* #
HE-4.6-7 ..... N85-36044* #
HE-4.6-8 ..... N85-36045* #
HE-4.6-9 ..... N85-36046* #
HE-4.6-10 ..... N85-36047* #
HE-4.6-11 ..... N85-36048* #
HE-4.6-13 ..... N85-36049* #
HE-4.6-14 ..... N85-36050* #
HE-4.6-15 ..... N85-36051* #
HE-4.7-1 ..... N85-36052* #
HE-4.7-2 ..... N85-36053* #
HE-4.7-3 ..... N85-36054* #
HE-4.7-4 ..... N85-36055* #
HE-4.7-5 ..... N85-36056* #
HE-4.7-6 ..... N85-36057* #
HE-4.7-7 ..... N85-36058* #
HE-4.7-8 ..... N85-36059* #
HE-4.7-9 ..... N85-36060* #
HE-4.7-10 ..... N85-36061* #
HE-4.7-12 ..... N85-36062* #
HE-4.7-13 ..... N85-36063* #
HE-4.7-14 ..... N85-36064* #
HE-4.7-15 ..... N85-36065* #
HE-5.1-1 ..... N85-36067* #
HE-5.1-2 ..... N85-36068* #
HE-5.1-4 ..... N85-36069* #
HE-5.1-5 ..... N85-36070* #
HE-5.1-6 ..... N85-36071* #
HE-5.1-7 ..... N85-36072* #
HE-5.1-10 ..... N85-36073* #
HE-5.1-12 ..... N85-36074* #
HE-5.1-13 ..... N85-36075* #
HE-5.1-14 ..... N85-36076* #
HE-5.1-15 ..... N85-36077* #
HE-5.1-16 ..... N85-36078* #
HE-5.2-1 ..... N85-36079* #
HE-5.2-2 ..... N85-36080* #
HE-5.2-3 ..... N85-36081* #
HE-5.2-4 ..... N85-36082* #
HE-5.2-5 ..... N85-36083* #
HE-5.2-7 ..... N85-36084* #
HE-5.2-8 ..... N85-36085* #
HE-5.2-10 ..... N85-36086* #
HE-5.2-11 ..... N85-36087* #
HE-5.2-12 ..... N85-36088* #
HE-5.2-13 ..... N85-36089* #
HE-5.2-14 ..... N85-36090* #
HE-5.2-15 ..... N85-36091* #
HE-5.2-16 ..... N85-36092* #
HE-5.2-17 ..... N85-36093* #
HE-5.2-18 ..... N85-36094* #
HE-5.2-19 ..... N85-36095* #
HE-5.2-20 ..... N85-36096* #
HE-5.2-21 ..... N85-36097* #
HE-5.3-1 ..... N85-36098* #
HE-5.3-5 ..... N85-36099* #
HE-5.3-6 ..... N85-36100* #
HE-5.3-7 ..... N85-36101* #
HE-5.3-8 ..... N85-36102* #
HE-5.3-9 ..... N85-36103* #
HE-5.3-10 ..... N85-36104* #
HE-5.3-11 ..... N85-36105* #
HE-5.3-12 ..... N85-36106* #
HE-5.3-13 ..... N85-36107* #
HE-5.3-14 ..... N85-36108* #
HE-5.3-15 ..... N85-36109* #
HE-5.3-16 ..... N85-36110* #
HE-5.3-17 ..... N85-36111* #
HE-5.3-21 ..... N85-36112* #
HE-5.3-22 ..... N85-36113* #
HE-5.3-23 ..... N85-36114* #
HE-5.3-24 ..... N85-36115* #
HE-5.4-1 ..... N85-36116* #
HE-5.4-4 ..... N85-36117* #
HE-5.4-7 ..... N85-36118* #
HE-5.4-8 ..... N85-36119* #
HE-5.4-9 ..... N85-36120* #
HE-5.4-10 ..... N85-36121* #
HE-5.4-10 ..... N85-36122* #
HE-5.4-13 ..... N85-36123* #
HE-5.4-14 ..... N85-36124* #
HE-5.4-15 ..... N85-36125* #
HE-5.4-16 ..... N85-36126* #
HE-6.1-1 ..... N85-36127* #
HE-6.1-2 ..... N85-36128* #
HE-6.1-3 ..... N85-36129* #
HE-6.1-4 ..... N85-36130* #
HE-6.1-5 ..... N85-36131* #
HE-6.1-6 ..... N85-36132* #
HE-6.1-7 ..... N85-36133* #
HE-6.1-8 ..... N85-36134* #
HE-6.1-9 ..... N85-36135* #
HE-6.1-11 ..... N85-36136* #
HE-6.1-12 ..... N85-36137* #
HE-6.2-2 ..... N85-36138* #
HE-6.2-3 ..... N85-36139* #
HE-6.2-4 ..... N85-36140* #
HE-6.2-5 ..... N85-36141* #
HE-6.2-6 ..... N85-36142* #
HE-6.2-7 ..... N85-36143* #
HE-6.2-8 ..... N85-36144* #
HE-6.2-9 ..... N85-36145* #
HE-6.2-10 ..... N85-36146* #
HE-6.2-11 ..... N85-36147* #
HE-6.2-12 ..... N85-36148* #
HE-6.2-13 ..... N85-36149* #
HE-6.2-14 ..... N85-36150* #
HE-6.2-15 ..... N85-36151* #
HE-6.2-16 ..... N85-36152* #
HE-6.2-17 ..... N85-36153* #
HE-6.2-18 ..... N85-36154* #
HE-7.1-1 ..... N85-36155* #
HE-7.1-2 ..... N85-36156* #
HE-7.1-3 ..... N85-36157* #
HE-7.1-4 ..... N85-36158* #
HE-7.1-5 ..... N85-36159* #
HE-7.1-6 ..... N85-36160* #
HE-7.1-7 ..... N85-36161* #
HE-7.1-12 ..... N85-36162* #

HEDL-TME-84-29 ..... N85-35382 #

HEL-TM-6-85 ..... N85-35613 #

IA-TR-85-27 ..... N85-35717 #

IAF-85-164 ..... N85-35225* #

ICASE-85-31 ..... N85-35675* #
ICASE-85-33 ..... N85-35676* #
ICASE-85-34 ..... N85-35375* #

IFSR-171 ..... N85-35777 #
IFSR-187 ..... N85-35846 #

IS-4876 ..... N85-35867 #

ISBN-0-643-03866-3 ..... N85-35518 #
ISBN-0-643-03867-1 ..... N85-35587 #
ISBN-0-644-03541-2 ..... N85-35530 #
ISBN-87-7478-247-9 ..... N85-35541 #
ISBN-90-6144-999-5 ..... N85-35339 #

ISFR-190 ..... N85-35760 #

ISL-CO-211/84 ..... N85-35344 #

ISSN-0067-5882 ..... N85-35387 #
ISSN-0081-3397 ..... N85-35717 #
ISSN-0084-7100 ..... N85-35530 #
ISSN-0176-7739 ..... N85-35542 #
ISSN-0340-7608 ..... N85-35361 #
ISSN-0340-7608 ..... N85-35399 #
ISSN-0340-7608 ..... N85-35400 #
ISSN-0340-7608 ..... N85-35496 #
ISSN-0340-7608 ..... N85-35668 #
ISSN-0343-7639 ..... N85-35473 #

ITOP-1-2-601 ..... N85-35188 #

ITR-3 ..... N85-35799 #

JHU/APL/CP-086/TPR/047 ..... N85-35830 #

JPL-PUB-85-25 ..... N85-35750* #
JPL-PUB-85-33 ..... N85-35322* #
JPL-PUB-85-45 ..... N85-35323* #
JPL-PUB-85-47 ..... N85-35795* #
JPL-PUB-85-51 ..... N85-35324* #
JPL-PUB-85-53 ..... N85-35219* #

JUEL-SPEZ-278 ..... N85-35473 #

KFK-1638 ..... N85-35742 #
KFK-3910 ..... N85-35384 #

KU-FRL-417-24 ..... N85-35695* #

L-15965 ..... N85-35307* #

LA-TR-85-26 ..... N85-35384 #

LA-UR-84-4017 ..... N85-35431 #
LA-UR-85-942 ..... N85-35381 #
LA-UR-85-1055 ..... N85-35379 #
LA-UR-85-1436 ..... N85-35733 #
LA-UR-85-1584 ..... N85-35766 #
LA-UR-85-1606 ..... N85-35762 #
LA-UR-85-1607 ..... N85-35721 #
LA-UR-85-1611 ..... N85-35405 #
LA-UR-85-1612 ..... N85-35661 #
LA-UR-85-1613 ..... N85-35779 #
LA-UR-85-1622 ..... N85-35784 #
LA-UR-85-1624 ..... N85-35663 #
LA-UR-85-1654 ..... N85-35757 #
LA-UR-85-1735 ..... N85-35775 #
LA-UR-85-1736 ..... N85-35765 #
LA-UR-85-1817 ..... N85-35656 #
LA-UR-85-1831 ..... N85-35778 #
LA-UR-85-1994 ..... N85-35359 #
LA-UR-85-2001 ..... N85-35786 #
LA-UR-85-2014 ..... N85-35360 #
LA-UR-85-2042 ..... N85-35787 #
LA-UR-85-2171 ..... N85-35525 #

LA-10367-MS ..... N85-35383 #

LARS-CR-060185 ..... N85-35463* #

LBL-18225 ..... N85-35700 #
LBL-18944 ..... N85-35732 #
LBL-19150 ..... N85-35494 #
LBL-19538 ..... N85-35260 #
LBL-19619 ..... N85-35261 #
LBL-19648 ..... N85-35746 #

LC-84-600281 ..... N85-35291 #
LC-84-600301 ..... N85-35290 #

LIDS-P-1473 ..... N85-35332 #

LMSC-HREC-TM-D697786 ..... N85-35236* #
LMSC-HREC-TM-D697818 ..... N85-35220* #
LMSC-HREC-TM-D697896 ..... N85-35221* #
LMSC-HREC-TM-D784643 ..... N85-35223* #
LMSC-HREC-TM-D784644 ..... N85-35423* #
LMSC-HREC-TM-D784769 ..... N85-35407* #
LMSC-HREC-TM-D784773 ..... N85-35237* #

LMSC-HREC-TN-D697613 ..... N85-35294* #
LMSC-HREC-TN-D697757 ..... N85-35222* #
LMSC-HREC-TN-D867570 ..... N85-35238* #
LMSC-HREC-TN-D867571 ..... N85-35224* #
LMSC-HREC-TN-D867576 ..... N85-35239* #
LMSC-HREC-TN-D867581 ..... N85-35240* #
LMSC-HREC-TN-D867582 ..... N85-35295* #

LR-30380-PHASE-1 ..... N85-35241* #

M-499 ..... N85-35371* #

MA-RD-760-85009 ..... N85-35388 #

MANPA-506(85) ..... N85-35226 #

MDC-J3789 ..... N85-35162* #

MECH-68 ..... N85-35426 #

MIM-3252 ..... N85-35309 #

MITT-41 ..... N85-35387 #

MPAE-W-79-84-27 ..... N85-35847 #

MR-RX-5377 ..... N85-35315 #

MT-CWR-85-001 ..... N85-35409 #

MTR-WP-85W00174 ..... N85-35179 #

MTR-9067 ..... N85-35633 #

NADC-85040-60 ..... N85-35609 #

NAS 1.15:77673 ..... N85-35296* #
NAS 1.15:77869 ..... N85-35272* #
NAS 1.15:77883 ..... N85-35161* #
NAS 1.15:77896 ..... N85-35245* #
NAS 1.15:77906 ..... N85-35242* #
NAS 1.15:77912 ..... N85-35163* #
NAS 1.15:77920 ..... N85-35164* #
NAS 1.15:86671 ..... N85-35623* #
NAS 1.15:86681 ..... N85-35834* #
NAS 1.15:86712 ..... N85-35573* #
NAS 1.15:86721 ..... N85-35832* #
NAS 1.15:86722 ..... N85-35833* #
NAS 1.15:86756 ..... N85-35578* #
NAS 1.15:86780 ..... N85-35372* #
NAS 1.15:86820 ..... N85-35210* #
NAS 1.15:87069 ..... N85-35225* #
NAS 1.15:87503 ..... N85-35831* #
NAS 1.15:87505 ..... N85-35206*
NAS 1.15:87576 ..... N85-35204* #
NAS 1.15:87577 ..... N85-35637* #
NAS 1.15:87594 ..... N85-35424* #
NAS 1.15:87596 ..... N85-35374* #
NAS 1.19:197 ..... N85-35839* #
NAS 1.21:7037(190) N85-35152*
NAS 1.21:7039(27)-SECTION-2 ..... N85-35820*
NAS 1.21:7046(12) N85-35209*
NAS 1.26:3917 ..... N85-35184* #
NAS 1.26:3925 ..... N85-35158* #
NAS 1.26:3926 ..... N85-35159* #
NAS 1.26:3929 ..... N85-35371* #
NAS 1.26:3930 ..... N85-35160* #
NAS 1.26:166091 ..... N85-35241* #
NAS 1.26:167862 ..... N85-35534* #
NAS 1.26:167863 ..... N85-35535* #
NAS 1.26:167864 ..... N85-35536* #
NAS 1.26:167865 ..... N85-35537* #
NAS 1.26:167866 ..... N85-35538* #
NAS 1.26:167884 ..... N85-35539* #
NAS 1.26:168037 ..... N85-35199* #
NAS 1.26:170881 ..... N85-35236* #
NAS 1.26:170882 ..... N85-35220* #
NAS 1.26:170883 ..... N85-35221* #
NAS 1.26:170884 ..... N85-35294* #
NAS 1.26:170885 ..... N85-35222* #
NAS 1.26:170886 ..... N85-35423* #
NAS 1.26:170887 ..... N85-35407* #
NAS 1.26:170888 ..... N85-35223* #
NAS 1.26:170889 ..... N85-35237* #
NAS 1.26:170890 ..... N85-35238* #
NAS 1.26:170891 ..... N85-35224* #
NAS 1.26:170892 ..... N85-35295* #
NAS 1.26:170893 ..... N85-35239* #
NAS 1.26:170894 ..... N85-35240* #
NAS 1.26:172618 ..... N85-35642* #
NAS 1.26:174696 ..... N85-35726* #
NAS 1.26:174724 ..... N85-35471* #
NAS 1.26:174766-VOL-1 ..... N85-35197* #
NAS 1.26:174766-VOL-2 ..... N85-35198* #
NAS 1.26:174927 ..... N85-35185* #
NAS 1.26:174960 ..... N85-35389* #
NAS 1.26:174963 ..... N85-35472* #
NAS 1.26:174973 ..... N85-35391* #
NAS 1.26:174975 ..... N85-35162* #
NAS 1.26:175308 ..... N85-35213*
NAS 1.26:175309 ..... N85-35641* #
NAS 1.26:176151 ..... N85-35844* #
NAS 1.26:176166 ..... N85-35201* #
NAS 1.26:176167 ..... N85-35533* #
NAS 1.26:176168 ..... N85-35840* #
NAS 1.26:176169 ..... N85-35749* #
NAS 1.26:176170 ..... N85-35517* #
NAS 1.26:176171 ..... N85-35794* #
NAS 1.26:176172 ..... N85-35841* #
NAS 1.26:176173 ..... N85-35845* #
NAS 1.26:176174 ..... N85-35186* #
NAS 1.26:176175 ..... N85-35214* #
NAS 1.26:176176 ..... N85-35244* #
NAS 1.26:176177 ..... N85-35594* #
NAS 1.26:176178 ..... N85-35695* #
NAS 1.26:176179 ..... N85-35395* #
NAS 1.26:176180 ..... N85-35215* #
NAS 1.26:176181 ..... N85-35591* #
NAS 1.26:176182 ..... N85-35590* #
NAS 1.26:176183 ..... N85-35589* #
NAS 1.26:176184 ..... N85-35588* #
NAS 1.26:176185 ..... N85-35713* #
NAS 1.26:176186 ..... N85-35320* #
NAS 1.26:176189 ..... N85-35321* #
NAS 1.26:176190 ..... N85-35342* #
NAS 1.26:176192 ..... N85-35373* #
NAS 1.26:176193 ..... N85-35343* #
NAS 1.26:176194 ..... N85-35324* #
NAS 1.26:176195 ..... N85-35325* #
NAS 1.26:176196 ..... N85-35795* #
NAS 1.26:176197 ..... N85-35323* #
NAS 1.26:176199 ..... N85-35322* #
NAS 1.26:176200 ..... N85-35750* #
NAS 1.26:176201 ..... N85-35219* #
NAS 1.26:176227 ..... N85-35306* #
NAS 1.26:176264 ..... N85-35463* #
NAS 1.26:176265 ..... N85-35464* #
NAS 1.26:177374 ..... N85-35639* #
NAS 1.26:177375 ..... N85-35640* #
NAS 1.26:177930 ..... N85-35643* #
NAS 1.26:177941 ..... N85-35675* #
NAS 1.26:177943-VOL-1 ..... N85-35202* #
NAS 1.26:177943-VOL-2 ..... N85-35203* #
NAS 1.26:177944 ..... N85-35676* #
NAS 1.26:177947 ..... N85-35375* #
NAS 1.26:177953 ..... N85-35390* #
NAS 1.26:177958 ..... N85-35243* #
NAS 1.26:178522 ..... N85-35540* #
NAS 1.55:2376-VOL-6 ..... N85-35848* #
NAS 1.55:2376-VOL-7 ..... N85-35968* #
NAS 1.55:2376-VOL-8 ..... N85-36066* #
NAS 1.60:2464 ..... N85-35307* #

NASA-CASE-LAR-13019-1 ..... N85-35194*
NASA-CASE-LAR-13076-1 ..... N85-35200*

NASA-CASE-LEW-13562-2 ..... N85-35195*
NASA-CASE-LEW-13923-1 ..... N85-35267*
NASA-CASE-LEW-14057-1 ..... N85-35233*

NASA-CASE-NPO-15924-1 ..... N85-35253*
NASA-CASE-NPO-16203-1 ..... N85-35227*

NASA-CP-2376-VOL-6 ..... N85-35848* #
NASA-CP-2376-VOL-7 ..... N85-35968* #
NASA-CP-2376-VOL-8 ..... N85-36066* #

NASA-CR-3917 ..... N85-35184* #
NASA-CR-3925 ..... N85-35158* #
NASA-CR-3926 ..... N85-35159* #
NASA-CR-3929 ..... N85-35371* #
NASA-CR-3930 ..... N85-35160* #
NASA-CR-166091 ..... N85-35241* #
NASA-CR-167862 ..... N85-35534* #
NASA-CR-167863 ..... N85-35535* #
NASA-CR-167864 ..... N85-35536* #
NASA-CR-167865 ..... N85-35537* #
NASA-CR-167866 ..... N85-35538* #
NASA-CR-167884 ..... N85-35539* #
NASA-CR-168037 ..... N85-35199* #
NASA-CR-170881 ..... N85-35236* #
NASA-CR-170882 ..... N85-35220* #
NASA-CR-170883 ..... N85-35221* #
NASA-CR-170884 ..... N85-35294* #
NASA-CR-170885 ..... N85-35222* #
NASA-CR-170886 ..... N85-35423* #
NASA-CR-170887 ..... N85-35407* #
NASA-CR-170888 ..... N85-35223* #
NASA-CR-170889 ..... N85-35237* #
NASA-CR-170890 ..... N85-35238* #
NASA-CR-170891 ..... N85-35224* #
NASA-CR-170892 ..... N85-35295* #
NASA-CR-170893 ..... N85-35239* #
NASA-CR-170894 ..... N85-35240* #
NASA-CR-172618 ..... N85-35642* #
NASA-CR-174696 ..... N85-35726* #
NASA-CR-174724 ..... N85-35471* #
NASA-CR-174766-VOL-1 ..... N85-35197* #
NASA-CR-174766-VOL-2 ..... N85-35198* #
NASA-CR-174927 ..... N85-35185* #
NASA-CR-174960 ..... N85-35389* #
NASA-CR-174963 ..... N85-35472* #
NASA-CR-174973 ..... N85-35391* #
NASA-CR-174975 ..... N85-35162* #
NASA-CR-175308 ..... N85-35213*
NASA-CR-175309 ..... N85-35641* #
NASA-CR-176151 ..... N85-35844* #
NASA-CR-176166 ..... N85-35201* #
NASA-CR-176167 ..... N85-35533* #
NASA-CR-176168 ..... N85-35840* #
NASA-CR-176169 ..... N85-35749* #
NASA-CR-176170 ..... N85-35517* #
NASA-CR-176171 ..... N85-35794* #
NASA-CR-176172 ..... N85-35841* #
NASA-CR-176173 ..... N85-35845* #
NASA-CR-176174 ..... N85-35186* #
NASA-CR-176175 ..... N85-35214* #
NASA-CR-176176 ..... N85-35244* #
NASA-CR-176177 ..... N85-35594* #
NASA-CR-176178 ..... N85-35695* #
NASA-CR-176179 ..... N85-35395* #
NASA-CR-176180 ..... N85-35215* #
NASA-CR-176181 ..... N85-35591* #
NASA-CR-176182 ..... N85-35590* #
NASA-CR-176183 ..... N85-35589* #
NASA-CR-176184 ..... N85-35588* #
NASA-CR-176185 ..... N85-35713* #
NASA-CR-176186 ..... N85-35320* #
NASA-CR-176189 ..... N85-35321* #
NASA-CR-176190 ..... N85-35342* #
NASA-CR-176192 ..... N85-35373* #
NASA-CR-176193 ..... N85-35343* #
NASA-CR-176194 ..... N85-35324* #
NASA-CR-176195 ..... N85-35325* #
NASA-CR-176196 ..... N85-35795* #
NASA-CR-176197 ..... N85-35323* #
NASA-CR-176199 ..... N85-35322* #
NASA-CR-176200 ..... N85-35750* #
NASA-CR-176201 ..... N85-35219* #
NASA-CR-176227 ..... N85-35306* #
NASA-CR-176264 ..... N85-35463* #
NASA-CR-176265 ..... N85-35464* #
NASA-CR-177374 ..... N85-35639* #
NASA-CR-177375 ..... N85-35640* #
NASA-CR-177930 ..... N85-35643* #
NASA-CR-177941 ..... N85-35675* #
NASA-CR-177943-VOL-1 ..... N85-35202* #
NASA-CR-177943-VOL-2 ..... N85-35203* #
NASA-CR-177944 ..... N85-35676* #
NASA-CR-177947 ..... N85-35375* #
NASA-CR-177953 ..... N85-35390* #
NASA-CR-177958 ..... N85-35243* #
NASA-CR-178522 ..... N85-35540* #

NASA-EP-197 ..... N85-35839* #

NASA-SP-7037(190) N85-35152*
NASA-SP-7039(27)-SECTION-2 ..... N85-35820*
NASA-SP-7046(12) N85-35209*

NASA-TM-77673 ..... N85-35296* #
NASA-TM-77869 ..... N85-35272* #
NASA-TM-77883 ..... N85-35161* #
NASA-TM-77896 ..... N85-35245* #
NASA-TM-77906 ..... N85-35242* #
NASA-TM-77912 ..... N85-35163* #
NASA-TM-77920 ..... N85-35164* #
NASA-TM-86671 ..... N85-35623* #
NASA-TM-86681 ..... N85-35834* #
NASA-TM-86712 ..... N85-35573* #
NASA-TM-86721 ..... N85-35832* #
NASA-TM-86722 ..... N85-35833* #
NASA-TM-86756 ..... N85-35578* #
NASA-TM-86780 ..... N85-35372* #
NASA-TM-86820 ..... N85-35210* #
NASA-TM-87069 ..... N85-35225* #
NASA-TM-87503 ..... N85-35831* #
NASA-TM-87505 ..... N85-35206*

NASA-TM-87576 ..... N85-35204* #
NASA-TM-87577 ..... N85-35637* #
NASA-TM-87594 ..... N85-35424* #
NASA-TM-87596 ..... N85-35374* #

NASA-TP-2464 ..... N85-35307* #

NAVTRAEQUIPC-IH-355 ..... N85-35632 #

NAVTRAEQUIPC-81-C-0105-16 ..... N85-35611 #

NBS-TN-1078 ..... N85-35364 #

NBS/TN-910-8 ..... N85-35754 #
NBS/TN-1080 ..... N85-35755 #
NBS/TN-1202 ..... N85-35753 #

NBSIR-84/2877-3 ..... N85-35363 #
NBSIR-84/2989-NASA ..... N85-35306* #
NBSIR-85/3118 ..... N85-35317 #
NBSIR-85/3135 ..... N85-35526 #
NBSIR-85/3153 ..... N85-35827 #

NCAR/CT-85 ..... N85-35568 #
NCAR/CT-86 ..... N85-35567 #

NCEL-TN-1723 ..... N85-35488 #

NEPRF-CR-84-09 ..... N85-35561 #

NMERDI-2-71-4333 ..... N85-35468 #

NOAA-TM-ERL-ESG-9 ..... N85-35571 #

NOAA-TM-ERL-PMEL-60 ..... N85-35570 #

NOAA-TR-NESDIS-19 ..... N85-35218 #

NOAA/TM-NESDIS-9 ..... N85-35566 #

NORDA-90 ..... N85-35576 #
NORDA-108 ..... N85-35577 #

NPS68-85-017 ..... N85-35560 #

NRL-MR-5534 ..... N85-35402 #
NRL-MR-5575 ..... N85-35682 #

NRL-8697 ..... N85-35627 #

NSF/CEE-84027 ..... N85-35527 #

NSF/ENG-85003 ..... N85-35433 #
NSF/ENG-85007 ..... N85-35434 #

NSMRL-1045 ..... N85-35616 #

NSWC/TR-84-360 ..... N85-35348 #
NSWC/TR-84-364 ..... N85-35208 #

NTIA-84-168 ..... N85-35340 #
NTIA-85-171 ..... N85-35331 #

NUREG/CR-3721-1-VOL-1 ..... N85-35259 #
NUREG/CR-4180 ..... N85-35806 #

NUSC-TM-811061 ..... N85-35696 #

NWC-TP-6490 ..... N85-35427 #
NWC-TP-6621 ..... N85-35330 #

ONRL-C-3-85 ..... N85-35692 #
ONRL-C-4-85 ..... N85-35715 #

ORAU/IEA-85-3(M) ..... N85-35818 #

ORNL-6152 ..... N85-35228 #

ORNL/CDIC-10 ..... N85-35562 #

ORNL/CSD-78/R1 ..... N85-35659 #

ORNL/SUB-83/43374/1/V3 ..... N85-35771 #

ORNL/TM-9381 ..... N85-35299 #
ORNL/TM-9573 ..... N85-35287 #
ORNL/TM-9649 ..... N85-35232 #

OSU/DGSS-358 ..... N85-35519 #

PB85-157766 ..... N85-35266 #
PB85-185072 ..... N85-35819 #
PB85-185387 ..... N85-35340 #
PB85-187052 ..... N85-35565 #
PB85-187904 ..... N85-35571 #
PB85-187938 ..... N85-35570 #

PB85-188050 ..... N85-35569 #
PB85-188233 ..... N85-35830 #
PB85-188332 ..... N85-35310 #
PB85-188340 ..... N85-35316 #
PB85-188944 ..... N85-35503 #
PB85-189108 ..... N85-35568 #
PB85-190866 ..... N85-35567 #
PB85-191393 ..... N85-35363 #
PB85-191419 ..... N85-35364 #
PB85-191815 ..... N85-35566 #
PB85-191971 ..... N85-35311 #
PB85-192755 ..... N85-35470 #
PB85-193068 ..... N85-35828 #
PB85-193522 ..... N85-35501 #
PB85-193910 ..... N85-35502 #
PB85-194363 ..... N85-35433 #
PB85-194736 ..... N85-35755 #
PB85-195279 ..... N85-35218 #
PB85-195303 ..... N85-35754 #
PB85-195766 ..... N85-35434 #
PB85-196376 ..... N85-35500 #
PB85-196871 ..... N85-35529 #
PB85-196889 ..... N85-35528 #
PB85-197887 ..... N85-35527 #
PB85-198562 ..... N85-35291 #
PB85-198570 ..... N85-35290 #
PB85-198695 ..... N85-35388 #
PB85-199545 ..... N85-35317 #
PB85-199602 ..... N85-35315 #
PB85-199636 ..... N85-35318 #
PB85-200186 ..... N85-35753 #
PB85-200210 ..... N85-35264 #
PB85-200228 ..... N85-35265 #
PB85-204345 ..... N85-35262 #
PB85-204394 ..... N85-35314 #
PB85-204600 ..... N85-35263 #
PB85-204717 ..... N85-35306* #
PB85-208494 ..... N85-35526 #
PB85-208502 ..... N85-35827 #

PH-272 ..... N85-35694

PM/84/18 ..... N85-35677 #

PNL-SA-12909 ..... N85-35738 #

PREPRINT-SER-027 ..... N85-35834* #

PWA-5594-251-VOL-2 ..... N85-35198* #
PWA-5594-258-VOL-1 ..... N85-35197* #
PWA-5914-39 ..... N85-35391* #

QR-1 ..... N85-35650 #
QR-2 ..... N85-35499 #
QR-2 ..... N85-35649 #
QR-4 ..... N85-35215* #

QTR-36 ..... N85-35216 #

RADC-TR-84-225 ..... N85-35350 #
RADC-TR-85-50 ..... N85-35335 #

REPT-2-SUPPL-9 ..... N85-35574 #
REPT-80 ..... N85-35638 #
REPT-83-1 ..... N85-35380 #
REPT-85-6 ..... N85-35342* #
REPT-110 ..... N85-35673 #
REPT-6546 ..... N85-35350 #
REPT-85129 ..... N85-35834* #
REPT-85208 ..... N85-35573* #
REPT-85222 ..... N85-35832* #
REPT-85223 ..... N85-35833* #
REPT-85264 ..... N85-35578* #
REPT-85350 ..... N85-35372* #
REPT-85375 ..... N85-35210* #

RFP-3728 ..... N85-35284 #
RFP-3780 ..... N85-35397 #

RNASCHQ8401 ..... N85-35329 #

RPT50220 ..... N85-35799 #

R82AEB293 ..... N85-35199* #

SAIC-85/1676-PRI-91 ..... N85-35353 #

SAND-83-7037 ..... N85-35495 #
SAND-84-2097C ..... N85-35414 #
SAND-84-2287C ..... N85-35302 #
SAND-84-2366C ..... N85-35769 #
SAND-84-2374C ..... N85-35564 #
SAND-84-2412C ..... N85-35768 #
SAND-84-2443C ..... N85-35782 #
SAND-84-2457C ..... N85-35780 #
SAND-84-2458C ..... N85-35355 #
SAND-84-2520C ..... N85-35756 #
SAND-84-2538C ..... N85-35720 #
SAND-84-2578C ..... N85-35354 #
SAND-84-8192 ..... N85-35380 #
SAND-85-0132 ..... N85-35338 #
SAND-85-0151C ..... N85-35396 #
SAND-85-0173C ..... N85-35412 #
SAND-85-0302C ..... N85-35398 #
SAND-85-0391C ..... N85-35808 #
SAND-85-0428C ..... N85-35386 #
SAND-85-0548 ..... N85-35393 #
SAND-85-7194 ..... N85-35489 #
SAND-85-05080 ..... N85-35357 #

SAPR-1 ..... N85-35749* #
SAPR-2 ..... N85-35749* #
SAPR-3 ..... N85-35840* #

SD-TR-85-25 ..... N85-35685 #
SD-TR-85-33 ..... N85-35351 #

SERI/TP-252-2693 ..... N85-35492 #

SME-ENG-HOR3 ..... N85-35213*

SR-1 ..... N85-35523 #
SR-2 ..... N85-35522 #
SR-2 ..... N85-35524 #
SR-4 ..... N85-35684 #
SR-7 ..... N85-35519 #
SR-7 ..... N85-35648 #

SRI-MP-85-024 ..... N85-35264 #

SU-AIM-352 ..... N85-35630 #

SU-SLAC-PUB-3546 ..... N85-35792 #
SU-SLAC-PUB-3608 ..... N85-35772 #
SU-SLAC-PUB-3609 ..... N85-35790 #
SU-SLAC-PUB-3610 ..... N85-35356 #
SU-SLAC-PUB-3612 ..... N85-35789 #
SU-SLAC-PUB-3631 ..... N85-35793 #
SU-SLAC-PUB-3633 ..... N85-35664 #
SU-SLAC-PUB-3640 ..... N85-35774 #
SU-SLAC-PUB-3646 ..... N85-35763 #
SU-SLAC-PUB-3658 ..... N85-35843 #
SU-SLAC-PUB-3659 ..... N85-35723 #
SU-SLAC-PUB-3668 ..... N85-35722 #
SU-SLAC-PUB-3673 ..... N85-35211 #
SU-SLAC-PUB-3683 ..... N85-35724 #
SU-SLAC-PUB-3690 ..... N85-35785 #

SU-SLAC-TN-84-1-REV ..... N85-35758 #

SU-STAN-CS-85-1041 ..... N85-35630 #

SU-TR-33 ..... N85-35681 #
SU-TR-233 ..... N85-35681 #
SU-TR-358 ..... N85-35686 #

SYRU/DECE/TR-85/1 ..... N85-35326 #

TACOM-TR-13090 ..... N85-35644 #
TACOM-TR-13091 ..... N85-35408 #

TE-4367-24-85 ..... N85-35318 #

TI85-002629 ..... N85-35414 #
TI85-003048 ..... N85-35283 #
TI85-008674 ..... N85-35806 #
TI85-009899 ..... N85-35259 #

TN-84-7104-101-13 ..... N85-35640* #
TN-84-7104-101-16 ..... N85-35639* #

TOP-1-2-601-REV ..... N85-35188 #
TOP-6-2-090 ..... N85-35207 #

TR-AAE-85-4 ..... N85-35389* #

TR-6 ..... N85-35297 #
TR-7 ..... N85-35798 #
TR-14 ..... N85-35679 #
TR-24 ..... N85-35298 #
TR-25 ..... N85-35803 #
TR-26 ..... N85-35252 #
TR-85-2 ..... N85-35529 #
TR-85-4 ..... N85-35528 #
TR-85-8 ..... N85-35320* #
TR-716 ..... N85-35634 #
TR-0084(4409-13)-1 ..... N85-35685 #
TR-0084A(5902-04)-1 ..... N85-35351 #
TR-84428-VOL-2 ..... N85-35184* #

UCB/SESM-85/02 ..... N85-35660 #

UCID-19912-REV-1 ..... N85-35662 #
UCID-20443 ..... N85-35404 #

UCRL-15679 ..... N85-35660 #
UCRL-91626 ..... N85-35563 #
UCRL-91968 ..... N85-35783 #
UCRL-92155 ..... N85-35743 #
UCRL-92236 ..... N85-35791 #
UCRL-92672 ..... N85-35842 #
UCRL-92682 ..... N85-35305 #
UCRL-92725 ..... N85-35740 #
UCRL-92855 ..... N85-35289 #

UDR-TR-82-156-VOL-1 ..... N85-35257 #
UDR-TR-85-94 ..... N85-35540* #

UHMET-84-1 ..... N85-35561 #

UILU-ENG-85-0504 ..... N85-35389* #
UILU-ENG-85-1710 ..... N85-35658 #
UILU-ENG-85-2543 ..... N85-35328 #
UILU-ENG-85-2565 ..... N85-35342* #

UMTA-MD-06-0047-84-1 ..... N85-35830 #

US-PATENT-APPL-SN-375784 ..... N85-35233*
US-PATENT-APPL-SN-493179 ..... N85-35227*
US-PATENT-APPL-SN-500651 ..... N85-35195*
US-PATENT-APPL-SN-523297 ..... N85-35233*
US-PATENT-APPL-SN-526768 ..... N85-35253*
US-PATENT-APPL-SN-532342 ..... N85-35200*
US-PATENT-APPL-SN-571617 ..... N85-35267*
US-PATENT-APPL-SN-576308 ..... N85-35194*
US-PATENT-APPL-SN-612952 ..... N85-35300 #
US-PATENT-APPL-SN-625323 ..... N85-35301 #
US-PATENT-APPL-SN-640712 ..... N85-35233*
US-PATENT-APPL-SN-662645 ..... N85-35736 #

US-PATENT-CLASS-44-1-SR N85-35253*
US-PATENT-CLASS-60-39.23 ..... N85-35195*
US-PATENT-CLASS-60-748 ..... N85-35195*
US-PATENT-CLASS-201-17 ..... N85-35253*
US-PATENT-CLASS-239-402.5 ..... N85-35195*
US-PATENT-CLASS-244-55 ..... N85-35194*
US-PATENT-CLASS-244-75-R N85-35200*
US-PATENT-CLASS-244-113 ..... N85-35200*
US-PATENT-CLASS-244-139 ..... N85-35200*
US-PATENT-CLASS-244-199 ..... N85-35194*
US-PATENT-CLASS-427-191 ..... N85-35267*
US-PATENT-CLASS-427-228 ..... N85-35267*
US-PATENT-CLASS-427-294 ..... N85-35267*
US-PATENT-CLASS-427-376.2 ..... N85-35267*
US-PATENT-CLASS-427-380 ..... N85-35267*
US-PATENT-CLASS-427-397.7 ..... N85-35267*
US-PATENT-CLASS-428-633 ..... N85-35233*
US-PATENT-CLASS-428-656 ..... N85-35233*
US-PATENT-CLASS-428-678 ..... N85-35233*
US-PATENT-CLASS-428-679 ..... N85-35233*
US-PATENT-CLASS-428-680 ..... N85-35233*
US-PATENT-CLASS-428-681 ..... N85-35233*
US-PATENT-CLASS-428-682 ..... N85-35233*
US-PATENT-CLASS-428-698 ..... N85-35267*
US-PATENT-CLASS-428-704 ..... N85-35267*
US-PATENT-CLASS-435-160 ..... N85-35227*
US-PATENT-CLASS-435-842 ..... N85-35227*

US-PATENT-4,485,151 ..... N85-35233*
US-PATENT-4,511,362 ..... N85-35253*
US-PATENT-4,533,101 ..... N85-35194*
US-PATENT-4,534,166 ..... N85-35195*
US-PATENT-4,535,033 ..... N85-35233*
US-PATENT-4,535,035 ..... N85-35267*
US-PATENT-4,538,778 ..... N85-35200*
US-PATENT-4,539,293 ..... N85-35227*

USAFSAM-TR-85-23 ..... N85-35606 #

USARIEM-M28/85 ..... N85-35614 #
USARIEM-M29/85 ..... N85-35612 #

USGS-CIRC-883 ..... N85-35465 #

USGS/WRI-84-4344 ..... N85-35469 #

UVA/525393/SE85/107 ..... N85-35680 #

WES/IR/K-84-10-1 ..... N85-35428 #
WES/IR/K-84-10-2 ..... N85-35429 #

WES/MP/GL-85-1 ..... N85-35411 #

WGR-85-5 ..... N85-35321* #

WIS-15 ..... N85-35575 #

WSR-3 ..... N85-35541 #

X-725-84-18 ..... N85-35206*

☆ U.S. GOVERNMENT PRINTING OFFICE: 1985-491-575/20023

FEDERAL DEPOSITORY LIBRARY PROGRAM

The Federal Depository Library Program provides Government publications to designated libraries throughout the United States. The Regional Depository Libraries listed below receive and retain at least one copy of nearly every Federal Government publication, either in printed or microfilm form, for use by the general public. These libraries provide reference services and inter-library loans; however, they are *not* sales outlets. You may wish to ask your local library to contact a Regional Depository to help you locate specific publications, or you may contact the Regional Depository yourself.

ARKANSAS STATE LIBRARY
One Capitol Mall
Little Rock, AR 72201
(501) 371-2326

AUBURN UNIV. AT MONTGOMERY LIBRARY
Documents Department
Montgomery, AL 36193
(205) 279-9110, ext. 253

UNIV. OF ALABAMA LIBRARY
Documents Dept.—Box S
University, AL 35486
(205) 348-7369

DEPT. OF LIBRARY, ARCHIVES AND PUBLIC RECORDS
Third Floor—State Cap.
1700 West Washington
Phoenix, AZ 85007
(602) 255-4121

UNIVERSITY OF ARIZONA LIB.
Government Documents Dept.
Tucson, AZ 85721
(602) 626-5233

CALIFORNIA STATE LIBRARY
Govt. Publications Section
P.O. Box 2037
Sacramento, CA 95809
(916) 322-4572

UNIV. OF COLORADO LIB.
Government Pub. Division
Campus Box 184
Boulder, CO 80309
(303) 492-8834

DENVER PUBLIC LIBRARY
Govt. Pub. Department
1357 Broadway
Denver, CO 80203
(303) 571-2131

CONNECTICUT STATE LIBRARY
Government Documents Unit
231 Capitol Avenue
Hartford, CT 06106
(203) 566-4971

UNIV. OF FLORIDA LIBRARIES
Library West
Documents Department
Gainesville, FL 32611
(904) 392-0367

UNIV. OF GEORGIA LIBRARIES
Government Reference Dept.
Athens, Ga 30602
(404) 542-8951

UNIV. OF HAWAII LIBRARY
Govt. Documents Collection
2550 The Mall
Honolulu, HI 96822
(808) 948-8230

UNIV. OF IDAHO LIBRARY
Documents Section
Moscow, ID 83843
(208) 885-6344

ILLINOIS STATE LIBRARY
Information Services Branch
Centennial Building
Springfield, IL 62706
(217) 782-5185

INDIANA STATE LIBRARY
Serials Documents Section
140 North Senate Avenue
Indianapolis, IN 46204
(317) 232-3686

UNIV. OF IOWA LIBRARIES
Govt. Documents Department
Iowa City, IA 52242
(319) 353-3318

UNIVERSITY OF KANSAS
Doc. Collect—Spencer Lib.
Lawrence, KS 66045
(913) 864-4662

UNIV. OF KENTUCKY LIBRARIES
Govt. Pub. Department
Lexington, KY 40506
(606) 257-3139

LOUISIANA STATE UNIVERSITY
Middleton Library
Govt. Docs. Dept.
Baton Rouge, LA 70803
(504) 388-2570

LOUISIANA TECHNICAL UNIV. LIBRARY
Documents Department
Ruston, LA 71272
(318) 257-4962

UNIVERSITY OF MAINE
Raymond H. Fogler Library
Tri-State Regional Documents Depository
Orono, ME 04469
(207) 581-1680

UNIVERSITY OF MARYLAND
McKeldin Lib.—Doc. Div.
College Park, MD 20742
(301) 454-3034

BOSTON PUBLIC LIBRARY
Government Docs. Dept.
Boston, MA 02117
(617) 536-5400 ext. 226

DETROIT PUBLIC LIBRARY
Sociology Department
5201 Woodward Avenue
Detroit, MI 48202
(313) 833-1409

MICHIGAN STATE LIBRARY
P.O. Box 30007
Lansing, MI 48909
(517) 373-0640

UNIVERSITY OF MINNESOTA
Government Pubs. Division
409 Wilson Library
309 19th Avenue South
Minneapolis, MN 55455
(612) 373-7813

UNIV. OF MISSISSIPPI LIB.
Documents Department
University, MS 38677
(601) 232-5857

UNIV. OF MONTANA
Mansfield Library
Documents Division
Missoula, MT 59812
(406) 243-6700

NEBRASKA LIBRARY COMM.
Federal Documents
1420 P Street
Lincoln, NE 68508
(402) 471-2045
In cooperation with University of Nebraska-Lincoln

UNIVERSITY OF NEVADA LIB.
Govt. Pub. Department
Reno, NV 89557
(702) 784-6579

NEWARK PUBLIC LIBRARY
5 Washington Street
Newark, NJ 07101
(201) 733-7812

UNIVERSITY OF NEW MEXICO
Zimmerman Library
Government Pub. Dept.
Albuquerque, NM 87131
(505) 277-5441

NEW MEXICO STATE LIBRARY
Reference Department
325 Don Gaspar Avenue
Santa Fe, NM 87501
(505) 827-2033, ext. 22

NEW YORK STATE LIBRARY
Empire State Plaza
Albany, NY 12230
(518) 474-5563

UNIVERSITY OF NORTH CAROLINA AT CHAPEL HILL
Wilson Library
BA/SS Documents Division
Chapel Hill, NC 27515
(919) 962-1321

UNIVERSITY OF NORTH DAKOTA
Chester Fritz Library
Documents Department
Grand Forks, ND 58202
(701) 777-2617, ext. 27
(In cooperation with North Dakota State Univ. Library)

STATE LIBRARY OF OHIO
Documents Department
65 South Front Street
Columbus, OH 43215
(614) 462-7051

OKLAHOMA DEPT. OF LIB.
Government Documents
200 NE 18th Street
Oklahoma City, OK 73105
(405) 521-2502

OKLAHOMA STATE UNIV. LIB.
Documents Department
Stillwater, OK 74078
(405) 624-6546

PORTLAND STATE UNIV. LIB.
Documents Department
P.O. Box 1151
Portland, OR 97207
(503) 229-3673

STATE LIBRARY OF PENN.
Government Pub. Section
P.O. Box 1601
Harrisburg, PA 17105
(717) 787-3752

TEXAS STATE LIBRARY
Public Services Department
P.O. Box 12927—Cap. Sta.
Austin, TX 78753
(512) 471-2996

TEXAS TECH UNIV. LIBRARY
Govt. Documents Department
Lubbock, TX 79409
(806) 742-2268

UTAH STATE UNIVERSITY
Merrill Library, U.M.C. 30
Logan, UT 84322
(801) 750-2682

UNIVERSITY OF VIRGINIA
Alderman Lib.—Public Doc.
Charlottesville, VA 22901
(804) 924-3133

WASHINGTON STATE LIBRARY
Documents Section
Olympia, WA 98504
(206) 753-4027

WEST VIRGINIA UNIV. LIB.
Documents Department
Morgantown, WV 26506
(304) 293-3640

MILWAUKEE PUBLIC LIBRARY
814 West Wisconsin Avenue
Milwaukee, WI 53233
(414) 278-3000

ST. HIST LIB. OF WISCONSIN
Government Pub. Section
816 State Street
Madison, WI 53706
(608) 262-4347

WYOMING STATE LIBRARY
Supreme Ct. & Library Bld.
Cheyenne, WY 82002
(307) 777-6344

National Aeronautics and
Space Administration
Code NIT-4
Washington, D.C.
20546

Official Business

Penalty for Private Use, $300

SPECIAL FOURTH-CLASS RATE
POSTAGE & FEES PAID
NASA
WASHINGTON, D.C.
PERMIT No. G 27

NASA

POSTMASTER: If Undeliverable (Section 158
Postal Manual) Do Not Return